Scientific and Technical Aerospace Reports

STAR

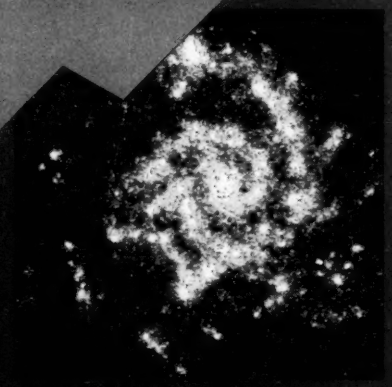

An Abstract Journal

Volume 30, Number 22
November 23, 1992
N92-31238 to N92-32242

Scientific and Technical Aerospace Reports

Scientific and Technical Aerospace Reports (STAR) is an abstract journal that provides comprehensive coverage of worldwide aerospace-related reports. It is a major product of the International Aerospace Database managed by the NASA Scientific and Technical Information (STI) Program. The coverage includes reports on aeronautics, space, and supporting disciplines. *STAR* lists current, publicly available reports entered into the NASA STI Database during the 2-week period preceding publication. A typical citation and abstract appear on page viii. They explain how to read the items that are announced in this journal.

NASA sponsors a companion journal, *International Aerospace Abstracts (IAA)* (*NOVA* for internal NASA use) that lists abstracts of the open literature on aerospace subjects available worldwide. *IAA* is available for sale through the AIAA.

Entries found in *STAR* and *IAA* are available through NASA's online service, RECON, as the International Aerospace Database and through DIALOG as the Aerospace Database.

Information on aerospace and related subjects is gathered by the NASA STI Program through national and international agreements and exchanges and is made available to the NASA community as well as to the public in many forms through various outlets. The section on NASA STI Program Products and Services contains additional information.

For further information please contact:
NASA Center for AeroSpace Information (CASI)
P.O. Box 8757
Baltimore, Maryland 21240-0757
(301) 621-0390

US ISSN 0036-8741

Volume 30 Number 22 / November 23, 1992

TABLE OF CONTENTS

AERONAUTICS For related information see also *Astronautics.*

01 AERONAUTICS (GENERAL) **3745**

02 AERODYNAMICS **3750**
Includes aerodynamics of bodies, combinations, wings, rotors, and control surfaces; and internal flow in ducts and turbomachinery. For related information see also *34 Fluid Mechanics and Heat Transfer.*

03 AIR TRANSPORTATION AND SAFETY **3755**
Includes passenger and cargo air transport operations; and aircraft accidents. For related information see also *16 Space Transportation* and *85 Urban Technology and Transportation.*

04 AIRCRAFT COMMUNICATIONS AND NAVIGATION **3756**
Includes digital and voice communication with aircraft; air navigation systems (satellite and ground based); and air traffic control. For related information see also *17 Space Communications, Spacecraft Communications, Command and Tracking* and *32 Communications and Radar.*

05 AIRCRAFT DESIGN, TESTING AND PERFORMANCE **3756**
Includes aircraft simulation technology. For related information see also *18 Spacecraft Design, Testing and Performance* and *39 Structural Mechanics.* For land transportation vehicles see *85 Urban Technology and Transportation.*

06 AIRCRAFT INSTRUMENTATION **3758**
Includes cockpit and cabin display devices; and flight instruments. For related information see also *19 Space craft Instrumentation* and *35 Instrumentation and Photography.*

07 AIRCRAFT PROPULSION AND POWER **3759**
Includes prime propulsion systems and systems components, e.g., gas turbine engines and compressors; and onboard auxiliary power plants for aircraft. For related information see also *20 Spacecraft Propulsion and Power, 28 Propellants and Fuels,* and *44 Energy Production and Conversion.*

08 AIRCRAFT STABILITY AND CONTROL **3760**
Includes aircraft handling qualities; piloting; flight controls; and autopilots. For related information see also *05 Aircraft Design, Testing and Performance.*

09 RESEARCH AND SUPPORT FACILITIES (AIR) **3762**
Includes airports, hangars and runways; aircraft repair and overhaul facilities; wind tunnels; shock tubes; and aircraft engine test stands. For related information see also *14 Ground Support Systems and Facilities (Space).*

ASTRONAUTICS For related information see also *Aeronautics.*

12 ASTRONAUTICS (GENERAL) **3762**
For extraterrestrial exploration see *91 Lunar and Planetary Exploration.*

13 ASTRODYNAMICS **3765**
Includes powered and free-flight trajectories; and orbital and launching dynamics.

14 GROUND SUPPORT SYSTEMS AND FACILITIES (SPACE) ..... **N.A.**
Includes launch complexes, research and production facilities; ground support equipment, e.g., mobile transporters; and simulators. For related information see also *09 Research and Support Facilities (Air).*

15 LAUNCH VEHICLES AND SPACE VEHICLES **3765**
Includes boosters; operating problems of launch/space vehicle systems; and reusable vehicles. For related information see also *20 Spacecraft Propulsion and Power.*

16 SPACE TRANSPORTATION **3766**
Includes passenger and cargo space transportation, e.g., shuttle operations; and space rescue techniques. For related information see also *03 Air Transportation and Safety* and *18 Spacecraft Design, Testing and Performance.* For space suits see *54 Man/System Technology and Life Support.*

17 SPACE COMMUNICATIONS, SPACECRAFT COMMUNICATIONS, COMMAND AND TRACKING . **N.A.**
Includes telemetry; space communications networks; astronavigation and guidance; and radio blackout. For related information see also *04 Aircraft Communications and Navigation* and *32 Communications and Radar.*

N.A.—no abstracts were assigned to this category for this issue.

18 SPACECRAFT DESIGN, TESTING AND PERFORMANCE **3766**
Includes satellites; space platforms; space stations; spacecraft systems and components such as thermal and environmental controls; and attitude controls. For life support systems see *54 Man/System Technology and Life Support.* For related information see also *05 Aircraft Design, Testing and Performance, 39 Structural Mechanics,* and *16 Space Transportation.*

19 SPACECRAFT INSTRUMENTATION **3768**
For related information see also *06 Aircraft Instrumentation* and *35 Instrumentation and Photography.*

20 SPACECRAFT PROPULSION AND POWER **3769**
Includes main propulsion systems and components, e.g., rocket engines; and spacecraft auxiliary power sources. For related information see also *07 Aircraft Propulsion and Power, 28 Propellants and Fuels, 44 Energy Production and Conversion,* and *15 Launch Vehicles and Space Vehicles.*

CHEMISTRY AND MATERIALS

23 CHEMISTRY AND MATERIALS (GENERAL) **3772**

24 COMPOSITE MATERIALS **3772**
Includes physical, chemical, and mechanical properties of laminates and other composite materials. For ceramic materials see *27 Nonmetallic Materials.*

25 INORGANIC AND PHYSICAL CHEMISTRY **3777**
Includes chemical analysis, e.g., chromatography; combustion theory; electrochemistry; and photochemistry. For related information see also *77 Thermodynamics and Statistical Physics.*

26 METALLIC MATERIALS **3786**
Includes physical, chemical, and mechanical properties of metals, e.g., corrosion; and metallurgy.

27 NONMETALLIC MATERIALS **3791**
Includes physical, chemical, and mechanical properties of plastics, elastomers, lubricants, polymers, textiles, adhesives, and ceramic materials. For composite materials see *24 Composite Materials.*

28 PROPELLANTS AND FUELS **3798**
Includes rocket propellants, igniters and oxidizers; their storage and handling procedures; and aircraft fuels. For related information see also *07 Aircraft Propulsion and Power, 20 Spacecraft Propulsion and Power,* and *44 Energy Production and Conversion.*

29 MATERIALS PROCESSING **3802**
Includes space-based development of products and processes for commercial application. For biological materials see *55 Space Biology.*

ENGINEERING For related information see also *Physics.*

31 ENGINEERING (GENERAL) **3802**
Includes vacuum technology; control engineering; display engineering; cryogenics; and fire prevention.

32 COMMUNICATIONS AND RADAR **3803**
Includes radar; land and global communications; communications theory; and optical communications. For related information see also *04 Aircraft Communications and Navigation* and *17 Space Communications, Spacecraft Communications, Command and Tracking.* For search and rescue see *03 Air Transportation and Safety,* and *16 Space Transportation.*

33 ELECTRONICS AND ELECTRICAL ENGINEERING **3811**
Includes test equipment and maintainability; components, e.g., tunnel diodes and transistors; microminiaturization; and integrated circuitry. For related information see also *60 Computer Operations and Hardware* and *76 Solid-State Physics.*

34 FLUID MECHANICS AND HEAT TRANSFER **3818**
Includes boundary layers; hydrodynamics; fluidics; mass transfer and ablation cooling. For related information see also *02 Aerodynamics* and *77 Thermodynamics and Statistical Physics.*

35 INSTRUMENTATION AND PHOTOGRAPHY **3826**
Includes remote sensors; measuring instruments and gauges; detectors; cameras and photographic supplies; and holography. For aerial photography see *43 Earth Resources and Remote Sensing.* For related information see also *06 Aircraft Instrumentation* and *19 Spacecraft Instrumentation.*

36 LASERS AND MASERS **3830**
Includes parametric amplifiers. For related information see also *76 Solid-State Physics.*

37 MECHANICAL ENGINEERING **3832**
Includes auxiliary systems (nonpower); machine elements and processes; and mechanical equipment.

38 QUALITY ASSURANCE AND RELIABILITY **3836**
Includes product sampling procedures and techniques; and quality control.

39 STRUCTURAL MECHANICS **3838**
Includes structural element design and weight analysis; fatigue; and thermal stress. For applications see *05 Aircraft Design, Testing and Performance* and *18 Spacecraft Design, Testing and Performance.*

GEOSCIENCES For related information see also *Space Sciences.*

42 GEOSCIENCES (GENERAL) **3843**

43 EARTH RESOURCES AND REMOTE SENSING **3843**
Includes remote sensing of earth resources by aircraft and spacecraft; photogrammetry; and aerial photography. For instrumentation see *35 Instrumentation and Photography.*

44 ENERGY PRODUCTION AND CONVERSION **3845**
Includes specific energy conversion systems, e.g., fuel cells; global sources of energy; geophysical conversion; and windpower. For related information see also *07 Aircraft Propulsion and Power, 20 Spacecraft Propulsion and Power,* and *28 Propellants and Fuels.*

45 ENVIRONMENT POLLUTION **3849**
Includes atmospheric, noise, thermal, and water pollution.

46 GEOPHYSICS **3855**
Includes aeronomy; upper and lower atmosphere studies; ionospheric and magnetospheric physics; and geomagnetism. For space radiation see *93 Space Radiation.*

47 METEOROLOGY AND CLIMATOLOGY **3858**
Includes weather forecasting and modification.

48 OCEANOGRAPHY **3863**
Includes biological, dynamic, and physical oceanography; and marine resources. For related information see also *43 Earth Resources and Remote Sensing.*

LIFE SCIENCES

51 LIFE SCIENCES (GENERAL) **3866**

52 AEROSPACE MEDICINE **3868**
Includes physiological factors; biological effects of radiation; and effects of weightlessness on man and animals.

53 BEHAVIORAL SCIENCES **3870**
Includes psychological factors; individual and group behavior; crew training and evaluation; and psychiatric research.

54 MAN/SYSTEM TECHNOLOGY AND LIFE SUPPORT **3872**
Includes human engineering; biotechnology; and space suits and protective clothing. For related information see also *16 Space Transportation.*

55 SPACE BIOLOGY ..... **N.A.**
Includes exobiology; planetary biology; and extraterrestrial life.

MATHEMATICAL AND COMPUTER SCIENCES

59 MATHEMATICAL AND COMPUTER SCIENCES (GENERAL) ..... **N.A.**

60 COMPUTER OPERATIONS AND HARDWARE **3873**
Includes hardware for computer graphics, firmware, and data processing. For components see *33 Electronics and Electrical Engineering.*

61 COMPUTER PROGRAMMING AND SOFTWARE **3874**
Includes computer programs, routines, algorithms, and specific applications, e.g., CAD/CAM.

62 COMPUTER SYSTEMS **3881**
Includes computer networks and special application computer systems.

63 CYBERNETICS **3884**
Includes feedback and control theory, artificial intelligence, robotics and expert systems. For related information see also *54 Man/System Technology and Life Support.*

64 NUMERICAL ANALYSIS **3886**
Includes iteration, difference equations, and numerical approximation.

65 STATISTICS AND PROBABILITY **3888**
Includes data sampling and smoothing; Monte Carlo method; and stochastic processes.

66 SYSTEMS ANALYSIS **3889**
Includes mathematical modeling; network analysis; and operations research.

67 THEORETICAL MATHEMATICS ..... **N.A.**
Includes topology and number theory.

PHYSICS For related information see also *Engineering.*

70 PHYSICS (GENERAL) **3889**
For precision time and time interval (PTTI) see *35 Instrumentation and Photography;* for geophysics, astrophysics or solar physics see *46 Geophysics, 90 Astrophysics,* or *92 Solar Physics.*

71 ACOUSTICS **3891**
Includes sound generation, transmission, and attenuation. For noise pollution see *45 Environment Pollution.*

72 ATOMIC AND MOLECULAR PHYSICS **3892**
Includes atomic structure, electron properties, and molecular spectra.

73 NUCLEAR AND HIGH-ENERGY PHYSICS **3899**
Includes elementary and nuclear particles; and reactor theory. For space radiation see *93 Space Radiation.*

74 OPTICS **3900**
Includes light phenomena and optical devices. For lasers see *36 Lasers and Masers.*

75 PLASMA PHYSICS **3903**
Includes magnetohydrodynamics and plasma fusion. For ionospheric plasmas see *46 Geophysics.* For space plasmas see *90 Astrophysics.*

76 SOLID-STATE PHYSICS **3907**
Includes superconductivity. For related information see also *33 Electronics and Electrical Engineering* and *36 Lasers and Masers.*

77 THERMODYNAMICS AND STATISTICAL PHYSICS **3914**
Includes quantum mechanics; theoretical physics; and Bose and Fermi statistics. For related information see also *25 Inorganic and Physical Chemistry* and *34 Fluid Mechanics and Heat Transfer.*

SOCIAL SCIENCES

80 SOCIAL SCIENCES (GENERAL) **3916**
Includes educational matters.

81 ADMINISTRATION AND MANAGEMENT **3916**
Includes management planning and research.

82 DOCUMENTATION AND INFORMATION SCIENCE **3917**
Includes information management; information storage and retrieval technology; technical writing; graphic arts; and micrography. For computer documentation see *61 Computer Programming and Software.*

83 ECONOMICS AND COST ANALYSIS ..... **N.A.**
Includes cost effectiveness studies.

84 LAW, POLITICAL SCIENCE AND SPACE POLICY **3922**
Includes NASA appropriation hearings; aviation law; space law and policy; international law; international cooperation; and patent policy.

85 URBAN TECHNOLOGY AND TRANSPORTATION **3922**
Includes applications of space technology to urban problems; technology transfer; technology assessment; and surface and mass transportation. For related information see *03 Air Transportation and Safety, 16 Space Transportation,* and *44 Energy Production and Conversion.*

SPACE SCIENCES For related information see also *Geosciences.*

88 SPACE SCIENCES (GENERAL) ..... **N.A.**

89 ASTRONOMY **3923**
Includes radio, gamma-ray, and infrared astronomy; and astrometry.

90 ASTROPHYSICS **3923**
Includes cosmology; celestial mechanics; space plasmas; and interstellar and interplanetary gases and dust. For related information see also *75 Plasma Physics.*

91 LUNAR AND PLANETARY EXPLORATION **3924**
Includes planetology; and manned and unmanned flights. For spacecraft design or space stations see *18 Spacecraft Design, Testing and Performance.*

92 SOLAR PHYSICS **3925**
Includes solar activity, solar flares, solar radiation and sunspots. For related information see *93 Space Radiation.*

93 SPACE RADIATION **3926**
Includes cosmic radiation; and inner and outer earth's radiation belts. For biological effects of radiation see *52 Aerospace Medicine.* For theory see *73 Nuclear and High-Energy Physics.*

GENERAL

Includes aeronautical, astronautical, and space science related histories, biographies, and pertinent reports too broad for categorization; histories or broad overviews of NASA programs.

99 GENERAL **3926**

SUBJECT INDEX **I-1**

PERSONAL AUTHOR INDEX **I-85**

CORPORATE SOURCE INDEX **I-93**

CONTRACT NUMBER INDEX **I-107**

REPORT NUMBER INDEX **I-111**

ACCESSION NUMBER INDEX **I-121**

APPENDIX **A-1**

TYPICAL CITATION AND ABSTRACT

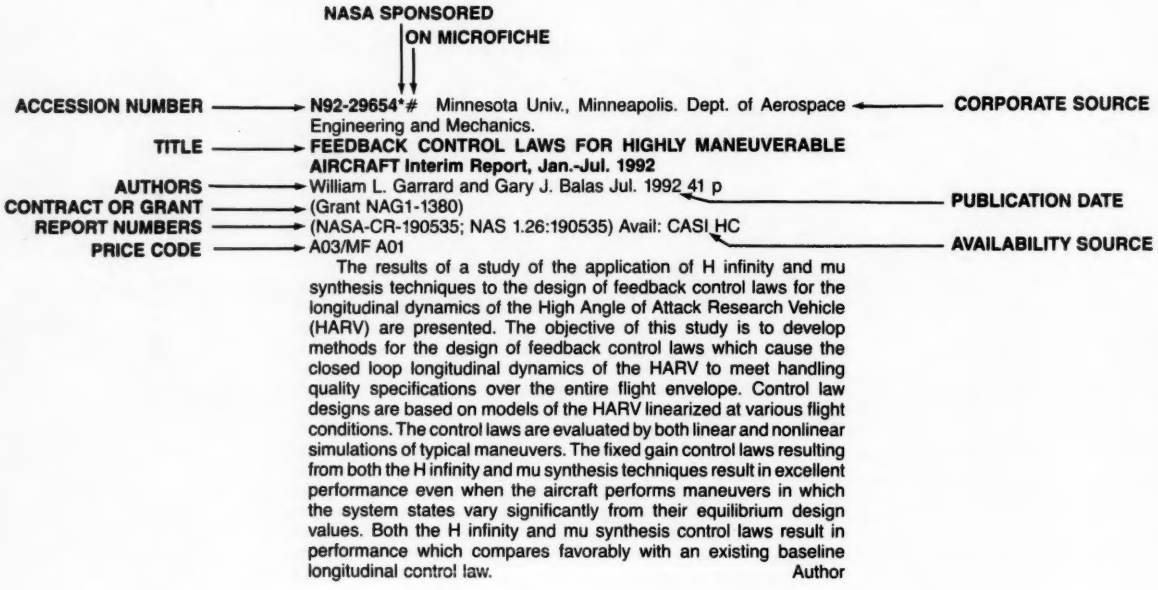
NASA SPONSORED
ON MICROFICHE
ACCESSION NUMBER
N92-29654*# Minnesota Univ., Minneapolis. Dept. of Aerospace Engineering and Mechanics.
CORPORATE SOURCE
TITLE
FEEDBACK CONTROL LAWS FOR HIGHLY MANEUVERABLE AIRCRAFT Interim Report, Jan.-Jul. 1992
AUTHORS
William L. Garrard and Gary J. Balas Jul. 1992 41 p
PUBLICATION DATE
CONTRACT OR GRANT
(Grant NAG1-1380)
REPORT NUMBERS
(NASA-CR-190535; NAS 1.26:190535) Avail: CASI HC
AVAILABILITY SOURCE
PRICE CODE
A03/MF A01
The results of a study of the application of H infinity and mu synthesis techniques to the design of feedback control laws for the longitudinal dynamics of the High Angle of Attack Research Vehicle (HARV) are presented. The objective of this study is to develop methods for the design of feedback control laws which cause the closed loop longitudinal dynamics of the HARV to meet handling quality specifications over the entire flight envelope. Control law designs are based on models of the HARV linearized at various flight conditions. The control laws are evaluated by both linear and nonlinear simulations of typical maneuvers. The fixed gain control laws resulting from both the H infinity and mu synthesis techniques result in excellent performance even when the aircraft performs maneuvers in which the system states vary significantly from their equilibrium design values. Both the H infinity and mu synthesis control laws result in performance which compares favorably with an existing baseline longitudinal control law.
Author

VOLUME 30 NUMBER 22 / NOVEMBER 23, 1992

Scientific and Technical Aerospace Reports

A Semimonthly Publication of the National Aeronautics and Space Administration

01 AERONAUTICS (GENERAL)

N92-31267*# National Aeronautics and Space Administration. Lewis Research Center, Cleveland, OH.
PRELIMINARY EVALUATION OF ADHESION STRENGTH MEASUREMENT DEVICES FOR CERAMIC/TITANIUM MATRIX COMPOSITE BONDS
Bobby Pohlchuck (Kent State Univ., OH.) and Mary V. Zeller Aug. 1992 24 p
(Contract NCC3-189; RTOP 763-22-51)
(NASA-TM-105803; E-7233; NAS 1.15:105803) Avail: CASI HC A03/MF A01

The adhesive bond between ceramic cement and a titanium matrix composite substrate to be used in the National Aerospace Plane program is evaluated. Two commercially available adhesion testers, the Sebastian Adherence Tester and the CSEM REVETEST Scratch Tester, are evaluated to determine their suitability for quantitatively measuring adhesion strength. Various thicknesses of cements are applied to several substrates, and bond strengths are determined with both testers. The Sabastian Adherence Tester has provided limited data due to an interference from the sample mounting procedure, and has been shown to be incapable of distinguishing adhesion strength from tensile and shear properties of the cement itself. The data from the scratch tester has been found to be difficult to interpret due to the porosity and hardness of the cement. Recommendations are proposed for a more reliable adhesion test method. Author

N92-31456* National Aeronautics and Space Administration, Washington, DC.
AERONAUTICAL ENGINEERING: A CONTINUING BIBLIOGRAPHY WITH INDEXES (SUPPLEMENT 280)
Jul. 1992 172 p
(NASA-SP-7037(280); NAS 1.21:7037(280)) Avail: CASI HC A08

This bibliography lists 647 reports, articles, and other documents introduced into the NASA scientific and technical information system in June, 1991. Subject coverage includes: aerodynamics, air transportation safety, aircraft communication and navigation, aircraft design and performance, aircraft instrumentation, aircraft propulsion, aircraft stability and control, research facilities, astronautics, chemistry and materials, engineering, geosciences, computer sciences, physics, and social sciences. Author

N92-31615# Federal Aviation Administration, Atlantic City, NJ.
GNAS MAINTENANCE CONTROL CENTER (GMCC) DESIGN QUALIFICATION TEST AND EVALUATION (DQT/E) TEST REPORT
Richard VanSuetendael Jul. 1992 133 p
(DOT/FAA/CT-TN91/39) Avail: CASI HC A07/MF A02

This report presents the results of Design Qualification Test and Evaluation (DQT&E) testing of the General National Airspace System (GNAS) Maintenance Control Center (GMCC). As Test Director, ACN-250 conducted testing at the Federal Aviation Administration (FAA) Technical Center, Atlantic City International Airport, New Jersey. The purpose of DQT&E testing is to verify that the phase 1 and phase 2 GMCC design requirements are met. The requirements were successfully demonstrated with some minor problems. However, due to an incomplete test configuration, ACN-250 recommended retesting the system with a four GMCC network. Author

N92-31861# Israel Society of Aeronautics and Astronautics, Tel Aviv.
COLLECTION OF PAPERS OF THE 31ST ISRAEL ANNUAL CONFERENCE ON AVIATION AND ASTRONAUTICS
22 Feb. 1990 239 p Conference held in Tel-Aviv, Israel, February 21-22, 1990; sponsored by Technion - Israel Inst. of Tech., Tel-Aviv Univ., Ben Gurion Univ. of the Negev, Rafael Armament Development Authority, National Committee for Space Research, Israel Space Agency, Aircraft Industries Ltd. El Al Israel Airlines Ltd., Israel Military Idustries, and the Society of Aerospace Engineers in Israel
(ITN-92-85124) Avail: CASI HC A11/MF A03

Subjects covered by the 28 papers include aging aircraft maintenance, automatic airfoil design, computerized aircraft design and manufacture, single-rotor helicopter simulation, robotics, skewed sensor arrays in flight-control systems, combustion chambers and processes in rocket and ramjet systems, orbital vehicle control and guidance, aluminum alloy testing, structural design, missile guidance, unmanned air vehicle trajectories, single and two-target differential games, fuel combustion, turbulent flow vortices, and Euler codes for aerodynamic problems. For individual titles, see N92-31862 through N92-31889.

N92-31862# Boeing Commercial Airplane Co., Seattle, WA.
AGING FLEET: MAINTAINING AIRWORTHINESS **c03**
B. A. Cosgrove *In* Israel Society of Aeronautics and Astronautics, 31st Israel Annual Conference on Aviation and Astronautics 22 Feb. 1990 p 1-4 Previously announced in IAA as A91-43077 (For primary document see N92-31861 22-01)
Avail: CASI HC A01/MF A03

In the U.S., airliner safety involves information exchange among the manufacturer, the airline, and the Federal Aviation Administration (FAA). Results of airline inspections are reported to the manufacturer and the FAA and may result in service recommendations from the manufacturer and airworthiness directives from the FAA. Since 1985, Boeing has operated a system of inspecting long-service airliners, paying special attention to fatigue effects. Where corrosion cracks have been found unexpectedly early, the cause was usually corrosion. In 1988, the manufacturers, the FAA and the National Aeronautics and Space Administration (NASA) formed an aging aircraft task force which established working groups for each aircraft model. These groups can recommend mandatory actions to the FAA. ISA

N92-31863# Princeton Univ., NJ.
AUTOMATIC DESIGN OF TRANSONIC AIRFOILS TO REDUCE THE SHOCK INDUCED PRESSURE DRAG **c02**
Antony Jameson *In* Israel Society of Aeronautics and Astronautics, 31st Israel Annual Conference on Aviation and Astronautics 22 Feb. 1990 p 5-17 Previously announced in IAA as A91-43078 (For primary document see N92-31861 22-01)
Avail: CASI HC A03/MF A03

This paper discusses the use of control theory for optimum design of aerodynamic configurations. Examples are presented of the application of this method to the reduction of shock induced pressure drag on airfoils in two-dimensional transonic flow. ISA

N92-31864# Boeing Commercial Airplane Co., Seattle, WA.
INTEGRATED COMPUTER SYSTEMS IN AIRCRAFT DESIGN AND MANUFACTURE: DIFFICULTIES AND IMPLICATIONS **c61**

W. W. Braithwaite *In* Israel Society of Aeronautics and Astronautics, 31st Israel Annual Conference on Aviation and Astronautics 22 Feb. 1990 p 18-26 Previously announced in IAA as A91-43079 (For primary document see N92-31861 22-01)
Avail: CASI HC A02/MF A03

Boeing's aircraft design process begins with a mathematical model of the aircraft shell, implemented on CDC/CYBER equipment and IBM mainframe computers. A model extraction system is used to extract contours from the model onto desired planes. Analyses of element kinematics, section properties and structural members is based on the model or on detail design. Drawing preparation involves interactive graphics, an automatically programmed tool (APT) system. Boeing has developed interface systems for data exchange among the various design and engineering systems, and network interface processors for converting data for exchange among several networks. The CATIA system enables solid and wireframe models to be simulated and digital mockups of structural units to be constructed. Use of such digital mockups yields considerable cost and time savings in routing cables, wiring, tubes, etc. ISA

N92-31865# Technion - Israel Inst. of Tech., Haifa. Faculty of Aerospace Engineering.
A SIMULATION MODEL OF A SINGLE ROTOR HELICOPTER **c08**

Z. Beigelman and A. Rosen *In* Israel Society of Aeronautics and Astronautics, 31st Israel Annual Conference on Aviation and Astronautics 22 Feb. 1990 p 27-37 Previously announced in IAA as A91-43080 (For primary document see N92-31861 22-01)
Avail: CASI HC A03/MF A03

The paper presents a model suitable for helicopter flight mechanics purposes. The different components of the vehicle are treated separately, and thus a modular model is obtained. The complete dynamic model is highly nonlinear and is used for trim calculations and calculations of the dynamic response to arbitrary pilot's input, or different external disturbances. Linearization of the model leads to an eigenvalue problem for analyzing the stability of different trim positions. For validation purposes the results of the new model are compared to flight test results and results of other numerical models of the AH-1G Cobra helicopter. Fair agreement is presented, while deviations are discussed and explained. ISA

N92-31866# Lehigh Univ., Bethlehem, PA. Intelligent Systems Lab.
DESIGN AND AUTOMATED MANUFACTURING **c61**

Kenneth Preiss (Ben Gurion Univ. of the Negev, Beersheva, Israel) *In* Israel Society of Aeronautics and Astronautics, 31st Israel Annual Conference on Aviation and Astronautics 22 Feb. 1990 p 38-40 (For primary document see N92-31861 22-01)
Avail: CASI HC A01/MF A03

A 'factory' has until now been associated with one physical site, and 'industry' has been associated with a country. We are beginning to see the emergence of an industrial enterprise as a virtual, distributed, global entity. This is made possible by the equipment, software and work methods developed to create, transmit and use electronic data. These developments are changing the traditional work environment for the design engineer. The basic disciplines of the design work are no different, but the need to interact, rapidly, with different nodes in a design network, and with various manufacturing and marketing functions, is requiring new capabilities. The paper will explore the implications of these developments, especially for Israel, with its unusual makeup of manpower and resources. ISA

N92-31867# Tel-Aviv Univ. (Israel). Faculty of Engineering.
SINGULARITY AVOIDANCE FOR SCARA-TYPE ROBOTS **c37**

L. Beiner *In* Israel Society of Aeronautics and Astronautics, 31st Israel Annual Conference on Aviation and Astronautics 22 Feb. 1990 p 41-43 Previously announced in IAA as A91-43081 (For primary document see N92-31861 22-01)
Avail: CASI HC A01/MF A03

This paper addresses the following problem: for a SCARA robot and a task specified at a number of discrete points on a workpiece of given shape, find the workpiece location for which the robot remains as far away as possible from singular configurations. The problem is solved by minimizing an objective function related to the robot Jacobian, subject to workspace boundary constraints. Examples are presented in which the optimum location is found using the Hooke-Jeeves direct search algorithm. ISA

N92-31868# Israel Aircraft Industries Ltd., Lod. Flight Control Dept.
FCS SKEWED SENSORS ARRAY: PRACTICAL CONSIDERATIONS **c06**

D. Agami and H. Yahia *In* Israel Society of Aeronautics and Astronautics, 31st Israel Annual Conference on Aviation and Astronautics 22 Feb. 1990 p 44-50 Previously announced in IAA as A91-43082 (For primary document see N92-31861 22-01)
Avail: CASI HC A02/MF A03

Several papers published in this area during the past years describe computational methods which solve the basic problem of the Skewed Sensors Array (SSA), i.e., how to resolve the orthogonal inputs based on the skewed sensor data, and how to detect and isolate a failed sensor. In general, various transformation methods from the sensor vector space to the orthogonal input space are described, and failed sensor isolation techniques are offered - based on consistency tests. In this paper, a further step was made to analyze the inaccuracies in the context of the effects on an aircraft which employs an SSA. The results point out the main deficiencies of the SSA in practice. Given flight control grade sensors with reasonable static error bands, it is foreseen that considerable effort will be required during the design and test phases of a project, in order to satisfy the flight control accuracy requirements, through the use of sophisticated and time-consuming voter/monitor algorithms. The choice of an SSA for flight control is, therefore, a serious matter of risk and cost trade-off for any specific application. ISA

N92-31869# Technion - Israel Inst. of Tech., Haifa. Dept. of Aerospace Research.
STUDY OF A SPHERICAL SPINNING COMBUSTION CHAMBER FOR ORBIT INSERTION **c20**

G. Avital, J. B. Greenberg, D. Laredo, Y. Levy, Y. Tambour, and Y. M. Timnat *In* Israel Society of Aeronautics and Astronautics, 31st Israel Annual Conference on Aviation and Astronautics 22 Feb. 1990 p 51-61 Previously announced in IAA as A91-43083 (For primary document see N92-31861 22-01)
Avail: CASI HC A03/MF A03

The study of spray dynamics and fuel vapor distributions in a spinning spherical combustion chamber is of great interest to designers of orbital transfer motors, particularly within the context of residual thrust that can be important for the final staging of such vehicles. In this work we present a theoretical investigation of the evolution in droplet size distributions within such a combustor and spatial distribution of fuel vapors, as the droplets vaporize. The modelling of the spray is performed using a sectional approach that provides the means for handling the large number of droplets in any realistic system by dividing them into size-defined sections and dealing with one integral quantity in each section. However, both droplet transfer to the host gaseous phase and inter- and intra-sectional transfer, through droplet vaporization and coalescence, are rigorously accounted for. The governing two-phase flow equations are solved numerically using split-operator finite difference methods. A wide variety of injection conditions are considered. Computed results highlight the effects of these conditions coupled with spinning rates, and vaporization and coalescence rates on the way in which fuel vapors are formed and become distributed in the combustion chamber. Finally, a

description is given of an experimental rig that is to be used for analyzing the flow field and the spatial and size distribution of particles in a spinning chamber. ISA

N92-31870# Rafael Armament Development Authority, Haifa (Israel).
SIZING SUPERSONIC FREEJET NOZZLE AND INLET LOCATION FOR SIMULATION OF THE TRANSITION PHASE IN INTEGRAL ROCKET RAMJET **c07**
I. Greenberg and E. Shokron (Israel Aircraft Industries Ltd., Lod.) *In* Israel Society of Aeronautics and Astronautics, 31st Israel Annual Conference on Aviation and Astronautics 22 Feb. 1990 p 62-65 Previously announced in IAA as A91-43084 (For primary document see N92-31861 22-01)
Avail: CASI HC A01/MF A03

The semi-freejet testing technique is used to demonstrate transition from rocket booster to ramjet sustainer at a specific flight condition with a maximum model size. For an existing ramjet model, three conditions limit optimal freejet nozzle sizing. First, the inlet model should be located in such a manner that the freejet nozzle will 'start' during the booster phase. Second, in the ramjet phase the oblique shock wave at the exit of the freejet nozzle will impinge on the inlet without disturbing the flow to the engine. Lastly, the maximum air flow rate that is available for the test is limited by the facility air reservoir. The design conditions and limits are summarized in a graph which defines the boundaries of the regime for sizing freejet nozzle and inlet axial location. A supersonic nozzle was constructed for a ramjet with an axisymmetric, external compression nose inlet. Successful transition tests were conducted in a low cost facility. ISA

N92-31871# Naval Weapons Center, China Lake, CA. Research Dept.
EFFECT OF INLET GEOMETRY ON THE FLOW AND COMBUSTION PROCESSES IN A SOLID FUEL RAMJET **c07**
K. J. Wilson, K. C. Schadow, E. Gutmark, P. A. O. G. Korting (Prins Maurits Lab. TNO, Rijswijk, Netherlands), and F. Dijkstra (Technische Hogeschool, Deift, Netherlands) *In* Israel Society of Aeronautics and Astronautics, 31st Israel Annual Conference on Aviation and Astronautics 22 Feb. 1990 p 66-72 Previously announced in IAA as A91-43085 (For primary document see N92-31861 22-01)
Avail: CASI HC A02/MF A03

A passive control method to enhance combustion in a solid fuel ramjet was investigated by injecting air through a small-aspect-ratio elliptical orifice at the entrance of the dump combustion chamber. The non-circular injector changes the shear-flow dynamics. This results in enhanced mixing between the air and fuel added from the combustor side wall, as compared with circular injectors. When such an elliptic injector has the proper dimensions, the elliptic vortices issuing from the orifice bend around their small axis, followed by self-induction. This results in a high jet spread along the minor axis. This process causes switch over of the axes (axis switching) and high entrainment of fluid into the wide and narrow sections of the jet. The occurrence of axis switching, however, depends critically on the shape of the elliptic injector or the initial shear-flow conditions at the injector, for example, momentum thickness and its circumferential distribution. In the present paper, the effect of differently shaped elliptic injectors with varying initial conditions on the flow and combustion characteristics in a solid fuel ramjet with plexiglas (PMMA) as a fuel was studied. For reasons of comparison, combustion tests with various circular injectors were also performed. The effect on regression rate behavior was emphasized. The results are supported by thermocouple measurements in a dump combustor, where ethylene was injected through a porous wall, and by measurements made in free-jets. ISA

N92-31872# Tel-Aviv Univ. (Israel). Dept. of Mechanics, Materials and Structures.
J(SUB 2) FRACTURE TOUGHNESS TESTING OF Al 707 5-T7351 **c26**
Leslie Banks-Sills and Dov Sherman *In* Israel Society of Aeronautics and Astronautics, 31st Israel Annual Conference on Aviation and Astronautics 22 Feb. 1990 p 73-75 Previously announced in IAA as A91-43086 (For primary document see N92-31861 22-01)
Avail: CASI HC A01/MF A03

Since the load-displacement curve recorded for a perspex fracture specimen could not be applied to the more ductile 7075-T7351 aluminum alloy, a rigid plastic analysis was carried out for a mode 2 fracture specimen, to determine the J-integral under mode 2 loading in terms of the area under the load/crack sliding displacement record, the uncracked ligament and the specimen thickness. An elasto-plastic finite element analysis helped to determine the proper position for the crack sliding displacement gauge. For nominal specimen thicknesses of 5, 7.5, and 9 mm, J(sub 1c) was determined to be 10.5, 10.8, and 10.2 kN/m, respectively. Mode 1, plane strain fracture toughness testing on the same material gave a K(sub 2c) value equivalent to a J(sub 1c) value of 10.8 kN/m. Preliminary J(sub 2c) test methods were developed and led to a tentative value of 43 kN/m for J(sub 2c). Further tests are being performed on thinner specimens. ISA

N92-31873# Tel-Aviv Univ. (Israel). Dept. of Solid Mechanics, Materials and Structures.
THE DESIGN AND TESTING OF AN OPTIMAL BEAM COMPOSED OF UNIMODAL ELEMENTS **c39**
Moshe B. Fuchs, Gideon Benyamini, and Ehud Bousso *In* Israel Society of Aeronautics and Astronautics, 31st Israel Annual Conference on Aviation and Astronautics 22 Feb. 1990 p 76-80 Previously announced in IAA as A91-43087 (For primary document see N92-31861 22-01)
Avail: CASI HC A01/MF A03

Flexural structures are intrinsically inefficient from a structural weight point of view. This is largely due to an ineffective use of the material of the beam elements. The variation of the stresses in the transverse direction of a beam is palliated by the use of I type cross sections. However, in the presence of shear loads, the bending moment varies along the longitudinal direction of the beam and, consequently, flexural systems are usually largely understressed. The present theory is based on the finding that a beam element is structurally equivalent to two basic elements acting in parallel. A 'moment' element which carries the average bending moment, and a 'shear' element, which carries the differential part of the bending moment distribution. Since these unimodal elements are uniformly stressed they are very efficient structural elements. Theoretical results have shown that in many cases substantial weight reductions can be expected when unimodal elements are employed to carry flexural loads. This paper describes the design and the practical implementation of an optimal beam composed of unimodal elements. Preliminary results indicate that the success of these structures depends largely on a judicious design of the unimodal components. ISA

N92-31874# Israel Aircraft Industries Ltd., Yehud.
A NOVEL CONTROL-GUIDANCE LAW FOR LOW-THRUST ORBIT MANEUVER **c18**
Marcel Sidi *In* Israel Society of Aeronautics and Astronautics, 31st Israel Annual Conference on Aviation and Astronautics 22 Feb. 1990 p 81-88 Previously announced in IAA as A91-43088 (For primary document see N92-31861 22-01)
Avail: CASI HC A02/MF A03

A simple control-guidance law for low-thrust coplanar orbital transfer maneuvers is investigated. The law is based on classical control theory, and is intended to circumvent the two-point boundary value problem difficulties encountered in the optimal control approach as applied to orbit maneuvering. The proposed guidance law is fairly insensitive to uncertainties in control parameters such as thrust level, thrust direction, and the initial time of the maneuver. The performance index is based on a trade-off between time and fuel expenditure, for missions in which the maneuver must be performed in one single phase because of operational time constraints. Constant or variable thrusts are admitted. ISA

N92-31875# Rafael Armament Development Authority, Haifa (Israel).
AN INNOVATIVE TWO AXIS RATE GYRO: THEORY AND PRINCIPLES OF OPERATION **c35**
J. Rosenberg, E. Netzer, P. Bar-Avi, and I. Porat *In* Israel Society of Aeronautics and Astronautics, 31st Israel Annual Conference on Aviation and Astronautics 22 Feb. 1990 p 89-91 Previously announced in IAA as A91-43089 (For primary document see N92-31861 22-01)
Avail: CASI HC A01/MF A03

A new gyro sensor capable of measuring angular rate motion about two perpendicular axes was developed. The gyro has small dimensions and simple structure. The principle of operation is explained as well as its main sub-structure components. The theory, including the equations of motion and their solution is stated. Brief specifications for three units that differ in their measurement ranges are included. ISA

N92-31876*# National Aeronautics and Space Administration. Goddard Space Flight Center, Greenbelt, MD.
EXTENDED KALMAN FILTER FOR ATTITUDE ESTIMATION OF THE EARTH RADIATION BUDGET SATELLITE **c19**
Julie Deutschmann and Itzhack Y. Bar-Itzhack (Technion - Israel Inst. of Tech., Haifa.) *In* Israel Society of Aeronautics and Astronautics, 31st Israel Annual Conference on Aviation and Astronautics 22 Feb. 1990 p 92-106 Previously announced in IAA as A91-43090 and N90-13433 (For primary document see N92-31861 22-01)
Avail: CASI HC A03/MF A03

This paper describes the design and testing of an Extended Kalman Filter (EKF) for ground attitude determination, misalignment estimation, and sensor calibration of the Earth Radiation Budget Satellite (ERBS). Attitude is represented by the quaternion of the rotation and the attitude estimation error is defined as an additive error. Quaternion normalization is used for increasing the convergence rate and for minimizing the need for filter tuning. The development of the filter dynamic model, the gyro error model and the measurement models of the Sun sensors, and the infrared scanner and the magnetometers which are used to generate vector measurements is presented. The filter is applied to real data transmitted by ERBS sensors. Results are presented and analyzed and the EKF advantages as well as sensitivities are discussed. On the whole the filter meets the expected synergism, accuracy, and robustness. ISA

N92-31877# Maryland Univ., College Park. Dept. of Aerospace Engineering.
THE USE OF HIGH LIFT-TO-DRAG HYPERSONIC VEHICLES FOR AERO-ASSISTED ORBITAL MANEUVERING **c18**
Mark J. Lewis *In* Israel Society of Aeronautics and Astronautics, 31st Israel Annual Conference on Aviation and Astronautics 22 Feb. 1990 p 107-119 Previously announced in IAA as A91-43091 (For primary document see N92-31861 22-01)
Avail: CASI HC A03/MF A03

The benefits of using a hypersonic waverider for spacecraft trajectory modification are presented. A waverider is a hypersonic vehicle specifically designed so that the undersurface bow shock is attached to the leading edge, which provides for the highest known lift-to-drag ratios achievable at high Mach number flight. Several viable space missions are suggested which could use such configurations for low-drag aeroassisted maneuvers in planetary atmospheres. It is shown that large changes in the spacecraft velocity vector can be accomplished with acceptably small losses in energy due to drag using a waverider aeroshell. The primary advantage of an aeroassisted maneuver is suggested by comparison with a traditional gravity assist trajectory. Some scaling laws are presented for comparing waveriders designed for different planetary atmospheres, and it is shown that the compositional differences among the terrestrial planets have a minimal impact on waverider design. ISA

N92-31878*# National Aeronautics and Space Administration. Goddard Space Flight Center, Greenbelt, MD.
TRUE COVARIANCE SIMULATION OF THE EUVE (EXTREME ULTRA VIOLET EXPLORER) UPDATE FILTER **c19**
I. Y. Bar-Itzhack (Technion - Israel Inst. of Tech., Haifa.) and R. R. Harman *In* Israel Society of Aeronautics and Astronautics, 31st Israel Annual Conference on Aviation and Astronautics 22 Feb. 1990 p 120-126 Previously announced in IAA as A91-43092 (For primary document see N92-31861 22-01)
Avail: CASI HC A02/MF A03

This paper presents a covariance analysis of the performance and sensitivity of the attitude determination Extended Kalman Filter (EKF) used by the onboard computer (OBC) of the Extreme Ultra Violet Explorer (EUVE) spacecraft. The linearized dynamics and measurement equations of the error states are used in formulating the 'truth model' describing the order of the systems involved. The 'design model' used by the OBC EKF is then obtained by reducing the order of the truth model. The covariance matrix of the EKF which uses the reduced order model is not the correct covariance of the EKF estimation error. A 'true covariance analysis' has to be carried out in order to evaluate the correct accuracy of the OBC generated estimates. The results of such analysis are presented which indicate both the performance and the sensitivity of the OBC EKF. ISA

N92-31879# Rafael Armament Development Authority, Haifa (Israel).
DISCRETE OPTIMAL GUIDANCE FOR HIGH ORDER MISSILE AND MANEUVERING TARGET **c08**
Ilan Rusnak *In* Israel Society of Aeronautics and Astronautics, 31st Israel Annual Conference on Aviation and Astronautics 22 Feb. 1990 p 127-131 Previously announced in IAA as A91-43093 (For primary document see N92-31861 22-01)
Avail: CASI HC A01/MF A03

Explicit, closed form formula of a discrete optimal guidance law for a linear, time-invariant acceleration commanded and arbitrary order missile and a linear, time-invariant, arbitrary order maneuvering target is derived. The formula is given in terms of the missile's and target's transfer functions and responses to initial conditions. Examples are explicitly solved for zero lag and for 1st order missiles. It is shown that the discrete proportional navigation ratio is higher and time varying rather than equal to 3 as in the continuous case. ISA

N92-31880# Israel Military Industries, Ramat-Hasharon (Israel). Systems Div.
OPTIMAL TRAJECTORIES FOR AN UNMANNED AIR VEHICLE **c05**
Joseph Z. Ben-Asher *In* Israel Society of Aeronautics and Astronautics, 31st Israel Annual Conference on Aviation and Astronautics 22 Feb. 1990 p 132-140 Previously announced in IAA as A91-43094 (For primary document see N92-31861 22-01)
Avail: CASI HC A02/MF A03

Time-optimal trajectories for the Delilah Unmanned Air Vehicle (UAV) were studied. Delilah is a 400-lb, turbojet-powered decoy carrying active and passive radio-frequency (RF) payloads; its dash speed is 770 kt and its flight ceiling is 30,000 ft. The Pontryagin Minimum Principle was applied to the minimum-time point-to-point maneuvering problem and a new technique was demonstrated, to perform the Jacobi test. The technique is based on a singular value decomposition of the transition matrix and is simpler and more reliable than the old technique of evaluating sub-determinants. Two approximations to the problem, the energy model and the intermediate model, were shown to agree well with the exact solution. ISA

N92-31881# Technion - Israel Inst. of Tech., Haifa. Faculty of Aerospace Engineering.
ESTIMATION OF AIRCRAFT ATTITUDE BY ANGULAR RATE MEASUREMENTS **c05**
M. Koifman and S. J. Merhav *In* Israel Society of Aeronautics and Astronautics, 31st Israel Annual Conference on Aviation and

Astronautics 22 Feb. 1990 p 141-152 Previously announced in IAA as A91-43095 Sponsored by Ministry of Defence and Precision Instrument Industries (For primary document see N92-31861 22-01)
Avail: CASI HC A03/MF A03

A method for on-board aircraft attitude estimation based on the measurements of an orthogonal triad of strapdown low-cost gyros, airspeed, barometric attitude, and magnetic heading sensors is presented. A reduced-order, computationally simplified, Extended Kalman Filter is shown to provide on-line attitude estimates with bounded errors not exceeding 0.5 degree at output rates of the order of 20 Hz. Considerations for order reduction and computational simplifications which facilitate on-line operation are presented. Off-line computer simulations including uncertain atmospheric turbulence and time-varying gyro drift demonstrate precision and robustness. Actual on-line simulations including real rate gyros are described. The results validate the feasibility of the concept. ISA

N92-31882# Technion - Israel Inst. of Tech., Haifa. Faculty of Aerospace Engineering.
AN AUTOMATED COMPUTATIONAL METHOD FOR BARRIER CONSTRUCTION IN SINGLE AND TWO-TARGET DIFFERENTIAL GAMES c66
L. Breuer, B. Kantor (Aerobyte Engineering, Tel Aviv, Israel), and J. Shinar *In* Israel Society of Aeronautics and Astronautics, 31st Israel Annual Conference on Aviation and Astronautics 22 Feb. 1990 p 153-161 (For primary document see N92-31861 22-01)
Avail: CASI HC A02/MF A03

The solution of qualitative differential games consists of a partition of the space of admissible initial conditions to regions of a possible outcome. These regions are separated from each other by closed semipermeable barrier surfaces. The paper presents an automated computational method to construct and visualize the barriers in such games. The most important element of the method is to identify the intersections between different families of optimal barrier trajectories. The computer program is a modular one and allows for user interaction for verifying, via the visualization, the closure of the barrier, as well as for manually completing eventually missing parts. Examples of a single-target pursuit-evasion game of the kind using the dynamic model of the 'Game of Two Cars' and the corresponding two-target game are presented. ISA

N92-31883# Oregon State Univ., Corvallis. Dept. of Mechanical Engineering.
INCIPIENT AND TOTAL GROUP COMBUSTION OF FUEL SPRAYS IN AIR c25
I. Peleg (Rafael Armament Development Authority, Haifa, Israel) and A. M. Kanury *In* Israel Society of Aeronautics and Astronautics, 31st Israel Annual Conference on Aviation and Astronautics 22 Feb. 1990 p 162-170 Previously announced in IAA as A91-43096 (For primary document see N92-31861 22-01)
Avail: CASI HC A02/MF A03

Combustion in sprays of liquid fuels generally involves burning of a collection of droplets together in a cloud surrounded by a common flame. The droplets within the flame undergo vaporization, the vapors diffuse to the edge of the cloud to meet oxygen, and the flame evolves. This is known as total group combustion (TGC). If the spray contains only a few droplets, oxygen can diffuse to the interior of the cloud to permit each droplet to burn individually with its own envelope flame, as if it existed in isolation from its neighbors. The conditions under which droplets cease to burn individually signal incipient group combustion (IGC). The conditions under which the communal flame resides at the edge of the cloud compose the so-called TGC criterion. These IGC and TGC criteria are important from both the theoretical and practical points of view. In this work, a simple model is presented to predict the IGC and TGC criteria. This method adapts the earlier work of Labowsky and Rosner, which is based on an analytical solution of steady oxidant mass conservation in which convection is ignored. The criteria are then applied to sprays of different common hydrocarbon fuels to represent the conditions for IGC and TGC in terms of dimensionless separation distance between drops and the total number of drops in the cloud. The results compare well with those of Labowsky when the fuel of concern is dodecane. Comparison with the work of Chiu, Kim and Croke for n-butylbenzene indicates good agreement in TGC conditions. ISA

N92-31884# Technion - Israel Inst. of Tech., Haifa. Faculty of Aerospace Engineering.
TRANSPORT AND EVAPORATION EFFECTS IN COUNTERFLOW SPRAY DIFFUSION FLAMES c25
N. Sarig and J. B. Greenberg *In* Israel Society of Aeronautics and Astronautics, 31st Israel Annual Conference on Aviation and Astronautics 22 Feb. 1990 p 171-178 Previously announced in IAA as A91-43097 (For primary document see N92-31861 22-01)
Avail: CASI HC A02/MF A03

A new theoretical study of a counterflow spray diffusion flame is presented. The fuel is introduced into the system in the form of liquid droplets suspended homogeneously in a nitrogen host environment. Hitherto unexamined effects of transport properties and evaporation are accounted for explicitly. Calculated results point to the sensitivity of flame location and temperature to the type of liquid fuel employed, coupled to the initial spray injection conditions (initial droplet size distribution and velocity of injection). The relative roles of convective and diffusive transport of fuel vapors are also examined. ISA

N92-31885# Israel Military Industries, Ramat-Hasharon (Israel).
FLAMMABILITY LIMITS AND BALLISTIC PROPERTIES OF FUEL-RICH PROPELLANTS c28
Abraham Shalom and Alon Gany (Technion - Israel Inst. of Tech., Haifa.) *In* Israel Society of Aeronautics and Astronautics, 31st Israel Annual Conference on Aviation and Astronautics 22 Feb. 1990 p 179-184 Previously announced in IAA as A91-39558 (For primary document see N92-31861 22-01)
Avail: CASI HC A02/MF A03

The flammability limits and ballistic properties of composite fuel-rich propellants were studied experimentally, using polybutadiene acrylic acid acrylonitrile (PBAN) terpolymer with ammonium perchlorate (AP) oxidizer (PBAN/AP) propellant formulations. Higher pressures and AP contents as well as smaller AP particle size were found to promote sustained combustion and to increase burning rate. The addition of potassium perchlorate (KP) in place of AP increased the burning rate exponent from about 0.3 to over 0.7 at optimum conditions. Ferric oxide and copper chromite catalysts caused an increase of the burning rate by a factor of 2, while the addition of aluminum powder at the expense of the fuel binder was found to have a remarkable effect on the burning rate, with a maximum increase of as high as fivefold. ISA

N92-31886# Israel Aircraft Industries Ltd., Ben-Gurion Airport.
THE CALCULATION OF INCOMPRESSIBLE SEPARATED TURBULENT BOUNDARY LAYERS c34
A. Kogan and S. Migemi *In* Israel Society of Aeronautics and Astronautics, 31st Israel Annual Conference on Aviation and Astronautics 22 Feb. 1990 p 185-196 Previously announced in IAA as A90-51025 (For primary document see N92-31861 22-01)
Avail: CASI HC A03/MF A03

The algebraic turbulent model of Baldwin-Lomax was incorporated into the incompressible Navier-Stokes code FIDAP. This model has been extensively tested in the past in finite difference codes. We believe that the incorporation of the model into the finite element code also has resulted in a practical method to compute a variety of separated turbulent two-dimensional flows. Firstly, the model is used to compute the attached flow about an airfoil. Next, the application of the model to separated flows is presented, by computing the flows at high angles of attack up to maximum lift. It is shown that the model is capable of predicting separation, steady stall and C(sub L MAX). As a difficult test of the model, we compute the laminar separation bubble development

directly, using the full Navier-Stokes finite elements code. As far as we know, this approach has not been reported previously. The importance of using an appropriate upwinding is discussed. When possible, comparison of computed results with experiments is presented and the agreement is good. ISA

N92-31887# Technion - Israel Inst. of Tech., Haifa. Faculty of Aerospace Engineering.

THE STABILITY OF A SLIGHTLY ECCENTRIC STRAIGHT VORTEX FILAMENT IN A CIRCULAR TUBE **c34**

Z. Rusak and A. Seginer *In* Israel Society of Aeronautics and Astronautics, 31st Israel Annual Conference on Aviation and Astronautics 22 Feb. 1990 p 197-204 Previously announced in IAA as A91-43099 (For primary document see N92-31861 22-01)

Avail: CASI HC A02/MF A03

The three-dimensional stability of a straight vortex that runs down a circular tube, parallel with its axis but slightly displaced from it, was investigated experimentally. The vortex flow was modelled by an infinitely long concentrated potential vortex filament. The interaction of the vortex flow field with the tube walls, because of its small initial eccentricity, makes the vortex autorotate about the axis of the tube at a constant angular velocity. The walls of the tube are modelled by a surface distribution of potential sources. Small three-dimensional waves are imposed on the vortex filament, concurrently with fluctuations in the intensity of the surface distribution of the sources over the tube walls. A prescribed unsteady longitudinal perturbation to the radius of the tube is also considered. A linearization of the flow-field equations results in a system of first-order linear differential equations for the time history of the vortex perturbations. The development of the perturbations is shown to be analogous to the motion of a mass on a spring-damper combination. The 'generalized damping' of the off-center vortex-tube system governs the dynamic stability of the vortex, whereas its 'rigidity' governs its static stability. It is shown that the vortex develops a dynamic instability in a narrow range of wave numbers, as a direct result of its small eccentricity. Unexplained oscillations, which were previously observed in vortex flows in tubes, can be attributed to this dynamic instability of the vortex. ISA

N92-31888# Israel Aircraft Industries Ltd., Ben-Gurion Airport. Aerodynamics Dept.

EULER SOLVER FOR ARBITRARY CONFIGURATIONS: FURTHER APPLICATIONS **c02**

B. Epstein, A. L. Luntz, and A. Nachshon *In* Israel Society of Aeronautics and Astronautics, 31st Israel Annual Conference on Aviation and Astronautics 22 Feb. 1990 p 205-216 Previously announced in IAA as A91-43100 (For primary document see N92-31861 22-01)

Avail: CASI HC A03/MF A03

Further applications of a three-dimensional Euler code which is able to treat arbitrary aerodynamic configurations in a wide range of flight conditions are presented. Previous publications have demonstrated the ability of the code to handle complex aircraft configurations. The present applications verify the code in flight regimes not covered by potential codes (e.g., high supersonic flow and vortex flow) by comparison with reliable, internationally reported wind tunnel experiments and analytical solutions (where available). A short description of the code is also included. ISA

N92-31889# Technion - Israel Inst. of Tech., Haifa. Faculty of Aerospace Engineering.

THE THREE-DIMENSIONAL STABILITY OF THE FOEPPL VORTICES **c02**

Z. Rusak and A. Seginer *In* Israel Society of Aeronautics and Astronautics, 31st Israel Annual Conference on Aviation and Astronautics 22 Feb. 1990 p 217-225 Previously announced in IAA as A91-43101 (For primary document see N92-31861 22-01)

Avail: CASI HC A02/MF A03

The three-dimensional stability of a vortex pair in the cross flow behind an infinite solid circular cylinder (the Foeppl vortices), is investigated. The vortices are assumed to be parallel potential vortex filaments, and the cylinder is modelled by a potential source surface distribution. Small three-dimensional waves are imposed on the vortex filaments, concurrently with fluctuations in the intensity of the source distribution, and with a prescribed unsteady perturbation of the radius of the cylinder. A linearization of the flow-field equations results in first-order linear differential equations, that describe the time-history of the vortex perturbations in their symmetric and anti-symmetric modes. The development of the perturbations in both modes is analogous to the motion of a unit mass on a spring-and-damper combination. The generalized damping in each mode governs the static stability of the vortices. Results show that the well-known anti-symmetric two-dimensional dynamic instability of the Foeppl vortices vanishes as the wave number of the perturbations increases and they become stable, whereas the symmetric mode becomes unstable in a limited range of wave-numbers, and is governed mainly by the Crow instability of a free vortex pair. The Foeppl vortices can also tend to diverge statically at certain wave numbers and swirl ratios that characterize the vortices. ISA

02 AERODYNAMICS

Includes aerodynamics of bodies, combinations, wings, rotors, and control surfaces; and internal flow in ducts and turbomachinery.

For related information see also *34 Fluid Mechanics and Heat Transfer.*

N92-31239*# National Aeronautics and Space Administration. Langley Research Center, Hampton, VA.

CFD METHODS DEVELOPMENT CONSIDERATIONS FOR UNSTEADY AERODYNAMIC ANALYSIS

John T. Batina Jul. 1992 31 p Presented at the Workshop on Computational Aeroacoustics, Hampton VA, 6-9 Apr. 1992

(RTOP 505-63-50-12)

(NASA-TM-107644; NAS 1.15:107644) Avail: CASI HC A03/MF A01

The development of computational fluid dynamics (CFD) methods for unsteady aerodynamic analysis is described. Special emphasis is placed on considerations that are required for application of the methods to unsteady aerodynamic flow problems. Two broad categories of topics are presented to illustrate the major points. Although primary application of these CFD methods is to relatively low frequency oscillatory phenomena such as flutter, the ideas that are presented may be of value to developers of computational aeroacoustic methods for predicting high frequency acoustics. Author

N92-31246*# National Aeronautics and Space Administration. Langley Research Center, Hampton, VA.

HIGH REYNOLDS NUMBER TEST OF THE BOEING TR77 AIRFOIL IN THE LANGLEY 0.3-METER TRANSONIC CRYOGENIC TUNNEL

Julio Chu, Stuart G. Flechner, Acquilla S. Hill, and Roger A. Rozendaal (Boeing Commercial Airplane Co., Seattle, WA.) Jul. 1990 79 p

(RTOP 505-61-01-01)

(NASA-TM-4189; L-16724; NAS 1.15:4189) Avail: CASI HC A05/MF A01

A Boeing TR77 airfoil associated with the Advanced Technology Airfoil Test (ATAT) program was tested in the Langley 0.3 m Transonic Cryogenic Tunnel. Limited analysis of the data indicated that increasing Reynolds number for a fixed Mach number resulted in increased normal-force, nose-down pitching moment, and decreased drag coefficient. Increasing Mach number while keeping the Reynolds number constant yielded the expected increase in normal-force slopes, nose-down pitching moment coefficients, and decrease in angle of attack associated with maximum normal-force coefficient. Turbulent boundary layer flow was achieved over the airfoil at low Reynolds numbers for the test Mach number range using aluminum discs. Author

N92-31276*# National Aeronautics and Space Administration. Hugh L. Dryden Flight Research Facility, Edwards, CA.
IN-FLIGHT LEADING-EDGE EXTENSION VORTEX FLOW-FIELD SURVEY MEASUREMENTS ON A F-18 AIRCRAFT AT HIGH ANGLE OF ATTACK
David M. Richwine (PRC Kentron, Inc., Edwards, CA.) and David F. Fisher Sep. 1992 49 p Presented at the AIAA 9th Applied Aerodynamics Conference, Baltimore, MD, 23-25 Sep. 1991 Previously announced in IAA as A91-53759
(RTOP 505-68-71)
(NASA-TM-4398; H-1783; NAS 1.15:4398) Avail: CASI HC A03/MF A01

Flow-field measurements on the leading-edge extension (LEX) of the F-18 High Alpha Research Vehicle (HARV) were obtained using a rotating rake with 16 hemispherical-tipped five-hole probes. Detailed pressure, velocity, and flow direction data were obtained through the LEX vortex core. Data were gathered during 1-g quasi-stabilized flight conditions at angles of attack alpha from 10 degrees to 52 degrees and at Reynolds numbers based on mean aerodynamic cord up to 16 x 10(exp 6). Normalized dynamic pressures and crossflow velocities clearly showed the primary vortex above the LEX and formation of a secondary vortex at higher angles of attack. The vortex was characterized by a ring of high dynamic pressure surrounding a region of low dynamic pressure at the vortex core center. The vortex core, subcore diameter, and vertical location of the core above the LEX increased with angle of attack. Minimum values for static pressure were obtained in the vortex subcore and decreased nearly linearly with increasing angle of attack until vortex breakdown. Rake-measured static pressures were consistent with previously documented surface pressures and showed good agreement with flow visualization flight test results. Comparison of the LEX vortex flight test data to computational solutions at alpha approximately equals 19 degrees and 30 degrees showed fair correlation. Author

N92-31300# Naval Postgraduate School, Monterey, CA.
A COMPUTATIONAL INVESTIGATION OF AIRFOIL STALL FLUTTER M.S. Thesis
Jeffrey D. Clarkson Mar. 1992 191 p
(AD-A247302) Avail: CASI HC A09/MF A02

A fully factorized two-dimensional Navier-Stokes flow solver has been developed and applied to the problem of predicting subsonic airfoil flutter in the light stall regime. The inviscid fluxes are evaluated with a central difference ADI scheme and fourth and second order numerical dissipation is used to obtain oscillation-free solutions. The performance of algebraic and one-equation turbulence models in predicting separated flow is explored for computing high Reynolds number steady flow and unsteady flows over an oscillating NACA 0012 airfoil. Comparisons of the computed results with available experimental data indicate that even though the lift response is fairly well predicted, the computation of the pitching moment hysteresis loops is very sensitive to turbulence modeling. Results computed with several current models are in good agreement whenever the steady stall angle is exceeded only slightly. However, they fail to capture the vortex shedding process leading to the onset of stall flutter. GRA

N92-31508# Laboratoire d'Aerothermique du CNRS, Meudon (France).
FLAT PLATES PLACED IN DEPLETED HYPERSONIC FLOW [PLAQUES PLANES PLACEES EN ECOULEMENTS HYPERSONIQUES RAREFIES: ANNEXE]
J. Allegre (Societe d'Etudes et de Services pour Souffleries et Installations Aerothermodynamiques, Paris, France), M. Raffin (Societe d'Etudes et de Services pour Souffleries et Installations Aerothermodynamiques, Paris, France), J. C. Lengrand, A. Chpoun (Institut Univ. de Technologie, Evry, France), and L. Gottesdiener (Paris VI Univ., France) Mar. 1991 41 p In FRENCH
(Contract DRET-88-521)
(SESSIA-430/91.960; CNRS-RC-91-1; ETN-92-91319) Avail: CASI HC A03/MF A01

The present volume is the annex of the project's final report. It contains the experimental data obtained during wind tunnel tests. The purpose of the project was to measure the heat flow and the wall pressure of flat plates under hypersonic flow and low Reynolds number. Experimental and theoretical data, calculated by the Monte Carlo and Navier-Stokes methods, were compared. The three flow conditions were characterized by a Mach number approximately equal to 20 and Reynolds (Re) number equal to 2850, 8380, and 72770. Good agreement was observed between the theoretical and experimental values in the following cases: for Re = 2850, the best approach was the direct simulation Monte Carlo; for Re = 8380 and 72770, the best approach was obtained by the Navier Stokes method. ESA

N92-31514# Cranfield Inst. of Tech., Bedford (England). College of Aeronautics.
AN INVESTIGATION INTO THE INTERFACE BETWEEN THREE CLOSELY SPACED AXI-SYMMETRIC BODIES AT SUBSONIC SPEED
D. I. T. P. Llewelyn-Davies Sep. 1991 200 p Sponsored by RAE/Defence Research Agency, Farnborough, England
(Cranfield-Aero-9114; ISBN-1-871564-387; ETN-92-91727) Avail: CASI HC A09/MF A03

An experimental investigation into the interference effects present between three closely spaced bodies, over a range of 0 to 6 deg of either pitch or yaw, is presented. Detailed C(sub p) (pressure coefficient (p-p0(q))) distributions were obtained over the bodies and these were successively integrated to obtain the loading distribution along the bodies and the overall forces and moments. By analysis of contour maps representing the C(sub p) distribution over the bodies, the loading diagrams, and the overall loads, the extent of the interference regions and their effect on the aerodynamic characteristics of the bodies were determined. A panel method was used to estimate the C(sub p) distributions over the bodies and, as previously, the loading distributions along the bodies and the overall forces. Estimates were also made of the characteristics of the bodies when the attitude of the body combination was varied between 0 and -6 deg pitch, and when yaw was varied between 0 and +6 deg at pitch angles of +6 and -6 deg. ESA

N92-31532*# National Aeronautics and Space Administration. Langley Research Center, Hampton, VA.
WIND TUNNEL AERODYNAMIC CHARACTERISTICS OF A TRANSPORT-TYPE AIRFOIL IN A SIMULATED HEAVY RAIN ENVIRONMENT
Gaudy M. Bezos, R. Earl Dunham, Jr., Garl L. Gentry, Jr., and W. Edward Melson, Jr. (National Aeronautics and Space Administration. Wallops Flight Facility, Wallops Island, VA.) Aug. 1992 68 p
(RTOP 505-68-01-02)
(NASA-TP-3184; L-16959; NAS 1.60:3184) Copyright Avail: CASI HC A04/MF A01

The effects of simulated heavy rain on the aerodynamic characteristics of an NACA 64-210 airfoil section equipped with leading-and trailing-edge high-lift devices were investigated in the Langley 14- by 22-Foot Subsonic Tunnel. The model had a chord of 2.5 ft, a span of 8 ft, and was mounted on the tunnel centerline between two large endplates. Aerodynamic measurements in and out of the simulated rain environment were obtained for dynamic pressures of 30 and 50 psf and an angle-of-attack range of 0 to 20 degrees for the cruise configuration. The rain intensity was varied to produce liquid water contents ranging from 16 to 46 gm/cu m. The results obtained for various rain intensity levels and tunnel speeds showed significant losses in maximum lift capability and increases in drag for a given lift as the liquid water content was increased. The results obtained on the landing configuration also indicate a progressive decrease in the angle of attack at which maximum lift occurred and an increase in the slope of the pitching-moment curve as the liquid water content was increased. The sensitivity of test results to the effects of the water surface tension was also investigated. A chemical was introduced into the rain environment that reduced the surface

tension of water by a factor of 2. The reduction in the surface tension of water did not significantly alter the level of performance losses for the landing configuration. Author

N92-31533*# MCAT Inst., San Jose, CA.
HYPERSONIC CODE EFFICIENCY AND VALIDATION STUDIES Progress Report
Bradford C. Bennett Aug. 1992 25 p Original contains color illustrations
(Contract NCC2-522)
(NASA-CR-190680; NAS 1.26:190680; MCAT-92-014) Avail: CASI HC A03/MF A01; 10 functional color pages

Renewed interest in hypersonic and supersonic flows spurred the development of the Compressible Navier-Stokes (CNS) code. Originally developed for external flows, CNS was modified to enable it to also be applied to internal high speed flows. In the initial phase of this study CNS was applied to both internal flow applications and fellow researchers were taught to run CNS. The second phase of this research was the development of surface grids over various aircraft configurations for the High Speed Research Program (HSRP). The complex nature of these configurations required the development of improved surface grid generation techniques. A significant portion of the grid generation effort was devoted to testing and recommending modifications to early versions of the S3D surface grid generation code. Author

N92-31555# Arizona State Univ., Tempe.
STABILITY AND TRANSITION OF HYPERSONIC BOUNDARY-LAYER FLOWS Final Report
Helen L. Reed and William S. Saric Apr. 1992 32 p
(Contract F49620-88-C-0076)
(AD-A250279; AFOSR-92-0399TR) Avail: CASI HC A03/MF A01

This final report describes our research of hypersonic and supersonic boundary-layer flows. In spite of its extreme importance to the accurate prediction of drag and heating requirements in high-speed flow, the study of boundary-layer transition in hypersonic (NASP) and supersonic (fighter and high-speed civil transport) flows is still very much in its infancy. Transition is well known, however, to depend strongly on such effects as pressure gradient, wall curvature, sweep, roughness, wall mass transfer, freestream and wall temperature, nose radius, nonequilibrium chemistry, and freestream disturbances. (These effects have been discussed in any number of workshops and U.S. Transition Study Group meetings under the direction of Eli Reshotko.) We have completed detailed studies of the stability of the laminar basic state of 2-D and axisymmetric boundary layers with non-equilibrium chemistry included and 3-D boundary-layer flows of an ideal gas. (Relatively simple geometries were considered due to the anticipated difficulties in performing basic-state analyses.) GRA

N92-31622# Air Force Academy, CO. Research Lab.
ACTIVE CONTROL OF THE SEPARATION REGION ON A TWO-DIMENSIONAL AIRFOIL
Julie A. Lovato Mar. 1992 145 p
(AF Proj. 2300)
(AD-A249739; FJSRL-TR-92-0001) Avail: CASI HC A07/MF A02

This experimental analysis presents a comprehensive study of the separating boundary layer over a static airfoil under natural and actively controlled conditions. Near-surface hot-film and surface pressure measurements, as well as flow visualization are used to analyze the large-scale nature of the flow over a two-dimensional NACA-0015 airfoil and determine forcing effects. Results from the static study are then extended for an initial evaluation of unsteady airfoil control. Results show that the fundamental frequency associated with free shear layer instabilities for this case is an integral multiple of the frequency associated with wake structures. The static separating boundary layer response to active control confirms that it is a boundary layer transitioning to a free shear layer. Qualitative analyses show that significant reduction in overall static separation can be achieved under forcing conditions. Upper airfoil surface suction values are also significantly increased over the natural values. Applying tangential pulsed air control at static fundamental frequencies to a dynamic airfoil results in delay of the dynamic stall vortex formation and a delay of dynamic stall. These discoveries indicate that the developed control methodology may prove successful in increasing unsteady aircraft maneuverability. GRA

N92-31674# Wright Lab., Wright-Patterson AFB, OH.
PRESSURE AND TEMPERATURE FOR B-1B TRANSPARENCY TEST
Elijah W. Turner and John T. Riechers May 1992 122 p
(AF Proj. 2401)
(AD-A252711; WL-TM-92-312-FIBE) Avail: CASI HC A06/MF A02

Pressure and temperature data are presented for life cycle testing of the B-1B transparency. For each of three mission types, contour plots of pressure and temperature are presented for each mission segment. Potential flow theory was used to calculate pressure. Isentropic flow was assumed for calculating temperature. GRA

N92-31777# Boeing Aerospace and Electronics Co., Seattle, WA.
LOW DENSITY REAL GAS FLOWS ABOUT HYPERSONIC VEHICLES Final Report
J. J. Hoffman, R. S. Wong, and J. K. Krauss Nov. 1991 104 p
(Contract F33615-86-C-3006)
(AD-A250048; WL-TR-91-3072) Avail: CASI HC A06/MF A02

This document represents the final report for Air Force contract F33615-86-C-3006, 'Low Density Real Gas Flows About Hypersonic Vehicles'. The focus of this contract was the development of a computer code capable of predicting trends in hypersonic vehicle flowfield properties to support design trade studies for improved hypersonic vehicles. This report provides details of the Hypersonic Low Density Analysis (HYLDA) code developed for this contract. Included in this report are summaries of the HYLDA code, details of the HYLDA fully-coupled Navier-Stokes/finite rate chemistry solution algorithm, details of the thermochemistry models used by the code, and results from three Government-supplied demonstration cases. Code summaries discussed include code features, code design, and multiprocessing capability, while the algorithm discussion includes governing equations, development of the solution algorithm, and boundary conditions. The thermochemistry discussion includes details of the chemistry model transport properties model, and species thermodynamics properties model developed for the HYLDA code. The Government-supplied demonstration cases consist of a Mach 16 wedge flow, a Mach 12 biconic, and a Mach 5 catalytic hemisphere. GRA

N92-31808*# National Aeronautics and Space Administration. Hugh L. Dryden Flight Research Facility, Edwards, CA.
IN-FLIGHT EVALUATION OF AERODYNAMIC PREDICTIONS OF AN AIR-LAUNCHED SPACE BOOSTER
Robert E. Curry, Michael R. Mendenhall (Nielsen Engineering and Research, Inc., Mountain View, CA.), and Bryan Moulton (PRC Kentron, Inc., Edwards, CA.) Apr. 1992 21 p Presented at the AGARD Symposium on Theoretical and Experimental Methods in Hypersonic Flows, Torino, Italy, 4-7 May 1992
(RTOP 505-02-40)
(NASA-TM-104246; H-1803; NAS 1.15:104246) Avail: CASI HC A03/MF A01

Several analytical aerodynamic design tools that were applied to the Pegasus (registered trademark) air-launched space booster were evaluated using flight measurements. The study was limited to existing codes and was conducted with limited computational resources. The flight instrumentation was constrained to have minimal impact on the primary Pegasus missions. Where appropriate, the flight measurements were compared with computational data. Aerodynamic performance and trim data from the first two flights were correlated with predictions. Local measurements in the wing and wing-body interference region were correlated with analytical data. This complex flow region includes the effect of aerothermal heating magnification caused by the

presence of a corner vortex and interaction of the wing leading edge shock and fuselage boundary layer. The operation of the first two missions indicates that the aerodynamic design approach for Pegasus was adequate, and data show that acceptable margins were available. Additionally, the correlations provide insight into the capabilities of these analytical tools for more complex vehicles in which the design margins may be more stringent. Author

N92-31853# Catholic Univ. of America, Washington, DC. Dept. of Mechanical Engineering.
ORGANIZED TURBULENT STRUCTURES AND THEIR INDUCED WALL PRESSURE FLUCTUATIONS Ph.D. Thesis Interim Report, Jun. 1991 - May 1992
Vincent Wilczynski 8 May 1992 286 p
(Contract N00014-91-J-1925)
Copyright Avail: CASI HC A13/MF A03

The interaction between the velocity fluctuations within and the wall pressure below a turbulent boundary layer was experimentally investigated. Simultaneous measurements of the velocity and wall pressure fluctuations were obtained using hot-wire anemometers and an acoustic microphone, respectively. The spectral, statistical, and temporal characteristics of the data were analyzed using long time averaging techniques and event detection methods. Five of the known classes of coherent structure were identified in the collected data by more than one signal processing method. Large scale structure was observed outside the boundary layer, transmitted across the boundary layer, and produced low frequency oscillations in the wall pressure signature. Intermittent, short duration velocity events, which are related to the production and dissipation of turbulence were identified across the boundary layer. These fluctuations produced a discernable pattern in the wall pressure signature, and the observations were used to produce a model of the wall pressure fluctuations during the turbulence production process. Author

N92-32062# Naval Postgraduate School, Monterey, CA.
EXPLORATORY EXPERIMENTAL INVESTIGATION OF A WAVE PROPELLER M.S. Thesis
Carl W. Dane Mar. 1992 67 p
(AD-A252175) Avail: CASI HC A04/MF A01

A low-speed wind tunnel investigation was conducted to determine if a small secondary airfoil, or wave propeller, oscillating in a rotary plunging motion, could significantly affect the airflow over a lifting airfoil surface enough to delay the onset of stall. The lifting airfoil shape was a NACA 66(215)-216, chosen for its chordwise pressure instrumentation. Testing consisted of measuring the pressure distribution of the NACA 66(215)-216 airfoil past the stall angle-of-attack, and then again in combination with the wave propeller. The wave propeller was located in two different positions: above the lifting airfoils trailing edge, and aft of the trailing edge. The propeller was operated in both clockwise and counter-clockwise directions. The propeller effectiveness was evaluated by comparing the pressure distributions and computed lift curve slopes with and without propeller operation. Reynolds number varied from 1.28 x 10(exp 5) to 2.56 x 10(exp 5). Mechanical limitations resulted in testing to only ten percent of the desired wave propeller speeds. Results indicated that the wave propeller acted to block the air flow over the lifting wing causing early separation and loss of lift. GRA

N92-32114*# Virginia Polytechnic Inst. and State Univ., Blacksburg.
A COMPUTATIONAL EXAMINATION OF DIRECTIONAL STABILITY FOR SMOOTH AND CHINED FOREBODIES AT HIGH-ALPHA Report, 15 Aug. 1990 - 15 Aug. 1991
Ramakrishnan Ravi and William H. Mason Washington NASA. Langley Research Center Aug. 1992 84 p
(Grant NAG1-1037; RTOP 505-68-30-03)
(NASA-CR-4465; NAS 1.26:4465; VPI-Aero-182) Avail: CASI HC A05/MF A01

Computational Fluid Dynamics (CFD) has been used to study aircraft forebody flowfields at low-speed, angle-of-attack conditions with sideslip. The purpose is to define forebody geometries which provide good directional stability characteristics under these conditions. The flows over the experimentally investigated F-5A forebody and chine type configuration, previously computed by the authors, were recomputed with better grid topology and resolution. The results were obtained using a modified version of CFL3D (developed at NASA Langley) to solve either the Euler equations or the Reynolds equations employing the Baldwin-Lomax turbulence model with the Degani-Schiff modification to account for massive crossflow separation. Based on the results, it is concluded that current CFD methods can be used to investigate the aerodynamic characteristics of forebodies to achieve desirable high angle-of-attack characteristics. An analytically defined generic forebody model is described, and a parametric study of various forebody shapes was then conducted to determine which shapes promote a positive contribution to directional stability at high angle-of-attack. An unconventional approach for presenting the results is used to illustrate how the positive contribution arises. Based on the results of this initial parametric study, some guidelines for aerodynamic design to promote positive directional stability are presented. Author

N92-32162*# Texas Univ., Arlington. Dept. of Mechanical and Aerospace Engineering.
EXPERIMENTAL STUDIES OF HYPERSONIC SHOCK-WAVE BOUNDARY-LAYER INTERACTIONS Final Report
Frank K. Lu 10 Sep. 1992 66 p
(Grant NAG1-891)
(NASA-CR-190731; NAS 1.26:190731) Avail: CASI HC A01/MF A01

Two classes of shock-wave boundary-layer interactions were studied experimentally in a shock tunnel in which a low Reynolds number, turbulent flow at Mach 8 was developed on a cold, flat test surface. The two classes of interactions were: (1) a swept interaction generated by a wedge ('fin') mounted perpendicularly on the flat plate; and (2) a two-dimensional, unseparated interaction induced by a shock impinging near an expansion corner. The swept interaction, with wedge angles of 5-20 degrees, was separated and there was also indication that the strongest interactions prossessed secondary separation zones. The interaction spread out extensively from the inviscid shock location although no indication of quasi-conical symmetry was evident. The surface pressure from the upstream influence to the inviscid shock was relatively low compared to the inviscid downstream value but it rose rapidly past the inviscid shock location. However, the surface pressure did not reach the downstream inviscid value and reasons were proposed for this anomalous behavior compared to strongly separated, supersonic interactions. The second class of interactions involved weak shocks impinging near small expansion corners. As a prelude to studying this interaction, a hypersonic similarity parameter was identified for the pure, expansion corner flow. The expansion corner severely damped out surface pressure fluctuations. When a shock impinged upstream of the corner, no significant changes to the surface pressure were found as compared to the case when the shock impinged on a flat plate. But, when the shock impinged downstream of the corner, a close coupling existed between the two wave systems, unlike the supersonic case. This close coupling modified the upstream influence. Regardless of whether the shock impinged ahead or behind the corner, the downstream region was affected by the close coupling between the shock and the expansion. Not only was the mean pressure distribution modified but the unsteadiness in the surface pressure was reduced compared to the flat-plate case. Author

N92-32177*# MCAT Inst., San Jose, CA.
CONTROL OF UNSTEADY SEPARATED FLOW ASSOCIATED WITH THE DYNAMIC STALL OF AIRFOILS Final Report, 2 Mar. - 15 Jul. 1992
Michael C. Wilder Aug. 1992 32 p
(Contract NCC2-637)
(NASA-CR-190688; NAS 1.26:190688; MCAT-92-015) Avail: CASI HC A03/MF A01

The two principal objectives of this research were to achieve

an improved understanding of the mechanisms involved in the onset and development of dynamic stall under compressible flow conditions, and to investigate the feasibility of employing adaptive airfoil geometry as an active flow control device in the dynamic stall engine. Presented here are the results of a quantitative (PDI) study of the compressibility effects on dynamic stall over the transiently pitching airfoil, as well as a discussion of a preliminary technique developed to measure the deformation produced by the adaptive geometry control device, and bench test results obtained using an airfoil equipped with the device. Author

N92-32213*# National Aeronautics and Space Administration. Ames Research Center, Moffett Field, CA.
TRANSONIC WIND TUNNEL TEST OF A 14 PERCENT THICK OBLIQUE WING
Robert A. Kennelly, Jr., Ilan M. Kroo (Stanford Univ., CA.), James M. Strong, and Ralph L. Carmichael Aug. 1990 430 p
(RTOP 533-06-01)
(NASA-TM-102230; A-89236; NAS 1.15:102230) Avail: CASI HC A19/MF A04

An experimental investigation was conducted at the ARC 11-by 11-Foot Transonic Wind Tunnel as part of the Oblique Wing Research Aircraft Program to study the aerodynamic performance and stability characteristics of a 0.087-scale model of an F-8 airplane fitted with an oblique wing designed by Rockwell International. The 10.3 aspect ratio, straight-tapered wing of 0.14 thickness/chord ratio was tested at two different mounting heights above the fuselage. Additional tests were conducted to assess low-speed behavior with and without flaps, aileron effectiveness at representative flight conditions, and transonic drag divergence with 0 degree wing sweep. Longitudinal stability data were obtained at sweep angles of 0, 30, 45, 60, and 65 degrees, at Mach numbers ranging from 0.25 to 1.40. Test Reynolds numbers varied from 3.2 to 6.6 x 10 exp 6/ft. and angle of attack ranged from -5 to +18 degrees. Most data were taken at zero sideslip, but a few runs were at sideslip angles of +/- 5 degrees. The raised wing position proved detrimental overall, although side force and yawing moment were reduced at some conditions. Maximum lift coefficient with the flaps deflected was found to fall short of the value predicted in the preliminary design document. The performance and trim characteristics of the present wing are generally inferior to those obtained for a previously tested wing designed at ARC. Author

N92-32226*# Boeing Commercial Airplane Co., Seattle, WA.
AN INSTALLED NACELLE DESIGN CODE USING A MULTIBLOCK EULER SOLVER. VOLUME 1: THEORY DOCUMENT Final Report
H. C. Chen Sep. 1992 59 p
(Contract NAS1-18703)
(NASA-CR-189652-Vol-1; NAS 1.26:189652-Vol-1) Avail: CASI HC A04/MF A01

An efficient multiblock Euler design code was developed for designing a nacelle installed on geometrically complex airplane configurations. This approach employed a design driver based on a direct iterative surface curvature method developed at LaRC. A general multiblock Euler flow solver was used for computing flow around complex geometries. The flow solver used a finite-volume formulation with explicit time-stepping to solve the Euler Equations. It used a multiblock version of the multigrid method to accelerate the convergence of the calculations. The design driver successively updated the surface geometry to reduce the difference between the computed and target pressure distributions. In the flow solver, the change in surface geometry was simulated by applying surface transpiration boundary conditions to avoid repeated grid generation during design iterations. Smoothness of the designed surface was ensured by alternate application of streamwise and circumferential smoothings. The capability and efficiency of the code was demonstrated through the design of both an isolated nacelle and an installed nacelle at various flow conditions. Information on the execution of the computer program is provided in volume 2.
Author

N92-32228*# Boeing Commercial Airplane Co., Seattle, WA.
AN INSTALLED NACELLE DESIGN CODE USING A MULTIBLOCK EULER SOLVER. VOLUME 2: USER GUIDE Final Report
H. C. Chen Sep. 1992 74 p
(Contract NAS1-18703)
(NASA-CR-189652-Vol-2; NAS 1.26:189652-Vol-2) Avail: CASI HC A04/MF A01

This is a user manual for the general multiblock Euler design (GMBEDS) code. The code is for the design of a nacelle installed on a geometrically complex configuration such as a complete airplane with wing/body/nacelle/pylon. It consists of two major building blocks: a design module developed by LaRC using directive iterative surface curvature (DISC); and a general multiblock Euler (GMBE) flow solver. The flow field surrounding a complex configuration is divided into a number of topologically simple blocks to facilitate surface-fitted grid generation and improve flow solution efficiency. This user guide provides input data formats along with examples of input files and a Unix script for program execution in the UNICOS environment. Author

N92-32240*# Sverdrup Technology, Inc., Brook Park, OH.
THREE-DIMENSIONAL COMPRESSIBLE TURBULENT COMPUTATIONS FOR A NONDIFFUSING S-DUCT Final Report
G. J. Harloff, J. R. DeBonis, C. F. Smith, and J. E. Bruns Washington NASA. Lewis Research Center Apr. 1992 31 p
(Contract NAS3-25266; RTOP 533-02-30)
(NASA-CR-4391; E-6173; NAS 1.26:4391) Avail: CASI HC A03/MF A01

The PARC3D code was used to compute the compressible turbulent flow within a three dimensional, nondiffusing S-duct. A frame of reference is provided for future computational fluid dynamics studies of internal flows with strong secondary flows and provides an understanding of the performance characteristics of a typical S-duct with attached flow. The predicted results, obtained with both H- and O-grids, are compared with the experimental wall pressure, static and total pressure fields, and velocity vectors. Additionally, computed boundary layer thickness, velocity profiles in wall coordinates, and skin friction values are presented. Author

N92-31863# Princeton Univ., NJ.
AUTOMATIC DESIGN OF TRANSONIC AIRFOILS TO REDUCE THE SHOCK INDUCED PRESSURE DRAG
Antony Jameson *In* Israel Society of Aeronautics and Astronautics, 31st Israel Annual Conference on Aviation and Astronautics 22 Feb. 1990 p 5-17 Previously announced in IAA as A91-43078 (For primary document see N92-31861 22-01)
Avail: CASI HC A03/MF A03

N92-31888# Israel Aircraft Industries Ltd., Ben-Gurion Airport. Aerodynamics Dept.
EULER SOLVER FOR ARBITRARY CONFIGURATIONS: FURTHER APPLICATIONS
B. Epstein, A. L. Luntz, and A. Nachshon *In* Israel Society of Aeronautics and Astronautics, 31st Israel Annual Conference on Aviation and Astronautics 22 Feb. 1990 p 205-216 Previously announced in IAA as A91-43100 (For primary document see N92-31861 22-01)
Avail: CASI HC A03/MF A03

N92-31889# Technion - Israel Inst. of Tech., Haifa. Faculty of Aerospace Engineering.
THE THREE-DIMENSIONAL STABILITY OF THE FOEPPL VORTICES
Z. Rusak and A. Seginer *In* Israel Society of Aeronautics and Astronautics, 31st Israel Annual Conference on Aviation and Astronautics 22 Feb. 1990 p 217-225 Previously announced in IAA as A91-43101 (For primary document see N92-31861 22-01)
Avail: CASI HC A02/MF A03

03 AIR TRANSPORTATION AND SAFETY

Includes passenger and cargo air transport operations; and aircraft accidents.

For related information see also *16 Space Transportation* and *85 Urban Technology and Transportation.*

N92-31453# General Accounting Office, Washington, DC. Resources, Community, and Economic Development Div.
AVIATION SAFETY: CHANGES NEEDED IN FAA'S SERVICE DIFFICULTY REPORTING PROGRAM
Mar. 1991 18 p
(GAO/RCED-91-24; B-238393) Avail: CASI HC A03/MF A01; GAO, PO Box 6015, Gaithersburg, MD 20877 HC

As requested, this group has evaluated the effectiveness of the FAA's Service Difficulty Reporting (SDR) program. The programs objective is to help airline and FAA personnel to promptly correct conditions that could adversely affect air safety. This is accomplished by distributing reports on aircraft malfunctions to airline and FAA personnel. This report centered on the SDR program's impact on the safety of aging airliners in commercial aviation and excluded general aviation. This evaluation covered: (1) the usefulness of the SDR data to FAA and airline personnel; (2) factors affecting the SDR program's usefulness; and (3) changes needed to improve the program, if warranted. H.A.

N92-31549*# Clemson Univ., SC. Radar Systems Lab.
SPECTRUM MODAL ANALYSIS FOR THE DETECTION OF LOW-ALTITUDE WINDSHEAR WITH AIRBORNE DOPPLER RADAR Final Report
Matthew W. Kunkel Washington NASA. Langley Research Center Aug. 1992 97 p
(Grant NAG1-928; RTOP 505-64-12-02)
(NASA-CR-4457; NAS 1.26:4457; CU-TR-15; DOT/FAA/RD-92/21) Avail: CASI HC A05/MF A02

A major obstacle in the estimation of windspeed patterns associated with low-altitude windshear with an airborne pulsed Doppler radar system is the presence of strong levels of ground clutter which can strongly bias a windspeed estimate. Typical solutions attempt to remove the clutter energy from the return through clutter rejection filtering. Proposed is a method whereby both the weather and clutter modes present in a return spectrum can be identified to yield an unbiased estimate of the weather mode without the need for clutter rejection filtering. An attempt will be made to show that modeling through a second order extended Prony approach is sufficient for the identification of the weather mode. A pattern recognition approach to windspeed estimation from the identified modes is derived and applied to both simulated and actual flight data. Comparisons between windspeed estimates derived from modal analysis and the pulse-pair estimator are included as well as associated hazard factors. Also included is a computationally attractive method for estimating windspeeds directly from the coefficients of a second-order autoregressive model. Extensions and recommendations for further study are included. Author

N92-31562# Royal Australian Air Force, Victoria. Inst. of Aviation Medicine.
IMMERSION SUIT USAGE WITHIN THE RAAF
D. B. Watson Jan. 1992 28 p
(AD-A250645; AVMED-8-92; DODA-AR-006-814) Avail: CASI HC A03/MF A01

Military aircrews flying over oceans or lakes are constantly at risk of ditching or ejecting into cold water. Immersion in sufficiently cold water for a sufficient time results in death through hypothermia. Apart from water temperature and time, other factors that influence survival in cold water include the insulation and water proofing of the victim's garments, the activity and posture of the victim, the calmness of the water surface, and individual factors such as fitness and body fat. It is possible to improve the survival chances of immersed aircrew through the wearing of protective insulative garments that reduce the rate of heat loss to the surrounding water. Such immersion suits may be constantly worn during a flight or donned only during particularly risky phases of an overwater flight or once an emergency has been identified. These immersion suits are respectively known as either constant wear immersion suits (CWIS) or quick-don immersion suits (QDIS). This paper discusses general aspects of immersion hypothermia and its prevention as well as immersion suit usage within the RAAF. A series of brief recommendations concerning the future use of immersion suits within the RAAF are made. GRA

N92-31813# Deutsche Forschungsanstalt fuer Luft- und Raumfahrt, Oberpfaffenhofen (Germany, F.R.). Abtteilung Wolkenphysik.
THE ICING OF THE ELEVATOR OF THE DLR ICING RESEARCH AIRCRAFT OF Do 28 TYPE [DIE VEREISUNG DES HOEHENRUDERS DES VEREISUNGSFORSCHUNGSFLUGZEUGS DER DLR VOM TYP DO 28]
Hans-Eberhard Hoffmann, Johann Demmel, and Joachim Schuster Aug. 1991 67 p In GEORGIAN
(DLR-Mitt-91-12; ISSN-0939-298X; ETN-92-91732) Avail: CASI HC A04/MF A01; DLR, Wissenschaftlisches Berichtswesen, Postfach 90 60 58, 5000 Cologne, Fed. Republic of Germany, HC

Observations of the icing of the elevator for information on the type of accretion are addressed. Most of the coarse ice structures observed until now could be related to the following icing classes: 1st stripe of rime ice; 52 stripes of rime ice as borders of one stripe of clear ice; 3 stripes of rime ice with and without clear ice between them; and 3 stripes of rime ice growing together. The maximum extension of ice accretion on the upper and bottom side of the elevator amounted to 80 mm. In this case, the temperature was about -2.5 C, the median volume diameter of the cloud particles about 400 micrometers, and the total water content between 0.02 and 0.10 g/cu m. The roughness had its maximum value of 19 mm after an incomplete pneumatic deicing. Without influence of pneumatic deicing the maximum roughness was 15 mm. ESA

N92-31928# Department of Energy, Washington, DC.
REPORT OF THE AVIATION SAFETY REVIEW OF DEPARTMENT OF ENERGY HELICOPTER OPERATIONS
Feb. 1992 123 p
(DE92-016346; DOE/EH-0242P) Avail: CASI HC A06/MF A02

In a memorandum dated November 27, 1991, the Secretary of Energy directed the Office of Environment, Safety and Health (EH) to lead, with Program Secretarial Office participation, an aviation safety review of the safe operation of the Department's helicopter program. The Aviation Safety Review Team comprised of aviation experts from the US Army, the Federal Aviation Administration, private consulting organizations, and Department of Energy (DOE) staff was assembled. The scope of the Aviation Safety Review Team's appraisals included the following as applicable: policy; operations; maintenance; crew training; previous appraisals; contract requirements; aviation safety analysis reports; refueling facilities and management; night vision goggle (NVG) operations; helicopter limited standdown initiative; Secretary of Energy Notice (SEN) -6D-91 Compliance; and, DOE/contractor organizational structures and responsibilities. The appraisals at each site included a review of aviation policy, manuals, procedures, facilities, and documentation pertaining to management, safety, operations, maintenance, and quality control. DOE

N92-31943# European Space Agency, Paris (France).
ANALYSIS OF THREE ICING TEST FLIGHTS REACHING THE AIRCRAFT-REFERRED ICING DEGREE OF SEVERE
Hans-Eberhard Hoffmann (Deutsche Forschungsanstalt fuer Luft- und Raumfahrt, Oberpfaffenhofen, Germany, F.R.) and Johann Demmel (Deutsche Forschungsanstalt fuer Luft- und Raumfahrt, Oberpfaffenhofen, Germany, F.R.) Mar. 1992 107 p Transl. into ENGLISH of Eine Analyse von drei Vereisungsfluegen mit Erreichen des Luftfahrzeugbezogenen Vereisungsgrades Severe (Oberpfaffenhofen, Germany, DLR), Aug. 1990 118 p Original language document was announced as N91-21123

(ESA-TT-1254; DLR-FB-90-34; ETN-92-91711) Avail: CASI HC A06/MF A02

Three test flights in icing conditions are discussed: one in the range of a high pressure area, and the other two in the range of warm fronts, where the aircraft-referred icing degree of 'severe' was reached. The ice accretion on the underside of the wing of the Do28 extended (at 50 to 70 cm) beyond the area which can be pneumatically deiced. In the area of the pneumatic deicing boots, the deicing was totally ineffective or incomplete. The mean values of the cloud physics parameters which produced the aircraft referred icing degree of 'severe' were: total water content 0.20, 0.22, 0.30 g/cu m; temperature -1.8, -2.0, -4.5 C; and median volume diameter 20, 180, and 300 microns. The cloud flight paths in the range of the warm fronts were only 1/10 to 3/10 of the cloud flight path in the range of high pressure areas when it came to attaining the maximum icing characteristics achieved in the range of a high pressure area. The reason for this was the considerably higher value of the median volume diameter in the range of the warm fronts. ESA

N92-32219# Defence and Civil Inst. of Environmental Medicine, Downsview (Ontario).
CANADIAN AIRCREW SEA WATER SURVIVAL, 1952-1987
C. J. Brooks Sep. 1988 36 p
(DCIEM-88-RR-39; CTN-92-60344) Avail: CASI HC A03/MF A01

A 36-year retrospective study of all Canadian military aircraft has been conducted. There have been 55 aircraft accidents where aircrew or passengers have landed in the sea. One hundred and fifty-eight personnel have been involved with 68 fatalities, an overall survival rate of 57 percent. Survivors were rescued in under 15 minutes in 40 percent of cases; the remainder were rescued in under three hours. The longest time spent in a life raft was 2 hours and 45 minutes. Seventy percent of aircrew had less than 15 seconds warning of impending water immersion. There were five cases where crew and passengers probably died from a combination of cold, drowning, and cardiac arrythmias. Immersion suits were worn in only six accidents and in two of these, leakage was reported. Aircrew who have received training in water survival, underwater escape trainers, who are strong swimmers or sports divers, have a better chance of survival. Therefore, it is strongly recommended that aircrew, particularly helicopter pilots flying over water, should receive underwater escape training. Author (CISTI)

N92-31862# Boeing Commercial Airplane Co., Seattle, WA.
AGING FLEET: MAINTAINING AIRWORTHINESS
B. A. Cosgrove *In* Israel Society of Aeronautics and Astronautics, 31st Israel Annual Conference on Aviation and Astronautics 22 Feb. 1990 p 1-4 Previously announced in IAA as A91-43077
(For primary document see N92-31861 22-01)
Avail: CASI HC A01/MF A03

04 AIRCRAFT COMMUNICATIONS AND NAVIGATION

Includes digital and voice communication with aircraft; air navigation systems (satellite and ground based); and air traffic control.

For related information see also *17 Space Communications, Spacecraft Communications, Command and Tracking* and *Communications and Radar.*

N92-31746# Sandia National Labs., Albuquerque, NM.
TECHNIQUES FOR AUTONOMOUS NAVIGATION
R. H. Byrne, P. R. Klarer, and J. B. Pletta Mar. 1992 83 p
(Contract DE-AC04-76DP-00789)
(DE92-013458; SAND-92-0457) Avail: CASI HC A05/MF A01

Based on the growing need to develop physical security systems which are more flexible and less manpower intensive, the US Army has defined the Required Operational Capability (ROC) for a Mobile Detection Assessment Response System (MDARS). This report evaluates potential technical approaches for implementing the portion of the MDARS robotic path-following system. To address the wide range of available technologies, the report is broken into two main sections, path sensing and position location. Path sensing techniques discussed include: vision, ultrasonic ranging, scanning lasers, inductive wire-following, and stripe-following. Position location systems covered include: CPS, Loran-C, Omega, transit, RF beacons, and laser reflectors. A cost-risk trade-off analysis of the systems described is provided along with recommendations on the best technical approach to meet the MDARS path-following requirements using proven technology. DOE

N92-31838# Federal Aviation Administration, Atlantic City, NJ.
GLOBAL POSITIONING SYSTEM RUNWAY INCURSION PROGRAM STATIC GROUND TESTS Technical Report, Feb. - Mar. 1991
Carl Caruso May 1992 25 p
(Contract FAA-T0704-E)
(DOT/FAA/CT-TN91/44) Avail: CASI HC A03/MF A01

Described here are the ground tests of the Global Positioning System (GPS) in the terminal area at the Atlantic City International Airport. The purpose of the Runway Incursion Program is to investigate the application of GPS as a navigation aid to allow the pilot to safely transverse airport taxiways and runways under poor visibility conditions. The primary objective of the tests was to resolve the critical issue of differential GPS accuracy as a function of the differential update rate. Author

N92-32054# Naval Postgraduate School, Monterey, CA.
DECISION-MAKING GUIDE FOR THE PROPOSED COAST GUARD DIFFERENTIAL GLOBAL POSITIONING SYSTEM M.S. Thesis
Robert J. Wilson Jun. 1991 168 p
(AD-A246046) Avail: CASI HC A08/MF A02

The Coast Guard has begun an initiative to deploy a nationwide Differential Global Positioning System (DGPS) to support Coast Guard missions and to enhance maritime safety in harbor navigation. DGPS service is expected to provide accuracy to within ten meters (95 percent of the time) to suitably equip vessels. It would do this by broadcasting corrections to GPS navigation satellite signals, thereby, improving accuracy by a factor of ten over standard GPS. The primary emphasis is on showing how decision making and planning for the DGPS project may be aided by comparing technological alternatives using Cost Effectiveness Analysis (CEA). This method is essentially a means of quantifying effectiveness per dollar of cost. The author consolidates the discussion of key issues within one document, identifies the technical decision criteria, estimates alternative system life-cycle costs, and makes a preliminary finding as to the merits of radiobeacon transmission over a dedicated satellite channel. In order to quantify effectiveness, many performance criteria are consolidated under five figures of merit: accuracy, availability, coverage, integrity, and adaptability. The inclusion of user equipment prices in life-cycle costs proves to be critical to the preliminary finding in favor of the radiobeacon-based alternative. This CEA model is especially suited to decision making in an environment of technological and policy change, since it can be easily refined and updated. Author (GRA)

05 AIRCRAFT DESIGN, TESTING AND PERFORMANCE

Includes aircraft simulation technology.

For related information see also *18 Spacecraft Design, Testing and Performance* and *39 Structural Mechanics.* For land transportation vehicles see *85 Urban Technology and Transportation.*

N92-31261*# National Aeronautics and Space Administration. Hugh L. Dryden Flight Research Facility, Edwards, CA.
OVERVIEW OF THE NASA DRYDEN FLIGHT RESEARCH FACILITY AERONAUTICAL FLIGHT PROJECTS
Robert R. Meyer, Jr. Aug. 1992 20 p Presented at the

AGARD Flight Mechanics Panel, Chania, Crete, Greece, 11 May 1992
(RTOP 505-68-50)
(NASA-TM-104254; H-1847; NAS 1.15:104254; AGARD-16)
Avail: CASI HC A03/MF A01

Several principal aerodynamics flight projects of the NASA Dryden Flight Research Facility are discussed. Key vehicle technology areas from a wide range of flight vehicles are highlighted. These areas include flight research data obtained for ground facility and computation correlation, applied research in areas not well suited to ground facilities (wind tunnels), and concept demonstration. Author

N92-31264*# National Aeronautics and Space Administration. Langley Research Center, Hampton, VA.
A SUMMARY OF THE ACTIVE FLEXIBLE WING PROGRAM
Boyd Perry, III, Stanley R. Cole, and Gerald D. Miller (Rockwell International Corp., Los Angeles, CA.) Jul. 1992 12 p Presented at the AIAA Dynamic Specialists' Conference, Dallas, TX, 16-17 Apr. 1992 Previously announced in IAA as A92-35652
(RTOP 505-63-50-15)
(NASA-TM-107655; NAS 1.15:107655) Avail: CASI HC A03/MF A01

A summary of the NASA/Rockwell Active Flexible Wing Program is presented. Major elements of the program are presented. Key program accomplishments included single- and multiple-mode flutter suppression, load alleviation and load control during rapid roll maneuvers, and multi-input/multi-output multiple-function active controls tests above the open-loop flutter boundary. Author

N92-31350*# National Aeronautics and Space Administration. Langley Research Center, Hampton, VA.
FLUTTER SUPPRESSION DIGITAL CONTROL LAW DESIGN AND TESTING FOR THE AFW WIND-TUNNEL MODEL
Vivek Mukhopadhyay Jul. 1992 8 p Presented at the AIAA Dynamics Specialists' Conference, Dallas, TX, 16-17 Apr. 1992 Previously announced in IAA as A92-35668
(RTOP 505-63-50-15)
(NASA-TM-107652; NAS 1.15:107652; AIAA Paper 92-2095-CP)
Avail: CASI HC A02/MF A01

Design of a control law for simultaneously suppressing the symmetric and antisymmetric flutter modes of a string mounted fixed-in-roll aeroelastic wind tunnel model is described. The flutter suppression control law was designed using linear quadratic Gaussian theory and involved control law order reduction, a gain root-locus study, and the use of previous experimental results. A 23 percent increase in open-loop flutter dynamic pressure was demonstrated during the wind tunnel test. Rapid roll maneuvers at 11 percent above the symmetric flutter boundary were also performed when the model was in a free-to-roll configuration. Author

N92-31351*# National Aeronautics and Space Administration. Langley Research Center, Hampton, VA.
ROLLING MANEUVER LOAD ALLEVIATION USING ACTIVE CONTROLS
Jessica A. Woods-Vedeler and Anthony S. Pototzky (Lockheed Engineering and Sciences Co., Hampton, VA.) Jul. 1992 11 p Presented at the AIAA Dynamics Specialists' Conference, Dallas, TX, 16-17 Apr. 1992 Previously announced in IAA as A92-35670
(RTOP 505-63-50-15)
(NASA-TM-107654; NAS 1.15:107654) Avail: CASI HC A03/MF A01

Rolling Maneuver Load Alleviation (RMLA) was demonstrated on the Active Flexible Wing (AFW) wind tunnel model in the LaRC Transonic Dynamics Tunnel. The design objective was to develop a systematic approach for developing active control laws to alleviate wing incremental loads during roll maneuvers. Using linear load models for the AFW wind-tunnel model which were based on experimental measurements, two RMLA control laws were developed based on a single-degree-of-freedom roll model. The RMLA control laws utilized actuation of outboard control surface pairs to counteract incremental loads generated during rolling maneuvers and roll performance. To evaluate the RMLA control laws, roll maneuvers were performed in the wind tunnel at dynamic pressures of 150, 200, and 250 psf and Mach numbers of .33, .38, and .44, respectively. Loads obtained during these maneuvers were compared to baseline maneuver loads. For both RMLA controllers, the incremental torsion moments were reduced by up to 60 percent at all dynamic pressures and performance times. Results for bending moment load reductions during roll maneuvers varied. In addition, in a multiple function test, RMLA and flutter suppression system control laws were operated simultaneously during roll maneuvers at dynamic pressures 11 percent above the open-loop flutter dynamic pressure. Author

N92-31515# Cranfield Inst. of Tech., Bedford (England). College of Aeronautics.
ASTOVL COMBAT AIRCRAFT DESIGN SYNTHESIS AND OPTIMIZATION
N. Kehayas Jan. 1992 279 p Sponsored by RAE
(Cranfield-Aero-9201; ISBN-1-871564-360; ETN-92-91728) Avail: CASI HC A13/MF A03

The development of a baseline configuration for an Advanced Short Take Off and Vertical Landing (ASTOVL) combat aircraft is presented. The design synthesis and coding of these baseline configuration (code VERTI), the interfacing of the design synthesis code VERTI with the optimizer code RQPMIN, and the optimization of the baseline configuration, are presented. ESA

N92-31736# Sandia National Labs., Albuquerque, NM.
B-1B NUCLEAR CERTIFICATION TASKS PERFORMED BY THE AIRCRAFT COMPATIBILITY DEPARTMENT AT SANDIA NATIONAL LABORATORIES
J. A. Jackson and S. E. Pink May 1992 41 p
(Contract DE-AC04-76DP-00789)
(DE92-016750; SAND-92-0912) Avail: CASI HC A03/MF A01

The B-1B aircraft, also called the Lancer, is a multi-role, long range strategic bomber belonging to the USAF's Strategic Air Command. Its primary purpose is to fly intercontinental missions with a large payload of nuclear gravity bombs and short range attack missiles and deliver them to pre-determined targets. Through the efforts of engineers in the Aircraft Compatibility Department, and members of the B-1B Project Officers Group, a reliable nuclear weapon capability has been proven and maintained on this aircraft. This document will give the reader an overview of the B-1B nuclear weapon capability. This will include a brief discussion of the aircraft, the AMAC and suspension systems used, the weapon interfaces, and the test and analysis that were required and completed by Sandia National Laboratories Aircraft Compatibility Department before the recommendation was made to add the B-1B to the bomb ACCDs. The responsible B-1B Aircraft Compatibility personnel will update this report on a yearly basis. DOE

N92-31793# Wright Lab., Wright-Patterson AFB, OH.
AN ASSESSMENT OF THE B-747'S CAPABILITY TO OPERATE ON ROUGH SURFACES
Elijah W. Turner and John T. Riechers May 1992 98 p
(AD-A250134; WL-TM-92-313-FIBE) Avail: CASI HC A05/MF A02

A study has been conducted to determine the capability of the Boeing 747 to operate on rough runways; specifically, runways that have been damaged by bombing and repaired rapidly using current Air Force procedures. The quality of the repairs has been determined that will allow the aircraft to operate from the repaired surface without being subjected to loads on the landing gears that exceed design limit load. This study indicates that the B-747 is capable of taking off on a repaired runway at 836,000 lbs gross weight provided that repairs in the first 500 feet of the takeoff roll are at least class B. Repairs further down the runway only need to be class E. If the aircraft will traverse two repairs, tables are provided that give the minimum spacing between repairs. Consideration is not given to traversing more than two repairs. Analysis indicates that the ability of the nose gear to withstand loads produced by traversing repair profiles can be significantly improved by increasing the precharge pressure in the shock strut.

A nose gear precharge of 185 psi will reduce the peak loads sufficiently to permit a class C repair to be at any position on the runway, including the first 500 feet. Increasing the precharge pressure to 272 psi will permit class E repairs to be located anywhere. At the maximum landing gross weight of 666,000 lbs, none of the repairs A through E produced loads that exceeded design limit load during taxi at any speed. GRA

N92-32053# Naval Postgraduate School, Monterey, CA.
DYNAMIC MODELING AND MODAL ANALYSIS OF AN AIR-TO-AIR MISSILE M.S. Thesis
Michael A. Shutty Sep. 1991 111 p
(AD-A245957) Avail: CASI HC A06/MF A02

The P-3 Orion patrol airplane has a need for an air-to-air missile system for defense against enemy aircraft on its long-range missions. In response to this need, the Naval Air Test Center was tasked in 1989 to conduct a P-3/AIM-9 (Sidewinder) integration program. In support of this program, a vibration test stand was established at NPS, and a ground vibration characterization was conducted to determine if a potential flutter problem existed. This test resulted in the development of a two degree-of-freedom lumped-mass model and experimental determination of the missile's resonance modes in pitch. With the recent termination of the P-7A, the P-3 community is now looking at the Orion 2 program to carry it into the 21st century. The Orion 2 will most likely have a beefed-up wing structure, necessitating an analysis of this wing in conjunction with the AIM-9 missile. This investigation responds to that requirement by concurrently developing a mathematical model of the AIM-9 missile using finite element methods to analytically determine its modal parameters, and setting up a modal test system to quantify the parameters of this model by experimentally determining the missile's natural frequencies, mode shapes, and transient response. This fully instrumented test system and associated methodologies could then be the basis for conducting a comprehensive modal test of the AIM-9 missile system, as well as to quantify the vibration characteristics of other candidate missile systems. GRA

N92-32111*# National Aeronautics and Space Administration. Langley Research Center, Hampton, VA.
TIME SIMULATION OF FLUTTER WITH LARGE STIFFNESS CHANGES
Mordechay Karpel (Israel Inst. of Tech., Haifa.) and Carol D. Wieseman Jul. 1992 11 p Presented at the AIAA Structures, Structural Dynamics, and Materials Conference, Dallas, TX, 13-15 Apr. 1992 Previously announced in IAA as A92-34467
(Contract NAS1-18605; NAGw-1708; RTOP 505-63-50-15)
(NASA-TM-107650; NAS 1.15:107650) Avail: CASI HC A03/MF A01

Time simulation of flutter, involving large local structural changes, is formulated with a state-space model that is based on a relatively small number of generalized coordinates. Free-free vibration modes are first calculated for a nominal finite-element model with relatively large fictitious masses located at the area of structural changes. A low-frequency subset of these modes is then transformed into a set of structural modal coordinates with which the entire simulation is performed. These generalized coordinates and the associated oscillatory aerodynamic force coefficient matrices are used to construct an efficient time-domain, state-space model for a basic aeroelastic case. The time simulation can then be performed by simply changing the mass, stiffness, and damping coupling terms when structural changes occur. It is shown that the size of the aeroelastic model required for time simulation with large structural changes at a few apriori known locations is similar to that required for direct analysis of a single structural case. The method is applied to the simulation of an aeroelastic wind-tunnel model. The diverging oscillations are followed by the activation of a tip-ballast decoupling mechanism that stabilizes the system but may cause significant transient overshoots. Author

N92-31880# Israel Military Industries, Ramat-Hasharon (Israel). Systems Div.
OPTIMAL TRAJECTORIES FOR AN UNMANNED AIR VEHICLE
Joseph Z. Ben-Asher *In* Israel Society of Aeronautics and Astronautics, 31st Israel Annual Conference on Aviation and Astronautics 22 Feb. 1990 p 132-140 Previously announced in IAA as A91-43094 (For primary document see N92-31861 22-01)
Avail: CASI HC A02/MF A03

N92-31881# Technion - Israel Inst. of Tech., Haifa. Faculty of Aerospace Engineering.
ESTIMATION OF AIRCRAFT ATTITUDE BY ANGULAR RATE MEASUREMENTS
M. Koifman and S. J. Merhav *In* Israel Society of Aeronautics and Astronautics, 31st Israel Annual Conference on Aviation and Astronautics 22 Feb. 1990 p 141-152 Previously announced in IAA as A91-43095 Sponsored by Ministry of Defence and Precision Instrument Industries (For primary document see N92-31861 22-01)
Avail: CASI HC A03/MF A03

06 AIRCRAFT INSTRUMENTATION

Includes cockpit and cabin display devices; and flight instruments.

For related information see also *19 Spacecraft Instrumentation* and *35 Instrumentation and Photography.*

N92-32051# Naval Postgraduate School, Monterey, CA.
A CONTINUING STUDY OF ALTITUDE DETERMINATION DEFICIENCIES OF THE SERVICE AIRCRAFT INSTRUMENTATION PACKAGE (SAIP) M.S. Thesis
Robert J. Russell Sep. 1991 79 p
(AD-A245952) Avail: CASI HC A05/MF A01

After correcting test equipment used in a previous study of the SAIP for an ambiguous grounding requirement, research was continued on aerodynamic factors affecting SAIP altitude measurement. Existing equations for incompressible flow over a cylinder and a sphere were used to model the static-pressure probe located on the front of the SAID pod and an algorithm was derived for the computation of the pressure coefficient, Cp. Our low-speed wind tunnel data show an overpressure at the static pressure ports when the angle of attack (phi) is less than 14 deg. The five-inch diameter body of the SAIP, located aft of the static pressure probe, is responsible for creating a stagnation-like region at the front of the SAIP probe which envelops the static-port location. Calculation of the altitude error (delta zeta) using the model for Cp, corrected for compressibility, is within + or - 15 percent of the error observed in flight at Mach 0.60. Improvements in the compressibility correction as well as analyses using an aero-panel method are suggested before sufficiently reliable fixes to the SAIP can be proposed. GRA

N92-31868# Israel Aircraft Industries Ltd., Lod. Flight Control Dept.
FCS SKEWED SENSORS ARRAY: PRACTICAL CONSIDERATIONS
D. Agami and H. Yahia *In* Israel Society of Aeronautics and Astronautics, 31st Israel Annual Conference on Aviation and Astronautics 22 Feb. 1990 p 44-50 Previously announced in IAA as A91-43082 (For primary document see N92-31861 22-01)
Avail: CASI HC A02/MF A03

07 AIRCRAFT PROPULSION AND POWER

Includes prime propulsion systems and systems components, e.g., gas turbine engines and compressors; and onboard auxilliary power plants for aircraft.

For related information see also *20 Spacecraft Propulsion and Power, 28 Propellants and Fuels,* and *44 Energy Production and Conversion.*

N92-31250*# National Aeronautics and Space Administration. Lewis Research Center, Cleveland, OH.

NASA. LEWIS RESEARCH CENTER SUPERSONIC THROUGHFLOW FAN PROGRAM

Royce D. Moore, Daniel L. Tweedt, and Rodrick V. Chima 1990 17 p Presented at the 1990 JANNAF Propulsion Meeting, Anaheim, CA, 3-5 Oct. 1990

(RTOP 505-62-61)

(NASA-TM-103248; E-5675; NAS 1.15:103248) Avail: CASI HC A03/MF A01

Recent studies have indicated the need for a commercial supersonic transport which can cruise at Mach 2 to 3. Various propulsion systems to power this new generation transport were examined and include supersonic throughflow fan engines which show the largest potential payoff. This concept also shows advantages for other types of aircraft including fighters. Another potential application of the supersonic throughflow fan is its use in conjunction with an air turboramjet engine. A fan that can operate with supersonic inlet Mach numbers would reduce the inlet losses incurred in diffusing the flow from supersonic to subsonic velocities at the fan face. In addition, the size and weight of an all-supersonic inlet will be substantially lower than that of a conventional inlet. In order to furnish the required information for assessing the potential for this type of fan, NASA-Lewis began a program to design, analyze, build, and test a fan stage that is capable of operation with supersonic axial velocities from inlet to exit. The objectives of this program are to demonstrate the feasibility and potential of supersonic throughflow fans, to gain a fundamental understanding of the flow physics associated with such systems, and to develop an experimental data base for design and analysis code validation. An overview is presented of the NASA-Lewis supersonic throughflow fan program. The fan's aerodynamic design is summarized and some results from initial testing of a proof-of-concept supersonic throughflow fan are discussed. Finally, the experimental results are compared with those calculated from two viscous codes. Author

N92-31275*# National Aeronautics and Space Administration. Hugh L. Dryden Flight Research Facility, Edwards, CA.

SUBSONIC FLIGHT TEST EVALUATION OF A PERFORMANCE SEEKING CONTROL ALGORITHM ON AN F-15 AIRPLANE

Glenn B. Gilyard and John S. Orme Aug. 1992 20 p Presented at the 28th AIAA/SAE/ASME/ASEE Joint Propulsion Conference, Nashville, TN, 6-8 Jul. 1992

(RTOP 533-02-36)

(NASA-TM-4400; H-1808; NAS 1.15:4400) Avail: CASI HC A03/MF A01

The subsonic flight test evaluation phase of the NASA F-15 (powered by F 100 engines) performance seeking control program was completed for single-engine operation at part- and military-power settings. The subsonic performance seeking control algorithm optimizes the quasi-steady-state performance of the propulsion system for three modes of operation. The minimum fuel flow mode minimizes fuel consumption. The minimum thrust mode maximizes thrust at military power. Decreases in thrust-specific fuel consumption of 1 to 2 percent were measured in the minimum fuel flow mode; these fuel savings are significant, especially for supersonic cruise aircraft. Decreases of up to approximately 100 degree R in fan turbine inlet temperature were measured in the minimum temperature mode. Temperature reductions of this magnitude would more than double turbine life if inlet temperature was the only life factor. Measured thrust increases of up to approximately 15 percent in the maximum thrust mode cause substantial increases in aircraft acceleration. The system dynamics of the closed-loop algorithm operation were good. The subsonic flight phase has validated the performance seeking control technology, which can significantly benefit the next generation of fighter and transport aircraft. Author

N92-31439# Aeronautical Research Labs., Melbourne (Australia).

RESEARCH INTO IMPROVING THE DURABILITY OF THE HOT SECTION IN THE AIRCRAFT TURBINE ENGINE

N. S. Swansson Dec. 1991 24 p

(AD-A250342; ARL-PROP-TM-473; DODA-AR-006-651) Avail: CASI HC A03/MF A01

Propulsion Branch at ARL is reviewing the direction of its research activities into the integrity, durability, and life extension of aircraft turbine engine components. Hot section repairs dominate the costs of engine overhaul, so resources are being redeployed from other programs on life of engine components toward this area of high potential benefit. Engine hot section life is an area of great complexity and wide scope. Despite the technical difficulties and limits in resources, the branch can make a useful contribution with carefully selected research. New proposed areas or extensions are structural analysis of high temperature components under cycles of thermal loading, and thermal analysis of components to determine temperature distribution which characterizes the thermomechanical loading. While structural analysis can build upon existing related expertise, little experience exists in thermal analysis and its core discipline of heat transfer, so a program to build up this technology base is proposed and options are examined. GRA

N92-31534*# United Technologies Corp., East Hartford, CT.

LIFE PREDICTION AND CONSTITUTIVE MODELS FOR ENGINE HOT SECTION ANISOTROPIC MATERIALS PROGRAM Interim Report

D. M. Nissley and T. G. Meyer Aug. 1992 177 p

(Contract NAS3-23939)

(NASA-CR-189222; NAS 1.26:189222; PWA-5968-80) Avail: CASI HC A09/MF A02

This report presents the results from a 35 month period of a program designed to develop generic constitutive and life prediction approaches and models for nickel-based single crystal gas turbine airfoils. The program is composed of a base program and an optional program. The base program addresses the high temperature coated single crystal regime above the airfoil root platform. The optional program investigates the low temperature uncoated single crystal regime below the airfoil root platform including the notched conditions of the airfoil attachment. Both base and option programs involve experimental and analytical efforts. Results from uniaxial constitutive and fatigue life experiments of coated and uncoated PWA 1480 single crystal material form the basis for the analytical modeling effort. Four single crystal primary orientations were used in the experiments: (001), (011), (111), and (213). Specific secondary orientations were also selected for the notched experiments in the optional program. Constitutive models for an overlay coating and PWA 1480 single crystal material were developed based on isothermal hysteresis loop data and verified using thermomechanical (TMF) hysteresis loop data. A fatigue life approach and life models were selected for TMF crack initiation of coated PWA 1480. An initial life model used to correlate smooth and notched fatigue data obtained in the option program shows promise. Computer software incorporating the overlay coating and PWA 1480 constitutive models was developed. Author

N92-31817# Los Alamos National Lab., NM.

ANALYTICAL AND EXPERIMENTAL STUDIES OF HEAT PIPE RADIATION COOLING OF HYPERSONIC PROPULSION SYSTEMS

R. A. Martin, M. A. Merrigan, M. G. Elder, J. T. Sena, E. S. Keddy, and C. C. Silverstein (CCS Associates, Bethel Park, PA.) 1992 7 p Presented at the 28th Joint Propulsion Conference, Nashville, TN, 6-8 Jul. 1992

(Contract W-7405-eng-36)
(DE92-013428; LA-UR-92-1390; CONF-920747-2) Avail: CASI HC A02/MF A01

Preliminary, research-oriented, analytical and experimental studies were completed to assess the feasibility of using high-temperature heat pipes to cool hypersonic engine components. This new approach involves using heat pipes to transport heat away from the combustor, nozzle, or inlet regions, and to reject it to the environment by thermal radiation from an external heat pipe nacelle. For propulsion systems using heat pipe radiation cooling (HPRC), it is possible to continue to use hydrocarbon fuels into the Mach 4 to Mach 6 speed range, thereby enhancing the economic attractiveness of commercial or military hypersonic flight. In the second-phase feasibility program recently completed, we found that heat loads produced by considering both convection and radiation heat transfer from the combustion gas can be handled with HPRC design modifications. The application of thermal insulation to ramburner and nozzle walls was also found to reduce the heat load by about one-half and to reduce peak HPRC system temperatures to below 2700 F. In addition, the operation of HPRC at cruise conditions of around Mach 4.5 and at an altitude of 90,000 ft lowers peak hot section temperatures to around 2800 F. An HPRC heat pipe was successfully fabricated and tested at Mach 5 conditions of heat flux, heat load, and temperature. DOE

N92-31910*# Massachusetts Inst. of Tech., Cambridge. Gas Turbine Lab.
TURBINE BLADE TIP AND SEAL CLEARANCE EXCITATION FORCES
M. Martinez-Sanchez and B. Jaroux 27 May 1992 372 p
(Contract NAS8-35018)
(NASA-CR-184341; NAS 1.26:184341) Avail: CASI HC A16/MF A03

Experimental and theoretical work done as Phase 3 of a program sponsored by MSFC to investigate the magnitude, origin, and parametric variations of destabilizing forces which arise in high power turbines due to blade-tip leakage effects are described. The two facilities which were built for this purpose are first described. The larger one is a closed, 2 atm pressurized Freon-12 flow loop in which is installed a 1:1 replica of the SSME first stage hydrogen turbine, which can be driven by the flow, and which generates about 14 KW of power into a load-absorbing DC generator. The smaller facility is used to measure the forces on labyrinth seals of the same type as those used in our turbine tests with a shrouded turbine. The seals can be kinematically whirled and spun (independently), and the inlet swirl can be set to a variety of values. Air is the working fluid (with atmospheric discharge) and the data are real-time pressure distributions in the seal glands. The five different unshrouded turbine configurations were tested with static offsets, plus one with a shroud band and a two-ridge seal. Theoretical models of various degrees of complexity were developed to help interpreting and extrapolating the data. The notion of partial work done by the fluid leaking through the tip gaps was put on a quantitative basis by examining the leakage vortex roll-up dynamics. This was used to obtain a theory of the work loss due to a uniform gap. Perturbation and multiple scale arguments were then used to extend this to the case of an eccentric turbine. This yields an unsteady, 3-D theory which can predict the distribution of the approach flow, and its effect on work defect, cross-forces, pressure patterns, and dynamic damping. The predictions agree qualitatively with the data and exhibit the correct trends, but the cross-forces are generally under-predicted. Author

N92-32059# Purdue Univ., West Lafayette, IN. School of Mechanical Engineering.
RESEARCH ON AERO-THERMODYNAMIC DISTORTION INDUCED STRUCTURAL DYNAMIC RESPONSE OF MULTISTAGE COMPRESSOR BLADING Final Report, Nov. 1987 - May 1991
Sanford Fleeter Mar. 1992 220 p
(Contract F49620-88-C-0022)
(AD-A250865; TSPC-TR-92-10; AFOSR-92-0403TR) Avail: CASI HC A10/MF A03

The overall objective of this basic research program was the quantitative investigation of the fundamental phenomena relevant to aerothermodynamic distortion-induced structural dynamic blade responses in multistage gas turbine engines. The technical approach involved unique benchmark experiments and analyses. In particular, the flow physics of multistage blade row interactions were investigated, with unique unsteady aerodynamic data obtained and analyses developed to understand, quantify, and discriminate the fundamental flow phenomena as well as to direct the modeling of advanced analyses. Data obtained define the flow interactions and the effects on both the aerodynamic forcing function and the resulting unsteady aerodynamics of compressor rotor blades and stator vanes in a multistage environment over a wide range of realistic reduced frequency values for the first time. GRA

N92-31870# Rafael Armament Development Authority, Haifa (Israel).
SIZING SUPERSONIC FREEJET NOZZLE AND INLET LOCATION FOR SIMULATION OF THE TRANSITION PHASE IN INTEGRAL ROCKET RAMJET
I. Greenberg and E. Shokron (Israel Aircraft Industries Ltd., Lod.) *In* Israel Society of Aeronautics and Astronautics, 31st Israel Annual Conference on Aviation and Astronautics 22 Feb. 1990 p 62-65 Previously announced in IAA as A91-43084 (For primary document see N92-31861 22-01)
Avail: CASI HC A01/MF A03

N92-31871# Naval Weapons Center, China Lake, CA. Research Dept.
EFFECT OF INLET GEOMETRY ON THE FLOW AND COMBUSTION PROCESSES IN A SOLID FUEL RAMJET
K. J. Wilson, K. C. Schadow, E. Gutmark, P. A. O. G. Korting (Prins Maurits Lab. TNO, Rijswijk, Netherlands), and F. Dijkstra (Technische Hogeschool, Delft, Netherlands) *In* Israel Society of Aeronautics and Astronautics, 31st Israel Annual Conference on Aviation and Astronautics 22 Feb. 1990 p 66-72 Previously announced in IAA as A91-43085 (For primary document see N92-31861 22-01)
Avail: CASI HC A02/MF A03

08 AIRCRAFT STABILITY AND CONTROL

Includes aircraft handling qualities; piloting; flight controls; and autopilots.

For related information see also *05 Aircraft Design, Testing and Performance.*

N92-31240*# National Aeronautics and Space Administration. Langley Research Center, Hampton, VA.
DESIGN AND EXPERIMENTAL VALIDATION OF A FLUTTER SUPPRESSION CONTROLLER FOR THE ACTIVE FLEXIBLE WING
Martin R. Waszak and S. Srinathkumar (National Aeronautical Lab., Bangalore, India) Aug. 1992 19 p
(RTOP 505-64-20-01)
(NASA-TM-4381; L-16977; NAS 1.15:4381) Avail: CASI HC A03/MF A01

The synthesis and experimental validation of an active flutter suppression controller for the Active Flexible Wing wind tunnel model is presented. The design is accomplished with traditional root locus and Nyquist methods using interactive computer graphics tools and extensive simulation based analysis. The design approach uses a fundamental understanding of the flutter mechanism to formulate a simple controller structure to meet stringent design specifications. Experimentally, the flutter suppression controller succeeded in simultaneous suppression of two flutter modes, significantly increasing the flutter dynamic pressure despite modeling errors in predicted flutter dynamic pressure and flutter

frequency. The flutter suppression controller was also successfully operated in combination with another controller to perform flutter suppression during rapid rolling maneuvers. Author

N92-31656*# Douglas Aircraft Co., Inc., Long Beach, CA.
DESIGN AND ANALYSIS ISSUES OF INTEGRATED CONTROL SYSTEMS FOR HIGH-SPEED CIVIL TRANSPORTS Final Report
Craig A. McCarty, John B. Feather, John R. Dykman, Mark A. Page, and John Hodgkinson Washington NASA May 1992 73 p Prepared for PRC Kentron, Inc., Edwards, CA
(Contracts NAS2-12722; ATD-91-DAC-7103)
(NASA-CR-186022; H-1787; NAS 1.26:186022) Avail: CASI HC A04/MF A01

A study was conducted to identify, rank, and define development plans for the critical guidance and control design and analysis issues as related to economically viable and environmentally acceptable high-speed civil transport. The issues were identified in a multistep process. First, pertinent literature on supersonic cruise aircraft was reviewed, and experts were consulted to establish the fundamental characteristics and problems inherent to supersonic cruise aircraft. Next, the advanced technologies and strategies being pursued for the high-speed civil transport were considered to determine any additional unique control problems the transport may have. Finally, existing technologies and methods were examined to determine their capabilities for the design and analysis of high-speed civil transport control systems and to identify the shortcomings and issues. Three priority levels - mandatory, highly beneficial, and desirable - were established. Within each of these levels, the issues were further ranked. Technology development plans for each issue were defined. Each plan contains a task breakdown and schedule. Author

N92-31966# Virginia Polytechnic Inst. and State Univ., Blacksburg. Dept. of Mathematics.
AN INTEGRATED RESEARCH PROGRAM FOR THE MODELING, ANALYSIS AND CONTROL OF AEROSPACE SYSTEMS Final Report, 31 Aug. 1987 - 30 Sep. 1991
J. A. Burns, E. M. Cliff, and T. L. Herdman 3 Mar. 1992 30 p
(Grant AF-AFOSR-0292-92)
(AD-A250199; AFOSR-92-0292TR) Avail: CASI HC A03/MF A01

The following is a summary list of accomplishments under this contract: (1) ICAM was established in August of 1987; (2) an interactive computer system was developed; (3) over 85 research papers were produced; (4) over 33 students were supported in part by the contract; (5) more than 12 PhD's and 5 MS students were produced; (6) seven Post Doctoral Associates were supported; (7) more than 65 short term visitors came to Virginia Tech (16 of these were long term visitors); and (8) over 100 scientists attended the conference on numerical methods for partial differential equations. GRA

N92-31967# Stanford Univ., CA. Dept. of Mechanical Engineering.
MATHEMATICAL MODELING AND NUMERICAL SIMULATION OF THE DYNAMICS OF FLEXIBLE STRUCTURES UNDERGOING LARGE OVERALL MOTIONS Final Report, 15 Feb. 1989 - 14 May 1991
J. C. Simo 14 May 1991 11 p
(Grant AF-AFOSR-0294-89)
(AD-A250202; AFOSR-92-0287TR) Avail: CASI HC A03/MF A01

A multidisciplinary effort aimed at the development of analytical and computational tools for the modeling and simulation of very flexible structures is reported. This research is concerned with three main areas: (1) mathematical aspects with special emphasis on nonlinear stability analysis; (2) modeling aspects with emphasis in very flexible slender structures; and (3) numerical analysis aspects with emphasis on methodologies suitable for large scale and accurate simulation. The present research effort has resulted in 36 publications, two conferences, and a strong collaboration (in a related research effort also sponsored by AFOSR) with groups at UC Berkeley and University of Maryland. GRA

N92-32175*# Boeing Commercial Airplane Co., Seattle, WA.
ENGINE MONITORING DISPLAY STUDY Final Report
Mary E. Hornsby Washington NASA. Langley Research Center Aug. 1992 96 p
(Contract NAS1-18027; RTOP 505-66-41-04)
(NASA-CR-4463; NAS 1.26:4463) Avail: CASI HC A05/MF A01

The current study is part of a larger NASA effort to develop displays for an engine-monitoring system to enable the crew to monitor engine parameter trends more effectively. The objective was to evaluate the operational utility of adding three types of information to the basic Boeing Engine Indicating and Crew Alerting System (EICAS) display formats: alphanumeric alerting messages for engine parameters whose values exceed caution or warning limits; alphanumeric messages to monitor engine parameters that deviate from expected values; and a graphic depiction of the range of expected values for current conditions. Ten training and line pilots each flew 15 simulated flight scenarios with five variants of the basic EICAS format; these variants included different combinations of the added information. The pilots detected engine problems more quickly when engine alerting messages were included in the display; adding a graphic depiction of the range of expected values did not affect detection speed. The pilots rated both types of alphanumeric messages (alert and monitor parameter) as more useful and easier to interpret than the graphic depiction. Integrating engine parameter messages into the EICAS alerting system appears to be both useful and preferred. Author

N92-32241*# National Aeronautics and Space Administration. Lewis Research Center, Cleveland, OH.
A PARAMETER OPTIMIZATION APPROACH TO CONTROLLER PARTITIONING FOR INTEGRATED FLIGHT/PROPULSION CONTROL APPLICATION
Phillip Schmidt (Akron Univ., OH.), Sanjay Garg, and Brian Holowecky (Akron Univ., OH.) Aug. 1992 30 p
(RTOP 505-62-50)
(NASA-TM-105826; E-7260; NAS 1.15:105826) Avail: CASI HC A03/MF A01

A parameter optimization framework is presented to solve the problem of partitioning a centralized controller into a decentralized hierarchical structure suitable for integrated flight/propulsion control implementation. The controller partitioning problem is briefly discussed and a cost function to be minimized is formulated, such that the resulting 'optimal' partitioned subsystem controllers will closely match the performance (including robustness) properties of the closed-loop system with the centralized controller while maintaining the desired controller partitioning structure. The cost function is written in terms of parameters in a state-space representation of the partitioned sub-controllers. Analytical expressions are obtained for the gradient of this cost function with respect to parameters, and an optimization algorithm is developed using modern computer-aided control design and analysis software. The capabilities of the algorithm are demonstrated by application to partitioned integrated flight/propulsion control design for a modern fighter aircraft in the short approach to landing task. The partitioning optimization is shown to lead to reduced-order subcontrollers that match the closed-loop command tracking and decoupling performance achieved by a high-order centralized controller. Author

N92-31865# Technion - Israel Inst. of Tech., Haifa. Faculty of Aerospace Engineering.
A SIMULATION MODEL OF A SINGLE ROTOR HELICOPTER
Z. Beigelman and A. Rosen *In* Israel Society of Aeronautics and Astronautics, 31st Israel Annual Conference on Aviation and Astronautics 22 Feb. 1990 p 27-37 Previously announced in IAA as A91-43080 (For primary document see N92-31861 22-01)
Avail: CASI HC A03/MF A03

N92-31879# Rafael Armament Development Authority, Haifa (Israel).
DISCRETE OPTIMAL GUIDANCE FOR HIGH ORDER MISSILE AND MANEUVERING TARGET
Ilan Rusnak *In* Israel Society of Aeronautics and Astronautics, 31st Israel Annual Conference on Aviation and Astronautics 22 Feb. 1990 p 127-131 Previously announced in IAA as A91-43093 (For primary document see N92-31861 22-01)
Avail: CASI HC A01/MF A03

09 RESEARCH AND SUPPORT FACILITIES (AIR)

Includes airports, hangars and runways; aircraft repair and overhaul facilities; wind tunnels; shock tubes; and aircraft engine test stands.

For related information see also *14 Ground Support Systems and Facilities (Space).*

N92-31252*# Rochester Inst. of Tech., NY. Center for Imaging Science.
DIGITAL ANALYSIS OF WIND TUNNEL IMAGERY TO MEASURE FLUID THICKNESS Final Report
Roger L. Easton, Jr. and James Enge Aug. 1992 41 p Original contains color illustrations
(Grant NAG3-1202)
(NASA-CR-189234; NAS 1.26:189234) Avail: CASI HC A03/MF A01; 1 functional color page

Documented here are the procedure and results obtained from the application of digital image processing techniques to the problem of measuring the thickness of a deicing fluid on a model airfoil during simulated takeoffs. The fluid contained a fluorescent dye and the images were recorded under flash illumination on photographic film. The films were digitized and analyzed on a personal computer to obtain maps of the fluid thickness. Author

N92-31640*# National Aeronautics and Space Administration. Lewis Research Center, Cleveland, OH.
SUPERSONIC THROUGHFLOW FAN TEST FACILITY AT NASA. LEWIS RESEARCH CENTER
Donald C. Urasek, Walter S. Cunnan, Richard L. Lantz, Dennis L. Fronek, Ronald A. Dawson, and Jeffrey C. Brown Sep. 1990 25 p
(RTOP 505-62-61)
(NASA-TP-3038; E-5398; NAS 1.60:3038) Avail: CASI HC A03/MF A01

The increased need for efficient supersonic flight has revived interest in supersonic throughflow fans for advanced high-speed propulsion systems. NASA LeRC recently began a program to design, build, and test a single-stage fan that will operate with supersonic air velocity sustained through the blade rows. In a major revamping of the LeRC Multistage Compressor Facility, NASA has built a 20 in. diameter annular wind tunnel with a 0.7 hub-to-tip ratio. The wind tunnel houses a high-speed rotating fan package. The objectives of this research program are to demonstrate feasibility, to gain an understanding of the flow physics, and to create a data base. The facility, test package, and instrumentation for supporting the operation of the supersonic throughflow fan program are described. Author

N92-31900*# National Aeronautics and Space Administration. Langley Research Center, Hampton, VA.
DATA REDUCTION FORMULAS FOR THE 16-FOOT TRANSONIC TUNNEL: NASA LANGLEY RESEARCH CENTER, REVISION 2
Charles E. Mercer, Bobby L. Berrier, Francis J. Capone, and Alan M. Grayston (Wyle Labs., Inc., Hampton, VA.) Jul. 1992 288 p Revised Supersedes NASA-TM-86319, revision 1
(RTOP 505-62-30-01)
(NASA-TM-107646; NAS 1.15:107646) Avail: CASI HC A13/MF A03

The equations used by the 16-Foot Transonic Wind Tunnel in the data reduction programs are presented in nine modules. Each module consists of equations necessary to achieve a specific purpose. These modules are categorized in the following groups: (1) tunnel parameters; (2) jet exhaust measurements; (3) skin friction drag; (4) balance loads and model attitudes calculations; (5) internal drag (or exit-flow distribution); (6) pressure coefficients and integrated forces; (7) thrust removal options; (8) turboprop options; and (9) inlet distortion. Author

N92-32026# Los Alamos National Lab., NM.
PROBLEMS ASSOCIATED WITH LAUNCHING HYPERVELOCITY PROJECTILES FROM THE FAST SHOCK TUBE
J. F. Kerrisk and J. K. Meier 1992 23 p
(Contract W-7405-eng-36)
(DE92-015276; LA-UR-92-1529) Avail: CASI HC A03/MF A01

Modeling and experiments are being done with the goal of understanding the physics of projectile acceleration at high driving pressures (megabar range) and short acceleration times (a few microseconds) well enough to design and test successful hypervelocity launch systems. The Fast Shock Tube, a cylindrically convergent high-explosive driver, has been used to accelerate projectiles. Detailed modeling of the experiments, including high-pressure gas flow, projectile instability, and projectile fracture, has been done with MESA/2D. Modeling results show quantitative agreement with the average behavior of the system. However, details of projectile behavior are not predicted well. Observed velocity distributions across the diameter of a projectile or projectile shapes are only in qualitative agreement with calculations. This, then, presents the major constraint on the successful design of a launch system: that the processes that limit projectile integrity depend on the details of the drive conditions, and these details are not quantitatively modeled at this time. DOE

N92-32201*# National Aeronautics and Space Administration. Hugh L. Dryden Flight Research Facility, Edwards, CA.
SYSTEM OVERVIEW OF THE NASA DRYDEN INTEGRATED TEST FACILITY
Robert L. Binkley and Dale Mackall Aug. 1992 12 p Presented at the Society of Flight Test Engineers 23rd Annual Symposium, Hauppage, NY, Aug. 1992
(RTOP 505-68-27)
(NASA-TM-104250; H-1831; NAS 1.15:104250) Avail: CASI HC A03/MF A01

The Integrated Test Facility, built at the NASA Dryden Flight Research Facility, provides new real-time test capabilities for emerging research aircraft. An overview of the test facility and the real-time systems developed to operate this unique facility is presented. The facility will reduce flight test risk by minimizing the difference between the flight and ground test environments. This ground test environment is provided by combining real-time flight simulation with the actual aircraft. A brief introduction to the facility is followed by a discussion of the generic capabilities of its real-time systems. The simulation system with flight hardware and the remotely augmented vehicle system is described. An overview of many hardware systems developed for the facility follows. The benefits of applying simulation to hardware-in-the-loop testing on the X-31 Flight Research Program are presented. Author

12 ASTRONAUTICS (GENERAL)

For extraterrestrial exploration see *91 Lunar and Planetary Exploration.*

N92-31634*# National Aeronautics and Space Administration, Washington, DC.
INTEGRATED TECHNOLOGY PLAN FOR THE CIVIL SPACE PROGRAM, 1991
1991 137 p
(PB92-181692) Avail: CASI HC A07/MF A02

The purpose of the Integrated Technology Plan (ITP) is to serve as a strategic plan for the OAST space research and

technology (R&T) program, and as a strategic planning framework for other NASA and national participants in advocating and conducting technology developments that support future U.S. civil space missions. The ITP begins with a discussion of the national policy and NASA organization which establishes the overall framework for civil space R&T planning. The second chapter provides a top-level review of the potential users of civil space R&T, their strategic mission plans, and the technologies they have identified as needed to achieve those plans. The overall methodology used to develop a civil space technology strategy is discussed. The technical details of the 1991 strategic plan are described, ending with a review of civil space R&T priorities. The fourth chapter describes how the strategic plan is annually translated into the OAST Space R&T Program, with a summary of the fiscal year 1992 program. The ITP concludes with a discussion of requirements for technology development coordination and strategies for facilitating the transfer of civil space technology to the private sector. Several appendices also are attached that provide further information regarding budget implications of the strategic plan, organizational roles, and other topics. Author

N92-32009 Huntsville Association of Technical Societies, AL.
TABES 92: 8TH ANNUAL TECHNICAL AND BUSINESS EXHIBITION AND SYMPOSIUM. EXECUTIVE SUMMARIES AND SUBMITTED PAPERS
1992 201 p Symposium held in Huntsville, AL, 12-13 May 1992
Copyright Avail: Issuing Activity

The Small Space Missions sessions presented some relatively inexpensive alternatives to current mission approaches. The alternatives discussed included: robotic, low orbit missions; a permanent return to the moon and then on to Mars with manned missions; and interplanetary exploration. The Space Technologies sessions discussed speedier vehicles, complex research, needs for efficient and exotic fuels and structures materials, and the need for multi-language abilities for joint international missions. For individual titles, see N92-32010 through N92-32021.

N92-32010 Cynetics Corp., Rapid City, SD.
ADVANCES IN SMALL SATELLITE COMMUNICATION SYSTEMS **c18**
Don K. Lefevre *In* Huntsville Association of Technical Societies, TABES 92: 8th Annual Technical and Business Exhibition and Symposium. Executive Summaries and Submitted Papers 1992 8 p (For primary document see N92-32009 22-12)
(TABES Paper 92-411) Copyright Avail: Issuing Activity

The recent interest in small satellites has produced many exciting new proposals for these systems. However, small satellite communication systems have unique constraints when compared to large geostationary systems. These constraints often include the following: (1) very limited available power; (2) lower data rates; (3) relatively large Doppler shifts for low-earth orbit (LEO) satellites; and (4) uncertain frequency allocations. Author

N92-32011* National Aeronautics and Space Administration. Marshall Space Flight Center, Huntsville, AL.
SPACECRAFT STABILITY AND CONTROL **c18**
Chris Barret *In* Huntsville Association of Technical Societies, TABES 92: 8th Annual Technical and Business Exhibition and Symposium. Executive Summaries and Submitted Papers 1992 9 p (For primary document see N92-32009 22-12)
(TABES Paper 92-414) Copyright Avail: Issuing Activity

The Earth's first artificial satellite, Sputnik 1, slowly tumbled in orbit. The first U.S. satellite, Explorer 1, also tumbled out of control. Today, satellite stability and control has become a higher priority. For a satellite design that is to have a life expectancy of 14 years, appropriate spacecraft flight control systems will be reviewed, stability requirements investigated, and an appropriate flight control system recommended in order to see the design process. Disturbance torques, including aerodynamic, magnetic, gravity gradient, solar, micrometeorite, debris, collision, and internal torques, will be assessed to quantify the disturbance environment so that the required compensating torques can be determined. The control torques, including passive versus active, momentum control, bias momentum, spin stabilization, dual spin, gravity gradient, magnetic, reaction wheels, control moment gyros, inertia augmentation techniques, three-axis control, and reaction control systems (RCSs), will be considered. Conditions for stability will also be considered. Author

N92-32012 Essex Corp., Columbia, MD.
OPTICAL PROCESSING ARCHITECTURES FOR SPACEBORNE SAR IMAGE GENERATION AND RF ARRAY BEAM FORMING **c74**
Terry M. Turpin, Leslie H. Gesell, and James L. Lafuse *In* Huntsville Association of Technical Societies, TABES 92: 8th Annual Technical and Business Exhibition and Symposium. Executive Summaries and Submitted Papers 1992 7 p (For primary document see N92-32009 22-12)
(TABES Paper 92-444) Copyright Avail: Issuing Activity

The extremely high computing performance obtainable with optical processors, as well as their inherently small size, make them especially applicable to spaceborne applications where size, weight, and power constraints are severe. Essex has developed and patented optical computing systems that are applicable to a number of spaceborne applications. These include an optical processor for generating images from spaceborne synthetic aperture radar (SAR) for remote sensing applications, and an optical processor for RF array beam forming applicable for COMSAT and spacebased radar. This paper will focus on these processors as well as the potential for other spaceborne optical computing applications. Author

N92-32013 Rockwell International Corp., Downey, CA. Space Systems Div.
ROBOTICS DEVELOPMENT FOR THE ENHANCEMENT OF SPACE ENDEAVORS **c37**
A. J. Mauceri and Margaret M. Clarke *In* Huntsville Association of Technical Societies, TABES 92: 8th Annual Technical and Business Exhibition and Symposium. Executive Summaries and Submitted Papers 1992 5 p (For primary document see N92-32009 22-12)
(TABES Paper 92-445) Copyright Avail: Issuing Activity

Telerobotics and robotics development activities to support NASA's goal of increasing opportunities in space commercialization and exploration are described. The Rockwell International activities center is using robotics to improve efficiency and safety in three related areas: remote control of autonomous systems, automated nondestructive evaluation of aspects of vehicle integrity, and the use of robotics in space vehicle ground reprocessing operations. In the first area, autonomous robotic control, Rockwell is using the control architecture, NASREM, as the foundation for the high level command of robotic tasks. In the second area, we have demonstrated the use of nondestructive evaluation (using acoustic excitation and lasers sensors) to evaluate the integrity of space vehicle surface material bonds, using Orbiter 102 as the test case. In the third area, Rockwell is building an automated version of the present manual tool used for Space Shuttle surface tile re-waterproofing. The tool will be integrated into an orbiter processing robot being developed by a KSC-led team. Author

N92-32014 Alabama Univ., Huntsville. Atmospheric Science Program.
THE UNCERTAINTIES OF GLOBAL TEMPERATURES IN THE GLOBAL WARMING CONTEXT **c45**
John R. Christy *In* Huntsville Association of Technical Societies, TABES 92: 8th Annual Technical and Business Exhibition and Symposium. Executive Summaries and Submitted Papers 1992 7 p (For primary document see N92-32009 22-12)
(TABES Paper 92-447) Copyright Avail: Issuing Activity

Long-term surface temperature records have large enough uncertainties and contain enough uncertainties and contain enough natural variability that conclusions about global warming due to greenhouse gas emissions are not possible based on these data. Comparison with newly developed data from satellites indicates the surface temperatures measured today do not provide the

accuracy necessary for assessing climate trends for over half of the globe. Though warm and cool years generally coincide between satellite and surface measurements, the subtle differences are sufficient to cause one to rethink the conclusions of excessive warmth of the past two years (1990-91) and decade. Author

N92-32015 Nissho Iwai Corp., Tokyo (Japan).
THE TRADING COMPANY IN SPACE DEVELOPMENT IN JAPAN
Toshi N. Gonda *In* Huntsville Association of Technical Societies, TABES 92: 8th Annual Technical and Business Exhibition and Symposium. Executive Summaries and Submitted Papers 1992 6 p (For primary document see N92-32009 22-12)
(TABES Paper 92-424) Copyright Avail: Issuing Activity

Trading companies have a unique status in the Japanese market and a really deep involvement in Japanese trade. They are also involved in space development and the space industry as well. An overview of trading companies activities and, more specifically, a way of involving them more in the space industry are presented. The activities of Nissho Iwai Corporation, one of the Sogo Shosha, are described in detail. Their activities in the space industry have two aspects, one is social and the other is commercial. They have been stimulating space projects in these aspects. There are several international cooperative space projects between Japan and the U.S. These projects are proceeding on a government to government basis. But, it is worthwhile to realize that the Sogo Shosha may create trade flow through increased international space cooperation in the private sector. Author

N92-32016 Italian Space Agency, Rome.
SPACE STATION MINI PRESSURISED LOGISTICS MODULES: AN OPPORTUNITY TO ENLARGE AND REINFORCE INTERNATIONAL COOPERATION **c18**
Luciano Guerriero and Ernesto Vallerani *In* Huntsville Association of Technical Societies, TABES 92: 8th Annual Technical and Business Exhibition and Symposium. Executive Summaries and Submitted Papers 1992 7 p Prepared in cooperation with Alenia Spazio S.p.A., Rome, Italy (For primary document see N92-32009 22-12)
(TABES Paper 92-425) Copyright Avail: Issuing Activity

Italy will provide two Mini Pressurized Logistics Modules to NASA as part of its contribution to the Space Station Freedom program. The development of the pressurized modules will support access to the Space Station during its development phases and will assure maintenance of the Space Station later on. Furthermore, the pressurized modules will constitute a first step in providing a logistics system to support Columbus in orbit and a future European Space Station. The pressurized modules of the logistics system are essential elements of the entire complex system for the future expansion of space activities, including missions to the Moon and Mars. Author

N92-32017 Tennessee Univ. Space Inst., Tullahoma. Commercial Experiment Transporter Program.
COMET: COMMERCIAL SPACE OPPORTUNITIES THROUGH DEVELOPED TECHNOLOGIES **c81**
Carter H. Myers *In* Huntsville Association of Technical Societies, TABES 92: 8th Annual Technical and Business Exhibition and Symposium. Executive Summaries and Submitted Papers 1992 7 p (For primary document see N92-32009 22-12)
(TABES Paper 92-453) Copyright Avail: Issuing Activity

The Commercial Experiment Transporter (COMET) is a set of hardware and related infrastructure used to support orbital experiments of the Commercial Centers for the Development of Space (CCDS) and their industrial partners. The COMET program was established as the cutting edge of the U.S. Space Commercialization efforts. The COMET program takes off-the-shelf equipment, integrates the pieces, and offers access to space for scientific experimentation at reduced cost. Described here is the COMET vehicle, where off-the-shelf hardware was used, and where new designs were developed. An update on the program status is given. Author

N92-32018 McDonnell-Douglas Corp., Huntsville, AL. SPACEHAB Program.
SPACEHAB: A GIANT STEP IN THE COMMERCIAL DEVELOPMENT OF SPACE **c18**
James E. Shepard *In* Huntsville Association of Technical Societies, TABES 92: 8th Annual Technical and Business Exhibition and Symposium. Executive Summaries and Submitted Papers 1992 7 p (For primary document see N92-32009 22-12)
(TABES Paper 92-454) Copyright Avail: Issuing Activity

SPACEHAB is a privately developed and operated system offering customers a crew-tended microgravity environment for experimentation and product development. The first SPACEHAB flight module was delivered to the SPACEHAB Payload Processing Facility (SPPF) in Florida and 22 experiments are being integrated for an April 1993 mission. SPACEHAB modules are flown in the forward quarter-bay of the NASA Orbiter and are supported by two crew members. The paylaod accommodations include up to 61 experiment lockers, double and single racks and standard mounting plates for mounting unique payload containers directly to the module structure. Experiments designed for the Orbiter mid-deck, Spacelab or Space Station Freedom can be flown in SPACEHAB. The 24-month integration cycle is currently the shortest for any crew-tended carrier; a goal of 18 months is being actively pursued. Author

N92-32019 Alenia Spazio S.p.A., Turin (Italy).
ITALIAN-US COOPERATION IN SPACE: THE CASE OF TETHERED, IRIS/LAGEOS, AND SPACEHAB **c54**
Paolo Piantella *In* Huntsville Association of Technical Societies, TABES 92: 8th Annual Technical and Business Exhibition and Symposium. Executive Summaries and Submitted Papers 1992 21 p (For primary document see N92-32009 22-12)
(TABES Paper 92-467) Copyright Avail: Issuing Activity

Cooperation between the U.S. and Italy is discussed in three space missions: (1) the Tethered Satellite System; (2) the Italian Research Interim Stage (IRIS) launcher and Laser Geodynamic Satellite (LAGEOS) satellite; and (3) the SPACEHAB modules. Each of these programs is described in detail, including: project overview; instrumentation; objectives; and international cooperation to achieve goals. H.A.

N92-32020 Ocean Planet Odyssey, New York, NY.
ONE THOUSAND DAYS NON-STOP AT SEA: LESSONS FOR A MISSION TO MARS **c53**
Reid Stowe and Albert A. Harrison (California Univ., Davis.) *In* Huntsville Association of Technical Societies, TABES 92: 8th Annual Technical and Business Exhibition and Symposium. Executive Summaries and Submitted Papers 1992 14 p (For primary document see N92-32009 22-12)
(TABES Paper 92-462) Copyright Avail: Issuing Activity

Plans for the exploration and settlement of space include a manned mission to Mars in the early twenty-first century. Among the many issues that must be addressed prior to the departure of the first Mars crew, are those regarding crewmember adaptation to a three year mission. During fall of 1993, the schooner Anne, bearing a crew of six to eight members will undertake a 1000 day voyage without touching land or receiving supplies from another craft. The purpose of this expedition includes the evaluation of equipment, supplies, and humans under conditions of isolation and confinement that will resemble some of those of the initial Mars voyage. The present paper describes some of the psychological support and research activities planned for the three year mission and the schooner's value as a laboratory for life in space. Author

N92-32021 Army Strategic Defense Command, Huntsville, AL. GBR Project Office.
GROUND BASED RADAR **c32**
William W. Ryan *In* Huntsville Association of Technical Societies, TABES 92: 8th Annual Technical and Business Exhibition and Symposium. Executive Summaries and Submitted Papers 1992 7 p (For primary document see N92-32009 22-12)
(TABES Paper 92-213) Copyright Avail: Issuing Activity

The current state of turmoil in the world of ballistic missile technology dictates that the U.S. be prepared to deal with a growing ballistic missile threat. To meet this challenge the U.S. Army is developing a new family of ground based radar to support both the Theater Missile Defense and the Strategic Defense Initiatives. This class of radar provides affordable, reliable tracking and discrimination based on mature technology and commonality of design. The commonality of design concept uses technology and components that can be scaled in number, size, and capability. This approach allows ground based radar to support the near term requirements of both tactical and strategic defense and also provide flexibility for more sophisticated future threats. Author

N92-32148*# National Aeronautics and Space Administration. Marshall Space Flight Center, Huntsville, AL.
ANALYSIS OF DEBRIS FROM SPACELAB SPACE LIFE SCIENCES-1
S. V. Caruso, E. B. Rodgers, and T. L. Huff (Sverdrup Technology, Inc., Huntsville, AL.) Jul. 1992 90 p
(NASA-TM-103593; NAS 1.15:103593) Avail: CASI HC A05/MF A01

Airborne microbiological and particulate contamination generated aboard Spacelab modules is a potential safety hazard. In order to shed light on the characteristics of these contaminants, microbial and chemical/particulate analyses were performed on debris vacuumed from cabin and avionics air filters in the Space Life Sciences-1 (SLS-1) module of the Space Transportation System 40 (STS-40) mission 1 month after landing. The debris was sorted into categories (e.g., metal, nonmetal, hair/fur, synthetic fibers, food particles, insect fragments, etc.). Elemental analysis of particles was done by energy dispersive analysis of x rays (metals) and Fourier transform infrared spectroscopy (nonmetals). Scanning electron micrographs were done of most particles. Microbiological samples were grown on R2A culture medium and identified. Clothing fibers dominated the debris by volume. Other particles, all attributed to the crew, resulted from abrasions and impacts during missions operations (e.g., paint chips, plastic, electronic scraps and clothing fibers). All bacterial species identified are commonly found in the atmosphere or on the human body. Bacillus sp. was the most frequently seen bacterium. One of the bacterial species, Enterobacter agglomerans, could cause illness in crew members with depressed immune systems. Author

N92-32238# Lockheed Missiles and Space Co., Calabasas, CA.
NASA PROGRAMS
[1991] 25 p Original contains color illustrations
Avail: CASI HC A03/MF A01; 22 functional color pages

A brief, but comprehensive, overview is presented of Lockheed's participation in NASA space programs. A short description is combined with colorful illustrations describing specific projects in which Lockheed has participated. The NASA space programs discussed include the following: Mission to Planet Earth; Hubble Space Telescope; Space Station Freedom; Assured Crew Return Vehicle; Mars Cargo Transfer Vehicle; National Launch System; Stratospheric Observatory for Infrared Astronomy (SOFIA); Gravity Probe-B; and Space Infrared Telescope Facility. Technology transfer from NASA space programs to civilian use is also discussed. H.A.

13 ASTRODYNAMICS

Includes powered and free-flight trajectories; and orbital and launching dynamics.

N92-31685# National Aerospace Lab., Tokyo (Japan).
GPS SATELLITE ORBIT DETERMINATION USING PSEUDORANGE DATA: EXPERIMENTS AND RESULTS
M. Murata, T. Yamamoto, and Y. Hamada May 1991 20 p
(PB92-178870; NAL-TR-1110T) Avail: CASI HC A03/MF A01

A GPS orbit determination software system called Multi-Satellite Orbit Processor (MSPO) has been developed, and uses pseudorange data to determine accurate orbits for the GPS satellite constellation. Methods and strategies specific to the precise orbit determination of GPS satellites are described, with special emphasis placed on force modeling of the solar radiation pressure and y-bias. The orbit accuracy was evaluated from analysis of P-code pseudorange data collected by the Cooperative International GPS Network (CIGNET), being primarily based on a direct comparison with the precise ephemerides generated at the Naval Surface Warfare Center (NSWC). Methods leading to an orbit accuracy of better than 0.5 ppm were demonstrated. Author

14 GROUND SUPPORT SYSTEMS AND FACILITIES (SPACE)

Includes launch complexes, research and production facilities; ground support equipment, e.g., mobile transporters; and simulators.

For related information see also *09 Research and Support Facilities (Air).*

No abstracts in this category.

15 LAUNCH VEHICLES AND SPACE VEHICLES

Includes boosters; operating problems of launch/space vehicle systems; and reusable vehicles.

For related information see also *20 Spacecraft Propulsion and Power.*

N92-31251*# National Aeronautics and Space Administration. Lewis Research Center, Cleveland, OH.
GRAPHITE/EPOXY COMPOSITE ADAPTERS FOR THE SPACE SHUTTLE/CENTAUR VEHICLE
Harold J. Kasper and Darryl S. Ring (General Dynamics Corp., San Diego, CA.) Sep. 1990 34 p
(Contract NAS3-2290)
(NASA-TP-3014; E-4969; NAS 1.60:3014) Avail: CASI HC A03/MF A01

The decision to launch various NASA satellite and Air Force spacecraft from the Space Shuttle created the need for a high-energy upper stage capable of being deployed from the cargo bay. Two redesigned versions of the Centaur vehicle which employed a graphite/epoxy composite material for the forward and aft adapters were selected. Since this was the first time a graphite/epoxy material was used for Centaur major structural components, the development of the adapters was a major effort. An overview of the composite adapter designs, subcomponent design evaluation test results, and composite adapter test results from a full-scale vehicle structural test is presented. Author

N92-31542# Sandia National Labs., Albuquerque, NM.
SOLID-ARMATURE RAILGUNS WITHOUT THE VELOCITY-SKIN EFFECT
M. Cowan 1991 6 p Presented at the 6th Symposium on Electromagnetic Launch Technology, Austin, TX, 28-30 Apr. 1992
(Contract DE-AC04-76DP-00789)
(DE92-012630; SAND-91-2208C; CONF-9204102-8) Avail: CASI HC A02/MF A01

If the velocity-skin effect could be eliminated, solid-armature railguns might reach high velocity (greater than or equil to 6 km/s) without forcing most of the armature current to pass through an arc. Even then, magnetic diffusion (the 'normal' skin effect) will limit acceleration. In this paper, the performance limits for railguns which are free from the velocity-skin effect are investigated by deriving the upper limits for a specific kind of power supply. Previous performance estimates made for solid-armature railguns are examined in the light of these results and are found to be relatively

very optimistic. A railgun design which limits the velocity-skin effect and which may allow improved performance for solid armatures is described. DOE

N92-31735# Lawrence Livermore National Lab., CA.
PROJECTILE DEVELOPMENT FOR RAILGUNS USING HYPERVELOCITY PREACCELERATION
A. R. Susoeff, R. S. Hawke, J. A. Ang, J. R. Asay, C. A. Hall, C. H. Konrad (Sandia National Labs., Albuquerque, NM.), and G. L. Sauve (EG and G Washington Analytical Services Center, Inc., Albuquerque, NM.) 20 Mar. 1992 22 p
(Contracts W-7405-eng-48; DE-AC04-76DP-00789)
(DE92-016741; UCRL-ID-109283-Rev-1) Avail: CASI HC A03/MF A01

The STARFIRE Project is a joint Lawrence Livermore National Laboratory (LLNL) and Sandia National Laboratories (SNL) effort to achieve hypervelocity projectile launches up to 15 km/s. The apparatus used to achieve this goal is a three stage acceleration system made up of a two-stage light-gas gun (2SLGG) coupled to a railgun. The 2SLGG is used as a preaccelerator capable of injecting 2 gram projectiles at velocities of 6 km/s or more. Projectiles used in this environment are subject to many conditions. Some of these which effect projectile design include acceleration loading, structural response, barrel condition and alignment. Development of a projectile to satisfy the programmatic requirements is underway. This report covers the evolution of design and fabrication for railgun projectiles from previous experimentation at LLNL to the replenished plasma armature and projectile now used on STARFIRE. Projectile design, development and fabrication methods which use off-the-shelf materials and standard techniques to meet the operational criteria of the experimental program are discussed in this paper. Initial work involving the design and fabrication of skirted projectiles, which are expected to further reduce interaction phenomena between the plasma armature and railgun barrel, is also described. DOE

16 SPACE TRANSPORTATION

Includes passenger and cargo space transportation, e.g., shuttle operations; and space rescue techniques.

For related information see also *03 Air Transportation and Safety* and *18 Spacecraft Design, Testing and Performance.* For space suits see *54 Man/System Technology and Life Support.*

N92-32130*# Martin Marietta Corp., Denver, CO.
INTERPLANETARY PROGRAM TO OPTIMIZE SPACE TRAJECTORIES (IPOST). VOLUME 3: PROGRAMMER'S MANUAL Final Report
P. E. Hong, P. D. Kent, D. W. Olson, and C. A. Vallado 31 Jul. 1992 62 p
(Contract NAS1-18147; RTOP 506-49-11-02)
(NASA-CR-189653-Vol-3; NAS 1.26:189653-Vol-3) Avail: CASI HC A04/MF A01

The Interplanetary Program to Optimize Space Trajectories (IPOST) is intended to support many analysis phases, from early interplanetary feasibility studies through spacecraft development and operations. Here, information is given on the IPOST code. Author

17 SPACE COMM., SPACECRAFT COMM., COMMAND & TRACKING

Includes telemetry; space communications networks; astronavigation and guidance; and radio blackout.

For related information see also *04 Aircraft Communications and Navigation* and *32 Communications and Radar.*

No abstracts in this category.

18 SPACECRAFT DESIGN, TESTING AND PERFORMANCE

Includes satellites; space platforms; space stations; spacecraft systems and components such as thermal and environmental controls; and attitude controls.

For life support systems see *54 Man/System Technology and Life Support.* For related information see also *05 Aircraft Design, Testing and Performance, 39 Structural Mechanics,* and *16 Space Transportation.*

N92-31260*# Dayton Univ., OH. Dept. of Engineering Management and Systems.
THE DETERMINATION OF OPERATIONAL AND SUPPORT REQUIREMENTS AND COSTS DURING THE CONCEPTUAL DESIGN OF SPACE SYSTEMS Final Report
Charles Ebeling and Kenneth D. Beasley Aug. 1992 269 p
(Grant NAG1-1327)
(NASA-CR-190626; NAS 1.26:190626) Avail: CASI HC A12/MF A03

The first year of research to provide NASA support in predicting operational and support parameters and costs of proposed space systems is reported. Some of the specific research objectives were (1) to develop a methodology for deriving reliability and maintainability parameters and, based upon their estimates, determine the operational capability and support costs, and (2) to identify data sources and establish an initial data base to implement the methodology. Implementation of the methodology is accomplished through the development of a comprehensive computer model. While the model appears to work reasonably well when applied to aircraft systems, it was not accurate when used for space systems. The model is dynamic and should be updated as new data become available. It is particularly important to integrate the current aircraft data base with data obtained from the Space Shuttle and other space systems since subsystems unique to a space vehicle require data not available from aircraft. This research only addressed the major subsystems on the vehicle. K.S.

N92-31457*# National Aeronautics and Space Administration. Langley Research Center, Hampton, VA.
COMPARISON OF EFFECTS OF COPROPAGATED AND PRECOMPUTED ATMOSPHERE PROFILES ON MONTE CARLO TRAJECTORY SIMULATION
Eric M. Queen and Thomas M. OMara (PRC Kentron, Inc., Hampton, VA.) Aug. 1990 47 p
(RTOP 506-46-21-01)
(NASA-TM-102600; NAS 1.15:102600) Avail: CASI HC A03/MF A01

A realization of a stochastic atmosphere model for use in simulations is presented. The model provides pressure, density, temperature, and wind velocity as a function of latitude, longitude, and altitude, and is implemented in a three degree of freedom simulation package. This implementation is used in the Monte Carlo simulation of an aeroassisted orbital transfer maneuver and results are compared to those of a more traditional approach. Author

N92-31632# Bureau of Land Management, Washington, DC.
SATELLITE POSITIONING SYSTEMS: A REPORT TO THE DIRECTOR
Sep. 1991 84 p
(PB92-181270) Avail: CASI HC A05/MF A01

New and remarkable positioning and communications technology from the age of satellites is now available for wide application. Its promise and potential blending for Bureau of Land Management (BLM) purposes will virtually apply to all functions and will gradually change methods of operation. Although space based technologies have been in use in BLM to a minor extent for many years, the coming-of-age of the NAVSTAR Global Positioning System (Navigation Satellite Timing and Ranging, or GPS) dramatically points up an enormous operational resource from Satellite Positioning Technology (SPT). Here, an overview is given of the SPT world with emphasis on GPS. The bureau-wide use of SPT is strongly advocated, while also recognizing some limitations. Noted is a simplicity of use. But complexities in need of management direction are pointed out. Volumes of scientific and technical information exist as to the theory and application of SPT. Very little of that type of data is included. The BLM SPT bridge described here is an attempt to bring the area of present and future capabilities together with BLM user needs and operations. Author

N92-31677*# Boeing Co., Seattle, WA. Defense and Space Group.
ANALYSIS OF SYSTEMS HARDWARE FLOWN ON LDEF. RESULTS OF THE SYSTEMS SPECIAL INVESTIGATION GROUP
Harry W. Dursch, W. Steve Spear, Emmett A. Miller, Gail L. Bohnhoff-Hlavacek, and Joel Edelman Apr. 1992 307 p Sponsored in part by Strategic Defense Initiative Organization Original contains color illustrations
(Contract NAS1-19247; RTOP 506-48-91-08)
(NASA-CR-189628; NAS 1.26:189628) Avail: CASI HC A14/MF A03; 11 functional color pages

The Long Duration Exposure Facility (LDEF) was retrieved after spending 69 months in low Earth orbit (LEO). LDEF carried a remarkable variety of mechanical, electrical, thermal, and optical systems, subsystems, and components. The Systems Special Investigation Group (Systems SIG) was formed to investigate the effects of the long duration exposure to LEO on systems related hardware and to coordinate and collate all systems analysis of LDEF hardware. Discussed here is the status of the LDEF Systems SIG investigation through the end of 1991. Author

N92-31822# Air Force Inst. of Tech., Wright-Patterson AFB, OH.
HIGH-LATITUDE SPACECRAFT CHARGING IN LOW-EARTH POLAR ORBIT M.S. Thesis
Thomas B. Frooninckx 1991 114 p
(AD-A249868; AFIT/CI/CIA-91-119) Avail: CASI HC A06/MF A02

Spacecraft charging within the upper ionosphere is commonly thought to be insignificant and thus has received little attention. Recent experimental evidence has shown that electric potential differences as severe as 680 volts can develop between Defense Meteorological Satellite Program (DMSP) polar-orbiting (840 kilometers) spacecraft and their high-latitude environment. To explore space vehicle charging in this region more fully, an analysis was performed using DMSP F6, F7, F8, and F9 satellite precipitating particle and ambient plasma measurements taken during the winters of 1986-87 (solar minimum) and 1989-90 (solar maximum). An extreme solar cycle dependence was discovered as charging occurred more frequently and with greater severity during the period of solar minimum. One hundred seventy charging events ranging from -46 to 1,430 volts were identified, and satellite measurements and Time Dependent Ionospheric Model (TDIM) output were used to characterize the environments which generated and inhibited these potentials. All current sources were considered to determine the cause of the solar cycle dependence. GRA

N92-31997# Southwest Research Inst., San Antonio, TX.
A PENETRATION MECHANICS DATABASE Final Report
Charles E. Anderson, Jr., Bruce L. Morris, and David L. Littlefield 31 Jan. 1992 459 p
(Contracts DAAL03-91-C-0021; DE-AC04-90AL-58770)
(AD-A246351; SwRI-3593/001) Avail: CASI HC A20/MF A04

A penetration mechanics database has been compiled that contains experimental results from a variety of researchers of different nationalities (German, French, English, Canadian, and American), during different decades (the 1960's to the 1990's), and with different purposes or objectives (space debris impact, armor design and evaluation, penetrator design and evaluation, and theoretical verification). The data fall naturally into three subgroupings: (1) penetration into semi-infinite targets; (2) perforation of finite-thickness targets; and (3) penetration from multiple impact (segmented rods). Data collection was primarily limited to experiments conducted against generic type targets, and emphasis was placed on data that would be more relevant to heavy armor issues. This diverse collection of data for metallic targets has been tabulated; data tables include the initial impact conditions, the projectile and target geometries and materials, and the measured response. Information on the materials, e.g., hardness of yield strength, along with impact information such as yaw has been tabulated if available. Graphical displays of the data have been used to summarize the data, and cross-plotting that combines data from different sources has also been provided. GRA

N92-32073# Research Inst. of National Defence, Stockholm (Sweden). Dept. of Information Technology.
MONITORING THREATS TO SATELLITE FUNCTIONS
U. Ekblad and T. Orhaug Jan. 1992 33 p Sponsored by Royal Ministry for Foreign Affairs, Stockholm, Sweden
(PB92-195445; FOA-C-30647-9.4) Avail: CASI HC A03/MF A01

Satellite functions are briefly described before the possible threats with which satellites can be confronted are discussed. Monitoring possibilities and various monitoring techniques which could be used for obtaining information concerning threats to satellites and for determining causes and identifying aggressors are discussed. Author

N92-32082# Nova Univ., Dania, FL. Oceanographic Center.
SATELLITE-TO-SATELLITE TRACKING IN THE HIGH-LOW MODE: LINE-OF-SIGHT ACCELERATION IN A RESIDUAL GRAVITY FIELD Report No. 3
Georges Blaha Jul. 1991 34 p
(Contract F19628-89-K-0016)
(PL-TR-91-2209) Avail: CASI HC A03/MF A01

The residual line-of-sight acceleration for a general satellite configuration is developed that is rigorous to within the first-order differentials. In addition to the usual 'basic term' treated in geophysical literature, two kinds of corrective terms are derived: the term c sub 1 (related to satellite velocities) and the combined term c(sub 2)+c(sub 3)+c(sub 4) (related to satellite positions). Subsequently, the general formulation is specialized for a high-low configuration. The outcome of computer simulations performed for this configuration confirms the first-order formulation. In all cases examined (two arcs of up to three minutes in duration, three different reference gravity fields), the first-order results agree with the known 'true' values to within 0.00001 mgal. These results clearly indicate that the basic term lacks the accuracy to represent alone a valid mathematical model. However, when this term is corrected by c(sub 1), its accuracy improves significantly, attaining the level of 0.01 mgal or better. The practical significance of this finding, as well as a possibility to exploit it efficiently in the future, are indicated. Author

N92-32100*# Lockheed Missiles and Space Co., Sunnyvale, CA.
DESIGN, ANALYSIS, AND TESTING OF THE PHASE 1 CSI EVOLUTIONARY MODEL ERECTABLE TRUSS
M. J. Gronet, D. A. Davis, D. H. Kintis, R. D. Brillhart (Structural

Dynamics Research Corp., San Diego, CA.), and E. M. Atkins (Structural Dynamics Research Corp., San Diego, CA.) Washington NASA. Langley Research Center Aug. 1992 379 p
(Contract NAS1-19241; RTOP 590-14-61-01)
(NASA-CR-4461; NAS 1.26:4461; LMSC/P024859) Avail: CASI HC A17/MF A03

This report addressed the design, analysis, and testing of the erectable truss structure for the Phase 1 CSI Evolutionary Model (CEM) testbed. The Phase 1 CEM testbed is the second testbed to form part of an ongoing program of focused research at NASA/LaRC in the development of Controls-Structures Integration (CSI) technology. The Phase 1 CEM contains the same overall geometry, weight, and sensor locations as the Phase 0 CEM, but is based in an integrated controller and structure design, whereby both structure and controller design variables are sized simultaneously. The Phase 1 CEM design features seven truss sections composed of struts with tailored mass and stiffness properties. A common erectable joint is used and the strut stiffness is tailored by varying the cross-sectional area. To characterize the structure, static tests were conducted on individual struts and 10-bay truss assemblies. Dynamic tests were conducted on 10-bay truss assemblies as well as the fully-assembled CEM truss. The results indicate that the static and dynamic properties of the structure are predictable, well-characterized, and within the performance requirements established during the Phase 1 CEM integrated controller/structure design analysis. Author

N92-31874# Israel Aircraft Industries Ltd., Yehud.
A NOVEL CONTROL-GUIDANCE LAW FOR LOW-THRUST ORBIT MANEUVER
Marcel Sidi *In* Israel Society of Aeronautics and Astronautics, 31st Israel Annual Conference on Aviation and Astronautics 22 Feb. 1990 p 81-88 Previously announced in IAA as A91-43088 (For primary document see N92-31861 22-01)
Avail: CASI HC A02/MF A03

N92-31877# Maryland Univ., College Park. Dept. of Aerospace Engineering.
THE USE OF HIGH LIFT-TO-DRAG HYPERSONIC VEHICLES FOR AERO-ASSISTED ORBITAL MANEUVERING
Mark J. Lewis *In* Israel Society of Aeronautics and Astronautics, 31st Israel Annual Conference on Aviation and Astronautics 22 Feb. 1990 p 107-119 Previously announced in IAA as A91-43091 (For primary document see N92-31861 22-01)
Avail: CASI HC A03/MF A03

N92-32010 Cynetics Corp., Rapid City, SD.
ADVANCES IN SMALL SATELLITE COMMUNICATION SYSTEMS
Don K. Lefevre *In* Huntsville Association of Technical Societies, TABES 92: 8th Annual Technical and Business Exhibition and Symposium. Executive Summaries and Submitted Papers 1992 8 p (For primary document see N92-32009 22-12)
(TABES Paper 92-411) Copyright Avail: Issuing Activity

N92-32011* National Aeronautics and Space Administration. Marshall Space Flight Center, Huntsville, AL.
SPACECRAFT STABILITY AND CONTROL
Chris Barret *In* Huntsville Association of Technical Societies, TABES 92: 8th Annual Technical and Business Exhibition and Symposium. Executive Summaries and Submitted Papers 1992 9 p (For primary document see N92-32009 22-12)
(TABES Paper 92-414) Copyright Avail: Issuing Activity

N92-32016 Italian Space Agency, Rome.
SPACE STATION MINI PRESSURISED LOGISTICS MODULES: AN OPPORTUNITY TO ENLARGE AND REINFORCE INTERNATIONAL COOPERATION
Luciano Guerriero and Ernesto Vallerani *In* Huntsville Association of Technical Societies, TABES 92: 8th Annual Technical and Business Exhibition and Symposium. Executive Summaries and Submitted Papers 1992 7 p Prepared in cooperation with Alenia Spazio S.p.A., Rome, Italy (For primary document see N92-32009 22-12)
(TABES Paper 92-425) Copyright Avail: Issuing Activity

N92-32018 McDonnell-Douglas Corp., Huntsville, AL. SPACEHAB Program.
SPACEHAB: A GIANT STEP IN THE COMMERCIAL DEVELOPMENT OF SPACE
James E. Shepard *In* Huntsville Association of Technical Societies, TABES 92: 8th Annual Technical and Business Exhibition and Symposium. Executive Summaries and Submitted Papers 1992 7 p (For primary document see N92-32009 22-12)
(TABES Paper 92-454) Copyright Avail: Issuing Activity

19 SPACECRAFT INSTRUMENTATION

For related information see also *06 Aircraft Instrumentation* and *35 Instrumentation and Photography.*

N92-31675# Air Force Inst. of Tech., Wright-Patterson AFB, OH.
AN INVESTIGATION OF SPINUP DYNAMICS OF AXIAL GYROSTATS USING ELLIPTIC INTEGRALS AND THE METHOD OF AVERAGING Ph.D. Thesis
Christopher D. Hall 1991 225 p
(AD-A249728; AFIT/CI/CIA-91-026D) Avail: CASI HC A10/MF A03

A gyrostat is a rigid body containing an internal source of angular momentum which does not alter the geometry of the system. Because of their relative simplicity, gyrostats are frequently used to model dual-spin spacecraft. An axial gyrostat is composed of two rigid bodies: an asymmetric platform and an axisymmetric rotor aligned with a principal axis of the platform. Rotation of the rotor relative to the platform provides a source of internal angular momentum, and does not affect the moment of inertia tensor of the gyrostat. In this thesis, we consider the dynamics of axial gyrostats in the absence of energy dissipation and external torques. Spinup of the rotor is effected by a small constant internal axial torque, g(sub a). The dynamics are described by four first-order ordinary differential equations, which admit exact solutions in terms of elliptic functions for g(sub a) = 0. Application of the method of averaging reduces the problem to a single first-order differential equation, which is studied analytically and numerically. This single equation accurately describes most spinup trajectories. However, when spinup trajectories cross the instantaneous separatrices of the g(sub a) = 0 system, the Omicron(1) frequency of the unaveraged system vanishes. The averaged equations are not valid near these separatrix crossings, and we develop an approximate equation valid in a neighborhood of the separatrix, which we use to connect the averaged solutions across the separatrix. When applied iteratively in a neighborhood of the separatrix, the approximation equation agrees qualitatively with the exact solution. GRA

N92-31846# Pacific Northwest Lab., Richland, WA.
USE OF TISSUE EQUIVALENT PROPORTIONAL COUNTERS TO CHARACTERIZE RADIATION QUALITY ON THE SPACE SHUTTLE
L. A. Braby, T. J. Conroy, D. C. Elegy, and L. W. Brackenbush Apr. 1992 7 p Presented at the Meeting on New Horizons in Radiation Protection and Shielding, Pasco, WA, 26 Apr. - 1 May 1992
(Contract DE-AC06-76RL-01830)
(DE92-012347; PNL-SA-19981; CONF-920431-24) Avail: CASI HC A02/MF A01

Tissue equivalent proportional counters (TEPC) are essentially cavity ionization chambers operating at low pressure and with gas gain. A small, battery powered, TEPC spectrometer, which records lineal energy spectra at one minute intervals, was used on several space shuttle missions. The data it has collected clearly show the South Atlantic anomaly and indicate a mean quality factor somewhat higher than expected. An improved type of instrument

was developed with sufficient memory to record spectra at 10 second intervals, and with increased resolution for low LET events. This type of instrument will be used on most future space shuttle flights and in some international experiments. DOE

N92-32204*# National Aeronautics and Space Administration. Langley Research Center, Hampton, VA.
GROUND AND FLIGHT CALIBRATION ASSESSMENT OF HiRAP ACCELEROMETER DATA FROM MISSIONS STS-35 AND STS-40
Robert C. Blanchard, Kevin T. Larman (Lockheed Engineering and Sciences Co., Hampton, VA.), and Christina D. Moats (Lockheed Engineering and Sciences Co., Hampton, VA.) Apr. 1992 31 p (RTOP 506-48-11-05)
(NASA-TM-107602; NAS 1.15:107602) Avail: CASI HC A03/MF A01

A method of removing non-aerodynamic signals and calibrating the High Resolution Accelerometer Package (HiRAP) flight data was developed and is discussed for Shuttle Orbiter missions STS-35 and STS-40. These two mission data sets were analyzed using ground (dynamic) calibration data and flight calibrations using a flight calibration technique that was developed and refined over the HiRAP operational lifetime. This technique evolved early in the flight program, since it was recognized that ground calibration factors are insufficient to determine absolute low acceleration levels. The application of flight calibration factors to the data sets from these missions produced calibrated acceleration levels within an accuracy of less than plus or minus 1.5 micro-g of zero during a time in the flight when the acceleration level was known to be less than 1 micro-g. This analysis further confirms the theory that flight calibrations are required in order to obtain the absolute measurement of low-frequency, low-acceleration flight signals.
Author

N92-31876*# National Aeronautics and Space Administration. Goddard Space Flight Center, Greenbelt, MD.
EXTENDED KALMAN FILTER FOR ATTITUDE ESTIMATION OF THE EARTH RADIATION BUDGET SATELLITE
Julie Deutschmann and Itzhack Y. Bar-Itzhack (Technion - Israel Inst. of Tech., Haifa.) *In* Israel Society of Aeronautics and Astronautics, 31st Israel Annual Conference on Aviation and Astronautics 22 Feb. 1990 p 92-106 Previously announced in IAA as A91-43090 and N90-13433 (For primary document see N92-31861 22-01)
Avail: CASI HC A03/MF A03

N92-31878*# National Aeronautics and Space Administration. Goddard Space Flight Center, Greenbelt, MD.
TRUE COVARIANCE SIMULATION OF THE EUVE (EXTREME ULTRA VIOLET EXPLORER) UPDATE FILTER
I. Y. Bar-Itzhack (Technion - Israel Inst. of Tech., Haifa.) and R. R. Harman *In* Israel Society of Aeronautics and Astronautics, 31st Israel Annual Conference on Aviation and Astronautics 22 Feb. 1990 p 120-126 Previously announced in IAA as A91-43092 (For primary document see N92-31861 22-01)
Avail: CASI HC A02/MF A03

20 SPACECRAFT PROPULSION AND POWER

Includes main propulsion systems and components, e.g., rocket engines; and spacecraft auxilliary power sources.

For related information see also *07 Aircraft Propulsion and Power, 28 Propellants and Fuels, 44 Energy Production and Conversion,* and *15 Launch Vehicles and Space Vehicles.*

N92-31245*# Sunpower, Inc., Athens, OH.
FREE-PISTON STIRLING ENGINE CONCEPTUAL DESIGN AND TECHNOLOGIES FOR SPACE POWER, PHASE 1 Final Report
L. Barry Penswick, William T. Beale, and J. Gary Wood (Wood, J. Gary, Albany, OH) Jan. 1990 139 p
(Contract NAS3-23885; RTOP 586-01-11)
(NASA-CR-182168; NAS 1.26:182168) Avail: CASI HC A07/MF A02

As part of the SP-100 program, a phase 1 effort to design a free-piston Stirling engine (FPSE) for a space dynamic power conversion system was completed. SP-100 is a combined DOD/DOE/NASA program to develop nuclear power for space. This work was completed in the initial phases of the SP-100 program prior to the power conversion concept selection for the Ground Engineering System (GES). Stirling engine technology development as a growth option for SP-100 is continuing after this phase 1 effort. Following a review of various engine concepts, a single-cylinder engine with a linear alternator was selected for the remainder of the study. The relationships of specific mass and efficiency versus temperature ratio were determined for a power output of 25 kWe. This parametric study was done for a temperature ratio range of 1.5 to 2.0 and for hot-end temperatures of 875 K and 1075 K. A conceptual design of a 1080 K FPSE with a linear alternator producing 25 kWe output was completed. This was a single-cylinder engine designed for a 62,000 hour life and a temperature ratio of 2.0. The heat transport systems were pumped liquid-metal loops on both the hot and cold ends. These specifications were selected to match the SP-100 power system designs that were being evaluated at that time. The hot end of the engine used both refractory and superalloy materials; the hot-end pressure vessel featured an insulated design that allowed use of the superalloy material. The design was supported by the hardware demonstration of two of the component concepts - the hydrodynamic gas bearing for the displacer and the dynamic balance system. The hydrodynamic gas bearing was demonstrated on a test rig. The dynamic balance system was tested on the 1 kW RE-1000 engine at NASA Lewis. Author

N92-31249*# National Aeronautics and Space Administration. Lewis Research Center, Cleveland, OH.
CYCLIC HOT FIRING RESULTS OF TUNGSTEN-WIRE-REINFORCED, COPPER-LINED THRUST CHAMBERS
John M. Kazaroff and Robert S. Jankovsky Sep. 1990 16 p (RTOP 505-01-11)
(NASA-TM-4214; E-5337; NAS 1.15:4214) Avail: CASI HC A03/MF A01

An advanced thrust liner material for potential long life reusable rocket engines is described. This liner material was produced with the intent of improving the reusable life of high pressure thrust chambers by strengthening the chamber in the hoop direction, thus avoiding the longitudinal cracking due to low cycle fatigue that is observed in conventional homogeneous copper chambers, but yet not reducing the high thermal conductivity that is essential when operating with high heat fluxes. The liner material produced was a tungsten wire reinforced copper composite. Incorporating this composite into two hydrogen-oxygen test rocket chambers was done so that its performance as a reusable liner material could be evaluated. Testing results showed that both chambers failed prematurely, but the crack sites were perpendicular to the normal direction of cracking indicating a degree of success in containing the tremendous thermal strain associated with high temperature rocket engines. The failures, in all cases, were associated with drilled instrumentation ports and no other damages or deformations were found elsewhere in the composite liners.
Author

N92-31342*# National Aeronautics and Space Administration. Lewis Research Center, Cleveland, OH.
THE EVOLUTIONARY DEVELOPMENT OF HIGH SPECIFIC IMPULSE ELECTRIC THRUSTER TECHNOLOGY
James S. Sovey, John A. Hamley, Michael J. Patterson, Vincent K. Rawlin, and Roger M. Myers (Sverdrup Technology, Inc., Brook Park, OH.) 1992 28 p Presented at the Space Programs and Technologies Conference, Huntsville, AL, 24-27 Mar. 1992; sponsored by AIAA Previously announced in IAA as A92-38650
(Contract NAS3-25266; RTOP 506-42-31)

(NASA-TM-105712; E-7104; NAS 1.15:105712; AIAA Paper 92-1556) Avail: CASI HC A03/MF A01

Electric propulsion flight and technology demonstrations conducted primarily by Europe, Japan, China, the U.S., and the USSR are reviewed. Evolutionary mission applications for high specific impulse electric thruster systems are discussed, and the status of arcjet, ion, and magnetoplasmadynamic thrusters and associated power processor technologies are summarized.

Author

N92-31474# Colorado Univ., Boulder. Center for Combustion Research.

SOLID ROCKET COMBUSTION PHENOMENA Final Report, 1 Oct. 1988 - 30 Sep. 1991

David R. Kassoy, Meng Wang, and Qing Zhao 9 Jan. 1992 100 p

(Grant AF-AFOSR-0023-89)

(AD-A248006; CCR-92-01; AFOSR-92-0208TR) Avail: CASI HC A05/MF A02

This Final Technical Report describes completed research accomplishments and ongoing activities that are focused on the evolution of boundary driven acoustic disturbances in a low Mach number shear flow like that found in the chamber of a solid rocket engine. The completed work (manuscripts in Appendices A and B) focuses on the relatively complex wave systems that appear in a two-dimensional planar shear flow following the refraction of very simple, initially planar axial disturbances. Work in progress emphasizes: (1) the characteristics of acoustic disturbances driven by sidewall mass addition in semi-confined channels and tubes; (2) the role of strongly injected Stokes boundary layers in providing a transition from the acoustic flow to the no-slip condition on the wall; and (3) mathematical methods required to deal with nonlinear processes within an acoustically disturbed flow. The review of our work emphasizes the importance of studying the evolution of boundary driven acoustic disturbances, primarily to gain an understanding of how small burning rate transients (modeled by unsteady wall injection) lead to large engine chamber responses observed in unstable solid rockets. GRA

N92-31503# Sandia National Labs., Albuquerque, NM.

SPACE NUCLEAR POWER, PROPULSION, AND RELATED TECHNOLOGIES

Marshall Berman, ed. and John A. Stikar, ed. Jan. 1992 63 p Original contains color illustrations

(SAND91-2617) Avail: CASI HC A04/MF A01

Sandia National Laboratories is one of the nation's largest research and development (R&D) facilities and is responsible for national security programs in defense and energy with a primary emphasis on nuclear weapon R&D. However, Sandia also supports a wide variety of projects ranging from basic materials research to the design of specialized parachutes. As a multiprogram national laboratory, Sandia has much to offer both industrial and government customers in pursuing space nuclear technologies. A brief summary of Sandia's technical capabilities, test facilities, and example programs that relate to military and civilian objectives in space is presented. K.S.

N92-31507*# National Aeronautics and Space Administration. Lewis Research Center, Cleveland, OH.

A DEMONSTRATION OF AN INTELLIGENT CONTROL SYSTEM FOR A REUSABLE ROCKET ENGINE

Jeffrey L. Musgrave, Daniel E. Paxson, Jonathan S. Litt, and Walter C. Merrill Jun. 1992 11 p Submitted for publication Prepared in cooperation with Army Aviation Systems Command, Cleveland, OH

(RTOP 582-01-11)

(NASA-TM-105794; E-7224; NAS 1.15:105794) Avail: CASI HC A03/MF A01

An Intelligent Control System for reusable rocket engines is under development at NASA Lewis Research Center. The primary objective is to extend the useful life of a reusable rocket propulsion system while minimizing between flight maintenance and maximizing engine life and performance through improved control and monitoring algorithms and additional sensing and actuation. This paper describes current progress towards proof-of-concept of an Intelligent Control System for the Space Shuttle Main Engine. A subset of identifiable and accommodatable engine failure modes is selected for preliminary demonstration. Failure models are developed retaining only first order effects and included in a simplified nonlinear simulation of the rocket engine for analysis under closed loop control. The engine level coordinator acts as an interface between the diagnostic and control systems, and translates thrust and mixture ratio commands dictated by mission requirements, and engine status (health) into engine operational strategies carried out by a multivariable control. Control reconfiguration achieves fault tolerance if the nominal (healthy engine) control cannot. Each of the aforementioned functionalities is discussed in the context of an example to illustrate the operation of the system in the context of a representative failure. A graphical user interface allows the researcher to monitor the Intelligent Control System and engine performance under various failure modes selected for demonstration. Author

N92-31550*# GenCorp Aerojet, Sacramento, CA. Propulsion Div.

PRESSURE FED THRUST CHAMBER TECHNOLOGY PROGRAM Final Report

Glen M. Dunn Jul. 1992 126 p Original contains color illustrations

(Contract NAS8-37365)

(NASA-CR-190666; NAS 1.26:190666) Avail: CASI HC A07/MF A02; 2 functional color pages

This is the final report for the Pressure Fed Technology Program. It details the design, fabrication, and testing of subscale hardware which successfully characterized Liquid Oxygen Rocket Propulsion (LOX/RP) combustion for low cost pressure fed design. The innovative modular injector design is described in detail as well as hot-fire test results which showed excellent performance. The program summary identifies critical LOX/RP design issues that have been resolved in this testing, and details the low risk development requirements for low cost engines for future Expandable Launch Vehicles (ELV). Author

N92-31897# Oak Ridge National Lab., TN.

POTASSIUM RANKINE CYCLE NUCLEAR POWER SYSTEMS FOR SPACECRAFT AND LUNAR-MASS SURFACE POWER

R. S. Holcomb 1992 10 p Presented at the Nuclear Technologies for Space Exploration, Jackson, WY, 16-19 Aug. 1992

(Contract DE-AC05-84OR-21400)

(DE92-016163; CONF-920803-10) Avail: CASI HC A02/MF A01

The potassium Rankine cycle has high potential for application to nuclear power systems for spacecraft and surface power on the moon and Mars. A substantial effort on the development of Rankine cycle space power systems was carried out in the 1960's. That effort is summarized and the status of the technology today is presented. Space power systems coupling Rankine cycle power conversion to both the SP-100 reactor and thermionic reactors as a combined power cycle are described. DOE

N92-31901*# National Aeronautics and Space Administration. Lewis Research Center, Cleveland, OH.

KRYPTON ION THRUSTER PERFORMANCE

Michael J. Patterson and George J. Williams Aug. 1992 13 p Presented at the 28th Joint Propulsion Conference and Exhibit, Nashville, TN, 6-8 Jul. 1992; sponsored by AIAA, SAE, ASME, and ASEE

(RTOP 506-42-31)

(NASA-TM-105818; E-7249; JPC-92-3144; NAS 1.15:105818)

Copyright Avail: CASI HC A03/MF A01

Preliminary data were obtained from a 30 cm ion thruster operating on krypton propellant over the input power range of 0.4 to 5.5 kW. The data presented are compared and contrasted to the data obtained with xenon propellant over the same input power envelope. Typical krypton thruster efficiency was 70 percent at a

specific impulse of approximately 5000 s, with a maximum demonstrated thrust to power ratio of approximately 42 mN/kW at 2090 s specific impulse and 1580 watts input power. Critical thruster performance and component lifetime issues were evaluated. Order of magnitude power throttling was demonstrated using a simplified power-throttling strategy. Author

N92-31916*# National Aeronautics and Space Administration. Lewis Research Center, Cleveland, OH.
AN OVERVIEW OF THE LEWIS RESEARCH CENTER CSTI THERMAL MANAGEMENT PROGRAM
Albert J. Juhasz 1991 13 p Presented at the Conference on Advanced Space Exploration Initiative Technologies, Cleveland, OH, 4-6 Sep. 1991; sponsored in part by NASA, AIAA, and OAI Previously announced in IAA as A91-52422
(RTOP 590-13-21)
(NASA-TM-105310; E-6542; NAS 1.15:105310; AIAA Paper 91-3528) Avail: CASI HC A03/MF A01

An integrated multi-element project effort, currently being carried out at NASA LeRC, for the development of space heat rejection subsystems, with special emphasis on lightweight radiators, in support of SEI power system technology, and in particular the SP-100 program, is reported. Principal project elements include both contracted and in-house efforts. Included in the first category are two contracts aimed at the development of advanced radiator concepts, and demonstration of a flexible fabric heat pipe radiator concept. In-house work is designed to guide and support the overall program by system integration studies, heat pipe testing and analytical code development, radiator surface morphology alteration for emissivity enhancement, and composite materials research focused on the development of lightweight high conductivity fins. Author

N92-32030# Sandia National Labs., Albuquerque, NM.
A PHILOSOPHY FOR SPACE NUCLEAR SYSTEMS SAFETY
A. C. Marshall 1992 6 p Presented at the Nuclear Technologies for Space Exploration, Jackson, WY, 16-19 Aug. 1992
(Contract DE-AC04-76DP-00789)
(DE92-016501; SAND-92-1223C; CONF-920803-12) Avail: CASI HC A02/MF A01

The unique requirements and contraints of space nuclear systems require careful consideration in the development of a safety policy. The Nuclear Safety Policy Working Group (NSPWG) for the Space Exploration Initiative has proposed a hierarchical approach with safety policy at the top of the hierarchy. This policy allows safety requirements to be tailored to specific applications while still providing reassurance to regulators and the general public that the necessary measures have been taken to assure safe application of space nuclear systems. The safety policy used by the NSPWG is recommended for all space nuclear programs and missions. DOE

N92-32108*# National Aeronautics and Space Administration. Lewis Research Center, Cleveland, OH.
SP-100 REACTOR WITH BRAYTON CONVERSION FOR LUNAR SURFACE APPLICATIONS
Lee S. Mason, Carlos D. Rodriguez, Barbara I. McKissock, James C. Hanlon (Sverdrup Technology, Inc., Brook Park, OH.), and Brian C. Mansfield (Dayton Univ., OH.) 1992 18 p Presented at the Ninth Symposium on Space Nuclear Power Systems, Albuquerque, NM, 12-16 Jan. 1992
(RTOP 506-49-11)
(NASA-TM-105637; E-6983; NAS 1.15:105637) Avail: CASI HC A03/MF A01

Examined here is the potential for integrating Brayton-cycle power conversion with the SP-100 reactor for lunar surface power system applications. Two designs were characterized and modeled. The first design integrates a 100-kWe SP-100 Brayton power system with a lunar lander. This system is intended to meet early lunar mission power needs while minimizing on-site installation requirements. Man-rated radiation protection is provided by an integral multilayer, cylindrical lithium hydride/tungsten (LiH/W) shield encircling the reactor vessel. Design emphasis is on ease of deployment, safety, and reliability, while utilizing relatively near-term technology. The second design combines Brayton conversion with the SP-100 reactor in a erectable 550-kWe powerplant concept intended to satisfy later-phase lunar base power requirements. This system capitalizes on experience gained from operating the initial 100-kWe module and incorporates some technology improvements. For this system, the reactor is emplaced in a lunar regolith excavation to provide man-rated shielding, and the Brayton engines and radiators are mounted on the lunar surface and extend radially from the central reactor. Design emphasis is on performance, safety, long life, and operational flexibility. Author

N92-32129*# GenCorp Aerojet, Sacramento, CA. Propulsion Div.
ORBITAL TRANSFER ROCKET ENGINE TECHNOLOGY: ADVANCED ENGINE STUDY Final Report, Oct. 1988 - Mar. 1990
Warren R. Hayden Jun. 1992 282 p
(Contract NAS3-23772)
(NASA-CR-187216; NAS 1.26:187216; Aerojet-2459-31-1) Avail: CASI HC A13/MF A03

An advanced LOX/LH2 engine study for the use of NASA and vehicle prime contractors in developing concepts for manned missions to the Moon, Mars, and Phobos is documented. Parametric design data was obtained at five engine thrusts from 7.5K lbf to 50K lbf. Also, a separate task evaluated engine throttling over a 20:1 range and operation at a mixture ratio of 12 plus or minus 1 versus the 6 plus or minus 1 nominal. Cost data was also generated for DDT&E, first unit production, and factors in other life cycle costs. The major limitation of the study was lack of contact with vehicle prime contractors to resolve the issues in vehicle/engine interfaces. The baseline Aerojet dual propellant expander cycle was shown capable of meeting all performance requirements with an expected long operational life due to the high thermal margins. The basic engine design readily accommodated the 20:1 throttling requirement and operation up to a mixture ratio of 10 without change. By using platinum for baffled injector construction the increased thermal margin allowed operation up to mixture ratio 13. An initial engine modeling with an Aerojet transient simulation code (named MLETS) indicates stable engine operation with the baseline control system. A throttle ratio of 4 to 5 seconds from 10 percent to 100 percent thrust is also predicted. Performance predictions are 483.1 sec at 7.5K lbf, 487.3 sec at 20K lbf, and 485.2 sec at 50K lbf with a mixture ratio of 6 and an area ratio of 1200. Engine envelopes varied from 120 in. length/53 in. exit diameter at 7.5K lbf to 305 in. length/136 in. exit diameter at 50 K lbf. Packaging will be an important consideration. Continued work is recommended to include more vehicle prime contractor/engine contractor joint assessment of the interface issues. Author

N92-32237*# National Aeronautics and Space Administration. Lewis Research Center, Cleveland, OH.
LOW-Isp DERATED ION THRUSTER OPERATION
Michael J. Patterson Aug. 1992 18 p Presented at the 28th Joint Propulsion Conference and Exhibit, Nashville, TN, 6-8 Jul. 1992; sponsored by AIAA, SAE, ASME, and ASEE
(RTOP 506-42-31)
(NASA-TM-105787; E-7217; JPC-92-3203; NAS 1.15:105787)
Copyright Avail: CASI HC A03/MF A01

The performance and lifetime expectations of 30 cm xenon ion thruster technology at low values of specific impulse were evaluated, with emphasis on 1000-2500 s operation. Power levels of up to 2.0 kW, appropriate for auxiliary and orbit maneuvering propulsion, were processed at thrust-to-power ratios up to 57 mN/kW. These tests were conducted using a derated 30 cm ion thruster with high-perveance design two-grid ion optics with xenon propellent. Lifetime projections were made based on a simple analysis of critical component erosion rates, and it was found that a strong correlation exists with the ratio of the specific impulse-to-input power. Under all operating conditions for which the projected thruster lifetime is less than 10,000 hrs, the life-limiting

component of this technology is erosion of the accelerator grid due to charge-exchange ions. The use of alternative grid materials such as carbon is estimated to increase useful thruster lifetimes by as much as an order of magnitude and may enable long-life high thrust-density, sub-2500 s Isp operation. The performance and life of the derated thruster appears similar to that of the Russian SPT-100 thruster in the 1.0-2.0 kW, 1600-2000 s operational envelope. Author

N92-32239*# Sverdrup Technology, Inc., Brook Park, OH.
NUMERICAL SIMULATION OF GEOMETRIC SCALE EFFECTS IN CYLINDRICAL SELF-FIELD MPD THRUSTERS Final Report
M. LaPointe Aug. 1992 28 p Presented at the 28th Joint Propulsion Conference and Exhibit, Nashville, TN, 6-8 Jul. 1992; sponsored by AIAA, SAE, ASME, and ASEE
(Contract NAS3-25266)
(NASA-CR-189224; E-7277; NAS 1.26:189224) Avail: CASI HC A03/MF A01

A 2-D, two-temperature, single fluid magnetohydrodynamic code which incorporates classical plasma transport coefficients and Hall effects was developed to predict steady-state, self-field magnetoplasmadynamic (MPD) thruster performance. The governing equations and numerical methods of solution are outlined and discussed. Experimental comparisons are used to validate model predictions. The model accurately predicts thrust and reproduces trends in the discharge voltage for discharge currents below experimentally measured onset values. However, because the model does not include electrode effects, the calculated voltage drops are significantly lower than experimentally measured values. Predictions of thrust and flow efficiency are made for a matrix of fifteen cylindrical thruster geometries, assuming a fully ionized argon propellant. A maximum predicted specific impulse of 1680 s is obtained for a thruster with an anode radius of 2.5 cm, a cathode radius of 0.5 cm, and equal electrode lengths of 2.5 cm. A scaling relation is developed to predict, within limits, the onset of cylindrical, self-field thruster instability as a function of geometry and operating condition. Author

N92-31869# Technion - Israel Inst. of Tech., Haifa. Dept. of Aerospace Research.
STUDY OF A SPHERICAL SPINNING COMBUSTION CHAMBER FOR ORBIT INSERTION
G. Avital, J. B. Greenberg, D. Laredo, Y. Levy, Y. Tambour, and Y. M. Timnat *In* Israel Society of Aeronautics and Astronautics, 31st Israel Annual Conference on Aviation and Astronautics 22 Feb. 1990 p 51-61 Previously announced in IAA as A91-43083 (For primary document see N92-31861 22-01)
Avail: CASI HC A03/MF A03

23 CHEMISTRY AND MATERIALS (GENERAL)

N92-31850# Vermont Univ., Burlington. Dept. of Chemistry.
INORGANIC RINGS ON CARBON CHAINS
Christopher W. Allen 22 May 1992 22 p
(Contract N00014-89-J-1041)
(AD-A251043; TR-19) Avail: CASI HC A03/MF A01

We have developed a new class of inorganic polymers in which inorganic rings are substituents on carbon backbone polymers. There are features of interest in the chemistry of the inorganic ring systems in, or leading to, these polymers. The reactivity of the substituent on the inorganic ring which leads to polymerization gives valuable insights into the electronic interactions involving exocyclic groups. The reactivity of an inorganic ring system in a polymeric environment can be exploited and lastly new applications of inorganic ring systems were proposed. Synthesis of the new polymers was accomplished by chain polymerization of an olefin affixed to a cyclophosphazene or a cycloborazine. In cyclophosphazene chemistry, propenyl, ethoxyvinyl, vinyloxy, methacryloyl ethenedioxy, and alpha-methylenthenyl substituents undergo co- or homopolymerization. In cycloborazine systems both p-vinylphenyl and vinyl derivatives were examined. Reactivity data in copolymerization reactions show, in general, that the cyclophosphazene acts as a strong sigma electron withdrawing substituent when bonded to unsaturated organic moieties. Nucleophilic substitution reactions of the cyclophosphazene unit have been explored for both poly(propenyl- pentafluorocyclotriphospha zene- co-styrene) and poly(vinyloxypentachlorocycla- triphosphazene). The reactions of the latter with fluoroalkoxides, aryloxides, and amines were explored in detail with an emphasis on degrees of substitution and substituent effects on the thermal decomposition process of the polymers. GRA

24 COMPOSITE MATERIALS

Includes physical, chemical, and mechanical properties of laminates and other composite materials.
For ceramic materials see *27 Nonmetallic Materials.*

N92-31266*# Case Western Reserve Univ., Cleveland, OH. Dept. of Physics.
ELECTRONIC AND TOTAL ENERGY PROPERTIES OF TERNARY AND QUATERNARY SEMICONDUCTOR COMPOUNDS, ALLOYS, AND SUPERLATTICES: THEORETICAL STUDY OF Cu/GRAPHITE BONDING Technical Report, Jan. 1991 - Jan. 1992
Walter R. L. Lambrecht 28 Aug. 1992 22 p
(Grant NAG3-954)
(NASA-CR-190691; NAS 1.26:190691) Avail: CASI HC A03/MF A01

The goals of the research were to provide a fundamental science basis for why the bonding of Cu to graphite is weak, to critically evaluate the previous analysis of the wetting studies with particular regard to the values used for the surface energies of Cu and graphite, and to make recommendations for future experiments or other studies which could advance the understanding and solution of this technological problem. First principles electronic structure calculations were used to study the problem. These are based on density functional theory in the local density approximation and the use of the linear muffin-tin orbital band structure method. Calculations were performed for graphite monolayers, single crystal graphite with the hexagonal AB stacking, bulk Cu, Cu(111) surface, and Cu/graphite superlattices. The study is limited to the basal plane of graphite because this is the graphite plane exposed to Cu and graphite surface energies and combined with the measured contact angles to evaluate the experimental adhesion energy. Author

N92-31274*# Virginia Polytechnic Inst. and State Univ., Blacksburg. Dept. of Engineering Science and Mechanics.
COMPOSITE MATERIAL SHEAR PROPERTY MEASUREMENT USING THE IOSIPESCU SPECIMEN
Henjen Ho, Haryanto T. Budiman, Ming-Yi Tsai, John Morton, and Gary L. Farley (National Aeronautics and Space Administration. Langley Research Center, Hampton, VA.) 30 Apr. 1992 36 p Presented at the 11th Symposium on Composite Materials: Testing and Design, Hampton, VA
(Grants NAG1-1053; NSF DMR-88-09714)
(NASA-CR-190661; NAS 1.26:190661) Avail: CASI HC A03/MF A01

A detailed evaluation of the suitability of the Iosipescu specimen tested in the modified Wyoming fixture is presented. Finite element analysis and moire interferometry are used to assess the uniformity of the shear stress field in the test section of unidirectional and cross-ply graphite-epoxy composites. The nonuniformity of the strain field and the sensitivity of some fiber orientations to the specimen/fixture contact mechanics are discussed. The shear responses obtained for unidirectional and cross-ply graphite-epoxy composites are discussed and problems associated with anomalous behavior are addressed. An experimental determination of the shear

response of a range of material systems using strain gage instrumentation and moire interferometry is performed. Author

N92-31305# Massachusetts Inst. of Tech., Cambridge. Dept. of Mechanical Engineering.
THE 3-D ANALYSIS AND VERIFICATION OF FRACTURE GROWTH MECHANISMS IN FIBER-REINFORCED CERAMIC COMPOSIES Final Report, 31 Oct. 1988 - 30 Sep. 1991
M. P. Cleary, M. C. Larson, W. D. Keat, and F. T. Patterson 31 Mar. 1992 28 p
(Grant AF-AFOSR-0005-89)
(AD-A250893; AFOSR-92-0417TR) Avail: CASI HC A03/MF A01

This final report documents a 3-D computational and experimental investigation into the mechanics of toughening a brittle matrix by incorporating long brittle fibers. Computationally, small scale failure, mechanisms ahead of a crack are explicitly modeled and merged with a continuum representation of the far field outside the process zone. Particular attention is given to the interfacial decohesion and frictional slipping near the tip of a matrix crack which is impinging upon an inclusion. The surface integral and finite element (SIFEH) method, which employs the principle of superposition to combine the best features of two powerful numerical techniques, provides an extremely flexible and efficient computational platform for modeling linear elastic fractures near material inhomogeneities. Applications to general 3-D fracture growth in multimaterial media demonstrate the capabilities of the computational technique and are also described. The computational simulation is being guided by laboratory experiments. Crack growth observations made on a model (microstructure) structure comprising a glass rod embedded in a cement matrix show the toughening mechanisms of crack pinning and crack bridging in operation. In a second experiment, interfacial slip evolution was modeled experimentally for planar bimaterial interfaces. This combined experimental and numerical program is providing insight into optimal combinations of the key parameters (e.g., residual stresses at interface, friction coefficient, strength of fibers) to maximize toughness. GRA

N92-31307# Ohio State Univ., Columbus.
A FINITE ELEMENT PROCEDURE FOR ANALYSIS OF LAMINATED COMPOSITE PLATES Final Report, 1 Jul. 1985 - 30 Jun. 1990
R. S. Sandhu, W. E. Wolfe, and M. Moazzami 18 Jun. 1991 144 p
(Contract F33615-85-C-3213)
(AD-A250902; WL-TR-91-3023) Avail: CASI HC A07/MF A02

A variational formulation and finite-element implementation of the well-known discrete laminate theory of laminated composite plates is presented. To allow for varying properties of different layers with respect to the fixed reference frame used in the analysis, a linear variation of 'in-plane' displacements over each layer is assumed. The rate of variation can be different for each layer. The coupling between 'in-plane' and 'transverse' deformation is allowed for as is deformation due to shear. The mathematical model essentially assumes the laminated plate to be a stacking of Mindlin's orthotropic plates allowing for interfacial continuity of displacement. A finite element scheme implementing the foregoing concepts is described. Through the thickness, nodal points are used to reduce the problem to one of two-dimensional geometry. Three different interpolation schemes viz., the eight-point serendipity, the nine-point Lagrangian, and the four-point Lagrangian are used in the isoparametric elements and their effectiveness is compared. The numerical procedure is verified against available solutions and then applied to analysis of stresses in a multi-ply free-edge delamination specimen. The procedure does not satisfy the traction-free edge condition and, therefore, the approach cannot be used to predict delamination and its growth. GRA

N92-31315# New Mexico Inst. of Mining and Technology, Socorro. Dept. of Metallurgical and Materials Engineering.
INTERFACE ENGINEERING IN ALUMINA/GLASS COMPOSITES Final Report, 1 Mar. 1989 - 29 Feb. 1992
K. K. Chawla 29 Feb. 1992 170 p
(Contract N00014-89-J-1459)
(AD-A248587) Avail: CASI HC A08/MF A02

The work done in the past three years has demonstrated the feasibility of developing alumina fiber based glass matrix composites for structural applications by applying an interface engineering approach. Composites consisting of a glass matrix containing coated and uncoated continuous alumina type fibers, were produced by a slurry impregnation method. A tin dioxide coating was used for the PRD-166 (alumina + zirconia) fiber, while a boron nitride coating was used for the Nextel 480 (alumina + silica + boria) fiber. Coatings were applied by chemical vapor deposition (CVD). Important parameters in the coating process, in order to obtain a uniform coating on the fiber surface, are the deposition temperature and time. Tin dioxide coating forms an effective barrier between alumina and glass, and thereby prevents strong chemical bonding between the components of this composite system. Improvements in mechanical properties can be achieved by incorporation of such fibers into a brittle matrix. The primary mode of toughening in coated PRD-166/glass composites is crack deflection and fiber bridging while in coated Nextel/glass and Saphikon/glass composites, fiber pullout also occurs. A strong potential exists for enhancing toughness even further, provided the surface roughness of the interfaces can be controlled. Preliminary tests carried out on smooth single crystal alumina fiber reinforced glass matrix composites have indicated that extensive fiber matrix debonding and pullout can result. GRA

N92-31361# Illinois Univ., Urbana-Champaign. National Center for Composite Materials Research.
A PROPOSAL FOR THE ESTABLISHMENT OF A CENTER FOR ADVANCED COMPOSITE MATERIALS RESEARCH Final Report
James Economy Mar. 1992 59 p
(Contract N00014-86-K-0799)
(AD-A250072) Avail: CASI HC A04/MF A01

A key objective of the ONR-URI Center is to conduct basic research on critical materials science, mechanics, and structural problems currently confronting the Navy and to be encountered in its future use of advanced composite materials. The current emphasis of the Center's research thrust is placed on thick-section structural composites and composite structures, since these subjects have been identified as major potential problem areas of concern in the present and future high-performance Navy structural systems. The research program had three major thrusts, namely: (1) materials design and selection; (2) processing of thick filament wound cylinders; and (3) mechanical behavior of thick section composites. GRA

N92-31378# New York Univ., New York. Inst. of Mathematical Sciences.
MATHEMATICAL PROBLEMS IN MICROMECHANICS AND COMPOSITE MATERIALS Final Report, 1 Feb. 1989 - 31 Jan. 1992
Robert V. Kohn, Marco Avellaneda, and Graeme W. Milton 1991 26 p
(Contract DAAL03-91-G-0084)
(AD-A249584; ARO-28283.3-EG) Avail: CASI HC A03/MF A01

This is the final technical report on ARO Contract DAAL03-89-K-0039, which began February 1, 1989 and terminated January 31, 1992. The scientific focus of this work is at the frontier where mathematics meets the materials sciences. Physically, we are concerned with the effective moduli of composites, the formation of fine scale structure in coherent phase transitions, and with oscillatory solutions of nonlinear partial differential equations from continuum mechanics. Mathematically, we bring to bear a variety of tools including homogenization, the calculus of variations, and the theory of stochastic processes. Our

accomplishments include: (1) new bounds on the effective moduli of two-component and polycrystalline composites; (2) a new understanding of the role of surface energy in coherent phase transitions; and (3) rigorous results on the effective diffusivity due to a turbulent velocity field. The training of young scientists, both postdocs and students, has been a major part of our activity.
GRA

N92-31382# Naval Air Development Center, Warminster, PA. Air Vehicle and Crew Systems Technology Dept.
CORROSION BEHAVIOR OF SQUEEZE CAST ALUMINUM METAL MATRIX COMPOSITES Final Report
Vinod S. Agarwala and Alan S. Fabiszewski Dec. 1991 36 p
(AD-A250486; NADC-91122-60) Avail: CASI HC A03/MF A01

Corrosion behavior of metal matrix composites (MMC) vary greatly with the reinforcement material type, processing conditions, and methods of fabrication into engineering parts. The corrosion susceptibilities for the MMC arise from the segregations of the reinforcement material during fluid flow (extrusion) and/or processing, and from the resulting compositional differences in the alloy, the matrix material. These differences set-up galvanic cells and cause preferential corrosion. The metal matrix composites studied were Al 6061/Al2O3 and Al 356/SiC. In particular, the effects of near-net-shape processing called squeeze casting (solidification of liquid under pressure) was investigated. The results showed that regions which were clustered with SiC or Al203 were microstructurally sensitive to preferential corrosion. Electrochemical - potentiodynamic polarization and controlled potential corrosion behavior measurements were made and related to microstructural segregation through metallographic optical microscopic analysis.
GRA

N92-31506*# National Aeronautics and Space Administration. Lewis Research Center, Cleveland, OH.
COMPUTATIONAL SIMULATION OF INTERMINGLED-FIBER HYBRID COMPOSITE BEHAVIOR
Subodh K. Mital (Toledo Univ., OH.) and Christos C. Chamis Mar. 1992 11 p Presented at the 37th International SAMPE Symposium and Exhibition, Anaheim, CA, 9-12 Mar. 1992
(RTOP 510-01-50)
(NASA-TM-105666; E-7028; NAS 1.15:105666) Avail: CASI HC A03/MF A01

Three-dimensional finite-element analysis and a micromechanics based computer code ICAN (Integrated Composite Analyzer) are used to predict the composite properties and microstresses of a unidirectional graphite/epoxy primary composite with varying percentages of S-glass fibers used as hydridizing fibers at a total fiber volume of 0.54. The three-dimensional finite-element model used in the analyses consists of a group of nine fibers, all unidirectional, in a three-by-three unit cell array. There is generally good agreement between the composite properties and microstresses obtained from both methods. The results indicate that the finite-element methods and the micromechanics equations embedded in the ICAN computer code can be used to obtain the properties of intermingled fiber hybrid composites needed for the analysis/design of hybrid composite structures. However, the finite-element model should be big enough to be able to simulate the conditions assumed in the micromechanics equations.
Author

N92-31566*# Virginia Polytechnic Inst. and State Univ., Blacksburg. Dept. of Engineering Science and Mechanics.
AN EXPERIMENTAL PROCEDURE FOR THE IOSIPESCU COMPOSITE SPECIMEN TESTED IN THE MODIFIED WYOMING FIXTURE
Henjen Ho, Ming-Yi Tsai, John Morton, and G. L. Farley (National Aeronautics and Space Administration. Langley Research Center, Hampton, VA.) 1991 24 p
(Grant NAG1-1053)
(NASA-CR-190660; NAS 1.26:190660) Avail: CASI HC A03/MF A01

A detailed description is given of the experimental procedure for testing composite Iosipescu specimens in the modified Wyoming fixture. Specimen preparation and strain gage instrumentation are addressed. Interpretation of the experimental results is discussed. With the proper experimental procedure and setup, consistent and repeatable shear properties are obtained.
Author

N92-31604# Virginia Polytechnic Inst. and State Univ., Blacksburg. Dept. of Engineering Science and Mechanics.
ROLE OF INTERFACES AND INTERPHASES IN THE EVOLUTION MECHANICS OF MATERIAL SYSTEMS Final Report, 1 Dec. 1990 - 1 Dec. 1991
K. Reifsnider, W. Stinchcomb, D. Dillard, R. Swain, and K. Jayaraman 26 Mar. 1992 173 p
(Grant AF-AFOSR-0216-89)
(AD-A250410; AFOSR-92-0398TR) Avail: CASI HC A08/MF A02

The general objective of this investigation was to apply the discipline of mechanics to the prediction and description of the long-term behavior of composite materials by developing experimental information, conceptual understanding, and analytical representations of the evolution of the properties of constituent materials and interfaces in composite material systems as a function of time during the application of time-variable mechanical, thermal, and chemical loadings. The general approach to this objective was to develop mechanistic representations of the 'state of the material' under those conditions, and to join those descriptions with micromechanical descriptions of the 'state of stress' in 'critical elements' to support an estimate of remaining strength, and thereby, to predict remaining life. The current program focused on the role of interfaces and interphases in the evolution mechanics of material systems. The objective of the program was to achieve accurate and realistic representations of the geometry, arrangement, properties, and property distributions (as a function of space) associated with the region between fibers and matrix material in continuous and short fiber reinforced composite materials, to develop engineering methods of characterizing the interphasal strength, and to use a critical element method to extend these findings to the prediction of the changes in stiffness and strength.
GRA

N92-31609# National Inst. of Standards and Technology, Boulder, CO. Materials Reliability Div.
CRYOGENIC 4.4 MN MECHANICAL TEST SYSTEM FOR LARGE SCALE TESTS OF COMPOSITE SUPPORT STRUTS
R. P. Walsh, R. P. Reed, J. D. McColskey, W. Fehringer, and J. R. Berger Mar. 1992 40 p
(PB92-181148; NISTIR-3966; B91-0161) Avail: CASI HC A03/MF A01

Details of a large mechanical test program undertaken by the NIST Materials Reliability Division are presented. These tests were intended to validate the full scale structural behavior of the composite support struts in a thermal and mechanical environment identical to actual service conditions. Two types of tests were performed: ultimate compressive strength and fatigue. Thermal conditions for the tests ranged from isothermal, room temperature tests to an imposed thermal gradient of cryogenic-to-room temperatures. The development of the unique facility necessary for the large scale cryogenic tests is detailed.
Author

N92-31716# Messerschmitt-Boelkow-Blohm G.m.b.H., Munich (Germany, F.R.).
CUTTING TREATMENT BY DRILLING OF FIBER BOUND SYNTHETIC MATERIALS [SPANENDE BEARBEITUNG DURCH BOHREN VON FASERVERBUND-KUNSTSTOFFEN]
J. Pelzl 1991 73 p In GERMAN Presented at the Deutsche Industrieforum fuer Technologie Conference, Berlin, Fed. Republic of Germany, 11-12 Nov. 1991
(MBB-UD-0609-91-PUB; ETN-92-91889) Avail: CASI HC A04/MF A01

It is shown that the quality of bore holes in fiber bound synthetic materials is influenced by a number of limiting conditions. The most important factors affecting the use are related to the type of fiber and matrix system, fiber structure and laminate texture, laminate thickness and bore hole diameter, other materials in hybrid

texture, accessibility and usable machines, used cutting geometry and cutting material, selected cutting velocities and forward feeding. It is not possible to give a general 'recipe' for the boring of fiber bound synthetic materials. ESA

N92-31806# Northwestern Univ., Evanston, IL. Dept. of Physics and Astronomy.
ENERGETICS, BONDING MECHANISM AND ELECTRONIC STRUCTURE OF METAL/CERAMIC INTERFACES
A. J. Freeman 1992 6 p
(Contract DE-FG02-88ER-45372)
(DE92-013401; DOE/ER-45372/4) Avail: CASI HC A02/MF A01

Among the tremendous variety of oxide materials currently used for technological applications, those based on titanium and vanadium oxides are not only among the most important, but are also the most intriguing. Relatively small changes in crystallographic modifications and valencies of metal atoms, as the wide class of Magnelli phases and related compounds, may result in abrupt metal-insulator transitions and sharp changes of magnetic ordering with critical temperatures that may vary in the hundreds of degrees range. When doped by other transition, or s and p metals, these oxides exhibit a vast variety of complicated cooperative phenomena, starting from unusual ferroelectricity up to superconductivity at moderately high temperatures. Most of these unusual materials have been extensively studied and used in the bulk or polycrystalline thin film form. For the fabrication of novel devices of micron or submicron sizes; however, single crystal films and superlattices are preferred or required. Moreover, one may expect that such 'man-made' artificial structures will reveal new and unusual physical properties. These are the reasons for the renaissance in experimental and theoretical investigations of these oxides that is now occurring. DOE

N92-31823# Air Force Inst. of Tech., Wright-Patterson AFB, OH.
THERMOMECHANICAL FATIGUE BEHAVIOR OF A SILICONE CARBIDE FIBER-REINFORCED CALCIUM ALUMINOSILICATE GLASS-CERAMIC MATRIX COMPOSITE M.S. Thesis
Lawrence M. Butkus 1991 139 p
(AD-A249870; AFIT/CI/CIA-91-126) Avail: CASI HC A07/MF A02

Ceramic matrix composites are being considered for use in advanced turbine engines and other applications where thermomechanical fatigue (TMF) conditions exist. Isothermal fatigue and in-phase TMF tests were performed on a unidirectional, continuous-fiber, Nicalon reinforced calcium aluminosilicate glass-ceramic material (O16, SiC/CAS-11). Monotonic tensile tests were performed at 1100 C (2012 F) and 100 MPa/sec to determine the material's ultimate strength and proportional limit. Isothermal fatigue tests at 1100 C (2012 F) employed two loading profiles, a triangular waveform with ramp times of 60 seconds, and a similar profile with a superimposed 60 second hold time. These tests used a maximum stress of 100 MPa (40 percent of sigma(sub pl)), R = 0.1. TMF loading profiles were identical to the isothermal loading profiles. During the TMF tests, the temperature was cycled between 500 and 1100 C (932 and 2012 F) in time with the load. Run out was arbitrarily set at 1000 cycles for all fatigue profiles. All fatigued specimens reached run out and were tested in tension at 1100 C and 100 MPa/sec immediately following the isothermal and thermomechanical tests. Residual modulus, residual strength, hysteretic modulus, and strain accumulation were all explored as possible damage indicators. Strain accumulation appeared to be the parameter which allowed for the greatest distinction to be made among the types of tests performed. Author

N92-31854*# Sverdrup Technology, Inc., Brook Park, OH.
TAILORED METAL MATRIX COMPOSITES FOR HIGH-TEMPERATURE PERFORMANCE
M. R. Morel, D. A. Saravanos (Ohio Aerospace Inst., Brook Park.), and C. C. Chamis (National Aeronautics and Space Administration. Lewis Research Center, Cleveland, OH.) Mar. 1992 24 p
Presented at the 37th International SAMPE Symposium and Exhibition, Anaheim, CA, 9-12 Mar. 1992; sponsored by the Society for the Advancement of Materials and Processing Engineering Sponsored by NASA. Lewis Research Center
(RTOP 510-01-08)
(NASA-TM-105816; E-7247; NAS 1.15:105816) Avail: CASI HC A03/MF A01

A multi-objective tailoring methodology is presented to maximize stiffness and load carrying capacity of a metal matrix cross-ply laminated at elevated temperatures. The fabrication process and fiber volume ratio are used as the design variables. A unique feature is the concurrent effects from fabrication, residual stresses, material nonlinearity, and thermo-mechanical loading on the laminate properties at the post-fabrication phase. For a (0/90)(sub s) graphite/copper laminate, strong coupling was observed between the fabrication process, laminate characteristics, and thermo-mechanical loading. The multi-objective tailoring was found to be more effective than single objective tailoring. Results indicate the potential to increase laminate stiffness and load carrying capacity by controlling the critical parameters of the fabrication process and the laminate. Author

N92-31912# Oak Ridge National Lab., TN.
RADIATION DAMAGE IN CARBON-CARBON COMPOSITES
T. D. Burchell, W. P. Eartherly, and G. E. Nelson 1992 4 p
Presented at the International Conference on Carbon: Carbon 1992, Essen, Fed. Republic of Germany, 22-26 Jun. 1992
(Contract DE-AC05-84OR-21400)
(DE92-011778; CONF-920628-2-Extd-Abst) Avail: CASI HC A01/MF A01

Graphite and carbon-carbon composite materials are widely used in plasma facing applications in current tokamak devices such as TFTR and D3D in the USA, JET, Tore Supra and TEXTOR in Europe, and JT-60U in Japan. Carbon-carbon composites are attractive choices for tokamak limiters and diverters because of their low atomic number, high thermal shock resistance, high melting point, and high thermal conductivity. Next generation machines such as the International Thermonuclear Experimental Reactor (ITER) will utilize carbon-carbon composites in their first wall and diverter. ITER will be an ignition machine and thus will produce substantial neutron fluences from the D-T fusion reaction. The resultant high energy neutrons will cause carbon atom displacements in the plasma facing materials which will markedly affect their structure and physical properties. The effect of neutron damage on graphite has been studied for over forty years. Recently the effects of neutron irradiation on the fusion relevant graphite GraphNOL N3M was reviewed. In contrast to graphite, relatively little work has been performed to elucidate the effects of neutron irradiation on carbon-carbon composites. The results of our previous irradiation experiments have been published elsewhere. Here the irradiation induced dimensional changes in 1D, 2D, and 3D carbon-carbon composites are reported for fluences up to 4.7 dpa at an irradiation temperature of 600 C. DOE

N92-31940# Factory Mutual Research Corp., Norwood, MA.
FLAMMABILITY CHARACTERISTICS OF GLASS REINFORCED EPOXY COMPOSITE MATERIALS Final Report, Oct. 1990 - Dec. 1991
Archibald Tewarson Feb. 1992 31 p
(Contract DAAL04-90-M-0746; DA Proj. 162-63102-D-071)
(AD-A251009; MTL-TR-92-8) Avail: CASI HC A03/MF A01

Fiber reinforced composite (FRC) materials are used extensively because of their favorable physico-chemical properties and high strength-to-weight ratio. The use of composites in Army vehicles as a means of decreasing weight and enhancing survivability, without reducing personnel safety, has been under study for some time. Although FRC materials are very attractive in terms of their physico-chemical properties, concern for possible fire hazards is understandable, as organic polymers are a major constituent of the materials. This report presents flammability evaluation results for three FRC materials (MTL 6 to 7). In this evaluation, the latest technology developed at Factory Mutual Research Corporation (FMRC) was used. In comparison to ordinary combustibles, such as cellulosics and most non-fire retarded

plastics, the three FRC materials have higher resistance to ignition and flame propagation. In comparison to the FRC materials (MTL 1 to 5) investigated in the previous study for the Army Materials Technology Lab, the three FRC materials were found to ignite more easily, and flame propagated beyond the ignition zone. Also, these three materials generated significantly higher amounts of material vapors, CO, smoke, and heat than the materials examined earlier (MTL 1 to 5). Thus passive fire protection is required for these materials. This protection can be provided by surface coatings or by surface lamination using highly fire resistant FRC materials such as the fiberglass phenolic examined in the previous study. GRA

N92-31979# FIMOD Corp., Blacksburg, VA.
OPTICAL FIBER SENSORS FOR ORGANIC MATRIX COMPOSITE MATERIAL CURE MONITORING Final Report
Bernd D. Zimmermann 15 Apr. 1991 67 p
(Contract DAAL04-90-C-0013)
(AD-A247114) Avail: CASI HC A04/MF A01

The report describes experiments that were conducted to demonstrate the feasibility of a novel optical fiber based composite cure monitoring technique. Preliminary investigations were conducted using a fast cure, industrial grade epoxy in a neat resin environment. Neat resin tests were demonstrated using a more common composite resin, Hercules' 3501-6 material. A neat resin cure monitoring station, which allowed repeatable cure monitoring results, was developed. A cure monitor assembly which addressed practical feasibility issues, was also developed. This assembly made it possible to interface the relatively fragile resin fiber elements with standard all-silica lead fibers without requiring micro-positioning equipment for alignment. In order to simplify the data acquisition process during the cure monitoring cycle, a PC-Basic routine was written which allowed continuous retrieval of data from a multi-channel optical meter as well as conventional thermocouples. This routine was used to perform cure monitoring measurements on Hercules 3501-6/AS4 composite coupons. Normalized transmitted power as a function of cure was monitored and showed correlation to the neat resin experiments conducted earlier. GRA

N92-32047# Northrop Corp., Hawthorne, CA. Aircraft Div.
COMPOSITE FAILURE ANALYSIS HANDBOOK. VOLUME 1: PROGRAM REVIEW Final Report, 1 Jan. 1987 - 31 Oct. 1990
R. J. Kar Feb. 1992 184 p
(Contract F33615-87-C-5212)
(AD-A250520; WL-TR-91-4032-Vol-1; DOT/FAA/CT-91/23-Vol-1) Avail: CASI HC A09/MF A02

The objective of this program was to create a comprehensive handbook for use in conducting failure analysis investigations on failed composite structure. This program builds upon previous efforts as documented in the 'Compendium of Post-Failure Analysis Techniques for Composite Materials'. The purpose of creating this handbook was to document the techniques, the fractographic and material property data, and case history studies currently being utilized in the analysis of failed composite structure. The major tasks on this program included: (1) procedural guidelines for field investigation techniques; (2) an expanded fractographic data base for carbon/epoxy materials tested under known conditions; (3) a fractographic data base for resin based composite materials other than carbon/epoxy; (4) fractographic documentation of composite material and processing defects; (5) documentation of fracture characteristics in adhesive and mechanical joint failures; (6) compilation of material property data for composite materials; and (7) documentation of case histories recently conducted on failed composite structure. GRA

N92-32048# Northrop Corp., Hawthorne, CA. Aircraft Div.
COMPOSITE FAILURE ANALYSIS HANDBOOK. VOLUME 2: TECHNICAL HANDBOOK. PART 1: PROCEDURES AND TECHNIQUES Final Report, 1 Jan. 1987 - 31 Oct. 1990
R. J. Kar Feb. 1992 266 p
(Contract F33615-87-C-5212)
(AD-A250521; WL-TR-91-4032-Vol-2-Pt-1;
DOT/FAA/CT-91-23-Vol-2-Pt-1) Avail: CASI HC A12/MF A03

The objective of this program was to create a comprehensive handbook for use in conducting failure analysis investigations on failed composite structure. This program builds upon previous efforts as documented in the 'Compendium of Post-Failure Analysis Techniques for Composite Materials'. The purpose of creating this handbook was to document the techniques, the fractographic and material property data and case history studies currently being utilized in the analysis of failed composite structure. The major tasks of this program included: (1) procedural guidelines for field investigation techniques; (2) an expanded fractographic data base for carbon/epoxy materials tested under known conditions; (3) a fractographic data base for resin based composite materials other than carbon/epoxy; (4) fractographic documentation of composite material and processing defects; (5) documentation of fracture characteristics in adhesive and mechanical joint failures; (6) compilation of material property data for composite materials; and (7) documentation of case histories recently conducted on failed composite structure. GRA

N92-32064# Naval Postgraduate School, Monterey, CA.
THE EFFECT OF THERMOMECHANICAL PROCESSING PARAMETERS ON THE AMBIENT BEHAVIOR OF 10 PERCENT VOLUME 6061 Al-ALUMINA M.S. Thesis
David Eastwood, Jr. Mar. 1992 88 p
(AD-A252177) Avail: CASI HC A05/MF A01

Thermomechanical processing was conducted on a 10 percent (by volume) 6061 Alumina particle reinforced metal matrix composite (MMC). The TMP employed consisted of isothermal rolling with intermediate annealing, using a schedule of reduction with constrain strain per pass. The as-processed material exhibited high strength while simultaneously achieving ductility comparable to that of the unreinforced 6061 matrix alloy. In the fully annealed condition, the composite's strength and ductility were essentially equal to those of the unreinforced aluminum. An aging study showed accelerated aging and greater peak strength for the composite. Finally, a process and heat treatment combination was established in an attempt to optimize simultaneously the strength and ductility of the composite. It was found that the composite could be aged to a peak strength of 340 MPA while retaining a ductility of 14 percent elongation to failure. GRA

N92-32075# Texas A&M Univ., College Station. Dept. of Mechanical Engineering.
THE MECHANICS OF FRACTAL DAMAGE Final Report
Ted L. Anderson and Sun Yongqi 30 Mar. 1992 35 p
(Grant AF-AFOSR-0373-90)
(AD-A250518; CMC-6730-15; AFOSR-92-0397TR) Avail: CASI HC A03/MF A01

This report describes a preliminary investigation of the applicability of fractal geometry to damage modeling. Microstructural heterogeneity, both the size distribution and spatial distribution of microstructural features, can be modeled simply and compactly with a fractal dimension. The ultimate goal of this research is the development of an alternative to continuum damage and micromechanics models. The scaling nature of fractal geometry may aid the development of models that connect microscale damage with global mechanical response. An assumed fractal size distribution of microcracks in a brittle solid was used to derive the Weibull distribution for strength, and a relationship between the Weibull shape parameter and the fractal dimension of the flaw distribution was obtained. Published data on the strength of glass fibers were consistent with a fractal flaw distribution. Stable damage evolution in tougher materials with fractal microstructures was also considered. Although preliminary results are promising, further work is necessary to develop the concepts of fractal damage more fully. GRA

N92-32104# Howard Univ., Washington, DC. Dept. of Mechanical Engineering.
EIGENSENSITIVITY ANALYSIS OF COMPOSITE LAMINATES: EFFECT OF MICROSTRUCTURE Final Report, 1 Nov. 1989 - 31 Oct. 1990
Robert Reiss and Taft H. Broome Feb. 1992 77 p
(Contract F49620-89-C-0003)
(AD-A250864; AFOSR-92-0401TR) Avail: CASI HC A05/MF A01

The purpose of this research is to develop new methods to determine how the frequency of laminates depends upon the microstructure of each individual layer. Toward this end, modern methods of sensitivity analysis are employed to develop new closed-form representations for the frequency response of laminates, where the governing eigenvalue equation is represented either in distributed parameter or discrete form. Solutions are obtained for both damped and undamped structures in terms of the aggregate micromechanical properties (stiffnesses and damping coefficients). Thus the solutions are valid for all macromechanical models of the microstructure. One new method for determining the effective stiffness and mass properties of the laminate - the Load Correction Method - is developed in detail and some of the computational issues associated with this method are discussed.
GRA

N92-32135# Allied-Signal Aerospace Co., Kansas City, MO.
TITANIUM CARBON NITRIDE COATING
S. D. Nance Apr. 1992 9 p
(Contract DE-AC04-76DP-00613)
(DE92-013158; KCP-613-4650) Avail: CASI HC A02/MF A01

The purpose of this investigation was to determine the advantages of titanium carbon nitride (TiCN) coated tools. Cutting tests were conducted comparing TiCN coating directly against titanium nitride (TiN) coated and uncoated T-15 CPM end mills.
DOE

N92-32159*# Washington Univ., Seattle. Dept. of Mechanical Engineering.
AN INVESTIGATION OF THE THERMOVISCOPLASTIC BEHAVIOR OF A METAL MATRIX COMPOSITE AT ELEVATED TEMPERATURES Final Report
John R. Rogacki and Mark E. Tuttle Sep. 1992 160 p
(Grant NAG1-974)
(NASA-CR-190700; NAS 1.26:190700) Avail: CASI HC A08/MF A02

The response of a fiberless thirteen layer hot isostatically pressed Ti-15-3 laminate to creep, constant strain rate, and cyclic constant strain rate loading at temperatures ranging from 482 to 649 C was investigated. Creep stresses from 48 to 260 MPa and strain rates of .0001 to .01 m/m/sec were used. Material parameters for three unified constitutive models (Bodner-Partom, Miller, and Walker models) were determined for Ti-15-3 from the experimental data. Each of the three models was subsequently incorporated into a rule of mixtures and evaluated for accuracy and ease of use in predicting the thermoviscoplastic response of unidirectional metal matrix composite laminates (both 0 and 90 degrees). The laminates were comprised of a Ti-15-3 matrix with 29 volume percent CSC6 fibers. The predicted values were compared to experimentally determined creep and constant strain rate data. It was found that all three models predicted the viscoplastic response of the 0 degree specimens reasonably well, but seriously underestimated the viscoplastic response of the 90 degree specimens. It is believed that this discrepancy is due to compliant and/or weak fiber-matrix interphase. In general, it was found that of the three models studied the Bodner-Partom model was easiest to implement, primarily because this model does not require the use of cyclic constant strain rate tests to determine the material parameters involved. However, the version of the Bodner-Partom model used in this study does not include back stress as an internal state variable, and, hence, may not be suitable for use with materials which exhibit a pronounced Baushinger effect. The back stress is accounted for in both the Walker and Miller models; determination of the material parameters associated with the Walker model was somewhat easier than in the Miller model.
Author

N92-32215# Defence Research Establishment Pacific, Victoria (British Columbia). Research and Development Branch.
MOTION MODEL FOR THE CORRECTION OF POINT SOURCE DISTORTION IN RADIOGRAPHS OF HONEYCOMB
J. E. Boyd Sep. 1988 18 p
(DREP-88-14; CTN-92-60337) Avail: CASI HC A03/MF A01

Problems are encountered from point-source, non-parallel radiation when a honeycomb material is radiographed. Radiation passing through the honeycomb parallel to cell walls forms a clear and undistorted image of the structure. Other radiation forms a distorted image of the structure. The distortion is manifested as blurring of the cell walls. This report proposes a numerical method which can be applied to digital image processing to compensate for distortion in honeycomb radiographs due to point-source radiation. The method is based on a model for the system which assumes that the radiation source is parallel, and that the distortion is caused by motion during the integration of the radiograph. Models for motion blurring are well understood, so a motion blur can be corrected. The result is that by treating the point-source distortion as motion blurring, the distortion can be corrected, within the constraints of the model. The theoretical basis of the motion model for point-source distortion in honeycomb is presented, and the technique used to correct the distortion is outlined. Results from computer simulation and from actual radiographs are presented.
CISTI

N92-32234*# National Aeronautics and Space Administration. Lewis Research Center, Cleveland, OH.
EFFECTS OF FIBER AND INTERFACIAL LAYER ARCHITECTURES ON THE THERMOPLASTIC RESPONSE OF METAL MATRIX COMPOSITES
Marek-Jerzy Pindera (Virginia Univ., Charlottesville.), Alan D. Freed, and Steven M. Arnold Aug. 1992 38 p
(RTOP 519-01-50)
(NASA-TM-105802; E-7232; NAS 1.15:105802) Avail: CASI HC A03/MF A01

Examined here is the effect of fiber and interfacial layer morphologies on thermal fields in metal matrix composites (MMCs). A micromechanics model based on an arbitrarily layered concentric cylinder configuration is used to calculate thermal stress fields in MMCs subjected to spatially uniform temperature changes. The fiber is modelled as a layered material with isotropic or orthotropic elastic layers, whereas the surrounding matrix, including interfacial layers, is treated as a strain-hardening, elastoplastic, von Mises solid with temperature-dependent parameters. The solution to the boundary-value problem of an arbitrarily layered concentric cylinder under the prescribed thermal loading is obtained using the local/global stiffness matrix formulation originally developed for stress analysis of multilayered elastic media. Examples are provided that illustrate how the morphology of the SCS6 silicon carbide fiber and the use of multiple compliant layers at the fiber/matrix interface affect the evolution of residual stresses in SiC/Ti composites during fabrication cool-down.
Author

25 INORGANIC AND PHYSICAL CHEMISTRY

Includes chemical analysis, e.g., chromatography; combustion theory; electrochemistry; and photochemistry.

For related information see also *77 Thermodynamics and Statistical Physics.*.

N92-31268 Department of the Navy, Washington, DC.
WAVEGUIDE-BINDING SENSOR FOR USE WITH ASSAYS Patent
Richard B. Thompson, inventor (to Navy) and Carl A. Villarruel, inventor (to Navy) 29 Oct. 1991 8 p Filed 9 Nov. 1990

(AD-D015230; US-Patent-5,061,857; US-Patent-Appl-SN-610895; US-Patent-Class-250-458.1) Avail: US Patent and Trademark Office

An optical waveguide-binding sensor which increases sensor sensitivity to fluorescence detection during assays of liquids based on adjustments in the V number along the optical waveguide are presented. The sensing waveguide includes a mode converting section where the V number of the waveguide gradually increases from the distal sensing end of the mode converting section to the proximal end of the mode converting section. The gradually change in V number can be accomplished by either gradually inwardly tapering waveguide along the sensor portion from the proximal end, or by gradually varying the dopant concentration along the sensing portion. The sensor tapers in diameter to change the V number along the distal end of the optical waveguide. The present invention increases the efficiency of fluorescence detection by converting weakly-guided high-order modes of fluorescence radiation at the distal end into lower-order modes at the proximal and increases the efficiency of fluorescent excitation by converting the low order mode entering the proximal end into weakly-guided high order modes at the sensing end. At the sensing end, these weakly guided modes strengthen the evanescent excitation wave. GRA

N92-31292# University of Northern Illinois, De Kalb. Dept. of Chemistry.

INTERFACIAL ION TRANSPORT BETWEEN IMMISCIBLE LIQUIDS

Petr Vanysek 24 Jun. 1992 52 p

(Contract N00014-91-J-1058)

(AD-A252424; TR-042) Avail: CASI HC A04/MF A01

The interface between two immiscible liquids is used as a characteristic boundary for study of charge equilibrium, adsorption and transport. Interfacial potential differences across the liquid/liquid boundary are explained theoretically and documented in experimental studies with fluorescent, potential sensitive dyes. The results show that presence of an inert salt or a physiological electrolyte is essential for the function of the dyes. Impedance measurements are used for studies of bovine serum albumin adsorption on the interface. Ways of determining liquid/liquid capacitance influenced by BSA presence are shown. The potential of zero charge of the interface was obtained for zero to 200 ppm of BSA. The impedance behavior is also discussed as a function of pH. A recent new approach, using microinterface for interfacial ion transport, is outlined. GRA

N92-31301# Army Lab. Command, Watertown, MA. Material Technology Lab.

CHARACTERIZATION OF OXIDE FORMED ON SILICON BY EXPOSURE TO ATOMIC OXYGEN IN SPACE Final Report

Louise C. Sengupta, Judith S. Brodkin, Wolfgang Frnzen, and Paul L. Sagalyn Feb. 1992 23 p

(AD-A249787; MTL-TR-92-1) Avail: CASI HC A03/MF A01

The oxide formed on silicon by exposure to space on the long duration exposure facility (LDEF) has been examined using variable angle spectroscopic ellipsometry (VASE), Fourier transform infrared spectroscopy (FTIR), and X-ray photoelectron spectroscopy (XPS). The position of the silicon specimen on the satellite resulted in the formation of an oxide whose thickness varied with distance along the sample surface. Each transverse section of the surface was studied separately and compared to a region on the sample shielded from the oxygen flux in space by an aluminum bar. Film thickness and composition of the oxide were determined by a least square fit of the VASE data to a model surface using an effective medium approximation. The results revealed a nonporous oxide film with a thickness that increased from 350 A to 1200 A almost linearly along the sample. Furthermore, all of the experiments revealed an oxygen deficiency that increases with film thickness. Several other techniques were also performed on the sample to confirm these results. These results can be used to identify some of the oxide deposition parameters which occurred in the environment of the LDEF. GRA

N92-31393# Ballistic Research Labs., Aberdeen Proving Ground, MD.

TOMOGRAPHIC RECONSTRUCTION OF INFRARED SPECTRA OF NONHOMOGENEOUS MEDIA: APPLICATIONS TO A FLAT FLAME BURNER Final Report, Sep. - Dec. 1991

Kevin L. McNesby and Robert A. Fifer Apr. 1992 31 p

(DA Proj. 1L1-61102-AH-43)

(AD-A249999; BRL-TR-3333) Avail: CASI HC A03/MF A01

We are using computed tomography, a radiological imaging technique, to obtain species profiles within a flame as a function of height above the burner surface and lateral position at that height. This information is extracted from parallel line-of-sight absorbance data using a technique known as Abel inversion. This process yields two dimensional 'slices' of the flame. At any point within each slice the infrared spectrum of the species present may be obtained. Abel inversion is a special application of computerized tomography which may be applied only to systems possessing axial symmetry. We have used this technique to evaluate line-of-sight spectra of a low pressure (less than 100 torr) premixed methane/nitrous oxide burner flame. The flame is supported on a water-cooled, stainless steel cylindrical frit which sits inside a low pressure chamber. Parallel line-of-sight infrared spectra through the low pressure chamber are inverted to give the radial dependence of infrared absorption at each wavelength of the spectrum. This data is used to evaluate the performance of the low pressure burner and to discriminate against cold gases which may obscure absorbances of trace species within the flame. GRA

N92-31414# Lawrence Livermore National Lab., CA.

PROPANE OXIDATION THROUGH THE NEGATIVE TEMPERATURE COEFFICIENT REGION AT 10 AND 15 ATMOSPHERES: RESULTS OF EXPERIMENTAL AND MODELING STUDIES

D. N. Koert, K. Jaouabi, D. L. Miller, N. P. Cernansky (Drexel Univ., Philadelphia, PA.), W. J. Pitz, and C. K. Westbrook 10 Dec. 1991 21 p Presented at the 24th International Symposium on Combustion, Sydney (Australia), 5-10 Jul. 1992

(Contract W-7405-eng-48)

(DE92-007902; UCRL-JC-109757; CONF-920707-23) Avail: CASI HC A03/MF A01

A detailed chemical kinetic mechanism for propane oxidation was used to successfully model experimental data through the range of temperatures (650 - 800 K) corresponding to the negative temperature coefficient (NTC) region encountered by engine end-gas just prior to knocking. An important feature of the mechanism is that it models alkylperoxy radical reactions using only uncoupled, parallel reaction paths. The results show that the overall mechanism is most sensitive to changes in the rate of the reactions which produce diperoxy radicals, i.e., that low temperature branching is dominated by decomposition of diperoxy radicals instead of alkylhydroperoxide branching. The calculated concentration versus temperature profiles for all species qualitatively reproduced the NTC behavior indicated by the experimental species data. The fuel consumption and the major product species, propene and carbon monoxide, were accurately predicted over the entire temperature range. While the calculations accurately reproduced the qualitative behavior of the profiles for the minor species, the concentration levels of these species were generally overpredicted. An attempt was made to model the experimental data using another propane oxidation mechanism which employs a coupled, multichannel unimolecular scheme to model alkylperoxy radical reactions and was found to be unable to reproduce the NTC behavior. However, when a direct path for the reaction R + O2 (yields) olefin + HO2 was added to the mechanism, NTC behavior emerged. DOE

N92-31415# Lawrence Livermore National Lab., CA.

HIGH-TEMPERATURE IGNITION OF PROPANE WITH MTBE AS AN ADDITIVE: SHOCK-TUBE EXPERIMENTS AND MODELING

J. A. Gray (Sandia National Labs., Livermore, CA.) and C. K. Westbrook Dec. 1991 22 p Presented at the 24th International

Symposium on Combustion, Sydney (Australia), 5-10 Jul. 1992
(Contract W-7405-eng-48)
(DE92-008933; UCRL-JC-106910; CONF-920707-22) Avail: CASI HC A03/MF A01

Ignition of propane was studied in a shock tube and by computational modeling to determine the effect of methyl tert-butyl ether (MTBE) as a fuel additive. MTBE and isobutene were added in amounts up to 25 percent of the fuel to propane-oxygen-argon mixtures to shock-tube experiments covering a range of temperatures between 1450 and 1800 K. Ignition delays were measured from chemiluminescence at 432 nm due to excited CH radicals. The temperature dependence of the ignition rates was analyzed to yield Arrhenium parameters of E(sub a) is approximately 40 kcal/mol and log(A) is approximately 9.0 sec(exp -1) for the overall reaction. Reactions involving MTBE and its decomposition products were combined with an established propane mechanism in a numerical model to describe the kinetic interaction of this additive with a typical hydrocarbon fuel. The experiments and the kinetic model both show that MTBE and isobutene retard propane ignition with nearly equal efficiency. The kinetic model demonstrates that isobutene kinetics are responsible for inhibition by both MTBE and isobutene, and the specific elementary reactions which produce this behavior are identified. DOE

N92-31416# Lawrence Livermore National Lab., CA.
TWO-STAGE N-BUTANE FLAME: A COMPARISON BETWEEN EXPERIMENTAL MEASUREMENTS AND MODELING RESULTS
C. Corre, F. L. Dryer (Princeton Univ., NJ.), W. J. Pitz, and C. K. Westbrook Feb. 1992 25 p Presented at the 24th International Symposium on Combustion, Sydney (Australia), 5-10 Jul. 1992
(Contracts W-7405-eng-48; DE-FG04-87AL-43771)
(DE92-009457; UCRL-JC-109756; CONF-920707-25) Avail: CASI HC A03/MF A01

Two stage autoignition processes in unburned end-gases are generally considered to be responsible for homogeneously-initiated engine knock phenomena. Two-stage flame processes were investigated to achieve a better understanding of the low temperature and high temperature chemistry responsible for this type of autoignition behavior. A stabilized n-butane two-stage flame was numerically simulated, utilizing a detailed kinetic mechanism involving 141 species and 850 elementary reactions, and results are compared with experimental data obtained from a one dimensional, two-stage flame burner. With the exception of those for butenes and hydroperoxyl radicals, calculated and experimental profiles are found to agree within a factor of two over the entire flame region. Under the fuel rich conditions studied, CH3O and OH radicals are found to be the principal reactive radicals in the cool flame region. A decrease in the estimated rate of reactions R + HO2 = RO + OH (R = C3H5, CH3, C2H5, and C4H7) is required to obtain agreement of fuel profiles between the two flame zones. In the second stage region, predicted reaction profiles are in general agreement with the experiment, with the exception of formaldehyde and C4-oxygenated species, for which consumptions are substantially underestimated. This study suggests that the reaction channel for direct metathesis and stabilized hot adduct formation for the overall process C4H9 + O2 (yields) C4H8 + HO2 need further attention. DOE

N92-31417# California Univ., Berkeley. Lawrence Berkeley Lab.
FLAME FRONT GEOMETRY IN PREMIXED TURBULENT FLAMES
I. G. Shepherd and W. T. Ashurst (Sandia National Labs., Livermore, CA.) Dec. 1991 18 p Presented at the 24th International Symposium on Combustion, Sydney (Australia), 5-10 Jul. 1992
(Contracts DE-AC03-76SF-00098; DE-AC04-76DR-00789)
(DE92-010310; LBL-31590; CONF-920707-26; SAND-92-8504C)
Avail: CASI HC A03/MF A01

Experimental and numerical determinations of flame front curvature and orientation in premixed turbulent flames are presented. The experimental data is obtained from planar, cross sectional images of stagnation point flames at high Damkoehler number. A direct numerical simulation of a constant energy flow is combined with a zero-thickness, constant density flame model to provide the numerical results. The computational domain is a 32(exp 3) cube with periodic boundary conditions. The two-dimensional curvature distributions of the experiments and numerical simulations compare well at similar q'/S(sub L) values with means close to zero and marked negative skewness. At higher turbulence levels the simulations show that the distributions become symmetric about zero. These features are also found in the three dimensional distributions of curvature. The simulations support assumptions which make it possible to determine the mean direction cosines from the experimental data. This leads to a reduction of 12 percent in the estimated flame surface area density in the middle of the flame brush. DOE

N92-31434# South Carolina Univ., Columbia. Dept. of Chemistry.
SYNTHESIS OF SOLUBLE ALPHA-THIOPHENE OLIGOMERS. MONOMER TO OCTAMER
James M. Tour and Ruilian Wu 25 Apr. 1992 31 p
(Contract N00014-89-J-3062)
(AD-A250082; TR-9) Avail: CASI HC A03/MF A01

Described is the detailed synthesis of alpha-thiophene oligomers ranging from the monomer to the octamer that are silylated at the alpha' and omega positions. The terminal trimethylsilyl groups allow the monomer, dimer, and trimer to be freely soluble in numerous organic solvents. The higher homologs, trimer through octamer have, in addition to the terminal trimethylsilyl groups, methyl groups symmetrically substituting one or more of the thiophene units in order to enhance the solubility of the systems. Methyl substitution can not be on the 3-position of terminal thiophene units or else rapid protodesilylation occurs in thiophene oligomeric intermediates greater than two units long. The UV-visible spectroscopic characteristics of the synthesized oligomers suggest that, in solution, electrochemically prepared poly(3alkyl-a-thiopbene) effectively has only 6-7 contiguous conjugated alpha-thiophene units. However, in the solid state, the effective conjugation path in the polymer is much longer. The effect of d(pi)-p(pi)-conjugation between the terminal silicon atom and the conjugated system was also investigated by executing the quantitative protodesilylation of the pentameric oligothiophene. GRA

N92-31441# Argonne National Lab., IL.
ECONOMICS OF MICROWAVE PLASMA DISSOCIATION OF H2S
E. J. Daniels, J. B. L. Harkness, and R. D. Doctor 1992 10 p Presented at the American Institute of Chemical Engineers Spring Meeting, New Orleans, LA, 29 Mar. - 2 Apr. 1992
(Contract W-31-109-eng-38)
(DE92-014846; ANL/CP-76034; CONF-920310-10) Avail: CASI HC A02/MF A01

The conventional treatment technology for hydrogen-sulfide is based on Claus chemistry; elemental sulfur is recovered but the hydrogen is lost as water, although the fuel value of the hydrogen is recovered as heat. A new waste treatment technology, reported in the Soviet literature, has been validated in an experimental program at Argonne National Laboratory. The new technology uses microwave energy to dissociate hydrogen-sulfide and recovers both elemental sulfur and hydrogen. Recovery of the hydrogen provides for its reuse for its chemical value. A comparative economic analysis of the microwave technology and conventional sulfur recovery and tail-gas treatment technology such as Claus/SCOT is presented. The sensitivity of the comparative economics to process variables such as dissociation energy and conversion rate, and cost variables, such as the value of hydrogen and the cost-of-electricity is evaluated. Under the conditions of this analysis, the conclusion is that it is more cost-effective to recover the hydrogen for its chemical value via microwave dissociation rather than to accept its conversion to water and effective use as a fuel. DOE

N92-31524# Massachusetts Inst. of Tech., Cambridge. Dept. of Chemistry.

F Mo(CHCMe2Ph)(NAr)(OR)2 AND RELATIVE REACTIVITY TOWARD 2,3-BIS(TRIFLUOROMETHYL) NORBORNADIENE IENE

John H. Oskam and Richard R. Schrock 1 May 1992 15 p
(Contract N00014-89-J-1542)
(AD-A250234; MIT-TR-17) Avail: CASI HC A03/MF A01

Anti rotamers of Mo(CHCMe2Ph)(NAr)(OR)2 complexes (Ar = 2,6-C6H3-i-Pr2; OR = OCMe2(CF3), OCMe(CF3)2, and OC(CF3)2(CF2CF2CF3)) can be generated at -80 deg in toluene by photolysis at 366 nm and the rate of conversion of anti to syn rotamers determined by NMR methods. At equilibrium the anti rotamers can be observed by high field proton NMR at 250 after many transients and values for Keq(syn/anti) thereby determined. Keq can be determined at O deg when OR = OCMe3 and k anti/syn estimated. The rate of conversion of the anti to the syn rotamer in toluene is found to vary by at least five orders of magnitude as the alkoxide is changed from t-butoxide to OC(CF3)2(CF2CF2CF3). The results in TBF are analogous, although the rates of rotamer interconversion are much slower for any given alkoxide. Addition of 2,3-bis(trifluoromethyl)norbornadiene to mixtures containing both anti and syn Mo(CHCMe2Ph)-(NAr)(OCMe(CF3)2)2 showed that in both toluene and TBF the anti-rotamer was orders of magnitude more reactive than the syn rotamer.

GRA

N92-31565# Ames Lab., IA.

ROBOTIC SOIL SAMPLER FOR HAZARDOUS WASTE CLEAN UP

E. J. Jaselskis 1992 9 p Presented at the 9th International Symposium on Automation and Robotics in Construction, Tokyo (Japan), 3-5 Jun. 1992
(Contract W-7405-eng-82)
(DE92-012693; IS-M-703; CONF-9206157-1) Avail: CASI HC A02/MF A01

An innovative field sampling system using LA-ICP-AES (laser ablation-inductively coupled plasma -- atomic emission spectrometry) technology is currently being developed through an integrated team approach at Ames Laboratory to provide in-situ, real time analysis of inorganic hazardous waste. This sampling approach is conducted through a mobile testing facility which consists of an instrumentation vehicle called the Mobile Demonstration Laboratory for Environmental Screening Technologies (MDLEST), and an attached trailer called the Robotic Sampling Accessory (RSA). The RSA provides automated sampling capabilities through an attached three-degree-of-freedom robot that will be equipped with surface and subsurface sampling probes. The probes are currently being designed by a multidisciplinary team consisting of engineers and scientists at Ames Laboratory, Iowa State University, and Lockheed. This system is expected to improve sample quality assurance, reduce sampling time and cost, and improve worker safety. Limitations and future areas of research for the MDLEST-RSA are also discussed.

DOE

N92-31607# Lawrence Livermore National Lab., CA.

HYDROCARBON IGNITION: AUTOMATIC GENERATION OF REACTION MECHANISMS AND APPLICATIONS TO MODELING OF ENGINE KNOCK

C. Chevalier (Stuttgart Univ., Germany, F.R.), J. Warnatz (Stuttgart Univ., Germany, F.R.), W. J. Pitz, and C. K. Westbrook Feb. 1992 23 p Presented at the 24th International Symposium on Combustion, Sydney (Australia), 5-10 Jul. 1992
(Contract W-7405-eng-48)
(DE92-011943; UCRL-JC-109758; CONF-920707-29) Avail: CASI HC A03/MF A01

A computational technique is described which automatically develops detailed chemical kinetic reaction mechanisms for large aliphatic hydrocarbon fuel molecules. This formulation uses the LISP language to apply general rules which identify the chemical species produced, the reactions between these species, and the elementary reaction rates for each reaction step. Reaction mechanisms for cetane (n-hexadecane) and most alkane fuels C(sub 7) and smaller are developed using this automatic technique, and detailed sensitivity analyses for n-heptane and cetane are described. These reaction mechanisms are then applied to calculation of knock tendencies in internal combustion engines. The model is used to study the influence of fuel molecule size and structure on knock tendency, to examine knocking properties of fuel mixtures, and to determine the mechanisms by which pro-knock and anti-knock additives change knock properties.

DOE

N92-31671# California Univ., Berkeley. Lawrence Berkeley Lab.

PERFORMANCE OF MULTIPLE STREAM PULSED JET COMBUSTION SYSTEMS

J. A. Maxson, D. M. Hensinger, K. Hom, and A. K. Oppenheim 1991 12 p
(Contract DAAL03-87-K-0123)
(AD-A249722; ARO-25245.4-EG) Avail: CASI HC A03/MF A01

In the course of our studies on pulsed jet combustion (PJC) a series of tests were carried out to determine the performance of multi-stream systems. This included multi-jet efflux, as well as dual-generator aggregates. The essential performance indicator of a PJC system is the pressure transducer record, yielding, in particular, data on the rise time and amplitude of the pressure pulse, as well as the rate of pressure rise. Concomitantly with pressure measurements, a sequence of schlieren records were obtained to reveal the salient features of the fluid mechanical phenomena of the PJC process. Elucidated thereby are the effects of entrainment induced by large scale vortex structures of turbulent jet plumes, and their decisive role in governing the process of combustion, as influenced by their particular configuration. Our tests demonstrated the capability of multiple stream PJC systems to shorten the rise time and increase the amplitude of the pressure pulse, both effects of obvious potential benefit to engine performance.

GRA

N92-31678# California Univ., Berkeley. Dept. of Mechanical Engineering.

IGNITION AND FLAME PROPAGATION STUDIES OVER A FLAT FUEL SURFACE Ph.D. Thesis

B. T. Amos Mar. 1992 149 p
(Grant NANB7D737)
(PB92-181056; NIST/GCR-92/604) Avail: CASI HC A07/MF A02

Numerical studies are performed which show the evolution of the combustion process over a flat fuel surface subjected to an external source of radiation. Ignition is caused either by the high temperature of the fuel surface or by radiation absorption by the fuel vapor. The surface is assumed to be either in a zero gravity, initially stagnant air environment or in a stagnation point flow field. Regardless of the source of ignition considered or the type of the flow field, the same sequence of events is predicted. The sequence of events begins with a pre-ignition, radiation dominated phase in which fuel and air mix above the fuel surface. After ignition occurs, there is a period of weak chemical reaction, which is followed by a period of stronger reaction in which a premixed flame front develops. Before dying out the premixed flame front separates the fuel from the oxygen and leaves behind a diffusion flame. The combustion and radiation processes are shown to have a large effect on the flow field in the stagnation point flow cases. For the case in which ignition is caused by gas phase absorption, the radiation required to cause ignition is so high that an opposed jet flow is created. In the case in which ignition is caused by the hot surface, the radiation is lower and the boundary layer remains almost intact. For both types of ignition the premixed flame fronts produced heat fast enough that the expanding gas is able to drive the incoming flow back from the fuel surface. After the premixed flame front dies out, leaving the diffusion flame, the incoming flow again dominates and a boundary layer reappears.

Author

N92-31683# Environmental Protection Agency, Research Triangle Park, NC. Air and Energy Engineering Research Lab.
DEVELOPMENT OF A CORE COMBUSTION RESEARCH PROGRAM PLAN FOR EPA Final Report, Sep. 1989 - Feb. 1990
G. B. Martin May 1992 44 p
(Contract EPA-68-02-3365)
(PB92-180868; EPA/600/R-92/084) Avail: CASI HC A03/MF A01

Described here is a plan, evolving from a review of the state of the art in combustion research, for a long term research program in combustion and thermal destruction. A strawman plan was prepared and reviewed by a panel of representatives from industry, academia, and government organizations. The plan identifies four cornerstone areas where technology gaps are perceived to exist and a keystone of basic and engineering research needed to generalize the technological developments to a variety of systems. Author

N92-31717# Massachusetts Univ., Amherst. Dept. of Chemical Engineering.
THEORETICAL STUDIES OF SOLID-FLUID PHASE EQUILIBRIA
P. A. Monson Jun. 1992 6 p
(Contract DE-FG02-90ER-14150)
(DE92-016598; DOE/ER-14150/2) Avail: CASI HC A02/MF A01

This report summarizes research on the molecular theory of solid-fluid phase equilibria. This research has focused upon the influence of molecular shape upon solid-fluid coexistence and on development of a theory for the free energy of mixtures in the solid state. We have completed our extension of the cell model to the case of hard diatomic molecules in the solid state. We have completed an extensive study of the solid-fluid coexistence properties using this theory. Extensive Monte Carlo simulations studies have also been made providing a comprehensive picture of how molecular shape influences the stable crystal structure and solid-fluid equilibria. Comparison of the results from the cell theory confirms the accuracy of the theoretical approach. Using the information from our studies of hard dumbbell systems as a reference system, a generalized van der Waals treatment of solid-fluid equilibria in nonspherical molecules has been made. This theory provides a systematic basis for understanding the dependence upon molecular shape, upon solid-fluid equilibria in general, and upon triple point to critical point property ratios in particular. A cell theory of the free energy of hard sphere mixtures in the solid state has been formulated. The theory correctly predicts the positive volume mixing of hard sphere mixtures in the solid state. DOE

N92-31725# Johns Hopkins Univ., Baltimore, MD. Dept. of Chemistry.
THEORETICAL STUDIES OF THE REACTIONS AND SPECTROSCOPY OF RADICAL SPECIES RELEVANT TO COMBUSTION REACTIONS AND DIAGNOSTICS
D. R. Yarkony Apr. 1992 12 p
(Contract DE-FG02-91ER-14189)
(DE92-013484; DOE/ER-14189/1) Avail: CASI HC A03/MF A01

This report describes the use of our electronic structure algorithms to treat nonadiabatic processes relevant to combustion diagnostics and combustion reactions during the first nine months of Department of Energy grant DE-FG02-91ER14189 and outlines future work to be performed. During this period problems have been addressed in detail: (1) the possibility of using photoionization spectroscopy to detect CH3O; (2) the lifetimes of the individual ro-vibronic levels in OH(v = 3) a state that has been suggested as a fluorescence probe of OH produced in combustion environments; and (3) the basic mechanism for the spin-forbidden initiating step in the Fenimore mechanism for the production of NO in flame fronts. DOE

N92-31729# General Atomic Co., San Diego, CA.
A GLOBAL FITTING CODE FOR MULTICHORDAL NEUTRAL BEAM SPECTROSCOPIC DATA
R. P. Seraydarian, K. H. Burrell, and R. J. Groebner May 1992 11 p Presented at the 9th Topical Conference on High-Temperature Plasma Diagnostics, Santa Fe, NM, 15-19 Mar. 1992
(Contract DE-AC03-89ER-51114)
(DE92-014258; GA-A-20915; CONF-920362-32) Avail: CASI HC A03/MF A01

Knowledge of the heat deposition profile is crucial to all transport analysis of beam heated discharges. The heat deposition profile can be inferred from the fast ion birth profile which, in turn, is directly related to the loss of neutral atoms from the beam. This loss can be measured spectroscopically by the decrease in amplitude of spectral emissions from the beam as it penetrates the plasma. The spectra are complicated by the motional Stark effect which produces a manifold of nine bright peaks for each of the three beam energy components. A code has been written to analyze this kind of data. In the first phase of this work, spectra from tokamak shots are fit with a Stark splitting and Doppler shift model that ties together the geometry of several spatial positions when they are fit simultaneously. In the second phase, a relative position-to-position intensity calibration will be applied to these results to obtain the spectral amplitudes from which beam atom loss can be estimated. This paper reports on the computer code for the first phase. Sample fits to real tokamak spectral data are shown. DOE

N92-31748# Sandia National Labs., Albuquerque, NM.
A SEMICONDUCTOR BRIDGE IGNITED GAS GENERATOR
M. C. Grubelich and R. W. Bickes, Jr. 1992 8 p Presented at the 18th International Pyrotechnics Seminar, Breckenridge, CO, 13-17 Jul. 1992
(Contract DE-AC04-76DP-00789)
(DE92-014049; SAND-92-0021C; CONF-920796-1) Avail: CASI HC A02/MF A01

Compact, lightweight, self-contained gas generator systems are required for a variety of inflation or deployment applications. We designed a generic gas generator employing a semiconductor bridge (SCB) igniter to evaluate the characteristics of the black powder propellant selected. Because of the low ignition energy requirements and rugged design of SCB's, they are ideally suited to the volume, mass, and severe environments for the gas generator applications. In our design, an SCB ignited a pyrotechnic (TiH(1.68)KClO4) which was used to ignite an end-burning consolidated black powder grain. We evaluated the performance of the gas generator using a computer program developed to simulate the combustion of the end-burning propellant grain. This model is in good agreement with the data from our test firings. In addition, we examined direct SCB ignition of black powder as a function of loading pressure and firing-set current. DOE

N92-31752# Clarkson Univ., Potsdam, NY.
ANALYSIS AND COMPUTER TOOLS FOR SEPARATION PROCESSES INVOLVING NONIDEAL MIXTURES
A. Lucia May 1992 10 p
(Contract DE-FG02-86ER-13552)
(DE92-015298; DOE/ER-13552/7) Avail: CASI HC A02/MF A01

The objectives of this research were to continue to further both the theoretical understanding of and the development of computer tools (algorithms) for separation processes involving nonideal mixtures. These objectives were divided into three interrelated major areas: the mathematical analysis of the number of steady-state solutions to multistage separation processes; the numerical analysis of general; related fixed-point methods; and the development and implementation of computer tools for process simulation. DOE

N92-31763# Lawrence Livermore National Lab., CA.
AUTOIGNITION BEHAVIOR OF LEAN MIXTURES: CHEMICAL AND THERMODYNAMICS EFFECTS

P. D. Ronney, M. Shoda, S. T. Waida, C. K. Westbrook, and W. J. Pitz 15 Jan. 1992 19 p Presented at the 24th International Symposium on Combustion, Sydney (Australia), 5-10 Jul. 1992
(Contract W-7405-eng-48)
(DE92-009690; UCRL-JC-109673; CONF-920707-24) Avail: CASI HC A03/MF A01

Knock characteristics of natural gas (NG), 89 octane unleaded gasoline, 2,2-dimethyl butane (22DMB), and methyl tert-butyl ether (MTBE) in stoichiometric and lean fuel-air mixtures were studied in a production 4-cylinder automotive engine. The intake temperature at the knock limit (ITKL) was different for each fuel but always higher in lean mixtures. Gasoline and 22DMB exhibited much greater increases in ITKL than MTBE and NG at lean conditions. Surprisingly, for lean mixtures 22DMB exhibited higher ITKL than MTBE and was almost as high as NG. Comparison with detailed numerical modeling was very favorable. Computations show that both differences in chemistry and end-gas temperature and pressure histories are responsible for these trends. This behavior is interpreted in terms of the negative temperature coefficient behavior of hydrocarbon oxidation. The implication of these results for the specification of optimal fuels for lean-burn engine is discussed. DOE

N92-31772# Ames Lab., IA.
REAL-TIME INFRARED SPECTROSCOPY OF MOVING SOLIDS FOR ON-LINE ANALYSES
R. W. Jones, S. Luo, and J. F. McClelland 1991 4 p Presented at the 8th International Conference on Fourier Tranform Spectroscopy, Lubeck-Travemunde (Germany), 1-6 Sep. 1991
(Contract W-7405-eng-82)
(DE92-012156; IS-M-686; CONF-9109297-2) Avail: CASI HC A01/MF A01

Two related methods, transient infrared emission spectroscopy and transient infrared transmission spectroscopy, can obtain good spectra from opaque, moving solids by using a transient thermal gradient to isolate spectroscopically a thin layer of material. The basic elements of the methods, the ability to depth profile, and an application involving monitoring coating cure are described. DOE

N92-31773# Sandia National Labs., Livermore, CA.
SATURATION EFFECTS IN DEGENERATE FOUR-WAVE MIXING SPECTROSCOPY: NONPERTURBATIVE CALCULATIONS
R. P. Lucht, R. L. Farrow, and D. J. Rakestraw 1992 4 p Presented at the CLEO/QELS 1992, Anaheim, CA, 10-17 May 1992
(Contract DE-AC04-76DR-00789)
(DE92-012253; SAND-92-8495C; CONF-920573-8) Avail: CASI HC A01/MF A01

Saturation, collisional, and Doppler effects for gas-phase degenerate four-wave mixing (DFWM) are investigated through nonperturbative solution of the density matrix equations. The calculated lineshapes and pressure dependence are in excellent agreement with nitric oxide DFWM experiments. DOE

N92-31776# Energy and Environmental Research Corp., Irvine, CA.
TECHNOLOGY ADVANCING RESEARCH COMBUSTION IN BURNERS Annual Report, Aug. 1990 - Jul. 1991
R. Payne and G. S. Samuelsen Apr. 1991 45 p Prepared in cooperation with California Univ., Irvine
(Contract GRI-5089-260-1828)
(PB92-164359; GRI-92/0068) Avail: CASI HC A03/MF A01

The first phase of a three-phase program, the design of a Burner Engineering Research Laboratory (BERL), has been completed. The BERL will be installed at the Sandia National Laboratories Combustion Research Facility in Livermore, California, and will permit the use of advanced laser diagnostics for the study of industrial gas flames. An Industrial and Academic Advisory Group (IAAG) was established to critically review the BERL design. Comments and recommendations from the first meeting of the IAAG are summarized and have been incorporated into the final design. The BERL provides optical access to the combustion zone of 0.1-3.0 MMBtu/h gas burners. The modular design consists of five spool sections, a burner quarl and an exhaust transition. Interchangeable panels containing refractory insulation, windows, probe ports, or cooled walls provide a range of thermal environments and diagnostic access. The design also includes a vertical traverse to move the combustion chamber through the optical diagnostic path and a horizontal traverse to move the diagnostic volume through the furnace. Operational specifications of the BERL for a baseline 1 MMBtu/h firing rate include: 100 percent excess air, 50 percent FGR, 1450 F air preheat, and steam injection at 11 b/lb-fuel. Author

N92-31803# Ballistic Research Labs., Aberdeen Proving Ground, MD.
ABSORPTION SPECTROSCOPY THROUGH THE DARK ZONE OF SOLID PROPELLANT FLAMES Final Report, Oct. 1990 - Oct. 1991
John A. Vanderhoff, M. W. Teague, and Anthony J. Kotlar Apr. 1992 48 p
(DA Proj. 1L1-61102-AH-43)
(AD-A250033; BRL-TR-3334) Avail: CASI HC A03/MF A01

A windowed strand burner with a propellant feed mechanism has been used to characterize the steady state combustion of solid propellants over a pressure environment of 0.1-2.0 MPa nitrogen. Under conditions where a line of sight measurement is meaningful, temperatures and absolute concentrations can be extracted from optical absorption spectra. An arc lamp light source and spectrometer-intensified photodiode array detector systems provided the means to absorption spectra for NO through the dark zone burning solid propellants. Additionally, OH absorption spectra were obtained in the luminous flame region. A least squares fitting program applied to these absorption spectra resulted in a determination of temperature profiles and absolute NO concentrations for JA-2, M-9, and HMX2 solid propellants over a pressure range of 0.3-2.0 MPa. Measured dark zone temperatures ranged from about 1,300 K to 1,600 K and NO concentrations varied from about 15 to 30 mole percent depending upon the propellant type and pressure. Where possible these values are compared with literature data. Temperatures in the luminous flame computed from OH absorption spectra reached values in agreement with adiabatic flame temperatures. Video records of each propellant burn allowed a determination of the propellant burn rate and length of the dark zone as a function of pressure. GRA

N92-31805# Lawrence Livermore National Lab., CA.
NUMERICAL SIMULATION OF TULIP FLAME DYNAMICS
L. D. Cloutman 30 Nov. 1991 20 p Presented at the 24th International Symposium on Combustion, Sydney (Australia), 5-10 Jul. 1992
(Contract W-7405-eng-48)
(DE92-008553; UCRL-JC-109083; CONF-920707-20) Avail: CASI HC A03/MF A01

A finite difference reactive flow hydrodynamics program based on the full Navier-Stokes equations was used to simulate the combustion process in a homogeneous-charge, constant-volume combustion bomb in which an oddly shaped flame, known as a 'tulip flame' in the literature, occurred. The 'tulip flame' was readily reproduced in the numerical simulations, producing good agreement with the experimental flame shapes and positions at various times. The calculations provide sufficient detail about the dynamics of the experiment to provide some insight into the physical mechanisms responsible for the peculiar flame shape. Several factors seem to contribute to the tulip formation. The most important process is the baroclinic production of vorticity by the flame front, and this rate of production appears to be dramatically increased by the nonaxial flow generated when the initial semicircular flame front burns out along the sides of the chamber. The vorticity produces a pair of vortices behind the flame that advects the flame into the tulip shape. Boundary layer effects contribute to the details of the flame shape next to the walls of the chamber, but are otherwise not important. DOE

N92-31816# Oak Ridge K-25 Site, TN.
CERAMIC MEMBRANES FOR HIGH TEMPERATURE HYDROGEN SEPARATION
D. E. Fain, G. E. Roettger, and D. E. White 1992 11 p Presented at the 6th Annual Fossil Energy Materials Conference, Oak Ridge, TN, 12-14 May 1992
(Contract DE-AC05-84OT-21400)
(DE92-013342; K/TCD-1020; CONF-9205123-1) Avail: CASI HC A03/MF A01

Considerable progress has been made toward the development of a porous ceramic membrane that can be used to separate hydrogen from coal gas at temperatures above 1000 F. The essential mechanism for the gas separation is molecular sieving. The pores in the membrane are made so small that the small hydrogen molecules can pass through the membrane much faster than other molecules. Membranes have been made with mean pore diameters of 10 Angstroms. Ideally, the membranes should have a pore diameter of less than 4 and greater than 2.5 Angstroms. There is currently no means for measuring pore diameters of less than about 10 Angstroms. Experiments are under way to evaluate the pore size by measuring the flow rates of gases with spherical symmetry and of different size. For example, helium, argon, methane, carbon tetrafluoride, and sulfur hexafluoride are a good series of gases to use for that purpose. Surface flow and other transport modes complicate the interpretation of the data. A theoretical model will be discussed that is being developed to help interpret the flow and separation data. Flow and separation measurements need to be made at higher temperatures to understand adequately the membrane character. The status of the membrane development, the status of the theoretical model, and some fundamentals of gas separation are discussed. DOE

N92-31820# California Univ., Los Angeles.
CORRELATION FROM RANDOMNESS: QUANTITATIVE ANALYSIS OF SPUTTERED GRAPHITE SURFACES USING THE SCANNING TUNNELING MICROSCOPE Technical Report, 1 Jun. 1991 - 31 May 1992
E. A. Eklund, E. J. Snyder, and R. S. Williams 10 Mar. 1992 62 p
(Contract N00014-90-J-1178)
(AD-A252420; TR-16) Avail: CASI HC A04/MF A01

The Scanning Tunneling Microscope (STM) was used to quantitatively examine the surface morphology of highly oriented pyrolytic graphite (HOPG) surfaces bombarded with 5 key Ar(+) ions. Constant current topographs clearly showed that the morphology of the resulting nonequilibrium surfaces depended sensitively on the ion flux, the ion fluence, and the sample temperature. For low and intermediate ion fluence, an increase in surface roughness with increasing ion flux was observed. For constant ion flux, the surfaces developed structures with heights proportional to the ion fluence and separations characterized by a correlation length that diverged with increasing fluence. Increasing the sample temperature during bombardment produced smoother surfaces as a result of enhanced surface diffusion. The autocovariance function G(L) and the height correlation function, h(q) exp 2, in reciprocal space were calculated directly from the STM topographs. The latter was then compared with a linear response theory for the formation of rough surfaces under nonequilibrium conditions and a scaling analysis. The fluence dependence of the surface roughening of graphite could not be explained by shot noise alone in a linear theory, whereas surface diffusion and redeposition of sputtered material satisfactorily accounted for the correlation observed in the bombardment-induced features. GRA

N92-31857# Argonne National Lab., IL.
ANALYSES AND PREDICTIONS OF THE THERMODYNAMIC PROPERTIES AND PHASE DIAGRAMS OF SILICATE SYSTEMS
M. Blander, A. Pelton (Ecole Polytechnique, Montreal, Quebec), and G. Eriksson (Ecole Polytechnique, Montreal, Quebec) 1992 6 p Presented at the 4th International Conference on Molten Slags and Fluxes, Sendai (Japan), 8-11 Jun. 1992
(Contract W-31-109-eng-38)
(DE92-016177; ANL/CP-76308; CONF-9206196-1) Avail: CASI HC A02/MF A01

Molten silicates are ordered solutions which can not be well-represented by the usual polynomial representation of deviations from ideal solution behavior (i.e., excess free energies of mixing). An adaptation of quasichemical theory which is capable of describing the properties of ordered solutions represents the measured properties of binary silicates over broad ranges of composition and temperature. For simple silicates such as the MgO-FeO-SiO2 ternary system, in which silica is the only acid component, a combining rule generally leads to good predictions of ternary solutions from those of the binaries. In basic solutions, these predictions are consistent with those of the conformal ionic solution theory. Our results indicate that our approach could provide a potentially powerful tool for representing and predicting the properties of multicomponent molten silicates. DOE

N92-31860# Sandia National Labs., Livermore, CA.
UNIMOLECULAR REACTION MECHANISMS INVOLVING C3H4, C4H4, AND C6H6 HYDROCARBON SPECIES
C. F. Melius, J. A. Miller, and E. M. Evleth 1991 28 p Presented at the 24th International Symposium on Combustion, Sydney (Australia), 5-10 Jul. 1992
(Contract DE-AC04-76DR-00789)
(DE92-005326; SAND-91-8718; CONF-920707-5) Avail: CASI HC A03/MF A01

The unimolecular rearrangement processes of unsaturated aliphatic hydrocarbons representative of intermediates in rich hydrocarbon flames have been investigated using the quantum chemical BAC-MP4 method. In particular, we have investigated the unimolecular reaction mechanisms involving (1) allene cyclopropene propyne rearrangement, (2) vinylacetylene pyrolysis leading to acetylene and diacetylene, and (3) various C6H6 compounds, including 1,5-hexadiyne, 1,2,4,5-hexatetraene, and 1,2-hexadin-5-yne leading to 3,4-dimethylenecyclobutene, fulvene, benzene, 2-ethynyl-1,3-butadiene, and other C6H6 species. Rate constants for various reaction steps give good agreement with available experimental measurements. The reaction mechanisms are also consistent with various deuterium isotope labeling experiments. The results indicate that many different types of reaction mechanisms occur, including concerted pathways involving carbene and vinylidene intermediates and insertion reactions of vinylidenes into C-H bonds and C-C multiple bonds. New decomposition pathways are presented for vinylacetylene pyrolysis, for conversion of 1,2-hexadien-5-yne to fulvene, and for conversion of fulvene to benzene. DOE

N92-31891# Colorado State Univ., Fort Collins.
DIOSMACYCLOALKANES AS MODELS FOR THE FORMATION OF HYDROCARBONS FROM SURFACE METHYLENES
J. R. Norton May 1992 4 p
(Contract DE-FG02-84ER-13299)
(DE92-014588; DOE/ER-13299/8) Avail: CASI HC A01/MF A01

We are making progress on our investigation of the mechanism of olefin exchange with Os2(C2H4)(CO) (sub 8). We are probing this system by a kinetic study of the reaction of Os2(C2H4)(CO) (sub 8) with butyl acrylate (BA) under various pressures of ethylene. DOE

N92-31918# Georgia Inst. of Tech., Atlanta. School of Aerospace Engineering.
PULSE COMBUSTION ENGINEERING RESEARCH LABORATORY: EXHAUST ENERGY Annual Report, 1 Sep. 1990 - 31 Aug. 1991
B. T. Zinn, B. R. Daniel, and J. I. Jagoda Oct. 1991 85 p
(Contract GRI-5089-260-1839)
(PB92-172402; GIT-AER-E-16-616; GRI-91/0352) Avail: CASI HC A05/MF A01

A Pulse Combustion Engineering Laboratory (PERL) for the study of novel applications of pulse combustion technology has been established. The laboratory is equipped with state-of-the-art

diagnostic capabilities for investigating oscillatory combustion, fluid mechanics and transport processes. Investigations carried out during the contract period included the determination of the acoustic properties of various pulse combustor components and configurations with and without combustion, using an impedance tube technique. The results were used to explain the contrasting operating characteristics of Helmholtz and Schmidt pulse combustors. A model for predicting the performance of pulse combustors is under development. The PC based model will serve as a long overdue design tool for the development of highly loaded pulse combustors. In addition, the effects of pulsations upon the evaporation of sprays and individual droplets are being investigated. This will lead to a better understanding of the mechanisms by which pulsations enhance heat and mass transfer. The staff of the PERL has initiated numerous interactions with industrial organizations in order to encourage their use of the laboratory's facilities and expertise. Author

N92-31942# European Space Agency, Paris (France).
CONTRIBUTION TO THE MODELLING OF TURBULENT COMBUSTION IN THE CASE OF STABILISATION BY FLAME-LOCK [CONTRIBUTION A LA MODELISATION DE LA COMBUSTION TURBULENTE DANS LE CAS D'UNE STABILISATION PAR ACCROCHE-FLAMMES]
Pascale Gilbank (Office National d'Etudes et de Recherches Aerospatiales, Paris, France) Nov. 1991 208 p Transl. into ENGLISH of French document (Paris, France, ONERA), 1989 Original language document was announced as N91-11090
(ESA-TT-1229; ONERA-NT-1989-8; ETN-92-91387) Avail: CASI HC A10/MF A03

A method for predicting turbulent reactive flows, capable of describing various combustion regimes and of being adapted to realistic reactive schemes, is suggested. In industrial configurations such as the afterburning combustors of aircraft engines, various turbulent combustion regimes can coexist at various locations of the combustor or at various times. The chemical kinetics in these flows are complex and it can be important to predict the variation of the various species involved, both intermediate species which determine the overall reaction rate, and the production of contaminating species. The particular feature of this method, called the PEUL model, is the use of Eulerian balance equations to describe the variation of the variables characterizing the flow; the source term involved in the Eulerian balance equations for the mass fractions of the chemical species is determined by Lagrangian equations. The Lagrangian approach has the advantage of describing the flow from a more phenomenological standpoint. The PEUL model thus allows numerical prediction of multireactive turbulent flows. The PEUL model is applied to a turbulent air/methane premixing flame developing in a two dimensional channel with constant section or in a channel possessing a step behind which a recirculation zone is established. ESA

N92-31959# Nebraska Univ., Lincoln. Dept. of Chemistry.
DIPOLAR INTERACTION ASSISTED EFFECTS ON SECOND HARMONIC GENERATION
H. W. Guan and C. H. Wang 1 Jun. 1992 17 p
(Contract N00014-90-J-1494)
(AD-A252487; TR-16) Avail: CASI HC A02/MF A01

The coefficients for second harmonic generation (SHG) for the 2-methyl 4-nitroaniline/ poly(methyl methacrylate) guest/host system were measured as a function of the NLO chromophore concentration and of the poling field strength. The orientational order parameters (OP) were calculated from the SHG coefficients. The OP's were found to depend on the NLO chromophore concentration. The concentration dependence was associated with Kirkwood's g-factor describing the orientational pair correlation. The ratio of order parameters L33/L31, measured in the weak poling field condition is 3, and independent of the NLO chromophore concentration. This is in agreement with the result of a recent calculation. GRA

N92-31976# Research Triangle Inst., Research Triangle Park, NC.
CATALYTIC CARBON MEMBRANES FOR HYDROGEN PRODUCTION
A. S. Damle and S. K. Gangwal Jan. 1992 71 p
(Contract DE-AC21-89MC-26034)
(DE92-001269; DOE/MC-26034/3083) Avail: CASI HC A04/MF A01

Commercial carbon composite microfiltration membranes may be modified for gas separation applications by providing a gas separation layer with pores in the 1- to 10-nm range. Several organic polymeric precursors and techniques for depositing a suitable layer were investigated. The in-situ polymerization technique was found to be the most promising, and pure component permeation tests with membrane samples prepared with this technique indicated Knudsen diffusion behavior. The gas separation factors obtained by mixed-gas permeation tests were found to depend strongly on gas temperature and pressure indicating significant viscous flow at high-pressure conditions. The modified membranes were used to carry out simultaneous water gas shift reaction and product hydrogen separation. These tests indicated increasing CO conversions with increasing hydrogen separation. A simple process model was developed to simulate a catalytic membrane reactor. A number of simulations were carried out to identify operating conditions leading to product hydrogen concentrations over 90 percent. DOE

N92-31998# Purdue Univ., West Lafayette, IN. Dept. of Chemistry.
ROLE OF THE DOUBLE-LAYER CATION ON THE POTENTIAL-DEPENDENT STRETCHING FREQUENCIES AND BINDING GEOMETRIES OF CARBON MONOXIDE AT PLATINUM-NONAQUEOUS INTERFACES
Joseph D. Roth and Michael J. Weaver Feb. 1992 36 p
(Contract N00014-91-J-1409)
(AD-A246980; TR-116) Avail: CASI HC A03/MF A01

The influences of the double-layer cation upon the electrode potential-dependent infrared spectral properties of saturated CO adlayers on polycrystalline platinum have been examined in acetonitrile, methanol, tetrahydrofuran (THF), and dichloromethane. These solvents were chosen to yield a range of dielectric and solvating environments. Two classes of electrolytes were examined that contain tetraalkylammonium and alkali metal cations. For each solvent containing the former electrolytes, near-exclusive terminal CO coordination was observed throughout the accessible potential range (from ca -2.5 to 1 V vs ferrocenium-ferrocene), as evidenced by a single potential-dependent C-O stretching band at ca 2040-2090/cm. The nus sub vo frequency-potential slopes depend significantly on the size of the tetraalkylammonium cation. This dependence is approximately consistent with the expectations of a simple doublelayer model featuring a linear potential drop throughout the inner layer, with the position of the outer Helmholtz plane being determined by the CO adlayer thickness plus the unsolvated cation radius. The infrared spectra in alkali metal (Li(+), Na(+), K(+)) electrolytes yielded a similar terminal nu sub vo feature, which is replaced entirely at relatively negative potentials by a band at ca 1730-1800/cm. This effect is ascribed to a potential-induced conversion from terminal to multifold CO coordination geometries, driven by Lewis acid-base interactions. GRA

N92-32029# Pittsburgh Univ., PA. Dept. of Chemical and Petroleum Engineering.
PROBE MOLECULE STUDIES: ACTIVE SPECIES IN ALCOHOL SYNTHESIS
D. G. Blackmond Apr. 1992 9 p
(Contract DE-FG22-90PC-90305)
(DE92-015430; DOE/PC-90305/T6) Avail: CASI HC A02/MF A01

The goal of this research is to develop a better understanding of the mechanisms of formation of alcohols and other oxygenates from syngas over supported catalysts. Probe molecules will be added in situ during the reaction to help delineate reaction pathways

and identify reaction intermediate species. The key of our study is to investigate how the species generated by these probe molecules interact with surface species present during oxygenate formation. DOE

N92-32057# Emory Univ., Atlanta, GA. Dept. of Chemistry.
UV PHOTOCHEMISTRY OF TRIVINYLANTIMONY ADSORBED ON QUARTZ
J. A. Tarr, S. P. Lee, and M. C. Lin 1991 22 p
(Contract N00014-89-J-1235)
(AD-A252215) Avail: CASI HC A02/MF A01

The surface photochemistry of trivinylantimony adsorbed on a cold quartz surface was investigated using pulsed, 193 nm excimer-laser radiation. The major desorption products observed were C2H2, C2H3, C2H4, C4H6, Sb, Sb(C2H3), Sb(C2H3)2, Sb(C2H3)3, and Sb2. Photoproduct distributions and their Maxwell Boltzmann characteristic temperatures were determined using time-of-flight mass spectrometry, incorporating both electron impact and, for Sb detection, resonance enhanced multiphoton ionization. Photoproduct yields and Maxwell-Boltzmann temperatures were dependent on photon fluence, sample dosage, and surface temperature. The Maxwell-Boltzmann temperatures of the CxHy products were substantially lower than those of the metallic and organometallic species, indicating that the desorption of the Sb-containing products probably occurs via electronically excited states. A mechanism is given for the photochemistry of adsorbed trivinylantimony. GRA

N92-32076# TRW Space Technology Labs., Redondo Beach, CA.
LASER-INITIATED CONICAL DETONATION WAVE FOR SUPERSONIC COMBUSTION, PART 3
G. F. Carrier, F. E. Fendell, and M. S. Chou Jul. 1992 12 p
(Contract F49620-90-C-0070)
(AD-A250522; AFOSR-92-0420TR) Avail: CASI HC A03/MF A01

Further theoretical and experimental studies are undertaken of the feasibility of an air-breathing supersonic combustor based on a stabilized, conically configured (oblique) detonation wave. The conical wave is the resultant of the interaction of a train of spherical detonation waves, each directly initiated by a brief, localized deposition of energy from a very-rapidly-repeated pulsed laser. The laser is tightly focused on a fixed site (in the combustor) where there is a steady uniform supersonic stream of combustible gas. Simple analysis and laboratory experiments on the (nonintrusive) direct initiation of an individual spherical detonation wave by a single laser pulse are reported, with emphasis on the pulse-energy and pulse-duration parameters. Then, an estimate is given of the entropy production associated with the interaction of spherical detonations created in a supersonic reactive stream by a train of laser pulses. The entropy production, which arises from reflected shocks in already-detonated mixture, is reduced either by increasing the repetition rate of the laser or by increasing the flow speed of the cold-gas mixture. GRA

N92-32080# Colorado State Univ., Fort Collins. Dept. of Chemistry.
NEAR-IR ABSORPTION SPECTRA FOR THE BUCKMINSTERFULLERENE ANIONS: AN EXPERIMENTAL AND THEORETICAL STUDY
Del R. Lawson, Daniel L. Feldheim, Colby A. Foss, Peter K. Dorhout, C. Michael Elliott, Bruce A. Parkinson, and Charles R. Martin 8 May 1992 12 p Submitted for publication
(Contract N00014-82-K-0612; NSF CHE-85-16904; NR Proj. 627838)
(AD-A250532; TR-71) Avail: CASI HC A03/MF A01

C60 can exist in a number of oxidation states including C60(sup 1-), C60(sup 2-) and C60(sup 3-). Ultraviolet-visible absorption data have been described. Near-infrared absorption data have not been presented for any of the oxidation states of C60. We have discovered that this is a serious oversight, because near-IR absorption peaks which are unique to C60(sup 1-), C60(sup 2-) and C60(sup 3-) are observed upon one, two and three electron electrochemical reductions of C60. We have rationalized the energies and intensities of these electronic absorptions based on modifications of the known molecular orbital diagram for C60. The near-IR absorptions reported here should provide a clear and unambiguous route for determining the oxidation state of C60 in solution. GRA

N92-32093# Midwest Research Inst., Golden, CO.
SYNTHESIS OF CRESOLS AND XYLENOLS FROM PHENOL AND METHANOL
H. W. Prengle, Jr., X. vanTran, K. Moinzadeh, F. A. Bricout, and S. Alam (Houston Univ., TX.) Apr. 1992 38 p
(Contract DE-AC02-83CH-10093)
(DE91-002141; NREL/TP-253-4276) Avail: CASI HC A03/MF A01

This report is the first of two reports that concern the manufacture of the same chemicals using two processes - a conventional catalytic process and a solar photothermal catalytic process - to determine the relative process economics. The results of a process study and evaluation for the synthesis of cresols and xylenols using a conventional catalytic process are presented. The solar photothermal catalytic process is evaluated in the second report on the synthesis of cresols and xylenols from benzene and methanol. The process was a vapor-phase methylation of phenol using a high mole ratio of methanol over a solid acidic catalyst. An arbitrary base case plant size (fresh feed) of about 7 million kg/y (15.3 million lbm/y) was chosen and then escalated to a breakeven size. It was concluded that if a chemical company could obtain a fair share of the market, an estimated profitable operation would result for a plant size greater than 12.80 E6 kg/y of fresh feed. DOE

N92-32113# Oregon Graduate Center for Study and Research, Beaverton.
FUNDAMENTAL STUDIES IN OXIDATION-REDUCTION IN RELATION TO WATER PHOTOLYSIS
J. K. Hurst 1991 11 p
(Contract DE-FG06-87ER-13664)
(DE92-014333; DOE/ER-13664/5) Avail: CASI HC A03/MF A01

Our research has been directed at understanding three elementary processes that are central to developing membrane-based integrated chemical systems for water photolysis. These are: (1) the role of interfaces in charge separation/recombination reactions, (2) pathways for transmembrane charge separation, and (3) mechanisms of water oxidation catalyzed by transition metal coordination complexes. Historically, the chemical dynamics of each of these processes has been poorly understood, with numerous unresolved issues and conflicting viewpoints appearing in the literature. Our experimental systems comprise primarily unilamellar vesicles that have been doped with amphiphilic viologens which function as transmembrane charge relays. These systems are experimentally highly tractable and versatile, are conceptually simple, and have been widely used in a variety of organized microphase media and prototypic devices. As such, they are ideal for identifying basic principles governing reactivity. DOE

N92-32117# UOP, Inc., Des Plaines, IL.
THE DEVELOPMENT OF PRECIPITATED IRON CATALYSTS WITH IMPROVED STABILITY
H. Abrevaya May 1992 14 p
(Contract DE-AC22-87PC-79812)
(DE92-014630; DOE/PC-79812/T7) Avail: CASI HC A03/MF A01

The objective of this program is to identify the chemical principles governing the deactivation of precipitated iron catalysts during Fischer-Tropsch synthesis and to use these chemical principles in the design of catalysts suitable for slurry reactors. The performance targets are 88 percent CO+H2 conversion with less than 1 percent deactivation/day for 1 month and a methane and ethane selectivity of no more than 7 percent (based on

hydrocarbons and oxygenates only) at a space velocity of at least 2 normal liters per hr gram iron (NL/hr/gFe) using a synthesis gas with 0.5-1.0 H(sub 2):Co ratio in a slurry reactor. DOE

N92-32141# Pennsylvania State Univ., University Park. Center for Advanced Materials.
CATALYST DISPERSION AND ACTIVITY UNDER CONDITIONS OF TEMPERATURE-STAGED LIQUEFACTION
A. Davis, H. H. Schobert, G. D. Mitchell, and L. Artok Feb. 1992 27 p
(Contract DE-AC22-89PC-89877)
(DE92-014112; DOE/PC-89877/9) Avail: CASI HC A03/MF A01

The general objectives of this research are as follows: (1) to investigate the use of highly dispersed catalysts for the pretreatment of coal by mild hydrogenation; (2) to identify the active forms of the catalysts under reaction conditions; and (3) to clarify the mechanisms of catalysis. The ultimate objective is to ascertain if mild catalytic hydrogenation resulting in very limited or no coal solubilization is an advantageous pretreatment for the transformation of coal into transportable fuels. The experimental program will focus upon the development of effective methods of impregnating coal with catalysts, evaluating the conditions under which the catalysts are most active and establishing the relative impact of improved impregnation on conversion and product distributions obtained from coal hydrogenation. DOE

N92-32145# Lawrence Livermore National Lab., CA.
EVOLUTION OF REACTANTS FLUID VOLUME IN TURBULENT JETS
A. L. Kuhl, J. Bell, R. E. Ferguson (Naval Surface Warfare Center, Silver Spring, MD.), K. Y. Chien (Naval Surface Warfare Center, Silver Spring, MD.), and J. P. Collins (Naval Surface Warfare Center, Silver Spring, MD.) Jan. 1992 14 p Presented at the 24th International Symposium on Combustion, Sydney (Australia), 5-10 Jul. 1992
(Contract W-7405-eng-48)
(DE92-011298; UCRL-JC-108986; CONF-920707-27) Avail: CASI HC A03/MF A01

Numerical simulations of the evolution of an axisymmetric gaseous fuel jet penetration into a liquid oxidizer were performed with a multifluid version of a high-order Godunov code. The fuel jet was unstable and rapidly broke up into mixing structures with a variety of length scales. The complexity of the mixing increased with increased grid resolution. However, grid refinement studies demonstrated that the reactants volume (i.e., the fuel volume within specified concentration limits) rapidly converged to a solution that was insensitive to the mesh size. DOE

N92-31883# Oregon State Univ., Corvallis. Dept. of Mechanical Engineering.
INCIPIENT AND TOTAL GROUP COMBUSTION OF FUEL SPRAYS IN AIR
I. Peleg (Rafael Armament Development Authority, Haifa, Israel) and A. M. Kanury *In* Israel Society of Aeronautics and Astronautics, 31st Israel Annual Conference on Aviation and Astronautics 22 Feb. 1990 p 162-170 Previously announced in IAA as A91-43096 (For primary document see N92-31861 22-01)
Avail: CASI HC A02/MF A03

N92-31884# Technion - Israel Inst. of Tech., Haifa. Faculty of Aerospace Engineering.
TRANSPORT AND EVAPORATION EFFECTS IN COUNTERFLOW SPRAY DIFFUSION FLAMES
N. Sarig and J. B. Greenberg *In* Israel Society of Aeronautics and Astronautics, 31st Israel Annual Conference on Aviation and Astronautics 22 Feb. 1990 p 171-178 Previously announced in IAA as A91-43097 (For primary document see N92-31861 22-01)
Avail: CASI HC A02/MF A03

26 METALLIC MATERIALS

Includes physical, chemical, and mechanical properties of metals, e.g., corrosion; and metallurgy.

N92-31243# Polish Academy of Sciences, Warsaw. Inst. Podstawowych Problemow Techniki.
STUDIES OF THE EFFECT OF STRAIN VELOCITY ON MECHANICAL PROPERTIES OF THE 34GS STEEL [BADANIE WPLYWU PREDKOSCI ODKSZTALCENIA NA WLASCIWOSCI MECHANICZNE STALI 34 GS]
Lech Dietrich and Marek Sliwowski 1992 50 p In POLISH
Avail: CASI HC A03/MF A01

Results of dynamic tests performed on 34GS steel for moderate strain velocities up to 2 l/s are presented. The relationship between the upper yield point and plastic flow delay time versus strain velocity was determined. A digital measuring technique was used and processing of experimental data was automated. Author

N92-31360# Pratt and Whitney Aircraft, West Palm Beach, FL.
FATIGUE IN SINGLE CRYSTAL NICKEL SUPERALLOYS Interim Report, 16 Mar. - 15 Apr. 1992
Charles Annis 15 Apr. 1992 10 p
(Contract N00014-91-C-0124)
(AD-A250068; PWA-FR2198-06) Avail: CASI HC A02/MF A01

This program investigates the seemingly unusual behavior of single crystal airfoil materials. The fatigue initiation processes in single crystal (SC) materials are significantly more complicated and involved than fatigue initiation and subsequent behavior of a (single) macrocrack in conventional, isotropic materials. To understand these differences is the major goal of this project. GRA

N92-31391# Lawrence Livermore National Lab., CA.
THE SYNTHESIS AND CHARACTERIZATION OF NEW COPPER COORDINATION COMPLEXES CONTAINING AN ASYMMETRIC COORDINATING CHELATE LIGAND: APPLICATION TO ENZYME ACTIVE SITE MODELING
M. W. Droege, J. H. Satcher, Jr., R. A. Reibold, and T. J. R. Weakely (Oregon Univ., Eugene.) Jan. 1992 9 p Presented at the American Chemical Society National Meeting, San Francisco, CA, 5-10 Apr. 1992
(Contract W-7405-eng-48)
(DE92-011532; UCRL-JC-109210; CONF-920444-21) Avail: CASI HC A02/MF A01

A new class of ligand which produces a binuclear metal complex with coordination asymmetry was designed and synthesized. A binuclear copper complex was prepared and characterized including a single crystal x-ray structure analysis. The structure reveals that one copper is 5-coordinate (distorted square pyramidal) while the other copper is only 4-coordinate (distorted square planar), and they are separated by an endogenous (mu)-alkoxo oxygen and a bridging acetate. Although this structural type of chelator has been found in biological systems, it has not been previously described for inorganic coordination complexes prepared by design. It is anticipated that this ligand and derivatives of it will play an important role in mimicking chemical reactivity of enzyme active sites that function by substrate interaction at only one metal of a multimetal active site. DOE

N92-31418# Oak Ridge National Lab., TN.
EXPERIMENTAL STUDIES OF ALUMINUM SOLUBILITY AND SPECIATION IN BRINES
D. J. Wesolowski and D. A. Palmer 1992 4 p Presented at the 7th Water-Rock Interaction Conference, Park City, UT, 9-23 Jul. 1992
(Contract DE-AC05-84OR-21400)
(DE92-010448; CONF-920761-4) Avail: CASI HC A01/MF A01

The solubility of gibbsite, AlOH3, was measured in the following: (1) Na(+)-H(+) -Al3(+)-Cl(-) brines to 70 C and 5 molal ionic strength; (2) Na(+)K(+)-OH(-)-Cl(-) -AlOH4(-) brines to 80 C and 5 molal; and (3) at 50 C in 0.1 molal NaCl with the H(+) concentration controlled by acetate, bis-tris, and tris buffers at -log(H(+)) - 3 to 9. The activity coefficient ratios, ((gamma)Al3(+))

/ ((gamma)H(+))(exp 3) and ((gamma)AlOH4(-)) / ((gamma)OH(-)), were modeled in the 0 - 100 C range using the Pitzer ion interaction treatment. Complexes of Al3(+) with acetate and AlOH4(-) with bis-tris were identified. Our results indicate that complexation of Al3(+) by chloride is insignificant in this temperature range. The formation constants of AlOH2(+) were quantitatively determined by potentiometric titrations in the range 25 - 125 C and 0 - 5 molal ionic strength in NaCl media. After correcting for complexation of aluminum ions with the buffers, our solubility data at near neutral pH's are shown to be in quantitative agreement with the potentiometric results. DOE

N92-31575# Argonne National Lab., IL.
RADIATION-INDUCED CRYSTALLINE-TO-AMORPHOUS TRANSITION IN INTERMETALLIC COMPOUNDS OF THE Cu-Ti ALLOY SYSTEM
N. Q. Lam, P. R. Okamoto, R. Devanathan, and M. J. Sabochick (Gulf States Utilities Co., Beaumont, TX.) Feb. 1992 26 p Presented at the Fall Meeting of the Minerals, Metals and Materials Society of AIME and Materials Week of the American Society of Metals, Cincinnati, OH, 20-24 Oct. 1991 Submitted for publication
(Contract W-31-109-eng-38)
(DE92-010276; ANL/CP-75586; CONF-911003-24) Avail: CASI HC A03/MF A01

Recent progress in molecular-dynamics studies of radiation-induced crystalline-to-amorphous transition in the ordered intermetallic compounds of the Cu-Ti system is discussed. The effect of irradiation was simulated by the generation of Frenkel pairs, which resulted in both the formation of stable point defects and chemical disorder upon defect recombination. The thermodynamic, structural and mechanical responses of the compounds during irradiation were determined by monitoring changes in the system potential energy, volume expansion, pair correlation function, diffraction patterns, and elastic constants. It was found that the intermetallics Cu4Ti3, CuTi, and CuTi2 could be rendered amorphous by the creation of Frenkel pairs, but Cu4Ti could not, consistent with experimental observations during electron irradiation. However, the simulations showed that Cu4Ti did become amorphous when clusters of Frenkel pairs were introduced, indicating that this compound may be susceptible to amorphization by heavy-ion bombardment. A generalization of the Lindemann criterion was used to develop a thermodynamic description of solid-state amorphization as a disorder-induced melting process. DOE

N92-31584# Joint Publications Research Service, Arlington, VA.
JPRS REPORT: SCIENCE AND TECHNOLOGY. CENTRAL EURASIA: MATERIALS SCIENCE
30 Jun. 1992 40 p Transl. into ENGLISH from various Russian articles
(JPRS-UMS-92-010) Avail: CASI HC A03/MF A01

Given here is a bibliography of Central Eurasian materials science. Topics covered include analysis and testing, protective coatings, ferrous and nonferrous metals, alloys, nonmetallic materials, metal working, and mining. Author

N92-31610# Helsinki Univ. of Technology, Espoo (Finland). Lab. of Materials Processing and Powder Metallurgy.
THERMODYNAMIC ASSESSMENT OF THE Cr-Zr SYSTEM
K. Zeng, M. Haemaelaeinen, and R. Luoma 1992 19 p
(PB92-180645; TKK-V-B66; ISBN-951-22-0857-1) Avail: CASI HC A03/MF A01

An optimized set of thermodynamic functions of the Cr-Zr system was obtained using phase diagram data from the literature. The excess free energies of the solution phases, liquid and three terminal solid solutions, were described by the Redlich-Kister formula. The Laves phases, (alpha)Cr2Zr, (beta)Cr2Zr, and (gamma)Cr2Zr, were described by the Wagner-Schottky model: (alpha)Cr2Zr was treated with a two-sublattice model assuming antistructure atoms on both sublattices; and (beta)Cr2Zr and (gamma)Cr2Zr were described with three sublattices after the formula (Cr,Zr)6(Zr,Cr)4(Cr)2, where the second atoms on the first two brackets are antistructure atoms. The calculated phase diagram agrees well with the experimental values. The predicted homogeneity range of (alpha)Cr2Zr is in excellent agreement with the experimentally observed one. Author

N92-31612# Illinois Univ., Urbana. Dept. of Mechanical and Industrial Engineering.
NON-EQUILIBRIUM SYNTHESIS BY LASER CLADDING OF Ni, Nb AND Mg ALLOYS FOR IMPROVED ENVIRONMENTAL RESISTANCE Final Report, Nov. 1988 - Oct. 1991
J. Mazumder, A. Kar, S. K. Tewari, and C. R. Ribaudo 30 Mar. 1992 91 p
(Grant AF-AFOSR-0061-89)
(AD-A250552; AFOSR-92-0305TR) Avail: CASI HC A05/MF A01

The technique of laser surface modification provides a unique means of synthesizing novel nonequilibrium materials in near net shape. The goal of the proposed program is to develop a science base for synthesis of nonequilibrium metastable alloys by laser processing. This report summarizes experimental and theoretical studies carried out during the period of November 1988 to October 1991 on laser surface modification of Ni, Nb, and Mg alloys for improved environmental resistance at high temperature. A microstructural evolution model of NbAl3 was developed and the relative oxidation resistance of claddings of several Nb-based alloys were investigated. Initial work with V revealed that V increases the ductility, and decreases the oxidation resistance of laser clad NbAl3. Oxidation behavior of alloys with Ti, B, and Hf as a ternary alloy addition were identified. GRA

N92-31667# Lawrence Livermore National Lab., CA.
SUPERPLASTICITY IN A NICKEL SILICIDE ALLOY, Ni3Si(V, Mo) Ph.D. Thesis
S. L. Stoner Dec. 1991 103 p
(Contract W-7405-eng-48)
(DE92-011651; UCRL-LR-109425) Avail: CASI HC A06/MF A02

The fundamentals of superplasticity, including mechanical and microstructural characteristics are reviewed. The interest in developing intermetallic alloys for high temperature, structural applications is discussed. The superplastic properties of an intermetallic alloy based on nickel silicide were investigated. A duplex microstructure is shown with a third phase present as dispersions. The beta phase is ordered and the (alpha + beta) phase is a mixture of a solid solution phase and beta dispersions. The mechanical behavior of the material is presented. The maximum strain-rate sensitivity is approximately 0.5. The stress/strain curve varies with temperature, strain-rate, and orientation of the tension with respect to the microstructure. Steady-state behavior is shown in Region II as well as strain hardening caused by dynamic growth of the beta phase. The (alpha + beta) grains refine with deformation. Growth and refinement are enhanced at slower strain-rates. The nickel silicide alloy cavitates during superplasticity and shows increasing cavitation with decreasing strain-rate. The failure mechanism is intergranular and the final failure occurs by cavity coalescence. Annealing the material prior to testing produced a more uniform microstructure and improved the superplastic performance of the alloy. DOE

N92-31695# Laboratoire d'Automatique et d'Analyse des Systemes, Toulouse (France). Groupe Composants et Circuits a Effet de Champ.
CONTROL OF RAPID THERMAL PROCESSING EQUIPMENT FOR MICROELECTRONICS APPLICATIONS Ph.D. Thesis - Institut National des Sciences Appliquees [CONTROLE DES PROCEDES THERMIQUES RAPIDES APPLIQUES A LA MICROELECTRONIQUE]
Nicolas Nolhier 1992 154 p In FRENCH
(LAAS-92013; ETN-92-91683) Avail: CASI HC A08/MF A02

The control of rapid thermal processing equipment using infrared radiation is addressed. Thermal uniformity, temperature measurement, and temperature control are considered. A model giving the wafer temperature profile during rapid thermal process

is developed. This model calculates the light flux onto the wafer and resolves the heat transfer equation. Two methods to improve thermal uniformity are consequently suggested and simulated. Time resolved reflectivity is applied to the melting point detection of a germanium thin film, to provide a means for optical pyrometer calibration. The temperature control issue is addressed by studying the furnace open loop response and by using various control methods (PID, PID with parameter scheduling, and adaptive predictive control law). The feasibility of in situ characterization of wafer transformations based upon an estimation of the process transfer function is considered. ESA

N92-31733# Massachusetts Inst. of Tech., Cambridge. Dept. of Materials Science and Engineering.
DETERMINISTIC ANALYSIS OF PROCESSES AT CORRODING METAL SURFACES AND THE STUDY OF ELECTROCHEMICAL NOISE IN THESE SYSTEMS
R. M. Latanision Jun. 1992 55 p
(Contract DE-FG02-89ER-45388)
(DE92-016286; DOE/ER-45388/T1) Avail: CASI HC A04/MF A01

The control of metal dissolution processes is important in fields ranging from battery technology to corrosion. Nevertheless, metal dissolution remains a poorly understood class of electrochemical reactions. Although the reaction sequence for dissolution of many metals has been elucidated, kinetic descriptions are based on area averaged values of parameters that describe the relationship between the rate of reaction and the activation energy. Theoretical and experimental research on metal dissolution has focused traditionally on macroscopic processes and features. However, in the last few years there has been considerable interest in examining these processes on a microscopic scale. This proposal describes a research program to continue our work on theoretical modelling of metal dissolution. Over the next few years, results from theoretical modelling of dissolution, in conjunction with new experimental techniques such as in situ scanning tunneling microscopy, are expected to provide a new insight into the processes controlling metal dissolution and corrosion. DOE

N92-31744# Sandia National Labs., Livermore, CA.
THE STRUCTURE AND PROPERTIES OF GRAIN BOUNDARIES IN Ni3Al
M. J. Mills, S. H. Goods, and S. M. Foiles 1991 13 p Presented at the Annual Fall Meeting of the Materials Research Society, Boston, MA, 2-6 Dec. 1991
(Contract DE-AC04-76DR-00789)
(DE92-012143; SAND-92-8411C; CONF-911202-77) Avail: CASI HC A03/MF A01

The mechanical behavior of polycrystalline intermetallic compounds are often strongly influenced by the properties of the interfaces present. A classic example of this is the intergranular fracture exhibited by polycrystalline Ni3Al, and the dramatic increase in ductility upon the addition of small amounts of boron. It has been proposed that boron may promote the transmission of slip across grain boundaries by inducing the formation of a local region of compositional disorder. The results of experimental efforts to characterize the effect of boron on the structure and chemistry of these grain boundaries are summarized. Recent high resolution transmission electron microscopy studies using oriented bicrystals are described which indicate that there is no apparent change in the compositional ordering to within 0.5 nm from the boundary. These experimental results are compared with the results of atomistic calculations which were used to examine the effect of stoichiometry and boron content on the energy and degree of ordering of these boundaries. The proposed mechanisms of intergranular fracture in Ni3Al are discussed based on this experimental and theoretical work. DOE

N92-31759# Lawrence Livermore National Lab., CA.
A FAST LASER ALLOYING PROCESS FOR THE SELECTIVE ELECTROPLATING OF METAL ON SiO2 AND POLYIMIDE
V. Malba and A. F. Bernhardt 18 Dec. 1991 8 p Presented at the Annual Fall Meeting of the Materials Research Society, Boston, MA, 2-6 Dec. 1991
(Contract W-7405-eng-48)
(DE92-011764; UCRL-JC-109268; CONF-911202-76) Avail: CASI HC A02/MF A01

A new laser direct-write process for patterning of metal on multichip modules has been developed. The process involves the laser modification of the non-conductive surface of a seed multilayer, converting it to a conductive surface, which can be electroplated with metal. The seed multilayer is composed of a TiW adhesion layer, onto which a Au film is sputtered, followed by an a-Si layer, which forms the non-conductive surface. The laser modifies the surface by alloying (or mixing) the Si and Au to form the conductive surface. This laser process has been shown to be capable of writing speeds of 2.5 m/s. With a silicon dioxide interlevel dielectric layer, the process works over a large range of laser power (P(sub max)/P(sub min) approximately = 5). A polyimide interlevel dielectric layer can be used without damage or loss of adhesion, although the process margin is substantially reduced (P(sub max)/P(sub min) approximately = 2). DOE

N92-31795# Harvard Univ., Cambridge, MA. Dept. of Chemistry.
TRIS-TRIPHENYLSILOXY COMPOUNDS OF ALUMINUM
Allen W. Apblett, Alison C. Warren, and Andrew R. Barron 12 May 1992 30 p
(Contract N00014-91-J-1934)
(AD-A250141) Avail: CASI HC A03/MF A01

The reaction of AlMe3 with three equivalents of HOSiPh3 in THF results in the formation of the solvent complex A1(OSiPh3)(sub 3)(THF). Hydrolysis of 1 yields the stable water complex A1(OSiPh3)(sub 3)(H2O)(THF)(sub 2) in which the THF molecules are hydrogen bonded to the coordinated water ligand. These compounds have been fully characterized by H-1, C-13, O-17, Al-27, and Si-29 and 29 Si nuclear magnetic resonance (NMR) and IR spectroscopy. In addition, variable temperature 1H NMR of 2 has been employed to investigate the steric interactions between the phenyl rings of adjacent siloxide ligands. The molecular structures of the solvates have been determined by x-ray crystallography. GRA

N92-31796# Harvard Univ., Cambridge, MA. Dept. of Chemistry.
THE PREPARATION OF (Al2O3)x(SiO2)y THIN FILMS USING (Al(OSiEt3))2 AS A SINGLE SOURCE PRECURSOR
Christopher C. Landry, Linda K. Cheatham, Andrew N. MacInnes, and Andrew R. Barron 12 May 1992 34 p
(Contract N00014-91-J-1934)
(AD-A250142) Avail: CASI HC A03/MF A01

Aluminum silicates, (Al2O3)(SiO2)(y), are attractive candidates as corrosion and wear-resistant coatings for metals and other substrates, due to their superior properties of creep resistance, thermal expansion, and chemical stability. Recently, it has been proposed that amorphous alumina-silica films would find application as insulators in multilevel interconnections, and as encapsulants for active devices and thin film components, because they do not suffer the temperature instability of alumina films while retaining the desirable insulating characteristics. Thin films of aluminum silicates have been previously prepared by either sol-gel techniques or the pyrolysis of aluminum-silicon containing polymers. However, there remain some difficulties in obtaining homogeneous and continuous films. Metal-organic chemical vapor deposition (MOCVD) offers an attractive alternative to these methods, since contiguous, homogeneous thin films can be deposited at low temperatures with high growth rates. GRA

N92-31797# Bureau of Mines, Washington, DC. Div. of Ferrous Metals.
CHROMIUM, NICKEL, AND OTHER ALLOYING ELEMENTS IN US-PRODUCED STAINLESS AND HEAT-RESISTING STEEL
J. F. Papp 1991 49 p
(PB92-178623; BUMINES-IC-9275; LC-88-600144) Avail: CASI HC A03/MF A01

The objective of the U.S. Bureau of Mines study is to calculate

an accurate, reliable estimate of chromium and nickel content of stainless and heat-resisting steel produced in the United States. The columbium, manganese, molybdenum, titanium, tungsten, and vanadium contents of this steel are also calculated. Such contents are required for estimating the quantity of alloying element recovered from recycled stainless steel and consumed by market sectors. In the investigation, the elemental fraction of stainless and heat-resisting steel was calculated as the ratio of the weight of element contained in stainless steel to the weight of stainless steel produced. The elemental fraction was calculated as a time-averaged, grade-averaged value. The elemental fraction was averaged from 1962 through 1983, and averaged over the grades for which production was reported by the American Iron and Steel Institute during that time period. Author

N92-31898# Oak Ridge National Lab., TN.
IMPURITY EFFECTS ON THE MAGNETIC ORDERING IN CHROMIUM
R. S. Fishman and S. H. Liu May 1992 5 p Presented at the International Conference on the Physics of Transition Metals, Darmstadt (Germany), 20-24 Jul. 1992
(Contract DE-AC05-84OR-21400)
(DE92-016165; CONF-920762-2) Avail: CASI HC A01/MF A01

It is well-known that impurities profoundly alter the magnetic properties of chromium. While vanadium impurities suppress the Neel temperature T(sub N), manganese impurities enhanced T(sub N) substantially. As evidenced by neutron scattering experiments, doping with as little as 0.2 percent vanadium changes the transition from weakly first order to second order. Young and Sokoloff explained that the first-order transition in pure chromium is caused by a charge-density wave which is the second harmonic of the spin-density wave. By examining the subtle balance between the spin-density and charge-density wave terms in the mean-field free energy, we find that the first-order transition is destroyed when the vanadium concentration exceeds about 0.15 percent in agreement with experiments. DOE

N92-31924# Argonne National Lab., IL.
OXIDATION/SULFIDATION BEHAVIOR OF Fe-Cr ALLOYS: A REACTIVE-ELEMENT EFFECT
K. Natesan and J. H. Park Apr. 1992 11 p Presented at the 6th Annual Fossil Energy Materials Conference, Oak Ridge, TN, 12-14 May 1992
(Contract W-31-109-eng-38)
(DE92-016172; ANL/CP-75787; CONF-9205123-7) Avail: CASI HC A03/MF A01

Corrosion resistance of a number of structural alloys in high-temperature environments is achieved by the formation of a continuous chromium oxide scale. Research on high-temperature corrosion of structural alloys has been in progress to reduce the rate of oxidation, improve the adhesion of oxide scale to the substrate alloy, and to stabilize the oxide scale against other corrosive agents such as sulfur, chlorine, alkalies, and ash/sorbent deposits. Extensive research is being conducted at Argonne National Laboratory to (1) evaluate mechanisms of oxidation, sulfidation, and break-away corrosion of chromia- and alumina-forming alloys exposed to mixed-gas atmospheres that span a wide range of oxygen, sulfur, and chlorine activities typical of combustion and gasification systems; (2) develop an understanding of the role of several microalloy constituents (e.g., Zr, Nb, Y, Ce, V) in oxidation/sulfidation processes and scale breakdown; (3) characterize the physical, chemical and mechanical properties of surface scales that are resistant to sulfidation attack; and (4) evaluate the role of deposits, such as alkali sulfates, alkali chlorides, ash, and sulfur sorbents, in the corrosion behavior or metallic alloys, selected coatings, and ceramic materials. DOE

N92-31987# National Materials Property Data Network, Inc., Columbus, OH.
MARINE STRUCTURAL STEEL TOUGHNESS DATA BANK, VOLUME 1 Final Report
J. G. Kaufman and Martin Prager 28 Aug. 1991 455 p
(Contract DTCG23-86-C-20062)
(AD-A247923; SSC-352-Vol-1; SSC-SSR-1311-Vol-1) Avail: CASI HC A20/MF A04

Despite the substantial number of data available on the toughness of a wide variety of steels which may be used for marine applications, there has been no comprehensive source to which one might go to readily find well-documented numeric data for the full range of materials and types of data of interest. Steps were taken to begin the establishment of such a source, with first priority given to toughness data for high strength, low alloy steels. This handbook provides the initial compilation for the Marine Structural Toughness Data Bank, a summary of data from about 10,000 tensile and toughness tests of hundreds of samples representing eleven steels of importance for marine applications. The result of this program is not only a source of reliable and well-documented numeric data on the toughness of steels, but also the nucleus of a system which may be expended to include other properties of these steels and other materials which might be considered for such applications. The source will be of value to all segments of the marine industry, commercial and military, and to a number of other industry groups which utilize these steels, as well as to the steel industry itself. GRA

N92-32004# Los Alamos National Lab., NM.
LASER-ABLATED COPPER CONDENSATION IN HELIUM
G. L. Strobel Jun. 1992 20 p
(Contract W-7405-eng-36)
(DE92-016685; LA-12291-MS) Avail: CASI HC A03/MF A01

The expansion of laser-ablated copper into room temperature helium to saturation and the subsequent copper condensation is analyzed. At saturation, the copper number density is about three orders of magnitude less than the helium number density. Saturation of the copper in this cooling, variable concentration mixture occurs at about 2000 K. Validity conditions for classical homogeneous nucleation rate theory are not met in this copper expansion. The room temperature helium quickly supercools the more dilute copper atoms, resulting in a critical drop consisting of two or fewer atoms that signals the lack of validity for classical homogeneous nucleation rate theory. Chemical reaction rate equations are used to analyze the copper dimer concentration time dependence. Partial defocusing of the laser may bring about copper condensation conditions more appropriate for homogeneous nucleation rate theory. DOE

N92-32032# Allied-Signal Aerospace Co., Kansas City, MO.
METALLIZATION OF FERRITE CERAMIC COUPLINGS
J. Burden Jun. 1992 88 p
(Contract DE-AC04-76DP-00613)
(DE92-016573; KCP-613-4747) Avail: CASI HC A05/MF A01

Tests were conducted to determine the optimum sputtering conditions for which the strongest metallization adherence could be achieved for the ferrite safing wheel assemblies. The conditions were varied through four separate test runs with a fifth verification run conducted using parameters selected from the first four runs. The parameters tested were the effects of etching, precleaning, chamber pressures, plating materials, plating thickness, soldering pressures, and cooling rates. The results increased the strength of the metallization to two pounds, well in excess of the required one pound minimum. It was also determined that the gold should be sputtered on and not thermally deposited, which caused cracking in the ferrite material. DOE

N92-32052# Naval Postgraduate School, Monterey, CA.
A STUDY OF THE MICROSTRUCTURAL BASIS FOR THE STRENGTH AND TOUGHNESS PROPERTIES OF WATER-QUENCHED AND AIR-COOLED HSLA-100, HSLA-100 WITH INCREASED COPPER, AND A ULCB STEEL M.S. Thesis
Thomas C. Mohr Sep. 1991 97 p
(AD-A245955) Avail: CASI HC A05/MF A02

The microstructural basis for strength of the water-quenched and air-cooled HSLA-100, HSLA-100 with increased copper, and a ULCB steel was investigated by conducting an inclusion study and characterizing the microstructure of each of the steels. For

the inclusion study, the SEM was used to examine a large number of fields and determine inclusion morphology while the EDX was used to determine inclusion composition. The microstructure of both the water-quenched and air-cooled steels was characterized using the optical microscope, SEM, and TEM. The HSLA-100 with increased copper steel was adequately calcium treated and aluminum deoxidized as evidenced by the low sulfur content, few MnS stringers, and lack of large oxide arrays. The ULCB steel was not calcium treated or Al-killed; nor was it thermomechanically processed as shown by the lack of lipped, broken, or elongated stringers. Both MnS and oxide inclusions were present, and consequently, ladle metallurgy would have to be used before the ULCB steel was hot-worked. The microstructural basis for the strength of the as-quenched HSLA-100, HSLA-100 with increased copper, and ULCB steels is the transformation product packet size, small lath width, and high dislocation density. The as-quenched increased copper steel also contained e-copper precipitates which added to its high level of strength and toughness. The as-quenched ULCB steel did not reach the desired strength level. GRA

N92-32066# Pratt and Whitney Aircraft, West Palm Beach, FL.
FATIGUE IN SINGLE CRYSTAL NICKEL SUPERALLOYS Report, 16 May - 15 Jun. 1992
15 Jun. 1992 7 p
(AD-A252492; PWA-FR21998-08) Avail: CASI HC A02/MF A01

This program investigates the seemingly unusual behavior of single crystal airfoil materials. The fatigue initiation processes in single crystal (SC) materials are significantly more complicated and involved than fatigue initiation and subsequent behavior of a (single) macrocrack in conventional, isotropic materials. To investigate these differences is the major aim of this project. GRA

N92-32084# Northwestern Univ., Evanston, IL.
QUANTUM MECHANICAL APPROACH TO UNDERSTANDING MICROSTRUCTURAL AND MECHANICAL PROPERTIES IN INTERMETALLICS Final Report, 1 Oct. 1988 - 30 Sep. 1991
Arthur J. Freeman 22 Apr. 1992 15 p
(Grant AF-AFOSR-0346-88)
(AD-A250550; AFOSR-92-0414TR) Avail: CASI HC A03/MF A01

The primary goal of the proposed research is to study and develop alloying concepts for understanding intermetallic alloys as derived from a first principles quantum mechanical approach. Thus, a major part of our effort will be to study and determine ductilizing effects of alloying elements in several intermetallic compounds and to work closely with experimental efforts to evaluate the applicability of the theoretical approach to alloy design. Specifically, highly precise all-electron quantum mechanical electronic structure methods will be applied to the study of a number of materials problems in order to obtain from first principles information of relevance to alloy stability and the design of structural materials. Using our recently developed state-of-the-art all-electron self-consistent total energy methods which give precise solutions of the local density equations, fundamental information will be sought about the structural and electronic properties of these alloys in order to predict stable and metastable phases and how alloying affects bonding, crystal ordering and crystal symmetry. The first principles approach used here will address questions of a metallurgical nature, such as phase stability, crystal structure, equilibrium lattice constants, and mechanical properties, including the effect of atomic relaxation. The proposed research seeks to explore a new capability for modeling materials and their properties on a computer which have not yet been performed. GRA

N92-32096# Pennsylvania State Univ., University Park. Dept. of Materials Science and Engineering.
PREDICTION OF HYDROGEN ENTRY AND PERMEATION IN METALS AND ALLOYS Annual Report, 1 Oct. 1990 - 30 Sep. 1991
Howard W. Pickering Jan. 1992 21 p
(Contract N00014-91-J-1189)
(AD-A245286) Avail: CASI HC A03/MF A01

This report summarizes results of the past year on our continuing in-situ experiments directed to the problem of hydrogen entry and degradation of materials both for planar surfaces and for the more complicated recessed surface. For the planar surface, the hydrogen permeation and scanning tunneling microscopy (STM) techniques are being used, and for the recessed surface, the study uses a combined microscopy/electrochemical probe technique and a crevice geometry. Further modeling of the hydrogen permeation technique has led to an experimental procedure that yields two previously unattainable rate constants that are important for controlling hydrogen absorption into a material from an aqueous environment, the hydrogen absorption (entry) and desorption (exiting) constants. STM has been further developed for in-situ study of hydrogen bonding at the atomic scale by successfully imaging hydrogen adsorption on the model Si(100)2X1 surface from a low pressure hydrogen gas phase. For the recessed surface hydrogen, entry from an aqueous solution occurs for a much wider range of conditions than previous believed. Chloride ion and acidification indirectly promote hydrogen ion reduction and entry on the recessed surface through their direct effect on promoting the IR-induced mechanism of crevicing. GRA

N92-32139# Sandia National Labs., Albuquerque, NM.
A BAN ON USE OF LEAD-BEARING SOLDERS: IMPLICATIONS FOR THE ELECTRONICS INDUSTRY
P. T. Vianco and F. G. Yost Apr. 1992 11 p
(Contract DE-AC04-76DP-00789)
(DE92-013291; SAND-92-0211) Avail: CASI HC A03/MF A01

This white paper addresses the issue of banning lead from solders used in electronics manufacturing. The current efforts by legislative bodies and regulatory agencies to curtail the use of lead in manufactured goods, including solders, are described. In response to a ban on lead or the imposition of a tax which makes lead uneconomical for use in solder alloys, alternative technologies including lead-free solders and conductive epoxies are presented. The recommendation is made that both users and producers of solder materials join together as partners in a consortium to address this issue in a timely and cost-effective manner. DOE

N92-32156*# Eloret Corp., Sunnyvale, CA.
COMPUTATIONAL STUDIES OF METAL-METAL AND METAL-LIGAND INTERACTIONS Report, 1 Oct. - 31 May 1992
Leslie A. Barnes 25 Aug. 1992 36 p
(Contract NCC2-741)
(NASA-CR-190674; NAS 1.26:190674) Avail: CASI HC A03/MF A01

The geometric structure of Cr(CO)6 is optimized at the modified coupled-pair functional (MCPF), single and double excitation coupled-cluster (CCSD) and CCSD(T) levels of theory (including a perturbational estimate for connected triple excitations), and the force constants for the totally symmetric representation are determined. The geometry of Cr(CO)5 is partially optimized at the MCPF, CCSD and CCSD(T) levels of theory. Comparison with experimental data shows that the CCSD(T) method gives the best results for the structures and force constants, and that remaining errors are probably due to deficiencies in the one-particle basis sets used for CO. A detailed comparison of the properties of free CO is therefore given, at both the MCPF and CCSD/CCSD(T) levels of treatment, using a variety of basis sets. With very large one-particle basis sets, the SSCD(T) method gives excellent results for the bond distance, dipole moment and harmonic frequency of free CO. The total binding energies of Cr(CO)6 and Cr(CO)5 are also determined at the MCPF, CCSD and CCSD(T) levels of theory. The CCSD(T) method gives a much larger total binding energy than either the MCPF or CCSD methods. An analysis of the basis set superposition error (BSSE) at the MCPF level of treatment points out limitations in the one-particle basis used here and in a previous study. Calculations using larger basis sets reduced the BSSE, but the total binding energy of Cr(CO)6 is still significantly smaller than the experimental value, although the first CO bond

dissociation energy of Cr(CO)6 is well described. An investigation of 3s3p correlation reveals only a small effect. The remaining discrepancy between the experimental and theoretical total binding energy of Cr(CO)6 is probably due to limitations in the one-particle basis, rather than limitations in the correlation treatment. In particular an additional d function and an f function on each C and O are needed to obtain quantitative results. This is underscored by the fact that even using a very large primitive se (1042 primitive functions contracted to 300 basis functions), the superposition error for the total binding energy of Cr(CO)6 is 22 kcal/mol at the MCPF level of treatment. Author

N92-31872# Tel-Aviv Univ. (Israel). Dept. of Mechanics, Materials and Structures.
J(SUB 2) FRACTURE TOUGHNESS TESTING OF Al 707 5-T7351
Leslie Banks-Sills and Dov Sherman *In* Israel Society of Aeronautics and Astronautics, 31st Israel Annual Conference on Aviation and Astronautics 22 Feb. 1990 p 73-75 Previously announced in IAA as A91-43086 (For primary document see N92-31861 22-01)
Avail: CASI HC A01/MF A03

27 NONMETALLIC MATERIALS

Includes physical, chemical, and mechanical properties of plastics, elastomers, lubricants, polymers, textiles, adhesives, and ceramic materials.

For composite materials see *24 Composite Materials*.

N92-31270 Department of the Navy, Washington, DC.
NONLINEAR OPTICAL ACRYLIC POLYMERS AND USE THEREOF IN OPTICAL AND ELECTRO-OPTIC DEVICES
Patent
Leslie H. Sperling, inventor (to Navy), Clarence J. Murphy, inventor (to Navy), Warren A. Rosen, inventor (to Navy), Himanshu Jain, inventor (to Navy), and Warren N. Herman, inventor (to Navy) 7 Jan. 1992 11 p Filed 16 Jul. 1990
(AD-D015236; US-Patent-5,079,321; US-Patent-Appl-SN-552658; US-Patent-Class-526-311) Avail: US Patent and Trademark Office

This invention relates to acrylic polymers and more specifically to polyacrylamides and polyacrylates such as poly(2-N-2-methyl-5-nitrophenylamino) ethyl acrylate and poly(N-2-methyl-4-nitrophenyl) acrylamide. These acrylic polymers are particularly useful as nonlinear optical components in various electrical devices for processing optical signals including interferometers, optical switches, optical amplifiers, generators, computational devices, and the like. This invention relates to acrylic polymers and more specifically to polyacrylamides and polyacrylates capable of exhibiting nonlinear optical responses in an electric or electromagnetic field. Specifically, this invention is directed to the use of these acrylic polymers as the nonlinear optical component in various electrical devices for purposes of processing optical signals. Recent developments have led to increased use of optical components in various electrical and optoelectronic devices, i.e., devices containing optical components with either active or passive components. These devices include, for example, the use of optical materials in second harmonic generators, modulators, e.g., spatial light modulators, phase shifters, optical amplifiers, laser technology, interferometers, optical switches, logic gates, communications and computational devices, etc. GRA

N92-31278*# National Aeronautics and Space Administration. Marshall Space Flight Center, Huntsville, AL.
GIBBS FREE ENERGY OF REACTIONS INVOLVING SiC, Si3N4, H2, AND H2O AS A FUNCTION OF TEMPERATURE AND PRESSURE
M. A. Isham Aug. 1992 18 p
(RTOP 593-71-51)
(NASA-TP-3275; M-694; NAS 1.60:3275) Avail: CASI HC A03/MF A01

Silicon carbide and silicon nitride are considered for application as structural materials and coating in advanced propulsion systems including nuclear thermal. Three-dimensional Gibbs free energy were constructed for reactions involving these materials in H2 and H2/H2O. Free energy plots are functions of temperature and pressure. Calculations used the definition of Gibbs free energy where the spontaneity of reactions is calculated as a function of temperature and pressure. Silicon carbide decomposes to Si and CH4 in pure H2 and forms a SiO2 scale in a wet atmosphere. Silicon nitride remains stable under all conditions. There was no apparent difference in reaction thermodynamics between ideal and Van der Waals treatment of gaseous species. Author

N92-31318# Utah State Univ., Logan. Dept. of Chemistry and Biochemistry.
ORGANOMETALLIC NONLINEAR OPTICAL (NLO) POLYMERS. PART 2: SYNTHESIS OF MAIN-CHAIN ORGANOMETALLIC POLYMERS AND A STRUCTURAL STUDY OF FERROCENE NLO-PHORES
Michael E. Wright and Edward G. Toplikar 10 May 1992 27 p
(Contract N00014-91-J-1625)
(AD-A250655; TR-7) Avail: CASI HC A03/MF A01

A detailed structural analysis of several ferrocene based NLO-phores were examined by x ray diffraction. The study illustrated that electron-withdrawing groups favor and control planarity of the Pi system. Through selective functionalization of the cyclopentadienyl rings of ferrocene new monomers, were prepared in the study. One monomer was suitable for Lewis acid catalyzed transesterification polymerization using Ti(OC4H9)4 and others were appropriate for a Knoevenagel polycondensation. The transesterification polymerization resulted in formation of an intractable polymeric material of unknown structure. The homopolymerization by the Knoevenagel technique afforded the desired polymer. The polymer was characterized by GPC and spectroscopic data. A major by-product in the polymerization was the macrocyclic lactone 10a produced from an intramolecular Knoevenagel condensation. The lactone structure was confirmed by single-crystal x ray diffraction. GRA

N92-31356# Naval Ocean Systems Center, San Diego, CA. Research, Development, Test and Evaluation Div.
SYNTHESIS OF DIAMOND FILMS WITH PULSED PLASMA
M. Aklufi and D. Brock Mar. 1992 9 p Sponsored by ONR
(AD-A250058) Avail: CASI HC A02/MF A01

Diamond films were grown in plasmas that were formed with microwaves and modulated with a pulsed generator. Films obtained with the use of pulse periods in the nanosecond, microsecond, and millisecond ranges were compared to baseline films which were obtained with a CW plasma. The deposited films were examined with SEM, XRD, and Micro-Raman spectroscopy. For the experimental conditions used, the diamond films' growth rates and quality improved with increasing pulse duration while maintaining a duty cycle at nearly 50 percent and reached a maximum with CW generated films. This was attributed primarily to an increasing degree of supersaturation of atomic hydrogen at the growth surface with increasing pulse time. GRA

N92-31358# North Carolina Univ., Chapel Hill. Dept. of Chemistry.
CHARGE TRANSFER PROCESSES IN MULTIPLE SITE CHEMICAL SYSTEMS Final Report, 2 Aug. 1988 - 31 Jan. 1992
Thomas J. Meyer 31 Mar. 1992 11 p
(Contract DAAL03-88-K-0192)
(AD-A249538; ARO-25586.14-CH) Avail: CASI HC A03/MF A01

Based on support from AROD, we have investigated redox and photochemical events in polypyrrole based polymeric films, and charge transfer processes in systems containing more than one redox site covalently attached to either soluble polymer or to solid supports. Binding and electrode position of metal particles into vinyl-bipyridyl based films were also achieved. Optical and

thermal electron transfer in mixed-valence dimeric systems were studied in some detail. GRA

N92-31377# Arizona State Univ., Tempe.
SURFACE STRUCTURES AND SURFACE PROCESSES OF CERAMICS WITH ATOMIC RESOLUTIONS: A STUDY BY SCANNING TUNNELING MICROSCOPY Final Report, 1 Jun. 1988 - 30 Sep. 1991
Ignatius S. Tsong and William T. Petuskey 10 Dec. 1991 18 p
(Contract DAAL03-88-K-0098)
(AD-A249581; ARO-24845.15-MS) Avail: CASI HC A03/MF A01

We applied a new technique for surface imaging, scanning tunneling microscopy (STM) to study the atomic and electronic structures of ceramic surfaces. The model ceramic chosen for this study was SiC. STM imaging was possible when the SiC single crystals were doped with nitrogen to render them semiconducting. Atomically resolved images were successfully taken on surfaces of cubic Beta-SiC(100) and (111), which showed a variety of reconstructions. In particular, the STM images of the Beta-SiC(III) surface showed a 6 x 6 geometry, in contrast to a 6 square root of 3 x 6 square root of 3 geometry when measured by low-energy electron diffraction (LEED). We found that this discrepancy was due to a graphite monolayer incommensurately grown on top of the Si-terminated Beta-SiC(111) surface. This conclusion was reached after probing the electronic structure of the surface by scanning tunneling spectroscopy (STS). On a larger scale, i.e. over distances between 50 and 500 nano-m, the surface topographics observed by STM were correlated with the initial growth modes of the SiC simple crystals. In addition to the STM studies, we conducted experimental and theoretical investigations on the thermochemistry and interfacial displacement reactions of the Ti-Si-C and Ti-Si-N systems in order to refine the understanding of thermodynamic and phase equilibria characteristics of ceramic-metal composite systems. GRA

N92-31388# Implant Sciences Corp., Wakefield, MA.
STRONGLY ADHERENT CERAMIC SURFACE LAYERS BY ION IMPLANTATION Final Report, Mar. - Sep. 1991
Stephen N. Bunker 15 Dec. 1991 28 p
(Contract DAAL03-91-C-0014)
(AD-A248882; ARO-28436.1-MS-SBI) Avail: CASI HC A03/MF A01

Many applications exist for specialized coatings which must never debond during their working life. Ceramic coatings on metals are particularly important for this special category, but the dissimilar properties of the two types of materials make most existing coating techniques unacceptable. Ion implantation is well-known to produce totally adherent depositions of atoms, because the high energy of the ion beam causes the atoms to come to rest inside the target material rather than lay upon it. Thus, there is no discrete surface for debonding. Unfortunately, it has rarely been possible to accumulate enough ion implanted atoms in one place to form a pure layer because the sputtering coefficient is usually greater than unity. This research has developed a technique of codepositing a sacrificial layer together with ion implantation in order to create an effective sputtering coefficient of zero. Implanted atoms can accumulate to arbitrarily thick layers which are physically merged to the substrate. A demonstration of the general techniques has been performed using Zirconium as the ion. GRA

N92-31394# Massachusetts Inst. of Tech., Cambridge. Dept. of Chemistry.
SYNTHESIS OF SIDE CHAIN LIQUID CRYSTAL POLYMERS BY LIVING RING OPENING METATHESIS POLYMERIZATION. 4: SYNTHESIS OF AMORPHOUS AND SIDE CHAIN LIQUID CRYSTAL AB BLOCK COPOLYMERS
Zen Komiya, Coleen Pugh (Carnegie-Mellon Univ., Pittsburgh, PA.), and Richard R. Schrock 1 May 1992 27 p
(Contract N00014-89-J-1542)
(AD-A250353; MIT-TR-16) Avail: CASI HC A03/MF A01

Di-block copolymers, with well defined block length, yield ordered phase separation. Morphology of the microphase separation is controllable by varying the weight ratio of the two blocks and the length of each block. If one of the blocks is a side chain liquid crystalline polymer (SCLCP), microphase separated systems with liquid crystalline microphases may be realized. Such systems are of fundamental as well as practical interest. The effect of size and type on the liquid crystalline microphase transition is one of the fundamental questions. This effect is recently investigated by the polymer system in which low molecular weight liquid crystals are dispersed. Different from the low molecular weight liquid crystals dispersed systems, the block copolymer can give several types of microdomains (lamellae, cylinders, or spheres). GRA

N92-31404# Army Lab. Command, Watertown, MA. Material Technology Lab.
HIGH STRENGTH GLASS SECOND SOURCE QUALIFICATION TO COMPOSITE ARMOR SPECIFICATION MIL-L-46197(MR) Final Report
William E. Haskell, III Apr. 1992 16 p
(AD-A252114; MTL-TR-92-30) Avail: CASI HC A02/MF A01

Vetrotex RH glass woven roving fabric impregnated with Cyanamid CYCOM 4102 polyester resin was evaluated for structural armor applications. The mechanical and ballistic properties of this system were compared to MIL-L-46197 (MR) requirements. The specific lot of RH glass evaluated under this effort met MIL-L-46197 (MR) requirements. S-2 and RH fiberglass/polyester systems should meet specification requirements when manufactured and processed in strict compliance with MIL-L-46197 (MR). The identification of this second high strength fiberglass source will generate pricing competition and cost savings for the Government. MIL-L-46197 (MR) has been amended and is now entitled Laminate: High Strength Glass, Fabric-Reinforced, Polyester Resin Impregnated, Amendment No. 1, 22 November 1991. GRA

N92-31408# University of Southern Mississippi, Hattiesburg. Dept. of Polymer Science.
LINEAR AND STAR-BRANCHED SILOXY-SILANE POLYMERS: ONE POT A-B POLYMERIZATION AND END-CAPPING Technical Report, Jun. 1992
Lon J. Mathias and Ralph M. Bozen 29 May 1992 3 p
(Contract N00014-89-J-1225)
(AD-A252195; TR-45) Avail: CASI HC A02/MF A01

Silane and siloxane polymers form an important family of commercial materials. They pose a unique combination of thermal stability, hydrophobicity, and segmental mobility which gives them low temperature flexibility and properties useful in demanding application where their high cost is justified. Recent reports of silicone dendrimers make available single-molecule structures which greatly extend these potential uses. We have developed an alternative approach to siloxy-silane hyperbranched polymers that uses an A-B3 monomer possessing one alkene moiety and three Si-H groups. Addition of a platinum hydrosilation catalyst leads to rapid formation of polymer with a high relative content of terminal Si-H groups that can be reacted (end-capped) with a variety of alkenes such as allyl phenyl ether and the allyl ether-monomethyl ether of oligooxyethylene. GRA

N92-31419# HCC Science and Technology Co., Summit, NJ.
POLYMER BLENDS, VOLUME 1 Final Report
Michael Jaffe May 1992 119 p
(Contract F49620-88-C-0014)
(AD-A252112; AFOSR-92-0415TR) Avail: CASI HC A06/MF A01

Three generations of PBI and polyamide blends have been evaluated for use as high temperature matrix resins for carbon fiber composites in aerospace applications. To enable property testing, a neat resin molding cycle was developed to produce plagues with less than 2 percent void volume. Phthalic anhydride end-capping of the PBI was shown to significantly reduce crosslinking as measured by the change in Tg after high temperature exposure. This reduction in end-group chemistry provided for maximum thermoplasticity of the blend during molding. Thermo-oxidative stability studies indicated that at 60 F and above,

the weight loss of the blend was approximately proportional to its PBI content. Attempts to mitigate this effect by incorporating 6F moiety into the PBI backbone were unsuccessful. Phosphoric acid treatment of 85/15 molded blend samples was shown to provide a four-fold increase in weight retention. However, this effect was due to surface oxidation barrier effect. A series of nine copolymer polyimides were synthesized and evaluated. The blend of 10/90 ecPBI/6FcoPI-2 was chosen to be moved forward for aerospace evaluations. The blend with end capped chemistry was scaled up in steps from gram quantities to 50 kilograms. Prepregging of the neat resin onto plain weave AS-4 carbon fabric and onto AS-4 unidirectional tape was successfully demonstrated by YLA Incorporated. Three prepregging trials produced a total of 1450 linear feet of fabric and over 450 feet of unidirectional prepregs. Composite laminate fabrication was demonstrated by both Lockheed and Hoechst Celanese. Composite properties were demonstrated which either approached or exceeded GE Aircraft Engines specifications for PMR-15 composites. GRA

N92-31435# Cornell Univ., Ithaca, NY.
NOVEL CHEMICALLY AMPLIFIED DRY-DEVELOPING IMAGING MATERIALS FOR HIGH RESOLUTION MICROLITHOGRAPHY
J. M. Frechet, J. Fahey, S. M. Lee, S. Matuszczak, and Y. Shacham-Diamond 20 Apr. 1992 14 p
(Contract N00014-91-J-1338)
(AD-A250085; TR-6) Avail: CASI HC A03/MF A01

Several new polymers, copolymers, and polyfunctional crosslinkers that can be used to formulate chemically amplified resist materials were prepared, characterized, and tested in combination with suitable photoactive compounds. All of the materials operate on the basis of acid catalyzed processes involving alkylation, dehydration, or isomerization reactions. Sensitivities below 0.1 mJ/sq cm were measured with deep-UV irradiation, while most of the materials also operate effectively after E-beam or X-ray exposure. The resist materials are useful in dry development and top-surface imaging processes. Depending on the nature of the matrix polymer and the design of the resist material, both positive and negative tone images can be obtained. Dry development using an oxygen plasma can be achieved following selective silylation of the resists after exposure and post-baking. Those areas of the films that are silylated resist etching by the oxygen plasma providing access to high resolution images that also benefit from the high sensitivity of the chemically amplified resists. GRA

N92-31436# Cornell Univ., Ithaca, NY.
THE PHOTOGENERATION OF POLYMERIC AMINES: SYNTHESIS AND PHOTOCROSSLINKING OF COPOLYMERS CONTAINING PHOTOACTIVE CARBAMATE PENDANT GROUPS
J. E. Beecher, J. F. Cameron, and J. M. Frechet 20 Apr. 1992 26 p
(Contract N00014-91-J-1338)
(AD-A250086; TR-7) Avail: CASI HC A03/MF A01

Two families of copolymers containing 4-(2-NITROBENZYLOXY) CARBAMOYL-styrene as the photoactive component, with styrene or methyl methacrylate as the other component are described. The polymers are prepared by chemical modification of copolymers of 4-amino-styrene with styrene and methyl methacrylate, respectively, using 2-nitrobenzyl chloroformate. The photoactive carbamate groups of both copolymers can be removed by irradiation with UV light below 320 nm. Quantum yield measurements and comparisons with small molecule model compounds confirm that attachment to the polymer has no effect on the photolability of the 2-nitrobenzyl carbamoyl protecting group. Quantum yield values near 0.10 also compare favorably with those obtained for related small molecules. The photoactive polymers were tested successfully in the UV induced crosslinking of formulations containing epoxy groups. GRA

N92-31473# University of Southern California, Los Angeles. Dept. of Materials Science and Engineering.
DEVELOPMENT OF AN ELECTROCHEMICAL METHOD FOR FIELD TESTING OF PROTECTIVE COATINGS Final Report, 1 Jul. 1990 - 31 Dec. 1991
Florian Mansfeld 31 Dec. 1991 50 p
(Contract N00014-90-J-4123)
(AD-A245872) Avail: CASI HC A03/MF A01

Nine different coating systems on cold rolled steel have been tested by recording of EIS data during immersion in 0.5 N NaCl (open to air). One set of samples has been tested in the as received condition and after application of an artificial defect. Another set was tested after outdoor exposure for two years at Cape Canaveral, Florida. For this set the susceptibility to cathodic delamination was also evaluated. For the set which was tested in the as-received condition for one year, the sample with an all latex coating was eliminated from further testing since the coating was so porous that the impedance spectra resembled those usually found for bare steel. In long term testing, coating damage was observed only for the alkyd enamel, the alkyd enamel Si-alkyd, and the zinc-rich primer epoxy polyamide polyurethane systems. For the set which was tested for 55 d after outdoor exposure, significant coating damage could only be detected for the alkyd enamel Si-alkyd coating. The coating properties degraded faster than for the as received sample indicating that outdoor exposure had weakened the coating. In the cathodic delamination tests the largest damage occurred for the other alkyd based coatings. GRA

N92-31538# Northwestern Univ., Evanston, IL.
CERAMIC SURFACES AND SINTERING
L. D. Marks Aug. 1991 18 p
(Contract DE-FG02-87ER-45309)
(DE92-011570; DOE/ER-45309/4) Avail: CASI HC A03/MF A01

We produced ultrafine faceted alumina particles (UFPs), 20-50 nm in diameter, by an arc-discharge method and sintered small clusters of them as they were carried through a tube furnace by flowing gas. The experiment was conducted under near UHV clean environment and specimens were examined in a UHV H9000 TEM. The UFPs produced in this study were transition alumina phases gamma, delta and theta. We found new delta and theta phases which were different from those in earlier studies. We developed two computer programs to simulate the shape, 3-D arrangement, and random contact of UFPs. Gaps were discovered to exist between particles due to random contact and possibly rotation and slip after contact. As no shrinkage was found, surface diffusion was identified as the dominant mechanism that was responsible for the formation of 'necks' by filling in the gaps. These necks had well-defined, atomically-sharp contact angles, which suggest that the neck growth process was controlled by faceting. DOE

N92-31539# Sandia National Labs., Albuquerque, NM.
CHARACTERIZATION OF POLYMERS FOR MICROCELLULAR FOAMS
D. A. Schneider and R. A. Assink Mar. 1992 39 p
(Contract DE-AC04-76DP-00789)
(DE92-012444; SAND-91-1591) Avail: CASI HC A03/MF A01

We have measured, by H-1 and C-13 nuclear magnetic resonance (NMR), the percent deuteration, the tacticity and the purity of several polymers and one solvent used in the preparation of microcellular foams. The percent deuteration was measured for polystyrene, polyacrylonitrile and polyethylene. The tacticities of polystyrene and polyacrylonitrile were determined. The purity and degradation products of polyacrylonitrile and maleic anhydride were examined. This report documents the experimental procedures and results of these measurements. DOE

N92-31557# Massachusetts Inst. of Tech., Cambridge. Dept. of Chemistry.
CYCLOPOLYMERIZATION OF METALLOID-CONTAINING ALPHA, OMEGA-DIENES. 1,3-DIVINYLTETRAMETHYLDISILOXANE, 1,3-DIVINYLTETRAMETHYLDISILAZANE AND 1,3-DIVINYLPENTAMETHYLDISILAZANE
Dietmar Seyferth and Jennifer L. Robison 5 Apr. 1992 51 p
(Contract N00014-91-J-1590)
(AD-A250347) Avail: CASI HC A04/MF A01

The di-tert-butyl peroxide-initiated cyclopolymerization of (CH2=CHMe2Si)2X (X = 0, NH, NMe) gives polymers of relatively low molecular weight. Their IR, H-1, and Si-29 NMR spectroscopy provided some structural information when they were compared with spectroscopic data for model cyclic and acyclic organosilicon compounds. These studies indicated the presence of 5- and 6-membered cyclic units in the polymer chain, possibly also of 7-membered cyclic and of acyclic units. The Si-NH-Si functions in the cyclopolymer derived from (CH2=CHMe2Si)2NH reacted readily with HF and HCl to open the ring and introduce SiMe2F and SiMe2Cl substituents, respectively, onto the polymer backbone. Reactions of the former with LiAlH4, MeLi, n-BuLi, and CH2=CHMgBr converted them to SiMe2H, SiMe3, SiMe2Bu-n, and SiMe2(CH=CH2) substituents, respectively. GRA

N92-31560# Lawrence Livermore National Lab., CA.
SOL-GEL MULTILAYERS APPLIED BY A MENISCUS COATING PROCESS
J. A. Britten and I. M. Thomas 19 Mar. 1992 9 p Presented at the Material Research Society Spring Meeting, San Francisco, CA, 27 Apr. - 2 May 1992
(Contract W-7405-eng-48)
(DE92-012697; UCRL-JC-110152; CONF-920402-1) Avail: CASI HC A02/MF A01

We describe a meniscus coating method to produce high-laser damage threshold, silica/alumina sol-gel multilayer reflectors on 30 (plus) cm substrates for laser-fusion applications. This process involves forcing a small suspension flow through a porous applicator tube, forming a falling film on the tube. A substrate contacts this film to form a meniscus. Motion of the substrate relative to the applicator entrains a thin film on the substrate, which leaves behind a porous, optical quality film upon solvent evaporation. We develop a solution for the entrained film thickness as a function of geometry, flow and fluid properties by an analysis similar to that of the classical dip-coating problem. This solution is compared with experimental measurements. Also, preliminary results of multilayer coating experiments with a prototype coater are presented, which focus on coating uniformity and laser damage threshold (LDT). DOE

N92-31618# National Inst. of Standards and Technology, Gaithersburg, MD. Polymers Div.
DEVELOPMENT OF CHARACTERIZATION TECHNIQUES FOR POLYURETHANES 1. CHARACTERIZATION OF SRM 1480, A LOW MOLECULAR WEIGHT POLYURETHANE FOR SEC CALIBRATION
C. M. Guttman, J. R. Maurey, P. H. Verdier, C. C. Han, and F. W. Wang Apr. 1992 28 p
(PB92-172485; NISTIR-4788) Avail: CASI HC A03/MF A01

The characterization of a polyurethane standard reference material, SRM 1480, is described. The weight average molecular weight of SRM 1480 by light scattering was determined to be 47,000 g/mole. The intrinsic viscosity of SRM 1480 in the THF was also measured and found to be 43.8 mL/g. The size exclusion chromatography (SEC) of SRM 1480 in the tetrahydrofuran (THF) as received in the bottle was found to exhibit concentration dependent peak positions, even at low concentrations. The addition of 0.01 moles per liter LiBr to the THF was found to alleviate the problem. This low concentration of LiBr did not change the polystyrene calibration of the SEC columns. GRA

N92-31624# Army Lab. Command, Watertown, MA. Material Technology Lab.
RECENT DEVELOPMENTS IN THE FUNDAMENTALS OF GAS PERMEATION IN RUBBERY POLYMERS Final Report
C. R. Desper Mar. 1992 14 p
(DA Proj. 1L1-61102-AH-42)
(AD-A249745; MTL-TR-92-14) Avail: CASI HC A03/MF A01

The ability to predict the gas permeation behavior in rubbery polymers requires knowledge of both the equilibrium solubility and the diffusion constant. The methods for predicting the solubility and diffusion constants from first principles have been assessed. The dissolution process is best addressed by the methods of statistical mechanics using the lattice-fluid (LF) equation of state. This treatment requires experimental PVT data on the pure components, but not on mixtures, assuming ideal gas behavior. Departure from ideality would require knowledge of the X interaction parameter. The diffusion part of the problem is best addressed by molecular dynamics (MD) simulation. Some difficulties have been experienced in obtaining agreement between diffusion behavior predicted by MD, associated with unrealistically low amorphous density values predicted by MD, but the anisotropic united atom (AUA) approach to nonbonded potentials seems to resolve this problem. GRA

N92-31631# Sandia National Labs., Albuquerque, NM.
SURFACE CHEMISTRY OF MoS2 LUBRICANT FILMS: EFFECTS OF HIGH HUMIDITY STORAGE ON SPUTTERED FILMS
D. E. Peebles and J. A. Ohlhausen May 1992 50 p
(Contract DE-AC04-76DP-00789)
(DE92-015392; SAND-92-0052) Avail: CASI HC A03/MF A01

Many MoS2 lubricant film formulations exhibit tribological performance degradation after extended storage in high humidity ambient environments. As a part of an extensive study of the effects of high humidity storage on a wide variety of MoS2 lubricant film formulations, the effects of high humidity storage on sputtered MoS2 films have been examined. The surface chemistries of a series of ten different commercially deposited MoS2 lubricant film formulations on 440C stainless steel have been examined before and after 1 month of storage at 98 percent relative humidity. While the films varied greatly in film chemistry prior to high humidity storage, many smaller differences were observed after high humidity storage. Addition of Ni to the films affects the film chemistry far more dramatically than the addition of AuPd or SbO(x), facilitating oxidation of the MoS2 and enhancing formation of sulfate species. All of the films are adequately characterized by considering only MoS2 and MoO3 species, with the exception of the films co-sputtered with Ni and ion implanted with N(sup +), where some MoO2 or MoS(2-x)O(x) must also be present. DOE

N92-31792* National Aeronautics and Space Administration. Langley Research Center, Hampton, VA.
IMIDE/ARYLENE ETHER COPOLYMERS Patent
Brian J. Jensen, inventor (to NASA), Paul M. Hergenrother, inventor (to NASA), and Robert G. Bass, inventor (to NASA) 12 May 1992 9 p Filed 21 Nov. 1989 Supersedes N90-26953 (27 - 21, p 2983)
(NASA-Case-LAR-14159-1-CU; US-Patent-5,112,923; US-Patent-Appl-SN-439317; US-Patent-Class-525-420; US-Patent-Class-525-434; US-Patent-Class-525-436; Int-Patent-Class-C08L-79/08) Avail: US Patent and Trademark Office

Imide/arylene ether block copolymers are prepared by reacting anhydride terminated poly(amic acids) with amine terminated poly(arylene ethers) in polar aprotic solvents and by chemically or thermally cyclodehydrating the resulting intermediate poly(amic acids). The resulting block copolymers have one glass transition temperature or two, depending upon the particular structure and/or the compatibility of the block units. Most of these block copolymers form tough, solvent resistant films with high tensile properties.
Official Gazette of the U.S. Patent and Trademark Office

N92-31810# Cornell Univ., Ithaca, NY.
PHOTOGENERATED BASE AS CATALYST FOR IMIDIZATION REACTIONS: DESIGN OF PHOTOSENSITIVE POLYIMIDES
J. M. Frechet, J. F. Cameron, C. M. Chung, S. A. Haque, and C. G. Willson 20 Apr. 1992 8 p
(Contract N00014-91-J-1338)
(AD-A250067; TR-8) Avail: CASI HC A02/MF A01

The photogeneration of free amines or diamines from soluble organic precursors such as photoactive 2-nitrobenzyl carbamates is useful for the imidization of polymers containing amic acid or amic ester groups as part of their main-chain or their side-chain. The base-catalyzed reaction occurs at lower temperatures than the noncatalyzed thermal process and is applicable to the patterning of thin film coatings. GRA

N92-31840*# National Aeronautics and Space Administration. Lewis Research Center, Cleveland, OH.
LIQUID LUBRICATION FOR SPACE APPLICATIONS
Robert L. Fusaro and Michael M. Khonsari (Pittsburgh Univ., PA.) Jul. 1992 34 p
(RTOP 505-63-5B)
(NASA-TM-105198; E-6500; NAS 1.15:105198) Avail: CASI HC A03/MF A01

Reviewed here is the state of the art of liquid lubrication for space applications. The areas discussed are types of liquid lubrication mechanisms, space environmental effects on lubrication, classification of lubricants, liquid lubricant additives, grease lubrication, mechanism materials, bearing anomalies and failures, lubricant supply techniques, and application types and lubricant needs for those applications. Author

N92-31917# Oak Ridge National Lab., TN.
SUBSTRATE SURFACE EFFECTS ON THE PROPERTIES OF SPUTTER-DEPOSITED AND LASER-IRRADIATED FILMS
A. J. Pedraza (Tennessee Univ., Knoxville.), M. J. Godbole (Tennessee Univ., Knoxville.), and L. Romana 1991 7 p Presented at the Annual Fall Meeting of the Materials Research Society, Boston, MA, 2-6 Dec. 1991
(Contract DE-AC05-84OR-21400)
(DE92-013850; CONF-911202-79) Avail: CASI HC A02/MF A01

Sapphire substrates, mechanically polished to an optical finish, were annealed for two days at either 1000 or 1350 C. The near surface condition of as-polished and of the annealed substrates was analyzed by Rutherford backscattering/channeling (RBS-C) and by scanning electron microscopy/channeling (SEM-C), by transmission electron microscopy (TEM), and by scanning tunneling microscopy (STM). The polished substrates were found to be RBS-amorphous up to 100 nm, and heavily damaged at larger depths. In agreement with these results, no electron channeling was obtained from polished samples. TEM, however, showed that the damaged region was crystalline, and the only defects detected were microtwins. Both RBS-C and SEM-C analyses revealed that the damage is removed when the sapphire substrates are annealed for 48 hrs. at 1350 C. The condition of the near-surface region, viz., as-polished or annealed, is found to strongly affect the morphology of the laser-irradiated copper films deposited on sapphire substrates. A correlation is found between the threshold for film evaporation and for film rupture upon laser irradiation, both being a function of the substrate condition. It is concluded that the near-surface damaged layer acts as a thermal barrier for heat transport across the substrate. DOE

N92-31938# Argonne National Lab., IL.
RADIOLYTIC GAS PRODUCTION IN THE ALPHA PARTICLE DEGRADATION OF PLASTICS
D. T. Reed, J. Hoh, J. Emery, and D. Hobbs (Westinghouse Savannah River Co., Aiken, SC.) 1992 11 p Presented at the Waste Management 1992, Tucson, AZ, 1-5 Mar. 1992
(Contract W-31-109-eng-38)
(DE92-011846; ANL/CP-75684; CONF-920307-72) Avail: CASI HC A03/MF A01

Net gas generation due to alpha particle irradiation of polyethylene and polyvinyl chloride was investigated. Experiments were performed in an air environment at 30, 60, and 100 C. The predominant radiolytic degradation products of polyethylene were hydrogen and carbon dioxide with a wide variety of trace organic species noted. Irradiation of polyvinyl chloride resulted in the formation of HCl in addition to the products observed for polyethylene. For both plastic materials, a strong enhancement of net yields was noted at 100 C. DOE

N92-31941# Carnegie-Mellon Univ., Pittsburgh, PA. Dept. of Chemistry.
RING-OPENING POLYMERIZATION OF STRAINED CYCLOTETRASILANES AS A NEW ROUTE TOWARDS WELL DEFINED POLYSILYLENES
Krzysztof Matyjaszewski, Marek Cypryk, Jerezy Chrusciel, and Eric Fossum 25 May 1992 12 p
(Contract N00014-90-J-1186)
(AD-A251020; TR-34) Avail: CASI HC A03/MF A01

Ring-opening polymerization of cyclic silanes is described as a new synthetic route to well defined high molecular weight polysilylenes. Strained cyclotetra-silanes with phenyl and methyl substituents at each Si atom in the four-membered ring are prepared by partial dephenylation of octaphenylcyclotetrasilane with triflic acid and subsequent treatment with methylmagnesium bromide. Chemoselectivity, regioselectivity, and stereoselectivity of monomer synthesis is discussed in detail. In addition to classic anionic initiators for the ring-opening process, new catalysts and initiators based on transition metals (Cu, Pd, Pt) are described. They provide much better control of the microstructure than systems with Li(+) counterion. GRA

N92-31951# Georgetown Univ., Washington, DC. Dept. of Chemistry.
DEVELOPMENT OF EFFECTIVE QUANTUM CHEMICAL METHOD FOR POLYMERS AND SOLID Final Report, Dec. 1988 - Nov. 1991
M. Kertesz 15 May 1992 9 p
(Grant AF-AFOSR-0229-89)
(AD-A250976; AFOSR-92-0457TR) Avail: CASI HC A02/MF A01

Applications of the chemical-molecular viewpoint in the calculation of properties of polymeric systems proved very fruitful in this project. In the area of methodology, we have perfected the band theory code MOSOL, which is based on the semiempirical MNDO (and its closely related versions, AM1 and PM3). These codes were all developed with some AFOSR support. In the course of this work we have included a screw axis of symmetry for polymers. Subsequently, we extended the method to metallic systems and improved the convergence of the calculations. We have introduced methodology applicable to a wide class of polymers and properties based on the oligomer approach. We have developed a new analytical theory for the calculation of the elastic modulus, Y, of polymers. GRA

N92-31952# Florida Univ., Gainesville. Dept. of Chemistry.
THE EFFECT OF SURFACE PRESSURE ON LANGMUIR-BLODGETT POLYMERIZATION OF 2-PENTADECYL ANILINE
H.-C. Zhou and R. S. Duran 19 May 1992 2 p
(Contract N00014-91-J-1655)
(AD-A250993; TR-3) Avail: CASI HC A01/MF A01

In this paper the effect of applied surface pressure upon the Langmuir-Blodgett polymerization of 2-pentadecyl aniline is investigated. Increasing the surface pressure was found to increase the polymerization rate dramatically. Experiments were performed to elucidate the underlying cause of this effect. GRA

N92-31954# Florida Univ., Gainesville. Dept. of Chemistry.
REAL TIME INVESTIGATIONS OF THE POLYMERIZATION OF 2-PENTADECYL ANILINE ON THE LANGMUIR-BLODGETT TROUGH
H. C. Zhou and R. S. Duran 19 May 1992 4 p

(Contract N00014-91-J-1655)
(AD-A250994; TR-6) Avail: CASI HC A01/MF A01

The monomer, 2-pentadecyl aniline, was spread at air-aqueous interfaces to produce stable monolayer films. Its surface pressure and surface potential isotherms are discussed. Polymerization of 2-pentadecyl aniline confined to a monolayer with a Langmuir trough was also studied. By using the trough itself as an instrument to probe the polymerization, the effects of initiator concentration and subphase acid concentration on the polymerization reaction are discussed. GRA

N92-31960# Nebraska Univ., Lincoln. Dept. of Chemistry.
ELECTRO-OPTICS AND SECOND HARMONIC GENERATION OF NONLINEAR OPTICAL POLYMERS
C. H. Wang and H. W. Guan 1 Jun. 1992 10 p
(Contract N00014-90-J-1494)
(AD-A252488; TR-17) Avail: CASI HC A02/MF A01

The susceptibilities for second harmonic generation (SHG) chi(sub 31)(sup (2)) and chi(sub 33)(sup (2)) of a new high T(sub g) polymer, 1,2-benzyl-1,2-cyclohexy l-bridged syndioregic a-cyanocinncimamide (BCSCCA) were measured by using a Maker fringe apparatus. The BCSCCA was spin coated on a quartz substrate. The film of about 1 micron thickness has shown a large birefringence before poling, thus indicating molecular alignment due to spin coating. The polar order was induced by poling the film at 215 C with the corona discharge. The SHG coefficient d(sub 33) = 3.54 pm/V and d(sub 13) = 0.95 pm/V at 532 nm. The d-coefficients are stable and show negligible decay over one month. The SHG intensities at 532, 528, 476, 403, and 366 mn are also observed. A large resonance enhancement in the SHG intensity was observed inside the absorption band. GRA

N92-31961# Nebraska Univ., Lincoln. Dept. of Chemistry.
DIFFUSION OF CAMPHORQUINONE IN UNIAXIALLY DRAWN POLYCARBONATE FILMS
J. L. Xia and C. H. Wang 1 Jun. 1992 16 p
(Contract N00014-90-J-1494)
(AD-A252489; TR-14) Avail: CASI HC A02/MF A01

Employing the laser induced holographic grating relaxation technique, we have measured tracer diffusion coefficients of a photochromous dye, camphorquinone (CQ), in uniaxially drawn polycarbonate films as a function of stretch ratio. Anisotropy in the tracer diffusion coefficient was observed with D greater than D by at least a factor of 4 for the film stretched to the stretch ratio delta = 2.3. The diffusion coefficient along the direction of stretch D increases significantly with increasing delta, whereas D decreases slightly with increasing delta. The stretch ratio dependence of D and D is interpreted according to a modified free volume theory. The strain rate and stretch temperature dependence of the anisotropic tracer diffusion coefficient was also investigated. GRA

N92-31968# Utah Univ., Salt Lake City. Dept. of Materials Science and Engineering.
DECOMPOSITION STUDIES OF TRIISOPROPYLANTIMONY AND TRIALLYLANTIMONY
S. H. Li, C. A. Larsen, G. B. Stringfellow, and R. W. Gedridge, Jr. 22 May 1992 26 p
(Contract N00014-91-J-1447)
(AD-A250671; TR-22) Avail: CASI HC A03/MF A01

The pyrolysis of triisopropylantimony ((C3H7)3SB) and triallylantimony ((C3H5)3Sb) has been investigated mass-spectrometrically in He and D2 using an SiO2 flow tube reactor at atmospheric pressure. Both temperature and time dependencies of percent decomposition were studied and the reaction products were analyzed. The overall decomposition processes for both compounds were found to be homogeneous and first order. (C3H7)3Sb pyrolyzes at 250-350 C with no effect of the ambient gas. However, C3H6, C3H8, and C6H14 (2,3-dimethylbutane) were produced in He, whereas C3H7D appeared in D2. The pyrolysis is believed to begin via bond cleavage to generate the free C3H7 radicals that, in turn, recombine and disproportionate. Isopropyl radicals react slowly with D2, producing the C3H7D detected. For (C3H5)3Sb, the pyrolysis takes place at 100-160 C. The only major product is C6HI0 (1,5-hexadiene). Both the pyrolysis rate and products were independent of the ambient. Two possible mechanisms, homolysis and reductive coupling, are discussed. Assuming that homolysis is the rate-limiting step for the pyrolysis of both (C3H7)3Sb and (C3H5)3Sb, bond strengths of 30.8 and 21.6 kcal/mole for C3H7-Sb and C3H5-Sb were determined from the experimental data. When either (C3H7)3Sb or (C3H5)3Sb was mixed with trimethylindium, a nonvolatile, liquid material, probably an adduct, was formed. GRA

N92-32001# Pittsburgh Univ., PA. Dept. of Chemistry.
THE SYNTHESIS AND CHARACTERIZATION OF TRIBOPHYSICAL LAYERS ON DIAMOND AND SILICON CARBIDE SURFACES Final Report, 1 May 1989 - 31 Jan. 1992
John T. Yates, Jr. May 1992 44 p
(Grant AF-AFOSR-0364-89)
(AD-A250983; AFOSR-92-0444TR) Avail: CASI HC A03/MF A01

A new ultrahigh vacuum apparatus, dedicated to the study of the surface chemistry of diamond single crystals, has been completed and the first scientific experiments have been done. This apparatus incorporates XPS, LEED, ESDIAD, HREELS, and TPD facilities for the study of the fluorination and hydrogenation of diamond single crystals. The apparatus is being employed for studies of atomic hydrogen/deuterium adsorption on diamond(100) in initial experiments prior to the use of XeF2 as a fluorinating agent. It is proposed to study the formation of CHx and CFx surface species, the thermal desorption products from these species, the resistance to oxidation by these species, and the functionalization of the diamond surface by fluorinated molecules such as C2F4, NF3, and CF3CF. Collaborative AFM studies of diamond AFM tips sliding over our diamond(100) single crystal are underway. Frictional studies completed on the non-modified surface will be compared to studies on fluorinated diamond(100). GRA

N92-32045# Aeronautical Research Labs., Melbourne (Australia).
POLYALPHAOLEFINS: A NEW IMPROVED COST EFFECTIVE AIRCRAFT RADAR COOLANT Aircraft Materials Report
Michael A. Stropki Jun. 1991 21 p
(AD-A250517; ARL-MAT-R-124; DODA-AR-006-607) Avail: CASI HC A03/MF A01

The use and potential problems associated with silicate ester (Coolanol) dielectric coolants in U.S. military applications such as aircraft radar and missile systems are highlighted. These fluids have caused significant and sometimes catastrophic problems due to their hygroscopic nature and subsequent formation of flammable alcohols and silica gel. In some of the more advanced stages, a gelatinous precipitate has caused component malfunctions such as electrical arcing, filter clogging, and fires. Extensive and costly fluid monitoring procedures have brought the malfunction under control, but this has not eliminated the problem. The U.S. Air Force and Navy have investigated the replacement of these silicate-ester-based fluids with a hydrogenated polyalphaole-fin-based (PAO) fluid in order to solve these material system problems. This report includes a brief historical perspective of silicate-ester related problems, the advantages and disadvantages of PAO, specific U.S. Air Force/Navy aircraft system flight test programs, and current status of the U.S. PAO conversion. GRA

N92-32079# Colorado State Univ., Fort Collins. Dept. of Chemistry.
EFFECT OF SYNTHESIS TEMPERATURE IN THE STRUCTURE, DOPING LEVEL AND CHARGE-TRANSPORT PROPERTIES OF POLYPYRROLE
Wenbin Liang, Junting Lei, and Charles R. Martin 8 May 1992 30 p

(Contract N00014-82-K-0612)
(AD-A250531; TR-72) Avail: CASI HC A03/MF A01

Polypyrrole perchlorate was chemically synthesized at various temperatures and the resulting polymers were investigated by elemental analysis, Fourier transform infrared spectroscopy (FTIR), x-ray photoelectron spectroscopy (XPS) and conductivity measurements. A correlation between conductivity, doping level and synthesis temperature was observed. The doping level of the polymer is higher when the synthesis is conducted at lower temperature exhibit longer conjugation length, fewer structural defects, higher charge carrier hopping frequency and higher conductivity. Furthermore, the results of this study indicate that the positive charges of doped polypyrrole are preferentially localized on the nitrogen atoms which are adjacent to the doping anions, as opposed to being uniformly delocalized along the polymer backbone. GRA

N92-32089# Oak Ridge National Lab., TN.
RHEOLOGY OF ZIRCONIA-ALUMINA GELCASTING SLURRIES
A. Bleier, O. O. Omatete, and C. G. Westmoreland 1992 9 p Presented at the Material Research Society Spring Meeting, San Francisco, CA, 27 Apr. - 2 May 1992
(Contract DE-AC05-84OR-21400)
(DE92-016787; CONF-920402-39) Avail: CASI HC A02/MF A01

The rheology of zirconia-alumina composite slurries for gelcasting was studied in order to maximize the solids loading. The viscosity and yield stress were controlled by adjusting the pH. This approach allows the solids loading to be maximized for the gelcasting of near-net-shape composites. A strong correspondence exists among the rheological behavior, the surface charge on the particles, colloidal stability, and the maximum solids loading. The best pH conditions for gelcasting composites depends on the specific binary composition. DOE

N92-32094# Oak Ridge National Lab., TN.
EFFECT OF SURFACE MODIFICATIONS ON THE PROPERTIES OF SILICON NITRIDE CERAMICS
S. Natansohn (GTE Labs., Inc., Waltham, MA.), A. E. Pasto (GTE Labs., Inc., Waltham, MA.), and W. J. Rourke (GTE Labs., Inc., Waltham, MA.) 1992 39 p Presented at the 94th Annual Meeting and Exposition of the American Ceramic Society, Minneapolis, MN, 12-16 Apr. 1992
(Contract DE-AC05-84OR-21400)
(DE92-013848; CONF-920448-5) Avail: CASI HC A03/MF A01

The effect of surface oxygen concentration of silicon nitride powders on the properties of resulting ceramics was studied. A high purity silicon nitride powder was treated physically and chemically to modify its surface oxygen content. The resulting powders were hot-pressed into dense ceramics using 6 w/o yttria as sintering aid. Strength and oxidation resistance of these ceramics were measured and correlated with the powder and ceramic compositions as well as the resulting intergranular phases. Results show that the phases developed in yttria-containing silicon nitride ceramics vary with slight changes in the initial powder oxygen content, as predicted, and that strength can be correlated to initial oxygen concentration. The mechanical strength vs. oxygen content curve has a definite maximum, i.e., there is a small oxygen concentration range at which optimum ceramic strength is realized. Best results are obtained when the oxygen content is increased by thermal oxidation; other techniques, such as chemical oxidation or addition of silica, are not as effective, particularly in attaining high strength at elevated temperatures. DOE

N92-32095# Arizona State Univ., Tempe. Dept. of Chemistry.
SOLID ELECTROLYTES AND IMPACT-RESISTANT CERAMICS
C. A. Angell Aug. 1991 20 p
(Contract DE-FG02-89ER-45398)
(DE92-015297; DOE/ER-45398/3) Avail: CASI HC A03/MF A01

In this proposal, we describe a program to exploit recent achievements in two distinct areas of materials science, both of them dependent on the independent motion of singly charged ions through an immobile matrix. The first is the area of non-crystalline solid electrolytes in which this laboratory has gained prominence over the past decade. The second is an area proposed for study in our previous proposal and now verified as a principle worthy of considerable further investigation: it involves the use of mobile ions for fast absorption of mechanical energy from short time impacts, hence, inhibition of crack nucleation and failure in glassy substances. In the first area, we will study both glassy and polymeric systems. For glassy solid electrolytes, we will perform the first electrochemical measurements of cation and anion self-diffusion coefficients in glasses, to provide data to compare with neutron scattering results and, thereby, to resolve a theoretical dispute. We will look for an important but so-far-unstudied relationship between conductivity/viscosity decoupling in fast ion glasses, and fragility of the liquid above the glass transition temperature. In polymer-salt systems, we will perform both diagnostic and developmental studies. We will try to demonstrate a continuity of behavior, as a function of solvent content, between highly decoupled glass and over-coupled salt/polymer solution behavior. This will incorporate a study of polymer-salt liquid immiscibility at high temperatures to seek the relationship between salts and molecular diluent as additives to the polymer solvent. We propose also to study the effects of perfluorination on both polymer fragility and glass transition, and also on carboxylate basicity for possible improvements in overall polymer-salt performance. DOE

N92-32136# Allied-Signal Aerospace Co., Kansas City, MO.
HIGH DENSITY THIN-WALLED SYNTACTIC FOAM
W. A. Staggs Apr. 1992 28 p
(Contract DE-AC04-76DP-00613)
(DE92-013159; KCP-613-4661) Avail: CASI HC A03/MF A01

Silicone rubber/glass microballoon syntactic foams (0.64 g/cm(sup 3)) were prepared using two different silicone rubber resin systems. Physical and thermodynamic properties were characterized for both syntactic foam systems. The mold was modified, and mold filling and handling techniques were varied to reduce the number and size of voids. DOE

N92-32146# Pacific Northwest Lab., Richland, WA.
ELECTRONIC STRUCTURE AND PHOTOPHYSICAL PROPERTIES OF POLYIMIDES
J. P. LaFemina and S. A. Kafafi (Johns Hopkins Univ., Baltimore, MD.) Apr. 1992 7 p Presented at the American Chemical Society National Meeting, San Francisco, CA, 5-10 Apr. 1992
(Contract DE-AC06-76RL-01830)
(DE92-012353; PNL-SA-20358; CONF-920444-27) Avail: CASI HC A02/MF A01

The quantum mechanical AM1 and CNDO/S3 models were used to examine the effect of iso-electronic substitutions on the conformation, electronic structure, and optical absorption spectra for a series of aromatic polyimides. An analysis of the geometric changes at the substitution site and its effect on the electronic structure allowed for the prediction of changes in the ICT band of the optical absorption spectra. DOE

N92-32151# Cornell Univ., Ithaca, NY. Dept. of Computer Science.
ON DEXTEROUS ROTATIONS OF POLYGONS
Daniela Rus Dec. 1991 27 p
(Contracts N00014-88-K-0591; N00014-89-J-1946)
(AD-A250967; TR-91-1258) Avail: CASI HC A03/MF A01

Dexterous manipulation, which is the reorientation of objects inside robot hands, is an active area of robotics research, whose progress has been slow. In this paper we present an algorithm for dexterous rotations of polygons by finger tracking. The algorithm involves simple finger motions. It can achieve arbitrarily large rotations and it is robust in the presence of computational uncertainties. GRA

N92-32153# Carnegie-Mellon Univ., Pittsburgh, PA. Dept. of Chemistry.
CATIONIC RING OPENING POLYMERIZATION OF OXAZOLINES INITIATED BY TRIMETHYLSILYL DERIVATIVES
Krzysztof Matyjaszewski and Jeffrey S. Hrkach 25 May 1992 10 p
(Contract N00014-90-J-1186)
(AD-A251109; TR-31) Avail: CASI HC A02/MF A01

Cationic polymerization of oxazolines was initiated by trimethylsilyl triflate and trimethylsilyl iodide. Initiation is slow due to the formation of a imine dimeric cation which is very unreactive toward oxazoline. The presence of the imine dimeric cation was confirmed by NMR and FAB-MS. GRA

N92-32194# Florida Univ., Gainesville. Dept. of Chemistry.
POLYMERIZATION OF CONDUCTING POLYMERS CONFINED TO FREE SURFACES: A COMPARISON OF THE LANGMUIR-BLODGETT POLYMERIZATION OF 3-ALKYL PYRROLES AND 2-ALKYL ANILINES
H. C. Zhou and R. S. Duran 19 May 1992 20 p
(Contract N00014-91-J-1655)
(AD-A250966) Avail: CASI HC A03/MF A01

The Langmuir-Blodgett polymerization of two monomers, 2-pentadecyl aniline and 3-hexadecyl pyrrole, is compared. Both monomers reacted to form polymers at air/aqueous interfaces. The aniline monomer showed autoacceleration upon polymerization and polymerized much faster as the applied surface pressure increased. The pyrrole monomer polymerized faster than the aniline, but showed little dependence on applied surface pressure. A new Langmuir-Blodgett polymerization experiment where the monomers were preoriented in a double compartment trough before chemical polymerization is introduced. The differences in the polymerization behavior of the two monomers is discussed in terms of their conformation. GRA

N92-32197# Rensselaer Polytechnic Inst., Troy, NY. Dept. of Chemistry.
PREPARATION OF NON-OXIDE CERAMICS BY PYROLYSIS OF ORGANOMETALLIC PRECURSORS
L. V. Interrante, W. R. Schmidt, P. S. Marchetti, and G. E. Maciel 25 May 1992 12 p
(Contract N00014-91-J-1917)
(AD-A251112) Avail: CASI HC A03/MF A01

Molecular precursors to non-oxide ceramics are of increasing interest for applications where conventional processing methods fail to provide the ceramic product in the required purity, microstructure and/or final form. The thermoplasticity, volatility, solubility, and/or molecular-level homogeneity of such precursor systems can provide, for example, high surface area powders of pure phases or of homogeneous nanocomposites; thin films and coatings by CVD and by pyrolysis of solution-applied precursor films; and continuous ceramic fiber less than 10 micro in diameter. Selected examples from our research on precursors to AlN, Si3N4 and SiC, including the synthesis of new precursors and solid state NMR studies of the precursor-to ceramic conversion process, will be used to illustrate the potential advantages of this approach to non-oxide ceramics. GRA

N92-32198# Harvard Univ., Cambridge, MA. Dept. of Chemistry.
SUPERSONIC PYROLYSIS JETS FOR DIAMOND FILM DEPOSITION Annual Report, 1 Jun. 1991 - 31 May 1992
Peter Chen 1 Jun. 1992 8 p
(Contract N00014-91-J-1012)
(AD-A251125; TR-2) Avail: CASI HC A02/MF A01

We have constructed and tested new higher-temperature ceramic (ZrO2 and SiC) pyrolysis nozzles that can operate continuously at 1700 C for several hours. The two successful designs were used to generate intense (1016 sec-1) beams of CH3 by thermal decomposition of azomethane. We probed the pyrolysate by vacuum-UV photoionization mass spectroscopy and (mass-resolved) resonant multiphoton ionization spectroscopy and determined that the ratio of CH3/C2H2 in our source is greater than 100:1. This should-make it an ideal source of methyl radicals for deposition. A chamber with the pyrolysis nozzle and a separate electric discharge nozzle source of H was constructed. The two jets were directed onto a thermostatted molybdenum foil. Micro-Raman assays (NRL with Jim Butler) of deposited material showed good-quality diamond, but we could not rule out Raman signals from diamond seed crystals with which the surface was scratched. We designed an efficient synthesis for 13CH3-N = N-CH3 as a source of 50 percent 13C-enriched methyl radicals. Micro-Raman showed no evidence 13C-enriched diamond, from which we conclude that we were previously seeing only the seed crystals. We are currently working on in situ probes to quantify the H concentration, and also trying different substrates. GRA

N92-32199# Instituto de Pesquisas Espaciais, Sao Jose dos Campos (Brazil). Lab. Associado de Plasma.
TETRAGONAL ZIRCONIA CERAMICS IN ZrO2-CeO2 SYSTEM (Ce-TZP): PREPARATION, CHARACTERIZATION AND MECHANICAL PROPERTIES [CERAMICAS DE ZIRCONIA TETRAGONAL POLICRISTALINA NO SISTEMA ZRO2-CEO2 (CE-TZP): PREPARACAO, CARACTERISTICAS E PROPRIEDADES MECANICAS]
Maria doCarmodeANono 1992 10 p In PORTUGESE
Presented at the 36th Congresso Brasileiro de Ceramica, Caxambu, Brazil, 7-10 Jun. 1992
(INPE-5372-PRE/1746) Avail: CASI HC A02/MF A01

The results achieved in a study about Ce-TZP ceramics prepared from conventional powder mixtures of ZrO2 and CeO2 (with composition in the range of 8 to 16 mol percent CeO2) are discussed. Physical and chemical characteristics were related with the powder compactation behavior and with the sinterization state. The sintered ceramics showed a level of high porosity (approx. equals 4 percent), mainly due to the fairly adequate powder characteristics and compactation. The crystalline phases were analyzed from x-ray diffraction data. The phases showed that these ceramics can present tetragonal-to-monoclinic stress induced transformation. The bending strength, fracture toughness and Vickers hardness results were influenced by CeO2 content microstructure and sintering temperature. These Ce-TZP ceramics showed mechanical strength results comparable to those published in the international literature. Author

28 PROPELLANTS AND FUELS

Includes rocket propellants, igniters, and oxidizers; their storage and handling procedures; and aircraft fuels.

For related information see also *07 Aircraft Propulsion and Power, 20 Spacecraft Propulsion and Power,* and *44 Energy Production and Conversion.*

N92-31399# Pennsylvania State Univ., University Park.
ADVANCED THERMALLY STABLE JET FUEL DEVELOPMENT PROGRAM. VOLUME 2: COMPOSITIONAL FACTORS AFFECTING THERMAL DEGRADATION OF JET FUELS Final Annual Report, Jul. 1990 - Jul. 1991
C. Song, S. Eser, H. H. Schobert, P. G. Hatcher, and M. M. Coleman May 1992 187 p
(Contract FY1455-89-N-0635)
(AD-A252656; WL-TR-91-2117-Vol-2) Avail: CASI HC A09/MF A02

This project focuses on the compositional factors affecting jet fuel thermal stability at high temperatures. The chemical composition of the four jet fuel samples (JP-8C, JP-8P, JP-7P, and Jet A1) and Wilsonville middle distillates was characterized by using selective ion monitoring technique in GC-MS analysis. The thermal treatment tests have been performed on jet fuels and a series of model compounds including tetralin, decalin, ethylcyclohexane, butylcyclohexane, nbutylbenzene, t-butylbenzene, n-octane, n-decane, and n-tetradecane. Deposit samples from an actual aircraft fuel system as well as those produced from jet fuels and model compounds in microautoclaves were characterized by FTIR and polarized-light microscopy.

Experiments were conducted to find the optimum amount of antioxidant 2,6-di-tert-butyl-4-methylphenol necessary to minimize the solid formation upon thermal stressing of JP8 neat and Jet A-1 fuel samples. The chemistry of thermal degradation of the fuel and antioxidant mixtures was studied by using FTIR to characterize the liquid products from thermal stressing. GRA

N92-31442# Argonne National Lab., IL. Energy Systems Div.
EXPERIMENTAL EVALUATION OF OXYGEN-ENRICHED AIR AND EMULSIFIED FUELS IN A SINGLE-CYLINDER DIESEL ENGINE. VOLUME 1: CONCEPT EVALUATION
R. R. Sekar, W. W. Marr, R. L. Cole, and T. J. Marciniak Nov. 1991 46 p
(Contract W-31-109-eng-38)
(DE92-015999; ANL/ESD/TM-30-Vol-1) Avail: CASI HC A03/MF A01

The performance of a single-cylinder, direct-injection diesel engine was measured with intake oxygen levels of up to 35 percent and fuel water contents of up to 20 percent. Because a previous study indicated that the use of a less-expensive fuel would be more economical, two series of tests with No. 4 diesel fuel and No. 2 diesel fuel were conducted. To control the emissions of nitrogen oxides (NOx), water was introduced into the combustion process in the form of water-emulsified fuel, or the fuel injection timing was retarded. In the first series of tests, compressed oxygen was used; in the second series of tests, a hollow-tube membrane was used. Steady-state engine performance and emissions data were obtained. Test results indicated a large increase in engine power density, a slight improvement in thermal efficiency, and significant reductions in smoke and particulate-matter emissions. Although NOx emissions increased, they could be controlled by introducing water and retarding the injection timing. The results further indicated that thermal efficiency is slightly increased when moderately water-emulsified fuels are used, because a greater portion of the fuel energy is released earlier in the combustion process. Oxygen-enriched air reduced the ignition delay and caused the heat-release rate and cumulative heat-release rates to change measurably. Even at higher oxygen levels, NOx emissions decreased rapidly when the timing was retarded, and the amount of smoke and the level of particulate-matter emissions did not significantly increase. The single-cylinder engine tests confirmed the results of an earlier technical assessment and further indicated a need for a low-pressure-drop membrane specifically designed for oxygen enrichment. DOE

N92-31462# Sandia National Labs., Albuquerque, NM.
ADVANCED THERMALLY STABLE, JET FUELS DEVELOPMENT PROGRAM ANNUAL REPORT. VOLUME 1: MODEL AND EXPERIMENT SYSTEM DEVELOPMENT Interim Report, Jun. 1990 - Jun. 1991
Elmer Klavetter, Wayne Trott, Tim OHern, and Steve Martin Jan. 1992 58 p
(AF Proj. 3048)
(AD-A249625; WL-TR-91-2099) Avail: CASI HC A04/MF A01

A program entitled Thermally Stable Jet Fuels Development was initiated in FY-89 by the U.S. Air Force, Aero Propulsion and Power Directorate, working jointly with the Department of Energy, Pittsburgh Energy Technology Center. Aviation turbine fuel thermal stability is of concern because of the potential operational problems arising from the degradation of fuels when used to cool aircraft components. Within this program, investigations are proceeding to develop candidate advanced thermally stable fuels, kinetic models of fuel degradation and to measure parameters for computational fluid dynamic models to predict the degradation of fuel under various conditions. This report summarizes the development and testing of instrumentation systems to measure solid particle formation during fuel thermal stressing and to measure the accumulation rates of solids on a surface, and describes analyses of jet fuel liquids and formed solids. GRA

N92-31570# Sandia National Labs., Albuquerque, NM.
THE COLLECTION, HANDLING, TRANSPORTATION, AND THERMAL DESORPTION OF EXPLOSIVE VAPOR USING QUARTZ COLLECTION TUBES
P. J. Rodacy and D. Ingersoll Apr. 1992 26 p
(Contract DE-AC04-76DP-00789)
(DE92-011441; SAND-90-1326) Avail: CASI HC A03/MF A01

This work describes the collection, handling, transportation, thermal desorption, and analysis of explosive vapors using quartz collection tubes. A description of the sampling system is presented, along with the collection efficiency of the quartz tubes and some of the precautions necessary to maintain the sample integrity. The design and performance characteristics of the thermal desorption system are also discussed. Collection of explosive vapor using empty, 0.25 inch O.D. by 5.25 inch long quartz tubes at a flow rate of 200 mL/min is quite different. Thermal desorption of the explosive vapor molecules using a furnace that allows control of the gas phase chemistry in the IMS has been shown to provide a reliable, reproducible means of analysis. Empty quartz tubes provide a sharper desorption profile than packed collection tubes, resulting in a better signal-to-noise ratio, and perhaps, a lower detection limit than packed quartz tubes. Both the ion drift time of the explosive and its desorption characteristics can provide a means of identification. Sample handling, packaging, and transportation methods which minimize sample loss and contamination have been developed and evaluated. DOE

N92-31593# Midwest Research Inst., Golden, CO.
CATALYST AND FEEDSTOCK EFFECTS IN THE THERMOCHEMICAL CONVERSION OF BIOMASS TO LIQUID TRANSPORTATION FUELS
B. Rejai, F. A. Agblevor, R. J. Evans, and D. Wang May 1992 5 p Presented at the National Solar Energy Conference, Cocoa Beach, FL, 13-18 Jun. 1992
(Contract DE-AC02-83CH-10093)
(DE92-010569; NREL/TP-431-4831; CONF-920678-7) Avail: CASI HC A01/MF A01

The thermochemical conversion of biomass feedstocks to liquid transportation fuels can be accomplished by three processes, namely gasification, high-pressure liquefaction, and pyrolysis. In this study, the pyrolysis option is selected which is followed by the catalytic upgrading of pyrolysis vapors to aromatic and olefinic hydrocarbons (PYROCAT process). The aromatics constitute a high-octane gasoline blend, while the olefins can be utilized as feedstocks for various chemicals. The PYROCAT process has been studied in a laboratory-scale fixed-bed catalytic reactor. Consecutive biomass samples were pyrolyzed rapidly in steam at 550 C and atmospheric pressure, and then the pyrolysis vapors were passed over a zeolite catalyst. The catalytic upgrading products were monitored in real-time using molecular-beam mass-spectrometry (MBMS). The yields of major products were estimated from mass-spectral data. Several zeolite catalysts were screened in the upgrading process and promising catalysts with high yields were identified. Feedstocks studied included the woody biomass species aspen (Populus tremuloides), basswood (Tilia americana), and willow (Salix alba); the three isolated components of wood lignin, xylan and cellulose; and the herbaceous species bagasse (Saccharum spp. hybrid), wheat straw (Triticum aestivum), and Sericea lespedeza (Lespedeza cuneata). DOE

N92-31751# Sun Oil Co., Marcus Hook, PA. Research and Development Dept.
LIGHT ALKANE CONVERSION PROCESSES: SUPRABIOTIC CATALYST SYSTEMS FOR SELECTIVE OXIDATION OF LIGHT ALKANE GASES TO FUEL OXYGENATES
J. E. Lyons 1992 15 p Presented at the US Department of Energy Contractor Review Meeting on Natural Gas Research and Development, Morgantown, WV, 5-6 May 1992
(Contract DE-FC21-90MC-26029)
(DE92-015229; DOE/MC-26029/92/C0037; CONF-920584-22)
Avail: CASI HC A03/MF A01

The objective of the work presented in this paper is to develop new, efficient catalysts for the selective transformation of the light

alkanes in natural gas to alcohols for use as liquid transportation fuels, fuel precursors, and chemical products. There currently exists no DIRECT one-step catalytic air-oxidation process to convert these substrates to alcohols. Such a one-step route would represent superior useful technology for the utilization of natural gas and similar refinery-derived light hydrocarbon streams. Processes for converting natural gas or its components (methane, ethane, propane, and the butanes) to alcohols for use as motor fuels, fuel additives, or fuel precursors will not only add a valuable alternative to crude oil but will produce a clean-burning, high octane alternative to conventional gasoline. DOE

N92-31800# Army Missile Command, Redstone Arsenal, AL. Weapons Science Directorate.

SELECTIVE NITRATIONS: THE LASER-INDUCED NITRATION OF THREE CYCLOALKANES, 1 Summary Report, May 1988 - Jul. 1991

Ann E. Stanley, Susan E. Godbey, Judith M. Bonicamp, and Larry M. Ludwick Feb. 1992 49 p

(Contract DAAL03-86-D-0001)

(AD-A249942; AD-E951775; AMSMI/TR-RD-WS-91-12) Avail: CASI HC A03/MF A01

The Army uses nitrated compounds as explosives and propellants. There is a special need for propellants with the chemical composition necessary to burn exactly with a minimum of side products which create smoke, but with high energy production. An important part of this process is the ability to selectively nitrate materials. Laser-induced chemistry possesses the potential to drive some reactions in an efficient and selective manner, and may be useful in driving nitration reactions toward specific products. Reported herein are the results of several successful attempts to laser-induce the reaction of nitrogen dioxide with three cycloalkanes. Specifically, the carbon dioxide infrared laser was used to drive the reaction between cyclopropane, cyclobutane, and cyclopentane under a variety of reaction conditions. The major products resulted from either ring cleavage or product dissociation, and nitration or oxidation. The qualitative spectrochemical analysis of the product mixtures is presented. Optimal conditions were found for producing products. The array of products was found to be highly sensitive to the specific reaction conditions. GRA

N92-31804# Ballistic Research Labs., Aberdeen Proving Ground, MD.

SHOCK TUBE STUDY OF THE REACTION OF TRIETHANOL AMMONIUM NITRATE WITH N2O Final Report, Sep. 1989 - Dec. 1990

Richard A. Beyer Apr. 1992 27 p

(DA Proj. 1L1-61102-AH-43)

(AD-A250034; BRL-TR-3329) Avail: CASI HC A03/MF A01

The ignition of triethanol ammonium nitrate in O2 and N2O has been studied in a shock tube over the temperature range from 1,300 K to 1,950 K. The ignition threshold for TEAN in 5 percent N20 is above 1,300 K. The reactions can be described by Arrhenius kinetics with activation energies of 17.0 kcal/mol and 20.7 kcal/mol, respectively. GRA

N92-31969# Andrulis Research Corp., Salt Lake City, UT.

DEVELOPMENT OF METHODOLOGY AND TECHNOLOGY FOR IDENTIFYING AND QUANTIFYING EMISSION PRODUCTS FROM OPEN BURNING AND OPEN DETONATION THERMAL TREATMENT METHODS. BANGBOX TEST SERIES. VOLUME 1. TEST SUMMARY Final Report, Dec. 1988 - Jan. 1992

MacDonald Johnson Jan. 1992 85 p

(Contract DAAD09-87-D-0008)

(AD-A250733) Avail: CASI HC A05/MF A01

The report addresses the gaseous and particulate sampling of TNT detonations and double-base and manufactures residue propellant burns. All trials were accomplished in an air supported building (BangBox). Sampling was accomplished with real time instruments for CO2, CO, NOx, 03, and SO2; canister samplers for SF6, CO2, CO, and volatile hydrocarbons; Quartz fiber filters with backup XAD-2 resin cartridges for semivolatile organics, and various instruments for size and mass of particles. For each analyte measured an emission factor was calculated by the concentration times volume of the building and by the carbon balance method. The carbon balance method is based on the conservation of carbon in the detonation or burn and thus becomes the trace element used as the basis for determining emission factors. The mass balance of carbon in the TNT detonation was established in the BangBox with CO, contributing 97 percent of the total carbon, CO carbon (0.50 percent), semivolatile and non volatile organics carbon (0.57 percent), and soot (1.7 percent). GRA

N92-31970# Andrulis Research Corp., Salt Lake City, UT.

DEVELOPMENT OF METHODOLOGY AND TECHNOLOGY FOR IDENTIFYING AND QUANTIFYING EMISSION PRODUCTS FROM OPEN BURNING AND OPEN DETONATION THERMAL TREATMENT METHODS. BANGBOX TEST SERIES. VOLUME 2: TEST DEVELOPMENT Final Report, Dec. 1988 - Jan. 1992

MacDonald Johnson Jan. 1992 192 p

(Contract DAAD09-87-D-0008)

(AD-A250734) Avail: CASI HC A09/MF A02

The report covers in detail the test and the supporting data and analyses used to answer the objectives. The supporting data and analyses are provided for the test development, selection of equipment and procedures, determination of BangBox volume, aerosol homogeneity, and the detonation products of TNT, the burn products of double-base propellant and composite propellant, and the detonation products of foam-attenuated TNT. All trials were accomplished in an air supported building (BangBox). Sampling was accomplished with real time instruments for CO2, CO, NOx, O3, and SO; canister samplers for SF6, C02, CO, and volatile hydrocarbons; Quartz fiber filters with backup XAD-2 resin cartridges for semivolatile organics, and various instruments for size and mass of particulates. For each analyte measured an emission factor was calculated by the concentration times volume of the building and by the carbon balance method. The carbon balance method is based on the conservation of carbon in the detonation or burn and thus become the trace element used as the basis for determining emission factors. GRA

N92-31971# Andrulis Research Corp., Salt Lake City, UT.

DEVELOPMENT OF METHODOLOGY AND TECHNOLOGY FOR IDENTIFYING AND QUANTIFYING EMISSION PRODUCTS FROM OPEN BURNING AND OPEN DETONATION THERMAL TREATMENT METHODS. FIELD TEST SERIES A, B, AND C. VOLUME 1: TEST SUMMARY Final Report, Dec. 1988 - Jan. 1992

MacDonald Johnson Jan. 1992 290 p

(Contract DAAD09-87-D-0008)

(AD-A250735) Avail: CASI HC A13/MF A03

The report covers the OB/OD field tests A, B, and C using the methodology and technology developed in the BangBox (BB) test for use on the fixed-wing aircraft (FWAC). Field test A was a checkout of the equipment and sampling selected from the BB test, and the development of procedures for sampling the TNT detonation crater soil, and the particle fallout in the surrounding area. Triple-base propellant was also burned in pans with the area sampled to 30-m with fallout pans. The analytes in both the air emission and the soil were identified and quantified. Field test B used TNT as the explosive and manufacturing residue as the burn material. Air sampling with the FWAC and soil sampling provided estimates of emission factors (EF) and soil contaminates that were detected above background levels. Suspended TNT detonations and manufacturing residue burns were also characterized for emission products. Phase C test using refinements in sampling and analysis from the previous phases provided data for TNT, composition B, explosive D, and RDX detonations and manufacturing residue single-base (M1,M6) propellant burns. The EF data from the TNT field tests were examined and compared with BB data; the results were comparable in the analytes detected and the level of analytes detected. The results indicate an efficiency for the detonation greater than 92 percent. GRA

N92-31972# Andrulis Research Corp., Salt Lake City, UT.
DEVELOPMENT OF METHODOLOGY AND TECHNOLOGY FOR IDENTIFYING AND QUANTIFYING EMISSION PRODUCTS FROM OPEN BURNING AND OPEN DETONATION THERMAL TREATMENT METHODS. FIELD TEST SERIES A, B, AND C. VOLUME 2, PART A: QUALITY ASSURANCE AND QUALITY CONTROL Final Report, Dec. 1988 - Jan. 1992
MacDonald Johnson Jan. 1992 138 p
(Contract DAAD09-87-D-0008)
(AD-A250736) Avail: CASI HC A07/MF A02

The report describes the quality assurance/quality control program conducted during 1990 field testing which supported the OB/OD Thermal Treatment Methods Study. The QA/QC program encompassed sample collection, preparation, storage, extraction, analytical instrument operation, data reduction, statistical data analyses and interpretation. Samples included atmosphere collected in evacuated stainless steel canisters, soil, and Teflon coated-glass-fiber media. The supercritical fluid chromatograph and gas chromatograph with mass spectrometers were the principal laboratory analytical instruments used during these field tests. Real-time instruments detected and quantified CO, CO2, NO, NO2, and NOx. Near-real-time analyses were accomplished by use of a Teflon bag in which samples of the plume were collected for analyses during testing operations. Sample-tracking was conducted using a system which permitted precise identification of individual specimens from collection through analyses or archiving. Analysis of atmosphere and soil samples spiked by the U.S. Environment Protection Agency (EPA) reflected a degree of accuracy well within acceptable limits. GRA

N92-31973# Andrulis Research Corp., Salt Lake City, UT.
DEVELOPMENT OF METHODOLOGY AND TECHNOLOGY FOR IDENTIFYING AND QUANTIFYING EMISSION PRODUCTS FROM OPEN BURNING AND OPEN DETONATION THERMAL TREATMENT METHODS. FIELD TEST SERIES A, B, AND C. VOLUME 2, PART B: QUALITY ASSURANCE AND QUALITY CONTROL. APPENDICES Final Report, Dec. 1988 - Jan. 1992
MacDonald Johnson Jan. 1992 367 p
(Contract DAAD09-87-D-0008)
(AD-A250737) Avail: CASI HC A16/MF A03

The report describes the quality assurance/quality control program conducted during 1990 field testing which supported the OB/OD Thermal Treatment Methods Study. The QA/QC program encompassed sample collection, preparation, storage, extraction, analytical instrument operation, data reduction, statistical data analyses and interpretation. Samples included atmosphere collected in evacuated stainless steel canisters, soil, and Teflon coated-glass-fiber media. The supercritical fluid chromatograph and gas chromatograph with mass spectrometers were the principal laboratory analytical instruments used during these field tests. Real-time instruments detected and quantified CO, CO2, NO, NO2, and NOx. Near-real-time analyses were accomplished by use of a Teflon bag in which samples of the plume were collected for analyses during testing operations. Sample-tracking was conducted using a system which permitted precise identification of individual specimens from collection through analyses or archiving. Analysis of atmosphere and soil samples spiked by the U.S. Environmental Protection Agency (EPA) reflected a degree of accuracy well within acceptable limits. GRA

N92-31982# Phasex Corp., Lawrence, MA.
SUPERCRITICAL FLUID FRACTIONATION OF JP-8 Final Report, Aug. 1990 - Jun. 1991
James J. Watkins and V. J. Krukonis 26 Dec. 1991 60 p
(Contract F33615-90-C-2075)
(AD-A247835; WL-TR-91-2083) Avail: CASI HC A04/MF A01

The fractionation of military aviation fuels with supercritical methane for purposes of separating multi-ring heteroaromatic and multi-ring aromatic compounds was demonstrated. It was shown that fractionated fuel possesses cleaner combustion properties, and it is anticipated that fractionated fuel will demonstrate enhanced thermal stability due to the absence of the heterocyclic compounds. Because supercritical fluids fractionate on the basis of solute/solvent interactions it is possible to separate compounds of similar vapor pressure but slightly different chemical natures. Trace quantities of heterocyclic and multi-ring aromatic compounds, therefore, may be removed without significantly altering the balance of the fuel. Distribution coefficients and selectivities (in methane) were obtained for several heteroaromatic compounds in JP-8, and calculations using this data indicate that a 95 percent reduction in heteroaromatic content with a 97 percent yield will be possible in a continuous, counter-current extraction column with an effective separation zone of less than 10 feet operating at ambient temperature and at pressures of less than 3800 psi. GRA

N92-32098# Naval Surface Warfare Center, Silver Spring, MD.
ESTIMATION OF METAL ACCELERATION BY AN SF5 CONTAINING EXPLOSIVE
Horst G. Adolph and G. W. Lawrence 30 Jun. 1991 22 p
(AD-A245338; NAVSWC-TR-91-250) Avail: CASI HC A03/MF A01

A two-inch cylinder expansion test was performed on a composition containing HMX, an energetic binder and 19 percent of a compound containing SF5 groups. The experimental cylinder wall energies were compared with calculated data for an analogous composition devoid of SF5. The results suggest that replacing hydrogen by the SF5 oxidizer moiety in a C, H, N, O explosive neither increases or decreases its metal accelerating ability substantially. The purpose of the work described here was to obtain an estimate of the relative metal accelerating ability of an SF5 containing explosive. The work is part of a continuing effort to assess the potential of the SF5 moiety as an energetic group. The approach taken was to perform a cylinder expansion test on a composition containing a significant amount of an SF5 compound and to compare the results with the calculated performance of a corresponding composition containing an equal volume of an SF5-free analog (H substituted for SF5). A lack of heat of formation data on SF5 compounds prevented calculation of the performance of the SF5 composition and direct comparison with the experimental data. GRA

N92-32230*# National Aeronautics and Space Administration. Lewis Research Center, Cleveland, OH.
DEMONSTRATED SURVIVABILITY OF A HIGH TEMPERATURE OPTICAL FIBER CABLE ON A 1500 POUND THRUST ROCKET CHAMBER
Amy L. Sovie Sep. 1992 11 p Proposed for presentation at the SPIE's International Symposium OE/Fibers 1992, Boston, MA, 8-11 Sep. 1992; sponsored by the International Society for Optical Engineering
(RTOP 590-21-41)
(NASA-TM-105835; E-7270; NAS 1.15:105835) Avail: CASI HC A03/MF A01

A demonstration of the ability of an existing optical fiber cable to survive the harsh environment of a rocket engine was performed at the NASA Lewis Research Center. The intent of this demonstration was to prove the feasibility of applying fiber optic technology to rocket engine instrumentation systems. Extreme thermal transient tests were achieved by wrapping a high temperature optical fiber, which was cablized for mechanical robustness, around the combustion chamber outside wall of a 1500 lb Hydrogen-Oxygen rocket engine. Additionally, the fiber was wrapped around coolant inlet pipes which were subject to near liquid hydrogen temperatures. Light from an LED was sent through the multimode fiber, and output power was monitored as a function of time while the engine was fired. The fiber showed no mechanical damage after 419 firings during which it was subject to transients from 30 K to 350 K, and total exposure time to near liquid hydrogen temperatures in excess of 990 seconds. These extreme temperatures did cause attenuation greater than 3 dB, but the signal was fully recovered at room temperature. This experiment demonstrates that commercially available optical fiber cables can survive the environment seen by a typical rocket engine instrumentation system, and disclose a temperature-dependent attenuation observed during exposure to near liquid hydrogen temperatures. Author

N92-31885# Israel Military Industries, Ramat-Hasharon (Israel).
FLAMMABILITY LIMITS AND BALLISTIC PROPERTIES OF FUEL-RICH PROPELLANTS
Abraham Shalom and Alon Gany (Technion - Israel Inst. of Tech., Haifa.) *In* Israel Society of Aeronautics and Astronautics, 31st Israel Annual Conference on Aviation and Astronautics 22 Feb. 1990 p 179-184 Previously announced in IAA as A91-39558
(For primary document see N92-31861 22-01)
Avail: CASI HC A02/MF A03

29 MATERIALS PROCESSING

Includes space-based development of products and processes for commercial applications.
For biological materials see *55 Space Biology.*

N92-31826# Utah State Univ., Logan. Dept. of Chemistry and Biochemistry.
ORGANIC MAIN-CHAIN NLO POLYMERS. 1: COPOLYMERIZATION OF BIS(ARYLCARBOXALDEHYDE) AND BIS(CYANOACETATE) MONOMERS VIA THE KNOEVENAGEL CONDENSATION Technical Report No. 9, 15 Apr. 1991 - 15 Apr. 1992
Michael E. Wright and Sanjoy Mullick 10 May 1992 24 p
(Contract N00014-91-J-1625)
(AD-A250215) Avail: CASI HC A03/MF A01

Two monomers, 4-(CO2Et(CN)C=CH)C6H4O(CH2)6OH (2) and 4-(CHO)C6H40(CH2)602CCH2CN (3), both containing NLO-phores, were prepared and polymerized by different methods. The Knoevenagel polycondensation technique provided polymers of good molecular weight and tractable in organic solvents. A series of bis(carboxaldehyde) comonomers were prepared in the study, and copolymerized with CNCH2CO2(CH2)6O2CCH2CN to afford a new series of accordion polymers (6) which contains NLO-phores. The copolymers were obtained with molecular weights in the range of 3100 to 30,100. We did not observe Tgs for the copolymers above 10 C. Author (GRA)

31 ENGINEERING (GENERAL)

Includes vacuum technology; control engineering; display engineering; cryogenics; and fire prevention.

N92-31242# Polish Academy of Sciences, Warsaw. Inst. Podstawowych Problemow Techniki.
EFFECT OF OUTER TEMPERATURE CHANGES AND SOLAR RADIATION ON EFFECTIVE HEAT LOSSES THROUGH EXTERNAL PARTITIONS OF BUILDINGS [WPLYW ZMIAN TEMPERATURY ZEWNETRZNEJ ORAZ PROMIENIOWANIA SLONECZNEGO NA EFEKTYWNE STRATY CIEPLA PRZEZ PRZEGRODY ZEWNETRZNE BUDYNKU]
Zbyslaw Pluta 1992 29 p In POLISH
Avail: CASI HC A03/MF A01

Problems related to modeling the thermal dynamics of buildings are discussed. The methods used for approaching this problem were found in the literature; they are presented along with my own description of the thermal phenomena in buildings. The description is based on results from the application of transport equations. The results of the calculations for a model room are presented. Author

N92-31263*# National Aeronautics and Space Administration. Lewis Research Center, Cleveland, OH.
LIFE EXTENDING CONTROL FOR ROCKET ENGINES
C. F. Lorenzo, J. R. Saus, A. Ray (Pennsylvania State Univ., University Park.), M. Carpino (Pennsylvania State Univ., University Park.), and M.-K. Wu (Pennsylvania State Univ., University Park.) Aug. 1992 19 p
(RTOP 590-21-11)
(NASA-TM-105789; E-7219; NAS 1.15:105789) Avail: CASI HC A03/MF A01

The concept of life extending control is defined. A brief discussion of current fatigue life prediction methods is given and the need for an alternative life prediction model based on a continuous functional relationship is established. Two approaches to life extending control are considered: (1) the implicit approach which uses cyclic fatigue life prediction as a basis for control design; and (2) the continuous life prediction approach which requires a continuous damage law. Progress on an initial formulation of a continuous (in time) fatigue model is presented. Finally, nonlinear programming is used to develop initial results for life extension for a simplified rocket engine (model). Author

N92-31580# Sandia National Labs., Albuquerque, NM.
CONTROLLED ATMOSPHERE SOLDERING SYSTEM
D. M. Keicher, C. L. Hernandez, D. R. Frear, and F. M. Hosking 1992 10 p Presented at the National Electronic Packaging and Production Conference (NEPCON), Boston, MA, 16 Jun. 1992
(Contract DE-AC04-76DP-00789)
(DE92-012633; SAND-92-0849C; CONF-9206154-1) Avail: CASI HC A02/MF A01

We have developed a controlled environment system in which to perform wetting experiments to analyze the effects of various atmospheres, both inert and reducing, on solder processing. This system consists of a custom designed vacuum chamber, an apparatus for heating specimens and a video system for data acquisition. The system design allows for rapid changes to various processing atmospheres. Specimens can be heated to soldering temperature from room temperature rapidly. The temperature is regulated by a controller which gives a maximum heating rate of 23 C/second while minimizing the amount of overshoot, thereby quickly achieving a stabilized temperature. A video system is used to acquire the data in the form of both numerical data and real-time video images. The video system allows multiple views of the wetting process to be captured and simultaneously records time and temperature information. The recorded information is suitable for digital analysis. The controlled atmosphere soldering system was used to perform experiments that examine the effect of inert and acid vapor atmospheres on solder wetting behavior. DOE

N92-31830# Science Applications International Corp., San Diego, CA. Foreign Applied Sciences Assessment Center.
SOVIET PRECISION TIMEKEEPING RESEARCH AND TECHNOLOGY
R. F. C. Vessot, D. W. Allan, S. J. B. Crampton, L. S. Cutler, and R. H. Kern Aug. 1991 338 p
(PB92-173046) Avail: CASI HC A15/MF A03

Soviet progress in precision timekeeping research and timekeeping capability during the last two decades is discussed. The study was conducted by a panel of seven U.S. scientists who have expertise in timekeeping, frequency control, time dissemination, and the direct applications of these disciplines to scientific investigation. The following topics are addressed: generation of time by atomic clocks at the present level of their technology; new and emerging technologies related to atomic clocks; time and frequency transfer technology; statistical processes involving metrological applications of time and frequency; applications of precise time and frequency to scientific investigations supporting timekeeping technology; and a comparison of Soviet research efforts with those of the United States and the West. The number of Soviet professionals working in the field is roughly 10 times that in the United States. The Soviet Union has facilities for large-scale production of frequency standards and has concentrated its efforts on developing and producing rubidium gas cell devices (relatively compact, low-cost frequency standards of modest accuracy and stability) and atomic hydrogen masers (relatively large, high-cost standards of modest accuracy and high stability). Author

N92-31890# Aerospace Medical Research Labs., Wright-Patterson AFB, OH.
CONSTRUCTION OF A DUAL AXIS FORCE REFLECTION STICK AND TEST STATION Final Report, Oct. 1989 - Sep. 1991
Daniel E. Repperger, Eric L. Scarborough, and Tamara L. Chelette Nov. 1991 29 p
(AD-A250731; AL-TR-1992-0041) Avail: CASI HC A03/MF A01

This report describes the construction of a dual axis force reflecting stick controller and test station which was constructed through the use of basic research funds (ILIR monies). The prototype described in this report is powered only by electric motors and used the latest technology in computers. This was an advancement over a previous prototype which involved pneumatic devices and was very large, bulky, and awkward to use. An experiment was conducted with 5 subjects as described herein to test the overall system for its use in experimental design. The motivation for developing such a small test station for the use of force reflection in stick controllers is because with this new compact and portable system, many new applications now appear for this technology. The system described herein minimizes both weight and electric power requirements to produce the same force reflection. By upgrading the technology in the components used in this test station, wider use of force reflection is now available for a host of new applications. GRA

N92-31908# Lawrence Livermore National Lab., CA.
CAPABILITIES OF THE 3-AXES MODIFIED FP42 DECKEL MILLING MACHINE
E. Villarreal May 1991 20 p
(Contract W-7405-eng-48)
(DE92-011737; UCRL-ID-107571) Avail: CASI HC A03/MF A01

This report is a technical guide containing information on the design and performance of the modified FP42 Deckel milling machine and associated tooling used in conjunction with the Deckel. The main modification consists of an aluminum head assembly bolted to the Deckel headstock. The head assembly supports two milling spindles. The spindles may be oriented in the X, Y and Z coordinate axes. The associated tooling includes a tool set station and precision workpiece clamping base. DOE

N92-32125# Brookhaven National Lab., Upton, NY.
THIN POLYMER ICEMAKER DEVELOPMENT AND TEST PROGRAM
R. W. Leigh (Pratt Inst., Brooklyn, NY.) Aug. 1991 21 p
(Contract DE-AC02-76CH-00016)
(DE92-016941; BNL-47549) Avail: CASI HC A03/MF A01

We have constructed and tested a small device to produce ice in ice/water mixtures using a cold fluid as the heat sink. The device is a flexible heat exchanger constructed from a thin film of a suitable polymer. When filled with circulating liquid coolant the heat exchanger consists of an inflated series of parallel tubes; ice forms on the outside in complementary half cylinders. When the circulation is cut off, gravity drains the coolant and the static head of the water bath crushes the tubes, freeing them from the ice which floats to the surface. Brine circulation is then re-started and the cycle begins again. Here we report recent testing of this device: it makes ice readily under water and easily sheds the semi-cylinders of ice over many cycles of operation. It produces ice at a rate of 10 kg/m(exp 2)-hour. It offers substantial benefits in simplicity and reliability over mechanical harvester ice making systems, and the potential for significant improvements in energy efficiency compared to systems which use a re-heat cycle to harvest the ice. A reliable method of leak detection has been developed. The device should be of substantial value to systems where efficiency and reliability are at a premium, such as slush ice for district cooling. DOE

32 COMMUNICATIONS AND RADAR

Includes radar; land and global communications; communications theory; and optical communications.

For related information see also *04 Aircraft Communications and Navigation* and *17 Space Communications, Spacecraft Communications, Command and Tracking.* For search and rescue see *03 Air Transportation and Safety,* and *16 Space Transportation.*

N92-31238*# Michigan Univ., Ann Arbor. Radiation Lab.
ELECTROMAGNETIC SCATTERING BY COATED CONVEX SURFACES AND WEDGES SIMULATED BY APPROXIMATE BOUNDARY CONDITIONS Ph.D. Thesis Technical Report, Feb. - Sep. 1992
H. H. Syed and John L. Volakis Jun. 1992 172 p Sponsored by Dynetics, Inc. and Pacific Missile Test Center
(Grant NAG2-541)
(NASA-CR-190540; NAS 1.26:190540; UMICH-025921-30-T)
Avail: CASI HC A08/MF A02

Asymptotic/high-frequency solutions are developed for analyzing the non-specular scattering mechanisms associated with coated convex surfaces and edges simulated by approximate boundary conditions. In particular, the standard impedance boundary conditions (SIBC's) and the second order generalized impedance boundary conditions (GIBC's) are employed for a characterization of the edge diffraction, creeping wave, and surface diffracted wave contributions. To study the creeping wave and surface diffracted wave mechanisms, rigorous UTD (uniform geometrical theory of diffraction) diffraction coefficients are developed for a convex coated cylinder simulated with SIBC's and GIBC's. The ray solutions obtained remain valid in the transition region and reduce uniformly to those in the deep lit and shadow regions. A uniform asymptotic solution is also presented for observations in the close vicinity of the cylinder. The diffraction coefficient for a convex cylinder are obtained via a generalization of the corresponding ones of the circular cylinder. To validate the asymptotic/high-frequency solution, integral equations are derived for both E and H-polarization and solved numerically using the method of moments. Results are presented for a single and three layered coated convex cylinder. Some insights are also provided on the accuracy of the employed GIBC's versus SIBC's for application to curved surfaces. To characterize the scattering by impedance wedges illuminated at skew incidence, diffraction coefficients are derived from an approximate solution of the governing functional difference equations. This solution exactly recovers the known ones for an impedance half plane or an arbitrary wedge at normal incidence, and to validate it for other wedge angles, a moment method code was used. Finally, to test the usefulness of the approximate skew incidence impedance wedge diffraction coefficient for three dimensional structures, equivalent currents are derived in the context of the physical theory of diffraction (PTD) for a finite length impedance wedge of arbitrary internal angles. These are incorporated in a standard general purpose PTD code and results are presented for a number of different impedance structures. Author

N92-31257*# National Aeronautics and Space Administration. Langley Research Center, Hampton, VA.
FLEXIBLE HEATING HEAD FOR INDUCTION HEATING APPARATUS AND METHOD Patent Application
Robert L. Fox, inventor (to NASA), Samuel D. Johnson, inventor (to NASA) (Inductron Corp., Yorktown, VA.), Robert H. Coultrip, inventor (to NASA) (Inductron Corp., Yorktown, VA.), and W. Morris Phillips, inventor (to NASA) (Inductron Corp., Yorktown, VA.) 31 Oct. 1991 17 p
(NASA-Case-LAR-14418-1; NAS 1.71:LAR-14418-1; US-Patent-Appl-SN-790723) Avail: CASI HC A03/MF A01

An induction heating head includes a length of wire having first and second opposite ends and being wound in a flat spiral shape to form an induction coil, a capacitor connected to the first and second ends of the wire, the induction coil and capacitor defining a tank circuit, and a flexible, elastomeric body molded to

encase the induction coil. When a susceptor is placed in juxtaposition to the body, and the tank circuit is powered, the susceptor is inductively heated. NASA

N92-31273*# Arizona State Univ., Tempe. Coll. of Engineering and Applied Science.
HIGH-FREQUENCY TECHNIQUES FOR RCS PREDICTION OF PLATE GEOMETRIES Semiannual Progress Report, 1 Feb. - 31 Jul. 1992
Constantine A. Balanis and Lesley A. Polka 31 Jul. 1992 21 p (Grant NAG1-562)
(NASA-CR-190656; NAS 1.26:190656) Avail: CASI HC A03/MF A01

Given here are hard polarization diffraction coefficients for the special case of a wedge that is coated with a lossy dielectric on one face and is perfectly conducting on the other face. Expressions for plane-wave incidence, far-field observation; for cylindrical-wave incidence, far-field observation; and for plane-wave incidence, near-field observation are presented for regular diffractions. In addition, terms for surface-wave and surface-wave transition fields are presented. These expressions are derived from the Uniform Theory of Diffraction (UTD) coefficients for a generalized impedance wedge and are simplified for rapid calculation for the case of one perfectly conducting face. Results from a first-order model for a coated, rectangular plate are examined; and potential problems in extending this modeling approach to more complicated coated structures are identified. Author

N92-31284# Naval Postgraduate School, Monterey, CA.
DESIGN AND SPECIFICATION OF A HIGH SPEED TRANSPORT PROTOCOL M.S. Thesis
Robert C. McArthur 26 Mar. 1992 92 p
(AD-A248323) Avail: CASI HC A05/MF A01

Due to the increase in data throughout potential provided by high speed (fiber optic) networks, existing transport protocols are becoming increasingly incapable of providing reliable and timely transfer of data. Whereas in networks of the past it was the transmission medium that caused the greatest communications delay, it is the case today that the transport protocols themselves have become the bottleneck. This thesis provides detailed insight into the issues that are affecting the development of the next generation of high speed transport protocols, and includes a formal specification and limited analysis of one such protocol. Through a dissection of transport protocol functions, this thesis illustrates some of the problems which are hindering optimal performance, and demonstrates some of the design considerations of new transport protocols which are providing significant gains in efficiency. Three of the most promising lightweight transport protocol research projects are surveyed to provide a frame of reference for the newly emerging design paradigm: taking advantage of the low error rate of fiber optic media to optimize success, rather than compensate for failure. GRA

N92-31314# Naval Postgraduate School, Monterey, CA.
ANALYSIS AND EVALUATION OF PROJECT EVERGREEN DATA M.S. Thesis
Antonio Gala Sep. 1991 193 p
(AD-A245983) Avail: CASI HC A09/MF A03

Project Evergreen was an experiment conducted to evaluate antenna responses to nanosecond pulses and the capability of broadband equipment to capture them. The two antennas tested were a log periodic antenna modified by Lawrence Livermore National Laboratories and a TEM horn antenna. Analysis of the data collected by the Naval Postgraduate School test site personnel indicated the following. (1) The antenna output response characteristic is different for the log periodic antenna and the TEM horn antenna. (2) The received polarization is a function of the transmitted polarization and the orientation of the receiving site relative to the transmitting site. (3) Signal strength and capture are a function of the polarization alignment of the transmitting and receiving antenna. (4) Pulses on the order of 1 to 10 nanoseconds require bandwidth exceeding 1 Gigahertz (GHz) in the transmitting and receiving equipment. (5) Broadband equipment with minimum bandwidths of 1 GHz are required to adequately capture and process extremely short time duration signals. GRA

N92-31317# Los Alamos National Lab., NM.
WAVENUMBERS FOR CURRENTS ON INFINITE- AND FINITE-LENGTH WIRES IN A CHIRAL MEDIUM
A. K. Bhattacharyya (New Mexico State Univ., University Park.), G. J. Burke (Lawrence Livermore National Lab., CA.), and E. K. Miller (Los Alamos National Lab., NM.) 1992 5 p Presented at the IEEE-American Physical Society International Symposium, Chicago, IL, 18-25 Jul. 1992
(Contract W-7405-eng-36)
(DE92-007565; LA-UR-92-296; CONF-920750-2) Avail: CASI HC A01/MF A01

There is increasing interest in determining the electromagnetic properties of material media differing from free space and the effects thereof on the radiation, propagation, and scattering of electromagnetic fields. A material property of special present interest is that of chirality. Chirality manifests itself as a 'handedness' wherein a chiral medium does not support propagation of a linearly-polarized plane wave, but which instead decomposes into two circularly-polarized waves that propagate at different speeds. Initial work in this area was devoted to developing various analytical solutions to some basic problems such as the Green's Dyadic for a point current source. Attention is now being increasingly devoted to using this early work for a variety of applications such as analyzing antennas in chiral media scattering from chiral objects; scattering from objects having chiral coatings; and reflection from planar chiral interfaces. The focus of the work described here is determining the wavenumbers (= minus alpha minus j beta) of the current waves excited on wire antennas located in an infinite chiral medium using two complementary approaches. One is to use an extension of an existing computer model (NEC) that permits modeling of arbitrary wire objects located in an infinite chiral medium. The other is to develop a solution for an infinitely long cylindrical antenna also located in an infinite chiral medium. The latter canonical problem is of interest in its own right as well as providing a means for achieving mutual validation with the NEC model. DOE

N92-31333# Connecticut Univ., Storrs. Dept. of Electrical and Systems Engineering.
ESTIMATION WITH MULTISENSOR/MULTISCAN DETECTION FUSION Final Report, 1 Aug. 1991 - 31 Jan. 1992
Y. Bar-Shalom and K. R. Pattipati 28 Mar. 1992 19 p
(Grant AF-AFOSR-0292-91)
(AD-A250496; AFOSR-92-0372TR) Avail: CASI HC A03/MF A01

In this paper we present an algorithm to solve the static problem of associating data from three spatially distributed heterogeneous sensors, each with a set of detections at the same time. The sensors could be active (3D or 2D radars) or passive (EO sensors measuring the azimuth and elevation angles of the source). The source of a detection can be either a real target, in which case the measurement is the true observation variable of the target plus measurement noise, or a spurious one, i.e., a false alarm. In addition, the sensors may have nonunity detection probabilities. The problem is to associate the measurements from the sensors to identify the 'real' targets, and to obtain their position estimates. Mathematically, this (static) measurement-target association problem leads to a generalized three-dimensional (3-D) matching problem, which is known to be NP-hard. In this paper, we present a fast, but near-optimal 3-D matching algorithm suited for estimating the positions of a large number of targets (greater than 50) in a dense cluster for real-time applications. Performance results on several representative test cases solved by the algorithm are presented. Author (GRA)

N92-31354# Oak Ridge National Lab., TN.
MITIGATION OF MAGNETOHYDRODYNAMIC ELECTROMAGNETIC PULSE (MHD-EMP) EFFECTS FROM COMMERCIAL ELECTRIC POWER SYSTEMS

P. R. Barnes, F. M. Tesche, and E. F. Vance Mar. 1992 99 p
(Contracts DNA0046-C156-AI; DE-AC05-84OR-21400)
(AD-A249577; ORNL-6709) Avail: CASI HC A05/MF A02

A large nuclear detonation at altitudes of several hundred kilometers above the earth distorts the earth's magnetic field and produces a strong magnetohydrodynamic electromagnetic pulse (MHD-EMP). This can adversely affect electrical power systems. In this report, the effects of this nuclear environment on critical facilities connected to the commercial power system are considered. Methods of mitigating the MHD-EMP impacts are investigated, and recommended protection schemes are presented. Guidelines for testing facilities to determine the effects of MHD-EMP and to validate the mitigation methods also are discussed. GRA

N92-31368# National Inst. of Standards and Technology, Boulder, CO. Electromagnetic Fields Div.
PHASE CHARACTERISTICS AND TIME RESPONSES OF UNKNOWN LINEAR SYSTEMS DETERMINED FROM MEASURED CW AMPLITUDE DATA
M. T. Ma and J. W. Adams Nov. 1991 26 p
(PB92-183722; NIST/TN-1349) Avail: CASI HC A03/MF A01

An alternative but simpler technique for calculating the complete time and frequency characteristics of an unknown linear system from the measured amplitude response to cw excitations is described. The associated system transfer function so determined may or may not be at minimum phase. A comparison of the time responses shows the worst case. Results also indicate that the susceptibility of the minimum-phase system to damage by pulsed excitation is the greatest during the initial period of excitation. GRA

N92-31369# Naval Command, Control and Ocean Surveillance Center, San Diego, CA. RDT/E Div.
USING THE BURST DERIVATIVE MEASURE TO IMPROVE THE COMPUTATIONAL EFFICIENCY OF ISAR MOTION COMPENSATION ALGORITHMS Final Report
R. P. Bocker and S. A. Jones Apr. 1992 38 p
(AD-A250850; NRAD-TD-2278) Avail: CASI HC A03/MF A01

This technical report describes the use of the burst derivative measure in motion compensation ISAR algorithms for estimating both the slant-range translational motion and rotational kinematic quantities of an uncooperative airborne target. Tests have been performed on simulated as well as actual ISAR data using both a Sun 4 SPARCstation 2 and a parallel processing transputer array. Preliminary results indicate that the burst derivative measure gives significant improvement in processing speed over the traditional entropy measure presently employed. GRA

N92-31376# California Univ., Los Angeles. Dept. of Electrical Engineering.
SIGNAL LOCATION USING GENERALIZED LINEAR CONSTRAINTS Final Report, 1 Aug. 1989 - 31 Jan. 1992
Lloyd J. Griffiths and D. D. Feldman Jan. 1992 13 p
(Contract DAAL03-89-K-0127)
(AD-A249580; ARO-27032.1-EL) Avail: CASI HC A03/MF A01

This report has presented a two-part method for estimating the directions of arrival of uncorrelated narrowband sources when there are arbitrary phase errors and angle independent gain errors. The signal steering vectors are estimated in the first part of the method; in the second part, the arrival directions are estimated. It should be noted that the second part of the method can be tailored to incorporate additional information about the nature of the phase errors. For example, if the phase errors are known to be caused solely by element misplacement, the element locations can be estimated concurrently with the DOA's by trying to match the theoretical steering vectors to the estimated ones. Simulation results suggest that, for general perturbation, the method can resolve closely spaced sources under conditions for which a standard high-resolution DOA method such as MUSIC fails. GRA

N92-31381# West Chester Univ., PA. Dept. of Mathematics and Computer Science.
ALGORITHMS FOR THE DETERMINATION OF SPATIAL AND SPECTRAL DISTRIBUTION OF ELECTROMAGNETIC ENERGY IN A SIMULATED BIOSTRUCTURE SUBJECTED TO TRANSIENT SPATIALLY HETEROGENEOUS RADIATION WITH APPLICATIONS TO RADAR HAZARD ASSESSMENT AND CANCER THERAPY
D. K. Cohoon 1992 310 p
(Grant AF-AFOSR-0183-90)
(AD-A250447; AFOSR-92-0290TR) Avail: CASI HC A14/MF A03

There is concern that high power sources of electromagnetic radiation may cause physical harm to an exposed individual even when the frequencies are below those of x rays. Specifically concerns arise in the use of microwave equipment, radars, lasers, active imaging devices, and transmitters. Early efforts to address this question considered total absorbed power and then local internal temperature increases; computer algorithms to make these predictions were developed by USAF/SAM. Recently, as equipment with small duty cycles and very high peak power have been developed, concerns over the effect of sweeping fields and electromagnetic transients on biological structures have arisen. The algorithm developed in this report has as its purpose a highly accurate benchmark code which will predict the response of an N layer bianisotropic spherical structure to multiple plane waves with different amplitudes, frequencies, polarizations, and directions of travel and full wave solutions involving all of the p(sup m)(sub n). GRA

N92-31387# Sandia National Labs., Albuquerque, NM.
AN EVALUATION OF IONIZING RADIATION EMITTED BY HIGH POWER MICROWAVE GENERATORS
C. David Lovell (School of Aerospace Medicine, Brooks AFB, TX.) and W. Emmett Bolch (Florida Univ., Gainesville.) Feb. 1992 23 p
(Contract DE-AC04-76DP-00789)
(DE92-016160; SAND-91-7061) Avail: CASI HC A03/MF A01

Ionizing radiation emitted by electron-beam driven high power microwave (HPM) generators were measured in the near and far-field using lithium fluoride (LiF) thermoluminescent dosimeters (TLD's). Simplified photon energy spectra were determined by measuring radiation transmission, at electron beam energies of 300 to 650 keV, through various thicknesses of steel and lead attenuators. These data were used to calculate the effective energy of the x-rays produced by interactions between the electrons and the walls or other structures of the HPM generators. Operators were polled to determine locations of burn marks or other visible damage to locate potential ionizing radiation source regions. DOE

N92-31413# Naval Postgraduate School, Monterey, CA. Dept. of Electrical and Computer Engineering.
EXPONENTIAL REPRESENTATION AND CONSISTENCY CHECKING FOR M LAYER
Hung-Mou Lee and Yin Y. Han Mar. 1992 70 p
(AD-A250423; NPSEC-92-005) Avail: CASI HC A04/MF A01

M-layer, the tropospheric propagation effect prediction program is revised for greater accuracy, speed, and stability. This is achieved through converting the extended complex number representation into the representation by complex exponent, improving the accuracy in Airy function computation, introducing a new mode locating algorithm, and implementing a consistency checking procedure for determining the proper method to evaluate the height gain function. The revision has been documented and the new program source code has been delivered. It is recommended that the mode search protocol, not just the mode locating algorithm introduced in this revision, be completely revised. Unlike the current approach of blanketing the whole possible region until exhaustion, modes should be searched according to their range attenuation rates one by one along a well defined path. This should result in a faster and even more stable program. The program size can also be reduced. GRA

N92-31449# Los Alamos National Lab., NM.
READILY IMPLEMENTED ENHANCED SINUSOID DETECTION IN NOISE
K. V. Lindsay Mar. 1992 45 p
(Contract W-7405-eng-36)
(DE92-011359; LA-UR-92-789) Avail: CASI HC A03/MF A01

Significant efforts have been devoted, spanning many years, to the problem of sinusoid detection in noise. Many of these efforts have produced superb, yet complex, algorithms which may be difficult to use for a wide segment of the Digital Signal Processing (DSP) community. This paper presents a simple, easily implemented and highly effective method which solves this problem. This method severely degrades non-sinusoidal noise while leaving the embedded sinusoid(s) relatively undisturbed. The algorithm, simply put, exploits the difference between the net effect of integration and differentiation of sinusoids versus the effect of these operations on random noise and other signal sequences. The cross-correlation of sine wave with its differentiated (and/or integrated) self is quite high. Conversely, the cross-reduction of a noise sequence with its differentiated (and/or integrated) self is much lower. Therefore, it is reasonable to assume that for sequences consisting of a sinusoid in noise, significant signal-to-noise-ratios (SNRs) in the correlation results are achievable using a combination of differentiation (and/or integration) and cross-correlation operations on such sequences. This technique has been applied to actual Doppler radar data, as well as to synthesized data, with excellent improvement in signal detection capability. DOE

N92-31468*# New Mexico State Univ., Las Cruces. Dept. of Electrical Engineering.
THE INVESTIGATION OF BANDWIDTH EFFICIENT CODING AND MODULATION TECHNIQUES Final Annual Report
2 Sep. 1992 133 p
(Grant NAG5-1392)
(NASA-CR-190685; NAS 1.26:190685) Avail: CASI HC A07/MF A02

The New Mexico State University Center for Space Telemetering and Telecommunications systems has been, and is currently, engaged in the investigation of trellis-coded modulation (TCM) communication systems. In particular, TCM utilizing M-ary phase shift keying is being studied. The study of carrier synchronization in a TCM environment, or in MPSK systems in general, has been one of the two main thrusts of this grant. This study has involved both theoretical modelling and software simulation of the carrier synchronization problem. H.A.

N92-31470# Defence Research Establishment, Ottawa (Ontario). Nuclear Effects Section.
DESIGN OF A TEM CELL EMP SIMULATOR
Pete Sevat Jun. 1991 115 p
(DREO-1084; CTN-92-60311) Avail: CASI HC A06/MF A02

Electromagnetic pulse (EMP) simulators are designed to simulate the EMP generated by a nuclear weapon and are used to harden equipment against the effects of EMP. A transverse electromagnetic (TEM) cell is a square or rectangular coaxial transmission line tapered at each end to form a closed cell. The cell is fed at one end with a signal generator, a continuous wave or pulse generator, and terminated at the other end with a resistor equal to the characteristic impedance of the line. An advantage of the TEM cell is that the field is well characterized and reasonably uniform. A small, symmetric, TEM cell EMP simulator is described which is intended for applications such as susceptibility testing of small equipment, calibration of sensors, design and testing of countermeasures, measurement of transfer functions, and research and development. A detailed design is presented for a 50 ohm and 100 ohm TEM cell with an inner volume of 4 m(exp 3) and a test volume of 0.24 m(exp 3). The pulse generator and terminating network are integrated into the cell to form a completely shielded structure. In this way no interference from the inside of the cell to the outside, or vice versa, will occur. Author (CISTI)

N92-31471# McMaster Univ., Hamilton (Ontario). Communications Research Lab.
DETECTION OF SIGNAL HARMONIC SETS
Mehmet Zeytinoglu and Kon M. Wong May 1989 125 p
(Contract DREA-W7707-7-7926)
(DREA-CR-89-420; CTN-92-60315) Avail: CASI HC A06/MF A02

This report examines the problem of detecting signals consisting of harmonically related and partially correlated components. The received signal is assumed to have undergone multipath propagation and to be embedded in noise. Fast Fourier transform based detection algorithms that utilize this structure to enhance detection performance are investigated. Two basic detection algorithms is considered. In the case of the coherent detector, spectral components corresponding to harmonic frequencies are first combined, then the resulting expression is used to estimate total signal power. This approach stands in contrast to an incoherent detector which is a generalization of conventional detectors and is based on the principle of independently estimating the power at each harmonic frequency bin. Statistical laws governing these detection algorithms are delineated and theoretical and simulation results are presented. It is concluded that harmonic detector structures are inherently superior in their performance to single bin detectors. Author (CISTI)

N92-31543# Atmospheric Sciences Lab., White Sands Missile Range, NM.
ENERGY BALANCE MODEL FOR IMAGERY AND ELECTROMAGNETIC PROPAGATION Final Report
Henry Rachele and Arnold Tunick May 1992 41 p
(AD-A250884; ASL-TR-0311) Avail: CASI HC A03/MF A01

The optical turbulence structure parameter C2n typically appears in formulations used to estimate the effects of temperature and moisture (gradients) on imagery and electromagnetic propagation. Temperature and moisture gradients can be approximated from sensible and latent heat flux estimates, and these fluxes can be obtained from radiation/energy balance equations. Numerous energy balance models exist requiring different kinds and numbers of inputs. The semiempirical model developed and presented in this report was constrained to require a minimum number of conventional measurements at a reference level (2 m). These measurements include temperature, pressure, relative humidity, and windspeed. The model also requires a judgment of soil type and moisture (dry, moist, or saturated), cloud characteristics (tenths of cloud cover and density and an estimate of cloud height), day of the year, time of day, and longitude and latitude of the site of interest. Model estimates of net radiation, sensible and latent heat fluxes and C2n are compared with measured values. GRA

N92-31568# Instituto de Pesquisas Espaciais, Sao Jose dos Campos (Brazil).
CHANGES IN THE REFLECTANCE OF EX SITU LEAVES: A METHODOLOGICAL APPROACH [ALTERACOES NA REFLECTANCIA DE FOLHAS EX SITU: UMA ABORDAGEM METOLOGICA]
Flavio Jorge Ponzoni and Mario Takao Inoe Apr. 1992 59 p In PORTUGESE
(INPE-5407-PUD/051) Avail: CASI HC A04/MF A01

The main aspects of the interaction between electromagnetic radiation and detached leaves are presented. An experiment with Eucalipto and Araucaria detached leaves is described, including the description of the methodologies utilized in the collection and storage of the reflectance. Author

N92-31569# Wright Lab., Wright-Patterson AFB, OH.
ANALYSIS OF RANDOM INDUCED CROSS POLARIZATION
Daniel T. McGrath Mar. 1992 66 p
(AD-A249773; WL-TM-92-700-XPN) Avail: CASI HC A04/MF A01

Streamlined radomes will always introduce depolarization because of the fact that any material surface viewed at an oblique angle has different transmission coefficients for fields polarized

parallel and perpendicular to the plane of incidence, a phenomenon known as divorce. The cross polarized fields are similar in nature to those responsible for Condon lobes of parabolic reflectors, and which are known to make those antennas susceptible to cross polarization jamming. The relative strength of those lobes is directly related to the amount of divorce, and is quite sensitive to the phase difference of parallel and perpendicular transmission coefficients. A mere 20 deg of phase divorce has a comparable effect to 3 dB of amplitude divorce. This paper presents a detailed analysis for general radome shapes, based on geometrical optics (ray tracing). Example results are presented for conical and tangent ogive radome geometries used in conjunction with a circular-aperture antenna that is mechanically scanned. The results show that when the antenna is scanned off axis, the cross polarized pattern changes from a Condon lobe structure to a difference pattern in the direction orthogonal to the axis of scan, e.g.: under azimuth scanning the cross polarized sum pattern resembles an elevation difference pattern, while the cross polarized elevation difference resembles a sum beam. Hence, interference in the cross polarization will introduce a tracking error in the direction orthogonal to the scan plane. GRA

N92-31614*# Michigan Univ., Ann Arbor. Radiation Lab.
A FINITE ELEMENT-BOUNDARY INTEGRAL METHOD FOR CONFORMAL ANTENNA ARRAYS ON A CIRCULAR CYLINDER Final Report
Leo C. Kempel and John L. Volakis Jul. 1992 35 p Sponsored by Pacific Missile Test Center, Pt. Mugu, CA
(Contract NCA2-543)
(NASA-CR-190534; NAS 1.26:190534; UMICH-027723-6-T)
Avail: CASI HC A03/MF A01

Conformal antenna arrays offer many cost and weight advantages over conventional antenna systems. In the past, antenna designers have had to resort to expensive measurements in order to develop a conformal array design. This was due to the lack of rigorous mathematical models for conformal antenna arrays. As a result, the design of conformal arrays was primarily based on planar antenna design concepts. Recently, we have found the finite element-boundary integral method to be very successful in modeling large planar arrays of arbitrary composition in a metallic plane. We are extending this formulation to conformal arrays on large metallic cylinders. In doing so, we will develop a mathematical formulation. In particular, we discuss the finite element equations, the shape elements, and the boundary integral evaluation. It is shown how this formulation can be applied with minimal computation and memory requirements. Author

N92-31617# Federal Aviation Administration, Atlantic City, NJ.
EFFECT OF GUARD BAND REDUCTION ON MARKER BEACON RECEIVER PERFORMANCE
Martin Badinelli, Sam Barto, Arthur Cushman, and Y. Viet Truong Jul. 1992 46 p
(DOT/FAA/CT-TN92/18) Avail: CASI HC A03/MF A01

Aircraft Marker Beacon Receivers, which are a part of the Instrument Landing System, operate at a frequency of 75 megahertz (MHz) and until 1 Jan. 1990, were protected by a guard band of +/- 400 kilohertz (kHz). After this date, the guard band was reduced to +/- 200 kHz. This report details testing performed at the Federal Aviation Administration (FAA) Technical Center to assess the effect emitters, using this new guard band, will have on Marker Beacon Receivers. The effect of the interference on the Marker Beacon Receivers was determined by performing a desensitization test, a no-desired signal test, and a selectivity measurement on five general aviation Marker Beacon Receivers. For these tests, emitters that use amplitude modulation, frequency modulation, pulse modulation, and continuous wave were simulated. It was found that emitters using these new frequencies can cause interference to Marker Beacon Receivers. Recommendations for limiting the interference effect are provided in the body of the report. Author

N92-31629# Aerospace Corp., El Segundo, CA. Technical Operations.
DICKE NARROWING IN STRONG FIELDS: THE ATOM-AS-ANTENNA ANALOGY
J. C. Camparo, R. P. Frueholz, and H. G. Robinson (Duke Univ., Durham, NC.) 13 May 1992 21 p
(Contract F04701-88-C-0089)
(AD-A252321; TR-0089(4945-05)-1; SSD-TR-92-10) Avail: CASI HC A03/MF A01

When a radiator (or absorber) suffers velocity-changing collisions that do not perturb its internal state, the oscillator's successive Doppler shifts are motionally averaged. This process (Dicke narrowing) gives rise to a homogeneously broadened sub-Doppler resonance, which is often astride a broad, apparently Doppler width, pedestal. It has long been held that this pedestal is an inhomogeneous remnant of Doppler broadening, but no evidence has ever been obtained to substantiate this expectation. In the present study, we investigate the behavior of Dicke-narrowed lineshapes in strong fields in an evacuated wall-coated cell. Our experimental results indicate that the hypothesis of an inhomogeneous Doppler remnant pedestal is invalid. Rather, the pedestal is homogeneously broadened, and is best understood in terms of the oscillator's response to the electromagnetic field's power spectral density as observed in its rest frame. This conclusion suggests an intimate relationship between the process of Dicke narrowing and the behavior of quantum systems in the presence of stochastic fields. By envisioning the quantum system as a narrow-band antenna that only absorbs a small portion of the field's energy, we develop a simple intuitive model to account for the interaction of the atom with the nonmonochromatic field; the appeal of this simple theory is that it removes the need for extensive computation. Agreement between this atom-as-antenna analogy and experiment is very good. GRA

N92-31691# Air Force Inst. of Tech., Wright-Patterson AFB, OH.
SCATTERING FROM A FINITE COLLECTION OF TRANSVERSE DIPOLE AND AXIAL SLOT ARRAYS WITH EDGE EFFECTS Ph.D. Thesis
J. P. Skinner 1991 227 p
(AD-A249622; AFIT/CI/CIA-91-025D) Avail: CASI HC A11/MF A03

A moment method based solution for the electromagnetic radiation and scattering from geometries composed of transverse dipole column arrays and a finite collection of axial slot arrays is developed. Each 'array' is an infinite column of periodic elements, with transverse referring to a dipole orientation perpendicular to the infinite axis and axial denoting that thin linear slots are directed along the infinite axis. The slots are mounted in infinite ground planes, which may be surrounded by an arbitrary stack of infinite lossless dielectric slabs, simulating a hybrid frequency selective radome (i.e., periodic surface) in one linear polarization, which is infinite in one dimension and finite in another. Transverse dipole arrays are used to simulate phased array antennas in a similar 'finite by infinite' model. Independent modes in scattering current expansions are defined along single columns of periodic elements, with Floquet's theorem governing the current fluctuation along the infinite axis. A coupling matrix is developed with nine sub-blocks, representing mutual admittances, mutual impedances, unitless voltage gains, and unitless current gains. GRA

N92-31715# Utrecht State Univ. (Netherlands). Dept. of Computer Science.
TOWARDS A COMPLETE HIERARCHY OF COMPOSITIONAL DATAFLOW MODELS
Bengt Jonsson (Swedish Inst. of Computer Science, Uppsala.) and Joost N. Kok Dec. 1991 24 p
(Contract STU-89-01220P)
(RUU-CS-91-45; ETN-92-91811) Avail: CASI HC A03/MF A01

An investigation on trace models of dataflow networks, with the aim of characterizing compositional and noncompositional models, is presented. Several compositional trace models, which differ in whether they model liveness, termination or divergence,

are studied. The models are related into a hierarchy, according to their capability to distinguish networks. A hierarchy is called 'complete' if any gap between two models in the hierarchy contains no compositional models. The main contribution is to prove that most of the gaps in the hierarchy do not contain compositional models. Several full abstraction results in the literature follow directly from the gaps in the hierarchy. By restricting the networks to contain less powerful nondeterministic processes, additional models are shown to become compositional. This means that additional models are added to the hierarchy. ESA

N92-31722# Lawrence Livermore National Lab., CA.
IONOSPHERIC COMMUNICATIONS CHANNEL MODELLING
R. K. Bahr (Arizona Univ., Tucson.) and B. R. Ward (Arizona Univ., Tucson.) Feb. 1992 40 p
(Contract W-7405-eng-48)
(DE92-013039; UCRL-CR-110002) Avail: CASI HC A03/MF A01

The general scope of this work has been to investigate ionospheric communications channel modeling. Specifically, we have developed a simple model to study the detection and time-of-arrival (TOA) estimation of an earth-based, transient electromagnetic pulse by a satellite-borne receiver. The complete channel model divides naturally into four parts: the electromagnetic pulse signal model, the ionospheric propagation mode, the noise model, and the detector/TOA estimator. The described model is admittedly very crude. Numerous simplifications and outright omissions have been made. Nevertheless, we hope that this provides a sufficient basis for any interested researchers wishing to pursue the study of transient pulse detection and estimation. Below each of the four, sub-models are detailed. We alert the reader to some of the simplifications/omissions made in the model development. DOE

N92-31738# Sandia National Labs., Albuquerque, NM.
MODELING ARBITRARILY DIRECTED SLOTS THAT ARE NARROW BOTH IN WIDTH AND DEPTH WITH REGARD TO THE FDTD SPATIAL CELL
D. J. Riley and C. D. Turner 1991 5 p Presented at the IEEE-American Physical Society International Symposium, Chicago, IL, 18-25 Jul. 1992
(Contract DE-AC04-76DP-00789)
(DE92-008015; SAND-91-2910C; CONF-920750-3) Avail: CASI HC A01/MF A01

The Hybrid Thin-Slot Algorithm (HTSA) integrates a transient integral-equation solution for an aperture in an infinite plane into a finite-difference time-domain (FDTD) code. The technique was introduced for linear apertures and was extended to include wall loss and lossy internal gaskets. A general implementation for arbitrary thin slots is described here. The 3-D FDTD-code TSAR was selected for the implementation. The HTSA does not provide universal solutions to the narrow slot problem, but has merits appropriate for particular applications. The HTSA is restricted to planar slots, but can solve the important case that both the width and depth of the slot are narrow compared to the FDTD spatial cell. In addition, the HTSA is not bound to the FDTD discrete spatial and time increments, and therefore, high-resolution solutions for the slot physics are possible. The implementation of the HTSA into TSAR is based upon a 'slot data file' that includes the cell indices where the desired slots are exist within the FDTD mesh. For an HTSA-defined slot, the wall region local to the slot is shorted, and therefore, to change the slot's topology simply requires altering the file to include the desired cells. DOE

N92-31801# Army Missile Command, Redstone Arsenal, AL. Weapons Science Directorate.
DESIGN AND DEVELOPMENT OF MINILINK VIDEO: A FIBER-OPTIC COUPLED VIDEO SYSTEM Summary Report, Feb. - Oct. 1991
Darryl Holder Feb. 1992 21 p
(AD-A249945; AD-E951785; AMSMI/TR-RD-WS-92-2) Avail: CASI HC A03/MF A01

This report documents the in-house design, construction, and testing of a battery powered video camera which transmits its signal along a fiber-optic cable to the monitoring station. Certain types of testing require that a video camera be placed in close proximity to the test article, which results in the camera being subjected to the full force of the test environment, which often impairs its performance or causes it to fail entirely. In commercially available units, power and video cables which connect to the camera pose an electric shock hazard in some tests and can be a source of unwanted pickup of electromagnetic fields. The necessity for in-house design of this system was realized after a survey showed that no one manufacturer offers a system meeting all of the requirements for video monitoring. Because of these factors, a battery powered video camera which transmits its signal along a fiber-optic cable to the monitoring station has been designed in-house. The experimental version of this camera proved to be resistant to the environment, provided better contrast, higher resolution, and greater capability of operation at low light levels. This unit was successful for its intended purpose, and is a generally useful device with no changes. Future plans are to further extend the experimental design of the system to allow test monitoring with greater efficiency while yielding superior images.
Author (GRA)

N92-31809# Naval Postgraduate School, Monterey, CA.
MULTIMEDIA ELECTRONIC MAIL: STANDARDS AND PERFORMANCE SIMULATION M.S. Thesis
Nag J. Choi Mar. 1992 94 p
(AD-A250047) Avail: CASI HC A05/MF A01

This thesis surveys the current multimedia electronic mail (e-mail) related standards. The increasing demands for interoperability pushed the international standardization organizations to develop standards for e-mail. The multimedia e-mail related standards include X.400 and ODA. ODA supports formatted text, raster graphics, and geometric graphics. The future standards will be able to support high bandwidth uses such as high resolution color still-image, full-motion video, voice, and audio. The future components of multimedia e-mail include TIFF for raster graphics, CGM for geometric graphics, JPEG for high resolution color still-image, and MPEG for full-motion video. These multimedia data require vast amounts of storage, processing time, and transmission bandwidth. The standardization efforts can be viewed as selecting the best combination of these three factors. According to this view, the standard for each component is reviewed with frame of background, coding, compression, and current status. With the information from the survey study, a simulation study is conducted to investigate the performance of LAN where multimedia data are transmitted. The simulation results show that the high resolution image browsing activity in a LAN will burden the low speed LANs. The adoption of compression chips or high speed LANs such as FDDI will make such high bandwidth activities feasible. GRA

N92-31855*# National Aeronautics and Space Administration. Lewis Research Center, Cleveland, OH.
HIGH-PERFORMANCE PACKAGING FOR MONOLITHIC MICROWAVE AND MILLIMETER-WAVE INTEGRATED CIRCUITS
K. A. Shalkhauser, K. Li (Hughes Aircraft Co., Torrance, CA.), and Y. C. Shih (Hughes Aircraft Co., Torrance, CA.) 1992 11 p Presented at the 14th International Communications Satellite Systems Conference, Washington, DC, 22-26 Mar. 1992; sponsored by AIAA Previously announced in IAA as A92-31706
(Contract NAS3-25870; RTOP 506-72-1C)
(NASA-TM-105744; E-7149; NAS 1.15:105744) Copyright Avail: CASI HC A03/MF A01

Packaging schemes were developed that provide low-loss, hermetic enclosure for advanced monolithic microwave and millimeter-wave integrated circuits (MMICs). The package designs are based on a fused quartz substrate material that offers improved radio frequency (RF) performance through 44 gigahertz (GHz). The small size and weight of the packages make them appropriate for a variety of applications, including phased array antenna systems. Packages were designed in two forms; one for housing

a single MMIC chip, the second in the form of a multi-chip phased array module. The single chip array module was developed in three separate sizes, for chips of different geometry and frequency requirements. The phased array module was developed to address packaging directly for antenna applications, and includes transmission line and interconnect structures to support multi-element operation. All packages are fabricated using fused quartz substrate materials. As part of the packaging effort, a test fixture was developed to interface the single chip packages to conventional laboratory instrumentation for characterization of the packaged devices. The package and test fixture designs were both developed in a generic sense, optimizing performance for a wide range of possible applications and devices. Author

N92-31920# Science Applications International Corp., San Diego, CA. Foreign Applied Sciences Assessment Center.
SOVIET SATELLITE COMMUNICATIONS SCIENCE AND TECHNOLOGY
J. N. Birch, S. J. Campanella, G. S. Gordon, D. R. McElroy, and W. L. Pritchard Aug. 1991 161 p
(PB92-173038) Avail: CASI HC A08/MF A02

The current state of the art and projections of future Soviet satellite communications technologies are discussed. A panel of six U.S. scientists and engineers assessed the Soviet ability to support high-data-rate space missions at 128 Mbps by evaluating current and projected Soviet satellite communications technologies. A variety of space missions were considered, including Earth-to-Earth communications via satellites in geostationary or highly elliptical orbits, those missions that require space-to-Earth communications via a direct path, and those missions that require space-to-Earth communications via a relay satellite. Soviet satellite communications capability, in most cases, is 10 years behind that of the United States and other industrialized nations such as Japan, Italy, and France. However, based upon an analysis of communications links needed to support these missions, using current Soviet capabilities, it is well within the current Soviet technology to support certain space missions outlined above at rates of 128 Mbps or higher, although the published literature clearly shows that the Soviet Union has not exceeded 60 Mbps in its current space system. In response to decreased governmental support, the Soviet communications satellite industry is showing signs of some internal competition, is working on increasing communications satellite lifetime, and is also striving to develop joint ventures with Western firms. Author

N92-31921# Defence Research Establishment, Ottawa (Ontario). SATCOM Section.
SQUARE-LAW DEVICE ANALYSIS FOR THE DETECTION AND TIMING ESTIMATION OF A BURST BPSK SIGNAL
W. R. Seed Jun. 1991 29 p
(DREO-91-6; CTN-92-60331) Avail: CASI HC A03/MF A01

A square-law device is often found in the receiver front end of radar and communication devices. The two outputs of a square law device were analyzed in terms of output signal to noise ratio (SNR) for a burst binary phase shift keyed (BPSK) modulated pulse. After first deriving the device's output for a general BSPK signal, a closer examination was performed for a 13 bit Barker code which was selected for its good autocorrelation properties. The baseband component was shown to have a 2-3 dB performance advantage over the bandpass component. This SNR advantage increases as the frequency uncertainty of the input signal and hence, the input filter bandwidth, increases. The SNR of a BPSK modulated pulse following the enveloped detector and lowpass filter is compared to that obtained from a CW pulse having an equal power and duration. From the comparison, an expression is derived that transforms the E(sub b)/N(sub o) for a burst BPSK modulated signal to an equivalent E(sub b)/N(sub o) for a CW pulse. This can be utilized in parameter estimation and signal detection analyses for BPSK modulated pulses. Author (CISTI)

N92-31944# California Univ., Los Angeles. Dept. of Electrical Engineering.
COMPACT MILLIMETER-WAVE DEVICES: DIELECTRIC LOADED CARM, HIGH VOLTAGE CARM, SLOW WAVE CRM AND HIGH HARMONIC GYROTRON Final Report, 1 Dec. 1989 - 30 Nov. 1991
Neville Luhmann, Jr. 30 Nov. 1991 12 p
(Grant AF-AFOSR-0005-90)
(AD-A250497; AFOSR-92-0350TR) Avail: CASI HC A03/MF A01

A gyro-BWO can provide broadband slow timescale tunability by adjusting the magnetic field and fast narrowband tunability by varying the gun's voltage. This device depends on the internal feedback of the fast wave interaction between the electro beam's cyclotron resonance wave and a backward electromagnetic wave. Although the previous two experiments were operated at kW power levels, a gyro-BWO is capable of much higher power. GRA

N92-31993# Naval Postgraduate School, Monterey, CA.
COHERENT/NONCOHERENT DETECTION OF COHERENT OPTICAL HETERODYNE DPSK-CDMA AND MFSK-CDMA SIGNALS M.S. Thesis
David A. Jakubek Dec. 1991 103 p
(AD-A246215) Avail: CASI HC A06/MF A02

The system performance of a coherent optical heterodyne communication system is analyzed for MFSK-CDMA and DPSK-CDMA signalling. The analysis determines the effect that receiver thermal noise, photodetector shot noise, laser phase noise, and multiple user noise has on the system performance. For the single user system performance, the probability of bit error of the system is calculated as a function of Eb/No for laser linewidth-to-bit rate ratios from 0.1 to 0.01. For both MFSK and DPSK, the system performance is most affected by laser phase noise at higher linewidth-to-bit rate ratios. The multiple user analysis for MFSK-CDMA and DPSK-CDMA is determined by calculating the probability of bit error as a function of the number of users for various laser linewidth-to-bit rate ratios and codelengths. The observations made for the single user case concerning the effects of laser phase noise are also observed for the multiple user case. When the effects of the laser phase noise no longer dominate system performance, then MFSK-CDMA and DPSK-CDMA can be used to increase the user capacity of optical fiber systems.
Author (GRA)

N92-31996# IIT Research Inst., Chicago, IL.
EXTREMELY LOW FREQUENCY (ELF) COMMUNICATIONS SYSTEM ECOLOGICAL MONITORING PROGRAM SUMMARY OF 1990 PROGRESS Technical Report, 1 Jan. - 31 Dec. 1990
M. M. Abromavage and J. E. Zapotosky Dec. 1991 63 p
(Contract N00039-88-C-0065)
(AD-A246344; IITRI-D06200-1) Avail: CASI HC A04/MF A01

A long term ecological monitoring program is being conducted to monitor for possible electromagnetic effects that operation of the U.S. Navy's ELF Communications System might have to resident biota and their ecological relationships. Monitoring studies were selected through a peer reviewed and a competitive bidding process in mid-1982, and work on most studies began in late summer of that year. Preliminary activities of the program consisted of site selection, characterization of critical study aspects, and validation of assumptions made in original proposals. Data collection for studies at the Naval Radio Transmitting Facility (NRTF)-Clam Lake, Wisconsin was completed, as scheduled, during 1990. Data collection for studies at the NRTF-Republic, Michigan is planned to continue through 1992. This report summarizes the progress of the monitoring program during 1990. To date, investigators conclude that effects have occurred on biota exposed to EM fields produced by either a fully operational or an intermittently energized ELF transmission produced by either a fully operational or an intermittently energized ELF transmitting facility. GRA

N92-32043# Mitre Corp., Bedford, MA.
VALIDATION OF THE NUMERICAL ELECTRO-MAGNETICS CODE (NEC) FOR ANTENNA WIRE ELEMENTS IN PROXIMITY TO EARTH
M. M. Weiner Sep. 1991 60 p
(Mitre RP-91260)
(AD-A250507; MTR-11278) Avail: CASI HC A04/MF A01

This paper summarizes recent MITRE efforts to validate the NEC-3, NEC-GS, and NEC-3I versions of the Numerical Electromagnetics Code (NEC) developed by Lawrence Livermore National Laboratory for predicting the performance of antenna wire elements in close proximity to flat earth. In an early version (NEC-1), the effect of the air-ground interface was included by applying a plane-wave Fresnel reflection coefficient approximation to the field of a point source. The NEC-2 version, while still retaining the Fresnel reflection coefficient model as an option, provides a more accurate ground model by numerically evaluating Sommerfeld integrals. The version NEC-3 extends the NEC-2 version to cases for bare wire segments below the air-earth interface. Version NEC-GS utilizes rotational symmetry to provide a more efficient version of NEC-3 for the case of a monopole element with a uniform radial wire groundscreen (GS). Version NEC-3I extends NEC-3 to include the case of insulated wires. Author (GRA)

N92-32070# Research Inst. of National Defence, Linkoeping (Sweden). Huvudavdelning foer Informationsteknologi.
CALIBRATION NETWORK INTENDED FOR PHASED-ARRAY ANTENNAS AT 3 GHz [KALIBRERINGSNAET FOER DIGITALA GRUPPANTENNER VID 3 GHZ]
A. Bergquist Mar. 1992 46 p In SWAHILI
(PB92-195429; FOA-C-30650-8.4,3.2) Avail: CASI HC A03/MF A01

A study was made of a calibration network intended for phased-array antennas in a multistatic radar project. The output of the network was calculated, and an analysis was made of how the neglect of multiple reflections of higher orders affects the result. Author

N92-32101# Kansas Univ., Lawrence. Radar Systems and Remote Sensing Lab.
RADAR BACKSCATTER FROM THE SEA: CONTROLLED EXPERIMENTS Final Report
R. K. Moore Apr. 1992 5 p
(Contract N00014-90-J-4044)
(AD-A250858; RSL-TR-8960-1) Avail: CASI HC A01/MF A01

The subwindowing method of modelling synthetic-aperture-radar (SAR) imaging of ocean waves was extended to allow wave propagation in arbitrary directions. Simulated images show that the SAR image response to swells that are imaged by velocity bunching is reduced by random smearing due to wind-generated waves. The magnitude of this response is not accurately predicted by introducing a finite coherence time in the radar backscatter. The smearing does not affect the imaging of waves by surface radar cross-section modulation, and is independent of the wind direction. Adjusting the focus of the SAR processor introduces an offset in the image response of the surface scatters. When adjusted by one-half the azimuthal phase velocity of the wave, this compensates the incoherent advance of the wave being imaged, leading to a higher image contrast. The azimuthal cut-off and range rotation of the spectral peak are predicted when the imaging of wind-generated wave trains is simulated. The simulated images suggest that velocity bunching and azimuthal smearing are strongly interdependent, and cannot be included in a model separately. GRA

N92-32134# Brookhaven National Lab., Upton, NY.
CONVERSION OF POWER AND FREQUENCY
A. G. Ruggiero and J. Wei 1992 3 p Presented at the 3rd European Particle Accelerator Conference, Berlin (Germany), 24-28 Mar. 1992
(Contract DE-AC02-76CH-00016)
(DE92-012543; BNL-46678; CONF-920315-33) Avail: CASI HC A01/MF A01

This paper deals with a novel idea to excite electrons to radiate energy in the short (millimeter) wavelength range. A short electron bunch is made to travel along the axis of a waveguide where a TM electromagnetic wave is also traveling and causes the beam to perform transverse oscillations. The electrons radiate energy as a consequence of the oscillations. It is found that a convenient mode of operation is to drive the waveguide in proximity of the cut-off. DOE

N92-32161# Research Inst. of National Defence, Linkoeping (Sweden). Huvudavdelning foer Informationsteknologi.
REALIZATION OF LATTICE NETWORKS AT MHz- AND GHz-FREQUENCIES [REALISERING AV KORSLAENKSKOMPONENTER 1 MHZ-OCH GHZ-OMRADET]
A. Bergquist Feb. 1992 40 p In SWAHILI
(PB92-195437; FOA-C-30649-3.2) Avail: CASI HC A03/MF A01

A theoretical study of lattice networks is reported, together with results from measurements on such networks at MHz frequencies. It is shown how a considerable gain in bandwidth can be attained by using lattice networks for components instead of conventional transmission line- or lumped pi- and T-networks. Author

N92-32176# Defence Research Establishment, Ottawa (Ontario). EHF SATCOM Section.
A PROTOTYPE DND Ku BAND SATCOM SYSTEM FOR ANIK-C2 (PROJECT MASTER/MM2)
James D. Lambert and Allen H. McEwen May 1990 154 p
(DREO-1034; CTN-92-60332) Avail: CASI HC A08/MF A02

This report describes the construction, operation, and intended use of two complete Dept. of National Defense (Canada) satellite communications (SATCOM) terminals which are capable of point to point demonstration communications with each other using the Ku-band Canadian domestic satellite, Anik C-2. The two terminals consist of a fixed and a mobile unit, both of which were built to commercial standards to maximize the opportunities for DND benefit from the existing Canadian domestic SATCOM technology. The fixed terminal is assembled in a small shelter and uses a 12 foot antenna system. The mobile unit is contained in a small trailer mounted shelter with an integral, steerable 6 foot antenna center and a message center. This unit is suitable for operation on land or in a single C130 Hercules aircraft. The two terminals operate together to provide a secure point to point full duplex 19.2 kilobytes per second multiplexed data circuit over the Anik C-2 satellite. Both terminals will normally operate at a low transmit level of about +3 dBw. Northern trials are planned for the system. Since the satellite antenna gain rolls off rapidly north of the 60th parallel, both the mobile and fixed station Tx and Rx powers will have to be increased to illuminate the transponder with the same flux levels. Author (CISTI)

N92-32203# Toronto Univ. (Ontario).
EXPERIMENT ON A THREE-BEAM ADAPTIVE ARRAY FOR EHF FREQUENCY-HOPPED SIGNALS USING A FAST ALGORITHM, PHASE-D
J. L. Yen, P. Kremer, N. Amin, and J. Fung 1 May 1989 18 p
(Contract DSS-36001-8-3527-01-SS)
(CTN-92-60322) Avail: CASI HC A03/MF A01

The Department of National Defence (Canada) has been conducting studies into multi-beam adaptive arrays for extremely high frequency (EHF) frequency hopped signals. A three-beam 43 GHz adaptive antenna and a beam control processor is under development. An interactive software package for the operation of the array, capable of applying different control algorithms is being written. A maximum signal to jammer plus noise ratio (SJNR) was found to provide superior performance in preventing degradation of user signals in the presence of nearby jammers. A new fast algorithm using a modified conjugate gradient approach was found to be a very efficient way to implement anti-jamming arrays based on maximum SJNR criterion. The present study was intended to refine and simplify this algorithm and to implement the algorithm on an experimental array for real-time evaluation of

anti-jamming performance. A three-beam adaptive array was used. A simulation package was used in the evaluation of multi-beam systems using more than three beams and different user-jammer scenarios. An attempt to further reduce the computation burden through continued analysis of maximum SJNR met with limited success. A method to acquire and track an incoming laser beam is proposed. Author (CISTI)

N92-32214# Juszko Scientific Services, Victoria (British Columbia).
PARAMETERIZATION OF DIRECTIONAL SPECTRA, PART 2, VOLUME 1 Final Report
Barbara-Ann Juszko 31 Dec. 1989 120 p
(Contract DREA-W77707-9-0214-01-OCS)
(DREA-CR-89-445-Pt-2-Vol-1; CTN-92-60327) Avail: CASI HC A06/MF A02

The description of complex directional wave spectra using a limited number of parameters would reduce data storage requirements and facilitate the theoretical and practical use of spectral characteristics. The present work assessed the ability of a 10 parameter model developed in the WAVEC study and the existing OGDP hindcast model to represent hindcast directional wave spectra observed at a single location near Hibernia. The parametric model acceptably reproduced the hindcast spectra over 90 percent of the time. There was little loss of information as indicated by the behavior of the spectral statistics. A significant correlation was observed between energy levels, peak wave direction and vector mean direction between hindcast and observed behavior. No definite conclusions could be formed on specific frequency direction features due to intrinsic limitations in directional spectral techniques. A coherence analysis between hindcast and measured winds indicated that the man machine mix of hindcast input wind did provide an improvement over a purely geostrophic estimate. The coherence squared dropped below acceptable levels at frequencies above 0.75 cycles per day (cpd). This behavior was reflected in the coherence of the vector mean wave field. Limiting the analysis to selected wave frequency bands, indicated that the hindcast model did not reproduce the observed swell signature with any statistical confidence while the set showed acceptable coherence to frequencies between 0.75 and 1.0 cpd.
Author (CISTI)

N92-32217# Defence Research Establishment Valcartier (Quebec).
CHARACTERISTICS OF SELECTED REFERENCE TARGETS FOR CALIBRATING 10.6 MICRON LASER RADARS
H. Henshall and J. M. Cruickshank Nov. 1988 44 p
(DREV-R-4487/88; CTN-92-60339) Avail: CASI HC A03/MF A01

The reflective characteristics of several materials have been examined in an effort to develop a 10.6-micron reflectivity standard for field measurements on twelve different target materials, showing that many materials have components of diffuse reflectivity, specular reflectivity, and retroreflectivity. For each material examined, both the effective Lambertian reflectivity and the beam depolarization were determined. It was also found that because of the strong retroreflection component present in many materials, the practice of estimating the effective diffuse reflectivity from measurements of total reflectivity could lead to erroneous reflectivity values for laser radar systems. One of the preferred reference targets found for 10.6-micron field measurements was canvas tarpaulin. Author (CISTI)

N92-32231# Defence Research Establishment, Ottawa (Ontario). EHF SATCOM Section.
EHF SATCOM FREQUENCY HOPPING PATTERN GENERATOR: PROOF OF CONCEPT
Claude Belisle (Communications Research Centre, Ottawa, Ontario) and Claude Brochu Nov. 1989 35 p
(DREO-89-32; CTN-92-60323) Avail: CASI HC A03/MF A01

The Department of National Defence (Canada) has undertaken investigations aimed at the design and fabrication of a payload and two ground terminal simulators for the Functional Advanced EHF (extremely high frequencies) SATCOM System for Evaluation and Test (FASSET) project. This report describes the design of the frequency hopping pattern generator for the simulator project. The frequency hopping pattern is defined by a pseudo-random (PN) sequence of maximal length called a m-sequence. A precise time synchronization between the PN sequence produced at the transmitter and the one produced at the receiver must be obtained to recover the transmitted data. This report describes a system which can rapidly set the output bit pattern of a PN sequence of maximal length to simulate the desired time of day, given the PN sequence code and the initial condition of the sequence. This system can be used for synchronizing the frequency hopping pattern generator of the receiver to that of the transmitter. The operator enters the PN sequence generating polynomial, the initial condition of the sequence, the time of day when the sequence was initiated, and the time of day to which the sequence is to be set. The computer program evaluates all required connections inside each chip and downloads that information. Subsequently, an external clock is used in conjunction with the hardware circuit to produce the PN sequence bit pattern at the required rate.
Author (CISTI)

N92-32232# Defence Research Establishment, Ottawa (Ontario). EHF SATCOM Section.
A FREQUENCY HOPPING SYNTHESIZER CONTROLLER FOR EHF SATCOM
Claude Brochu Jul. 1989 64 p
(DREO-89-29; CTN-92-60324) Avail: CASI HC A04/MF A01

The Ground Terminal Simulator is one of the inhouse test facilities being developed at the Department of National Defence (Canada) for the system and technology evaluation phase of the Functional Advanced EHF (extremely high frequency) SATCOM System for Evaluation and Test (FASSET) project. The frequency hopping subsystem is a critical part of the simulator. A synthesizer controller was built to test this subsystem. This report describes the components of the synthesizer controller, its assembly and operation, and areas where improvement is possible. The frequency hopping synthesizer controller is composed of a high performance personal computer, a digital I/O board, an interface board, and software required to perform tests of the synthesizer in a number of modes. A performance analysis was done on the controller and the synthesizer operating in frequency hopping mode. It demonstrated that real time operation could not be supported by a personal computer due to speed constraints. However, the system should be of value in testing the frequency hopping subsystems in the construction stage of the ground terminal simulator.
Author (CISTI)

N92-32021 Army Strategic Defense Command, Huntsville, AL. GBR Project Office.
GROUND BASED RADAR
William W. Ryan *In* Huntsville Association of Technical Societies, TABES 92: 8th Annual Technical and Business Exhibition and Symposium. Executive Summaries and Submitted Papers 1992 7 p (For primary document see N92-32009 22-12)
(TABES Paper 92-213) Copyright Avail: Issuing Activity

33 ELECTRONICS AND ELECTRICAL ENGINEERING

Includes test equipment and maintainability; components, e.g., tunnel diodes and transistors; microminiaturization; and integrated circuitry.

For related information see also *60 Computer Operations and Hardware* and *76 Solid-State Physics.*

N92-31244# Polish Academy of Sciences, Warsaw. Inst. Podstawowych Problemow Techniki.
PIEZOELECTRIC RADIANT-TO-AIR ULTRASONIC TRANSDUCERS [PIEZOELEKTRYCZNE PRZETWORNIKI ULTRADZWIEKOWE PROMIENIUJACE DO POWIETRZA]

Wincenty Pajewski and Marek Szalewski 1992 80 p In POLISH
Avail: CASI HC A05/MF A01

Piezoelectric ultrasonic transducers used in robotics for sound echo location, identification of objects, and position of manipulators are discussed. The transducers radiate to air the ultrasonic waves at frequencies ranging from several tens to several hundreds of kHz. The following are discussed: the properties of the air as a medium for propagation of ultrasonic waves are discussed; resonant vibrations of various piezoelectric elements used in ultrasonic transducers and the methods used to analyze those vibrations; the methods used to obtain the parameters required for robotic applications; the shape of the directional response pattern of radiation; and measuring methods of transducer properties. Some basic properties of radiant-to-air transducers are presented: acoustic impedance, bandwidth, and power response. Designs and characteristics of the following types of ultrasonic transducers are presented: transducers with flexurally vibrating piezoelectric elements, transducers with piezoelectric elements of thickness-oriented vibrations (or with packs of such elements), transducers with annular piezoelectric elements, and composite transducers. Parameters of these transducers are shown. Author

N92-31282*# National Aeronautics and Space Administration. Lewis Research Center, Cleveland, OH.
STABILITY TESTING AND ANALYSIS OF A PMAD DC TEST BED FOR THE SPACE STATION FREEDOM
Robert M. Button and Andrew S. Brush (Sverdrup Technology, Inc., Brook Park, OH.) Aug. 1992 8 p Presented at the 27th Intersociety Energy Conversion Engineering Conference, San Diego, CA, 3-7 Aug. 1992; sponsored by ANS, SAE, ACS, AIAA, ASME, and IEEE
(RTOP 474-42-10)
(NASA-TM-105846; E-7289; NAS 1.15:105846) Avail: CASI HC A02/MF A01

The Power Management and Distribution (PMAD) DC Test Bed at the NASA Lewis Research Center is introduced. Its usefulness to the Space Station Freedom Electrical Power (EPS) development and design are discussed in context of verifying system stability. Stability criteria developed by Middlebrook and Cuk are discussed as they apply to constant power DC to DC converters exhibiting negative input impedance at low frequencies. The utility-type Secondary Subsystem is presented and each component is described. The instrumentation used to measure input and output impedance under load is defined. Test results obtained from input and output impedance measurements of test bed components are presented. It is shown that the PMAD DC Test Bed Secondary Subsystem meets the Middlebrook stability criterion for certain loading conditions. Author

N92-31289# Stanford Linear Accelerator Center, CA.
A THREE-GAP KLYSTRON OUTPUT CAVITY AT X-BAND
K. Ko, T. G. Lee, S. Tonegawa, and N. Kroll Mar. 1992 11 p Presented at the Soc. of Photo-Optical Instrumentation Engineers' International Symposium on Laser Spectroscopy as Part of SPIE's Symposium on Optics, Electro-optics and Laser Applications in Science and Engineering, Los Angeles, CA, 19-25 Jan. 1992
(Contracts DE-AC03-76SF-00515; DE-AS03-89ER-40527)
(DE92-012417; SU-SLAC-PUB-5760; CONF-920124-23) Avail: CASI HC A03/MF A01

A high-power X-band klystron employing a double-gap output cavity has been operating at SLAC. Multi-gap output circuits have lower surface gradients at the interaction gaps than single-gap ones but are prone to self-oscillate due to negative loading and trapped higher-order modes. In the double-gap circuit design, considerable attention had been directed to deal with these stability problems. The performance of the present tube appears to be limited by gap breakdown and beam interception, particularly at long pulses. A three-gap output cavity is currently under development to further reduce the gap surface gradient. Another new feature of the circuit is an enlarged downstream drift tube to improve on beam clearance. This paper discusses the considerations involved in designing a multi-gap output cavity and presents the cold test measurements on the three-gap circuit. The experimental data is compared with numerical results from the 3-D simulation code ARGUS. DOE

N92-31334# Lawrence Livermore National Lab., CA.
CALCULATIONAL PREDICTION OF ULTRAWIDEBAND ELECTROMAGNETIC PULSES BY LASER-INITIATED AIR AVALANCHE SWITCHES
D. J. Mayhall and J. H. Yee Dec. 1991 17 p Presented at the Society of Photo-Optical Instrumentation Engineers' International Symposium on Laser Spectroscopy as part of SPIE's Symposium on Optics, Electro-Optics and Laser Applications in Science and Engineering, Los Angeles, CA
(Contract W-7405-eng-48)
(DE92-011732; UCRL-JC-107443; CONF-920124-21) Avail: CASI HC A03/MF A01

The gas avalanche switch is a recently conceived, laser-activated, high-voltage, picosecond-speed switch. It basically consists of a set of pulse-charged electrodes immersed in a gas at high-pressure (2-800 atm). A picosecond-scale laser pulse initiates an avalanche discharge in the gas between the electrodes. With the proper configuration, the avalanche, which is fueled by the immense number of electrons available in the gas, causes the applied voltage to collapse in picoseconds and generates electromagnetic waves. A two-dimensional electron fluid computer code solves Maxwell's curl equations and a set of electron fluid equations for transverse magnetic modes in air between parallel plate conductors. Collision frequencies for ionization and momentum and energy exchange to neutral molecules are taken to scale directly with neutral pressure. Calculations are performed for a Blumlein pulse generator geometry, featuring a charged rectangular center electrode between grounded parallel plates spaced 2 mm apart. In one mode of operation, initial electrons are induced in the lower air gap, the gap between the center electrode and the lower plate. At 292 kV on the center electrode, 27 atm pressure, and uniform ionization under the full width of the center electrode, induced voltage pulses of 300 kV, 2.4 ps rise time, 9.1 ps full width at half maximum (FWHM), 38 ps duration, and 22 GHz bandwidth at 3 dB occur at the ends of the parallel plates. Reduction of the initial electron number over eleven orders of magnitude has very little gross effect on these pulses. Concentration of the initial electrons into a narrow, centered column generally results in reductions in rise time, FWHM, and pulse duration, as well as increases in peak voltage. Movement of the narrow column to the extreme left of the center electrode causes the voltage pulses at the left and right sides of the parallel plates to differ somewhat in their characteristics. DOE

N92-31355# Naval Postgraduate School, Monterey, CA.
THE PREDICTION OF THE PERFORMANCE OF A MICROCIRCUIT HEAT SINK IN THE BOILING MODE M.S. Thesis
John W. Larkin Mar. 1992 61 p
(AD-A250045) Avail: CASI HC A04/MF A01

As microcircuit technology advances, there is an increased need for the dissipation of the heat which is generated. Extended surfaces are a useful tool in fulfilling the heat sink requirements for a microcircuit element. Heat transfer is very effective in the boiling mode and this thesis focuses on the analysis of a spine-shaped extended surface in a boiling liquid. Because the heat transfer in the spine and the propagation of signals on a transmission line are governed by identical differential equations, an analysis procedure based on the cascading of electrical transmission lines is used to predict the performance of the spine. The result of the analysis is a computer program that can assist the circuit designer in meeting any heat transfer requirements. GRA

N92-31367# National Inst. of Standards and Technology, Gaithersburg, MD. Electronics and Electrical Engineering Lab. Office.
ELECTRONICS AND ELECTRICAL ENGINEERING LABORATORY TECHNICAL PUBLICATION ANNOUNCEMENTS COVERING LABORATORY PROGRAMS, JULY TO SEPTEMBER 1991, WITH 1992 EEEL EVENTS CALENDAR Report, Jul. - Sep. 1991
J. A. Gonzales Mar. 1992 25 p
(PB92-181239; NISTIR-4803) Avail: CASI HC A03/MF A01

This is the 13th issue of the quarterly publication providing information on the technical work of the National Institute of Standards and Technology, Electronics and Electrical Engineering Laboratory (EEEL). The issue of the EEEL Technical Publication Announcements covers the third quarter of calendar year 1991. Abstracts are provided by technical area for papers published this quarter. Major subject headings include the following: Fundamental Electrical Measurements; Semiconductor Microelectronics; Signal Acquisition; Processing and Transmission; Electrical Systems; and Electromagnetic Interference. GRA

N92-31373# Virginia Univ., Charlottesville. Dept. of Electrical Engineering.
INTERNATIONAL SEMICONDUCTOR DEVICE RESEARCH SYMPOSIUM (ISDRS-91) Final Report, Oct. 1991 - Mar. 1992
Michael Shur Mar. 1992 7 p Symposium held in Charlottesville, VA, 4-6 Dec. 1991
(Contract DAAL03-91-G-0338)
(AD-A249348; UVA/525291/EE92/101; ARO-29342.2-EL-CF)
Avail: CASI HC A02/MF A01

The First International Semiconductor Device Research Symposium (ISDRS-91) took place in Charlottesville, Va on December 4-6, 1991 for the purpose of providing a convenient forum for the exchange of information and new ideas for researchers from industry, university, and government laboratories with leading researchers from the United States, Canada, Europe, Asia, and the former Soviet Union. As the first international conference of its kind to take place after the August 1991 coup attempt in the Soviet Union, it was unique with the presence of an unusually large contingent of Russian scientists. The emphasis of the program was on novel ideas such as advanced semiconductor technologies still in their infancy whose tangible technological outcomes are not expected for another five to ten years. Some of the technologies discussed at the symposium included bandgap engineering, large area semiconductor electronics, new millimeter wave and opto-electronics technologies, and silicon carbide and diamond devices. GRA

N92-31374# Physical Optics Corp., Torrance, CA.
A MICROPRISM ARRAY FOR LARGE-SCALE, WIDE-BAND INTERCONNECTION OF OPTOELECTRONIC SYSTEMS Final Report, 1 Jul. - 31 Dec. 1991
Ray T. Chen 15 Mar. 1992 33 p
(Contract DAAL03-91-C-0030)
(AD-A249380; Rept-3128; ARO-29005.1-EL-SBI) Avail: CASI HC A03/MF A01

In contrast to any existing means of interconnection for a large-scale, high-speed optoelectronic system, Physical Optics Corporation (POC) proposes fabricating and using a microprism (-100 micro-m in size,) array (MPA) as a wide-band coupler for two-dimensional and three-dimensional system integration. The flexibility of MPA's angles allows implementation of the MPA to any point to point interconnects. Realizing that the major bottle neck of hologram-based interconnection is the intrinsic limitation of coupling bandwidth (-10 micro-m), we demonstrated a microprism coupler (MPA) with larger than 200 micro-m bandwidth from free space to optical data bus (ODB). For example, LED-based transmission from a single-mode guide to a multimode fiber can be solved only by using the MPA. Unlike the conventional prism which has a dimension of mm to cm, the MPA has miniscule dimensions. An MPA with -100 Jim in size is demonstrated. The proposed MPA is immune from electromagnetic interference (EMI). Furthermore, the cost of the microprism is less than $1 a piece in mass production, significantly less than holograms. In Phase 1, fabrication of the MPA will be upgraded followed by a demonstration of large-scale board-to-board MAP-based 3-D interconnection. GRA

N92-31431# Westinghouse Defense and Electronic Systems Center, Baltimore, MD. Advanced Technology Div.
STABLE INTEGRATED MICROWAVE TO OPTICAL MODULATOR
31 Dec. 1991 14 p
(Contract N00014-90-C-0073)
(AD-A249974) Avail: CASI HC A03/MF A01

The key technical objective for this research program is to integrate quantum well lasers (QWL's), detectors, and GaAs MESFET's to produce a monolithic integrated microwave-to-optical modulator on semi-insulating GaAs substrates. GRA

N92-31440# Pacific Northwest Lab., Richland, WA.
FINAL REPORT ON DSA METHODS FOR MONITORING ALUMINA IN ALUMINUM REDUCTION CELLS WITH CERMET ANODES
C. F. Windisch, Jr. Apr. 1992 59 p
(Contract DE-AC06-76RL-01830)
(DE92-013599; PNL-8076) Avail: CASI HC A04/MF A01

The Sensors Development Program was conducted at the Pacific Northwest Laboratory (PNL) for the US Department of Energy, Office of Industrial Processes. The work was performed in conjunction with the Inert Electrodes Program at PNL. The objective of the Sensors Development Program in FY 1990 through FY 1992 was to determine whether methods based on digital signal analysis (DSA) could be used to measure alumina concentration in aluminum reduction cells. Specifically, this work was performed to determine whether useful correlations exist between alumina concentration and various DSA-derived quantification parameters, calculated for current and voltage signals from laboratory and field aluminum reduction cells. If appropriate correlations could be found, then the quantification parameters might be used to monitor and, consequently, help control the alumina concentration in commercial reduction cells. The control of alumina concentration is especially important for cermet anodes, which have exhibited instability and excessive wear at alumina concentrations removed from saturation. DOE

N92-31451# Westinghouse Science and Technology Center, Pittsburgh, PA.
HIGH TEMPERATURE SUPERCONDUCTING FILMS AND MULTILAYERS FOR ELECTRONICS Annual Report, 20 Feb. 1991 - 20 Feb. 1992
John R. Gavaler and John Talvacchio 20 Feb. 1992 23 p
(Contract F49620-91-C-0034)
(AD-A250732; Rept-92-9SL2-Super-R1; AFOSR-92-0286TR)
Avail: CASI HC A03/MF A01

The four tasks of this three-year program address properties fundamental to (1) enhancing the superconducting properties of HTS films, (2) the application of HTS films in passive microwave circuits, (3) the realization of HTS digital electronics, and (4) the development of new superconducting devices. Progress during the first year included significant enhancements in the properties of superconducting YBCO films. One of these, the elimination of surface roughness due to Cu particles, was essential for the subsequent growth of high quality multilayer structures. For the first time, uniform large-area YBCO films were sputtered on both sides of a substrate with properties equal or superior to those of single-sided smaller-area films. Two new device configurations were developed: the integration of a ferroelectric film on a YBCO electrode compatible with ferroelectric memory cells and a step-edge S-N-S Josephson junction using in-situ deposited gold as the normal metal. SQUIDs fabricated with such junctions had the highest yield of any HTS junction configuration. Epitaxial superconducting Ba-K-Bi-O films were deposited and the gap energy was measured as a function of temperature in low-leakage S-I-N tunnel junctions. GRA

N92-31461# Naval Weapons Center, China Lake, CA.
THE SIXTEENTH ANNUAL ELECTRONICS MANUFACTURING SEMINAR PROCEEDINGS
21 Feb. 1992 373 p Proceedings held in Ridgecrest, CA, 19-21 Feb. 1992
(AD-A247920; NWC-TP-7163) Avail: CASI HC A16/MF A03

Presented are the proceedings of the 16th Annual Electronics Manufacturing Seminar, held on 19-21 February 1922, in Ridgecrest, Calif. The proceedings include the papers presented at the Seminar and cover all aspects of soldering technology and electronics manufacturing. The proceedings are a compilation of information provided by both nongovernment and government sources. The proceedings are published in the interest of furthering communication and broadening awareness of current activities among soldering technology and electronics manufacturing specialists. Author (GRA)

N92-31464# Spire Corp., Bedford, MA.
SiGe Si QUANTUM WIRES FOR EFFICIENT, ROOM TEMPERATURE, TUNABLE LUMINESCENCE Final Report, 1 Jul. - 31 Dec. 1991
Fereydoon Namavar, H. P. Maruska, and Nader M. Kalkhoran 3 Mar. 1992 31 p
(Contract DAAL03-91-C-0033)
(AD-A249651; SPIRE-FR-60208; ARO-29008.1-EL-SBI) Avail: CASI HC A03/MF A01

A porous silicon visible light emitting diode has been developed. Porous silicon was prepared by electrochemically etching p-type silicon wafers in hydrofluoric acid solutions. Photoluminescence spectroscopy of these samples revealed intense light emission at wavelengths throughout the visible spectrum, as well as unusually strong emission at the band edge energy of bulk crystalline silicon. Emission intensities were comparable to those usually exhibited by high quality reference samples of GaAs. Thus, quantum confinement of carriers in silicon nanostructures, created by the etch procedure, is indicated. Electroluminescence is observed from diode structures fabricated as heterojunctions between porous silicon and the transparent conductor indium-tin oxide, which serves as a window to allow light emission from the top surface of the device. Luminescence only occurs under forward electrical bias, while photovoltaic effects are seen under reverse bias. After the data are corrected for series resistance effects, the electroluminescent devices are shown to operate at junction biases of about 3-4 volts. A model based on minority carrier injection has been developed. Porous silicon light emitting diodes offer great promise for wafer scale integration of optical interconnects in high speed data processor applications, and to allow the construction of low cost flat panel displays, entirely in silicon. GRA

N92-31490# University of Southern California, Los Angeles. Dept. of Electrical Engineering and Electrophysics.
PROPOSAL FOR A WORKSHOP IN THE PHYSICS AND APPLICATION OF HOLLOW ELECTRODE GLOW SWITCHES Final Report, 1 May 1989 - 30 Sep. 1991
Martin Gundersen 6 Dec. 1991 26 p
(Grant AF-AFOSR-0342-89)
(AD-A247139; AFOSR-92-0149TR) Avail: CASI HC A03/MF A01

The purpose of the 1989 NATO ARW was to develop applications for and an improved understanding of the physics for high current emission and conduction observed in hollow cathode-hollow anode switches including the pseudospark and back-lighted thyratron (BLT). New applications include highly emissive cathodes for microwave devices, accelerators and free electron lasers, high power tubes, electron and ion-beams, microlithography, accelerators, and other plasma devices. Recent research has produced this new generation of gas-phase plasma switches that are characterized by very high current emission and conduction while operating in a glow mode. The cathode properties are especially remarkable - about 2 orders of magnitude larger emission than existing thermionic cathodes. Part of the meeting was devoted to understanding these properties and exploiting applications of this cathode. These results disserve study in order to understand the underlying physical mechanisms and to develop ideas and insight into future applications, and foster coherent research in this area. This meeting was also motivated by the fact that there are many new applications of these devices under consideration. These include new types of ion and electron beams for microelectronic technology, accelerators, other plasma loaded devices, plasma lenses for high energy physics, plasma accelerators, applications requiring very high cathode emission such as cathodes for pulsed accelerators, and microwave sources. GRA

N92-31499# Oak Ridge National Lab., TN.
A COMPARISON OF THREE SELF-TUNING CONTROL ALGORITHMS DEVELOPED FOR THE BRISTOL-BABCOCK CONTROLLER
P. A. Tapp Apr. 1992 185 p
(Contract DE-AC05-84OR-21400)
(DE92-014472; ORNL/TM-12040) Avail: CASI HC A09/MF A02

A brief overview of adaptive control methods relating to the design of self-tuning proportional-integral-derivative (PID) controllers is given. The methods discussed include gain scheduling, self-tuning, auto-tuning, and model-reference adaptive control systems. Several process identification and parameter adjustment methods are discussed. Characteristics of the two most common types of self-tuning controllers implemented by industry (i.e., pattern recognition and process identification) are summarized. The substance of the work is a comparison of three self-tuning proportional-plus-integral (STPI) control algorithms developed to work in conjunction with the Bristol-Babcock PID control module. The STPI control algorithms are based on closed-loop cycling theory, pattern recognition theory, and model-based theory. A brief theory of operation of these three STPI control algorithms is given. Details of the process simulations developed to test the STPI algorithms are given, including an integrating process, a first-order system, a second-order system, a system with initial inverse response, and a system with variable time constant and delay. The STPI algorithms' performance with regard to both setpoint changes and load disturbances is evaluated, and their robustness is compared. The dynamic effects of process deadtime and noise are also considered. Finally, the limitations of each of the STPI algorithms are discussed, some conclusions are drawn from the performance comparisons, and a few recommendations are made. DOE

N92-31525# Midwest Research Inst., Golden, CO.
RESEARCH ON STABLE, HIGH-EFFICIENCY AMORPHOUS SILICON MULTIJUNCTION MODULES
A. Banerjee, E. Chen, R. Clough, T. Glatfelter, S. Guha, G. Hammond, M. Hopson, N. Jackett, M. Lycette, and J. Noch et al Apr. 1992 85 p Prepared in cooperation with United Solar Systems Corp., Troy, MI
(Contract DE-AC02-83CH-10093)
(DE92-001244; NREL/TP-411-4840) Avail: CASI HC A05/MF A01

This report describes the progress made during phase 1 of a research and development program to obtain high-efficiency amorphous silicon alloy multijunction modules. Using a large-area deposition system, double-and triple-junction cells were made on stainless steel substrates of over 1 sq. ft. with Ag and ZnO predeposited back reflector. Modules of over 1 sq. ft. were produced with between 9.2 and 9.9 percent initial aperture-area efficiencies as measured under a USSC Spire solar simulator. Efficiencies as measured under the NREL Spire solar simulator were found to be typically 15 to 18 percent lower. The causes for this discrepancy are now being investigated. The modules show about 15 percent degradation after 600 hours of one-sun illumination at 50 C. To optimize devices for higher stabilized efficiency, a new method was developed by which the performance of single-junction cells after long-term, one-sun exposure at 50 C can be predicted by exposing cells to short-term intense light at different temperatures. This method is being used to optimize the

component cells of the multijunction structure to obtain the highest light-degraded efficiency. DOE

N92-31548# Lawrence Livermore National Lab., CA.
HIGH-PRESSURE GAS SWITCH FOR A WIDEBAND SOURCE
P. A. Pincosy, P. Poulsen, and W. R. Cravey 20 May 1992 6 p Presented at the 9th International Conference on High Power Particle Beams, Washington, DC, 25-29 May 1992
(Contract W-7405-eng-48)
(DE92-015822; UCRL-JC-108827; CONF-920515-19) Avail: CASI HC A02/MF A01

High-power ultrawideband pulses with equivalent center frequencies around 10 GHz require switching in a time scale of about a hundred picoseconds. We are developing a high-pressure gas switch that is designed to store a few joules of energy. Energy is stored in the transmission line upstream of the switch. The switch is a gap in a short transmission line of low impedance. The line is pulse charged to store the desired energy before the electric field across the gap collapses from the avalanche buildup of electrons. To ensure a relatively uniform voltage collapse across the width of the gap, initial electrons are produced by radiation from a bare spark. The switching repeatability is very good when the spark provides the initial electrons. Gap electric fields greater than 1 MV/cm were achieved for a 10-atm switch pressure in air with a voltage collapse less than 150 ps over 6 cm of switch length. The switch was tested with repetitive pulses up to 1 kHz. In a pulse charging mode, the collapse time of the gap will typically be 5 times less than the charging time. For applications where a switching time of tens of picoseconds is desired, a second switch would be required. DOE

N92-31650# Oak Ridge National Lab., TN.
WHAT CAN WE LEARN FROM MAGNETIZATION EXPERIMENTS ON HIGH T(SUB c) SUPERCONDUCTORS? AN OVERVIEW
J. R. Thompson (Tennessee Univ., Knoxville.) Apr. 1992 13 p Presented at the Material Research Society Spring Meeting, San Francisco, CA, 27 Apr. - 2 May 1992
(Contract DE-AC05-84OR-21400)
(DE92-014465; CONF-920402-11) Avail: CASI HC A03/MF A01

Magnetization studies provide a facile and convenient means for investigating high temperature superconductors. This work provides an overview and some specific examples of the types of information attainable through magnetic experiments. Regimes to be discussed include the Meissner region with low applied magnetic fields; the mixed state in higher fields at high temperatures, where equilibrium superconductive properties are accessible, and the magnetically irreversible mixed state at lower temperatures, often with large critical current densities J(sub c). Generally, the critical currents in the last region are metastable. The associated flux creep phenomenon also provides insight into the last region that is metastable. The associated flux creep phenomenon also provides insight into the materials problem of optimizing the pinning of vortices, in order to maximize J(sub c). DOE

N92-31651# Brookhaven National Lab., Upton, NY.
UNDERSTANDING AND MANAGING THE EFFECTS OF BATTERY CHARGER AND INVERTER AGING
W. Gunther and S. Aggarwal (Nuclear Regulatory Commission, Washington, DC.) 1992 11 p Presented at the Aging Research Information Conference, Rockville, MD, 24-27 Mar. 1992
(Contract DE-AC02-76CH-00016)
(DE92-014473; BNL-NUREG-47472; CONF-920375-18) Avail: CASI HC A03/MF A01

An aging assessment of battery chargers and inverters was conducted under the auspices of the NRC's Nuclear Plant Aging Research (NPAR) Program. The intentions of this program are to resolve issues related to the aging and service wear of equipment and systems at operating reactor facilities and to assess their impact on safety. Inverters and battery chargers are used in nuclear power plants to perform significant functions related to plant safety and availability. The specific impact of a battery charger or inverter failure varies with plant configuration. Operating experience data have demonstrated that reactor trips, safety injection system actuations, and inoperable emergency core cooling systems have resulted from inverter failures; and dc bus degradation leading to diesel generator inoperability or loss of control room annunication and indication have resulted from battery and battery charger failures. For the battery charger and inverter, the aging and service wear of subcomponents have contributed significantly to equipment failures. This paper summarizes the data and then describes methods that can be used to detect battery charger and inverter degradation prior to failure, as well as methods to minimize the failure effects. In both cases, the managing of battery charger and inverter aging is emphasized. DOE

N92-31664# Superconducting Super Collider Lab., Dallas, TX.
IMPROVED FERRITE BIASING SCHEME FOR BOOSTER RF CAVITIES
G. Schaffer Mar. 1992 5 p Presented at the 3rd European Particle Accelerator Conference, Berline, Fed. Republic of Germany, 24-28 Mar. 1992
(Contract DE-AC35-89ER-40486)
(DE92-011650; SSCL-Preprint-79; CONF-920315-20) Avail: CASI HC A01/MF A01

A new engineering design of ferrite tuners for rapid-cycling-booster rf cavities is proposed. The basic concept is to divide a perpendicularly biased ferrite tuner into two (or more) successive or parallel sections which are magnetically biased in opposite directions. This approach aims at several improvements with respect to existing designs: (1) reduction of magnet weight; (2) lower eddy currents; (3) reduction (or cancellation) of magnetic fields on beam axis; and (4) possibility of increasing the tuner breakdown voltage by stepwise widening of airgaps between ferrite layers of successive tuner sections. Some details are illustrated for stripline tuners, especially for the Low-Energy- and Medium-Energy-Boosters (LEB and MEB) in the Supercollider injector scenario. DOE

N92-31681# Los Alamos National Lab., NM.
ANTHEM SIMULATIONAL STUDIES OF THE PLASMA OPENING SWITCH
Rodney J. Mason 1992 7 p Presented at the 9th International Conference on High Power Particle Beams, Washington, DC, 25-29 May 1992
(Contract W-7405-eng-36)
(DE92-015247; LA-UR-92-1705; CONF-920515-12) Avail: CASI HC A02/MF A01

For a deeper understanding of the physical processes governing the Plasma Opening Switch (POS) we use the ANTHEM 2D implicit simulation code to study ion dynamical effects on electrohydrodynamic (EHD) waves propagating along steep density interfaces in the switch plasmas. At radial interfaces where the density jumps toward the anode, these waves can drive a finger of magnetic field into the plasma toward the load. Ion dynamics can open the rear of such fingers into a wedge-like density gap. Then we examine ion effects in uniform switch plasmas. These first develop potential hill structures at the drive edge of the cathode from the competition between electron velocity advection and EHD magnetic exclusion waves. Magnetic pressure gradients at the hill periphery and EHD effects then establish a density gap propagating along the cathode with radial electron emission from its tip. Similar results are obtained under both multi-fluid and PIC modeling of the plasma components. DOE

N92-31697# Laboratoire d'Automatique et d'Analyse des Systemes, Toulouse (France). Groupe Circuits et Composants a Effets de Champ.
STATIC AND DYNAMIC PROPERTIES OF CURRENT SENSING POWER VDMOS TRANSISTOR Ph.D. Thesis - Toulouse Univ. [PROPRIETES STATIQUES ET DYNAMIQUES DU TRANSISTOR VDMOS DE PUISSANCE A MIROIR DE COURANT]
Kamel Djellabi 1992 178 p In FRENCH
(LAAS-92032; ETN-92-91684) Avail: CASI HC A09/MF A02

The properties of current sensing power metal-oxide semiconductor field effect transistors (MOSFETs) were studied. The functioning principle of this device was analyzed and conclusions were drawn concerning the 'current mirror' capability of such integrated structures. An equivalent electric circuit compatible with the simulation program SPICE was established. The parameter extraction method was specified. A model that accounts for the temperature dependence of the device parameters was developed. In order to validate the established model a switching of the device in resistive and inductive loads was simulated. The behavior of the model was tested on a conventional power electronics circuit, the H bridge leg. Simulations of temperature dependences were presented. ESA

N92-31718# Sandia National Labs., Albuquerque, NM.
TORQUE LINEARIZING HARDWARE FOR THE ELECTRIC JOINT MOTORS OF A DIRECT-DRIVE ROBOT
P. F. Muir and J. R. Bryan 1991 10 p Presented at the Ideas in Science and Electronics (ISE) Symposium, Albuquerque, NM, 14 May 1992
(Contract DE-AC04-76DP-00789)
(DE92-012681; SAND-91-2350C; CONF-9205141-2) Avail: CASI HC A02/MF A01

Many emerging high-performance robot control algorithms require the command of the joint torques, yet no known commercial robots provide such a capability. We describe the design, development, testing, and application of a VMEbus-based torque linearizing joint interface board (JIB). One JIB resides between the robot control processor and each joint motor amplifier. The JIB provides the control processor with the capability to read the motor position and apply accurate motor torques. The torque command capability derives from the application of a 128k x 8 EPROM lookup table for each motor phase. Because joint motor torque is dependent upon the torque command and the motor position, the hardware is designed to utilize the torque command and the current motor position as the address to retrieve the proper pulse-width for the PWM motor amplifier. The table look-up cycle operates independently of the robot controller at a 40KHz rate to provide constant joint torque as the motor rotates. We identify the proper table entries by an automated in situ data collection procedure. Static torque generation results show that the torque deviations are reduced from as much as 76 percent to below 5 percent for each of the three direct-drive motors (two are variable reluctance motors and one is brushless DC) on an AdeptTwo robot. These torque deviations are reduced below 2.5 percent if only the upper 90 percent of the torque range is considered. The torque deviations of the non-direct-drive joint are reduced by 50 percent. Dynamic robot edge following experiments show that the robot speed of operation can be more than doubled for a given applied force accuracy by utilizing the joint torque linearizing boards. DOE

N92-31760# Superconducting Super Collider Lab., Dallas, TX.
BEAM POSITION MONITOR ELECTRONICS USING DC COUPLED DEMODULATING LOGARITHMIC AMPLIFIERS
G. R. Aiello and M. R. Mills Mar. 1992 5 p Presented at the 3rd European Particle Accelerator Conference, Berlin (Germany), 24-28 Mar. 1992 Submitted for publication
(Contract DE-AC35-89ER-40486)
(DE92-011697; SSCL-Preprint-74; CONF-920315-18) Avail: CASI HC A01/MF A01

An electronics circuit operating up to 120 MHz suitable for Beam Position Monitor signal processing is described. Two different channels process signals from the electrodes. Each channel is realized with two cascaded DC coupled demodulating logarithmic amplifiers, providing an output voltage proportional to the logarithm of the input signal amplitude. The outputs from the two channels are processed by differential and summing amplifiers. The difference output produces a voltage proportional to the beam displacement between the electrodes, but both the difference and sum outputs are digitized in order to allow for a software correction of the gain and offset mismatches. The electronics show better characteristics than previous implementations utilizing log-amp circuits. The dynamic range has been increased, keeping the linearity error smaller than 1 percent over a 65 dB input signal range. The noise characteristics have been improved providing good resolution at low currents. The RF burst response has also been tested showing good characteristics for use on a Linac or transfer line. One prototype, working at 60 MHz, has been built and is planned for use on one or more machines at the SSC. DOE

N92-31780# Naval Postgraduate School, Monterey, CA.
ROUNDOFF ALGORITHMS FOR DIGITAL PHASE SHIFTERS THAT MINIMIZE BEAM SHIFT M.S. Thesis
Stanley E. Engle Mar. 1992 161 p
(AD-A250094) Avail: CASI HC A08/MF A02

The performance of a phased array antenna depends upon the phase and amplitude distribution across the aperture. A continuous 13-near phase distribution is required for an efficient focussed beam, but practical phase shifters are digital devices and can only provide an approximation to a linear phase distribution. Consequently some type of roundoff criteria must be established. The method of roundoff affects the radiation pattern characteristics such as beam location and sidelobe level. Accurate target tracking requires that a radar have a small beam pointing error. Low sidelobes are also desirable to prevent jamming and the illumination of clutter. Therefore the goal was to select a roundoff criterion that provides a phase distribution across the aperture to minimize both the beam shift and the sidelobe levels, while simultaneously maximizing the gain. The methods examined are referred to regular roundoff, weighted random roundoff, running sum roundoff and symmetric running sum roundoff. The first two are in common use, but the third and fourth are new methods examined in this paper. It was demonstrated that the latter two, of the four roundoff methods, have the beam shift without significantly degrading the other pattern properties. GRA

N92-31791# SRI International Corp., Menlo Park, CA.
FIELD-EMITTER ARRAYS FOR RF VACUUM MICROELECTRONICS Quarterly Technical Report No. 1, 1 Oct. - 31 Dec. 1991
C. A. Spindt and A. Rosengreen Feb. 1992 27 p
(Contract MDA972-91-C-0029; ARPA Order 8162)
(AD-A250101) Avail: CASI HC A03/MF A01

This report covers the first quarter of a program to develop field-emitter arrays for vacuum micro-electronics. The goals of the effort are 5 mA total current at 5 A/sq cm for at least 1 h, and demonstrated modulation of the emission at 1 GHz. Efforts for this period have been directed toward developing a suitable anode structure for this application, designing a low-capacitance cathode structure capable of being driven at GHz frequencies, and designing test apparatus for operation of the cathodes in the GHz range (microstrip lines, etc.). The results of the development to date are that 1,000-tip cathodes have been operated with carefully processed, close-spaced nickel anodes at 15 mA and 23 A/sq cm for over 1000 h. In addition, low-capacitance cathode structures have been fabricated, and although there have been some difficulties with dielectric depositions, one cathode has been tested with very encouraging results. A low-capacitance 625-tip linear array with a 4 micro-m x 1.25-mm electrode area has been tested at up to 25 mA total current at 1000 A/sq cm with a 5 percent duty cycle and modulated at 20 MHz (the limit of the function generator available at the time of the experiment). GRA

N92-31799# Notre Dame Univ., IN. Dept. of Physics.
THEORY OF SEMICONDUCTING SUPERLATTICES AND MICROSTRUCTURES Final Report, 15 Oct. 1988 - 14 Oct. 1991
John D. Dow 1 Mar. 1992 76 p LIMITED REPRODUCIBILITY: Availability: Document partially illegible
(Contract N00014-89-J-1136)
(AD-A248758) Avail: CASI HC A05/MF A01

This final report of work summarizes the theoretical development of semiconducting superlattices and microstructures. These include the first theory of Hjalmarson-Frenkel core excitons

in superlattices; it is applied to strained-layer systems. This theory will be useful in characterizing phenomena in such superlattices, using synchrotron radiation. A unified theory of dopants in II-VI materials, with emphasis on ZnSe and candidates for blue-green lasers is discussed. This explains why Ga is no longer an effective dopant in ZnI-xMnxSe for greater than 0.1, with a theory that also provides a natural explanation of why ZnTe is almost unique among the II-VI semiconductors in that it is naturally p-type. This work provides a theoretical framework for viewing and understanding the recent successes at 3M by Haas et al. in obtaining blue emission from ZnSe. It also provides strong evidence against the thirty-year-old explanation that self-compensation is responsible for the inability to make a p-n junction in II-VI semiconductors. A general theory of substitutional impurities in superlattices that predicts anomalous changes of dopant character with layer thicknesses, and establishes an intellectual framework for understanding the properties of impurities in superlattices is covered. GRA

N92-31834# Eagle-Picher Industries, Inc., Joplin, MO. Couples Dept.
RESEARCH AND DEVELOPMENT OF ADVANCED NICKEL-IRON BATTERIES FOR ELECTRIC VEHICLE PROPULSION
1991 68 p
(Contracts DE-AC02-92CH-10510; W-31-109-eng-38)
(DE92-014099; DOE/CH-10510-01) Avail: CASI HC A04/MF A01

The purpose of this program was to develop and demonstrate an advanced nickel-iron battery suitable for use in electric vehicles. During the course of this contract various steps were taken to improve nickel-iron battery performance while reducing cost. Improvement of the nickel electrode through slurry formulations and substrate changes, as seen with the fiber electrode, were investigated. Processing parameters for impregnation and formation were also manipulated to improve efficiency. Impregnation saw the change of anode type from platinized titanium to the consumable nickel anode. Formation changes were also made allowing for doubled processing capabilities of positive electrodes, a savings in both time and money. A final design change involved the evolution of the NIF-200 from the NIF-220. This change permitted the use of 1.2 mm iron electrodes and maintained the necessary performance characteristics for electric vehicle propulsion. Emphasis on a pilot plant became the main focus during the late 1989 - 90 period. The pilot plant facility would be a culmination of the program providing the best product at the lowest price. DOE

N92-31849# Naval Command, Control and Ocean Surveillance Center, San Diego, CA. Research, Development, Test and Evaluation Div.
FABRICATION OF AN INSULATED GATE DIAMOND FET FOR HIGH TEMPERATURE APPLICATIONS
J. R. Zeidler, R. Nguyen, C. A. Hewett, and C. R. Zeisse Apr. 1992 9 p
(AD-A251042) Avail: CASI HC A02/MF A01

A type IIa natural diamond was implanted with boron to form a p-type channel layer. This layer was then used to fabricate an insulated gate field effect transistor. This is the first reported use of ion implantation to successfully fabricate a field effect device in diamond. Testing was carried out from room temperature to 550 K. Both saturation and pinch-off were observed at room temperature, with a measured transconductance of 6.9 micron S/mm. Device failures at elevated temperatures were attributed to gate current leakage through the SiO2 insulator layer. GRA

N92-31946# Allied-Signal Aerospace Co., Kansas City, MO.
LOW THERMAL COEFFICIENT OF EXPANSION PRINTED WIRING BOARDS
J. K. Desch May 1992 27 p
(Contract DE-AC04-76DP-00613)
(DE92-013704; KCP-613-4748) Avail: CASI HC A03/MF A01

Production processes have been established and the reliability has been successfully proven for multilayer printed wiring boards manufactured from polyimide/quartz laminates. The polyimide/quartz is a construction of polyimide resin reinforced with quartz fabric. The polyimide/quartz has a lower thermal coefficient of expansion (TCE) in the X-Y plane at 9-10 ppm/C than standard production laminates (polyimide/glass and epoxy/glass) at 15-16 ppm/C and is intended for use in conjunction with surface mount devices (SMD). The lower TCE of polyimide/quartz provides a closer match to the TCE of the SMD, thereby reducing thermal stresses during temperature cycling. Surface mount technology is being used in the current programs with future applications now being considered. DOE

N92-32002# California Univ., Santa Barbara. Dept. of Chemistry.
THE CHEMISTRY AND PACKAGING OF NANOCOMPOSITE CONFINED ARRAYS Technical Report, 1 Jun. 1991 - 31 May 1992
G. D. Stucky 15 May 1992 9 p
(Contract N00014-90-J-1159)
(AD-A250991) Avail: CASI HC A02/MF A01

The miniaturization of electronic and optic devices has revolutionized response times, energy loss, and transport efficiency. An additional bonus is that as one approaches the nanosize regime the presence or absence of a few atoms and the geometrical disposition of each atom can significantly modify electronic and photonic properties. This control can be further supplemented by packaging assemblies of atoms or molecules into thin film or nanocomposite bulk materials to define surface states, cluster environment and geometry, intercluster interactions, and consequently, a wide tunable range of optical and charge carrier responses. The chemist is presented with an intriguing challenge. First the clusters must be unisized with identical geometries. Secondly, the atom or molecular assemblies should ideally have perfect periodicity in order to rigorously define optoelectronic densities and intercluster tunnelling. A third requirement is that the nanocomposite be processable, generally in the form of thin films or single crystals. Numerous approaches are being undertaken in achieving these goals, including molecular beam and atomic layer epitaxy, molecular sieve inclusion chemistry, molecular capping of inorganic clusters, porous glass, and aerosol synthesis. This paper presents a brief review of the interface chemistry associated with nanophase confinement and packaging and some features of three dimensional surface confinement using molecular sieves and zeolites. GRA

N92-32033# Allied-Signal Aerospace Co., Kansas City, MO.
FLEX CIRCUIT LAMINATION
L. Wolfe Jun. 1992 12 p
(Contract DE-AC04-76DP-00613)
(DE92-016574; KCP-613-4804) Avail: CASI HC A03/MF A01

Lamination process characteristics -- load, relative humidity, and lamination press pad -- were investigated as they relate to dimensional stability, voids, and 90-degree peel strength. Quantitative data was gathered for dimensional stability and voids. A predictive model was developed for peel strength. At the completion of the above activities, it was evident that a better understanding of the fundamental lamination process was needed. A Machine/Process Capability Study will be performed on the lamination process. DOE

N92-32074# California Univ., Los Angeles.
VLSI FOR HIGH-SPEED DIGITAL SIGNAL PROCESSING Quarterly Progress Report, 1 Jan. - 31 Mar. 1992
Alan N. Willson, Jr. 31 Mar. 1992 4 p
(Contract N00014-91-J-1852)
(AD-A250365) Avail: CASI HC A01/MF A01

We have continued our development of the 12-bit by 11-bit multiplier for our multiprocessor-ring chip. Since the multiplier's performance is the single most important factor in determining the maximum speed at which our system can operate, it is essential that this task be performed in the best possible manner. Our goal was that this multiplier operate in approximately 30 nano-s so

that our overall chip speed could reach 30 MHz. The multiplier was designed to accommodate eleven-bit data and twelve-bit coefficients. In addition to the above-cited operating speed goal, we needed to make the multiplier small enough that five complete processors, including five multipliers, can be included on a single IC (which employs 2-microns CMOS technology). As mentioned in the previous progress report, after completing the multiplier's layout and verifying its correct functioning via logic simulation, we performed SPICE simulations on the various multiplier critical-path components. These simulations indicated an operating speed well under 30 nano-s. We next fabricated a MOSIS TinyChip (2.22 mm x 2.25 mm, in 2-micron technology) with this 12-bit by 11-bit multiplier and a small block of coefficient RAM as well as a small dual-port register block. This allowed us to test the multiplier's performance in an environment that closely simulated the five-processor-ring system. GRA

N92-32200# Instituto de Pesquisas Espaciais, Sao Jose dos Campos (Brazil). Lab Associado de Plasma.
Ba2Ti9O20 MICROWAVE DIELECTRIC RESONATOR: PROCESSING, PHASE SYNTHESIS AND CHARACTERIZATION [RESSOADORES DIELETRICOS PARA MICROONDAS DE BA2TI9O20: PROCESSAMENTO, SINTESE E CARACTERIZACAO]
Maria doCarmoANono and Pedro Jose deCastro 1992 10 p In PORTUGESE Presented at the 36th Congresso Brasileiro de Ceramica, Caxambu, Brazil, 7-10 Jun. 1992
(INPE-5373-PRE/1747) Avail: CASI HC A02/MF A01

A Ba2Ti9O20 dielectric resonator was produced with Brazilian initial materials and characterized for microwave application as oscillators and filters. The powder mixture with 0, 82 BaCO3.0,818TiO2 composition was prepared. Cylindrical samples were compacted by uniaxial and isostatic pressing, and phase synthesis and ceramic sintering was made at 1300 C in air. Structural phases and qualitative chemical analysis were made on sintered ceramics. Density and some microwave dielectric parameters, such as dielectric constant, quality factor due to dielectric loss, and resonant frequency were measured. A commercial imported Ba2Ti9O20 dielectric resonator (Trans-Tech, USA) was characterized by identical methods. The results presented show that Brazilian and imported dielectric resonators are in good agreement. Author

N92-32233*# National Aeronautics and Space Administration. Lewis Research Center, Cleveland, OH.
MONOLITHIC AND MECHANICAL MULTIJUNCTION SPACE SOLAR CELLS
Raj K. Jain and Dennis J. Flood Aug. 1992 13 p
(RTOP 506-41-11)
(NASA-TM-105832; E-7009-1; NAS 1.15:105832) Avail: CASI HC A03/MF A01

High-efficiency, lightweight, radiation-resistant solar cells are essential to meet the large power requirements of future space missions. Single-junction cells are limited in efficiency. Higher cell efficiencies could be realized by developing multijunction, multibandgap solar cells. Monolithic and mechanically stacked tandem solar cells surpassing single-junction cell efficiencies have been fabricated. This article surveys the current status of monolithic and mechanically stacked multibandgap space solar cells, and outlines problems yet to be resolved. The monolithic and mechanically stacked cells each have their own problems related to size, processing, current and voltage matching, weight, and other factors. More information is needed on the effect of temperature and radiation on the cell performance. Proper reference cells and full-spectrum range simulators are also needed to measure efficiencies correctly. Cost issues are not addressed, since the two approaches are still in the developmental stage. Author

34 FLUID MECHANICS AND HEAT TRANSFER

Includes boundary layers; hydrodynamics; fluidics; mass transfer; and ablation cooling.

For related information see also *02 Aerodynamics* and *77 Thermodynamics and Statistical Physics.*

N92-31247*# National Aeronautics and Space Administration. Langley Research Center, Hampton, VA.
COMPUTER PROGRAM TO SOLVE TWO-DIMENSIONAL SHOCK-WAVE INTERFERENCE PROBLEMS WITH AN EQUILIBRIUM CHEMICALLY REACTING AIR MODEL
Christopher E. Glass Aug. 1990 148 p
(RTOP 506-40-21-01)
(NASA-TM-4187; L-16709; NAS 1.15:4187) Avail: CASI HC A07/MF A02

The computer program EASI, an acronym for Equilibrium Air Shock Interference, was developed to calculate the inviscid flowfield, the maximum surface pressure, and the maximum heat flux produced by six shock wave interference patterns on a 2-D, cylindrical configuration. Thermodynamic properties of the inviscid flowfield are determined using either an 11-specie, 7-reaction equilibrium chemically reacting air model or a calorically perfect air model. The inviscid flowfield is solved using the integral form of the conservation equations. Surface heating calculations at the impingement point for the equilibrium chemically reacting air model use variable transport properties and specific heat. However, for the calorically perfect air model, heating rate calculations use a constant Prandtl number. Sample calculations of the six shock wave interference patterns, a listing of the computer program, and flowcharts of the programming logic are included. Author

N92-31256# National Inst. for Fusion Science, Nagoya (Japan).
STATISTICAL ANALYSIS OF ANOMALOUS TRANSPORT IN RESISTIVE INTERCHANGE TURBULENCE
Hideo Sugama and Masahiro Wakatani (Kyoto Univ., Uji, Japan) Dec. 1991 27 p Submitted for publication
(NIFS-125) Avail: CASI HC A03/MF A01

A new anomalous transport model for resistive interchange turbulence is derived from statistical analysis applying two-scale direct-interaction approximation to resistive magnetohydrodynamic equations with a gravity term. Our model is similar to the K sigma model for eddy viscosity of turbulent shear flows in that anomalous transport coefficients are expressed in terms of the turbulent kinetic energy K and its dissipation rate sigma, while K and sigma are determined by transport equations. This anomalous transport model can describe some nonlocal effects such as those from boundary conditions which cannot be treated by conventional models based on the transport coefficients represented by locally determined plasma parameters. Author

N92-31265*# Institute for Computer Applications in Science and Engineering, Hampton, VA.
ADAPTIVE MESH STRATEGIES FOR THE SPECTRAL ELEMENT METHOD Final Report
Catherine Mavriplis (George Washington Univ., Washington, DC.) Jul. 1992 22 p Submitted for publication
(Contract NAS1-19480; RTOP 505-90-52-01)
(NASA-CR-189686; NAS 1.26:189686; ICASE-92-36) Avail: CASI HC A03/MF A01

An adaptive spectral method was developed for the efficient solution of time dependent partial differential equations. Adaptive mesh strategies that include resolution refinement and coarsening by three different methods are illustrated on solutions to the 1-D viscous Burger equation and the 2-D Navier-Stokes equations for driven flow in a cavity. Sharp gradients, singularities, and regions of poor resolution are resolved optimally as they develop in time using error estimators which indicate the choice of refinement to be used. The adaptive formulation presents significant increases in efficiency, flexibility, and general capabilities for high order spectral methods. Author

N92-31281*# National Aeronautics and Space Administration. Langley Research Center, Hampton, VA.
STAGNATION-POINT HEAT-TRANSFER RATE PREDICTIONS AT AEROASSIST FLIGHT CONDITIONS
Roop N. Gupta, Jim J. Jones (Analytical Mechanics Associates, Inc., Hampton, VA.), and William C. Rochelle (Lockheed Engineering and Sciences Co., Houston, TX.) Sep. 1992 21 p
(RTOP 506-40-91-02)
(NASA-TP-3208; L-17039; NAS 1.60:3208) Avail: CASI HC A03/MF A01

The results are presented for the stagnation-point heat-transfer rates used in the design process of the Aeroassist Flight Experiment (AFE) vehicle over its entire aeropass trajectory. The prediction methods used in this investigation demonstrate the application of computational fluid dynamics (CFD) techniques to a wide range of flight conditions and their usefulness in a design process. The heating rates were computed by a viscous-shock-layer (VSL) code at the lower altitudes and by a Navier-Stokes (N-S) code for the higher altitude cases. For both methods, finite-rate chemically reacting gas was considered, and a temperature-dependent wall-catalysis model was used. The wall temperature for each case was assumed to be radiative equilibrium temperature, based on total heating. The radiative heating was estimated by using a correlation equation. Wall slip was included in the N-S calculation method, and this method implicitly accounts for shock slip. The N-S/VSL combination of projection methods was established by comparison with the published benchmark flow-field code LAURA results at lower altitudes, and the direct simulation Monte Carlo results at higher altitude cases. To obtain the design heating rate over the entire forward face of the vehicle, a boundary-layer method (BLIMP code) that employs reacting chemistry and surface catalysis was used. The ratio of the VSL or N-S method prediction to that obtained from the boundary-layer method code at the stagnation point is used to define an adjustment factor, which accounts for the errors involved in using the boundary-layer method. Author

N92-31283# Aerometrics, Inc., Sunnyvale, CA.
DIAGNOSTICS FOR RESEARCH IN ATOMIZATION AND TURBULENT TWO-PHASE FLOWS Final Report, 1 Jul. 1986 - 31 Jan. 1991
William D. Bachalo 23 Dec. 1991 210 p
(Contract F49620-86-C-0078)
(AD-A247201; AFOSR-92-0034TR) Avail: CASI HC A10/MF A03

This investigation focussed on the development of instrumentation for the study of atomization and two-phase turbulent flows, including sprays in reacting turbulent flow. Four methods were investigated: the phase Doppler method, ratiometric light scatter detection, Lagrangian frame particle dynamics analyzer, and scattered light heterodyne interferometry. For the phase Doppler technique, the physics of the dual beam light scattering phenomena, the effects of particle morphology on the light scattering, the effects of the nonuniform illumination of the particle, and the consequences of the random particle trajectories were investigated. Sampling statistics were also considered. The ratiometric light scatter detection method was used to size irregular shaped and inhomogeneous particles using the scattered light intensity in the near forward direction. The uncertainty due to the particle trajectory through the beams was removed using an optical deconvolution approach. A Lagrangian method for tracking individual particles was investigated. A rapidly swept light sheet produced a series of images of an individual particle on an array detector, from which the particles, position, and velocity were obtained. This method is feasible given sufficient laser power and/or a large enough particle. Scattered light heterodyne interferometry posed significant limitations which indicated that it would not offer significant advantages. GRA

N92-31286# Calspan-Buffalo Univ. Research Center, NY.
FUNDAMENTAL STUDIES OF THE STRUCTURE OF HYPERSONIC ATTACHED AND SEPARATED BOUNDARY LAYERS OVER SMOOTH, ROUGH AND TRANSPIRATION-COOLED SURFACES Final Technical Report, 15 May 1988 - 29 Aug. 1991
Michael S. Holden Nov. 1991 196 p
(Grant AF-AFOSR-0223-88)
(AD-A250284; AFOSR-92-0394TR) Avail: CASI HC A09/MF A03

A program of fundamental experimental research and analysis has been conducted to examine two key areas associated with the design of hypersonic vehicles for re-entry and sustained hypervelocity flight. In the first, and major, segment of the program, detailed measurements were obtained to examine the thermo-fluid dynamics of transpiration-cooling and the separate and combined effects of surface roughness and blowing on the fluid mechanics of transpiration and ablative thermal protection systems. In the second segment of the program, we embarked on a detailed experimental examination of turbulent compressibility effects in regions of attached and separated flows. The first phase of this program was devoted to studies associated with developing the models and instrumentation to obtain highly resolved high frequency measurements in fully turbulent boundary layer at Mach 11, 13, and 15. In the second phase of this program, segments were concentrated on the development of the direct measurement of density fluctuations using high pressure electron beam techniques. During this contract we also took the opportunity to analyze and publish important measurements made in an earlier program demonstrating compressibility effects in hypersonic turbulent wakes. GRA

N92-31287# EG and G Energy Measurements, Inc., Idaho Falls.
EMISSIVITY MEASUREMENTS IN SUPPORT OF EXPERIMENTS ON NATURAL CONVECTION BETWEEN A VERTICAL CYLINDER AND A SURROUNDING ARRAY
J. E. OBrien Dec. 1991 31 p
(Contract DE-AC07-76ID-01570)
(DE92-012321; EGG-NE-10083) Avail: CASI HC A03/MF A01

Experimental measurements of surface emissivities of three metallic samples have been obtained in support of an experiment aimed at determining natural convection and total heat transfer for a heated vertical cylinder surrounded by an array of cooled vertical tubes. In some cases, the heated stainless steel cylinder was shrouded by a perforated aluminum outer cylinder. The surrounding cooled tubes were also aluminum. In this experiment, heat transfer from the heated tube and the surrounding outer cylinder will occur by a combination of natural convection and radiation. At temperatures near the melting point of aluminum, the radiant contribution is particularly important, accounting for 50 percent or more of the total heat transfer. Consequently, accurate knowledge of surface emissivities of the heated rods, outer cylinders and surrounding structures is needed in order to predict the system thermal response during the transient. Direct measurements of surface emissivities have been obtained for one stainless steel and two aluminum samples. The measurements were obtained using an infrared pyrometer sensitive to the 8-14 micron wavelength range. A procedure for estimating total hemispherical emissivities based on the measured spectral, normal results is also provided. DOE

N92-31306# Ohio State Univ., Columbus.
STABILITY OF BOUNDARY LAYERS AT HIGH SUPERSONIC AND HYPERSONIC SPEEDS Final Report, 30 Jun. - 31 Oct. 1991
Thorwald Herbert 12 May 1992 24 p
(Contract F49620-88-C-0082)
(AD-A250900; AFOSR-92-0416TR) Avail: CASI HC A03/MF A01

The thrust of this research program has been the improvement of our capabilities for analyzing stability and transition of boundary layers at supersonic speeds. During the first phase, our efforts were primarily directed toward analytical studies, establishing the

elements of the numerical approach, and evaluating existing and new concepts to tackle the variety of problems. The second, and final, phase has been devoted to combining selected elements into codes, verification of these codes, comparison with previous results, and computing the basic flow over realistic geometries. The latter task has consumed the bulk of our resources. Analytical and numerical studies have been performed to investigate the role of the shock on both stability and receptivity characteristics of the flow. Development of the parabolized stability equations (PSE) for compressible flows has been a major goal. A new code incorporating many of the latest concepts and open to extensions is largely completed. GRA

N92-31322# California Univ., Los Angeles. School of Engineering and Applied Science.
ADAPTIVE AND NONADAPTIVE FEEDBACK CONTROL OF GLOBAL INSTABILITIES WITH APPLICATION TO A HEATED 2-D JET Final Technical Report, 15 Jun. 1989 - 31 Dec. 1991
Peter A. Monkewitz and D. L. Mingori Apr. 1992 63 p
(Grant AF-AFOSR-0421-89)
(AD-A250700; UCLA-ENG-92-28; AFOSR-92-0427TR) Avail: CASI HC A04/MF A01

Close to the onset of self-excited fluid oscillations the generic complex Ginzburg-Landau is proposed as the lowest order model for the plant. Its linear part which provides the stability boundaries is derived from first principles for both doubly-infinite and semi-infinite flow domains. Concentrating on a single global mode, the model is further simplified to the Stuart-Landau equation. For this latter model, a methodology is developed for the design of single-input single-output controllers. The so designed controllers have been implemented on a self-excited, heated two-dimensional jet with one hot wire as sensor and an acoustic speaker as actuator, and are shown to be effective within their limitations in suppressing or enhancing limit-cycle oscillations. Finally, the effect of of a controller designed to suppress the most unstable global mode on other modes is investigated experimentally in the wake of a cylinder at low Reynolds number, where an encouraging semi-quantitative correspondence to the Ginzburg-Landau model is found. GRA

N92-31352*# Ohio Univ., Athens. Center for Stirling Technology Research.
OSCILLATING-FLOW REGENERATOR TEST RIG: WOVEN SCREEN AND METAL FELT RESULTS Status Report, 1 Apr. 1991 - 30 Jun. 1992
D. Gedeon (Gedeon Associates, Athens, OH.) and J. G. Wood 29 Jul. 1992 38 p
(Grant NAG3-1269)
(NASA-CR-190689; NAS 1.26:190689) Avail: CASI HC A03/MF A01

We present correlating expressions, in terms of Reynolds or Peclet numbers, for friction factors, Nusselt numbers, enhanced axial conduction ratios, and overall heat flux ratios in four porous regenerator samples representative of stirling cycle regenerators: two woven screen samples and two random wire samples. Error estimates and comparison of data with others suggest our correlations are reliable, but we need to test more samples over a range of porosities before our results will become generally useful. Author

N92-31420# Westinghouse Savannah River Co., Aiken, SC.
TWO-COMPONENT FLOW STUDY IN LARGE-DIAMETER HORIZONTAL PIPE
D. A. Eghbali 3 Dec. 1991 28 p Presented at the American Society of Mechanical Engineers National Heat Transfer Conference and Exposition, San Diego, CA, 9-12 Aug. 1992
(Contract DE-AC09-89SR-18035)
(DE92-013196; WSRC-MS-91-393; CONF-920804-9) Avail: CASI HC A03/MF A01

Westinghouse Savannah River Company, Idaho National Engineering Laboratory, and Wyle Laboratory cooperated in a series of single- and two-component calibration tests conducted to obtain sufficient information for calibrating flowmeters, to observe flow patterns, and to estimate void functions. Testing, conducted in large-diameter horizontal pipe, covered total flows of 0.19 to 1.89 m(exp 3)/s (3000 to 30000 gpm) and inlet void fractions up to 40 percent. A flow regime map, constructed using video images of the flow patterns and void fraction data, was compared with maps from the literature, with generally good agreement for interpretation of flow patterns. DOE

N92-31421# Westinghouse Savannah River Co., Aiken, SC.
FLOW INSTABILITY IN A VERTICAL ANNULUS UNDER STEADY STATE AND TRANSIENT CONDITIONS
C. Fighetti (Columbia Univ., New York, NY.), S. Kokolis (Columbia Univ., New York, NY.), C. Maciuca (Columbia Univ., New York, NY.), D. G. Reddy (Columbia Univ., New York, NY.), B. Yang (Columbia Univ., New York, NY.), V. Carrano (Columbia Univ., New York, NY.), E. McAssey, Jr. (Villanova Univ., PA.), and Z. Qureshi 1992 19 p Presented at the American Society of Mechanical Engineers National Heat Transfer Conference and Exposition, San Diego, CA, 9-12 Aug. 1992
(Contract DE-AC09-89SR-18035)
(DE92-013217; WSRC-MS-92-132; CONF-920804-7) Avail: CASI HC A03/MF A01

Experimental data have been obtained for the occurrence of flow instability in a vertical annulus under steady state and transient down-flow conditions. The results show that the primary factor affecting the onset of flow instability is the Q(sub ratio) parameter (a measure of the void production in a channel). In addition, it is shown that for steady state conditions good agreement exists between the single annulus data and single tube data based upon the same L/D ratio. The results also indicate that under transient operation the Q(sub ratio) can be used as a stability criterion. DOE

N92-31424# Los Alamos National Lab., NM.
A MODEL FOR THE INTERFACIAL SHEAR IN VERTICAL, ADIABATIC, ANNULAR-MIST FLOW
M. W. Cappiello 1992 12 p Presented at the American Society of Mechanical Engineers National Heat Transfer Conference and Exposition, San Diego, CA, 9-12 Aug. 1992
(Contract W-7405-eng-36)
(DE92-013537; LA-UR-92-1271; CONF-920804-8) Avail: CASI HC A03/MF A01

A model is developed for the interfacial shear in upward, vertical, adiabatic, annular-mist flow. The model accounts for the momentum of both the droplet and film components and is applicable to the two-fluid approximation. Three computer programs are developed to evaluate the sensitivity of the droplet drag coefficient on the droplet velocity calculation, to solve the two-fluid set of equations by iteration, and to evaluate the required film friction factor from the data. The results of the sensitivity calculation show that a constant drag coefficient of 0.44 for the droplet is sufficient for estimating the droplet velocity over a typical range of gas velocities. Several film friction factor correlations from the literature were tested against the existing data of Hossfeld and Barathan. It was found that a modified effective roughness correlation proposed by Wallis performs the best overall in predicting the data for both small- and large-diameter pipes. The Electrical Power Research Institute drift-flux correlation and the Barathan correlation consistently underpredict the data. The use of the Henstock and Hanratty correlation predicts an incorrect trend. A new correlation is developed that better predicts the data over the entire range of gas injection rates. DOE

N92-31425# Worcester Polytechnic Inst., MA. Dept. of Mechanical Engineering.
GRANULAR FLOWS DOWN BUMPY INCLINES
M. W. Richman and R. E. Martin 1991 12 p Presented at the 3rd Joint Department of Energy/National Science Foundation (DOE/NSF) Workshop on Flow of Particulates and Fluids, Worcester, MA, 22-24 Oct. 1991
(Contract DE-AC22-91PC-90185)
(DE92-013568; CONF-9110369-1) Avail: CASI HC A03/MF A01

We are concerned here with steady, fully developed, gravity-driven flows of smooth, identical spheres down bumpy inclines. We summarize the analysis of these flows carried out by Richman and Marciniec (1990), who employed a kinetic constitutive theory and replaced the solid volume fraction by its depth-averaged value wherever it occurred in the balance equations. In the same manner, we obtain approximate closed form expressions for the normal stress, shear stress, and granular temperature, which when employed in the constitutive relations determine the solid volume fraction and mean velocity profiles. We then reparameterize the solutions to obtain, for fixed angles of inclination and boundary characteristics, the variations of mass flow rate with mass-hold up. In addition, we determine the corresponding variations of flow depth, depth-averaged solid volume fraction, and depth-averaged mean velocity. With the results presented in this manner, it is easy to make qualitative comparisons between predictions made by the theory and experimental results obtained by Johnson et. al. (1990). DOE

N92-31426# Pittsburgh Energy Technology Center, PA.
STEADY FLOW OF A FLUID-SOLID MIXTURE BETWEEN PARALLEL PLATES
G. Johnson (Pittsburgh Univ., PA.), K. R. Rajagopal (Pittsburgh Univ., PA.), M. Massoudi, and M. P. Mathur 1992 73 p
(Contract DE-AC05-76OR-00033)
(DE92-013645; DOE/OR-00033/T476) Avail: CASI HC A04/MF A01

In Part 1, a mathematical description for a flowing mixture of solid particulates and a fluid is developed within the context of Mixture Theory. Specifically, the equations governing the flow of a two-component mixture of a Newtonian fluid and a granular solid are derived. These relatively general equations are then reduced to a system of coupled ordinary differential equations describing steady flow of the mixture between flat plates. The resulting boundary value problem is solved numerically and results are presented for cases in which drag and lift interactions are important. Part 2 gives an overview of the methods used to obtain the numerical solutions. Multiple shooting, finite difference, and collocation methods for solving boundary value problems involving ordinary differential equations are discussed. A method for applying integral boundary conditions is then presented. Finally, the relative efficiency and effectiveness of the methods is discussed. DOE

N92-31452# Virginia Polytechnic Inst. and State Univ., Blacksburg. Dept. of Aerospace and Ocean Engineering.
DESCRIPTION OF A 1000 SENSOR CONSTANT CURRENT ANEMOMETER SYSTEM FOR LOCATING THREE-DIMENSIONAL TURBULENT BOUNDARY LAYER SEPARATIONS
R. L. Simpson, D. A. Walker, and K. A. Shinpaugh Dec. 1991 53 p
(Contract MDA972-90-C-0013)
(AD-A250827; VPI-AOE-185) Avail: CASI HC A04/MF A01

The location of three-dimensional separation on bodies such as submarines is important diagnostic information. Considerable changes in the side forces and moments occur with the undesirable phenomenon of separation. Three-dimensional flow separations occur very close to local minima in the magnitude of the wall shear stress. A 1000-flush-surface-sensor constant-current-anemometer separation location system is described here for locating these local minima along the axis of a body. As shown here, the convective heat transfer coefficient from a sensor is proportional to the one-third power of the local skin friction magnitude for the directionally-insensitive sensors described here. The constant-current anemometer design permits the use of strips of serially-connected sensors that require only one current source per strip. These compact electronics can be housed inside the body. The voltage drop across each sensor is measured for a number of different computer-controlled currents and related to the local heat transfer coefficient and the fixed parameters for that sensor. Each sensor mounted on the body forms a first order dynamic thermal system whose time constants can be experimentally determined. Thereafter, such as in transient flow separation conditions, measurements only for one current are necessary for a given precalibrated sensor. Results are presented for two sets of tests: (1) flow in the VPI and SU Water Tunnel over a 20 deg angle-of-attack circular cylinder, and (2) a 6:1 prolate spheroid at 15 deg angle of attack towed in the David Taylor Research Center 140' Basin. The separation location results are in close agreement with those from earlier wind tunnel tests by other investigators. GRA

N92-31484*# National Aeronautics and Space Administration. Lewis Research Center, Cleveland, OH.
A GENERAL NUMERICAL MODEL FOR WAVE ROTOR ANALYSIS
Daniel W. Paxson Jul. 1992 38 p
(RTOP 505-62-10)
(NASA-TM-105740; E-7141; NAS 1.15:105740) Avail: CASI HC A03/MF A01

Wave rotors represent one of the promising technologies for achieving very high core temperatures and pressures in future gas turbine engines. Their operation depends upon unsteady gas dynamics and as such, their analysis is quite difficult. This report describes a numerical model which has been developed to perform such an analysis. Following a brief introduction, a summary of the wave rotor concept is given. The governing equations are then presented, along with a summary of the assumptions used to obtain them. Next, the numerical integration technique is described. This is an explicit finite volume technique based on the method of Roe. The discussion then focuses on the implementation of appropriate boundary conditions. Following this, some results are presented which first compare the numerical approximation to the governing differential equations and then compare the overall model to an actual wave rotor experiment. Finally, some concluding remarks are presented concerning the limitations of the simplifying assumptions and areas where the model may be improved. I.I.C.

N92-31513# Technische Univ., Delft (Netherlands). Faculty of Technical Mathematics and Informatics.
THE DISCRETIZATION OF THE 2D INCOMPRESSIBLE NAVIER-STOKES EQUATIONS ON A COLLOCATED GRID
W. Couzy and P. Wilders 1991 41 p Sponsored by Delft Hydraulics Lab.
(Rept-91-61; ETN-92-91425) Copyright Avail: CASI HC A03/MF A01

A collocated discretization of the instationary incompressible Navier-Stokes equations in two dimensions is presented. The discretization is based on the method of Rhie and Chow extended to unsteady flows. Some topics of the curvilinear coordinate system are addressed. An identity that ensures the accuracy of our discretization for constant vector fields is ensured. The Navier-Stokes equations are presented in tensor formulation. The discretization in space is derived. The discretization in time and the pressure correction algorithm are given. The suppression of spurious pressure oscillations is treated. A modified pressure correction method, which is based on the method of Rhie and Chow, is presented. The equations with Cartesian unknowns are derived from the invariant equations in tensor formulation and mathematical details of the modified pressure correction method are given. ESA

N92-31528# Lawrence Livermore National Lab., CA.
PLANE STOKES FLOW DRIVEN BY CAPILLARITY ON A FREE SURFACE: OVERVIEW AND STATUS
R. W. Hopper 25 Oct. 1991 6 p Presented at the 5th International Colloquium on Free Boundary Problems: Theory and Applications, Montreal (Canada), 13-22 Jun. 1990 Revised
(Contract W-7405-eng-48)
(DE92-011469; UCRL-JC-103243-Rev-2; CONF-900684-1-Rev-2)
Avail: CASI HC A02/MF A01

This article summarizes some recent work on the creeping viscous incompressible plane flow in a region bounded by a simple smooth closed curve and driven solely by surface tension. Such problems are self-contained in that the applied tractions are intrinsic in the geometry. The objective is to determine exactly the time

evolution of the shape of the region. The problems are fundamentally nonlinear due to the large changes in shape, and it is emphasized that no mathematical approximations are made. For finite regions, the shape in the complex z-plane is described in terms of a time-dependent conformal mapping function. In practice, it has been necessary to conjecture an explicit parametric form whose validity must be verified using the shape-evolution equation. Suitable parameterizations are not always obvious. When the conjectured form holds and the equations can be solved, the evolution of the shape with time is obtained in simple, exact, and closed form except for the value of the time, which requires a mere quadrature. Internal velocity and stress fields can be obtained. DOE

N92-31535*# Institute for Computer Applications in Science and Engineering, Hampton, VA.
SENSITIVITY ANALYSIS OF HYDRODYNAMIC STABILITY OPERATORS Final Report
Peter J. Schmid (Massachusetts Inst. of Tech., Cambridge.), Dan S. Henningson (Massachusetts Inst. of Tech., Cambridge.), Mehdi R. Khorrami (High Technology Corp., Hampton, VA.), and Mujeeb R. Malik (High Technology Corp., Hampton, VA.) Jul. 1992 27 p Submitted for publication; sponsored in part by the Aeronautical Research Inst. of Sweden (FFA)
(Contracts NAS1-18605; NAS1-19480; NAS1-18240; RTOP 505-90-52-01)
(NASA-CR-189683; NAS 1.26:189683; ICASE-92-33) Avail: CASI HC A03/MF A01

The eigenvalue sensitivity for hydrodynamic stability operators is investigated. Classical matrix perturbation techniques as well as the concept of epsilon-pseudoeigenvalues are applied to show that parts of the spectrum are highly sensitive to small perturbations. Applications are drawn from incompressible plane Couette, trailing line vortex flow and compressible Blasius boundary layer flow. Parametric studies indicate a monotonically increasing effect of the Reynolds number on the sensitivity. The phenomenon of eigenvalue sensitivity is due to the non-normality of the operators and their discrete matrix analogs and may be associated with large transient growth of the corresponding initial value problem. Author

N92-31559# Arizona Univ., Tucson.
AN EXPERIMENTAL INVESTIGATION OF THE FORMATION OF SECONDARY VORTICES AND THE GENERATION OF SMALL-SCALE MOTION IN A SPANWISE FORCED PLANE MIXING LAYER Final Report, 1 Aug. 1988 - 30 Sep. 1991
A. Glezer Mar. 1992 177 p
(Grant AF-AFOSR-0271-88)
(AD-A250350; AFOSR-92-0361TR) Avail: CASI HC A09/MF A02

The evolution of spanwise instability modes and 3-D pulsed disturbances leading to the formation of streamwise vortices in a plane mixing layer and subsequently to the onset of small-scale 3-D motion were studied in a closed-return water facility. Streamwise vortices may result from a spanwise core instability of the primary vortices, or a spanwise instability of the nominally 2-D strain field between them. These two instability modes were excited by time-harmonic wavetrains with spanwise phase or amplitude variations, respectively, synthesized by a mosaic of surface film heaters flush-mounted on the flow partition. The appearance of the streamwise vortices is accompanied by significant distortion in the transverse distribution of the streamwise velocity component. Inflection points, which are not present in corresponding velocity distributions of the unforced flow, indicate the formation of locally unstable regions of large shear in which broadband perturbations already present in the base flow undergo rapid amplification which is followed by breakdown to turbulence and mixing transition. The core instability of the primary vortices suggests itself as a viable mechanism for the continuation of the mixing process far downstream of mixing transition. Pulsed excitation was produced by pulsed spanwise amplitude modulation of a spanwise-uniform time-harmonic carrier wave train synthesized by the surface film heaters. GRA

N92-31564*# Institute for Computer Applications in Science and Engineering, Hampton, VA.
DEVELOPMENT OF WAVELET ANALYSIS TOOLS FOR TURBULENCE Final Report
A. Bertelrud, G. Erlebacher, Ph. Dussouillez (Aix-Marseilles Univ., France), M. P. Liandrat, J. Liandrat (Aix-Marseilles Univ., France), F. Moret Bailly (Aix-Marseilles Univ., France), and Ph. Tchamitchian (Centre National de la Recherche Scientifique, Marseilles, France) Jul. 1992 22 p
(Contract NAS1-18605; RTOP 505-90-52-01)
(NASA-CR-189674; NAS 1.26:189674; ICASE-IR-23) Avail: CASI HC A03/MF A01

Presented here is the general framework and the initial results of a joint effort to derive novel research tools and easy to use software to analyze and model turbulence and transition. Given here is a brief review of the issues, a summary of some basic properties of wavelets, and preliminary results. Technical aspects of the implementation, the physical conclusions reached at this time, and current developments are discussed. Author

N92-31625# Lawrence Livermore National Lab., CA.
TURBULENT DUSTY BOUNDARY LAYER IN AN ANFO SURFACE-BURST EXPLOSION
A. L. Kuhl, R. E. Ferguson, K. Y. Chien, and J. P. Collins Jan. 1992 39 p Presented at the 24th International Symposium on Combustion, Sydney (Australia), 5-10 Jul. 1992
(Contract W-7405-eng-48)
(DE92-012101; UCRL-JC-108985; CONF-920707-28) Avail: CASI HC A03/MF A01

This paper describes the results of numerical simulations of the dusty, turbulent boundary layer created by a surface burst explosion. The blast wave was generated by the detonation of a 600-T hemisphere of ANFO, similar to those used in large-scale field tests. The surface was assumed to be ideally noncratering but contained an initial loose layer of dust. The dust-air mixture in this fluidized bed was modeled as a dense gas (i.e., an equilibrium model, valid for very small-diameter dust particles). The evolution of the flow was calculated by a high-order Godunov code that solves the nonsteady conservation laws. Shock interactions with dense layer generated vorticity near the wall, a result that is similar to viscous, no-slip effects found in clean flows. The resulting wall shear layer was unstable, and rolled up into large-scale rotational structures. These structures entrained dense material from the wall layer and created a chaotically striated flow. The boundary layer grew due to merging of the large-scale structures and due to local entrainment of the dense material from the fluidized bed. The chaotic flow was averaged along similarity lines (i.e., lines of constant values of x = r/Rs and y = z/Rs where R(sub s) = ct(exp alpha)) to establish the mean-flow profiles and the r.m.s. fluctuating-flow profiles of the boundary layer. DOE

N92-31687*# Institute for Computer Applications in Science and Engineering, Hampton, VA.
ON THE SPATIAL EVOLUTION OF LONG-WAVELENGTH GOERTLER VORTICES GOVERNED BY A VISCOUS-INVISCID INTERACTION Final Report
Meelan Choudhari (High Technology Corp., Hampton, VA.), Philip Hall (Manchester Univ., England), and Craig Streett (National Aeronautics and Space Administration. Langley Research Center, Hampton, VA.) Jul. 1992 29 p Submitted for publication
(Contract NAS1-18605; RTOP 505-90-52-01)
(NASA-CR-189681; NAS 1.26:189681; ICASE-92-31) Avail: CASI HC A03/MF A01

The generation of long-wavelength, viscous-inviscid interactive Goertler vortices is studied in the linear regime by numerically solving the time-dependent governing equations. It is found that time-dependent surface deformations, which assume a fixed nonzero shape at large times, generate steady Goertler vortices that amplify in the downstream direction. Thus, the Goertler instability in this regime is shown to be convective in nature, contrary to the earlier findings of Ruban and Savenkov. The disturbance pattern created by steady and streamwise-elongated surface obstacles on a concave surface is examined in detail,

and also contrasted with the flow pattern due to roughness elements with aspect ratio of order unity on flat surfaces. Finally, the applicability of the Briggs-Bers criterion to unstable physical systems of this type is questioned by providing a counterexample in the form of the inviscid limit of interactive Goertler vortices.
Author

N92-31696# George Washington Univ., Washington, DC. School of Engineering and Applied Science.
DEVELOPMENT AND APPLICATION OF NEW ALGORITHMS FOR THE SIMULATION OF COMPRESSIBLE FLOWS WITH MOVING BODIES IN THREE DIMENSIONS Final Report, 15 Sep. 1990 - 14 Sep. 1991
Rainald Lohner and Jean Cabello 3 Mar. 1992 59 p
(Grant AF-AFOSR-0540-89)
(AD-A250232; AFOSR-92-0369TR) Avail: CASI HC A04/MF A01

A new CFD capability for compressible flows with moving bodies was developed. The salient features of this capability are (1) fast and reliable 3-D unstructured grid generation, (2) flow solvers for moving frames of reference, (3) adaptive mesh regeneration during transient runs, (4) on-line display of results, and (5) post-processing and movie-making capability.
GRA

N92-31701# Los Alamos National Lab., NM.
ESTABLISHING LOW-POWER OPERATING LIMITS FOR LIQUID METAL HEAT PIPES
J. Secary (Phillips Lab., Kirkland AFB, NM.), M. A. Merrigan, and M. D. Keddy 1992 9 p Presented at the 8th International Heat Pipe Conference, Bejing (China), 14-18 Sep. 1992
(Contract W-7405-eng-36)
(DE92-011367; LA-UR-92-849; CONF-920981-1) Avail: CASI HC A02/MF A01

Liquid metal heat pipes operated at power throughputs well below their design point for long durations may fail as a result of the working fluid migrating to a cold region within the pipe, freezing there, and returning hot to the evaporator section. Eventually, sufficient working fluid inventory may be lost to the cold region to cause a local dry-out condition in the evaporator. A joint experimental and analytical effort between the Air Force Phillips Laboratory and Los Alamos National Laboratory is underway to investigate the phenomena. Experiments include both high temperature liquid metal and low temperature organic heat pipes. To date, a low temperature working fluid has been selected and its performance in a heat pipe validated. Additionally, a low-temperature heat pipe has been fabricated and is presently being tested.
DOE

N92-31726# Massachusetts Inst. of Tech., Cambridge. Dept. of Chemical Engineering.
MACROSTATISTICAL HYDRODYNAMICS
H. Brenner 1992 15 p
(Contract DE-FG02-88ER-13896)
(DE92-013589; DOE/ER-13896/4) Avail: CASI HC A03/MF A01

During the course of these efforts we have been studying the suspension of particles in Newtonian and non-Newtonian liquids, embodying a combination of analysis, experiments, and numerical simulations. Experiments primarily involved tracking small balls as they fall slowly through otherwise quiescent suspensions of neutrally buoyant particles. Detailed trajectories of the balls, obtained either with new experimental techniques or by numerical simulation, were statistically interpreted in terms of the mean settling velocity and the dispersion about the mean. We showed that falling-ball rheometry, using small balls relative to the suspended particles, could be a means of measuring the macroscopic zero-shear-rate viscosity without significantly disturbing the original microstructure; therefore, falling-ball rheometry can be a powerful tool for use in studying the effects of microstructures on the macroscopic properties of suspensions. We plan to extend this work to the study of more complex, structured fluids, and to use other tools (e.g., rolling-ball rheometry) to study boundary effects. We also propose to study flowing suspensions to obtain non-zero-shear-rate viscosities. The intent is to develop an understanding of the basic principles needed to treat generic multiphase flow problems, through a detailed study of model systems.
DOE

N92-31770# Stanford Univ., CA. Center for Space Science and Astrophysics.
INTERACTION OF FAST STEADY FLOW WITH SLOW TRANSIENT FLOW: A NEW CAUSE OF INTERPLANETARY Bz EVENTS
Xuepu Zhao 16 Dec. 1991 16 p
(Contract N00014-89-J-1024)
(AD-A250273) Avail: CASI HC A03/MF A01

The occurrence of the nonspiral magnetic field, (high helium density) Cold Magnetic Enhancement and counterstreaming suprathermal electron flux in the slow flow around the forward shock indicates that the slow flow is a CME in interplanetary space (ICME). The characteristics of the field and plasma in the fast flow around the reverse shock is typical for a high speed stream. Thus the shock pair here appears to be caused by the interaction of a high speed stream with a slow ICME. The fact that a -Bz event occurred in such a shock pair suggests that the slow ICME is disconnected from the Sun. It is shown that compression alone appears to be adequate to explain the large southward IMF component within the shocked plasma because of the large southward field component present in the ICME ahead of the forward shock. In addition, a new method to infer the shock angle and Mach number from the observed upstream plasma B and the jump ratios of proton density and total magnetic flux density across a shock is described.
GRA

N92-31785# Argonne National Lab., IL.
HEAT EXCHANGER PERFORMANCE CALCULATIONS FOR ENHANCED-TUBE CONDENSER APPLICATIONS
T. J. Rabas 1992 10 p Presented at the American Society of Mechanical Engineers National Heat Transfer Conference and Exposition, San Diego, CA, 9-12 Aug. 1992
(Contract W-31-109-eng-38)
(DE92-016603; ANL/CP-75985; CONF-920804-17) Avail: CASI HC A02/MF A01

The lack of a prediction method is sometimes used for the rejection of enhanced tubes for some condenser applications even though there is ample data from single-tube condensing experiments. Three methods are discussed that can be used to rate and/or size these multitube units based on the single-tube experimental results. The Kern vertical-number correction appears to be quite adequate for most operating conditions, the exceptions being large sizes and/or deep vacuum operation. The bundle-factor method is preferred for these applications; however, field test results are required to obtain this factor. If performance data are not available, pointwise or numerical methods are required, but special care must be taken to insure that the adverse effects of noncondensable gas pockets and the saturation-temperature depression are properly addressed.
DOE

N92-31824# Princeton Univ., NJ.
THE STRUCTURE AND CONTROL OF THREE-DIMENSIONAL SHOCK WAVE TURBULENT BOUNDARY LAYER INTERACTIONS Final Report, 1 Oct. 1988 - 31 Aug. 1991
Seymour M. Bogdonoff and Alexander J. Smits 20 Mar. 1992 30 p
(Grant AF-AFOSR-0033-89)
(AD-A250209; AFOSR-92-0388TR) Avail: CASI HC A03/MF A01

The three year period covered in the subject report was a considerable shift from the previous years of work on shock wave turbulent boundary layer interactions. The earlier work concentrated on simple building block experiments and a search for a fundamental understanding of the flow phenomena. In the subject research, most of the work on fundamentals for the simple configurations was stopped. The main emphasis for the first two years of the current program was on complex configurations and the final year was a close-out program on a new approach. The

work on complex configurations was limited to two geometries which used the much studied single sharp fin interaction as the initial conditions. This shift in emphasis had two main purposes: (1) block experiments in more complex interactions required for applications and (2) to provide a more critical test of computation which, although giving the general characteristics for the building block experiments, did not give highly quantitative results. The primary activities for the first two years will be discussed in three major groupings: (1) and (2) discussions of the two complex configurations, and (3) a description of the boundary layer conditions which are critical to the definition of the experiment and the check by computational fluid dynamics. GRA

N92-31832# Sandia National Labs., Albuquerque, NM.
USE OF A GENETIC ALGORITHM TO SOLVE FLUID FLOW PROBLEMS ON AN NCUBE/2 MULTIPROCESSOR COMPUTER
R. J. Pryor and D. D. Cline Apr. 1992 49 p
(Contract DE-AC04-76DP-00789)
(DE92-014044; SAND-91-2532) Avail: CASI HC A03/MF A01

This paper presents a method to solve partial differential equations governing two-phase fluid flow by using a genetic algorithm on the NCUBE/2 multiprocessor computer. Genetic algorithms represent a significant departure from traditional approaches of solving fluid flow problems. The inherent parallelism of genetic algorithms offers the prospect of obtaining solutions faster than ever possible. The paper discusses the two-phase flow equations, the genetic representation of the unknowns, the fitness function, the genetic operators, and the implementation of the genetic algorithm on the NCUBE/2 computer. The paper investigates the implementation efficiency using a pipe blowdown test and presents the effects of varying both the genetic parameters and the number of processors. The results show that genetic algorithms provide a major advancement in methods for solving two-phase flow problems. A desired goal of solving these equations for a specific simulation problem in real time or faster requires computers with an order of magnitude more processors or faster than the NCUBE/2's 1024. DOE

N92-31839# National Inst. of Standards and Technology, Boulder, CO. Chemical Engineering Div.
EFFECTS OF FLOW CONDITIONERS AND TAP LOCATION ON ORIFICE FLOWMETER PERFORMANCE Technical Report, Feb. - Dec. 1990
J. L. Scott, C. F. Sindt, M. A. Lewis, and J. A. Brennan Oct. 1991 73 p
(Contract GRI-5088-271-1680)
(PB92-183730; NIST/TN-1352; B91-0281; GRI-91/0229) Avail: CASI HC A04/MF A01

Current research is being conducted to provide information which will be used to improve the existing industry standards for proper installation of orifice meters. The research includes experimental investigation of a Zanker, an etoile, and several tube bundle flow conditioners at various positions relative to the orifice plate. Also included are the effects of pressure tap location, both with and without flow conditioning, as reflected in determination of discharge coefficients. Of the flow conditioners tested at approximately 11 pipe diameters upstream of the orifice plate, the Zanker flow conditioner resulted in discharge coefficients most similar to baseline values. There was only a slight difference in orifice meter performance when a flanged or an in-line tube bundle flow conditioner was used at the tested location upstream of the orifice plate. The effect of pressure tap location was found to be significant with the 0.73 beta ratio plate. Recommendations for future research, as a result of these findings, are included.
Author

N92-31895# Pittsburgh Energy Technology Center, PA.
HEAT TRANSFER AND FLOW OF A MODIFIED SECOND GRADE FLUID
G. Gupta (Pittsburgh Univ., PA.) and M. Massoudi May 1992 37 p
(DE92-014744; DOE/PETC-TR/92/6) Avail: CASI HC A03/MF A01

We examine the fully developed flow of a generalized fluid of second grade between heated parallel plates, due to a pressure gradient along the plate. The constant coefficient coefficient of shear viscosity of a fluid of second grade is replaced by a shear dependent viscosity with an exponent, m. If the normal stress coefficients are set equal to zero, this reduces to the standard power-law model. We obtain the solution for the case when the temperature changes only in the direction normal to the plates for the two most commonly used viscosity models: (1) when the viscosity does not depend on temperature; and (2) when the viscosity is an exponentially decaying function of temperature.
DOE

N92-31933# Sandia National Labs., Albuquerque, NM.
AXISYMMETRIC BLUFF-BODY FLOW: A VORTEX SOLVER FOR THIN SHELLS
J. H. Strickland May 1992 67 p
(Contract DE-AC04-76DP-00789)
(DE92-016748; SAND-91-2760) Avail: CASI HC A04/MF A01

A method which is capable of solving the axisymmetric flow field over bluff bodies consisting of thin shells such as disks, partial spheres, rings, and other such shapes is presented in this report. The body may be made up of several shells whose edges are separated by gaps. The body may be moved axially according to arbitrary velocity time histories. In addition, the surfaces may possess axial and radial degrees of flexibility such that points on the surfaces may be allowed to move relative to each other according to some specified function of time. The surfaces may be either porous or impervious. The present solution technique is based on the axisymmetric vorticity transport equation. Physically, this technique simulates the generation of vorticity at body surfaces in the form of discrete ring vortices which are subsequently diffused and convected into the boundary layers and wake of the body. Relatively large numbers of vortices (1000 or more) are required to obtain good simulations. Since the direct calculation of perturbations from large numbers of ring vortices is computationally intensive, a fast multipole method was used to greatly reduce computer processing time. Several example calculations are presented for disks, disks with holes, hemispheres, and vented hemispheres. These results are compared with steady and unsteady experimental data. DOE

N92-31977# Brookhaven National Lab., Upton, NY.
CONDENSATION IN A TWO-PHASE POOL
R. B. Duffey and E. D. Hughes (Edgerton, Germeshausen and Grier, Inc., Idaho Falls, ID.) 1991 9 p Presented at the First European Thermal Sciences Conference and 3rd UK National Heat Transfer Conference and 460th Event of the European Federation of Chemical Engineering, Birmingham, England, 16-18 Sep. 1992
(Contracts DE-AC02-76CH-00016; DE-AC07-76ID-01570)
(DE92-010048; BNL-47120; CONF-920928-1) Avail: CASI HC A02/MF A01

We consider the case of vapor condensation in a liquid pool, when the heat transfer is controlled by heat losses through the walls. The analysis is based on drift flux theory for phase separation in the pool, and determines the two-phase mixture height for the pool. To our knowledge, this is the first analytical treatment of this classic problem that gives an explicit result (previous work having established the result for the evaporative case). From conservation of mass and energy in a one-dimensional steady flow, together with a void relation between the liquid and vapor fluxes, we determine the increase in the mixture level from the base level of the pool. It can be seen that the thermal and hydrodynamic influences are separable. Thus, the thermal influence of the wall heat transfer appears through its effect on the condensing length, so that at high condensation rates the pool is all liquid, and at low rates overflows (the level swell or foaming effect). Similarly, the phase separation effect hydrodynamically determines the height via the relative velocity of the mixture to the entering flux. We examine some practical applications of this result to level swell in condensing flows, and also examine some limits in ideal cases. DOE

N92-32000# Grumman Aerospace Corp., Bethpage, NY.
HIGHLY ACCURATE PREDICTION OF UNSTEADY VISCOUS FLOWS Final Report, 1 Jan. 1991 - 1 Jan. 1992
F. Marconi and Gino Moretti Apr. 1992 45 p
(Contract F49620-91-C-0015)
(AD-A250982; AFOSR-92-0429TR) Avail: CASI HC A03/MF A01

This report describes a detailed investigation of the effects of computational accuracy on the prediction of shock wave/boundary layer interaction. In particular, the result of inaccuracies in the computation of the shock and the flow in its vicinity is studied. A new computational procedure computes all shocks as discontinuities while including all viscous effects. This scheme is used as a standard against which the accuracy of widely used shock capturing schemes is measured. The effect of the numerical error generated by spreading a shock over a few mesh intervals (instead of a few mean free paths) is evaluated with regard to shock/boundary layer interaction. We consider the spreading error, as well as the error produced by reducing the formal accuracy of these schemes near shocks (in order to eliminate wiggles). In this report, we present the computational scheme and results for a number of flow configurations. GRA

N92-32003# Argonne National Lab., IL.
HEAT AND MASS TRANSFER CONSIDERATIONS IN ADVANCED HEAT PUMP SYSTEMS
C. B. Panchal and K. J. Bell 1992 7 p Presented at the 27th Intersociety Energy Conversion Engineering Conference, San Diego, CA, 3-7 Aug. 1992
(Contract W-31-109-eng-38)
(DE92-016635; ANL/CP-75330; CONF-920801-13) Avail: CASI HC A02/MF A01

Advanced heat-pump cycles are being investigated for various applications. However, the working media and associated thermal design aspects require new concepts for maintaining high thermal effectiveness and phase equilibrium for achieving maximum possible thermodynamic advantages. In the present study, the heat- and mass-transfer processes in two heat-pump systems -- those based on absorption processes, and those using refrigerant mixtures -- are analyzed. The major technical barriers for achieving the ideal performance predicted by thermodynamic analysis are identified. The analysis provides general guidelines for the development of heat- and mass-transfer equipment for advanced heat-pump systems. DOE

N92-32008# Los Alamos National Lab., NM.
FEHMN 1.0: FINITE ELEMENT HEAT AND MASS TRANSFER CODE
G. Zyvoloski, Z. Dash, and S. Kelkar May 1992 113 p
(Contract W-7405-eng-36)
(DE92-013998; LA-12062-MS-Rev-1) Avail: CASI HC A06/MF A02

A computer code is described which can simulate nonisothermal multiphase multicomponent flow in porous media. It is applicable to natural-state studies of geothermal systems and groundwater flow. The equations of heat and mass transfer for multiphase flow in porous and permeable media are solved using the finite element method. The permeability and porosity of the medium are allowed to depend on pressure and temperature. The code also has provisions for movable air and water phases and noncoupled tracers; that is, tracer solutions that do not affect the heat and mass transfer solutions. The tracers can be passive or reactive. The code can simulate two-dimensional, two-dimensional radial, or three-dimensional geometries. A summary of the equations in the model and the numerical solution procedure are provided in this report. A user's guide and sample problems are also included. The FEHMN (Finite Element Heat and Mass Nuclear) code, described in this report, is a version of FEHM (Finite Element Heat and Mass, Zyvoloski et al., 1988) developed for the Yucca Mountain Site Characterization Project (YMP). The main use of FEHMN will be to assist in the understanding of flow fields in the saturated zone below the potential Yucca Mountain repository. DOE

N92-32022# Los Alamos National Lab., NM.
CAVEAT: A COMPUTER CODE FOR FLUID DYNAMICS PROBLEMS WITH LARGE DISTORTION AND INTERNAL SLIP
F. L. Addessio, J. R. Baumgardner, J. K. Dukowicz, N. L. Johnson, B. A. Kashiwa, R. M. Rauenzahn, and C. Zemach May 1992 167 p
(Contract W-7405-eng-36)
(DE92-014078; LA-10613-MS-Rev-1) Avail: CASI HC A08/MF A02

This report is a description of the two-dimensional version of CAVEAT, a computer code which solves numerically the equations of transient, multimaterial, compressible fluid dynamics. CAVEAT is written to treat a wide variety of problems. It has the ability, for example, to describe material interfaces and the large slip along interfaces, to describe complex geometries without sacrificing vector processing, and to apply tabular equations of state. Its numerical methods were chosen to minimize numerical diffusion, achieve a high degree of vectorization, and facilitate extension to three dimensions. CAVEAT uses an explicit time-marching, conservative finite-volume numerical technique in which all state variables, including velocity, are cell centered; values at vertices and cell faces are derived. The technique is a variation of the Godunov method that uses an approximate Riemann solver and accommodates arbitrary equations of state. Spatial differencing may either be first order or second order with a choice of limiters of the gradient in an attempt to preserve monotonicity. The formulation is spatially two-dimensional with options for Cartesian and curvilinear geometries. Discretization is achieved with a mesh of arbitrary quadrilateral cells whose vertices can move with time. Arbitrary mesh motion is supported by allowing transport of material between cells according to the Arbitrary Lagrangian-Eulerian technique. This report is a second edition of an earlier report on CAVEAT. Because of the maturity and expanded use of CAVEAT, this report includes new sections directed toward first-time users. We have chosen to document in this report only the hydrodynamics part of the much larger version of CAVEAT. DOE

N92-32038# Carnegie-Mellon Univ., Pittsburgh, PA. Dept. of Mathematics.
NEW TECHNIQUES IN COMPUTATIONAL FLUID DYNAMICS: ALGORITHMS, ANALYSIS, APPLICATIONS Final Report, 1 Jun. 1989 - 31 Dec. 1991
R. A. Nicolaides 31 Dec. 1991 5 p
(Grant AF-AFOSR-0359-89)
(AD-A250498; AFOSR-92-0353TR) Avail: CASI HC A01/MF A01

The overall goal of this research was the development and application of covolume methodology in computational fluid dynamics (CFD) and related areas. The main framework of the covolume approach is now in place and its major characteristics are reasonably well understood. The research shows the algorithm to be a stable and accurate approach to computing viscous fluids on unstructured meshes. The covolume approach has several unique features, including an associated discrete vector field theory, which in turn permits covolume discretizations to exhibit important physical characteristics, for example being free of artificial vorticity creation. There is still need for work in compressible and three dimensional flows. GRA

N92-32115# Westinghouse Savannah River Co., Aiken, SC.
HEAT TRANSFER AND PRESSURE DROP IN AN ANNULAR CHANNEL WITH DOWNFLOW
F. X. Dolan (Creare, Inc., Hanover, NH.), C. J. Crowley (Creare, Inc., Hanover, NH.), and Z. H. Qureshi 1992 29 p Presented at the American Society of Mechanical Engineers National Heat Transfer Conference and Exposition, San Diego, CA, 9-12 Aug. 1992
(Contract DE-AC09-89SR-18035)
(DE92-014363; WSRC-MS-92-123; CONF-920804-10) Avail: CASI HC A03/MF A01

The onset of a flow instability (OFI) determines the minimum flow rate for cooling in the flow channels of a nuclear fuel assembly. A test facility was constructed with full-scale models (length and

diameter) of annular flow channels incorporating many instruments to measure heat transfer and pressure drop with downflow in the annulus. Tests were performed both with and without axial centering ribs at prototypical values of pressure, flow rate and uniform wall heat flux. The axial ribs have the effect of subdividing the annulus into quadrants, so the problem becomes one of parallel channel flow, unlike previous experiments in tubes (upflow and downflow). Other tests were performed to determine the effects if any of asymmetric and non-uniform circumferential wall heating, operating pressure level and dissolved gas concentration. Data from the tests are compared with models for channel heat transfer and pressure drop profiles in several regimes of wall heating from single-phase forced convection through partially and fully developed nucleate boiling. Minimum stable flow rates were experimentally determined as a function of wall heat flux and heat distribution and compared with the model for the transition to fully developed boiling which is a key criterion in determining the OFI condition in the channel. The heat transfer results in the channel without ribs are in excellent agreement with predictions from a computer model of the flow in the annulus and with empirical correlations developed from similar tests. The test results with centering ribs show that geometrical variations between the channels can lead to differences in subchannel behavior which can make the effect of the ribs and the geometry an important factor when assessing the power level at which the fuel assembly (and the reactor) can be operated to prevent overheating in the event of a loss-of-coolant-accident (LOCA). DOE

N92-32158*# Institute for Computer Applications in Science and Engineering, Hampton, VA.
REYNOLDS STRESS CALCULATIONS OF HOMOGENEOUS TURBULENT SHEAR FLOW WITH BOUNDED ENERGY STATES Final Report
Charles G. Speziale and R. Abid (High Technology Corp., Hampton, VA.) Jul. 1992 18 p Submitted for publication
(Contracts NAS1-18605; NAS1-19480; RTOP 505-90-52-01)
(NASA-CR-189682; NAS 1.26:189682; ICASE-92-32) Avail: CASI HC A03/MF A01

Reynolds stress calculations of homogeneous turbulent shear flow are conducted with a second-order closure model modified to account for non-equilibrium vortex stretching in the dissipation rate transport equation, as recently proposed by Bernard and Speziale. As with the earlier reported k-epsilon model calculations incorporating this vortex streching effect, a production-equals-dissipation equilibrium is obtained with bounded turbulent kinetic energy and dissipation. However, this equilibrium is not achieved until the dimensionless time greater than 60, an elapsed time that is at least twice as large as any of those considered in previous numerical and physical experiments on homogeneous shear flow. Direct quantitative comparisons between the model predictions and the results of experiments are quite favorable. In particular, it is shown that the inclusion of this non-equilibrium vortex stretching effect has the capability of explaining the significant range of production to dissipation ratios observed in experiments. Author

N92-32242*# Analytical Services and Materials, Inc., Hampton, VA.
TOWARDS UNDERSTANDING TURBULENT SCALAR MIXING
Sharath S. Girimaji Washington NASA. Langley Research Center Jul. 1992 55 p
(Contract NAS1-18599; RTOP 505-62-40-06)
(NASA-CR-4446; NAS 1.26:4446) Avail: CASI HC A04/MF A01

In an effort towards understanding turbulent scalar mixing, we study the effect of molecular mixing, first in isolation and then by accounting for the effects of the velocity field. The chief motivation for this approach stems from the strong resemblance of the scalar probability density function (PDF) obtained from the scalar field evolving from the heat conduction equation that arises in a turbulent velocity field. However, the evolution of the scalar dissipation is different for the two cases. We attempt to account for these differences, which are due to the velocity field, using a Lagrangian frame analysis. After establishing the usefulness of this approach, we use the heat-conduction simulations (HCS), in lieu of the more expensive direct numerical simulations (DNS), to study many of the less understood aspects of turbulent mixing. Comparison between the HCS data and available models are made whenever possible. It is established that the beta PDF characterizes the evolution of the scalar PDF during mixing from all types of non-premixed initial conditions. Author

N92-31886# Israel Aircraft Industries Ltd., Ben-Gurion Airport.
THE CALCULATION OF INCOMPRESSIBLE SEPARATED TURBULENT BOUNDARY LAYERS
A. Kogan and S. Migemi *In* Israel Society of Aeronautics and Astronautics, 31st Israel Annual Conference on Aviation and Astronautics 22 Feb. 1990 p 185-196 Previously announced in IAA as A90-51025 (For primary document see N92-31861 22-01)
Avail: CASI HC A03/MF A03

N92-31887# Technion - Israel Inst. of Tech., Haifa. Faculty of Aerospace Engineering.
THE STABILITY OF A SLIGHTLY ECCENTRIC STRAIGHT VORTEX FILAMENT IN A CIRCULAR TUBE
Z. Rusak and A. Seginer *In* Israel Society of Aeronautics and Astronautics, 31st Israel Annual Conference on Aviation and Astronautics 22 Feb. 1990 p 197-204 Previously announced in IAA as A91-43099 (For primary document see N92-31861 22-01)
Avail: CASI HC A02/MF A03

35 INSTRUMENTATION AND PHOTOGRAPHY

Includes remote sensors; measuring instruments and gages; detectors; cameras and photographic supplies; and holography.

For aerial photography see *43 Earth Resources and Remote Sensing.* For related information see also *06 Aircraft Instrumentation,* and *19 Spacecraft Instrumentation.*

N92-31298# Analysis and Measurement Services Corp., Knoxville, TN.
NEW TECHNOLOGY FOR REMOTE TESTING OF RESPONSE TIME OF INSTALLED THERMOCOUPLES. VOLUME 2: RESEARCH DATA Final Report, Sep. 1987 - Dec. 1990
H. M. Hashemian and D. W. Mitchell Jan. 1992 267 p
(Contract F40600-87-C-0003)
(AD-A245821; AEDC-TR-91-26-Vol-2) Avail: CASI HC A12/MF A03

A comprehensive research and development project was completed to provide new technology for remote testing of response time of thermocouples as installed in operating processes. A significant portion of this development depended on the Loop Current Step Response (LCSR) method. This method is based on heating the thermocouple internally by applying an electric current to its extension leads. The current produces Joule heating in the thermocouple and causes the thermocouple junction to settle several degrees above the ambient temperature. The current is then cut off and the thermocouple output is recorded as it cools to the ambient temperature. It has been established by experimental research and theoretical development carried out in this project that this cooling transient can be analyzed to provide the response time of the thermocouple under the conditions tested. With little additional effort, the equipment that was developed in this project can be adapted to provide a capability for in-situ assessment of static health, reliability, and accuracy of installed thermocouples. GRA

N92-31313# Fermi National Accelerator Lab., Batavia, IL.
INVESTIGATION OF FACTORS AFFECTING THE CALIBRATION OF STRAIN GAGE BASED TRANSDUCERS (GOODZEIT GAGES) FOR SSC MAGNETS

M. Davidson, A. Gilbertson, and M. Dougherty Mar. 1991 9 p Presented at the 3rd Annual International Industrialization Symposium on the Super Collider (IISSC), Atlanta, GA, 13-15 Mar. 1991
(Contract DE-AC02-76CH-03000)
(DE92-010722; FNAL-TM-1724; CONF-910340-54) Avail: CASI HC A02/MF A01

These transducers are designed to measure stresses on SSC collared coils. They are individually calibrated with a bonded ten-stack of SSC inner coil cable by applying a known load and reading corresponding output from the gages. The transducer is supported by a notched 'backing plate' that allows for bending of the gage beam during calibration or in use with an actual coil. Several factors affecting the calibration and use of the transducers are the number of times a 'backing plate' is used, the similarities or difficulties between bonded ten-stacks, and the differences between the ten-stacks and the coil they represent. The latter is probably the most important because a calibration curve is a model of how a transducer should react within a coil. If the model is wrong, the calibration curve is wrong. Information will be presented regarding differences in calibrations between Brookhaven National Labs (also calibrating these transducers) and Fermilab -- what caused these differences, the investigation into the differences between coils and ten-stacks and how they relate to transducer calibration, and some suggestions for future calibrations. DOE

N92-31340# National Inst. for Fusion Science, Nagoya (Japan).
NEW HIGH VOLTAGE PARALLEL PLATE ANALYZER
Y. Hamada, Y. Kawasumi, K. Masai, H. Iguchi, A. Fujisawa, and Y. Abe (Iwate Univ., Morioka, Japan) Jan. 1992 16 p Submitted for publication
(NIFS-128; ISSN-0915-633X) Avail: CASI HC A03/MF A01

A new modification of the parallel plate analyzer for 500 keV heavy ions designed to eliminate the effect of the intense UV and visible radiations was successfully conducted. The principle of the modification and the results are discussed. Author

N92-31370# National Inst. of Standards and Technology, Gaithersburg, MD. Automated Production Technology Div.
AUTOMATION OF STRAIN-GAUGE LOAD-CELL FORCE CALIBRATION
Kenneth W. Yee Apr. 1992 13 p
(PB92-187087; NISTIR-4823) Avail: CASI HC A03/MF A01

The National Institute of Standards and Technology (NIST) has six dead-weight machines (DWMs), used for force calibration up to 4.4 meganewtons (MN), which were all placed in service ca. 1965. More than 20 years later, five of these machines were automated. The authors now automatically apply programmed force values to the strain gauge load cell and record the output using a high precision digital voltmeter, all controlled by a PC-XT class computer. Subsequently, environmental chambers have been added to three machines to perform automatically the type of evaluation testing of load cells used in scales in commerce. GRA

N92-31475# MCR Technology, Inc., Chicago, IL.
HIGH BRIGHTNESS X RAY SOURCE FOR DIRECTED ENERGY AND HOLOGRAPHIC IMAGING APPLICATIONS, PHASE 2
Final Report
Armon McPherson and Charles K. Rhodes 31 Mar. 1992 169 p
(Contract N00014-89-C-2274)
(AD-A248858) Avail: CASI HC A08/MF A02

Advances in x-ray imaging technology and x-ray sources are such that a new technology can be brought to commercialization enabling the three-dimensional (3-D) microvisualization of hydrated biological specimens. The Company is engaged in a program whose main goal is the development of a new technology for direct three dimensional (3-D) x-ray holographic imaging. It is believed that this technology will have a wide range of important applications in the defense, medical, and scientific sectors. For example, in the medical area, it is expected that biomedical science will constitute a very active and substantial market, because the application of physical technologies for the direct visualization of biological entities has had a long and extremely fruitful history. GRA

N92-31502# Brookhaven National Lab., Upton, NY.
THE NSLS 100 ELEMENT SOLID STATE ARRAY DETECTOR
L. R. Furenlid, H. W. Kraner, L. C. Rogers, D. Stephani, R. H. Beuttenmuller, J. Beren, and S. P. Cramer (California Univ., Davis.) 1991 17 p Presented at the 7th National Conference and Exhibition on Synchrotron Radiation Instrumentation, Baton Rouge, LA, 28-31 Oct. 1991
(Contract DE-AC02-76CH-00016)
(DE92-014477; BNL-47475; CONF-9110146-18) Avail: CASI HC A03/MF A01

X-ray absorption studies of dilute samples require fluorescence detection techniques. Since signal-to-noise ratios are governed by the ratio of fluorescent to scattered photons counted by a detector, solid state detectors which can discriminate between fluorescence and scattered photons are the instruments of choice for trace element measurements. Commercially available 13 element Ge array detectors permitting total count rates of less than 500,000 counts per second are now in routine use. Since x-ray absorption beamlines at high brightness synchrotron sources can already illuminate most dilute samples with enough flux to saturate the current generation of solid state detectors, the development of next-generation instruments with significantly higher total count rates is essential. We present the design and current status of the 100 element Si array detector being developed in a collaboration between the NSLS and the Instrumentation Division at Brookhaven National Laboratory. The detecting array consists of a 10 by 10 matrix of 4 mm by 4 mm elements laid out on a single piece of ultra-high purity silicon mounted at the front end of a liquid nitrogen dewar assembly. A matrix of charge sensitive integrating preamplifiers feed signals to an array of shaping amplifiers, single channel analyzers, and scalers. An electronic switch, delay amplifier, linear gate, digital scope, peak sensing A to D converter, and histogramming memory module provide for complete diagnostics and channel calibration. The entire instrument is controlled by a LabView 2 application on a MacII ci; the software also provides full control over beamline hardware and performs the data collection. DOE

N92-31633# National Inst. of Standards and Technology, Gaithersburg, MD. Building and Fire Research Lab.
CALIBRATION AT 24 C OF A HEAT-FLOW-METER APPARATUS HAVING 610 mm SQUARE PLATES
R. R. Zarr and B. A. Licitra May 1991 29 p
(Contract DE-AI01-90CE-21041)
(DE92-015954; NISTIR-4539) Avail: CASI HC A03/MF A01

Results are summarized for 38 individual calibration measurements conducted at 24 C and atmospheric conditions for a heat-flow-meter apparatus having 610 mm square plants. The apparatus was calibrated using a 26.2-mm-thick specimen of fibrous-glass broad having a density of 139 kg/m(exp 3). The specimen was selected from an internal lot (Lot 1970) of Standard Reference Material (SRM) similar to SRMs 1450, 1450a, and 1450b. Values of apparent thermal conductivity were predicted using a regression equation developed for this lot of fibrous-glass insulation. Calibration measurements varied plus or minus 0.4 percent with a small drift of 0.4 percent over 250 days. The apparent thermal conductivity of the calibration specimen was also measured using the National Institute of Standards and Technology's one-metre Line-Heat-Source Guarded Hot Plate. Agreement between measurements of thermal conductivity of the guarded hot plate and predicted values were within +0.2 to -0.3 percent at 24 C. The report describes the heat-flow-meter apparatus and the computer data-acquisition-system used to collect data from the apparatus. DOE

N92-31694# Texas Univ. at Dallas, Richardson. Dept. of Chemistry.
DUAL GATED IMAGING SYSTEM FOR ENHANCED FLUORESCENT DIAGNOSTICS MEASUREMENTS Final Report, 15 May 1991 - 15 Jan. 1992
Lynn A. Melton 13 Mar. 1992 22 p
(Contract DAAL03-91-G-0148)
(AD-A249673; ARO-28890.1-EG-EQ) Avail: CASI HC A03/MF A01

This report describes the purchase specifications and initial use of a dual gated imaging system capable of intensified imaging with gate times as short as 1 nano-sec. The system consists of two primary subsystems: (1) dual fast gated image intensifiers; and (2) a sensitive CCD camera and readout/computer system. With dual images, it is possible to measure the fluorescent lifetimes of the dopant which is the marker for the fuel, fluoranthene, in a two dimensional image, and subsequently to correct the fuel intensity image for oxygen quenching. From the fuel and oxygen images, the equivalence ratio image can be calculated. In initial experiments, the system has been used to capture instantaneous (less than 50 nano-s) equivalence ratio images for gaseous methane jets and for diffusion flames. GRA

N92-31790* National Aeronautics and Space Administration. Marshall Space Flight Center, Huntsville, AL.
HOLLOW FIBER CLINOSTAT FOR SIMULATING MICROGRAVITY IN CELL CULTURE Patent
Percy H. Rhodes, inventor (to NASA), Teresa Y. Miller, inventor (to NASA), and Robert S. Snyder, inventor (to NASA) 14 Apr. 1992 5 p Filed 28 Jul. 1989 Supersedes N89-28793 (27 - 23, p 3294)
(NASA-Case-MFS-28370-1; US-Patent-5,104,802; US-Patent-Appl-SN-386175; US-Patent-Class-435-286; US-Patent-Class-435-311; US-Patent-Class-435-312; Int-Patent-Class-C12M-3/02; Int-Patent-Class-C12M-3/00; Int-Patent-Class-C12M-1/12; Int-Patent-Class-C12M-1/10) Avail: US Patent and Trademark Office

A clinostat for simulating microgravity on cell systems carried in a fiber fixedly mounted in a rotatable culture vessel is disclosed. The clinostat is rotated horizontally along its longitudinal axis to simulate microgravity or vertically as a control response. Cells are injected into the fiber and the ends of the fiber are sealed and secured to spaced end pieces of a fiber holder assembly which consists of the end pieces, a hollow fiber, a culture vessel, and a tension spring with three alignment pins. The tension spring is positioned around the culture vessel with its ends abutting the end pieces for alignment of the spring. After the fiber is secured, the spring is decompressed to maintain tension on the fiber while it is being rotated. This assures that the fiber remains aligned along the axis of rotation. The fiber assembly is placed in the culture vessel and culture medium is added. The culture vessel is then inserted into the rotatable portion of the clinostat and subjected to rotate at selected rpms. The internal diameter of the hollow fiber determines the distance the cells are from the axis of rotation.
Official Gazette of the U.S. Patent and Trademark Office

N92-31794# Naval Medical Research Inst., Bethesda, MD.
A DETECTOR FOR STATIONARY GAS BUBBLES: FEASIBILITY STUDIES Technical Report, Aug. 1989 - Jan. 1991
G. Albin, P. Massell, W. Mints, and J. Himm Apr. 1992 95 p
(NR Proj. MM3-3-P-30)
(AD-A250135; NMRI-92-25) Avail: CASI HC A05/MF A01

Work progresses on developing operating procedures for a system intended to detect stationary gas bubbles of diameters 0.9 to 6 micron using ultrasonic interrogation. The original system has been redesigned and is now configured for menu-driven remote control from a PC. Signal averaging and subtraction of measured background noise are available for the signal/noise (S/N) ratio. The output signal is now a spectrum consisting of the amplitude of the 2nd harmonic distortion component of the output signal versus the frequency of the input signal. For well-characterized physical systems, it should be possible to deduce bubble sizes from this spectrum. Calibration standards, consisting of stable bubbles in the 0.9 to 6 micron size range, have proven difficult to prepare. The reason for this difficulty is that size changes in such small spherical bubbles usually are fast relative to the measurement time, as has been studied using a mathematical simulation. Nonetheless, work will now proceed without calibration, using less well-defined bubble populations to test the system's ability to detect bubbles categorically (i.e., 'bubbles' or 'no bubbles'). To predict the S/N ratio for single bubbles in water, we have used mathematical simulations of vibrating bubbles in conjunction with measurements of the system noise. GRA

N92-31828# Nebraska Univ., Lincoln. Dept. of Chemistry.
HOLOGRAPHIC GRATING RELAXATION AND PHOTON CORRELATION SPECTROSCOPIC STUDIES OF VISCOELASTIC LIQUIDS ABOVE THE GLASS TRANSITION
C. H. Wang and S. S. Gong 1 Jun. 1992 5 p
(Contract N00014-90-J-1494)
(AD-A252485; TR-12) Avail: CASI HC A02/MF A01

Photon correlation spectroscopic (PCS) and holographic grating relaxation (HGR) techniques are used to measure the dynamics of density fluctuations in liquid orthoterphenyl, salol, and poly(propylene glycol) oligomers in both the normal and supercooled liquid regimes down to their glass transition temperatures. In the PCS study, a strongly temperature dependent nonhydrodynamic mode due to structural relaxation is observed in each of the above mentioned glass forming liquid. The shape of the nonhydrodynamic mode is nonexponential and can be fit to a stretch exponential function for each liquid. The nonhydrodynamic mode measured in PCS is shown to be the dynamic longitudinal compliance of the liquid. The tracer diffusion coefficients of camphorquinone in the above glass forming liquids do not obey the Stokes-Einstein equation. The slowness of the structural relaxation of the host liquid and the finite size of the tracer are identified to be the cause for the departure from the Stokes Einstein equation. GRA

N92-31909# Lawrence Livermore National Lab., CA.
DISPERSIVE-INFRARED GAS SENSOR SYSTEM DESIGN AND OPERATION MANUAL
T. J. Kulp, T. G. McRae, R. Kennedy, and D. Garvis Oct. 1991 127 p
(Contract W-7405-eng-48)
(DE92-011766; UCRL-CR-103698) Avail: CASI HC A07/MF A02

The objective of this project was to develop nondispersive infrared (IR) gas sensor capable of detecting and quantifying gaseous HCl emitted during the launch of rockets using solid propellants. To satisfy the practical requirements of this application, the sensor must be capable of unmanned field operation, remotely addressable, field calibratable, and able to measure low concentrations (1 ppm) of HCl at relatively rapid rates. DOE

N92-31919# Michigan Univ., Ann Arbor. Dept. of Nuclear Engineering.
DEVELOPMENT OF GAMMA RAY IMAGING CAMERAS
D. K. Wehe and G. F. Knoll 28 May 1992 31 p
(Contract DE-FG02-90ER-12932)
(DE92-015305; DOE/ER-12932/2) Avail: CASI HC A03/MF A01

In January 1990, the Department of Energy initiated this project with the objective to develop the technology for general purpose, portable gamma ray imaging cameras useful to the nuclear industry. The ultimate goal of this R&D initiative is to develop the analog to the color television camera where the camera would respond to gamma rays instead of visible photons. The two-dimensional real-time image would be displayed and indicate the geometric location of the radiation relative to the camera's orientation, while the brightness and 'color' would indicate the intensity and energy of the radiation and, hence, identify the emitting isotope. There is a strong motivation for developing such a device for applications within the nuclear industry, for both high- and low-level waste

repositories, for environmental restoration problems, and for space and fusion applications. At present, there are no general purpose radiation cameras capable of producing spectral images for such practical applications. At the time of this writing, work on this project has been underway for almost 18 months. Substantial progress has been made in the project's two primary areas: mechanically-collimated (MCC) and electronically-collimated camera (ECC) designs. We present developments covering the mechanically-collimated design, and then discuss the efforts on the electronically-collimated camera. The renewal proposal addresses the continuing R&D efforts for the third year effort. DOE

N92-32086# Oak Ridge National Lab., TN.
INCOHERENCE EFFECTS IN REFLECTION ELECTRON MICROSCOPY
A. Howie (Cambridge Univ., England), M. Y. Lanzerotti (Cambridge Univ., England), and Z. L. Wang 1992 8 p Presented at the 5th Asia-Pacific Electron Microscopy Conference, Beijing (China), 1-6 Aug. 1992
(Contract DE-AC05-84OR-21400)
(DE92-016161; CONF-920891-2) Avail: CASI HC A02/MF A01

The phase contrast imaging of surface steps in reflection electron microscopy is analyzed. It is shown that the typical images are seriously affected by incoherence effects and that this arises, not from the strong inelastic scattering which is often present, but from the effective angular spread in the illumination which is frequently determined by the width of the Bragg reflection. DOE

N92-32128*# Allied-Signal Aerospace Co., Teterboro, NJ. Guidance Systems Div.
RL-34 RING LASER GYRO LABORATORY EVALUATION FOR THE DEEP SPACE NETWORK ANTENNA APPLICATION
28 Nov. 1991 147 p
(Contract JPL-959072)
(NASA-CR-190481; JPR-9950-1368; NAS 1.26:190481) Avail: CASI HC A07/MF A02

The overall results of this laboratory evaluation are quite encouraging. The gyro data is in good agreement with the system's overall pointing performance, which is quite close to the technical objectives for the Deep Space Network (DSN) application. The system can be calibrated to the levels required for millidegree levels of pointing performance, and initialization performance is within the required 0.001 degree objective. The blind target acquisition performance is within a factor of two of the 0.0001 degree objective, limited only by a combination of the slow rate (0.5 deg/sec) and the existing production quantization logic (0.38 arc-sec/pulse). Logic circuitry exists to better this performance such that it will better the objective by 50 percent. Representative data with this circuitry has been provided for illustration. Target tracking performance is about twice the one millidegree objective, with several factors contributing. The first factor is the bias stability of the gyros, which is exceptional, but will limit performance to the 0.001 and 0.002 degree range for long tracking periods. The second contributing factor is the accelerometer contributions when the system is elevated. These degrade performance into the 0.003 to 0.004 degree range, which could be improved upon with some additional changes. Finally, we have provided a set of recommendations to improve performance closer to the technical objectives. These recommendations include gyro, electronics, and system configurational changes that form the basis for additional work to achieve the desired performance. In conclusion, we believe that the RL-34 ring laser gyro-based advanced navigation system demonstrated performance consistent with expectations and technical objectives, and it has the potential for even further enhancement for the DSN application. Author

N92-32138# EG and G Rocky Flats, Inc., Golden, CO.
IMPROVEMENTS TO THE ROCKY FLATS METROLOGY LABORATORIES VELOCITY METER CALIBRATION SYSTEM
K. R. Abercrombie 12 Mar. 1992 16 p
(Contract DE-AC34-90DP-62349)
(DE92-013162; RFP-4529) Avail: CASI HC A03/MF A01

The Rocky Flats Standards Laboratory has undertaken a project to improve calibration of air velocity meters by reducing the uncertainty of the Velocity Meter Calibration System. The project was accomplished by analyzing the governing equation in order to determine which areas within the system contributed most to the overall system uncertainty. Then, based upon this new analysis, new components were selected to replace the components identified in the analysis. Finally, the system was re-evaluated to determine the new systematic uncertainty for the system. DOE

N92-32174# Sandia National Labs., Albuquerque, NM.
DEVICE FOR MONITORING THE THICKNESS OF A DIELECTRIC COATING ON A DIELECTRIC SUBSTRATE
Yu. A. Skripnik (Kiev Technological Inst. of Light Industry, USSR), A. N. Dykov (Kiev Technological Inst. of Light Industry, USSR), and N. M. Sviridov (Kiev Technological Inst. of Light Industry, USSR) Mar. 1992 7 p Transl. into ENGLISH of Russian Patent Application No. SU-1186935 (23 Oct. 1985) 3 p
(Contract DE-AC04-76DP-00789)
(DE92-014741; ALS/TR-92-008) Avail: CASI HC A02/MF A01

This invention is comprised of a device for monitoring the thickness of a dielectric coating on a dielectric substrate, comprising a capacitive sensor in the form of a dielectric substrate on which are mounted a high-potential and low-potential electrode, made in the form of coplanar, concentric rings. An additional electrode is located in such fashion that the initial capacitances between the high-potential electrode and the additional electrodes and between the additional electrode and the low-potential electrode are equal. Additional components are a switch whose middle contact is connected with the additional electrode, and the edge contacts are connected with high-potential and low-potential electrodes, a high-frequency generator, a bridge circuit connected to said generator, and a recorder. The invention may be used to monitor the thickness of a dielectric coating applied to a dielectric substrate, for example paint and polymer coatings on leather and textiles. The goal of the invention is to increase measurement accuracy. DOE

N92-32218# Defence Research Establishment Valcartier (Quebec).
ABSOLUTE CALIBRATION OF THE FOURIER INTERFEROMETRIC TRANSMISSOMETER
J.-M. Theriault and P. L. Roney Apr. 1988 29 p
(DREV-R-4511/88; CTN-92-60343) Avail: CASI HC A03/MF A01

The design and the ultimate performance of many electro-optical systems can be strongly affected by atmospheric conditions. It is often difficult to decide which atmospheric transmission model is the most appropriate or accurate in obtaining estimates of the performance of active and passive systems. In order to be able to make a quantitative evaluation of the accuracy and applicability of models, it is necessary to have a data bank of accurate measurements of high spectral resolution transmission at long paths and over a wide range of atmospheric conditions. Defence Research Establishment Valcartier (DREV) has set up a 5.7-km transmission range which includes a high-resolution Fourier transform spectrometer system and an infrared source which will be used to measure atmospheric transmittance. This report presents a detailed analysis of the method used to calibrate the Fourier Interferometric Transmissometer (FIT). Derivation of the calibration equation is based on a fundamental relation of radiometry, the radiance conservation law prime N = TN. Thus, the calibrated spectrum of atmospheric transmission is simply determined by obtaining the ratio of a source signal to a local reference signal and then correcting it by the calibration factor. In addition, this report discusses an experimental procedure to evaluate the quality of collimating systems used as a source in transmissometers. CISTI

N92-31875# Rafael Armament Development Authority, Haifa (Israel).
AN INNOVATIVE TWO AXIS RATE GYRO: THEORY AND PRINCIPLES OF OPERATION

J. Rosenberg, E. Netzer, P. Bar-Avi, and I. Porat *In* Israel Society of Aeronautics and Astronautics, 31st Israel Annual Conference on Aviation and Astronautics 22 Feb. 1990 p 89-91 Previously announced in IAA as A91-43089 (For primary document see N92-31861 22-01)
Avail: CASI HC A01/MF A03

36 LASERS AND MASERS

Includes parametric amplifiers.
For related information see also *76 Solid-State Physics.*

N92-31319# Xerox Palo Alto Research Center, CA.
PULSED LASER DEPOSITION OF HIGH Tc SUPERCONDUCTING THIN FILMS Final Report
J. B. Boyce and G. A. Connell 15 Apr. 1992 159 p
(Contract F49620-90-C-0069)
(AD-A250657; AFOSR-92-0345TR) Avail: CASI HC A08/MF A02

Superconducting thin films have been deposited in-situ on several substrate materials using pulsed excimer laser deposition. The major accomplishments were in four separate areas: (1) We were the first to grow excellent quality YBa2Cu3O7 on Si and on silicon-on-sapphire. The quality of these films has enabled several applications and other studies to be realized. These include infrared detectors and superconducting metal-insulator-semiconductor structures, as well as flux motion studies. (2) We were the first to grow excellent quality YBCO on GaAs. This success allows superconductors to be combined with high-speed GaAs for future device applications. (3) We were the first to grow a-axis oriented YBCO films using monolayer buffers of PrO2. This structural orientation favors technical applications, such as, Josephson devices or tunnel junctions. (4) We were the first to observe an extreme sensitivity of T sub c to cool-down rate for epitaxial Fe-doped YBCO films. These results not only may yield information on the role of the Cu-O chains and planes in the superconductivity of this material but also may lead to procedures to increase the flux pinning. GRA

N92-31411# Texas Univ., Austin. Inst. for Fusion Studies.
AMPLIFICATION MECHANISM OF ION-RIPPLE LASERS AND ITS POSSIBLE APPLICATION
K. R. Chen and J. M. Dawson (California Univ., Los Angeles.) May 1992 16 p
(Contracts DE-FG05-80ET-53088; DE-FG03-86ER-53225)
(DE92-016155; DOE/ET-53088/554; IFSR-554) Avail: CASI HC A03/MF A01

The IRL is an advanced scheme for generating coherent high-power radiation, in which a relativistic electron beam propagates obliquely through an ion ripple in a plasma. Its amplification mechanism is described by a low gain theory while the linear growth rate is given by the dispersion relation. The efficiency of the lasing is determined by the nonlinear saturation mechanism discussed. By proper choice of device parameters, sources of microwaves, optical, and perhaps even x-rays can be made. The availability of tunable sources for wide wavelength regimes, coherence and high-power, as well as lower cost and simplicity of equipment are emphasized. DOE

N92-31605# Air Force Inst. of Tech., Wright-Patterson AFB, OH.
STUDIES IN DYNAMIC CHARACTERIZATION AND CONTROL OF A FLEXIBLE STRUCTURE AND OPTICAL BEAMPATH M.S. Thesis
Marcus R. Schulthess 1991 106 p
(AD-A250555; AFIT/CI/CIA-91-130) Avail: CASI HC A06/MF A02

The dynamic characterization and control of a flexible structure and optical beampath is explored. The experiment is motivated by the expanding demand for structurally mounted space based laser pointing and tracking systems. The setup of the cantilevered UWAA planar truss is based on a similar setup at the Air Force Academy. An existing finite element model is modified to reflect the characteristics of the UWAA truss and experimentally validated. A reduced order truss model suitable for simulation is developed and validated with the hardware. The formulation of linear and nonlinear models for the AJT and tilting mirror actuators are explored. The design and implementation of the mirror and structural control is manifested in the form of proportional-integral (PI) feedback to a tilting control mirror to actively reject line of sight disturbances and velocity feedback to on-off AJT actuators to supress large amplitude low frequency lateral structural vibrations. Good line of sight disturbance rejection is demonstrated for the first four lateral modes of the flexible truss structure. The AJT velocity feedback controller was used to supress large amplitude low frequency oscillations to bring structural vibrational motions to within limited range of the tilting mirror platform. A baseline theoretical model of the reduced order truss and control actuators was constructed in SIMULAB and thoroughly validated. GRA

N92-31684# Argonne National Lab., IL.
ELEMENTARY REACTION RATE MEASUREMENTS AT HIGH TEMPERATURES BY TUNABLE-LASER FLASH-ABSORPTION
J. P. Hessler 20 Mar. 1992 5 p Presented at the DOE Combustion Contractors Meeting, Tahoe City, CA, 15-17 Jun. 1992
(Contract W-31-109-eng-38)
(DE92-015269; ANL/CP-75935; CONF-9206180-3) Avail: CASI HC A01/MF A01

The major objective of this program is to measure thermal rate coefficients and branching ratios of elementary reactions. To perform these measurements, we have constructed an ultrahigh-purity shock tube to generate temperatures between 1000 and 5500 K. The tunable-laser flash-absorption technique is used to measure the rate of change of the concentration of species which absorb below 50,000 cm(exp -1) e.g.: OH, CH, and CH3. This technique is being extended into the vacuum-ultraviolet spectral region where we can measure atomic species (H, D, C, O, and N) and diatomic species (O2, CO, and OH). DOE

N92-31698# Laboratoire d'Automatique et d'Analyse des Systemes, Toulouse (France).
PHASE-LOCKED ARRAYS OF ANTIGUIDED DIODE LASERS: MODELLING, DESIGN, EVALUATION OF PERFORMANCE LIMITS Ph.D. Thesis - Toulouse Univ. [RESEAU DE DIODES LASER A ANTIGUIDES: MODELISATION, CONCEPTION, EVALUATION DES LIMITES DE PERFORMANCES]
Muriel Reglat 1992 123 p In FRENCH
(LAAS-92034; ETN-92-91685) Avail: CASI HC A06/MF A02

The modal behavior of gallium arsenide/aluminum gallium arsenide (GaAs/AlGaAs) phase locked arrays of antiguided diode lasers and a method for designing these kind of devices are considered. Both complex refractive index method and effective index method are used to develop a methodology to analyze material modes with the aim of bringing out criteria of an in-phase mode operation. This type of component presents a specific mode operation: the resonance of its in-phase mode which, after a systematic study of parameters of different kinds of arrays, appears to be the best situation to achieve coherent and power light sources. A method of design of such phase locked arrays of antiguided diode lasers is established. ESA

N92-31755# Textron Defense Systems, Everett, MA.
CO2 LASER FREQUENCY MULTIPLICATION
Mar. 1992 2 p
(Contract N00014-91-C-2279)
(AD-A248574) Avail: CASI HC A01/MF A01

The duration of the mode-locked CO2 laser pulses was measured to be 0.9 + or - nsec by the technique of second harmonic autocorrelation. Knowing the pulse duration, the spot size, and the harmonic conversion efficiency, a detailed fit of experiment to theory gave an estimate of the nonlinear coefficient of AgGaSe2, d36 = 31 + or - V(1), in agreement with the most accurate literature values. A number of experiments were made

with longer pulse trains in which the highest harmonic energy conversion reached 78 percent. The damage threshold was measured, and it turned out to be related much more strongly to fluence than intensity. The shorter pulse trains had peak intensities of close to 300 MW 1/cm squared, whereas the longer trains (3 usec) had intensities up to 40 MW 1/cm squared. GRA

N92-31762# Edgerton, Germeshausen and Grier, Inc., Idaho Falls, ID.
APPLICATION OF REACTOR-PUMPED LASERS TO POWER BEAMING
T. E. Repetti Oct. 1991 20 p
(Contract DE-AC07-76ID-01570)
(DE92-012370; EGG-PHY-9978) Avail: CASI HC A03/MF A01

Power beaming is the concept of centralized power generation and distribution to remote users via energy beams such as microwaves or laser beams. The power beaming community is presently performing technical evaluations of available lasers as part of the design process for developing terrestrial and space-based power beaming systems. This report describes the suitability of employing a nuclear reactor-pumped laser in a power beaming system. Although there are several technical issues to be resolved, the power beaming community currently believes that the AlGaAs solid-state laser is the primary candidate for power beaming because that laser meets the many design criteria for such a system and integrates well with the GaAs photodiode receiver array. After reviewing the history and physics of reactor-pumped lasers, the advantages of these lasers for power beaming are discussed, along with several technical issues which are currently facing reactor-pumped laser research. The overriding conclusion is that reactor-pumped laser technology is not presently developed to the point of being technically or economically competitive with more mature solid-state technologies for application to power beaming. DOE

N92-31769# Maryland Univ., College Park.
MICROWAVE GENERATION FOR MAGNETIC FUSION ENERGY APPLICATIONS
T. M. Antonsen, Jr., W. W. Destler, V. L. Granatstein, and B. Levush Jan. 1992 45 p
(Contract DE-FG05-87ER-52147)
(DE92-011424; DOE/ER-52147/5) Avail: CASI HC A03/MF A01

This progress report encompasses work on two separate projects, both related to developing sources for electron cyclotron resonance heating of magnetic fusion plasmas. The report is therefore divided into two parts as follows: free electron laser with small period wigglers; and theory and modeling of high frequency, high power gryotron operation. Task A is experimental and eventually aims at developing continuously tunable, CW sources for ECRH with power per unit as high as 5 megawatts. Task B provides gryotron theory and modeling in support of the gryotron development programs at MIT and Varian. DOE

N92-31775# Ames Lab., IA.
LASER DECONTAMINATION: A NEW STRATEGY FOR FACILITY DECOMMISSIONING
H. M. Pang, R. J. Lipert, Y. M. Hamrick, S. Bayrakal, K. Gaul, B. Davis, D. P. Baldwin, and M. C. Edelson 1992 7 p Presented at the Spectrum 1992: Nuclear and Hazardous Waste Management International Topical Meeting, Boise, ID, 23-27 Aug. 1992
(Contract W-7405-eng-82)
(DE92-014113; IS-M-709; CONF-920851-12) Avail: CASI HC A02/MF A01

Lasers can be employed to remove both surface and bulk contamination from metals. Experiments demonstrate that approximately 5 microns can be removed from an Al surface by one powerful laser pulse. Focusing with cylindrical lenses is shown to result in good surface coverage and reduced surface redeposition. High-resolution laser spectroscopy in a small atomic beam device is demonstrated and discussions of bulk decontamination by AVLIS-like methods are described. A plan for estimating the cost-effectiveness of laser decontamination technology is discussed. DOE

N92-31788* National Aeronautics and Space Administration. Langley Research Center, Hampton, VA.
METHOD AND CIRCUIT FOR CONTROLLING THE EVOLUTION TIME INTERVAL OF A LASER OUTPUT PULSE Patent
Norman P. Barnes, inventor (to NASA) 7 Jul. 1992 6 p Filed 31 May 1989 Supersedes N89-28816 (27 - 23, p 3298)
(NASA-Case-LAR-13772-1; US-Patent-5,128,949;
US-Patent-Appl-SN-359460; US-Patent-Class-372-25;
US-Patent-Class-372-30; Int-Patent-Class-H01S-3/10) Avail: US Patent and Trademark Office

The invention is a method and circuit for controlling the evolution time interval of a laser output pulse used for making precise spectral measurements. It comprises the means for pumping a laser medium in a resonator that includes a Q-switch and polarizer that act in combination to control the loss in the resonator. A photodiode senses the resulting fluorescence which is applied to a two level Q-switch and polarizer from high to intermediate to substantially zero loss states to control the evolution time interval of the resulting laser output pulse.
Official Gazette of the U.S. Patent and Trademark Office

N92-31798# Columbia Univ., New York, NY.
LASER ENHANCED CHEMICAL REACTION STUDIES
1992 6 p
(Contract DE-FG02-88ER-13937)
(DE92-010772; DOE/ER-13937/4) Avail: CASI HC A02/MF A01

Experimental studies of dynamic molecular processes are described with particular emphasis on the use of a powerful infrared diode laser probe technique developed in our laboratory. This technique allows us to determine the final states of CO2 (and other molecules) produced by collisions, photofragmentation, or chemical reactions with a spectral resolution of 0.0003 cm(exp -1) and a time resolution of 10(exp -7) sec. Such high spectral resolution provides a detailed picture of the vibrational and rotational states of molecules produced by these dynamic events. We have used this experimental method to probe collisions between hot hydrogen/deuterium atoms and CO2, between O((exp 1)D) atoms and CO2, to study the final states of DC1 molecules produced as a result of the reactions of hot Cl atoms, and to investigate the dynamics of the reaction between OH and CO molecules. Advances in our techniques over the past two years have allowed us to identify and study more than 200 final rotational states in ten different vibrational levels of CO2 encompassing all three normal modes, many overtones, and combination states of the molecule. We have extended the technique to probe a variety of new molecules such as OCS, N2O, DCl, and CS2. All of this work is aimed at providing experimental tests for polyatomic molecule potential energy surfaces, chemical transition states in complex systems, and theories of reaction dynamic in molecules with more than three atoms. DOE

N92-31802# New Mexico Univ., Albuquerque. Center for High Technology Materials.
LASER MATERIAL INTERACTIONS Annual Technical Report, period ending 15 Apr. 1991
S. R. Brueck 13 Apr. 1992 36 p
(Grant AF-AFOSR-0337-89)
(AD-A250028; AFOSR-92-0312TR) Avail: CASI HC A03/MF A01

The Laser-Materials Interaction Laboratory at the Center for High Technology Materials at the University of New Mexico, which is devoted to a broad range of laser spectroscopic probes of semiconductor and nonlinear materials, fabrication processes, and opto-electronic devices, carries out much of this work in conjunction with the Opto-electronics Research Center Program, also funded by AFOSR. During the period of this report significant progress was made in a number of areas, including ultrafast operation of optically pumped resonant periodic-gain GaAs surface-emitting

lasers, grating coupling to surface-plasma waves, and high-speed Si Schottky photodiodes. GRA

N92-31902# Lawrence Livermore National Lab., CA.
HIGH PERFORMANCE OF COPPER PUMPED DYE LASERS
R. P. Hackel 1 Feb. 1992 10 p Presented at the Lasers 1991, San Diego, CA, 8-13 Dec. 1991
(Contract W-7405-eng-48)
(DE92-011763; UCRL-JC-108146; CONF-911296-9) Avail: CASI HC A02/MF A01

Narrowband, spectrally formatted and near diffraction limited light from dye master-oscillator-power amplifier chains pumped by copper lasers support several missions including Atomic Vapor Laser Isotope Separation, laser guide star experiments and laser materials processing studies. DOE

N92-31935# Maryland Univ., College Park. Lab. for Plasma Research.
MILLIMETER WAVE FREE ELECTRON LASER AMPLIFIERS: EXPERIMENTS AND DESIGNS
S. W. Bidwell, Z. X. Zhang, T. M. Antonsen, Jr., D. M. Bensen, W. W. Destler, V. L. Granatstein, P. E. Lantham, B. Levush, J. Rodgers, and H. P. Freund et al 1991 3 p Presented at the 16th International Conference on Infrared and Millimeter Waves, Lausanne, Switzerland, 26-30 Aug. 1991
(Contract DE-FG05-87ER-52147)
(DE92-011813; CONF-9108146-2) Avail: CASI HC A01/MF A01

Free electron laser amplifiers are investigated as sources of high average-power (1 MW) millimeter to submillimeter wave radiation (200-600 GHz) for application to electron cyclotron resonance heating of magnetically confined fusion plasmas. As a stepping-stone to higher frequencies and cw operation a pulsed amplifier ((tau)(sub pulse) approx. equal to 80 nano-s) at 98 GHz is being developed. Status is reported on this experiment which investigates linear gain amplification with use of sheet electron beam (transverse cross section = 0.1 x 2.0 cm, V(sub beam) = 440 keV, I(sub beam) approx. equal to 10 A) and short-period wiggler ((ell)(sub w) = 0.96 cm) and with expected output of 140 W. Predictions of gain and efficiency from a 1-D universal formulation are presented. Beam propagation results, with wiggler focusing as a means of sheet beam confinement in both transverse dimensions, through the 54 cm (56 period) pulsed electromagnet wiggler are discussed. Peak wiggler fields of 5.1 kG on-axis have been achieved. DOE

N92-32042# Massachusetts Inst. of Tech., Cambridge. Research Lab. of Electronics.
FEMTOSECOND PHOTONICS: FUNDAMENTAL PHENOMENA AND DEVICE BEHAVIOR Final Report, 1 Aug. 1988 - 31 Jul. 1991
E. P. Ippen, J. G. Fujimoto, and H. A. Haus 10 Feb. 1992 24 p
(Contract F49620-88-C-0089)
(AD-A250506; AFOSR-92-0282TR) Avail: CASI HC A03/MF A01

This report describes a number of different research projects carried out under this contract. Emphasis is placed on progress made during the third and final year, but a listing of publications and reports covering all three years of the contract is attached. Titles of the individual projects include: Picosecond Optical Switching, Additive Pulse Modelocking in Diode Pumped Nd:YAG and YLF, Multistage High Repetition Rate Femtosecond Amplifiers, Control and Spontaneous Emission with Semi-conductor Microcavities, Carrier Dynamics in Metals and Semiconductors, Time Domain Interferometry, Nonlinear Dynamics in Active Semiconductor Devices, Four Wave Mixing and Information in Photorefractive Crystals, and Impulsive Excitation of Coherent Phonons. Author (GRA)

N92-32061# Naval Postgraduate School, Monterey, CA.
THEORY FOR THE CEBAF INFRARED AND SHIPBOARD FELS M.S. Thesis
Darwin L. Clark Mar. 1992 80 p
(AD-A252174) Avail: CASI HC A05/MF A01

The continuing development of the free electron laser (FEL), as a powerful and versatile source of coherent radiation, steadily drives toward the goal of high efficiency and broad tunability at shorter wavelengths. New experiments provide significant data and insight for analysis by theoreticians and experimentalists. Two important areas of study are short electron pulse effects, and the dynamics of optical mode distortion by intense beam currents. The initial part of this thesis examines one aspect of the projected task of FEL application as a military weapon. The advantages of the FEL over other directed energy sources are detailed, as well as the challenge presented by the effects of the marine atmosphere to high energy laser propagation. The remainder of this thesis examines several effects of long wavelength FELS. Chapter IV examines the proposed parameters of the CE-OAF IR FEL, and the analysis leads to predictions describing system performance. Chapter V examines the effects of single pass optical mode distortion for FELs with narrow electron beams. Single-mode theory states that gain is proportional to the product of electron beam current and filling factor, but three dimensional simulations show that gain is a function of electron beam-filling factor alone. Also examined is a phenomenon of destructive interference of light in the FEL modulator. GRA

37 MECHANICAL ENGINEERING

Includes auxiliary systems (nonpower); machine elements and processes; and mechanical equipment.

N92-31271 Department of the Navy, Washington, DC.
REPLACEABLE VALVE SEAT Patent
Raymond W. Jordan, inventor (to Navy) 14 Jan. 1992 5 p Filed 25 Apr. 1991
(AD-D015250; US-Patent-5,080,120; US-Patent-Appl-SN-691287; US-Patent-Class-137-1) Avail: US Patent and Trademark Office

A valve with an O-ring, a disk seal, and a replaceable valve seat is presented. A groove in the bottom on the valve seat flange forms an inner and outer drip ledge with the inner and outer periphery of the flange. If leakage occurs at the valve seat O-ring, fluid droplets will form on the out drip ledge. If leakage occurs at the disk seal, fluid droplets will form on the inner drip ledge. A visual inspection of these drip ledges through an access port, or by a borescope placed in an inspection port, can discriminate between a leak which originates in the O-ring and a leak which originates in the disk seal. When conventional replaceable valve seats leak, fluid droplets form at the bottom on the valve seat. In the present invention, such a valve seat is modified by machining a groove on the bottom surface of the valve seat flange. This groove and the inner and outer surfaces of the flange intersect and form drip ledges. If leakage occurs at the valve seat seal, shown as an O-ring in the preferred embodiment, fluid droplets will form on the outer drip ledge. If leakage occurs at the valve disk seal, fluid droplets will form on the inner drip ledge. The drip ledges can be inspected either through an access port or by passing a borescope through a small inspection port in the valve case. Visual inspection of the bottom on the drip ledge will positively identify the required repair action. GRA

N92-31349*# National Aeronautics and Space Administration. Lewis Research Center, Cleveland, OH.
EXPERIMENTAL TESTING OF PROTOTYPE FACE GEARS FOR HELICOPTER TRANSMISSIONS
R. Handschuh, D. Lewicki, and R. Bossler (Lucas Western, Inc., City of Industry, CA.) 1992 15 p Proposed for presentation at the Gearbox Configurations of the 1990's, Solihull, England, 28 Oct. 1992; sponsored by Inst. of Mechanical Engineers Prepared in cooperation with Army Aviation Systems Command, Cleveland, OH

(RTOP 505-63-36; DA Proj. 1L1-62211-A-47-A)
(NASA-TM-105434; E-7084; NAS 1.15:105434; AVSCOM-TR-92-C-008) Avail: CASI HC A03/MF A01

An experimental program to test the feasibility of using face gears in a high-speed and high-power environment was conducted. Four face gear sets were tested, two sets at a time, in a closed-loop test stand at pinion rotational speeds to 19,100 rpm and to 271 kW. The test gear sets were one-half scale of the helicopter design gear set. Testing the gears at one-eighth power, the test gear set had slightly increased bending and compressive stresses when compared to the full scale design. The tests were performed in the LeRC spiral bevel gear test facility. All four sets of gears successfully ran at 100 percent of design torque and speed for 30 million pinion cycles, and two sets successfully ran at 200 percent of torque for an additional 30 million pinion cycles. The results, although limited, demonstrated the feasibility of using face gears for high-speed, high-load applications. Author

N92-31363# Connecticut Univ., Storrs.
TRIBOLOGY OF LANGMUIR-BLODGETT FILMS Interim Report
C. L. Mirley and J. T. Koberstein Mar. 1992 29 p
(Contract DAAL03-91-G-0139)
(AD-A250075; TR-1; ARO-27863.1-MS) Avail: CASI HC A03/MF A01

This report reviews some of the current theories of lubrication, friction and wear, and how these effects are measured. Special emphasis is placed on polymeric systems and the use of Langmuir-Blodgett films as lubricants. GRA

N92-31384# Oak Ridge National Lab., TN.
EVALUATION OF PROPOSED INSERVICE TESTING PROCEDURES FOR CHECK VALVES
J. C. Moyers and D. A. Casada 1992 19 p Presented at the Symposium on Testing of Pumps and Valves in Nuclear Power Plants, Washington, DC, 21-23 Jul. 1992
(Contract DE-AC05-84OR-21400)
(DE92-014502; CONF-920732-4) Avail: CASI HC A03/MF A01

The results of an evaluation of proposed inservice testing procedures intended to provide full-stroke exercising of two sets of check valves in a PWR plant is presented. One set consists of three valves in the three parallel combined high and low head cold leg safety injection lines. The other set consists of valves installed in the safety injection accumulator discharge lines. The proposed acceptance criteria for the parallel-line valves was based on total flow and pressure drop determination for the three-line system proving that each line is functioning satisfactorily. The proposed acceptance criteria for the accumulator discharge valves is based on the valve flow rate as determined by two methods, the rate of accumulator pressure decay and the rate of pressurizer level change. The conclusions of the evaluation are that full stroking is not positively demonstrated for either set of valves, that total system flow/pressure drop is an insensitive indicator of flow through each of the parallel lines, and that temperature transients during accumulator blowdown testing should be evaluated for potential structural damage. DOE

N92-31433# Connecticut Univ., Storrs.
TRIBOLOGY OF FUNCTIONALLY-TERMINATED OLIGOMER FILMS Interim Report
C. L. Mirley and J. T. Koberstein 18 Mar. 1992 16 p
(Contract DAAL03-91-G-0139)
(AD-A250076; TR-2; ARO-27863.2-MS) Avail: CASI HC A03/MF A01

A research outline is described in a dissertation prospectus. An investigation into the applicability of Langmuir-Blodgett films of functionally terminated oligomers as specialized lubricants is proposed. GRA

N92-31437# Martin Marietta Labs., Baltimore, MD.
SURFACE ANALYSIS OF STAINLESS STEEL OUTER RACE BEARING SPECIMENS Final Report
D. K. Schaffer and H. M. Hand Oct. 1991 36 p
(Contract N62269-90-M-7269)
(AD-A250088; MML-TR-91-16c; NADC-91093-60) Avail: CASI HC A03/MF A01

The results of analysis of R-4 stainless steel instrument bearings, subjected to various wear cycles, are reported to describe the fate of a synthetic Schiff base lubricant additive at the bearing wear track surfaces. The surfaces were monitored by x-ray, photoelectron spectroscopy (XPS), and Fourier infrared (FTIR) spectroscopy to characterize all lubricant (and grease) species of interest. The data indicate a general modification or degradation of both the lubricant and ubiquitous fluorinated grease ('Kryto-x') additive during the wear stages. Chemical and structural compositions are described for residual derivatives at the bearing track surfaces. Further studies are recommended that will enable confirmation of both the chemical fate and the molecular mechanism of lubricant additives candidates. GRA

N92-31460# Air Force Academy, CO. Dept. of Mathematics.
BUILDING AN EDUCATIONAL ROBOT ARM FOR UNDER $1,000 Final Report
Kenneth A. Lillie 20 Feb. 1992 22 p
(AD-A247499; USAFA-TR-92-1) Avail: CASI HC A03/MF A01

Undergraduate research in robotics has blossomed in the last decade, primarily because of the wide diversity of disciplines involved, such as mathematics, computer science, electrical and mechanical engineering. The colleges and universities that have the best robotics programs have the largest budgets. Typical educational robots cost from $3,000 to $10,000. This particular project is specially aimed at producing an educational robot structural design for under $1,000, thereby making robotic research more accessible to the smaller schools. Foremost in the high-level design philosophy was the idea of making the architecture as open as possible--providing the widest possible dissemination of information. Secondly, the building materials had to be easily acquired within the continental United States, preferably by mail order or local purchase. The preliminary design included choosing the structural materials. A decision to use plastic for arm construction resulted from an appropriate trade-off study. Next, the most logical actuators were chosen, based on speed, size, and type. The detailed design included making specific choices for building materials, specific motors/gears, dimensions, range of motions, and end-effector design. GRA

N92-31469# National Research Council of Canada, Ottawa (Ontario). Engine Lab.
A PRELIMINARY STUDY IN THE USE OF PHASE DEMODULATION TECHNIQUES FOR THE ANALYSIS OF GEAR VIBRATION DATA [ETUDE PRELIMINAIRE SUR L'UTILISATION DE TECHNIQUES DE DEMODULATION DE PHASE POUR L'ANALYSE DES DONNEES VIBRATOIRES DES ENGRENAGES]
J. Nicks and G. Krishnappa Oct. 1990 52 p
(NRC-32083; NRC-TR-ENG-005; CTN-92-60310) Avail: CASI HC A04/MF A01

The assessment of component health by vibration analysis is an integral part of monitoring of gas turbine engines. This report presents a preliminary study of a vibration analysis method for the early detection of gear tooth damage. Using a phase demodulation technique, the condition of a gear based on the characteristics of the phase component of the vibration signal is evaluated. Vibration data from both a high-speed test rig and from a commercial aero-engine gearbox were examined. Preliminary results indicate that phase modulation analysis can provide very early and reliable detection of faults in gears. It is important that the analysis procedure be performed on a gear when it is in good condition to establish an acceptable baseline. Any mesh harmonic may be demodulated about, providing that stable baseline analysis results can be obtained. This analysis method appears to be more suited for trend monitoring, to obtain the earliest possible fault warning, rather than single-shot assessment. It is shown that kurtosis is not a reliable analysis parameter for use with phase demodulation. Combining the percent modulation of the unwrapped

phase function with the maximum kurtosis of the wrapped and unwrapped phase function resulted in more reliable diagnosis of faults. CISTI

N92-31485*# National Aeronautics and Space Administration. Lewis Research Center, Cleveland, OH.
MODAL SIMULATION OF GEARBOX VIBRATION WITH EXPERIMENTAL CORRELATION
Fred K. Choy (Akron Univ., OH.), Yeefeng F. Ruan (Akron Univ., OH.), James J. Zakrajsek, and Fred B. Oswald 1992 17 p Presented at the 28th Joint Propulsion Conference and Exhibit, Nashville, TN, 6-8 Jul. 1992; sponsored by AIAA, SAE, ASME, and ASEE
(DA Proj. 1L1-62211-A-47-A; RTOP 505-63-36)
(NASA-TM-105702; E-7090; NAS 1.15:105702;
AVSCOM-TR-92-C-018; AIAA Paper 92-3494) Avail: CASI HC A03/MF A01

A newly developed global dynamic model was used to simulate the dynamics of a gear noise rig at NASA Lewis Research Center. Experimental results from the test rig were used to verify the analytical model. In this global dynamic model, the number of degrees of freedom of the system are reduced by transforming the system equations of motion into modal coordinates. The vibration of the individual gear-shaft system are coupled through the gear mesh forces. A three-dimensional, axial-lateral coupled, bearing model was used to couple the casing structural vibration to the gear-rotor dynamics. The coupled system of modal equations is solved to predict the resulting vibration at several locations on the test rig. Experimental vibration data was compared to the predictions of the global dynamic model. There is excellent agreement between the vibration results from analysis and experiment. Author

N92-31500# Oak Ridge National Lab., TN.
MOTOR-OPERATED GLOBE VALVE PERFORMANCE IN A LIQUID SODIUM ENVIRONMENT
D. H. Wood, M. S. Smith, and J. D. Drischler 1992 14 p Presented at the Bi-Annual Nuclear Energy Meeting of the American Nuclear Society and the American Society of Mechanical Engineers, San Diego, CA, 23-26 Aug. 1992
(Contract DE-AC05-84OR-21400)
(DE92-014456; CONF-920818-2) Avail: CASI HC A03/MF A01

This study investigates motor-operated globe valve (MOV) performance in a liquid sodium environment as reported to the Centralized Reliability Data Organization (CREDO) from site representatives at several liquid metal reactors and liquid metal test facilities. The CREDO data base contains engineering histories for 179 motor-operated glove valves. Thirty-nine failures have been documented for these components in over 8.7 million hours of operation. The most common MOV events were anomalies with the limit and torque switches, although human initiated problems were also frequent causes of failures. The failure data suggest that an improved preventive maintenance program with a higher frequency of inspection of the limit and torque switches should increase MOV availability and reliability. The event rate for all failure modes was computed as 4.47 events per 10(exp 8) operating hours by assuming a Poisson distribution of failure over valve operating time. The 5 percent and 95 percent confidence limits based on a chi-squared probability distribution function were computed as 3.36 and 5.83 events per 10(exp 6) operating hours, respectively. The operating performance of these liquid metal MOVs was compared to similar data for MOVs in commercial light water reactors and was found to exhibit similar failure rates. DOE

N92-31536*# National Aeronautics and Space Administration. Lewis Research Center, Cleveland, OH.
EFFECT OF OUT-OF-ROUNDNESS ON THE PERFORMANCE OF A DIESEL ENGINE CONNECTING-ROD BEARING
D. Vijayaraghavan, D. E. Brewe, and T. G. Keith, Jr. (Ohio Aerospace Inst., Brook Park.) Oct. 1991 19 p Presented at the STLE/ASME Tribology Conference, St. Louis, MO, 17-19 Oct. 1991; sponsored by the ASME Journal of Tribology
(RTOP 505-63-5A)
(NASA-TM-105600; E-6863; NAS 1.15:105600;
AVSCOM-TR-92-C-029) Avail: CASI HC A03/MF A01

In this paper, the dynamic performance of the Ruston and Hornsby VEB diesel engine connecting-rod bearing with circular and out-of-round profiles is analyzed. The effect of cavitation is considered by using a cavitation algorithm, which mimics JFO boundary conditions. The effect of mass inertia is accounted for by solving coupled nonlinear equations of motion. The journal profiles considered are circular, elliptical, semi-elliptical, and three lobe epicycloid. The predicted journal trajectory and other performance parameters for one complete load cycle are presented for all of the out-of-round profiles and are also compared with the predictions for the circular bearing. Author

N92-31653# Department of Energy, Washington, DC. Office of Transportation Technologies.
ELECTRIC AND HYBRID VEHICLES PROGRAM
May 1992 56 p
(DE92-015200; DOE/CE-0357P) Avail: CASI HC A04/MF A01

The Department of Energy's (DOE) Electric and Hybrid Vehicles (EHV) Program is conducting research, development, testing, and evaluation activities to encourage the use of electricity and alternative fuels for transportation. This program supports the expanded DOE involvement as recommended in the National Energy Strategy. The transportation sector is the single largest user of petroleum; it consumed 63 percent of all petroleum used in the United States last year. Only a small fraction (5 percent) of electricity is generated from petroleum. Electric vehicles, which are themselves virtually pollution-free, could play a key role in helping to reduce both urban pollution and our dependence on petroleum imports. The program's goals are to develop, in cooperation with industry, the technology that will lead to the production and introduction of pollution-free electric vehicles into the Nation's transportation fleet and substitute domestic sources of energy for petroleum-based fuels. This report describes progress achieved in developing electric and hybrid vehicle technologies, beginning with highlights of recent accomplishments in FY-91. Detailed descriptions are provided of program activities during FY-91 in the areas of battery, fuel-cell, and propulsion system development, and testing and evaluation of new technology in fleet site operations and in laboratories. In accordance with the reporting requirements of the Act, this annual report contains a status report on incentives and use of foreign components and concludes with a list of publications resulting from the DOE program. DOE

N92-31720# Argonne National Lab., IL. Energy Systems Div.
POTENTIAL IMPACT OF HIGH TEMPERATURE SUPERCONDUCTORS ON MAGLEV TRANSPORTATION
J. R. Hull Feb. 1992 21 p
(Contract W-31-109-eng-38)
(DE92-012683; ANL/ESD/TM-27) Avail: CASI HC A03/MF A01

This report describes the potential impact that high-temperature superconductors (HTS's) may have on transportation by magnetically levitated vehicles. It is not intended as a planning document, but rather as an overview of potential HTS applications to magnetic-levitation (maglev) transportation. The present maglev program in the United States is summarized, and the present status of development of HTS's is described. Areas identified for possible impact on maglev technology are: (1) liquid-nitrogen-cooled levitation magnets; (2) magnetic-field shielding of the passenger compartment; (3) superconducting magnetic energy storage for wayside power; (4) superconducting bearings for flywheel energy storage for wayside power; (5) downleads to continuously powered liquid-helium-cooled levitation magnets; and (6) liquid-hydrogen-cooled levitation magnets and linear motor propulsion windings. Major technical issues that remain to be resolved for the use of HTS's in maglev applications include thermal magnetic stability, mechanical properties, and critical current density at liquid-nitrogen temperatures. DOE

N92-31774# Argonne National Lab., IL.
PRELIMINARY DESIGN FOR A MAGLEV DEVELOPMENT FACILITY
H. T. Coffey, J. L. He, S. L. Chang, J. X. Bouillard, S. S. Chen, Y. Cai, L. O. Hoppie, S. A. Lottes, D. M. Rote, and Z. Y. Zhang (Polytechnic Inst. of New York, Brooklyn.) et al Apr. 1992 200 p
(Contract W-31-109-eng-38)
(DE92-012259; ANL/ESD-14) Avail: CASI HC A09/MF A03

A preliminary design was made of a national user facility for evaluating magnetic-levitation (maglev) technologies in sizes intermediate between laboratory experiments and full-scale systems. A technical advisory committee was established and a conference was held to obtain advice on the potential requirements of operational systems and how the facility might best be configured to test these requirements. The effort included studies of multiple concepts for levitating, guiding, and propelling maglev vehicles, as well as the controls, communications, and data-acquisition and -reduction equipment that would be required in operating the facility. Preliminary designs for versatile, dual 2-MVA power supplies capable of powering attractive or repulsive systems were developed. Facility site requirements were identified. Test vehicles would be about 7.4 m (25 ft) long, would weigh from 3 to 7 metric tons, and would operate at speeds up to 67 m/s (150 mph) on a 3.3-km (2.05-mi) elevated guideway. The facility would utilize modular vehicles and guideways, permitting the substitution of levitation, propulsion, and guideway components of different designs and materials for evaluation. The vehicle would provide a test cell in which individual suspension or propulsion components or subsystems could be tested under realistic conditions. The system would allow economical evaluation of integrated systems under varying weather conditions and in realistic geometries. DOE

N92-31807# Edgerton, Germeshausen and Grier, Inc., Idaho Falls, ID.
PERFORMANCE TESTS OF A FAST-ACTING VALVE FOR THE DRIVER TUBES OF A LARGE BLAST/THERMAL SIMULATOR Final Report, Jan. 1991 - Jan. 1992
Marcela R. Stacey May 1992 65 p
(Contract DE-AC07-76ID-01570)
(AD-A250035; EGG-ME-10066; BRL-CR-687) Avail: CASI HC A04/MF A01

This document describes the testing of a fast-acting throat valve element designed by Eaton Consolidated Controls for use in driver tubes, (blast generators) of a Large Blast/Thermal Simulator (LB/TS). An LB/TS is used to simulate decaying blast waves such as are generated by nuclear explosions. The Eaton Throat Valve Element (ETVE) was tested at the Idaho National Engineering Laboratory (INEL) to evaluate its performance against the design criteria. The ETVE was mounted at the end of a driver tube and actuated 16 times at 6 different driver pressures ranging from 396 kPa to 12.4 MPa (57.5 psi to 1,800 psi). The valve seals survived successfully all 16 tests with the driver gas at room temperature and maintained an acceptable leak rate throughout the test program. The average valve lag time was determined to vary from 36 to 120 ms; however, the valve was found to chatter, going through several (up to 20) opening/closing cycles after actuation before settling in the open position. An increase in the pneumatic supply pressure driving the valve showed a minor decrease in the number of chattering cycles. When the valve was actuated with no pressure in the driver tube, no chattering was observed. At the conclusion of the test sequence, the valve seals were inspected and were in good condition. The shock waves appeared to agree with code predictions when the chattering effects were disregarded. GRA

N92-31841# Solar Turbines, Inc. San Diego, CA.
GAS ENGINE HEAT RECOVERY UNIT Final Report, Sep. 1983 - Jul. 1991
A. J. Kubasco Jul. 1991 73 p
(Contract GRI-5083-243-0787)
(PB92-184373; SR83-R-5092-90; GRI-91/0354) Avail: CASI HC A04/MF A01

The objective of Gas Engine Heat Recovery Unit was to design, fabricate, and test an efficient, compact, and corrosion resistant heat recovery unit (HRU) for use on exhaust of natural gas-fired reciprocating engine-generator sets in the 50-500 kW range. The HRU would be a core component of a factory pre-packaged cogeneration system designed around component optimization, reliability, and efficiency. The HRU uses finned high alloy, stainless steel tubing wound into a compact helical coil heat exchanger. The corrosion resistance of the tubing allows more heat to be taken from the exhaust gas without fear of the effects of acid condensation. One HRU is currently installed in a cogeneration system at the Henry Ford Hospital Complex in Dearborn, Michigan. A second unit underwent successful endurance testing for 850 hours. The plan was to commercialize the HRU through its incorporation into a Caterpillar pre-packaged cogeneration system. Caterpillar is not proceeding with the concept at this time because of a downturn in the small size cogeneration market. Author

N92-31892*# Rockwell International Corp., Canoga Park, CA. Rocketdyne Div.
ORBIT TRANSFER VEHICLE ENGINE TECHNOLOGY PROGRAM. TASK B-6 HIGH SPEED TURBOPUMP BEARINGS Final Report, Jun. 1987 - Sep. 1989
Jan. 1992 97 p
(Contract NAS3-23773)
(NASA-CR-189230; NAS 1.26:189230; RI/RD-92-114; Rept-92-RC-09071) Avail: CASI HC A05/MF A02

Bearing types were evaluated for use on the Orbit Transfer Vehicle (OTV) high pressure fuel pump. The high speed, high load, and long bearing life requirements dictated selection of hydrostatic bearings as the logical candidate for this engine. Design and fabrication of a bearing tester to evaluate these cryogenic hydrostatic bearings was then conducted. Detailed analysis, evaluation of bearing materials, and design of the hydrostatic bearings were completed resulting in fabrication of Carbon P5N and Kentanium hydrostatic bearings. Rotordynamic analyses determined the exact bearing geometry chosen. Instrumentation was evaluated and data acquisition methods were determined for monitoring shaft motion up to speeds in excess of 200,000 RPM in a cryogenic atmosphere. Fabrication of all hardware was completed, but assembly and testing was conducted outside of this contract. Author

N92-31929# Maryland Univ., College Park.
BACKLASH CONTROL VIA REDUNDANT DRIVES: AN EXPERIMENTAL VERIFICATION
L. W. Tsai and S. L. Chang 1992 9 p Presented at the 22nd ASME Biennial Mechanisms Conference, Scottsdale, AZ, Sep. 1992
(Contract DE-FG05-88ER-13977)
(DE92-016368; CONF-9209143-1) Avail: CASI HC A02/MF A01

In this paper, a novel concept for the control of backlash in geared servo-mechanisms is demonstrated with a prototype manipulator. The concept utilizes unidirectional redundant drives to assure positive coupling of gear meshes at all times and, thereby, eliminates backlash completely. To establish a proof of concept, a two-DOF prototype manipulator with three unidirectional drives is designed and tested. A dynamic model based on Language's formulation is established. A PID controller using a computed torque control technique is developed. Two experiments, one with redundant drives and the other without redundant drives, are conducted. The experimental results demonstrate that use of unidirectional redundant drives improves the repeatability of a manipulator by an order of magnitude. DOE

N92-32121# Lawrence Livermore National Lab., CA.
MODELING AND DESIGN OF A CLOSED KINEMATIC CHAIN ROBOTIC MECHANISM
K. D. Young Dec. 1991 10 p Presented at the Singapore International Conference on Intelligent Control and Instrumentation,

Singapore (Singapore), 17-21 Feb. 1992
(Contract W-7405-eng-48)
(DE92-014777; UCRL-JC-109152; CONF-9202113-1) Avail: CASI HC A02/MF A01

In this paper, we model and design a class of deployable closed kinematic chains for the purpose of understanding the engineering issues in highly redundant robotic mechanisms. An approach to modeling of the constrained mechanical system is introduced for the design of decentralized controllers. A variable structure control algorithm is introduced to insure the dynamic decoupling among the active degrees of freedom of the system, and to provide highly robust, and disturbance insensitive closed loop dynamic performance. We show a hardware design of the decentralized variable structure controller for which prototype electronic controller boards are fabricated and tested. Preliminary experiment data validate the theoretically predicted robustness and insensitivity in the closed loop system. DOE

N92-32173# Harry Diamond Labs., Adelphi, MD.
EXTERNAL COMBUSTION ENGINE TECHNOLOGY (VAPOR AND LIQUID CYCLES) FOR INDIVIDUAL SOLDIER POWER SYSTEMS Final Report, Jan. - Dec. 1991
David L. Overman Apr. 1992 96 p
(AD-A252754; HDL-TR-2212) Avail: CASI HC A05/MF A01

Soldiers of the future will be equipped with electronic and electro-mechanical hardware to enhance their capabilities that will require individual power. There are several potential methods of supplying these power requirements. This report is an initial study of advanced vapor-cycle and liquid-cycle engine systems directed at this application. Results of the study indicated that miniature external combustion vapor-cycle engines in the 1- to 10-horsepower class, employing modern materials and design practices, have the potential to provide a compact, high-efficiency, quiet, and multi-fuel (especially military diesel fuel) power source to meet individual soldier and special operations requirements. A major appendix presents a thermodynamic analysis of the performance of a high-compression uniflow steam engine and the associated Rankine vapor cycle. GRA

N92-31867# Tel-Aviv Univ. (Israel). Faculty of Engineering.
SINGULARITY AVOIDANCE FOR SCARA-TYPE ROBOTS
L. Beiner *In* Israel Society of Aeronautics and Astronautics, 31st Israel Annual Conference on Aviation and Astronautics 22 Feb. 1990 p 41-43 Previously announced in IAA as A91-43081 (For primary document see N92-31861 22-01)
Avail: CASI HC A01/MF A03

N92-32013 Rockwell International Corp., Downey, CA. Space Systems Div.
ROBOTICS DEVELOPMENT FOR THE ENHANCEMENT OF SPACE ENDEAVORS
A. J. Mauceri and Margaret M. Clarke *In* Huntsville Association of Technical Societies, TABES 92: 8th Annual Technical and Business Exhibition and Symposium. Executive Summaries and Submitted Papers 1992 5 p (For primary document see N92-32009 22-12)
(TABES Paper 92-445) Copyright Avail: Issuing Activity

38 QUALITY ASSURANCE AND RELIABILITY

Includes product sampling procedures and techniques; and quality control.

N92-31336# Auburn Univ., AL. Dept. of Mechanical Engineering.
WELD PENETRATION AND DEFECT CONTROL
B. A. Chin 15 May 1992 42 p
(Contract DE-FG02-88ER-12817)
(DE92-015310; DOE/ER-12817/T1) Avail: CASI HC A03/MF A01

Highly engineered designs increasingly require the use of improved materials and sophisticated manufacturing techniques. To obtain optimal performance from these engineered products, improved weld properties and joint reliability are a necessity. This requirement for improved weld performance and reliability has led to the development of high-performance welding systems in which pre-programmed parameters are specified before any welding takes place. These automated systems however lack the ability to compensate for perturbations which arise during the welding process. Hence, the need for systems which monitor and control the in-process status of the welding process. This report discusses work carried out on weld penetration indicators and the feasibility of using these indicators for on-line penetration control. DOE

N92-31479# Naval Postgraduate School, Monterey, CA.
SEQUENTIAL ESTIMATION OF OPTIMAL AGE REPLACEMENT POLICIES WHEN DISTRIBUTION OF LIFETIMES IS PHASE TYPE M.S. Thesis
Patchara Pumpiched Mar. 1992 73 p
(AD-A249020) Avail: CASI HC A04/MF A01

Optimal age replacement policies are designed to cut down system failures and minimize maintenance cost. By scheduling planned replacements, a system is replaced at a scheduled time or at failure, whichever comes first, and the cost of replacement before failure (planned) is less than the cost after failure (unplanned). In this thesis, the distribution of lifetimes is a known, increasing failure rate phase type distribution. To find the optimal time of replacement, the parameters of underlying phase type distribution must be estimated. An optimal age sequential procedure is developed. In particular, the phase type distribution parameters are estimated using a matching moments nonlinear programming approach. Since there are many parameters associated with phase type distributions and the distributions include matrix exponential terms, the parameters are, in general, difficult to estimate. A specific case where the phase type distribution has initial probability vector = (1,0,0) is studied for different sample sizes and compared with a similar nonparametric procedure. GRA

N92-31647# Superconducting Super Collider Lab., Dallas, TX.
UTILIZATION OF GAMMA RAY INSPECTION SYSTEM FOR TOMOGRAPHIC IMAGING AND DIMENSIONAL ANALYSIS OF COMPLETE MODEL MAGNET COLD MASSES AND COLLARED COIL SECTIONS
D. Bein, J. Zbasnik, J. Bolger (International Digital Modeling Corp., Austin, TX.), B. Firey (International Digital Modeling Corp., Austin, TX.), B. Rice (International Digital Modeling Corp., Austin, TX.), B. Crane (International Digital Modeling Corp., Austin, TX.), G. Rabaey (International Digital Modeling Corp., Austin, TX.), J. Wesick (International Digital Modeling Corp., Austin, TX.), and L. Morgan (International Digital Modeling Corp., Austin, TX.) Mar. 1992 8 p Presented at the International Industrial Symposium on the Super Collider, New Orleans, LA, 4-6 Mar. 1992 Submitted for publication
(Contract DE-AC35-89ER-40486)
(DE92-013466; SSCL-Preprint-57; CONF-920331-5) Avail: CASI HC A02/MF A01

Non-destructive digital photon transmission imaging can be performed with the IRIS system to provide internal component dimensions and locations of manufactured superconducting magnets and sub-assemblies. With non-destructive evaluation of the magnet components, and sub-assemblies at critical stages of the manufacturing process, it is possible to assess the quality at each stage with the goal of improving manufacturing reproducibility and reliability. Evaluations of the feasibility of the IRIS system have been performed on a NbTi billet used for the production of monofilament rods used in the manufacturing of multifilament strand. It has also been used to perform inspections on collared coil sections, both 40 mm and 50 mm, as well as cold masses. The dimensional accuracy for locating the conductor winding positions in a collared coil section has been found to be plus or minus 80 microns. Non-destructive analysis using the IRIS system offers in-process inspection, as well as post assembly examination capabilities previously unavailable except through destructive physical analysis by sectioning and polishing for optical inspection

after vacuum impregnation. This novel inspection tool may give us deep insights into the validity of our mechanical and electromagnetic models currently used to evaluate magnet design and may lead to substantial savings per magnet analysis. DOE

N92-31657# Pacific Northwest Lab., Richland, WA.
REAL-TIME STATISTICAL QUALITY CONTROL AND ARM
D. K. Blough May 1992 8 p Presented at the 46th American Society for Quality Control (ASQC) Congress, Nashville, TN, 18-20 May 1992
(Contract DE-AC06-76RL-01830)
(DE92-015253; PNL-SA-19989; CONF-9205190-1) Avail: CASI HC A02/MF A01

An important component of the Atmospheric Radiation Measurement (ARM) Program is real-time quality control of data obtained from meteorological instruments. It is the goal of the ARM program to enhance the predictive capabilities of global circulation models by incorporating in them more detailed information on the radiative characteristics of the earth's atmosphere. To this end, a number of Cloud and Radiation Testbeds (CART's) will be built at various locations worldwide. Each CART will consist of an array of instruments designed to collect radiative data. The large amount of data obtained from these instruments necessitates real-time processing in order to flag outliers and possible instrument malfunction. The Bayesian dynamic linear model (DLM) proves to be an effective way of monitoring the time series data which each instrument generates. It provides a flexible yet powerful approach to detecting in real-time sudden shifts in a non-stationary multivariate time series. An application of these techniques to data arising from a remote sensing instrument to be used in the CART is provided. Using real data from a wind profiler, the ability of the DLM to detect outliers is studied. DOE

N92-31693# Laboratoire d'Automatique et d'Analyse des Systemes, Toulouse (France).
CONTINUOUS TIME AND DISCRETE TIME HYPEREXPONENTIAL MODEL FOR DEPENDABILITY GROWTH MODELING Ph.D. Thesis - Toulouse Univ. [MODELE HYPEREXPONENTIEL EN TEMPS CONTINU EN TEMPS DISCRET POUR L'EVALUATION DE LA CROISSANCE DE LA SURETE DE FONCTIONNEMENT]
Mohamed Kaaniche 1992 190 p In FRENCH
(LAAS-92002; ETN-92-91682) Avail: CASI HC A09/MF A02

Theoretical and practical results on computer system reliability and availability growth modeling are presented. Two kinds of system behavior characterizations are considered, one with respect to time and the other with respect to the number of executions performed. Attention is centered on two reliability growth models: the continuous time hyperexponential model and the discrete time hyperexponential model. For each of these models, single component systems and multicomponent systems are considered such that the reliability growth of each component of the considered system is characterized by the hyperexponential model. The discrete time hyperexponential model is also used to account for some characteristics of the software environment to evaluate dependability measures of the software that are particular to the environment in which it is executed. ESA

N92-31753# Sandia National Labs., Albuquerque, NM.
GUIDELINES FOR GENERATING ACCEPTANCE SAMPLING PLANS FOR CONTINUOUS PRODUCTION
R. R. Prairie Mar. 1992 29 p
(Contract DE-AC04-76DP-00789)
(DE92-010763; SAND-88-3185) Avail: CASI HC A03/MF A01

This report provides guidance for developing sampling plans for products that follow continuous rather than lot production. The basic concept of the plans is to test 100 percent of the initial phase of production and then, after the product has shown itself to be concordant with the reliability requirement, to monitor the product at a reduced sampling rate. Plan parameters are provided as a function of reliability requirement, and characteristics of the plan are described. DOE

N92-32143# Atomic Energy of Canada Ltd., Chalk River (Ontario). Nuclear Labs.
EWE: A COMPUTER MODEL FOR ULTRASONIC INSPECTION
S. R. Douglas and K. R. Chaplin Nov. 1991 55 p Prepared in cooperation with Ontario Hydro, Toronto, Ontario
(DE92-627145; AECL-10507; COG-91-261) Avail: CASI HC A04/MF A01

The computer program EWE simulates the propagation of elastic waves in solids and liquids. It was applied to ultrasonic testing to study the echoes generated by cracks and other types of defects. A discussion of the elastic wave equations is given, including the first-order formulation, shear and compression waves, surface waves and boundaries, numerical method of solution, models for cracks and slot defects, input wave generation, returning echo construction, and general computer issues. DOE

N92-32172# Maryland Univ., Baltimore.
TOTAL QUALITY MANAGEMENT: A MANAGEMENT PHILOSOPHY FOR PROVIDING HIGH QUALITY CONSTRUCTION
Paul D. Beckwith 1992 83 p
(AD-A252743) Avail: CASI HC A05/MF A01

Total Quality Management (TQM) is not a new concept. Only recently (within the past ten years or so) have American companies started to realize the potential of TQM as a means of ensuring high quality products and services. With this realization has come implementation in manufacturing and service companies. A commercial construction company, like any other business, must provide a top quality finished product to its customer if it intends to stay in business. TQM is one way to work to that end. This report explores the quality problems facing my fictitious construction company, which I believe are fairly typical among the commercial construction industry, existing management methods, and the TQM method to ensure top quality production. It will be shown why I believe TQM or a variation thereof is the best method for controlling the quality of products and service during the construction process. Under the philosophy of TQM, we build quality into the finished product. GRA

N92-32202# Defence Research Establishment Pacific, Victoria (British Columbia). Research and Development Branch.
INVESTIGATION INTO THE ULTRASONIC NDE OF ADHESIVELY BONDED JOINTS
K. I. McRae May 1989 18 p
(DREP-90-02; CTN-92-60321) Avail: CASI HC A03/MF A01

At present a reliable nondestructive evaluation (NDE) technique to detect poor bonding conditions does not exist. The present study investigated techniques by which the adhesive properties of bonds may be degraded and examined ultrasonic methods capable of detecting the subsequent degradation of bond quality. The adhesive strength of most metal-metal bonds is primarily dependent on the quality of the thin (a few microns) oxide layer at the metal surface. It seems unlikely that standard ultrasonic techniques which use millimeter length waves could detect poor bond quality. The application of the leaky Lamb wave using an ultrasonic spectroscopic technique was investigated in the present study. A theoretical evaluation indicated that the leaky Lamb technique should be useful in determining bond quality. Despite this prediction, the existence of an adhesive bond had little apparent effect on the resulting Lamb wave propagation. All bonds appeared to be evaluated as bad, regardless of the result of mechanical tests. Furthermore, a significant variation between spectra within each specimen was observed. Further investigation of these phenomena is recommended. CISTI

39 STRUCTURAL MECHANICS

Includes structural element design and weight analysis; fatigue; and thermal stress.

For applications see *05 Aircraft Design, Testing and Performance* and *18 Spacecraft Design, Testing and Performance.*

N92-31279*# National Aeronautics and Space Administration. Langley Research Center, Hampton, VA.
ANALYSIS AND PREDICTION OF MULTIPLE-SITE DAMAGE (MSD) FATIGUE CRACK GROWTH
D. S. Dawicke (Analytical Mechanics Associates, Inc., Hampton, VA.) and J. C. Newman, Jr. Aug. 1992 18 p
(RTOP 505-63-50-04)
(NASA-TP-3231; L-17006; NAS 1.60:3231) Avail: CASI HC A03/MF A01

A technique was developed to calculate the stress intensity factor for multiple interacting cracks. The analysis was verified through comparison with accepted methods of calculating stress intensity factors. The technique was incorporated into a fatigue crack growth prediction model and used to predict the fatigue crack growth life for multiple-site damage (MSD). The analysis was verified through comparison with experiments conducted on uniaxially loaded flat panels with multiple cracks. Configuration with nearly equal and unequal crack distribution were examined. The fatigue crack growth predictions agreed within 20 percent of the experimental lives for all crack configurations considered.
Author

N92-31280*# National Aeronautics and Space Administration. Marshall Space Flight Center, Huntsville, AL.
APPLICATIONS OF FEM AND BEM IN TWO-DIMENSIONAL FRACTURE MECHANICS PROBLEMS
J. B. Min, B. E. Steeve, and G. R. Swanson Aug. 1992 23 p
(NASA-TP-3277; M-695; NAS 1.60:3277) Avail: CASI HC A03/MF A01

A comparison of the finite element method (FEM) and boundary element method (BEM) for the solution of two-dimensional plane strain problems in fracture mechanics is presented in this paper. Stress intensity factors (SIF's) were calculated using both methods for elastic plates with either a single-edge crack or an inclined-edge crack. In particular, two currently available programs, ANSYS for finite element analysis and BEASY for boundary element analysis, were used.
Author

N92-31303# Allied-Signal Aerospace Co., Kansas City, MO.
COMPUTER-AIDED MODELING TOOLS FOR FORGING PROCESS FEASIBILITY STUDIES
A. S. El-Gizawy (Missouri Univ., Columbia.) Mar. 1992 53 p
(Contract DE-AC04-76DP-00613)
(DE92-012116; KCP-613-4503) Avail: CASI HC A04/MF A01

Equations were developed to express stress distributions for a variety of deformation configurations. Strain equations were developed as they apply to forged workpieces, as were strain rate equations. The flow stress equation was introduced. The shear criterion was established to minimize the amount of energy that deforming metal flow consumes. An equation was developed relating flash width and thickness using the concept of constant volume. Force equations were developed for lateral and converging flow. From these equations, the closed-die axisymmetric forging process was simulated in two cases: constant ram speed and constant strain rate. Fortran programs were developed for both cases. Software employed to present on-screen interactive graphics was FIGARO by MEGATEK. The feasibility of producing a particular part was studied by comparing net shape, near net shape, and conventional forging/machining methods. A near net shape design with some machining was recommended as most economical.
DOE

N92-31331# Army Armament Research, Development and Engineering Center, Watervliet, NY.
A GENERALIZED PLANE-STRAIN ELASTIC STRESS SOLUTION FOR A MULTIORTHOTROPIC-LAYERED CYLINDER Final Report
Mark D. Witherell Mar. 1992 27 p
(AD-A250487; ARCCB-TR-92013) Avail: CASI HC A03/MF A01

A methodology is presented for constructing an exact stress solution for a multiorthotropic-layered cylinder for which all layers have equivalent axial strain. Combined loadings of internal pressure, external pressure, and axial force are included in the solution's formulation. The multilayered solution is developed by applying the proper boundary conditions to a three-dimensional elasticity solution for a monolayered orthotropic cylinder. Theoretical results for multilayered cylinders with selected material layups and loading conditions are compared with finite element results to verify the accuracy of the solution's formulation. The software implementation of this solution provides the design engineer with a powerful tool for efficiently using composite materials in cylindrical pressure vessels.
GRA

N92-31335# Argonne National Lab., IL.
MODE METHODS FOR STRAIN-HARDENING STRUCTURES
C. K. Youngdahl Apr. 1992 9 p Presented at the 10th Symposium on Energy Engineering Sciences, Argonne, IL, 11-13 May 1992
(Contract W-31-109-eng-38)
(DE92-014855; ANL/CP-76120; CONF-9205147-1) Avail: CASI HC A02/MF A01

An approximation method is being developed to predict the dynamic plastic response of rigid, strain-hardening structures. This method is analogous to the instantaneous mode techniques used to treat rigid, perfectly plastic structures in that a deflection shape involving a number of arbitrary functions of time is selected, based on static deformation profiles. Two stress fields are associated with the deflection shape: one satisfies the equations of motion with appropriate boundary and continuity conditions, and the other satisfies the strain-hardening constitutive relation with appropriate boundary and smoothness conditions. The method is illustrated using the case of a simply-supported beam with a central plastic region.
DOE

N92-31337# Maryland Univ., College Park. Dept. of Mechanical Engineering.
ON THE FEASIBILITY OF A TRANSIENT DYNAMIC DESIGN ANALYSIS METHOD Annual Progress Report, 1 May 1991 - 30 Apr. 1992
George J. OHara and Patrick F. Cunniff Apr. 1992 10 p
(Contract N00014-91-J-4059)
(AD-A250406) Avail: CASI HC A02/MF A01

This Annual Report summarizes the progress that was made during the first year of the two-year grant from the Office of Naval Research. The dynamic behavior of structures subjected to mechanical shock loading provides a continuing problem for design engineers concerned with shipboard foundations supporting critical equipment. There are two particular problems associated with shock response that are currently under investigation. The first topic explores the possibilities of developing a transient design analysis method that does not degrade the current level of the Navy's shock-proofness requirements for heavy shipboard equipment. The second topic examines the prospects of developing scaling rules for the shock response of simple internal equipment of submarines subjected to various attack situations. This effort has been divided into two tasks: chemical explosive scaling for a given hull; and scaling of equipment response across different hull sizes. The computer is used as a surrogate shock machine for these studies. Hence, the results of the research can provide trends, ideas, suggestions, and scaling rules to the Navy. In using these results, the shock-hardening program should use measured data rather than calculated data.
GRA

N92-31339*# Georgia Inst. of Tech., Atlanta. School of Aerospace Engineering.
MODELING OF COMPOSITE BEAMS AND PLATES FOR STATIC AND DYNAMIC ANALYSIS Semiannual Interim Report, 17 Jan. - 16 Jul. 1992
Dewey H. Hodges 16 Jul. 1992 27 p
(Grant NAG1-1094)
(NASA-CR-190536; NAS 1.26:190536) Avail: CASI HC A03/MF A01

A rigorous theory and the corresponding computational algorithms were developed for through-the-thickness analysis of composite plates. This type of analysis is needed in order to find the elastic stiffness constants of a plate. Additionally, the analysis is used to post-process the resulting plate solution in order to find approximate three-dimensional displacement, strain, and stress distributions throughout the plate. It was decided that the variational-asymptotical method (VAM) would serve as a suitable framework in which to solve these types of problems. Work during this reporting period has progressed along two lines: (1) further evaluation of neo-classical plate theory (NCPT) as applied to shear-coupled laminates; and (2) continued modeling of plates with nonuniform thickness. Author

N92-31383# Oak Ridge National Lab., TN.
RESIDUAL STRESS AND STRAIN MEASUREMENTS IN AN AUSTENITIC STEEL PLATE CONTAINING A MULTIPASS WELD
S. Spooner, S. A. David, J. H. Root (Atomic Energy of Canada Ltd., Chalk River, Ontario), T. M. Holden (Atomic Energy of Canada Ltd., Chalk River, Ontario), M. A. M. Bourke (Los Alamos National Lab., NM.), and J. Goldstone (Los Alamos National Lab., NM.) 1992 6 p Presented at the 3rd International Conference on Trends in Welding Research, Gatlinburg, TN, 1 Jun. 1992
(Contract DE-AC05-84OR-21400)
(DE92-014478; LA-UR-92-1528; CONF-9206173-1) Avail: CASI HC A02/MF A01

Residual stresses and strains in a 2.4 by 30.5 by 30.5-cm type 304 stainless steel plate containing a multiple-pass gas tungsten arc weld were measured with the neutron diffraction technique at a reactor (Chalk River) and a pulsed source (Los Alamos). At Chalk River, three orthogonal strain components were obtained at each sampling point from the average of the strains measured with (111) and (200) Bragg peaks. Points along the top and bottom of the plate running transverse to the welding direction and points along a through-thickness path in the weld and in the heat affected zone were measured. At the top, the longitudinal stress reached 260 MPa in tension at the fusion line. All three components became compressive in the fusion zone. Measurement of longitudinal and normal strains through the thickness in the fusion zone was difficult because of large grain size and strong preferred orientation. However, the transverse strains in the fusion zone were measured as a function of depth at the Los Alamos pulsed source and were compared with corresponding results obtained at Chalk River. DOE

N92-31389# New Hampshire Univ., Durham. Dept. of Mechanical Engineering.
EFFECT OF FRACTURE SURFACE INTERFERENCE ON SHEAR CRACK GROWTH
T. S. Gross, D. W. Watt, and D. A. Mendelsohn (Ohio State Univ., Columbus.) Feb. 1992 9 p
(Contract DE-FG02-90ER-45433)
(DE92-011431; DOE/ER-45433/1) Avail: CASI HC A02/MF A01

A joint analytical-experiment program to investigate the effect of fracture surface interference on shear modes of crack growth is progressing satisfactorily. A general two-dimensional, boundary element model was formulated by the group at Ohio State University. The model is capable of calculating the effective Mode I and Mode II stress intensity factors for flat or curved cracks with small scale yielding. The model can calculate K(sub I) and K(sub II) for an arbitrary constitutive law for displacement of the crack faces. The constitutive law proposed in our earlier work is being used in the new boundary element model. The experimental portion of the effort at UNH was to use an as-yet undeveloped electro-optic holographic interferometry (EOH) system to measure the crack face displacement field while the crack is loaded in shear. The algorithms for obtaining the interferograms were developed, the testing machine modifications necessary for interferometric measurements are complete, and interferograms of specimens under load were obtained. Techniques for digitizing the fracture surface profile were developed and preliminary numerical experiments were conducted to determine the (Delta)K dependence of fracture asperity interference on an actual crack. DOE

N92-31400# Carnegie-Mellon Univ., Pittsburgh, PA.
THE EFFECT OF ELASTIC STRESS ON OSTWALD RIPENING PHENOMENA
W. C. Johnson 1992 8 p
(Contract DE-FG02-84ER-45166)
(DE92-015291; DOE/ER-45166/4) Avail: CASI HC A02/MF A01

The purpose of our research program is to understand the influence of elastic misfit strain and applied stress on the development of microstructure in two-phase coherent alloys. The long-term goal of our research is to identify those materia! parameters that promote microstructural stability in multiphase systems at elevated temperatures. Our efforts since the last progress report in February 1991 have been twofold. First, we have continued performing coarsening simulations of elastically and diffusionally interacting particles in an infinite matrix. In addition, we have been performing simulations of unstressed systems during coarsening. Secondly, we have begun to develop an experimental component to the research that would allow a careful comparison between theory, computer simulations, and experiment. We have continued to focus our computer simulations of stressed systems on elastically homogeneous and isotropic systems containing tetragonally misfitting particles. DOE

N92-31501# Oak Ridge National Lab., TN.
RESIDUAL STRESSES IN A MULTIPASS FERRITIC WELDMENT
J. H. Root (Atomic Energy of Canada Ltd., Chalk River, Ontario), T. M. Holden (Atomic Energy of Canada Ltd., Chalk River, Ontario), J. Schroeder (Atomic Energy of Canada Ltd., Chalk River, Ontario), S. Spooner, C. A. Hubbard, T. A. Dodson, and S. A. David 1992 5 p Presented at the 3rd International Conference on Trends in Welding Research, Gatlinburg, TN, 1 Jun. 1992
(Contract DE-AC05-84OR-21400)
(DE92-014467; CONF-9206173-2) Avail: CASI HC A01/MF A01

The distribution of residual stresses associated with a multipass, gas-tungsten arc weld, joining two 2.5 percent Cr 1 percent Mo steel plates of thickness 13 mm, was measured non-destructively by neutron diffraction. The large tensile longitudinal stress (400-500 MPa) in the weld and in the plates immediately adjacent to the weld are balanced by compressive stresses (-150 MPa) in the periphery of the plate. The stress components normal to the plate surface and transverse to the weld are everywhere equal in magnitude. In the fusion zone of the weld, these components are tensile at the top surface and middle of the plate and zero at the back surface of the plate (i.e., near the root pass of the weld). DOE

N92-31504*# National Aeronautics and Space Administration. Langley Research Center, Hampton, VA.
FINITE-ELEMENT ANALYSES AND FRACTURE SIMULATION IN THIN-SHEET ALUMINUM ALLOY
J. C. Newman, Jr., D. S. Dawicke (Analytical Services and Materials, Inc., Hampton, VA.), and C. A. Bigelow Aug. 1992 22 p Presented at the International Workshop on Structural Integrity of Aging Airplanes, Atlanta, GA, 31 Mar. - 2 Apr. 1992 Submitted for publication
(RTOP 538-02-10)

(NASA-TM-107662; NAS 1.15:107662) Avail: CASI HC A03/MF A01

A two-dimensional, elastic-plastic finite-element analysis was used with a critical crack-tip-opening angle (CTOA) fracture criterion to model stable crack growth in thin-sheet 2024-T3 aluminum alloy under monotonic loading after precracking at different cyclic stress levels. Tests were conducted on three types of specimens: middle-crack, three-hole-crack and blunt-notch tensile specimens. An experiment technique was developed to measure CTOA during crack growth initiation and stable tearing using a high-resolution video camera and recorder. Crack front shapes were also measured during initiation and stable tearing using a fatigue marker-load technique. Three-dimensional elastic-plastic finite-element analyses of these crack shapes for stationary cracks were conducted to study the crack-front opening displacements. Predicted load against crack extension on middle-crack tension specimens agreed well with test results even for large-scale plastic deformations. The analyses were able to predict the effects of specimen size and precracking stress history on stable tearing. Predicted load against load-line displacements agreed well with test results up to maximum load bu the analyses tended to overpredict displacements as crack grew beyond the maximum load under displacement-controlled conditions. During the initiation phase, the measured CTOA values were high but decreased and remained nearly constant after a small amount of stable tearing. The constant value of CTOA agree well with the calculated value from the finite-element analysis. The larger CTOA values measured at the sheet surface during the initiation phase may be associated with the crack tunneling observed in the tests. Three-dimensional analyses for nonstraight crack fronts predicted much higher displacements near the free surface than in the interior. Author

N92-31505*# National Aeronautics and Space Administration. Lewis Research Center, Cleveland, OH.

A DIFFERENTIAL CDM MODEL FOR FATIGUE OF UNIDIRECTIONAL METAL MATRIX COMPOSITES

S. M. Arnold and S. Kruch (Office National d'Etudes et de Recherches Aerospatiales, Paris, France) 1992 22 p Proposed for presentation at the ASME, Anaheim, CA, 8-13 Nov. 1992

(RTOP 510-01-50)

(NASA-TM-105726; E-7128; NAS 1.15:105726) Avail: CASI HC A03/MF A01

A multiaxial, isothermal, continuum damage mechanics (CDM) model for fatigue of a unidirectional metal matrix composite volume element is presented. The model is phenomenological, stress based, and assumes a single scalar internal damage variable, the evolution of which is anisotropic. The development of the fatigue damage model, (i.e., evolutionary law) is based on the definition of an initially transversely isotropic fatigue limit surface, a static fracture surface, and a normalized stress amplitude function. The anisotropy of these surfaces and function, and therefore the model, is defined through physically meaningful invariants reflecting the local stress and material orientation. This transversely isotropic model is shown, when taken to it's isotropic limit, to directly simplify to a previously developed and validated isotropic fatigue continuum damage model. Results of a nondimensional parametric study illustrate (1) the flexibility of the present formulation in attempting to characterize a class of composite materials, and (2) the capability of the formulation in predicting anticipated qualitative trends in the fatigue behavior of unidirectional metal matrix composites. Also, specific material parameters representing an initial characterization of the composite system SiC/Ti 15-3 and the matrix material (Ti 15-3) are reported. Author

N92-31512# Aeronautical Research Inst. of Sweden, Stockholm. Structures Dept.

THE INFLUENCE OF VARIOUS SPECTRUM PARAMETERS ON FATIGUE LIFE AND RESIDUAL STRESS RELAXATION

Jonas Bogren, Luis LopezMartinez (Swedish Steel A.B., Oxeloesund, Sweden), and Mats Brunnberg (Linkoeping Univ., Sweden) Nov. 1991 33 p Sponsored by Swedish National Board for Industrial and Technical Development; Nordic Industrial Fund; ABB, Hafo A.B.; Saab-Scania; Swedish Steel A.B.; and VME

(FFA-TN-1991-44; ETN-92-91393) Avail: CASI HC A03/MF A01

The influence of spectrum parameters on fatigue life and residual stress relaxation were studied. The specimen is a non load carrying fillet weld. Four different spectra were applied and an additional spectrum was used when residual stress relaxation was investigated. All these five spectra have similar range pair distributions and the same block length of 500,000 cycles. The following spectrum parameters were varied: stress ratio, irregularity factor, and mean stress. Two different stress levels were used in the tests. Residual stresses were measured using X-ray diffraction. The levels and distributions of the measured welding induced residual stresses are in agreement with other investigations. The residual stresses were found to relax very rapidly. Fifty percent or more of the initial stresses are relaxed within the first 7 percent of the total specimen life. The initial level is close to the yield stress of the material and at 7 percent or less of the specimen life the levels are relaxed to about 50 to 80 Mpa. The rate of relaxation is much lower for the spectrum with R = -1, based on percent of total life, compared to the other spectra. Large scatter in fatigue life is observed at the lower stress level. Large retardation effects were found for the spectrum with R = 0, compared to constant amplitude loading. Life ratios, tested to predicted life, are in the range of 0.5 to 4.7. The only spectrum parameter that had large influence on fatigue life was the stress ratio. The irregularity factor and stress ratio were of less significance. ESA

N92-31516# Cranfield Inst. of Tech., Bedford (England). College of Aeronautics.

DYNAMICS OF SHUTTLE BASED FLEXIBLE ANTENNA SYSTEM Thesis - Stuttgart Univ.

M. Moch and C. L. Kirk Jan. 1992 234 p

(Cranfield-Aero-9203; ISBN-1-871564-379; ETN-92-91729) Avail: CASI HC A11/MF A03

The Lagrangian approach was used to model a complex flexible antenna/astromast system. In order to keep the open and closed loop dynamic models to a reasonable size a reduced model with four degrees of freedom was selected. The possibility of using the DC servomotor in a closed loop system, to damp the oscillations produced by the step function motors' torque (required for acceleration and deceleration), was investigated. Using the dynamical model, an open loop pitching maneuver was simulated, eigenvalue analysis was applied, and residual oscillations at the end of the maneuver were damped out by the DC servomotor using closed loop feedback control. ESA

N92-31619*# Vermont Univ., Burlington. Dept. of Mathematics and Statistics.

CSM SOLUTIONS OF ROTATING BLADE DYNAMICS USING INTEGRATING MATRICES Final Report, 1 Mar. 1991 - 28 Feb. 1992

William D. Lakin 28 Feb. 1992 14 p

(Grant NAG1-1097)

(NASA-CR-190577; NAS 1.26:190577) Avail: CASI HC A03/MF A01

The dynamic behavior of flexible rotating beams continues to receive considerable research attention as it constitutes a fundamental problem in applied mechanics. Further, beams comprise parts of many rotating structures of engineering significance. A topic of particular interest at the present time involves the development of techniques for obtaining the behavior in both space and time of a rotor acted upon by a simple airload loading. Most current work on problems of this type use solution techniques based on normal modes. It is certainly true that normal modes cannot be disregarded, as knowledge of natural blade frequencies is always important. However, the present work has considered a computational structural mechanics (CSM) approach to rotor blade dynamics problems in which the physical properties of the rotor blade provide input for a direct numerical solution of the relevant boundary-and-initial-value problem. Analysis of the dynamics of a given rotor system may require solution of the governing equations over a long time interval corresponding to

many revolutions of the loaded flexible blade. For this reason, most of the common techniques in computational mechanics, which treat the space-time behavior concurrently, cannot be applied to the rotor dynamics problem without a large expenditure of computational resources. By contrast, the integrating matrix technique of computational mechanics has the ability to consistently incorporate boundary conditions and 'remove' dependence on a space variable. For problems involving both space and time, this feature of the integrating matrix approach thus can generate a 'splitting' which forms the basis of an efficient CSM method for numerical solution of rotor dynamics problems. Author

N92-31638# Pacific Northwest Lab., Richland, WA.
MECHANICAL STRENGTH AND STABILITY OF LITHIUM ALUMINATE
J. L. Brimhall Jun. 1992 25 p
(Contract DE-AC06-76RL-01830)
(DE92-015998; PNL-8088) Avail: CASI HC A03/MF A01

Pacific Northwest Laboratory (PNL) investigated the strength and resistance to thermal shock of lithium aluminate annular pellets. The room temperature, axial compressive fracture strength of pellets made at Westinghouse Advanced Energy Systems (WAES) varied from 80 to 133 ksi. The strength at 430 C (806 F) was to 30 to 40 percent lower. The strength at 900 C (1652 F) showed a wide variation with one measurement near 90 ksi. These strength values are consistent with other data and predictions made in the literature when the grain size and porosity of the microstructure are taken into account. In diametral compression tests, the fracture strengths were much lower due to the existence of tensile stresses in some pellet regions from this type of loading. However, the fracture stresses were still generally higher than those reported in the literature; this fracture resistance probably reflects the better quality of the pellets tested in this study. Measurements on pellets made at PNL indicated lower strengths compared to the WAES material. This strength difference could be accounted for by different processing technologies: material made at PNL was cold-pressed and sintered with high porosity whereas the WAES material was isostatically hot-pressed with high density. Thermal shocking of the material by ramping to 900 C in two minutes did not have an observable effect on the microstructure or the strength of any of the pellets. DOE

N92-31658# Sydney Univ. (Australia). School of Civil and Mining Engineering.
STRENGTH TESTS OF COLD-FORMED CHANNEL SECTIONS UNDERGOING LOCAL AND DISTORTIONAL BUCKLING
Y. B. Kwon and G. J. Hancock Jun. 1991 92 p
(PB92-180835; R-640) Avail: CASI HC A05/MF A01

In this report, the results of compression tests of thin-walled channel section columns formed by brake-precessing are described. Two different section geometries, a simple lipped channel and a lipped channel with an intermediate stiffener in the web, were tested between fixed-ended boundary conditions. The geometries and yield strength were chosen to ensure that a substantial post-buckling strength reserve occurred in the distortional mode and that local buckling might occur simultaneously at a shorter wavelength. The deformations were measured using a movable frame on which linear displacement transducers were mounted. The residual stresses and material properties were also measured. Distortional or mixed local distortional buckling stresses obtained from testing are compared with theoretical buckling stresses. Design curves for the maximum strength of the columns undergoing distortional or mixed modes of buckling are proposed and compared with the test results. GRA

N92-31745# Westinghouse Savannah River Co., Aiken, SC.
COMPUTER APPLICATIONS FOR ENGINEERING/STRUCTURAL ANALYSIS
M. Zaslawsky and S. K. Samaddar 1991 19 p Presented at the Westinghouse Computer Symposium, Monroeville, PA, 21-22 Oct. 1991 Revised
(Contract DE-AC09-89SR-18035)
(DE92-013070; WSRC-MS-91-230-Rev-1;
CONF-9110344-8-Rev-1) Avail: CASI HC A03/MF A01

Analysts and organizations have a tendency to lock themselves into specific codes with the obvious consequence of not addressing the real problem and thus reaching the wrong conclusion. This paper discusses the role of the analyst in selecting computer codes. The participation and support of a computation division in modifying the source program, configuration management, and pre- and post-processing of codes are among the subjects discussed. Specific examples illustrating the computer code selection process are described in the following problem areas: soil structure interaction, structural analysis of nuclear reactors, analysis of waste tanks where fluid structure interaction is important, analysis of equipment, structure-structure interaction, analysis of the operation of the superconductor supercollider which includes friction and transient temperature, and 3D analysis of the 10-meter telescope being built in Hawaii. Validation and verification of computer codes and their impact on the selection process are also discussed. DOE

N92-31844# Brookhaven National Lab., Upton, NY.
ELECTRICALLY-INDUCED STRESSES AND DEFLECTION IN MULTIPLE PLATES
Jih-Perng Hu and P. R. Tichler 1992 8 p Presented at the 11th Symposium on Engineering Applications of Mechanics, Saskatchewan (Canada), 11 May 1992
(Contract DE-AC02-76CH-00016)
(DE92-012303; BNL-47331; CONF-9205145-1) Avail: CASI HC A02/MF A01

Thermohydraulic tests are being planned at the High Flux Beam Reactor of Brookhaven National Laboratory, in which direct electrical heating of metal plates will simulate decay heating in parallel plate-type fuel elements. The required currents are high if plates are made of metal with a low electrical resistance, such as aluminum. These high currents will induce either attractive or repulsive forces between adjacent current-carrying plates. Such forces, if strong enough, will cause the plates to deflect and so change the geometry of the coolant channel between the plates. Since this is undesirable, an analysis was made to evaluate the magnitude of the deflection and related stresses. In contrast to earlier publications in which either a concentrated or a uniform load was assumed, in this paper an exact force distribution on the plate is analytically solved and then used for stress and deflection calculations, assuming each plate to be a simply supported beam. Results indicate that due to superposition of the induced forces between plates in a multiple-and-parallel plate array, the maximum deflection and bending stress occur at the midpoint of the outermost plate. The maximum shear stress, which is inversely proportional to plate thickness, occurs at both ends of the outermost plate. DOE

N92-31847# Wright Lab., Wright-Patterson AFB, OH.
VAASEL-ANSYS COMPARISON FOR A THERMALLY LOADED BEAM Report, Apr. - May 1991
Estelle R. Anselmo Aug. 1991 16 p
(AD-A251003; WL-TM-92-308-FIBE) Avail: CASI HC A03/MF A01

This report presents the results of calculating the deflection and stresses in a thermally loaded beam. Three different methods were used for the calculation: classical beam theory, ANSYS (Version 4.4), and VAASEL (Version 1.1). Comparisons between each of the methods are presented. GRA

N92-31911*# Cincinnati Univ., OH. Dept. of Aerospace Engineering and Engineering Mechanics.
STRUCTURAL SIMILITUDE AND SCALING LAWS FOR LAMINATED BEAM-PLATES
George J. Simitses and Jalil Rezaeepazhand Jul. 1992 78 p
(Grant NAG1-1280)
(NASA-CR-190585; NAS 1.26:190585) Avail: CASI HC A05/MF A01

The establishment of similarity conditions between two structural systems is discussed. Similarity conditions provide the relationship

between a scale model and its prototype and can be used to predict the behavior of the prototype by extrapolating the experimental data of the corresponding small-scale model. Since satisfying all the similarity conditions simultaneously is difficult or even impossible, distorted models with partial similarity (with at least one similarity condition relaxed) are more practical. Establishing similarity conditions based on both dimensional analysis and direct use of governing equations is discussed, and the possibility of designing distorted models is investigated. The method is demonstrated through analysis of the cylindrical bending of orthotropic laminated beam-plates subjected to transverse line loads. Author

N92-31989# Air Force Inst. of Tech., Wright-Patterson AFB, OH.
EXPERIMENTAL FEEDBACK OF FRACTIONAL ORDER STATES OF A LIGHTLY DAMPED STRUCTURE M.S. Thesis
Robert C. McCall Mar. 1992 100 p
(AD-A248027; AFIT/GA/92M/01; AFIT/GA/ENY/90M-01) Avail: CASI HC A05/MF A02

The purpose of this study was to investigate the effectiveness of using fractional order time derivatives of position feedback signals in the active control of vibration. To that end, circuitry was built and evaluated that finds the half order derivative of an input signal. The magnitude responses of the fractional derivative circuits is very good, but there are large phase shifts present that may degrade the performance of the controllers. Two methods of incorporating the fractional derivative signals into the controller were examined. One method involved developing a similarity transformation that transforms an integer order state controller into an equivalent controller using fractional or mixed fractional and integer order signals. The second method was a form of traditional pole placement techniques that allowed the direct designs of a controller using fractional and integer order feedback signals. Designs were tested on an inverted cantilever beam, with control provided by a shaker, and compared to theoretical predictions and to traditional integer order controllers. There is a discrepancy in the modeling that manifests itself as a large offset in magnitude, particularly at very low frequencies. However, controllers utilizing fractional order feedback provided nearly identical control authority to the traditional integer order designs. GRA

N92-32088# Sandia National Labs., Albuquerque, NM.
A GENERALIZATION TO STOCHASTIC AVERAGING IN RANDOM VIBRATION
J. R. Red-Horse Jun. 1992 32 p
(Contract DE-AC04-76DP-00789)
(DE92-016747; SAND-89-2608) Avail: CASI HC A03/MF A01

Stochastic Averaging is applied to a class of randomly excited single degree-of-freedom oscillators possessing linear damping and nonlinear stiffness terms. The assumed excitation form involves an externally applied evolutionary Gaussian stochastic process. Special emphasis is placed on casting the problem in a more formal mathematical framework than that traditionally used in engineering applications. For the case under consideration, it is shown that a critical step involves the selection of an appropriate period of oscillation over which the temporal averaging can be performed. As an example, this averaging procedure is performed on a Duffing oscillator. The validity of the derived result is partially confirmed by reducing it is to special case, for which there is a known solution, and comparing both solutions. DOE

N92-32168# Arizona Univ., Tucson. Engineering Experiment Station.
INSTABILITIES OF DAMAGE AND SURFACE DEGRADATION MECHANISMS IN BRITTLE MATERIAL STRUCTURAL SYSTEMS Final Report, 1 Jul. 1989 - 31 Dec. 1991
F. F. Tang, G. N. Frantziskonis, and C. S. Desai 15 Mar. 1992 313 p
(Grant AF-AFOSR-0460-89)
(AD-A250785; AFOSR-92-0366TR) Avail: CASI HC A14/MF A03

A review of the theoretical and experimental information on surface degradation and related instabilities is presented, and the physical significance of surface or skin effects is identified. The research involves study of relation between surface degradation and scale or size as well as shape effects, and surface damage growth instabilities and related bursting in brittle materials. A theory is developed to trace growth of surface degradation and to identify onset of relevant instabilities. Here, internal length is also estimated based on available experimental results. A comprehensive series of laboratory compression tests are performed on rectangular specimens with different dimensions of an artificial rock-like material. Simultaneous nondestructive ultrasonic measurements are obtained at various locations on the specimens. The damage and instability distributions obtained by using a finite element procedure and symbolic computation are related to the dissipated energy derived from ultrasonic measurements. Comparisons of theoretical predictions and nondestructive measurements correlate very well. GRA

N92-32206# Polish Academy of Sciences, Warsaw. Inst. Podstawowych Problemow Techniki.
ACOUSTIC EMISSION METHOD APPLIED TO TESTS ON CONCRETE [METODA EMISJI AKUSTYCZNEJ W ZASTOSOWANIU DO BADANIA BETONU]
Jerzy Hola (Wroclaw Univ., Poland) and Zbigniew Ranachowski 1991 29 p In POLISH
Avail: CASI HC A03/MF A01

The possibilities of using the acoustic emission method in testing concrete are demonstrated. Basic information on acoustic emission as a phenomenon, a research-method description of measuring parameters and measuring systems, and a description of foreign and domestic equipment are presented. A cross-sectional review of the results of experiments and research works obtained in our country during the last ten years is provided. References containing detailed data related both to the description of experiments and works performed and to the results obtained are included. Author

N92-32235*# Virginia Polytechnic Inst. and State Univ., Blacksburg. Dept. of Engineering Science and Mechanics.
OPTIMAL DESIGN OF GEODESICALLY STIFFENED COMPOSITE CYLINDRICAL SHELLS Report, Sep. 1989 - Sep. 1991
G. Gendron and Z. Guerdal Aug. 1992 222 p
(Grant NAG1-643)
(NASA-CR-190706; NAS 1.26:190706; CCMS-92-23; VPI-E-92-20)
Avail: CASI HC A10/MF A03

An optimization system based on the finite element code Computations Structural Mechanics (CSM) Testbed and the optimization program, Automated Design Synthesis (ADS), is described. The optimization system can be used to obtain minimum-weight designs of composite stiffened structures. Ply thickness, ply orientations, and stiffener heights can be used as design variables. Buckling, displacement, and material failure constraints can be imposed on the design. The system is used to conduct a design study of geodesically stiffened shells. For comparison purposes, optimal designs of unstiffened shells and shells stiffened by rings and stingers are also obtained. Trends in the design of geodesically stiffened shells are identified. An approach to include local stress concentrations during the design optimization process is then presented. The method is based on a global/local analysis technique. It employs spline interpolation functions to determine displacements and rotations from a global model which are used as 'boundary conditions' for the local model. The organization of the strategy in the context of an optimization process is described. The method is validated with an example. Author

N92-32236*# Duke Univ., Durham, NC. Dept. of Mechanical Engineering.
ASYMPTOTIC MODAL ANALYSIS AND STATISTICAL ENERGY ANALYSIS Final Report, 15 Oct. 1986 - 15 Feb. 1992
Earl H. Dowell Jul. 1992 59 p

(Grant NAG1-709)
(NASA-CR-190516; NAS 1.26:190516) Avail: CASI HC A04/MF A01

Asymptotic Modal Analysis (AMA) is a method which is used to model linear dynamical systems with many participating modes. The AMA method was originally developed to show the relationship between statistical energy analysis (SEA) and classical modal analysis (CMA). In the limit of a large number of modes of a vibrating system, the classical modal analysis result can be shown to be equivalent to the statistical energy analysis result. As the CMA result evolves into the SEA result, a number of systematic assumptions are made. Most of these assumptions are based upon the supposition that the number of modes approaches infinity. It is for this reason that the term 'asymptotic' is used. AMA is the asymptotic result of taking the limit of CMA as the number of modes approaches infinity. AMA refers to any of the intermediate results between CMA and SEA, as well as the SEA result which is derived from CMA. The main advantage of the AMA method is that individual modal characteristics are not required in the model or computations. By contrast, CMA requires that each modal parameter be evaluated at each frequency. In the latter, contributions from each mode are computed and the final answer is obtained by summing over all the modes in the particular band of interest. AMA evaluates modal parameters only at their center frequency and does not sum the individual contributions from each mode in order to obtain a final result. The method is similar to SEA in this respect. However, SEA is only capable of obtaining spatial averages or means, as it is a statistical method. Since AMA is systematically derived from CMA, it can obtain local spatial information as well. Author

N92-31873# Tel-Aviv Univ. (Israel). Dept. of Solid Mechanics, Materials and Structures.
THE DESIGN AND TESTING OF AN OPTIMAL BEAM COMPOSED OF UNIMODAL ELEMENTS
Moshe B. Fuchs, Gideon Benyamini, and Ehud Bousso *In* Israel Society of Aeronautics and Astronautics, 31st Israel Annual Conference on Aviation and Astronautics 22 Feb. 1990 p 76-80 Previously announced in IAA as A91-43087 (For primary document see N92-31861 22-01)
Avail: CASI HC A01/MF A03

42 GEOSCIENCES (GENERAL)

N92-32132# Joint Publications Research Service, Arlington, VA.
JPRS REPORT: SCIENCE AND TECHNOLOGY. CENTRAL EURASIA: EARTH SCIENCES
23 Jul. 1992 40 p Transl. into ENGLISH from various Russian articles
(JPRS-UES-92-004) Avail: CASI HC A03/MF A01

A bibliography of Central Eurasian research in Earth sciences is given. Topics covered include oceanography, atmospheric physics, and ecology. Author

43 EARTH RESOURCES AND REMOTE SENSING

Includes remote sensing of earth resources by aircraft and spacecraft; photogrammetry; and aerial photography.

For instrumentation see *35 Instrumentation and Photography.*

N92-31277# Instituto de Pesquisas Espaciais, Sao Jose dos Campos (Brazil).
PROCEDURES AND ERRORS IN THE DETERMINATION OF THE BI-DIRECTIONAL REFLECTANCE FACTOR AND OTHER RADIOMETRIC QUANTITIES M.S. Thesis [PROCESSOS E ERROS NA DETERMINACAO DO FATOR DE REFLECTANCIA BIDIRECIONAL E DE OUTRAS GRANDEZAS RADIOMETRICAS]
Pedro NevesdaSilvaFilho Apr. 1992 158 p In PORTUGESE
(INPE-5386-TDI/475) Avail: CASI HC A08/MF A02

To determine the reflectance factor of important targets through irradiance and/or radiance measurements is necessary for many applications of remote sensing. For other applications, it is enough to measure absolute radiometric quantities. In the measurement procedures, many errors can be introduced. Through radiance measurements, computations of bi-directional reflectance factor and diffuse directional reflectance factor, the errors which some parameters can introduce in the measured values of radiometric quantities were studied and analyzed. The obtained results show the necessity of using correct measurement procedures such as: (1) calibration of reference plates and radiometers; (2) inter-calibration of radiometers; (3) attention to irradiance variations due to atmospheric changes or the presence of neighboring targets; and (4) geometric modifications of radiation during the measurement. Author

N92-31323# Mitre Corp., Bedford, MA.
COMPRESSION OF DIGITIZED MAP IMAGES Final Report
D. A. Southard Mar. 1992 55 p
(Contract F19628-89-C-0001)
(AD-A250707; MTR-11201; ESD-TR-92-052) Avail: CASI HC A04/MF A01

The Air Force Mission Support System (AF MSS) will display digital images of navigational charts. The Defense Mapping Agency's (DMA) Equal Arc-Second Raster Chart (ARC) Digitized Raster Graphics (ADRG) products will be the primary source of data. System cost and performance goals require a storage reduction ratio of 48:1 for these images. This reduction will be obtained through a combination of spatial reduction, image compression, and color quantization. The AF MSS system specification admits many possible implementations at each step. Some combinations of options do not yield satisfactory results. This report describes a series of investigations into these three areas. We evaluate alternative algorithms, and identify a set of choices that offer the best image quality and performance, based on our prototype tests. GRA

N92-31329# Air Force Inst. of Tech., Wright-Patterson AFB, OH.
SUN-VIEW-TARGET GEOMETRY EFFECTS ON SPECTRALLY-DERIVED VEGETATIVE INDEX ESTIMATES OF ABSORBED RADIATION AND LEAF AREA M.S. Thesis
Daniel Cornell Jun. 1991 146 p
(AD-A249984; AFIT/CI/CIA-91-114) Avail: CASI HC A07/MF A02

Estimating the quantity and quality of vegetation is a primary goal of remote sensing. The impact of changing sun-view-target geometry on spectral measures of vegetative amount (vegetative indices, VIs) is a major source of concern with this pursuit. A field experiment was conducted to test the statistical significance of solar and view zenith angle effects on the regression coefficients of relationships established between the simple ratio and normalized difference vegetation indices and the biophysical parameters fraction of absorbed photosynthetically active radiation (APAR) and leaf area index (LAI). Measurements of spectral

bidirectional reflectance and biophysical parameters were made in an alfalfa (Medicago Sativa, L.) field located near Mead, NE throughout the 1990 growing season. View and solar zenith angle effects on VIs were found to statistically affect (at a - 0.05) the regression coefficients for relationships established between VIs and APAR and LAI. While APAR was best estimated with nadir or near nadir-derived VIs for all solar zenith angles, no one view zenith angle at all solar zenith angles best estimated LAI from the two VIs. Despite the statistical significance of view and solar zenith angle effects on regression parameters, estimation of APAR and LAI with VIs derived from off-nadir spectral data used in nadir derived regression relationships resulted in D-indices of agreement greater than 0.94 with measured values of APAR and LAI. GRA

N92-31357*# Wyoming Univ., Laramie. Dept. of Atmospheric Science.
AN AIRBORNE STUDY OF BOUNDARY LAYER HEAT AND MOISTURE FLUXES FOR PROJECT FIFE Final Report
Robert D. Kelly 1992 7 p
(Grant NAG5-913)
(NASA-CR-190665; NAS 1.26:190665) Avail: CASI HC A02/MF A01

A summary of work accomplished during the first International Satellite Cloud Climatology Project (ISLSCP) Field Experiment is presented. The Wyoming King Air participated in Intensive Field Campaigns (IFCs) 3 and 4 in 1987, which were committed to a combination of airborne sensible and latent heat flux measurements and soil moisture mappings, with the University of Kansas' X-band side-looking airborne radar (SLAR). A total of 9 flux missions were flown in 1987 using several different flight designs. A critical decision in the first round of aircraft flux analyses, agreed to by all the flux aircraft investigators, was to pass the aircraft data through a high-pass filter prior to the eddy-correlation flux calculations. Several conclusions were drawn from this study: (1) boundary layer (BL) profiles of heat fluxes were usually linear; (2) high-pass filtering applied to the aircraft data did not add to the disagreement between the profile; (3) undersampling at high frequencies could have accounted for as much as a 15 percent underestimate of surface fluxes; (4) disagreement between the aircraft and surface latent heat fluxes changed signs between summer and fall; (5) magnitude and sign of disagreement between aircraft and surface heat fluxes varied systematically with BL depth or height of aircraft profile; and (6) Bowen ratios from both detrended and filtered aircraft data agreed with surface values better for moist, summer cases than for dry cases. H.A.

N92-31362# Naval Ocean Systems Center, San Diego, CA.
REMOTE SENSING OF TRAPPING LAYER BASE HEIGHT USING ATIS TRANSMISSIONS
T. M. Vuong Dec. 1991 26 p
(AD-A250074; NOSC/TR-1487) Avail: CASI HC A03/MF A01

This report describes an experiment that examined the method of determining a trapping layer directly from VHF and UHF radio measurements. The experiment used existing radio broadcasts along the coast of southern California. Some strong correlations between the observed signal strengths and the inferred trapping layer base heights of the various radio paths were shown, indicating the height of the trapping layer is an important factor in controlling radio propagation on over-the-horizon paths. GRA

N92-31621# Army Engineer School, Fort Leonard Wood, MO.
RESULTS OF EARTH OBSERVATION STUDY ON STS-31 FOR TERRA GEODE, JANUARY 1987 - JUNE 1991
John Karpiscak, III May 1992 28 p
(AD-A250750; TEC-0009) Avail: CASI HC A03/MF A01

Terra Geode is a MMIS experiment developed by the U.S. Army Engineer School. The experiment is designed to evaluate the utility of a trained military space-based observer providing information for tactical movement. The experiment is being done in four phases: (1) military astronaut observations, (2) geologist-astronaut observations, (3) military payload specialist observations, and (4) permanent manned presence in space. Phase 1 consisted of the planning stages and informal discussions with military astronauts who had been asked to observe certain geological features. It was determined that further investigations were warranted for future phases. A geologist-astronaut flying on STS-31 agreed to conduct Phase 2 on a time-available basis. The flight of STS-31 was 5 days long, from 24 April to 1 May 1990. Many data points were observed during STS-31's high altitude, short duration flight. It was determined that it is feasible to identify and record the various elements that comprise a mobility prediction, and to explore the degree of accuracies that can reasonably be expected from a trained observer in orbit. GRA

N92-32127*# National Aeronautics and Space Administration. Langley Research Center, Hampton, VA.
MISSION DESCRIPTION AND IN-FLIGHT OPERATIONS OF ERBE INSTRUMENTS ON ERBS, NOAA 9, AND NOAA 10 SPACECRAFT Report, Feb. 1986 - Jan. 1987
William L. Weaver, Kathryn A. Bush (ST Systems Corp., Hampton, VA.), Keith T. Degnan (ST Systems Corp., Hampton, VA.), Clayton E. Howerton (ST Systems Corp., Hampton, VA.), and Carol J. Tolson (ST Systems Corp., Hampton, VA.) Aug. 1992 217 p
(RTOP 665-45-20)
(NASA-RP-1279; L-17069; NAS 1.61:1279) Avail: CASI HC A10/MF A03

Instruments of the Earth Radiation Budget Experiment (ERBE) are operating on three different Earth-orbiting spacecraft. The Earth Radiation Budget Satellite (ERBS) is operated by NASA, and NOAA 9 and NOAA 10 weather satellites are operated by the National Oceanic and Atmospheric Administration (NOAA). This paper is the second in a series that describes the ERBE mission, and data processing and validation procedures. This paper describes the spacecraft and instrument operations for the second full year of in-orbit operations, which extend from February 1986 through January 1987. Validation and archival of radiation measurements made by ERBE instruments during this second year of operation were completed in July 1991. This period includes the only time, November 1986 through January 1987, during which all ERBE instruments aboard the ERBE, NOAA 9, and NOAA 10 spacecraft were simultaneously operational. This paper covers normal and special operations of the spacecraft and instruments, operational anomalies, and the responses of the instruments to in-orbit and seasonal variations in the solar environment. Author

N92-32216# Defence Research Establishment Pacific, Victoria (British Columbia). Research and Development Branch.
OSRMS: THE DREP NEAR-NADIR SCATTEROMETER
L. C. Rempel, B. A. Hughes, and S. J. Hughes Aug. 1988 43 p
(DREP-88-15; CTN-92-60338) Avail: CASI HC A03/MF A01

The ocean surface roughness measurement system (OSRMS) is a near-nadir directed infrared (IR) scatterometer specially constructed for and operated by the Defence Research Establishment Pacific (DREP). It has been used to measure ocean surface parameters and particularly for the examination from an aircraft of internal waves. This paper gives a description of the configuration and operation of the OSRMS including the mechanical, electrical, electronic, optical, and software components. A brief overview of the trials in which the OSRMS took part is included, with the main focus on the 1987 trial, SCATTMOD III and the data obtained in that trial. An infrared laser system at a wavelength of 1.06 micrometers operating on a Convair-580 aircraft was used for the trials. This frequency puts a limitation on the weather conditions since infrared is attenuated and scattered by aerosols and water vapor, and particularly by clouds. Lower frequencies have a high transmission through cloud but require larger and more complicated transmitters and receivers. The OSRMS was shown to be capable of taking quantitative measurements of ocean surface roughness parameters over a 100-meter swath at 200 knots aircraft speed. The equipment functioned very well (the roll compensation circuitry and the beam angle versus roll ramp linearity), yet areas for potential improvement still remain (hard disk drive problems and system noise). Also, the weather related limitations of this system were clearly evident. Data collected clearly showed internal waves, ship wakes, and

wind speed effects. The speckle noise level for data taken in open ocean conditions under moderate wind speeds was larger than that predicted by previous measurements in inshore waters. CISTI

N92-32220# Instituto de Pesquisas Espaciais, Sao Jose dos Campos (Brazil).
IMAGES SIMULATION OF SENSORS WITH LARGE FIELD OF VIEW FROM IMAGES OF SENSORS WITH LESS FIELD OF VIEW: THE SSR/TM CASE M.S. Thesis [SIMULACAO DE IMAGENS DE SENSORES COM LARGO CAMPO DE VISADA A PARTIR DE IMAGENS DE SENSORES COM MENOR CAMPO DE VISADA: O CASO SSR/TM]
Ailton CruzdosSantos Mar. 1992 134 p In PORTUGESE (INPE-5378-TDI/473) Avail: CASI HC A07/MF A02

In this work, the simulation of the raw image obtained by an orbital sensor with large field of view, under an approximate model for the SSR (Remote Sensing Satellite) of MECB (Brazilian Complete Spatial Mission) from a set of images obtained by a sensor with smaller field of view is presented. Actually, a set of images obtained by the LANDSAT/TM (Thematic Mapper) constructed under geometric control in a cartographic projection and corrected by control points was used. Using an earth surface model, the points within the surface corresponding to each detector center projection (in geodetic coordinates - latitude and longitude) are determined. The values of the pixels of the image with large field of view are calculated from the pixels of the TM image in the neighborhood of these points. This calculation is done using an adaptive simulation filter. The results appear to be satisfactory from the geometric point of view adopted in this work. Author

N92-32223*# Cambridge Research and Instrumentation, Inc., MA.
WAVELENGTH-TUNABLE LIQUID CRYSTAL IMAGING FILTERS FOR REMOTE SENSING FROM GEOSYNCHRONOUS PLATFORMS Interim Report
Peter Foukal 26 Aug. 1992 16 p Sponsored by NASA. Marshall Space Flight Center
(Contract NAS7-1170; NASA Order H-11987-D)
(NASA-CR-190698; NAS 1.26:190698; CRI-P45-1) Avail: CASI HC A03/MF A01

We have reviewed spectral requirements of planned NASA geosynchronous remote sensing missions and identified several applications of the liquid crystal tunable filter (LCTF) technology. We have modeled the LCTF performance in the visible and near-infrared and carried out a literature study on space-hardening of the filter components to evaluate the suitability of LCTF's for geosynchronous missions. We have also compared the power consumption, weight, size, reliability, and optical performance of an imaging spectrophotometer using a LCTF monochromator to other instruments that have been put forward for remote sensing from geosynchronous platforms. We put forward some conceptual designs for LCTF's that seem to offer important advantages in wavelength-flexibility, tuning speed, power consumption, and reliability over the mechanical filter wheels presently baselined for the High Resolution Earth Processes Imager (HEPI) and the Advanced Lightning Mapper (ALM) experiments. The extremely wide acceptance angle achievable with LCTF's could also avoid the need for large-aperture interference filters in the ALM (and LIS) experiments. Author

44 ENERGY PRODUCTION AND CONVERSION

Includes specific energy conversion systems, e.g., fuel cells; global sources of energy; geophysical conversion; and windpower.

For related information see also *07 Aircraft Propulsion and Power, 20 Spacecraft Propulsion and Power,* and *28 Propellants and Fuels.*

N92-31262*# National Aeronautics and Space Administration. Lewis Research Center, Cleveland, OH.
A FREE-PISTON STIRLING ENGINE/LINEAR ALTERNATOR CONTROLS AND LOAD INTERACTION TEST FACILITY
Jeffrey S. Rauch (Sverdrup Technology, Inc., Brook Park, OH.), M. David Kankam, Walter Santiago, and Frank J. Madi (Sverdrup Technology, Inc., Brook Park, OH.) Aug. 1992 8 p Presented at the 27th Intersociety Energy Conversion Conference, San Diego, CA, 3-7 Aug. 1992; sponsored by SAE
(Contract NAS3-25266; RTOP 590-13-11)
(NASA-TM-105825; E-7259; NAS 1.15:105825) Avail: CASI HC A02/MF A01

A test facility at LeRC was assembled for evaluating free-piston Stirling engine/linear alternator control options, and interaction with various electrical loads. This facility is based on a 'SPIKE' engine/alternator. The engine/alternator, a multi-purpose load system, a digital computer based load and facility control, and a data acquisition system with both steady-periodic and transient capability are described. Preliminary steady-periodic results are included for several operating modes of a digital AC parasitic load control. Preliminary results on the transient response to switching a resistive AC user load are discussed. Author

N92-31290# National Association of Regulatory Utility Commissioners, Washington, DC.
NATIONAL CONFERENCE ON INTEGRATED RESOURCE PLANNING: PROCEEDINGS
1991 586 p Conference held in Santa Fe, NM, 8-10 Apr. 1991
(Contract DE-FG01-89CE-28301)
(DE92-013573; CONF-9104196) Avail: CASI HC A25/MF A05

Until recently, state regulators have focused most of their attention on the development of least-cost or integrated resource planning (IRP) processes for electric utilities. A number of commissions are beginning to scrutinize the planning processes of local gas distribution companies (LDCs) because of the increased control that LDCs have over their purchased gas costs (as well as the associated risks) and because of questions surrounding the role and potential of gas end-use efficiency options. Traditionally, resource planning (LDCs) has concentrated on options for purchasing and storing gas. Integrated resource planning involves the creation of a process in which supply-side and demand-side options are integrated to create a resource mix that reliably satisfies customers' short-term and long-term energy service needs at the lowest cost. As applied to gas utilities, an integrated resource plan seeks to balance cost and reliability, and should not be interpreted simply as the search for lowest commodity costs. The National Association of Regulatory Utility Commissioners' (NARUC) Energy Conservation committee asked Lawrence Berkeley Laboratory (LBL) to survey state PUCs to determine the extent to which they have undertaken least cost planning for gas utilities. The survey included the following topics: status of state PUC least-cost planning regulations and practices for gas utilities; type and scope of natural gas DSM programs in effect, including fuel substitution; economic tests and analysis methods used to evaluate DSM programs; relationship between prudency reviews of gas utility purchasing practices and integrated resource planning; and key regulatory issues facing gas utilities during the next five years. DOE

N92-31481# Midwest Research Inst., Golden, CO. National Renewable Energy Lab.
SOLAR SYNTHESIS OF ADVANCED MATERIALS: A SOLAR INDUSTRIAL PROGRAM INITIATIVE

A. Lewandowski Jun. 1992 6 p
(Contract DE-AC02-83CH-10093)
(DE92-010575; NREL/TP-432-4734) Avail: CASI HC A02/MF A01

This is an initiative for accelerating the use of solar energy in the advanced materials manufacturing industry in the United States. The initiative will be based on government-industry collaborations that will develop the technology and help US industry compete in the rapidly expanding global advanced materials marketplace. Breakthroughs in solar technology over the last 5 years have created exceptional new tools for developing advanced materials. Concentrated sunlight from solar furnaces can produce intensities that approach those on the surface of the sun and can generate temperatures well over 2000 C. Very thin layers of illuminated surfaces can be driven to remarkably high temperatures in a fraction of a second. Concentrated solar energy can be delivered over large areas, allowing for rapid processing and high production rates. By using this technology, researchers are transforming low-cost raw materials into high-performance products. Solar synthesis of advanced materials uses bulk materials and energy more efficiently, lowers processing costs, and reduces the need for strategic materials -- all with a technology that does not harm the environment. The Solar Industrial Program has built a unique, world class solar furnace at NREL to help meet the growing need for applied research in advanced materials. Many new advanced materials processes have been successfully demonstrated in this facility, including metalorganic deposition, ceramic powders, diamond-like carbon materials, rapid heat treating, and cladding (hard coating). DOE

N92-31497# Midwest Research Inst., Golden, CO. National Renewable Energy Lab.
MODULE PROCESS OPTIMIZATION AND DEVICE EFFICIENCY IMPROVEMENT FOR STABLE, LOW-COST, LARGE-AREA, CADMIUM TELLURIDE-BASED PHOTOVOLTAIC MODULE PRODUCTION
S. P. Albright, B. Ackerman, R. R. Chamberlin, and J. F. Jordan (Photon Energy, Inc., El Paso, TX.) Apr. 1992 22 p
(Contract DE-AC02-83CH-10093)
(DE92-010564; NREL/TP-413-4873) Avail: CASI HC A03/MF A01

This report describes work under a three-year phased subcontract to develop CdS/CdTe devices and modules and to further improve the technology base at Photon Energy, Inc. (PEI) to better address the commercialization issues and objectives of the PEI and the US Department of Energy. During this reporting period we (1) achieved efficiencies of 12.7 percent on small area devices, (2) achieved 1-ft(exp 2) modules with over 8 percent aperture-area efficiency (and active area efficiencies up to approximately 10 percent, (3) tested 4-ft(exp 2) modules at NREL at 23.1 (21.3) watts, normalized (6.3 percent efficiency), and (4) found no inherent stability problems with CdTe technology during life testing, at both NREL and PEI. DOE

N92-31498# Midwest Research Inst., Golden, CO. National Renewable Energy Lab.
A SURFACE DEFINITION CODE FOR TURBINE BLADE SURFACES
S. L. Yang (Michigan Technological Univ., Houghton.), D. Oryang, and M. J. Ho (Tuskegee Inst., AL.) May 1992 207 p
(Contract DE-AC02-83CH-10093)
(DE92-010574; NREL/TP-257-4099) Avail: CASI HC A10/MF A03

A numerical interpolation scheme has been developed for generating the three-dimensional geometry of wind turbine blades. The numerical scheme consists of (1) creating the frame of the blade through the input of two or more airfoils at some specific spanwise stations and then scaling and twisting them according to the prescribed distributions of chord, thickness, and twist along the span of the blade; (2) transforming the physical coordinates of the blade frame into a computational domain that complies with the interpolation requirements; and finally (3) applying the bi-tension spline interpolation method, in the computational domain, to determine the coordinates of any point on the blade surface. Detailed descriptions of the overall approach to and philosophy of the code development are given along with the operation of the code. To show the usefulness of the bi-tension spline interpolation code developed, two examples are given, namely CARTER and MICON blade surface generation. Numerical results are presented in both graphic data forms. The solutions obtained in this work show that the computer code developed can be a powerful tool for generating the surface coordinates for any three-dimensional blade. DOE

N92-31526# Midwest Research Inst., Golden, CO.
DEVELOPMENT OF A COMPUTER MODEL FOR POLYCRYSTALLINE THIN-FILM CuInSe2 AND CdTe SOLAR CELLS
J. L. Gray (Purdue Univ., West Lafayette, IN.), R. J. Schwartz (Purdue Univ., West Lafayette, IN.), and Y. J. Lee (Purdue Univ., West Lafayette, IN.) Apr. 1992 36 p
(Contract DE-AC02-83CH-10093)
(DE92-001242; NREL/TP-413-4835) Avail: CASI HC A03/MF A01

This report describes work to develop a highly accurate numerical model for CuInSe2 and CdTe solar cells. ADEPT (A Device Emulation Program and Toolbox), a one-dimensional semiconductor device simulation code developed at Purdue University, was used as the basis of this model. An additional objective was to use ADEPT to analyze the performance of existing and proposed CuInSe2 and CdTe solar cell structures. The work is being performed in two phases. The first phase involved collecting device performance parameters, cell structure information, and material parameters. This information was used to construct the basic models to simulate CuInSe2 and CdTe solar cells. This report is a tabulation of information gathered during the first phase of this project on the performance of existing CuInSe2 and CdTe solar cells, the material properties of CuInSr2, CdTe, and CdS, and the optical absorption properties of CuInSe2, CdTe, and CdS. The second phase will entail further development and the release of a version of ADEPT tailored to CuInSe2 and CdTe solar cells that can be run on a personal computer. In addition, ADEPT will be used to analyze the performance of existing and proposed CuInSe2 and CdTe solar cell structures. DOE

N92-31531# Argonne National Lab., IL.
SODIUM HEAT ENGINE DEVELOPMENT PROGRAM
J. P. Singh, D. S. Kupperman, S. Majumdar, S. Dorris, N. Gopalsami, S. L. Dieckman, R. A. Jaross, D. L. Johnson, J. S. Gregar, and R. B. Poeppel et al Jan. 1992 138 p
(Contract W-31-109-eng-38)
(DE92-012398; ANL-91/45) Avail: CASI HC A07/MF A02

The Sodium Heat Engine (SHE) is an efficient thermoelectric conversion device which directly generates electricity from a thermally regenerative electrochemical cell that relies on the unique conduction properties of beta''-alumina solid electrolyte (BASE). Laboratory models of a variety of SHE devices have demonstrated the feasibility and efficiency of the system; engineering development of large prototype devices has been slowed by a series of materials and fabrication problems. Failure of the electrolyte tubes has been a recurring problem and a number of possible causes have been postulated. To address these issues, a two-phase engineering development program was undertaken. This report summarizes the final results of the first phase of the program, which included extensive materials characterization activities, a study of applicable nondestructive evaluation methods, an investigation of possible stress states that would contribute to fracture, and certain operational issues associated with the electromagnetic pumps used in the SHE prototype. Mechanical and microstructural evaluation of commercially obtained BASE tubes revealed that they should be adequate for SHE applications and that sodium exposure produced no appreciable deleterious strength effects. Processing activities to produce a more uniform and smaller grain size for the BASE tubes were completed using isostatic pressing, extrusion, and slip casting. Green tubes were sintered by conventional and microwave plasma methods. Of

particular interest is the residual stress state in the BASE tubes, and both analysis and nondestructive evaluation methods were employed to evaluate these stresses. X-ray and neutron diffraction experiments were performed to determine the bulk residual stresses in commercially fabricated BASE tubes; however, tube-to-tube variations and variations among the various methods employed did not allow formulation of a definitive definition of the as-fabricated stress state. DOE

N92-31571# Los Alamos National Lab., NM.
BATTERIES AND FUEL CELLS Working Group Report
J. Eberhardt (Department of Energy, Washington, DC.) and A. Landgrebe (Department of Energy, Washington, DC.) 1991 12 p Presented at the Surface Processing Applications to Transportation and Utilities Technologies, Washington, DC, 10-12 Dec. 1991
(Contract W-7405-eng-36)
(DE92-011493; LA-UR-92-984; CONF-9112112-1) Avail: CASI HC A03/MF A01

Electrochemical energy systems are dominated by interfacial phenomena. Catalysis, corrosion, electrical and ionic contact, and wetting behavior are critical to the performance of fuel cells and batteries. Accordingly, development of processing techniques to control these surface properties is important to successful commercialization of advanced batteries and fuel cells. Many of the surface processing issues are specific to a particular electrochemical system. Therefore, the working group focused on systems that are of specific interest to DOE/conservation and renewable energy. These systems addressed were: polymer electrolyte membrane (PEM) fuel cells, direct methanol oxidation (DMO) fuel cells, and lithium/polymer batteries. The approach used by the working group for each of these systems was to follow the current path through the system and to identify the principal interfaces. The function of each interface was specified together with its desired properties. The degree to which surface properties limit performance in present systems was rated. Finally, the surface processing needs associated with the performance limiting interfaces were identified. This report summarizes this information. DOE

N92-31579# Midwest Research Inst., Golden, CO.
COOPERATIVE FIELD TEST PROGRAM FOR WIND SYSTEMS
W. S. Bollmeier, II and D. M. Dodge Mar. 1992 38 p
(Contract DE-AC02-83CH-10093)
(DE92-001209; NREL/TP-253-4252) Avail: CASI HC A03/MF A01

The objectives of the Federal Wind Energy Program, managed by the US Department of Energy (DOE), are (1) to assist industry and utilities in achieving a multi-regional US market penetration of wind systems, and (2) to establish the United States as the world leader in the development of advanced wind turbine technology. In 1984, the program conducted a series of planning workshops with representatives from the wind energy industry to obtain input on the Five-Year Research Plan then being prepared by DOE. One specific suggestion that came out of these meetings was that the federal program should conduct cooperative research tests with industry to enhance the technology transfer process. It was also felt that the active involvement of industry in DOE-funded research would improve the state of the art of wind turbine technology. DOE established the Cooperative Field Test Program (CFTP) in response to that suggestion. This program was one of the first in DOE to feature joint industry-government research test teams working toward common objectives. DOE

N92-31594# Energy Information Administration, Washington, DC. Office of Integrated Analysis and Forecasting.
WORLD ENERGY PROJECTION SYSTEM: MODEL DOCUMENTATION
Jun. 1992 62 p
(DE92-014206; DOE/EIA-M050(92)) Avail: CASI HC A04/MF A01

The World Energy Project System (WEPS) is an accounting framework that incorporates projects from independently documented models and assumptions about the future energy intensity of economic activity (ratios of total energy consumption divided by gross domestic product) and about the rate of incremental energy requirements met by hydropower, geothermal, coal, and natural gas to produce projections of world energy consumption published annually by the Energy Information Administration (EIA) in the International Energy Outlook (IEO). Two independently documented models presented in Figure 1, the Oil Market Simulation (OMS) model and the World Integrated Nuclear Evaluation System (WINES), provide projections of oil and nuclear power consumption published in the IEO. Output from a third independently documented model, and the International Coal Trade Model (ICTM), is not published in the IEO but is used in WEPS as a supply check on projections of world coal consumption produced by WEPS and published in the IEO. A WEPS model of natural gas production documented in this report provides the same type of implicit supply check on the WEPS projections of world natural gas consumption published in the IEO. Two additional models are included in Figure 1, the OPEC Capacity model and the Non-OPEC Oil Production model. These WEPS models provide inputs to the OMS model and are documented in this report. DOE

N92-31623# Midwest Research Inst., Golden, CO. National Renewable Energy Lab.
OUTDOOR TESTING OF ADVANCED OPTICAL MATERIALS FOR SOLAR THERMAL ELECTRIC APPLICATIONS
T. J. Wendelin, G. Jorgensen, and R. M. Goggin May 1992 5 p Presented at the National Solar Energy Conference, Cocoa Beach, FL, 13-18 Jun. 1992
(Contract DE-AC02-83CH-10093)
(DE92-010567; NREL/TP-441-4801; CONF-920678-5) Avail: CASI HC A01/MF A01

The development of low-cost, durable advanced optical materials is an important element in making solar energy viable for electricity production. It is important to determine the expected lifetime of candidate reflector materials in real-world service conditions. The demonstration of the optical durability of such materials in outdoor environments is critical to the successful commercialization of solar thermal electric technologies. For many years, optical performance data have been collected and analyzed by the National Renewable Energy Laboratory (NREL) for candidate reflector materials subjected to simulated outdoor exposure conditions. Much of this testing is accelerated in order to predict service durability. Some outdoor testing has occurred, but not in a systematic manner. To date, simulated/accelerated testing has had limited correlation with actual outdoor exposure testing. Such a correlation is desirable to provide confidence in lifetime predictions based upon accelerated weathering methods. To obtain outdoor exposure data for realistic environments and to establish a data base for correlating simulated/accelerated outdoor exposure data with actual outdoor exposure data, the development of an expanded outdoor testing program has recently been initiated by NREL. Several outdoor test sites will be selected based on the solar climate, potential for solar energy utilization by industry, and cost of installation. Test results are site dependent because exposure conditions vary with geographical location. The importance of this program to optical materials development is outlined, and the process used to determine and establish the outdoor test sites is described. Candidate material identification and selection is also discussed. DOE

N92-31646# Midwest Research Inst., Golden, CO.
PHOTOVOLTAIC SUBCONTRACT PROGRAM, FY 1991
Mar. 1992 325 p
(Contract DE-AC02-83CH-10093)
(DE92-001248; NREL/TP-410-4724) Avail: CASI HC A14/MF A03

This report summarizes the FY-91 (October 1, 1990, through September 30, 1991) progress of the subcontracted photovoltaic (PV) research and development (R&D) performed under the Photovoltaic Advanced Research and Development Project at the National Renewable Energy Laboratory (NREL) - formerly the Solar

Energy Research Institute (SERI). The mission of the national PV program is to develop PV technology for large-scale generation of economically competitive electric power in the United States. The technical sections of the report cover the main areas of the subcontract program: the Amorphous Silicon Research Project, Polycrystalline Thin Films, Crystalline Silicon Materials Research, High-Efficiency Concepts, the New Ideas Program, the University Participation Program, and the Photovoltaic Manufacturing Technology (PVMaT) project. Technical summaries of each of the subcontracted programs provide a discussion of approaches, major accomplishments in FY-91, and future research directions. DOE

N92-31845# Pacific Northwest Lab., Richland, WA.
CHEMICAL ENERGY STORAGE SYSTEM FOR SEGS SOLAR THERMAL POWER PLANT
D. R. Brown, J. L. LaMarche, and G. E. Spanner Apr. 1992 20 p Presented at the International Solar Energy Conference, Honolulu, HI, 4-8 Apr. 1992
(Contract DE-AC06-76RL-01830)
(DE92-012327; PNL-SA-19467; CONF-920429-2) Avail: CASI HC A03/MF A01

The Pacific Northwest Laboratory evaluated the potential feasibility of using chemical energy storage at the Solar Electric Generating System (SEGS) power plants developed by Luz International. Like sensible or latent heat energy storage systems, chemical energy storage can be beneficially applied to solar thermal power plants to dampen the impact of cloud transients, extend the daily operating period, and/or allow a higher fraction of power production to occur during high-valued peak demand periods. Higher energy storage densities make chemical energy storage a potentially attractive option. The results of the evaluation indicated that a system based on the reversible reaction, CaO + H2O = Ca(OH)2, could be technically and economically feasible for this application, but many technical and economic issues must be resolved. DOE

N92-31893# Midwest Research Inst., Golden, CO.
ADVANCED HIGH EFFICIENCY CONCENTRATOR CELLS
R. Gale Jun. 1992 45 p Prepared in cooperation with Varian Associates, Palo Alto, CA
(Contract DE-AC02-83CH-10093)
(DE92-010559; NREL/TP-451-4855) Avail: CASI HC A03/MF A01

This report describes research to develop the technology needed to demonstrate a monolithic, multijunction, two-terminal, concentrator solar cell with a terrestrial power conversion efficiency greater than 35 percent. Under three previous subcontracts, Varian developed many of the aspects of a technology needed to fabricate very high efficiency concentrator cells. The current project was aimed at exploiting the new understanding of high efficiency solar cells. Key results covered in this report are as follows: (1) a 1.93-eV AlGaAs/1.42-eV GaAs metal-interconnected cascade cell was manufactured with a one-sun efficiency at 27.6 percent at air mass 1.5 (AM1.5) global; (2) a 1.0eV InGaAs cell was fabricated on the 'reverse' side of a low-doped GaAs substrate with a one-sun efficiency of 2.5 percent AM1.5 diffuse and a short-circuit current of 14.4 mA/cm(exp 2); (3) small-scale manufacturing of GaAs p/n concentrator cells was attempted and obtained an excellent yield of high-efficiency cells; (4) grown-in tunnel junction cell interconnects that are transparent and thermally stable using C and Si dopants were developed. DOE

N92-31903# Missouri Univ., Rolla. Dept. of Ceramic Engineering.
CHARACTERIZATION OF OXIDES FOR LOW TEMPERATURE SOLID OXIDE FUEL CELLS Annual Report, Sep. 1990 - Aug. 1991
H. U. Anderson and M. M. Nasrallah Oct. 1991 70 p Presented in part at GRI Annual Contractors Meeting, Chicago, IL, Oct. 1991
(Contract GRI-5090-260-2069)
(PB92-152883; GRI-91/0397) Avail: CASI HC A04/MF A01

The program has two major objectives: first, to identify appropriate processing techniques for thin film components to be used in solid oxide fuel cells (SOFC) operating at intermediate temperatures, and second, to develop and characterize potential mixed conducting oxides to be used as cathodes in intermediate temperature SOFC applications. Interaction studies between YSZ and LSM revealed the presence of La2Zr2O7 at the interface and the interdiffusion of ions. These interactions were significantly reduced by introducing a CeO2-based buffer layer between LSM and YSZ. Dense and porous LSM was produced using tape casting techniques. Thin films of YSZ and ZrO2 were successfully deposited on various substrates using spin coating and chemical vapor deposition techniques. Correlations between TEC, free volume, ionic radii and defect structure of various perovskites for cathode applications were developed. Potential mixed conducting compositions within the system La(1-x)Sr(x)(Co(1-y)Fe(y))O3 were prepared; their structure and phase stability were identified. TEC measurements on the system have been carried out and related to previously mentioned parameters. Author

N92-31922# Interfacial Sciences, Inc., Santa Clara, CA.
ELECTROCHEMICAL OXIDATION OF METHANE FOR FUEL CELLS Annual Report, 15 Feb. 1990 - 31 Dec. 1990
K. W. Frese, F. Wang, and C. Chen 28 Dec. 1991 39 p
(Contract GRI-5090-260-2048)
(PB92-172303; GRI-92/0021) Avail: CASI HC A03/MF A01

Methane is an abundant raw material that may be converted to electrical energy in fuel cells or it may be transformed to a liquid fuel such as methanol by suitable electrochemical processes. At present, catalytic electrode materials for methane oxidation are limited to Pt and a few Pt-based alloys. More efficient and cheaper electrode materials are desired to improve the performance and lower the cost of methane anodes in fuel cells. The costs associated with gas reforming would be eliminated in a direct methane fuel cell. A basic research program is being conducted to investigate the factors controlling the performance of various anode materials with the goal of identifying improved electrocatalysts. A specific goal is to improve the oxidation kinetics of CO(ad), a known intermediate in CH4 oxidation. DSA-type conducting oxides containing RuO2 or RuO2 + SnO2 were used as substrates for thin films of Pt and small particles of Ag. Both Pt and Ag are active for methane oxidation. The resulting electrodes were used as anodes for electrochemical methane oxidation. The most important property of these oxide substrate materials are proven electrochemical stability in Cl2 evolution and the low lying empty electronic levels. Author

N92-32087# Sandia National Labs., Albuquerque, NM.
DESIGN, FABRICATION, AND TESTING OF A 30 kW(SUB t) SCREEN-WICK HEAT-PIPE SOLAR RECEIVER
C. E. Andraka, R. B. Diver, and D. A. Wolf (Dynatherm Corp., Cockeysville, MD.) 1992 6 p Presented at the 27th Intersociety Energy Conversion Engineering Conference, San Diego, CA, 3-7 Aug. 1992
(Contract DE-AC04-76DP-00789)
(DE92-016500; SAND-92-0795C; CONF-920801-5) Avail: CASI HC A02/MF A01

Heat-Pipe reflux receivers have been identified as a desirable interface to couple a Stirling engine with a parabolic dish solar concentrator. The reflux receiver provides power uniformly and nearly isothermally to the engine heater heads while de-coupling the heater head design from the solar absorber surface design. Therefore, the heat pipe reflux receiver allows the receiver and heater head to be independently thermally optimized, leading to high receiver thermal transport efficiency. Dynatherm Corporation designed and fabricated a screen-wick heat-pipe receiver for possible application to the Cummins Power Generation, Inc. first-generation 4 kW(sub e) free-piston dish-Stirling system, which required up to 30 kW(sub t). The receiver features a composite absorber wick and a homogeneous sponge-wick on the aft dome to provide sodium to the absorber during hot restarts. The screen wick is attached to the absorber dome by spot welds. Refluxing troughs collect the condensate in a cylindrical condenser and return it directly to the absorber surface. The receiver was fabricated

and lamp tested to 16 kW(sub t) throughput by Dynatherm. The receiver has been tested on Sandia's 60 kW(sub t) solar furnace to a throughput power of 27.5 kW(sub t) and vapor space temperature up to 780 C. Infrared thermography was used to monitor the entire absorber dome for impending dryout while the receiver was tested. The receiver was started using solar input, without the assistance of electrical pre-heaters. The power was extracted with a gas-gap cold-water calorimeter to simulate the operation of a Stirling engine. The receiver design, thermal performance analysis, flux distribution analysis, test results, and post-test analysis are presented. DOE

N92-32091# Oak Ridge National Lab., TN.
SOLAR THERMAL ENERGY STORAGE IN PHASE CHANGE MATERIALS
C. K. Jotshi, D. Y. Goswami (Florida Univ., Gainesville.), and J. J. Tomlinson 1992 6 p Presented at the National Solar Energy Conference, Cocoa Beach, FL, 13-18 Jun. 1992
(Contract DE-AC05-84OR-21400)
(DE92-016908; CONF-920678-8) Avail: CASI HC A02/MF A01

This paper describes the thermophysical properties and thermal behavior of the phase change materials (PCMs) that have been identified as potential materials for solar thermal energy storage applications. PCMs that undergo solid-liquid and solid-solid phase transformation have been described. PCMs which include salt hydrates, paraffins, non-paraffins, eutectics of inorganic and/or organic compounds, and polyalcohols are discussed. The containment requirement for these PCMs are also described in this paper. DOE

N92-32110# Midwest Research Inst., Golden, CO.
COMPUTER SIMULATION OF SHADING AND BLOCKING: DISCUSSION OF ACCURACY AND RECOMMENDATIONS
F. W. Lipps (Houston Univ., TX.) Apr. 1992 37 p
(Contract DE-AC02-83CH-10093)
(DE91-002146; NREL/TP-253-4281) Avail: CASI HC A03/MF A01

A field of heliostats suffers losses caused by shading and blocking by neighboring heliostats. The complex geometry of multiple shading and blocking events suggests that a processing code is needed to update the boundary vector for each shading or blocking event. A new version, RSABS, (programmer's manual included) simulates the split-rectangular heliostat. Researchers concluded that the dominant error for the given heliostat geometry is caused by the departure from planarity of the neighboring heliostats. It is recommended that a version of the heliostat simulation be modified to include losses due to nonreflective structural margins, if they occur. Heliostat neighbors should be given true guidance rather than assumed to be parallel, and the resulting nonidentical quadrilateral images should be processed, as in HELIOS, by ignoring overlapping events, rare in optimized fields. DOE

N92-32112# Midwest Research Inst., Golden, CO.
DESICCANT COOLING USING UNGLAZED TRANSPIRED SOLAR COLLECTORS
A. A. Pesaran and K. Wipke (Stanford Univ., CA.) May 1992 7 p Presented at the National Solar Energy Conference, Cocoa Beach, FL, 13-18 Jun. 1992
(Contract DE-AC02-83CH-10093)
(DE92-010568; NREL/TP-432-4827; CONF-920678-6) Avail: CASI HC A02/MF A01

The use of unglazed solar collectors for desiccant regeneration in a solid desiccant cooling cycle was investigated because these collectors are lower in cost than conventional glazed flat-plate collectors. Using computer models, the performance of a desiccant cooling ventilation cycle integrated with either unglazed transpired collectors or conventional glazed flat-plate collectors was obtained. We found that the thermal performance of the unglazed system was lower than the thermal performance of the glazed system because the unglazed system could not take advantage of the heat of adsorption released during the dehumidification process. For a 3-ton cooling system, although the area required for the unglazed collector was 69 percent more than that required for the glazed collector, the cost of the unglazed collector array was 44 percent less than the cost of the glazed collector array. The simple payback period of the unglazed system was half of the payback period of the glazed collector when compared to an equivalent gas-fired system. Although the use of unglazed transpired collectors makes economic sense, some practical considerations may limit their use in desiccant regeneration. DOE

N92-32118# Brookhaven National Lab., Upton, NY.
MATERIALS FOR GEOTHERMAL PRODUCTION
L. E. Kukacka 1992 13 p
(Contract DE-AC02-76CH-00016)
(DE92-014691; BNL-47508) Avail: CASI HC A03/MF A01

Advances in the development of new materials continue to be made in the geothermal materials project. Many successes have already been accrued and the results used commercially. In FY-91, work was focused on reducing well drilling, fluid transport and energy conversion costs. Specific activities performed included lightweight CO2 resistant well cements, thermally conductive and scale resistant protective liner systems, chemical systems for lost circulation control, corrosion mitigation in process components at The Geysers, and elastomer-metal bonding systems. Efforts to transfer the technologies developed in these efforts to other energy-related sectors of the economy continued, and considerable success was achieved. DOE

N92-32124# Brookhaven National Lab., Upton, NY.
GEOTHERMAL MATERIALS DEVELOPMENT
L. E. Kukacka Dec. 1991 16 p
(Contract DE-AC02-76CH-00016)
(DE92-016940; BNL-47529) Avail: CASI HC A03/MF A01

Advances in the development of new materials, the commercial availabilities of which are essential for the attainment of Hydrothermal Category Level 1 and 2 Objectives, continue to be made in the Geothermal Materials Development Project. Many successes have already been accrued and the results used commercially. In FY-91, utility company sponsored 'full cost' recovery programs based upon materials technology developed in this project were initiated on topics such as condensing heat exchangers, high temperature composites for utility vaults used in district heating systems, and corrosion resistant coatings for use in oil-fired electric generating processes. In FY-91, the DOE/GD-sponsored R&D project was focused on reducing well drilling, fluid transport and energy conversion costs. Specific activities being performed included lightweight CO2-resistant well cements, chemical systems for lost circulation control, thermally conductive and scale resistant protective linear systems, corrosion mitigation in process components at The Geysers, and elastomer-metal bonding systems needed for use in high temperature well drilling and safety related applications. DOE

45 ENVIRONMENT POLLUTION

Includes atmospheric, noise, thermal, and water pollution.

N92-31258*# National Aeronautics and Space Administration, Washington, DC.
THE DETECTION OF CLIMATE CHANGE DUE TO THE ENHANCED GREENHOUSE EFFECT
Robert A. Schiffer and Sushel Unninayar 1991 60 p Presented at the GEDEX Atmospheric Temperature Workshop, Columbia, MD, 9-11 Jul. 1991
(NASA-TM-107965; NAS 1.15:107965) Avail: CASI HC A04/MF A01

The greenhouse effect is accepted as an undisputed fact from both theoretical and observational considerations. In Earth's atmosphere, the primary greenhouse gas is water vapor. The specific concern today is that increasing concentrations of anthropogenically introduced greenhouse gases will, sooner or

later, irreversibly alter the climate of Earth. Detecting climate change has been complicated by uncertainties in historical observations and measurements. Thus, the primary concern for the GEDEX project is how can climate change and enhanced greenhouse effects be unambiguously detected and quantified. Specifically examined are the areas of: Earth surface temperature; the free atmosphere (850 millibars and above); space-based measurements; measurement uncertainties; and modeling the observed temperature record. H.A.

N92-31259*# National Science Foundation, Washington, DC. Committee on Earth and Environmental Sciences.
OUR CHANGING PLANET: THE FY 1993 US GLOBAL CHANGE RESEARCH PROGRAM. A SUPPLEMENT TO THE US PRESIDENT'S FISCAL YEAR 1993 BUDGET
1992 89 p Revised Sponsored in part by NASA, Washington; NOAA; DOE; and EPA Original contains color illustrations
(NASA-CR-190675; NAS 1.26:190675) Avail: CASI HC A05/MF A01; 2 functional color pages

An improved predictive understanding of the integrated Earth system, including human interactions, will provide direct benefits by anticipating and planning for possible impacts on commerce, agriculture, energy, resource utilization, human safety, and environmental quality. The central goal of the U.S. Global Change Research Program (USGCRP) is to help establish the scientific understanding and the basis for national and international policymaking related to natural and human-induced changes in the global Earth system. This will be accomplished through: (1) establishing an integrated, comprehensive, long-term program of documenting the Earth system on a global scale; (2) conducting a program of focused studies to improve our understanding of the physical, geological, chemical, biological, and social processes that influence the Earth system processes; and (3) developing integrated conceptual and predictive Earth system models. H.A.

N92-31297# Lawrence Livermore National Lab., CA.
EFFECTS OF ANTHROPOGENIC SULFUR AEROSOLS ON CLIMATE
C. C. Chuang and J. E. Penner May 1992 4 p Presented at the 13th International Conference on Nucleation and Atmospheric Aerosols and Nucleation Symposium, Salt Lake City, UT, 24-28 Aug. 1992
(Contract W-7405-eng-48)
(DE92-016158; UCRL-JC-108521; CONF-9208100-1) Avail: CASI HC A01/MF A01

The potential effect of atmospheric aerosols from anthropogenic sulfur emissions on climate has received a considerable amount of attention recently. Concerns are expressed regarding a possible change in the global energy budget of variations in the clear sky albedo as well as variations in the cloud optical properties. A climate model is coupled with a 3-D global chemistry model to investigate the climate response to anthropogenic sulfur aerosols. Our preliminary study indicates that the global change in the reflected solar radiation due to the increase of sulfate particles offsets part of the warming resulting from the increase of greenhouse gases. DOE

N92-31304# Alaska Univ., Fairbanks. Water Research Center.
ANNUAL DYNAMICS WITHIN THE ACTIVE LAYER
1991 22 p
(Contract DE-FG06-84ER-60247)
(DE92-013520; DOE/ER-60247/T1) Avail: CASI HC A03/MF A01

We have continued our meteorological and hydrologic data collection in support of our process-oriented research. The six years of data collected to date is unique in its scope and continuity in a North Hemisphere Arctic setting. This valuable data base has allowed us to further our understanding of the interconnections and interactions among the atmosphere, hydrosphere, biosphere, and lithosphere. The increased understanding of the heat and mass transfer processes has allowed us to increase our model-oriented research efforts. Examples of applications are the following. (1) Spring snowmelt on the North Slope of Alaska is the dominant hydrologic event of the year. This event provides most of the moisture for use by vegetation in the spring and early summer period. The mechanisms and timing of snowmelt are important factors in predicting runoff, the migrations of birds and large mammals and the diversity of plant communities. It is important globally due to the radical and abrupt change in the surface energy balance over vast areas. (2) We were able to explore the trends and differences in the snowmelt process along a transect from the Brooks Range to the Arctic Coastal plain. Snowpack ablation was monitored at three sites. These data were analyzed along with meteorologic data at each site. The initiation of ablation was site specific, being largely controlled by the complementary addition of energy from radiation and sensible heat flux. DOE

N92-31312# Ohio State Univ., Columbus.
HYDROLOGICAL AND GEOCHEMICAL RESPONSE AND RECOVERY IN DISTURBED ARCTIC ECOSYSTEMS
1992 5 p
(Contract DE-FG02-84ER-60246)
(DE92-016223; DOE/ER-60246/5) Avail: CASI HC A01/MF A01

This progress report is a funding extension request to continue the database work for the Hydrological and Geochemical Response and Recovery in Disturbed Arctic Ecosystems Program. Throughout the period from 1985 to 1992, the Department of Energy supported research on the hydrology and geochemistry of the headwater basin of Imnavait Creek that focused on the quantification of the input from atmospheric sources of biologically significant and other related chemical variables; the transport of these variables in surface and subsurface flow, and their efflux from the basin; and the development of geochemical budgets. The acquisition of multi-year data sets (the longest and most detailed sets in the Arctic) have made it possible to define seasonal ranges and amplitudes; determine spatial and temporal relationships within the different flow compartments; and to begin to model the pathways and rates of movement through and across different landscape units. The length of record has also made it possible to examine the quantity and influence of local and extra-regional additions. DOE

N92-31324# Lawrence Livermore National Lab., CA.
THE VALIDATION OF ATMOSPHERIC MODELS
W. L. Gates Mar. 1992 17 p Presented at the 1st Demetra Conference on the Dilemmas of Global Warming, Chianciano Terme, Italy, 28 Oct. - 1 Nov. 1991
(Contract W-7405-eng-48)
(DE92-013254; UCRL-ID-109810; CONF-9110374-1) Avail: CASI HC A03/MF A01

The validation of atmospheric models is a key part of the modeling enterprise, but one to which increased attention needs to be given if systematic progress is to be made in the development of predictive climate models. The validation of current AGCM's in terms of the mean seasonal distribution of primary variables such as pressure, temperature, and wind shows a reasonable ability to simulate the observed large-scale features, while at the same time identifying a number of systematic errors. More recent validations have included the simulation of variability, which reveals a modest level of skill but with further systematic errors. Recent results from mesoscale models nested within AGCM's, however, have shown substantial skill in the simulation of regional climate. In addition to conventional data sources of various resolutions, current model validation is enriched by the use of satellite observations and other special data sets, as well as by the analyses from operational models. A comprehensive atmospheric model validation program includes examination of not only the mean and variance, but of the complete frequency distribution. Moreover, in addition to the primary dynamical and physical variables, the various derived quantities associated with fluxes and processes and the occurrence of specific events should also be evaluated. A complete validation would also include evaluation of a model's ability to simulate more than just the present climate and/or its ability to simulate observed

climate change (the latter aspect necessarily including the oceans). DOE

N92-31422# Brookhaven National Lab., Upton, NY.
APPLICATION OF FREE-AIR CO2 ENRICHMENT (FACE) TECHNOLOGY TO A FOREST CANOPY: A SIMULATION STUDY
F. W. Lipfert, G. R. Hendrey, K. L. Lewin, and Y. Alexander (Israel Inst. for Biological Research, Ness-Ziona.) Mar. 1992 12 p Presented at the 9th World Clean Air Congress and Exhibition: Towards the Year 2000 - Critical Issues in the Global Environment, Montreal (Canada), 30 Aug. - 4 Sep. 1992
(Contract DE-AC02-76CH-00016)
(DE92-013308; BNL-47392; CONF-920814-4) Avail: CASI HC A03/MF A01

Forest ecosystems constitute an important part of the planet's land cover. Understanding their exchanges of carbon with the atmosphere is crucial in projecting future net atmospheric CO2 increases. It is also important that experimental studies of these processes be performed under conditions which are as realistic as possible, particularly with respect to photosynthesis and evapotranspiration. New technology and experimental protocols now exist which can facilitate studying an undisturbed forest canopy under long-term enriched CO2 conditions. The International Geosphere Biosphere Program of the International Council of Scientific Unions has established a subprogram on Global Change and Terrestrial Ecosystems (GCTE). This program is driven by two major concerns: to be able to predict the effects of global change on the structure and function of ecosystems, and to predict how these changes will control both atmospheric CO2 and climate, through various feedback pathways. Brookhaven National Laboratory (BNL) has developed a system for exposing field-grown plants to controlled elevated concentrations of atmospheric gases, without use of confining chambers that alter important atmospheric exchange processes. This system is called FACE (Free Air CO2 Enrichment). This paper focuses on the fluid mechanics of free-air fumigation and uses a numerical simulation model based on superposed gaussian plumes to project how the present ground-based system could be used to fumigate an elevated forest canopy. DOE

N92-31423# Lawrence Livermore National Lab., CA.
NUMERICAL SIMULATION OF PRECIPITATION SCAVENGING AND COMPARISON WITH OBSERVATION OF PRESCRIBED FOREST FIRES
C. R. Molenkamp and M. M. Bradley Apr. 1992 6 p Presented at the 11th International Conference on Clouds and Precipitation, Montreal (Canada), 17-21 Aug. 1992
(Contract W-7405-eng-48)
(DE92-013513; UCRL-JC-109179; CONF-920881-1) Avail: CASI HC A02/MF A01

The primary mechanism by which aerosol particles are removed from the atmosphere is precipitation scavenging. Because of our interest in understanding the processes by which aerosol particles are scavenging as well as basic cloud dynamic and microphysical interactions, we have developed a numerical model that simulates these processes. This model was developed as part of our study of the global climatic effects of smoke from a large number of massive fires. One of the ways that we have attempted to validate the accuracy of the model is to perform simulations of prescribed forest burns where there is information on the source characteristics and fire morphology, and observations of the cloud dynamics and microphysics. In this paper we describe simulations of the Hardiman township and Batterby township Ontario, Canada, prescribed fires. Our numerical model, OCTET, is a system of eight progressively more complex models designed to simulate plumes, clouds, and mesoscale system. OCTET has a three-dimensional, nonhydrostatic, compressible dynamic framework originally based on a convective storm model. DOE

N92-31427# Sandia National Labs., Albuquerque, NM.
ENVIROTRADE: ITS ROLE IN THE CLEANUP OF THE ENVIRONMENT
M. W. Harrington and C. P. Harlan 1992 4 p Presented at the Spectrum 1992: Nuclear and Hazardous Waste Management International Topical Meeting, Boise, ID, 23-27 Aug. 1992
(Contract DE-AC04-76DP-00789)
(DE92-013691; SAND-92-0458C; CONF-920851-8) Avail: CASI HC A01/MF A01

In support of the US Department of Energy's commitment to the remediation of waste sites throughout its complex, the DOE has recognized that it can accelerate its technology development efforts and leverage the expenditure of available funds through an international cooperation among government entities, private industry, and educational institutions. To support the technology transfer of environmental information, the DOE has sponsored the development of EnviroTRADE -- an international information system that will facilitate the exchange of environmental restoration and waste management technologies worldwide. The system will contain profiles on both environmental restoration/waste management needs and foreign/domestic technologies. Users will be able to identify matches between worldwide needs and available or emerging technologies. Where matches between needs and existing technologies are not found, the system will identify the potential for development of new and innovative technologies to address environmental problems. EnviroTRADE will also provide general information on international environmental restoration and waste management organizations, sites, activities, and contacts. DOE

N92-31527# Oak Ridge National Lab., TN. Carbon Dioxide Information Analysis Center.
TWO LONG-TERM INSTRUMENTAL CLIMATIC DATA BASES OF THE PEOPLE'S REPUBLIC OF CHINA
D. P. Kaiser Nov. 1991 188 p
(Contract DE-AC05-84OR-21400)
(DE92-010378; ORNL/CDIAC-47; NDP-039; ESDP-3747) Avail: CASI HC A09/MF A02

Two long-term instrumental data bases containing meteorological observations from the People's Republic of China (PRC) are described. These data sets were compiled in accordance with a joint research agreement signed by the United States Department of Energy (DOE) and the PRC Chinese Academy of Sciences (CAS) on August 19, 1987. CAS has provided records from 265 stations, partitioned into networks of 60 and 205 stations which each provide good geographical coverage of the PRC. The 60-station network data contain monthly measurements of barometric pressure, air temperature, precipitation amount, relative humidity, sunshine duration, cloud amount, wind direction and speed, and number of days with snow cover. Detailed station histories are presented for all 60 stations. The 205-station network data contain monthly mean temperatures and monthly precipitation totals; however, station histories are not currently available. Sixteen stations from these data sets (13 from the 60-station and 3 from the 205-station) have temperature and/or precipitation records which begin prior to 1900, whereas the remaining stations began observing in the early to mid-1900's. Records from the 262 stations extend through 1988; the remaining three station records extend through the early 1980's. These data can be used in defining regional climate changes, establishing relationships between regional and large-scale climates, and in studying the climatic impacts of urbanization and increased concentrations of greenhouse gases. Additional uses could include examining impacts of periodic events such as volcanic eruptions or the El Nino/Southern Oscillation (ENSO). These data sets represent the most comprehensive, long-term instrumental Chinese climate data presently available. DOE

N92-31556# Naval War Coll., Newport, RI. Dept. of Operations.
ANTI-ENVIRONMENTAL WARFARE: PROTECTING THE ENVIRONMENT DURING WARTIME Final Report
Richard O. Gamble, II 19 Jun. 1992 39 p
(AD-A250337) Avail: CASI HC A03/MF A01

This paper analyzes the operational impact resulting from the growing legal and political concerns over the environment during

wartime. Current international law and national policies are examined to determine their potential effect on Rules of Engagement, and the resulting operational impact on means and methods of warfare. As illustrated during the recent Persian Gulf War, coalition leaders will be operationally constrained by political demands to protect the environment, and to mitigate ecological destruction caused by an opposing force. These constraints will effect how offensive action is conducted against environmentally sensitive industries including nuclear, chemical, and petroleum. Commanders must adhere to the current environmental policies and place more emphasis on the principles of discrimination and military necessity in selecting and striking targets. Concurrently, commanders must balance protecting the environment and the requisite minimum casualties to obtain the objectives and preserve public support. GRA

N92-31574# Pacific Northwest Lab., Richland, WA.
ENERGY CONSERVATION: THE MAIN FACTOR FOR REDUCING GREENHOUSE GAS EMISSIONS IN THE FORMER SOVIET UNION
I. A. Bashmakov and V. P. Chupyatov Dec. 1991 29 p
(Contract DE-AC06-76RL-01830)
(DE92-012355; PNL-SA-20400) Avail: CASI HC A03/MF A01

The energy intensity of the former Soviet Union is more than twice that of other market economics in similar stages of economic development. Low energy efficiency in the Soviet Union has contributed significantly to global carbon and other greenhouse gas emissions. The technological potential for energy conservation in the former Soviet Union is the largest in the world. The inefficiencies of the previous command-system economy, however, have provided little incentive for conserving energy. The present transition to a market-based economy should encourage the incorporation of energy-efficiency improvements in order for the former Soviet Union to successfully lower its energy intensity. There are several obstacles that limit implementing energy conservation; for example, energy prices and discount rates influence the volume of investment in energy efficiency. Nevertheless, cost-effective measures for energy conservation do exist even in the most energy-intensive sectors of the Soviet economy and should form the core of any energy conservation program. The overall cost-effective potential for carbon savings in the former Soviet Union is estimated to be 280 to 367 million tons of carbon per year by the year 2005, or 23 to 29 percent of 1988 energy-related emissions. DOE

N92-31591# Argonne National Lab., IL.
MINORITIES AND AIR QUALITY NON-ATTAINMENT AREAS: A PRELIMINARY GEO-DEMOGRAPHIC ANALYSIS
D. Wernette and L. Nieves Jun. 1991 22 p Presented at the Socioeconomic Energy Research and Analysis Conference, Baltimore, MD, 27-28 Jun. 1992
(Contract W-31-109-eng-38)
(DE92-013054; ANL/CP-75440; CONF-9206158-3) Avail: CASI HC A03/MF A01

A major section of the Clean Air Act Amendments (CAAA) focuses on reducing air pollution through extending and modifying the provisions for states and localities with US Environmental Protection Agency (EPA)-designated non-attainment areas. Specifically, Title 1 of the CAAA is concerned with non-attainment areas, as defined relative to the National Ambient Air Quality Standards for atmospheric ozone, carbon monoxide, and particulate matter; Title 2 is concerned with mobile sources or air pollution, which produce carbon monoxide, contribute to ozone concentrations, and in the past have been a major source of airborne lead; and Title 4 is concerned with acid deposition, mainly due to sulfur dioxide emissions. This paper has its origin in the question of the potential benefits for minorities--relative to the majority non-Black, non-Hispanic population--of reductions in air pollution that may result from these amendments. It is part of a larger effort to identify and assess the costs and benefits of the CAAA for minorities, relative to the majority population. The focus of this paper centers on comparing Black and Hispanic populations to White, non-Hispanic populations living in EPA-designated non-attainment area counties in the contiguous United States, which excludes Alaska and Hawaii. Subsequent comparisons of majority populations with Native Americans and Asian-Americans will include these two states. DOE

N92-31592# Virginia Polytechnic Inst. and State Univ., Blacksburg. Management Systems Labs.
RESEARCH AND DEVELOPMENT OF METHODS AND TOOLS FOR ACHIEVING AND MAINTAINING CONSENSUS PROCESSES IN THE FACE OF CHANGE WITHIN AND AMONG GOVERNMENT OVERSIGHT AGENCIES, VOLUME 1
Mar. 1992 138 p
(Contract DE-FG02-88DP-48058)
(DE92-014179; DOE/DP-48058/4-Vol-1) Avail: CASI HC A07/MF A02

This progress report summarizes our research activities under our consensus grant. In year four of the grant, we continued to capitalize on and benefit from historical events which drove our early emphasis on group process studies. Following our work on various procedures for bringing together groups such as the State and Tribal Government Working Group and the Stakeholders' Forum (both of which provide input to the Five-Year Waste Plan), we continue to observe these groups and collect data. We also began a configuration study involving the complex modeling of DOE's Office of Environmental Restoration and Waste Management (EM). Related to group process studies is the issue of the information requirements for individuals making decisions in consensus groups. Our information studies examined the requirements for decision-related information, frameworks for such information, and the effectiveness of information portrayed for decision making. However, we were able not only to continue studying consensus groups in action and related information issues, but also to focus considerable attention on the fundamental side of our research. The fundamental or basic research conducted in year four included: (1) expanding our literature database; (2) beginning the writing of the literature review summary document and the consensus guide; (3) developing frameworks and models such as the Environmental Trilogy model and a structural equations model of the consensus process; and (4) conducting laboratory studies concerning the effects of the presence of an expert, met expectations, opportunity to express views, incentive structure and conflict type (competitive versus collaborative) on consensus outcomes. DOE

N92-31598# National Acid Precipitation Assessment Program, Washington, DC.
ACID DEPOSITION: STATE OF SCIENCE AND TECHNOLOGY. SUMMARY REPORT OF THE US NATIONAL ACID PRECIPITATION ASSESSMENT PROGRAM, VOLUMES 1-4
P. M. Irving and E. Smith Sep. 1991 270 p
(PB92-100353; ISBN-0-16-035925-2) Avail: CASI HC A12/MF A03; SOD HC

The 27 State-of-Science and State-of-Technology (SOS/T) Reports published in 1990 as the definitive scientific and technical synthesis of information obtained during the first decade of the U.S. National Acid Precipitation Assessment Program (NAPAP) are summarized. In most cases, the summaries were the first chapters of the complete SOS/T Report. Author

N92-31620# Federal Coordinating Council for Science, Engineering and Technology, Washington, DC. Committee on Earth and Environmental Sciences.
OUR CHANGING PLANET: THE FY 1993 US GLOBAL CHANGE RESEARCH PROGRAM. A REPORT BY THE COMMITTEE ON EARTH AND ENVIRONMENTAL SCIENCES, A SUPPLEMENT TO THE US PRESIDENT'S FISCAL YEAR 1993 BUDGET
Jan. 1992 90 p
(PB92-156892) Avail: CASI HC A05/MF A01

The U.S. Global Change Reasearch Program (USGCRP) was established as a Presidential initiative in the FY-1990 Budget to help develop sound national and international policies related to global environmental issues, particularly global climate change.

The USGCRP is implemented through a priority-driven scientific research agenda that is designed to be integrated, comprehensive, and multidisciplinary. It is designed explicitly to address scientific uncertainties in such areas as climate change, ozone depletion, changes in terrestrial and marine productivity, global water and energy cycles, sea level changes, the impact of global changes on human health and activities, and the impact of anthropogenic activities on the Earth system. The USGCRP addresses three parallel but interconnected streams of activity: documenting global change (observations); enhancing understanding of key processes (process research); and predicting global and regional environmental change (integrated modeling and prediction).

Author

N92-31626# San Diego State Univ., CA.

RESPONSE OF A TUNDRA ECOSYSTEM TO ELEVATED ATMOSPHERIC CARBON DIOXIDE AND CO2-INDUCED CLIMATE CHANGE

W. C. Oechel Apr. 1992 18 p

(Contract DE-FG03-86ER-60479)

(DE92-013925; DOE/ER-60479/T1) Avail: CASI HC A03/MF A01

This report presents the progress on the DOE funded project: 'Response of a Tundra Ecosystem to Elevated Atmospheric Carbon Dioxide and CO2 Induced Climate Change.' The current funding cycle was initiated on September 1, 1989, to run through August 31, 1992. There was an initial reduction in scope dictated by budget availabilities, primarily manipulations of CO2, temperature, and nutrients at a wet tundra located at Barrow, Alaska. These experiments still need to be done over the mid- to longer term in order to accurately predict, apriori, the effects of climate change on the arctic tundra as well as possible feedbacks. Coordination and cooperation with other agencies was initiated in 1990 and formally proposed in our 1991 renewal at the national and international level and has become an important aspect of the research. To accurately and precisely scale, plot, and transect measurements to the circumpolar tundra is beyond the scope of the current DOE project. It is possible, however to determine the patterns and controls of CO2 flux from the current circumpolar arctic tundra with the involvement of additional agencies and governments. Results from the past two years of this project confirm that the arctic has become a source of CO2 to the atmosphere. This change coincides with recent climatic variation in the arctic, and suggests a positive feedback of arctic ecosystems on atmospheric CO2 and global change. Measurements along a latitudinal gradient across the north slope of Alaska indicate a loss of carbon from tussock tundra and wet tundra, decreasing in magnitude along a decreasing gradient of temperature, but an increasing gradient in soil moisture. These data are in agreement with work done on tussock tundra in 1983-85, and 1987. DOE

N92-31648# Corvallis Environmental Research Lab., OR.

METHODS OF ASSESSING RESPONSES OF TREES, STANDS AND ECOSYSTEMS TO AIR POLLUTION

K. W. Stolte, D. M. Duriscoe, E. R. Cook, and S. P. Cline 1992 73 p Prepared in cooperation with Forest Service, Research Triangle Park, NC; Lamont-Doherty Geological Inst., Palisades, NY; ManTech Environmental Technology International, Inc., Corvallis, OR; and National Park Service, Three Rivers, CA

(PB92-180231; EPA/600/A-92/104) Avail: CASI HC A04/MF A01

The focus is on three main types of assessments of pollution effects used in the case studies chronicled in chapters 8-12 (regional studies of conifer forests in the west). These are measures of crown conditions of individual trees; impacts on populations and communities; and temporal patterns in radial growth. The concepts behind the development of each approach are introduced with references to previous work, leading to a discussion of the state of science. The importance of quality assurance techniques to the success of any assessment of air pollution effects is also discussed. Author

N92-31649*# National Center for Atmospheric Research, Boulder, CO. Atmospheric Chemistry Div.

GLOBAL ATMOSPHERIC CIRCULATION STATISTICS, 1000-1 mb

William J. Randel Feb. 1992 253 p Sponsored in part by NSF

(Contract NASw-16215)

(PB92-186196; NCAR/TN-366+STR) Avail: CASI HC A12/MF A03

The atlas presents atmospheric general circulation statistics derived from twelve years (1979-90) of daily National Meteorological Center (NMC) operational geopotential height analyses; it is an update of a prior atlas using data over 1979-1986. These global analyses are available on pressure levels covering 1000-1 mb (approximately 0-50 km). The geopotential grids are a combined product of the Climate Analysis Center (which produces analyses over 70-1 mb) and operational NMC analyses (over 1000-100 mb). Balance horizontal winds and hydrostatic temperatures are derived from the geopotential fields. GRA

N92-31732# Pacific Northwest Lab., Richland, WA.

EVOLUTION OF ENVIRONMENTAL PROTECTION STRATEGIES IN THE SOVIET UNION

A. M. Lesperance May 1992 9 p Presented at the 17th Annual Conference of the National Association of Environmental Professionals, Seattle, WA, 5-8 May 1992

(Contract DE-AC06-76RL-01830)

(DE92-015090; PNL-SA-20767; CONF-920519-3) Avail: CASI HC A02/MF A01

In performing this work, interviews were conducted with members of the Supreme Soviet Committee for Rational Use of Natural Resources, Moscow, City Council, and St. Petersburg City Council. These officials provided their views on the current status of environmental protection in the former Soviet Union. Literature published in English, although limited, supplemented these discussions. In addition, a literature search was conducted of recent articles about this topic. Although the research for this paper was conducted before and during the August 1991 coup attempt in the Soviet Union, and after the formation of the Commonwealth of Independent States (CIS), many of the observations expressed in this report may be relevant to the new states. This report provides historical perspective on the barriers encountered while attempting to develop environmental policy in the former Soviet Union and establishes a context for problems facing the new states in developing their environmental policies. Organization changes that have occurred in environmental protection since the August coup are included to the extent they are known. DOE

N92-31782# Oak Ridge National Lab., TN.

A DYNAMIC MODEL OF TERRESTRIAL CARBON CYCLING

W. R. Emanuel, A. W. King, and W. M. Post 1992 24 p Presented at the 2nd Ciocco Global Cycle Meeting, Ciocco (Italy), 8-20 Sep. 1991

(Contract DE-AC05-84OR-21400)

(DE92-015130; CONF-9109340-4) Avail: CASI HC A03/MF A01

A model of terrestrial carbon cycling as it is affected by land-use activities such as forest harvest and clearing is described. A compartment model simulates carbon cycling responses of ecosystems to harvest and clearing perturbations. An area distribution function summarizes the extent of ecosystems according to carbon density in vegetation per unit area. Through time, plant growth and land use alter this area distribution function with opposing tendencies. Simulations agree reasonably well with previous studies. Discrepancies appear to be associated with dead organic matter responses. DOE

N92-31896# Oak Ridge National Lab., TN.

ITERATIVE FUNCTIONALISM AND CLIMATE MANAGEMENT REGIMES: FROM INTERGOVERNMENTAL PANEL ON CLIMATE CHANGE TO INTERGOVERNMENTAL NEGOTIATING COMMITTEE

D. L. Feldman (Tennessee Univ., Knoxville.) 1992 27 p

Presented at the 4th North American Symposium on Society and Resource Management, Madison, WI, 17-20 May 1992
(Contract DE-AC05-84OR-21400)
(DE92-014798; CONF-9205167-1) Avail: CASI HC A03/MF A01

This paper contends that an iterative functionalist regime -- comprised of international organizations that monitor the global climate and perform scientific and policy research on prevention, mitigation, and adaptation strategies for response to possible global warming -- has developed over the past decade. A common global effort by scientists, diplomats, and others to negotiate a framework convention that would reduce emissions of carbon dioxide and other greenhouse gases has been brought about by this regime. Individuals that participate in this regime are engaged in several cooperative activities including: (1) international research on the causes and consequences of global change; (2) global environmental monitoring and standard-setting for analyses of climate data; and (3) negotiating a framework convention that places limits on greenhouse gas emissions by countries. The implications of this iterative approach for successful implementation of a treaty to forestall global climate change are discussed. DOE

N92-31907# Oak Ridge National Lab., TN. Carbon Dioxide Information Analysis Center.
TRENDS 1991: A COMPENDIUM OF DATA ON GLOBAL CHANGE
T. A. Boden, ed., R. J. Sepanski, ed., and F. W. Stoss, ed. Dec. 1991 694 p
(Contract DE-AC05-84OR-21400)
(DE92-011733; ORNL/CDIAC-46; ESD-3746) Avail: CASI HC A99/MF A06

This document is a source of frequently used global change data. This second issue of the Trends series expands the coverage of sites recording atmospheric concentrations of carbon dioxide (CO2) and methane, (CH4), and it updates records reported in the first issue. New data for other trace atmospheric gases have been included in this issue; historical data on nitrous oxide (N2) from ice cores, modern records of atmospheric concentrations of chlorofluorocarbons (CFC-11 and CFC-12) and N2O and estimates of global estimates of CFC-11 and CFC-12. The estimates for global and national CO2 emissions from the burning of fossil fuels, the production of cement, and gas flaring have been revised and updated. Regional CO2 emission estimates have been added, and long-term temperature records have been updated and expanded. Data records are presented in four- to six-page formats, each dealing with a specific site, region, or emissions species. The data records include tables and graphs; discussion of methods for collecting, measuring, and reporting the data; trends in the data; and references to literature that provides further information. All data appearing in the document are available on digital media from the Carbon Dioxide Information Analysis Center. DOE

N92-31930# Department of Energy, Washington, DC.
MULTI-YEAR STRATEGIC PLAN FOR THE ATMOSPHERIC STUDIES IN COMPLEX TERRAIN: ASCOT PROGRAM
Jun. 1992 40 p
(DE92-016646; DOE/ER-0549T) Avail: CASI HC A03/MF A01

The Atmospheric Studies in Complex Terrain (ASCOT) program was developed by the Office of Health and Environmental Research of the Office of Energy Research in the Department of Energy (DOE). The program was originally designed to study atmospheric process in regions of complex terrain and the impact of energy sources on air quality in those regions. The ASCOT program has been the principal atmospheric boundary layer research program of DOE. This document contains a description of the ASCOT program's objectives over the next five years and beyond, placing them in the context of current and anticipated needs of DOE and initiatives described in the National Energy Strategy. DOE

N92-31931# Sandia National Labs., Albuquerque, NM.
ENERGY AND ENVIRONMENT: A SANDIA TECHNOLOGY BULLETIN
L. Parrott, ed., N. S. Hey, ed., and H. Floyd, ed. Apr. 1992 8 p
(Contract DE-AC04-76DP-00789)
(DE92-016740; SAND-92-0467) Avail: CASI HC A02/MF A01

The Planning and Staff Support of the Sandia National Laboratories publishes a monthly bulletin entitled, Energy and Environment. The bulletin facilitates technology exchange with industries, universities, and with other government agencies. This bulletin is for the month of April 1992 and covers such things as new methods of soldering which reduce environmental threats by avoiding chlorofluorocarbon solvents. Some technologies developed are soldering in controlled atmospheres, acid-vapor soldering, and laser soldering. Another topic in this bulletin is the designing of catalysts of chemical reactions by computers. Biomimetic catalysts are being created by Computer-Aided Molecular Design. These biomimetic catalysts can aid in fuel conversion. In-situ remediation of soils contaminated by heavy metals was another topic in this bulletin. This in-situ process is called, electrokinetic remediation. It uses electrodes to induce a metal-attracting electric field in the ground. The last topic in this bulletin is the design of a semiconductor bridge (SCB) which is used to improve the timing and effectiveness of blasting. Timing and accuracy is important; and the blasting industry is no exception. This SCB gives a low-energy pulse which causes a doped region on a polysilicon substrate into a bright plasma. This plasma discharge causes the ignition and produces an accurate explosion in microseconds. DOE

N92-32071# National Oceanographic Data Center, Rockville, MD. Library and Information Services Div.
ECOSYSTEMS OF THE FLORIDA KEYS: A BIBLIOGRAPHY
L. Pikula and S. Elswick Apr. 1992 197 p
(PB92-198910; Current-Ref-92-1) Avail: CASI HC A09/MF A03

Given here is the bibliography that was originally prepared for the Florida Keys National Marine Sanctuary located in Key Largo, Florida by the NOAA Regional Library in Miami, Florida. It was prepared with the idea that it would be used by scientists and educators interested in the Keys. The majority of citations are references to works about marine invertebrates and flora, with a substantial number of citations to works about oceanography, geology, meteorology, marine mammals and fishes, and terrestrial flora and fauna. Author

N92-32083# Argonne National Lab., IL.
THE POTENTIAL OF PASSIVE-REMOTE FOURIER TRANSFORM INFRARED (FTIR) SPECTROSCOPY TO DETECT ORGANIC EMISSIONS UNDER THE CLEAN AIR ACT
J. C. Demirgian, C. L. Hammer, and R. T. Kroutil (Chemical Research and Development Center, Aberdeen Proving Ground, MD.) 1992 12 p Presented at the Optical Remote Sensing and Applications To Environmental and Industrial Safety Problems, Houston, TX, 6-9 Apr. 1992
(Contract W-31-109-eng-38)
(DE92-015224; ANL/CP-75853; CONF-920443-1) Avail: CASI HC A03/MF A01

The Clean Air Act of 1990 regulates the emission of 198 air toxics. Currently, there is no existing technology by which a regulatory agency can independently determine if a facility is in compliance. We have successfully tested the ability of passive-remote Fourier transform infrared (FTIR) spectroscopy to detect chemical plumes released in the field. Additional laboratory releases demonstrated that FTIR spectroscopy can detect target analytes in mixtures containing components which have overlapping absorbances. The FTIR spectrometer was able to identify and quantify each component released with an average quantitative error of less than 20 percent using partial least squares (PLS) analysis and 40 percent using classical least squares analysis (CLS) when calibration files containing pure components and mixtures were used. Calibration files containing only pure analytes resulted in CLS outperforming PLS analyses. DOE

N92-32147*# Lawrence Livermore National Lab., CA.
NASA HIGH SPEED RESEARCH PROGRAM, EMISSIONS SCENARIOS COMMITTEE REPORT OF MEETINGS ON 26 SEPTEMBER 1991 AND 9 JANUARY 1992
D. J. Wuebbles 23 Mar. 1992 11 p Sponsored by NASA, Washington
(Contract W-7405-eng-48)
(NASA-CR-190379; NAS 1.26:190379; DE92-012409; UCRL-ID-109860) Avail: CASI HC A03/MF A01

An important step in the process of assessing the environmental effects of possible future High-Speed Civil Transports (HSCTs) is the definition of scenarios for the emissions from a fleet of such aircraft. These scenarios are then used in numerical models of the chemistry and physics of the global atmosphere to determine potential environmental effects, including concerns about changes in ozone and in climate. The Emissions Scenarios Committee was formed to provide a forum for meeting the combined needs of the atmospheric science community, the aircraft industry, NASA and the federal government in undertaking the development of scenarios for such assessments. DOE

N92-32155# Lawrence Livermore National Lab., CA.
GLOBAL TRENDS IN ENERGY USE: INDICATIONS FOR RESEARCH
R. N. Schock Oct. 1991 7 p Presented at the Conference on Global Climate Change: Its Mitigation Through Improved Production and Utilization of Energy, Los Alamos, NM, 21-24 Oct. 1991
(Contract W-7405-eng-48)
(DE92-014773; UCRL-JC-109018; CONF-9110127-4) Avail: CASI HC A02/MF A01

This report discusses global energy consumption and energy sources. Forecasts of energy usage are made based on current growth rates. DOE

N92-32222*# Massachusetts Inst. of Tech., Cambridge. Dept. of Civil Engineering.
A TEST OF ECOLOGICAL OPTIMALITY FOR SEMIARID VEGETATION M.S. Thesis
Guido D. Salvucci, Peter S. Eagleson, and Edmund K. Turner 8 May 1992 196 p
(Grant NAGw-1696)
(NASA-CR-190705; NAS 1.26:190705; MIT-R92-17; MIT-335) Avail: CASI HC A09/MF A03

Three ecological optimality hypotheses which have utility in parameter reduction and estimation in a climate-soil-vegetation water balance model are reviewed and tested. The first hypothesis involves short term optimization of vegetative canopy density through equilibrium soil moisture maximization. The second hypothesis involves vegetation type selection again through soil moisture maximization, and the third involves soil genesis through plant induced modification of soil hydraulic properties to values which result in a maximum rate of biomass productivity. Author

N92-32014 Alabama Univ., Huntsville. Atmospheric Science Program.
THE UNCERTAINTIES OF GLOBAL TEMPERATURES IN THE GLOBAL WARMING CONTEXT
John R. Christy *In* Huntsville Association of Technical Societies, TABES 92: 8th Annual Technical and Business Exhibition and Symposium. Executive Summaries and Submitted Papers 1992 7 p (For primary document see N92-32009 22-12)
(TABES Paper 92-447) Copyright Avail: Issuing Activity

46 GEOPHYSICS

Includes aeronomy; upper and lower atmosphere studies; ionospheric and magnetospheric physics; and geomagnetism.

For space radiation see *93 Space Radiation.*

N92-31476# Massachusetts Inst. of Tech., Cambridge. Earth Resources Lab.
RESEARCH IN REGIONAL SEISMOLOGY: THE EFFECT OF ANISOTROPY Scientific Report No. 1
M. N. Toksoz and Richard L. Gibson, Jr. 19 Nov. 1991 84 p
(Contract F19628-90-K-0057)
(AD-A248940; AD-E200990; Rept-74527; PL-TR-91-2297) Avail: CASI HC A05/MF A01

The objective of this study is to examine the influence of fracturing and anisotropy in the source medium or near the source of radiation, especially the generation of SV and SH. One effect is scattering near the source. We present a ray-Born method for the computation of scattered wavefields in a general 3-D, anisotropic medium. This approach applied ray methods to the computation of Green's tensors for a background earth model and uses the Born approximation to determine the scattered wavefield from each volume element within a discretized model of heterogeneity. The application of these two approximate methods requires that the background model be relatively smooth compared to a wavelength for the validity of ray theory, but that the scattering heterogeneity have short characteristic length compared to the propagating wavelength for accurate use of the Born approximation. Comparisons of ray-Born results to the complete solution for scattering from an elastic sphere show that this methods works fairly well for wavelengths on the order of five times larger than the length scales typical of the heterogeneity, but then breaks down due to the failure of the Born approximation. With this restriction in mind, the method is applied to a hypothetical layered earth model containing a thin, laterally extensive fracture zone. GRA

N92-31478# Boston Univ., MA. Center for Space Physics.
THE EFFECTS OF MAGNETIC STORM PHASES ON F-LAYER IRREGULARITIES FROM AURORAL TO EQUATORIAL LATITUDES Quarterly Report, 1 Jan. - 31 Mar. 1992
Jules Aarons and Michael Mendillo 31 Mar. 1992 3 p
(Contract N00014-89-J-1754)
(AD-A249011) Avail: CASI HC A01/MF A01

Determining the morphology of F layer irregularities as a function of longitude in the equatorial region is vital for understanding the physics of the development of these irregularities. We aim to lay the observational basis which can then be used to test theoretical models. Theoretical models were developed in earlier works. The question is whether the models are consistent with the morphology as we see it. According to our criteria, the data used should be confined to observations taken near the magnetic equator during quiet magnetic periods and at times within a few hours after sunset. Anomaly region data should be omitted for studying the generation mechanism. The questions to be answered by the proposed mechanisms concern levels of occurrence at various longitudes. GRA

N92-31509# Woodward-Clyde Consultants, Pasadena, CA.
TIME DOMAIN REGIONAL DISCRIMINANTS Scientific Report No. 1, 1 Nov. 1990 - 1 Nov. 1991
L. J. Burdick, E. J. Garnero, C. K. Saikia, and D. V. Helmberger 1 Nov. 1991 86 p
(Contract F19628-90-C-0194)
(AD-A249949; PL-TR-91-2278; AD-E200945) Avail: CASI HC A05/MF A01

Most regional discriminants developed to date have been based purely on empirics, and many rely on the characteristics of spectra. At Woodward Clyde, a unique type of time domain discriminant has been developed based on a theoretical understanding of wave propagation and the direct identification of depth phases in P sub n and Pg. This work has involved original basic research into the nature of the short period P sub n waveform and the effect of pP

sub n on it; development of an understanding of the nature of P sub n propagation; and inquiries into the relation of pP sub n and spall. The studies of Pg have involved identification of a frequency band in which the waveform is stable; a forward modeling study of NTS regional data; and a careful breakdown of the wavenumber integration synthetics into the generalized rays that compose them. This work has led to direct identification of depth phase effects in Pg and a preliminary indication of how to detect and discriminate with them. This is the first report on a multi-year effort to complete development of the P discriminants, to extend the technology to S sub n and Sg and to test the power of the discriminants on the new data bases from the Soviet Union. Strong efforts to analyze the new data from the Soviet Union have been undertaken including studies of both the older hand digitized analog records and of the digital data from the new IRIS stations. GRA

N92-31510# Systems Science and Software, La Jolla, CA.
TWO-DIMENSIONAL AXISYMMETRIC CALCULATIONS OF SURFACE WAVES GENERATED BY AN EXPLOSION IN AN ISLAND, MOUNTAIN, AND SEDIMENTARY BASIN
J. L. Stevens, K. L. McLaughlin, S. M. Day, and B. Shkoller Oct. 1991 50 p
(Contract F08606-89-C-0022)
(AD-A249971; SSS-TR-91-12833) Avail: CASI HC A03/MF A01

The generation of long period (20-50 second) surface waves by an explosion on an island, inside a mountain, or near a material discontinuity is studied using two-dimensional axisymmetric finite difference calculations. The generation of surface waves can be reduced substantially if the explosion is close to a vertical boundary such as a material velocity reduction, mountain slope, or island/ocean boundary. This occurs because the horizontal components of the static stress field are reduced at the boundary. Three sets of finite difference calculations were performed for an island surrounded by an ocean of air, water, and a low velocity solid. Calculations include ocean depths of 3 km and 6 km, and the island varies in diameter from 6 km to 48 km. For a 48 km island material boundary has little effect on the surface waves. For an island width equal to the ocean depth, however, the surface wave generation is reduced by an order of magnitude for air and water, and reduced by more than a factor of 2 for the low velocity solid. Comparisons with the geography of the Amchitka and Mururoa island test sites show that this effect is small for explosions at those sites, however, the effect appears to be important for Novaya Zemlya and other sites where explosions are detonated inside mountains, and at sites with strong material variations. GRA

N92-31522# Technische Univ., Delft (Netherlands). Faculty of Technical Mathematics and Information.
COMPARISON OF RESULTS: TECHNISCHE UNIV., DELFT-ORGANISATIE VOOR TOEGEPAST NATUURWETENSCHAPPELIJK ONDERZOEK EXPERT JUDGEMENT STUDY OF DISPERSION-DEPOSITION Final Report
Roger M. Cooke 1992 38 p
(Rept-92-11; ETN-92-91863) Copyright Avail: CASI HC A03/MF A01

A summary analysis of the data gathered for an expert elicitation independent of an expert judgement study of atmospheric dispersion and deposition is given. The purpose of this effort was to determine whether it was possible to use an elicitator who was not intimately involved with the modeling and question formulation. It was also of interest to determine whether the assessment of experts consulted by the accident consequence modeling community were presentative of the community at large. Both questions are suggested as being answered in the affirmative. The results of the 'optimized decision maker', formed by combining the experts' assessment according to the 'classical model' with that of the final summary of the whole project, are compared. ESA

N92-31551*# Alabama Univ., Huntsville.
COMBINED RELEASE AND RADIATION EFFECTS SATELLITE (CRRES) EXPERIMENTS DATA COLLECTION, ANALYSIS, AND PUBLICATION Final Report
Terry N. Long and Melanie O. Alzmann 25 Apr. 1992 35 p
(Contract NAS8-38609)
(NASA-CR-184361; Rept-5-32746; NAS 1.26:184361) Avail: CASI HC A03/MF A01

The Combined Release and Radiation Effects Satellite (CRRES) program experiments data collection, analysis, and publication activities are described. These activities were associated with both the satellite chemical release and a planned Puerto Rico sounding rocket campaign. To coordinate these activities, a working group meeting was organized and conducted. Author

N92-31636# Lamont-Doherty Geological Observatory, Palisades, NY.
LAMONT-DOHERTY GEOLOGICAL OBSERVATORY Report, 1990 - 1991
M. Langseth and R. Jellineck 1992 157 p
(PB92-185040) Avail: CASI HC A08/MF A02

This report features a series of articles whose titles are: Topography and Faulting in the Western U.S. - An example of digital map making; Profile of the Hudson River; Responses to Impending Continent-Continent Collision in the Mediterranean; Ocean Ridges as Active Volcanoes; The Role of Thermohaline Circulation in Global Climate Change; El Nino and Natural Short-Term Climate Variability; The El Nino/Southern Oscillation System and the Record of Past Climate Change; Sedimentary Basins as Thermochemical Reactors; Modeling the Stratigraphy of Continental Margins; The Role of Late-Stage Sedimentation in the Generation of GAs, Gulf of Mexico; and Conjuring Up the Red Planet. H.A.

N92-31637# National Geophysical Data Center, Boulder, CO.
SOLAR-GEOPHYSICAL DATA NUMBER 572, APRIL 1992. PART 1: (PROMPT REPORTS). DATA FOR MARCH, FEBRUARY 1992, AND LATE DATA
Helen E. Coffey, ed. Apr. 1992 162 p
(PB92-187723; SGD-572-Pt-1; LC-79-640375; ISSN-0038-0911)
Avail: CASI HC A08/MF A02

The contents of this report include a detailed index for 1991-1992 and data for February and March 1992. This data includes: solar terrestrial environment; IUWDS alert periods; solar activity indices; solar flares; solar radio emission; Stanford mean solar field; solar active regions; sudden ionosphere disturbances; solar radio spectral observations; cosmic ray measurements by neutron monitor; geomagnetic indices; provisional Dst indices for Jan.-Nov. 1991; and Pioneer Venus solar wind for Oct. 1990 to Dec. 1991. H.A.

N92-31639# National Geophysical Data Center, Boulder, CO.
SOLAR-GEOPHYSICAL DATA NUMBER 572, APRIL 1992. PART 2: (COMPREHENSIVE REPORTS). DATA FOR OCTOBER 1991 AND MISCELLANEOUS
Helen E. Coffey, ed. Apr. 1992 120 p
(PB92-187731; SGD-572-Pt-2; LC-79-640375; ISSN-0038-0911)
Avail: CASI HC A06/MF A02

The contents include a detailed index for 1991-1992, and data for Oct. 1991 on: solar flares; solar x-ray radiation from GEOS satellite; mass ejections from the sun; active prominence; and filaments. H.A.

N92-31662# Lawrence Livermore National Lab., CA.
ANALYSIS OF THE EFFECTS OF AEROSOL DISTRIBUTION IN THE ATMOSPHERE ON SURFACE RADIATIVE MEASUREMENTS
L. C. Rosen and J. Hobson Apr. 1992 26 p
(Contract W-7405-eng-48)
(DE92-014189; UCRL-ID-110395) Avail: CASI HC A03/MF A01

The distribution of atmospheric aerosols in the atmosphere may have important effects on the radiative properties of the

atmosphere and thereby on the climate. The Atmospheric and Geophysical Sciences Division of the Lawrence Livermore National Laboratory is working with the Atmospheric Radiation Measurements (ARM) program to advise the program as to the importance of aerosols to the ARM measurement plan. The ARM Program established a set of goals which highlight the important areas of scientific needs associated with the understanding and prediction of global climate change. This report summarizes the initial studies performed to assess the importance and effects of atmospheric aerosols on the measurements of atmospheric radiation. To accomplish this, three interlinked models were employed which calculated the MIE parameters, averaged over the appropriate size distributions, and computed the solar radiation at the surface. These models are discussed. A number of computations were performed using different aerosol scenarios and size distributions. These results are discussed and a summary of these initial calculations and future directions of research are outlined. DOE

N92-31766# Michigan Univ., Ann Arbor. Dept. of Naval Architecture and Marine Engineering.
COMPUTATION OF NONLINEAR GRAVITY WAVES BY A DESINGULARIZED BOUNDARY INTEGRAL METHOD
Yusong Cao Oct. 1991 169 p
(Contract N00014-86-K-0684)
(AD-A251149; TR-91-13) Avail: CASI HC A08/MF A02

A desingularized boundary integral equation method combined with an Eulerian-Lagrangian time-stepping technique is developed for nonlinear gravity wave problems. The desingularization distance between the boundary and the sources is related to the local mesh size to ensure convergence. Tests for some simple problems show that desingularization significantly reduces the computer time required to compute the influence matrix of the resulting algebraic system. The algebraic system is still adequately well-conditioned to allow fast iterative solutions. Accurate solutions can be obtained for a large range of desingularization distances on the order of the mesh size. Several nonlinear water wave problems are then investigated. The first problem considers upstream runaway solitons due to a disturbance moving near critical speed in two-dimensional shallow water. Results from the desingularized method with the fully nonlinear free surface boundary condition agree well with those using the fKdV model for weak disturbances. The fully nonlinear model predicts larger solitons than the fKdV model for strong disturbances and also predicts the breaking of waves for some stronger disturbances. GRA

N92-31906# Air Force Inst. of Tech., Wright-Patterson AFB, OH.
UPPER TROPOSPHERIC JET STREAMS OVER NORTH AMERICA DURING SUMMER 1988 M.S. Thesis
David E. Landers 1991 113 p
(AD-A249871; AFIT/CI/CIA-91-115) Avail: CASI HC A06/MF A02

Much has been written describing the jet stream. Most previous works dwell on the characteristics of the winter jet stream, when jets are faster and more easily discerned. This paper will instead focus on the jet streams over North America during the summer of 1988. During July 1988 the predominant jet regime over North America (70 percent of the observations at 250 millibars) was that of a single jet along the United States/Canada border. During August 1988, however, the single jet regime was only present 26 percent of the time, with a two jet regime occurring 53 percent of the time. The southern jet during August appeared in a location similar to the winter season subtropical jet, but generally had the characteristics of a polar front jet stream. GRA

N92-31932# Air Force Inst. of Tech., Wright-Patterson AFB, OH.
IMPULSIVE MAGNETIC PERTURBATIONS OF THE HIGH LATITUDE, DAYSIDE IONOSPHERE M.S. Thesis
Michael D. Krajnak 1991 106 p
(AD-A249872; AFIT/CI/CIA-91-110) Avail: CASI HC A06/MF A02

Recently interest has grown in the study of dayside magnetic impulse events observed at high latitude ground stations. These signals may be signatures of dayside magnetopause processes in the ionosphere. Successful identification of the ground signature of any process means that its contribution to the magnetospheric environment can be monitored with ground stations. Recent work has focused on signals that are expected to accompany mesoscale field-aligned currents moving through the ionosphere. The actual source of these currents remains controversial, with Flux Transfer Events (FTEs) and solar wind pressure enhancements being the primary candidates. We use a data set from the Ninth Coordinated Data Analysis Workshop which includes observations of the type that have been associated with dayside magnetic impulse events. We focus on the morphology and dynamics of this event which appear unique. For example, the inferred velocity across a chain of station near 1400 local time is two to ten times faster than reported near the terminator. We compare solar wind plasma and magnetic field parameters with models that relate the impulsive events to solar wind pressure perturbations of FTEs. There is an increase of the dynamic pressure prior to the event and the solar wind magnetic field is southward throughout the entire interval. GRA

N92-31964# Cooperative Inst. for Research in the Atmosphere, Fort Collins, CO.
ARO GEOSCIENCE CENTER FELLOWSHIPS Final Report, 1 Sep. 1986 - 30 Nov. 1991
Thomas H. VonderHaar, Jan L. Behunek, Viswanathan N. Bringi, Thomas H. Brubaker, and Pierre Y. Julien Jan. 1992 30 p
(Contract DAAL03-86-G-0190)
(AD-A249225; ARO-24610.1-GS-UIF) Avail: CASI HC A03/MF A01

The fellowship grant was supported by the ARO Center for Geosciences located at the Foothills Campus at Colorado State University under the auspices of the Cooperative Institute for Research in the Atmosphere (CIRA). The center for Geosciences at Colorado State University was established in collaboration with the Army Research Office on October 1, 1986. The center brought together a wide range of expertise into one focused multidisciplinary research framework. Under the administrative structure of CIRA, the center involved investigators from the University's Departments of Atmospheric Science, Civil Engineering, Electrical Engineering, Earth Resources, Forest and Wood Science, Physics, and Psychology. The technical components of the center are in atmospheric and surface remote and in-situ sensing; atmospheric modeling; hydrologic modeling; and geoscience information extraction. GRA

N92-31986# ST Systems Corp., Pacific Grove, CA.
NAVY ATMOSPHERIC BOUNDARY LAYER (NABL) MODEL SYSTEM: SOFTWARE/INTERFACE DESIGN DOCUMENT Final Report
Pierre A. Petit Dec. 1991 107 p
(Contract N00014-88-D-0333)
(AD-A247903; NOARL-TN-204) Avail: CASI HC A06/MF A02

This design documents applies to the Naval Atmospheric Boundary Layer (NABL) Model Systems which is identified and abbreviated as NABLS. The NABL model was developed to produce short-range (0 to 36 hour) forecasts of meteorological conditions in the atmospheric boundary layer. Although NABL is a one-dimensional stick model, it uses turbulence parametrizations and a vertical resolution which are superior to those in the current Navy operational regional and global atmospheric prediction model systems (NORAPS and NOGAPS respectively). NABL obtains adiabatic tendencies of temperature and moisture from NORAPS or NOGAPS, giving it three-dimensional character, although NABL does not interact in a two-way sense with either of the larger-scale prediction model systems. NABL has demonstrated superior skill at predicting the vertical structure of temperature and refractivity in the boundary layer. The NABLS will permit a system user to specify where geographically and for what forecast intervals and times the NABL model will be run; will cause the requisite initial condition and tendency information from one of the larger-scale

models to be made available for input to NABLS; and will provide for saving the resultant, high-resolution NABL model output in a convenient format(s) for use by other such applications (external to NABLS) which may now or in the future have need for such information. GRA

N92-32027# Hawaii Univ., Honolulu. Dept. of Geology and Geophysics.
PHYSICAL CHARACTERIZATION OF MAGMATIC LIQUIDS
M. H. Manghnani Jun. 1992 13 p
(Contract DE-FG03-85ER-13418)
(DE92-015302; DOE/ER-13418/T1) Avail: CASI HC A03/MF A01

This report describes a research project that was conducted from August 15, 1985 to February 28, 1992. The project was based on the ultrasonic studies of natural and synthetic silicate melts, and the study of Brillouin scattering of synthetic silicates and oxides. Measurements of the compressional wave velocity and attenuation can be established using the ultrasonic methods. Temperature dependences of silicates can be established by the Brillouin scattering. DOE

N92-32055# Utah State Univ., Logan. Center for Atmospheric and Space Sciences.
USU CENTER OF EXCELLENCE IN THEORY AND ANALYSIS OF THE GEO-PLASMA ENVIRONMENT Annual Report, 1 Oct. 1990 - 30 Sep. 1991
Robert W. Schunk 25 May 1992 26 p
(Grant AF-AFOSR-0026-90)
(AD-A252189; AFOSR-92-0547TR) Avail: CASI HC A03/MF A01

A team of ten Ph.D. scientists and several graduate students were assembled at USU to work in close collaboration with scientists at the Air Force Geophysics Laboratory on a number of problems that are relevant to Air Force systems, including OTH radars, communications, and orbiting space structures. The overall goal of the research is to obtain a better understanding of the basic chemical and physical processes operating in the geoplasma environment, including the ionosphere, thermosphere, and magnetosphere. Some of our specific tasks include the following: (1) studies of ionospheric structure and irregularities; (2) study of the feasibility of developing better operational ionospheric models; (3) conduct model/data comparisons in order to validate the ionospheric models; (4) study plasma electrodynamics in the high latitude ionosphere; (5) study magnetosphere-ionosphere coupling problems; (6) continue the development of our thermospheric circulation model; (7) study plasmasphere refilling problems; (8) study OTH ray tracing problems at high latitudes; and (9) study certain spacecraft-environment interaction problems, including those related to high-voltage power sources, spacecraft outgassing, artificial plasma cloud expansion, and spacecraft charging at LEO altitudes. GRA

N92-32195*# Massachusetts Inst. of Tech., Cambridge. Research Lab. of Electronics.
ADVANCED MICROWAVE SOUNDING UNIT STUDY FOR ATMOSPHERIC INFRARED SOUNDER Final Technical Report, 29 Mar. 1990 - 14 Jan. 1992
Philip W. Rosenkranz and David H. Staelin 12 Aug. 1992 41 p
(Contract NAS5-30791)
(NASA-CR-190628; NAS 1.26:190628) Avail: CASI HC A03/MF A01

The Atmospheric Infrared Sounder (AIRS), the Advanced Microwave Sounding Unit (AMSU-A), and the Microwave Humidity Sounder (MHS, formerly AMSU-B) together constitute the advanced sounding system facility for the Earth Observing System (EOS). A summary of the EOS phase B activities are presented. Author

47 METEOROLOGY AND CLIMATOLOGY

Includes weather forecasting and modification.

N92-31320# Army Lab. Command, White Sands Missile Range, NM. Atmospheric Sciences Lab.
UNIFIED VERY LOW STRATUS CLOUD/SUBCLOUD MICROPHYSICS MODEL Final Report
Henry Rachele Apr. 1992 73 p
(AD-A250662; ASL-TR-0309) Avail: CASI HC A04/MF A01

A model is presented for simulating very low stratus clouds and their associated subcloud regions. This model is based on the assumption that the atmosphere contains particles that can be chemically and physically characterized and that grow in the presence of moisture as a function of relative humidity, temperature, and the size and chemistry of the particles. Components of this model include droplet growth and evaporation, phase change and mass balance of total water, thermodynamics, and ascent of a cluster of drops enclosed in moist air. The model requires only limited user input: some conventional meteorological values at a reference height (2 m above ground level) and some parameter values and other specifications. Input values for a visibility parameter and relative humidity are used with a choice of air mass type to define the parameters of a truncated bimodal lognormal drop size distribution at the reference height. Vertical profiles of drop size distributions can be simulated and used for further analysis. Examples are shown for modeled vertical profiles of lapse rate, temperature, potential temperature, mass loading, relative humidity, drop size, and drop concentration. GRA

N92-31432# Air Force Inst. of Tech., Wright-Patterson AFB, OH.
BALANCED, POTENTIAL VORTICITY DYNAMICS IN THE TROPICS M.S. Thesis
Kenneth W. Harding 16 Apr. 1991 82 p
(AD-A249981; AFIT/CI/CIA-91-105) Avail: CASI HC A05/MF A01

A scheme for describing tropical atmospheric flow is analyzed. Based on the quasi-balanced approximation from Stevens et al. (1990), attempts are made to test the validity of the approximation. Isentropic potential vorticity, being a critical variable in the approximation, is calculated using data gathered during phase 2 of the Australian Meteorological Experiment (AMEX). These isentropic potential vorticity fields are then examined in terms of the Charney-Stern theorem for instability. It is found that there is a consistent area of reversed equator-to-pole gradient of potential vorticity. This area is susceptible to combined barotropic-baroclinic instability. After reviewing several previous attempts to quantify tropical atmospheric flow, the quasi-balanced approximation from Stevens et al. (1990) is tested using archived data for several different time frames and levels in the atmosphere. It is found that the quasi-balanced approximation works very well for areas not dominated by convection. In these convective areas, however, there appears to be a weakness in the approximation. GRA

N92-31493# Air Force Inst. of Tech., Wright-Patterson AFB, OH.
CLOUD-TO-GROUND LIGHTNING CHARACTERISTICS IN MESOSCALE CONVECTIVE SYSTEMS M.S. Thesis
Carolyn D. Morgenstern 1991 124 p
(AD-A250418; AFIT/CI/CIA-91-120) Avail: CASI HC A06/MF A02

Cloud-to-ground (CG) lightning characteristics were examined in 25 Mesoscale Convective Systems (MCS's) that occurred during the warm season of 1986. Lightning strike locations were superimposed on infrared (IR) satellite imagery to examine lightning ground strike patterns relative to cold cloud-tops of MCS's. Lightning strikes frequently indicated thunderstorms more than 1 hr before cold clouds were apparent on IR satellite imagery. Time series of the area within various temperature contours were compared to time series of positive and negative flash rates. The patterns of variations in negative cloud-to-ground flash rates appeared most similar to variations in the area within temperatures of -60 to -70 C on satellite imagery. Positive flashes occurred in

two different modes, a stratiform/dissipating mode and a convective mode. In the stratiform/dissipating mode, positive flashes occurred during the mature and dissipating stages of an MCS and peaked near or after the peak in negative flash rates. Ground strike locations were generally dispersed across a large area and were usually associated with either a dissipating convective region or a stratiform region on radar and with decaying and warming cloud-top temperatures on satellite imagery. The stratiform/dissipating mode appeared during all months on the warm season. GRA

N92-31521# Technische Univ., Delft (Netherlands). Faculty of Technical Mathematics and Information.

COMBINING EXPERT PROBABILISTIC WEATHER FORECASTS: RESULTS OF POST-HOC ANALYSES OF THE ZIERIKZEE EXPERIMENT

D. Roeleven, R. M. Cooke, and M. Kok (Delft Hydraulics Lab., Emmeloord, Netherlands) 1991 59 p

(Rept-91-101; ETN-92-91851) Copyright Avail: CASI HC A04/MF A01

The so called classical model for combining expert judgements is reviewed. Its application to a very large set of weather forecasting data is discussed and forecasts to those of other combination rules are compared. The notion of proper scoring rules is discussed and a generalization of this motion employed in the classical model motivated. An application of the classical model to probabilistic meteorological forecasts in The Netherlands is discussed. It emerges that the classical model produces a decision maker whose forecasts outperform the experts' individual forecasts, and outperform other rules for combining expert assessments found in the literature, namely simple averaging and log odds averaging. These results contrast with a conclusion of Clemen and Winkler that simple averaging of expert judgments produces best results. A heuristic optimization method with some favorable results is presented and conclusions drawn. ESA

N92-31523# Air Force Inst. of Tech., Wright-Patterson AFB, OH.

THE STRUCTURE AND ENERGETICS OF AMAZON SQUALL LINES Ph.D. Thesis

Harold L. Massie, Jr. Aug. 1991 211 p

(AD-A250182; AFIT/CI/CIA-91-027D) Avail: CASI HC A10/MF A03

The role of the Amazon Basin as a global center of action for deep convection is quantified in the context of the planet's heat balance. Mesoscale heat and moisture budgets are presented for three synoptic-scale coastal originating systems (COS) over the Amazon Basin during the 1987 wet season. The budgets are obtained from volumetric analyses of mesoscale rawinsonde data from the April-May 1987 Amazon Boundary Layer Experiment (ABLE-2B). Classification of cloud and rainfall components is based on data from Portable Automated Mesonet (PAM) Towers, GOES images, and radar. Satellite measurements of the total active cloud area, coupled with the mesoscale budget calculations, are used to determine the system-wide vertical transport of heat as a function of the COS life cycle. Maximum heat transport occurs in the COS mature stage when the system has its maximum spatial extent. The instantaneous heat transport for the 300-100 mb layer in a mature COS equals nearly 20 percent of the theoretical heat export requirement for the equatorial trough zone. A little more than half of the system-wide transport occurs in the dynamically active anvil cloud. GRA

N92-31540# Naval Postgraduate School, Monterey, CA. Dept. of Physics.

AMENDING THE W* VELOCITY SCALE FOR SURFACE LAYER, ENTRAINMENT ZONE, AND BAROCLINIC SHEAR IN MIXED FORCED/FREE TURBULENT CONVECTION Final Report, Oct. 1990 - Sep. 1991

R. F. Kamada 30 Mar. 1992 19 p Sponsored by AF

(Contract MIPR-FY76169100412)

(AD-A250389; NPS-PH-92-007) Avail: CASI HC A03/MF A01

We amend the free convective mixed layer velocity scale, w* to w*s to include mechanical turbulence from forced convection. W*s has discrete surface layer, entrainment zone, and baroclinic components and requires the length scales: zo, L, Delta h, zi, and zb, a newly defined baroclinic length. To close the system we offer simple models for delta h, the entrainment zone depth. The delta h models show realistic diurnal hysteresis, using a critical bulk Richardson number which exceeds unity. GRA

N92-31583# Colorado State Univ., Fort Collins. Dept. of Atmospheric Science.

UPDATED FORECAST OF ATLANTIC SEASONAL HURRICANE ACTIVITY FOR 1992

William M. Gray 5 Aug. 1992 17 p

Avail: CASI HC A03/MF A01

Presented here are the details of the author's updated forecast of tropical cyclone activity for the Atlantic Ocean region including the Caribbean Sea and the Gulf of Mexico during 1992. This updated forecast includes meteorological data for June and July and is based on the ongoing research activities which relates the amount of seasonal Atlantic tropical cyclone activity to five factors: (1) three measures of the Quasi-Biennial Oscillation of equatorial stratospheric zonal wind (QBO) at 50 mb (20 km) and 30 mb (23 km) and the absolute value of the shear between these levels; (2) the El Nino (EN) as specified by the Equatorial East Pacific Sea Surface Temperature Anomaly (SSTA) and the value of the Southern Oscillation Index (SOI); (3) Caribbean basin Sea-Level Pressure Anomalies (SLPAs) and upper tropospheric 200 mb Zonal Wind Anomalies (ZWA); (4) two measures of West African Rainfall (AR) anomalies, one of June-July in the western Sahel region, and the other the previous year August through November precipitation in the Gulf of Guinea region; and (5) the surface west to east pressure and temperature gradients across the western Sahel region of Africa. Information received by the author through 4 August 1992 indicates that the 1992 hurricane season should be below average with about 4 hurricanes, 8 named storms of at least tropical storm intensity, about 15 hurricane days, a total of 35 named storm days, and a Hurricane Destruction Potential of 35. Because the western Sahel is expected to be dry again this year, it is anticipated that there will be only one intense hurricane of Saffir/Simpson intensity category 3, 4, or 5 this season. This year's forecast is for the same amount of hurricane activity that was previously forecasted on 26 November 1991. Author

N92-31602# Air Force Inst. of Tech., Wright-Patterson AFB, OH.

A CASE STUDY OF A PROLONGED SLEET EVENT: 16-17 FEBRUARY 1987 AND CLIMATOLOGY OF SLEET EVENTS FOR NORTH CAROLINA, 1949-1989 M.S. Thesis

David R. Musick 1991 82 p

(AD-A250184; AFIT/CI/CIA-91-112) Avail: CASI HC A05/MF A01

Winter storms in the southeastern region of the United States have the potential to produce widespread regions of mixed and frozen precipitation with serious economic and social ramifications. Due to the relative infrequency of these storms, most southeastern states are ill prepared to deal with their effects, thus, increasing the need for accurate and timely forecasts of the type and duration of precipitation in this region. An investigation was undertaken of an unusually prolonged sleet event that affected North Carolina on 16-17 February 1987, to identify the synoptic and mesoscale features that governed the formation and duration of the frozen and mixed precipitation. Sleet was observed from Kansas eastward across the Appalachian Mountains to the western third of the coastal plain, with accumulations of more than 20 cm occurring in the eastern portions of the Piedmont region. These accumulations resulted in collapsed roofs and the closing of some businesses and schools for more than a week. Easterly flow on the south side of a New England high pressure center resulted in unusually strong cold-air damming that forced a shallow layer of cold air at the surface south along the east slopes of the Appalachians, across Georgia and into the Gulf of Mexico. Convective activity over the Gulf of Mexico infused significant moisture into a warm southwesterly airstream in the mid-troposphere that overran the cold air. GRA

N92-31603# Air Force Inst. of Tech., Wright-Patterson AFB, OH.

A COMPARATIVE ANALYSIS OF THE TEMPORAL VARIABILITY OF LIGHTNING OBSERVATIONS AND GOES IMAGERY M.S. Thesis

Peter B. Roohr 1991 249 p

(AD-A250185; AFIT/CI/CIA-91-109) Avail: CASI HC A11/MF A03

The chronological understanding of lightning and the development of lightning detection devices dates back to the pre World War 2 era. The fitting of thunderstorms and lightning into the global electrical circuit and the correlation of lightning to the radar characteristics and cloud features of varied convection has been the focus of research for many years. Most of the earlier systems provided localized data for research into the electrical phenomena associated with tornadic development, isolated thunderstorms, and various mesoscale interactions. With the advent of high-altitude aircraft and satellite technology came the study of lightning in a climatological sense. While polar orbiters (namely the DMSP) and the Vela satellite enabled researchers to discover certain hot spots for lightning activity around the globe, the U-2 experiments provided the criteria for a proposed geosynchronous lightning mapper. Over the last twenty years advances in electronics, the discovery of a correlation between the location of a lightning strike to ground and the peak in the return-stroke waveform, and the elimination of intracloud flashes due to their frequency characteristics led to the development of lightning detection via magnetic direction-finders and time-of-arrival systems. The magnetic direction-finder system (manufactured by Lightning Location and Protection, Inc.) determines azimuths to a lightning strike from two or more stations and triangulates to locate the strike. GRA

N92-31641# National Oceanic and Atmospheric Administration, Boulder, CO. Wave Propagation Lab.

FEASIBILITY STUDY FOR A LOW-ALTITUDE WIDE AND TEMPERATURE PROFILER

J. R. Jordan and R. J. Lataitis May 1992 28 p

(PB92-188200; NOAA-TM-ERL-WPL-222) Avail: CASI HC A03/MF A01

The feasibility of constructing a high-resolution, portable, wind and temperature profiling radar for boundary layer studies is examined. With the proposed five-beam radio acoustic sounding system, the sound speed difference between two opposed pairs of symmetric off-zenith beams can be used to profile the horizontal wind speed. The speed of sound as measured with a fifth vertical beam can be used to profile the temperature. The type of profiler can be operated in high-clutter urban environments, and can measure winds and temperature to 600 m under favorable conditions using reasonable levels of radar transmitter power. A radar equation for signal-to-noise ratio is used to calculate the maximum range for two sets of meteorological parameters corresponding to the best and worst case conditions. Author

N92-31670# Naval Postgraduate School, Monterey, CA.

A NUMERICAL, ANALYTICAL, AND OBSERVATIONAL STUDY OF THE EFFECT OF CLOUDS ON SURFACE WIND AND WIND STRESS DURING THE CENTRAL ARCTIC WINTER Ph.D. Thesis

Peter S. Guest 13 Mar. 1992 187 p

(AD-A252706) Avail: CASI HC A09/MF A02

Results of measurements from several Arctic field programs and numerical models show that clouds affect wind stress during the central Arctic winter by changing the longwave cooling of the surface and cloud layers. The longwave cooling alters the thermodynamic structure of the lower atmosphere which in turn affects the efficiency of momentum transfer to the surface. For typical Arctic conditions, wind stress is changed by about 40 percent one hour after a cloud condition change, due to changes in both the surface layer stability and surface layer wind speed. The actual wind stress effect due to clouds during this time is a function of wind speed, thermal wind, atmospheric boundary layer depth, magnitude of radiation change, snow age and, sometimes, snow depth. After several hours, surface heat fluxes are no longer important, but the structure of the atmosphere has been permanently altered. This affects the wind stress by about 10 percent to 20 percent during certain situations, but can vary depending on the initial atmospheric structure. Measurements of these effects show variations in wind stress associated with clouds. Operational and research studies of ice and ocean dynamics will benefit from consideration of cloud effects on wind stress. GRA

N92-31702# Freie Univ., Berlin (Germany, F.R.). Arbeitsgruppe Stratosphaere.

METEOROLOGICAL DATA, NEW SERIES B BASIC MATERIAL. VOLUME 53, NO. 1: DAILY ALTITUDE MAPS OF THE 30-hPa-AREA AND MONTHLY MEAN MAPS FOR THE YEAR 1986, PART 1 Quarterly Report [METEOROLOGISCHE ABHANDLUNGEN NEUE FOLGE SERIE B, GRUNDLAGENMATERIAL. BAND 53, HEFT 1: TAEGLICHE HOEHENKARTEN DER 30-HPA-FLAECHE SOWIE MONATLICHE MITTELKARTEN FUER DAS JAHR 1986. TEIL 1,1: VIERTELJAHR]

Barbara Naujokat 1986 132 p In GERMAN

(QR-1-Vol-53-No-1-Pt-1; ETN-92-91690) Copyright Avail: CASI HC A07/MF A02

Height and temperature analyses of constant pressure levels for the first quarter of the whole Northern Hemisphere are presented. These analyses are based on rawinsonde, rocket sonde, and satellite data and were performed by means of a hydrostatic build-up method. The daily charts were digitized and the values were obtained as grid points on a geographical grid. The computed monthly mean values are included in tables and supplemented with the climatological values reported from the radiosonde stations. Distributions of the standard deviations, monthly variations, deviations from the parallel mean, and the long term mean are presented. The stratospheric circulation is described for polar, mid, and tropical latitudes. ESA

N92-31704# Freie Univ., Berlin (Germany, F.R.). Arbeitsgruppe Stratosphaere.

METEOROLOGICAL DATA, NEW SERIES B BASIC MATERIAL. VOLUME 53, NO. 2: DAILY ALTITUDE MAPS OF THE 30-hPa-AREA AND MONTHLY MEAN MAPS FOR THE YEAR 1986, PART 2 Quarterly Report [METEOROLOGISCHE ABHANDLUNGEN NEUE FOLGE SERIE B GRUNDLAGENMATERIAL. BAND 53, HEFT 2: TAEGLICHE HOEHENKARTEN DER 30-HPA-FLAECHE SOWIE MONATLICHE MITTELKARTEN FUER DAS JAHR 1986. TEIL 2,2: VIERTELJAHR]

Barbara Naujokat 1986 85 p In GERMAN

(QR-2-Vol-53-No-2-Pt-2; ETN-92-91691) Copyright Avail: CASI HC A05/MF A01

Height and temperature analyses of constant pressure levels for the second quarter of the whole Northern Hemisphere are presented. These analyses were based on rawinsonde, rocket sonde, and satellite data and were performed by means of a hydrostatic build up method. The daily charts were digitized and the values were obtained as grid points on a geographical grid. The computed monthly mean values are included on tables and supplemented with the climatological values reported from the radiosonde stations. Distributions of the standard deviations, monthly variations, deviations from the parallel mean, and the long term mean are presented. The stratospheric circulation is described for polar, mid, and tropical latitudes. ESA

N92-31706# Freie Univ., Berlin (Germany, F.R.). Arbeitsgruppe Stratosphaere.
METEOROLOGICAL DATA, NEW SERIES B BASIC MATERIAL. VOLUME 53, NO. 4: DAILY ALTITUDE MAPS OF THE 30-hPa-AREA AND MONTHLY MEAN MAPS FOR THE YEAR 1986, PART 4 Quarterly Report [METEOROLOGISCHE ABHANDLUNGEN, NEUE FOLGE SERIE B GRUNDLAGENMATERIAL. BAND 53, HEFT 4: TAEGLICHE HOEHENKARTEN DER 30-HPA-FLAECHE SOWIE MONATLICHE MITTELKARTEN FUER DAS JAHR 1986. TEIL 4,4: VIERTELJAHR]
Barbara Naujokat 1986 117 p In GERMAN
(QR-4-Vol-53-No-4-Pt-4; ETN-92-91692) Copyright Avail: CASI HC A06/MF A02

Height and temperature analyses of constant pressure levels for the fourth quarter of the whole Northern Hemisphere are presented. These analyses were based on rawinsonde, rocket sonde, and satellite data and were performed by means of a hydrostratic buildup method. The daily charts were digitized and the values were obtained as grid points on a geographical grid. The computed, monthly mean values are included in tables and supplemented with the climatological values reported from the radiosonde stations. Distributions of the standard deviations, monthly variations, deviations from the parallel mean, and the long term mean are presented. The stratospheric circulation is described for polar, mid, and tropical latitudes. ESA

N92-31708# Freie Univ., Berlin (Germany, F.R.). Inst. fuer Meteorologie.
METEOROLOGICAL DATA, NEW SERIES A MONOGRAPHS. VOLUME 5, NO. 4: A THREE DIMENSIONAL MODEL SIMULATION OF THE CIRCULATION IN THE MIDDLE ATMOSPHERE WITH CCONSIDERATION OF TROPOSPHERICAL-STRATOSPHERICAL INTERACTIONS Ph.D. Thesis [METEOROLOGISCHE ABHANDLUNGEN NEUE FOLGE SERIE A MONOGRAPHIEN. BAND 5, HEFT 4: EINE DREIDIMENSIONALE MODELLSIMULATION DER ZIRKULATION IN DER MITTLEREN ATMOSPHAERE MIT ASPEKTEN TROPOSPHAERISCH STRATOSPHAERISCHER WECHSELWIRKUNGEN]
Ulrike Langematz Sep. 1991 182 p In GERMAN
(Contract BMFT-KF-20128)
(ETN-92-91693) Copyright Avail: CASI HC A09/MF A02

A global, nonlinear three dimensional primitive equation model designed to perform simulations of the middle atmosphere circulation is presented. The model was based on the spectral ECMWF (European Centre for Medium Weather Forecasts) forecast model and was vertically extended to 0.01 hPa (near 80 km). Physical processes in the troposphere were unchanged. In the stratosphere and mesosphere parametrizations of radiative processes and small scale dissipation were added. The ability of the model to reproduce the characteristic climatological structure in the middle atmosphere was shown by analyzing a perpetual January integration. Model deficiencies were explained by the crude parameterization in longwave cooling rates and by the missing gravity wave parameterization. The effects of raising the upper boundary on the tropospheric climate were investigated by parallel integrations of the extended and two unextended model versions. In the stratosphere the original model shows evidence of reflecting vertically propagating planetary waves. The climate of the extended version is close to reality. In the troposphere there are only small differences. The introduction of a relaxation term for the zonal wind in the two top model layers which is often used in numerical models to avoid energy reflection from the upper boundary is shown to be of considerable negative influence on the lower troposphere climate of the original ECMWF model. ESA

N92-31709# Sandia National Labs., Albuquerque, NM.
USING TRANSFER FUNCTIONS AS A METHOD FOR PREDICTING LIGHTNING EFFECTS ON MUNITIONS STORAGE BUNKERS
J. K. Struck (Picatinny Arsenal, Dover, NJ.), M. A. Chiefa (Picatinny Arsenal, Dover, NJ.), J. E. Grenert (Picatinny Arsenal, Dover, NJ.), R. E. Jorgenson, and M. E. Morris 1992 5 p Presented at the 21st International Conference on Lightning Protection, Berlin (Germany), 22-25 Sep. 1992
(Contract DE-AC04-76DP-00789)
(DE92-012627; SAND-92-1008C; CONF-9209107-1) Avail: CASI HC A01/MF A01

Measurements have recently been conducted and computer models constructed to determine the coupling of lightning energy into munition storage bunkers as detailed in companion conference papers. In this paper, transfer functions from the incident current to the measured parameters are used to construct simple circuit models that explain much of the important observed quantitative and qualitative information and differences in transfer functions are used to identify nonlinearities in the response data. In particular, V(sub oc) - the open-circuit voltage generated between metal objects in the structure, I(sub sc) - the short-circuit current generated in a wire connecting metal objects in the structure, and a typical current measurement in the buried counterpoise system behave in a relatively simple manner explainable by one or several circuit elements. The circuit elements inferred from measured data are comparable in magnitude with those developed from simple analytical models for inductance and resistance. These analytical models are more useful in predicting bounding electromagnetic environment values rather than providing exact time domain waveforms. DOE

N92-31710# Freie Univ., Berlin (Germany, F.R.). Inst. fuer Meteorologie.
METEOROLOGICAL DATA, NEW SERIES A MONOGRAPHS. VOLUME 6, NO. 2: CASE STUDY ON THE CONGRUENCE OF PRECIPITATION DATA FROM SYNOP-MODELL AND METEOSAT DATA Ph.D. Thesis [METEOROLOGISCHE ABHANDLUNGEN NEUE FOLGE SERIE A MONOGRAPHIEN. BAND 6, HEFT 2: FALLSTUDIE UEBER DIEK ONGRUENZ VON NIEDERSCHLAGSINFORMATION AUS SYNOP-, MODELL- UND METEOSAT-DATEN]
Margit Christa Scholl May 1991 181 p In GERMAN
(ETN-92-91694) Copyright Avail: CASI HC A09/MF A02

An empirical process for the meteorological data integration in the regional grid is studied. The possibility of deriving the distribution of precipitation on ground under European conditions from satellite data is examined. A method which uses the usual satellite data of the visible and infrared spectral area in a trispectral form and directly refers to ground observations as an a priori knowledge to obtain regional forecasting is proposed. The data were integrated in a modular program system which contains procedures for structuration, interpolation, correction and inclusion of three dimensional analyses. The method is proved to be helpful for a good local and regional weather diagnosis. ESA

N92-31714# Air Force Inst. of Tech., Wright-Patterson AFB, OH.
SIMULATION OF DIURNALLY VARYING DOWNSLOPE WINDS OVER NORTHERN UTAH M.S. Thesis
Kim M. Rigling Jun. 1991 73 p
(AD-A250568; AFIT/CI/CIA-91-116) Avail: CASI HC A04/MF A01

A relatively complete regional model is utilized to simulate downslope winds in two dimensions. The purpose of this study is to investigate the applicability of conclusions gained by prior investigators using simpler models that lacked diurnal solar cycles and have not explicitly included boundary layer physics. The model used in this study retains turbulent kinetic energy and surface energy budgets as well as longwave and shortwave radiative effects, and is applied to a realistic section to topography over Northern Utah. The diurnal cycle, established by the radiation calculations and reinforced with the prognostic turbulence closure terms, is found to be a first order effect and, therefore, essential for the evolution of windstorm events. These events are characterized by a nocturnal maximum in the forecast wind fields and development of a strong low level temperature inversion. Winds are weakest in the early afternoon at the time of strongest vertical turbulent mixing and most unstable stratification. This study

confirms previous findings on the importance of the vertical wind and stability profiles to the amplification of downslope winds. It also investigates the dynamics of the momentum equation, and finds that, over most of the region of strong winds, the Bernoulli and dissipation terms oppose the pressure gradient and terrain following terms, and the Coriolis term is negligible. Preliminary results for the three-dimensional case are presented. GRA

N92-31734# National Climatic Data Center, Asheville, NC.
COMPREHENSIVE AEROLOGICAL REFERENCE DATA SET (CARDS)
R. E. Eskridge 1992 79 p
(Contract DE-AI05-90ER-61011)
(DE92-016469; DOE/ER-61011/T2) Avail: CASI HC A05/MF A01

Under the CO2 doubling scenario, the current numerical climate models are robust in predicting that surface temperatures will rise markedly in the polar regions and that stratospheric temperatures will decrease markedly. The goal of the CARDS project is to produce an upper air data set based on radiosonde and pibal observations suitable for use in evaluating climate models and detecting climate change. We are taking a number of steps to achieve this goal: we have begun collecting upper air data from various sources, we are developing plans to digitize (key) selected older data, we are developing station histories, we have developed version 1.0 of a quality control (QC) program, and we are developing methods for removing biases (systematic errors) from these data. A final step to ensure data integrity will consist of an analysis of these data in the context of greenhouse-gas induced climate modification. DOE

N92-31750# Sandia National Labs., Albuquerque, NM.
MEASURED RESPONSES OF A MUNITIONS STORAGE BUNKER TO ROCKET-TRIGGERED LIGHTNING
G. H. Schnetzer and R. J. Fisher 1991 6 p Presented at the 21st International Conference on Lightning Protection, Berlin (Germany), 22-25 Sep. 1992
(Contract DE-AC04-76DP-00789)
(DE92-012628; SAND-91-2061C; CONF-9209107-2) Avail: CASI HC A02/MF A01

During the summer of 1991, a rocket-triggered lightning test was performed on an earth-covered munitions bunker located at Ft. McClellan, Alabama. Nine negative cloud-to-ground lightning flashes, comprising a total of 38 individual return strokes, were successfully initiated and directed to designated attachment points on the structure. High resolution measurements were simultaneously made of the incident flash currents, both return-stroke and continuing current components, and of responses at 24 test points located throughout the bunker. The response quantities that were recorded included currents, voltages, and electric and magnetic fields. The maximum responses observed at each test point, both as measured and as linearly scaled to median and severe return-stroke incident current amplitudes, are presented and discussed. DOE

N92-31784# Air Force Inst. of Tech., Wright-Patterson AFB, OH.
A COMPARATIVE STUDY OF THE DYNAMIC PERFORMANCE OF THREE BIVANES M.S. Thesis
William G. Coats, Jr. May 1991 181 p
(AD-A250096; AFIT/CI/CIA-91-107) Avail: CASI HC A09/MF A02

The dynamic performances of three multi-directional wind vanes, or bivanes, are studied and compared for the purpose of determining which bivane responds the fastest to changes in wind direction, with acceptable accuracy. The procedures for testing the bivanes include evaluations on the static and dynamic characteristics of each bivane, and comparing how well each conforms to published standards. The static tests determined the accuracy and linearity of each bivane. Deviations from the ideal linear response were used to correct the dynamic test data. The dynamic tests were performed in the large Civil Engineering wind tunnel at wind speeds of 5 and 10 m/s. The bivanes were released from six positions and allowed to return to the equilibrium angle. All three bivanes produced second-order underdamped responses necessary to rapidly adjust to a change in wind direction. Using the times of the first peak and second zero-crossing, the damping ratio, and natural wavelength, were calculated. These parameters described how well and fast the bivane responds to changes in wind direction. Apart from technical irregularities in a portion of the electronics, the Climatronics Dual Annulus Bivane responded the quickest and appears to be the best bivane for yielding wind components. GRA

N92-31894# Maryland Univ., College Park.
A STUDY OF LONGWAVE RADIATION CODES FOR CLIMATE STUDIES: VALIDATION WITH ARM OBSERVATIONS AND TESTS IN GENERAL CIRCULATION MODELS
R. G. Ellingson and F. Baer 1992 6 p
(Contract DE-FG05-90ER-61075)
(DE92-014100; DOE/ER-61075/T1) Avail: CASI HC A02/MF A01

Research by the US Department of Energy (DOE) has shown that cloud radiative feedback is the single most important effect determining the magnitude of possible climatic responses to human activity. However, these effects are still not known at the levels needed for climate prediction. Consequently, DOE has launched a major initiative -- the Atmospheric Radiation Measurements (ARM) Program -- directed at improving the parameterization of the physics governing cloud and radiative processes in general circulation models (GCM's). One specific goal of ARM is to improve the treatment of radiative transfer in GCM's under clear-sky, general overcast, and broken cloud conditions. Our approach to developing the radiation model is to test existing models in an iterative, predictive fashion. We will supply the Clouds and Radiative Testbed (CART) with a set of models to be compared with operationally observed data. The differences we find will lead to the development of new models to be tested with new data. Similarly, our GCM studies will use existing GCM's to study the radiation sensitivity problem. We anticipate that the outcome of this approach will provide both a better longwave radiative forcing algorithm and a better understanding of how longwave radiative forcing influences the equilibrium climate of the atmosphere. DOE

N92-31978# Naval Postgraduate School, Monterey, CA.
A DIAGNOSTIC STUDY OF RAPIDLY DEVELOPING CYCLONES USING SURFACE-BASED Q VECTORS M.S. Thesis
David W. Titley Jun. 1991 138 p
(AD-A246993) Avail: CASI HC A07/MF A02

Accurate short-term (0-6 h) forecasts of rapid cyclogenesis are important to both civilian and military maritime interests. Because upper-air observations over the ocean are sparse, the relatively plentiful surface synoptic data must be used for diagnostic analysis. Surface pressure and temperature data for two Intensive Observation Periods (IOP's) that occurred during the Experiment on Rapidly Intensifying Cyclones over the Atlantic (ERICA) are objectively analyzed and Q vectors--a measure of the low-level ageostrophic flow required to restore geostrophic balance--are calculated. Areas of Q vector convergence, which imply upward vertical motion, were compared to satellite imagery and to the future 3-h and 6-h pressure tendencies. When the storms were intensifying most rapidly, satellite imagery showed cold-topped stratiform clouds over areas of Q vector convergence. Areas of strong Q vector convergence (divergence) showed significant (95 percent confidence level) pressure falls (rises) 3 h and 6 h in the future. Surface Q vectors are shown to have qualitative value in short-range forecasts of the location of the storm, but do not forecast storm intensity. The surface Q vector interpretations are less useful near landmasses, as the surface temperature field becomes less representative of the mean tropospheric temperature. GRA

N92-32097# Polish Academy of Sciences, Warsaw. Inst. Podstawowych Problemow Techniki.
PROBABILISTIC ANALYSIS OF TWENTY-FOUR HOUR WEATHER DATA FOR WARSAW [ANALIZA PROBABLISTYCZNA DOBOWYCH DANYCH POGODOWYCH DLA WARSZAWY]
Dorota Bzowska and Elzbieta Kossecka 1992 58 p In POLISH
Avail: CASI HC A04/MF A01

Weather data recorded for Warsaw during a period of 10 years was used for determining the probabilistic characteristics of daily changes in weather variables which affect the heat exchange processes in buildings. Their mutual correlations were also analyzed. Author

N92-32103# Massachusetts Inst. of Tech., Cambridge.
A COMPARISON OF THE PERFORMANCE OF TWO GUST FRONT DETECTION ALGORITHMS USING A LENGTH-BASED SCORING TECHNIQUE
D. L. Klingle-Wilson, M. F. Donovan, S. H. Olson, and F. W. Wilson 8 May 1992 45 p
(Contract DTFA01-89-Z-02033)
(AD-A250862; ATC-185; DOT/FAA/NR-92/1) Avail: CASI HC A03/MF A01

The Terminal Doppler Weather Radar (TDWR) Gust Front Algorithm provides, as products, estimates of the current locations of gust fronts, their future locations, the wind speed and direction behind the gust fronts, and the wind shear hazard to landing or departing aircraft. These products are used by air traffic controllers and supervisors to warn pilots of potentially hazardous wind shears during take-off and landing and to plan runway reconfigurations. Until recently, an event-based scoring scheme was used to evaluate the performance of the algorithm. With the event-based scoring scheme, if any part of a gust front was detected, a valid detection was declared. Unfortunately, this scheme gave no indication of how much of the gust front length was detected, nor could the probabilities be easily related to the probability of issuing a wind shear alert for a specific approach or departure path which was being impacted by a gust front. To make the scoring metric more nearly reflect the operational use of the product, a new length-based scoring scheme was devised. This scheme computes the length of the gust front detected by the algorithm. When computed over a large number of gust fronts, this length-based scoring scheme yields the probability that any part of the gust front will be detected. GRA

N92-32212# Instituto de Pesquisas Espaciais, Sao Jose dos Campos (Brazil).
A COORDINATED STUDY OF A STORM SYSTEM OVER THE SOUTH AMERICAN CONTINENT M.S. Thesis [ESTUDO COORDENADO DE UM SISTEMA DE TEMPESTADE SOBRE A AMERICA DO SUL]
Rosangela Barreto Bi Gin Apr. 1992 161 p In PORTUGESE
(INPE-5388-TDI/477) Avail: CASI HC A08/MF A02

A coordinated study of a storm system over South America is presented. Data were obtained by a stratospheric balloon borne electric field detector launched from Cachoeira Paulista (22 degrees 39 minutes S, 47 degrees 9 minutes W) on December 13, 1989. The data were supported by synoptic information, local meteorological balloon soundings, GOES-7 infrared imagery, conventional meteorological radars and a lightning detector and tracking system. The analysis of results showed that the storm consisted of large thunderstorm cells with very high cloud tops. In the edge of the storm, some thunderclouds were distributed along squall lines. From the electric field balloon data, it was estimated that the thunderstorm cells had charges in excess of a hundred of coulombs. Also it was not found evidence of the presence of a shielding layer. The stratosferic temperature data showed perturbations associated with the storm, perhaps due to thunderstorm generated gravity waves. The lightning related ground data showed that most of the flashes come from the edge of the storm and are positive. These results seem to indicate that the electrical structure of thunderstorms in South America has some peculiarities. The importance of these peculiarities on the global atmospheric electric circuit remains to be investigated. Author

N92-32224# Instituto de Pesquisas Espaciais, Sao Jose dos Campos (Brazil).
RAINWATER AND THROUGHFALL CHEMISTRY IN A TERRA FIRME RAIN FOREST: CENTRAL AMAZONIA
Maria Cristina Forti and Lycia Maria Moreira-Nordemann 1992 27 p Previously announced in IAA as A91-34858 Submitted for publication Sponsored by GTE/ABLE and Financiadora de Estudos e Projetos
(INPE-5364-PRE/1744) Avail: CASI HC A03/MF A01

During the Global Tropospheric Experimental (GTE) Amazon Boundary Layer Experiment (ABLE) 2B campaign in the Amazon basin, samples of rainwater and throughfall were obtained in a 'terra firme' (non-flooded forest) rainforest at the Ducke Reserve. The samples were collected during one wet period (April 1 to May 13, 1987) and one dry period (August 1 to October 1, 1987). All samples were analyzed for Na(+), K(+), Mg(+), Ca(2+), NH4(+), Cl(-) and SO4(2-), and pH. The rainwater was acidic, with a volume-weighted mean pH of 4.6 for the two periods. Rainwater input from the dry period was two times greater for Na(+), Mg(2+), NH4(+) and SO4(2-) and about four times greater for K(+) than from the wet period. The ionic concentrations in throughfall were higher than those in rainwater, except for NH4(+) during the dry period. This enrichment of throughfall is attributed to the interaction of precipitation with the forest canopy. Author

48 OCEANOGRAPHY

Includes biological, dynamic, and physical oceanography; and marine resources.

For related information see also *43 Earth Resources and Remote Sensing.*

N92-31308# Institute for Naval Oceanography, Bay Saint Louis, MS.
SYNTHETIC TEMPERATURE PROFILE IN THE GULF OF MEXICO. PART 1: STATISTICAL RELATIONSHIP BETWEEN MODAL AMPLITUDES AND DYNAMIC HEIGHT AT SURFACE
D. S. Ko May 1992 25 p
(AD-A252701; INO-TM-8-Pt-1) Avail: CASI HC A03/MF A01

The feasibility of estimating temperature profiles (synthetic temperature profiles) from Geodetic Earth Orbiting Satellite (GEOSAT) altimeter-derived sea-surface heights in the Gulf Stream region has been explored. The scheme was based on a statistical relationship between sea surface heights and subsurface temperature profiles derived by deWitt. DeWitt found that the first two empirical orthogonal functions (EOFs) of the temperature profiles represented more than 95 percent of the overall temperature variance. Furthermore, he found that there is a tight relationship between relative dynamic height and amplitude of the first two EOF modes. This relationship was used to generate the synthetic temperature profiles from GEOSAT data. The synthetic temperature profiles compared well with the expendable bathythermograph (XBT) measurements. In this study the temperature and salinity profiles in the Gulf of Mexico were collected and analyzed. Then the deWitt scheme was employed. The feasibility of using sea-surface heights to estimate temperature profiles (synthetic profiles) in the Gulf of Mexico was investigated. GRA

N92-31406# Harvard Univ., Cambridge, MA. Div. of Applied Sciences.
MODELLING AND PREDICTION OF REGIONS OF THE NORTH PACIFIC Final Technical Report, 1 Jul. 1987 - 1 Oct. 1989
Allan R. Robinson 1991 11 p
(Contract N00014-87-K-6009)
(AD-A252144; NOARL-CR-044-91) Avail: CASI HC A02/MF A01

This was a project for the identification and description of the

phenomenology and research into the development of a nowcast and forecast scheme for the frontal location and predominant features of the sub-arctic frontal region of the North Pacific Ocean. The potential coupling of the Harvard Open Ocean Model (HOOM) to a regional ocean model was investigated. The lead scientist at Harvard and Co-Principal Investigator was Dr. Richard Schmalz until March 1989, followed by Dr. Carlos Lozano. Mr. Wayne Leslie also participated. Professor Gunnar Roden of the University of Washington participated in the project as a principal scientist. GRA

N92-31407# Naval Postgraduate School, Monterey, CA.
SENSITIVITY OF THE TOMOGRAPHIC INVERSE SOLUTION TO ACOUSTIC PATH VARIABILITY M.S. Thesis
Gary E. English Mar. 1992 40 p
(AD-A252146) Avail: CASI HC A03/MF A01

As part of the Greenland Sea Project, Woods Hole Oceanographic Institution and Scripps Institute of Oceanography deployed six acoustic tomography transceiver moorings to measure variability of the Greenland Sea gyre through a cooling cycle from September 1988 to August 1989. Using a set of Greenland Sea acoustic tomography data provided by Woods Hole Oceanographic Institution, this thesis investigated the importance of incorporating acoustic path changes in the construction of the tomographic inverse solution. A comparison of the inverse solutions for changes in sound speed using non-corrected and corrected acoustic multipaths was conducted. Although the two inverse solutions are qualitatively similar, significant quantitative differences exist. These differences indicate that it is necessary to account for changes in the acoustic multipaths for the generation of accurate Greenland Sea acoustic tomography maps. GRA

N92-31429# Institute of Ocean Sciences, Sidney (British Columbia).
ACOUSTIC STUDIES OF OCEAN SURFACE PROCESSES IN SWAPP Final Report
D. M. Farmer 5 Feb. 1992 12 p
(Contract N00014-91-J-1036)
(AD-A247519) Avail: CASI HC A03/MF A01

This report covers work done as a result of participation in the SWAPP cruise in conjunction with FLIP. We participated with the IOS vessel PARIZEAU and obtained extensive data sets using two rather novel approaches. We used active sonar systems to detect bubble clouds and bubble size distributions, and passive hydrophones to map the distribution and properties of breaking surface waves. Each of these approaches not only involved the development of specialized hardware, but also required development of novel signal processing schemes so as to handle the very high data rates. Each approach is described in sequence. A publication list resulting from this work is also included. GRA

N92-31495# Naval Postgraduate School, Monterey, CA. Dept. of Oceanography.
HYDROGRAPHIC AND ACOUSTIC DOPPLER CURRENT PROFILER (ADCP) DATA FROM THE FARALLONES SHELF AND SLOPE STUDY Technical Report, 13-18 Feb. 1991
Paul F. Jessen, Steven R. Ramp, Curtis A. Collins, Newell Arfield, and Leslie K. Rosenfeld Mar. 1992 179 p
(AD-A250834; NPS-OC-92-003) Avail: CASI HC A09/MF A02

This data report presents hydrographic (CTD) and Acoustic Doppler Current Profiler (ADCP) data from a cruise to the Continental Shelf and slope region near the Gulf of the Farallones National Marine Sanctuary during 13-18 February 1991. The study area encompassed a region from 75 km south of San Francisco (Pigeon Point) north to about 38 deg 0.0' N (Point Reyes) extending from the coast to about 90 km offshore. The sampling grid consisted of five across-shore transects 20 km apart, with nine or ten CTD stations from 5 to 15 km apart each transect. A total of forty-eight CTD's were made to within approximately 25 m of the bottom. ADCP data were collected during the occupation of the sampling grid as well during a separate ADCP survey conducted at the end of the cruise. The data are presented as vertical sections, property distributions on horizontal surfaces, and waterfall plots. GRA

N92-31544# Florida Univ., Gainesville. Dept. of Geography.
GEOMORPHIC VARIABILITY IN THE COASTAL ZONE Final Report
Joann Mossa, Edward P. Meisburger, and Andrew Morang May 1992 123 p Sponsored by Corps of Engineers
(AD-A252713; CREC-TR-92-4) Avail: CASI HC A06/MF A02

The coastlines of the world's oceans encompass a tremendous variety of geomorphic and geologic structures. They range from rocky cliffs to sandy barrier beaches to low-lying swampy wetlands. The geomorphic forms were created by the interaction of antecedent geology, physical dynamic processes, and man-made intervention. Variable features are usually composed of unconsolidated materials that respond rapidly to changes in the dynamic environment. More stable features are usually associated with consolidated rock or occur in quiescent environments. The geologic history of shorelines can be inferred from a careful study of geomorphic structures, coupled with additional data on physical processes and historic events. Many of the study techniques are relatively simple, consisting of analysis of existing maps and historical sources. An understanding of the processes which have shaped the shore is crucial to the design of coastal structures and to the intelligent management of coastal resources and habitats. In addition, understanding of the form/process relationships between geomorphology and dynamics may allow coastal scientists to more accurately predict the results of construction or other modifications along the shore. GRA

N92-31572# Lamont-Doherty Geological Inst., Palisades, NY.
STEADY-STATE AND TRANSIENT MODELING OF TRACER AND NUTRIENT DISTRIBUTIONS IN THE GLOBAL OCEAN
T. F. Stocker and W. S. Broecker 26 Mar. 1992 22 p
(Contract DE-FG02-91ER-61202)
(DE92-011805; DOE/ER-61202/1) Avail: CASI HC A03/MF A01

The deep circulation model developed by Wright and Stocker has been used to represent the latitude-depth distributions of temperature, salinity, radiocarbon, and color tracers in the Pacific, Atlantic, and Indian Oceans. Restoring temperature and salinity to observed surface data, the model shows a global thermohaline circulation where deep water is formed in the North Atlantic and in the Southern Ocean. A parameter study reveals that the high-latitude surface salinity determines the composition of deep water and its flow in the global ocean. Increasing Southern Ocean surface salinity by 0.4 ppt, the circulation changes from a present-day mode where North Atlantic deep water is one where Antarctic bottom water is dominant. An inorganic carbon cycle with surface carbonate chemistry is included, and gas exchange is parameterized in terms of pCO2 differences. Pre-industrial conditions are achieved by adjusting the basin-mean alkalinity. A classical 2 x CO2 experiment yields the intrinsic time scales for carbon uptake of the ocean; they agree with those obtained from simple box models or 3-dimensional ocean general circulation models. Using the estimated industrial anthropogenic input of CO2 into the atmosphere the model requires, consistent with other model studies, an additional carbon flux to match the observed increase of atmospheric pCO2. We use more realistic surface boundary conditions which reduce sensitivity to freshwater discharges into the ocean. In a glacial-to-interglacial experiment rapid transitions of the deep circulation between two different states occur in conjunction with a severe reduction of the meridional heat flux and sea surface temperature during peak melting. After the melting the conveyor belt circulation restarts. DOE

N92-31630# Walcoff and Associates, Inc., Alexandria, VA.
PROCEEDINGS OF THE 4TH ATLANTIC OCS REGION INFORMATION TRANSFER MEETING Final Report
R. Ainger, L. Atkinson, T. Berger, S. Broome, and G. Brown Feb. 1992 199 p Meeting held in Wilmington, NC, 24-25 Sep. 1991 Sponsored in part by Minerals Management Service
(Contract DI-14-12-0001-30583)
(PB92-177690; OCS/MMS-92/0001) Avail: CASI HC A09/MF A03

The area of industry interest is known as the Manteo Prospect,

while the activities surrounding the proposed drilling are referred to collectively as the Manteo Project. The wildcat wellsite is 2,690 ft (857 m) of water near the edge of the Gulf Stream. It is also near a fishing ground known locally as 'The Point'. The area is believed to be gas prone rather than oil prone. The estimated size of the resource could be as high as 5 trillion cubic feet of gas. The purpose of the meeting was to exchange information to the leasing background, legislative activities, scientific results, and socioeconomic studies. Legislative-related reports include descriptions of the Oil Pollution Act of 1990, the Outer Banks Protection Act, the Environmental Studies Review Panel, and the North Carolina Physical Oceanography Panel. Reports of studies on marine life include benthic diatoms, benthic fauna, pelagic seabirds, sea turtles, and right whales. One report describes the use of airships (blimps) for ocean research - a capability relevant to North Carolina because the east coast airship facility is located in the state. Local marine science facilities described include NOAA's National Undersea Research Center at the University of North Carolina at Wilmington (NURC/UNCW) and the National Marine Fisheries Service Laboratory in Beaufort. Developments in oil spill cleanup technology and capabilities are described by both the Coast Guard and the industry. A socioeconomic report describes the effects of the oil and gas activities on the tourist industry. Author

N92-31644# Woods Hole Oceanographic Inst., MA.
HYDROGRAPHIC OBSERVATIONS FROM THE US/PRC COOPERATIVE PROGRAM IN THE WESTERN EQUATORIAL PACIFIC OCEAN: CRUISES 5-8
B. J. Lake, K. Yang, Z. Luizhi, R. C. Millard, and S. Pu Jul. 1991 414 p
(Contract NA85AA-D-AC117)
(PB92-177054; WHOI-91-19) Avail: CASI HC A18/MF A04

In support of the Tropical Ocean and Global Atmosphere (TOGA) program, investigators from the Woods Hole Oceanographic Institution (WHOI), NOAA Pacific Marine Environmental Laboratory (PMEL), and the State Oceanic Administration (SOA) from both Qingdao (First Institute) and Guangzhou (South China Sea Branch) conducted hydrographic observations aboard the Chinese R/V Xiang Yang Hong 14 in the western equatorial Pacific Ocean. The objective of the component of the TOGA program was to document the water mass property distributions of the western equatorial Pacific and describe the oceanic velocity field. The four cruises summarized here were conducted during the period November 1988 to July 1990 and are the final half of an eight cruise repeated survey of the region begun in 1985. Conductivity-Temperature Depth-Oxygen (CTD/O2) stations were collected to a minimum cast depth of 2500m or the bottom when shallower. The cruise reoccupied the same stations to provide temporal information. Summarized listings of CTD/O2 data together with selected physical properties of sea water for these cruises are provided here, as well as a description of the hardware used and an explanation of the data reduction techniques employed. Author

N92-31821# Systems Science and Software, La Jolla, CA.
THREE-DIMENSIONAL FINITE DIFFERENCE MODELING OF SURFACE WAVE PROPAGATION ACROSS THE BARENTS SHELF
K. L. McLaughlin, T. G. Barker, J. L. Stevens, B. Shkoller, and S. M. Day Oct. 1991 74 p
(Contract F08606-89-C-0022)
(AD-A249865; SSS-TR-91-12828) Avail: CASI HC A04/MF A01

A three-dimensional (3D) finite difference simulation has been conducted of surface waves propagating across a laterally heterogeneous velocity and density model of the Barents Shelf. The 3D model encompasses a region of 1620 by 810 km to a depth of 210 km. The calculations were designed to model 0.02 to 0.05 Hz surface waves from an isotropic source at Novaya Zemlya in a 3D heterogeneous model. Extensive focusing/defocusing of surface waves are observed for the entire bandwidth from 0.02 to 0.05 Hz. Focusing/defocusing is observed to frequency dependent such that the amplitude patterns of 0.02 and 0.05 Hz are not correlated. A hybrid Fresnel-Kirchoff technique is used to project Rayleigh wave amplitudes to teleseismic distances. About 25 percent of the variance of the far-field Rayleigh wave amplitude scatter from Novaya Zemlya events can be explained by near-source (within 800 km) scattering. Multipathing was observed to occur for 0.04 to 0.05 Hz Rayleigh waves, consistent with observations of Novaya Zemlya events observed at the Norwegian Seismic Array (NORSAR). Rayleigh-to-Love conversion is observed in the simulation in localized regions along structural boundaries. Such scattered Love waves should be observable at narrow azimuthal ranges. GRA

N92-31842# Woods Hole Oceanographic Inst., MA. Hydrographic Programme Office.
WORLD OCEAN CIRCULATION EXPERIMENT. WOCE CHLOROFLUOROCARBON INTERCOMPARISON CRUISE REPORT
Douglas W. R. Wallace (Brookhaven National Lab., Upton, NY.), R. Weiss (Scripps Institution of Oceanography, San Diego, CA.), and T. Joyce Mar. 1992 39 p
(Contract DE-AC02-76CH-00016; NSF OCE-86-13321; NSF OCE-92-06184)
(PB92-185974; WOCE-83/92; WHPO-92-1) Avail: CASI HC A03/MF A01

Measurements of the anthropogenic chlorofluorocarbons (CFC's), F11 (CCl3F), and F12 (CCl2F2) were identified as a priority measurement to be made on all WOCE-WHP legs. The utility of these compounds lies in their conservative behavior in sea water, their transient atmospheric and surface ocean history, and in their being amenable to rapid and cost-effective analysis at sea. An at-sea comparison of chlorofluorocarbon (CFC) measurements was conducted aboard the R/V New Horizon at the GEOSECS intercalibration station at 28 degrees 31.0 N 122 degrees 10.0 W in the eastern Pacific during December, 1989. Nine laboratories from the USA and Europe took part. The intercomparison between laboratories was based on water samples collected at the station, analysis of marine air, and analyses of laboratory-prepared gas mixtures and equilibrated water samples. Despite shipping-related and instrumental difficulties encountered by several groups, results of the first intercomparison were encouraging. For F11 (CCl3F), 6-7 groups shared agreement at levels approaching WOCE accuracy standards (1 percent or 0.01 pmol/kg). For F12 (CCl2F2) agreement was poorer (2.5-3 percent or 0.02 pmol/kg), approximately a factor of 2 outside WOCE guidelines. The study identified shipping and equipment setup procedures as a critical aspect of ocean-going CFC analyses that requires more attention. Author

N92-31988# Naval Postgraduate School, Monterey, CA. Dept. of Oceanography.
SEASONAL WIND AND OCEAN THERMAL FORCING INFLUENCES ON THE GENERATION OF THE LEEUWIN CURRENT AND ITS EDDIES M.S. Thesis
Eric J. Bayler Sep. 1991 209 p
(AD-A246992; NPS-OC-91-003) Avail: CASI HC A10/MF A03

A high-resolution, multi-level, primitive equation ocean model is used to examine the response of an idealized, flat-bottomed, eastern boundary oceanic regime on a beta-plane to constant ocean thermal and wind forcing by annual mean and seasonal mean climatologies. The focus of the study is the Leeuwin current along the coastal region, from 200 S to 350 S, off Western Australia. The annual mean ocean thermal forcing is sufficient to produce a poleward surface coastal current and an equatorward undercurrent. Seasonal variation of the ocean thermal forcing provides little enhancement to the current structure, although the seasonal variation does enhance eddy generation during the periods of stronger thermal gradient. Wind forcing by annual mean climatology significantly inhibits the poleward coastal flow, but does not eliminate it. Seasonal wind forcing generates a strong seasonal signal in the poleward coastal flow, but never dominates over the pressure gradient forcing. The combination of wind and thermal cycles allows the formation of the North West Shelf waters and,

subsequently, triggers the release of poleward flowing North West Shelf waters. This additional forcing produces a strong surge in poleward flow during the austral autumn. A nonlinear feedback mechanism acts to extend the duration of this flow through the austral winter. GRA

N92-32050# Naval Oceanographic and Atmospheric Research Lab., Bay Saint Louis, MS.
DEVELOPMENT, TESTING AND OPERATION OF A LARGE SUSPENDED OCEAN MEASUREMENT STRUCTURE FOR DEEP-OCEAN USE Final Report
M. G. Fagot, R. C. Swenson, T. A. Howell, G. D. McCardle, and D. L. Walton May 1992 8 p
(AD-A252188; NOARL-PR-91-132-253) Avail: CASI HC A02/MF A01

A large, suspended ocean measurement structure was developed and operated. The structure was a tripod configuration 5100 m high with a base footprint of 6190 m, all of which is suspended by a single 6150-lb buoyant float. The three 6200-m legs contained environmental measurement instrumentation and engineering sensors located in the top 2150 m of the legs. Communications with the system was via a single steel coaxial cable, which also moored the tending vessel during operation. This paper focuses on the ocean engineering for developing, testing, and operating the system. A new, lightweight cable design facilitated storage, deployment, and retrieval of more than 18,600 m (10 nmi) of cable from a relatively small, 210-foot-long tending vessel. The deployment scenario was optimized to allow this single vessel to transport and deploy over 67 tons of system equipment. An acoustic positioning system was employed to 'fly' the 7000-lb anchors to precise bottom locations. The system was the largest ocean measurement structure to be successfully deployed in the deep ocean (5200 m). GRA

N92-32056# Naval Postgraduate School, Monterey, CA.
AN ANALYSIS OF HYDROGRAPHIC DATA COLLECTED OFF POINT SUR, CALIFORNIA IN JUNE 1990 M.S. Thesis
Georgios Th. Tziagidis Sep. 1991 70 p
(AD-A246060) Avail: CASI HC A04/MF A01

The data collected in June 1990 from the R/V Point Sur are used to study the California Undercurrent and California Current in the area off Point Sur. The area of study is a coastal region starting 3 km off Point Sur and extending westward 102 km. At that distance the orientation of the line of the stations changes to southwest, extending to 228 km offshore. The cruise took place from 16-22 of June under upwelling favorable weather conditions. The results help illustrate the great variability of the currents in the area. In June 1990 the California Undercurrent exists, is strong (max speed 36 cm/sec), is confined to the first 65 km from the shore, and carries equatorial type waters northward in depths less than 650 dbars. The estimated transport is 2.9 Sv. The California Current is broad, slower than the undercurrent (max speed 28 cm/sec), shallower, and carries Subarctic North Pacific waters. The coastal upwelling looks strong starting from the depth of 100 dbars, and contributes to the inshore coastal jet which is observed in the first 8 km from the shore and in the upper 20 dbars. Unlike previous analyses based on CalCOFI data, the undercurrent appears robust in June. Its strong surface and sub-surface signature had not previously been reported for this month. This may be due, in part, to the determination that 700 dbar is a more appropriate reference level than either 500 or 1000 dbar. GRA

N92-32069# Research Inst. of National Defence, Linkoeping (Sweden). Huvudavdelning foer Informationsteknologi.
REAL TIME DETECTION IN A LASER BATHYMETRY SYSTEM [REALTIDSDETEKTERING I LASERBATYMETRISYSTEM]
C. Larsson Feb. 1992 42 p In SWAHILI
(PB92-195452; FOA-C-30642-3.1) Avail: CASI HC A03/MF A01

A special echo extraction algorithm for real time detection in a laser bathymetry system is described in detail. The theoretical connections for optimizing the parameters involved are also discussed. Also covered are the calculation and comparison of the signal to noise relation to a directly derivating system. Furthermore, two adaptive methods of threshold detection are described in detail. A summary is given of a certain number of Monte Carlo simulations of the laser echo. Author

N92-32106# National Marine Fisheries Service, Honolulu, HI.
BIOLOGY, OCEANOGRAPHY, AND FISHERIES OF THE NORTH PACIFIC TRANSITION ZONE AND SUBARCTIC FRONTAL ZONE
J. A. Wetherall Dec. 1991 117 p Presented at the North Pacific Transition Zone Workshop, Honolulu, HI, 9-11 May 1988 Prepared in cooperation with Joint Inst. for Marine and Atmospheric Research, Honolulu, HI
(PB92-178128; NOAA-TM-NMFS-105) Avail: CASI HC A06/MF A02

The topics covered include the following: subarctic-subtropical transition zone of the North Pacific; large-scale aspects and mesoscale structure; biology of the transition region; review of the biology and distribution of the neon flying squid (Ommastrephes bartrami) in the North Pacific; North Pacific albacore ecology and oceanography; zonal variability in salmonid driftnet catch rates in the central North Pacific; and the fisheries for neon flying squid in the central North Pacific. GRA

51 LIFE SCIENCES (GENERAL)

N92-31302# Northwestern Univ., Chicago, IL. Dept. of Cellular Molecular and Structural Biolog y.
CELLULAR LOCALIZATION OF INFRARED SOURCES Final Report, 12 Jan. 1989 - 11 Jan. 1992
Guenter Albrecht-Buehler 1 Jan. 1992 3 p
(Contracts MIPR-122-89; MIPR-113-90)
(AD-A249795; ARO-26385.6-LS) Avail: CASI HC A01/MF A01

During the past grant period we developed a special phase-contrast light microscope with an infrared spot illuminator. Using this microscope, we were able to show that cultured mammalian tissue cells such as 3T3 cells appeared capable of locating distant, microscopic infrared light sources and aiming for them. The strongest responses were observed if the infrared light sources emitted light of wavelengths in the range of 800-900 nm intermittently at rates of 30-60 pulses per min. In addition, we found that the irradiation of small spots of the cell body induced one or several changes of cell polarity in locomoting 3T3 cells. This kind of infrared 'vision' of single cells has never been observed before. It may have important conceptual implications for our approach to eukaryotic cells as well as practical implications for the control of wound healing and metastasis. GRA

N92-31465# Wayne State Univ., Detroit, MI. Dept. of Biochemistry.
EVOLUTION AND ANALYSIS OF THE FUNCTIONAL DOMAINS OF THE CHIMERIC PROTEINS THAT INITIATE PYRIMIDINE BIOSYNTHESIS Final Report, 1 Dec. 1986 - 31 Jul. 1990
David R. Evans 10 Jan. 1992 10 p
(Contract N00014-87-K-0081; NR Proj. RR0-4106)
(AD-A250069) Avail: CASI HC A02/MF A01

The objective of this project is to test the hypothesis that the complex proteins with novel functions arose in the course of evolution by combining structural domains having partial functions. The research focuses on the enzymes that catalyze de novo pyrimidine biosynthesis. While the reactions are the same in most organisms, there are striking differences in the structure and regulation of these enzymes. This year we completed the sequence of the mammalian protein CAD, a 243 kDa polypeptide which carries glutamine dependent (GLN) carbamyl phosphate synthetase (CPS), aspartate transcarbamylase (ATC) and dihydroorotase (DHO) activities. Phylogenetic analysis suggests that the mammalian chimeric protein was formed by stepwise translocation and fusion of ancestral genes that occurred prior to the major radiation that lead to fungi, plants, and animals. The sequence

divergence suggests that the fused and monofunctional DHO domains have a different evolutionary history. In contrast, sequence studies and molecular modeling of the mammalian ATC domain and a reexamination of the subunit structure of a class A ATCase, thought to have a radically different structure, showed that the ATCase catalytic domain is a trimer of identical 34 kDa polypeptides that has been highly conserved throughout the course of evolution. GRA

N92-31590# Wright State Univ., Dayton, OH. Dept. of Chemistry.
A STUDY OF THE EFFECT OF HYDROCARBON STRUCTURE ON THE INDUCTION OF MALE RAT NEPHROPATHY AND METABOLITE STRUCTURE Annual Report, 1 Jun. 1991 - 31 May 1992
M. P. Serve 31 May 1992 5 p
(Grant AF-AFOSR-0396-89)
(AD-A252192; AFOSR-92-0559TR) Avail: CASI HC A02/MF A01

Male Fischer 344 rats were dosed with the saturated branched chain hydrocarbon 3-methylheptane. Pathological examination of the kidneys of the dosed animals compared to the kidneys of control rats dosed with water indicated that there was a noticeable difference in the ability of the hydrocarbon to induce the classic nephrotoxicity produced by 2,2,4-trimethylpentane and other branched chain hydrocarbons. Hyaline droplet formation was used as the principal indicator of kidney damage. There was little indication of any cast formation in the corticomedullary junction area of the kidney. Identification of the rat urinary metabolites of 3-methylheptane yielded 3,5-diethyl 2,3-dihydrofuran, 3-ethyl-6-methyl 2,3-dihydropyran, 3-methyl-2-heptanol, 5-methyl-2-heptanol, 2-n-butyl 1,3-butanediol, 2-ethyl 1,3-hexanediol, B-methyl-8-enantholactone, 3-methyl 3,4-heptanediol, 3-methyl 2,3-heptanediol, 3-methyl 3,5-heptanediol,2-ethyl 1,4-hexanediol, 8-methyl-8-enantholactone, 5-methyl 2,5-heptanediol, 2-ethyl 1,5-hexanediol and 2-ethyl1-hexanoic acid. GRA

N92-31711# Pacific Northwest Lab., Richland, WA.
STATIC MAGNETIC FIELDS: A SUMMARY OF BIOLOGICAL INTERACTIONS, POTENTIAL HEALTH EFFECTS, AND EXPOSURE GUIDELINES
T. S. Tenforde May 1992 19 p Presented at the 8th International Radiation Protection Association (IRPA) World Congress, Vancouver (Canada), 10-22 May 1992
(Contract DE-AC06-76RL-01830)
(DE92-015218; PNL-SA-20340; CONF-920501-22) Avail: CASI HC A03/MF A01

Interest in the mechanisms of interaction and the biological effects of static magnetic fields has increased significantly during the past two decades as a result of the growing number of applications of these fields in research, industry and medicine. A major stimulus for research on the bioeffects of static magnetic fields has been the effort to develop new technologies for energy production and storage that utilize intense magnetic fields (e.g., thermonuclear fusion reactors and superconducting magnet energy storage devices). Interest in the possible biological interactions and health effects of static magnetic fields has also been increased as a result of recent developments in magnetic levitation as a mode of public transportation. In addition, the rapid emergence of magnetic resonance imaging as a new clinical diagnostic procedure has, in recent years, provided a strong rationale for defining the possible biological effects of magnetic fields with high flux densities. In this review, the principal interaction mechanisms of static magnetic fields will be described, and a summary will be given of the present state of knowledge of the biological, environmental, and human health effects of these fields. DOE

N92-31747# Columbia Univ., New York, NY. Center for Radiological Research.
THE RADIOLOGICAL RESEARCH ACCELERATOR FACILITY
E. J. Hall May 1992 21 p
(Contract DE-FG02-88ER-60631)
(DE92-013674; DOE/ER-60631/9) Avail: CASI HC A03/MF A01

The Radiological Research Accelerator Facility (RARAF) is based on a 4-MV Van de Graaff accelerator, which is used to generate a variety of well-characterized radiation beams for research in radiobiology, radiological physics, and radiation chemistry. It is part of the Center for Radiological Research (CRR) of Columbia University, and its operation is supported as a National Facility by the US Department of Energy (DOE). As such, RARAF is available to all potential users on an equal basis, and scientists outside the CRR are encouraged to submit proposals for experiments at RARAF. The operation of the Van de Graaff is supported by the DOE, but the research projects themselves must be supported separately. Experiments performed from May 1991-April 1992 are described. DOE

N92-31778# Rochester Univ., NY.
FUNCTION OF P AND M PATHWAYS IN PRIMATES Annual Report
William Merigan 13 Apr. 1992 3 p
(Grant AF-AFOSR-0041-89)
(AD-A250055; AFOSR-92-0310TR) Avail: CASI HC A01/MF A01

Psychophysical threshold measures were used in combination with precisely located lesions of the sub-cortical visual pathway to examine segregation of function between P and M pathways. Scleral search coils monitored fixation locus in the tested monkeys, to insure that test stimuli were presented in visual field regions corresponding to the lesion location. Results of these studies indicated that the P pathway (or color-opponent pathway) is the major contributor to visual acuity, color vision, and luminance contrast sensitivity. On the other hand, the M pathway (or broadband pathway) appeared crucial for the visibility of low spatial frequencies (broad contours), as well as sensitivity to rapidly drifting visual stimuli. GRA

N92-31980# Topical Testing, Inc., Salt Lake City, UT.
A BIOLOGICAL MODEL OF THE EFFECTS OF TOXIC SUBSTANCES Annual Technical Report No. 1, 1 Nov. 1990 - 31 Oct. 1991
Robert P. Tuckett 29 Nov. 1991 62 p
(Contract F49620-91-C-0012)
(AD-A247138; AFOSR-92-0004TR) Avail: CASI HC A04/MF A01

Due to the basic nature of military operations, it is sometimes necessary for Air Force personnel to be exposed to toxic chemicals in their work environment, either as a protracted low-level exposure or as a high-level, acute exposure. The Draize rabbit eye test for acute irritancy has come under severe criticism by the animal rights movement and has undergone legislative restrictions. Therefore, the tissue culture test being developed is likely to commercial as well as scientific benefit. Progress by topical testing during the past year has been on a number of technical fronts including the development of data collection software and a method for delivery of microquantities of toxic chemicals to individual nerve cells in tissue culture. The neuronal cultures are now viable and reproducible, and their response to a variety of chemical stimuli has been recorded. Corneal epithelial cultures have been viable for a number of months. A number of strategies have been explored to expand the corneal epithelial culture and, thus, make it a viable commercial system. In summary, topical testing has made substantial gains in the development of a commercial assay system, and next year will focus on testing the system's response to different classes of toxic chemicals. GRA

N92-32120# Princeton Univ., NJ.
DEVELOPMENT AND APPLICATION OF PHOTOSENSITIVE DEVICE SYSTEMS TO STUDIES OF BIOLOGICAL AND ORGANIC MATERIALS
S. M. Gruner and G. T. Reynolds 15 May 1992 13 p
(Contract DE-FG02-87ER-60522)

(DE92-014728; DOE/ER-60522/6) Avail: CASI HC A03/MF A01

This report describes progress as of the third year of a 3-year DoE grant for 1/1/92 to 12/31/92. Because this is the last year of a 3-year grant cycle, this report will summarize progress over the entire 3-year period. The overall goals of the grant are to develop novel instrumentation and techniques for the performance of biological and materials research, and especially for the development of x-ray detectors suitable for use at storage ring sources. Research progress has been excellent and the overall goals, as well as most of the specific goals have been successfully met. DOE

52 AEROSPACE MEDICINE

Includes physiological factors; biological effects of radiation; and effects of weightlessness on man and animals.

N92-31326# Maryland Univ., Baltimore. School of Medicine.
ACETYLCHOLINESTERASE INHIBITORS ON THE SPINAL CORD Final Report, 1 Feb. 1986 - 30 Sep. 1989
Jordan E. Warnick 22 Nov. 1991 79 p
(Contract DAMD17-86-C-66030; DA Proj. 3MI-62770-A-871)
(AD-A252694) Avail: CASI HC A05/MF A01

This report describes studies on organophosphorus (OP) inhibitors of acetylcholinesterase (AChE) in the mammalian spinal cord in which the mechanism and site of action of the OPs on synaptic transmission were studied with selective agonists and antagonists of putative central neurotransmitters. Spinal cords isolated from neonatal rats 5- to 9-days old were hemisected and placed in experimental chambers. Electrodes attached to dorsal and ventral root pairs recorded the monosynaptic (MSR) and polysynaptic reflexes (PSR). The roles of N-methyl-D-aspartate (NMDA) and non-NMDA receptors in the generation of MSRs and PSRs and in the action of AChE inhibitors were examined. Utilizing specific receptor inhibitors, it was found that the AChE inhibitors caused depression through muscarinic, not nicotinic receptors, that oximes antagonize AChE inhibitors by virtue of their anticholinergic actions, and not regeneration of ChE, and that thyrotropin releasing hormone can effectively reverse the depression of reflex activity. The facilitation caused by the AChE inhibitors was found to be caused by a block of bicuculline-sensitive inhibition. In addition, it was found that NMDA and non-NMDA receptors are present at synapses between the dorsal root afferent neuron and the excitatory interneuron in the PSR and between the dorsal root afferent neuron and motoneuron of the MSR. GRA

N92-31409# Oak Ridge National Lab., TN.
RADIATION PROTECTION FOR HUMAN EXPLORATION OF THE MOON AND MARS: APPLICATION OF THE MASH CODE SYSTEM
J. O. Johnson, R. T. Santoro, J. D. Drischler, and J. M. Barnes 1992 11 p Presented at the Nuclear Technologies for Space Exploration, Jackson, WY, 16-19 Aug. 1992
(Contract DE-AC05-84OR-21400)
(DE92-014416; CONF-920803-5) Avail: CASI HC A03/MF A01

The Monte Carlo Adjoint Shielding Code System (MASH), developed for the Department of Defense for calculating radiation protection factors for armored vehicles against neutron and gamma radiation, has been used to assess the dose from reactor radiation to an occupant in a habitat on Mars. The capability of MASH to reproduce measured data is summarized to demonstrate the accuracy of the code. The estimation of the radiation environment in an idealized reactor-habitat model is reported to illustrate the merits of the adjoint Monte Carlo procedure for space related studies. The reactor radiation dose for different reactor-habitat surface configurations to a habitat occupant is compared with the natural radiation dose acquired during a 500-day Mars mission. DOE

N92-31491# Medical Coll. of Virginia, Richmond. Dept. of Neurology.
THE EFFECTS OF HYDRAZINES OF NEURONAL EXCITABILITY Annual Report, 1 May 1989 - 31 May 1990
Robert J. DeLorenzo 10 Jan. 1992 32 p
(Grant AF-AFOSR-0235-87)
(AD-A247142; AFOSR-92-0111TR) Avail: CASI HC A03/MF A01

Hydrazines (HZ) are toxic compounds which have numerous industrial applications including their use as missile propellants in advanced aircraft such as the F-16 and space vehicles. The extremely high toxicity of HZ's and the recurrent accidental exposure due to routine storage, use, and disposal of these compounds have created a significant health hazard among aerospace and defense industry personnel. HZ exposure can result in lethal complications involving repeated seizures and eventual respiratory collapse. Acute HZ exposure produces repeated tonic-clonic seizures in animals and man due to the strong convulsant properties of these compounds. In order to develop effective therapies for HZ toxicity, it is important to determine the mechanisms by which HZ's produce their neuronal excitatory effects. Initial studies in our laboratory of the electrophysiological effects of HZ's have shown that HZ exposure induces spontaneous and evoked epileptiform activity in mammalian hippocampus, recorded in vitro. In cultured hippocampal neurons, we have found that HZ's decrease the postburst after hyperpolarization, a primary postsynaptic mechanism utilized by many types of neurons to terminate bursts, and maintain a check on hyperexcitability. As expected, this AHP reduction by HZ's increases the rate of sustained repetitive firing in these neurons, and may be one mechanism contributing to HZ convulsant actions. GRA

N92-31492# Naval Health Research Center, San Diego, CA.
BODY WATER HOMEOSTASIS AND HUMAN PERFORMANCE IN HIGH HEAT ENVIRONMENTS: FLUID HYDRATION RECOMMENDATIONS FOR OPERATION DESERT STORM Final Report, Feb. - Nov. 1991
B. L. Bennett Nov. 1991 21 p
(DA Proj. M00-94)
(AD-A249772; NHRC-91-13) Avail: CASI HC A03/MF A01

Sustained operations during high temperatures increase the risk of heat illness. This risk can be lessened so that degradation in human performance does not impact substantially on military operations. Military personnel should obtain adequate heat acclimatization prior to moderate or heavy workloads, maintain strict fluid and food intake schedules, and alter workload to relative changes in air temperature. These factors will assist in maintaining body fluid balance. Prior to prolonged heat exposure, emphasis should be placed on achieving high aerobic fitness, becoming fully heat acclimated, and learning correct fluid hydration procedures. This will assist in greater physical performance at a lower core temperature in heat. These physiological benefits are ineffective during exposure to heat when individuals become dehydrated. Forced fluid hydration schedules will ensure that fluid intake will match fluid loss as sweat, thereby preventing the negative physiological effects of dehydration. GRA

N92-31554# Human Systems Div., Brooks AFB, TX.
MICRO SAINT MODEL OF FATIGUE ASSESSMENT Annual Report, 1 Oct. 1990 - 30 Sep. 1991
Jonathan French 14 Jan. 1992 27 p
(DA Proj. 3M2-63002-D-995)
(AD-A249976) Avail: CASI HC A03/MF A01

Opportunities for fatigue-related accidents are greatest when extended duty cycles must be maintained. A means to plan for the influence of fatigue would be useful to best utilize crew resources. An equation was derived that predicts performance degradation associated with fatigued cognitive abilities. During a 30 hour sleep deprivation study, 9 male subjects were required to perform a 45 minute performance battery every 120 minutes and variables sensitive to fatigue were determined. Plasma melatonin levels also were obtained. Composite response time and accuracy scores were then derived. The equation that best described the

composite scores included a linear component (hours awake weighting) and a circadian component (melatonin weighting). The respective prediction equations accounted for 36.7 and 36.9 percent of the variance in response time performance and 12.4 and 19.9 percent of the accuracy performance (p .001). These percentages indicate that accuracy predictions were more enhanced by the circadian component than were those for response time. This work represents a mathematical description of fatigued performance that is sensitive to circadian cycles and requires minimal input data. The results might be used to recommend when additional crew should be employed as performance falls below critical thresholds or the best crew rest times during sustained operations. GRA

N92-31558# California Univ., Irvine. Dept. of Electrical and Computer Engineering.
MODELING OF LEARNING-INDUCED RECEPTIVE FIELD PLASTICITY IN AUDITORY NEOCORTEX Final Report, 1 Aug. 1989 - 31 Dec. 1991
Norman M. Weinberger and Jack Sklansky 31 Dec. 1991 52 p
(Contract N00014-89-J-3187)
(AD-A250348) Avail: CASI HC A04/MF A01

A motivating assumption of this research is that insights into the structure and operation of the brain can inspire important ideas for the design of intelligent machines, in particular, machines that detect and classify auditory and visual signals buried in noise. In this project, we focus on the ability of the auditory cortex to adapt its sensitivity to pure tones. Our objective is a model of learning that will enable us to predict changes in the receptive fields of pyramidal cells in the auditory cortex in response to conditioning. Our model is constructed in two major parts: a local process that accounts for the preconditioned states of the pyramidal neurons, and a global process that accounts for the dispersed impact of conditioning across the pyramidal neurons. Recent findings in awake behaving animals have shown that neuronal tuning to acoustic features, e.g., frequency, is systematically altered in the auditory cortex as a result of learning. Responses to training signals are increased whereas responses to other stimuli are decreased, often enough to make the training signal become the most potent stimulus for a cell. This adaptive filtering appears to be a fundamental property of auditory signal processing. GRA

N92-31589# Brookhaven National Lab., Upton, NY.
MICRODISTRIBUTION OF LEAD IN BONE: A NEW APPROACH
K. W. Jones, R. S. Bockman (Cornell Univ., New York, NY.), and F. Bronner (Connecticut Univ., Farmington.) 1991 17 p Presented at the Workshop on Lead: Metabolism and Bone Deposition, Upton, NY, 10-12 Apr. 1991
(Contract DE-AC02-76CH-00016)
(DE92-013036; BNL-47370; CONF-9104363-1) Avail: CASI HC A03/MF A01

A knowledge of the microdistribution of lead in bone is important in order to understand the mechanisms for accumulation and release of lead. The availability of the synchrotron x-ray microscope for sensitive measurements of bone content and distribution of lead provides a valuable tool which, when combined with kinetic, balance, and tissue measurements, can lead to better evaluation of lead toxicity. It may also provide the basis for the development of a suitable model of how lead behaves in the human body. An outline of an experimental protocol for exploitation of the x-ray microscope is given, along with synchrotron x-ray microscope measurements of the distribution of gallium in rat bone that demonstrate the feasibility of the experimental approach. DOE

N92-31608# Lawrence Livermore National Lab., CA.
BIODOSIMETRY OF IONIZING RADIATION IN HUMANS USING THE GLYCOPHORIN A GENOTOXICITY ASSAY
R. H. Jensen, R. G. Langlois, S. G. Grant, and W. L. Bigbee 26 Jul. 1991 5 p Presented at the 9th International Congress of Radiation Research (ICRR) Conference, Toronto (Canada), 7-12 Jul. 1991
(Contract W-7405-eng-48)
(DE92-011974; UCRL-JC-108024; CONF-9107136-11) Avail: CASI HC A01/MF A01

Our assay for determining somatic mutations in humans detects variant erythrocytes that occur as a result of in vivo allele loss at the glycophorin A (GPA) locus in erythroid precursor cells in the bone marrow. This gene codes for a cell surface sialoglycoprotein that occurs in two allelic forms, named the M and N forms, and is codominantly expressed on erythrocytes in peripheral blood of people who are heterozygous at the GPA locus. With our assay, which is performed only on GPA(MN) heterozygotes, we are able to detect rare variant erythrocytes that have lost expression of one of the two GPA alleles. Two different variant cell types are detected. One termed N(O) variant cells, is hemizygous. Such cells might arise by mutation, deletion or inactivation of the GPA(M) allele or loss of chromosome carrying that allele in erythroid precursor cells. Our assay also detects homozygous variant erythrocytes that have lost expression of the GPA(M) allele and express the GPA(N) allele at twice the heterozygous level. These NN variant cells would be generated by chromosomal loss and duplication, gene conversion or mitotic recombination in erythroid precursor cells. The GPA assay requires expression of GPA(N), thus guaranteeing that all variant cells are capable of normally expressing this cell surface antigen. The result of this assay is an enumeration of the frequency of N(O) and NN variant cell types for each individual analyzed. Such variant cell frequencies provide a measure of the quantity of somatic cell mutations that have occurred at the GPA locus. If the relationship between the mutations expressed at the GPA locus and the onset of cancer induced by radiation can be developed, this assay may serve as an effective monitoring method for people at high risk for exposure to ionizing radiation with a cancer risk estimation linked to the results of this monitor. DOE

N92-31905# Pittsburgh Univ., PA. Dept. of Psychiatry.
ORGANIZATION OF THE HUMAN CIRCADIAN SYSTEM Annual Report, 1 Feb. 1991 - 31 Jan. 1992
Robert Y. Moore 31 Jan. 1992 5 p
(Grant AF-AFOSR-0175-91)
(AD-A247498; AFOSR-92-0219TR) Avail: CASI HC A01/MF A01

As in the prior material, the largest population of neurons in the Human SCN contains NT. These are distributed throughout the nucleus and are accompanied by a dense axonal plexus which is probably intrinsic. The NT plexus is uniformly dense throughout the SCN with numerous, small varicosities. These are distributed in a pattern that indicates the synapses are predominantly axodendritic. The second largest population of neurons is VP-containing. These also are widely distributed but perikarya are not present in the ventral-medial portion of the nucleus. The VP plexus is also dense and the distribution of axons also indicates a predominantly axodendritic synapse organization. NPY-containing neurons are found predominantly in the central part of the SCN. There is a dense, and quite coarse, plexus of varicosities and axons peripherally with many fewer axons in the area of NPY cell bodies. The plexus includes a set of very fine fibers and varicosities that presumably arise either from the SCN neurons or the lateral geniculate. VIP perikarya are located very ventrally and medially in the nucleus. Axons project through the nucleus and out into the adjacent interior hypothalamus. The area innervated by these VIP fibers appears much wider than in the rat and includes the paraventricular nucleus. GRA

N92-31962# Air Force Inst. of Tech., Wright-Patterson AFB, OH.
NONTHERMAL INHALATION INJURY M.S. Thesis
Patricia M. Miller 1992 68 p
(AD-A252532; AFIT/CI-CIA-92-010) Avail: CASI HC A04/MF A01

Inhalation injury is one of the leading factors in the deaths of burn patients and is the leading cause of death at the scene of fires. Research into sepsis and burn care have taken precedence since 1960. Only recently have researchers taken a closer look at smoke inhalation and its effects. With the increased use of synthetic

materials in buildings, furniture, and clothes there is a need for emergency personnel to understand the effects of the various byproducts of combustion on the human body. A thorough knowledge of the physiological mechanisms, relevant assessment parameters, and treatment modalities related to smoke inhalation enables the emergency CNS to provide expert care. The CNS must then use this knowledge to provide education to emergency and prehospital staff. The emergency CNS may also play a large role in the current research on new treatments. This paper reviews the physiology, assessment, and treatment of inhalation injuries. Suggestions are also made regarding how the emergency CNS can incorporate this knowledge into the roles of the CNS. GRA

N92-31963# Naval Biodynamics Lab., New Orleans, LA.
NAVAL BIODYNAMICS LABORATORY: 1989 AND 1990 COMMAND HISTORY
Jul. 1991 95 p
(AD-A247185) Avail: CASI HC A05/MF A01

The Naval Biodynamics Laboratory (NAVBIODYNLAB) was established as the Naval Aerospace Medical Research Laboratory Detachment (NAMRLD) in April 1971 by the Bureau of Medicine and Surgery (BUMED). NAMRLD was a detachment of the Naval Aerospace Medical Research Laboratory which is located at the Naval Air Station, Pensacola, Florida. The initial purpose of the Detachment was to study human response to impact acceleration. In 1975, the mission was expanded to include human response to vibration, ship motion, and human performance. NAVBIODYNLAB was designed a separate command by the Secretary of the Navy in February, 1980, and officially established by OPNAV NOTICE 5450 on 28 February 1980. GRA

N92-32107# Research Triangle Inst., Research Triangle Park, NC.
NONINVASIVE AMBULATORY ASSESSMENT OF CARDIAC FUNCTION AND MYOCARDIAL ISCHEMIA IN HEALTHY SUBJECTS EXPOSED TO CARBON MONOXIDE Midterm Report, 8 Apr. 1991 - 7 Feb. 1992
Paul N. Kizakevich, Michael L. McCartney, and Milan J. Hazucha 6 Mar. 1992 32 p
(Contract DAMD17-91-C-1007; DA Proj. 3M1-62787-A-878)
(AD-A252264) Avail: CASI HC A03/MF A01

Carbon monoxide is of continuing interest to the military community. The transient nature of weapons firing, the spatial distribution of CO concentration, and differences in individual physiology will cause the CO dose to vary significantly among crewmembers. Continuous and noninvasive ambulatory monitoring of cardiopulmonary measurements in situ may provide an understanding of the effects of CO exposure among crewmembers in the field environment. This project evaluates the utility of combined impedance and electrocardiographic estimators of cardiac function during exercise in air and with exposure to CO. Treadmill exercise is included on test subjects for comparison with the existing body of data on exercise performance in asymptomatic patients and the body of data which reflects performance decrements with exercise and CO in normals. Upper body exercise is included to test the hypothesis that this form of exercise places a greater strain on the cardiovascular system than lower body exercise, both with and without CO exposure. All of the accomplished work to date has involved preparatory tasks, therefore no experimental results are reported. The midterm report does discuss the literature review, the experiment plan, and the development of a human exposure facility for executing the planned experiments. GRA

53 BEHAVIORAL SCIENCES

Includes psychological factors; individual and group behavior; crew training and evaluation; and psychiatric research.

N92-31291# Reading Univ. (England).
THEORY AND TEST OF STRESS RESISTANCE Final Report, Nov. 1990 - Nov. 1991
Frank P. McKenna and Dinkar Sharma Apr. 1992 41 p
(Contract DAJA45-90-C-0031)
(AD-A250741; ARI-RN-92-22) Avail: CASI HC A03/MF A01

In this report, we developed a laboratory model to test hypotheses concerning the disruptive effects of emotional stimuli. The research assesses the potential of the computerized emotional Stroop task. We discovered that the task was sensitive to two important elements of stress resistance, threat and habituation. The Stroop task is sensitive to the nature of the stimuli, namely that threatening stimuli can be distinguished from nonthreatening stimuli and that with stimulus repetition the stimuli show effects of habituation. Important findings emerged from the research in the following areas. Time pressure and task difficulty. One of the most important findings demonstrates the importance of time pressure and information load on overall performance and the adaptive process that eliminates emotional interference. When an individual is under time pressure and/or is performing a difficult task, there is greater emotional interference than when there is no time pressure or the task is easy. The important role that time pressure and task difficulty play in tasks such as this has not, to this point, been acknowledged. GRA

N92-31321# Eagle Technology, Inc., Winter Park, FL.
DEVELOPMENT OF QUANTITATIVE SPECIFICATIONS FOR SIMULATING THE STRESS ENVIRONMENT Final Report, Jul. 1989 - May 1991
James E. Driskell, Brian Mullen, Craig Johnson, Sandy Hughes, and Cheryl L. Batchelor Mar. 1992 210 p
(Contract F33615-89-C-0008)
(AD-A250669; AL-TR-1991-0109) Avail: CASI HC A10/MF A03

This report is a culmination of work originally started in 1988. The combat maintenance environment is an environment that, to date, has not yet been clearly defined but is extremely important to our success in future combat. These maintenance personnel, although highly trained and skilled technicians, receive little preparation for the extreme stresses of the combat environment. To determine the parameters of that environment, the literature has offered few solutions. However, by utilizing a meta-analytic technique to identity the stress factors that restrict or limit effective performance, we can develop specifications for simulating the stress environment. This report identifies specific ranges to induce stress in the areas of noise, time, pressure, group pressure, threat, uncontrollability, fatigue, dual tasks, and heat and cold. In addition, further research avenues are recommended. GRA

N92-31341*# Georgia Inst. of Tech., Atlanta. Center for Human-Machine Systems Research.
ACQUISITION AND PRODUCTION OF SKILLED BEHAVIOR IN DYNAMIC DECISION-MAKING TASKS Status Report, 31 Jan. - 31 Jul. 1992
Alex Kirlik 31 Jul. 1992 159 p
(Grant NAG2-656)
(NASA-CR-190614; NAS 1.26:190614) Avail: CASI HC A08/MF A02

Detailed summaries of two NASA-funded research projects are provided. The first project was an ecological task analysis of the Star Cruiser model. Star Cruiser is a psychological model designed to test a subject's level of cognitive activity. Ecological task analysis is used as a framework to predict the types of cognitive activity required to achieve productive behavior and to suggest how interfaces can be manipulated to alleviate certain types of cognitive demands. The second project is presented in the form of a thesis for the Masters Degree. The thesis discusses the modeling of

decision-making through the use of neural network and genetic-algorithm machine learning technologies. D.R.D.

N92-31392# Air Force Inst. of Tech., Wright-Patterson AFB, OH.
IN-FLIGHT DECISION MAKING BY HIGH TIME AND LOW TIME PILOTS DURING INSTRUMENT OPERATIONS M.S. Thesis
Kenneth L. Kemper 1992 98 p
(AD-A249990) Avail: CASI HC A05/MF A02

This study examined decision-making in high and low-time pilots (n = 26) on a simulated IFR cross-country flight using MIDIS 3.0, a microcomputer-based flight-decision simulator. When confronted with situations which could endanger the safety and/or efficiency of the flight, it was hypothesized that high-time pilots would recognize the cues relevant to the problem, pattern match these cues with a situational schemata, or script, from long term memory (LTM), and choose to execute their first workable solution. It was hypothesized that low-time pilots would also attempt the same decision-making strategy, but because of their smaller experiential repertoires would fail to make a pattern match in LTM. It was posited that novices then are forced to use a utility strategy in which they must integrate cues with declarative knowledge, generate alternatives, evaluate outcomes, and finally choose the alternative calculated to bring the most utility. The difference in strategies was hypothesized to lead high-time pilots to choose more optimal solutions. The results clearly show that high-time pilots decision optimality is significantly better than low-time pilots. GRA

N92-31444# Educational Testing Service, Princeton, NJ.
PROBABILITY-BASED INFERENCE IN A DOMAIN OF PROPORTIONAL REASONING TASKS
Anne Beland and Robert J. Mislevy Jan. 1992 62 p
(Contracts N00014-88-K-0304; N00014-91-J-4101)
(AD-A247304; ETS-RR-92-15-ONR) Avail: CASI HC A04/MF A01

Educators and psychologists are increasingly interested in modelling the processes and knowledge structures by which people learn and solve problems. Progress has been made in developing cognitive models in several domains, and in devising observational settings that provided clues about subject's cognition from this perspective. Less attention has been paid to procedures for inference or decision making with such information, given that it provides only imperfect information about cognition - in short, test theory for cognitive assessment. This paper describes probability based inference in this context, and illustrates its application with an example concerning proportional reasoning. GRA

N92-31472# York Univ. (Ontario). Human Performance in Space Lab.
ILLUSORY SELF MOTION AND DISORIENTATION Final Report
Ian P. Howard 12 Sep. 1989 94 p
(Contract DCIEM-07SE-W7711-7-7012)
(CTN-92-60318) Avail: CASI HC A05/MF A01

An illusion of self motion and disorientation is experienced by persons viewing a large moving display. This report describes work undertaken to reinvestigate several of the assumed properties of such vection. These results relate to the practical problems of motion sickness and disorientation experienced in moving vehicles and to the fidelity of visual stimuli used to generate sensations of self-motion in simulators. Results of the investigations are as follows. The visual display presented in a flight simulator does not have to be large to generate a convincing sense of self motion. If a surrounding part of a large visual display is moving in one direction and a smaller central display is moving in the opposite direction, the direction of vection is determined by the surround display, even when the central display is the more distant. When the central display occupies the same area as the surround display, the sense of vection was controlled by whichever was more distant. Thus, factors of relative size and distance are more important to the sense of vection than is the factor of central or peripheral placement. Vection is driven more effectively by movement perceived in the upper visual field than in the lower. People with bilateral loss of vestibular function did not experience the limited degree of illusory tilt experienced by normal subjects when subjected to pitch and roll vection. Stationary objects were found to inhibit vection only when they were more distant than the moving display. CISTI

N92-31758# Rochester Univ., NY.
FUNCTION OF PANEL M PATHWAYS IN PRIMATES Final Technical Report, 1 Oct. 1988 - 30 Sep. 1991
William Merigan 13 Apr. 1992 4 p
(Grant AF-AFOSR-0041-89)
(AD-A250275; AFOSR-92-0347TR) Avail: CASI HC A01/MF A01

Psychophysical threshold measures were used in combination with precisely located lesions of the sub-cortical visual pathway to examine segregation of function between P and M pathways. Scleral search coils monitored fixation locus in the tested monkeys, to insure that test stimuli were presented in visual field regions corresponding to the lesion location. Results of these studies indicated that the P pathway (or color-opponent pathway) is the major contributor to visual acuity, color vision, and luminance contrast sensitivity. On the other hand, the M pathway (or broad contours), as well shows sensitivity to rapidly drifting visual stimuli. A special role for the M pathway in the processing of visual motion was ruled out by determining its contribution to directional and velocity sensitivity. GRA

N92-31779# Harvard Univ., Cambridge, MA. Dept. of Psychology.
FORMS OF MEMORY FOR REPRESENTATION OF VISUAL OBJECTS Annual Report, 15 Feb. 1991 - 14 Feb. 1992
Daniel L. Schacter 14 Feb. 1992 8 p
(Grant AF-AFOSR-0182-91)
(AD-A250056; AFOSR-92-0234TR) Avail: CASI HC A02/MF A01

Considerable progress has been made during the past year toward achieving the project's main goals of elucidating the representations and processes involved in implicit and explicit memory for novel visual objects. Experiments have been completed or initiated that: (1) clarify the effects of structural and functional encoding manipulations on priming and explicit memory; (2) help to specify the nature of the structural representation that underlies priming effects on the object decision task; (3) extend findings on priming of novel objects to tests other than possible/impossible object decision; (4) elucidate the extent to which implicit memory for novel objects is spared in subject populations with explicit memory deficits; and (5) examine conditions under which priming of novel objects may be observed. GRA

N92-32063# Naval Postgraduate School, Monterey, CA.
THE IMPACT OF COGNITIVE FEEDBACK ON THE PERFORMANCE OF INTELLIGENCE ANALYSTS M.S. Thesis
Geraldine S. Krotow Mar. 1992 74 p
(AD-A252176) Avail: CASI HC A04/MF A01

Human judgement and the process of decision making has been studied in depth for the past century. More recent research has revealed that feedback is a primary element in the decision making process. Feedback has been categorized according to its role in decision making. Some categories of feedback include cognitive, feedforward, and outcome. Cognitive feedback may hold the most promise for positively affecting the decision making process. Naval Intelligence analysis is a complex process which involves human judgement and decision making on a daily basis. This thesis sought to determine whether or not cognitive feedback would enable intelligence analysts to make optimal choices more consistently than if they were presented with just outcome feedback. Naval Intelligence analysts were the subjects of an unclassified experiment which captured a realistic task performed routinely by analysts in the Fleet. The experiment revealed that cognitive feedback produced the most accurate and optimal results, and indicates that intelligence analysis would benefit from decision

support systems that incorporate the element of cognitive feedback. GRA

N92-32105# California Univ., Santa Cruz. Dept. of Psychology and Psychobiology.
SPACE CONSTANCY ON VIDEO DISPLAY TERMINALS Annual Report, 1 Jan. - 31 Dec. 1991
Bruce Bridgeman 31 Dec. 1991 21 p
(Grant AF-AFOSR-0095-90)
(AD-A247290; AFOSR-92-0142TR) Avail: CASI HC A03/MF A01

Work for the grant's second year progressed in four projects. The first, a report of distorted space processing in flickering fields, concerns empirical work completed. The second project extended this work to high-speed flicker, at 480 adn 960 Hz. No evidence was found that these high flicker rates have any advantages over slower rates, though some technical issues were resolved. The third project examined reading rates on CRT screens at 60 and 500 Hz. The faster rate resulted in reading that was on average 0.6 msec faster, a difference that is neither statistically reliable nor of practical consequence. Technical problems in that study were addressed in the fourth study, using more subjects and a larger and more difficult sample of reading material, with eye movement monitoring and an automatized screen refresh procedure. Initial results showed a small advantage in reading speed at the higher frequency for 4 to 6 subjects, and an overall advantage of 5 words/min at 500 Hz. Data collection is continuing in this project. GRA

N92-32020 Ocean Planet Odyssey, New York, NY.
ONE THOUSAND DAYS NON-STOP AT SEA: LESSONS FOR A MISSION TO MARS
Reid Stowe and Albert A. Harrison (California Univ., Davis.) *In* Huntsville Association of Technical Societies, TABES 92: 8th Annual Technical and Business Exhibition and Symposium. Executive Summaries and Submitted Papers 1992 14 p (For primary document see N92-32009 22-12)
(TABES Paper 92-462) Copyright Avail: Issuing Activity

54 MAN/SYSTEM TECHNOLOGY AND LIFE SUPPORT

Includes human engineering; biotechnology; and space suits and protective clothing.

For related information see also *16 Space Transportation.*

N92-31294# Army Research Inst. for the Behavioral and Social Sciences, Alexandria, VA.
EMPIRICAL DEVELOPMENT OF A SCALE FOR THE PREDICTION OF PERFORMANCE ON A SUSTAINED MONITORING TASK Final Report, Jun. 1991 - Jan. 1992
Linda G. Pierce and Lloyd M. Crumley May 1992 28 p
(AD-A252443; ARI-RN-92-36) Avail: CASI HC A03/MF A01

Research on vigilance performance has been extensive, but few guidelines exist for selecting persons well suited to perform vigilance tasks. The focus of this pilot study was to determine if a subset of items from the Minnesota Multiphasic Personality Inventory (MMPI) that would discriminate between soldiers able to sustain an adequate level of performance and soldiers whose performance deteriorated over time could be identified. Thirty-nine items produced chi-squares with p values less than .05. A discriminant analysis correctly classified 88.5 percent of the soldiers maintaining their performance rate and 83.9 percent of the soldiers with performance degraded over time. If validation efforts are successful, it may be possible to use the 39-item scale to select soldiers who will, on average, detect 13 percent more targets and incorrectly identify 15 percent fewer targets. GRA

N92-31309# Midwest Research Inst., Golden, CO.
SIMPLIFIED AIR CHANGE EFFECTIVENESS MODELING
B. A. Rock, R. Anderson, and M. J. Brandemuehl (Colorado Univ., Boulder.) Jun. 1992 23 p
(Contract DE-AC02-83CH-10093)
(DE92-010577; NREL/TP-432-4737) Avail: CASI HC A03/MF A01

This paper describes recent progress in developing practical air change effectiveness modeling techniques for the design and analysis of air diffusion in occupied rooms. The ultimate goal of this continuing work is to develop a simple and reliable method for determining heating, ventilating, and air-conditioning (HVAC) system compliance with ventilation standards. In the current work, simplified two-region models of rooms are used with six occupancy patterns to find the air change effectiveness. A new measure, the apparent ACH effectiveness, yields the relative ventilation performance of an air diffusion system. This measure can be used for the prediction or evaluation of outside air delivery to the occupants. The required outside air can be greater or less than that specified by ventilation standards such as ASHRAE Standard 62-89. DOE

N92-31327# Naval Health Research Center, San Diego, CA.
STRESS REACTIVITY: FIVE-FACTOR REPRESENTATION OF A PSYCHOBIOLOGICAL TYPOLOGY Interim Report, Mar. - Aug. 1991
Ross R. Vickers, Jr. 26 Aug. 1991 37 p
(NR Proj. MR0-4101)
(AD-A252715; NHRC-91-26) Avail: CASI HC A03/MF A01

A typology contrasting stress reactive individuals with stress resistant individuals has been proposed based on studies of children and nonhuman primates. The present study tested for these hypothesized types in U.S. Navy recruits who completed the NEO Personality Inventory. Hierarchical agglomerative and partitioning cluster analyses were conducted in 10 samples of U.S. Navy recruits (n = 331-335). Replicability of clusters across subsamples was a primary criterion for choosing between alternative cluster solutions. Applying this criterion, up to five clusters could be identified reliably. The five-factor personality profiles for two types in the five-cluster solution approximated a priori predictions about reactive and resistant profiles well enough to indicate that a reactivity typology is a viable model of personality differences in this population. GRA

N92-31330# Minnesota Univ., Minneapolis. Dept. of Pschology.
HUMAN IMAGE UNDERSTANDING Final Report, 1 Jun. 1988 - 1 Jan. 1992
Irving Biederman 17 Apr. 1992 27 p
(Grant AF-AFOSR-0231-88)
(AD-A250401; AFOSR-92-0360TR) Avail: CASI HC A03/MF A01

An extensive series of experiments assessing the visual priming of briefly presented images indicates that the visual representation that mediates real-time object recognition specifies neither the image edges or vertices nor an overall model of the object but an arrangement of simple volumes (or geons) corresponding to the object's parts. This representation can be activated with no loss in efficiency when the image is projected onto the retina at another position, size, or orientation in depth from when originally viewed. Consideration of these invariances suggests a computational basis for the evolution of two extrastriate visual systems, one for recognition and the other subserving motor interaction. It may be possible to assess the functioning of these systems behaviorally, that is, to split the cortex horizontally, through a comparison of performance on naming and episodic memory tasks. We have developed a neural network model that captures the essential characteristics of human object recognition performance. GRA

N92-31458# Aerospace Medical Research Labs., Wright-Patterson AFB, OH.
VERTICAL IMPACT TESTS OF HUMANS AND ANTHROPOMORPHIC MANIKINS Interim Report, 28 Sep. 1987 - 19 Apr. 1991
John R. Buhrman Apr. 1991 147 p

(AF Proj. 7231)
(AD-A245866; AL-TR-1991-0129) Avail: CASI HC A07/MF A02

Small and large prototype Advanced Dynamic Anthropomorphic Manikins (ADAM's) along with CG-95 and CG-95 GARD manikins, were subjected to impacts up to +24 Gz on a vertical deceleration tower. Human subjects were also tested at levels of up to +10 Gz. The test variables were acceleration input and rise-time, seat-back angle, restraint harness, and seat cushion. Both the small and large ADAM's were found to be structurally sound at test up to +24 Gz. Data acquisition, however, was often incomplete, due mostly to broken wires, noisy channels, and circuit board failures. Both ADAM manikins demonstrated reasonable good repeatability of acceleration and force data in the direction of impact, although the channel sensitivities appeared to gradually change with repeated tests. The small ADAM appeared to demonstrate relatively consistent simulation of human dynamic response in the z-axis, but the large ADAM had a tendency to generate larger peak acceleration and seat force data than expected. Employing a Confor(TM) Foam seat cushion appeared to have almost no effect on human dynamic response. The X-Band 90 deg restraint harness appeared to outperform the PCU-15/P harness in the human tests. Varying the seat-back angle + or - 10 degree significantly effected only the peak magnitude of the x-axis chest acceleration data. GRA

N92-31974# University of Central Florida, Orlando. Inst. for Simulation and Training.
HEAD TRACKING AND HEAD MOUNTED DISPLAYS FOR TRAINING SIMULATIONS Report, 1990 - 1992
J. M. Moshell, Richard Dunn-Roberts, and Pat Moskal 5 Feb. 1992 168 p
(Contract N61339-90-C-0041)
(AD-A250866; IST-TR-92-12) Avail: CASI HC A08/MF A02

A two part task is presented. The first task constructs a six monitor display around a Simulated Abrams M1A1 Tank Commander location. The scene is simultaneously displayed on three monitors. The scene switches to the adjacent three monitors as a function of the Tank Commander's head motion. Production simulator difficulties were studied. The second task integrates 'eye phones' and CyberFace to various image generators, especially ESIG500 and SIMNET IG. Simulation usefulness issues were researched. GRA

N92-32023# Institute for Defense Analyses, Alexandria, VA.
PILOT ERRORS INVOLVING HEAD-UP DISPLAYS (HUDs), HELMET-MOUNTED DISPLAYS (HMDs), AND NIGHT VISION GOGGLES (NVGs) Final Report, Jun. - Nov. 1991
Lucien M. Biberman and Earl A. Alluisi Jan. 1992 166 p
(AD-A250719; IDA-P-2638; IDA/HQ-91-40259; AD-E501523)
Avail: CASI HC A08/MF A02

Having become aware of difficulties with night vision and display equipment in helicopters and fixed-wing aircraft, IDA staff members collected pertinent literature, interviewed aircrews, aeromedical research people, and cockpit designers, and then carried out display simulations. They found serious safety problems associated with the newer techniques of displaying information to aircrews. At highly task-loaded moments, pilots are often so stressed that they channelize attention and ignore indications of trouble. Thus, human-factors problems cancel the technological advances being introduced into modern aircraft cockpits. To help solve those problems, the investigators attempted to do the following: appraise the reality and severity of shortcomings in display instrumentation and its use; and arrange for specific laboratory research by the Army and the Air Force, followed by tests and demonstrations. They presented their findings and recommendations to the Air Staff and the Air Force Scientific Advisory Board, as well as the Army Deputy Under Secretary for Operations Research and the Commander of the Army Aviation Center and his aeromedical staff at Fort Rucker. GRA

N92-32031# Ottawa Univ. (Ontario). School of Human Kinetics.
PRELIMINARY DEVELOPMENT OF A PROTOCOL FOR DETERMINING HEAT STRESS CAUSED BY CLOTHING Final Report
J. S. Thoden, M. Jette, and J. Quenneville Jun. 1989 124 p
(Contract DREO-55SS.W7714-8-5725)
(DREO-PSD-EPS-05/89; CTN-92-60329) Avail: CASI HC A06/MF A02

A study was undertaken to develop an effective and efficient exercise protocol with which to evaluate the rates of change in body temperature under specific conditions of exercise while wearing different types of protective clothing. The specific objectives of the program were to determine if: (1) oesophagal, rectal and left middle finger-tip temperature followed the same response to serial exposures to steady state exercise and rest; (2) responses in oesophagal, rectal or finger-tip temperature during exercise were substantially affected by wearing clothing with different insulating properties; and (3) if repetitive cycles of steady-state exercise to produce the relatively unstressful change of rectal temperature of 38.5 C and 38.3 C would provide an effective protocol for the evaluation of change in rectal, oesophagal and finger-tip temperature in response to clothing with different insulating properties. It was concluded that different types of information can be derived from each thermistor location. Information from rectal and oesophagal thermometers is complementary but slightly out of phase and of different magnitude. The combination of thermistor locations and the exercise-rest cycle protocol is insufficiently sensitive to detect changes in body temperature caused by different types of insulation. CISTI

N92-32019 Alenia Spazio S.p.A., Turin (Italy).
ITALIAN-US COOPERATION IN SPACE: THE CASE OF TETHERED, IRIS/LAGEOS, AND SPACEHAB
Paolo Piantella *In* Huntsville Association of Technical Societies, TABES 92: 8th Annual Technical and Business Exhibition and Symposium. Executive Summaries and Submitted Papers 1992 21 p (For primary document see N92-32009 22-12)
(TABES Paper 92-467) Copyright Avail: Issuing Activity

55 SPACE BIOLOGY

Includes exobiology; planetary biology; and extraterrestrial life.

No abstracts in this category.

59 MATHEMATICAL AND COMPUTER SCIENCES (GENERAL)

No abstracts in this category.

60 COMPUTER OPERATIONS AND HARDWARE

Includes hardware for computer graphics, firmware, and data processing.

For components see *33 Electronics and Electrical Engineering.*

N92-31269 Department of the Navy, Washington, DC.
OPTICAL INTERCONNECTS IN THE COMPUTER ENVIRONMENT Patent

Todd A. Kline, inventor (to Navy), Warren A. Rosen, inventor (to Navy), William J. Bermingham, inventor (to Navy), and Eric A. Alfonsi, inventor (to Navy) 26 Nov. 1991 12 p Filed 6 Sep. 1990
(AD-D015235; US-Patent-5,068,880; US-Patent-Appl-SN-580043; US-Patent-Class-375-116) Avail: US Patent and Trademark Office

A method is provided for decoding an input data stream formed of data words having word boundaries and a synchronization word in a network interface unit of a high speed computer network. The input data stream is applied to a serial-to-parallel shift register to provide parallel boundary determination words for locating a word boundary within the data stream. There are no serial shifting of bits within the parallel boundary determination words. The parallel boundary determination words are shifted through a register file in parallel and applied to synchronization word detectors which provide a series of detecting windows shifted from each other by one bit. When one of the word detection windows detects the synchronization word, a word boundary is determined in accordance with the detection. Boundary detection data is, thus, effectively monitored in serial while it is shifted through the register file in parallel. This permits the use of slower and smaller logic in the register file. An encoder is also provided wherein a SYNCH bit pattern is transmitted in the absence of data words. If new data words arrive during transmission of the SYNCH bit pattern, at least a portion of the first data word is stored while the remainder of the SYNCH bit pattern is transmitted. After transmission of the remainder of the SYNCH bit pattern, the data word portion is retrieved and transmitted. GRA

N92-31366# National Inst. of Standards and Technology, Gaithersburg, MD.
OPERATING PRINCIPLES OF MULTIKRON PERFORMANCE INSTRUMENTATION FOR MIMD COMPUTERS
A. Mink and R. J. Carpenter Mar. 1992 29 p Sponsored by DARPA
(PB92-181072; NISTIR-4737) Avail: CASI HC A03/MF A01

The single-chip MULTIKRON design replaces the authors' earlier event trace (uTRAMS) and resource utilization (uREMS) performance instrumentation chips. It incorporates a longer timestamp, more bits of user-event and processor identification, and 16 counters for resource utilization measurement. The initial implementation uses a 64-bit processor bus, though the design allows simple modification to a 32-bit bus. The collection network output has a width of 11 bits (8 data, one parity, and two control), and can transfer up to 25 million data bytes per second. GRA

N92-32183# Defence Research Information Centre, Glasgow (Scotland).
LOCAL AREA NETWORKS (LAN)
G. Farquhar *In* AGARD, Bringing Down the Barriers to Information Transfer Feb. 1992 7 p (For primary document see N92-32182 22-82)
Copyright Avail: CASI HC A02/MF A02

61 COMPUTER PROGRAMMING AND SOFTWARE

Includes computer programs, routines, alogorithms, and specific applications, e.g., CAD/CAM.

N92-31299# Air Force Inst. of Tech., Wright-Patterson AFB, OH. School of Systems and Logistics.
REDUCING REQUIREMENTS ERRORS THROUGH THE USE OF COMPUTER-AIDED SOFTWARE ENGINEERING (CASE) TOOLS AND DURING REQUIREMENTS ANALYSIS M.S. Thesis
Marvin B. Key, Jr. Dec. 1991 155 p
(AD-A246879; AFIT/GSS/ENG/91D-07) Avail: CASI HC A08/MF A02

This study investigated whether using CASE tools in the requirements analysis phase of software development reduced the software coding errors attributable to requirement analysis. A survey of the population gathered data about current practices and efforts in CASE tools use. The data was gathered in two groups: a control group and a sample group. The data was analyzed by group and in various combinations to obtain a greater understanding into population trends and tendencies. The results of the research indicate that the Air Force does not use CASE tools to any great extent. Also, error and cost data are not tracked in a meaningful way either. The conclusion drawn from this research shows that CASE tool use is still in its infancy and needs to begin rapid growth in order to speed up developments and reduce costs with the constantly shrinking budget. The major recommendation is to perform a more detailed study of the population to determine exactly where CASE tools are being used and where improvements need to be made. GRA

N92-31348# Instituto de Pesquisas Espaciais, Sao Jose dos Campos (Brazil).
THE SWENDSEN-WANG DYNAMICS IN THE SIMULATION OF THE ISING MODEL
Alejandro C. Frery and Mauricio Marengoni 1992 13 p
(INPE-5394-PRE/1752) Avail: CASI HC A03/MF A01

We present some simulation results on the convergence properties of one of the available methods to simulate Markovian fields - the Swendsen-Wang algorithm. We use the observed values of the mean magnetization, the pseudo-likehood estimates, the observed short and long range correlations, and a number of connected subgraphs to study the problems associated with the stopping time of the algorithm for different values of the parameter. Author

N92-31353# Carnegie-Mellon Univ., Pittsburgh, PA. Dept. of Computer Science.
PROGRAMMING WITH INDUCTIVE AND CO-INDUCTIVE TYPES
John Greiner 27 Jan. 1992 37 p
(Contract N00014-84-K-0415; ARPA Order 5404)
(AD-A249562; CMU-CS-92-109) Avail: CASI HC A03/MF A01

We look at programming with inductive and co-inductive datatypes, which are inspired theoretically by initial algebras and final co-algebras, respectively. A predicative calculus which incorporates these datatypes as primitive constructs is presented. This calculus allows reduction sequences which are significantly more efficient for two dual classes of common programs than do previous calculi using similar primitives. Several techniques for programming in this calculus are illustrated with numerous examples. A short survey of related work is also included. GRA

N92-31379# Texas A&M Univ., College Station. Dept. of Chemistry.
A ROBUST ALGORITHM FOR ISOTROPIC RECONSTRUCTION OF MAGIC-ANGLE SPINNING SOLID-STATE NMR SPECTRA Technical Report, 1 Jan. - 22 Apr. 1992
Nick C. Elbaum and James F. Haw 23 Apr. 1992 33 p
(Contract N00014-91-J-1475)
(AD-A249610; TR-3) Avail: CASI HC A03/MF A01

Magic-angle spinning (MAS) is an essential component of most solid state NMR experiments. The use of finite spinning speeds results in spinning sidebands due to incomplete averaging of chemical shift anisotropy or quadrupole effects. Sidebands can seriously affect interpretation and quantitation, and the need to minimize them has had a pervasive influence on the practice of MAS NMR. We report a radically new approach for reconstructing spectra in the limit of infinite spinning speed from a set of experimental spectra obtained at various finite speeds. This is achieved using a robust algorithm that handles any number of sideband orders and deals with overlapping peaks. The full signal-to-noise advantage of acquiring multiple spectra is preserved in the reconstruction. Isotropic reconstruction is illustrated for C CP/MAS spectra for crystalline compounds and a representative polymer, P MAS spectra of a mixture, and 79Br MAS spectra of KBr. 19 orders of sidebands were used in the reconstruction of the latter example. A limitation of the present algorithm is that it

requires spectra to be obtained at speeds sufficient to resolve the sidebands from the isotropic peaks. It thus fails to reconstruct the C CP/MAS spectrum of a coal from experimental spectra at very slow spinning speeds. GRA

N92-31405# Mitre Corp., Bedford, MA.
A PERFORMANCE-BASED COMPARISON OF OBJECT-ORIENTED SIMULATION TOOLS
Edward H. Bensley, Victor T. Giddings, Jonathan I. Leivent, and Ronald J. Watro Apr. 1992 95 p Presented at the Object-Oriented Simulation Conference, Newport Beach, CA, 20-22 Jan. 1992 Submitted for publication
(AD-A252125) Avail: CASI HC A05/MF A01

This paper compares the performance and features of five different tools for object-oriented simulation. Three of the tools (MODSIM III, SES/workbench, and Sim++) are commercial products that are targeted exclusively at simulation work. Also examined are simulations in Smalltalk-80 and our own, non-commercial C++ simulation library, called MOOSE (MITRE Object-Oriented Simulation Executive). For each of the tools, we discuss the support for simulation, the support for object-oriented design and the degree to which these areas are effectively integrated. We report the results of performance testing of the tools using six concise benchmarks, each devised to test a specific feature, and one larger simulation, devised to compare general performance. Also included are partial results on ERIC, an object-oriented simulation tool developed at Rome Laboratories. GRA

N92-31410# Stanford Univ., CA. Systems Optimization Lab.
A STRICTLY IMPROVING PHASE 1 ALGORITHM USING LEAST-SQUARES SUBPROBLEMS
S. A. Leichner, G. B. Dantzig, and J. W. Davis Apr. 1992 44 p
(Contract DE-FG03-92ER-25116)
(DE92-015904; SU-SOL-92-1) Avail: CASI HC A03/MF A01

Although the simplex method's performance in solving linear programming problems is usually quite good, it does not guarantee strict improvement at each iteration on degenerate problems. Instead of trying to recognize and avoid degenerate steps in the simplex method, we have developed a new phase 1 algorithm that is completely impervious to degeneracy, with strict improvement attained at each iteration. It is also noted that the new phase 1 algorithm is closely related to a number of existing algorithms. When tested on the 30 smallest NETLIB linear programming test problems, the computational results for the new phase 1 algorithm were almost 3.5 times faster than the simplex method; on some problems, it was over 10 times faster. DOE

N92-31447# Oak Ridge National Lab., TN.
GRAPHICAL DEVELOPMENT TOOLS FOR NETWORK-BASED CONCURRENT SUPERCOMPUTING
A. Beguelin, J. Dongarra, A. Geist, and R. Manchek (Tennessee Univ., Knoxville.) 1991 11 p Presented at the Conference on Supercomputing 1991, Albuquerque, NM, 14-16 Nov. 1991
(Contract DE-AC05-84OR-21400)
(DE92-011144; CONF-911103-8) Avail: CASI HC A03/MF A01

This paper describes an X-window based software environment called HeNCE (Heterogeneous Network Computing Environment) designed to assist scientists in developing parallel programs that run on a network of computers. HeNCE is built on top of a software package called PVM which supports process management and communication between a network of heterogeneous computers. HeNCE is based on a parallel programming paradigm where an application program can be described by a graph. Nodes of the graph represent subroutines and the arcs represent data dependencies. HeNCE is composed of integrated graphical tools for creating, compiling, executing, and analyzing HeNCE programs. DOE

N92-31480# Colorado Univ., Denver.
THE DEVELOPMENT OF MODULARIZED SOFTWARE FOR EMPIRICAL TESTING OF NEW ALGORITHMS IN LINEAR PROGRAMMING Final Report, 1 Oct. 1987 - 30 Sep. 1991
Harvey J. Greenberg 31 Oct. 1991 10 p
(Contract N00014-88-K-0104)
(AD-A250811) Avail: CASI HC A02/MF A01

Empirical research into new strategies and tactics for linear programming requires realistic, large-scale problem-solving tools. The Workbench for Research In (linear) Programming, called WRIP, is a highly modularized system for generating, solving and analyzing instances of linear programs. The core of WRIP is OB1, an advanced optimizer that includes simplex and interior point methods. To support basic operations, OB1 contains a linear algebra library and related routines to process large, sparse matrices. Its modular structure enables algorithm experimentation by modifying one or more of its subroutines. In order to test ideas and gain insight into an algorithm's performance, WRIP includes a modeling language, called MODLER, and a controlled randomization module, called RANDMOD. These enable meaningful randomization on raw data elements and matrix operations, respectively, that preserve the realism of the structure of the linear programming model while applying statistical inference. In addition, an interactive analysis system, called ANALYZE, is included to gain insights into problem and solution properties for deeper analysis of results. All modules are written in FORTRAN/77 and have been tested in a variety of computing environments. WRIP has been distributed to about 30 academics engaged in mathematical programming research, in the U.S. and Europe. In addition, the principal investigators have extended their own insights into algorithm design through experimental rigor made possible by this software. GRA

N92-31486*# Research Inst. for Computing and Information Systems, Houston, TX.
SOURCES OF UNBOUNDED PRIORITY INVERSIONS IN REAL-TIME SYSTEMS AND A COMPARATIVE STUDY OF POSSIBLE SOLUTIONS
Sadegh Davari (Houston Univ., Clear Lake, TX.) and Lui Sha (Carnegie-Mellon Univ., Pittsburgh, PA.) May 1992 14 p
(Contract NCC9-16)
(NASA-CR-190711; NAS 1.26:190711) Avail: CASI HC A03/MF A01

In the design of real-time systems, tasks are often assigned priorities. Preemptive priority driven schedulers are used to schedule tasks to meet the timing requirements. Priority inversion is the term used to describe the situation when a higher priority task's execution is delayed by lower priority tasks. Priority inversion can occur when there is contention for resources among tasks of different priorities. The duration of priority inversion could be long enough to cause tasks to miss their dead lines. Priority inversion cannot be completely eliminated. However, it is important to identify sources of priority inversion and minimize the duration of priority inversion. In this paper, a comprehensive review of the problem of and solutions to unbounded priority inversion is presented. Author

N92-31487*# Research Inst. for Computing and Information Systems, Houston, TX.
MISSION AND SAFETY CRITICAL (MASC) PLANS FOR THE MASC KERNEL SIMULATION
15 Nov. 1991 10 p Prepared in cooperation with GHG Corp., Houston, TX
(Contract NCC9-16; RICIS Proj. SE-16)
(NASA-CR-190708; NAS 1.26:190708) Avail: CASI HC A02/MF A01

This report discusses a prototype for Mission and Safety Critical (MASC) kernel simulation which explains the intended approach and how the simulation will be used. Smalltalk is chosen for the simulation because of usefulness in quickly building working models of the systems and its object-oriented approach to software. A scenario is also introduced to give details about how the simulation works. The eventual system will be a fully object-oriented one implemented in Ada via Dragoon. To implement the simulation, a scenario using elements typical of those in the Space Station, was created. I.I.C.

N92-31488# Ballistic Research Labs., Aberdeen Proving Ground, MD.
MODULAR UNIX (TRADE NAME)-BASED VULNERABILITY ESTIMATION SUITE (MUVES) ANALYST'S GUIDE Final Report, Jul. 1988 - Oct. 1991
Phillip J. Hanes, Scott L. Henry, Gary S. Moss, Karen R. Murray, and Wendy A. Winner Dec. 1991 177 p
(AD-A245322; BRL-MR-3954) Avail: CASI HC A09/MF A02

Assessments of a target's susceptibility to damage in an encounter with a threat (vulnerability) and the capability of weapon systems to inflict damage on targets (lethality) have been conducted at the Ballistic Research Laboratory (BRL) for over forty years. Research and data from test firings have been incorporated in a series of computer models that predict the results of target-threat interactions. Prior to the Modular UNIX-based Vulnerability Estimation Suite (MUVES), many computer programs for predicting vulnerability/lethality assessments had evolved with their own blend of specially tailored algorithms and with their own code maintenance requirements. Even though these programs functionally employed many of the same different versions of the same code. In 1985, BRL's Vulnerability/Lethality Division (VLD) initiated discussions to develop an integrated software system for performing vulnerability/lethality assessments. These efforts have resulted in MUVES, a comprehensive software package for vulnerability/lethality analysis. MUVES is written primarily in C for the UNIX operating system environment. MUVES is a flexible platform able to accommodate existing vulnerability methodologies as well as future vulnerability applications. GRA

N92-31529# Allied-Signal Aerospace Co., Kansas City, MO.
PROTOTYPE CASTING FABRICATION BY STEREOLITHOGRAPHY
W. E. Cromwell Mar. 1992 103 p Presented at the Allied-Signal Aerospace Company Conference on Computer Aided Engineering, Torrence, CA, 29 Apr. 1992
(Contract DE-AC04-76DP-00613)
(DE92-011489; KCP-613-4837; CONF-9204114-1) Avail: CASI HC A06/MF A02

The evolution of the new technology of producing CAD models by ultraviolet solidification of resin materials (STEREOLITHOGRAPHY) continues to progress. The potential application area of rigid fabrication of prototype investment castings is becoming more feasible as we continue to successfully yield experimental castings by the 'SHELL' processing method. This supplemental (to 11/90 publication) report briefly reviews the original project objectives, activities related to these objectives since November 1990, and progress made through December 1991. We discuss several new case studies involving new resin materials (and other materials) tested along with investment casting processing results. The most recent success, the processing of the highly complex 'C' HOUSING design by the 'SHELL' mold process in both aluminum and steel, will be discussed. This is considered a major breakthrough toward establishing this new technology as a viable approach to the rapid development of prototype investment castings, employing the most common aerospace (precision) cast process. Our future planning calls for expanding the study to help the investment casting industry in refining related processing techniques and to continue our evaluation of new resins suitable for the casting process. Present project planning calls for the completion of this study by the third quarter FY-93 or sooner. We believe that with the continued excellent cooperation of our casting supplier study team and an accelerated effort by resin materials producers to further refine related materials, we can achieve all objectives during the planned time frame. DOE

N92-31541# Carnegie-Mellon Univ., Pittsburgh, PA. Software Engineering Inst.
REQUIREMENTS ENGINEERING AND ANALYSIS WORKSHOP PROCEEDINGS Final Report
Dec. 1991 281 p Workshop held in Pittsburgh, PA, 12-14 Mar. 1991
(Contract F19628-90-C-0003)
(AD-A250415; CMU/SEI-91-TR-30; ESD-TR-91-30) Avail: CASI HC A13/MF A03

Inadequate, incomplete, erroneous, and ambiguous system and software requirements are a major and ongoing source of problems in systems development. These problems manifest themselves in missed schedules, budget excesses, and systems that are to varying degrees unresponsive to the true needs of the sponsor. These difficulties are often attributed to the poorly defined and ill-understood processes used to elicit, specify, analyze, and validate requirements. The Software Engineering Institute (SEI) hosted the Requirements Engineering and Analysis Workshop in Pittsburgh, Pennsylvania, on March 12-14, 1991. The intention of the workshop was to focus discussion on issues and activities that could help the Department of Defense (DoD) to deal more effectively with the requirements of mission-critical systems. The workshop participants were divided into four working groups: requirements engineering process and products, requirements volatility, requirements elicitation, and requirements engineering techniques and tools. A summary of the findings of each working group follows. GRA

N92-31561*# Institute for Computer Applications in Science and Engineering, Hampton, VA.
PARTI PRIMITIVES FOR UNSTRUCTURED AND BLOCK STRUCTURED PROBLEMS Final Report
Alan Sussman, Joel Saltz, Raja Das, S. Gupta, Dimitri Mavriplis, Ravi Ponnusamy (Syracuse Univ., NY.), and Kay Crowley Jun. 1992 33 p Proposed for presentation at the Symposium on High Performance Computing for Flight Vehicles, 7-9 Dec. 1992 Original contains color illustrations
(Contract NAS1-18605; NSF ASC-88-19374; RTOP 505-90-52-01)
(NASA-CR-189662; NAS 1.26:189662; ICASE-IR-22) Avail: CASI HC A03/MF A01; 1 functional color page

Described here is a set of primitives (PARTI) developed to efficiently execute unstructured and block structured problems on distributed memory parallel machines. We present experimental data from a 3-D unstructured Euler solver run on the Intel Touchstone Delta to demonstrate the usefulness of our methods. Author

N92-31573# University of South Florida, Tampa. Coll. of Engineering.
DEVELOPMENT OF THE ASPECT GRAPH REPRESENTATION FOR USE IN R VERSION Final Report, 1 Nov. 1988 - 31 Oct. 1991
Kevin Bowyer 31 Oct. 1991 23 p
(Grant AF-AFOSR-0036-89)
(AD-A247109; AFOSR-92-0071TR) Avail: CASI HC A03/MF A01

Over the past few years, a number of researchers have presented algorithms for computing the aspect graph representation for polyhedra and curved-surface objects. However, currently it is computed from the theoretical standpoint of perfect resolution in the viewpoint, the projected image and the object shape. This means that the aspect graph may include details that an observer could never see in practice. This paper reviews a complete implementation of an algorithm to compute the exact aspect graph of solids of revolution under the perspective projection in 3D space. Then we explore the notion of introducing scale into the qualitative aspect graph framework, this providing a mechanism for selecting a level of detail that is large enough to merit explicit representation. Several alternative interpretations of the scale space aspect graph are examined in response to the results produced for an example object by the implemented system. GRA

N92-31586# Software Productivity Solutions, Inc., Indialantic, FL.
QUALITY EVALUATION SYSTEM (QUES), VOLUME 1 Final Report, Dec. 1987 - Sep. 1991
Karen A. Dyson Dec. 1991 102 p
(Contract F30602-88-C-0019)

(AD-A252679; A015-Vol-1; RL-TR-91-407-Vol-1) Avail: CASI HC A06/MF A02

Volume 1 presents the features of the Quality Evaluation System (QUES). QUES is a tool which automates the process of establishing, maintaining, and applying a software quality evaluation framework. Features are illustrated with examples and reports generated by the tool. The main features include framework creation, framework tailoring, project creation and data collection. QUES will support analysis of Fortran and Ada code on a DEC VAX and analysis of Ada code on a SUN SparcStation. Volume 2 summarizes the Rome Laboratory Software Quality Framework (RLSQF) as automated with the QUES tool. This volume upgrades the original RADC Software Quality Framework documented in 1985. The primary changes were improved objectivity of questions, improved automatability of questions, improved applicability to Ada, and consistency with DOD-STD-2167A lifecycle phases and terminology. GRA

N92-31587# Stanford Univ., CA. Dept. of Electrical Engineering.

OPTICAL OVERSAMPLED ANALOG-TO-DIGITAL CONVERSION Ph.D. Thesis

Barry L. Shoop 29 Jun. 1992 130 p Sponsored by Military Academy

(AD-A252695) Avail: CASI HC A07/MF A02

A new approach to optical analog-to-digital (A/D) conversion based on oversampling and error diffusion coding techniques is proposed. This new approach combines the high resolution capabilities of classical oversampled A/D conversion with the high speed of optical processing technology to extend the resolution and conversion rates beyond those currently possible with other electronic or optical converters. The optical approach is device independent, requiring only optical thresholding, subtraction, and digital logic for implementation. The underlying concept is to trade bandwidth for improved amplitude resolution using advanced signal processing techniques. This new approach to optical A/D conversion differs from classical Nyquist rate optical A/D conversion in that each signal sample is not necessarily quantized to the closest reconstruction level. The analog input signal is first optically sampled at a frequency much greater than the Nyquist frequency and is then quantized by a modulator which incorporates one-bit quantizers and linear filters in a negative feedback architecture for the purpose of reducing the quantization noise within the signal baseband. This in-band noise reduction is accomplished by spectrally shaping the quantization noise, forcing most of the noise power to frequencies above the signal's cutoff frequency. GRA

N92-31601# Naval Ocean Systems Center, San Diego, CA. Research, Development, Test and Evaluation Div.

PERFORMANCE MEASURES OF THE Ada RENDEZVOUS

A. Sterrett and M. Minei Mar. 1992 7 p Sponsored by ONR

(AD-A250060) Avail: CASI HC A02/MF A01

The Ada Programming Language was designed to meet the need for a standard computer programming language. Ada has the ability to take advantage of multiprocessor environments. One feature, known as the rendezvous, allows tasks to synchronize in such a environment. In this paper, we will look at the performance of the Ada rendezvous in a two-processor system. In a distributed Ada system, the rendezvous provides synchronized communication between asynchronous tasks. A system of this sort would consist of at least two processors, each serving various tasks. Presently, the performance behavior of tasks which synchronize and possibly communicate are not widely known. Developers of concurrent Ada systems will need to perform sensitivity studies of the Ada tasking environment to develop efficient time-critical programs. Therefore, we will discuss rendezvous response time from the point of view of a sensitivity study. We will show generalized performance curves of the rendezvous along with commentary on their performance elbows (or bottlenecks). Rendezvous response time is defined as the amount of time one task must wait until its rendezvous request to another task is completed. The discussion will be based on two separate computer simulations of a two-processor system. The tools to be used to build these simulations are ELSIR and APOSL. GRA

N92-31628# National Inst. of Standards and Technology, Gaithersburg, MD. Fabrication Technology Div.

SHOP OF THE 1990'S PROJECT: AN EVALUATION TOOL FOR WIREFRAME CAD SOFTWARE

B. Bluethmann and J. Johnson Apr. 1992 64 p

(PB92-181130; NISTIR-4813) Avail: CASI HC A04/MF A01

A methodology is given for small machine shops to benchmark Computer-Aided Design (CAD) packages. The initial step of the process is to determine a shop's CAD requirements, and to convert those requirements into specific CAD features. After determining the necessary features, the methodology is a three part process. Part one involves completing a checklist to determine which features are available on each CAD package. The second part consists of giving values to the features of the CAD package, biased toward the more important features. Part three generates a weighted tally of each package. Employing the evaluation tool simplifies the difficult process of determining the most suitable CAD package for each individual shop. Author

N92-31642# Michigan State Univ., East Lansing.

A SIMPLE LINEARIZED LEARNING ALGORITHM WHICH OUTPERFORMS BACK-PROPAGATION

J. R. Deller, Jr. and S. D. Hunt 1992 6 p Sponsored in part by an Ameritech Fellowship; and by Puerto Rico Univ.

(Contract N00014-91-J-1329; NSF MIP-90-16734)

(AD-A249697) Avail: CASI HC A02/MF A01

A class of algorithms is presented for training multilayer perceptrons using purely linear techniques. The methods are based upon linearizations of the network using error surface analysis, followed by a contemporary least squares estimation procedure. Specific algorithms are presented to estimate weights node-wise, layer-wise, and for estimating the entire set of network weights simultaneously. In several experimental studies, the node-wise method is superior to back-propagation and an alternative linearization method by Azimi-Sadjadi et al., in terms of number of convergences and convergence rate. The layer and network-wise updating offer further improvement. GRA

N92-31654# Argonne National Lab., IL.

ORACLE AND THE END-USER: PRACTICAL IMPLEMENTATION OF APPLICATIONS IN A MULTI-USER, MULTI-PLATFORM ENVIRONMENT

1992 13 p Presented at the Midwest Oracle Users Group Regional Meeting, Milwaukee, WI, 15 May 1992

(Contract W-31-109-eng-38)

(DE92-015223; ANL/CP-75955; CONF-9205200-1) Avail: CASI HC A03/MF A01

This presentation will describe methods used to develop a standard user-interface to ORACLE applications, to train users, and document these systems in a diverse multi-user, multi-platform environment. Implementation and documentation of applications and training of users can be difficult when the end-users have diverse levels of computer proficiency and work with a multiple array of hardware platforms. We will discuss common problems encountered in such an environment and the approaches used to solve them. The Advanced Photon Source at Argonne National Laboratory has over 300 users, using a variety of hardware: SUN workstations, Macintoshes, PCs running MS-Windows, VAXstations, DECstations, and a variety of terminal types. The perfect scenario would be to allow everyone to access the database using a particular workstation environment, or if using a terminal, access the database using the standard function keys. For example, a Macintosh user could use a true graphics version of SQL*FORMS; likewise a SUN workstation user. We are in the process of evaluating the use of utilities such as bit-mapped versions of SQL*FORMS for SUNs and Macintoshes, and intend to continue work in that direction. However, there are still some issues to be resolved, both technical and financial, before client-server technology becomes a realistic alternative in our mixed

environment. This presentation will have two components. Part 1 will address some technical issues concerned with providing a standard user interface. Part 2 will deal with administrative issues; specifically documentation, user training, and communications between users and developers. DOE

N92-31669# Sandia National Labs., Albuquerque, NM.
ADAPTIVE INVERSE FILTER
J. Kalb 1992 8 p Presented at the Ideas in Science and Electronics Symposium, Albuquerque, NM, 14 May 1992
(Contract DE-AC04-76DP-00789)
(DE92-011660; SAND-92-0816C; CONF-9205141-1) Avail: CASI HC A02/MF A01

The design of an inverse adaptive filter, using the Least-Mean-Square (LMS) algorithm, is described. The correct data is taken with an analog filter. The gradient estimate used in the LMS algorithm is based upon the instantaneous error, e(exp 2)(n). Minimizing the mean-squared-error does not provide an optimal solution in this specific case. Therefore, another performance criterion, error power, was developed to calculate the optimal inverse model. Despite using a different performance criterion, the inverse filter converges rapidly and gives a small mean-squared-error. Computer simulations of this filter are also shown. DOE

N92-31676# Naval Postgraduate School, Monterey, CA.
HYPER-NPSNET: A VIRTUAL WORLD WITH AN INTEGRATED 3-D HYPERTEXT M.S. Thesis
John A. Daley 26 Mar. 1992 53 p
(AD-A252726) Avail: CASI HC A04/MF A01

This thesis proposes an extension to the NPSNET 3D virtual world prototype to provide an integrated 3D hypertext. This hypertext would be embedded into the virtual world, and would provide the capability for real-time or non-realtime reference, aspect-change within or around vehicles, direct navigation to a specified 3D location, and other features. Hypermedia such as video or graphic animations, with or without sound, in addition to text files will be accessible through the hypertext. The hypertext elements will be embedded into the virtual world by the use of icons or other symbols, which become visible if selected by the user. Foreseeable applications include hypernavigation, historical reference visualization, direct access to higher-level analysis functions, and contextual referencing for training applications. A prototype of Hyper-NPSNET is planned for initial review in June 1992. GRA

N92-31689# Laboratoire d'Automatique et d'Analyse des Systemes, Toulouse (France). Groupe Systemes de Production.
ABOUT REAL TIME INDUSTRIAL PROCESSES CONTROL: A METHODOLOGY BASED ON OBJECTS AND PETRI NETS Ph.D. Thesis - Toulouse Univ. [SUR LA COMMANDE DE PROCEDES INDUSTRIELS: UNEMETHODOLOGIE BASEE OBJETS ET RESEAUX DE PETRI]
Mario Paludetto 1991 270 p In FRENCH
(LAAS-91467; ETN-92-91679) Avail: CASI HC A12/MF A03

The main phases of the life cycle of software dedicated to the real time control of industrial process are presented, specifically addressing analysis, design and coding. These three phases constitute Hierarchical Object Oriented Design/Petri Nets Object (HOOD/PNO) methodology and are all based on object concepts and Petri nets. A historic and critical panorama of object oriented analysis and design methods, specifically HOOD method, is presented. The current lack of object oriented requirements analysis methods for real time application design is underlined. Focus is on requirements analysis on the definition of object classes. Object oriented design method fundamentally allows objects compositions and decompositions based on their behavioral descriptions by means of Petri nets. Validation is addressed through a Petri nets analysis of object behaviors during requirements analysis and design phases. For lack of real time object oriented language with concurrency possibilities, implementation uses Ada language. It underlines semi automatic code generation. It suggests implementation rules in the case of Petri nets based descriptions of both operation control structures and object control structures. ESA

N92-31703# Los Alamos National Lab., NM.
SOME COMPUTATIONAL CHALLENGES OF DEVELOPING EFFICIENT PARALLEL ALGORITHMS FOR DATA-DEPENDENT COMPUTATIONS IN THERMAL-HYDRAULICS SUPERCOMPUTER APPLICATIONS
S. B. Woodruff 1992 13 p Presented at the International Topical Meeting on Reactor Thermal Hydraulics: Towards the Next Generation of Nuclear Power Plants, Salt Lake City, UT, 20-24 Sep. 1992
(Contract W-7405-eng-36)
(DE92-011368; LA-UR-92-859; CONF-920903-4) Avail: CASI HC A03/MF A01

The Transient Reactor Analysis Code (TRAC), which features a two-fluid treatment of thermal hydraulics, is designed to model transients in water reactors and related facilities. One of the major computational costs associated with TRAC and similar codes is calculating constitutive coefficients. Although the formulations for these coefficients are local, the costs are flow-regime or data-dependent; i.e., the computations needed for a given spatial node often vary widely as a function of time. Consequently, poor load balancing will degrade efficiency on either vector or data parallel architectures when the data are organized according to spatial location. Unfortunately, a general automatic solution to the load-balancing problem associated with data-dependent computations is not yet available for massively parallel architectures. This document discusses why developers should either wait for such solutions or consider alternative numercial algorithms, such as a neural net representation, that do not exhibit load-balancing problems. DOE

N92-31739# Lawrence Livermore National Lab., CA.
A TASK ADAPTIVE PARALLEL GRAPHICS RENDERING ALGORITHM
S. Whitman Dec. 1991 21 p Presented at the Siggraph 1992, Chicago, IL, 26-31 Jul. 1992
(Contract W-7405-eng-48)
(DE92-008062; UCRL-JC-109659; CONF-920759-1) Avail: CASI HC A03/MF A01

A parallel approach to computer graphics rendering is needed in order to generate images of highly complex data quickly. This paper presents an algorithm which can be used on general purpose multiprocessor computers. It was designed for a physically-distributed, logically-shared memory computer with features amenable to both shared memory and message passing implementation. The work decomposition strategy involves assigning rectangular screen space areas to processors initially. Then, as the computation proceeds, processors which have completed their work adaptively partition another processor's task in order to even the computational load. Results on the BBN TC2000 computer at LLNL for this algorithm indicate an efficiency ranging from 59 percent to 90 percent on 96 processors for a variety of test images. In fact, a rendering speed of almost 100,000 polygons per second (anti-aliased, specular highlighted) was achieved at this configuration using the software algorithm described here. DOE

N92-31742# Lawrence Livermore National Lab., CA.
THE MATRIX EDITOR FOR SYMBOLIC JACOBIANS IN ALPAL
J. F. Painter Dec. 1991 13 p Presented at the International Symposium on Symbolic and Algebraic Computation, Berkeley, CA, 27-29 Jul. 1992
(Contract W-7405-eng-48)
(DE92-008076; UCRL-JC-109266; CONF-920760-1) Avail: CASI HC A03/MF A01

ALPAL is a Macsyma-based tool that automatically generates code to solve nonlinear integro-differential equations, given a very high-level specification of the equations to be solved and the numerical methods to be used. The Matrix Editor is a graphical, interactive tool for specifying the handling of Jacobian matrices

and linear solvers. It automates such routine but difficult tasks as correctly converting from the data structures used for computing the Jacobian to data structures used by a linear solver. The user specifies what to do only at a high, natural level of abstraction.
DOE

N92-31743# Lawrence Livermore National Lab., CA.
NEW ALGORITHMS FOR THE MINIMAL FORM PROBLEM
J. S. Oliveira, G. O. Cook, Jr., and M. R. Purtill (Institute for Defense Analyses, Princeton, NJ.) 20 Dec. 1991 9 p Presented at the International Symposium on Symbolic and Algebraic Computation, Berkeley, CA, 27-29 Jul. 1992
(Contract W-7405-eng-48)
(DE92-011963; UCRL-JC-109225; CONF-920760-3) Avail: CASI HC A02/MF A01

It is widely appreciated that large-scale algebraic computation (performing computer algebra operations on large symbolic expressions) places very significant demands upon existing computer algebra systems. Because of this, parallel versions of many important algorithms have been successfully sought, and clever techniques have been found for improving the speed of the algebraic simplification process. In addition, some attention has been given to the issue of restructuring large expressions, or transforming them into 'minimal forms.' By 'minimal form,' we mean that form of an expression that involves a minimum number of operations in the sense that no simple transformation on the expression leads to a form involving fewer operations. Unfortunately, the progress that has been achieved to date on this very hard problem is not adequate for the very significant demands of large computer algebra problems. In response to this situation, we have developed some efficient algorithms for constructing 'minimal forms.' In this paper, the multi-stage algorithm in which these new algorithms operate is defined and the features of these algorithms are developed. In a companion paper, we introduce the core algebra engine of a new tool that provides the algebraic framework required for the implementation of these new algorithms.
DOE

N92-31783# Air Force Inst. of Tech., Wright-Patterson AFB, OH.
COMPUTER AIDED PROCESS PLANNING (CAPP): THE USER INTERFACE FOR THE FABRICATION MODULE OF THE RAPID DESIGN SYSTEM M.S. Thesis
Christine M. Cartaya 1991 131 p
(AD-A250095; AFIT/CI/CIA-91-129) Avail: CASI HC A07/MF A02

The Rapid Design System (RDS) is a feature based design, fabrication, and inspection system. Research and development of the RDS has been sponsored by the United States Air Force. The Fabrication Planning (FP) module of the RDS is being developed by the University of Dayton. The FP module automatically creates a process plan for machining a metal part. The research addressed herein deals with the User Interface for the review and modification of a process plan. The FP module automatically creates a plan using information from the Feature Based Design Environment (FBDE) of the RDS. It integrates this information with the information received from a program/database called MetCAPP(sup tm). The process plan is created in a series of steps: feature translation, feature sequencing, setup generation, and operations generation. The purpose of the Planning Window and User Interface is to give a designer, machinists, or process planner the ability to automatically generate and manipulate a complete process plan.
GRA

N92-31787*# Research Inst. for Computing and Information Systems, Houston, TX.
CONFIGURATION MANAGEMENT AND SOFTWARE MEASUREMENT IN THE GROUND SYSTEMS DEVELOPMENT ENVIRONMENT (GSDE)
Victor E. Church (Computer Sciences Corp., Beltsville, MD.), D. Long (Computer Sciences Corp., Beltsville, MD.), Ray Hartenstein (Computer Sciences Corp., Beltsville, MD.), and Alfredo Perez-Davila (Houston Univ., Clear Lake, TX.) Feb. 1992 20 p
(Contract NCC9-16; RICIS Proj. SE-34)
(NASA-CR-190716; NAS 1.26:190716) Avail: CASI HC A03/MF A01

A set of functional requirements for software configuration management (CM) and metrics reporting for Space Station Freedom ground systems software are described. This report is one of a series from a study of the interfaces among the Ground Systems Development Environment (GSDE), the development systems for the Space Station Training Facility (SSTF) and the Space Station Control Center (SSCC), and the target systems for SSCC and SSTF. The focus is on the CM of the software following delivery to NASA and on the software metrics that relate to the quality and maintainability of the delivered software. The CM and metrics requirements address specific problems that occur in large-scale software development. Mechanisms to assist in the continuing improvement of mission operations software development are described.
Author

N92-31825# California Univ., Davis. Dept. of Electrical Engineering and Computer Science.
SPECIFICATION AND VERIFICATION OF SECURE CONCURRENT AND DISTRIBUTED SOFTWARE SYSTEMS Final Technical Report, Jul. 1988 - Dec. 1989
M. Archer, G. Fisher, K. Levitt, R. Olsson, and J. Alves-Foss Feb. 1992 277 p
(Contract F30602-88-D-0025)
(AD-A252477; RL-TR-92-16) Avail: CASI HC A13/MF A03

This report describes an investigation of techniques to support the specification and verification of concurrent and distributed software systems, with special emphasis on issues of security. The investigation has focused on two major areas. The primary focus is a survey of existing methodologies and systems that are relevant to the specification and verification of concurrency. The secondary focus is on the initial design of a short-term workbench that embodies capabilities of existing systems together with new features that extend the current state of the art in the specification and verification of concurrency. The introduction summarizes survey results and presents overall conclusions about the current state of the art. Sections 2 and 3 of the present the details of the methodology and system surveys, respectively. The surveys include high level feature comparison tables accompanied by extended reviews. Section 4 describes a design for the short-term workbench that will support computer-aided specification and verification. Section 5 describes a set of extended examples that were developed to test the design ideas. Section 6 concludes with an overall summary and an overview of targets for future work.
GRA

N92-31833# Sparta, Inc., Lexington, MA.
USER'S GUIDE FOR TREETHERM: A 3-D THERMAL MODEL FOR SINGLE TREES Report No. 9, 1 Jul. - 31 Dec. 1990
James R. Jones 31 Mar. 1991 61 p
(Contract F19628-88-C-0038)
(LTR91-003; PL-TR-91-2109) Avail: CASI HC A04/MF A01

Energy budget modeling of vegetated surfaces is complicated by the extreme variability that can be encountered in the species that are present. A three dimensional thermal model of trees, TREETHERM, has been developed to understand the thermal properties of trees. The model has been developed for leafed and leafless conditions. This report presents a User's Guide for TREETHERM. Descriptions of the input requirements for the code are presented as well as examples of how to use the code.
Author

N92-31899# Argonne National Lab., IL.
ADIFOR: FORTRAN SOURCE TRANSLATION FOR EFFICIENT DERIVATIVES
C. Bischof, G. Corliss, A. Griewank, P. Hovland, and A. Carle 1992 12 p Presented at the ACM SIGARCH International Conference on Supercomputing, Washington, DC, 19-24 Jul. 1992
(Contract W-31-109-eng-38)
(DE92-016187; ANL/CP-75260; CONF-920730-4) Avail: CASI HC A03/MF A01

The numerical methods employed in the solution of many scientific computing problems require the computation of derivatives of a function f: R(sup n) yields R(sup m). Both the accuracy and the computational requirements of the derivative computation are usually of critical importance for the robustness and speed of the numerical method. ADIFOR (automatic differentiation in Fortran) is a source translation tool implemented using the data abstractions and program analysis capabilities of the ParaScope Parallel Programming Environment. ADIFOR accepts arbitrary Fortran-77 code defining the computation of a function and writes portable Fortran-77 code for the computation of its derivatives. In contrast to previous approaches, ADIFOR views automatic differentiation as a process of source translation that exploits computational context to reduce the cost of derivative computations. Experimental results show that ADIFOR can handle real-life codes, providing exact derivatives with a running time that is competitive with the standard divided-difference approximations of derivatives and which may perform orders of magnitude faster than divided-differences in cases. The computational scientist using ADIFOR is freed from worrying about the accurate and efficient computation of derivatives, even for complicated functions, and is able to concentrate on the more important issues of algorithm design or system modeling. DOE

N92-31939# Carnegie-Mellon Univ., Pittsburgh, PA. Dept. of Computer Science.
A LANGUAGE FOR HIGHER-ORDER EXPLANATION-BASED LEARNING Ph.D. Thesis
Scott Dietzen Jan. 1992 160 p
(Contract N00014-84-K-0415)
(AD-A251008; CMU/CS-92-110) Avail: CASI HC A08/MF A02

Certain tasks, such as formal program development and theorem proving, fundamentally rely upon the manipulation of higher-order objects such as functions and predicates. Computing tools intended to assist in performing these tasks are at present inadequate in both the amount of 'knowledge' they contain (i.e., the level of support they provide) and in their ability to 'learn' (i.e., their capacity to enhance that support over time). The application of a relevant machine learning technique - explanation-based generalization (EBG) - has thus far been limited to first-order problem representations. We extend EBG to generalize higher-order values, thereby enabling its application to higher-order problem encodings. Logic programming provides a uniform framework in which all aspects of explanation-based generalization and learning may be defined and carried out. First-order Horn logics (e.g., Prolog) are not, however, well suited to higher-order applications. Instead, we employ Lambda Prolog, a higher-order logic programming language, as our basic framework for realizing higher-order EBG. In order to capture the distinction between domain theory and training-instance, upon which EBG relies, we extend Lambda Prolog with the necessity operator of modal logic. We then provide a formal characterization of both the extended logic, Lambda Prolog, and of higher-order EBG over Lambda Prolog computation. We also illustrate applications of higher-order EBG within program development and theorem proving. GRA

N92-31991# Air Force Inst. of Tech., Wright-Patterson AFB, OH. School of Engineering.
CONFIDENCE INTERVAL ESTIMATION FOR OUTPUT OF DISCRETE-EVENT SIMULATIONS USING THE KALMAN FILTER M.S. Thesis
Randall B. Howard Mar. 1992 149 p
(AD-A248170; AFIT/GOR/ENS/92M-15) Avail: CASI HC A07/MF A02

Discrete-event simulation is computer modeling of stochastic, dynamic systems. The Kalman filter is a Bayesian stochastic estimation algorithm. Because of the correlated nature of simulation output, it is difficult to apply the methods of classical statistics directly when constructing confidence intervals of discrete-event simulation parameters. Through the determination of a dynamics equation and application of the Kalman filter to simulation output data, three new confidence interval construction techniques have been developed. One technique obtains an estimate of the mean value and its associated variance from an estimated Kalman filter. The second technique utilizes Multiple Model Adaptive Estimation (MMAE) techniques to obtain an estimate of the simulation output's mean value and its associated variance. The third technique also uses MMAE, but constructs a nonsymmetric confidence interval using the final MMAE filter probabilities. The purpose of this research was twofold. The first objective was to explore these new confidence interval construction techniques based on the information provided by Kalman filters. The second objective was to contrast these Kalman filter approaches to several accepted approaches. Both of these objectives were achieved and excellent results were obtained. GRA

N92-32039# Massachusetts Inst. of Tech., Cambridge.
NEW DIRECTIONS IN NETWORK FLOWS Final Report, 1 Jan. 1988 - 31 Dec. 1991
James B. Orlin 20 Mar. 1992 7 p
(Grant AF-AFOSR-0088-88)
(AD-A250499; AFOSR-92-0352TR) Avail: CASI HC A02/MF A01

An algorithm has been developed for the solution of problems using Lagrangian relaxation. This algorithm appears to improve running times by a factor of n-squared, where n is the number of variables. GRA

N92-32060# Naval Postgraduate School, Monterey, CA.
FITTING AND PREDICTION UNCERTAINTY FOR A SOFTWARE RELIABILITY MODEL M.S. Thesis
Thomas E. Dennison Mar. 1992 70 p
(AD-A252173) Avail: CASI HC A04/MF A01

The cost of system operational testing is steadily increasing. It is desirable for the software manager to know if the software is sufficiently well developed or reliable to support such testing. Current software reliability models provide only point estimates of the mean time to next failure or expected number of errors to occur in additional testing time. The goal of this thesis is to take into account prediction uncertainties of a software reliability model. Bootstrapping is used to provide the software manager with confidence limits of the predicted expected number of faults to occur for additional testing time. The results can be particularly useful to a software manager who must find out if the software is reliable enough to support system operational testing. The range of predicted/expected number of faults will be of more use to a software manager, who has to justify the answer to this question, than just a point estimate. Two software fault data sets are analyzed with this technique emphasizing how a software manager should analyze the results. GRA

N92-32122*# Virginia Univ., Charlottesville. Dept. of Electrical Engineering.
ARTIFICIAL NEURAL NETWORK IMPLEMENTATION OF A NEAR-IDEAL ERROR PREDICTION CONTROLLER Final Technical Report, 1 Jun. 1990 - 30 Jun. 1992
Eugene S. McVey and Lynore Denise Taylor Sep. 1992 8 p
(Grant NGT-70172)
(NASA-CR-190694; NAS 1.26:190694; UVA/528352/EE93/102)
Avail: CASI HC A02/MF A01

A theory has been developed at the University of Virginia which explains the effects of including an ideal predictor in the forward loop of a linear error-sampled system. It has been shown that the presence of this ideal predictor tends to stabilize the class of systems considered. A prediction controller is merely a system which anticipates a signal or part of a signal before it actually occurs. It is understood that an exact prediction controller is physically unrealizable. However, in systems where the input tends to be repetitive or limited, (i.e., not random) near ideal prediction is possible. In order for the controller to act as a stability compensator, the predictor must be designed in a way that allows it to learn the expected error response of the system. In this way, an unstable system will become stable by including the predicted error in the system transfer function. Previous and current prediction controller include pattern recognition developments and fast-time simulation which are applicable to the analysis of linear sampled

data type systems. The use of pattern recognition techniques, along with a template matching scheme, has been proposed as one realizable type of near-ideal prediction. Since many, if not most, systems are repeatedly subjected to similar inputs, it was proposed that an adaptive mechanism be used to 'learn' the correct predicted error response. Once the system has learned the response of all the expected inputs, it is necessary only to recognize the type of input with a template matching mechanism and then to use the correct predicted error to drive the system. Suggested here is an alternate approach to the realization of a near-ideal error prediction controller, one designed using Neural Networks. Neural Networks are good at recognizing patterns such as system responses, and the back-propagation architecture makes use of a template matching scheme. In using this type of error prediction, it is assumed that the system error responses be known for a particular input and modeled plant. These responses are used in the error prediction controller. An analysis was done on the general dynamic behavior that results from including a digital error predictor in a control loop and these were compared to those including the near-ideal Neural Network error predictor. This analysis was done for a second and third order system. Author

N92-32126# Oak Ridge National Lab., TN.
CGVIEW: A PROGRAM TO GENERATE ISOMETRIC AND PERSPECTIVE VIEWS OF COMBINATORIAL GEOMETRIES
T. J. Burns Jul. 1992 21 p
(Contract DE-AC05-84OR-21400)
(DE92-016979; ORNL/TM-12019) Avail: CASI HC A03/MF A01

The prototype of a graphical debugger for combinatorial geometry (CG) is described. The prototype debugger consists of two parts: a FORTRAN-based 'view' generator and a Microsoft Windows application for displaying the geometry. This document describes the code CGVIEW, which comprises the first part of the system. User-specified options permit the selection of an arbitrary viewpoint in space and the generation of either an isometric or perspective view. Additionally, any combination of zones, materials, or regions can be flagged as invisible to facilitate the inspection of internal details of the geometry. In the same manner, an arbitrary body can be cut away from the geometry to facilitate inspection and debugging. Examples illustrating the various options are described. DOE

N92-32150# EG and G Energy Measurements, Inc., Los Alamos, NM.
PROBLEMS WITH INTERLEAVED DIGITIZERS
1992 10 p Presented at the High Speed Digital Recorder Workshop, Las Vegas, NV, 21 Apr. 1992
(Contract DE-AC08-88NV-10617)
(DE92-013369; EGG-10617-5103; CONF-9204124-3) Avail: CASI HC A02/MF A01

At EG&G/EM, Los Alamos, part of our digitizer evaluation philosophy is to identify how digitization errors corrupt measurements. The impact of any specific error depends on its source, its size, and whether it's correlated or uncorrelated. Thus, identification of error sources, estimation of error sizes, and determination of errors as correlated or uncorrelated are crucial. Identification of error sources generally tags the errors as correlated or uncorrelated. We have identified several sources of errors and labelled them as correlated or uncorrelated. We will discuss how we have estimated these errors for an identified test unit. DOE

N92-32157*# Institute for Computer Applications in Science and Engineering, Hampton, VA.
A SWEEP ALGORITHM FOR MASSIVELY PARALLEL SIMULATION OF CIRCUIT-SWITCHED NETWORKS Final Report
Bruno Gaujal (Rutgers Univ., New Brunswick, NJ.), Albert G. Greenberg (Bell Telephone Labs., Inc., Murray Hill, NJ.), and David M. Nicol (College of William and Mary, Williamsburg, VA.) Jul. 1992 29 p Submitted for publication
(Contracts NAS1-18605; NAS1-19480; NAG1-1060; NAG1-995; NSF ASC-88-19373; NSF CCR-92-01195; RTOP 505-90-52-01)
(NASA-CR-189680; NAS 1.26:189680; ICASE-92-30) Avail: CASI HC A03/MF A01

A new massively parallel algorithm is presented for simulating large asymmetric circuit-switched networks, controlled by a randomized-routing policy that includes trunk-reservation. A single instruction multiple data (SIMD) implementation is described, and corresponding experiments on a 16384 processor MasPar parallel computer are reported. A multiple instruction multiple data (MIMD) implementation is also described, and corresponding experiments on an Intel IPSC/860 parallel computer, using 16 processors, are reported. By exploiting parallelism, our algorithm increases the possible execution rate of such complex simulations by as much as an order of magnitude. Author

N92-31864# Boeing Commercial Airplane Co., Seattle, WA.
INTEGRATED COMPUTER SYSTEMS IN AIRCRAFT DESIGN AND MANUFACTURE: DIFFICULTIES AND IMPLICATIONS
W. W. Braithwaite *In* Israel Society of Aeronautics and Astronautics, 31st Israel Annual Conference on Aviation and Astronautics 22 Feb. 1990 p 18-26 Previously announced in IAA as A91-43079 (For primary document see N92-31861 22-01)
Avail: CASI HC A02/MF A03

N92-31866# Lehigh Univ., Bethlehem, PA. Intelligent Systems Lab.
DESIGN AND AUTOMATED MANUFACTURING
Kenneth Preiss (Ben Gurion Univ. of the Negev, Beersheva, Israel) *In* Israel Society of Aeronautics and Astronautics, 31st Israel Annual Conference on Aviation and Astronautics 22 Feb. 1990 p 38-40 (For primary document see N92-31861 22-01)
Avail: CASI HC A01/MF A03

62 COMPUTER SYSTEMS

Includes computer networks and special application computer systems.

N92-31365# National Inst. of Standards and Technology, Gaithersburg, MD. Advanced Systems Div.
OVERVIEW OF INTEGRATED SERVICES DIGITAL NETWORK CONFORMANCE TESTING Final Report
L. A. Collica, K. M. Roberts, and D. Su Mar. 1992 21 p
(PB92-181015; NIST/SP-823/1) Avail: CASI HC A03/MF A01

The document introduces a series of documents which focus on the conformance test specifications for the various Integrated Services Digital Network (ISDN) Protocols. An overview of the current status of ISDN Conformance Testing, and the issues involved are also provided. GRA

N92-31428# Rochester Univ., NY. Dept. of Computer Science.
ARCHITECTURAL ADAPTABILITY IN PARALLEL PROGRAMMING
Lawrence A. Crowl May 1991 114 p
(Contracts N00014-87-K-0548; N00014-82-K-0193)
(AD-A247516; TR-381) Avail: CASI HC A06/MF A02

To create a parallel program, programmers must decide what parallelism to exploit, and choose the associated data distribution and communication. Since a typical algorithm has much more potential parallelism than any single architecture can effectively exploit, programmers usually express only the exploitation of parallelism appropriate to a single machine. Unfortunately, parallel architectures vary widely. A program that executes efficiently on one architecture may execute badly, if at all, on another architecture. To port such a program to a new architecture, we must rewrite the program to remove any ineffective parallelism, to introduce any parallelism appropriate for the new machine, to re-distribute data and processing, and to alter the form of communication. Architectural adaptability is the ease with which programmers can tune or port a program to a different architecture. The thesis of this dissertation is that control abstraction is

fundamental to architectural adaptability for parallel programs. With control abstraction, we can define and use a rich variety of control constructs to represent an algorithm's potential parallelism. Since control abstraction separates the definition of a construct from its implementation, a construct may have several different implementations, each providing different exploitations of parallelism. By selecting an implementation for each use of a control construct with annotations, we can vary the parallelism we choose to exploit without otherwise changing the source code.
GRA

N92-31443# Naval Postgraduate School, Monterey, CA.
SIMULATION OF A PARALLEL PROCESSOR BASED SMALL TACTICAL SYSTEM M.S. Thesis
Panurit Yuktadatta Dec. 1991 151 p
(AD-A245911) Avail: CASI HC A08/MF A02

The Simulation of A Parallel Processor Based Small Tactical System is a part of The Parallel Command and Decision System (PARCDS) Laboratory, which was established in the early 1980's to support research for the Navy's AEGIS combat system. The current U.S. Navy's AEGIS system, which uses standard AN/Uyk-7 computers, has four processors in the computer system. When one of them fails, the system automatically reloads the remaining three processors with software that has a reduced capability. But in probably less than one decade, they will not be capable of handling the increasing demand for some more complex software systems. Military command and decision systems of the next decade must be characterized be economy, speed, stability, reliability, and ease of repair. The transputer features all of these benefits and provides a scalable network of transputers which is relatively easy to design. The need for parallel processing grows more evident daily, since the best high-performance uniprocessor architectures are reaching their limits. The prime objective of this thesis is to model a small tactical system by using a network of transputers to develop the transputer version of the Ada programming language system which models a small tactical system.
GRA

N92-31445# Rochester Univ., NY. Dept. of Computer Science.
SYSTEMATIC DETECTION OF PARALLELISM IN ORDINARY PROGRAMS
Cesar A. Gonzalez May 1991 113 p
(Contract N00014-82-K-0193)
(AD-A247514; TR-351) Avail: CASI HC A06/MF A02

This dissertation discusses a general model for compilers that take imperative codes written for sequential machines (ordinary code) and detect the parallelism in that code that is compatible with the semantics of the underlying programming language. This model is based on the idea of separating the concerns of parallelism detection and parallelism exploitation. This separation is made possible by having the detection component provide an explicit representation of the parallelism available in the original code. This explicitly parallel representation is based on a formalization of the notion of permissible execution sequences for a given mass of code. The model discussed here prescribes the structure of the parallelism detector. This structure depends on (1) recognizing a hierarchical structure on a graph representation of the program, and (2) separately encoding parallelization conditions and effects. Opportunities for parallelization can then be discovered by traversing the hierarchical structure from the bottom up. During this traversal, progressively larger parts of the program are compared against the independently encoded conditions and transformed when the conditions are satisfied. The hierarchy guarantees that the results of transforming a piece of a program propagate in time to affect the possible parallelization of larger pieces. Although some of the algorithms used have exponential worst cases for general graphs, their observed behavior on real flow graphs is no worse than quadratic on the size of the original program.
GRA

N92-31466# Lawrence Livermore National Lab., CA.
DATA PARALLEL PROGRAMMING
B. C. Gorda Apr. 1992 5 p Presented at the 29th Semiannual CRAY User Group, Berlin (Germany), 6-10 Apr. 1992
(Contract W-7405-eng-48)
(DE92-013981; UCRL-JC-110439; CONF-9204136-2) Avail: CASI HC A01/MF A01

Parallel programming today can be a tedious and error prone activity. Specifically, with recent massively parallel systems, the coding investment in managing data layout and communication can easily exceed that required to describe the algorithm. The resulting algorithm is married to the data layout so tightly that changes in one require changes in the other. Optimizing the program involves careful handling of fragile algorithmic code which is dependent on the layout. The data parallel model with data distribution directives separates the algorithm from the data layout specification. The programmer can thus modify one with no effect on the other. The model holds the promise of reducing the code cost of well turned applications in addition to greatly increasing the portability among vendors supporting the impending industry standard. The model being worked on is briefly described, and some preliminary estimates on the BBN TC2000 are provided.
DOE

N92-31483*# Research Inst. for Computing and Information Systems, Houston, TX.
ISSUES IN DESIGNING TRANSPORT LAYER MULTICAST FACILITIES Interim Report
Bert J. Dempsey (Digital Technology, Inc., Champaign, IL.) and Alfred C. Weaver (Digital Technology, Inc., Champaign, IL.) Aug. 1990 33 p
(Contract NCC9-16; RICIS Proj. SE-31)
(NASA-CR-190639; NAS 1.26:190639) Avail: CASI HC A03/MF A01

Multicasting denotes a facility in a communications system for providing efficient delivery from a message's source to some well-defined set of locations using a single logical address. While modern network hardware supports multidestination delivery, first generation Transport Layer protocols (e.g., the DoD Transmission Control Protocol (TCP) (15) and ISO TP-4 (41)) did not anticipate the changes over the past decade in underlying network hardware, transmission speeds, and communication patterns that have enabled and driven the interest in reliable multicast. Much recent research has focused on integrating the underlying hardware multicast capability with the reliable services of Transport Layer protocols. Here, we explore the communication issues surrounding the design of such a reliable multicast mechanism. Approaches and solutions from the literature are discussed, and four experimental Transport Layer protocols that incorporate reliable multicast are examined.
Author

N92-31740# Lawrence Livermore National Lab., CA.
THE MULTICOMPUTER TOOLBOX: SCALABLE PARALLEL LIBRARIES FOR LARGE-SCALE CONCURRENT APPLICATIONS
A. Skjellum and C. Baldwin 10 Dec. 1991 51 p Presented at the ACM SIGARCH International Conference on Supercomputing, Washington, DC, 19-24 Jul. 1992
(Contract W-7405-eng-48)
(DE92-008068; UCRL-JC-109251; CONF-920730-2) Avail: CASI HC A04/MF A01

In this paper, we consider what is required to develop parallel algorithms for engineering applications on message-passing concurrent computers. At Caltech, the first author studied the concurrent dynamic simulation of distillation column networks. This research was accomplished with attention to portability, high performance, and reusability of the underlying algorithms. Emerging from this work are several key results: (1) a methodology for explicit parallelization of algorithms and for the evaluation of parallel algorithms in the distributed-memory context; (2) a set of portable, reusable numerical algorithms constituting a 'Multicomputer Toolbox,' suitable for use on both existing and future medium-grain concurrent computers; (3) a working prototype simulation system, Cdyn, for distillation problems, that can be enhanced to address more complex flowsheeting problems in chemical engineering; and (4) ideas for how to achieve higher performance with Cdvn, using

iterative methods for the underlying linear algebra. Of these, the chief emphasis in the present paper is the reusable collection of parallel libraries comprising the Toolbox. Concurrent algorithms for the solution of dense and sparse linear systems, and ordinary differential-algebraic equations were developed as part of this work. Importantly, we have embedded the notion of data distribution independence--support for algorithmic correctness independent of data locality choices--into the underlying methodology and practical software. This together with carefully designed message passing primitives, and concurrent data structures encapsulating data layout of matrices and vectors, provides an excellent basis for building and then tuning the performance of whole applications, rather than single computational steps. DOE

N92-31741# Lawrence Livermore National Lab., CA.
PDDP: DATA-DRIVEN PARALLELISM AND SHARED MEMORY
K. H. Warren and B. C. Gorda Dec. 1991 11 p Presented at the ACM SIGARCH International Conference on Supercomputing, Washington, DC, 19-24 Jul. 1992
(Contract W-7405-eng-48)
(DE92-008073; UCRL-JC-109496; CONF-920730-1) Avail: CASI HC A03/MF A01

The Parallel Data Distribution Preprocessor, PDDP, exploits the cycle time of local shared memory blocks to achieve efficient data parallelization on a MIMD distributed shared memory machine. Shared memory arrays are distributed among the processors. PDDP treats a subset of Fortran D primitives and provides semi-automatic parallelization when Fortran 90 array syntax is used. DOE

N92-31835*# Alabama Univ., Huntsville.
AUTOMATED PAYLOAD EXPERIMENT TOOL FEASIBILITY STUDY Final Technical Report, 10 Jan. - 30 Sep. 1991
Gary A. Maddux, James Clark, Harry Delugach, Charles Hammons, Julie Logan, and Anna Provancha Sep. 1991 153 p
(Contract NAS8-36955)
(NASA-CR-184256; NAS 1.26:184256; UAH-5-32559) Avail: CASI HC A08/MF A02

To achieve an environment less dependent on the flow of paper, automated techniques of data storage and retrieval must be utilized. The prototype under development seeks to demonstrate the ability of a knowledge-based, hypertext computer system. This prototype is concerned with the logical links between two primary NASA support documents, the Science Requirements Document (SRD) and the Engineering Requirements Document (ERD). Once developed, the final system should have the ability to guide a principal investigator through the documentation process in a more timely and efficient manner, while supplying more accurate information to the NASA payload developer. Author

N92-32034# Oak Ridge National Lab., TN.
THE HIERARCHICAL SPATIAL DECOMPOSITION OF THREE-DIMENSIONAL PARTICLE-IN-CELL PLASMA SIMULATIONS ON MIMD DISTRIBUTED MEMORY MULTIPROCESSORS
D. W. Walker Jul. 1992 12 p
(Contract DE-AC05-84OR-21400)
(DE92-016802; ORNL/TM-12071) Avail: CASI HC A03/MF A01

The hierarchical spatial decomposition method is a promising approach to decomposing the particles and computational grid in parallel particle-in-cell application codes, since it is able to maintain approximate dynamic load balance while keeping communication costs low. In this paper we investigate issues in implementing a hierarchical spatial decomposition on a hypercube multiprocessor. Particular attention is focused on the communication needed to update guard ring data, and on the load balancing method. The hierarchical approach is compared with other dynamic load balancing schemes. DOE

N92-32040# Princeton Univ., NJ. Dept. of Electrical Engineering and Computer Science.
FAULT TOLERANT PARALLEL COMPUTING IN ORTHOGONAL SHARED-MEMORY AND RELATED ARCHITECTURES Final Technical Report, 1 Jan. 1990 - 31 Dec. 1991
Niraj K. Jha and Isaac D. Scherson 2 Apr. 1992 11 p
(Grant AF-AFOSR-0144-90)
(AD-A250504; AFOSR-92-0368TR) Avail: CASI HC A03/MF A01

The aim of the research summarized in this final report was to investigate a class of orthogonal shared-memory architectures and interconnection networks, and to obtain generalized methods for implementing algorithm-based fault tolerance (ABFT) on multiprocessor architectures. We proposed a theory based on orthogonal graphs to represent many well-known interconnection networks such as the binary m-cube, spanning-bus meshes, multistage interconnection networks, etc. A previously proposed multiprocessor architecture called the Orthogonal Multiprocessor (OMP) is also a special case of this method. The simplicity of the graph construction rules permits us to characterize and understand the differences and similarities among networks like the SW-banyan, the baseline network, among others. This opens the way for discovering new structures by studying different possible combinations of the parameters which define orthogonal graphs. GRA

N92-32109# New York Univ., New York. Inst. of Mathematical Sciences.
WORKSHOP ON THE DERIVATION OF PARALLEL PROGRAMS AND ARCHITECTURES: CLOSING REPORT Technical Report, 1 Dec. 1989 - 30 Nov. 1991
Robert Paige 30 Nov. 1991 2 p Workshop held in New York, NY, 30 Aug. - 2 Sep. 1992
(Contract N00014-90-J-1421)
(AD-A252742) Avail: CASI HC A01/MF A01

This workshop took place at New York University, Courant Institute from 30 Aug. - 2 Sep. 1992. The aim of the workshop was to bring together computer scientists in transformational programming and parallel algorithm design in order to share ideas that might benefit both communities. It was hoped that exposure by the transformational people to algorithm design methods developed within the theoretical community would stimulate progress in software development for parallel architectures. It was also hoped that exposure to syntax directed methods and pragmatic programming concerns within the transformational community would encourage more realistic theoretical models of parallel architectures and more systematic and algebraic approaches for parallel algorithm design. GRA

N92-32152# Cornell Univ., Ithaca, NY. Dept. of Computer Science.
THE DATA STRUCTURE ACCELERATOR ARCHITECTURE
Richard Zippel Dec. 1991 29 p
(Contracts N00014-88-K-0591; N00014-89-J-1946)
(AD-A250968; TR-91-1256) Avail: CASI HC A03/MF A01

We present a fine grained, massively parallel SIMD architecture called the data structure accelerator and demonstrate its use in a number of problems in computational geometry. This architecture is extremely dense and highly scalable. Systems of 10,000,000 processing elements can be feasibly embedded in work stations. We advocate that this architecture be used in tandem with conventional single sequence machines and with small scale, shared memory multiprocessors. We present a language for programming such heterogeneous systems that smoothly encorporates the SIMD instructions of the data structure accelerator with conventional single sequence code. GRA

63 CYBERNETICS

Includes feedback and control theory, artificial intelligence, robotics and expert systems.

For related information see also *54 Man/System Technology and Life Support.*

N92-31254*# Massachusetts Inst. of Tech., Cambridge. Dept. of Aeronautics and Astronautics.

SPACECRAFT DYNAMICS CHARACTERIZATION AND CONTROL SYSTEM FAILURE DETECTION. VOLUME 3: CONTROL SYSTEM FAILURE MONITORING Final Report

Christiaan M. vanSchalkwyk 10 Feb. 1992 140 p

(Grant NAG1-968)

(NASA-CR-190529; NAS 1.26:190529) Avail: CASI HC A07/MF A02

We discuss the application of Generalized Parity Relations to two experimental flexible space structures, the NASA Langley Mini-Mast and Marshall Space Flight Center ACES mast. We concentrate on the generation of residuals and make no attempt to implement the Decision Function. It should be clear from the examples that are presented whether it would be possible to detect the failure of a specific component. We derive the equations from Generalized Parity Relations. Two special cases are treated: namely, Single Sensor Parity Relations (SSPR) and Double Sensor Parity Relations (DSPR). Generalized Parity Relations for actuators are also derived. The NASA Langley Mini-Mast and the application of SSPR and DSPR to a set of displacement sensors located at the tip of the Mini-Mast are discussed. The performance of a reduced order model that includes the first five models of the mast is compared to a set of parity relations that was identified on a set of input-output data. Both time domain and frequency domain comparisons are made. The effect of the sampling period and model order on the performance of the Residual Generators are also discussed. Failure detection experiments where the sensor set consisted of two gyros and an accelerometer are presented. The effects of model order and sampling frequency are again illustrated. The detection of actuator failures is discussed. We use Generalized Parity Relations to monitor control system component failures on the ACES mast. An overview is given of the Failure Detection Filter and experimental results are discussed. Conclusions and directions for future research are given. Author

N92-31293# Science Applications International Corp., San Diego, CA.

DATA TO TEST AND EVALUATE THE PERFORMANCE OF NEURAL NETWORK ARCHITECTURES FOR SEISMIC SIGNAL DISCRIMINATION, NEURAL COMPUTING FOR SEISMIC PHASE IDENTIFICATION, VOLUME 2

Gagan B. Patnaik and Thomas J. Sereno, Jr. 27 Sep. 1991 42 p

(Contract F19628-90-C-0156)

(AD-A252442; PL-TR-92-2110; SR-1) Avail: CASI HC A03/MF A01

This report describes the application of a neural computing approach for automated initial identification of seismic phases (P or S) recorded by 3-component stations. We use a 3-layer back-propagation neural network to identify phases on the basis of their polarization attributes. This approach is much easier to develop than a more traditional rule-based system because of the high-dimensionality of the input (8-10 polarization attributes), and because the data are station-dependent. The neural network approach also performs 3-7 percent better than a linear multivariate method. Most of the gain is for signals with low signal-to-noise ratio since the nonlinear neural network classifier is less sensitive to outliers (or noisy data) than the linear multivariate method. Another advantage of the neural network approach is that it is easily adapted to data recorded by new stations. For example, we find that we achieve 75-80 percent identification accuracy for a new station without system retraining (e.g., using a network derived from data from a different station). The data required for retraining can be accumulated in about two weeks of continuous operation of the new station, and training takes less than one hour on a Sun4 Sparc station. After this retraining, the identification accuracy increases to greater than 90 percent. We have recently added context (e.g., the number of arrivals before and after the arrival under consideration) to the input of the neural network, and we have found that this further improves the identification accuracy by 3-5 percent. This neural network approach performs better than competing technologies for automated initial phase identification, and it is amenable to machine-learning techniques to automate the process of acquiring new knowledge. GRA

N92-31332# Illinois Univ., Urbana. Center for Supercomputing Research and Development.

ANALYSIS AND DESIGN OF NEURAL NETWORKS Final Report, 30 Sep. 1989 - 29 Sep. 1991

George Cybenko and P. R. Kumar Jan. 1992 8 p

(Grant AF-AFOSR-0536-89)

(AD-A250495; AFOSR-92-0355TR) Avail: CASI HC A02/MF A01

The training problem for feedforward neural networks is a nonlinear parameter estimation that can be solved by a variety of optimization techniques. Much of the literature of neural networks has focused on variants of gradient descent. The training of neural networks using such techniques is known to be a slow process, however, more sophisticated techniques do not always perform better. It is shown that feedforward neural networks can have ill-conditioned Hessians and that this ill-conditioning can be quite common. The analysis and experimental results lead to the conclusion that many network training problems are ill-conditioned and may not be solved more efficiently by higher order optimization methods. The analyses are for completely connected layered networks, and they extend to networks with sparse connectivity as well. The results suggest that neural networks can have considerable redundancy in parameterizing the function space in a neighborhood of a local minimum, independently of whether or not the solution has a small residual. GRA

N92-31395# Army Electronic Proving Ground, Fort Huachuca, AZ.

METHODOLOGY INVESTIGATION FINAL REPORT: AUTOMATED REAL-TIME TEST SCENARIO GENERATION, PHASE 1 Final Report, Oct. 1990 - Oct. 1991

Curtis Massie Oct. 1991 91 p

(AD-A250439; USAEPG-FR-1425) Avail: CASI HC A05/MF A01

This report covered Phase I of an investigation to identify flexible and powerful designs for automated real-time test scenario test generation. This report will support development of new capabilities in the USAEPG family of test drivers. Current drivers need to be more interactive. Their scenarios need to change in response to messages received. This report identified other design enhancements including the following: graphical user interface, time-ordered event lists (TOELS) for message-oriented tests, scenario scripting in terms of message traffic loading for traffic-oriented tests, support for scripting an integrated scenario involving multiple nodes (instead of scripting each node separately), and an interface with an exercise driver (like the Corps Battle Simulator). GRA

N92-31511# Carnegie-Mellon Univ., Pittsburgh, PA. Dept. of Computer Science.

NEURAL NETWORK PERCEPTION FOR MOBILE ROBOT GUIDANCE Ph.D. Thesis

Dean A. Pomerleau 16 Feb. 1992 216 p

(Contracts DACA76-85-C-0002; DACA76-85-C-0003)

(AD-A249972; CMU-CS-92-115) Avail: CASI HC A10/MF A03

Vision based mobile robot guidance has proven difficult for classical machine vision methods because of the diversity and real time constraints inherent in the task. This thesis describes a connectionist system called ALVINN (Autonomous Land Vehicle In a Neural Network) that overcomes these difficulties. ALVINN learns to guide mobile robots using the back-propagation training algorithm. Because of its ability to learn from example, ALVINN can adapt to new situations and, therefore, cope with the diversity

of the autonomous navigation task. But real world problems like vision based mobile robot guidance presents a different set of challenges for the connectionist paradigm. Among them are: developing a general representation from a limited amount of real training data; understanding the internal representations developed by artificial neural networks; estimating the reliability of individual networks; combining multiple networks trained for different situations into a single system, and combining connectionist perception with symbolic reasoning. Solutions to these above problems are presented. Using these techniques, the ALVINN system can learn to control an autonomous van in under 5 minutes by watching a person drive. Once trained, individual ALVINN networks can drive in a variety of circumstances, including single-lane paved and unpaved roads, and multi-lane lined and unlined roads, at speeds of up to 55 miles per hour. GRA

N92-31597*# Research Inst. for Computing and Information Systems, Houston, TX.
USING NEURAL NETWORKS IN SOFTWARE REPOSITORIES
David Eichmann, ed. (West Virginia Univ., Morgantown.), Kankanahalli Srinivas (West Virginia Univ., Morgantown.), and G. Boetticher (West Virginia Univ., Morgantown.) 1 Jun. 1992 35 p
(Contract NCC9-16; RICIS Proj. SE-43)
(NASA-CR-190641; NAS 1.26:190641) Avail: CASI HC A03/MF A01

The first topic is an exploration of the use of neural network techniques to improve the effectiveness of retrieval in software repositories. The second topic relates to a series of experiments conducted to evaluate the feasibility of using adaptive neural networks as a means of deriving (or more specifically, learning) measures on software. Taken together, these two efforts illuminate a very promising mechanism supporting software infrastructures - one based upon a flexible and responsive technology. Author

N92-31680# National Inst. of Standards and Technology, Gaithersburg, MD. Robot Systems Div.
LOGARITHMIC RETINAE
D. Raviv, D. J. Orser, and J. S. Albus Apr. 1992 44 p Prepared in cooperation with Florida Atlantic Univ., Boca Raton
(PB92-183649; NISTIR-4807) Avail: CASI HC A03/MF A01

The paper suggests several iconic image 'warpings', or remappings, which facilitate computationally inexpensive measurements of moving 3-D points relative to a camera. Assuming translational motion of the camera, where the optical axis coincides with the direction of motion, and a stationary scene, points in 3-D space that lie on a particular 3-D surface produce a constant value for some nonlinear function of the optical flow. The function need not be computed after the image is formed, but rather can be implemented by hardware at the retinal level. Four sets of different surfaces are introduced and there is one optical-flow-based constant value for each surface. These values are called 'invariants'. For each invariant a logarithmic retina is defined which will cause optical flow on the surfaces to have identical values. The process of image remapping, called 'normalization', is defined for four 1-D parameterizations of space: range, depth, looming and clearance. For each invariant a camera-retina imaging model utilizing spherical projection and foveal peripheral resolution is described for analyzing optical flow. Computer simulation demonstrates how the now suggested retinae normalize the optical flow with respect to each one of the parameterizations. Author

N92-31811# Honeywell, Inc., Minneapolis, MN. Sensor and System Development Center.
ARTIFICIAL INTELLIGENCE IN TRAINING (AIT) Interim Report, Feb. - Oct. 1991
Charles P. Bloom, Peter T. Bullemer, Mohammed Nasiruddin, Jodi Ray, and Robin R. Penner Apr. 1992 61 p
(Contract F33615-90-C-0013)
(AD-A250145; AL-TP-1992-0010) Avail: CASI HC A04/MF A01

The objective of the current research program was to develop a prototype knowledge acquisition tool that could enable the investigation of knowledge acquisition issues for instructional systems. Our approach to accomplishing this objective entailed the identification of the types of knowledge to be acquired, the evaluation of methods of acquiring such knowledge, the specification of appropriate interaction metaphors for the direct acquisition of knowledge from multiple human sources, and the iterative development of an Artificial Intelligence in Training (AIT) prototype that operationalized the findings of the first three tasks. The AIT prototype demonstrated critical characteristics of a knowledge acquisition environment designed to acquire multiple types of knowledge using a simulated domain environment in which multiple, animated views of knowledge are completely introspective and manipulatable. In addition, strategic knowledge construction was demonstrated based on observations of user actions. We described sample knowledge acquisition scenarios to characterize the functionality supported by the AIT prototype. The following areas for additional research were recommended: acquisition of instructional heuristics, dynamic construction of justification knowledge, use of higher level problem representations such as the goal-action hierarchy, and most importantly, the veridicality of the expertise captured using these methods. GRA

N92-31827# Michigan State Univ., East Lansing.
SIGNAL AND NOISE MODELS ARISING FROM THE THEORY OF ERRORS Final Report
Raoul LePage and V. Mandrekar 1992 13 p
(Contract N00014-85-K-0150)
(AD-A250222) Avail: CASI HC A03/MF A01

Series constructions of stable random process and invariance principles; Gaussian slicing; point process approach to stable processes; seamless resampling; and optimality methods based on expected logarithm are discussed. GRA

N92-32036# Sandia National Labs., Albuquerque, NM.
EFFECTIVE PATH PLANNING THROUGH TASK RESTRICTION
C. P. Chen Jun. 1992 19 p
(Contract DE-AC04-76DP-00789)
(DE92-017351; SAND-91-1964) Avail: CASI HC A03/MF A01

We present a simple and effective path planning algorithm based on a series of plausible task restrictions. It is designed to solve 'realistic' problems very quickly, at the expense of not being able to solve every problem. First, the notion of 'realistic' problems is motivated with heuristic arguments and formalized through task restrictions. Next, an algorithm solving the resulting tasks of interest is provided. We prove its correctness and theoretical efficiency, and demonstrate empirically its effectiveness and speed. We expect our algorithm to be of practical significance based on its simplicity and predicted performance. DOE

N92-32041# Maryland Univ., College Park. Systems Research Center.
SIGNAL PROCESSING AND RECOGNITION IN ADAPTIVE NEURAL NETWORKS Final Report, 1 Aug. 1988 - 31 Jul. 1991
Shihab A. Shamma and P. S. Krishnaprasad 31 Jul. 1991 24 p
(Grant AF-AFOSR-0204-88)
(AD-A250505; AFOSR-92-0357TR) Avail: CASI HC A03/MF A01

The research reported here has been conducted over the last three years under the AFOSR grant (AFOSR-88-0204). It was divided into four general categories of projects: (1) cochlear models applications and implementations; (2) early auditory processing and binaural hearing and phonemic segmentation; (3) central auditory function, physiology, psychoacoustics, and mathematical models; and (4) analysis of neural networks in applications to tactile sensing. Mathematical formulations of the deconvolution problem were analyzed and solved using neural network structures.
Author (GRA)

64 NUMERICAL ANALYSIS

Includes iteration, difference equations, and numerical approximation.

N92-31241# Instituto de Pesquisas Espaciais, Sao Jose dos Campos (Brazil).
THE VEHICLE ROUTING PROBLEM: SOME COMPUTATIONAL TESTS OF SAVINGS METHOD AND ITS VARIATIONS [O PROBLEMA DE ROTEAMENTO DE VEICULOS: ALGUNS TESTES COMPUTACIONAIS DO METODO DAS ECONOMIAS E VARIACOES]
Horacio Hideki Yanasse and Iamara Virginia deMendoncaMotta Dec. 1991 28 p In PORTUGESE
(INPE-5361-RPQ/656) Avail: CASI HC A03/MF A01

Some computational tests were performed with several heuristics that use the Clarke and Wright basic savings principle. The tests show that, among the heuristics analyzed, one cannot pick one as being better than the other. There is a big compromise between the quality of solution and computational time; for small gains in quality, a great computational effort is required. Author

N92-31311# Argonne National Lab., IL.
ADIFOR: AUTOMATIC DIFFERENTIATION IN A SOURCE TRANSLATOR ENVIRONMENT
C. Bischof, G. Corliss, A. Griewank, and A. Carle 1992 10 p Presented at the International Symposium on Symbolic and Algebraic Computation, Berkeley, CA, 27-29 Jul. 1992
(Contract W-31-109-eng-38)
(DE92-016185; ANL/CP-75497; CONF-920760-5) Avail: CASI HC A02/MF A01

The numerical methods employed in the solution of many scientific computing problems require the computation of derivatives of a function f: R(sup n) yields R(sup m). ADIFOR (Automatic Differentiation in FORtran) is a source transformation tool that accepts Fortran 77 code for the computation of a function and writes portable Fortran 77 code for the computation of the derivatives. In contrast to previous approaches, ADIFOR views automatic differentiation as a source transformation problem and employs the data analysis capabilities of the ParaScope Fortran programming environment. Experimental results show that ADIFOR can handle real-life codes and that ADIFOR-generated codes are competitive with divided-difference approximations of derivatives. In addition, studies suggest that the source-transformation approach to automatic differentation may improve the time required to compute derivatives by orders of magnitude. DOE

N92-31520# Technische Univ., Delft (Netherlands). Faculty of Technical Mathematics and Information.
PHASE PORTRAITS OF NON DEGENERATE QUADRATIC SYSTEMS WITH ZERO FINITE MULTIPLICITY
J. W. Reyn 1991 34 p
(Rept-91-96; ETN-92-91846) Copyright Avail: CASI HC A03/MF A01

For nondegenerate quadratic systems, without (real or complex) finite singular points, the 30 different phase portraits are derived. The corresponding conditions on the 12 coefficients in the system are given. ESA

N92-31553*# Cornell Univ., Ithaca, NY. Dept. of Computer Science.
USING CONSISTENT SUBCUTS FOR DETECTING STABLE PROPERTIES
Keith Marzullo and Laura Sabel Apr. 1992 28 p Supersedes TR-91-1205
(Grant NAG2-593)
(NASA-CR-190443; NAS 1.26:190443; TR-92-1277; TR-91-1205) Avail: CASI HC A03/MF A01

We present a general protocol for detecting whether a property holds in a distributed system, where the property is a member of a subclass of stable properties we call the locally stable properties. Our protocol is based on a decentralized method for constructing a maximal subset of the local states that are mutually consistent, which in turn is based on a weakened version of vectored time stamps. The structure of our protocol lends itself to refinement, and we demonstrate its utility by deriving some specialized property-detection protocols, including two previously known protocols that are known to be effective. Author

N92-31567# Maryland Univ., College Park. Dept. of Computer Science.
ITERATIVE METHODS FOR LARGE SPARSE LINEAR SYSTEMS ARISING FROM PARTIAL DIFFERENTIAL EQUATIONS Final Report, 1 Dec. 1988 - 31 Jan. 1992
Howard C. Elman Mar. 1992 5 p
(Contract DAAL03-89-K-0016)
(AD-A249524; ARO-26391.10-MA) Avail: CASI HC A01/MF A01

The objective of this project was to study numerical methods for solving sparse linear systems of equations of the type that arise from discretized partial differential equations. Such systems arise in mathematical models of numerous physical processes including turbulent flow, chemical reactive flow, semiconductor device simulation, and structural mechanics. For many such problems, analytic solutions are not available, so the only way of obtaining insight into the model is through numerical approximation and solution. The solution of sparse linear systems is often the most costly task, in terms of both computer time and storage, required by this process, so that improving the efficiency of such computations is of critical importance for the construction of accurate numerical models. Emphasis was on sparse iterative methods for solving these systems and implementation of linear system solvers on parallel computers. Major results are summarized in the final report. GRA

N92-31690# Laboratoire d'Automatique et d'Analyse des Systemes, Toulouse (France).
MATHEMATICAL STRUCTURES FOR QUALITATIVE CALCULUS, A CONTRIBUTION TO QUALITATIVE SIMULATION Ph.D. Thesis - Toulouse Univ. [STRUCTURES MATHEMATIQUES POUR LE CALCUL QUALITATIF, CONTRIBUTION A LA SIMULATION QUALITATIVE]
Antoine Missier 1991 133 p In FRENCH
(LAAS-91475; ETN-92-91680) Avail: CASI HC A07/MF A02

A mathematical structure called 'qualitative space', which associates a set of qualities to a set of objects is defined. It allows for arithmetic and logic manipulations of these qualities. This structure defines a general framework for order of magnitude qualitative algebras, including the particular case of sign algebra which is commonly used in qualitative physics. The properties of these algebras with respect to qualitative calculus are studied; leading to general results for qualitative equation set resolution, which is a prime step in environment type qualitative simulation. A qualitative simulator named SQUALE, based on qualitative differential equations and using sign algebra is reported. Production of spurious behaviors is the major problem encountered with this type of simulation. Further development reduces the behavioral explosion. SQUALE was developed according to a new approach, using constraint resolution, which considerably reduces the combinatorial aspect. Some other improvements arising from mathematical analysis are proposed and implemented. ESA

N92-31956# Loughborough Univ. of Technology (England). Dept. of Mathematical Sciences.
NONLINEAR PARTIAL DIFFERENTIAL EQUATIONS AND SOLITONS
C. Hoenselaers Jan. 1992 16 p
(MATHS-Rept-A-152; ETN-92-91725) Avail: CASI HC A03/MF A01

An introduction to the method of prolongation structures as a tool to solve nonlinear partial differential equations are given. For equations amenable to this method, Baecklund transformations can be derived which allow an exact solution of the equation under study to be written in terms of another exact solution and certain functions derived from it. ESA

N92-31957# Loughborough Univ. of Technology (England). Dept. of Mathematical Sciences.
A FUNDAMENTAL NOTION OF EQUIVALENCE FOR LINEAR MULTIVARIABLE SYSTEMS
A. C. Pugh, N. P. Karampetakis (Aristotle Univ. of Thessaloniki. Greece), A. I. G. Vardulakis (Aristotle Univ. of Thessaloniki, Greece), and G. E. Hayton (Hull Univ., England) Mar. 1992 37 p Presented at 31st IEEE Conference on Decision and Control Sponsored in part by Greek National Foundation
(MATHS-Rept-A-153; ETN-92-91726) Avail: CASI HC A03/MF A01

A fundamental form of equivalence between polynomial matrix descriptions (PMD's) of linear multivariable systems is defined. This notion of equivalence is based on the existence of a certain ojective map between the finite and infinite solution sets of the differential equations describing the two systems. The connection with the system matrix relationship of full system equivalence transformation is established and, as a consequence, the role of all the conditions appearing in the latter form of equivalence are fully ascribed. ESA

N92-32081# Tennessee Univ., Knoxville. Dept. of Mathematics.
NON-CONVEX PROBLEMS IN PDE: EQUILIBRIUM THEORY AND DYNAMICS Final Report, 1 Apr. - 30 Sep. 1991
Nicholas Alikakos 30 Sep. 1991 8 p
(Grant AF-AFOSR-0232-91)
(AD-A250549; AFOSR-92-0412TR) Avail: CASI HC A02/MF A01

The main goal of the research discussed in this conference is a mathematical understanding of nonlinear dynamics appropriate for models of continua which admit phase transitions. The mathematical problems that were discussed addressed the general questions of: how do nonlinear systems relax to equilibrium; and how do interfaces and transition zones propagate? The speakers represented different aspects of the subject. The group included theoreticians as well as numerical analysts. GRA

N92-32163# Massachusetts Inst. of Tech., Cambridge. Computer Science Lab.
FULL ABSTRACTION AND THE CONTEXT LEMMA
Trevor Jim and Albert R. Meyer Dec. 1991 49 p
(Contract N00014-89-J-1988)
(AD-A247062; MIT/LCS/TR-524) Avail: CASI HC A03/MF A01

It is impossible to add a combinator to PCF to achieve full abstraction for models such as Berry's stable domains in a way analogous to the addition of the parallel-or combinator that achieves full abstraction for the familiar cpo model. In particular, we define a general notion of rewriting systems of the kind used for evaluating simply typed lambda-terms in Scott's PCF. Any simply typed lambda-calculus with such a PCF-like rewriting semantics is shown necessarily to satisfy Milner's Context Lemma. A simple argument demonstrates that any denotational semantics that is adequate for PCF, and in which certain simple Boolean functionals exist, cannot be fully abstract for any extension of PCF satisfying the Context Lemma. An immediate corollary is that stable domains cannot be fully abstract for any extension of PCF definable by PCF-like rules. GRA

N92-32164*# Institute for Computer Applications in Science and Engineering, Hampton, VA.
NONLINEARLY STABLE COMPACT SCHEMES FOR SHOCK CALCULATIONS Final Report
Bernardo Cockburn (Minnesota Univ., Minneapolis.) and Chi-Wang Shu (Brown Univ., Providence, RI.) May 1992 26 p Submitted for publication
(Contracts NAS1-18605; NAG1-1145; DAAL03-91-G-0123; NSF DSM-91-03997; RTOP 505-90-52-01)
(NASA-CR-189663; NAS 1.26:189663; ICASE-92-21) Avail: CASI HC A03/MF A01

The applications of high-order, compact finite difference methods in shock calculations are discussed. The main concern is to define a local mean which will serve as a reference for introducing a local nonlinear limiting to control spurious numerical oscillations while maintaining the formal accuracy of the scheme. For scalar conservation laws, the resulting schemes can be proven total-variation stable in one space dimension and maximum-norm stable in multiple space dimensions. Numerical examples are shown to verify accuracy and stability of such schemes for problems containing shocks. These ideas can also be applied to other implicit schemes such as the continuous Galerkin finite element methods. Author

N92-32171# Carnegie-Mellon Univ., Pittsburgh, PA. Dept. of Computer Science.
POLYMORPHIC TYPE ASSIGNMENT AND CPS CONVERSION
Robert Harper and Mark Lillibridge Apr. 1992 17 p
(Contract F19628-91-C-0168)
(AD-A250954; CMU/CS-92-122) Avail: CASI HC A03/MF A01

Meyer and Wand established that the type of a term in the simply typed lambda-calculus may be related in a straightforward manner to the type of its call-by-value CPS transform. This typing property may be extended to Scheme-like continuation-passing primitives, from which the soundness of these extensions follows. We study the extension of these results to the Damas-Milner polymorphic type assignment system under both the call-by-value and call-by-name interpretations. We obtain CPS transforms for the call-by-value interpretation, provided that the polymorphic let is restricted to values, and for the call-by-name interpretation with no restrictions. We prove that there is no call-by-value CPS transform for the full Damas-Milner language that validates the Meyer-Wand typing property and is equivalent to the standard call-by-value transform up to beta eta-conversion. GRA

N92-32205# National Inst. for Fusion Science, Nagoya (Japan).
KERNEL OPTIMUM NEARLY-ANALYTICAL DISCRETIZATION (KOND) METHOD APPLIED TO PARABOLIC EQUATIONS KOND-P SCHEME
Y. Kondoh (Gunma Univ., Japan) and Y. Hosaka (Gunma Univ., Japan) Nov. 1991 25 p Submitted for publication
(NIFS-118) Avail: CASI HC A03/MF A01

A KOND-P scheme, which is the application of the Kernel Optimum Nearly-analytical Discretization (KOND) method for the construction of numerical schemes to the parabolic type partial differential equation, is presented. Typical numerical results are shown to clarify that the KOND-P scheme is more accurate than the conventional explicit scheme by 2-3 orders of magnitude, as measured by the root mean square deviation from analytical solutions. Author

N92-32210# Polish Academy of Sciences, Warsaw. Inst. Podstawowych Problemow Techniki.
DETERMINATION OF THE MATRIX CONDITIONING INDICATOR. COMPARISON OF APPROXIMATE METHODS [WYZNACZANIE WSKAZNIKA UWARUNKOWANIA MACIERZY POROWNANIE METOD PRZYBLIZONYCH]
Elzbieta Tyrkiel 1992 64 p In POLISH
Avail: CASI HC A04/MF A01

Numerical determination of the conditioning indicator cond (A) for a system of linear equations as a product of the matrix spectral norms and the inverse of the system: cond (A) = matrix A (dot) the inverse matrix A. An approximate iterative method for determining the value of each norm was tested. Two versions of this method, differing in the method of selecting the starting vector for the iterative process, were taken into consideration. Calculation tests were performed for matrices of various degrees (n = 10/100). Consumption of both indicator calculating methods was estimated in cases when the system is solved by means of the QR orthogonal-triangular distribution and the LU triangular distribution. Accuracy of the results was estimated on the basis of spectral norm values, obtained by the singular matrix distribution method. The method tested makes possible effective estimation of the order of magnitude of the conditioning indicator which is basic information required for practical calculations. A significant restriction of the conclusions presented is the fact that the random

matrices tested are for the most part well-conditioned (indicator values do not exceed the order of 10 exp 3). Author

65 STATISTICS AND PROBABILITY

Includes data sampling and smoothing; Monte Carlo method; and stochastic processes.

N92-31517# Center for Mathematics and Computer Science, Amsterdam (Netherlands). Dept. of Operations Research, Statistics and System Theory.
ON A CHARACTERIZATION OF THE EXPONENTIAL DISTRIBUTION BASED ON A TYPE 2 RIGHT CENSORED SAMPLE
Julian Leslie (MacQuarie Univ., Sydney, Australia) and Constance vanEeden (British Columbia Univ., Vancouver.) Jul. 1991 20 p Sponsored by Natural Sciences and Engineering Research Council of Canada; FCAR, Quebec; and University College, London, England
(CWI-BS-R9117; ETN-92-91784) Copyright Avail: CASI HC A03/MF A01

Dufour (1982) gives a conjecture concerning a characterization of the exponential distribution based on type 2 right censored samples. This conjecture, if true, generalized the characterization based on complete samples of earlier works. It is shown that Dufour's conjecture is true if the number of censored observations is no larger than (n/3) - 1, where n is the sample size. ESA

N92-31518# Technische Univ., Delft (Netherlands). Faculty of Technical Mathematics and Information.
TWO PROPERTIES OF UNIFORM DISTRIBUTIONS, WITH APPLICATIONS TO SOME NONPARAMETRIC ESTIMATION PROBLEMS
R. Gruebel 1991 16 p
(Rept-91-94; ETN-92-91844) Copyright Avail: CASI HC A03/MF A01

A nonnegative random variable X with decreasing density may be represented in distribution as X = U(dot)Y, with U uniformly distributed on (0,1) and Y a random variable which is independent of U. Based on a simple explicit formula for the distribution of Y, three nonparametric maximum likelihood problems are related: estimation of distribution functions from uniform random fractions, exponential deconvolution, and estimation of decreasing densities. The solution of the last one is the well known Grenander estimator; the approach leads to simple explicit solutions of the other two. A second property of uniform distributions, related to the first, deals with censoring: the influence of the distribution of Y outside the censoring interval on the distribution of the censored random fraction U(dot)Y is investigated. A process of line segments of random length on the real line where uniform random fractions arise in connection with censored observations is considered. The results can then be applied to a problem from stereology. ESA

N92-31519# Technische Univ., Delft (Netherlands). Faculty of Technical Mathematics and Information.
NONPARAMETRIC ESTIMATION IN RENEWAL THEORY, 1: THE EMPIRICAL RENEWAL FUNCTION
Rudolf Gruebel and Susan M. Pitts (University Coll., London, England) 1991 32 p
(Rept-91-95; ETN-92-91845) Copyright Avail: CASI HC A03/MF A01

A nonparametric estimator for the renewal function is introduced and its properties, including consistency, asymptotic normality, asymptotic validity of bootstrap confidence regions, and associated implementation methods, are discussed. The underlying theme is that stochastic models can be regarded as functionals or nonlinear operators. This view leads to nonparametric estimators in a natural way and statistical properties of the estimators can be related to the local behavior of the functionals. The implementation method is based on the fast Fourier transform algorithm. ESA

N92-31600# Stanford Univ., CA. Dept. of Operations Research.
INDEPENDENT SAMPLING OF A STOCHASTIC PROCESS
Peter W. Glynn and Karl Sigman Nov. 1991 12 p
(Contract DAAL03-91-G-0101)
(AD-A249712; SU-TR-74; ARO-28809.6-MASDI) Avail: CASI HC A03/MF A01

We investigate when sampling a stochastic process X = (X(t) : t greater than 0) at the times of an independent point process, leads to the same empirical distribution as the time average limiting distribution of X. We considered two cases. The first is when X is an asymptotically stationary process and satisfies a mixing and coupling condition. In this case, the entire limiting distribution in function space are shown to be the same. The second case is when X is only assumed to have a constant finite time average and is assumed a positive t renewal with a spread-out cycle length distribution. In this non-ergodic case, the averages are shown to be the same when some further condition is placed on X and Psi. GRA

N92-31757# Stanford Univ., CA. Dept. of Operations Research.
IMPORTANCE SAMPLING FOR MARKOV CHAINS: ASYMPTOTICS FOR THE VARIANCE
Peter W. Glynn Oct. 1991 27 p
(Contract DAAL03-91-G-0101)
(AD-A249804; ARO-28809.5-MA-SDI) Avail: CASI HC A03/MF A01

In this paper, we apply the Perron-Frobenius theory for non-negative matrices to the analysis of variance asymptotics for simulations of finite state Markov chains to which importance sampling is applied. The results show that we can typically expect the variance to grow (at least) exponentially rapidly in the length of the time horizon simulated. The exponential rate constant is determined by the Perron-Frobenius eigenvalue of a certain matrix. Applications to cumulative costs, terminal costs, steady-state costs, and the like ratio gradient estimator are presented. In addition, the implications for general discrete-event simulations are presented. GRA

N92-31768# Carnegie-Mellon Univ., Pittsburgh, PA. Graduate School of Industrial Administration.
DECOMPOSITION OF BALANCED MATRICES. PART 4: CONNECTED SQUARES
Michele Conforti, Gerard Cornuejols, and M. R. Rao Oct. 1991 27 p
(Grants NSF DDM-89-01495; NSF DDM-88-00281; NSF DDM-90-01705)
(AD-A247308; MSRR-572) Avail: CASI HC A03/MF A01

There exist two complete bipartite graphs K1, K2 in G having disjoint node sets, with the property that the removal of the edges in K1, K2 disconnects G. There exists a subset S of the nodes of G with the property that the removal of S disconnects G, where S can be partitioned into three disjoint sets T, A, N, such that T is not equal to 0, some nodes T are adjacent to every node, and every node of T is adjacent to every node of A. A 0,1 matrix is balanced if it does not contain a square submatrix of odd order with two ones per row and per column. Balanced matrices are important in integer programming and combinatorial optimization, since the associated set packing and set covering polytopes have integral vertices. To a 0,1 matrix A we associate a bipartite graph as follows: The node nets Vr and Vc represent the row set and the column set of A, and edge ij belongs to E if and only if ay=1. Since a 0,1 matrix is balanced if and only if the associated bipartite graph does not contain a chordless cycle of length 4k+2, the above theorem provides a decomposition of balanced matrices into elementary matrices whose associated bipartite graphs have no cycle of length 4k + 2. GRA

N92-31981# Cognitech, Inc., Santa Monica, CA.
A REAL TIME SYSTEM FOR MULTISENSOR IMAGE ANALYSIS THROUGH PYRAMIDAL SEGMENTATION Final Report, 1 Jun. - 30 Nov. 1991

L. Rudin, S. Osher, G. Koepfler, and J. M. Morel 30 Jan. 1992 32 p
(Contract F49620-91-C-0036)
(AD-A247169; AFOSR-92-0021TR) Avail: CASI HC A03/MF A01

A state of the art, fully functional, multi-scale, and multichannel segmentation tool has been developed. It is based on the recently developed computational theory of the 2-normal segmentations. A fast multiscale pyramidal algorithm has been designed and applied to the theoretical variational segmentation model of Mumford-Shah. This algorithm has a multichannel capability, as well as a much more general class of solutions. Namely, a piecewise polynomial segmentation is natural to the pyramidal multichannel framework. The piecewise affine segmentation has been implemented and tested. Application specific channels include: gray scale information, two-dimensional wavelet channels for texture discrimination, and multiscale singular feature channels. The accuracy of the pyramidal segmentation algorithm has been experimentally compared to the accuracy of two other modern segmentation algorithms. The performance of the pyramidal algorithm has shown an average four-fold reduction in error measurements. Computational experiments with reconnaissance photography, multisensor satellite imagery, medical CT, and MRI multi-band data have shown a great practical potential of this technique. Preliminary experimentation in clutter removal via multichannel segmentation points to a totally new class of feature preserving decluttering algorithms. GRA

N92-32225# Instituto de Pesquisas Espaciais, Sao Jose dos Campos (Brazil).
MARKOVIAN FIELDS AS LIMITS OF MARKOV CHAINS
Oscar H. Bustos and Alejandro C. Frery 1992 16 p
(INPE-5395-PRE/1753) Avail: CASI HC A03/MF A01

Markovian fields are useful stochastic models for statistical treatment of digitized images, among other applications. In this paper we present some simulation results about the convergence properties of one of the available methods to simulate Markovian fields: the Gibbs sampler. We use the observed values of the mean magnetization, the pseudo-likehood estimates, and the observed short and long range correlations to study the problems associated with the stopping time of the algorithm for different values of the parameter. Author

66 SYSTEMS ANALYSIS

Includes mathematical modeling; network analysis; and operations research.

N92-32119# Lawrence Livermore National Lab., CA.
OPTIMAL TARGETING OF EVADING OBJECTS
S. A. Erickson, Jr. Oct. 1991 18 p Presented at the 1991 Operations Research Society of America/Technical Institute of Management Sciences (ORSA/TIMS) Conference, Anaheim, CA, 3-6 Nov. 1991
(Contract W-7405-eng-48)
(DE92-014719; UCRL-JC-108771; CONF-9111227-1) Avail: CASI HC A03/MF A01

The work reported here concerns a competitive game in the area of weapon targeting. Over the last several decades, a number of games abstracted from combat have been studied with operations research techniques. Well-known examples include duels where the object is to maximize the probability of hitting an approaching target which can also shoot, search games where one player tries to locate the chosen position of another, offense and defense resource allocation problems, maneuver problems leading to differential games and others dating back to World War II. The problem we discuss here, aiming at a knowledgeable, evading target does not seem to have been dealt with before. However, it has close connections with other games and optimization. Optimal strategies for both aiming and evasion are simultaneously determined using a variant of minmax optimization. A method of parametric optimization is discussed which leads to efficient solution of the minmax problem. Several examples are used to illustrate the theory. DOE

N92-32229# Advisory Group for Aerospace Research and Development, Neuilly-Sur-Seine (France). Guidance and Control Panel.
PROCEEDINGS OF THE 53RD SYMPOSIUM ON AIR VEHICLE MISSION CONTROL AND MANAGEMENT [LA GESTION ET LE CONTROLE DES MISSIONS DES VEHICULES AERIENS]
Duncan E. McIver Jul. 1992 14 p Symposium held in Amsterdam, Netherlands, 22-25 Oct. 1991
(AGARD-AR-310; ISBN-92-835-0678-2; CP-504; CP-504S)
Copyright Avail: CASI HC A03/MF A01

This document gives summaries of papers presented at the Guidance and Control Panel 53rd Symposium held from Oct. 22 to Oct. 25, 1991. Topics covered by these papers include: operational mission considerations; situation assessment; route planning; planning techniques; and implementation aspects. H.A.

N92-31882# Technion - Israel Inst. of Tech., Haifa. Faculty of Aerospace Engineering.
AN AUTOMATED COMPUTATIONAL METHOD FOR BARRIER CONSTRUCTION IN SINGLE AND TWO-TARGET DIFFERENTIAL GAMES
L. Breuer, B. Kantor (Aerobyte Engineering, Tel Aviv, Israel), and J. Shinar *In* Israel Society of Aeronautics and Astronautics, 31st Israel Annual Conference on Aviation and Astronautics 22 Feb. 1990 p 153-161 (For primary document see N92-31861 22-01)
Avail: CASI HC A02/MF A03

67 THEORETICAL MATHEMATICS

Includes topology and number theory.

No abstracts in this category.

70 PHYSICS (GENERAL)

For precision time and time interval (PTTI) see *35 Instrumentation and Photography;* for geophysics, astrophysics or solar physics see *46 Geophysics, 90 Astrophysics,* or *92 Solar Physics.*

N92-31359# Boston Univ., MA.
ENHANCEMENT OF FRACTURE TOUGHNESS USING HIGH INTENSITY ELECTRIC CURRENTS Final Report, 1 Aug. 1991 - 31 Jan. 1992
V. K. Sarin and J. Gurland Feb. 1992 8 p
(Contract DAAL03-91-G-0240)
(AD-A249809; ARO-28821.1-MS) Avail: CASI HC A02/MF A01

The object of this research is to conduct exploratory experiments on the effects of electric current on the fracture characteristics of materials prone to microcracking and catastrophic failure. It is anticipated that under controlled conditions, the applied electric current may result in localized heating at the highly stressed zones around the tips of the microcracks, and/or electroplastic effects. If so, the resulting stress relief and microstructural modifications could be utilized to inhibit crack growth under subsequent loading, and thereby in effect, increase the fracture toughness of the damaged microstructure, without necessarily affecting bulk hardness, flow strength, and ductility. GRA

N92-31686# Air Force Inst. of Tech., Wright-Patterson AFB, OH.
MAXIMUM LIKELIHOOD ESTIMATION OF FRACTIONAL BROWNIAN MOTION AND MARKOV NOISE PARAMETERS M.S. Thesis
Matthew E. Skeen 1991 139 p
(AD-A249623; AFIT/CI/CIA-91-132) Avail: CASI HC A07/MF A02

Maximum likelihood estimation and power spectral density analysis are developed as tools for the analysis of stochastic processes. Some useful results from the theory of Markov stochastic processes are then presented followed by the introduction of fractional Brownian motion and fractional Gaussian noise as non-Markov models for systems with power spectral density proportional to fBeta, where -3 less than Beta less than -1 and -1 less than Beta less than 1 over all frequencies. Maximum likelihood system identification is applied to estimating the unknown parameters in a Markov model which approximates fractional Brownian motion. The algorithm runs a Kalman filter on states and a maximum likelihood estimator on parameters. Results are presented from estimating trend, white noise, random walk, and exponentially correlated noise parameters from fits to simulated and real test data. Maximum likelihood estimation is applied to the batch estimation of parameters in the non-Markov fractional Brownian motion model. New in this thesis is the use of partial derivatives to minimize the resulting likelihood function, and the capability to estimate the unknown parameters of additional trend and Markov noise processes. Results are presented from fits to computer simulated sample paths. GRA

N92-31925# Institut des Hautes Etudes Scientifiques, Bures-sur-Yvette (France).
FEYNMAN DIAGRAMS AND VASSILIEV INVARIANTS
A. B. Sossinsky Feb. 1992 20 p
(PB92-178284; IHES/M/92/13) Avail: CASI HC A03/MF A01

A brief exposition of the theory of V. Vassiliev's know invariants and their relationships with other invariants and with theoretical physics, based on Vassiliev's original paper and preprints by J. Birman, X.-S. Lin and D. Bar Natan, is presented. The main connection between Vassiliev invariants and physics is via the Feynman diagram of a singular knot, a notion implicitly contained in Vassiliev's work and more explicitly in Bar Natan's. Author

N92-32035# Ohio State Univ., Columbus.
THE PHYSICS OF CELLULAR AUTOMATA AND COHERENCE AND CHAOS IN CLASSICAL MANY-BODY SYSTEMS
24 Jun. 1992 6 p
(Contract DE-FG02-88ER-13916)
(DE92-016834; DOE/ER-13916/4) Avail: CASI HC A02/MF A01

This report contains short discussions on the following topics: non-variational effects in a Ginzburg-Landau equation; algebraic correlations in conserved chaotic systems; chaotic interface models of turbulence; algebraic correlations in coupled order parameter systems; and dynamics of Josephson Junction arrays. DOE

N92-32046# Aware, Inc., Cambridge, MA.
WAVELET SIGNAL PROCESSING FOR TRANSIENT FEATURE EXTRACTION Final Report, 15 Sep. 1991 - 14 Jan. 1992
Karl B. Jagler 15 Mar. 1992 84 p
(Contract F49620-91-C-0089)
(AD-A250519; AD-920315; AFOSR-92-0402TR) Avail: CASI HC A05/MF A01

Research was conducted to evaluate the feasibility of applying Wavelets and Wavelet Transform methods to transient signal feature extraction problems. Wavelet transform techniques were developed to extract low dimensional feature data that allowed a simple classification scheme to easily separate the various signals of interest. Additional development of these techniques will lead to robust feature extraction methods for transient signals. GRA

N92-32099# Clarkson Univ., Potsdam, NY.
EXPERIMENTAL STUDIES OF FRICTION AND HEAT TRANSFER IN ENHANCED PASSAGES
N. T. Obot, E. B. Esen, and L. Das Mar. 1992 9 p
(Contract DE-FG02-89CE-90029)
(DE92-011607; DOE/CE-90029/7) Avail: CASI HC A02/MF A01

The objectives of this research are two-fold. One is to carry out an extensive experimental investigation of pressure drop and heat transfer for internally enhanced passages in laminar, transitional, and turbulent flow. The laminar and transition regions have received very meager treatment in the past. In addition to the effects of Reynolds number and the geometric characteristics of the enhanced surfaces, a comprehensive investigation of the effect of fluid properties, which is usually expressed in terms of the Prandtl number, is one of the central features of this research program. The influence of Prandtl number on friction and heat transfer is undoubtedly the least understood because only a handful of studies considered more than one fluid. Also, there has been no consistent investigation of the Prandtl number effect for laminar or transitional flow. The second objective is to develop a general method that will aid data correlation and prediction which, in turn, will provide a better understanding of friction and heat transfer characteristics for smooth and enhanced passage. More specifically, the aim is to validate the frictional law of corresponding states using the present experimental data. DOE

N92-32116# Ames Lab., IA.
A SELF CONSISTENT GENERALIZED MODEL FOR THE CALCULATION OF MINOR LOOP EXCURSIONS IN THE THEORY OF HYSTERESIS
D. C. Jiles 1992 4 p Presented at the International Magnetics Conference, St. Louis, MO, 13-16 Apr. 1992
(Contract W-7405-eng-82)
(DE92-014394; IS-M-711; CONF-920408-2) Avail: CASI HC A01/MF A01

In the previous work it has been shown that the magnetization curves of a wide range of ferromagnetic materials can be calculated from a simple theory which invokes a constant energy loss per unit change in magnetization. The energy loss, which is therefore proportional to the change in magnetization, leads to hysteresis loops which are obtained from first principles. In the paper it will be shown how the model has been generalized to provide completely self consistent minor hysteresis loop excursions. By minor loop we mean any excursion for which either the range of magnetization (Delta)M or the range of magnetic field (Delta)H is not symmetric about zero. The resulting model solutions show that both crossing and partially coincident minor loops emerge naturally from the theory. This is known to occur in experimental observations and has been noted by Mayergoyz. The generalization of the theory of hysteresis to cover the minor loop excursions has resulted from the use of an effective volume fraction of active domains determined from the location of the minor loop reversal points on the M,H plane. Such a concept is well known in the use of Preisach models for describing hysteresis. This paper describes a generalization of the theory of hysteresis to cover asymmetric, or minor hysteresis loop excursions. The original description of the model was found to be particularly useful because it enabled hysteresis loops of magnetic materials to be successfully modelled with a limited set of only five physically based parameters. The extension of the model presented here is completely self consistent with the original formulation and requires no additional parameters to describe the minor loops. DOE

N92-32140# Superconducting Super Collider Lab., Dallas, TX.
THE PHYSICAL SOLUTION TO THE LORENTZ-DIRAC EQUATIONS IN A CONSTANT MAGNETIC FIELD
D. Endres (New Mexico Univ., Albuquerque.) Mar. 1992 20 p
(Contract DE-AC35-89ER-40486)
(DE92-013299; SSCL-530) Avail: CASI HC A03/MF A01

The somewhat controversial Lorentz-Dirac equations for the motion of a radiating relativistic electron are shown to admit a unique physical solution in a constant uniform magnetic field

perpendicular to the particle motion. In particular, the stable manifold of the origin in a four-dimensional velocity-acceleration phase space is shown to be globally the graph of a function mapping velocity to acceleration; solutions not in this manifold are shown to exhibit unphysical accelerations. Consequently, to each velocity there corresponds a unique physical acceleration determined by the stable manifold. DOE

N92-32211# Purdue Univ., West Lafayette, IN. Dept. of Physics.
DIFFUSION IN ORDERED AND DISORDERED MEDIA Final Report
Hisao Nakanishi 11 May 1992 14 p
(Contract N00014-90-J-1028)
(AD-A250949) Avail: CASI HC A03/MF A01

In this project, we have investigated the Brownian motion taking place in ordered and disordered media using various complementary approaches. These include the analysis of the eigenvalues and eigenvectors of the transition probability matrix (which represents both the media geometry and the kinetics of Brownian motion). This matrix is typically a large, random, Markov matrix and is shown to possess eigenspectrum with scaling properties which has been analyzed numerically. Secondly, the same matrix has been used to evaluate autocorrelation functions directly and exactly, taking advantage of high speed vector computation. Thirdly, the Langevin approach to diffusion has been extended to incorporate the anomalous diffusion on fractal media. Lastly, the frequency dependent conductivity of inhomogeneous media has been investigated using a persistent random walk model and the aforementioned numerical technique of the calculation of step autocorrelation functions. This last work has already revealed the unexpected effects of the interplay between the mean free path of the diffusing particle (carrier), the carrier density, and the length scale of inhomogeneity, in the media. This work represents what we believe to be the coherent efforts to understand the diffusion and transport in disordered media. GRA

71 ACOUSTICS

Includes sound generation, transmission and attenuation. For noise pollution see *45 Environmental Pollution.*

N92-31248*# General Electric Co., Cincinnati, OH. Aircraft Engines.
HIGH SPEED TURBOPROP AEROACOUSTIC STUDY (COUNTERROTATION). VOLUME 2: COMPUTER PROGRAMS
C. E. Whitfield, R. Mani, and P. R. Gliebe Jul. 1990 177 p
(Contract NAS3-23721; RTOP 535-05-01)
(NASA-CR-185242; NAS 1.26:185242) Avail: CASI HC A09/MF A02

The isolated counterrotating high speed turboprop noise prediction program developed and funded by GE Aircraft Engines was compared with model data taken in the GE Aircraft Engines Cell 41 anechoic facility, the Boeing Transonic Wind Tunnel, and in the NASA-Lewis 8 x 6 and 9 x 15 wind tunnels. The predictions show good agreement with measured data under both low and high speed simulated flight conditions. The installation effect model developed for single rotation, high speed turboprops was extended to include counter rotation. The additional effect of mounting a pylon upstream of the forward rotor was included in the flow field modeling. A nontraditional mechanism concerning the acoustic radiation from a propeller at angle of attack was investigated. Predictions made using this approach show results that are in much closer agreement with measurement over a range of operating conditions than those obtained via traditional fluctuating force methods. The isolated rotors and installation effects models were combined into a single prediction program. The results were compared with data taken during the flight test of the B727/UDF (trademark) engine demonstrator aircraft. Author

N92-31454# General Accounting Office, Washington, DC. Resources, Community, and Economic Development Div.
AVIATION NOISE: COSTS OF PHASING OUT NOISY AIRCRAFT
Jul. 1991 58 p
(GAO/RCED-91-128; B-239410) Avail: CASI HC A04/MF A01; GAO, PO Box 6015, Gaithersburg, MD 20877 HC

In Sept. 1990 this group testified on the costs of phasing out older, relatively noisy aircraft and on how these costs would be affected by the independent adoption of noise restrictions by airports. In Nov. 1990 the Airport Noise and Capacity Act of 1990 was enacted. This act phased out the noisiest jets currently in use by the year 2000 and limits the discretion of airports to adopt their own noise restrictions. This report briefly describes the likely effects of this Act on the costs to the airline industry of aviation noise restrictions. H.A.

N92-31563# Woods Hole Oceanographic Inst., MA.
A DATA PROCESSING MODULE FOR ACOUSTIC DOPPLER CURRENT METERS
Albert J. Plueddemann, Andrea L. Olen, Robin C. Singer, and Stephen P. Smith Jan. 1992 72 p
(Contract N00014-89-J-1288)
(AD-A250901; WHOI-92-05) Avail: CASI HC A04/MF A01

This report describes the development of a Data Processing Module (DPM) designed for use with an RD Instruments Acoustic Doppler Current Meter (ADCM). The DPM is a self-powered unit in its own pressure case and its use requires no modification to the current meter. The motivation for this work was the desire for real-time monitoring and data transmission from an ADCM deployed at a remote site. The DPM serves as an interface between the ADCM and a satellite telemetry package consisting of a controller, an Argos Platform Transmit Terminal, and an antenna. The DPM accepts the data stream from the ADCM, processes the data, and sends out the processed data upon request from the telemetry controller. The output of the ADCM is processed by eliminating unnecessary data, combining quality control information into a small number of summary parameters, and averaging the remaining data in depth and time. For the implementation described here, eight data records of 719 bytes each (output from the ADCM at 15 minute intervals) were processed and averaged over 2 hr intervals to produce a 34 byte output array. GRA

N92-31588# Colorado Univ., Boulder. Dept. of Mechanical Engineering.
ADVANCED DAA METHODS FOR SHOCK RESPONSE ANALYSIS Technical Report, 1 Jun. 1988 - 31 Mar. 1991
Thomas L. Geers, Peizhen Zhang, and Brett A. Lewis 1 Jul. 1992 116 p
(Contract DNA001-88-C-0057)
(AD-A252696; DNA-TR-91-69) Avail: CASI HC A06/MF A02

Doubly asymptotic approximations (DAA's) are approximate contact-surface relations for the dynamic interaction between a body and an adjacent medium. In this report, first- and second-order DAA's are formulated for an internal acoustic domain, and a first-order DAA is formulated and implemented in boundary-element form for a semi-infinite elastic domain. The new DAA's constitute extensions of DAA's previously formulated and implemented for external acoustic and infinite elastic domains. The accuracy of the internal DAA's is evaluated by comparing DAA and exact solutions for a canonical problem, namely, the excitation of a fluid-filled spherical shell submerged in an infinite acoustic medium by a plane step-wave; in this evaluation, the second-order DAA exhibits satisfactory accuracy. A preliminary evaluation of the first-order DAA for a semi-infinite elastic medium is conducted by comparing boundary-element DAA results with results in the literature for a suddenly pressurized spherical cavity; marginal accuracy is observed. GRA

N92-31672# Naval Postgraduate School, Monterey, CA. Dept. of Oceanography.
COMPUTER SIMULATION OF ACOUSTIC FLUCTUATIONS DUE TO FINESCALE TEMPERATURE PERTURBATIONS MEASURED BY THERMISTOR CHAIN M.S. Thesis
Gregory D. Crabtree Mar. 1992 56 p
(AD-A252709) Avail: CASI HC A04/MF A01

Finescale temperature features in the oceanic mixed layer (OML) modify acoustic propagation by perturbing the index of refraction. A thermistor chain measures temperature from the surface to 250 m with 2 m vertical resolution and 1.85 m horizontal resolution. Thermistor data is converted to high resolution sound velocity profiles for input to an implicit finite difference parabolic equation (IFD-PE) model. The control case is a surface duct with a horizontally averaged sound velocity profile. The IFD-PE model is run with monofrequency sources from 500 Hz to 10 kHz. The acoustic fluctuations and average acoustic pressure are computed each 20 km to a range of 100 km. Acoustic propagation through the temperature varying OML is contrasted with acoustic propagation through the temperature invariant OML. Finescale temperature randomly alters the average acoustic pressure by up to a factor of two and the acoustic fluctuations by up to a factor of five. GRA

N92-31789# Naval Undersea Warfare Center, New London, CT. Submarine Sonar Dept.
NEAR-FIELD AND FAR-FIELD SOUND RADIATION FROM A LINE-DRIVEN FLUID-LOADED INFINITE FLAT PLATE HAVING PERIODIC AND NON-PERIODIC ATTACHED RIB STIFFENERS Ph.D. Thesis - North Carolina State Univ. Final Report
Benjamin A. Cray 4 Mar. 1992 134 p
(AD-A250100; NUWC-NL-TD-10023) Avail: CASI HC A07/MF A02

The far-field and near-field solutions for the radiated acoustic pressure from a line-driven fluid-loaded, rib-stiffened thin elastic plate have been obtained. The plate has been configured to have two sets of rib-stiffeners, though the formulation given may be extended to include additional rib-stiffener sets. The stiffeners composing a given set are identical and are spaced periodically with distance l. However, one set of stiffeners is shifted by an amount from the other set. In this manner, portions of the plate may be configured with repeating sections having non-periodic rib spacing. The stiffeners exert reactive forces upon the plate, but not angular moments. Fluid loading is included on the upper surface of the plate while the lower surface is unloaded, except for a time harmonic line force applied normal to the lower surface. Expressions are derived, for the special case of periodic inter-rib spacing, which give the wavenumbers at which the magnitude of the wavenumber response obtains relative maximum and minimum values. For a stiffened plate, it is seen that excitation frequencies below coincidence generate large magnitude supersonic wavenumber components. GRA

N92-31818# Naval Research Lab., Washington, DC.
THE KRAKEN NORMAL MODE PROGRAM
M. B. Porter 22 May 1992 99 p
(DA Proj. RJ1-4-C-02)
(AD-A252409; NRL/MR/5120-92-6920) Avail: CASI HC A05/MF A01

In the late 1970's, several normal-mode models existed which were widely used for predicting acoustic transmission-loss in the ocean; however, each had its own problems. Typical difficulties included numerical instabilities for certain types of sound-speed profiles and failures to compute a complete set of ocean modes. In short, there was a need for a model that was robust, accurate, and efficient. In order to resolve these problems, a new algorithm was developed forming the basis for the KRAKEN normal mode model. Over subsequent years, KRAKEN was greatly extended, with options for modeling ocean environments that are range-independent, range-dependent, or fully 3-dimensional. The current version offers the specialist a vast number of options for treating ocean-acoustics problems (or more generally acousto-elastic waveguides). On the other hand, it is easy for a less sophisticated user to learn the small subset of tools needed for the common problem of transmission-loss modeling in range-independent ocean environments. This report addresses the need for a more complete user's guide to supplement the on-line help files. The first chapters give a fairly technical description of the mathematical and numerical basis of the model. Additional chapters give a simpler description of its use and installation in a manner that is accessible to less scientifically-oriented readers. GRA

N92-32044# Naval Research Lab., Washington, DC.
AN EMPIRICAL PREDICTION ALGORITHM FOR LOW-FREQUENCY ACOUSTIC SURFACE SCATTERING STRENGTHS Interim Report
Peter M. Ogden and Fred T. Erskine 28 Apr. 1992 19 p
(AD-A250508; NRL/FR/5160-92-9377) Avail: CASI HC A03/MF A01

We propose an algorithm for calculating surface backscattering strength for grazing angles between 0 and 40 degrees, for wind speeds between 0 and 40 knots and for frequencies between 50 and 1000 Hz. The algorithm is based on broadband SUS data collected during the Critical Sea Test series of at-sea experiments. It is intended as a replacement for the Chapman-Harris empirical formula presently used in virtually all low-frequency acoustics reverberation models. The algorithm represents an interim step between the original Chapman-Harris formula and a more detailed description of surface scattering that will take into account a wider variety of environmental factors. GRA

N92-32178*# Piersol Engineering Co., Woodland Hills, CA.
OPTIMUM DATA ANALYSIS PROCEDURES FOR TITAN 4 AND SPACE SHUTTLE PAYLOAD ACOUSTIC MEASUREMENTS DURING LIFT-OFF
Allan G. Piersol 23 Dec. 1991 45 p
(Contract JPL-9950-1365)
(NASA-CR-190479; JPR-584243; NAS 1.26:190479) Avail: CASI HC A03/MF A01

Analytical expressions have been derived to describe the mean square error in the estimation of the maximum rms value computed from a step-wise (or running) time average of a nonstationary random signal. These analytical expressions have been applied to the problem of selecting the optimum averaging times that will minimize the total mean square errors in estimates of the maximum sound pressure levels measured inside the Titan IV payload fairing (PLF) and the Space Shuttle payload bay (PLB) during lift-off. Based on evaluations of typical Titan IV and Space Shuttle launch data, it has been determined that the optimum averaging times for computing the maximum levels are (1) T (sub o) = 1.14 sec for the maximum overall level, and T(sub oi) = 4.88 f (sub i) (exp -0.2) sec for the maximum 1/3 octave band levels inside the Titan IV PLF, and (2) T (sub o) = 1.65 sec for the maximum overall level, and T (sub oi) = 7.10 f (sub i) (exp -0.2) sec for the maximum 1/3 octave band levels inside the Space Shuttle PLB, where f (sub i) is the 1/3 octave band center frequency. However, the results for both vehicles indicate that the total rms error in the maximum level estimates will be within 25 percent the minimum error for all averaging times within plus or minus 50 percent of the optimum averaging time, so a precise selection of the exact optimum averaging time is not critical. Based on these results, linear averaging times (T) are recommended for computing the maximum sound pressure level during lift-off. Author

72 ATOMIC AND MOLECULAR PHYSICS

Includes atomic structure, electron properties, and molecular spectra.

N92-31255# National Inst. for Fusion Science, Nagoya (Japan).
ELECTRON IMPACT EXCITATION OF POSITIVE IONS: PARTIAL WAVE APPROACH IN COULOMB-EIKONAL APPROXIMATION
Wen-Jia Qian (Liaoning Inst. of Metrology, Shenyang, China),

Yun-Bo Duan (Liaoning Inst. of Metrology, Shenyang, China), Rong-Long Wang (Liaoning Inst. of Metrology, Shenyang, China), and H. Narumi (Hiroshima Univ., Japan) Sep. 1991 17 p
(NIFS-106) Avail: CASI HC A03/MF A01

The eikonal partial wave theory for the electron impact excitation of positive ions is formulated firstly and is demonstrated in the 1s to 2s, 2p excitations of hydrogen-like ions. Author

N92-31316# California Univ., Davis. Dept. of Chemistry.
APPLICATION OF THE MEAN SPHERICAL APPROXIMATION TO THE ESTIMATIONS OF SINGLE ION THERMODYNAMIC QUANTITIES OF SOLVATION FOR MONOATOMIC MONOVALENT IONS IN AQUEOUS SOLUTIONS
W. R. Fawcett and Lesser Blum 24 Apr. 1992 14 p
(Contract N00014-90-J-1235)
(AD-A250190; TR-24) Avail: CASI HC A03/MF A01

The expression for the Gibbs energy of solvation for simple 1-1 electrolytes within the mean spherical approximation has been fitted to data for 20 alkali metal halides in water. In performing this fit, one needs to assume a radius for each ion, the Pauling values often having been chosen in the past. The MSA parameters appear as corrections to these radii and are different for cations and anions. Two sets of ionic radii were considered, the Pauling values from crystallographic data and values based on x-ray diffraction results obtained in aqueous solutions. Excellent fits between theory and experiment were obtained, the results with the latter set of radii being preferred. This analysis provides an extrathermodynamic route to single ion solvation free energies and yields results which are very close to the real free energy of solvation measured by Randles. GRA

N92-31328# California Univ., Davis. Dept. of Chemistry.
THE ROLE OF METAL STRUCTURE IN DETERMINING SOLVENT ORIENTATION AT THE ELECTRODE/SOLUTION INTERFACE
W. R. Fawcett 24 Apr. 1992 4 p
(Contract N00014-90-J-1235)
(AD-A249751; CU-TR-26) Avail: CASI HC A01/MF A01

The role of molecular packing on the dielectric properties of a solvent monolayer at a polarizable interface is examined for a hexagonally close packed system and a less well packed square lattice. Dipole-dipole interactions within the monolayer are considered both perpendicular and parallel to the geometrical electrode/solution interface. In both systems, dipoles with their vectors parallel to the interface predominate near the point of zero charge on the metal. As the charge on the metal increases, a capacity peak is observed whose value is much larger for the hexagonal lattice than the square one. Comparison with experimental data for single crystal silver electrodes demonstrates that the differences observed between capacity data on different low index faces cannot be due to differences in solvent molecule packing, but instead can be attributed to the presence of chemisorbed solvent molecules. GRA

N92-31385# San Francisco State Univ., CA.
RESEARCH IN ELEMENTARY PARTICLE PHYSICS
R. W. Bland and J. Greensite 1992 53 p
(Contract DE-AC03-81ER-40009)
(DE92-014585; DOE/ER-40009/T3) Avail: CASI HC A04/MF A01

Research in the area of elementary particle physics, using cryogenic particle detectors, is discussed. We have developed superconducting aluminum tunnel-junction detectors sensitive to a variety of particle signals. The detectors have potential applications in a number of particle-physics problems. We have extended our range of technologies in the areas of niobium tri-layer junctions and high-(Tc) superconducting bolometers. We have new data on response to low-energy x-rays and to alpha-particle signals from large-volume detectors. Our theoretical work is a continued investigation of nonperturbative aspects of quantum gravity. A Monte Carlo calculation is proposed for Euclidian quantum gravity, based on the 'fifth-time action' stabilization procedure. Results from the last year include a set of seven papers, summarized below, that address various aspects of nonperturbative quantum gravity and QCD. Among the issues addressed is the so-called 'problem of time' in canonical quantum gravity. DOE

N92-31386# Argonne National Lab., IL.
DEPENDENCE OF SECONDARY ION EMISSION FROM ORGANIC MATERIAL ON THE ENERGY LOSS OF THE IMPACTING HEAVY ION
J. E. Hunt and K. Wien (Technische Hochschule, Darmstadt, Germany, F.R.) 1991 16 p Presented at the Latin American School of Physics, Caxambu (Brazil), 4-24 Aug. 1991
(Contract W-31-109-eng-38)
(DE92-014845; ANL/CP-76036; CONF-9108199-1) Avail: CASI HC A03/MF A01

Samples of the amino acid valine were irradiated by 2.5 MeV-Ar, 0.8 MeV-Kr, and 1.0 MeV-Xe beams from the Argonne Dynamitron accelerator in order to study the energy distributions of ejected secondary ions. For Kr and Xe, the nuclear stopping power exceeded the electronic stopping power by a factor 2 or 3, respectively, but the functional shape of the energy distributions and the mean ejection energies (0.9-1.4 eV) indicated that the molecular ions (M +/- H)(+/-) are desorbed by an electronic sputter process. Contributions of atomic collision cascades were observed for the H(-) ion. In the second part of the article, the overall dependence of molecular ion yields on the electronic energy loss is discussed in the framework of recent desorption models and the structure of the nuclear track. DOE

N92-31463# Wisconsin Univ., Madison. Dept. of Chemistry.
THE PATHWAYS AND DYNAMICS OF MOLECULAR DECOMPOSITION Final Report, 1 Aug. 1988 - 31 Oct. 1991
F. F. Crim 12 Dec. 1991 25 p
(Contract DAAL03-88-K-0189)
(AD-A249627; ARO-26049.2-CH) Avail: CASI HC A03/MF A01

Molecular decompositions often control complex chemical reactions by producing a highly reactive fragment that determines the subsequent chemistry. Despite the importance of such processes, there is little detailed information available for testing theoretical models and guiding the analysis of practical systems. This report describes experiments that produce, characterize, and dissociate highly energized molecules in order to uncover the details of molecular decomposition. These experiments create highly energized molecules either by vibrational overtone excitation or electronic excitation and detect the products either by a state-resolved laser detection technique, such as laser induced fluorescence, or by energy-selective ionization using vacuum ultraviolet photons. The state-resolved measurements probe the decomposition dynamics by determining the quantum state populations in the products and their appearance rates. These data provide a particularly good point of comparison with theoretical models and are a test of the applicability of statistical theories. The energy-selective ionization studies can also provide rate information but are most valuable as a means of identifying the primary dissociation products and their recoil energies. The use of vacuum ultraviolet photons makes our apparatus very sensitive. We have proven the technique on electronic photodissociation of a series of nitroalkanes and on nitrobenzene. GRA

N92-31552# Florida Univ., Gainesville. Dept. of Physics.
A TUMBLING TOP-QUARK CONDENSATE MODEL
S. P. Martin 1992 16 p
(Contract DE-FG05-86ER-40272)
(DE92-016194; DOE/ER-40272/T1; UFIFT-HEP-92-07) Avail: CASI HC A03/MF A01

We propose a renormalizable model with no fundamental scalars which breaks itself in the manner of a 'tumbling' gauge theory down to the standard model with a top-quark condensate. Because of anomaly cancellation requirements, this model contains two color sextet fermions (quixes), which are vector-like with respect to the standard model gauge group. The model also has a large number of pseudo-Nambu-Goldstone bosons, some of which can be light. The top-quark condensate is responsible for breaking the electroweak gauge symmetry and gives the top quark

a large mass. We discuss the qualitative features and instructive shortcomings of the model in its present form. We also show that this model can be naturally embedded into an aesthetically pleasing model in which the standard model fermion appears symmetrically. DOE

N92-31595# Argonne National Lab., IL.
EDGE-ON ION IRRADIATION OF ELECTRON MICROSCOPE SPECIMENS
M. P. Otero (Fundacao de Technologia Industrial, Rio de Janeiro, Brazil) and C. W. Allen 1992 7 p Presented at the Material Research Society Spring Meeting, San Francisco, CA, 27 Apr. - 2 May 1992
(Contract W-31-109-eng-38)
(DE92-014847; ANL/CP-74821; CONF-920402-25) Avail: CASI HC A02/MF A01

A special technique is described for in situ transmission electron microscope (TEM) experiments involving simultaneous ion irradiation, in which the resultant phenomena are observed as in a cross-section TEM specimen. That is, instead of ion-irradiating the film or foil specimen normal to the major surfaces and observing in plan view (i.e., in the same direction), the specimen is irradiated edge-on (i.e., parallel to the major surfaces) and is observed normal to the depth direction with respect to the irradiation. The results of amorphization of Si, irradiated in this orientation by 1 or 1.5 MeV Kr, are presented and briefly compared with the usual plan view observations. The limitations of the technique are discussed and several experiments which might profitably employ this technique are suggested. DOE

N92-31606# Aerospace Corp., El Segundo, CA. Engineering and Technology Group.
EXPERIMENTAL AND COMPUTER MODELING STUDIES OF ISOTOPICALLY SELECTIVE TWO-STEP LASER PHOTODISSOCIATION OF SMALL MOLECULES
P. F. Zittel 25 Mar. 1992 25 p
(Contract DE-FG03-87ER-13657)
(DE92-011427; DOE/ER-13657/T1) Avail: CASI HC A03/MF A01

The approach to laser isotope separation taken in this study is based on isotopically selective, two-step, laser photodissociation of small molecules. A primary goal of this study is the measurement of fundamental molecular processes which control the two-step, photodissociative isotope enrichment process. This objective has led to experimental measurements of uv photodissociation cross sections for vibrationally excited states of several small molecules, including the first cross section reported for any neutral molecule in a specific, excited vibrational state. A second goal of this study has been the laboratory demonstration of isotope enrichment for isotopes of practical interest and for processes with a potential for larger scale production. Where possible, efforts have focussed on the separation of middle isotopes, such as O-17 and S-33, which are expensive and difficult to separate using other techniques. Considerable success has been achieved in demonstrating the enrichment of isotopes of bromine, carbon, oxygen, and a third goal of this study has been the application of computer modeling to the two-step enrichment process. Experimental measurements define as many as possible of the critical photophysical and chemical parameters required by an ab initio computer model of the enrichment process. Progress toward these goals has been documented in detail in a variety of journal articles and technical reports. It is not the objective of this final report to discuss each aspect of the work done under this contract/grant in detail. A general overview of the program, touches briefly on each of the problems addressed by the study and provides references to more detailed discussions. DOE

N92-31673# Air Force Inst. of Tech., Wright-Patterson AFB, OH.
MANY BODY PERTURBATION THEORY USING A RESTRICTED OPEN-SHELL HARTREE-FOCK (ROHF) REFERENCE FUNCTION Ph.D. Thesis
Walter J. Lauderdale 1991 137 p
(AD-A249725; AFIT/CI/CIA-91-028D) Avail: CASI HC A07/MF A02

One of the most common reference functions used for open shell molecules is the unrestricted Hartree-Fock (UHF) reference. While this reference is useful for many molecular systems, it can sometimes suffer from the mixing of high multiplicity states into the state of interest. This phenomenon is termed spin contamination. A number of projection techniques have been developed to correct the UHF reference at the SCF and correlated levels. General implementation of gradients for these projected methods, however, can be complex and computationally expensive. Nor are such methods rigorously extensive, as required for many-electron methods. These facts limit the usefulness of these methods. This work presents the development of an alternative approach. Rather than attempting to correct the deficiencies in the UHF reference, we start with a reference (ROHF) which is an eigenfunction of spin. The treatment of electron correlation is introduced using many body perturbation theory (MBPT), which is perhaps the most efficient way of adding the critical effects of electron correlation. GRA

N92-31679# Oak Ridge National Lab., TN.
COMPARISON OF DOUBLE AND SINGLE IONIZATION IN He BY PHOTONS AND BY CHARGED PROJECTILES
I. Sellin (Tennessee Univ., Knoxville.), J. Levin (Tennessee Univ., Knoxville.), R. Miller (Tennessee Univ., Knoxville.), N. Keller (Tennessee Univ., Knoxville.), Y. Azuma (Argonne National Lab., IL.), H. G. Berry (Argonne National Lab., IL.), and N. Berrah-Mansour (University of Western Michigan, Kalamazoo.) 1992 11 p Presented at the Spring-8 Workshop on Atomic Physics at High Brilliance, Himejii (Japan), 23-24 Mar. 1992
(Contracts DE-AC05-84OR-21400; W-31-109-eng-38; DE-AC02-76CH-00016)
(DE92-013411; CONF-9203146-1) Avail: CASI HC A03/MF A01

Recognizing that the term 'electron correlation' is a subject of central interest in current discussions of both photoionization and atomic collision physics, we adopt here the simplified definitions used by James McGuire in his recent article in Adv. At. Mol. Opt. Physics: (1) any effect arising from the Coulomb interaction between electrons; (2) any deviation of the electronic wave function from a product of single-particle orbitals. Within these definitions, double photoionization in He is exclusively attributable to electron correlation, since a single photon interacts with only one target electron. It is interesting to compare single and double photoionization cross sections with corresponding charged particle interaction cross sections. In the limit of high photon energies and projectile particle energies, the native expectation is that apart from kinematic factors the single ionization cross sections for particles and photons converge to the same values. Because of its specific sensitivity to electron correlation in double ionization, and because common factors drop out, it has become customary to compare the ratio of the double to single ionization cross sections rather than the raw cross sections themselves. Yet this ratio has been found experimentally to lie in the range R(h(nu)) = 4 to 5 percent in the photon energy range from 100 to 600 eV, and R (protons, antiprotons, electrons) in the range 0.2 to 0.4 percent in the corresponding limit for high velocity charged particles. These values are more than an order of magnitude different. DOE

N92-31700# Oak Ridge National Lab., TN.
TEMPERATURE-ENHANCED AUTODETACHMENT FROM LONG-LIVED PARENT NEGATIVE IONS OF GASEOUS DIELECTRICS
P. G. Datskos (Tennessee Univ., Knoxville.), L. G. Christophorou (Tennessee Univ., Knoxville.), and J. G. Carter (Tennessee Univ., Knoxville.) 1992 12 p Presented at the 10th International Conference on Gas Discharges and Their Applications, Swansea, England, 13-18 Sep. 1992
(Contract DE-AC05-84OR-21400)
(DE92-011108; CONF-920939-1) Avail: CASI HC A03/MF A01

At ambient temperature, T, a number of excellent gas dielectrics

attach electrons nondissociatively producing long-lived (autodetachment lifetime greater than 10(exp -6) s) parent anions. As T is increased above ambient, the dielectric strength of such gas dielectrics was found to decrease. This was attributed to the decrease in stable anion formation with increasing temperature. In this paper, we report on the effect of T on both the electron attachment and the autodetachment processes in gas dielectrics, which at low energies (less than 1 eV) attach electrons predominantly nondissociatively. The reduction in stable parent anion formation at elevated T is principally due to the large increase in autodetachment with increasing T. Results are presented with specific reference to perfluorobutene. The enhanced autodetachment at high T is expected to influence other dielectric gas properties as unstable parent anions become sources of electrons at T above ambient. DOE

N92-31705# Lawrence Livermore National Lab., CA.
PHOTON AND ELECTRON DATA BASES AND THEIR USE IN RADIATION TRANSPORT CALCULATIONS
D. E. Cullen, S. T. Perkins, and S. M. Seltzer (National Inst. of Standards and Technology, Gaithersburg, MD.) Feb. 1992 8 p Presented at the 2nd Topical Meeting on Industrial Radiation and Radioisotope Measurement Applications, Raleigh, NC, 8-11 Sep. 1992
(Contract W-7405-eng-48)
(DE92-011458; UCRL-JC-109763; CONF-920919-1) Avail: CASI HC A02/MF A01

The ENDF/B-VI photon interaction library includes data to describe the interaction of photons with the elements Z = 1 to 100 over the energy range 10 eV to 100 MeV. This library has been designed to meet the traditional needs of users to model the interaction and transport of primary photons. However, this library contains additional information which used in a combination with our other data libraries can be used to perform much more detailed calculations, e.g., emission of secondary fluorescence photons. This paper describes both traditional and more detailed uses of this library. DOE

N92-31721# Louisiana State Univ., Baton Rouge. Dept. of Physics and Astronomy.
THE STRUCTURE OF NUCLEI FAR FROM BETA STABILITY
E. F. Zganjar 1992 26 p
(Contract DE-FG05-84ER-40159)
(DE92-012598; DOE/ER-40159/182) Avail: CASI HC A03/MF A01

This report discusses shape coexistence and intruder states; the electric monopole transition in nuclei; gold isotopes; platinum isotopes; iridium isotopes; search for superdeformation in Hg-192; search for population of superformed states in Pb-194 using Bi-194 beta (sup +)-decay; detailed nuclear structure studies far from stability; prototype internal pair spectrometer; and picosecond lifetime spectrometer. DOE

N92-31724# Rice Univ., Houston, TX.
THEORETICAL ATOMIC COLLISION PHYSICS
N. F. Lane Mar. 1992 3 p
(Contract DE-FG05-87ER-13751)
(DE92-013571; DOE/ER-13751/5) Avail: CASI HC A01/MF A01

The current focus of the research is low-energy (collision v is less than bound v(sub e)) inelastic collisions for selected systems that possess the characteristic that many intermediate states are strongly coupled, such as can occur in classes of excited-atom (including Rydberg atom) collisions with atoms, molecules and positive and negative ions. We are interested in the dependence of various differential and total cross sections on the angular momentum of the initial excited state and on the alignment of the initial electron charge distribution (for non-spherical initially excited states). We wish to understand how characteristics of the classical trajectories (in CTMC calculations), e.g. multiple encounters, quasi-periodicity, and chaos, relate to characteristics of the probability (scattering) amplitudes obtained from semiclassical (quantum mechanical) treatments. In particular, in order to investigate a range of 'interaction regimes', we have proposed to study low-Rydberg-atom collisions with the following: ions and polar molecules (long range interaction); non-polar molecules and atoms (short-range interaction); and electron-attaching atoms/molecules (transient electron capture possible). We plan to look for observable signatures of possibly novel intracollisional interference effects and quasi-vibrational resonance effects that may occur in low-Rydberg collisions. DOE

N92-31728# Kyoto Univ., Kumatori (Japan). Research Reactor Inst.
PROCEEDINGS OF THE 2ND KUR SYMPOSIUM ON HYPERFINE INTERACTIONS
M. Mekata, ed. (Fukui Univ., Japan), T. Minamisono, ed., and Y. Kawase, ed. Oct. 1991 95 p Presented at the 2nd KUR Symposium on Hyperfine Interactions, Kumatori (Japan), 29-31 Jul. 1991
(DE92-789024; KURRI-TR-358; CONF-9107216) Avail: CASI HC A05/MF A01

Hyperfine interactions between a nuclear spin and an electronic spin discovered from hyperfine splitting in atomic optical spectra have been utilized not only for the determination of nuclear parameters in nuclear physics but also for novel experimental techniques in many fields such as solid state physics, chemistry, biology, mineralogy, and for diagnostic methods in medical science. Experimental techniques based on hyperfine interactions yield information about microscopic states of matter so that they are important in material science. Probes for material research using hyperfine interactions have been nuclei in the ground state and radioactive isotopes prepared with nuclear reactors or particle accelerators. But the use of muons generated from accelerators is growing. Such wide spread application of hyperfine interaction techniques gives rise to some difficulty in collaboration among various research fields. This report summarizes the KUR symposium in the hope that this information will help to alleviate the problem. DOE

N92-31765# Los Alamos National Lab., NM.
PROBLEMS IN NEUTRINO ELECTRON SCATTERING WITH 1-GeV NEUTRINOS
D. H. White 1992 6 p Presented at the TRIUMF Neutrino Workshop, Lake Louise (Canada), 18-21 Feb. 1992
(Contract W-7405-eng-36)
(DE92-013535; LA-UR-92-1302; CONF-9202106-1) Avail: CASI HC A02/MF A01

Neutrino physics has often been limited by lack of events. This limitation has been not so much for events in total, but for events in selected channels. The basic strategy for dealing with this issue has been to build massive detectors in which target and event detection have been combined. This strategy has been very successful, but it does carry the difficulty that, given a large detector mass, financial limitations apply to the detail with which events may be detected and reconstructed. At KAON, some of these difficulties will be alleviated by the increase in neutrino flux, which may make the construction of smaller and more specialized detectors feasible. At the Lake Louise workshop, a great deal of interest was expressed in neutrino electron scattering; we shall describe here the limitations of the BNL detector as they emerged in the measurement of sin(exp 2)(theta)(sub w) at BNL. In this context, the knowledge of the beam was an intrinsic part of this experimental systematic error. We start with a description of the beam. DOE

N92-31812# Oregon Univ., Eugene. Inst. of Theoretical Science.
PARTICLE PHYSICS CONFRONTS THE SOLAR NEUTRINO PROBLEM
P. B. Pal Jun. 1991 82 p
(Contract DE-FG06-85ER-40224)
(DE92-014013; DOE/ER-40224/205; OITS-470) Avail: CASI HC A05/MF A01

This review has four parts. In Part 1, we describe the reactions that produce neutrinos in the sun and the expected flux of those

neutrinos on the earth. We then discuss the detection of these neutrinos, and how the results obtained differ from the theoretical expectations, leading to what is known as the solar neutrino problem. In Part 2, we show how neutrino oscillations can provide a solution to the solar neutrino problem. This includes vacuum oscillations, as well as matter enhanced oscillations. In Part 3, we discuss the possibility of time variation of the neutrino flux and how a magnetic moment of the neutrino can solve the problem. We also discuss particle physics models which can give rise to the required values of magnetic moments. In Part 4, we present some concluding remarks and an outlook for the near future.
DOE

N92-31814# Nationaal Inst. voor Kernfysica en Hoge Energiefysica, Amsterdam (Netherlands).
EFFICIENCY CALCULATIONS OF THE HADRON DETECTOR
Paul vonSpreckelsen Nov. 1991 21 p
(NIKHEF-K-EMIN-92-01; ETN-92-91738) Avail: CASI HC A03/MF A01

Two plastic scintillator detectors (hadron detectors), box 1 and box 2, were developed for (electron, positron proton proton) reactions. The hadron detectors were designed to detect protons emitted in the energy range of 25 to 158 MeV and 37 to 198 MeV, respectively. The layout of the detector and its dimensions are described. The calculation of the efficiency of each element of one of the detectors is described. Tests performed to check the calculation method are presented. Conclusions on the efficiency are given.
ESA

N92-31836# International Centre for Theoretical Physics, Trieste (Italy).
RIGID ROTATIONS IN TWO-ELECTRON ATOMS IN A UNIFORM MAGNETIC FIELD
J. MahechaG Dec. 1991 37 p
(DE92-624981; LAMP-91/10) Avail: CASI HC A03/MF A01

Two exact rigid body solutions for a rotating two-electron atom under the influence of a magnetic field directed along the rotation axis were obtained using a classical approach. A solution gives at zero field the same result previously known as a rigid rotor. The other solution at zero field gives the previous result known as an asymmetric top or Langmuir solution. A stability analysis of the linearized motions near each of these equilibrium motions was made for different values of the magnetic field intensity. It was found that they are unstable but can exist during certain times for certain combinations of the magnetic field intensity and the angular momentum. The experimental realization of these classical states are the resonant states which would manifest in the spectrum as a subset of the quasi-Landau resonances. An examination of the energy levels near the ionization threshold shows that, in fact, they are similar to the quasi-Landau resonances. Also analytical expressions for the diamagnetic susceptibility of the two-excited states reported in this work were found. For the purpose of comparison, a study of the classical diamagnetism in one-electron atoms is presented.
DOE

N92-31837# Flinders Univ., Adelaide (Australia). Electronic Structure of Materials Centre.
ELECTRON SCATTERING BY ATOMIC HYDROGEN: ELASTIC AND INELASTIC PHENOMENA AT 13.9 TO 200 eV
Igor Bray, D. A. Konovalov, and I. E. McCarthy Jun. 1991 27 p
(DE92-625004; ESM-31) Avail: CASI HC A03/MF A01

A six state coupled-channel optical potential method for electron-atom scattering is applied to electron-hydrogen scattering at energies of 13.87, 16.46, 19.58, 35, 40, 54.4, 100, and 200 eV. The n = 1, 2, and 3 channels are coupled explicitly whereas the rest of the excited states of the atom including the continuum are taken into account via the 'ab initio' complex non-local polarization potential. The differential and integrated cross sections, as well as the exchange asymmetries for n = 1 and 2 channels, the total cross section, and the lambda, R, and I parameters for the 2p excitation are presented at each energy. The ratio of differential cross sections for n = 1 to n = 2, and for 2s to 2p, and the 2s + 2p differential cross sections are found to be in good agreement with experiment. There are still some discrepancies between experiment and theory for the 2p angular correlation parameters lambda, R, and I.
DOE

N92-31858# Florida Univ., Gainesville.
MOLECULAR INTERACTIONS AND PROPERTIES WITH MANY-BODY METHODS Annual Technical Report, 1 Dec. 1990 - 30 Nov. 1991
Rodney J. Bartlett 21 Jan. 1992 7 p
(Grant AF-AFOSR-0079-90)
(AD-A247052; AFOSR-92-0126TR) Avail: CASI HC A02/MF A01

The crucial component needed to understand molecular reactions is the potential energy surfaces (PES) that serve to describe the attractions among the atoms and molecules. However, such information is not easy to obtain. In many cases, the most direct approach to obtaining accurate potential surfaces for molecules, and detailed information about their excited states, vibrational spectra, and a wealth of other quantities, is high level ab initio solutions of the Schrodinger equation. However, more so than in most other areas, the ability to provide reliable quantum mechanical results for increasingly large molecules depends critically on improved method development. Whereas supercomputers can enable us to make much larger computations with old methods, the simultaneous development of new methods can increase computational capability by further orders of magnitude. In this regard, many-body perturbation theory (MBPT) and its infinite-order extensions termed coupled-cluster (CC) methods offer a number of attractive features that the more traditional configuration interaction approaches lack. Under AFOSR support, we have established these CC/MBPT theories as being among the most accurate available, and have developed very efficient and generally applicable computer programs to perform CC/MBPT calculations. Also, we have employed these methods for the first time in large-scale ab initio calculations of potential energy surfaces.
GRA

N92-31904# Gosudarstvennyi Komitet po Ispolzovaniyu Atomnoi Energii, Obninsk (USSR). Fiziko-Ehnergeticheskij Inst.
RESOLUTION FUNCTION OF AN INELASTIC SCATTERING SPECTROMETER WITH A PULSED NEUTRON SOURCE
A. I. Stupak 1991 27 p In RUSSIAN
(DE92-620889; FEI-2187) Avail: CASI HC A03/MF A01

The relationships for the resolution function calculation of an inelastic scattering spectrometer with a pulsed neutron source have been obtained. The calculated and experimental spectra of the elastic scattering on the vanadium sample are shown.
DOE

N92-31923# Oak Ridge National Lab., TN.
ALTERATIONS OF MULTIPHOTON-RESONANT PROCESSES THROUGH WAVE-MIXING EFFECTS
W. R. Garrett 1992 8 p Presented at the 6th International Symposium on Resonance Ionization Spectroscopy and its Applications, Santa Fe, NM, 24-29 May 1992
(Contract DE-AC05-84OR-21400)
(DE92-016164; CONF-920574-7) Avail: CASI HC A02/MF A01

A number of the manifestations of quantum interference effects on resonant multiphoton excitation processes are described. Examples of observations and predictions involving simple systems are summarized and discussed in the context of analytical applications.
DOE

N92-31926# Pittsburgh Univ., PA. Dept. of Physics and Astronomy.
EXPERIMENTAL PARTICLE PHYSICS AT THE UNIVERSITY OF PITTSBURGH
W. E. Cleland, E. Engels, Jr., T. J. Humanic, U. Perera, P. F. Shepard, and J. A. Thompson May 1992 29 p
(Contract DE-AC02-80ER-10667)
(DE92-016182; DOE/ER-10667/11) Avail: CASI HC A03/MF A01

The University of Pittsburgh High Energy Physics Group was

begun in 1970 under a National Science Foundation Science Development Grant, and NSF support of the research activities of this group was provided during the period 1972 through 1981. The activities supported by the contract, completed or continuing on beyond the contract, have included both instrumentation development and high energy physics experiments. Instrumentation development has included an optical trigger processor, a silicon microstrip detector system, silicon drift chamber development, and SSC ionization calorimetry and trigger strategy studies. Experiments supported by the contract that have been completed or are still in progress are: (1) axial field spectrometer experiment at CERN; (2) HELIOS experiment NA34 at the CERN SPS; (3) Novosibirsk Phi Factory; (4) BNL experiment E865 -- rare kaon decays; (5) Fermilab E706 -- direct photon production in Hadron-Hadron collisions; (6) Fermilab CDF -- physics at 2 TeV; and (7) search for fractionally charged particles in semiconductors. DOE

N92-31927# Maryland Univ., College Park. Dept. of Physics.
THEORETICAL STUDIES IN NUCLEAR REACTIONS AND NUCLEAR STRUCTURE
May 1992 72 p
(Contract DE-FG05-87ER-40322)
(DE92-016204; DOE/ER-40322/165) Avail: CASI HC A04/MF A01

Research in the Maryland Nuclear Theory Group focusses on problems in four basic areas of current relevance: hadrons in nuclear matter; the structure of hadrons; relativistic nuclear physics and heavy ion dynamics; and related processes. The section on hadrons in nuclear matter groups together research items which are aimed at exploring ways in which the properties of nucleons and the mesons which play a role in the nuclear force are modified in the nuclear medium. A very interesting result has been the finding that QCD sum rules supply a new insight into the decrease of the nucleon's mass in the nuclear medium. The quark condensate, which characterizes spontaneous chiral symmetry breaking of the late QCD vacuum, decreases in nuclear matter and this is responsible for the decrease of the nucleon's mass. The section on the structure of hadrons contains progress reports on our research aimed at understanding the structure of the nucleon. Widely different approaches are being studied, e.g., lattice gauge calculations, QCD sum rules, quark-meson models with confinement and other hedgehog models. A major goal of this type of research is to develop appropriate links between nuclear physics and QCD. The section on relativistic nuclear physics represents our continuing interest in developing an appropriate relativistic framework for nuclear dynamics. A Lorentz-invariant description of the nuclear force suggests a similar decrease of the nucleon's mass in the nuclear medium as has been found from QCD sum rules. Work in progress extends previous successes in elastic scattering to inelastic scattering of protons by nuclei. The section on heavy ion dynamics and related processes reports on research into the e(+) e(-) problem and heavy ion dynamics. DOE

N92-31936# Arizona State Univ., Tempe. Dept. of Mechanical and Aerospace Engineering.
PARTICLE DIAGNOSTICS IN OPTICALLY THICK SPRAYS
Final Report, 15 Aug. 1990 - 29 Feb. 1992
E. D. Hirleman and S. B. Kenney 5 Feb. 1992 49 p
(Grant AF-AFOSR-0358-90)
(AD-A250981; AFOSR-92-0446TR) Avail: CASI HC A03/MF A01

The results of a one-year research effort addressing some fundamental scientific issues relevant to particle diagnostics in optically-thick sprays are presented. The objective of this research effort involved development and application of an experimental apparatus for studying scattering in optically thick media. The important technical contributions of this project included the following: (1) development of a fluidized bed approach for creating controlled optically thick media; and (2) characterization of performance of multi-element detectors and light-valve arrays. With respect to the former, we have developed a binary-particle-phase fluidized bed concept combined with refractive-index matching that will allow the bed to be fluid-dynamically very dense (with interparticle spacings on the order of two diameters as required for stable operation) but optically less thick (with interparticle spacings greater than five diameters where independent, as opposed to dependent, multiple scattering is in effect). Conditions for stable operation of the binaryparticle-phase fluidized bed have been identified. Regarding detector and light-valve arrays, the experimental results indicated that edge effects are important and that current-generation Faraday-effect light valve arrays do not have the performance specifications required for use in multi-angle interrogation schemes for diagnostics in optically thick sprays. GRA

N92-31950# Minnesota Univ., Minneapolis. Dept. of Chemistry.
VIBRATIONAL MODES AND THE DYNAMIC SOLVENT EFFECT IN ELECTRON AND PROTON TRANSFER
Paul F. Barbara, Gilbert C. Walker, and Terrance P. Smith 18 May 1992 8 p
(Contract N00014-89-J-1746)
(AD-A250727; TR-12) Avail: CASI HC A02/MF A01

This article discusses recent work on ultrafast experiments on excited state intramolecular electron and proton transfer, with an emphasis on experiments on chemical systems that have been analyzed theoretically. In particular, those systems that have been quantitatively characterized by static spectroscopy, which provides detailed information about the reaction potential energy surface and about other parameters that are necessary to make a direct comparison to theoretical predictions, are described. GRA

N92-31958 Tel-Aviv Univ. (Israel). Dept. of Physics and Astronomy.
NEUTRON RADIATION DAMAGE TO SILICON DETECTORS
M.S. Thesis
Rafael Darvas Feb. 1991 110 p In HEBREW
(ITN-92-85162) Copyright Avail: Tel-Aviv Univ., Exact Sciences Library, Ramat Aviv, 69978, Israel

Silicon radiation detectors used, e.g., in colliding beam machines and calorimetry, may be exposed to intense neutron irradiation, resulting in crystal defects which form deep energy levels within the band gap. This work emphasized the detection, identification and characterization of such deep energy levels. Theoretical and experimental investigations of the effects of these levels on the capacitance of the detectors were also conducted. Measurements included deep level transient spectroscopy (DLTS) and the dependence of capacitance on temperature (CT) and on frequency (CF), in silicon detectors which had been irradiated with 10(exp 10) to 10(exp 11) neutrons/sq cm, at 14.1 MeV. A theoretical model is presented which predicts that the frequency dependence of the capacitance is determined by the ratio between the frequency and the inverse of the deep level relaxation time, and its temperature dependence is induced by changes in the capture and emission rates and in the space charge. DLTS detected deep levels with energies of 0.17, 0.24, 0.40 and 0.46 eV below the conduction band, which were identified as the oxygen vacancy, the double-charged divacancy, the single-charged vacancy and the phosphorus-vacancy complexes, respectively. CT measurements at 90-320K yielded values for the energies and concentrations of four deep levels which agreed well with the theoretical model and the DLTS measurements. CF measurements revealed no significant frequency dependence of capacitance in the 1 kHz to 1 MHz range. ISA

N92-31999# Minnesota Univ., Minneapolis. Dept. of Chemistry.
ULTRAFAST STUDIES ON ELECTRON TRANSFER IN THE BETAINES: EVIDENCE FOR LOCAL HEATING
Nancy E. Levinger, Alan E. Johnson, Gilbert C. Walker, Eva Akesson, and Paul F. Barbara 18 May 1992 9 p
(Contract N00014-89-J-1746)
(AD-A250728; TR-13) Avail: CASI HC A02/MF A01

We have made ultrafast, time-resolved pump probe measurements on the intramolecular electron transfer (ET) of the betaines, specifically betaine-30 and penta-t-butyl betaine. The data have been analyzed to determine the ET rate in a range of solvent

environments, at various temperatures and at a variety of pump and probe wavelengths. In all cases, the observed ET rate is fast, often faster than predicted by common ET theories. As a result, we have extended some common theories to successfully predict the measured ET rates. In addition to the ET dynamics, the data also display evidence for local heat deposition in the immediate vicinity of the betaine molecule which our extended model qualitatively predicts. GRA

N92-32006# California Univ., Berkeley. Lawrence Berkeley Lab.
IMPLICATIONS OF THE 17 keV NEUTRINO
L. J. Hall Jun. 1991 6 p Presented at the 14th International Warsaw Meeting on Elementary Particle Physics: Puzzles on the Electroweak Scale, Kazimierz (Poland), 27-31 May 1991
(Contract DE-AC03-76SF-00098)
(DE92-017000; LBL-30841; CONF-9105121-2; UCB-PTH-91/28) Avail: CASI HC A02/MF A01

Constraints on the theoretical interpretation of the 17 keV neutrino are reviewed. A simple understanding of the 17 keV neutrino is provided by flavon models, which involve the spontaneous breaking of Abelian lepton symmetries and have only the usual three light neutrino species. Signatures for this class of models include neutrino oscillations, tau decay to an electron and a flavon, and invisible decay modes of the Higgs boson to two flavons. DOE

N92-32007# Syracuse Univ., NY. Dept. of Physics.
FUSION WITH HIGHLY SPIN POLARIZED HD AND D(2)
A. Honig 29 Jun. 1992 16 p
(Contract DE-FG03-91SF-18862)
(DE92-017030; DOE/SF-18862/T1) Avail: CASI HC A03/MF A01

This report discusses the following topics relating to inertial confinement with spin polarized hydrogen targets: low temperature implementation of mating a target to omega; dilution-refrigerator cold-entry and retrieval system; target shell tensile strength characterization at low temperatures; and proton and deuteron spin-lattice relaxation measurements in HD in the millikelvin temperature range. DOE

N92-32024# California Univ., Santa Barbara. Dept. of Chemistry.
NATURE OF SHORT Li-H-C CONTACT INTERACTIONS IN ORGANOLITHIUM COMPOUNDS AND ITS IMPLICATION
Technical Report, 1 Jun. 1991 - 31 May 1992
Juan J. Novoa, Myung-Hwan Whanbo, and Galen D. Stucky 15 May 1992 3 p
(Contract N00014-90-J-1159)
(AD-A250992) Avail: CASI HC A01/MF A01

Our study shows that short Li-H distances of intermolecular Li-H-C contacts occur when the carbon atom bears at least one Li atom. Such an Li-H-C contact interaction is strongly stabilizing, and the associated interaction energy is nearly half the binding energy of an isolated LiH. This finding provides a natural explanation for the observation that solid alkyllithium exists as oligomeric units containing lithium atom clusters, because formation of the lithium atom clusters leads to a large number of strongly stabilizing intermolecular Li-H-C contacts involving the Li-bearing carbon atoms. The present work shows that a C-H bond can be lengthened significantly when it makes several Li-H-C contacts close to right-angle arrangements. GRA

N92-32090# Oak Ridge National Lab., TN.
EXOTIC NUCLEAR SHAPES AND CONFIGURATIONS THAT CAN BE STUDIED AT HIGH SPIN USING RADIOACTIVE ION BEAMS
J. D. Garrett 1992 23 p Presented at the International Workshop on the Physics and Techniques of Secondary Nuclear Beams, Dourdan (France), 23-25 Mar. 1992
(Contract DE-AC05-84OR-21400)
(DE92-016800; CONF-9203164-1) Avail: CASI HC A03/MF A01

The variety of new research possibilities afforded by the culmination of the two frontier areas of nuclear structure: high spin and studies far from nuclear stability (utilizing intense radioactive ion beams) are discussed. Topics presented include new regions of exotic nuclear shape (e.g., superdeformation, hyperdeformation, and reflection-asymmetric shapes); the population of and consequences of populating exotic nuclear configurations; and complete spectroscopy (i.e., the overlap of state of the art low- and high-spin studies in the same nucleus). Likewise, the various beams needed for proton- and neutron-rich high spin studies also are discussed. DOE

N92-32165# Westinghouse Savannah River Co., Aiken, SC.
PROMPT NEUTRON LIFETIME IN A STRONGLY HETEROGENEOUS LATTICE
E. F. Trumble, N. P. Baumann, and W. E. Graves 1991 12 p Presented at the American Nuclear Society (ANS) Topical Meeting on Advances in Reactor Physics, Charleston, SC, 8-11 Mar. 1992
(Contract DE-AC09-89SR-18035)
(DE92-013212; WSRC-MS-91-313; CONF-920308-21) Avail: CASI HC A03/MF A01

The prompt neutron lifetime is an important input parameter to the solution of the point reactor kinetics equations. In the past, many methods of determining the prompt neutron lifetime included the assumption that the thermal neutron lifetime was a good approximation to the prompt neutron lifetime. It has been found that strong heterogeneities within a lattice cause the calculation of the thermal neutron lifetime to significantly overpredict the prompt neutron lifetime. Therefore, a new method for the calculation of the prompt neutron lifetime is presented. This new method, the Alpha Search Method (ASM), is based on the time eigenvalue and does not suffer from the overprediction of the neutron lifetime as approximated by the thermal neutron lifetime. The causes of this overprediction, as well as comparisons of lifetimes computed by the ASM and other methods will be presented. DOE

N92-32167# Fermi National Accelerator Lab., Batavia, IL.
RESONANT ENHANCEMENT OF FLAVOR-CHANGING NEUTRINO INTERACTIONS
E. Roulet Oct. 1991 3 p Presented at the 2nd International Workshop on Theoretical and Phenomenological Aspects of Underground Physics, Toledo (Spain), 9-13 Sep. 1991
(Contract DE-AC02-76CH-03000)
(DE92-013020; FNAL/C-91/295-A; CONF-9109182-2) Avail: CASI HC A01/MF A01

The resonant amplification of neutrino oscillations in the presence of flavor-changing neutrino interactions with matter is analyzed. It is shown that a significant mu-flavor conversion can take place even in the absence of neutrino mixing in vacuum. To account for the solar neutrino deficit, the strength of the new interactions should be approximately 10(sup -2) G(sub F) and the resulting neutrino suppression and spectrum is similar to that in the ordinary MSW effect. Discussed are some extensions of the standard model where these interactions can be present, taking into account the experimental constraints that arise mainly from the induced leptonic rare decays. DOE

N92-32169# Florida Univ., Gainesville. Dept. of Chemistry.
IONIZATION POTENTIALS AND ELECTRON AFFINITIES OF SEMICONDUCTOR CLUSTERS DETERMINED VIA CHARGE TRANSFER REACTIONS
S. H. Bach, J. E. Bruce, R. Ramanathan, C. H. Watson, and J. A. Zimmerman 28 May 1992 17 p
(Contract N00014-87-J-1248)
(AD-A250943; TR-38) Avail: CASI HC A03/MF A01

This chapter summarizes ONR-supported work in Prof. Eyler's laboratories involving small clusters of As, C, and P. Charge transfer bracketing experiments involving cluster ions and neutral molecules of known electron affinities (E.A.) and ionization potential (I.P.) lead to precise estimates of E.A.'s and I.P.'s for the clusters studied. GRA

N92-32196# North Carolina Univ., Chapel Hill. Dept. of Chemistry.
STRUCTURE AND DYNAMICS OF Cl(H2O)20 CLUSTERS. THE EFFECT OF THE POLARIZABILITY AND THE CHARGE OFTHE ION Technical Report, 1 Jul. 1991 - 30 Jun. 1992
L. Perera and M. Berkowitz May 1992 14 p
(Contract N00014-89-J-1169)
(AD-A251094; TR-8) Avail: CASI HC A03/MF A01

The effect of the polarizability and the sign of the ionic charge were studied in Cl(H2O)20 clusters using a molecular dynamics computer simulation technique. From our simulations, we concluded that the reduction in the ionic polarizability did not significantly change the structure and dynamics of Cl7(H2O)20 cluster, but the inversion of the sign of the ionic charge produced a large effect. The energetic considerations helped us to understand why Cl is located on the surface of the cluster. By being on the surface, the anion permits the creation of the hydrogen bonded network between water molecules and that lowers the total energy of the cluster. Simulations with the inverted sign of the ionic charge correspond to that with a hypothetical Cl ion which is similar in size and polarizability to a Cs+ ion. The dynamical structures and the quenched structures of Cl(H2O)20 clusters are compared with the idealized structure of Cs+(H2O)20 cluster proposed recently (A. Selinger and A. W. Castleman, Jr., J. Phys Chem. 95, 8442 (1991)). GRA

73 NUCLEAR AND HIGH-ENERGY PHYSICS

Includes elementary and nuclear particles; and reactor theory.

For space radiation see *93 Space Radiation.*

N92-31325# Air Force Inst. of Tech., Wright-Patterson AFB, OH.
TRANSIENT FISSION GAS BEHAVIOR IN URANIUM NITRIDE FUEL UNDER PROPOSED SPACE APPLICATIONS Ph.D. Thesis
Daniel L. Deforest Dec. 1991 249 p
(AD-A252577; AFIT/CI/CIA-92-001D) Avail: CASI HC A11/MF A01

In order to investigate whether fission gas swelling and release would be significant factors in a space based nuclear reactor operating under the Strategic Defense Initiative (SDI) program, the finite element program REDSTONE (Routine For Evaluating Dynamic Swelling in Transient Operational Nuclear Environments) was developed to model the 1-D, spherical geometry diffusion equations describing transient fission gas behavior in a single uranium nitride fuel grain. The equations characterized individual bubbles, rather than bubble groupings. This limited calculations to those scenarios where low temperatures, low burnups, or both were present. Instabilities in the bubble radii calculations forced the implementation of additional constraints limiting the bubble sizes to minimum and maximum (equilibrium) radii. The validity of REDSTONE calculations were checked against analytical solutions for internal consistency and against experimental studies for agreement with swelling and release results. GRA

N92-31390# Stanford Linear Accelerator Center, CA.
PULSE-BY-PULSE ENERGY MEASUREMENT AT THE STANFORD LINEAR COLLIDER
G. Blaylock (California Univ., Santa Cruz.), D. Briggs, B. Collins, and M. Petree Jan. 1992 24 p Presented at the SEAM 1992: Scientific and Engineering Applications of the Macintosh Technical Conference and Exposition, San Francisco, CA, 15-17 Jan. 1992
(Contract DE-AC03-76SF-00515)
(DE92-011520; SLAC-PUB-5649; CONF-9201101-1) Avail: CASI HC A03/MF A01

The Stanford Linear Collider (SLC) collides a beam of electrons and positrons at 92 GeV. It is the first colliding linac, and produces Z(sup 0) particles for High-Energy Physics measurements. The energy of each beam must be measured to one part in 10(exp 4) on every collision (120 Hz). An Energy Spectrometer in each beam line after the collision produces two stripes of high-energy synchrotron radiation with critical energy of a few MeV. The distance between these two stripes at an imaging plane measures the beam energy. The Wire-Imaging Synchrotron Radiation Detector (WISRD) system comprises a novel detector, data acquisition electronics, readout, and analysis. The detector comprises an array of wires for each synchrotron stripe. The electronics measure secondary emission charge on each wire of each array. A Macintosh II (using THINK C, THINK Class Library) and DSP coprocessor (using ANSI C) acquire and analyze the data, and display and report the results for SLC operation. DOE

N92-31712# Chicago Univ., IL.
THEORETICAL HIGH ENERGY PHYSICS RESEARCH AT THE UNIVERSITY OF CHICAGO, TASK A
J. L. Rosner, E. J. Martinec, and R. G. Sachs Apr. 1992 20 p
(Contract DE-FG02-90ER-40560)
(DE92-016288; DOE/ER-40560/3A) Avail: CASI HC A03/MF A01

This report discusses research conducted at the University of Chicago in theoretical high energy physics. Some of the areas included in this report are: cp violation and cabibbo-kobayashi-maskawa matrix; radiative corrections and electroweak observables; heavy quark symmetry; heavy meson spectroscopy; hadronic string theory; composite models of quarks and leptons; and pedagogical effects. DOE

N92-31815# Nationaal Inst. voor Kernfysica en Hoge Energiefysica, Amsterdam (Netherlands).
INJECTING INTO AmPS WHEN RING CAVITY OPERATES AT 476 MHz
R. Maas Dec. 1991 11 p
(NIKHEF-K/AmPS/91-08; ETN-92-91739) Avail: CASI HC A03/MF A01

The different requirements for the stretcher and storage modes of the AmPS (Amsterdam Pulse Stretcher) are addressed. It is shown that in storage mode it is more practical to operate at a lower RF frequency than 2856 MHz, which is the RF frequency in stretcher mode. A few consequences of operating the ring cavity at a lower frequency than the (injecting) linac frequency are reviewed. ESA

N92-31831# Oak Ridge National Lab., TN.
ANALYTIC ESTIMATION OF RADIATION EFFECTS IN SPACE USING SOLID ANGLES
S. N. Cramer 1992 10 p Presented at the Nuclear Technologies for Space Exploration, Jackson, WY, 16-19 Aug. 1992
(Contract DE-AC05-84OR-21400)
(DE92-013282; CONF-920803-3) Avail: CASI HC A02/MF A01

The void of space allows the possible simplification of certain integrals which describe the transport of radiation from a point to a surface or volume. The solid angle in this integral is investigated analytically for geometric figures associated with the conic sections, their volumes of revolution, and other plane surfaces. The selection of random directions within the solid angles and the difficulties associated with concave surfaces are discussed. The expression for each solid angle is manipulated into an integral form which can be found in an appropriate handbook reference. It is found that the solid angles are given as linear combinations of elliptic integrals and elementary functions. DOE

N92-31948# Superconducting Super Collider Lab., Dallas, TX.
THE 6-D PHASE SPACE TRACKING WITH ACCELERATION: MODELING LOW ENERGY PROTON SYNCHROTRONS, PART 1
S. Machida Mar. 1992 19 p
(Contract DE-AC35-89ER-40486)
(DE92-013744; SSCL-570) Avail: CASI HC A03/MF A01

Booster synchrotrons for high energy colliders and small proton synchrotrons mostly operate within the 'low-energy' range from 10 MeV up to about 10 GeV. A simulation code of both single-

and multi-particle tracking has been developed especially for such machines. For the first time this code allows investigation of beam dynamics issues such as: (1) acceleration and synchrotron oscillations in fully 6-D phase space; (2) transverse and longitudinal space-charge effects in 3-D real space; and (3) capture and bunching at injection and transition crossing with harmonic RF cavities. This paper describes the single-particle part of the code and presents some results on the Low Energy Booster (LEB) of the Superconducting Super Collider (SSC). DOE

N92-31975# Superconducting Super Collider Lab., Dallas, TX.
CONNECTIVITY AMONG COMPUTER-AIDED ENGINEERING METHODS, PROCEDURES, AND TOOLS USED IN DEVELOPING THE SSC COLLIDER MAGNETS
N. Kallas and A. R. Jalloh Mar. 1992 10 p Presented at the International Industrial Symposium on the Super Collider, New Orleans, LA, 4-6 Mar. 1992
(Contract DE-AC35-89ER-40486)
(DE92-013954; SSCL-Preprint-60; CONF-920331-10) Avail: CASI HC A02/MF A01

The accomplishment of functional productivity for the computer aided engineering (CAE) environment at the magnet engineering department (ME) of the magnet systems divisions (MSD) at the Superconducting Super Collider Laboratory (SSCL) involves most of the basic aspects of information engineering. It is highly desirable to arrive at a software and hardware topology that offers total, two-way (back and forth), automatic and direct software and hardware connectivity among computer-aided design and drafting (CADD), analysis codes, and office automation tools applicable to the disciplines involved. This paper describes the components, data flow, and practices employed in the development of the CAE environment from a systems engineering aspect rather than from the analytical angle. When appropriate, references to case studies are made in order to demonstrate the connectivity of the techniques used. DOE

N92-32028# Iowa State Univ. of Science and Technology, Ames.
INTERMEDIATE/HIGH ENERGY NUCLEAR PHYSICS
J. P. Vary 1992 23 p
(Contract DE-FG02-87ER-40371)
(DE92-015363; DOE/ER-40371/5) Avail: CASI HC A03/MF A01

This report discusses progress on the following research: quark cluster model; solving quantum field theories in non-perturbative regime; relativistic wave equations, quarkonia and electron-positron resonances; nuclear dependence at large transverse momentum; factorization at the order of power corrections; single-spin asymmetries; and hadronic photon production. DOE

N92-32123# Sandia National Labs., Albuquerque, NM.
SCALING OF IFR PROPAGATION PHYSICS WITH BEAM/CHANNEL PARAMETERS
I. R. Shokair May 1992 10 p
(Contract DE-AC04-76DP-00789)
(DE92-015389; SAND-92-0747) Avail: CASI HC A02/MF A01

The equations of motion of beam and channel particles are analyzed in the ion focused regime. Using the paraxial approximation and assuming only transverse electro-magnetostatic interactions between beam and channel particles for the equations of motion (the same equations solved in the BUCKSHOT code) are written in non-dimensional form and scaling relations are derived for propagation parameters, magnetic erosion, and evaporation. These relations are very useful in doing parameter studies with a limited number of computer simulations. DOE

N92-32131# Stanford Linear Accelerator Center, CA.
THE POLARIZED ELECTRON GUN FOR THE SLC
D. C. Schultz, J. Clendenin, J. Frisch, E. Hoyt, L. Klaisner, M. Woods, D. Wright, and M. Zolotorev Mar. 1992 3 p Presented at the 3rd European Particle Accelerator Conference, Berlin (Germany), 24-28 Mar. 1992
(Contract DE-AC03-76SF-00515)
(DE92-012418; SU-SLAC-PUB-5768; CONF-920315-23) Avail: CASI HC A01/MF A01

A new polarized electron gun for use on the SLC at SLAC has been built and tested. It is a diode gun with a laser driven GaAs photocathode. It is designed to provide short (2 nano-s) pulses of 10 A at 160 kV at 120 Hz. The design features of the gun and results from a testing program on a new and dedicated beam line are presented. Early results from operation on the SLC will also be shown. DOE

N92-32133# Stanford Linear Accelerator Center, CA.
CALCULATIONS OF EMITTANCE AND DAMPING TIME EFFECTS IN THE SLC DAMPING RINGS
T. Limberg, H. Moshammer, T. Raubenheimer, J. Spencer, and R. Siemann Mar. 1992 3 p Presented at the 3rd European Particle Accelerator Conference, Berlin (Germany), 24-28 Mar. 1992
(Contract DE-AC03-76SF-00515)
(DE92-012420; SU-SLAC-PUB-5789; CONF-920315-24) Avail: CASI HC A01/MF A01

In a recent NDR machine experiment the transverse emittance was studied as a function of store time and tune. To explain the observed transverse emittance damping time constants, the magnetic measurement data of the longitudinal field of the bending magnets had to be taken into account. The variation of the transverse emittances with tune due to misalignments and the associated anomalous dispersion is studied as well as the effect of synchrobetatron coupling due to dispersion in the RF cavities. DOE

N92-32170# Florida Univ., Gainesville. Dept. of Chemistry.
AN IMPROVED ION GUIDE FOR EXTERNAL ION INJECTION IN GLOW DISCHARGE-FOURIER TRANSFORM ION CYCLOTRON RESONANCE (GD-FTICR) MASS SPECTROMETRY Technical Report, Jan. - Dec. 1991
Christopher M. Barshick and John R. Eyler 28 May 1992 20 p
(Contract N00014-87-J-1248)
(AD-A250944; TR-37) Avail: CASI HC A03/MF A01

To improve the existing ion transport optics of our glow discharge-Fourier transform ion cyclotron resonance (GD-FTICR) mass spectrometer, we have simulated several ion trajectories between the glow discharge source region and the ICR analyzer cell. These calculations suggested that a number of simple improvements, including the use of an ion flight tube and an electrically isolated conductance limit, would increase the efficiency of ion transfer through the fringing fields of the FTICR superconducting magnet and into the ICR analyzer cell. Ion beam intensity was monitored before and after implementing these improvements as a function of the distance between the glow discharge source and the analyzer cell. A twenty-fold improvement in the transport efficiency, as well as a significant enhancement in detected FTICR signals, was observed. GRA

74 OPTICS

Includes light phenomena; and optical devices.
For lasers see *36 Lasers and Masers.*

N92-31295# Sandia National Labs., Albuquerque, NM.
DETECTION OF OBJECT EDGES IN IMAGES CONTAINING CAST SHADOWS
G. C. Osbourn 1992 8 p Presented at the Image VI Conference, Scottsdale, AZ, 14-17 Jul. 1992
(Contract DE-AC04-76DP-00789)
(DE92-016092; SAND-92-0830C; CONF-920795-2) Avail: CASI HC A02/MF A01

Detecting object boundaries in the presence of cast shadows is a difficult task for machine vision systems. A new edge detector is presented which responds to shadow penumbras and abrupt object edges with distinguishable signals. The detector requires the use of spatially extended light sources and sufficient video

resolution to resolve the shadow penumbras of interest. Detection of high frequency noise is suppressed without requiring image-dependent adjustment of signal thresholds. The ability of the edge operator to distinguish shadow penumbras from abrupt object boundaries while suppressing responses to high frequency noise and texture is illustrated with idealized shadow and object edge intensity profiles. Selective detection of object boundaries in a video scene with a cast shadow is also demonstrated. DOE

N92-31380# Stanford Univ., CA. Center for Materials Research.
DEVELOPMENT OF HIGH EFFICIENCY NONLINEAR OPTICAL MATERIALS Final Technical Report, 1 Sep. 1986 - 31 Dec. 1991
Robert S. Feigelson and Roger K. Route 20 Mar. 1992 35 p
(Contract DAAL03-86-K-0129)
(AD-A249612; CMR-92-2; ARO-23577.6-MS) Avail: CASI HC A03/MF A01

This report summarizes a five year program on the development of high efficiency nonlinear optical materials. A major objective of the program was the development of an effective crystal growth technology for barium borate (BBO) and lithium borate (LBO). A secondary objective was to grow high quality crystals to facilitate optical property determinations and nonlinear optical device development. A top-seeded solution growth technique for these two materials is described, along with an assessment of their respective growth rate limiting mechanisms. A thorough analysis of the optical scattering defects found in BBO is also included. A supplemental task involved further development of the heat-treatment technology used to eliminate optical scattering centers from as-grown crystals of silver gallium selenide. A microchemical analysis and a mass balance model that, together, explain the dynamics of the heat-treatment process, and suggest a potential improvement in the process, are also included. GRA

N92-31397# Wisconsin Univ., Madison. Center for X Ray Lithography.
[ACTIVITIES OF THE CENTER FOR X RAY LITHOGRAPHY, PHASE 1] Final Report, 25 Apr. 1989 - 28 Feb. 1991
Martin Peckerar 29 Apr. 1992 15 p
(Contract N00014-89-J-2017)
(AD-A250446) Avail: CASI HC A03/MF A01

Three principal tasks were assigned by the NRL to the University of Wisconsin-Madison Center for X-ray Lithography. The first task involves the integration of the SVG Lithography vertical-stage stepper to the synchrotron x-ray source, Aladdin. This task involves the design and construction of the beamline optics, electronics, vacuum, and mechanics to deliver stable and uniform x-ray flux over a 25 mm by 50 mm field to the SVG Lithography stepper. Incorporated in this task is the development of the instrumentation from the beamline to SVG Lithography Stepper, i.e. flux information, scan rate and position sensors, etc., and the appropriate in-situ monitors to the beamline, e.g. vacuum information, mirror contamination status, etc. The final aspect of this first task involves the installation and characterization of the SVG Lithography Stepper and beamline systems in the clean room at the CXrL. The second and third tasks involve the design and construction of two clean rooms: a stepper clean room to house and support the vertical-stage stepper and its instrumentation; and a process clean room facility, which will be used to perform x-ray resist processing, resist cleanup, and inspection. GRA

N92-31430# Washington Univ., Seattle.
MONTE CARLO SIMULATIONS OF RANDOM ROUGH SURFACE SCATTERING WITH FINITE ELEMENT AND FINITE DIFFERENCE METHODS Final Report, 15 Jul. - 4 Nov. 1991
Leung Tsang and Chi H. Chan 16 Jan. 1992 4 p
(Contract DAAL03-91-G-0217)
(AD-A247528; ARO-29276-GS) Avail: CASI HC A01/MF A01

Monte Carlo simulations of scattering of waves by one-dimensional random rough gold surfaces at optical frequencies are investigated by the use of the finite-element method. Both TE and TM plane wave incidences are considered. Backscattering enhancements are observed for all the cases studied in this report. GRA

N92-31611# Stanford Univ., CA. Space Telecommunications and Radioscience Lab.
THREE-WAVE ENVELOPE SOLITONS: CAN THE SPEED OF LIGHT IN THE FIBER BE CONTROLLED?
Y. N. Taranenko and L. G. Kazovsky 1991 11 p
(Contract N00014-91-J-1857)
(AD-A247615) Avail: CASI HC A03/MF A01

Theory predicts that three-wave envelope solitons (TWES) can be generated in dual-mode optical fibers by injecting two copropagating light waves or a light wave and a flexural acoustic wave. The mechanism of the three-wave interaction is the recently observed intermodal stimulated forward Brillouin scattering. The velocity of the TWES can be controlled by changing the pump power. Using 200 mW pump power for a typical dual-mode fiber, the average speed of the light pulse in the fiber can be made as low as 30,000 m/sec. A recent growth of interest in dual-mode (DM) optical fibers for a variety of nonlinear switching and modulation schemes stems from the long interaction lengths and from the two nondegenerate copropagating optical modes (at the same optical frequency) offered by these fibers. This letter presents theoretical results suggesting that the speed of light in optical fibers can be controlled by using a nonlinear resonant interaction between two copropagating light waves and an acoustic wave in a DM optical fiber. The second order nonlinearity involved in this process is the intermodal forward stimulated Brillouin scattering (FSBS) in DM optical fibers. FSBS has been observed recently for the first time. In our quantitative examples we use the fiber and wave parameters from that experiment. GRA

N92-31692# Laboratoire d'Automatique et d'Analyse des Systemes, Toulouse (France).
FROM PERCEPTION TO MODELIZATION IN ROBOTICS USING ACHROMATIC AND CHROMATIC CAMERAS Ph.D. Thesis - Toulouse Univ. [DE LA PERCEPTION A LA MODELISATION PAR LA VISION ACHROME ET TRICHROME EN ROBOTIQUE]
Thierry Baron 1991 147 p In FRENCH
(LAAS-91484; ETN-92-91681) Avail: CASI HC A07/MF A02

In order to enable robots to perform autonomous decision and motion on the basis of visual information, it is necessary to model the physical phenomena that produce the images and to build a three dimensional model of the environment with the primitives extracted from these images. The formalism of the physical and geometrical models associated with image formation are considered. A region attribute characteristic of planar specular surfaces, along with an experimental study of charged couple device cameras are presented. Extraction, structuring, and use of associated region and line segment primitives, semantically grouped in pertinent primitives, are considered. The improvements brought by this approach are validated by two experimental applications in three dimensional modeling. The region and line segments association was used as a matching criteria in passive stereovision in indoor environment (planar surfaces). A three dimensional range sensor camera cooperation was developed to improve three dimensional reconstruction of the range data and to identify the semantic of the line segments. ESA

N92-31737# Brookhaven National Lab., Upton, NY.
LATTICE GAUGEFIXING AND OTHER OPTICS IN LATTICE GAUGE THEORY Ph.D. Thesis
Ken Yee Jun. 1992 112 p
(Contract DE-AC02-76CH-00016)
(DE92-016958; BNL-47668) Avail: CASI HC A06/MF A02

We present results from four projects. In the first, quark and gluon propagators and effective masses and (Delta)I = 1/2 Rule operator matching coefficients are computed numerically in gaugefixed lattice QCD. In the second, the same quantities are evaluated analytically in the strong coupling, N yields infinity limit. In the third project, the Schwinger model is studied in covariant gauges, where we show that the effective electron mass varies

with the gauge parameter and that longitudinal gaugefixing ambiguities affect operator product expansion coefficients (analogous to (Delta)I = 1/2 Rule matching coefficients) determined by matching gauge variant matrix elements. However, we find that matching coefficients even if shifted by the unphysical modes are (xi) invariant. In the fourth project, we show that the strong coupling parallelogram lattice Schwinger model has a different thermodynamic limit than the weak coupling continuum limit. As a function of lattice skewness angle these models span the Delta = minus 1 critical line of 6-vertex models which, in turn, have been identified as c = 1 conformal field theories.

DOE

N92-31761# Lawrence Livermore National Lab., CA.
RESOLUTION LIMITS FOR GROUND BASED ASTRONOMICAL IMAGING USING ADAPTIVE OPTICS
S. S. Olivier, C. E. Max, D. T. Gavel, and J. M. Brase 10 Mar. 1992 6 p Presented at the Laser Guide Star Adaptive Optics Workshop, Albuquerque, NM, 10-12 Mar. 1992
(Contract W-7405-eng-48)
(DE92-011949; UCRL-JC-109219; CONF-9203139-1) Avail: CASI HC A02/MF A01

We study the residual jitter present in astronomical images after the effect of the earth's atmosphere has been compensated using a fast steering mirror. This residual jitter places a limit on the resolution that can be achieved for long exposure images even when more elaborate adaptive optics systems are used to correct the image. We assume that the fast guiding system uses a star as its reference source. Then, from the observed characteristics of galactic stellar populations, we are able to predict the optimal performance of the fast guiding system as a function of the sky covering factor: that is the fraction of the sky for which the given level of performance can be achieved. The performance for a particular sky covering factor is optimized by choosing the appropriate closed-loop bandwidth and guide star magnitude. The performance also depends on a number of atmospheric and system parameters; however, we find that the optimal performance is relatively insensitive to all but two of these parameters, the telescope aperture size, and the strength of the atmospheric turbulence. Therefore, we consider two specific examples: first, a ten meter telescope imaging an atmosphere with relatively weak turbulence (3/4 arcsecond seeing in V), and second, a one meter telescope imaging through an atmosphere with relatively strong turbulence (2 arcsecond seeing in V). For these cases we find, for example, that a residual jitter of less than 0.03 and 0.3 arcseconds respectively can be obtained over about half the sky for nominal choices of the other parameters. The required closed-loop bandwidths in these cases are about 5 and 20 Hz while the appropriate guide stars are approximately 18th and 14th magnitude in V.

DOE

N92-32077# Case Western Reserve Univ., Cleveland, OH. Dept. of Macromolecular Science.
APPLICATION OF OPTICAL THEORY TO QUANTITATIVE SURFACE FT-IR WITH EMPHASIS ON MOLECULAR DEPTH PROFILING
Hatsuo Ishida May 1992 26 p
(Contract N00014-88-R-0330)
(AD-A250525; CWRU/DMS/TR-45) Avail: CASI HC A03/MF A01

Applications of optical theory to the study of surface, thin films and coatings have been reviewed. Recent advances in personal computing has made the application of optical theory to an observed spectrum a nearly routine practice. With diversification of infrared techniques which rely on reflection techniques, band shape distortion and frequency shift are common occurrence and the ability to correct for the optical effects has become extremely useful. This article discusses selected topics to demonstrate the usefulness of the application of optical theory. Special emphasis is placed on the quantitative nature of the discussion as well as techniques related to molecular depth profiling. GRA

N92-32092# E-Tek Dynamics, Inc., San Jose, CA.
OPTICAL COMPUTING AND OPTICAL SIGNAL PROCESSING, PHASE 1 Final Report, Oct. 1991 - Apr. 1992
J. J. Pan Apr. 1992 143 p
(Contract F49620-91-C-0090)
(AD-A250551; AFOSR-92-0404TR) Avail: CASI HC A07/MF A02

High efficient nonlinear optical materials (NOMS) are highly required for optical computing and optical signal processing. However, currently no such practical NOMs are available. In this project, new organic NOMs have been researched and developed. New organic NOM design principle and approach have been reviewed and investigated. Four new organic NOMs, namely, CMVI, DVDA, MOHNS and HMONS have been synthesized and purified. Nonlinear optical responses of these four samples have been demonstrated and characterized. Device fabrication and application for optical computing and optical signal processing have been investigated. GRA

N92-32137 Department of the Navy, Washington, DC.
OPTICAL INTERFEROMETRIC SENSOR DETECTED INTENSITY NOISE REDUCTIONS MEANS Patent
Jeffrey C. Gremillion, inventor (to Navy) 5 Apr. 1992 5 p Filed 5 Feb. 1990
(AD-D015296; US-Patent-5,104,223; US-Patent-Appl-SN-474941) Avail: US Patent and Trademark Office

An apparatus for reducing the detected optical intensity noise received from an optical interferometric sensor is presented. One embodiment of the device comprises high pass and low pass filtering means and an arithmetic divider device arranged so as to receive a single signal S1 and to cancel unwanted intensity noise in signal S1 prior to the transmission of the noise free signal out to a receiver circuit. A second embodiment of the device further includes an adder and a subtractor to receive two signals, S1 and S2. The adder and subtractor are cross connected in such a way as to combine the two signals for further processing and to permit intensity noise cancellation in the event that one of the signals is not available. GRA

N92-32144# California Univ., San Diego. Marine Physical Lab.
A SENSITIVITY STUDY OF DAYTIME VISIBILITY DETERMINATION WITH THE HORIZON SCANNING IMAGER Report No. 2
J. E. Shields, R. W. Johnson, and M. E. Karr Jul. 1991 45 p
(Contract F19628-88-C-0154; AF Proj. 2688)
(SIO-91-15; MPL-U-25/91; PL-TR-91-2189) Avail: CASI HC A03/MF A01

The Horizon Scanning Imager is an automated imaging system for determination of visibility during the daytime. This is accomplished through evaluation of contrast transmission of the atmosphere, which is determined from the measured radiance of dark targets near the horizon. The determination of visibility during the daytime by the Horizon Scanning Imager is influenced by a number of parameters, some measured and others input by the operator. These include the measured target radiance, measured horizon radiance, and inherent contrast of the target with respect to the horizon. A sensitivity study is presented in which the impact of uncertainty in these parameters is determined. On the basis of this study, specific recommendations are made to improve the visibility determinations. The first set of recommendations relates to the sensor accuracy and includes ways to improve the measurements and also ways to mitigate the impact of the residual errors. The second set of recommendations details strategies to minimize the impact of non-ideal measurement conditions.

Author

N92-32149# Stanford Linear Accelerator Center, CA.
RESULTS OF IR WORKING GROUP
D. Ritson Mar. 1992 3 p Presented at the 19th INFN Eloisation Project: Maximizing Luminosity of Hadron Colliders At 100 TeV, Erice (Italy), 13-19 Nov. 1991
(Contract DE-AC03-76SF-00515)

(DE92-013294; SU-SLAC-PUB-5774; CONF-9111208-2) Avail: CASI HC A01/MF A01

The IP luminosity at the Eloisatron will direct very large fluxes of hadronic debris into the IR quads. For instance at 1.10(sup 35) cm(sup 2)/sec the flux corresponds to 180 kilowatts. Already at the SSC fluxes in the neighborhood of 2 kilowatts are expected to require special handling. Scaling from SSC design experience we propose a configuration for the first IR quads at the Eloisatron capable of handling the heat load and radiation problems. DOE

N92-32012 Essex Corp., Columbia, MD.
OPTICAL PROCESSING ARCHITECTURES FOR SPACEBORNE SAR IMAGE GENERATION AND RF ARRAY BEAM FORMING
Terry M. Turpin, Leslie H. Gesell, and James L. Lafuse *In* Huntsville Association of Technical Societies, TABES 92: 8th Annual Technical and Business Exhibition and Symposium. Executive Summaries and Submitted Papers 1992 7 p (For primary document see N92-32009 22-12)
(TABES Paper 92-444) Copyright Avail: Issuing Activity

75 PLASMA PHYSICS

Includes magnetohydrodynamics and plasma fusion.

For ionospheric plasmas see *46 Geophysics*. For space plasmas see *90 Astrophysics*.

N92-31310# Argonne National Lab., IL.
DYNAMIC MODELING OF PLASMA-VAPOR INTERACTIONS DURING PLASMA DISRUPTIONS
A. Hassanein and D. A. Ehst May 1992 19 p Presented at the 10th International Conference on Plasma-Surface Interactions in Controlled Fusion Devices, Monterey, CA, 30 Mar. - 3 Apr. 1992
(Contract W-31-109-eng-38)
(DE92-016183; ANL/CP-74880; CONF-920311-18) Avail: CASI HC A03/MF A01

Intense deposition of energy in short times on fusion reactor components during a plasma disruption may cause severe surface erosion due to ablation of these components. The exact amount of the eroded material is very important to the reactor design and its lifetime. During the plasma deposition, the vaporized wall material will interact with the incoming plasma particles and may shield the rest of the wall from damage. The vapor shielding may then prolong the lifetime of these components and increase the reactor duty cycle. To correctly evaluate the impact of vapor shielding effect, a comprehensive model is developed. In this model, the dynamic slowing down of the plasma particles, both ions and electrons, with the eroded wall material is established. Different interaction processes between the plasma particles and the ablated material is included. The generated photon radiation source and the transport of this radiation through the vapor to the wall is modeled. Recent experimental data on disruptions is analyzed and compared with model predictions. Vapor shielding may be effective in reducing the overall erosion rate for certain plasma disruption parameters and conditions. DOE

N92-31372# Tennessee Univ. Space Inst., Tullahoma.
MONITORING GAS TEMPERATURES ENTERING AN MHD SUPERHEATER
B. C. Winkleman, J. P. Foote, and T. V. Giel 1992 6 p Presented at the 30th Symposium on Engineering Aspects of Magnetohydrodynamics, Baltimore, MD, 29 Jun. - 2 Jul. 1992
(Contract DE-AC02-79ET-10815)
(DE92-014200; DOE/ET-10815/182; CONF-920677-3) Avail: CASI HC A02/MF A01

A line reversal system used to continuously monitor gas temperature entering the first superheater test module at the U.S. DOE Coal Fluid Flow Facility is described. Problems of implementing thermocouple probes and the line reversal technique for the 1480-1539K (2200-2300 F) gas temperature regime and the harsh physical environment are discussed. Evidence of large, rapid variations in the gas transmissivity is presented. Line reversal temperatures are compared with shielded-aspirated and bare thermocouple probe measurements. DOE

N92-31412# Texas Univ., Austin. Inst. for Fusion Studies.
VORTICES ASSOCIATED WITH TOROIDAL ION TEMPERATURE GRADIENT DRIVEN FLUCTUATIONS
W. Horton, D. Jovanovic (Belgrade Univ., Yugoslavia), and J. J. Rasmussen (Risoe National Lab., Roskilde, Denmark) May 1992 23 p
(Contract DE-FG05-80ET-53088)
(DE92-016180; DOE/ET-53088/549; IFSR-549) Avail: CASI HC A03/MF A01

The three nonlinear hydrodynamic equations for potential, parallel ion velocity, and ion pressure used in simulations of the toroidal ion temperature gradient driven fluctuations and transport in a shear magnetic field are analyzed for coherent vortex structures. Two types of vortex structures are found: one type for weak shear that is a generalization of the usual modon vortex construction, and the second type of solution for strong magnetic shear where the convective nonlinearity in the parallel velocity field generates a cubic trapping nonlinearity in the vorticity equation. These vortex structures show the possibility of explaining the saturated states observed in the numerical simulations as self-organized nonlinear states in contrast to wave turbulence. DOE

N92-31459# Washington Univ., Seattle. Aerospace and Energetics Research Program.
TRANSIENT INTERNAL PROBE DIAGNOSTIC Annual Technical Report No. 1, 15 Sep. 1990 - 14 Oct. 1991
Thomas R. Jarboe, Gregory G. Spanjers, Walter H. Christiansen, Glen A. Wurden, and Bradford L. Wright 12 Dec. 1991 44 p
(Grant AF-AFOSR-0345-90)
(AD-A247306; AFOSR-92-0101TR) Avail: CASI HC A03/MF A01

The Transient Internal Probe (TIP) diagnostic is a novel method for probing the interior of hot magnetic fusion plasmas that are inaccessible with ordinary stationary probes, by limiting the time that the probe is in the plasma, and by encasing the probe in a diamond cladding. In the TIP scheme, a probe is fired through a hot plasma at velocities in excess of 2.5 km/s, and makes direct, local measurements of the internal magnetic field structure. These measurements are relayed to the laboratory optical detection system, using an incident laser that is retroreflected through a Faraday rotator crystal payload that acs as a magneto-optic sensor. The individual tasks associated with the TIP development, construction a two-stage light gas gun, optical detection system and probe projectile, are currently being completed. Integration of these tasks is currently underway. It is expected that the integrated system will be functional in the first six months of 1992. A diamond ablation study has also been performed to measure the ablative effects of a hot plasma in contact with a diamond pellet. Studies are currently underway to develop a sabot stripping system, and to develop a vacuum interface between the TIP diagnostic and the plasma experiments' vacuum chamber. GRA

N92-31494# City Univ. of New York, Staten Island.
NON-GEOTHERMAL OPTICS STUDY OF WAVE PROPAGATION
K. Imre Mar. 1992 9 p
(Contract DE-FG02-91ER-54131)
(DE92-011806; DOE/ER-54131/1) Avail: CASI HC A02/MF A01

A statistical theory of growth curve analysis, which makes use of smoothing splines is formulated and coded for applications. We have tested our codes extensively using computer generated data superposed with random noise of various intensities, by simultaneously fitting all data with two independent variables. We are presently evaluating various experimental data in the MFE database by making use of our codes. Our preliminary results indicate that TFTR ohmic temperature profile shape depends almost exclusively on the edge plasma safety factor, q(sub a), as

was previously shown to be true for ASDEX plasma profiles. The main advantage of the utilization of a simultaneous fitting of all (appropriately normalized) profiles as a function of more than one plasma parameter, is to improve significantly the signal to noise ratio. We also determine the amount of smoothing to be applied during the curve fitting process. An optimally selected smoothing helps to reduce the random noise, but yet allows the predictions to stay close to the data. In addition, the use of a multi-dimensional parameter field provides us with a uniformly valid representation. The curve fitting technique we employ uses a piecewise polynomial spline representation. However, we have eliminated the usually adopted method of setting a simple knot at every data point, because the experimentally obtained data is usually confined to the values of the plasma parameters bunched together in small intervals which are widely separated. Presently, we are using equally spaced knots. DOE

N92-31530# Lawrence Livermore National Lab., CA.
YLIFE-2 INERTIAL FUSION ENERGY POWER PLANT DESIGN
R. W. Moir Mar. 1992 12 p Presented at the 10th Topical Meeting on Technology of Fusion Energy, Boston, MA, 7-12 Jun. 1992
(Contract W-7405-eng-48)
(DE92-011965; UCRL-JC-109522; CONF-920607-10) Avail: CASI HC A03/MF A01

The HYLIFE-2 inertial fusion power plant design study uses a liquid fall, in the form of jets, to protect the first structural wall from neutron damage, x rays, and blast to provide a 30-y lifetime. HYLIFE-1 used liquid lithium. HYLIFE-2 avoids the fire hazard of lithium by using a molten salt composed of fluorine, lithium, and beryllium (Li2BeF4) called Flibe. Access for heavy-ion beams is provided. Calculations for assumed heavy-ion beam performance show a nominal gain of 70 at 5 MJ producing 350 MJ, about 5.2 times less yield than the 1.8 GJ from a driver energy of 4.5 MJ with gain of 400 for HYLIFE-1. The nominal 1 GWe of power can be maintained by increasing the repetition rate by a factor of about 5.2, from 1.5 to 8 Hz. A higher repetition rate requires faster re-establishment of the jets after a shot, which can be accomplished in part by decreasing the jet fall height and increasing the jet flow velocity. In addition, although not adequately considered for HYLIFE-1, there is liquid splash that must be forcibly cleared because gravity is too slow, at higher repetition rates than 1 Hz. Splash removal is accomplished in the central region by oscillating jet flows. The cost of electricity is estimated to be 0.09 $/kWh in constant 1988 dollars, about twice that of future coal and light water reactor nuclear power. The driver beam cost is about one-half the total cost, that is, a zero cost driver would give a calculated cost of electricity of 0.045 $/kWh. DOE

N92-31545# Massachusetts Inst. of Tech., Cambridge. Plasma Fusion Center.
FUSION DEVELOPMENT AND TECHNOLOGY
D. B. Montgomery 1992 53 p
(Contract DE-FG02-91ER-54110)
(DE92-014352; DOE/ER-54110/2) Avail: CASI HC A04/MF A01

This report discusses the following: superconducting magnet technology; high field superconductors; advanced magnetic system and divertor development; poloidal field coils; gyrotron development; commercial reactor studies; ITER physics: alpha physics and R&D for ITER; lower hybrid current drive and heating in the ITER device; ITER superconducting PF scenario and magnet analysis; ITER systems studies; and safety, environmental and economic factors in fusion development. DOE

N92-31576# Pittsburgh Energy Technology Center, PA.
MHD CONTRACTORS' REVIEW MEETING: ABSTRACTS
1992 185 p Meeting held in Pittsburgh, PA, 21-23 Jan. 1992
(DE92-011549; CONF-9201102-Absts) Avail: CASI HC A09/MF A02

The objectives of the Integrated Topping Cycle project are to design, construct, and deliver all prototypical hardware necessary to conduct long duration integrated MHD topping cycle proof-of-concept tests at the Component Development and Integration Facility (CDIF) in Butte, Montana. The results of the long duration tests will augment the existing engineering data base on MHD power train reliability, maintainability, durability, and performance, and will serve as a basis for scaling up to the early commercial scale power plant retrofit. The components of the MHD power train to be designed, fabricated, and tested include the following three systems: (1) a slagging coal combustion subsystem with a rated capacity of 50 MW thermal input, capable of operation with eastern (Illinois) or western (Montana Rosebud) coal; (2) a channel subsystem consisting of a segmented supersonic nozzle, channel (with current controls), and diffuser, capable of power output of 1.5 MW(sub e); and (3) a current consolidation subsystem to interface the channel with the existing facility inverter. DOE

N92-31613# Georgia Inst. of Tech., Atlanta. Fusion Research Center.
POLOIDAL ROTATION AND DENSITY ASYMMETRIES IN A TOKAMAK PLASMA WITH STRONG TOROIDAL ROTATION
W. M. Stacey, Jr. Jan. 1992 41 p
(Contract DE-FG05-87ER-51112)
(PB92-182534; GTRF-101) Avail: CASI HC A03/MF A01

A neoclassical model for calculating poloidal rotation and poloidal density asymmetries in a tokamak plasma with V(sub phi) approx. equal to V(sub th) and E/B(sub theta) approx. equal to 0(1) is developed. Application is made to the analysis of a deuterium plasma with a dominant carbon impurity. The dependences of the results on collisionality, the radial deuterium flux and the toroidal rotation speed are evaluated. The implications of the calculated poloidal velocities and density asymmetries for the magnitude of the gyroviscous torque are discussed. Author

N92-31616# General Atomic Co., San Diego, CA.
REAL TIME ANALYSIS OF TOKAMAK DISCHARGE PARAMETERS
J. R. Ferron and E. J. Strait Mar. 1992 11 p Presented at the 9th Topical Conference on High-Temperature Plasma Diagnostics, Santa Fe, NM, 15-19 Mar. 1992
(Contract DE-AC03-89ER-51114)
(DE92-011394; GA-A-20860; CONF-920362-20) Avail: CASI HC A03/MF A01

The techniques used in implementing two applications of real time analysis of data from the DIII-D tokamak are described. These tasks, which are demanding in both the speed of data acquisition and the speed of computation, execute on hardware capable of acquiring 40 million data samples per second and executing 80 million floating point operations per second. In the first case, a feedback control algorithm executing at a 10 kHz cycle frequency is used to specify the current in the poloidal field coils in order to control the discharge shape. In the second, fast Fourier transforms of Mirnov probe data are used to find the amplitude and frequency of each of eight toroidal mode numbers as a function of time during the discharge. Data sampled continuously at 500 kHz are used to produce results at 2 msec intervals. DOE

N92-31659# National Inst. for Fusion Science, Nagoya (Japan).
THEORY OF ANOMALOUS TRANSPORT IN TOROIDAL HELICAL PLASMAS
K. Itoh, Sanae-I. Itoh, and A. Fukuyama (Okayama Univ., Japan) Mar. 1992 19 p Submitted for publication
(NIFS-140) Avail: CASI HC A03/MF A01

A theoretical model of the anomalous transport in Torsatron/Heliotron plasmas is developed, based on the current-diffusive interchange instability which is destabilized due to the averaged magnetic hill near edge. An analytic formula of a transport coefficient is derived. This model explains the high edge transport, the power degradation and energy confinement scaling law, and the enhanced heat pulse thermal conduction. Author

N92-31688# Rutgers - The State Univ., Newark, NJ. Dept. of Physics.
TIME AND SPACE RESOLVED ELECTRON IMPACT EXCITATION RATES IN AN RF GLOW DISCHARGE Final Report
Daniel E. Murnick and Yuan Li 28 Feb. 1992 29 p
(Contract DAAL03-91-G-0297)
(AD-A249614) Avail: CASI HC A03/MF A01

Research on rf glow discharge plasmas was carried out to better understand the fundamental physics and chemistry of important aspects of plasma deposition and etching. A standard reference system for rf plasma processing research was utilized. Power, voltage and current waveforms were monitored and time and space resolved measurements were made using plasma induced emission (PIE). Nanosecond time resolution for PIE greatly expanded the utility of these plasma diagnostics over previous studies. Measurements were carried out with a prototype rf model discharge, atomic argon, concentrating on the important 4s levels 11.5 eV above the ground state and the manifold of p levels coupled to these states by strong dipole transitions. Extensive analysis and computer modeling was carried out to reproduce the experimental data obtained and to test assumptions often used for this model system. Models of electron excitation waves were stringently tested and evaluated. The research concentrated on studying details of excitation waveforms as a function of pressure and rf power. Information on electron energy distribution functions were derived from the experimental results. New experimental techniques to enhance time and space resolution were developed. GRA

N92-31707# Sandia National Labs., Albuquerque, NM.
LIGHT ION DRIVEN INERTIAL CONFINEMENT FUSION
D. L. Cook, R. G. Adams, J. H. Aubert, L. D. Bacon, J. E. Bailey, D. D. Bloomquist, J. D. Boyes, G. A. Chandler, R. S. Coats, and J. P. Corley et al 1992 3 p Proposed for presentation at the 14th International Conference on Plasma Physics and Controlled Nuclear Fusion Research, Wuerzburg, Germany, 30 Sep. - 7 Oct. 1992
(Contract DE-AC04-76DP-00789)
(DE92-011662; SAND-92-0806C; CONF-920913-1) Avail: CASI HC A01/MF A01

Intense light ion beams are being developed to drive inertial confinement fusion (ICF) targets. Recently, intense proton beams have been used to drive two different types of targets in experiments on the Particle Beam Fusion Accelerator. The experiments focused separately on ion deposition physics and on implosion hydrodynamics. In the ion deposition physics experiments, a 3-4 TW/cm(exp 2) proton beam heated a low-density foam contained within a gold cylinder with a specific power deposition exceeding 100 TW/gm for investigating ion deposition, foam heating, and generation of x-rays. The significant results from these experiments included the following: the foam provided an optically thin radiating region, the uniformity of radiation across the foam was good, and the foam tamped the gold case, holding it in its original position for the 15 ns beam pulse width. DOE

N92-31727# Columbia Univ., New York, NY.
ION TEMPERATURE GRADIENT INSTABILITY AND TRANSPORT Progress Report
1992 3 p
(Contract DE-FG02-87ER-53257)
(DE92-013590; DOE/ER-53257/5) Avail: CASI HC A01/MF A01

Anomalous ion thermal conductivity remains an open physics issue for the present generation of high temperature tokamaks. It is now believed to be due to the Ion Temperature Gradient (ITG or n(sub i)) instability. The production and identification of this instability is being studied in the simpler and experimentally convenient configuration of the steady state Columbia Linear Machine (CLM). The slab branch of this instability was produced (by two different heating methods), identified, and reported for the first time. The transition of the slab branch to the toroidal branch (more relevant for tokamaks) has now been studied by turning on the mirror current and gradually increasing it in CLM. This has enabled us to identify the toroidal/trapped ion branch of the ITG mode for the first time. A preliminary measurement of the ion thermal conductivity due to the mode indicates a highly anomalous value. DOE

N92-31730# Wisconsin Univ., Madison.
ELECTROSTATIC TURBULENCE AND TRANSPORT IN THE RFP EDGE Ph.D. Thesis
C. W. Spragins May 1992 49 p
(Contract DE-FG02-85ER-53198)
(DE92-014322; DOE/ER-53198/196) Avail: CASI HC A03/MF A01

This thesis details measurements of electrostatic turbulence and transport in the Madison Symmetric Torus reversed field pinch. The electrostatic fluctuation levels are found to be large, with tilde n(sub e)/n(sub e) approximately = 30-55 percent and tilde T(sub e)/T(sub e) approximately = 15-40 percent. The frequency and wavenumber spectra are broad, with delta n approximately = 70-150 and delta m approximately = 3-6, and differ from measured magnetic fluctuation spectra. The transport inferred from coherence measurements indicates that electrostatic fluctuations can account for most of the observed particle losses, but contribute only approximately 20 percent to the observed electron energy loss. DOE

N92-31749# General Atomic Co., San Diego, CA.
DIVERTOR MATERIAL EVALUATION SYSTEM AT D3-D
C. P. C. Wong, R. Jungle, R. D. Phelps, P. Politzer, F. Puhn, W. P. West, R. Bastasz (Sandia National Labs., Albuquerque, NM.), D. Buchenauer (Sandia National Labs., Albuquerque, NM.), W. Hsu (Sandia National Labs., Albuquerque, NM.), and J. Brooks (Argonne National Lab., IL.) et al Apr. 1992 17 p Presented at the 10th International Conference on Plasma-Surface Interactions in Controlled Fusion Devices, Monterey, CA, 30 Mar. - 3 Apr. 1992
(Contract DE-AC03-89ER-52153)
(DE92-013696; GA-A-20877; CONF-920311-8) Avail: CASI HC A03/MF A01

The Divertor Material Evaluation System (DIMES) at D3-D is a collaborative program between General Atomics, Sandia National Laboratories (SNL), and Argonne National Laboratory (ANL). This program was initiated in response to the need for understanding the interaction between the plasma and divertor surface materials in tokamaks. Material erosion, tritium retention, disruption effects, and material transport are very important topics for the design of ITER. The first phase of the DIMES study is integral material exposure measurements. The second phase of the study is the installation of the DIMES sample changer mechanism. The mechanical design goal for the second phase is to allow the insertion of instrumented samples into the bottom divertor plate region of D3-D without venting the tokamak. Different material samples can then be exchanged overnight after as few as one plasma shot of exposure. This paper presents the results of the integral experiments, the design of the DIMES sample changer mechanism, and the planning of material evaluation experiments at D3-D using the DIMES mechanism. DOE

N92-31764# General Atomic Co., San Diego, CA.
A PHASE CONTRAST INTERFEROMETER ON D3-D
S. Coda (Massachusetts Inst. of Tech., Cambridge.), M. Porkolab (Massachusetts Inst. of Tech., Cambridge.), and T. N. Carlstrom Apr. 1992 9 p Presented at the 9th Topical Conference on High-Temperature Plasma Diagnostics, Santa Fe, NM, 15-19 Mar. 1992
(Contract DE-AC03-89ER-51114)
(DE92-012699; GA-A-20876; CONF-920362-24) Avail: CASI HC A02/MF A01

A novel imaging diagnostic has recently become operational on the D3-D tokamak for the study of density fluctuations at the outer edge of the plasma. The phase contrast imaging approach overcomes the limitations of conventional scattering techniques in the spectral range of interest for transport-related phenomena, by

allowing detection of long wavelength modes (up to 7.6 cm) with excellent spatial resolution (5 mm) in the radial direction. Additional motivation for the diagnostic is provided by wave-plasma interactions during heating and current drive experiments in the ion cyclotron range of frequencies. Density perturbations of 4 x 10(exp 7) cm(exp -3) with a 1 MHz bandwidth can be resolved. The diagnostic employs a 7.6 cm diameter CO2 laser beam launched vertically across the plasma edge. An image of the plasma is then created on a 16-element detector array: the detector signals are directly proportional to the density fluctuations integrated along each chord. Wavelengths and correlation lengths can be inferred from the spatial mapping. The phase contrast method and its application to D3-D are described and tests and first plasma data are presented. DOE

N92-31771# Sandia National Labs., Livermore, CA.
POWER SCALING OF DIVERTOR PLASMA CONDITIONS DURING H-MODE IN D3-D
D. Buchenauer, J. W. Cuthbertson, D. N. Hill (Lawrence Livermore National Lab., CA.), C. Klepper (Oak Ridge National Lab., TN.), and T. W. Petrie (General Atomic Co., San Diego, CA.) 1992 16 p Presented at the 10th International Conference on Plasma-Surface Interactions in Controlled Fusion Devices, Monterey, CA, 30 Mar. - 3 Apr. 1992
(Contract DE-AC04-76DR-00789)
(DE92-012148; SAND-92-8489C; CONF-920311-5) Avail: CASI HC A03/MF A01

An array of fixed Langmuir probes spanning the inner and outer divertor strike points were used to measure the electron temperature, plasma density, and particle/heat flux profiles of the divertor plasma in D3-D. We report here on observations made during the steady state phase of high-power neutral-beam heated H-mode plasmas. These data are important for predicting the expected impurity sources and target-plate material lifetimes in future high power tokamaks such as ITER. H-mode plasmas formed with a high divertor neutral pressure in the absence of external gas feed in D3-D were found to have beneficial consequences in reducing the peak values of divertor electron temperature without loss of core energy confinement. We have observed a steady-state, high density (n(sup pl,d) is approximately equal to 10(exp 14) cm(exp -3)), moderate temperature (less than 50 eV) divertor plasma in D3-D at ITER-like divertor power levels of 3 MW/m(exp 2). A better understanding of the importance of ion-neutral and charge-exchange collisions may be needed to interpret these results. DOE

N92-31829# Oak Ridge National Lab., TN.
FLOW GENERATION BY TURBULENCE
B. A. Carreras, V. E. Lynch, and L. Garcia (Universidad Complutense, Madrid, Spain) 1992 43 p Presented at the International Topical Conference on New Ideas in Tokamak Confinement, La Jolla, CA, 27-29 Jan. 1992
(Contract DE-AC05-84OR-21400)
(DE92-013276; CONF-920142-1) Avail: CASI HC A03/MF A01

The radial structure of poloidal flows and radial electric fields in the tokamak plasma edge plays an important role in determining global tokamak confinement properties, including the transition from L-mode to H-mode. In a turbulent plasma, apart from classical momentum sources, poloidal flows can be generated and/or amplified through the Reynolds stress. This requires a symmetry-breaking process, such as radial diamagnetic effects or an externally applied shear flow that acts as a 'seed' for the flow. The flow modifies the linear properties of the instabilities and can change the fluctuation levels of turbulence. The flow generation processes are particularly important at the plasma edge, where the fluctuation levels are large. DOE

N92-31843# National Inst. for Fusion Science, Nagoya (Japan).
SIMULATION STUDY OF STEPWISE RELAXATION IN A SPHEROMAK PLASMA
Ritoku Horiuchi, Masaya Uchida, and Tetsuya Sato Oct. 1991 44 p
(DE92-782101; NIFS-111) Avail: CASI HC A03/MF A01

The energy relaxation process of a spheromak plasma in a flux conserver is investigated by means of a three-dimensional magnetohydrodynamic simulation. The resistive decay of an initial force-free profile brings the spheromak plasma to an m = 1/n = 2 ideal kink unstable region. It is found that the energy relaxation takes place in two steps; namely, the relaxation consists of two physically distinguished phases, and there exists an intermediate phase in between, during which the relaxation becomes inactive temporarily. The first relaxation corresponds to the transition from an axially symmetric force-free state to a helically symmetric one with an n = 2 crescent magnetic island structure via the helical kink instability. The n = 2 helical structure is nonlinearly sustained in the intermediate phase. The helical twisting of the flux tube creates a reconnection current in the vicinity of the geometrical axis. The second relaxation is triggered by the rapid growth of the n = 1 mode when the reconnection current exceeds a critical value. The helical twisting relaxes through magnetic reconnection toward an axially symmetric force-free state. It is also found that the poloidal flux reduces during the helical twisting in the first relaxation and the generation of the toroidal flux occurs through the magnetic reconnection process in the second relaxation. DOE

N92-31913# Oak Ridge National Lab., TN.
SMALL TOKAMAKS FOR FUSION TECHNOLOGY TESTING
Y. K. M. Peng, J. D. Galambos, and P. C. Shipe 1992 10 p Presented at the 10th Topical Meeting on Technology of Fusion Energy, Boston, MA, 7-12 Jun. 1992
(Contract DE-AC05-84OR-21400)
(DE92-011790; CONF-920607-9) Avail: CASI HC A02/MF A01

Small steady-state tokamaks for testing divertors and fusion nuclear technologies are considered. Based on present physics and technology data and explanation to reduce R(sub 0)/a, H-D-fueled tokamaks with R(sub 0) approximately 0.6-0.75 m, R(sub 0)/a approximately 1.8-2.5, and B(sub t0) approximately 1.4-2.2 T can be driven with P(sub tot) approximately 4.5 MW to maintain I(sub p) approximately 0.5 MA and produce the ITER-level plasma edge and divertor conditions. Given an adequate steady-state divertor solution and Q approximately 1 operation based on fusion through the suprathermal component, D-T-fueled tokamaks with R(sub 0) approximately 0.8 m, R(sub 0)/a approximately 2, and B(sub t0) approximately 4 T can be driven with P(sub tot) approximately 15 MW to maintain I(sub p) approximately 4.6 MA and produce a peak neutron wall load W(sub L) approximately 1 MW/sq m. Such devices appear possible if the plasma properties at the power R(sub 0)/a remain tokamak-like and, for the D-T case, an unshielded center core is feasible. The use of a single conductor as the inboard leg of the toroidal field coils for this purpose is discussed. The physics issues and the design features are identified for such tokamaks with a testing duty for factor goal of 10-20 percent. DOE

N92-31949# Sandia National Labs., Albuquerque, NM.
PLASMA CHANNEL GENERATION USING LOW ENERGY ELECTRON BEAMS
P. D. Kiekel Feb. 1992 19 p
(Contract DE-AC04-76DP-00789)
(DE92-013770; SAND-91-1626) Avail: CASI HC A03/MF A01

Channel ions can focus and guide a relativistic electron beam. This report discusses the generation of plasma channels using magnetically confined low energy electron beams in a low pressure gas. The most significant advantages of these channels are that any gas can be ionized and that they can easily be made to follow a curved path. The major advantages are that the channel is less well confined than a laser produced channel and that a small solenoidal magnetic field is required. This report is intended to be a guide for those technicians and scientists who need to assemble and operate an e-beam generated plasma channel system. Hardware requirements are discussed in detail. There are brief discussions of operating techniques, channel diagnostic, and channel characteristics. DOE

N92-31983# California Univ., Berkeley. Electronics Research Lab.
EVIDENCE OF STOCHASTIC DIFFUSION ACROSS A CROSS-FIELD SHEATH DUE TO KELVIN-HELMHOLTZ VORTICES
S. E. Parker, X. Q. Xu, A. J. Lichtenberg, and C. K. Birdsall 30 Sep. 1991 57 p
(Contracts N00014-89-J-1097; N00014-90-J-1198)
(AD-A247847; UCB/ERL-M91/79) Avail: CASI HC A04/MF A01

We identify mechanisms for particle transport across a cross-field sheath. We present a study of E x B drift motion in a vortex in which the ion drifts are perturbed by their finite gyroradii, and electron drifts are perturbed by one or more traveling waves. Large scale vortices, which are the result of nonlinear saturation of the Kelvin-Helmholtz instability resulting from shear in the E x B drift velocity, have been observed in plasma simulations of the cross-field sheath. Small scale turbulence is also present, and ions and electrons are transported across the sheath. A vortex alone does not allow for the observed electron transport because the electron drift orbits simply circulate. On the other hand, the ion motion can be stochastic from resonant interaction between harmonics of the drift motion and the gyromotion, independent of the background turbulence. The fluctuations in the ion density would then give rise to a small amplitude wave spectrum. The combined action of the vortex fields and traveling wave fields on the electron motion can then lead to stochastic electron diffusion. We study these effects, showing that the values of vortex fields observed in the simulation are sufficient to lead to both ion and electron stochasticity. Furthermore, the rate of the resulting diffusion is sufficient to account for the diffusion observed in the simulation. GRA

N92-31990# Air Force Inst. of Tech., Wright-Patterson AFB, OH.
AN EXAMINATION OF THE FEASIBILITY OF A NUCLEAR-PUMPED LASER-DRIVEN INERTIAL CONFINEMENT FUSION REACTOR WITH MAGNETICALLY PROTECTED WALLS M.S. Thesis
John M. Jacobson Mar. 1992 62 p
(AD-A248163; AFIT/GNE/ENP/92M-4) Avail: CASI HC A04/MF A01

A preliminary design study of a nuclear-pumped laser-driven inertial confinement fusion reactor with a magnetically protected first wall using an advanced DT-ignited, DD-fueled pellet demonstrated the feasibility of such a concept. This paper presents a parametric study of the required energy multiplication in the blanket, the pellet injection rate, and the net efficiency of this in the conceptual reactor for advanced pellet yields. A model of the reactor energy balance yields a required energy multiplication of 2.4. A cylindrical design for a helium-cooled blanket demonstrates that natural uranium micropellets in a laser pump region provide a multiplication of 2.9 with a subcritical neutron multiplication factor of 0.14. A lithium-oxide layer outside of the laser pump region provides a tritium breeding ratio of up to 0.4, which is more than sufficient to produce enough tritium for advanced DD-fueled, DT-ignited pellets to fuel the reactor. This paper presents the analysis behind these conclusions and presents avenues for further research on this concept. GRA

N92-32181# National Inst. for Fusion Science, Nagoya (Japan).
ENERGY TRANSPORT IN THE STEADY STATE PLASMA SUSTAINED BY DC HELICITY CURRENT DRIVE
K. Itoh, S.-I. Itoh, and A. Fukuyama (Okayama Univ., Japan) Jan. 1992 17 p Submitted for publication
(NIFS-127) Avail: CASI HC A03/MF A01

The steady state operation of tokamaks which is sustained by the DC helicity current drive near edge is obtained. We studied the steady state toroidal plasma where the toroidal current is generated near the edge and transferred to the core region by the cross field transport of the plasma current. If the current diffusivity is high, such a scheme for DC helicity current drive allows enough plasma current at the axis. However, the quantitative estimate of the required value for the current diffusivity shows that the energy transport coefficient must also be high, so that the actual application to high temperature plasmas would be difficult. This indicates the importance of the method for transporting the current. The radio frequency (rf) helicity current drive was shown to work. Author

N92-32208# Polish Academy of Sciences, Warsaw. Inst. Podstawowych Problemow Techniki.
WEAK ION-ACOUSTIC SHOCK WAVES AND DOUBLE LAYERS IN NON-COLLISION PLASMA [SLABE FALE UDERZENIOWE JONOWO-AKUSTYCZNE I WARSTWY PODWOJNE W PLAZMIE BESSDERZENIOWEJ]
Krzysztof Zuchowski 1991 19 p In POLISH
Avail: CASI HC A03/MF A01

An outline of the theory of shock waves in plasma is presented with particular emphasis on waves in the collisionless plasma. In addition, a theory of ion-acoustic waves is presented on the basis of a two-fluid model with modifications resulting from the kinetic theory taken into consideration. The purpose of the work was to compare weak shock waves and double layers in the collisionless plasma because of the absence of explicit definitions and properties discriminating these structures with a low electric potential drop. Also, the permanent magnetic field was not taken into consideration. Identification of these structures is important from the viewpoint of outer space where a large variety of similar phenomena occur: shock waves, double layers, soliton waves, and abnormal resistivity. The difficulties in conducting direct measurements in outer space make it necessary to use additional conclusions. The basic differences between the shock waves and double layers are reflected on the phase plane of ion motion. The shock waves are in motion and the ions in these waves move with supersonic speed while only a small part of captured ions are found. The double layers contain a large amount of captured ions which are static, so a low mass flow occurs here. Author

76 SOLID-STATE PHYSICS

Includes superconductivity.

For related information, see also *33 Electronics and Electrical Engineering* and *36 Lasers and Masers.*

N92-31296# Brookhaven National Lab., Upton, NY.
SPIN POLARIZED PHOTOEMISSION STUDIES OF SURFACES AND THIN-FILMS
P. D. Johnson, N. Brookes, and Y. Chang 1991 10 p Presented at the Spring Meeting of the Materials Research Society, Anaheim, CA, 29 Apr. - 3 May 1991
(Contract DE-AC02-76CH-00016)
(DE92-016098; BNL-47636; CONF-910406-41) Avail: CASI HC A02/MF A01

Spin polarized photoemission is used to study the magnetic states associated with the clean iron (001) surface. These studies reveal evidence for a minority spin surface state in agreement with first principles calculation. Studies of the same surface with silver and chromium epitaxial overlayers reveal evidence for interface states derived from the states found on the clean surface. In the case of the silver overlayer, the binding energy of this state is found to be dependent on the layer thickness of the overlayer. With chromium overlayers the binding energy for the same interface state does not show the same thickness dependence. However, a second interface state is observed immediately below the Fermi level. DOE

N92-31375# Rice Univ., Houston, TX. Dept. of Electrical and Computer Engineering.
GALLIUM ARSENIDE CLUSTERS AND THEIR INTERFACIAL PHYSICS AND CHEMISTRY Final Report, 15 Mar. 1988 - 14 Sep. 1991
Richard E. Smalley, Robert F. Curl, and Frank K. Tittel 15 Jan.

1992 42 p
(Contract DAAL03-88-K-0039)
(AD-A249565; ARO-25222.8-CH) Avail: CASI HC A03/MF A01

Gallium arsenide clusters have been studied on a Fourier transform ion cyclotron resonance (FTICR) mass spectrometer with an external supersonic cluster source. Reaction of GaAs cluster cations with ammonia revealed that all cluster cations larger than seven atoms were most reactive near the 1/1 composition ratio of gallium/arsenic. The results suggest that even at this small size, the clusters begin to adopt the alternating gallium/arsenic bonding arrangement, characteristic of bulk GaAs crystal surfaces where gallium-arsenic bonding activates gallium atoms for ammonia chemisorption. With excess NH3, Ga(x)As(y)NH3(+)(sub z) with the same GaAs composition (x and y) was observed with several values of z, which is explained in terms of the existence of multiple isomers of GaAs clusters. However, the anions were found to be inert toward NH3. Nitric oxide was found to etch singly charged Gax4sy (x + y = 9 to 16) clusters. A pronounced even-odd alternation in cluster ion reactivity towards NO was observed with the odd numbered cluster ions which are believed to be closed shell singlets being much less reactive than the even numbered cluster ions which are of necessity open shell species. The local density calculations of small Ga(x)As(y)(x + y less than 10) have been carried out. Multiple low energy structures were found, and the electronic properties are in agreement with experimental results. GRA

N92-31403# Sandia National Labs., Albuquerque, NM.
A SEALED He-4 SUPERFLUID-TRANSITION FIXED-POINT DEVICE
R. V. Duncan and G. Ahlers (California Univ., Santa Barbara.) 1992 4 p Presented at the 7th International Symposium on Temperature: Its Measurement and Control in Science and Industry, Toronto (Canada), 28 Apr. - 1 May 1992
(Contract DE-AC04-76DP-00789)
(DE92-014271; SAND-91-1615C; CONF-920423-5) Avail: CASI HC A01/MF A01

The superfluid transition in pure He-4 under its saturated vapor pressure provides an ideal fixed-point reference for thermometry near 2 K. In practice, the transition may be located to within a few nanokelvin, and it is virtually immune to drift. Here we first review the properties of He-4 very near the transition which may affect the performance of this fixed-point reference. Then we report on the construction and use of a sealed fixed-point device that requires no external capillaries or valves. It is as easily used in a vacuum cryostat as are superconductive fixed-point devices. Unlike superconductors, it is virtually unaffected by magnetic fields and material purity. DOE

N92-31438# Massachusetts Inst. of Tech., Cambridge. Dept. of Electrical Engineering and Computer Science.
OPTIMIZED PHOTOREFRACTIVE BARIUM TITANATE Final Report, 20 Feb. 1987 - 31 May 1990
Cardinal Warde and Hans P. Jenssen 11 Mar. 1992 100 p
(Contract F19628-87-C-0173)
(AD-A250089) Avail: CASI HC A05/MF A02

The goal of this research program was to investigate new and modified crystal-growth techniques that would lead to high-optical-quality BaTiO3 with increased photorefractive speed and sensitivity. The research program consisted of four parts: (1) feed material purification; (2) crystal growth by the top-seeded-solution technique as well as by a barium borate flux technique; (3) new furnace design studies; and (4) photorefractive characterization experiments. Iron and nickel-doped BaTiO3 crystals were grown under the program. BaTiO3 is a promising photorefractive material due to its large electrooptic coefficient and excellent self-pumped phase conjugation. Our furnaces were limited by certain design and operating characteristics, and crystals grown in these furnaces were easily contaminated by the furnace itself. Two new furnaces, cylindrical and octagonal furnaces, were developed with commercially available parts that are cleaner, more mechanically reproducible, more uniform in temperature and more responsive to control action through reduced thermal mass. The two furnaces are equipped with precise computer control of the pulling and rotation system. The cylindrical furnace was found to be susceptible to cracking due to expansion when heated and to shrinkage after heating. To prevent cracking, expansion joints were provided and the insulation set was made of flat plates set up in an octagonal pattern. GRA

N92-31446# North Carolina State Univ., Raleigh.
GROWTH, NITROGEN VACANCY REDUCTION AND SOLID SOLUTION FORMATION IN CUBIC GaN THIN FILMS AND THE SUBSEQUENT FABRICATION OF SUPERLATTICE STRUCTURES USING AlN AND InN Final Technical Report, 1 Jun. 1986 - 31 Dec. 1991
Robert F. Davis Feb. 1992 58 p
(Contract N00014-86-K-0686)
(AD-A248058) Avail: CASI HC A04/MF A01

An atomic layer epitaxy deposition system configured for the growth of thin films of the III-V nitrides of Al, Ga and In has been designed, constructed and commissioned. The system allows the introduction of up to 16 gases without mixing. Self-terminating growth of crystalline GaN films has been achieved on single crystal wafers of (0001) alpha(6H)-SiC. Results of analyses via Auger spectroscopy, electron microscopy and electron diffraction are described. Deposition of AlN and GaN via gas-source MBE was also continued during this period. The principal emphasis concerned the initial stages of growth of both compounds on the substrates of (00001) alpha(6H)-SiC and (0001) sapphire, as determined using X-ray photoelectron spectroscopy. An initial layer of silicon nitride formed on the surface of SiC prior to the deposition of either nitride. The deposition of GaN on sapphire followed the Stranski-Krastanov mode of nucleation and growth, while on SiC, characteristics of three-dimensional growth were evident. By contrast, AlN grew initially in a layer-by-layer mode. Deposition of GaN on vicinal (100) Beta-SiC during UV irradiation resulted in the formation of a new 4H polytype of this material. Deposition of BN via gas-source MBE on Cu(110) resulted in nanocrystalline cBN; films grown on (111) Cu resulted in h-BN (graphitic phase). Similar studies using Si(100) substrates also resulted in the occurrence of cBN. The occurrence of the cubic polytype was enhanced while that of h-BN was discouraged with the use of the UV light at 400-500 C. GRA

N92-31496# Princeton Univ., NJ. Dept. of Electrical Engineering and Computer Science.
SUBMILLIMETER WAVE SPECTROSCOPY OF HETEROJUNCTION SUPERLATTICES Final Technical Report, 1 Oct. 1990 - 30 Sep. 1991
D. C. Tsui 2 Apr. 1992 11 p
(Grant AF-AFOSR-2048-88)
(AD-A250835; AFOSR-92-0304TR) Avail: CASI HC A03/MF A01

The general objectives of this research are to systematically investigate the interaction of electromagnetic radiation in the far infrared range with the charge carriers in semiconductor heterojunction superlattice structures. Experiments are performed on both the lattice-matched GaAs/Al(x)Ga(1-x)As/GaAs heterojunction material structures and the strained-layer material of In(x)Ga(1-x)As/GaAs heterostructure. In the former case, new electronic processes are discovered and their possible detector application is explored. In the latter case, the energy level structure is determined and the carrier dynamics are studied using the submillimeter wave spectroscopy. GRA

N92-31537# Virginia Univ., Charlottesville. School of Engineering and Applied Science.
INTERNATIONAL SEMICONDUCTOR DEVICE RESEARCH SYMPOSIUM (ISDRS-91)
Michael Shur and John M. Money Mar. 1992 7 p Symposium held in Charlottesville, VA, 4-6 Dec. 1991
(AD-A247394; UVA/525465/EE92/101) Avail: CASI HC A02/MF A01

The First International Semiconductor Device Research Symposium took place in Charlottesville, VA, on 4-6 Dec. 1991

for the purpose of providing a convenient forum for the exchange of information and new ideas for researchers from industry, university, and government laboratories with leading researchers from the US, Canada, Europe, Asia, and the former Soviet Union. As the first international conference of its kind to take place after the Aug. 1991 coup attempt in the Soviet Union, it was unique with the presence of an unusually large contingent of Russian scientists. The emphasis of the program was on advanced semiconductor technologies still in their infancy whose tangible technological outcomes are not expected for another five to ten years. Some of the technologies discussed at the symposium included bandgap engineering, large area semiconductor electronics, new millimeter wave and optoelectronic technologies, and silicon carbide and diamond devices. GRA

N92-31546# Argonne National Lab., IL.
COMPUTER SIMULATION OF SCATTERED ION AND SPUTTERED SPECIES EFFECTS IN ION BEAM SPUTTER-DEPOSITION OF HIGH TEMPERATURE SUPERCONDUCTING THIN FILMS
A. R. Krauss and O. Auciello (Microelectronics Center of North Carolina, Research Triangle Park.) 1992 10 p Presented at the Material Research Society Spring Meeting, San Francisco, CA, 17 Apr. - 2 May 1992
(Contract W-31-109-eng-38)
(DE92-015227; ANL/CP-76122; CONF-920402-31) Avail: CASI HC A02/MF A01

Ion beam sputter-deposition is a technique currently used by many groups to produce single and multicomponent thin films. This technique provides several advantages over other deposition methods, which include the capability for yielding higher film density, accurate stoichiometry control, and smooth surfaces. However, the relatively high kinetic energies associated with ion beam sputtering also lead to difficulties if the process is not properly controlled. Computer simulations have been performed to determine net deposition rates, as well as the secondary erosion, lattice damage, and gas implantation in the films, associated with primary ions scattered from elemental Y, Ba and Cu targets used to produce high temperature superconducting Y-Ba-Cu-O films. The simulations were performed using the TRIM code for different ion masses and kinetic energies, and different deposition geometries. Results are presented for primary beams of Ar(+), Kr(+), and Xe(+) incident on Ba and Cu targets at 0 degrees and 45 degrees with respect to the surface normal, with the substrate positioned at 0 degrees and 45 degrees. The calculations indicate that the target composition, mass and kinetic energy of the primary beam, angle of incidence on the target, and position and orientation of the substrate affect the film damage and trapped primary beam gas by up to 5 orders of magnitude. DOE

N92-31582# Utah Univ., Salt Lake City. Dept. of Materials Science and Engineering.
NEW SOURCES FOR OMVPE
G. B. Stringfellow 19 Jul. 1991 13 p Submitted for publication
(Contract N00014-91-J-1447)
(AD-A250903; TR-30) Avail: CASI HC A03/MF A01

Until recently, the choice of group III and group V source molecules for organometallic vapor phase epitaxy (OMVPE) of III/V semiconductors has been relatively simple. The group III precursors were either the trimethyl- or triethyl-alkyls and only AsH3 and PH3 produced device quality material. The hazard posed by the hydride group V sources, as well as the desire for precursor molecules producing higher quality epitaxial layers, has motivated the development of new, organometallic group V precursor molecules. Novel group III precursors are also under development for reduction of carbon contamination, reduction of the growth temperature, use for selective growth and atomic layer epitaxy, and for use at very low pressures. Fundamental knowledge of bond strengths between metal atoms and various radicals, as well as the reactivity of the radicals, has guided the development of these new source materials. Some knowledge of the actual chemical reactions occurring during growth is also necessary for the intelligent design of new precursor molecules. This paper reviews the status of several novel precursors as well as the pyrolysis and growth reactions occurring during their use in atmospheric pressure OMVPE growth. GRA

N92-31627# Brookhaven National Lab., Upton, NY.
OXYGEN ORDERING AND STRAIN-RELATED MORPHOLOGY IN YBa2Cu(3-x)O7 SYSTEMS
Zhi-Xiong Cha, Yimei Zhu, and D. O. Welch 1992 6 p Presented at the International Conference on Martensitic Transformations, Monterey, CA, 20-24 Jul. 1992
(Contract DE-AC02-76CH-00016)
(DE92-014476; BNL-47474; CONF-920722-1) Avail: CASI HC A02/MF A01

Monte Carlo simulations were performed on an anisotropic lattice gas model which represent well the interactions between oxygen atoms in YBa2Cu3O7 systems doped with trivalent impurity atoms M such as Fe or Al. Concentration wave amplitudes obtained from these simulations were used to calculate the diffuse X-ray scattering intensity caused by the resulting displacement field using a concentration wave/displacement wave approach, and the results are compared with X-ray and electron diffraction data. The results suggest that the small orthorhombic domains associated with the oxygen 'cross-links' around impurity atoms M cause the diffuse scattering intensity to fall off with the scattering wave vector difference q from a Bragg peak as 1/q(exp 2) for small q and as 1/q(exp 4) for larger q. We show that the average size of such domains can be obtained from diffuse X-ray scattering data. DOE

N92-31652# Argonne National Lab., IL.
ION BEAM SPECTROSCOPY AS A MEANS OF IN-SITU MONITORING OF THIN FILM DEPOSITION
A. R. Krauss, M. Rangaswamy, G. Lamich, D. M. Gruen, J. A. Schultz (Ionwerks, Houston, TX.), and H. Schmidt (Schmidt Instruments, Houston, TX.) 1992 12 p Presented at the International Conference on Metallurgical Coatings and Thin Films, San Diego, CA, 6-10 Apr. 1992
(Contract W-31-109-eng-38)
(DE92-014857; ANL/CP-75799; CONF-920439-7) Avail: CASI HC A03/MF A01

Low energy (5-15 keV) pulsed beam Ion Scattering Spectroscopy (ISS) and Direct Recoil Spectroscopy (DRS) are surface analytical tools which possess the ability to provide a remarkably wide range of information directly relevant to the growth of multi-component semiconductor, metal and metal oxide thin films and layered structures. Ion beam methods have not been widely used for this purpose because the design of existing commercial instrumentation is unsuitable in terms of vacuum requirements, data acquisition rate, geometric interference with the deposition equipment, and the magnitude of the ion beam dose and consequent film damage required for the acquisition of spectra with reasonable signal-noise ratios. Users of advanced custom-built Time-of-Flight (TOF) instruments have been largely interested in other problems and for the most part, unaware of some of the unique operational characteristics of TOF DR/ISS as they pertain to thin film growth. We discuss here some of the physical properties which may be measured by DR/ISS and describe a physical implementation of the technique which is suitable as a real-time probe of thin film deposition in terms of very low required beam dose, rapid data acquisition, physical non-interference with the deposition equipment and high ambient pressure operation. DOE

N92-31655# International Centre for Theoretical Physics, Trieste (Italy).
SCHWINGER BOSON STUDIES OF THE t-J MODEL BEYOND MEAN-FIELD APPROXIMATION
Y. M. Li (Warwick Univ., Coventry, England), L. Yu (Academia Sinica, Beijing, China), D. N. Sheng (Academia Sinica, Beijing, China), and Z. B. Su (Academia Sinica, Beijing, China) Dec. 1991 24 p
(DE92-630650; IC-91/391) Avail: CASI HC A03/MF A01

A self-consistent systematic expansion is developed for the t-J model in the Schwinger boson approach. We treat the fermion part beyond the mean-field approximation and study the effects of magnetic fluctuations on the normal state properties. It is found that the hole motion is strongly renormalized and incoherent bands are produced by magnetic fluctuations. The conductivity and the electron density of states are calculated and shown to be anomalous. The antiferromagnetic nature of fluctuations is found to be essential for these unusual properties. The relevance of the obtained results to oxide superconductors is also discussed. DOE

N92-31661# Lawrence Livermore National Lab., CA.
PHOTON ABSORPTION AND THE DECAY OF SURFACE EXCITATION ON SAPPHIRE (1120)-(3 X 1)
A. V. Hamza, R. S. Hughes, Jr., L. L. Chase, and H. W.H. Lee Oct. 1991 9 p Presented at the SPIE International Society for Optical Engineering Meeting, Boulder, CO, 23-25 Oct. 1991
(Contract W-7405-eng-48)
(DE92-011533; UCRL-JC-109627; CONF-911064-9) Avail: CASI HC A02/MF A01

A laser-based two-pulse correlation technique is used to investigate the mechanisms of photon absorption and the decay of surface excitation on Al2O3(1120). The mechanism for emission of positive or neutral particles depends on the wavelength and/or pulsewidth. In our previous study for a pulsewidth of 80 picoseconds at 1064 nm the lifetime of the surface excitation leading to detectable emission and further to optical surface damage was measured to be (approximately) 200 picoseconds. However, for 800 femtosecond pulses at 616 nm the measured lifetime is a few nanoseconds. In both cases a low-order absorption process is indicated. DOE

N92-31665# Pacific Northwest Lab., Richland, WA.
STRESS AND PHASE TRANSFORMATION PHENOMENA IN OXIDE FILMS
G. J. Exarhos and N. J. Hess Apr. 1992 12 p Presented at the Material Research Society Spring Meeting, San Francisco, CA, 27 Apr. - 2 May 1992
(Contract DE-AC06-76RL-01830)
(DE92-014702; PNL-SA-20854; CONF-920402-16) Avail: CASI HC A03/MF A01

In situ optical methods are reviewed for characterization of phase transformation processes and evaluation of residual stress in solution-deposited metastable oxide films. Such low density films most often are deposited as disordered phases making them prone to crystallization and attendant densification when subjected to increased temperature and/or applied pressure. Inherent stress imparted during film deposition and its evolution during the transformation are evaluated from phonon frequency shifts seen in Raman spectra (TiO2) or from changes in the laser-induced fluorescence emission spectra for films containing rare earth (Sm(sup +3):Y23Al5O3) or transition metal (Cr(sup +3):Al2O3) dopants. The data in combination with measured increases in line intensities intrinsic to the evolving phase are used to follow crystallization processes in thin films. In general, film deposition parameters are found to influence the crystallite ingrowth kinetics and the magnitude of stress and stress relaxation in the film during the transformation. The utility of these methods to probe crystallization phenomena in oxide films will be addressed. DOE

N92-31666# New York Univ., New York.
US-JAPAN SEMINAR ON MAGNETIC MULTILAYERED STRUCTURES: PROCEEDINGS
17 May 1992 75 p Seminar held in Kauai, HI, 15-17 May 1992
(Contract N00014-92-J-1386)
(AD-A252440) Avail: CASI HC A04/MF A01

To study structural aspects associated with its elastic anomaly in a superlattice, we developed a unique x-ray diffraction method on a synchrotron radiation source by using a diamond-anvil high-pressure cell (DAC). By applying hydrostatic pressure accessible to 10GPa to a superlattice specimen, we obtain its linear/bulk compressibility from the Bragg peak shift and analyze its structure from the Bragg intensities. By using this technique, we have studied elastic properties of two metallic superlattices Au/Ni(fcc/fcc)2 and Mo/Ni(bcc/fcc)3 as well as a semiconductive one, PbSe/SnSe4. The slope of the line drawn in the figure represents compressibility (inverse of elastic modulus) of each layer. GRA

N92-31668# Sandia National Labs., Albuquerque, NM.
A COMPARISON OF INTERSTITIAL OXYGEN CALCULATED BY DIFFERENT TECHNIQUES
J. W. Medernach and J. O. Stevenson 1992 3 p Presented at the 181st Meeting of the Electrochemical Society, Inc., St. Louis, MO, 17-22 May 1992
(Contract DE-AC04-76DP-00789)
(DE92-011658; SAND-91-2693C; CONF-920514-3) Avail: CASI HC A01/MF A01

Methods which report an ability to determine interstitial oxygen (O(sub i)) in heavily doped silicon include the short baseline (SBL) and the curved baseline (CBL) techniques. Both the SBL and CBL methods are similar with the exception of the calibration. We developed a FORTRAN software package to provide separate methods for calculating O(sub i). The strength of the software is its ability to rapidly compare methods. We report on a comparison of calculation methods including the ASTM standard test F1188-88 which is used in a calibration, and the SBL and the CBL methods, which are used for the heavily doped silicon to provide reliable results. The O(sub i) values calculated for both virgin and thermally processed silicon are reported. DOE

N92-31699# Minnesota Univ., Minneapolis. Dept. of Chemistry.
ULTRAFAST EXPERIMENTS ON THE ROLE OF VIBRATIONAL MODES IN ELECTRON TRANSFER
Alan E. Johnson, Nancy E. Levinger, Dahv A. Kliner, Keisuke Tominaga, and Paul F. Barbara 18 May 1992 7 p
(Contract N00014-89-J-1746)
(AD-A250630) Avail: CASI HC A02/MF A01

The role of vibrational modes in ultrafast photoinduced intramolecular electron transfer reactions is explored. Femtosecond resolved experiments on two chemical classes will be described, namely, metal-metal intervalence electron transfer in mixed valence compounds and intromolecular charge recombination/separation in organic door/acceptor compound class, the betaines. The results have been analyzed to reveal the complex interactions of intromolecular and intermolecular modes in electron transfer reactions. The study of charge transfer processes, and in particular homogeneous electron transfer (ET) in solution, is at the forefront of the study of the molecular details of chemical reactions in liquids. The last decade has brought progress to many central problems in ET research, including the role of the solvent in these reactions, the involvement of vibrational degrees of freedom, the role of nuclear tunnneling of the solvent and solute (and related quantum mechanical effects), the pathway and mechanism of electronic interactions, including long range ET, and other aspects of biological and heterogeneous ET. Recent reviews of the foundations of ET theories have been given by Newton and Sutin and Marcus and Sutin. Theories of ET reactions in solution are formulated in terms of a model in which the transferring electron is localized at a donor molecular site in the reactant and at a different acceptor molecular site in the product. GRA

N92-31719# Lawrence Livermore National Lab., CA.
SUBNANOSECOND PHOTOCONDUCTIVE SWITCHING IN GaAs
R. L. Druce, M. D. Pocha, and K. L. Griffin Apr. 1991 13 p Presented at the 1st Los Alamos Symposium on Ultra-wideband Radar, Los Alamos, NM, 5-8 Mar. 1990 Revised
(Contract W-7405-eng-48)
(DE92-011521; UCRL-JC-103782-Rev-1; CONF-900397-3-Rev-1) Avail: CASI HC A03/MF A01

We are conducting research in photoconductive switching for the purpose of generating microwave pulses with amplitudes up to 50 kV. This technology has direct application to impulse radar and HPM sources. We are exploiting the very fast recombination

rates of Gallium Arsenide (GaAs) to explore the potential of GaAs as an on-off switch when operating in the linear mode (the linear mode is defined such that one carrier pair is generated for each photon absorbed). In addition, we are exploring the potential GaAs to act as a closing switch in 'avalanche' mode at high fields. We have observed switch closing times of less than 200 psec with a 100 psec duration laser pulse and opening times of less than 400 psec with neutron irradiated GaAs at fields of tens of kV/cm. If the field is increased and the laser energy decreased, the laser can be used to trigger photoconductive switches into 'avalanche' mode of operation in which carrier multiplication occurs. This mode of operation is quite promising since the switches close in less than 1 nsec while realizing significant energy gain (ratio of electrical energy in the pulse to optical trigger energy). We are currently investigating both large area (1 sq cm) and small area (less than 1 sq mm) switches illuminated by GaAlAs laser diodes at 900 nm and Nd:YAG lasers at 1.06 micrometers. Preliminary results indicate that the closing time of the avalanche switches depends primarily on the material properties of the devices with closing times of 300-1300 psec at voltages of 6-35 kV. We will present experimental results for linear, lock on, and avalanche mode operation of GaAs photoconductive switches and how these pulses may be applied to microwave generation. DOE

N92-31723# Los Alamos National Lab., NM.
MICROSTRUCTURE AND PROPERTIES OF IN-SITU RF SPUTTERED YBa2Cu3O7 THIN FILMS FOR MICROWAVE APPLICATIONS
D. W. Reagor, R. J. Houlton, F. H. Garzon, M. Hawley, I. D. Raistrick, and M. E. Piza 1992 11 p Presented at the Material Research Society Spring Meeting, San Francisco, CA, 27 Apr. - 2 May 1992
(Contract W-7405-eng-36)
(DE92-013379; LA-UR-92-1435; CONF-920402-3) Avail: CASI HC A03/MF A01

The residual surface resistance of a number of films of YBa2Cu3O7, prepared by off-axis sputtering onto MgO substrates, has been measured using parallel-plate resonator technique. Deposition conditions were kept constant, apart from the substrate temperature. There is no correlation between surface resistance and other important microscopic parameters, such as T(sub c) and c-axis lattice parameter. There is, however, a trend to higher R(sub s) with increasing volume fraction of in-plane misoriented material, although the correlation is not perfect. Furthermore, we have found that most of the misoriented material is localized at the film substrate interface and, therefore, is probably not responsible for most of the RF losses. The data suggest that at higher deposition temperatures, there is an increasing tendency for 45 degree-misoriented material to appear in the films, and it may be that a significant fraction of this material is present closer to the free film surface. STM qualitatively supports this conclusion. DOE

N92-31819# Brown Univ., Providence, RI. Dept. of Chemistry.
THE CRYSTAL GROWTH AND CHARACTERIZATION OF THE SOLID SOLUTIONS (ZnS)(1-x)(CuMS2)(x)
Y. R. Do, K. Dwight, and A. Wold 24 Mar. 1992 19 p
(Contract N00014-89-J-1849)
(AD-A248029; TR-20) Avail: CASI HC A03/MF A01

Polycrystalline samples of members of the systems (ZnS)1-x(CuMS2)x(M = Al, In or Fe) were prepared by direct combination of the elements. Single crystals have been grown by chemical vapor transport using iodine as the transport agent. They all crystallize with the zinc blend structure. Their IR transmission range is narrower than that observed for pure Zinc Sulfide, but all, except for the ZnS-CuInS2 system, still show good transmission in the long wavelength IR range. The addition of small amounts of I-III-VI2 modifies the hardness and the thermal stability of ZnS. Zinc Sulfide has been studied extensively because it offers a variety of unique device applications. ZnS crystallizes with the cubic zinc blend structure below 1020 C and with the hexagonal wurtzite structure above this phase transition temperature. The ternary chalcogenides, CuMS2(M = Al, Ga, In or Fe) crystallize with the chalcopyrite structure, which is closely related to the cubic zinc blend structure. In the chalcopyrite structure, there is an ordering of Cu(I) and M(III) (M = Al, Ga, In Or Fe) which results in a doubling of the c-axis. There have been relatively few studies carried out on the preparation and characterization of solid solutions formed between ZnS and CuMS2(M = Al, Ga, In or Fe). GRA

N92-31848# Cornell Univ., Ithaca, NY. Dept. of Chemistry.
SYNTHESIS, STRUCTURE AND PROPERTIES OF Ba6Co25S27: A PEROVSKITE-LIKE SUPERSTRUCTURE OF Co8S6 AND Ba6S CLUSTERS
G. J. Snyder, Michael E. Badding, and F. J. DiSalvo 30 May 1992 36 p
(Contract N00014-91-J-1269)
(AD-A251041) Avail: CASI HC A03/MF A01

We have prepared single crystals of a new ternary barium cobalt sulfide, Ba6Co25S27 by cooling a melt containing BaS, CoS, and Co from 975 C. The structure, determined by single crystal X-ray diffraction, is cubic (Pm3M) with a = 10.033(3)A, Z = 1, and R = 2.6 percent, Rw = 2.4 percent. The structure contains an octahedrally coordinated cobalt atom, nearly cubic clusters of eight cobalt atoms, and an unusual arrangement of barium atoms. The electric resistivity and magnetic susceptibility measurements show that Ba6Co25S27 is a poor metal with a resistance minimum at 8 K, and Pauli paramagnetic with a small Curie contribution indicating that either the Co8 cluster or the octahedrally coordinated cobalt atom has a magnetic moment. GRA

N92-31851# Pittsburgh Univ., PA. Surface Science Center.
THE THERMAL DISSOCIATION OF DECABORANE ON Si(111)-(7X7) AND DOPING EFFECTS IN THE NEAR SURFACE REGION
P. J. Chen, M. L. Colaianni, and J. T. Yates, Jr. 1 May 1992 31 p
(Contract N00014-82-K-0280)
(AD-A251057; TR-44) Avail: CASI HC A03/MF A01

The thermal decomposition of decaborane (BIOH14) and its doping effects on Si(111)-(7 by 7) has been investigated by surface spectroscopies. Upon adsorption between 100-300 K, molecular decaborane was identified on the surface by HREELS by the absence of Si-H surface species production. The thermal decomposition of adsorbed decaborane molecules involves a preferential removal of hydrogen from the weaker B-H-B linkage. H2 thermal desorption was observed to cover a wide temperature range between 300-900 K. Clean boron deposition on the surface was achieved at approximately 900 K. Upon heating to approximately 1275 K, extensive boron diffusion into bulk silicon produced a highly B-doped region below the surface (approximately 10(exp 3) A) with a carrier hole concentration on the order of approximately 10(exp 19) cm(exp -3) depending upon the initial surface boron coverage and annealing conditions. The surface adopted a(square root of 3 by square root of 3)R30 deg reconstruction with a nominal 1/3 ML boron occupying subsurface substitutional sites. Both the localized B-Si vibration and carrier surface plasmon excitation were observed by HREELS at 100 K. GRA

N92-31914# Florida State Univ., Tallahassee.
He ATOM-SURFACE SCATTERING: SURFACE DYNAMICS OF INSULATORS, OVERLAYERS AND CRYSTAL GROWTH
1992 37 p
(Contract DE-FG05-85ER-45208)
(DE92-011810; DOE/ER-45208/7) Avail: CASI HC A03/MF A01

Investigations in this laboratory have focused on the surface structure and dynamics of ionic insulators and on epitaxial growth onto alkali halide crystals. In the latter the homoepitaxial growth of NaCl/NaCl(001) and the heteroepitaxial growth of KBr/NaCl(001), NaCl/KBr(001) and KBr/RbCl(001) have been studied by monitoring the specular He scattering as a function of the coverage and by measuring the angular and energy distributions of the scattered He atoms. These data provide information on the

surface structure, defect densities, island sizes and surface strain during the layer-by-layer growth. The temperature dependence of these measurements also provides information on the mobilities of the admolecules. He atom scattering is unique among surface probes because the low-energy, inert atoms are sensitive only to the electronic structure of the topmost surface layer and are equally applicable to all crystalline materials. It is proposed for the next year to exploit further the variety of combinations possible with the alkali halides in order to carry out a definitive study of epitaxial growth in the ionic insulators. The work completed so far, including measurements of the Bragg diffraction and surface dispersion at various stages of growth, appears to be exceptionally rich in detail, which is particularly promising for theoretical modeling. In addition, because epitaxial growth conditions over a wide range of lattice mismatches is possible with these materials, size effects in growth processes can be explored in great depth. Further, as some of the alkali halides have the CsCl structure instead of the NaCl structure, we can investigate the effects of the heteroepitaxy with materials having different lattice preferences. Finally, by using co-deposition of different alkali halides, one can investigate the formation and stability of alloys and even alkali halide superlattices. DOE

N92-31915# Minnesota Univ., Minneapolis. Dept. of Physics.
EPITAXIAL IRON FILMS Final Report, 15 Dec. 1988 - 15 Dec. 1991
E. D. Dahlberg and P. I. Cohen 15 Feb. 1992 13 p
(Grant AF-AFOSR-0248-89)
(AD-A250402; AFOSR-92-0276TR) Avail: CASI HC A03/MF A01

This research involved studies of the magnetic properties of multilayered magnetic films and high quality thin films. Ultra-high vacuum sputtering and molecular beam epitaxy techniques were utilized to prepare the films. Electrical transport and magneto-optic effects were used to measure the magnetic properties of the films. The focus was determination of the temperature dependence of the magnetic anisotropy energies of epitaxial iron films, the magnetization dynamics of thin films, and the transport properties of multilayers. In the anisotropy energy work the effects of interfacial strain and morphology were the focus. The dynamics effort has recently provided a model for slow dynamic systems. The transport effort utilized multilayers of magnetic and nonmagnetic metals to study the interfacial scattering. The combination of a magnetic and nonmagnetic metal in this work facilitates the origin of the scattering by use of the anisotropic magnetoresistance. GRA

N92-31937# California Univ., Santa Barbara.
ABSORPTION SPECTRA AND ELECTRONIC PROPERTIES OF ALKALI METAL DOPED C60 Technical Report No. 8, 1 Jun. 1991 - 31 May 1992
V. I. Srdanov, A. P. Saab, D. Margolese, E. Poolman, and K. C. Khemani 15 May 1992 9 p
(Contract N00014-90-J-1159)
(AD-A251006) Avail: CASI HC A02/MF A01

Changes in optical absorption spectra of approximately 500 A thick films of C60 during doping with alkali metals (A = Li, Na, K, and Rb) were recorded. The stoichiometry of the potassium-doped C60 films was monitored by simultaneous in situ measurements of electrical conductivity. The spectral changes indicate that the molecular solid behavior of C60 bulk is preserved in the A6C60 phase. Assignments for the C60 and K6C60 absorption spectra based on molecular orbitals of C60 are discussed. GRA

N92-31945# Ohio Univ., Athens. Dept. of Physics and Astronomy.
ELECTRONIC STATES IN SYSTEMS OF REDUCED DIMENSIONALITY
S. E. Ulloa 15 Apr. 1992 9 p
(Contract DE-FG02-87ER-45334)
(DE92-013588; DOE/ER-45334/5) Avail: CASI HC A02/MF A01

This report briefly discusses the following research: magnetically modulated systems, inelastic magnetotunneling, ballistic transport review, screening in reduced dimensions, raman and electron energy loss spectroscopy, and ballistic quantum interference effects. DOE

N92-31955# Argonne National Lab., IL.
RECENT ADVANCES IN HIGH-TEMPERATURE SUPERCONDUCTOR WIRE FABRICATION AND APPLICATIONS DEVELOPMENT
J. R. Hull and K. L. Uherka 1992 19 p Presented at the 27th Intersociety Energy Conversion Engineering Conference, San Diego, CA, 3-7 Aug. 1992
(Contract W-31-109-eng-38)
(DE92-016634; ANL/CP-75477; CONF-920801-12) Avail: CASI HC A03/MF A01

In this paper, recent advances in fabrication of HTS wires are summarized, and detailed discussion is provided for developments in near- and intermediate-term applications. Near-term applications, using presently obtainable current densities, include: liquid-nitrogen depth sensors, cryostat current leads, and magnetic bearings. Intermediate-term applications, using current densities expected to be available in the near future include fault-current limiters and short transmission lines. DOE

N92-31984# Rochester Univ., NY. Dept. of Mechanical Engineering.
MECHANICS OF THIN FILMS Final Report, 1 Jul. 1987 - 30 Jun. 1991
J. C. Lambropoulos 6 Feb. 1992 151 p
(Contract N00014-87-K-0488)
(AD-A247848) Avail: CASI HC A08/MF A02

Problems in the mechanics and thermomechanics of thin films have been addressed: anisotropic stresses in films of cubic anisotropy oriented along the group of zone axes (100), (111), or (110) normals on a substrate; and relaxation in thin films by time-independent plastic deformation along the film substrate interface, by cracking, or by stress-induced diffusional flow during film growth. The toughening effect on brittle components of thin films in residual compression has been calculated and compared to experimental data. Motivated by measurements (using the thermal comparator technique) of thin film thermal conductivity where the film conductivity was found to be up to two orders of magnitude lower than that of the corresponding solid, the thermal conductivity of thin dielectric films has been correlated to microstructural features such as grain size and film thickness. The implications of reduced film thermal conductivity were examined for laser damage where nonlinear effects were shown to be important. The effects of film anisotropy and interfacial thermal resistance have been analyzed, and the contribution of microporosity to interfacial thermal resistance has been calculated. For thermally anisotropic films, an equivalent isotropic film of properly chosen thickness and conductivity could be identified. Length scales have been established against which the film thickness is to be compared. GRA

N92-31994# George Washington Univ., Washington, DC. Dept. of Chemistry.
AUGER LINE SHAPES AS A PROBE OF ELECTRONIC STRUCTURE IN COVALENT SYSTEMS Interim Technical Report No. 57
David E. Ramaker Jan. 1992 14 p
(Contract N00014-91-J-1896)
(AD-A246329; TR-57) Avail: CASI HC A03/MF A01

Our goal has been to develop a generally applicable, semi-empirical approach for quantitatively interpreting Auger line shapes for covalently bonded systems. In this regard, we examine four main topics. First, because the Cini-Sawatzky theory was originally derived for initially filled, single bands in metals, we present our grounds for applying it to covalent systems. Second, we examine the problem of unfilled bands, and third, we emphasize the importance of satellites. The role of satellites are examined with regard to benzene, graphite, and the new carbon material, C60, often referred to as 'buckyball'. Finally, we present results of an application to 'carbidic' carbon on Ni, where fundamental

new information was obtained concerning the nucleation of graphite at higher temperatures. In our discussions, results from the interpretation of the C KVV Auger line shapes of five different gas phase hydrocarbons (methane, ethane, cyclohexane, benzene, and ethylene), five different solids (polyethylene, diamond, graphite, 'buckyball', and nickel carbides), and a molecularly chemisorbed system (ethylene/Ni) are included. GRA

N92-31995# George Washington Univ., Washington, DC. Dept. of Chemistry.
DISSOCIATIVE ELECTRON ATTACHMENT OF O2: A SOLID-STATE EFFECT ON POTENTIAL CURVE CROSSING Interim Technical Report No. 58
Hideo Sambe and David E. Ramaker Jan. 1992 11 p
(Contract N00014-91-J-1896)
(AD-A246331; TR-58) Avail: CASI HC A03/MF A01

Previously published data on electron stimulated desorption (ESD) from condensed oxygen or oxygen solid matrices are reanalyzed. In the gas phase, the resonant state at 8.5 eV is known to dissociate predominantly into the second lowest limit. In this paper, we point out that this dissociation requires a nonadiabatic curve crossing. In the condensed phase or solid matrices, this resonant state is found to dissociate adiabatically into the lowest limit as well as nonadiabatically into the second limit. Furthermore, we find that the branching ratio strongly depends on the kinetic energy of the dissociating atoms. The singlet excited oxygen atom formed upon dissociation into the second limit, is found to participate in an anion complex formation via incage recombination. According to the Wigner-Witmer correlation rule, the lowest state must dissociate adiabatically into the lowest limit. However, Belic and Hall found that the (lowest) state dissociates into the second lowest limit almost exclusively. This implies that the state must cross a curve in the dissociation terminating at the second lowest limit. GRA

N92-32065# Washington State Univ., Pullman.
PARTICLE EMISSION AND CHARGING EFFECTS INDUCED BY FRACTURE Final Report, 1 Jun. 1987 - 30 Jun. 1992
J. T. Dickinson 30 Jun. 1992 16 p
(Contract N00014-87-K-0514)
(AD-A252182; FRACTO-92) Avail: CASI HC A02/MF A01

We summarize three research areas that have focused on surface dynamics associated with fracture and UV laser bombardment of materials. These studies were based on our capabilities to (1) detect and characterize particle release from surfaces on fast time scales, and (2) obtain high resolution topographical information utilizing scanning tunneling and atomic force microscopy. Three principle areas of study have been fracto-emission, scanning tunneling microscopy studies of fracture surfaces of crystals and polymers, and UV laser interactions with surfaces. These studies have focused on the examination of the energetic processes accompanying fracture, particularly those involving heat generating mechanisms such as dislocation motion and plastic deformation, phenomena at interfaces (often involving charge transfer processes), and high energy UV lasers interacting with inorganic and organic materials. GRA

N92-32072# National Inst. of Standards and Technology, Gaithersburg, MD. Ceramics Div.
FERROELECTRIC THIN FILMS PREPARED BY PULSE LASER DEPOSITION PROCESSING AND CHARACTERIZATION
L. P. Cook, C. K. Chiang, and P. K. Schenck May 1992 124 p
(PB92-196088; NISTIR-4844) Avail: CASI HC A06/MF A02

Described here is the development of piezoelectric lead zirconate-titanate (PZT) and barium titanate (BT) thin films for application to non-volatile memories for electronic devices such as computers. The work was done in the period from January 1989 to December 1991 in the Ceramics and Metallurgy Divisions at the National Institute of Standards and Technology, under the partial support of the Department of the Army through the Harry Diamond Laboratory. Author

N92-32078# Army Lab. Command, Fort Monmouth, NJ. Electronics Technology and Devices Lab.
MOVEMENT OF DISLOCATIONS IN QUARTZ
R. A. Murray Apr. 1992 12 p Presented at the 45th Annual Symposium on Frequency Control, 1991
(DA Proj. 1L1-62705-AH-94)
(AD-A250527; SLCET-TR-92-2) Avail: CASI HC A03/MF A01

Dislocations in quartz crystals have been known to cause problems in the fabrication of resonators by the formation of etch channels. The etch channels are known to weaken the physical strength of quartz blanks and to reduce the yield in photolithographic production processes. While it is possible to reduce the etch channel density in quartz by post growth electro-diffusion, this does not reduce the dislocation density. It is suspected that dislocations contribute to acceleration sensitivity, thermal hysteresis, and possibly aging. The behavior of dislocations in quartz is also of interest to the fields of geophysics, seismology, and plate tectonics because it affects the underground movement of rock. Specifically, the movement of dislocations in quartz is the mechanism through which quartz can be plastically deformed. A large body of literature on the movement of dislocations in natural and cultured quartz has been published in various geophysical journals over the past thirty years. This paper is a review of this literature and its possible implications for frequency control. GRA

N92-32085# Oak Ridge National Lab., TN.
IMAGING AND SPECTROMETRY OF BULK CRYSTAL SURFACES AND SURFACE DYNAMICAL PROCESSES AT HIGH TEMPERATURES
Z. L. Wang and J. Bentley (Tennessee Univ., Knoxville.) 1992 4 p Presented at the 5th Asia-Pacific Electron Microscopy Conference, Beijing (China), 1-6 Aug. 1992
(Contract DE-AC05-84OR-21400)
(DE92-015235; CONF-920891-1) Avail: CASI HC A01/MF A01

The use of electron energy-loss spectrometry (EELS) in the glancing-incidence, surface reflection mode (i.e., REELS) for bulk samples is an attractive technique since the signal comes mostly from electrons that have penetrated just a few atomic layers. The analysis of the composition and structure of thin surface layers can form an important adjunct to high resolution surface imaging by reflection electron microscopy (REM) in a conventional TEM instrument. In REELS, the energy spectrum at energy-losses lower than 50 eV is mostly determined by the collective excitation of the valence electrons near the surface. In this paper, the emphasis is on the high energy-losses due to atomic core-shell excitations in the reflection mode and REM imaging. DOE

N92-32166# Lawrence Livermore National Lab., CA.
ALUMINUM TUNNEL JUNCTION DETECTOR OPERATION IN AN ADIABATIC DEMAGNETIZATION REFRIGERATOR
S. Labov, E. Silver, M. LeGros, R. W. Bland (San Francisco State Univ., CA.), S. C. Dickson (San Francisco State Univ., CA.), T. G. Dignan (San Francisco State Univ., CA.), K. Laws (San Francisco State Univ., CA.), R. T. Johnson (San Francisco State Univ., CA.), M. W. Simon (San Francisco State Univ., CA.), and D. A. Stricker (San Francisco State Univ., CA.) et al 30 Jan. 1992 7 p Presented at the 4th International Workshop on Low Temperature Detectors and Dark Matter, Oxford, England, 4-7 Sep. 1991
(Contract W-7405-eng-48)
(DE92-013441; UCRL-JC-110033; CONF-9109317-2) Avail: CASI HC A02/MF A01

Superconducting tunnel junction detectors are being developed as both particle and X-ray detectors. Aluminum junctions are desirable for detectors because of their strong native oxide barriers, and because the small energy gap of aluminum is a good match to ballistic phonons generated by particle interactions in single crystals of silicon or other low acoustic-loss insulating crystals. Aluminum tunnel junction detectors must be operated near 0.1 T(sub C) which is 110 mK for aluminum. To operate detectors at these temperatures, we have developed adiabatic demagnetization refrigerators (ADRs) for the laboratory and prototype ADRs for space based operation. These cryogenic systems are simpler, more

convenient and more portable than most dilution refrigerators. We have demonstrated that the magnetic field of the ADR need not compromise the performance of aluminum tunnel junctions. We have recently initiated a program to develop superconducting tunnel junctions (STJs) as high resolution X-ray detectors and low energy threshold particle detectors. This complements our existing program in which we are developing high resolution X-ray microcalorimeter detectors. One of our goals for both of these cryogenic detector development efforts is to observe X-ray emission from cosmic sources. This requires a refrigeration system that can operate under zero gravity space flight conditions. For the microcalorimeter project, temperatures of 100 mK and below are required to sufficiently reduce the heat capacity of the device. DOE

N92-32207# Lasergenics Corp., San Jose, CA.
SINGLE CRYSTAL GROWTH OPTIMIZATION OF MAGNESIUM-DOPED LITHIUM NIOBATE Final Report, Sep. 1988 - Dec. 1991
R. G. Schlecht, C. I. Zanelli, A. M. Schlecht, P. F. Bordui, and C. D. Bird Apr. 1992 52 p
(Contract DAAL04-88-C-0029)
(AD-A250781; MTL-TR-92-24) Avail: CASI HC A04/MF A01

The purpose of the Phase 2 program entitled Single Crystal Growth Optimization of Magnesium-Doped Lithium Niobate was to optimize the growth of MgO:LiNbO3. The first step in this direction consisted of developing means and methods to accurately measure absorption losses (scattering loss methods were previously developed under a Phase 1 contract). It was known at the outset that very sensitive instrumentation would be required to allow measurements on small samples. The results of the measurements of both types of photon loss would then be used to optimize the molar concentration of MgO in LiNbO3 to achieve crystals with low loss as well as high photorefractive damage threshold. Highly sensitive scattering and absorption facilities were developed and used in the process of optimizing crystal growth. The ability to accurately and routinely measure these parameters has allowed us to understand variability in the growth process, determine growth parameters, and, most importantly, to observe that specific propagation and polarization directions are significantly less lossy than others. Studies were performed on the growth, poling, and resulting properties of MgO-doped lithium niobate. Both photorefractive damage threshold and NLO phase-matching temperature were observed to vary with MgO concentration. For one crystal doped with a high MgO concentration, it was impossible to induce measurable photorefractive damage. GRA

N92-32209# Polish Academy of Sciences, Warsaw. Inst. Podstawowych Problemow Techniki.
INVESTIGATION OF ACOUSTIC PROPERTIES OF HIGH-TEMPERATURE CERAMIC SUPERCONDUCTORS [BADANIE AKUSTYCZNYCH WLASCIWOSCI WYSOKOTEMPERATUROWYCH NADPRZEWODNIKOW CERAMICZNYCH]
Aleksander Opilski (Silesian Technical Univ., Gliwice, Poland) and Jerzy Krzak (Silesian Technical Univ., Gliwice, Poland) 1991 38 p In POLISH
Avail: CASI HC A03/MF A01

Because of the unsatisfactory condition of the high temperature superconductivity theory, attention has been focused on the significance of experimental studies, in particular acoustic studies. Given here is a review of literature dealing with the results of these studies on ceramic samples of Y-Ba-Cu-O. The results of studies conducted by four methods are presented: superficial waves, resonance, volumetric waves, and acoustic emission. Author

77 THERMODYNAMICS AND STATISTICAL PHYSICS

Includes quantum mechanics; theoretical physics; and Bose and Fermi statistics.

For related information see also *25 Inorganic and Physical Chemistry* and *34 Fluid Mechanics and Heat Transfer.*

N92-31402# International Centre for Theoretical Physics, Trieste (Italy).
A DYNAMICAL MODEL OF THE BEHAVIOUR OF HADRONIC AND FUNDAMENTAL STRINGS AT FINITE DENSITIES
F. Lizzi, I. Senda, and R. R. Viswanathan Dec. 1991 31 p
(DE92-630245; IC-91/388) Avail: CASI HC A03/MF A01

A dynamical model of interacting strings with fixed total energy and finite energy density is studied. Results previously obtained for the case when the kinetic energy is small are extended by means of a fully relativistic analysis. The nonlinear dynamical equations of the model are solved numerically and the equilibrium configurations for the case of both fundamental strings and the flux tube model of hadrons are investigated as a function of the energy density. Our results strongly suggest the formation of a resonance dominated phase for sufficiently large energy densities. The model is applied to the study of the evolution of hadronic matter produced in ion collision experiments, where the formation of a resonance dominated phase is noted immediately after the collision. Our results indicate that this non-equilibrium state decays rapidly and relaxes to equilibrium very soon after the collision, with a typical time scale of T approximately = 1/m(sub pi) approximately = 5 x 10(exp -24)s. DOE

N92-31489# Naval Postgraduate School, Monterey, CA.
NATURAL CONVECTION IMMERSION COOLING OF AN ARRAY OF VERTICALLY ORIENTED HEATED PROTRUSIONS IN AN ENCLOSURE FILLED WITH A DIELECTRIC LIQUID: EFFECTS OF ENCLOSURE WIDTH, PRANDTL NUMBER AND COMPONENT ORIENTATION M.S. Thesis
Scott T. Matthews Dec. 1991 97 p
(AD-A245884) Avail: CASI HC A05/MF A02

The natural convection heat transfer characteristics of a 3 x 3 array of vertically oriented heated protrusions, immersed in a dielectric liquid, were investigated. Aluminum blocks, 24 x 8 x 6 mm, were used to simulate 20 pin dual in-line packages. Surface temperature measurements of the components were made by imbedding copper-constantan thermocouples below the surface of each component face. A constant heat flux was provided to each component using an Inconel foil heating element. Power supplied to each component varied from 0.115 to 2.90 W. The aluminum blocks were mounted on a plexiglass substrate to form a 3 x 3 array of simulated electronic components. The circuit board containing the components was placed in a rectangular, plexiglass enclosure with inner dimensions: L = 203.2 mm H = 152.0 mm W = 82.6 mm, and a wall thickness of 25.4 mm. The upper boundary was maintained at 10 C, while all other exterior surfaces were insulated. The chamber width, measured from the surface of the circuit board to the opposite, inner wall of the enclosure, was varied from 42 to 7 mm by inserting plexiglass spacers into the enclosure. Two dielectric liquids, FC-75 and FC-43, were used as working fluids. Nondimensional data from this study was combined with the data obtained for a horizontal component orientation, to develop an empirical correlation which predicts the Nusselt number as a function of Rayleigh number, Prandtl number, component orientation, and chamber width. GRA

N92-31577*# Texas A&M Univ., College Station.
AN APPROXIMATE LOCAL THERMODYNAMIC NONEQUILIBRIUM RADIATION MODEL FOR AIR
Thomas A. Gally and Leland A. Carlson 1992 20 p
(Grant NAG1-1003)
(NASA-CR-190580; NAS 1.26:190580) Copyright Avail: CASI HC A03/MF A01

A radiatively coupled viscous shock layer analysis program which includes chemical and thermal nonequilibrium is used to

calculate stagnation point flow profiles for typical aeroassisted orbital transfer vehicle conditions. Two methods of predicting local thermodynamic nonequilibrium radiation effects are used as a first and second order approximation to this phenomena. Tabulated results for both nitrogen and air freestreams are given with temperature, species, and radiation profiles for some air conditions. Two body solution results are shown for 45 and 60 degree hyperboloid bodies at 12 km/sec and 80 km altitude. The presented results constitute an advancement in the engineering modeling of radiating nonequilibrium reentry flows. Author

N92-31585# Brown Univ., Providence, RI. Div. of Applied Mathematics.

GEOMETRIC THEORY OF INFINITE DIMENSIONAL DYNAMICAL SYSTEMS Final Report, 15 Aug. 1988 - 14 Oct. 1991

C. Dafermos, J. Mallet-Paret, P. Souganidis, and W. A. Strauss 14 May 1992 9 p

(Contract F49620-88-C-0129)

(AD-A252190; AFOSR-92-0545TR) Avail: CASI HC A02/MF A01

A subject of investigation was the extent to which an entropy inequality (i.e., the Second Law of Thermodynamics) induces stabilization of solutions of hyperbolic systems of conservation laws. It was shown that the entropy inequality guarantees uniqueness of Lipschitz solutions within the class of BV solutions, provided that the entropy is convex just in certain directions compatible with the natural invariance of the system expressed in terms of involutions. It was proven that BV solutions of strictly hyperbolic systems with shocks of moderate strength, which satisfy the Liu admissibility condition, minimize the rate of total entropy production. The theory of generalized characteristics for a single conservation law, developed earlier by the author, was applied to conservation laws with inhomogeneity and fading memory. The theory of generalized characteristics was developed for systems of conservation laws and was used to obtain information on the large time behavior of solutions. This theory was employed to establish uniqueness of solutions for special systems of conservation laws in which shock and rarefaction wave curves coincide. GRA

N92-31645# National Inst. of Standards and Technology, Gaithersburg, MD.

NOISE-INDUCED CHAOS AND PHASE SPACE FLUX: A SAMPLE-THEORETIC STUDY

M. Frey and E. Simiu Mar. 1992 37 p Prepared in cooperation with Johns Hopkins Univ., Baltimore, MD Sponsored in part by Minerals Management Service, Washington, DC

(PB92-172733; NISTIR-4791) Avail: CASI HC A03/MF A01

The authors study the effect of additive noise on near-integrable second-order dynamical systems whose unperturbed flows have homoclinic or heteroclinic orbits. The noise is represented by a type of Shinozuka stochastic process capable of arbitrarily closely approximating Gaussian noise with any specified spectrum. The authors derive a formula for the flux factor applicable for any asymptotic mean stationary excitation. The derivation shows that, to first order, the effect of the external excitation on the system is mediated by a linear filter associated with the system homoclinic or heteroclinic orbit. It also shows that the stationary mean distribution of the filtered excitation determines the average phase space flux. This is true for both random and nonrandom excitations and indicates that, for the dynamical systems considered here, these two classes of excitation play substantially equivalent roles in the promotion of chaos. Author

N92-31660# Messerschmitt-Boelkow-Blohm G.m.b.H., Munich (Germany, F.R.).

PRESSURE LOSS AND HEAT TRANSFER IN A TOOTHED FINNED HEAT TRANSFER MEDIUM [DRUCKVERLUST UND WAERMEUEBERGANG IN EINEM ZAHNRIPPENWAERMEUEBERTRAGER]

W. D. Ebeling (Erno Raumfahrttechnik G.m.b.H. Bremen, Germany, F.R.) and B. J. G. Leidinger (Erno Raumfahrttechnik G.m.b.H. Bremen, Germany, F.R.) 1991 5 p Repr. from Brennstoff-Waerme-Kraft, v. 43, no. 11, 24-27 Sep. 1991 p 528-533 In GERMAN

(MBB-UO-0163-91-PUB; ETN-92-91891) Avail: CASI HC A01/MF A01

Thermohydraulic investigation was carried out in a special toothed-finned geometry, which was provided for increasing heat transfer in an evaporator cooler. The evaporator cooler has applications in space navigation. The toothed-finned heat carrier was used in a counter current, with a view to simplifying the heat transfer coefficient evaluation, from the temperature and volume flows measured. Test results obtained confirmed the suitability of this test arrangement. Relationships were derived from test results, for the pressure loss coefficient and the Nusselt number, with regard to the Reynolds number for this determined finned geometry. ESA

N92-31663# Stanford Linear Accelerator Center, CA.

THE RQM TRIANGLE: A PARADIGM FOR RELATIVISTIC QUANTUM MECHANICS

H. P. Noyes Feb. 1992 12 p Presented at the 8th Annual Western Regional Meeting of the Alternative Natural Philosophy Association (ANPA), Stanford, CA, 15-17 Feb. 1992

(Contract DE-AC03-76SF-00515)

(DE92-011583; SU-SLAC-PUB-5752; CONF-9202100-1) Avail: CASI HC A03/MF A01

A simple way to relate Lorentz transformations to a finite and discrete model of counter firings is presented. We first abstract from counter firings with finite resolution to rational fraction velocities and a finite step-length. Discrete Lorentz transformations and quantized rotations follow. These are encoded by three integers and a triangle with integer sides: the RQM Triangle. The double slit experiment allows us to observe quantized space steps and measure invariant step lengths for any particle in rational ratio to one such length for any convenient reference particle. A discrete version of the Mandelstam analysis of elastic and anelastic scattering is implied. The results fit naturally into the bit-string formalism used in earlier work. DOE

N92-31767# Naval Postgraduate School, Monterey, CA.

FURTHER STUDIES IN FILMWISE CONDENSATION OF STEAM ON HORIZONTAL FINNED TUBES M.S. Thesis

Keith A. Swensen Mar. 1992 141 p

(AD-A252705) Avail: CASI HC A07/MF A02

Over the years, there has been significant variation in the filmwise steam condensation data at NPS on horizontal low-integral finned tubes. With a view to increasing the accuracy of the data, inserts were used inside the tubes to reduce inside thermal resistance; however, significant discrepancies then occurred in the calculated outside heat-transfer coefficient when compared to data taken without an insert. These discrepancies arose due to the data reduction technique which assumes a known inside heat-transfer resistance and subtracts this from a measured overall resistance. If the assumed value on the inside is inaccurate, then the outside value is equally inaccurate. The present work uses an instrumented smooth tube to obtain accurate inside heat-transfer correlations both with and without inserts and uses these to obtain accurate outside coefficients for a family of uninstrumented finned tubes with a view to finding an optimum fin spacing for steam condensation. GRA

N92-31953# Rutherford Appleton Lab., Chilton (England).

MINIMAL SUPERSYMMETRIC UNIFICATION PREDICTIONS

G. G. Ross (Oxford Univ., England) and R. G. Roberts Jan. 1992 31 p

(RAL-92-005; ETN-92-91721) Avail: CASI HC A03/MF A01

The predictions for the gauge couplings in the minimal extension of the standard model, which result from the assumption that the model comes from a unified theory with a single scale of breaking, are reexamined. The effects of thresholds are considered both at the unification scale and at the low energy scale of the new supersymmetric states. The latter are found to be particularly important and are analyzed using the supergravity spectrum

corresponding to common scalar and gaugino masses plus other soft supersymmetry breaking terms corrected by gauge and Yakawa radiative corrections. The analysis is extended to include the prediction for the W boson mass coming from the radiatively induced spontaneous symmetry breaking of the standard model. The requirement that this be within the measured value without fine tuning strongly limits the magnitude of the supersymmetry breaking scale and the resulting predictions for the detailed mass spectrum of the supersymmetric states and the Higgs bosons. The bottom quark mass is also determined using the full two loop renormalization group equation with the unification prediction m(sub b) m(sub tau) at the compactification scale. ESA

80 SOCIAL SCIENCES (GENERAL)

Includes educational matters.

N92-32160# National Center for Education Statistics, Washington, DC.
INTERNATIONAL MATHEMATICS AND SCIENCE ASSESSMENTS: WHAT HAVE WE LEARNED
E. A. Medrich and J. E. Griffith Jan. 1992 148 p
(PB92-183599; NCES-92-011) Avail: CASI HC A07/MF A02

Over the past quarter century, there have been five major international studies of science and mathematics achievement at the elementary, middle, and secondary school levels. The studies have been conducted under the auspices of two different nongovernmental research consortia. More than 30 countries have participated in at least one of the surveys. The United States has been involved in every one. A great variety of findings have resulted from the work, and these studies represent valuable contributions to the ways in which schooling inputs and outcomes are understood. The research has challenged participating countries to examine the structure, practices, and curricula of their educational systems, and as a consequence, to envision the possibility of rethinking curriculum content and the ways in which students are taught. A description of the international assessments and some of their findings are presented, and issues surrounding the collection and analysis of these data are addressed. Further, it offers suggestions about ways in which new data collection standards could improve the quality of the surveys and the utility of the reports in the future. Author

81 ADMINISTRATION AND MANAGEMENT

Includes management planning and research.

N92-31253*# National Aeronautics and Space Administration, Washington, DC.
SMALL BUSINESS INNOVATION RESEARCH PROGRAM SOLICITATION. CLOSING DATE: JULY 21, 1992
1992 116 p
(NASA-TM-107795; NASA-SBIR-92-1; NAS 1.15:107795) Avail: CASI HC A06/MF A02

The National Aeronautics and Space Administration (NASA) invites small businesses to submit Phase 1 proposals in response to its Small Business Innovation Research (SBIR) Program Solicitation 92-1. Firms with research or research and development capabilities (R/R&D) in science or engineering in any of the areas listed are encouraged to participate. This, the tenth annual SBIR solicitation by NASA, describes the program, identifies eligibility requirements, describes the proposal evaluation and award selection process, and provides other information to assist those interested in participating in NASA's SBIR program. It also identifies, in Section 8.0, the technical topics and subtopics in which SBIR Phase 1 proposals are solicited in 1992. These topics and subtopics cover a broad range of current NASA interests but do not necessarily include all areas in which NASA plans or currently conducts research. The NASA SBIR program seeks innovative approaches that respond to the needs, technical requirements, and new opportunities described in the subtopics. The focus is on innovation through the use of emerging technologies, novel applications of existing technologies, exploitation of scientific breakthroughs, or new capabilities or major improvements to existing technologies. NASA plans to select about 320 high-quality research or research and development proposals for Phase 1 contract awards on the basis of this Solicitation. Phase 1 contracts are normally six months in duration and funded up to $50,000, including profit. Selections will be based on the competitive merits of the offers and on NASA needs and priorities. Author

N92-31364# Small Business Administration, Washington, DC. Office of Minority Small Business and Capital Ownership Development.
REPORT TO THE US CONGRESS ON MINORITY SMALL BUSINESS AND CAPITAL OWNERSHIP DEVELOPMENT AS REQUIRED BY THE BUSINESS OPPORTUNITY DEVELOPMENT REFORM ACT OF 1988
Oct. 1991 177 p
(PB92-173681) Avail: CASI HC A09/MF A02

This is the first report on the Minority Small Business and Capital Ownership Development program as required by the Business Opportunity Development Reform Act of 1988. Congress emphasized that section 8(a) of the Small Business Act will remain 'a primary tool for improving opportunities for small business concerns owned and controlled by socially and economically disadvantaged individuals'. To ensure that the progress of the 8(a) Program is effectively measured, Congress directed the U.S. Small Business Administration to develop and implement a process for the systematic collection of data on the operations of the program. GRA

N92-31547*# Research Inst. for Computing and Information Systems, Houston, TX.
A PROPOSED GROUP MANAGEMENT SCHEME FOR XTP MULTICAST Interim Report
Bert J. Dempsey (Digital Technology, Inc., Champaign, IL.) and Alfred C. Weaver (Digital Technology, Inc., Champaign, IL.) Aug. 1990 12 p
(Contract NCC9-16; RICIS Proj. SE-31)
(NASA-CR-190633; NAS 1.26:190633) Avail: CASI HC A03/MF A01

The purpose of a group management scheme is to enable its associated transfer layer protocol to be responsive to user determined reliability requirements for multicasting. Group management (GM) must assist the client process in coordinating multicast group membership, allow the user to express the subset of the multicast group that a particular multicast distribution must reach in order to be successful (reliable), and provide the transfer layer protocol with the group membership information necessary to guarantee delivery to this subset. GM provides services and mechanisms that respond to the need of the client process or process level management protocols to coordinate, modify, and determine attributes of the multicast group, especially membership. XTP GM provides a link between process groups and their multicast groups by maintaining a group membership database that identifies members in a name space understood by the underlying transfer layer protocol. Other attributes of the multicast group useful to both the client process and the data transfer protocol may be stored in the database. Examples include the relative dispersion, most recent update, and default delivery parameters of a group. H.A.

N92-31992# Naval Research Lab., Washington, DC.
DEVELOPMENT OF A FAULT ISOLATION SYSTEM DATABASE MANAGER Final Report, 1990-1992
C. B. Barclay and J. A. Molnar 10 Feb. 1992 69 p
(AD-A248346; NRL/MR/5524-92-6944) Avail: CASI HC A04/MF A01

The Fault Isolation System Database Manager (FISDM) is an interactive database interface developed to enhance data and configuration management of causal models. A causal model of a Unit Under T describes the interrelationship of the electronic

components composing the UUT. The interface, written in C, was integrated with the Empress data management software package to access data manipulation routines. Standard data manipulation features are incorporated to enhance the creation and management of the knowledge database. Output features allow delivery of the data in multiple formats. The format required for the Fault Isolation System (FIS) knowledge database is produced directly as an output option. Additionally, a comma delimited format compatible with other database and spreadsheet software provides portability and flexibility for configuration management. Data management is achieved through maintenance of a standard format which can be translated to working version in other formats. FISDM permits central management of expert systems that require occasional modifications from multiple sources. This is a situation which often occurs over the fielded lifetime of military electronic systems. GRA

N92-32037# Sandia National Labs., Albuquerque, NM.
HEURISTIC SAMPLING ON DAGS
Pang-Chieh Chen Jun. 1992 17 p
(Contract DE-AC04-76DP-00789)
(DE92-017359; SAND-90-0444) Avail: CASI HC A03/MF A01

Many problems in computer applications can in theory be solved by searching through a directed-acyclic graph (DAG). In practice, however, this approach has been hampered by our analytical inability to predict the search cost accurately without actually implementing and executing the program. To overcome this inability, a simple and quick heuristic procedure based on a stratified sampling approach is presented. In generalizes a tree sampling technique already shown to be useful in predicting the performance of tree-searching programs. With the addition of this DAG sampling procedure, we should be able to forecast the complexity and feasibility of alternative tree or DAG searching algorithms so that we may utilize our computational resources more effectively. DOE

N92-32017 Tennessee Univ. Space Inst., Tullahoma. Commercial Experiment Transporter Program.
COMET: COMMERCIAL SPACE OPPORTUNITIES THROUGH DEVELOPED TECHNOLOGIES
Carter H. Myers *In* Huntsville Association of Technical Societies, TABES 92: 8th Annual Technical and Business Exhibition and Symposium. Executive Summaries and Submitted Papers 1992 7 p (For primary document see N92-32009 22-12)
(TABES Paper 92-453) Copyright Avail: Issuing Activity

82 DOCUMENTATION AND INFORMATION SCIENCE

Includes information management; information storage and retrieval technology; technical writing; graphic arts; and micrography.

For computer documentation see *61 Computer Programming and Software.*

N92-31272*# Research Inst. for Computing and Information Systems, Houston, TX.
ASSESSING REPOSITORY TECHNOLOGY. WHERE DO WE GO FROM HERE?
David Eichmann (West Virginia Univ., Morgantown.) 28 Feb. 1992 22 p
(Contract NCC9-16; RICIS Proj. SE-43)
(NASA-CR-190630; NAS 1.26:190630) Avail: CASI HC A03/MF A01

Three sample information retrieval systems, archie, autoLib, and Wide Area Information Service (WAIS), are compared with regard to their expressiveness and usefulness, first in the general context of information retrieval, and then as prospective software reuse repositories. While the representational capabilities of these systems are limited, they provide a useful foundation for future repository efforts, particularly from the perspective of repository distribution and coherent user interface design. Author

N92-31285# Carnegie-Mellon Univ., Pittsburgh, PA.
TYPE EVOLUTION AND INSTANCE ADAPTATION Final Report
Stewart M. Clamen 2 Mar. 1992 24 p
(Contract N00014-88-K-0641)
(AD-A248435) Avail: CASI HC A03/MF A01

Schema evolution support is an important facility for object-oriented database (OODB) systems. While existing OODB systems provide for limited forms of evolution, including modification to the database schema and reorganization of affected instances, we find their support insufficient. Specific deficiencies are (1) the lack of compatibility support for old applications, and (2) the lack of ability to install arbitrary changes upon the schema and database. This paper examines the limitations of existing schemes, and offers a more general framework for specifying and reasoning about the evolution of class definitions and the adaptation of existing, persistent instances to those new definitions. GRA

N92-31288# Department of Energy, Washington, DC.
FEDIX: THE ON-LINE DATABASE RETRIEVAL SERVICE OF GOVERNMENT INFORMATION FOR COLLEGES, UNIVERSITIES, AND OTHER ORGANIZATIONS
1992 79 p
(DE92-012384; DOE/ER-0533P) Avail: CASI HC A05/MF A01

FEDIX is an on-line information service that links the higher education community and the federal government to facilitate research, education, and services. The system provides accurate and timely federal agency information to colleges, universities, and other research organizations. There are no registration fees and no access charges for using FEDIX. Agencies participating in the FEDIX system include Department of Energy (DOE), Federal Aviation Administration (FAA), National Aeronautics and Space Administration (NASA), Office of Naval Research (ONR), Air Force Office of Scientific Research (AFOSR), National Science Foundation (NSF), National Security Agency (NSA), Department of Commerce (DOC), Department of Education (DOEd), Department of Housing and Urban Development (HUD), and Agency for International Development (AID). Additional government agencies are expected to join FEDIX in the near future. This guide is intended to help users access and utilize the FEDIX system. Because the system is frequently updated, some menus and tables used as examples in this text may not exactly match those displayed on the live system. DOE

N92-31371# National Inst. of Standards and Technology, Gaithersburg, MD. Office Systems Engineering Group.
NEXT GENERATION DOCUMENTS
Ronald B. Wilson and Roger F. Sies Apr. 1992 20 p
(PB92-187103; NISTIR-4830) Avail: CASI HC A03/MF A01

The object of the report is to identify PB91-187773 the goals of the Next Generation Document (NGD). On March 25, 1991, the National Institute of Standards and Technology (NIST) presented a workshop on NGDs on behalf of the Computer-aided Logistics and Acquisition Support (CALS) project. Staff members from various Department of Defense (DoD) services came together to exchange information on topics concerning NGDs. These individuals were primarily supervisors working within the document processing field. NIST wanted to learn from them: (1) what is a next generation document, and (2) what requirements the NGD must meet in the future. The report discusses the current DoD environment, its need to alter its business practices, and the movement towards the Open Systems Environment (OSE). The report also illustrates a NGD scenario and provides a listing of NGD requirements/services. Author

N92-31396# Wright State Univ., Dayton, OH. Dept. of Computer Science and Engineering.
ARIEL DATABASE RULE SYSTEM PROJECT Final Report, 15 Apr. 1989 - 14 Jan. 1992
Eric N. Hanson 14 Jan. 1992 14 p
(Grant AF-AFOSR-0286-89)
(AD-A250443; AFOSR-92-0272TR) Avail: CASI HC A03/MF A01

The Ariel project has led to several advancements in active

database technology and the development of a working prototype active database system. Ariel is unique in its support for efficient rule condition testing based on a discrimination network and in its tight integration of rule processing with database transaction processing. An efficient index for testing single-relation selection predicates was developed, which also resulted in the development of two new types of interval index data structures, the interval binary search tree, and the interval skip-list. For testing join conditions, a modified version of the TREAT algorithm, called A-TREAT, was developed. A-TREAT is suitable for use in a database environment. It's major new feature is the concept of virtual alpha-memory nodes, which, unlike normal alpha-memories, do not contain the data matching the associated selection predicate. Instead, virtual alpha-memories contain only the predicate. GRA

N92-31398# Environmental Protection Agency, Washington, DC. Office of Solid Waste.
RCRIS DATA ELEMENT DICTIONARY, VERSION 3.0.0: DATA TAPE DOCUMENTATION
25 Nov. 1991 577 p
(PB92-145515) Avail: CASI HC A25/MF A06

The report is the data element dictionary for the Resource Conservation and Recovery Information System (RCRIS). The data includes each hazardous waste facility name, Environmental Protection Agency (EPA) number, address, owner and operator information, facility contact name and telephone number. GRA

N92-31448# EG and G Energy Measurements, Inc., Albuquerque, NM.
AN ALTERNATIVE TO SNEAKERNET
S. Orrell and S. Ralstin 1992 19 p Presented at the DOE Computer Security Group Conference, Las Vegas, NV, 4-7 May 1992
(Contract DE-AC08-88NV-10617)
(DE92-011146; EGG-10617-6085; CONF-9205130-1) Avail: CASI HC A03/MF A01

Many computer security plans specify that only a small percentage of the data processed will be classified. Thus, the bulk of the data on secure systems must be unclassified. Secure limited access sites operating approved classified computing systems sometimes also have a system ostensibly containing only unclassified files but operating within the secure environment. That system could be networked or otherwise connected to a classified system(s) in order that both be able to use common resources for file storage or computing power. Such a system must operate under the same rules as the secure classified systems. It is in the nature of unclassified files that they either came from, or will eventually migrate to, a non-secure system. Today, unclassified files are exported from systems within the secure environment typically by loading transport media and carrying them to an open system. Import of unclassified files is handled similarly. This media transport process, sometimes referred to as sneaker net, often is manually logged and controlled only by administrative procedures. A comprehensive system for secure bi-directional transfer of unclassified files between secure and open environments has yet to be developed. Any such secure file transport system should be required to meet several stringent criteria. It is the purpose of this document to begin a definition of these criteria. DOE

N92-31450# Naval Postgraduate School, Monterey, CA.
IMPLEMENTING RELATIONAL OPERATIONS IN AN OBJECT-ORIENTED DATABASE M.S. Thesis
Stephen C. Filippi Mar. 1992 176 p
(AD-A249332) Avail: CASI HC A09/MF A02

This thesis expands the concepts of relational/object-oriented database systems. There are two different approaches to combining relational and object-oriented databases. This thesis takes the approach of adding relational operations to an object-oriented database rather than building an object-oriented layer on top of an existing relational database. The system proposed in this thesis was developed in the object-oriented programming language Prograph. It was chosen because it contains primitive operations for reading and writing database files to secondary storage and for manipulating complex data types (e.g., sounds, and pictures). This thesis demonstrates that the limitations of current systems can be remedied and that the relational/object-oriented database management system is indeed a feasible solution. GRA

N92-31455* National Aeronautics and Space Administration, Washington, DC.
NASA PATENT ABSTRACTS BIBLIOGRAPHY: A CONTINUING BIBLIOGRAPHY. SECTION 2: INDEXES (SUPPLEMENT 41)
Jul. 1992 578 p
(NASA-SP-7039(41)-Sect-2; NAS 1.21:7039(41)-Sect-2) Avail: CASI HC A25

A subject index is provided for over 5200 patents and patent applications for the period May 1969 through June 1992. Additional indexes list personal authors, corporate authors, contract numbers, NASA case numbers, U.S. patent class numbers, U.S. patent numbers, and NASA accession numbers. Author

N92-31467# Naval Oceanographic and Atmospheric Research Lab., Bay Saint Louis, MS.
DEEP-TOW ACOUSTICS/GEOPHYSICS SYSTEM COMPRESSIONAL VELOCITY DATABASE Final Report
M. M. Rowe and J. F. Gettrust May 1992 22 p
(AD-A252700; NOARL-TN-257) Avail: CASI HC A03/MF A01

This technical note describes the Deep-Tow Acoustics/Geophysics System (DTAGS) compressional velocity database, a compilation of compressional velocity functions derived from DTAGS deep-tow multichannel seismic data. Three geologically distinct areas are represented by the velocity functions included in this database: thick turbidites on the Bermuda Rise, fine grained terrigenous sediments containing methane hydrate on the Blake Outer Ridge, and thin sediments overlying a young basement near the Juan de Fuca Ridge. Horizontal sampling frequency of the database ranges from 45 to 230 m. Vertical sampling frequency ranges from 20 to 300 m. These compressional velocity profiles, functions of geographic region, layer thickness and range along the ship track, were determined from the DTAGS multichannel seismic data using standard semblance velocity analysis procedures. The six ASCII files containing compressional velocity data are included on an MS-DOS 3-1/2 diskette which may be ordered from the authors using the form included with this technical note. Included on the disk with the data files are two test files containing a description of the data file format and a list of locations where the data were collected. GRA

N92-31482# Naval Command, Control and Ocean Surveillance Center, San Diego, CA.
STI HANDBOOK: GUIDELINES FOR PRODUCING, USING, AND MANAGING SCIENTIFIC AND TECHNICAL INFORMATION IN THE DEPARTMENT OF THE NAVY. A HANDBOOK FOR NAVY SCIENTISTS AND ENGINEERS ON THE USE OF SCIENTIFIC AND TECHNICAL INFORMATION
M. E. Cathcart 1 Feb. 1992 288 p
(AD-A252439) Avail: CASI HC A13/MF A01

Numerous and complex regulations govern scientific and technical information (STI). To help you understand these regulations and how they impact your work, the Office of Naval Technology had this handbook prepared. STI regulations - both the Navy's and DoD's - have been explained in the context of how STI is managed within the Department of the Navy. The information in this handbook is based on the concept that scientific and technical information is part of the entire RDT and E process. You, as a Navy scientist or engineer, are involved with STI from the conceptual phase of your project until its transfer as an operational system. The Navy operates its scientific and technical information program (STIP) to: (1) Assist Navy scientists and engineers in their work; (2) Ensure that scientific and technical information provides the maximum contribution to advancing science and engineering; (3) Expeditiously, effectively, and efficiently conduct and manage Navy research, engineering, and studies; (4) Eliminate unnecessary duplication of resources and

efforts; and (5) Encourage and expedite the exchange and use of STI. GRA

N92-31578# Sandia National Labs., Albuquerque, NM.
ENVIROTRADE: A TECHNICAL PERSPECTIVE ON THE DEVELOPMENT OF AN INFORMATION SYSTEM PROVIDING DATA ON ENVIRONMENTAL TECHNOLOGIES AND NEEDS WORLDWIDE
M. W. Harrington and C. P. Harlan 1992 6 p Presented at the Innovative Technologies for Cleaning the Environment: Air, Water, and Soil, Erice (Italy), 22-29 Apr. 1992
(Contract DE-AC04-76DP-00789)
(DE92-012625; SAND-92-0637C; CONF-9204121-2) Avail: CASI HC A02/MF A01

In support of the U.S. Department of Energy's commitment to the remediation of waste sites throughout its complex, the DOE has recognized that it can accelerate its technology development efforts and leverage the expenditure of available funds through an international cooperation among government entities, private industry, and educational institutions. To support the technology transfer of environmental information, the DOE has sponsored the development of EnviroTRADE - an international information system that will facilitate the exchange of environmental restoration and waste management technologies worldwide. The system will contain profiles on both environmental restoration/waste management needs and foreign/domestic technologies. Users will be able to identify matches between worldwide needs and available or emerging technologies. Where matches between needs and existing technologies are not found, the system will identify the potential for development of new and innovative technologies to address environmental problems. EnviroTRADE will also provide general information on international environmental restoration and waste management organizations, sites, activities, and contacts. DOE

N92-31581# Westinghouse Savannah River Co., Aiken, SC.
OBJECTS USED TO IMPLEMENT INTELLIGENT DATABASES
W. S. Parks 1991 24 p Presented at the Artificial Intelligence (AI) in the Department of Energy (DOE) Complex Meeting, Oak Ridge, TN, 29-31 Oct. 1991
(Contract DE-AC09-89SR-18035)
(DE92-013098; WSRC-MS-91-439; CONF-9110341-3) Avail: CASI HC A03/MF A01

This paper presents a database construction useful for a rapid-prototyping environment. Intelligent systems require a priori knowledge and accumulated data to perform heuristics. Often the types of information required to make decisions are scattered and not well formed. The accumulation of heterogeneous information into structured formats requires deliberation and these activities are contrary to rapid-prototyping principles. When systems require unstructured information the logical implementation may be objects which create structure upon data that may appear to be random or chaotic. This scheme associates classes of information based upon similarity rather than requiring the data to be cast in a rigid form. A mechanism was developed to accumulate heterogeneous information into entities that have function and which can be reasoned upon for heuristics problem solving. Using a functional representation of information allows the developer to capture raw data in its native form and assimilate the information into dynamic code units. The dynamic code units have autonomy while maintaining an open interface to the remainder of the system. This allows for easy maintenance, implementation, and reusability which assure the tenets of rapid-prototype development and aggregating the dynamic units a database in a content readily accessible to the inference control. DOE

N92-31596# Argonne National Lab., IL.
ENHANCING GRASS DATA COMMUNICATION WITH VIDEOGRAPHIC TECHNOLOGY
R. G. Sullivan, D. Gerdes (Army Construction Engineering Research Lab., Champaign, IL.), and D. Youngs (Army Construction Engineering Research Lab., Champaign, IL.) 1992 17 p Presented at the 7th Annual GRASS GIS Users' Conference, Denver, CO, 16-19 Mar. 1992
(Contract W-31-109-eng-38)
(DE92-014852; ANL/CP-75978; CONF-9203156-1) Avail: CASI HC A03/MF A01

Research at Argonne National Laboratory and the US Army Construction Engineering Research Laboratory has shown that computer videographic technology can be used to assist visualization and communication of GIS-generated geographic information. Videographic tools can be used to make results of GRASS analyses clear to decision-makers and to public interest groups, as well as to help GRASS users visualize geographic data more easily. Useful videographic visualization tools include graphic overlay of GRASS layers onto panchromatic images, allowing landscape features to be associated with GIS classifications; draping of GIS layers onto terrain models to create shaded relief maps; and incorporation of photographic imagery into GIS graphics. Useful videographic communications capabilities include convenient, direct interface to video formats, allowing incorporation of live video into GRASS graphics and output of GRASS graphics to video; convenient output of high-quality slides and prints; and enhanced labeling and editing of GRASS images. Conversion of GRASS imagery to standard videographic file formats also facilitates incorporation of GRASS images into other software programs, such as database and work-processing packages. DOE

N92-31682# Bureau of Reclamation, Denver, CO.
HYDROGENERATOR DESIGN MANUAL, CHAPTER 8
Dec. 1991 127 p
(PB92-173707) Avail: CASI HC A07/MF A02

The Hydrogenerator Design Manual has been prepared to provide information needed by design engineers to properly select and specify hydrogenerator requirements. Information is provided to assist in preparing powerplant layouts, developing requirements for generator renovation (rewind) and uprating, recognizing failure possibilities, and instituting machine maintenance. The manual is intended to be used primarily by Bureau of Reclamation engineers responsible for application design, specifications preparation, and technical review for hydrogenerators. However, other personnel engaged in planning, operation and maintenance, inspection, construction, electrical control, power system design, design of mechanical equipment associated with hydrogenerators, structural design and layout, and hydraulic systems will find the manual useful. Author

N92-31731# Morgantown Technology Center, WV.
THE 193-PIXEL, THREE-DIMENSIONAL CAPACITANCE IMAGING SYSTEM
G. E. Fasching, W. J. Loudin, and N. S. Smith Aug. 1991 136 p
(DE92-001253; DOE/METC-92-4109) Avail: CASI HC A07/MF A02

This is the third in a series of technical notes that describe the development of the capacitance imaging system (CIS). The CIS was designed at the Morgantown Energy Technology Center (METC) as a tool for use in fluidized-bed research. This report briefly reviews the electronic system used for data accumulation and manipulation. It also describes the data processing methods that have been developed for 3-dimensional, fluidized-bed density measurement, and display for the first-generation, 16-electrode, 49-pixel, 4-level CIS. The review outlines the basic structure of the first-generation CIS as it applies to the 32-electrode, 193-pixel, 4-level system. Emphasis is placed upon the modification in the electronic system needed to best utilize the improved resolution capabilities offered by the 32-electrode, second-generation system. The report also describes the changes and advances made in data processing made necessary by the increase from 104 to 400 in the number of interelectrode displacement current measurements. The larger number of measurements allow for the possibility of greater accuracy of density determination to take advantage of the higher resolution available with smaller pixel definition. DOE

N92-31754# Naval Postgraduate School, Monterey, CA.
A DICTIONARY OF ACQUISITION AND CONTRACTING TERMS M.S. Thesis
Mark A. Brown Jun. 1992 107 p
(AD-A247053) Avail: CASI HC A06/MF A02

This thesis is a continuation of research initiated by Lieutenant Commander Daniel F. Ryan, SC, USN to establish a basis for defining words and terms used in the field of contracting. Concurrent research in this area is being conducted by students at the Naval Postgraduate School, Monterey, CA and the Air Force Institute of Technology, Wright-Patterson Air Force Base, Dayton, OH. Published definitions of twenty five terms presently used in Government contracting were reviewed, and a synthesized definition was developed for each term. The synthesized definitions were then scrutinized by a selected group of contracting professionals. Their feedback was used to develop a revised definition based upon consensus. GRA

N92-31859# Japan Atomic Energy Research Inst., Tokyo.
CORRESPONDENCE DICTIONARY FROM FREE ENGLISH TERM TO INIS DESCRIPTORS
Dec. 1991 103 p
(DE92-782192; INIS-JP-002) Avail: CASI HC A06/MF A02

This dictionary is intended for the on-line users of the INIS database who select controlled terms (INIS descriptors) starting from free terms. The purpose of terminology control is (1) to reduce the ambiguity of the term use among different subject fields, and (2) to improve the recall by coordinating the synonyms. The controlled terms are collected in the thesaurus, but it is not always easy to find suitable descriptors. This dictionary was compiled by analyzing existing records, and provides the specialists' know-how of converting free terms to descriptors. The 5,000 records in the physics field were selected, and analyzed by the physicists from the Department of Physics, Ibaraki University. Besides the compilation of this dictionary, the characteristics of the assigned descriptors were also clarified. DOE

N92-31934# Lawrence Livermore National Lab., CA.
A MODEL FOR EXTENDING THE BEHAVIOR OF ANNOTATIONS Ph.D. Thesis
A. M. Garcia Dec. 1991 73 p
(Contract W-7405-eng-48)
(DE92-011731; UCRL-LR-109666) Avail: CASI HC A04/MF A01

This thesis explores the use of Extensible Annotations to assist users in performing procedural tasks described in guideline documents. Extensible Annotations (EA's) are regular annotations with extended properties and functionality. They contain attributes provided by the system or defined by the user; they include links to their anchor document or task, and perhaps to other documents or EA's. All Extensible Annotations are based on an Object-Oriented class hierarchy model, and links between EA's and documents follow a hypertext network model. A prototype implementation of the system has been created for demonstrating the effectiveness of the Extensible Annotational Facility. DOE

N92-32049# Wichita State Univ., KS.
DATABASE EXPLORER: LARGE SCALE DATABASE APPLICATION Final Report, 25 Jan. 1991 - 24 Jan. 1992
Jan M. Zytkow 24 Jan. 1992 48 p
(Contract N00014-91-J-1362)
(AD-A252183) Avail: CASI HC A03/MF A01

We describe Forty-Niner (49er), a computer system for automated mining of useful knowledge in relational databases, we evaluate 49er on a number of tests, and we describe the results of 49er's applications to two NPRDC databases. The basic form of knowledge discovered by 49er is regularities, that is patterns common in sets of data, analogous to scientific laws. In addition, 49er introduces simple concepts. We describe the general form of regularities and we analyze a variety of their types. Regularities discovered in databases can play a role analogous to scientific laws, allowing the users to make prediction, explanations, and justified decisions. There has been considerable interest in recent years in automated methods of mining databases for useful knowledge. Database mining is attractive for many reasons. There are many available databases, they are simple and uniform in structure, and a considerable amount of effort has been spent in designing them and collecting useful data. Many historical records are available in the form of databases, such as stock market prices and indexes, corporate records, census data, and weather records. The automated search for regularities is particularly attractive and useful for large databases, and the same algorithms apply to all relational databases, because of their similarity in structure. Because many databases are very large, and the forthcoming databases will encompass gigabytes or even terabytes of information, knowledge extraction on that scale must be automated. GRA

N92-32058# International Atomic Energy Agency, Vienna (Austria).
DIRECTORY OF IAEA DATABASES
Nov. 1991 118 p
(DE92-628395; INIS-MF-13154) Avail: CASI HC A06/MF A02

The first edition of the Directory of IAEA Databases is intended to describe the computerized information sources available to IAEA staff members. It contains a listing of all databases produced at the IAEA, together with information on their availability. DOE

N92-32102# Army Chemical Research and Development Center, Aberdeen Proving Ground, MD.
REMOTE DATA TRANSFER (RDT): AN INTERPROCESS DATA TRANSFER METHOD FOR DISTRIBUTED ENVIRONMENTS
Jerry A. Clarke May 1992 51 p
(AD-A250859) Avail: CASI HC A04/MF A01

The decomposition of an application into pieces that can be distributed across several platforms requires a mechanism for exchanging data in addition to orchestrating requests and responses. This paper describes a layer of portable software that can be used to distribute an application in an attempt to achieve maximum system performance. GRA

N92-32182# Advisory Group for Aerospace Research and Development, Neuilly-Sur-Seine (France). Technical Information Panel.
BRINGING DOWN THE BARRIERS TO INFORMATION TRANSFER [L'ABAISSEMENT DES BARRIERES S'OPPOSANT AU TRANSFERT DE L'INFORMATION]
Feb. 1992 143 p In ENGLISH and FRENCH Meeting held in Madrid, Spain, 8-9 Oct. 1991
(AGARD-CP-505; ISBN-92-835-0655-3) Copyright Avail: CASI HC A07/MF A02

The last few years have seen rapid advances in a number of new technologies aimed at improving the storage and retrieval of information. Information Scientists may be aware of their potential but may have reservations concerning the absence of suitable standards or the short life associated with some developments. This conference brought together a group of experts to explain the practicalities of applying these new, powerful technologies, their successes and failures. Topics addressed included Artificial Intelligence, CD ROM, Hypertext, and Local Area Networks. These topics were addressed within the framework of finding practical solutions to the problems of achieving efficient and effective information transfer. For individual titles, see N92-32183 through N92-32192.

N92-32183# Defence Research Information Centre, Glasgow (Scotland).
LOCAL AREA NETWORKS (LAN) **c60**
G. Farquhar *In* AGARD, Bringing Down the Barriers to Information Transfer Feb. 1992 7 p (For primary document see N92-32182 22-82)
Copyright Avail: CASI HC A02/MF A02

The discussion is confined to the Man Machine Interface problems encountered during implementation and post implementation. Various development aspects are considered, commencing with the definition of the users' requirement, as distinct

from the users' wishes, to the provision of adequate post implementation support. The LAN installed at the Defence Research Information Center (DRIC) during 1987 and subsequently enhanced in 1988 is taken as the model for the discussion.
Author

N92-32184# Institut National des Sciences et Techniques Nucleaires, Saclay (France).
INTELLIGENT GATEWAYS [GATEWAYS 'INTELLIGENTS']
Christian Fluhr and Claudine Machard *In* AGARD, Bringing Down the Barriers to Information Transfer Feb. 1992 8 p In FRENCH (For primary document see N92-32182 22-82)
Copyright Avail: CASI HC A02/MF A02

Documentary databases that are accessible on-line are, at the present time, underused. This is due to several causes such as the difficulty in efficiently manipulating query languages, the heterogeneity of such languages, the diversity of middle-men with whom one must sign a contract to access the information, the clumsiness of the connection procedures, the costs, and the difficulty associated with choosing the best database. The problem of cost should be resolved as databases are used more effectively. The resolution of the difficulties cited above can be realized along different points of the information chain. It is possible to imagine the placement of considerable intelligence in the workstation of the searcher, but this would require large amounts of computing power. As an alternative, this could be done on a powerful autonomous system: the gateway. It is probably at this level that the majority of the problems could be the most easily resolved. It is for this reason that, even though a large part of what we will develop here can be placed in the workstation, we prefer to concentrate on the possible functionalities of gateways. The goal is not to list the functionalities proposed by existing gateways, but to list the group that current technology allows in the short term.
Author

N92-32185# Orleans Univ. (France).
USE OF EXPERT SYSTEMS AS USER INTERFACES IN INFORMATION RETRIEVAL [UTILISATION DES SYSTEMES EXPERTS DANS DES INTERFACES POUR LA RECHERCHE DOCUMENTAIRE]
J.-C. Bassano, D. Archambault, G. Desrocques, and A. Makaouche *In* AGARD, Bringing Down the Barriers to Information Transfer Feb. 1992 14 p In FRENCH (For primary document see N92-32182 22-82)
Copyright Avail: CASI HC A03/MF A02

The interfaces in question present a text or a group of texts in response to the users' query. These interfaces provide the user with a wide variety of utilities. Efficient technologies for the progressive pairing of the 'sense' between the question and the document are discussed. In order to make the tools cooperate, it is suggested that we have passed from using monolithic interfaces to hybrid or 'multi-expert' architectures. The current evolution of research is in the area of 'connectionist' executions. Author

N92-32186# Technisch Documentatie en Informatie Centrum voor de Krijgsmacht, The Hague (Netherlands).
SEARCH STRATEGIES IN NATURAL LANGUAGE
B. H. A. Zijlstra *In* AGARD, Bringing Down the Barriers to Information Transfer Feb. 1992 39 p (For primary document see N92-32182 22-82)
Copyright Avail: CASI HC A03/MF A02

After a discussion of online searching problems, some methods for making online searching easy for end-users are described: Intelligent gateways, ZOOM, HYPERLINE, CD-ROM, and MENUS. Attention is given to parsing and natural language interfaces to databases, and then natural language projects such as CITE, OKAPI, PLEXUS/TOME/MITI, DIANEGUIDE/NL, DGIS/STINET, SPIRIT/EMIR, and Alpha DIDO are described. In the fourth chapter attention is given to Natural Language and Thesauri, such as the bilingual NATO Thesaurus. A bibliography was added. In an annex an example shows that End-users can start online searching with Natural Language terms, using ZOOM and HYPERLINE commands. Author

N92-32187# Glasgow Univ. (Scotland). Dept. of Computing Science.
NON BOOLEAN SEARCH METHODS IN INFORMATION RETRIEVAL
C. J. vanRijsbergen *In* AGARD, Bringing Down the Barriers to Information Transfer Feb. 1992 12 p (For primary document see N92-32182 22-82)
Copyright Avail: CASI HC A03/MF A02

Information retrieval is a wide, often loosely-defined term, but in these pages I shall be concerned only with automatic information retrieval systems; automatic as opposed to manual and information as opposed to data or fact. Unfortunately the word information can be very misleading. In the context of information retrieval (IR), information, in the technical meaning given in Shannon's theory of communication, is not readily measured. Nevertheless it has become apparent that there is a notion of information fundamental to the information retrieval process that underlies our intuitions about what it is we attempt to retrieve. In many cases one can adequately describe this kind of retrieval by simply substituting 'document' for 'information' where a document may be text, image, etc. This implies that the process is concerned with the identification of certain kinds of objects, viz. documents. It does not explain what is the basis of this identification process, and it is here that the notion of information plays a role. In the case of Boolean retrieval, an attempt is made to measure the extent to which the information is contained in a particular document by establishing whether a document satisfies the request. In the non-Boolean case, this process of satisfaction has a measure of uncertainty attached to it. This paper will explore methods for non-Boolean retrieval. Author

N92-32188*# National Aeronautics and Space Administration, Washington, DC.
HYPERTEXT AND HYPERMEDIA SYSTEMS IN INFORMATION RETRIEVAL
K. M. Kaye and A. D. Kuhn *In* AGARD, Bringing Down the Barriers to Informations Transfer Feb. 1992 5 p (For primary document see N92-32182 22-82)
Copyright Avail: CASI HC A01/MF A02

This paper opens with a brief history of hypertext and hypermedia in the context of information management during the 'information age.' Relevant terms are defined and the approach of the paper is explained. Linear and hypermedia information access methods are contrasted. A discussion of hyperprogramming in the handling of complex scientific and technical information follows. A selection of innovative hypermedia systems is discussed. An analysis of the Clinical Practice Library of Medicine NASA STI Program hypermedia application is presented. The paper concludes with a discussion of the NASA STI Program's future hypermedia project plans. Author

N92-32189# Fachhochschule, Darmstadt (Germany, F.R.). Dept. of Computer Science.
AUTOMATED INPUT INTO DATABASES: OCR AND DESCRIPTIVE CATALOGUING
Gerhard E. Knorz *In* AGARD, Bringing Down the Barriers to Information Transfer Feb. 1992 10 p Sponsored by BMFT (For primary document see N92-32182 22-82)
Copyright Avail: CASI HC A02/MF A02

The technology of automated input from written text into databases is discussed. The current emphasis in office automation and desktop publishing helped optical character recognition to become a useful and affordable method. Different approaches (pixel-oriented, feature-based, using dictionaries, using special algorithms for special problems, character transition probabilities, or grammars) form the basis for meeting different classes of requirements such as demanded by small fonts, large varieties of fonts, special characters, different layout structures with mixed text and graphics, difficult printed matters with ligatures and kerning, and poor printing quality. On the way to an automated (or semi-automated) input process from printed matters into databases (OCR) is nothing but a necessary step within the line of scanning, character recognition, descriptive cataloging, and (optional) content

analysis. Cataloging here is to be understood in a broader sense convering the identification and classification of the relevant pieces of input and the normalization process according to database-specific rules. The role of efficient input into bibliographic databases is discussed, as well as problems and techniques of optical character recognition. AUTOCAT, a software prototype for automated cataloging is introduced: its foundation, approach, and user interface. Author

N92-32190# National Aerospace Lab., Emmeloord (Netherlands).
DATA COMPRESSION TECHNIQUES
R. A. Hogendoorn *In* AGARD, Bringing Down the Barriers to Information Transfer Feb. 1992 3 p (For primary document see N92-32182 22-82)
Copyright Avail: CASI HC A01/MF A02

Data compression can be used to reduce the volume of documents. This results in considerable savings on storage capacity and in transmission time. In general, there are two classes of compression techniques: reversible compression or statistical compression, with which documents can exactly be reproduced, and non-reversible or noisy compression, with which documents can be reproduced up to a given fidelity. Non-reversible compression most often gives a higher compression factor, but, obviously, at a price. Reversible algorithms are suitable for text compression and black-and-white images. Non-reversible algorithms are suitable for images. This paper describes the advantages and caveats of data compression. What is to be expected if data compression is used and, more important, what is not to be expected. Author

N92-32191# Canada Inst. for Scientific and Technical Information, Ottawa (Ontario). Scientific Numeric Database Service.
COMPUTERIZED PROPERTY DATA FOR ENGINEERING MATERIALS: AN OVERVIEW
Gordon H. Wood *In* AGARD, Bringing Down the Barriers to Information Transfer Feb. 1992 6 p (For primary document see N92-32182 22-82)
Copyright Avail: CASI HC A02/MF A02

The special problems of materials property databases, as opposed to scientific numeric databases, are described. A review of progress towards materials property databases since the seminal workshop of 1982 in Fairfield Glade, Tennessee is given based on the recent Third International Symposium on the Computerization and Use of Materials Property Data. Topics include standards and data representation, standards and database development, expert systems and materials databases, data issues for engineering materials, industrial applications, and working and prototype systems. Author

N92-32192# Defense Technical Information Center, Alexandria, VA. Office of Information Systems and Technology.
FACILITATING THE TRANSFER OF SCIENTIFIC AND TECHNICAL INFORMATION WITH SCIENTIFIC AND TECHNICAL NUMERIC DATABASES
H. Haller *In* AGARD, Bringing Down the Barriers to Information Transfer Feb. 1992 13 p (For primary document see N92-32182 22-82)
Copyright Avail: CASI HC A03/MF A02

The Defense Technical Information Center (DTIC) provides services primarily to librarians and technical information specialists. In an effort to better serve engineers and scientists, the end users, DTIC conducted a technology assessment of users and developers of scientific and technical numeric databases. DTIC's Department of Defense Gateway Information System (DGIS) provides the access mechanism to databases and the Multi-Type Information, and Data Analysis System (MIDAS) will provide the capabilities to process bibliographic information and numeric data. Author

N92-32227# Instituto de Pesquisas Espaciais, Sao Jose dos Campos (Brazil).
GIS: GEOGRAPHIC INFORMATION SYSTEMS. STATE OF THE ART AND FUTURE TENDENCIES [SIG: SISTEMAS DE INFORMACOES GEOGRAFICAS. ESTADO DA ARTE E TENDENCIAS FUTURAS]
Hermann Johann Heinr Kux 1991 35 p In PORTUGESE
(INPE-5358-NTC/301) Avail: CASI HC A03/MF A01

The objective of this article is to inform on commercial geographical information systems (GIS) currently available on the market. Common characteristics of todays GIS's are presented and a prediction concerning the next product generation is made. Author

83 ECONOMICS AND COST ANALYSIS

Includes cost effectiveness studies.

No abstracts in this category.

84 LAW, POLITICAL SCIENCE AND SPACE POLICY

Includes NASA appropriation hearings; aviation law; space law and policy; international law; international cooperation; and patent policy.

N92-31947# European Space Agency, Paris (France).
PARTNERSHIP IN SPACE: AN INTRODUCTION TO CANADA'S SPECIAL RELATIONSHIP WITH THE EUROPEAN SPACE AGENCY [PARTENARIAT DANS L'ESPACE: LE CANADA ET L'AGENCE SPATIALE EUROPEENNE]
Norman Longdon, ed. Sep. 1991 40 p In ENGLISH and FRENCH Original contains color illustrations
(ESA-BR-79; ISBN-92-9092-095-5; ETN-92-91712) Copyright Avail: CASI HC A03/MF A01

The special relationship Canada has with Europe, and the benefits of this relationship for Europe are considered. The terms of the cooperation agreement between ESA and Canada are presented and Canadian participation in ESA activities discussed. Special attention is given to programs in which Canada has played a significant role. These include the Olympus communication satellite and Earth observation programs (ERS-1). Future involvement in Earth observation (ERS-2), telecommunications and the Hermes spaceplane is discussed. How Canadians can take advantage of opportunities offered by ESA is considered and a look to the future is made. Useful addresses in Canada are given. ESA

85 URBAN TECHNOLOGY AND TRANSPORTATION

Includes applications of space technology to urban problems; technology transfer; technology assessment; and surface and mass transportation.

For related information see also *03 Air Transportation and Safety, 16 Space Transportation,* and *44 Energy Production and Conversion.*

N92-31599# Office of Technology Assessment, Washington, DC.
ANNUAL REPORT TO THE CONGRESS, FISCAL YEAR 1991 (OFFICE OF TECHNOLOGY ASSESSMENT)
Mar. 1992 64 p
(PB92-166549; OTA-A-530) Avail: CASI HC A04/MF A01

The report to congress is required under Section 11 of the Technology Assessment Act of 1972. P.L. 92-484. The report

describes the activities of the Office in the fiscal year 1991 within the context of the legislative agenda of the 102nd Congress and the events in the United States and the world during 1991. GRA

N92-31643# National Inst. of Standards and Technology, Gaithersburg, MD.
TECHNOLOGY INTEGRATION WORKSHOP: SELECTED PAPERS
H. Tom Oct. 1991 150 p Presented at the NIST Geographic Information Systems Standards Laboratory's Technology Integration Workshop held in Gaithersburg, MD, 23-24 Aug. 1990
(PB92-158278; NISTIR-4703) Avail: CASI HC A07/MF A02

The report contains selected summaries of technical presentations and demonstrations given at the National Institute of Standards and Technology (NIST) Geographic Information Systems (GIS) Standards Laboratory's Technology Integration Workshop held at NIST, Gaithersburg, Maryland on August 23-24, 1990. The Technology Integration Working Group was formed within the GIS Lab as a cooperative technology transfer vehicle to share advances being made in applying expert systems, object-oriented database technologies, and GIS to practical problems in spatial data management and cartographic portrayal. The Workshop focused upon demonstrations of work-in-progress prototypes and technical discussions of progress in several on-going projects. The Workshop as well as other NIST GIS Standards Laboratory activities are focused on performing cooperative research in order to integrate existing, emerging, and the anticipatory development of spatial data and information technology standards. Author

N92-31965# Industrial Technology Inst., Ann Arbor, MI.
A PROGRAM FOR THE TRANSFER OF MANUFACTURING TECHNOLOGY FROM THE NATIONAL LABORATORIES
R. H. Shackson Mar. 1992 6 p
(Contract DE-FG02-90ER-75564)
(DE92-011905; DOE/ER-75564/9) Avail: CASI HC A02/MF A01

The objective of this project is to test a needs-driven approach to transfer of manufacturing technology from the National Laboratories. The first task was the development of a 250-page book, describing the durable goods industry and its technological needs. This book was used in three engagements with DOE labs, in which researchers were briefed on needs, and asked to nominate technologies to meet these needs. Of 47 nominations, approximately one-third were technologies that has not been recognized as having value, and were not listed on the laboratory's data base. After several evaluation steps, commercialization planning is underway for six, and one is being considered for prototype development. DOE

88 SPACE SCIENCES (GENERAL)

No abstracts in this category.

89 ASTRONOMY

Includes radio, gamma-ray, and infrared astronomy, and astrometry.

N92-31343# Instituto de Pesquisas Espaciais, Sao Jose dos Campos (Brazil). Div. de Astrofisica.
G305.8 - 0.2 WATER VAPOUR SOURCE: A YOUNG OBJECT
J. W. S. VilasBoas (Sao Paulo Univ., Brazil), E. Scalise, Jr., and C. G. Sanzovo (Universidade Estadual de Londrina, Brazil) Sep. 1991 19 p Previously announced in IAA as A92-11096 Submitted for publication Sponsored by FINEP and FAPESP
(INPE-5337-PRE/1736) Avail: CASI HC A03/MF A01

Observations of water vapor and silicon monoxide masers were conducted in the direction of G305.8-0.2. No SiO maser emission above 7 Jy of flux density was detected. The short-time variability of the H20 maser together with the absence of compact radio continuum emission suggests that the excitation energy of the maser could originate from an O7-O9 protostar in its earlier evolutionary stages. Author

N92-31344# Instituto de Pesquisas Espaciais, Sao Jose dos Campos (Brazil). Departamento de Astrofisica.
PHOTOMETRY OF NOVA MUSCAE 1983
Marcos P. Diaz (Sao Paulo Univ., Brazil) and Joao E. Steiner (Sao Paulo Univ., Brazil) Sep. 1991 7 p Submitted for publication
(INPE-5339-PRE/1738) Avail: CASI HC A02/MF A01

We present photometric observations of the GQ Mus at quiescence which reveal a strong orbital modulation. We also discuss recent spectroscopic observations which reveal a very short orbital period. On the basis of the results, we argue that the system belongs to the class of magnetized cataclysmic variables. Author

N92-31347# Instituto de Pesquisas Espaciais, Sao Jose dos Campos (Brazil). Departamento de Astrofisica.
ACCRETION DISK IMAGE RECONSTRUCTION IN CATACLYSMIC VARIABLES
Raymundo Baptista (Sao Paulo Univ., Brazil) and Joao E. Steiner (Sao Paulo Univ., Brazil) Sep. 1991 7 p Submitted for publication
(INPE-5343-PRE/1742) Avail: CASI HC A02/MF A01

We developed a program to map the accretion disk brightness distribution in Cataclysmic Variables (CV's) from their eclipse light curves. The results of performance tests for synthetic data are discussed. Author

N92-32005# Lawrence Livermore National Lab., CA.
INSTITUTE OF GEOPHYSICS AND PLANETARY PHYSICS, 1991 Annual Report, 1 Oct. 1990 - 30 Sep. 1991
W. J. Nellis, ed. and C. M. Budwine, ed. 10 May 1992 123 p
(Contract W-7405-eng-48)
(DE92-016981; UCRL-53809-91) Avail: CASI HC A06/MF A02

This report contains brief discussions on topics in the following areas: high-pressure sciences; astrophysics; and geosciences. DOE

90 ASTROPHYSICS

Includes cosmology; celestial mechanics; space plasmas; and interstellar and interplanetary gases and dust.
For related information see also *75 Plasma Physics*.

N92-31345# Instituto de Pesquisas Espaciais, Sao Jose dos Campos (Brazil). Departamento de Astrofisica.
THE ECLIPSING CATACLYSMIC VARIABLE AY PISCIUM
Marcos P. Diaz (Sao Paulo Univ., Brazil) and Joao E. Steiner Sep. 1991 6 p Repr. from Astronomy and Astrophysics, v. 238, 1990 p 170-172
(INPE-5340-PRE/1739) Avail: CASI HC A02/MF A01

Photometric observations of the cataclysmic variable AY Psc are presented. We found that the star shows deep eclipses with an orbital period of 5.2 h. The orbital ephemeris is given as well as an analysis of 30 h of fast photometry. Author

N92-31346# Instituto de Pesquisas Espaciais, Sao Jose dos Campos (Brazil). Departamento de Astrofisica.
THE ECLIPSING CATACLYSMIC VARIABLE NSV 12615 (V4041 Sgr)
Raymundo Baptista (Sao Paulo Univ., Brazil), Francisco J. Jablonski, and Joao E. Steiner (Sao Paulo Univ., Brazil) Sep. 1991 6 p Submitted for publication
(INPE-5342-PRE/1741) Avail: CASI HC A02/MF A01

Photometric and spectroscopic observations of NSV 12615 (V4041 Sgr) are presented. It is argued that this object is probably a magnetic cataclysmic variable. Author

N92-31401# International Centre for Theoretical Physics, Trieste (Italy).
MODIFIED BLACK HOLES IN TWO DIMENSIONAL GRAVITY
N. Mohammedi Nov. 1991 12 p
(DE92-630244; IC-91/384) Avail: CASI HC A03/MF A01

The SL(2,R)/U(1) gauged WZWN model is modified by a topological term and the accompanying change in the geometry of the two dimensional target space is determined. The possibility of this additional term arises from a symmetry in the general formalism of gauging an isometry subgroup of a nonlinear sigma model with an antisymmetric tensor. It is shown, in particular, that the space-time exhibits some general singularities for which the recently found black hole is just a special case. From a conformal field theory point of view and for special values of the unitary representation of SL(2,R), this topological term can be interpreted as a small perturbation by a (1,1) conformal operator of the gauged WZWN action. DOE

N92-31635# Onsala Space Observatory (Sweden).
MOLECULAR OUTFLOWS ASSOCIATED WITH HH52-54 AND IRAS 12496-7650
L. B. G. Knee 5 Jan. 1992 38 p
(PB92-184472) Avail: CASI HC A03/MF A01

Results are presented of CO-12(J = 1-0) and CO-13(J = 1-0) observations of HH52-54. Two molecular outflows associated with HH52-54 have been discovered. The column density structure of the cloud and the alignments of the molecular and optical outflows lead us to identify two faint Infrared Astronomy Satellite (IRAS) sources as the exciting stars of the HH objects. The well-collimated outflow associated with HH54 optical 'streamer' confirms that the streamer is an optical jet. A third, weaker outflow is associated with the Herbig Ae star IRAS 12496-7650. Comparison of the data to other observations permits one to construct a scenario of the star formation and mass loss activity near HH52-54. The observed high ratios of outflow mechanical luminosity to stellar luminosity provide a stringet test of current theories for the outflow driving mechanism: in the case of the HH52-54 outflows, the authors conclude that they are probably in an energy-driven mode, and that Alfven wave-driven stellar winds from convective low-mass stars are the most likely driving mechanism. Author

N92-31713# Chicago Univ., IL.
PARTICIPATION IN HIGH ENERGY PHYSICS. TASK C: PARTICLE PHYSICS AND COSMOLOGY
M. S. Turner May 1992 11 p
(Contract DE-FG02-90ER-40560)
(DE92-016290; DOE/ER-40560/3C) Avail: CASI HC A03/MF A01

Over the past year or so the research of our group has spanned many topics at the boundary of particle physics and cosmology. The major focus has been in the general areas of inflation, cosmological phase transitions, astrophysical constraints to particle physics theories, and dark matter/structure formation as it relates to particle physics. Narrative summaries of the research of the individual group members are given in this paper. DOE

N92-32142# Arizona Univ., Tucson.
A CHARACTERIZATION OF THE HOT INFRARED BACKGROUND: THE INFRARED CIRRUS, ZODIACAL DUST BANDS, AND SOLAR SYSTEM DUST TRAILS Final Report, 3 Jun. 1987 - 31 Dec. 1990
Frank J. Low, M. Sykes, and Roc M. Cutri 1 Apr. 1991 240 p
(Contract F19628-87-K-0045; AF Proj. S321)
(PL-TR-91-2065) Avail: CASI HC A11/MF A03

Utilizing data from the Infrared Astronomical Satellite (IRAS), we have completed an investigation into the nature and properties of the principal components of the hot thermal background. These include the warm infrared cirrus, zodiacal dust bands, and cometary dust trails. A large set of high galactic latitude IRAS Skyflux maps were 'cleaned' using an image-space processor which we have developed. Using these enhanced infrared maps, 44 fields were identified which exhibit 'hot' 12 micron cirrus emission. A cooler, 100 micron emission can be seen in all of the fields, and there is at least a qualitative correlation between the 12 micron cirrus and diffuse optical emission. The relationship between the 12 and 100 micron emission was examined in two prominent cirrus complexes. Author

91 LUNAR AND PLANETARY EXPLORATION

Includes planetology; and manned and unmanned flights. For spacecraft design or space stations see *18 Spacecraft Design, Testing and Performance.*

N92-31781*# National Aeronautics and Space Administration. Lyndon B. Johnson Space Center, Houston, TX.
USING SPACE RESOURCES
Thomas A. Sullivan and David S. McKay 1991 30 p Original contains color illustrations
(NASA-TM-107966; NAS 1.15:107966) Avail: CASI HC A03/MF A01; 8 functional color pages

The topics covered include the following: reducing the cost of space exploration; the high cost of shipping; lunar raw materials; some useful space products; energy from the moon; ceramic, glass, and concrete construction materials; mars atmosphere resources; relationship to the Space Exploration Initiative (SEI); an evolutionary approach to using space resources; technology development; and oxygen and metal coproduction. Author

N92-32179# Joint Publications Research Service, Arlington, VA.
JPRS REPORT: SCIENCE AND TECHNOLOGY. CENTRAL EURASIA: LIFE SCIENCES Abstracts Only
27 May 1992 47 p Transl. into ENGLISH from various Central Eurasian articles
(JPRS-ULS-92-015) Avail: CASI HC A03/MF A01

A number of life science studies from Central Eurasia are discussed. Topics covered include biochemistry, epidemiology, genetics, immunology, microbiology, physiology, public health, radiation biology, and methane producing microorganisms as components of the Mars biosphere. For individual title, see N92-32180.

N92-32180# Joint Publications Research Service, Arlington, VA.
METHANE-PRODUCING MICROORGANISMS: COMPONENT OF MARS BIOSPHERE Abstract Only
M. V. Ivanov and A. Yu. Lein *In its* JPRS Report: Science and Technology. Central Eurasia: Life Sciences 27 May 1992 p 10 Transl. into ENGLISH from Doklady Akademii Nauk SSSR (Moscow, USSR), v. 321, no. 6, Dec. 1991 p 1272-1276 (For primary document see N92-32179 22-91)
Avail: CASI HC A01/MF A01

Researchers have turned the focus of the search for life on Mars to autotrophs that do not need organic carbon. Because the poor ecological conditions on Mars make the possibility of finding photoautotrophs highly unlikely, researchers are now looking for chemolytoautotrophs. Fundamental to the proposed strategy for searching for life on Mars is concentration of efforts on searching for specific ecosystems suited to the functioning of specialized groups of microorganisms such as anaerobes, psychrophiles, and oligotrophs. The most perspective of these are chemolytoautotrophs, methane-producing bacteria which inhabit ecosystems with temperatures of 0-100 C and which can develop in a pH range of 6.0-9.0. It has been found that methane-producing bacteria can fractionate the stable isotopes C-12 and C-13. The results showed that the methane-producing bacteria label the products of their metabolism, methane and biomass, with an increased concentration of C-12. The authors conclude that the data they have cited on the fractionation of carbon isotopes in the chemolytoautotrophic assimilation of CO2 by methane-producing bacteria satisfactorily explain the isotopic composition of SNC meteorites. Finally, a complex of sulfate and isotope-heavy carbonate minerals in association with an isotope-light organic substance forms during a secondary change in the basalt-dunite rock of Mars under conditions of their surface

change on the mother planet when solutions containing hydrogen are discharged with active involvement of methane-producing bacteria. Author

92 SOLAR PHYSICS

Includes solar activity, solar flares, solar radiation and sunspots.

For related information see *93 Space Radiation.*

N92-31338*# Utah State Univ., Logan. Center for Atmospheric and Space Sciences.

THE FLOW OF PLASMA IN THE SOLAR TERRESTRIAL ENVIRONMENT Semiannual Technical Report, 15 Jun. 1991 - 31 Mar. 1992

R. W. Schunk and T. J. Birmingham Mar. 1992 21 p
(Grant NAG5-1484)
(NASA-CR-190200; NAS 1.26:190200) Avail: CASI HC A03/MF A01

The scientific goals of the program are outlined, and some of the papers submitted for publication within the last six months are briefly highlighted. Some of the topics covered include ionosphere-magnetosphere coupling, polar cap arcs, polar wind, convection vortices, ionosphere-plasmasphere coupling, and the validity of macroscopic plasma flow models. Author

N92-31786# Stanford Univ., CA. Center for Space Science and Astrophysics.

EVOLUTION OF THE SOLAR AND CORONAL FIELD STRUCTURE: 1976-1991

J. T. Hoeksema 1992 10 p
(Contract N00014-89-J-1024; NSF ATM-90-22249)
(AD-A250097) Avail: CASI HC A02/MF A01

The magnetic field of the Sun determines the structure of the corona and the interplanetary medium. Observations of the solar field made at the Wilcox Solar Observatory at Stanford from 1976 to the present have been used to model the field patterns in the corona, the source of the heliospheric magnetic field. The IMF polarity at Earth can be predicted with about 80 percent reliability throughout the solar cycle. However, the field in the ecliptic is just one slice of a three-dimensional structure that changes greatly during the solar cycle. Near solar minimum the heliospheric current sheet is confined to the Sun's equatorial region. As the polar fields decay and reverse near solar maximum, the geometry of the heliospheric field becomes much more complex. Model coronal fields can also be used to estimate the solar wind velocity, determine the solar origin of interplanetary structures, and predict the out-of-ecliptic component of the IMF at Earth. GRA

N92-31856*# Lockheed Missiles and Space Co., Palo Alto, CA. Research and Development Div.

A SOLAR MAGNETIC AND VELOCITY FIELD MEASUREMENT SYSTEM FOR SPACELAB 2: THE SOLAR OPTICAL UNIVERSAL POLARIMETER (SOUP) Final Report, Sep. 1977 - Jan. 1991

Theodore D. Tarbell and Alan M. Title Aug. 1992 56 p
(Contract NAS8-32805)
(NASA-CR-190683; NAS 1.26:190683; LMSC-F404726; LMSC-PO35355) Avail: CASI HC A04/MF A01

The Solar Optical Universal Polarimeter (SOUP) flew on the shuttle mission Spacelab 2 (STS-51F) in August, 1985, and collected historic solar observations. SOUP is the only solar telescope on either a spacecraft or balloon which has delivered long sequences of diffraction-limited images. These movies led to several discoveries about the solar atmosphere which were published in the scientific journals. After Spacelab 2, reflights were planned on the shuttle Sunlab mission, which was cancelled after the Challenger disaster, and on a balloon flights, which were also cancelled for funding reasons. In the meantime, the instrument was used in a productive program of ground-based observing, which collected excellent scientific data and served as instrument tests. Given here is an overview of the history of the SOUP program, the scientific discoveries, and the instrument design and performance. Author

N92-31985# Tufts Univ., Medford, MA. Dept. of Physics and Astronomy.

HIGH-RESOLUTION MICROWAVE OBSERVATIONS OF THE SUN Final Report, 1 Nov. 1988 - 30 Apr. 1992

Kenneth R. Lang 28 Feb. 1992 198 p
(Grant AF-AFOSR-0147-89)
(AD-A247869; AFOSR-92-0221TR) Avail: CASI HC A09/MF A03

This is the final technical report for grant AFOSR-89-0147 entitled high-resolution microwave observations of solar activity. This report covers the period from 1 November 1988 to 30 April 1992. It contains the abstracts for 24 presentations at professional meetings (section 2); and reprints of 17 papers (section 4). The 24 professional presentations included meetings of the American Astronomical Society (AAS), the American Geophysical Union (AGU), the Committee on Space Research (SOSPAR), the International Astronomical Union (IAU), and the Union Radio Scientific International (URSI). The Very Large Array (VLA) and the Arecibo Observatory are the world's largest radio telescopes, each operated at enormous expense by the National Science Foundation (NSF); the 21 successful proposals with these facilities, totaling 51 days, therefore, represent an extremely efficient method of carrying out research by the Air Force Office of Scientific Research (AFOSR) that essentially funds salaries for Tufts scientists who use these facilities, analyze the data, and publish the results. Some of the topics covered include: eruptions, flares, origin, and prediction of solar activity; radio emission from coronal loops and filaments; resolution of the pre-flare, impulsive and decay phases of solar flares; x-ray emission from coronal loops and flares; the Solar Maximum Mission satellite; NASA balloon flights of high-energy solar detection; and the Yohkoh solar satellite. GRA

N92-32025# Instituto de Pesquisas Espaciais, Sao Jose dos Campos (Brazil).

MULTIPLE ELECTRON POPULATIONS ACCELERATED IN SOLAR BURSTS Ph.D. Thesis [MULTIPLAS POPULACOES DE PARTICULAS ACELERADAS EM EXPLOSOES SOLARES]

Ana Maria Zodi Vaz Sep. 1991 94 p In PORTUGESE
(INPE-5377-TDI/472) Avail: CASI HC A05/MF A01

The solar burst of November 4, 1981, 1828 UT, was observed simultaneously at eight microwave frequencies (1.4-44 GHz) by the Sagamore Hill (AFGL), Algonquin (HIA) and Itapetinga (INPE) observatories, as well as at seven x-ray energy channels by the experiment on board of Hinotori satellite (28-375 keV). The radio spectra obtained at Sagamore Hill observatory (1.4-15.4 GHz) were processed with good time resolution (one spectrum/sec). Data from Algonquin (10.6 GHz) and Itapetinga (22 and 44 GHz) observatories are of high sensitivity and time resolution (limited to 30 ms in this study). The time profiles at x-rays are analyzed in the lowest energy channel (28-38 keV), with time resolution of 30 ms. X-ray spectra were also obtained every 5-10 s throughout the main face of the burst. This event received a diagnostics exceptionally complete, being particularly suitable for analysis with the objective to investigate the causes producing the observed spectral and time variations. It has been found that the commonly adopted assumption of a single homogeneous emitting source, with a single accelerated electron population, is not consistent with the data obtained at the various frequencies. The results indicate that the emission should have originated from more than one accelerated electron population in sources more complex than usually assumed. The results also show that for the unique determination of the emission components it is necessary that a more complete diagnostics, still unavailable so far, particularly on the spatial dynamic processes, which are likely to occur simultaneously, be performed. Author

N92-32154# Washington Univ., Seattle. Dept. of Physics.

SOLAR NEUTRINOS: THEORY VERSUS EXPERIMENT

W. C. Haxton 1991 7 p Presented at the 2nd International Workshop on Theoretical and Phenomenological Aspects of Underground Physics, Toledo (Spain), 9-13 Sep. 1991
(Contract DE-FG06-88ER-40427)
(DE92-014327; DOE/ER-40427/2-N92; CONF-9109182-6) Avail: CASI HC A02/MF A01

I review the standard solar model, the disparities between its predictions and the solar neutrino flux measurements of the Homestake and Kamioka II collaborations, and possible particle physics resolutions of this puzzle. The effects of matter, including density fluctuations and turbulence, on solar neutrino oscillations are reviewed, including possibilities for generating time variations in the solar neutrino flux. Finally, I consider possible outcomes and implications of the SAGE/GALLEX gallium experiments. DOE

N92-32221# Instituto de Pesquisas Espaciais, Sao Jose dos Campos (Brazil).
FINE STRUCTURE SUPERIMPOSED ON mm-WAVELENGTH (18-23 GHz) SPECTRA OF SOLAR ACTIVE REGION M.S. Thesis [ESTRUTURA FINA SUPERPOSTA EM ESPECTROS DE REGIAO ATIVA SOLAR EM COMPRIMENTOS DE ONDA MM (23-18 GHZ)]
Jose Roberto Cecatto Feb. 1991 125 p In PORTUGESE
(INPE-5371-TDI/470) Avail: CASI HC A06/MF A02

A mm-lambda, 23-18 GHz, variable frequency radiometer with frequency resolution of 1 GHz and time resolution of 0.6-16 sec. has been developed in conjunction with a 13.7 meter diameter antenna. Here, this new radiometer, the procedures of calibration and observations of active region are described in detail. Observations of active region have been carried out using the mm-lambda radiometer. So far, spectra of four active regions have been observed. Two of these spectra have exhibited frequency fine structures in emission as well as in absorption, of the order of 2 GHz wide in frequency and in amplitude less than or equal to 100 percent of the original flux value, lasting for about half an hour. The spectra of the center of the sun and those of the active region have been interpreted in terms of 'bremsstrahlung' as a process of emission. Fine structure in absorption has been interpreted in terms of presence of a neutral current sheet between the radio source and the observer. The superimposed fine structure in emission has been discussed in terms of two possible mechanisms: (1) the emission of cyclotron line, and (2) the radio signature of a mysterious temperature plateau in the chromosphere. Author

93 SPACE RADIATION

Includes cosmic radiation; and inner and outer earth's radiation belts.

For biological effects of radiation see *52 Aerospace Medicine.* For theory see *73 Nuclear and High-Energy Physics.*

N92-31477# Louisiana State Univ., Baton Rouge.
THE INTERPLANETARY HEAVY ION ENVIRONMENT FOR BOTH GALACTIC COSMIC RAYS AND SOLAR ENERGETIC PARTICLES DURING THE CRRES MISSION Scientific Report No. 1
John P. Wefel and T. G. Guzik 18 Oct. 1991 90 p
(Contract F19628-90-K-0026)
(AD-A248942; AD-E200988; PL-TR-91-2252) Avail: CASI HC A05/MF A01

A calculational model of the Interplanetary Heavy Ion Environment is being developed for the CRRES mission to include both galactic cosmic rays (GCR) and solar energetic particles (SEP). Data from the ONR-604 experiment on CRRES plus results from other experiments/spacecraft are being combined to evaluate the heavy ion radiation environment in near-Earth space in the 1990-1991 epoch. The modeling effort is described along with operation and performance of the ONR-604 experiment, including prelaunch accelerator calibrations and on-orbit response. The status of the data systems development for this effort is summarized, along with its use for the initial analysis of the data and the modeling effort. The preliminary working environment for the period 1 Sep. 90 - 28 Feb. 91 is characterized by a high level of solar modulation and correspondingly low flux of GCR and no significant component from SEP's. Both particle flux and LET spectra were calculated. The limitations and uncertainties inherent in this working model are presented, along with the effort to be undertaken to understand and reduce the uncertainties. GRA

N92-31756# California Univ., Berkeley. Lawrence Berkeley Lab.
RELATING SPACE RADIATION ENVIRONMENTS TO RISK ESTIMATES
S. B. Curtis Oct. 1991 24 p Presented at the NATO Advanced Studies Institute on the Biological Effects and Physics of Solar and Galactic Cosmic Radiation Conference, Faro, Portugal, 13-22 Oct. 1991
(Contract DE-AC03-76SF-00098)
(DE92-010256; LBL-31685; CONF-9110312-2) Avail: CASI HC A03/MF A01

This lecture will provide a bridge from the physical energy or LET spectra as might be calculated in an organ to the risk of carcinogenesis, a particular concern for extended missions to the moon or beyond to Mars. Topics covered will include (1) LET spectra expected from galactic cosmic rays, (2) probabilities that individual cell nuclei in the body will be hit by heavy galactic cosmic ray particles, (3) the conventional methods of calculating risks from a mixed environment of high and low LET radiation, (4) an alternate method which provides certain advantages using fluence-related risk coefficients (risk cross sections), and (5) directions for future research and development of these ideas. DOE

N92-32193*# National Aeronautics and Space Administration. Langley Research Center, Hampton, VA.
EFFECTS OF FRAGMENTATION PARAMETER VARIATIONS ON ESTIMATES OF GALACTIC COSMIC RAY EXPOSURE: DOSE SENSITIVITY STUDIES FOR ALUMINUM SHIELDS
Lawrence W. Townsend, Francis A. Cucinotta, Judy L. Shinn, and John W. Wilson Jul. 1992 10 p
(RTOP 593-42-21-01)
(NASA-TM-4386; L-17082; NAS 1.15:4386) Avail: CASI HC A02/MF A01

Initial studies of the sensitivities of estimates of particle fluence, absorbed dose, and dose equivalent to fragmentation parameter variations are undertaken by using the LaRC galactic cosmic ray transport code (HZETRN). The new results, presented as a function of aluminum shield thickness, include upper and lower bounds on dose/dose equivalent corresponding to the physically realistic extremes of the fragmentation process and the percentage of variation of the dose/dose equivalent as a function of fragmentation parameter variation. Author

99 GENERAL

N92-31852*# National Aeronautics and Space Administration. Ames Research Center, Moffett Field, CA.
NAS (NUMERICAL AERODYNAMIC SIMULATION PROGRAM) TECHNICAL SUMMARIES, MARCH 1989 - FEBRUARY 1990
Feb. 1990 221 p Original contains color illustrations
(NASA-TM-107960; NAS 1.15:107960) Avail: CASI HC A10/MF A03; 125 functional color pages

Given here are selected scientific results from the Numerical Aerodynamic Simulation (NAS) Program's third year of operation. During this year, the scientific community was given access to a Cray-2 and a Cray Y-MP supercomputer. Topics covered include flow field analysis of fighter wing configurations, large-scale ocean modeling, the Space Shuttle flow field, advanced computational fluid dynamics (CFD) codes for rotary-wing airloads and

performance prediction, turbulence modeling of separated flows, airloads and acoustics of rotorcraft, vortex-induced nonlinearities on submarines, and standing oblique detonation waves. Author

N92-32067# National Science Foundation of US, Tokyo (Japan).
NSF TOKYO REPORTS. 1991 SURVEY OF RESEARCH AND DEVELOPMENT IN JAPAN
L. H. Weber and M. Miyahara Dec. 1991 15 p
(PB92-192624; Rept-Memo-221) Avail: CASI HC A03/MF A01

A summary of statistical data on Japanese research and development expenditures for the Japanese FY-90 (April 1990 through March 1991) is given. The data are based on a survey conducted by the Statistics Bureau of the Management and Coordination Agency of the Japanese Government. The survey covered approximately 16,400 organizations, including 12,700 private companies, 2,200 universities and 1,500 research institutes. Author

N92-32068# National Science Foundation of US, Tokyo (Japan).
NSF TOKYO REPORTS. GENERAL OUTLINE OF JFY 1991 GOVERNMENT SCIENCE AND TECHNOLOGY BUDGET
L. H. Weber and M. Miyahara Jan. 1992 43 p
(PB92-192640; Rept-Memo-222) Avail: CASI HC A03/MF A01

The FY-91 gross total of the Japanese Government's annual budget for all science and technology activities amounted to 2,022.6 billion Japanese yen. This represents an increase of 5.3 percent over the previous fiscal year level. A detailed summary is given in both tabular and narrative form of how total funding was allocated by agency and by major project. Author

Typical Subject Index Listing

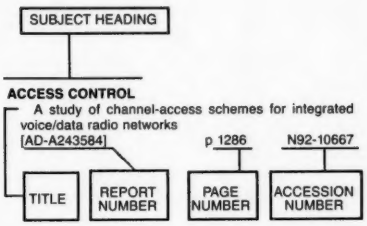

The subject heading is a key to the subject content of the document. Titles, report numbers, and accession numbers of pertinent documents are provided under each subject heading. When the title is insufficiently descriptive of the document content, a title extension has been added, separated from the title by three hyphens. The report number helps to indicate the type of document cited (e.g., NASA report, NASA translation, NASA contractor report). The accession number is the number by which the document abstracts are arranged in this journal and by which the document is sold or requested. The page number helps you locate the the citation in the abstract section. The titles, with title extensions if present, are arranged under each subject heading in ascending accession number order. The subject headings have been selected from the latest revision of the *NASA Thesaurus*.

A

A STARS
Molecular outflows associated with HH52-54 and IRAS 12496-7650
[PB92-184472] p 3924 N92-31635

ABLATION
Dynamic modeling of plasma-vapor interactions during plasma disruptions
[DE92-016183] p 3903 N92-31310
Transient internal probe diagnostic
[AD-A247306] p 3903 N92-31459
Laser-ablated copper condensation in helium
[DE92-016685] p 3789 N92-32004

ABSORPTION COOLING
Heat and mass transfer considerations in advanced heat pump systems
[DE92-016635] p 3825 N92-32003

ABSORPTION SPECTRA
Elementary reaction rate measurements at high temperatures by tunable-laser flash-absorption
[DE92-015269] p 3830 N92-31684
Absorption spectroscopy through the dark zone of solid propellant flames
[AD-A250033] p 3782 N92-31803
Absorption spectra and electronic properties of alkali metal doped C60
[AD-A251006] p 3912 N92-31937
Near-IR absorption spectra for the Buckminsterfullerene Anions: An experimental and theoretical study
[AD-A250532] p 3785 N92-32080
Electronic structure and photophysical properties of polyimides
[DE92-012353] p 3797 N92-32146

ABSORPTION SPECTROSCOPY
Absorption spectroscopy through the dark zone of solid propellant flames
[AD-A250033] p 3782 N92-31803

ACCELERATED LIFE TESTS
The effect of thermomechanical processing parameters on the ambient behavior of 10 percent volume 6061 Al-Alumina
[AD-A252177] p 3776 N92-32064

ACCELERATION (PHYSICS)
Projectile development for railguns using hypervelocity preacceleration
[DE92-016741] p 3766 N92-31735
Problems associated with launching hypervelocity projectiles from the fast shock tube
[DE92-015276] p 3762 N92-32026
Estimation of metal acceleration by an SF5 containing explosive
[AD-A245338] p 3801 N92-32098

ACCELERATION STRESSES (PHYSIOLOGY)
Naval Biodynamics Laboratory: 1989 and 1990 command history
[AD-A247185] p 3870 N92-31963

ACCELEROMETERS
Spacecraft dynamics characterization and control system failure detection. Volume 3: Control system failure monitoring
[NASA-CR-190529] p 3884 N92-31254
Ground and flight calibration assessment of HiRAP accelerometer data from missions STS-35 and STS-40
[NASA-TM-107602] p 3769 N92-32204

ACCEPTOR MATERIALS
Ultrafast experiments on the role of vibrational modes in electron transfer
[AD-A250630] p 3910 N92-31699

ACCRETION DISKS
The eclipsing cataclysmic variable NSV 12615 (V4041 Sgr)
[INPE-5342-PRE/1741] p 3923 N92-31346
Accretion disk image reconstruction in cataclysmic variables
[INPE-5343-PRE/1742] p 3923 N92-31347

ACCUMULATIONS
A case study of a prolonged sleet event: 16-17 February 1987 and climatology of sleet events for North Carolina, 1949-1989
[AD-A250184] p 3859 N92-31602

ACETATES
Experimental studies of aluminum solubility and speciation in brines
[DE92-010448] p 3786 N92-31418

ACETYL COMPOUNDS
Acetylcholinesterase inhibitors on the spinal cord
[AD-A252694] p 3868 N92-31326

ACETYLENE
Unimolecular reaction mechanisms involving C3H4, C4H4, and C6H6 hydrocarbon species
[DE92-005326] p 3783 N92-31860

ACID RAIN
Acid deposition: State of science and technology. Summary report of the US National Acid Precipitation Assessment Program, volumes 1-4
[PB92-100353] p 3852 N92-31598
Rainwater and throughfall chemistry in a terra firme rain forest: Central Amazonia
[INPE-5364-PRE/1744] p 3863 N92-32224

ACOUSTIC DUCTS
Asymptotic modal analysis and statistical energy analysis
[NASA-CR-190516] p 3842 N92-32236

ACOUSTIC EMISSION
Near-field and far-field sound radiation from a line-driven fluid-loaded infinite flat plate having periodic and non-periodic attached rib stiffeners
[AD-A250100] p 3892 N92-31789
Acoustic emission method applied to tests on concrete p 3842 N92-32206

ACOUSTIC EXCITATION
Advanced DAA methods for shock response analysis
[AD-A252696] p 3891 N92-31588
Noise-induced chaos and phase space flux: A sample-theoretic study
[PB92-172733] p 3915 N92-31645

ACOUSTIC MEASUREMENT
Development, testing and operation of a large suspended ocean measurement structure for deep-ocean use
[AD-A252188] p 3866 N92-32050
Optimum data analysis procedures for Titan 4 and Space Shuttle payload acoustic measurements during lift-off
[NASA-CR-190479] p 3892 N92-32178

ACOUSTIC PROPERTIES
Deep-tow acoustics/geophysics system compressional velocity database
[AD-A252700] p 3918 N92-31467
Hydrographic and Acoustic Doppler Current Profiler (ADCP) data from the Farallones shelf and slope study
[AD-A250834] p 3864 N92-31495
Pulse Combustion Engineering Research Laboratory: Exhaust energy
[PB92-172402] p 3783 N92-31918
Investigation of acoustic properties of high-temperature ceramic superconductors p 3914 N92-32209

ACOUSTIC SCATTERING
An empirical prediction algorithm for low-frequency acoustic surface scattering strengths
[AD-A250508] p 3892 N92-32044

ACOUSTIC VELOCITY
Sensitivity of the tomographic inverse solution to acoustic path variability
[AD-A252146] p 3864 N92-31407
Deep-tow acoustics/geophysics system compressional velocity database
[AD-A252700] p 3918 N92-31467
Computer simulation of acoustic fluctuations due to finescale temperature perturbations measured by thermistor chain
[AD-A252709] p 3892 N92-31672

ACOUSTICS
Sensitivity of the tomographic inverse solution to acoustic path variability
[AD-A252146] p 3864 N92-31407
Acoustic studies of ocean surface processes in SWAPP
[AD-A247519] p 3864 N92-31429
Deep-tow acoustics/geophysics system compressional velocity database
[AD-A252700] p 3918 N92-31467
Hydrographic and Acoustic Doppler Current Profiler (ADCP) data from the Farallones shelf and slope study
[AD-A250834] p 3864 N92-31495
A data processing module for acoustic Doppler current meters
[AD-A250901] p 3891 N92-31563
Computer simulation of acoustic fluctuations due to finescale temperature perturbations measured by thermistor chain
[AD-A252709] p 3892 N92-31672
NAS (Numerical Aerodynamic Simulation Program) technical summaries, March 1989 - February 1990
[NASA-TM-107960] p 3926 N92-31852

ACQUISITION
A dictionary of acquisition and contracting terms
[AD-A247053] p 3920 N92-31754
Optical fiber sensors for organic matrix composite material cure monitoring
[AD-A247114] p 3776 N92-31979

ACRYLATES
The photogeneration of polymeric amines: Synthesis and photocrosslinking of copolymers containing photoactive carbamate pendant groups
[AD-A250086] p 3793 N92-31436
Diosmacycloalkanes as models for the formation of hydrocarbons from surface methylenes
[DE92-014588] p 3783 N92-31891

ACRYLIC RESINS
Nonlinear optical acrylic polymers and use thereof in optical and electro-optic devices
[AD-D015236] p 3791 N92-31270

ACRYLONITRILES
Characterization of polymers for microcellular foams
[DE92-012444] p 3793 N92-31539
Flammability limits and ballistic properties of fuel-rich propellants p 3749 N92-31885

ACTIVATION ENERGY
Real time investigations of the polymerization of 2-pentadecyl aniline on the Langmuir-Blodgett trough
[AD-A250994] p 3795 N92-31954

ACTIVE CONTROL
A summary of the active flexible wing program
[NASA-TM-107655] p 3757 N92-31264
Rolling maneuver load alleviation using active controls
[NASA-TM-107654] p 3757 N92-31351
Active control of the separation region on a two-dimensional airfoil
[AD-A249739] p 3752 N92-31622
Spacecraft stability and control
[TABES PAPER 92-414] p 3763 N92-32011
Control of unsteady separated flow associated with the dynamic stall of airfoils
[NASA-CR-190688] p 3753 N92-32177

ACTUATORS
Modeling and design of a closed kinematic chain robotic mechanism
[DE92-014777] p 3835 N92-32121

ADA (PROGRAMMING LANGUAGE)
Quality Evaluation System (QUES), volume 1
[AD-A252679] p 3876 N92-31586
Performance measures of the Ada rendezvous
[AD-A250060] p 3877 N92-31601
About real time industrial processes control: A methodology based on objects and Petri nets
[LAAS-91467] p 3878 N92-31689

ADAPTATION
Theory and test of stress resistance
[AD-A250741] p 3870 N92-31291
Architectural adaptability in parallel programming
[AD-A247516] p 3881 N92-31428

ADAPTERS
Graphite/epoxy composite adapters for the Space Shuttle/Centaur vehicle
[NASA-TP-3014] p 3765 N92-31251

ADAPTIVE CONTROL
Adaptive mesh strategies for the spectral element method
[NASA-CR-189686] p 3818 N92-31265
Adaptive and nonadaptive feedback control of global instabilities with application to a heated 2-D jet
[AD-A250700] p 3820 N92-31322

ADAPTIVE FILTERS
Adaptive inverse filter
[DE92-011660] p 3878 N92-31669

ADAPTIVE OPTICS
Resolution limits for ground based astronomical imaging using adaptive optics
[DE92-011949] p 3902 N92-31761

ADDITIVES
Surface analysis of stainless steel outer race bearing specimens
[AD-A250088] p 3833 N92-31437
Experimental evaluation of oxygen-enriched air and emulsified fuels in a single-cylinder diesel engine. Volume 1: Concept evaluation
[DE92-015999] p 3799 N92-31442
Impurity effects on the magnetic ordering in chromium
[DE92-016165] p 3789 N92-31898

ADHESION
Electronic and total energy properties of ternary and quaternary semiconductor compounds, alloys, and superlattices: Theoretical study of Cu/graphite bonding
[NASA-CR-190691] p 3772 N92-31266
Preliminary evaluation of adhesion strength measurement devices for ceramic/titanium matrix composite bonds
[NASA-TM-105803] p 3745 N92-31267

ADHESION TESTS
Preliminary evaluation of adhesion strength measurement devices for ceramic/titanium matrix composite bonds
[NASA-TM-105803] p 3745 N92-31267

ADHESIVE BONDING
Preliminary evaluation of adhesion strength measurement devices for ceramic/titanium matrix composite bonds
[NASA-TM-105803] p 3745 N92-31267

ADHESIVES
Preliminary evaluation of adhesion strength measurement devices for ceramic/titanium matrix composite bonds
[NASA-TM-105803] p 3745 N92-31267

ADIABATIC CONDITIONS
A model for the interfacial shear in vertical, adiabatic, annular-mist flow
[DE92-013537] p 3820 N92-31424
Aluminum tunnel junction detector operation in an adiabatic demagnetization refrigerator
[DE92-013441] p 3913 N92-32166

ADIABATIC FLOW
A model for the interfacial shear in vertical, adiabatic, annular-mist flow
[DE92-013537] p 3820 N92-31424

ADSORPTION
Interfacial ion transport between immiscible liquids
[AD-A252424] p 3778 N92-31292
The role of metal structure in determining solvent orientation at the electrode/solution interface
[AD-A249751] p 3893 N92-31328
The thermal dissociation of decaborane on Si(111)-(7x7) and doping effects in the near surface region
[AD-A251057] p 3911 N92-31851
UV photochemistry of trivinylantimony adsorbed on quartz
[AD-A252215] p 3785 N92-32057
Prediction of hydrogen entry and permeation in metals and alloys
[AD-A245286] p 3790 N92-32096

AEROACOUSTICS
CFD methods development considerations for unsteady aerodynamic analysis
[NASA-TM-107644] p 3750 N92-31239
High speed turboprop aeroacoustic study (counterrotation). Volume 2: Computer programs
[NASA-CR-185242] p 3891 N92-31248

AEROASSIST
Stagnation-point heat-transfer rate predictions at aeroassist flight conditions
[NASA-TP-3208] p 3819 N92-31281
Comparison of effects of copropagated and precomputed atmosphere profiles on Monte Carlo trajectory simulation
[NASA-TM-102600] p 3766 N92-31457
An approximate local thermodynamic nonequilibrium radiation model for air
[NASA-CR-190580] p 3914 N92-31577
The use of high lift-to-drag hypersonic vehicles for aero-assisted orbital maneuvering p 3748 N92-31877

AERODYNAMIC BALANCE
A simulation model of a single rotor helicopter
p 3746 N92-31865

AERODYNAMIC CHARACTERISTICS
CFD methods development considerations for unsteady aerodynamic analysis
[NASA-TM-107644] p 3750 N92-31239
Wind tunnel aerodynamic characteristics of a transport-type airfoil in a simulated heavy rain environment
[NASA-TP-3184] p 3751 N92-31532
A computational examination of directional stability for smooth and chined forebodies at high-alpha
[NASA-CR-4465] p 3753 N92-32114
Transonic wind tunnel test of a 14 percent thick oblique wing
[NASA-TM-102230] p 3754 N92-32213

AERODYNAMIC CONFIGURATIONS
Euler solver for arbitrary configurations: Further applications p 3750 N92-31888

AERODYNAMIC DRAG
High Reynolds number test of the Boeing TR77 airfoil in the Langley 0.3-meter transonic cryogenic tunnel
[NASA-TM-4189] p 3750 N92-31246

AERODYNAMIC FORCES
Time simulation of flutter with large stiffness changes
[NASA-TM-107650] p 3758 N92-32111

AERODYNAMIC HEATING
In-flight evaluation of aerodynamic predictions of an air-launched space booster
[NASA-TM-104246] p 3752 N92-31808

AERODYNAMIC INTERFERENCE
An investigation into the interface between three closely spaced axi-symmetric bodies at subsonic speed
[CRANFIELD-AERO-9114] p 3751 N92-31514
In-flight evaluation of aerodynamic predictions of an air-launched space booster
[NASA-TM-104246] p 3752 N92-31808

AERODYNAMIC LOADS
A summary of the active flexible wing program
[NASA-TM-107655] p 3757 N92-31264
Rolling maneuver load alleviation using active controls
[NASA-TM-107654] p 3757 N92-31351

AERODYNAMIC STABILITY
Transonic wind tunnel test of a 14 percent thick oblique wing
[NASA-TM-102230] p 3754 N92-32213

AERODYNAMIC STALLING
A computational investigation of airfoil stall flutter
[AD-A247302] p 3751 N92-31300
Control of unsteady separated flow associated with the dynamic stall of airfoils
[NASA-CR-190688] p 3753 N92-32177

AERODYNAMICS
Overview of the NASA Dryden Flight Research Facility aeronautical flight projects
[NASA-TM-104254] p 3756 N92-31261
In-flight leading-edge extension vortex flow-field survey measurements on a F-18 aircraft at high angle of attack
[NASA-TM-4398] p 3751 N92-31276
Aeronautical engineering: A continuing bibliography with indexes (supplement 280)
[NASA-SP-7037(280)] p 3745 N92-31456
Automatic design of transonic airfoils to reduce the shock induced pressure drag p 3745 N92-31863
Axisymmetric bluff-body flow: A vortex solver for thin shells
[DE92-016748] p 3824 N92-31933
A continuing study of altitude determination deficiencies of the Service Aircraft Instrumentation Package (SAIP)
[AD-A245952] p 3758 N92-32051

AEROELASTIC RESEARCH WINGS
A summary of the active flexible wing program
[NASA-TM-107655] p 3757 N92-31264
Flutter suppression digital control law design and testing for the AFW wind-tunnel model
[NASA-TM-107652] p 3757 N92-31350
Rolling maneuver load alleviation using active controls
[NASA-TM-107654] p 3757 N92-31351

AEROELASTICITY
Flutter suppression digital control law design and testing for the AFW wind-tunnel model
[NASA-TM-107652] p 3757 N92-31350
Time simulation of flutter with large stiffness changes
[NASA-TM-107650] p 3758 N92-32111

AEROLOGY
Comprehensive Aerological Reference Data Set (CARDS)
[DE92-016469] p 3862 N92-31734

AEROMANEUVERING
The use of high lift-to-drag hypersonic vehicles for aero-assisted orbital maneuvering p 3748 N92-31877

AERONAUTICAL ENGINEERING
Aeronautical engineering: A continuing bibliography with indexes (supplement 280)
[NASA-SP-7037(280)] p 3745 N92-31456

AERONOMY
Combined Release and Radiation Effects Satellite (CRRES) experiments data collection, analysis, and publication
[NASA-CR-184361] p 3856 N92-31551

AEROSOLS
Effects of anthropogenic sulfur aerosols on climate
[DE92-016158] p 3850 N92-31297
Numerical simulation of precipitation scavenging and comparison with observation of prescribed forest fires
[DE92-013513] p 3851 N92-31423
Analysis of the effects of aerosol distribution in the atmosphere on surface radiative measurements
[DE92-014189] p 3856 N92-31662

AEROSPACE ENGINEERING
NASA patent abstracts bibliography: A continuing bibliography. Section 2: Indexes (supplement 41)
[NASA-SP-7039(41)-SECT-2] p 3918 N92-31455
Space nuclear power, propulsion, and related technologies
[SAND91-2617] p 3770 N92-31503
Integrated Technology Plan for the Civil Space Program, 1991
[PB92-181692] p 3762 N92-31634
An integrated research program for the modeling, analysis and control of aerospace systems
[AD-A250199] p 3761 N92-31966
TABES 92: 8th Annual Technical and Business Exhibition and Symposium. Executive summaries and submitted papers p 3763 N92-32009

AEROSPACE ENVIRONMENTS
Characterization of oxide formed on silicon by exposure to atomic oxygen in space
[AD-A249787] p 3778 N92-31301
Liquid lubrication for space applications
[NASA-TM-105198] p 3795 N92-31840

AEROSPACE INDUSTRY
Integrated Technology Plan for the Civil Space Program, 1991
[PB92-181692] p 3762 N92-31634
The trading company in space development in Japan
[TABES PAPER 92-424] p 3764 N92-32015

AEROSPACE SAFETY
The icing of the elevator of the DLR icing research aircraft of Do 28 type
[DLR-MITT-91-12] p 3755 N92-31813
A philosophy for space nuclear systems safety
[DE92-016501] p 3771 N92-32030
Analysis of debris from Spacelab Space Life Sciences-1
[NASA-TM-103593] p 3765 N92-32148

AEROSPACE SYSTEMS
The determination of operational and support requirements and costs during the conceptual design of space systems
[NASA-CR-190626] p 3766 N92-31260

Space nuclear power, propulsion, and related technologies
[SAND91-2617] p 3770 N92-31503
An integrated research program for the modeling, analysis and control of aerospace systems
[AD-A250199] p 3761 N92-31966

AEROSPACE TECHNOLOGY TRANSFER
Integrated Technology Plan for the Civil Space Program, 1991
[PB92-181692] p 3762 N92-31634
NASA programs --- nasa space programs
p 3765 N92-32238

AEROTHERMODYNAMICS
In-flight evaluation of aerodynamic predictions of an air-launched space booster
[NASA-TM-104246] p 3752 N92-31808
Research on aero-thermodynamic distortion induced structural dynamic response of multistage compressor blading
[AD-A250865] p 3760 N92-32059

AGGREGATES
Eigensensitivity analysis of composite laminates: Effect of microstructure
[AD-A250864] p 3777 N92-32104

AGING (MATERIALS)
Understanding and managing the effects of battery charger and inverter aging
[DE92-014473] p 3815 N92-31651

AIR
Experimental evaluation of oxygen-enriched air and emulsified fuels in a single-cylinder diesel engine. Volume 1: Concept evaluation
[DE92-015999] p 3799 N92-31442
An approximate local thermodynamic nonequilibrium radiation model for air
[NASA-CR-190580] p 3914 N92-31577

AIR BREATHING ENGINES
Laser-initiated conical detonation wave for supersonic combustion, part 3
[AD-A250522] p 3785 N92-32076

AIR CONDITIONING
Simplified air change effectiveness modeling
[DE92-010577] p 3872 N92-31309

AIR COOLING
A study of the microstructural basis for the strength and toughness properties of water-quenched and air-cooled HSLA-100, HSLA-100 with increased copper, and a ULCB steel
[AD-A245955] p 3789 N92-32052

AIR FLOW
Simplified air change effectiveness modeling
[DE92-010577] p 3872 N92-31309
Multi-year strategic plan for the atmospheric studies in complex terrain: ASCOT program
[DE92-016646] p 3854 N92-31930
Exploratory experimental investigation of a wave propeller
[AD-A252175] p 3753 N92-32062

AIR JETS
Effect of inlet geometry on the flow and combustion processes in a solid fuel ramjet p 3747 N92-31871

AIR POLLUTION
Effects of anthropogenic sulfur aerosols on climate
[DE92-016158] p 3850 N92-31297
Energy conservation: The main factor for reducing greenhouse gas emissions in the former Soviet Union
[DE92-012355] p 3852 N92-31574
Minorities and air quality non-attainment areas: A preliminary geo-demographic analysis
[DE92-013054] p 3852 N92-31591
Acid deposition: State of science and technology. Summary report of the US National Acid Precipitation Assessment Program, volumes 1-4
[PB92-100353] p 3852 N92-31598
Response of a tundra ecosystem to elevated atmospheric carbon dioxide and CO2-induced climate change
[DE92-013925] p 3853 N92-31626
Methods of assessing responses of trees, stands and ecosystems to air pollution
[PB92-180231] p 3853 N92-31648
Evolution of environmental protection strategies in the Soviet Union
[DE92-015090] p 3853 N92-31732
World ocean circulation experiment. WOCE chlorofluorocarbon intercomparison cruise report
[PB92-185974] p 3865 N92-31842
Iterative functionalism and climate management regimes: From intergovernmental panel on climate change to intergovernmental negotiating committee
[DE92-014798] p 3853 N92-31896
Multi-year strategic plan for the atmospheric studies in complex terrain: ASCOT program
[DE92-016646] p 3854 N92-31930
The potential of passive-remote Fourier Transform Infrared (FTIR) spectroscopy to detect organic emissions under the Clean Air Act
[DE92-015224] p 3854 N92-32083
NASA High Speed Research Program, Emissions Scenarios Committee report of meetings on 26 September 1991 and 9 January 1992
[NASA-CR-190379] p 3855 N92-32147

AIR QUALITY
Minorities and air quality non-attainment areas: A preliminary geo-demographic analysis
[DE92-013054] p 3852 N92-31591
The potential of passive-remote Fourier Transform Infrared (FTIR) spectroscopy to detect organic emissions under the Clean Air Act
[DE92-015224] p 3854 N92-32083

AIR SAMPLING
Development of an electrochemical method for field testing of protective coatings
[AD-A245872] p 3793 N92-31473
Trends 1991: A compendium of data on global change
[DE92-011733] p 3854 N92-31907

AIR TO AIR MISSILES
Dynamic modeling and modal analysis of an air-to-air missile
[AD-A245957] p 3758 N92-32053

AIR TRAFFIC CONTROL
Remote sensing of trapping layer base height using ATIS transmissions
[AD-A250074] p 3844 N92-31362

AIR TRANSPORTATION
NASA High Speed Research Program, Emissions Scenarios Committee report of meetings on 26 September 1991 and 9 January 1992
[NASA-CR-190379] p 3855 N92-32147

AIR WATER INTERACTIONS
Hydrographic observations from the US/PRC cooperative program in the western equatorial Pacific Ocean: Cruises 5-8
[PB92-177054] p 3865 N92-31644
A numerical, analytical, and observational study of the effect of clouds on surface wind and wind stress during the central Arctic winter
[AD-A252706] p 3860 N92-31670
Seasonal wind and ocean thermal forcing influences on the generation of the Leeuwin current and its eddies
[AD-A246992] p 3865 N92-31988

AIRBORNE EQUIPMENT
Spectrum modal analysis for the detection of low-altitude windshear with airborne Doppler radar
[NASA-CR-4457] p 3755 N92-31549

AIRBORNE RADAR
An airborne study of boundary layer heat and moisture fluxes for project FIFE
[NASA-CR-190665] p 3844 N92-31357

AIRBORNE RANGE AND ORBIT DETERMINATION
Charge transfer processes in multiple site chemical systems
[AD-A249538] p 3791 N92-31358

AIRCRAFT ACCIDENTS
Canadian aircrew sea water survival, 1952-1987
[DCIEM-88-RR-39] p 3756 N92-32219

AIRCRAFT CONFIGURATIONS
ASTOVL combat aircraft design synthesis and optimization
[CRANFIELD-AERO-9201] p 3757 N92-31515

AIRCRAFT CONTROL
A summary of the active flexible wing program
[NASA-TM-107655] p 3757 N92-31264
Design and analysis issues of integrated control systems for high-speed civil transports
[NASA-CR-186022] p 3761 N92-31656

AIRCRAFT DESIGN
ASTOVL combat aircraft design synthesis and optimization
[CRANFIELD-AERO-9201] p 3757 N92-31515
Collection of papers of the 31st Israel Annual Conference on Aviation and Astronautics
[ITN-92-85124] p 3745 N92-31861
Integrated computer systems in aircraft design and manufacture: Difficulties and implications
p 3746 N92-31864
An installed nacelle design code using a multiblock Euler solver. Volume 1: Theory document
[NASA-CR-189652-VOL-1] p 3754 N92-32226
An installed nacelle design code using a multiblock Euler solver. Volume 2: User guide
[NASA-CR-189652-VOL-2] p 3754 N92-32228

AIRCRAFT ENGINES
Polymer blends, volume 1
[AD-A252112] p 3792 N92-31419
Research into improving the durability of the hot section in the aircraft turbine engine
[AD-A250342] p 3759 N92-31439
Analytical and experimental studies of heat pipe radiation cooling of hypersonic propulsion systems
[DE92-013428] p 3759 N92-31817

AIRCRAFT FUELS
Advanced thermally stable, jet fuels development program annual report. Volume 1: Model and experiment system development
[AD-A249625] p 3799 N92-31462
Supercritical fluid fractionation of JP-8
[AD-A247835] p 3801 N92-31982

AIRCRAFT INDUSTRY
NASA High Speed Research Program, Emissions Scenarios Committee report of meetings on 26 September 1991 and 9 January 1992
[NASA-CR-190379] p 3855 N92-32147

AIRCRAFT INSTRUMENTS
Estimation of aircraft attitude by angular rate measurements p 3748 N92-31881
A continuing study of altitude determination deficiencies of the Service Aircraft Instrumentation Package (SAIP)
[AD-A245952] p 3758 N92-32051
Dynamic modeling and modal analysis of an air-to-air missile
[AD-A245957] p 3758 N92-32053

AIRCRAFT MAINTENANCE
GNAS Maintenance Control Center (GMCC) Design Qualification Test and Evaluation (DQT/E) test report
[DOT/FAA/CT-TN91/39] p 3745 N92-31615
Aging fleet: Maintaining airworthiness
p 3745 N92-31862

AIRCRAFT MANEUVERS
Rolling maneuver load alleviation using active controls
[NASA-TM-107654] p 3757 N92-31351
Discrete optimal guidance for high order missile and maneuvering target p 3748 N92-31879
Optimal trajectories for an unmanned air vehicle
p 3748 N92-31880

AIRCRAFT NOISE
Aviation noise: Costs of phasing out noisy aircraft
[GAO/RCED-91-128] p 3891 N92-31454

AIRCRAFT RELIABILITY
Aging fleet: Maintaining airworthiness
p 3745 N92-31862

AIRCRAFT SAFETY
Aviation safety: Changes needed in FAA's service difficulty reporting program
[GAO/RCED-91-24] p 3755 N92-31453
Aging fleet: Maintaining airworthiness
p 3745 N92-31862
Report of the aviation safety review of Department of Energy helicopter operations
[DE92-016346] p 3755 N92-31928

AIRCRAFT SPECIFICATIONS
Polymer blends, volume 1
[AD-A252112] p 3792 N92-31419

AIRCRAFT STRUCTURES
Aging fleet: Maintaining airworthiness
p 3745 N92-31862
Analysis of three icing test flights reaching the aircraft-referred icing degree of severe
[ESA-TT-1254] p 3755 N92-31943

AIRCRAFT SURVIVABILITY
Aging fleet: Maintaining airworthiness
p 3745 N92-31862

AIRFOIL OSCILLATIONS
A computational investigation of airfoil stall flutter
[AD-A247302] p 3751 N92-31300

AIRFOIL PROFILES
Automatic design of transonic airfoils to reduce the shock induced pressure drag p 3745 N92-31863

AIRFOILS
High Reynolds number test of the Boeing TR77 airfoil in the Langley 0.3-meter transonic cryogenic tunnel
[NASA-TM-4189] p 3750 N92-31246
Digital analysis of wind tunnel imagery to measure fluid thickness
[NASA-CR-189234] p 3762 N92-31252
Fatigue in single crystal nickel superalloys
[AD-A250068] p 3786 N92-31360
A surface definition code for turbine blade surfaces
[DE92-010574] p 3846 N92-31498
Wind tunnel aerodynamic characteristics of a transport-type airfoil in a simulated heavy rain environment
[NASA-TP-3184] p 3751 N92-31532
Active control of the separation region on a two-dimensional airfoil
[AD-A249739] p 3752 N92-31622
Automatic design of transonic airfoils to reduce the shock induced pressure drag p 3745 N92-31863
Exploratory experimental investigation of a wave propeller
[AD-A252175] p 3753 N92-32062
Control of unsteady separated flow associated with the dynamic stall of airfoils
[NASA-CR-190688] p 3753 N92-32177

AIRLINE OPERATIONS
Aviation safety: Changes needed in FAA's service difficulty reporting program
[GAO/RCED-91-24] p 3755 N92-31453
Aviation noise: Costs of phasing out noisy aircraft
[GAO/RCED-91-128] p 3891 N92-31454
An assessment of the B-747's capability to operate on rough surfaces
[AD-A250134] p 3757 N92-31793
AIRPORTS
GNAS Maintenance Control Center (GMCC) Design Qualification Test and Evaluation (DQT/E) test report
[DOT/FAA/CT-TN91/39] p 3745 N92-31615
Global positioning system runway incursion program static ground tests
[DOT/FAA/CT-TN91/44] p 3756 N92-31838
ALASKA
Annual dynamics within the active layer
[DE92-013520] p 3850 N92-31304
Hydrological and geochemical response and recovery in disturbed Arctic ecosystems
[DE92-016223] p 3850 N92-31312
Response of a tundra ecosystem to elevated atmospheric carbon dioxide and CO2-induced climate change
[DE92-013925] p 3853 N92-31626
ALBUMINS
Interfacial ion transport between immiscible liquids
[AD-A252424] p 3778 N92-31292
ALERTNESS
Empirical development of a scale for the prediction of performance on a sustained monitoring task
[AD-A252443] p 3872 N92-31294
ALGEBRA
The development of modularized software for empirical testing of new algorithms in linear programming
[AD-A250811] p 3875 N92-31480
Mathematical structures for qualitative calculus, a contribution to qualitative simulation
[LAAS-91475] p 3886 N92-31690
New algorithms for the minimal form problem
[DE92-011963] p 3879 N92-31743
ALGORITHMS
Subsonic flight test evaluation of a performance seeking control algorithm on an F-15 airplane
[NASA-TM-4400] p 3759 N92-31275
Estimation with multisensor/multiscan detection fusion
[AD-A250496] p 3804 N92-31333
Modeling of composite beams and plates for static and dynamic analysis
[NASA-CR-190536] p 3839 N92-31339
The Swendsen-Wang dynamics in the simulation of the Ising model
[INPE-5394-PRE/1752] p 3874 N92-31348
Using the burst derivative measure to improve the computational efficiency of ISAR motion compensation algorithms
[AD-A250850] p 3805 N92-31369
Signal location using generalized linear constraints
[AD-A249580] p 3805 N92-31376
A robust algorithm for isotropic reconstruction of magic-angle spinning solid-state NMR spectra
[AD-A249610] p 3874 N92-31379
Algorithms for the determination of spatial and spectral distribution of electromagnetic energy in a simulated biostructure subjected to transient spatially heterogeneous radiation with applications to radar hazard assessment and cancer therapy
[AD-A250447] p 3805 N92-31381
A strictly improving phase 1 algorithm using least-squares subproblems
[DE92-015904] p 3875 N92-31410
Architectural adaptability in parallel programming
[AD-A247516] p 3881 N92-31428
Detection of signal harmonic sets
[DREA-CR-89-420] p 3806 N92-31471
The development of modularized software for empirical testing of new algorithms in linear programming
[AD-A250811] p 3875 N92-31480
A comparison of three self-tuning control algorithms developed for the Bristol-Babcock controller
[DE92-014472] p 3814 N92-31499
Neural network perception for mobile robot guidance
[AD-A249972] p 3884 N92-31511
Spectrum modal analysis for the detection of low-altitude windshear with airborne Doppler radar
[NASA-CR-4457] p 3755 N92-31549
Development of the aspect graph representation for use in R version
[AD-A247109] p 3876 N92-31573
A simple linearized learning algorithm which outperforms back-propagation
[AD-A249697] p 3877 N92-31642
Logarithmic retinae
[PB92-183649] p 3885 N92-31680
Development and application of new algorithms for the simulation of compressible flows with moving bodies in three dimensions
[AD-A250232] p 3823 N92-31696
Some computational challenges of developing efficient parallel algorithms for data-dependent computations in thermal-hydraulics supercomputer applications
[DE92-011368] p 3878 N92-31703
Theoretical studies of the reactions and spectroscopy of radical species relevant to combustion reactions and diagnostics
[DE92-013484] p 3781 N92-31725
Modeling arbitrarily directed slots that are narrow both in width and depth with regard to the FDTD spatial cell
[DE92-008015] p 3808 N92-31738
A task adaptive parallel graphics rendering algorithm
[DE92-008062] p 3878 N92-31739
New algorithms for the minimal form problem
[DE92-011963] p 3879 N92-31743
Analysis and computer tools for separation processes involving nonideal mixtures
[DE92-015298] p 3781 N92-31752
Low density real gas flows about hypersonic vehicles
[AD-A250048] p 3752 N92-31777
Roundoff algorithms for digital phase shifters that minimize beam shift
[AD-A250094] p 3816 N92-31780
Use of a genetic algorithm to solve fluid flow problems on an NCUBE/2 multiprocessor computer
[DE92-014044] p 3824 N92-31832
Singularity avoidance for SCARA-type robots
p 3746 N92-31867
ADIFOR: Fortran source translation for efficient derivatives
[DE92-016187] p 3879 N92-31899
A real time system for multisensor image analysis through pyramidal segmentation
[AD-A247169] p 3888 N92-31981
New techniques in computational fluid dynamics: Algorithms, analysis, applications
[AD-A250498] p 3825 N92-32038
New directions in network flows
[AD-A250499] p 3880 N92-32039
Signal processing and recognition in adaptive neural networks
[AD-A250505] p 3885 N92-32041
An empirical prediction algorithm for low-frequency acoustic surface scattering strengths
[AD-A250508] p 3892 N92-32044
Database explorer: Large scale database application
[AD-A252183] p 3920 N92-32049
A comparison of the performance of two gust front detection algorithms using a length-based scoring technique
[AD-A250862] p 3863 N92-32103
Workshop on the Derivation of Parallel Programs and Architectures: Closing report
[AD-A252742] p 3883 N92-32109
A sweep algorithm for massively parallel simulation of circuit-switched networks
[NASA-CR-189680] p 3881 N92-32157
Data compression techniques p 3922 N92-32190
Experiment on a three-beam adaptive array for EHF frequency-hopped signals using a fast algorithm, phase-D
[CTN-92-60322] p 3810 N92-32203
Markovian fields as limits of Markov chains
[INPE-5395-PRE/1753] p 3889 N92-32225
A parameter optimization approach to controller partitioning for integrated flight/propulsion control application
[NASA-TM-105826] p 3761 N92-32241
ALIGNMENT
Analysis and evaluation of Project Evergreen data
[AD-A245983] p 3804 N92-31314
ALIPHATIC HYDROCARBONS
Trends 1991: A compendium of data on global change
[DE92-011733] p 3854 N92-31907
ALKALI HALIDES
He atom-surface scattering: Surface dynamics of insulators, overlayers and crystal growth
[DE92-011810] p 3911 N92-31914
ALKALI METALS
Application of the mean spherical approximation to the estimations of single ion thermodynamic quantities of solvation for monoatomic monovalent ions in aqueous solutions
[AD-A250190] p 3893 N92-31316
Absorption spectra and electronic properties of alkali metal doped C60
[AD-A251006] p 3912 N92-31937
Role of the double-layer cation on the potential-dependent stretching frequencies and binding geometries of carbon monoxide at platinum-nonaqueous interfaces
[AD-A246980] p 3784 N92-31998
ALKENES
Diosmacycloalkanes as models for the formation of hydrocarbons from surface methylenes
[DE92-014588] p 3783 N92-31891
Polyalphaolefins: A new improved cost effective aircraft radar coolant
[AD-A250517] p 3796 N92-32045
ALKYL COMPOUNDS
Polymerization of conducting polymers confined to free surfaces: A comparison of the Langmuir-Blodgett polymerization of 3-alkyl pyrroles and 2-alkyl anilines
[AD-A250966] p 3798 N92-32194
ALKYLATION
Novel chemically amplified dry-developing imaging materials for high resolution microlithography
[AD-A250085] p 3793 N92-31435
ALLOYING
A fast laser alloying process for the selective electroplating of metal on SiO2 and polyimide
[DE92-011764] p 3788 N92-31759
ALLOYS
Prediction of hydrogen entry and permeation in metals and alloys
[AD-A245286] p 3790 N92-32096
ALPHA PARTICLES
Radiolytic gas production in the alpha particle degradation of plastics
[DE92-011846] p 3795 N92-31938
ALTIMETERS
Estimation of aircraft attitude by angular rate measurements p 3748 N92-31881
ALTITUDE
A continuing study of altitude determination deficiencies of the Service Aircraft Instrumentation Package (SAIP)
[AD-A245952] p 3758 N92-32051
ALUMINATES
Mechanical strength and stability of lithium aluminate
[DE92-015998] p 3841 N92-31638
ALUMINUM
Natural convection immersion cooling of an array of vertically oriented heated protrusions in an enclosure filled with a dielectric liquid: Effects of enclosure width, Prandtl number and component orientation
[AD-A245884] p 3914 N92-31489
Tris-triphenylsiloxy compounds of aluminum
[AD-A250141] p 3788 N92-31795
Aluminum tunnel junction detector operation in an adiabatic demagnetization refrigerator
[DE92-013441] p 3913 N92-32166
ALUMINUM ALLOYS
Corrosion behavior of squeeze cast aluminum metal matrix composites
[AD-A250486] p 3774 N92-31382
The effect of elastic stress on Ostwald ripening phenomena
[DE92-015291] p 3839 N92-31400
Finite-element analyses and fracture simulation in thin-sheet aluminum alloy
[NASA-TM-107662] p 3839 N92-31504
The structure and properties of grain boundaries in Ni3Al
[DE92-012143] p 3788 N92-31744
J(sub 2) fracture toughness testing of Al 707 5-T7351
p 3747 N92-31872
ALUMINUM ARSENIDES
Advanced high efficiency concentrator cells
[DE92-010559] p 3848 N92-31893
ALUMINUM COMPOUNDS
Experimental studies of aluminum solubility and speciation in brines
[DE92-010448] p 3786 N92-31418
Thermomechanical fatigue behavior of a silicone carbide fiber-reinforced calcium aluminosilicate glass-ceramic matrix composite
[AD-A249870] p 3775 N92-31823
Quantum mechanical approach to understanding microstructural and mechanical properties in intermetallics
[AD-A250550] p 3790 N92-32084
ALUMINUM GALLIUM ARSENIDES
Phase-locked arrays of antiguided diode lasers: Modelling, design, evaluation of performance limits
[LAAS-92034] p 3830 N92-31698
Subnanosecond photoconductive switching in GaAs
[DE92-011521] p 3910 N92-31719
ALUMINUM NITRIDES
Growth, nitrogen vacancy reduction and solid solution formation in cubic GaN thin films and the subsequent fabrication of superlattice structures using AlN and InN
[AD-A248058] p 3908 N92-31446
ALUMINUM OXIDES
Interface engineering in alumina/glass composites
[AD-A248587] p 3773 N92-31315
Final report on DSA methods for monitoring alumina in aluminum reduction cells with cermet anodes
[DE92-013599] p 3813 N92-31440

Sodium Heat Engine Development Program
[DE92-012398] p 3846 N92-31531
Ceramic surfaces and sintering
[DE92-011570] p 3793 N92-31538
Non-equilibrium synthesis by laser cladding of Ni, Nb and Mg alloys for improved environmental resistance
[AD-A250552] p 3787 N92-31612
The effect of thermomechanical processing parameters on the ambient behavior of 10 percent volume 6061 Al-Alumina
[AD-A252177] p 3776 N92-32064

ALUMINUM SILICATES
The preparation of (Al2O3)x(SiO2)y thin films using (Al(OSiEt3))2 as a single source precursor
[AD-A250142] p 3788 N92-31796

AMAZON REGION (SOUTH AMERICA)
The structure and energetics of Amazon squall lines
[AD-A250182] p 3859 N92-31523
Rainwater and throughfall chemistry in a terra firme rain forest: Central Amazonia
[INPE-5364-PRE/1744] p 3863 N92-32224

AMINES
The photogeneration of polymeric amines: Synthesis and photocrosslinking of copolymers containing photoactive carbamate pendant groups
[AD-A250086] p 3793 N92-31436

AMINO ACIDS
Dependence of secondary ion emission from organic material on the energy loss of the impacting heavy ion
[DE92-014845] p 3893 N92-31386

AMMONIUM NITRATES
Turbulent dusty boundary layer in an ANFO surface-burst explosion
[DE92-012101] p 3822 N92-31625
Shock tube study of the reaction of triethanol ammonium nitrate with N2O
[AD-A250034] p 3800 N92-31804

AMMONIUM PICRATES
Development of methodology and technology for identifying and quantifying emission products from open burning and open detonation thermal treatment methods. Field test series A, B, and C. Volume 1: Test summary
[AD-A250735] p 3800 N92-31971

AMMUNITION
Using transfer functions as a method for predicting lightning effects on munitions storage bunkers
[DE92-012627] p 3861 N92-31709
Measured responses of a munitions storage bunker to rocket-triggered lightning
[DE92-012628] p 3862 N92-31750

AMORPHOUS MATERIALS
Synthesis of side chain liquid crystal polymers by living ring opening metathesis polymerization. 4: Synthesis of amorphous and side chain liquid crystal AB block copolymers
[AD-A250353] p 3792 N92-31394
Radiation-induced crystalline-to-amorphous transition in intermetallic compounds of the Cu-Ti alloy system
[DE92-010276] p 3787 N92-31575
The preparation of (Al2O3)x(SiO2)y thin films using (Al(OSiEt3))2 as a single source precursor
[AD-A250142] p 3788 N92-31796

AMORPHOUS SILICON
Research on stable, high-efficiency amorphous silicon multijunction modules
[DE92-001244] p 3814 N92-31525

AMPLIFICATION
Amplification mechanism of ion-ripple lasers and its possible application
[DE92-016155] p 3830 N92-31411

AMPLITUDES
Synthetic temperature profile in the Gulf of Mexico. Part 1: Statistical relationship between modal amplitudes and dynamic height at surface
[AD-A252701] p 3863 N92-31308
Phase characteristics and time responses of unknown linear systems determined from measured CW amplitude data
[PB92-183722] p 3805 N92-31368
Optical oversampled analog-to-digital conversion
[AD-A252695] p 3877 N92-31587

ANALOG TO DIGITAL CONVERTERS
Optical oversampled analog-to-digital conversion
[AD-A252695] p 3877 N92-31587
Problems with interleaved digitizers
[DE92-013369] p 3881 N92-32150

ANALOGIES
Dicke narrowing in strong fields: The atom-as-antenna analogy
[AD-A252321] p 3807 N92-31629

ANALYSIS OF VARIANCE
Importance sampling for Markov chains: Asymptotics for the variance
[AD-A249804] p 3888 N92-31757

ANALYZERS
Diagnostics for research in atomization and turbulent two-phase flows
[AD-A247201] p 3819 N92-31283
New high voltage parallel plate analyzer
[NIFS-128] p 3827 N92-31340

ANELASTICITY
The RQM triangle: A paradigm for relativistic quantum mechanics
[DE92-011583] p 3915 N92-31663

ANEMOMETERS
Description of a 1000 sensor constant current anemometer system for locating three-dimensional turbulent boundary layer separations
[AD-A250827] p 3821 N92-31452

ANGLE OF ATTACK
In-flight leading-edge extension vortex flow-field survey measurements on a F-18 aircraft at high angle of attack
[NASA-TM-4398] p 3751 N92-31276
Transonic wind tunnel test of a 14 percent thick oblique wing
[NASA-TM-102230] p 3754 N92-32213

ANGULAR CORRELATION
Electron scattering by atomic hydrogen: Elastic and inelastic phenomena at 13.9 to 200 eV
[DE92-625004] p 3896 N92-31837

ANGULAR DISTRIBUTION
Photon and electron data bases and their use in radiation transport calculations
[DE92-011458] p 3895 N92-31705

ANGULAR MOMENTUM
An investigation of spinup dynamics of axial gyrostats using elliptic integrals and the method of averaging
[AD-A249728] p 3768 N92-31675
Theoretical atomic collision physics
[DE92-013571] p 3895 N92-31724
Rigid rotations in two-electron atoms in a uniform magnetic field
[DE92-624981] p 3896 N92-31836

ANGULAR VELOCITY
FCS skewed sensors array: Practical considerations
p 3746 N92-31868
An innovative two axis rate gyro: Theory and principles of operation p 3748 N92-31875

ANIK SATELLITES
A prototype DND Ku band SATCOM system for ANIK-C2 (Project MASTER/MM2)
[DREO-1034] p 3810 N92-32176

ANILINE
The effect of surface pressure on Langmuir-Blodgett polymerization of 2-pentadecyl aniline
[AD-A250993] p 3795 N92-31952
Real time investigations of the polymerization of 2-pentadecyl aniline on the Langmuir-Blodgett trough
[AD-A250994] p 3795 N92-31954
Polymerization of conducting polymers confined to free surfaces: A comparison of the Langmuir-Blodgett polymerization of 3-alkyl pyrroles and 2-alkyl anilines
[AD-A250966] p 3798 N92-32194

ANIMALS
The effects of hydrazines of neuronal excitability
[AD-A247142] p 3868 N92-31491
Extremely Low Frequency (ELF) communications system ecological monitoring program summary of 1990 progress
[AD-A246344] p 3809 N92-31996

ANIONS
Application of the mean spherical approximation to the estimations of single ion thermodynamic quantities of solvation for monoatomic monovalent ions in aqueous solutions
[AD-A250190] p 3893 N92-31316
Temperature-enhanced autodetachment from long-lived parent negative ions of gaseous dielectrics
[DE92-011108] p 3894 N92-31700
Ring-opening polymerization of strained cyclotetrasilanes as a new route towards well defined polysilylenes
[AD-A251020] p 3795 N92-31941
Near-IR absorption spectra for the Buckminsterfullerene Anions: An experimental and theoretical study
[AD-A250532] p 3785 N92-32080
Structure and dynamics of Cl(H2O)20 clusters. The effect of the polarizability and the charge ofthe ion
[AD-A251094] p 3899 N92-32196

ANISOTROPIC MEDIA
Research in regional seismology: The effect of anisotropy
[AD-A248940] p 3855 N92-31476

ANISOTROPY
Research in regional seismology: The effect of anisotropy
[AD-A248940] p 3855 N92-31476
Mechanics of thin films
[AD-A247848] p 3912 N92-31984

ANNEALING
Substrate surface effects on the properties of sputter-deposited and laser-irradiated films
[DE92-013850] p 3795 N92-31917
The effect of thermomechanical processing parameters on the ambient behavior of 10 percent volume 6061 Al-Alumina
[AD-A252177] p 3776 N92-32064

ANNOTATIONS
A model for extending the behavior of annotations
[DE92-011731] p 3920 N92-31934

ANNUAL VARIATIONS
Annual dynamics within the active layer
[DE92-013520] p 3850 N92-31304
Meteorological data, new series B basic material. Volume 53, no. 1: Daily altitude maps of the 30-hPa-area and monthly mean maps for the year 1986, part 1
[QR-1-VOL-53-NO-1-PT-1] p 3860 N92-31702
Meteorological data, new series B basic material. Volume 53, no. 2: Daily altitude maps of the 30-hPa-area and monthly mean maps for the year 1986, part 2
[QR-2-VOL-53-NO-2-PT-2] p 3860 N92-31704
Meteorological data, new series B basic material. Volume 53, no. 4: Daily altitude maps of the 30-hPa-area and monthly mean maps for the year 1986, part 4
[QR-4-VOL-53-NO-4-PT-4] p 3861 N92-31706
Upper tropospheric jet streams over North America during summer 1988
[AD-A249871] p 3857 N92-31906
Seasonal wind and ocean thermal forcing influences on the generation of the Leeuwin current and its eddies
[AD-A246992] p 3865 N92-31988

ANODES
Proposal for a workshop in the physics and application of hollow electrode glow switches
[AD-A247139] p 3814 N92-31490

ANTENNA ARRAYS
A data processing module for acoustic Doppler current meters
[AD-A250901] p 3891 N92-31563
A finite element-boundary integral method for conformal antenna arrays on a circular cylinder
[NASA-CR-190534] p 3807 N92-31614
Scattering from a finite collection of transverse dipole and axial slot arrays with edge effects
[AD-A249622] p 3807 N92-31691
Roundoff algorithms for digital phase shifters that minimize beam shift
[AD-A250094] p 3816 N92-31780
High-performance packaging for monolithic microwave and millimeter-wave integrated circuits
[NASA-TM-105744] p 3808 N92-31855
Experiment on a three-beam adaptive array for EHF frequency-hopped signals using a fast algorithm, phase-D
[CTN-92-60322] p 3810 N92-32203

ANTENNA COMPONENTS
Validation of the Numerical Electro-magnetics Code (NEC) for antenna wire elements in proximity to Earth
[AD-A250507] p 3810 N92-32043

ANTENNA DESIGN
A finite element-boundary integral method for conformal antenna arrays on a circular cylinder
[NASA-CR-190534] p 3807 N92-31614
High-performance packaging for monolithic microwave and millimeter-wave integrated circuits
[NASA-TM-105744] p 3808 N92-31855

ANTENNA RADIATION PATTERNS
Roundoff algorithms for digital phase shifters that minimize beam shift
[AD-A250094] p 3816 N92-31780
Validation of the Numerical Electro-magnetics Code (NEC) for antenna wire elements in proximity to Earth
[AD-A250507] p 3810 N92-32043

ANTENNAS
Analysis and evaluation of Project Evergreen data
[AD-A245983] p 3804 N92-31314
Wavenumbers for currents on infinite- and finite-length wires in a chiral medium
[DE92-007565] p 3804 N92-31317
Dicke narrowing in strong fields: The atom-as-antenna analogy
[AD-A252321] p 3807 N92-31629

ANTIFERROMAGNETISM
Schwinger boson studies of the t-J model beyond mean-field approximation
[DE92-630650] p 3909 N92-31655

ANTIMONY
Decomposition studies of triisopropylantimony and triallylantimony
[AD-A250671] p 3796 N92-31968

ANTIOXIDANTS
Advanced thermally stable jet fuel development program. Volume 2: Compositional factors affecting thermal degradation of jet fuels
[AD-A252656] p 3798 N92-31399

APERTURES
Modeling arbitrarily directed slots that are narrow both in width and depth with regard to the FDTD spatial cell
[DE92-008015] p 3808 N92-31738
APPALACHIAN MOUNTAINS (NORTH AMERICA)
A case study of a prolonged sleet event: 16-17 February 1987 and climatology of sleet events for North Carolina, 1949-1989
[AD-A250184] p 3859 N92-31602
APPLICATIONS PROGRAMS (COMPUTERS)
Computer-aided modeling tools for forging process feasibility studies
[DE92-012116] p 3838 N92-31303
Exponential representation and consistency checking for M layer
[AD-A250423] p 3805 N92-31413
Hypersonic code efficiency and validation studies
[NASA-CR-190680] p 3752 N92-31533
The Matrix Editor for symbolic Jacobians in ALPAL
[DE92-008076] p 3878 N92-31742
User's guide for treetherm: A 3-D thermal model for single trees
[LTR91-003] p 3879 N92-31833
VAASEL-ANSYS comparison for a thermally loaded beam
[AD-A251003] p 3841 N92-31847
A study of longwave radiation codes for climate studies: Validation with ARM observations and tests in general circulation models
[DE92-014100] p 3862 N92-31894
Effects of fragmentation parameter variations on estimates of galactic cosmic ray exposure: Dose sensitivity studies for aluminum shields
[NASA-TM-4386] p 3926 N92-32193
Three-dimensional compressible turbulent computations for a nondiffusing S-duct
[NASA-CR-4391] p 3754 N92-32240
APPROPRIATIONS
NSF Tokyo reports. General outline of JFY 1991 government science and technology budget
[PB92-192640] p 3927 N92-32068
APPROXIMATION
Statistical analysis of anomalous transport in resistive interchange turbulence
[NIFS-125] p 3818 N92-31256
Balanced, potential vorticity dynamics in the tropics
[AD-A249981] p 3858 N92-31432
Advanced DAA methods for shock response analysis
[AD-A252696] p 3891 N92-31588
Schwinger boson studies of the t-J model beyond mean-field approximation
[DE92-630650] p 3909 N92-31655
Roundoff algorithms for digital phase shifters that minimize beam shift
[AD-A250094] p 3816 N92-31780
Determination of the matrix conditioning indicator. Comparison of approximate methods
p 3887 N92-32210
AQUATIC PLANTS
Ecosystems of the Florida Keys: A bibliography
[PB92-198910] p 3854 N92-32071
AQUEOUS SOLUTIONS
Application of the mean spherical approximation to the estimations of single ion thermodynamic quantities of solvation for monoatomic monovalent ions in aqueous solutions
[AD-A250190] p 3893 N92-31316
ARC JET ENGINES
The evolutionary development of high specific impulse electric thruster technology
[NASA-TM-105712] p 3769 N92-31342
ARC WELDING
Residual stresses in a multipass ferritic weldment
[DE92-014467] p 3839 N92-31501
ARCHITECTURE (COMPUTERS)
Data to test and evaluate the performance of neural network architectures for seismic signal discrimination, neural computing for seismic phase identification, volume 2
[AD-A252442] p 3884 N92-31293
Architectural adaptability in parallel programming
[AD-A247516] p 3881 N92-31428
Objects used to implement intelligent databases
[DE92-013098] p 3919 N92-31581
Optical oversampled analog-to-digital conversion
[AD-A252695] p 3877 N92-31587
Using neural networks in software repositories
[NASA-CR-190641] p 3885 N92-31597
Oracle and the end-user: Practical implementation of applications in a multi-user, multi-platform environment
[DE92-015223] p 3877 N92-31654
Some computational challenges of developing efficient parallel algorithms for data-dependent computations in thermal-hydraulics supercomputer applications
[DE92-011368] p 3878 N92-31703
Torque linearizing hardware for the electric joint motors of a direct-drive robot
[DE92-012681] p 3816 N92-31718
Optical processing architectures for spaceborne SAR image generation and RF array beam forming
[TABES PAPER 92-444] p 3763 N92-32012
Fault tolerant parallel computing in orthogonal shared-memory and related architectures
[AD-A250504] p 3883 N92-32040
Workshop on the Derivation of Parallel Programs and Architectures: Closing report
[AD-A252742] p 3883 N92-32109
The data structure accelerator architecture
[AD-A250968] p 3883 N92-32152
ARCTIC REGIONS
Annual dynamics within the active layer
[DE92-013520] p 3850 N92-31304
Hydrological and geochemical response and recovery in disturbed Arctic ecosystems
[DE92-016223] p 3850 N92-31312
Response of a tundra ecosystem to elevated atmospheric carbon dioxide and CO2-induced climate change
[DE92-013925] p 3853 N92-31626
A numerical, analytical, and observational study of the effect of clouds on surface wind and wind stress during the central Arctic winter
[AD-A252706] p 3860 N92-31670
ARGON
Correlation from randomness: Quantitative analysis of sputtered graphite surfaces using the scanning tunneling microscope
[AD-A252420] p 3783 N92-31820
ARID LANDS
A test of ecological optimality for semiarid vegetation
[NASA-CR-190705] p 3855 N92-32222
ARMATURES
Solid-armature railguns without the velocity-skin effect
[DE92-012630] p 3765 N92-31542
ARMED FORCES (UNITED STATES)
Ground based radar
[TABES PAPER 92-213] p 3764 N92-32021
Polyalphaolefins: A new improved cost effective aircraft radar coolant
[AD-A250517] p 3796 N92-32045
Decision-making guide for the proposed Coast Guard differential global positioning system
[AD-A246046] p 3756 N92-32054
External combustion engine technology (vapor and liquid cycles) for individual soldier power systems
[AD-A252754] p 3836 N92-32173
ARMOR
High strength glass second source qualification to composite armor specification MIL-L-46197(MR)
[AD-A252114] p 3792 N92-31404
AROMATIC COMPOUNDS
Supercritical fluid fractionation of JP-8
[AD-A247835] p 3801 N92-31982
Electronic structure and photophysical properties of polyimides
[DE92-012353] p 3797 N92-32146
ARRAYS
FCS skewed sensors array: Practical considerations
p 3746 N92-31868
ARTIFICIAL INTELLIGENCE
Detection of object edges in images containing cast shadows
[DE92-016092] p 3900 N92-31295
Objects used to implement intelligent databases
[DE92-013098] p 3919 N92-31581
Hydrocarbon ignition: Automatic generation of reaction mechanisms and applications to modeling of engine knock
[DE92-011943] p 3780 N92-31607
Artificial Intelligence in Training (AIT)
[AD-A250145] p 3885 N92-31811
ARTIFICIAL SATELLITES
Auger line shapes as a probe of electronic structure in covalent systems
[AD-A246329] p 3912 N92-31994
Spacecraft stability and control
[TABES PAPER 92-414] p 3763 N92-32011
Monitoring threats to satellite functions
[PB92-195445] p 3767 N92-32073
ASSAYING
Waveguide-binding sensor for use with assays
[AD-D015230] p 3777 N92-31268
Biodosimetry of ionizing radiation in humans using the glycophorin A genotoxicity assay
[DE92-011974] p 3869 N92-31608
ASSEMBLIES
Design, analysis, and testing of the Phase 1 CSI Evolutionary Model erectable truss
[NASA-CR-4461] p 3767 N92-32100
ASTRONAUTICS
Collection of papers of the 31st Israel Annual Conference on Aviation and Astronautics
[ITN-92-85124] p 3745 N92-31861
ASTRONAUTS
Results of earth observation study on STS-31 for Terra Geode, January 1987 - June 1991
[AD-A250750] p 3844 N92-31621
Relating space radiation environments to risk estimates
[DE92-010256] p 3926 N92-31756
ASTRONOMICAL PHOTOMETRY
Photometry of Nova Muscae 1983
[INPE-5339-PRE/1738] p 3923 N92-31344
The eclipsing cataclysmic variable AY Piscium
[INPE-5340-PRE/1739] p 3923 N92-31345
The eclipsing cataclysmic variable NSV 12615 (V4041 Sgr)
[INPE-5342-PRE/1741] p 3923 N92-31346
ASTRONOMICAL SPECTROSCOPY
Photometry of Nova Muscae 1983
[INPE-5339-PRE/1738] p 3923 N92-31344
The eclipsing cataclysmic variable NSV 12615 (V4041 Sgr)
[INPE-5342-PRE/1741] p 3923 N92-31346
ASTRONOMY
Resolution limits for ground based astronomical imaging using adaptive optics
[DE92-011949] p 3902 N92-31761
ASTROPHYSICS
Participation in high energy physics. Task C: Particle physics and cosmology
[DE92-016290] p 3924 N92-31713
Institute of Geophysics and Planetary Physics, 1991
[DE92-016981] p 3923 N92-32005
ASYMMETRY
The synthesis and characterization of new copper coordination complexes containing an asymmetric coordinating chelate ligand: Application to enzyme active site modeling
[DE92-011532] p 3786 N92-31391
Poloidal rotation and density asymmetries in a tokamak plasma with strong toroidal rotation
[PB92-182534] p 3904 N92-31613
ASYMPTOTIC METHODS
Asymptotic modal analysis and statistical energy analysis
[NASA-CR-190516] p 3842 N92-32236
ASYMPTOTIC PROPERTIES
Nonparametric estimation in renewal theory, 1: The empirical renewal function
[REPT-91-95] p 3888 N92-31519
ATLANTIC OCEAN
Updated forecast of Atlantic seasonal hurricane activity for 1992
p 3859 N92-31583
ATMOSPHERIC BOUNDARY LAYER
An airborne study of boundary layer heat and moisture fluxes for project FIFE
[NASA-CR-190665] p 3844 N92-31357
The structure and energetics of Amazon squall lines
[AD-A250182] p 3859 N92-31523
Feasibility study for a low-altitude wide and temperature profiler
[PB92-188200] p 3860 N92-31641
Navy Atmospheric Boundary Layer (NABL) model system: Software/Interface design document
[AD-A247903] p 3857 N92-31986
Rainwater and throughfall chemistry in a terra firme rain forest: Central Amazonia
[INPE-5364-PRE/1744] p 3863 N92-32224
ATMOSPHERIC CHEMISTRY
A study of longwave radiation codes for climate studies: Validation with ARM observations and tests in general circulation models
[DE92-014100] p 3862 N92-31894
ARO Geoscience Center fellowships
[AD-A249225] p 3857 N92-31964
Rainwater and throughfall chemistry in a terra firme rain forest: Central Amazonia
[INPE-5364-PRE/1744] p 3863 N92-32224
ATMOSPHERIC CIRCULATION
The validation of atmospheric models
[DE92-013254] p 3850 N92-31324
Balanced, potential vorticity dynamics in the tropics
[AD-A249981] p 3858 N92-31432
Global atmospheric circulation statistics, 1000-1 mb
[PB92-186196] p 3853 N92-31649
Real-time statistical quality control and ARM
[DE92-015253] p 3837 N92-31657
Analysis of the effects of aerosol distribution in the atmosphere on surface radiative measurements
[DE92-014189] p 3856 N92-31662
A numerical, analytical, and observational study of the effect of clouds on surface wind and wind stress during the central Arctic winter
[AD-A252706] p 3860 N92-31670

Meteorological data, new series A monographs. Volume 5, no. 4: A three dimensional model simulation of the circulation in the middle atmosphere with cconsideration of tropospherical-stratospherical interactions
[ETN-92-91693] p 3861 N92-31708
A study of longwave radiation codes for climate studies: Validation with ARM observations and tests in general circulation models
[DE92-014100] p 3862 N92-31894
Upper tropospheric jet streams over North America during summer 1988
[AD-A249871] p 3857 N92-31906
Multi-year strategic plan for the atmospheric studies in complex terrain: ASCOT program
[DE92-016646] p 3854 N92-31930

ATMOSPHERIC COMPOSITION
Application of Free-Air CO2 Enrichment (FACE) technology to a forest canopy: A simulation study
[DE92-013308] p 3851 N92-31422
Response of a tundra ecosystem to elevated atmospheric carbon dioxide and CO2-induced climate change
[DE92-013925] p 3853 N92-31626
Trends 1991: A compendium of data on global change
[DE92-011733] p 3854 N92-31907

ATMOSPHERIC EFFECTS
Analysis of the effects of aerosol distribution in the atmosphere on surface radiative measurements
[DE92-014189] p 3856 N92-31662

ATMOSPHERIC GENERAL CIRCULATION MODELS
A study of longwave radiation codes for climate studies: Validation with ARM observations and tests in general circulation models
[DE92-014100] p 3862 N92-31894

ATMOSPHERIC MODELS
The detection of climate change due to the enhanced greenhouse effect
[NASA-TM-107965] p 3849 N92-31258
Our changing planet: The FY 1993 US global change research program. A supplement to the US President's fiscal year 1993 budget
[NASA-CR-190675] p 3850 N92-31259
Effects of anthropogenic sulfur aerosols on climate
[DE92-016158] p 3850 N92-31297
Annual dynamics within the active layer
[DE92-013520] p 3850 N92-31304
Unified very low stratus cloud/subcloud microphysics model
[AD-A250662] p 3858 N92-31320
The validation of atmospheric models
[DE92-013254] p 3850 N92-31324
Remote sensing of trapping layer base height using ATIS transmissions
[AD-A250074] p 3844 N92-31362
Comparison of effects of copropagated and precomputed atmosphere profiles on Monte Carlo trajectory simulation
[NASA-TM-102600] p 3766 N92-31457
Two long-term instrumental climatic data bases of the People's Republic of China
[DE92-010378] p 3851 N92-31527
Real-time statistical quality control and ARM
[DE92-015253] p 3837 N92-31657
Analysis of the effects of aerosol distribution in the atmosphere on surface radiative measurements
[DE92-014189] p 3856 N92-31662
Comprehensive Aerological Reference Data Set (CARDS)
[DE92-016469] p 3862 N92-31734
ARO Geoscience Center fellowships
[AD-A249225] p 3857 N92-31964
Navy Atmospheric Boundary Layer (NABL) model system: Software/Interface design document
[AD-A247903] p 3857 N92-31986

ATMOSPHERIC MOISTURE
Unified very low stratus cloud/subcloud microphysics model
[AD-A250662] p 3858 N92-31320
The structure and energetics of Amazon squall lines
[AD-A250182] p 3859 N92-31523

ATMOSPHERIC PHYSICS
Comparison of results: Technische Univ., Delft-Organisatie voor Toegepast Natuurwetenschappelijk Onderzoek expert judgement study of dispersion-deposition
[REPT-92-11] p 3856 N92-31522
Energy balance model for imagery and electromagnetic propagation
[AD-A250884] p 3806 N92-31543
ARO Geoscience Center fellowships
[AD-A249225] p 3857 N92-31964
JPRS report: Science and technology. Central Eurasia: Earth sciences
[JPRS-UES-92-004] p 3843 N92-32132

ATMOSPHERIC RADIATION
Real-time statistical quality control and ARM
[DE92-015253] p 3837 N92-31657
Analysis of the effects of aerosol distribution in the atmosphere on surface radiative measurements
[DE92-014189] p 3856 N92-31662
A study of longwave radiation codes for climate studies: Validation with ARM observations and tests in general circulation models
[DE92-014100] p 3862 N92-31894

ATMOSPHERIC SOUNDING
Feasibility study for a low-altitude wide and temperature profiler
[PB92-188200] p 3860 N92-31641
Advanced microwave sounding unit study for atmospheric infrared sounder
[NASA-CR-190628] p 3858 N92-32195

ATMOSPHERIC TEMPERATURE
Effect of outer temperature changes and solar radiation on effective heat losses through external partitions of buildings p 3802 N92-31242
Feasibility study for a low-altitude wide and temperature profiler
[PB92-188200] p 3860 N92-31641
Seasonal wind and ocean thermal forcing influences on the generation of the Leeuwin current and its eddies
[AD-A246992] p 3865 N92-31988
The uncertainties of global temperatures in the global warming context
[TABES PAPER 92-447] p 3763 N92-32014

ATOMIC CLOCKS
Dicke narrowing in strong fields: The atom-as-antenna analogy
[AD-A252321] p 3807 N92-31629
Soviet precision timekeeping research and technology
[PB92-173046] p 3802 N92-31830

ATOMIC COLLISIONS
Theoretical atomic collision physics
[DE92-013571] p 3895 N92-31724
Laser enhanced chemical reaction studies
[DE92-010772] p 3831 N92-31798

ATOMIC SPECTRA
Proceedings of the 2nd KUR symposium on hyperfine interactions
[DE92-789024] p 3895 N92-31728

ATOMIC STRUCTURE
Electronic and total energy properties of ternary and quaternary semiconductor compounds, alloys, and superlattices: Theoretical study of Cu/graphite bonding
[NASA-CR-190691] p 3772 N92-31266
Surface structures and surface processes of ceramics with atomic resolutions: A study by scanning tunneling microscopy
[AD-A249581] p 3792 N92-31377
Submillimeter wave spectroscopy of heterojunction superlattices
[AD-A250835] p 3908 N92-31496
Theoretical studies of the reactions and spectroscopy of radical species relevant to combustion reactions and diagnostics
[DE92-013484] p 3781 N92-31725
Energetics, bonding mechanism and electronic structure of metal/ceramic interfaces
[DE92-013401] p 3775 N92-31806
He atom-surface scattering: Surface dynamics of insulators, overlayers and crystal growth
[DE92-011810] p 3911 N92-31914
Electronic states in systems of reduced dimensionality
[DE92-013588] p 3912 N92-31945
Auger line shapes as a probe of electronic structure in covalent systems
[AD-A246329] p 3912 N92-31994
Quantum mechanical approach to understanding microstructural and mechanical properties in intermetallics
[AD-A250550] p 3790 N92-32084
Electronic structure and photophysical properties of polyimides
[DE92-012353] p 3797 N92-32146

ATOMIZING
Diagnostics for research in atomization and turbulent two-phase flows
[AD-A247201] p 3819 N92-31283

ATOMS
Dicke narrowing in strong fields: The atom-as-antenna analogy
[AD-A252321] p 3807 N92-31629
Electron scattering by atomic hydrogen: Elastic and inelastic phenomena at 13.9 to 200 eV
[DE92-625004] p 3896 N92-31837
Molecular interactions and properties with many-body methods
[AD-A247052] p 3896 N92-31858

ATROPINE
Acetylcholinesterase inhibitors on the spinal cord
[AD-A252694] p 3868 N92-31326

ATTENTION
Theory and test of stress resistance
[AD-A250741] p 3870 N92-31291

ATTENUATION
Wavenumbers for currents on infinite- and finite-length wires in a chiral medium
[DE92-007565] p 3804 N92-31317

ATTITUDE GYROS
Estimation of aircraft attitude by angular rate measurements p 3748 N92-31881

ATTITUDE INDICATORS
Extended Kalman filter for attitude estimation of the Earth Radiation Budget Satellite p 3748 N92-31876
True covariance simulation of the EUVE (extreme ultra violet explorer) update filter p 3748 N92-31878
Estimation of aircraft attitude by angular rate measurements p 3748 N92-31881

AUDITORY SIGNALS
Modeling of learning-induced receptive field plasticity in auditory neocortex
[AD-A250348] p 3869 N92-31558

AUGER SPECTROSCOPY
Auger line shapes as a probe of electronic structure in covalent systems
[AD-A246329] p 3912 N92-31994

AUGMENTATION
Resonant enhancement of flavor-changing neutrino interactions
[DE92-013020] p 3898 N92-32167

AURORAL ZONES
The effects of magnetic storm phases on F-layer irregularities from auroral to equatorial latitudes
[AD-A249011] p 3855 N92-31478

AUSTENITIC STAINLESS STEELS
Residual stress and strain measurements in an austenitic steel plate containing a multipass weld
[DE92-014478] p 3839 N92-31383

AUSTRALIA
Seasonal wind and ocean thermal forcing influences on the generation of the Leeuwin current and its eddies
[AD-A246992] p 3865 N92-31988

AUTOCORRELATION
CO2 laser frequency multiplication
[AD-A248574] p 3830 N92-31755
Diffusion in ordered and disordered media
[AD-A250949] p 3891 N92-32211

AUTOMATA THEORY
The physics of cellular automata and coherence and chaos in classical many-body systems
[DE92-016834] p 3890 N92-32035

AUTOMATIC CONTROL
Estimation with multisensor/multiscan detection fusion
[AD-A250496] p 3804 N92-31333
Weld penetration and defect control
[DE92-015310] p 3836 N92-31336
Automation of strain-gauge load-cell force calibration
[PB92-187087] p 3827 N92-31370
An automated computational method for barrier construction in single and two-target differential games p 3749 N92-31882
Database explorer: Large scale database application
[AD-A252183] p 3920 N92-32049
Proceedings of the 53rd Symposium on Air Vehicle Mission Control and Management
[AGARD-AR-310] p 3889 N92-32229

AUTOMATIC TEST EQUIPMENT
Robotics development for the enhancement of space endeavors
[TABES PAPER 92-445] p 3763 N92-32013

AUTOMOBILE FUELS
Catalyst and feedstock effects in the thermochemical conversion of biomass to liquid transportation fuels
[DE92-010569] p 3799 N92-31593
Autoignition behavior of lean mixtures: Chemical and thermodynamics effects
[DE92-009690] p 3781 N92-31763

AUTONOMIC NERVOUS SYSTEM
Acetylcholinesterase inhibitors on the spinal cord
[AD-A252694] p 3868 N92-31326

AUTONOMOUS NAVIGATION
Neural network perception for mobile robot guidance
[AD-A249972] p 3884 N92-31511
Techniques for autonomous navigation
[DE92-013458] p 3756 N92-31746

AUTOROTATION
The stability of a slightly eccentric straight vortex filament in a circular tube p 3750 N92-31887

AUTOTROPHS
Methane-producing microorganisms: Component of Mars biosphere p 3924 N92-32180

AUXILIARY PROPULSION
Low-Isp derated ion thruster operation
[NASA-TM-105787] p 3771 N92-32237

AVERAGE
An investigation of spinup dynamics of axial gyrostats using elliptic integrals and the method of averaging
[AD-A249728] p 3768 N92-31675
AXES OF ROTATION
An innovative two axis rate gyro: Theory and principles of operation p 3748 N92-31875
AXIAL STRAIN
A generalized plane-strain elastic stress solution for a multiorthotropic-layered cylinder
[AD-A250487] p 3838 N92-31331
AXISYMMETRIC BODIES
An investigation into the interface between three closely spaced axi-symmetric bodies at subsonic speed
[CRANFIELD-AERO-9114] p 3751 N92-31514
AXISYMMETRIC FLOW
Axisymmetric bluff-body flow: A vortex solver for thin shells
[DE92-016748] p 3824 N92-31933
AZEOTROPES
Analysis and computer tools for separation processes involving nonideal mixtures
[DE92-015298] p 3781 N92-31752
AZIMUTH
Analysis of random induced cross polarization
[AD-A249773] p 3806 N92-31569
AZINES
The collection, handling, transportation, and thermal desorption of explosive vapor using quartz collection tubes
[DE92-011441] p 3799 N92-31570

B

B-1 AIRCRAFT
B-1B nuclear certification tasks performed by the Aircraft Compatibility Department at Sandia National Laboratories
[DE92-016750] p 3757 N92-31736
BACKGROUND NOISE
Readily implemented enhanced sinusoid detection in noise
[DE92-011359] p 3806 N92-31449
BACKGROUND RADIATION
A characterization of the hot infrared background: The infrared cirrus, zodiacal dust bands, and solar system dust trails
[PL-TR-91-2065] p 3924 N92-32142
BACKSCATTERING
Monte Carlo simulations of random rough surface scattering with finite element and finite difference methods
[AD-A247528] p 3901 N92-31430
Radar backscatter from the sea: Controlled experiments
[AD-A250858] p 3810 N92-32101
BACKWARD WAVE TUBES
Compact millimeter-wave devices: Dielectric loaded carm, high voltage carm, slow wave crm and high harmonic gyrotron
[AD-A250497] p 3809 N92-31944
BACKWARD WAVES
Compact millimeter-wave devices: Dielectric loaded carm, high voltage carm, slow wave crm and high harmonic gyrotron
[AD-A250497] p 3809 N92-31944
BACTERIA
Methane-producing microorganisms: Component of Mars biosphere p 3924 N92-32180
BALL BEARINGS
Surface analysis of stainless steel outer race bearing specimens
[AD-A250088] p 3833 N92-31437
BALLISTIC MISSILES
Ground based radar
[TABES PAPER 92-213] p 3764 N92-32021
Monitoring threats to satellite functions
[PB92-195445] p 3767 N92-32073
BALLOON SOUNDING
A coordinated study of a storm system over the South American continent
[INPE-5388-TDI/477] p 3863 N92-32212
BAND STRUCTURE OF SOLIDS
Schwinger boson studies of the t-J model beyond mean-field approximation
[DE92-630650] p 3909 N92-31655
Development of effective quantum chemical method for polymers and solid
[AD-A250976] p 3795 N92-31951
Auger line shapes as a probe of electronic structure in covalent systems
[AD-A246329] p 3912 N92-31994
BANDPASS FILTERS
Time domain regional discriminants
[AD-A249949] p 3855 N92-31509
BANDWIDTH
The investigation of bandwidth efficient coding and modulation techniques
[NASA-CR-190685] p 3806 N92-31468
Optical oversampled analog-to-digital conversion
[AD-A252695] p 3877 N92-31587
Realization of lattice networks at MHz- and GHz-frequencies
[PB92-195437] p 3810 N92-32161
BARENTS SEA
Three-dimensional finite difference modeling of surface wave propagation across the Barents Shelf
[AD-A249865] p 3865 N92-31821
BARIUM COMPOUNDS
Development of high efficiency nonlinear optical materials
[AD-A249612] p 3901 N92-31380
BARIUM FLUORIDES
Development of gamma ray imaging cameras
[DE92-015305] p 3828 N92-31919
BARIUM OXIDES
Oxygen ordering and strain-related morphology in YBa2Cu(3-x)O7 systems
[DE92-014476] p 3909 N92-31627
Ba2Ti9O20 microwave dielectric resonator: Processing, phase synthesis and characterization
[INPE-5373-PRE/1747] p 3818 N92-32200
BARIUM SULFIDES
Synthesis, structure and properties of Ba6Co25S27: A Perovskite-like superstructure of Co8S6 and Ba6S clusters
[AD-A251041] p 3911 N92-31848
BARIUM TITANATES
Optimized photorefractive barium titanate
[AD-A250089] p 3908 N92-31438
BAROCLINIC INSTABILITY
Balanced, potential vorticity dynamics in the tropics
[AD-A249981] p 3858 N92-31432
BAROCLINITY
Amending the w* velocity scale for surface layer, entrainment zone, and baroclinic shear in mixed Forced/Free turbulent convection
[AD-A250389] p 3859 N92-31540
BAROTROPIC FLOW
Balanced, potential vorticity dynamics in the tropics
[AD-A249981] p 3858 N92-31432
BASE FLOW
An experimental investigation of the formation of secondary vortices and the generation of small-scale motion in a spanwise forced plane mixing layer
[AD-A250350] p 3822 N92-31559
BATHYMETERS
Real time detection in a laser bathymetry system
[PB92-195452] p 3866 N92-32069
BATTERY CHARGERS
Understanding and managing the effects of battery charger and inverter aging
[DE92-014473] p 3815 N92-31651
BEACHES
Geomorphic variability in the coastal zone
[AD-A252713] p 3864 N92-31544
BEACONS
Effect of guard band reduction on marker beacon receiver performance
[DOT/FAA/CT-TN92/18] p 3807 N92-31617
BEAM INJECTION
New high voltage parallel plate analyzer
[NIFS-128] p 3827 N92-31340
Improved ferrite biasing scheme for booster RF cavities
[DE92-011650] p 3815 N92-31664
A global fitting code for multichordal neutral beam spectroscopic data
[DE92-014258] p 3781 N92-31729
Injecting into AmPS when ring cavity operates at 476 MHz
[NIKHEF-K/AMPS/91-08] p 3899 N92-31815
BEAM INTERACTIONS
Pulse-by-pulse energy measurement at the Stanford Linear Collider
[DE92-011520] p 3899 N92-31390
The 6-D phase space tracking with acceleration: Modeling low energy proton synchrotrons, part 1
[DE92-013744] p 3899 N92-31948
Scaling of IFR propagation physics with beam/channel parameters
[DE92-015389] p 3900 N92-32123
Calculations of emittance and damping time effects in the SLC damping rings
[DE92-012420] p 3900 N92-32133
Results of IR working group
[DE92-013294] p 3902 N92-32149
BEAM WAVEGUIDES
Plasma channel generation using low energy electron beams
[DE92-013770] p 3906 N92-31949
BEAMS (RADIATION)
Studies in dynamic characterization and control of a flexible structure and optical beampath
[AD-A250555] p 3830 N92-31605
Beam position monitor electronics using DC coupled demodulating logarithmic amplifiers
[DE92-011697] p 3816 N92-31760
Calculations of emittance and damping time effects in the SLC damping rings
[DE92-012420] p 3900 N92-32133
BEAMS (SUPPORTS)
Mode methods for strain-hardening structures
[DE92-014855] p 3838 N92-31335
VAASEL-ANSYS comparison for a thermally loaded beam
[AD-A251003] p 3841 N92-31847
The design and testing of an optimal beam composed of unimodal elements p 3747 N92-31873
Structural similitude and scaling laws for laminated beam-plates
[NASA-CR-190585] p 3841 N92-31911
BEARINGS
Effect of out-of-roundness on the performance of a diesel engine connecting-rod bearing
[NASA-TM-105600] p 3834 N92-31536
Orbit transfer vehicle engine technology program. Task B-6 high speed turbopump bearings
[NASA-CR-189230] p 3835 N92-31892
BEDS (PROCESS ENGINEERING)
The 193-pixel, three-dimensional capacitance imaging system
[DE92-001253] p 3919 N92-31731
BENDING
VAASEL-ANSYS comparison for a thermally loaded beam
[AD-A251003] p 3841 N92-31847
BENDING FATIGUE
Electrically-induced stresses and deflection in multiple plates
[DE92-012303] p 3841 N92-31844
BENDING MOMENTS
The design and testing of an optimal beam composed of unimodal elements p 3747 N92-31873
BENDING THEORY
A finite element procedure for analysis of laminated composite plates
[AD-A250902] p 3773 N92-31307
BENZENE
Analysis and computer tools for separation processes involving nonideal mixtures
[DE92-015298] p 3781 N92-31752
Unimolecular reaction mechanisms involving C3H4, C4H4, and C6H6 hydrocarbon species
[DE92-005326] p 3783 N92-31860
Auger line shapes as a probe of electronic structure in covalent systems
[AD-A246329] p 3912 N92-31994
BETA PARTICLES
The structure of nuclei far from beta stability
[DE92-012598] p 3895 N92-31721
BETAINES
Ultrafast studies on electron transfer in the betaines: Evidence for local heating
[AD-A250728] p 3897 N92-31999
BETATRONS
Calculations of emittance and damping time effects in the SLC damping rings
[DE92-012420] p 3900 N92-32133
BIAS
Improved ferrite biasing scheme for booster RF cavities
[DE92-011650] p 3815 N92-31664
BIBLIOGRAPHIES
NASA patent abstracts bibliography: A continuing bibliography. Section 2: Indexes (supplement 41)
[NASA-SP-7039(41)-SECT-2] p 3918 N92-31455
Aeronautical engineering: A continuing bibliography with indexes (supplement 280)
[NASA-SP-7037(280)] p 3745 N92-31456
JPRS report: Science and technology. Central Eurasia: Materials science
[JPRS-UMS-92-010] p 3787 N92-31584
Ecosystems of the Florida Keys: A bibliography
[PB92-198910] p 3854 N92-32071
JPRS report: Science and technology. Central Eurasia: Earth sciences
[JPRS-UES-92-004] p 3843 N92-32132
JPRS report: Science and technology. Central Eurasia: Life sciences
[JPRS-ULS-92-015] p 3924 N92-32179
Automated input into databases: OCR and descriptive cataloguing p 3921 N92-32189

BIDIRECTIONAL REFLECTANCE
Procedures and errors in the determination of the bi-directional reflectance factor and other radiometric quantities
[INPE-5386-TDI/475] p 3843 N92-31277

BINARY ALLOYS
Thermodynamic assessment of the Cr-Zr system
[PB92-180645] p 3787 N92-31610

BINARY MIXTURES
Analysis and computer tools for separation processes involving nonideal mixtures
[DE92-015298] p 3781 N92-31752

BINDING
Waveguide-binding sensor for use with assays
[AD-D015230] p 3777 N92-31268

BIOASSAY
A biological model of the effects of toxic substances
[AD-A247138] p 3867 N92-31980

BIOCHEMISTRY
JPRS report: Science and technology. Central Eurasia: Life sciences
[JPRS-ULS-92-015] p 3924 N92-32179

BIODYNAMICS
Naval Biodynamics Laboratory: 1989 and 1990 command history
[AD-A247185] p 3870 N92-31963

BIOLOGICAL EFFECTS
Algorithms for the determination of spatial and spectral distribution of electromagnetic energy in a simulated biostructure subjected to transient spatially heterogeneous radiation with applications to radar hazard assessment and cancer therapy
[AD-A250447] p 3805 N92-31381
Static magnetic fields: A summary of biological interactions, potential health effects, and exposure guidelines
[DE92-015218] p 3867 N92-31711
Relating space radiation environments to risk estimates
[DE92-010256] p 3926 N92-31756
Hollow fiber clinostat for simulating microgravity in cell culture
[NASA-CASE-MFS-28370-1] p 3828 N92-31790
A biological model of the effects of toxic substances
[AD-A247138] p 3867 N92-31980
Extremely Low Frequency (ELF) communications system ecological monitoring program summary of 1990 progress
[AD-A246344] p 3809 N92-31996

BIOLOGICAL EVOLUTION
Evolution and analysis of the functional domains of the chimeric proteins that initiate pyrimidine biosynthesis
[AD-A250069] p 3866 N92-31465

BIOLOGICAL MODELS (MATHEMATICS)
Micro saint model of fatigue assessment
[AD-A249976] p 3868 N92-31554
Modeling of learning-induced receptive field plasticity in auditory neocortex
[AD-A250348] p 3869 N92-31558

BIOMASS
Catalyst and feedstock effects in the thermochemical conversion of biomass to liquid transportation fuels
[DE92-010569] p 3799 N92-31593
Methane-producing microorganisms: Component of Mars biosphere p 3924 N92-32180
A test of ecological optimality for semiarid vegetation
[NASA-CR-190705] p 3855 N92-32222

BIOMASS ENERGY PRODUCTION
Catalyst and feedstock effects in the thermochemical conversion of biomass to liquid transportation fuels
[DE92-010569] p 3799 N92-31593

BIOSPHERE
Methane-producing microorganisms: Component of Mars biosphere p 3924 N92-32180

BIOSYNTHESIS
Evolution and analysis of the functional domains of the chimeric proteins that initiate pyrimidine biosynthesis
[AD-A250069] p 3866 N92-31465

BIREFRINGENCE
Electro-optics and second harmonic generation of nonlinear optical polymers
[AD-A252488] p 3796 N92-31960

BLACK HOLES (ASTRONOMY)
Modified black holes in two dimensional gravity
[DE92-630244] p 3924 N92-31401

BLADE TIPS
Turbine blade tip and seal clearance excitation forces
[NASA-CR-184341] p 3760 N92-31910

BLASIUS FLOW
Sensitivity analysis of hydrodynamic stability operators
[NASA-CR-189683] p 3822 N92-31535

BLOCK COPOLYMERS
Synthesis of side chain liquid crystal polymers by living ring opening metathesis polymerization. 4: Synthesis of amorphous and side chain liquid crystal AB block copolymers
[AD-A250353] p 3792 N92-31394
Imide/arylene ether copolymers
[NASA-CASE-LAR-14159-1-CU] p 3794 N92-31792

BLOCKING
Computer simulation of shading and blocking: Discussion of accuracy and recommendations
[DE91-002146] p 3849 N92-32110

BLUFF BODIES
Axisymmetric bluff-body flow: A vortex solver for thin shells
[DE92-016748] p 3824 N92-31933

BODY FLUIDS
Body water homeostasis and human performance in high heat environments: Fluid hydration recommendations for Operation Desert Storm
[AD-A249772] p 3868 N92-31492

BODY TEMPERATURE
Preliminary development of a protocol for determining heat stress caused by clothing
[DREO-PSD-EPS-05/89] p 3873 N92-32031

BOEING 747 AIRCRAFT
An assessment of the B-747's capability to operate on rough surfaces
[AD-A250134] p 3757 N92-31793

BOILING
The prediction of the performance of a microcircuit heat sink in the boiling mode
[AD-A250045] p 3812 N92-31355

BOLOMETERS
Research in elementary particle physics
[DE92-014585] p 3893 N92-31385

BONDING
Electronic and total energy properties of ternary and quaternary semiconductor compounds, alloys, and superlattices: Theoretical study of Cu/graphite bonding
[NASA-CR-190691] p 3772 N92-31266
Strongly adherent ceramic surface layers by ion implantation
[AD-A248882] p 3792 N92-31388
Energetics, bonding mechanism and electronic structure of metal/ceramic interfaces
[DE92-013401] p 3775 N92-31806
Geothermal materials development
[DE92-016940] p 3849 N92-32124

BONES
Microdistribution of lead in bone: A new approach
[DE92-013036] p 3869 N92-31589

BOOLEAN ALGEBRA
Non Boolean search methods in information retrieval p 3921 N92-32187

BOOSTER ROCKET ENGINES
Sizing supersonic freejet nozzle and inlet location for simulation of the transition phase in integral rocket ramjet p 3747 N92-31870

BORANES
The thermal dissociation of decaborane on Si(111)-(7x7) and doping effects in the near surface region
[AD-A251057] p 3911 N92-31851

BOREHOLES
Cutting treatment by drilling of fiber bound synthetic materials
[MBB-UD-0609-91-PUB] p 3774 N92-31716

BORING MACHINES
Cutting treatment by drilling of fiber bound synthetic materials
[MBB-UD-0609-91-PUB] p 3774 N92-31716

BORN APPROXIMATION
Research in regional seismology: The effect of anisotropy
[AD-A248940] p 3855 N92-31476

BORON
Fabrication of an insulated gate diamond FET for high temperature applications
[AD-A251042] p 3817 N92-31849
The thermal dissociation of decaborane on Si(111)-(7x7) and doping effects in the near surface region
[AD-A251057] p 3911 N92-31851

BOSONS
Pulse-by-pulse energy measurement at the Stanford Linear Collider
[DE92-011520] p 3899 N92-31390
Schwinger boson studies of the t-J model beyond mean-field approximation
[DE92-630650] p 3909 N92-31655

BOUNDARIES
Optical interconnects in the computer environment
[AD-D015235] p 3873 N92-31269
Applications of FEM and BEM in two-dimensional fracture mechanics problems
[NASA-TP-3277] p 3838 N92-31280

BOUNDARY CONDITIONS
Electromagnetic scattering by coated convex surfaces and wedges simulated by approximate boundary conditions
[NASA-CR-190540] p 3803 N92-31238
Statistical analysis of anomalous transport in resistive interchange turbulence
[NIFS-125] p 3818 N92-31256

BOUNDARY ELEMENT METHOD
Analysis and prediction of Multiple-Site Damage (MSD) fatigue crack growth
[NASA-TP-3231] p 3838 N92-31279
Applications of FEM and BEM in two-dimensional fracture mechanics problems
[NASA-TP-3277] p 3838 N92-31280

BOUNDARY INTEGRAL METHOD
A finite element-boundary integral method for conformal antenna arrays on a circular cylinder
[NASA-CR-190534] p 3807 N92-31614
Computation of nonlinear gravity waves by a desingularized boundary integral method
[AD-A251149] p 3857 N92-31766

BOUNDARY LAYER CONTROL
Fundamental studies of the structure of hypersonic attached and separated boundary layers over smooth, rough and transpiration-cooled surfaces
[AD-A250284] p 3819 N92-31286
Active control of the separation region on a two-dimensional airfoil
[AD-A249739] p 3752 N92-31622

BOUNDARY LAYER FLOW
Computer program to solve two-dimensional shock-wave interference problems with an equilibrium chemically reacting air model
[NASA-TM-4187] p 3818 N92-31247
Stability and transition of hypersonic boundary-layer flows
[AD-A250279] p 3752 N92-31555
Three-dimensional compressible turbulent computations for a nondiffusing S-duct
[NASA-CR-4391] p 3754 N92-32240

BOUNDARY LAYER SEPARATION
Fundamental studies of the structure of hypersonic attached and separated boundary layers over smooth, rough and transpiration-cooled surfaces
[AD-A250284] p 3819 N92-31286
Description of a 1000 sensor constant current anemometer system for locating three-dimensional turbulent boundary layer separations
[AD-A250827] p 3821 N92-31452
Active control of the separation region on a two-dimensional airfoil
[AD-A249739] p 3752 N92-31622
The calculation of incompressible separated turbulent boundary layers p 3749 N92-31686

BOUNDARY LAYER STABILITY
Stability of boundary layers at high supersonic and hypersonic speeds
[AD-A250900] p 3819 N92-31306

BOUNDARY LAYER TRANSITION
Stability of boundary layers at high supersonic and hypersonic speeds
[AD-A250900] p 3819 N92-31306
Stability and transition of hypersonic boundary-layer flows
[AD-A250279] p 3752 N92-31555

BOUNDARY LAYERS
Development of wavelet analysis tools for turbulence
[NASA-CR-189674] p 3822 N92-31564
Turbulent dusty boundary layer in an ANFO surface-burst explosion
[DE92-012101] p 3822 N92-31625

BOUNDARY VALUE PROBLEMS
Granular flows down bumpy inclines
[DE92-013568] p 3820 N92-31425
Steady flow of a fluid-solid mixture between parallel plates
[DE92-013645] p 3821 N92-31426

BOW WAVES
The use of high lift-to-drag hypersonic vehicles for aero-assisted orbital maneuvering p 3748 N92-31877

BRAIN
Modeling of learning-induced receptive field plasticity in auditory neocortex
[AD-A250348] p 3869 N92-31558

BRAYTON CYCLE
SP-100 reactor with Brayton conversion for lunar surface applications
[NASA-TM-105637] p 3771 N92-32108

BREEDER REACTORS
An examination of the feasibility of a nuclear-pumped laser-driven inertial confinement fusion reactor with magnetically protected walls
[AD-A248163] p 3907 N92-31990

BREMSSTRAHLUNG
Fine structure superimposed on mm-wavelength (18-23 GHz) spectra of solar active region
[INPE-5371-TDI/470] p 3926 N92-32221
BRIGHTNESS
High brightness x ray source for directed energy and holographic imaging applications, phase 2
[AD-A248858] p 3827 N92-31475
BRIGHTNESS DISTRIBUTION
Accretion disk image reconstruction in cataclysmic variables
[INPE-5343-PRE/1742] p 3923 N92-31347
BRILLOUIN EFFECT
Three-wave envelope solitons: Can the speed of light in the fiber be controlled?
[AD-A247615] p 3901 N92-31611
Physical characterization of magmatic liquids
[DE92-015302] p 3858 N92-32027
BRINES
Experimental studies of aluminum solubility and speciation in brines
[DE92-010448] p 3786 N92-31418
BRITTLE MATERIALS
Instabilities of damage and surface degradation mechanisms in brittle material structural systems
[AD-A250785] p 3842 N92-32168
BRITTLENESS
The 3-D analysis and verification of fracture growth mechanisms in fiber-reinforced ceramic composies
[AD-A250893] p 3773 N92-31305
BROADBAND
Analysis and evaluation of Project Evergreen data
[AD-A245983] p 3804 N92-31314
High-pressure gas switch for a wideband source
[DE92-015822] p 3815 N92-31548
BROADCASTING
Remote sensing of trapping layer base height using ATIS transmissions
[AD-A250074] p 3844 N92-31362
Issues in designing transport layer multicast facilities
[NASA-CR-190639] p 3882 N92-31483
Decision-making guide for the proposed Coast Guard differential global positioning system
[AD-A246046] p 3756 N92-32054
BROKEN SYMMETRY
A tumbling top-quark condensate model
[DE92-016194] p 3893 N92-31552
Flow generation by turbulence
[DE92-013276] p 3906 N92-31829
Implications of the 17 keV neutrino
[DE92-017000] p 3898 N92-32006
BROWNIAN MOVEMENTS
Maximum likelihood estimation of fractional Brownian motion and Markov noise parameters
[AD-A249623] p 3890 N92-31686
Diffusion in ordered and disordered media
[AD-A250949] p 3891 N92-32211
BUBBLES
A model for the interfacial shear in vertical, adiabatic, annular-mist flow
[DE92-013537] p 3820 N92-31424
Acoustic studies of ocean surface processes in SWAPP
[AD-A247519] p 3864 N92-31429
A detector for stationary gas bubbles: Feasibility studies
[AD-A250135] p 3828 N92-31794
BUCKLING
Strength tests of cold-formed channel sections undergoing local and distortional buckling
[PB92-180835] p 3841 N92-31658
Optimal design of geodesically stiffened composite cylindrical shells
[NASA-CR-190706] p 3842 N92-32235
BUCKMINSTERFULLERENE
Near-IR absorption spectra for the Buckminsterfullerene Anions: An experimental and theoretical study
[AD-A250532] p 3785 N92-32080
BUDGETS
NSF Tokyo reports. General outline of JFY 1991 government science and technology budget
[PB92-192640] p 3927 N92-32068
BUILDINGS
Effect of outer temperature changes and solar radiation on effective heat losses through external partitions of buildings p 3802 N92-31242
Probabilistic analysis of twenty-four hour weather data for Warsaw p 3863 N92-32097
BUNCHING
The 6-D phase space tracking with acceleration: Modeling low energy proton synchrotrons, part 1
[DE92-013744] p 3899 N92-31948
BURGER EQUATION
Nonlinearly stable compact schemes for shock calculations
[NASA-CR-189663] p 3887 N92-32164
BURNERS
Tomographic reconstruction of infrared spectra of nonhomogeneous media: Applications to a flat flame burner
[AD-A249999] p 3778 N92-31393
Technology advancing research combustion in burners
[PB92-164359] p 3782 N92-31776
BURNING RATE
Solid rocket combustion phenomena
[AD-A248006] p 3770 N92-31474
BUTADIENE
Unimolecular reaction mechanisms involving C3H4, C4H4, and C6H6 hydrocarbon species
[DE92-005326] p 3783 N92-31860
BUTANES
Light alkane conversion processes: Suprabiotic catalyst systems for selective oxidation of light alkane gases to fuel oxygenates
[DE92-015229] p 3799 N92-31751
BUTENES
Two-stage n-butane flame: A comparison between experimental measurements and modeling results
[DE92-009457] p 3779 N92-31416
Temperature-enhanced autodetachment from long-lived parent negative ions of gaseous dielectrics
[DE92-011108] p 3894 N92-31700

C

CADMIUM TELLURIDES
Module process optimization and device efficiency improvement for stable, low-cost, large-area, cadmium telluride-based photovoltaic module production
[DE92-010564] p 3846 N92-31497
Development of a computer model for polycrystalline thin-film CuInSe2 and CdTe solar cells
[DE92-001242] p 3846 N92-31526
CALCULUS
Programming with inductive and co-inductive types
[AD-A249562] p 3874 N92-31353
Mathematical structures for qualitative calculus, a contribution to qualitative simulation
[LAAS-91475] p 3886 N92-31690
Full abstraction and the context lemma
[AD-A247062] p 3887 N92-32163
Polymorphic type assignment and CPS conversion
[AD-A250954] p 3887 N92-32171
CALCULUS OF VARIATIONS
Mathematical problems in micromechanics and composite materials
[AD-A249584] p 3773 N92-31378
CALIBRATING
Investigation of factors affecting the calibration of strain gage based transducers (Goodzeit gages) for SSC magnets
[DE92-010722] p 3826 N92-31313
Automation of strain-gauge load-cell force calibration
[PB92-187087] p 3827 N92-31370
A sealed He-4 superfluid-transition fixed-point device
[DE92-014271] p 3908 N92-31403
Two-component flow study in large-diameter horizontal pipe
[DE92-013196] p 3820 N92-31420
Calibration at 24 C of a heat-flow-meter apparatus having 610 mm square plates
[DE92-015954] p 3827 N92-31633
A comparison of interstitial oxygen calculated by different techniques
[DE92-011658] p 3910 N92-31668
Calibration network intended for phased-array antennas at 3 GHz
[PB92-195429] p 3810 N92-32070
RL-34 ring laser gyro laboratory evaluation for the Deep Space Network antenna application
[NASA-CR-190481] p 3829 N92-32128
Improvements to the Rocky Flats Metrology Laboratories velocity meter calibration system
[DE92-013162] p 3829 N92-32138
Ground and flight calibration assessment of HiRAP accelerometer data from missions STS-35 and STS-40
[NASA-TM-107602] p 3769 N92-32204
Absolute calibration of the Fourier interferometric transmissometer
[DREV-R-4511/88] p 3829 N92-32218
CALIFORNIA
An analysis of hydrographic data collected off Point Sur, California in June 1990
[AD-A246060] p 3866 N92-32056
CAMERAS
Logarithmic retinae
[PB92-183649] p 3885 N92-31680
From perception to modelization in robotics using achromatic and chromatic cameras
[LAAS-91484] p 3901 N92-31692
Development of gamma ray imaging cameras
[DE92-015305] p 3828 N92-31919
CANADA
Partnership in space: An introduction to Canada's special relationship with the European Space Agency
[ESA-BR-79] p 3922 N92-31947
CANCER
Biodosimetry of ionizing radiation in humans using the glycophorin A genotoxicity assay
[DE92-011974] p 3869 N92-31608
CANOPIES (VEGETATION)
Application of Free-Air CO2 Enrichment (FACE) technology to a forest canopy: A simulation study
[DE92-013308] p 3851 N92-31422
A test of ecological optimality for semiarid vegetation
[NASA-CR-190705] p 3855 N92-32222
CANTILEVER BEAMS
Experimental feedback of fractional order states of a lightly damped structure
[AD-A248027] p 3842 N92-31989
CAPACITANCE
The 193-pixel, three-dimensional capacitance imaging system
[DE92-001253] p 3919 N92-31731
CAPACITORS
Flexible heating head for induction heating apparatus and method
[NASA-CASE-LAR-14418-1] p 3803 N92-31257
CAPILLARY FLOW
Plane stokes flow driven by capillarity on a free surface: Overview and status
[DE92-011469] p 3821 N92-31528
CARBAMATES (TRADENAME)
Photogenerated base as catalyst for imidization reactions: Design of photosensitive polyimides
[AD-A250067] p 3795 N92-31810
CARBON
Inorganic rings on carbon chains
[AD-A251043] p 3772 N92-31850
Catalytic carbon membranes for hydrogen production
[DE92-001269] p 3784 N92-31976
Near-IR absorption spectra for the Buckminsterfullerene Anions: An experimental and theoretical study
[AD-A250532] p 3785 N92-32080
CARBON COMPOUNDS
Nature of short Li-H-C contact interactions in organolithium compounds and its implication
[AD-A250992] p 3898 N92-32024
CARBON CYCLE
Application of Free-Air CO2 Enrichment (FACE) technology to a forest canopy: A simulation study
[DE92-013308] p 3851 N92-31422
Steady-state and transient modeling of tracer and nutrient distributions in the global ocean
[DE92-011805] p 3864 N92-31572
A dynamic model of terrestrial carbon cycling
[DE92-015130] p 3853 N92-31782
CARBON DIOXIDE
Application of Free-Air CO2 Enrichment (FACE) technology to a forest canopy: A simulation study
[DE92-013308] p 3851 N92-31422
Steady-state and transient modeling of tracer and nutrient distributions in the global ocean
[DE92-011805] p 3864 N92-31572
Energy conservation: The main factor for reducing greenhouse gas emissions in the former Soviet Union
[DE92-012355] p 3852 N92-31574
Response of a tundra ecosystem to elevated atmospheric carbon dioxide and CO2-induced climate change
[DE92-013925] p 3853 N92-31626
Comprehensive Aerological Reference Data Set (CARDS)
[DE92-016469] p 3862 N92-31734
Laser enhanced chemical reaction studies
[DE92-010772] p 3831 N92-31798
CARBON DIOXIDE CONCENTRATION
Response of a tundra ecosystem to elevated atmospheric carbon dioxide and CO2-induced climate change
[DE92-013925] p 3853 N92-31626
CARBON DIOXIDE LASERS
CO2 laser frequency multiplication
[AD-A248574] p 3830 N92-31755
CARBON FIBERS
Polymer blends, volume 1
[AD-A252112] p 3792 N92-31419
CARBON MONOXIDE
Laser enhanced chemical reaction studies
[DE92-010772] p 3831 N92-31798
Catalytic carbon membranes for hydrogen production
[DE92-001269] p 3784 N92-31976

Role of the double-layer cation on the potential-dependent stretching frequencies and binding geometries of carbon monoxide at platinum-nonaqueous interfaces
[AD-A246980] p 3784 N92-31998
Noninvasive ambulatory assessment of cardiac function and myocardial ischemia in healthy subjects exposed to carbon monoxide
[AD-A252264] p 3870 N92-32107

CARBON 14
Steady-state and transient modeling of tracer and nutrient distributions in the global ocean
[DE92-011805] p 3864 N92-31572

CARBON-CARBON COMPOSITES
Radiation damage in carbon-carbon composites
[DE92-011778] p 3775 N92-31912

CARBONACEOUS MATERIALS
New sources for OMVPE
[AD-A250903] p 3909 N92-31582
Auger line shapes as a probe of electronic structure in covalent systems
[AD-A246329] p 3912 N92-31994

CARCINOGENS
Biodosimetry of ionizing radiation in humans using the glycophorin A genotoxicity assay
[DE92-011974] p 3869 N92-31608
Relating space radiation environments to risk estimates
[DE92-010256] p 3926 N92-31756

CARDIOVASCULAR SYSTEM
Noninvasive ambulatory assessment of cardiac function and myocardial ischemia in healthy subjects exposed to carbon monoxide
[AD-A252264] p 3870 N92-32107

CARRIER DENSITY (SOLID STATE)
The thermal dissociation of decaborane on Si(111)-(7x7) and doping effects in the near surface region
[AD-A251057] p 3911 N92-31851

CASE HISTORIES
Composite failure analysis handbook. Volume 1: Program review
[AD-A250520] p 3776 N92-32047
Composite failure analysis handbook. Volume 2: Technical handbook. Part 1: Procedures and techniques
[AD-A250521] p 3776 N92-32048

CASTING
Corrosion behavior of squeeze cast aluminum metal matrix composites
[AD-A250486] p 3774 N92-31382
Prototype casting fabrication by stereolithography
[DE92-011489] p 3876 N92-31529
Rheology of zirconia-alumina gelcasting slurries
[DE92-016787] p 3797 N92-32089

CATACLYSMIC VARIABLES
Photometry of Nova Muscae 1983
[INPE-5339-PRE/1738] p 3923 N92-31344
The eclipsing cataclysmic variable AY Piscium
[INPE-5340-PRE/1739] p 3923 N92-31345
The eclipsing cataclysmic variable NSV 12615 (V4041 Sgr)
[INPE-5342-PRE/1741] p 3923 N92-31346
Accretion disk image reconstruction in cataclysmic variables
[INPE-5343-PRE/1742] p 3923 N92-31347

CATALYSIS
Organometallic Nonlinear Optical (NLO) polymers. Part 2: Synthesis of main-chain organometallic polymers and a structural study of ferrocene NLO-Phores
[AD-A250655] p 3791 N92-31318
The synthesis and characterization of new copper coordination complexes containing an asymmetric coordinating chelate ligand: Application to enzyme active site modeling
[DE92-011532] p 3786 N92-31391
Linear and star-branched siloxy-silane polymers: One pot A-B polymerization and end-capping
[AD-A252195] p 3792 N92-31408
Novel chemically amplified dry-developing imaging materials for high resolution microlithography
[AD-A250085] p 3793 N92-31435
Light alkane conversion processes: Suprabiotic catalyst systems for selective oxidation of light alkane gases to fuel oxygenates
[DE92-015229] p 3799 N92-31751
Catalytic carbon membranes for hydrogen production
[DE92-001269] p 3784 N92-31976
Probe molecule studies: Active species in alcohol synthesis
[DE92-015430] p 3784 N92-32029
Synthesis of cresols and xylenols from phenol and methanol
[DE91-002141] p 3785 N92-32093
Fundamental studies in oxidation-reduction in relation to water photolysis
[DE92-014333] p 3785 N92-32113

CATALYSTS
Catalyst and feedstock effects in the thermochemical conversion of biomass to liquid transportation fuels
[DE92-010569] p 3799 N92-31593
Light alkane conversion processes: Suprabiotic catalyst systems for selective oxidation of light alkane gases to fuel oxygenates
[DE92-015229] p 3799 N92-31751
Photogenerated base as catalyst for imidization reactions: Design of photosensitive polyimides
[AD-A250067] p 3795 N92-31810
Energy and Environment: A Sandia Technology Bulletin
[DE92-016740] p 3854 N92-31931
The development of precipitated iron catalysts with improved stability
[DE92-014630] p 3785 N92-32117
Catalyst dispersion and activity under conditions of temperature-staged liquefaction
[DE92-014112] p 3786 N92-32141

CATHODE GLOW
Proposal for a workshop in the physics and application of hollow electrode glow switches
[AD-A247139] p 3814 N92-31490

CATHODE RAY TUBES
Space constancy on video display terminals
[AD-A247290] p 3872 N92-32105

CATHODES
Batteries and fuel cells
[DE92-011493] p 3847 N92-31571

CATIONS
Application of the mean spherical approximation to the estimations of single ion thermodynamic quantities of solvation for monoatomic monovalent ions in aqueous solutions
[AD-A250190] p 3893 N92-31316
Correlation from randomness: Quantitative analysis of sputtered graphite surfaces using the scanning tunneling microscope
[AD-A252420] p 3783 N92-31820
Role of the double-layer cation on the potential-dependent stretching frequencies and binding geometries of carbon monoxide at platinum-nonaqueous interfaces
[AD-A246980] p 3784 N92-31998
Cationic ring opening polymerization of oxazolines initiated by trimethylsilyl derivatives
[AD-A251109] p 3798 N92-32153

CAVITATION FLOW
Effect of out-of-roundness on the performance of a diesel engine connecting-rod bearing
[NASA-TM-105600] p 3834 N92-31536

CAVITIES
A three-gap klystron output cavity at X-band
[DE92-012417] p 3812 N92-31289

CAVITY FLOW
Adaptive mesh strategies for the spectral element method
[NASA-CR-189686] p 3818 N92-31265

CAVITY RESONATORS
A three-gap klystron output cavity at X-band
[DE92-012417] p 3812 N92-31289
Improved ferrite biasing scheme for booster RF cavities
[DE92-011650] p 3815 N92-31664

CELL ANODES
Final report on DSA methods for monitoring alumina in aluminum reduction cells with cermet anodes
[DE92-013599] p 3813 N92-31440

CELLS (BIOLOGY)
Cellular localization of infrared sources
[AD-A249795] p 3866 N92-31302
Hollow fiber clinostat for simulating microgravity in cell culture
[NASA-CASE-MFS-28370-1] p 3828 N92-31790
A biological model of the effects of toxic substances
[AD-A247138] p 3867 N92-31980

CEMENTS
Preliminary evaluation of adhesion strength measurement devices for ceramic/titanium matrix composite bonds
[NASA-TM-105803] p 3745 N92-31267
The 3-D analysis and verification of fracture growth mechanisms in fiber-reinforced ceramic composies
[AD-A250893] p 3773 N92-31305
Materials for geothermal production
[DE92-014691] p 3849 N92-32118
Geothermal materials development
[DE92-016940] p 3849 N92-32124

CENTAUR LAUNCH VEHICLE
Graphite/epoxy composite adapters for the Space Shuttle/Centaur vehicle
[NASA-TP-3014] p 3765 N92-31251

CERAMIC COATINGS
Gibbs free energy of reactions involving SiC, Si3N4, H2, and H2O as a function of temperature and pressure
[NASA-TP-3275] p 3791 N92-31278
Strongly adherent ceramic surface layers by ion implantation
[AD-A248882] p 3792 N92-31388

CERAMIC FIBERS
Preparation of non-oxide ceramics by pyrolysis of organometallic precursors
[AD-A251112] p 3798 N92-32197

CERAMIC MATRIX COMPOSITES
The 3-D analysis and verification of fracture growth mechanisms in fiber-reinforced ceramic composies
[AD-A250893] p 3773 N92-31305
Thermomechanical fatigue behavior of a silicone carbide fiber-reinforced calcium aluminosilicate glass-ceramic matrix composite
[AD-A249870] p 3775 N92-31823

CERAMICS
Preliminary evaluation of adhesion strength measurement devices for ceramic/titanium matrix composite bonds
[NASA-TM-105803] p 3745 N92-31267
Interface engineering in alumina/glass composites
[AD-A248587] p 3773 N92-31315
Surface structures and surface processes of ceramics with atomic resolutions: A study by scanning tunneling microscopy
[AD-A249581] p 3792 N92-31377
Sodium Heat Engine Development Program
[DE92-012398] p 3846 N92-31531
Ceramic surfaces and sintering
[DE92-011570] p 3793 N92-31538
Energetics, bonding mechanism and electronic structure of metal/ceramic interfaces
[DE92-013401] p 3775 N92-31806
Ceramic membranes for high temperature hydrogen separation
[DE92-013342] p 3783 N92-31816
Metallization of ferrite ceramic couplings
[DE92-016573] p 3789 N92-32032
Ferroelectric thin films prepared by pulse laser deposition processing and characterization
[PB92-196088] p 3913 N92-32072
Effect of surface modifications on the properties of silicon nitride ceramics
[DE92-013848] p 3797 N92-32094
Solid electrolytes and impact-resistant ceramics
[DE92-015297] p 3797 N92-32095
Preparation of non-oxide ceramics by pyrolysis of organometallic precursors
[AD-A251112] p 3798 N92-32197
Tetragonal zirconia ceramics in ZrO2-CeO2 system (Ce-TZP): Preparation, characterization and mechanical properties
[INPE-5372-PRE/1746] p 3798 N92-32199
Ba2Ti9O20 microwave dielectric resonator: Processing, phase synthesis and characterization
[INPE-5373-PRE/1747] p 3818 N92-32200
Investigation of acoustic properties of high-temperature ceramic superconductors p 3914 N92-32209

CERMETS
Final report on DSA methods for monitoring alumina in aluminum reduction cells with cermet anodes
[DE92-013599] p 3813 N92-31440

CERTIFICATION
B-1B nuclear certification tasks performed by the Aircraft Compatibility Department at Sandia National Laboratories
[DE92-016750] p 3757 N92-31736

CESIUM IODIDES
Development of gamma ray imaging cameras
[DE92-015305] p 3828 N92-31919

CHAINS
Inorganic rings on carbon chains
[AD-A251043] p 3772 N92-31850

CHANGE DETECTION
The detection of climate change due to the enhanced greenhouse effect
[NASA-TM-107965] p 3849 N92-31258

CHANNELS
Strength tests of cold-formed channel sections undergoing local and distortional buckling
[PB92-180835] p 3841 N92-31658

CHANNELS (DATA TRANSMISSION)
Ionospheric communications channel modelling
[DE92-013039] p 3808 N92-31722

CHAOS
Noise-induced chaos and phase space flux: A sample-theoretic study
[PB92-172733] p 3915 N92-31645
The physics of cellular automata and coherence and chaos in classical many-body systems
[DE92-016834] p 3890 N92-32035

CHARACTER RECOGNITION
Automated input into databases: OCR and descriptive cataloguing p 3921 N92-32189
CHARACTERIZATION
On a characterization of the exponential distribution based on a type 2 right censored sample
[CWI-BS-R9117] p 3888 N92-31517
Development of characterization techniques for polyurethanes 1. Characterization of SRM 1480, a low molecular weight polyurethane for SEC calibration
[PB92-172485] p 3794 N92-31618
Tetragonal zirconia ceramics in ZrO2-CeO2 system (Ce-TZP): Preparation, characterization and mechanical properties
[INPE-5372-PRE/1746] p 3798 N92-32199
CHARGE CARRIERS
Submillimeter wave spectroscopy of heterojunction superlattices
[AD-A250835] p 3908 N92-31496
The chemistry and packaging of nanocomposite confined arrays
[AD-A250991] p 3817 N92-32002
Effect of synthesis temperature in the structure, doping level and charge-transport properties of polypyrrole
[AD-A250531] p 3796 N92-32079
CHARGE COUPLED DEVICES
Dual gated imaging system for enhanced fluorescent diagnostics measurements
[AD-A249673] p 3828 N92-31694
CHARGE TRANSFER
Interfacial ion transport between immiscible liquids
[AD-A252424] p 3778 N92-31292
Charge transfer processes in multiple site chemical systems
[AD-A249538] p 3791 N92-31358
Ultrafast experiments on the role of vibrational modes in electron transfer
[AD-A250630] p 3910 N92-31699
High-latitude spacecraft charging in low-Earth polar orbit
[AD-A249868] p 3767 N92-31822
Vibrational modes and the dynamic solvent effect in electron and proton transfer
[AD-A250727] p 3897 N92-31950
Ultrafast studies on electron transfer in the betaines: Evidence for local heating
[AD-A250728] p 3897 N92-31999
Particle emission and charging effects induced by fracture
[AD-A252182] p 3913 N92-32065
Effect of synthesis temperature in the structure, doping level and charge-transport properties of polypyrrole
[AD-A250531] p 3796 N92-32079
Fundamental studies in oxidation-reduction in relation to water photolysis
[DE92-014333] p 3785 N92-32113
Ionization potentials and electron affinities of semiconductor clusters determined via charge transfer reactions
[AD-A250943] p 3898 N92-32169
CHELATION
The synthesis and characterization of new copper coordination complexes containing an asymmetric coordinating chelate ligand: Application to enzyme active site modeling
[DE92-011532] p 3786 N92-31391
CHEMICAL ANALYSIS
Utilization of gamma ray inspection system for tomographic imaging and dimensional analysis of complete model magnet cold masses and collared coil sections
[DE92-013466] p 3836 N92-31647
Diosmacycloalkanes as models for the formation of hydrocarbons from surface methylenes
[DE92-014588] p 3783 N92-31891
Development of effective quantum chemical method for polymers and solid
[AD-A250976] p 3795 N92-31951
Effect of synthesis temperature in the structure, doping level and charge-transport properties of polypyrrole
[AD-A250531] p 3796 N92-32079
CHEMICAL BONDS
Nature of short Li-H-C contact interactions in organolithium compounds and its implication
[AD-A250992] p 3898 N92-32024
CHEMICAL COMPOSITION
Charge transfer processes in multiple site chemical systems
[AD-A249538] p 3791 N92-31358
Advanced thermally stable jet fuel development program. Volume 2: Compositional factors affecting thermal degradation of jet fuels
[AD-A252656] p 3798 N92-31399
Chromium, nickel, and other alloying elements in US-produced stainless and heat-resisting steel
[PB92-178623] p 3788 N92-31797
Vibrational modes and the dynamic solvent effect in electron and proton transfer
[AD-A250727] p 3897 N92-31950
Rainwater and throughfall chemistry in a terra firme rain forest: Central Amazonia
[INPE-5364-PRE/1744] p 3863 N92-32224
CHEMICAL ENERGY
Chemical energy storage system for SEGS solar thermal power plant
[DE92-012327] p 3848 N92-31845
CHEMICAL EVOLUTION
Evolution and analysis of the functional domains of the chimeric proteins that initiate pyrimidine biosynthesis
[AD-A250069] p 3866 N92-31465
CHEMICAL EXPLOSIONS
The collection, handling, transportation, and thermal desorption of explosive vapor using quartz collection tubes
[DE92-011441] p 3799 N92-31570
Turbulent dusty boundary layer in an ANFO surface-burst explosion
[DE92-012101] p 3822 N92-31625
Estimation of metal acceleration by an SF5 containing explosive
[AD-A245338] p 3801 N92-32098
CHEMICAL PROPERTIES
Autoignition behavior of lean mixtures: Chemical and thermodynamics effects
[DE92-009690] p 3781 N92-31763
CHEMICAL REACTIONS
The role of metal structure in determining solvent orientation at the electrode/solution interface
[AD-A249751] p 3893 N92-31328
The synthesis and characterization of new copper coordination complexes containing an asymmetric coordinating chelate ligand: Application to enzyme active site modeling
[DE92-011532] p 3786 N92-31391
The pathways and dynamics of molecular decomposition
[AD-A249627] p 3893 N92-31463
Characterization of polymers for microcellular foams
[DE92-012444] p 3793 N92-31539
New sources for OMVPE
[AD-A250903] p 3909 N92-31582
Elementary reaction rate measurements at high temperatures by tunable-laser flash-absorption
[DE92-015269] p 3830 N92-31684
Ultrafast experiments on the role of vibrational modes in electron transfer
[AD-A250630] p 3910 N92-31699
Laser enhanced chemical reaction studies
[DE92-010772] p 3831 N92-31798
Unimolecular reaction mechanisms involving C3H4, C4H4, and C6H6 hydrocarbon species
[DE92-005326] p 3783 N92-31860
Laser-ablated copper condensation in helium
[DE92-016685] p 3789 N92-32004
Probe molecule studies: Active species in alcohol synthesis
[DE92-015430] p 3784 N92-32029
CHEMICAL REACTORS
Propane oxidation through the negative temperature coefficient region at 10 and 15 atmospheres: Results of experimental and modeling studies
[DE92-007902] p 3778 N92-31414
Chemical energy storage system for SEGS solar thermal power plant
[DE92-012327] p 3848 N92-31845
The development of precipitated iron catalysts with improved stability
[DE92-014630] p 3785 N92-32117
CHEMICAL TESTS
The pathways and dynamics of molecular decomposition
[AD-A249627] p 3893 N92-31463
CHEMISORPTION
Gallium arsenide clusters and their interfacial physics and chemistry
[AD-A249565] p 3907 N92-31375
CHILDREN
Stress reactivity: Five-factor representation of a psychobiological typology
[AD-A252715] p 3872 N92-31327
CHINA
Two long-term instrumental climatic data bases of the People's Republic of China
[DE92-010378] p 3851 N92-31527
CHIPS (ELECTRONICS)
Operating principles of MULTIKRON performance instrumentation for MIMD computers
[PB92-181072] p 3874 N92-31366
High-performance packaging for monolithic microwave and millimeter-wave integrated circuits
[NASA-TM-105744] p 3808 N92-31855
CHLORIDES
Experimental studies of aluminum solubility and speciation in brines
[DE92-010448] p 3786 N92-31418
Structure and dynamics of Cl(H2O)20 clusters. The effect of the polarizability and the charge ofthe ion
[AD-A251094] p 3899 N92-32196
CHLOROCARBONS
World ocean circulation experiment. WOCE chlorofluorocarbon intercomparison cruise report
[PB92-185974] p 3865 N92-31842
CHLOROFLUOROCARBONS
World ocean circulation experiment. WOCE chlorofluorocarbon intercomparison cruise report
[PB92-185974] p 3865 N92-31842
CHLOROFORMATE
The photogeneration of polymeric amines: Synthesis and photocrosslinking of copolymers containing photoactive carbamate pendant groups
[AD-A250086] p 3793 N92-31436
CHOLINESTERASE
Acetylcholinesterase inhibitors on the spinal cord
[AD-A252694] p 3868 N92-31326
CHROMATOGRAPHY
Development of characterization techniques for polyurethanes 1. Characterization of SRM 1480, a low molecular weight polyurethane for SEC calibration
[PB92-172485] p 3794 N92-31618
CHROMIUM
Impurity effects on the magnetic ordering in chromium
[DE92-016165] p 3789 N92-31898
CHROMIUM ALLOYS
Thermodynamic assessment of the Cr-Zr system
[PB92-180645] p 3787 N92-31610
CHROMIUM OXIDES
Oxidation/sulfidation behavior of Fe-Cr alloys: A reactive-element effect
[DE92-016172] p 3789 N92-31924
CHROMIUM STEELS
Chromium, nickel, and other alloying elements in US-produced stainless and heat-resisting steel
[PB92-178623] p 3788 N92-31797
CHROMOSPHERE
Fine structure superimposed on mm-wavelength (18-23 GHz) spectra of solar active region
[INPE-5371-TDI/470] p 3926 N92-32221
CIRCADIAN RHYTHMS
Micro saint model of fatigue assessment
[AD-A249976] p 3868 N92-31554
Organization of the human circadian system
[AD-A247498] p 3869 N92-31905
CIRCUITS
Method and circuit for controlling the evolution time interval of a laser output pulse
[NASA-CASE-LAR-13772-1] p 3831 N92-31788
RL-34 ring laser gyro laboratory evaluation for the Deep Space Network antenna application
[NASA-CR-190481] p 3829 N92-32128
A sweep algorithm for massively parallel simulation of circuit-switched networks
[NASA-CR-189680] p 3881 N92-32157
CIRCULAR CYLINDERS
Electromagnetic scattering by coated convex surfaces and wedges simulated by approximate boundary conditions
[NASA-CR-190540] p 3803 N92-31238
A finite element-boundary integral method for conformal antenna arrays on a circular cylinder
[NASA-CR-190534] p 3807 N92-31614
The three-dimensional stability of the Foeppl vortices p 3750 N92-31889
CIRCULAR POLARIZATION
Analysis of random induced cross polarization
[AD-A249773] p 3806 N92-31569
CIVIL AVIATION
Integrated Technology Plan for the Civil Space Program, 1991
[PB92-181692] p 3762 N92-31634
Design and analysis issues of integrated control systems for high-speed civil transports
[NASA-CR-186022] p 3761 N92-31656
CLADDING
Transient internal probe diagnostic
[AD-A247306] p 3903 N92-31459
Non-equilibrium synthesis by laser cladding of Ni, Nb and Mg alloys for improved environmental resistance
[AD-A250552] p 3787 N92-31612
CLASSIFICATIONS
Type evolution and instance adaptation
[AD-A248435] p 3917 N92-31285
Using the burst derivative measure to improve the computational efficiency of ISAR motion compensation algorithms
[AD-A250850] p 3805 N92-31369

CLEAN ROOMS
Activities of the Center for X Ray Lithography, phase 1
[AD-A250446] p 3901 N92-31397
CLEARANCES
Turbine blade tip and seal clearance excitation forces
[NASA-CR-184341] p 3760 N92-31910
CLIMATE
Annual dynamics within the active layer
[DE92-013520] p 3850 N92-31304
Two long-term instrumental climatic data bases of the People's Republic of China
[DE92-010378] p 3851 N92-31527
Global atmospheric circulation statistics, 1000-1 mb
[PB92-186196] p 3853 N92-31649
Analysis of the effects of aerosol distribution in the atmosphere on surface radiative measurements
[DE92-014189] p 3856 N92-31662
Comprehensive Aerological Reference Data Set (CARDS)
[DE92-016469] p 3862 N92-31734
A study of longwave radiation codes for climate studies: Validation with ARM observations and tests in general circulation models
[DE92-014100] p 3862 N92-31894
Iterative functionalism and climate management regimes: From intergovernmental panel on climate change to intergovernmental negotiating committee
[DE92-014798] p 3853 N92-31896
Multi-year strategic plan for the atmospheric studies in complex terrain: ASCOT program
[DE92-016646] p 3854 N92-31930
The uncertainties of global temperatures in the global warming context
[TABES PAPER 92-447] p 3763 N92-32014
CLIMATE CHANGE
The detection of climate change due to the enhanced greenhouse effect
[NASA-TM-107965] p 3849 N92-31258
Our changing planet: The FY 1993 US global change research program. A supplement to the US President's fiscal year 1993 budget
[NASA-CR-190675] p 3850 N92-31259
Effects of anthropogenic sulfur aerosols on climate
[DE92-016158] p 3850 N92-31297
Our Changing Planet: The FY 1993 US Global Change Research Program. A report by the Committee on Earth and Environmental Sciences, a supplement to the US President's fiscal year 1993 budget
[PB92-156892] p 3852 N92-31620
Response of a tundra ecosystem to elevated atmospheric carbon dioxide and CO2-induced climate change
[DE92-013925] p 3853 N92-31626
Comprehensive Aerological Reference Data Set (CARDS)
[DE92-016469] p 3862 N92-31734
Iterative functionalism and climate management regimes: From intergovernmental panel on climate change to intergovernmental negotiating committee
[DE92-014798] p 3853 N92-31896
Trends 1991: A compendium of data on global change
[DE92-011733] p 3854 N92-31907
The uncertainties of global temperatures in the global warming context
[TABES PAPER 92-447] p 3763 N92-32014
NASA High Speed Research Program, Emissions Scenarios Committee report of meetings on 26 September 1991 and 9 January 1992
[NASA-CR-190379] p 3855 N92-32147
CLIMATOLOGY
Effects of anthropogenic sulfur aerosols on climate
[DE92-016158] p 3850 N92-31297
The validation of atmospheric models
[DE92-013254] p 3850 N92-31324
An airborne study of boundary layer heat and moisture fluxes for project FIFE
[NASA-CR-190665] p 3844 N92-31357
Two long-term instrumental climatic data bases of the People's Republic of China
[DE92-010378] p 3851 N92-31527
A case study of a prolonged sleet event: 16-17 February 1987 and climatology of sleet events for North Carolina, 1949-1989
[AD-A250184] p 3859 N92-31602
A comparative analysis of the temporal variability of lightning observations and GOES imagery
[AD-A250185] p 3860 N92-31603
Lamont-Doherty Geological Observatory
[PB92-185040] p 3856 N92-31636
Meteorological data, new series A monographs. Volume 5, no. 4: A three dimensional model simulation of the circulation in the middle atmosphere with cconsideration of tropospherical-stratospherical interactions
[ETN-92-91693] p 3861 N92-31708
Iterative functionalism and climate management regimes: From intergovernmental panel on climate change to intergovernmental negotiating committee
[DE92-014798] p 3853 N92-31896
Seasonal wind and ocean thermal forcing influences on the generation of the Leeuwin current and its eddies
[AD-A246992] p 3865 N92-31988
The uncertainties of global temperatures in the global warming context
[TABES PAPER 92-447] p 3763 N92-32014
CLINICAL MEDICINE
Hypertext and hypermedia systems in information retrieval p 3921 N92-32188
CLOSURE LAW
Reynolds stress calculations of homogeneous turbulent shear flow with bounded energy states
[NASA-CR-189682] p 3826 N92-32158
CLOSURES
An automated computational method for barrier construction in single and two-target differential games p 3749 N92-31882
CLOUD COVER
Energy balance model for imagery and electromagnetic propagation
[AD-A250884] p 3806 N92-31543
CLOUD HEIGHT INDICATORS
Cloud-to-ground lightning characteristics in mesoscale convective systems
[AD-A250418] p 3858 N92-31493
CLOUD PHYSICS
Unified very low stratus cloud/subcloud microphysics model
[AD-A250662] p 3858 N92-31320
CLOUDS
Numerical simulation of precipitation scavenging and comparison with observation of prescribed forest fires
[DE92-013513] p 3851 N92-31423
A study of longwave radiation codes for climate studies: Validation with ARM observations and tests in general circulation models
[DE92-014100] p 3862 N92-31894
CLUMPS
Structure and dynamics of Cl(H2O)20 clusters. The effect of the polarizability and the charge ofthe ion
[AD-A251094] p 3899 N92-32196
CLUSTER ANALYSIS
Compression of digitized map images
[AD-A250707] p 3843 N92-31323
CLUSTERS
Gallium arsenide clusters and their interfacial physics and chemistry
[AD-A249565] p 3907 N92-31375
CLUTTER
Spectrum modal analysis for the detection of low-altitude windshear with airborne Doppler radar
[NASA-CR-4457] p 3755 N92-31549
A real time system for multisensor image analysis through pyramidal segmentation
[AD-A247169] p 3888 N92-31981
CMOS
VLSI for high-speed digital signal processing
[AD-A250365] p 3817 N92-32074
COAL
MHD Contractors' Review Meeting: Abstracts
[DE92-011549] p 3904 N92-31576
World energy projection system: Model documentation
[DE92-014206] p 3847 N92-31594
COAL DERIVED GASES
Ceramic membranes for high temperature hydrogen separation
[DE92-013342] p 3783 N92-31816
COAL DERIVED LIQUIDS
Catalyst dispersion and activity under conditions of temperature-staged liquefaction
[DE92-014112] p 3786 N92-32141
COAL LIQUEFACTION
Catalyst dispersion and activity under conditions of temperature-staged liquefaction
[DE92-014112] p 3786 N92-32141
COASTAL WATER
An analysis of hydrographic data collected off Point Sur, California in June 1990
[AD-A246060] p 3866 N92-32056
COASTS
Geomorphic variability in the coastal zone
[AD-A252713] p 3864 N92-31544
Proceedings of the 4th Atlantic OCS Region Information Transfer Meeting
[PB92-177690] p 3864 N92-31630
An analysis of hydrographic data collected off Point Sur, California in June 1990
[AD-A246060] p 3866 N92-32056
COATINGS
Electromagnetic scattering by coated convex surfaces and wedges simulated by approximate boundary conditions
[NASA-CR-190540] p 3803 N92-31236
High-frequency techniques for RCS prediction of plate geometries
[NASA-CR-190656] p 3804 N92-31273
Interface engineering in alumina/glass composites
[AD-A248587] p 3773 N92-31315
Sol-gel multilayers applied by a meniscus coating process
[DE92-012697] p 3794 N92-31560
Electro-optics and second harmonic generation of nonlinear optical polymers
[AD-A252488] p 3796 N92-31960
Preparation of non-oxide ceramics by pyrolysis of organometallic precursors
[AD-A251112] p 3798 N92-32197
COAXIAL CABLES
Development, testing and operation of a large suspended ocean measurement structure for deep-ocean use
[AD-A252188] p 3866 N92-32050
COBALT
Synthesis, structure and properties of Ba6Co25S27: A Perovskite-like superstructure of Co8S6 and Ba6S clusters
[AD-A251041] p 3911 N92-31848
COCKPITS
Pressure and temperature for B-1B transparency test
[AD-A252711] p 3752 N92-31674
CODE DIVISION MULTIPLE ACCESS
Coherent/noncoherent detection of coherent optical heterodyne DPSK-CDMA and MFSK-CDMA signals
[AD-A246215] p 3809 N92-31993
CODING
Reducing requirements errors through the use of Computer-Aided Software Engineering (CASE) tools and during requirements analysis
[AD-A246879] p 3874 N92-31299
Systematic detection of parallelism in ordinary programs
[AD-A247514] p 3882 N92-31445
The investigation of bandwidth efficient coding and modulation techniques
[NASA-CR-190685] p 3806 N92-31468
Non-geothermal optics study of wave propagation
[DE92-011806] p 3903 N92-31494
COEFFICIENTS
High-frequency techniques for RCS prediction of plate geometries
[NASA-CR-190656] p 3804 N92-31273
COGNITION
Acquisition and production of skilled behavior in dynamic decision-making tasks
[NASA-CR-190614] p 3870 N92-31341
Probability-based inference in a domain of proportional reasoning tasks
[AD-A247304] p 3871 N92-31444
COHERENT RADIATION
Detection of signal harmonic sets
[DREA-CR-89-420] p 3806 N92-31471
Theory for the CEBAF infrared and shipboard FELS
[AD-A252174] p 3832 N92-32061
COLD ROLLING
Development of an electrochemical method for field testing of protective coatings
[AD-A245872] p 3793 N92-31473
COLD SURFACES
Experimental studies of hypersonic shock-wave boundary-layer interactions
[NASA-CR-190731] p 3753 N92-32162
COLD WATER
Immersion suit usage within the RAAF
[AD-A250645] p 3755 N92-31562
COLD WORKING
Development of an electrochemical method for field testing of protective coatings
[AD-A245872] p 3793 N92-31473
Strength tests of cold-formed channel sections undergoing local and distortional buckling
[PB92-180835] p 3841 N92-31658
COLLISION PARAMETERS
Electron scattering by atomic hydrogen: Elastic and inelastic phenomena at 13.9 to 200 eV
[DE92-625004] p 3896 N92-31837
COLLISIONLESS PLASMAS
Vortices associated with toroidal ion temperature gradient driven fluctuations
[DE92-016180] p 3903 N92-31412
Weak ion-acoustic shock waves and double layers in non-collision plasma p 3907 N92-32208

COLLISIONS
Dicke narrowing in strong fields: The atom-as-antenna analogy
[AD-A252321] p 3807 N92-31629
COLOR VISION
From perception to modelization in robotics using achromatic and chromatic cameras
[LAAS-91484] p 3901 N92-31692
Function of panel M pathways in primates
[AD-A250275] p 3871 N92-31758
COMBAT
Development of quantitative specifications for simulating the stress environment
[AD-A250669] p 3870 N92-31321
Simulation of a parallel processor based small tactical system
[AD-A245911] p 3882 N92-31443
COMBINATORIAL ANALYSIS
Decomposition of balanced matrices. Part 4: Connected squares
[AD-A247308] p 3888 N92-31768
COMBUSTIBLE FLOW
Contribution to the modelling of turbulent combustion in the case of stabilisation by flame-lock
[ESA-TT-1229] p 3784 N92-31942
COMBUSTION
Development of a core combustion research program plan for EPA
[PB92-180868] p 3781 N92-31683
Technology advancing research combustion in burners
[PB92-164359] p 3782 N92-31776
Pulse Combustion Engineering Research Laboratory: Exhaust energy
[PB92-172402] p 3783 N92-31918
Development of methodology and technology for identifying and quantifying emission products from open burning and open detonation thermal treatment methods. BangBox test series. Volume 1. Test summary
[AD-A250733] p 3800 N92-31969
Development of methodology and technology for identifying and quantifying emission products from open burning and open detonation thermal treatment methods. BangBox test series. Volume 2: Test development
[AD-A250734] p 3800 N92-31970
Development of methodology and technology for identifying and quantifying emission products from open burning and open detonation thermal treatment methods. Field test series A, B, and C. Volume 1: Test summary
[AD-A250735] p 3800 N92-31971
COMBUSTION CHAMBERS
Two-stage n-butane flame: A comparison between experimental measurements and modeling results
[DE92-009457] p 3779 N92-31416
MHD Contractors' Review Meeting: Abstracts
[DE92-011549] p 3904 N92-31576
Performance of multiple stream pulsed jet combustion systems
[AD-A249722] p 3780 N92-31671
Technology advancing research combustion in burners
[PB92-164359] p 3782 N92-31776
Study of a spherical spinning combustion chamber for orbit insertion p 3746 N92-31869
Pulse Combustion Engineering Research Laboratory: Exhaust energy
[PB92-172402] p 3783 N92-31918
Laser-initiated conical detonation wave for supersonic combustion, part 3
[AD-A250522] p 3785 N92-32076
COMBUSTION CHEMISTRY
Theoretical studies of the reactions and spectroscopy of radical species relevant to combustion reactions and diagnostics
[DE92-013484] p 3781 N92-31725
A semiconductor bridge ignited gas generator
[DE92-014049] p 3781 N92-31748
Autoignition behavior of lean mixtures: Chemical and thermodynamics effects
[DE92-009690] p 3781 N92-31763
COMBUSTION CONTROL
Two-stage n-butane flame: A comparison between experimental measurements and modeling results
[DE92-009457] p 3779 N92-31416
Effect of inlet geometry on the flow and combustion processes in a solid fuel ramjet p 3747 N92-31871
COMBUSTION EFFICIENCY
Development of methodology and technology for identifying and quantifying emission products from open burning and open detonation thermal treatment methods. Field test series A, B, and C. Volume 1: Test summary
[AD-A250735] p 3800 N92-31971
COMBUSTION PHYSICS
Solid rocket combustion phenomena
[AD-A248006] p 3770 N92-31474
Ignition and flame propagation studies over a flat fuel surface
[PB92-181056] p 3780 N92-31678
Numerical simulation of tulip flame dynamics
[DE92-008553] p 3782 N92-31805
Collection of papers of the 31st Israel Annual Conference on Aviation and Astronautics
[ITN-92-85124] p 3745 N92-31861
Pulse Combustion Engineering Research Laboratory: Exhaust energy
[PB92-172402] p 3783 N92-31918
Flammability characteristics of glass reinforced epoxy composite materials
[AD-A251009] p 3775 N92-31940
Contribution to the modelling of turbulent combustion in the case of stabilisation by flame-lock
[ESA-TT-1229] p 3784 N92-31942
COMBUSTION PRODUCTS
Nonthermal inhalation injury
[AD-A252532] p 3869 N92-31962
Development of methodology and technology for identifying and quantifying emission products from open burning and open detonation thermal treatment methods. BangBox test series. Volume 2: Test development
[AD-A250734] p 3800 N92-31970
Development of methodology and technology for identifying and quantifying emission products from open burning and open detonation thermal treatment methods. Field test series A, B, and C. Volume 2, part A: Quality assurance and quality control
[AD-A250736] p 3801 N92-31972
COMET TAILS
A characterization of the hot infrared background: The infrared cirrus, zodiacal dust bands, and solar system dust trails
[PL-TR-91-2065] p 3924 N92-32142
COMMAND AND CONTROL
Methodology investigation final report: Automated real-time test scenario generation, phase 1
[AD-A250439] p 3884 N92-31395
Simulation of a parallel processor based small tactical system
[AD-A245911] p 3882 N92-31443
COMMERCE
Report to the US Congress on minority small business and capital ownership development as required by the Business Opportunity Development Reform Act of 1988
[PB92-173681] p 3916 N92-31364
COMMERCIAL AIRCRAFT
Aviation safety: Changes needed in FAA's service difficulty reporting program
[GAO/RCED-91-24] p 3755 N92-31453
Aviation noise: Costs of phasing out noisy aircraft
[GAO/RCED-91-128] p 3891 N92-31454
COMMUNICATION NETWORKS
Issues in designing transport layer multicast facilities
[NASA-CR-190639] p 3882 N92-31483
Mission and Safety Critical (MASC) plans for the MASC Kernel simulation
[NASA-CR-190708] p 3875 N92-31487
GNAS Maintenance Control Center (GMCC) Design Qualification Test and Evaluation (DQT/E) test report
[DOT/FAA/CT-TN91/39] p 3745 N92-31615
Continuous time and discrete time hyperexponential model for dependability growth modeling
[LAAS-92002] p 3837 N92-31693
Towards a complete hierarchy of compositional dataflow models
[RUU-CS-91-45] p 3807 N92-31715
Soviet satellite communications science and technology
[PB92-173038] p 3809 N92-31920
COMMUNICATION SATELLITES
Soviet satellite communications science and technology
[PB92-173038] p 3809 N92-31920
Advances in small satellite communication systems
[TABES PAPER 92-411] p 3763 N92-32010
Decision-making guide for the proposed Coast Guard differential global positioning system
[AD-A246046] p 3756 N92-32054
A prototype DND Ku band SATCOM system for ANIK-C2 (Project MASTER/MM2)
[DREO-1034] p 3810 N92-32176
COMPARISON
A performance-based comparison of object-oriented simulation tools
[AD-A252125] p 3875 N92-31405
Titanium carbon nitride coating
[DE92-013158] p 3777 N92-32135
COMPATIBILITY
Imide/arylene ether copolymers
[NASA-CASE-LAR-14159-1-CU] p 3794 N92-31792
COMPILERS
Systematic detection of parallelism in ordinary programs
[AD-A247514] p 3882 N92-31445
COMPLEX COMPOUNDS
Tris-triphenylsiloxy compounds of aluminum
[AD-A250141] p 3788 N92-31795
COMPOSITE MATERIALS
The 3-D analysis and verification of fracture growth mechanisms in fiber-reinforced ceramic composies
[AD-A250893] p 3773 N92-31305
Mathematical problems in micromechanics and composite materials
[AD-A249584] p 3773 N92-31378
Composite failure analysis handbook. Volume 1: Program review
[AD-A250520] p 3776 N92-32047
Composite failure analysis handbook. Volume 2: Technical handbook. Part 1: Procedures and techniques
[AD-A250521] p 3776 N92-32048
The mechanics of fractal damage
[AD-A250518] p 3776 N92-32075
COMPOSITE STRUCTURES
Graphite/epoxy composite adapters for the Space Shuttle/Centaur vehicle
[NASA-TP-3014] p 3765 N92-31251
A finite element procedure for analysis of laminated composite plates
[AD-A250902] p 3773 N92-31307
A generalized plane-strain elastic stress solution for a multiorthotropic-layered cylinder
[AD-A250487] p 3838 N92-31331
A proposal for the establishment of a Center for Advanced Composite Materials Research
[AD-A250072] p 3773 N92-31361
Cryogenic 4.4 MN mechanical test system for large scale tests of composite support struts
[PB92-181148] p 3774 N92-31609
Catalytic carbon membranes for hydrogen production
[DE92-001269] p 3784 N92-31976
Composite failure analysis handbook. Volume 1: Program review
[AD-A250520] p 3776 N92-32047
Composite failure analysis handbook. Volume 2: Technical handbook. Part 1: Procedures and techniques
[AD-A250521] p 3776 N92-32048
Optimal design of geodesically stiffened composite cylindrical shells
[NASA-CR-190706] p 3842 N92-32235
COMPRESSED GAS
High-pressure gas switch for a wideband source
[DE92-015822] p 3815 N92-31548
COMPRESSIBILITY EFFECTS
Control of unsteady separated flow associated with the dynamic stall of airfoils
[NASA-CR-190688] p 3753 N92-32177
COMPRESSIBLE BOUNDARY LAYER
Sensitivity analysis of hydrodynamic stability operators
[NASA-CR-189683] p 3822 N92-31535
COMPRESSIBLE FLOW
Stability of boundary layers at high supersonic and hypersonic speeds
[AD-A250900] p 3819 N92-31306
Development and application of new algorithms for the simulation of compressible flows with moving bodies in three dimensions
[AD-A250232] p 3823 N92-31696
Automatic design of transonic airfoils to reduce the shock induced pressure drag p 3745 N92-31863
New techniques in computational fluid dynamics: Algorithms, analysis, applications
[AD-A250498] p 3825 N92-32038
Three-dimensional compressible turbulent computations for a nondiffusing S-duct
[NASA-CR-4391] p 3754 N92-32240
COMPRESSIBLE FLUIDS
Fundamental studies of the structure of hypersonic attached and separated boundary layers over smooth, rough and transpiration-cooled surfaces
[AD-A250284] p 3819 N92-31286
CAVEAT: A computer code for fluid dynamics problems with large distortion and internal slip
[DE92-014078] p 3825 N92-32022
COMPRESSING
Instabilities of damage and surface degradation mechanisms in brittle material structural systems
[AD-A250785] p 3842 N92-32168
COMPRESSION TESTS
Strength tests of cold-formed channel sections undergoing local and distortional buckling
[PB92-180835] p 3841 N92-31658
COMPRESSION WAVES
Deep-tow acoustics/geophysics system compressional velocity database
[AD-A252700] p 3918 N92-31467
COMPRESSIVE STRENGTH
Cryogenic 4.4 MN mechanical test system for large scale tests of composite support struts
[PB92-181148] p 3774 N92-31609

Mechanical strength and stability of lithium aluminate
[DE92-015998] p 3841 N92-31638
Strength tests of cold-formed channel sections undergoing local and distortional buckling
[PB92-180835] p 3841 N92-31658

COMPRESSOR BLADES

Research on aero-thermodynamic distortion induced structural dynamic response of multistage compressor blading
[AD-A250865] p 3760 N92-32059

COMPRESSOR ROTORS

NASA. Lewis Research Center supersonic throughflow fan program
[NASA-TM-103248] p 3759 N92-31250
Research on aero-thermodynamic distortion induced structural dynamic response of multistage compressor blading
[AD-A250865] p 3760 N92-32059

COMPUTATION

Computer applications for engineering/structural analysis
[DE92-013070] p 3841 N92-31745
A computational examination of directional stability for smooth and chined forebodies at high-alpha
[NASA-CR-4465] p 3753 N92-32114
Computational studies of metal-metal and metal-ligand interactions
[NASA-CR-190674] p 3790 N92-32156

COMPUTATIONAL CHEMISTRY

Analysis and computer tools for separation processes involving nonideal mixtures
[DE92-015298] p 3781 N92-31752

COMPUTATIONAL FLUID DYNAMICS

CFD methods development considerations for unsteady aerodynamic analysis
[NASA-TM-107644] p 3750 N92-31239
Adaptive mesh strategies for the spectral element method
[NASA-CR-189686] p 3818 N92-31265
Stagnation-point heat-transfer rate predictions at aeroassist flight conditions
[NASA-TP-3208] p 3819 N92-31281
Advanced thermally stable, jet fuels development program annual report. Volume 1: Model and experiment system development
[AD-A249625] p 3799 N92-31462
A general numerical model for wave rotor analysis
[NASA-TM-105740] p 3821 N92-31484
Hypersonic code efficiency and validation studies
[NASA-CR-190680] p 3752 N92-31533
PARTI primitives for unstructured and block structured problems
[NASA-CR-189662] p 3876 N92-31561
Development of wavelet analysis tools for turbulence
[NASA-CR-189674] p 3822 N92-31564
Development and application of new algorithms for the simulation of compressible flows with moving bodies in three dimensions
[AD-A250232] p 3823 N92-31696
In-flight evaluation of aerodynamic predictions of an air-launched space booster
[NASA-TM-104246] p 3752 N92-31808
The structure and control of three-dimensional shock wave turbulent boundary layer interactions
[AD-A250209] p 3823 N92-31824
NAS (Numerical Aerodynamic Simulation Program) technical summaries, March 1989 - February 1990
[NASA-TM-107960] p 3926 N92-31852
The calculation of incompressible separated turbulent boundary layers p 3749 N92-31886
Euler solver for arbitrary configurations: Further applications p 3750 N92-31888
Highly accurate prediction of unsteady viscous flows
[AD-A250982] p 3825 N92-32000
New techniques in computational fluid dynamics: Algorithms, analysis, applications
[AD-A250498] p 3825 N92-32038
A computational examination of directional stability for smooth and chined forebodies at high-alpha
[NASA-CR-4465] p 3753 N92-32114
Evolution of reactants fluid volume in turbulent jets
[DE92-011298] p 3786 N92-32145
An installed nacelle design code using a multiblock Euler solver. Volume 1: Theory document
[NASA-CR-189652-VOL-1] p 3754 N92-32226
Three-dimensional compressible turbulent computations for a nondiffusing S-duct
[NASA-CR-4391] p 3754 N92-32240

COMPUTATIONAL GRIDS

Adaptive mesh strategies for the spectral element method
[NASA-CR-189686] p 3818 N92-31265
The discretization of the 2D incompressible Navier-Stokes equations on a collocated grid
[REPT-91-61] p 3821 N92-31513
Hypersonic code efficiency and validation studies
[NASA-CR-190680] p 3752 N92-31533
Axisymmetric bluff-body flow: A vortex solver for thin shells
[DE92-016748] p 3824 N92-31933
New techniques in computational fluid dynamics: Algorithms, analysis, applications
[AD-A250498] p 3825 N92-32038

COMPUTER AIDED DESIGN

The determination of operational and support requirements and costs during the conceptual design of space systems
[NASA-CR-190626] p 3766 N92-31260
Reducing requirements errors through the use of Computer-Aided Software Engineering (CASE) tools and during requirements analysis
[AD-A246879] p 3874 N92-31299
A surface definition code for turbine blade surfaces
[DE92-010574] p 3846 N92-31498
Prototype casting fabrication by stereolithography
[DE92-011489] p 3876 N92-31529
Shop of the 1990's project: An evaluation tool for wireframe CAD software
[PB92-181130] p 3877 N92-31628
Computer Aided Process Planning (CAPP): The user interface for the fabrication module of the rapid design system
[AD-A250095] p 3879 N92-31783
Automatic design of transonic airfoils to reduce the shock induced pressure drag p 3745 N92-31863
Integrated computer systems in aircraft design and manufacture: Difficulties and implications p 3746 N92-31864
Energy and Environment: A Sandia Technology Bulletin
[DE92-016740] p 3854 N92-31931
Connectivity among computer-aided engineering methods, procedures, and tools used in developing the SSC collider magnets
[DE92-013954] p 3900 N92-31975
CGVIEW: A program to generate isometric and perspective views of combinatorial geometries
[DE92-016979] p 3881 N92-32126
A parameter optimization approach to controller partitioning for integrated flight/propulsion control application
[NASA-TM-105826] p 3761 N92-32241

COMPUTER AIDED MANUFACTURING

About real time industrial processes control: A methodology based on objects and Petri nets
[LAAS-91467] p 3878 N92-31689
Computer Aided Process Planning (CAPP): The user interface for the fabrication module of the rapid design system
[AD-A250095] p 3879 N92-31783
Integrated computer systems in aircraft design and manufacture: Difficulties and implications p 3746 N92-31864
Design and automated manufacturing p 3746 N92-31866
An integrated research program for the modeling, analysis and control of aerospace systems
[AD-A250199] p 3761 N92-31966
Connectivity among computer-aided engineering methods, procedures, and tools used in developing the SSC collider magnets
[DE92-013954] p 3900 N92-31975

COMPUTER AIDED MAPPING

Compression of digitized map images
[AD-A250707] p 3843 N92-31323

COMPUTER AIDED TOMOGRAPHY

Tomographic reconstruction of infrared spectra of nonhomogeneous media: Applications to a flat flame burner
[AD-A249999] p 3778 N92-31393

COMPUTER GRAPHICS

Compression of digitized map images
[AD-A250707] p 3843 N92-31323
Graphical development tools for network-based concurrent supercomputing
[DE92-011144] p 3875 N92-31447
Development of the aspect graph representation for use in R version
[AD-A247109] p 3876 N92-31573
Enhancing GRASS data communication with videographic technology
[DE92-014852] p 3919 N92-31596
A task adaptive parallel graphics rendering algorithm
[DE92-008062] p 3878 N92-31739
Automated payload experiment tool feasibility study
[NASA-CR-184256] p 3883 N92-31835
Integrated computer systems in aircraft design and manufacture: Difficulties and implications p 3746 N92-31864
CGVIEW: A program to generate isometric and perspective views of combinatorial geometries
[DE92-016979] p 3881 N92-32126

COMPUTER INFORMATION SECURITY

An alternative to sneakernet
[DE92-011146] p 3918 N92-31448
Specification and verification of secure concurrent and distributed software systems
[AD-A252477] p 3879 N92-31825

COMPUTER NETWORKS

Optical interconnects in the computer environment
[AD-D015235] p 3873 N92-31269
Data to test and evaluate the performance of neural network architectures for seismic signal discrimination, neural computing for seismic phase identification, volume 2
[AD-A252442] p 3884 N92-31293
Overview of integrated services digital network conformance testing
[PB92-181015] p 3881 N92-31365
Simulation of a parallel processor based small tactical system
[AD-A245911] p 3882 N92-31443
Graphical development tools for network-based concurrent supercomputing
[DE92-011144] p 3875 N92-31447
An alternative to sneakernet
[DE92-011146] p 3918 N92-31448
Enhancing GRASS data communication with videographic technology
[DE92-014852] p 3919 N92-31596
Real time analysis of tokamak discharge parameters
[DE92-011394] p 3904 N92-31616
Real-time statistical quality control and ARM
[DE92-015253] p 3837 N92-31657
Some computational challenges of developing efficient parallel algorithms for data-dependent computations in thermal-hydraulics supercomputer applications
[DE92-011368] p 3878 N92-31703
Fault tolerant parallel computing in orthogonal shared-memory and related architectures
[AD-A250504] p 3883 N92-32040
Remote Data Transfer (RDT): An interprocess data transfer method for distributed environments
[AD-A250859] p 3920 N92-32102
Intelligent gateways p 3921 N92-32184

COMPUTER PROGRAMMING

Programming with inductive and co-inductive types
[AD-A249562] p 3874 N92-31353
Graphical development tools for network-based concurrent supercomputing
[DE92-011144] p 3875 N92-31447
Performance measures of the Ada rendezvous
[AD-A250060] p 3877 N92-31601
Specification and verification of secure concurrent and distributed software systems
[AD-A252477] p 3879 N92-31825
ADIFOR: Fortran source translation for efficient derivatives
[DE92-016187] p 3879 N92-31899
Workshop on the Derivation of Parallel Programs and Architectures: Closing report
[AD-A252742] p 3883 N92-32109
Full abstraction and the context lemma
[AD-A247062] p 3887 N92-32163
Polymorphic type assignment and CPS conversion
[AD-A250954] p 3887 N92-32171

COMPUTER PROGRAMS

Computer program to solve two-dimensional shock-wave interference problems with an equilibrium chemically reacting air model
[NASA-TM-4187] p 3818 N92-31247
High speed turboprop aeroacoustic study (counterrotation). Volume 2: Computer programs
[NASA-CR-185242] p 3891 N92-31248
Reducing requirements errors through the use of Computer-Aided Software Engineering (CASE) tools and during requirements analysis
[AD-A246879] p 3874 N92-31299
Using the burst derivative measure to improve the computational efficiency of ISAR motion compensation algorithms
[AD-A250850] p 3805 N92-31369
A surface definition code for turbine blade surfaces
[DE92-010574] p 3846 N92-31498
A comparison of three self-tuning control algorithms developed for the Bristol-Babcock controller
[DE92-014472] p 3814 N92-31499
Development of a computer model for polycrystalline thin-film CuInSe2 and CdTe solar cells
[DE92-001242] p 3846 N92-31526
Two long-term instrumental climatic data bases of the People's Republic of China
[DE92-010378] p 3851 N92-31527
World energy projection system: Model documentation
[DE92-014206] p 3847 N92-31594

Using neural networks in software repositories
[NASA-CR-190641] p 3885 N92-31597
GPS satellite orbit determination using pseudorange data: Experiments and results
[PB92-178870] p 3765 N92-31685
Some computational challenges of developing efficient parallel algorithms for data-dependent computations in thermal-hydraulics supercomputer applications
[DE92-011368] p 3878 N92-31703
Computer applications for engineering/structural analysis
[DE92-013070] p 3841 N92-31745
Configuration management and software measurement in the Ground Systems Development Environment (GSDE)
[NASA-CR-190716] p 3879 N92-31787
Numerical simulation of tulip flame dynamics
[DE92-008553] p 3782 N92-31805
The KRAKEN normal mode program
[AD-A252409] p 3892 N92-31818
Integrated computer systems in aircraft design and manufacture: Difficulties and implications
p 3746 N92-31864
Euler solver for arbitrary configurations: Further applications p 3750 N92-31888
ADIFOR: Fortran source translation for efficient derivatives
[DE92-016187] p 3879 N92-31899
Data reduction formulas for the 16-foot transonic tunnel: NASA Langley Research Center, revision 2
[NASA-TM-107646] p 3762 N92-31900
An integrated research program for the modeling, analysis and control of aerospace systems
[AD-A250199] p 3761 N92-31966
Navy Atmospheric Boundary Layer (NABL) model system: Software/Interface design document
[AD-A247903] p 3857 N92-31986
FEHMN 1.0: Finite element heat and mass transfer code
[DE92-013998] p 3825 N92-32008
CAVEAT: A computer code for fluid dynamics problems with large distortion and internal slip
[DE92-014078] p 3825 N92-32022
Validation of the Numerical Electro-magnetics Code (NEC) for antenna wire elements in proximity to Earth
[AD-A250507] p 3810 N92-32043
Fitting and prediction uncertainty for a software reliability model
[AD-A252173] p 3880 N92-32060
EWE: A computer model for ultrasonic inspection
[DE92-627145] p 3837 N92-32143
An installed nacelle design code using a multiblock Euler solver. Volume 1: Theory document
[NASA-CR-189652-VOL-1] p 3754 N92-32226
An installed nacelle design code using a multiblock Euler solver. Volume 2: User guide
[NASA-CR-189652-VOL-2] p 3754 N92-32228
Numerical simulation of geometric scale effects in cylindrical self-field MPD thrusters
[NASA-CR-189224] p 3772 N92-32239

COMPUTER STORAGE DEVICES
Ferroelectric thin films prepared by pulse laser deposition processing and characterization
[PB92-196088] p 3913 N92-32072

COMPUTER SYSTEMS DESIGN
Sources of unbounded priority inversions in real-time systems and a comparative study of possible solutions
[NASA-CR-190711] p 3875 N92-31486
An integrated research program for the modeling, analysis and control of aerospace systems
[AD-A250199] p 3761 N92-31966
Fault tolerant parallel computing in orthogonal shared-memory and related architectures
[AD-A250504] p 3883 N92-32040

COMPUTER SYSTEMS PERFORMANCE
Overview of integrated services digital network conformance testing
[PB92-181015] p 3881 N92-31365
Continuous time and discrete time hyperexponential model for dependability growth modeling
[LAAS-92002] p 3837 N92-31693
Specification and verification of secure concurrent and distributed software systems
[AD-A252477] p 3879 N92-31825
New directions in network flows
[AD-A250499] p 3880 N92-32039

COMPUTER SYSTEMS PROGRAMS
Configuration management and software measurement in the Ground Systems Development Environment (GSDE)
[NASA-CR-190716] p 3879 N92-31787
Fitting and prediction uncertainty for a software reliability model
[AD-A252173] p 3880 N92-32060

COMPUTER SYSTEMS SIMULATION
Simulation of a parallel processor based small tactical system
[AD-A245911] p 3882 N92-31443
Mission and Safety Critical (MASC) plans for the MASC Kernel simulation
[NASA-CR-190708] p 3875 N92-31487
Confidence interval estimation for output of discrete-event simulations using the Kalman filter
[AD-A248170] p 3880 N92-31991

COMPUTER TECHNIQUES
The vehicle routing problem: Some computational tests of savings method and its variations
[INPE-5361-RPQ/656] p 3886 N92-31241
Computer-aided modeling tools for forging process feasibility studies
[DE92-012116] p 3838 N92-31303
Next generation documents
[PB92-187103] p 3917 N92-31371
Using consistent subcuts for detecting stable properties
[NASA-CR-190443] p 3886 N92-31553
Using neural networks in software repositories
[NASA-CR-190641] p 3885 N92-31597
Computer applications for engineering/structural analysis
[DE92-013070] p 3841 N92-31745
Computer Aided Process Planning (CAPP): The user interface for the fabrication module of the rapid design system
[AD-A250095] p 3879 N92-31783
An automated computational method for barrier construction in single and two-target differential games
p 3749 N92-31882
New techniques in computational fluid dynamics: Algorithms, analysis, applications
[AD-A250498] p 3825 N92-32038
Fault tolerant parallel computing in orthogonal shared-memory and related architectures
[AD-A250504] p 3883 N92-32040

COMPUTER VISION
Detection of object edges in images containing cast shadows
[DE92-016092] p 3900 N92-31295
Neural network perception for mobile robot guidance
[AD-A249972] p 3884 N92-31511
Development of the aspect graph representation for use in R version
[AD-A247109] p 3876 N92-31573
Logarithmic retinae
[PB92-183649] p 3885 N92-31680
From perception to modelization in robotics using achromatic and chromatic cameras
[LAAS-91484] p 3901 N92-31692

COMPUTERIZED SIMULATION
Wavenumbers for currents on infinite- and finite-length wires in a chiral medium
[DE92-007565] p 3804 N92-31317
Oscillating-flow regenerator test rig: Woven screen and metal felt results
[NASA-CR-190689] p 3820 N92-31352
Methodology investigation final report: Automated real-time test scenario generation, phase 1
[AD-A250439] p 3884 N92-31395
A performance-based comparison of object-oriented simulation tools
[AD-A252125] p 3875 N92-31405
Application of Free-Air CO2 Enrichment (FACE) technology to a forest canopy: A simulation study
[DE92-013308] p 3851 N92-31422
Numerical simulation of precipitation scavenging and comparison with observation of prescribed forest fires
[DE92-013513] p 3851 N92-31423
Comparison of effects of copropagated and precomputed atmosphere profiles on Monte Carlo trajectory simulation
[NASA-TM-102600] p 3766 N92-31457
The investigation of bandwidth efficient coding and modulation techniques
[NASA-CR-190685] p 3806 N92-31468
Modular UNIX (trade name)-based Vulnerability Estimation Suite (MUVES) analyst's guide
[AD-A245322] p 3876 N92-31488
A surface definition code for turbine blade surfaces
[DE92-010574] p 3846 N92-31498
Computational simulation of intermingled-fiber hybrid composite behavior
[NASA-TM-105666] p 3774 N92-31506
Computer simulation of scattered ion and sputtered species effects in ion beam sputter-deposition of high temperature superconducting thin films
[DE92-015227] p 3909 N92-31546
Experimental and computer modeling studies of isotopically selective two-step laser photodissociation of small molecules
[DE92-011427] p 3894 N92-31606
Recent developments in the fundamentals of gas permeation in rubbery polymers
[AD-A249745] p 3794 N92-31624
Oxygen ordering and strain-related morphology in YBa2Cu(3-x)O7 systems
[DE92-014476] p 3909 N92-31627
Computer simulation of acoustic fluctuations due to finescale temperature perturbations measured by thermistor chain
[AD-A252709] p 3892 N92-31672
Logarithmic retinae
[PB92-183649] p 3885 N92-31680
ANTHEM simulational studies of the plasma opening switch
[DE92-015247] p 3815 N92-31681
Maximum likelihood estimation of fractional Brownian motion and Markov noise parameters
[AD-A249623] p 3890 N92-31686
Mathematical structures for qualitative calculus, a contribution to qualitative simulation
[LAAS-91475] p 3886 N92-31690
Simulation of diurnally varying downslope winds over Northern Utah
[AD-A250568] p 3861 N92-31714
A semiconductor bridge ignited gas generator
[DE92-014049] p 3781 N92-31748
A detector for stationary gas bubbles: Feasibility studies
[AD-A250135] p 3828 N92-31794
Numerical simulation of tulip flame dynamics
[DE92-008553] p 3782 N92-31805
Multimedia electronic mail: Standards and performance simulation
[AD-A250047] p 3808 N92-31809
Three-dimensional finite difference modeling of surface wave propagation across the Barents Shelf
[AD-A249865] p 3865 N92-31821
NAS (Numerical Aerodynamic Simulation Program) technical summaries, March 1989 - February 1990
[NASA-TM-107960] p 3926 N92-31852
Mathematical modeling and numerical simulation of the dynamics of flexible structures undergoing large overall motions
[AD-A250202] p 3761 N92-31967
Confidence interval estimation for output of discrete-event simulations using the Kalman filter
[AD-A248170] p 3880 N92-31991
FEHMN 1.0: Finite element heat and mass transfer code
[DE92-013998] p 3825 N92-32008
Theory for the CEBAF infrared and shipboard FELS
[AD-A252174] p 3832 N92-32061
Computer simulation of shading and blocking: Discussion of accuracy and recommendations
[DE91-002146] p 3849 N92-32110
Scaling of IFR propagation physics with beam/channel parameters
[DE92-015389] p 3900 N92-32123
EWE: A computer model for ultrasonic inspection
[DE92-627145] p 3837 N92-32143
Images simulation of sensors with large field of view from images of sensors with less field of view: The SSR/TM case
[INPE-5378-TDI/473] p 3845 N92-32220
Markovian fields as limits of Markov chains
[INPE-5395-PRE/1753] p 3889 N92-32225
Numerical simulation of geometric scale effects in cylindrical self-field MPD thrusters
[NASA-CR-189224] p 3772 N92-32239

COMPUTERS
Ferroelectric thin films prepared by pulse laser deposition processing and characterization
[PB92-196088] p 3913 N92-32072

CONCENTRATION (COMPOSITION)
Final report on DSA methods for monitoring alumina in aluminum reduction cells with cermet anodes
[DE92-013599] p 3813 N92-31440

CONCENTRATORS
Outdoor testing of advanced optical materials for solar thermal electric applications
[DE92-010567] p 3847 N92-31623
Advanced high efficiency concentrator cells
[DE92-010559] p 3848 N92-31893

CONCENTRIC CYLINDERS
Effects of fiber and interfacial layer architectures on the thermoplastic response of metal matrix composites
[NASA-TM-105802] p 3777 N92-32234

CONCRETES
Instabilities of damage and surface degradation mechanisms in brittle material structural systems
[AD-A250785] p 3842 N92-32168
Acoustic emission method applied to tests on concrete p 3842 N92-32206

CONCURRENT PROCESSING
Sources of unbounded priority inversions in real-time systems and a comparative study of possible solutions
[NASA-CR-190711] p 3875 N92-31486
Specification and verification of secure concurrent and distributed software systems
[AD-A252477] p 3879 N92-31825
CONDENSATES
A tumbling top-quark condensate model
[DE92-016194] p 3893 N92-31552
CONDENSATION
Condensation in a two-phase pool
[DE92-010048] p 3824 N92-31977
CONDENSERS (LIQUEFIERS)
Heat exchanger performance calculations for enhanced-tube condenser applications
[DE92-016603] p 3823 N92-31785
CONDENSING
Further studies in filmwise condensation of steam on horizontal finned tubes
[AD-A252705] p 3915 N92-31767
Condensation in a two-phase pool
[DE92-010048] p 3824 N92-31977
Laser-ablated copper condensation in helium
[DE92-016685] p 3789 N92-32004
CONDITIONING
Determination of the matrix conditioning indicator. Comparison of approximate methods
p 3887 N92-32210
CONDUCTING POLYMERS
Polymerization of conducting polymers confined to free surfaces: A comparison of the Langmuir-Blodgett polymerization of 3-alkyl pyrroles and 2-alkyl anilines
[AD-A250966] p 3798 N92-32194
CONDUCTION BANDS
Neutron radiation damage to silicon detectors
[ITN-92-85162] p 3897 N92-31958
CONDUCTIVE HEAT TRANSFER
Theory of anomalous transport in toroidal helical plasmas
[NIFS-140] p 3904 N92-31659
Towards understanding turbulent scalar mixing
[NASA-CR-4446] p 3826 N92-32242
CONFERENCES
National Conference on Integrated Resource Planning: Proceedings
[DE92-013573] p 3845 N92-31290
International Semiconductor Device Research Symposium (ISDRS-91)
[AD-A249348] p 3813 N92-31373
The sixteenth annual electronics manufacturing seminar proceedings
[AD-A247920] p 3814 N92-31461
Proceedings of the 4th Atlantic OCS Region Information Transfer Meeting
[PB92-177690] p 3864 N92-31630
Lamont-Doherty Geological Observatory
[PB92-185040] p 3856 N92-31636
Technology Integration Workshop: Selected papers
[PB92-158278] p 3923 N92-31643
Proceedings of the 2nd KUR symposium on hyperfine interactions
[DE92-789024] p 3895 N92-31728
Collection of papers of the 31st Israel Annual Conference on Aviation and Astronautics
[ITN-92-85124] p 3745 N92-31861
TABES 92: 8th Annual Technical and Business Exhibition and Symposium. Executive summaries and submitted papers p 3763 N92-32009
Non-convex problems in PDE: Equilibrium theory and dynamics
[AD-A250549] p 3887 N92-32081
Bringing Down the Barriers to Information Transfer
[AGARD-CP-505] p 3920 N92-32182
Computerized property data for engineering materials: An overview p 3922 N92-32191
Proceedings of the 53rd Symposium on Air Vehicle Mission Control and Management
[AGARD-AR-310] p 3889 N92-32229
CONFIDENCE LIMITS
Confidence interval estimation for output of discrete-event simulations using the Kalman filter
[AD-A248170] p 3880 N92-31991
Fitting and prediction uncertainty for a software reliability model
[AD-A252173] p 3880 N92-32060
CONFIGURATION MANAGEMENT
Configuration management and software measurement in the Ground Systems Development Environment (GSDE)
[NASA-CR-190716] p 3879 N92-31787
Development of a fault isolation system database manager
[AD-A248346] p 3916 N92-31992
CONFORMAL MAPPING
Plane stokes flow driven by capillarity on a free surface: Overview and status
[DE92-011469] p 3821 N92-31528
CONGRESSIONAL REPORTS
Report to the US Congress on minority small business and capital ownership development as required by the Business Opportunity Development Reform Act of 1988
[PB92-173681] p 3916 N92-31364
Annual report to the Congress, fiscal year 1991 (Office of Technology Assessment)
[PB92-166549] p 3922 N92-31599
CONICS
Analytic estimation of radiation effects in space using solid angles
[DE92-013282] p 3899 N92-31831
CONIFERS
Methods of assessing responses of trees, stands and ecosystems to air pollution
[PB92-180231] p 3853 N92-31648
CONSERVATION
Geometric theory of infinite dimensional dynamical systems
[AD-A252190] p 3915 N92-31585
CONSISTENCY
Quality Evaluation System (QUES), volume 1
[AD-A252679] p 3876 N92-31586
CONSTRAINTS
Signal location using generalized linear constraints
[AD-A249580] p 3805 N92-31376
CONSTRUCTION INDUSTRY
Total quality management: A management philosophy for providing high quality construction
[AD-A252743] p 3837 N92-32172
CONSTRUCTION MATERIALS
Computerized property data for engineering materials: An overview p 3922 N92-32191
CONTAMINANTS
Analysis of debris from Spacelab Space Life Sciences-1
[NASA-TM-103593] p 3765 N92-32148
CONTAMINATION
Laser decontamination: A new strategy for facility decommissioning
[DE92-014113] p 3831 N92-31775
Analysis of debris from Spacelab Space Life Sciences-1
[NASA-TM-103593] p 3765 N92-32148
CONTINENTAL SHELVES
Hydrographic and Acoustic Doppler Current Profiler (ADCP) data from the Farallones shelf and slope study
[AD-A250834] p 3864 N92-31495
CONTINUOUS RADIATION
Phase characteristics and time responses of unknown linear systems determined from measured CW amplitude data
[PB92-183722] p 3805 N92-31368
CONTINUUM MECHANICS
Mathematical problems in micromechanics and composite materials
[AD-A249584] p 3773 N92-31378
A differential CDM model for fatigue of unidirectional metal matrix composites
[NASA-TM-105726] p 3840 N92-31505
CONTINUUM MODELING
A differential CDM model for fatigue of unidirectional metal matrix composites
[NASA-TM-105726] p 3840 N92-31505
The mechanics of fractal damage
[AD-A250518] p 3776 N92-32075
CONTRACT MANAGEMENT
Small Business Innovation Research program solicitation. Closing date: July 21, 1992
[NASA-TM-107795] p 3916 N92-31253
CONTRACTORS
MHD Contractors' Review Meeting: Abstracts
[DE92-011549] p 3904 N92-31576
NASA programs --- nasa space programs
p 3765 N92-32238
CONTRACTS
Small Business Innovation Research program solicitation. Closing date: July 21, 1992
[NASA-TM-107795] p 3916 N92-31253
A dictionary of acquisition and contracting terms
[AD-A247053] p 3920 N92-31754
CONTRAST
Function of panel M pathways in primates
[AD-A250275] p 3871 N92-31758
CONTROL EQUIPMENT
High performance of copper pumped dye lasers
[DE92-011763] p 3832 N92-31902
Backlash control via redundant drives: An experimental verification
[DE92-016368] p 3835 N92-31929
Modeling and design of a closed kinematic chain robotic mechanism
[DE92-014777] p 3835 N92-32121
CONTROL RODS
Emissivity measurements in support of experiments on natural convection between a vertical cylinder and a surrounding array
[DE92-012321] p 3819 N92-31287
CONTROL SIMULATION
EHF SATCOM frequency hopping pattern generator: Proof of concept
[DREO-89-32] p 3811 N92-32231
CONTROL STABILITY
A simulation model of a single rotor helicopter
p 3746 N92-31865
CONTROL STICKS
Construction of a dual axis force reflection stick and test station
[AD-A250731] p 3803 N92-31890
CONTROL SYSTEMS DESIGN
A free-piston Stirling engine/linear alternator controls and load interaction test facility
[NASA-TM-105825] p 3845 N92-31262
Flutter suppression digital control law design and testing for the AFW wind-tunnel model
[NASA-TM-107652] p 3757 N92-31350
Studies in dynamic characterization and control of a flexible structure and optical beampath
[AD-A250555] p 3830 N92-31605
Design and analysis issues of integrated control systems for high-speed civil transports
[NASA-CR-186022] p 3761 N92-31656
Hydrogenerator design manual, chapter 8
[PB92-173707] p 3919 N92-31682
Torque linearizing hardware for the electric joint motors of a direct-drive robot
[DE92-012681] p 3816 N92-31718
Method and circuit for controlling the evolution time interval of a laser output pulse
[NASA-CASE-LAR-13772-1] p 3831 N92-31788
Modeling and design of a closed kinematic chain robotic mechanism
[DE92-014777] p 3835 N92-32121
A frequency hopping synthesizer controller for EHF SATCOM
[DREO-89-29] p 3811 N92-32232
A parameter optimization approach to controller partitioning for integrated flight/propulsion control application
[NASA-TM-105826] p 3761 N92-32241
CONTROL THEORY
Flutter suppression digital control law design and testing for the AFW wind-tunnel model
[NASA-TM-107652] p 3757 N92-31350
A novel control-guidance law for low-thrust orbit maneuver p 3747 N92-31874
CONTROL VALVES
Evaluation of proposed inservice testing procedures for check valves
[DE92-014502] p 3833 N92-31384
Performance tests of a fast-acting valve for the driver tubes of a large blast/thermal simulator
[AD-A250035] p 3835 N92-31807
CONTROLLABILITY
A simulation model of a single rotor helicopter
p 3746 N92-31865
CONTROLLED ATMOSPHERES
Controlled atmosphere soldering system
[DE92-012633] p 3802 N92-31580
CONTROLLED FUSION
Transient internal probe diagnostic
[AD-A247306] p 3903 N92-31459
Kernel optimum nearly-analytical discretization (KOND) method applied to parabolic equations KOND-P Scheme
[NIFS-118] p 3887 N92-32205
CONTROLLERS
Design and experimental validation of a flutter suppression controller for the active flexible wing
[NASA-TM-4381] p 3760 N92-31240
Spacecraft dynamics characterization and control system failure detection. Volume 3: Control system failure monitoring
[NASA-CR-190529] p 3884 N92-31254
Stability testing and analysis of a PMAD DC test bed for the Space Station Freedom
[NASA-TM-105846] p 3812 N92-31282
A comparison of three self-tuning control algorithms developed for the Bristol-Babcock controller
[DE92-014472] p 3814 N92-31499
An investigation of spinup dynamics of axial gyrostats using elliptic integrals and the method of averaging
[AD-A249728] p 3768 N92-31675
Backlash control via redundant drives: An experimental verification
[DE92-016368] p 3835 N92-31929

Design, analysis, and testing of the Phase 1 CSI Evolutionary Model erectable truss
[NASA-CR-4461] p 3767 N92-32100
Artificial neural network implementation of a near-ideal error prediction controller
[NASA-CR-190694] p 3880 N92-32122
A parameter optimization approach to controller partitioning for integrated flight/propulsion control application
[NASA-TM-105826] p 3761 N92-32241

CONVECTION
Emissivity measurements in support of experiments on natural convection between a vertical cylinder and a surrounding array
[DE92-012321] p 3819 N92-31287
Cloud-to-ground lightning characteristics in mesoscale convective systems
[AD-A250418] p 3858 N92-31493
Amending the w* velocity scale for surface layer, entrainment zone, and baroclinic shear in mixed Forced/Free turbulent convection
[AD-A250389] p 3859 N92-31540

CONVECTIVE HEAT TRANSFER
Natural convection immersion cooling of an array of vertically oriented heated protrusions in an enclosure filled with a dielectric liquid: Effects of enclosure width, Prandtl number and component orientation
[AD-A245884] p 3914 N92-31489

CONVERGENCE
The Swendsen-Wang dynamics in the simulation of the Ising model
[INPE-5394-PRE/1752] p 3874 N92-31348

CONVEXITY
Electromagnetic scattering by coated convex surfaces and wedges simulated by approximate boundary conditions
[NASA-CR-190540] p 3803 N92-31238
Non-convex problems in PDE: Equilibrium theory and dynamics
[AD-A250549] p 3887 N92-32081

COOLANTS
Polyalphaolefins: A new improved cost effective aircraft radar coolant
[AD-A250517] p 3796 N92-32045

COOLING
Natural convection immersion cooling of an array of vertically oriented heated protrusions in an enclosure filled with a dielectric liquid: Effects of enclosure width, Prandtl number and component orientation
[AD-A245884] p 3914 N92-31489
Desiccant cooling using unglazed transpired solar collectors
[DE92-010568] p 3849 N92-32112

COOLING FINS
The prediction of the performance of a microcircuit heat sink in the boiling mode
[AD-A250045] p 3812 N92-31355

COOLING SYSTEMS
A model for the interfacial shear in vertical, adiabatic, annular-mist flow
[DE92-013537] p 3820 N92-31424
Desiccant cooling using unglazed transpired solar collectors
[DE92-010568] p 3849 N92-32112
Thin polymer icemaker development and test program
[DE92-016941] p 3803 N92-32125

COORDINATES
A surface definition code for turbine blade surfaces
[DE92-010574] p 3846 N92-31498
Time simulation of flutter with large stiffness changes
[NASA-TM-107650] p 3758 N92-32111

COPOLYMERIZATION
Organic main-chain NLO polymers. 1: Copolymerization of bis(arylcarboxaldehyde) and bis(cyanoacetate) monomers via the Knoevenagel condensation
[AD-A250215] p 3802 N92-31826
Inorganic rings on carbon chains
[AD-A251043] p 3772 N92-31850

COPOLYMERS
Polymer blends, volume 1
[AD-A252112] p 3792 N92-31419
Novel chemically amplified dry-developing imaging materials for high resolution microlithography
[AD-A250085] p 3793 N92-31435
The photogeneration of polymeric amines: Synthesis and photocrosslinking of copolymers containing photoactive carbamate pendant groups
[AD-A250086] p 3793 N92-31436
Imide/arylene ether copolymers
[NASA-CASE-LAR-14159-1-CU] p 3794 N92-31792

COPPER
Electronic and total energy properties of ternary and quaternary semiconductor compounds, alloys, and superlattices: Theoretical study of Cu/graphite bonding
[NASA-CR-190691] p 3772 N92-31266
The synthesis and characterization of new copper coordination complexes containing an asymmetric coordinating chelate ligand: Application to enzyme active site modeling
[DE92-011532] p 3786 N92-31391
Energetics, bonding mechanism and electronic structure of metal/ceramic interfaces
[DE92-013401] p 3775 N92-31806
The crystal growth and characterization of the solid solutions (ZnS)(1-x)(CuMS2)(x)
[AD-A248029] p 3911 N92-31819
High performance of copper pumped dye lasers
[DE92-011763] p 3832 N92-31902
Laser-ablated copper condensation in helium
[DE92-016685] p 3789 N92-32004

COPPER ALLOYS
Radiation-induced crystalline-to-amorphous transition in intermetallic compounds of the Cu-Ti alloy system
[DE92-010276] p 3787 N92-31575
A study of the microstructural basis for the strength and toughness properties of water-quenched and air-cooled HSLA-100, HSLA-100 with increased copper, and a ULCB steel
[AD-A245955] p 3789 N92-32052

COPPER OXIDES
Oxygen ordering and strain-related morphology in YBa2Cu(3-x)O7 systems
[DE92-014476] p 3909 N92-31627

COPPER SELENIDES
Development of a computer model for polycrystalline thin-film CuInSe2 and CdTe solar cells
[DE92-001242] p 3846 N92-31526

CORIOLIS EFFECT
Steady-state and transient modeling of tracer and nutrient distributions in the global ocean
[DE92-011805] p 3864 N92-31572

CORNEA
A biological model of the effects of toxic substances
[AD-A247138] p 3867 N92-31980

CORRECTION
Motion model for the correction of point source distortion in radiographs of honeycomb
[DREP-88-14] p 3777 N92-32215

CORRELATION
Lattice gaugefixing and other optics in lattice gauge theory
[DE92-016958] p 3901 N92-31737
Correlation from randomness: Quantitative analysis of sputtered graphite surfaces using the scanning tunneling microscope
[AD-A252420] p 3783 N92-31820

CORRELATION DETECTION
Problems with interleaved digitizers
[DE92-013369] p 3881 N92-32150

CORROSION
Corrosion behavior of squeeze cast aluminum metal matrix composites
[AD-A250486] p 3774 N92-31382
Surface chemistry of MoS2 lubricant films: Effects of high humidity storage on sputtered films
[DE92-015392] p 3794 N92-31631
Deterministic analysis of processes at corroding metal surfaces and the study of electrochemical noise in these systems
[DE92-016286] p 3788 N92-31733
Aging fleet: Maintaining airworthiness p 3745 N92-31862

CORROSION PREVENTION
Aging fleet: Maintaining airworthiness p 3745 N92-31862
Geothermal materials development
[DE92-016940] p 3849 N92-32124

CORROSION RESISTANCE
The preparation of (Al2O3)x(SiO2)y thin films using (Al(OSiEt3))2 as a single source precursor
[AD-A250142] p 3788 N92-31796
Oxidation/sulfidation behavior of Fe-Cr alloys: A reactive-element effect
[DE92-016172] p 3789 N92-31924
Materials for geothermal production
[DE92-014691] p 3849 N92-32118

COSMIC DUST
A characterization of the hot infrared background: The infrared cirrus, zodiacal dust bands, and solar system dust trails
[PL-TR-91-2065] p 3924 N92-32142

COSMIC RAYS
Relating space radiation environments to risk estimates
[DE92-010256] p 3926 N92-31756

COSMOLOGY
Participation in high energy physics. Task C: Particle physics and cosmology
[DE92-016290] p 3924 N92-31713

COST ANALYSIS
The determination of operational and support requirements and costs during the conceptual design of space systems
[NASA-CR-190626] p 3766 N92-31260
Energy conservation: The main factor for reducing greenhouse gas emissions in the former Soviet Union
[DE92-012355] p 3852 N92-31574
Fitting and prediction uncertainty for a software reliability model
[AD-A252173] p 3880 N92-32060

COST EFFECTIVENESS
Research and development of advanced nickel-iron batteries for electric vehicle propulsion
[DE92-014099] p 3817 N92-31834
TABES 92: 8th Annual Technical and Business Exhibition and Symposium. Executive summaries and submitted papers p 3763 N92-32009
Polyalphaolefins: A new improved cost effective aircraft radar coolant
[AD-A250517] p 3796 N92-32045

COST REDUCTION
Research and development of advanced nickel-iron batteries for electric vehicle propulsion
[DE92-014099] p 3817 N92-31834

COSTS
Aviation noise: Costs of phasing out noisy aircraft
[GAO/RCED-91-128] p 3891 N92-31454
Building an educational robot arm for under $1,000
[AD-A247499] p 3833 N92-31460
Sequential estimation of optimal age replacement policies when distribution of lifetimes is phase type
[AD-A249020] p 3836 N92-31479
Intelligent gateways p 3921 N92-32184

COUETTE FLOW
Sensitivity analysis of hydrodynamic stability operators
[NASA-CR-189683] p 3822 N92-31535

COUNTER ROTATION
High speed turboprop aeroacoustic study (counterrotation). Volume 2: Computer programs
[NASA-CR-185242] p 3891 N92-31248

COUNTERFLOW
Transport and evaporation effects in counterflow spray diffusion flames p 3749 N92-31884

COUPLINGS
Metallization of ferrite ceramic couplings
[DE92-016573] p 3789 N92-32032

COVARIANCE
True covariance simulation of the EUVE (extreme ultra violet explorer) update filter p 3748 N92-31878

CRACK PROPAGATION
Analysis and prediction of Multiple-Site Damage (MSD) fatigue crack growth
[NASA-TP-3231] p 3838 N92-31279
The 3-D analysis and verification of fracture growth mechanisms in fiber-reinforced ceramic composies
[AD-A250893] p 3773 N92-31305
Effect of fracture surface interference on shear crack growth
[DE92-011431] p 3839 N92-31389
Finite-element analyses and fracture simulation in thin-sheet aluminum alloy
[NASA-TM-107662] p 3839 N92-31504
Instabilities of damage and surface degradation mechanisms in brittle material structural systems
[AD-A250785] p 3842 N92-32168

CRACK TIPS
Applications of FEM and BEM in two-dimensional fracture mechanics problems
[NASA-TP-3277] p 3838 N92-31280
Finite-element analyses and fracture simulation in thin-sheet aluminum alloy
[NASA-TM-107662] p 3839 N92-31504

CRACKING (FRACTURING)
Cyclic hot firing results of tungsten-wire-reinforced, copper-lined thrust chambers
[NASA-TM-4214] p 3769 N92-31249
Analysis and prediction of Multiple-Site Damage (MSD) fatigue crack growth
[NASA-TP-3231] p 3838 N92-31279
Fatigue in single crystal nickel superalloys
[AD-A250068] p 3786 N92-31360

CRACKS
Aging fleet: Maintaining airworthiness p 3745 N92-31862

CRAY COMPUTERS
NAS (Numerical Aerodynamic Simulation Program) technical summaries, March 1989 - February 1990
[NASA-TM-107960] p 3926 N92-31852

CREEP PROPERTIES
Fatigue in single crystal nickel superalloys
[AD-A250068] p 3786 N92-31360

CREEP STRENGTH
The preparation of (Al2O3)x(SiO2)y thin films using (Al(OSiEt3))2 as a single source precursor
[AD-A250142] p 3788 N92-31796

CRESOLS
Synthesis of cresols and xylenols from phenol and methanol
[DE91-002141] p 3785 N92-32093
CREWS
One thousand days non-stop at sea: Lessons for a mission to Mars
[TABES PAPER 92-462] p 3764 N92-32020
Noninvasive ambulatory assessment of cardiac function and myocardial ischemia in healthy subjects exposed to carbon monoxide
[AD-A252264] p 3870 N92-32107
CROSS CORRELATION
Readily implemented enhanced sinusoid detection in noise
[DE92-011359] p 3806 N92-31449
CROSS FLOW
The three-dimensional stability of the Foeppl vortices
p 3750 N92-31889
A computational examination of directional stability for smooth and chined forebodies at high-alpha
[NASA-CR-4465] p 3753 N92-32114
CROSS POLARIZATION
A robust algorithm for isotropic reconstruction of magic-angle spinning solid-state NMR spectra
[AD-A249610] p 3874 N92-31379
Analysis of random induced cross polarization
[AD-A249773] p 3806 N92-31569
CROSSED FIELDS
Evidence of stochastic diffusion across a cross-field sheath due to Kelvin-Helmholtz vortices
[AD-A247847] p 3907 N92-31983
CROSSLINKING
Organic main-chain NLO polymers. 1: Copolymerization of bis(arylcarboxaldehyde) and bis(cyanoacetate) monomers via the Knoevenagel condensation
[AD-A250215] p 3802 N92-31826
Nature of short Li-H-C contact interactions in organolithium compounds and its implication
[AD-A250992] p 3898 N92-32024
CRYOGENIC EQUIPMENT
Orbit transfer vehicle engine technology program. Task B-6 high speed turbopump bearings
[NASA-CR-189230] p 3835 N92-31892
CRYOGENIC TEMPERATURE
Cryogenic 4.4 MN mechanical test system for large scale tests of composite support struts
[PB92-181148] p 3774 N92-31609
CRYOGENIC WIND TUNNELS
High Reynolds number test of the Boeing TR77 airfoil in the Langley 0.3-meter transonic cryogenic tunnel
[NASA-TM-4189] p 3750 N92-31246
CRYOGENICS
Orbit transfer vehicle engine technology program. Task B-6 high speed turbopump bearings
[NASA-CR-189230] p 3835 N92-31892
Aluminum tunnel junction detector operation in an adiabatic demagnetization refrigerator
[DE92-013441] p 3913 N92-32166
CRYOSTATS
Fusion with highly spin polarized HD and D(2)
[DE92-017030] p 3898 N92-32007
CRYSTAL DEFECTS
Substrate surface effects on the properties of sputter-deposited and laser-irradiated films
[DE92-013850] p 3795 N92-31917
Neutron radiation damage to silicon detectors
[ITN-92-85162] p 3897 N92-31958
CRYSTAL DISLOCATIONS
Movement of dislocations in quartz
[AD-A250527] p 3913 N92-32078
CRYSTAL FILTERS
Wavelength-tunable liquid crystal imaging filters for remote sensing from geosynchronous platforms
[NASA-CR-190698] p 3845 N92-32223
CRYSTAL GROWTH
Surface structures and surface processes of ceramics with atomic resolutions: A study by scanning tunneling microscopy
[AD-A249581] p 3792 N92-31377
Development of high efficiency nonlinear optical materials
[AD-A249612] p 3901 N92-31380
Optimized photorefractive barium titanate
[AD-A250089] p 3908 N92-31438
The crystal growth and characterization of the solid solutions (ZnS)(1-x)(CuMS2)(x)
[AD-A248029] p 3911 N92-31819
He atom-surface scattering: Surface dynamics of insulators, overlayers and crystal growth
[DE92-011810] p 3911 N92-31914
Mechanics of thin films
[AD-A247848] p 3912 N92-31984
Single crystal growth optimization of magnesium-doped lithium niobate
[AD-A250781] p 3914 N92-32207
CRYSTAL LATTICES
Oxygen ordering and strain-related morphology in YBa2Cu(3-x)O7 systems
[DE92-014476] p 3909 N92-31627
US-Japan seminar on magnetic multilayered structures: Proceedings
[AD-A252440] p 3910 N92-31666
Impurity effects on the magnetic ordering in chromium
[DE92-016165] p 3789 N92-31898
CRYSTAL OPTICS
Optimized photorefractive barium titanate
[AD-A250089] p 3908 N92-31438
Single crystal growth optimization of magnesium-doped lithium niobate
[AD-A250781] p 3914 N92-32207
CRYSTAL STRUCTURE
The synthesis and characterization of new copper coordination complexes containing an asymmetric coordinating chelate ligand: Application to enzyme active site modeling
[DE92-011532] p 3786 N92-31391
Ceramic surfaces and sintering
[DE92-011570] p 3793 N92-31538
Oxygen ordering and strain-related morphology in YBa2Cu(3-x)O7 systems
[DE92-014476] p 3909 N92-31627
CRYSTAL SURFACES
Imaging and spectrometry of bulk crystal surfaces and surface dynamical processes at high temperatures
[DE92-015235] p 3913 N92-32085
Supersonic pyrolysis jets for diamond film deposition
[AD-A251125] p 3798 N92-32198
CRYSTALLINITY
Tetragonal zirconia ceramics in ZrO2-CeO2 system (Ce-TZP): Preparation, characterization and mechanical properties
[INPE-5372-PRE/1746] p 3798 N92-32199
CRYSTALLIZATION
Stress and phase transformation phenomena in oxide films
[DE92-014702] p 3910 N92-31665
CRYSTALLOGRAPHY
Tris-triphenylsiloxy compounds of aluminum
[AD-A250141] p 3788 N92-31795
CRYSTALS
The role of metal structure in determining solvent orientation at the electrode/solution interface
[AD-A249751] p 3893 N92-31328
Imaging and spectrometry of bulk crystal surfaces and surface dynamical processes at high temperatures
[DE92-015235] p 3913 N92-32085
CUES
Acquisition and production of skilled behavior in dynamic decision-making tasks
[NASA-CR-190614] p 3870 N92-31341
In-flight decision making by high time and low time pilots during instrument operations
[AD-A249990] p 3871 N92-31392
CULTURE TECHNIQUES
Cellular localization of infrared sources
[AD-A249795] p 3866 N92-31302
Hollow fiber clinostat for simulating microgravity in cell culture
[NASA-CASE-MFS-28370-1] p 3828 N92-31790
A biological model of the effects of toxic substances
[AD-A247138] p 3867 N92-31980
CURING
Optical fiber sensors for organic matrix composite material cure monitoring
[AD-A247114] p 3776 N92-31979
CURRENT DENSITY
Recent advances in high-temperature superconductor wire fabrication and applications development
[DE92-016634] p 3912 N92-31955
CURVE FITTING
Non-geothermal optics study of wave propagation
[DE92-011806] p 3903 N92-31494
CURVES
Development of the aspect graph representation for use in R version
[AD-A247109] p 3876 N92-31573
CUSHIONS
Vertical impact tests of humans and anthropomorphic manikins
[AD-A245866] p 3872 N92-31458
CUTTING
Cutting treatment by drilling of fiber bound synthetic materials
[MBB-UD-0609-91-PUB] p 3774 N92-31716
Titanium carbon nitride coating
[DE92-013158] p 3777 N92-32135
CYCLIC HYDROCARBONS
Selective nitrations: The laser-induced nitration of three cycloalkanes, 1
[AD-A249942] p 3800 N92-31800
CYCLIC LOADS
Research into improving the durability of the hot section in the aircraft turbine engine
[AD-A250342] p 3759 N92-31439
CYCLOBUTANE
Selective nitrations: The laser-induced nitration of three cycloalkanes, 1
[AD-A249942] p 3800 N92-31800
CYCLOGENESIS
A diagnostic study of rapidly developing cyclones using surface-based Q vectors
[AD-A246993] p 3862 N92-31978
CYCLONES
A diagnostic study of rapidly developing cyclones using surface-based Q vectors
[AD-A246993] p 3862 N92-31978
CYCLOPROPANE
Selective nitrations: The laser-induced nitration of three cycloalkanes, 1
[AD-A249942] p 3800 N92-31800
CYCLOTRON RESONANCE
Gallium arsenide clusters and their interfacial physics and chemistry
[AD-A249565] p 3907 N92-31375
Millimeter wave free electron laser amplifiers: Experiments and designs
[DE92-011813] p 3832 N92-31935
An improved ion guide for external ion injection in glow discharge-Fourier transform ion cyclotron resonance (GD-FTICR) mass spectrometry
[AD-A250944] p 3900 N92-32170
CYCLOTRON RESONANCE DEVICES
Fusion development and technology
[DE92-014352] p 3904 N92-31545
Compact millimeter-wave devices: Dielectric loaded carm, high voltage carm, slow wave crm and high harmonic gyrotron
[AD-A250497] p 3809 N92-31944
CYCLOTRONS
An improved ion guide for external ion injection in glow discharge-Fourier transform ion cyclotron resonance (GD-FTICR) mass spectrometry
[AD-A250944] p 3900 N92-32170
CYLINDRICAL BODIES
Emissivity measurements in support of experiments on natural convection between a vertical cylinder and a surrounding array
[DE92-012321] p 3819 N92-31287
A generalized plane-strain elastic stress solution for a multiorthotropic-layered cylinder
[AD-A250487] p 3838 N92-31331
CYLINDRICAL SHELLS
Optimal design of geodesically stiffened composite cylindrical shells
[NASA-CR-190706] p 3842 N92-32235

D

DAMAGE
Analysis and prediction of Multiple-Site Damage (MSD) fatigue crack growth
[NASA-TP-3231] p 3838 N92-31279
Evaluation of proposed inservice testing procedures for check valves
[DE92-014502] p 3833 N92-31384
A differential CDM model for fatigue of unidirectional metal matrix composites
[NASA-TM-105726] p 3840 N92-31505
A study of the effect of hydrocarbon structure on the induction of male rat nephropathy and metabolite structure
[AD-A252192] p 3867 N92-31590
Using transfer functions as a method for predicting lightning effects on munitions storage bunkers
[DE92-012627] p 3861 N92-31709
Demonstrated survivability of a high temperature optical fiber cable on a 1500 pound thrust rocket chamber
[NASA-TM-105835] p 3801 N92-32230
DAMAGE ASSESSMENT
A preliminary study in the use of phase demodulation techniques for the analysis of gear vibration data
[NRC-32083] p 3833 N92-31469
Development of an electrochemical method for field testing of protective coatings
[AD-A245872] p 3793 N92-31473
Modular UNIX (trade name)-based Vulnerability Estimation Suite (MUVES) analyst's guide
[AD-A245322] p 3876 N92-31488
The mechanics of fractal damage
[AD-A250518] p 3776 N92-32075
Instabilities of damage and surface degradation mechanisms in brittle material structural systems
[AD-A250785] p 3842 N92-32168

DAMPING
Calculations of emittance and damping time effects in the SLC damping rings
[DE92-012420] p 3900 N92-32133
DARK MATTER
Participation in high energy physics. Task C: Particle physics and cosmology
[DE92-016290] p 3924 N92-31713
DATA ACQUISITION
A free-piston Stirling engine/linear alternator controls and load interaction test facility
[NASA-TM-105825] p 3845 N92-31262
Combined Release and Radiation Effects Satellite (CRRES) experiments data collection, analysis, and publication
[NASA-CR-184361] p 3856 N92-31551
Quality Evaluation System (QUES), volume 1
[AD-A252679] p 3876 N92-31586
Real time analysis of tokamak discharge parameters
[DE92-011394] p 3904 N92-31616
Hydrographic observations from the US/PRC cooperative program in the western equatorial Pacific Ocean: Cruises 5-8
[PB92-177054] p 3865 N92-31644
Real-time statistical quality control and ARM
[DE92-015253] p 3837 N92-31657
The 193-pixel, three-dimensional capacitance imaging system
[DE92-001253] p 3919 N92-31731
Comprehensive Aerological Reference Data Set (CARDS)
[DE92-016469] p 3862 N92-31734
Artificial intelligence in Training (AIT)
[AD-A250145] p 3885 N92-31811
Development of gamma ray imaging cameras
[DE92-015305] p 3828 N92-31919
Optical fiber sensors for organic matrix composite material cure monitoring
[AD-A247114] p 3776 N92-31979
A penetration mechanics database
[AD-A246351] p 3767 N92-31997
Probabilistic analysis of twenty-four hour weather data for Warsaw
[AD-A247290] p 3863 N92-32097
Space constancy on video display terminals
[AD-A247290] p 3872 N92-32105
International mathematics and science assessments: What have we learned
[PB92-183599] p 3916 N92-32160
Ground and flight calibration assessment of HiRAP accelerometer data from missions STS-35 and STS-40
[NASA-TM-107602] p 3769 N92-32204
A coordinated study of a storm system over the South American continent
[INPE-5388-TDI/477] p 3863 N92-32212
DATA BASE MANAGEMENT SYSTEMS
FEDIX: The on-line database retrieval service of government information for colleges, universities, and other organizations
[DE92-012384] p 3917 N92-31288
Ariel database rule system project
[AD-A250443] p 3917 N92-31396
STI handbook: Guidelines for producing, using, and managing scientific and technical information in the Department of the Navy. A handbook for Navy scientists and engineers on the use of scientific and technical information
[AD-A252439] p 3918 N92-31482
Two long-term instrumental climatic data bases of the People's Republic of China
[DE92-010378] p 3851 N92-31527
Oracle and the end-user: Practical implementation of applications in a multi-user, multi-platform environment
[DE92-015223] p 3877 N92-31654
Photon and electron data bases and their use in radiation transport calculations
[DE92-011458] p 3895 N92-31705
Comprehensive Aerological Reference Data Set (CARDS)
[DE92-016469] p 3862 N92-31734
A model for extending the behavior of annotations
[DE92-011731] p 3920 N92-31934
Development of a fault isolation system database manager
[AD-A248346] p 3916 N92-31992
Database explorer: Large scale database application
[AD-A252183] p 3920 N92-32049
Directory of IAEA databases
[DE92-628395] p 3920 N92-32058
DATA BASES
The determination of operational and support requirements and costs during the conceptual design of space systems
[NASA-CR-190626] p 3766 N92-31260
Type evolution and instance adaptation
[AD-A248435] p 3917 N92-31285
Ariel database rule system project
[AD-A250443] p 3917 N92-31396
Implementing relational operations in an object-oriented database
[AD-A249332] p 3918 N92-31450
Deep-tow acoustics/geophysics system compressional velocity database
[AD-A252700] p 3918 N92-31467
Non-geothermal optics study of wave propagation
[DE92-011806] p 3903 N92-31494
Time domain regional discriminants
[AD-A249949] p 3855 N92-31509
Two long-term instrumental climatic data bases of the People's Republic of China
[DE92-010378] p 3851 N92-31527
A proposed group management scheme for XTP multicast
[NASA-CR-190633] p 3916 N92-31547
Objects used to implement intelligent databases
[DE92-013098] p 3919 N92-31581
Quality Evaluation System (QUES), volume 1
[AD-A252679] p 3876 N92-31586
Technology Integration Workshop: Selected papers
[PB92-158278] p 3923 N92-31643
Hyper-NPSNET: A virtual world with an integrated 3-D hypertext
[AD-A252726] p 3878 N92-31676
Photon and electron data bases and their use in radiation transport calculations
[DE92-011458] p 3895 N92-31705
Correspondence dictionary from free English term to INIS descriptors
[DE92-782192] p 3920 N92-31859
Marine structural steel toughness data bank, volume 1
[AD-A247923] p 3789 N92-31987
A penetration mechanics database
[AD-A246351] p 3767 N92-31997
Composite failure analysis handbook. Volume 1: Program review
[AD-A250520] p 3776 N92-32047
Composite failure analysis handbook. Volume 2: Technical handbook. Part 1: Procedures and techniques
[AD-A250521] p 3776 N92-32048
Database explorer: Large scale database application
[AD-A252183] p 3920 N92-32049
Directory of IAEA databases
[DE92-628395] p 3920 N92-32058
Local Area Networks (LAN) p 3874 N92-32183
Intelligent gateways p 3921 N92-32184
Use of expert systems as user interfaces in information retrieval p 3921 N92-32185
Search strategies in natural language p 3921 N92-32186
Automated input into databases: OCR and descriptive cataloguing p 3921 N92-32189
Computerized property data for engineering materials: An overview p 3922 N92-32191
Facilitating the transfer of scientific and technical information with scientific and technical numeric databases p 3922 N92-32192
DATA COMPRESSION
Compression of digitized map images
[AD-A250707] p 3843 N92-31323
Data compression techniques p 3922 N92-32190
DATA CONVERTERS
Optical interconnects in the computer environment
[AD-D015235] p 3873 N92-31269
DATA FLOW ANALYSIS
Optical interconnects in the computer environment
[AD-D015235] p 3873 N92-31269
Towards a complete hierarchy of compositional dataflow models
[RUU-CS-91-45] p 3807 N92-31715
DATA INTEGRATION
Meteorological data, new series A monographs. Volume 6, no. 2: Case study on the congruence of precipitation data from SYNOP-MODELL and Meteosat data
[ETN-92-91694] p 3861 N92-31710
DATA LINKS
Design and development of minilink video: A fiber-optic coupled video system
[AD-A249945] p 3808 N92-31801
DATA MANAGEMENT
Optical interconnects in the computer environment
[AD-D015235] p 3873 N92-31269
DATA PROCESSING
Optical interconnects in the computer environment
[AD-D015235] p 3873 N92-31269
Comparison of results: Technische Univ., Delft-Organisatie voor Toegepast Natuurwetenschappelijk Onderzoek expert judgement study of dispersion-deposition
[REPT-92-11] p 3856 N92-31522
A proposed group management scheme for XTP multicast
[NASA-CR-190633] p 3916 N92-31547
A data processing module for acoustic Doppler current meters
[AD-A250901] p 3891 N92-31563
Hyper-NPSNET: A virtual world with an integrated 3-D hypertext
[AD-A252726] p 3878 N92-31676
Optimum data analysis procedures for Titan 4 and Space Shuttle payload acoustic measurements during lift-off
[NASA-CR-190479] p 3892 N92-32178
Facilitating the transfer of scientific and technical information with scientific and technical numeric databases p 3922 N92-32192
DATA PROCESSING TERMINALS
Space constancy on video display terminals
[AD-A247290] p 3872 N92-32105
DATA REDUCTION
Further studies in filmwise condensation of steam on horizontal finned tubes
[AD-A252705] p 3915 N92-31767
Data reduction formulas for the 16-foot transonic tunnel: NASA Langley Research Center, revision 2
[NASA-TM-107646] p 3762 N92-31900
Mission description and in-flight operations of ERBE instruments on ERBS, NOAA 9, and NOAA 10 spacecraft
[NASA-RP-1279] p 3844 N92-32127
DATA RETRIEVAL
Automated payload experiment tool feasibility study
[NASA-CR-184256] p 3883 N92-31835
Database explorer: Large scale database application
[AD-A252183] p 3920 N92-32049
DATA STORAGE
Implementing relational operations in an object-oriented database
[AD-A249332] p 3918 N92-31450
Automated payload experiment tool feasibility study
[NASA-CR-184256] p 3883 N92-31835
DATA STRUCTURES
Ariel database rule system project
[AD-A250443] p 3917 N92-31396
Objects used to implement intelligent databases
[DE92-013098] p 3919 N92-31581
The multicomputer toolbox: Scalable parallel libraries for large-scale concurrent applications
[DE92-008068] p 3882 N92-31740
PDDP: Data-driven parallelism and shared memory
[DE92-008073] p 3883 N92-31741
The Matrix Editor for symbolic Jacobians in ALPAL
[DE92-008076] p 3878 N92-31742
The data structure accelerator architecture
[AD-A250968] p 3883 N92-32152
DATA SYSTEMS
RCRIS data element dictionary, version 3.0.0: Data tape documentation
[PB92-145515] p 3918 N92-31398
Photon and electron data bases and their use in radiation transport calculations
[DE92-011458] p 3895 N92-31705
DATA TRANSFER (COMPUTERS)
A proposed group management scheme for XTP multicast
[NASA-CR-190633] p 3916 N92-31547
Design and automated manufacturing p 3746 N92-31866
DATA TRANSMISSION
Data parallel programming
[DE92-013981] p 3882 N92-31466
The investigation of bandwidth efficient coding and modulation techniques
[NASA-CR-190685] p 3806 N92-31468
A proposed group management scheme for XTP multicast
[NASA-CR-190633] p 3916 N92-31547
Enhancing GRASS data communication with videographic technology
[DE92-014852] p 3919 N92-31596
Bringing Down the Barriers to Information Transfer
[AGARD-CP-505] p 3920 N92-32182
Data compression techniques p 3922 N92-32190
DAYTIME
A sensitivity study of daytime visibility determination with the horizon scanning imager
[SIO-91-15] p 3902 N92-32144
DEBRIS
Analysis of debris from Spacelab Space Life Sciences-1
[NASA-TM-103593] p 3765 N92-32148
DECELERATION
Vertical impact tests of humans and anthropomorphic manikins
[AD-A245866] p 3872 N92-31458
DECISION MAKING
Acquisition and production of skilled behavior in dynamic decision-making tasks
[NASA-CR-190614] p 3870 N92-31341

In-flight decision making by high time and low time pilots during instrument operations
[AD-A249990] p 3871 N92-31392
Simulation of a parallel processor based small tactical system
[AD-A245911] p 3882 N92-31443
Probability-based inference in a domain of proportional reasoning tasks
[AD-A247304] p 3871 N92-31444
Combining expert probabilistic weather forecasts: Results of post-hoc analyses of the Zierikzee experiment
[REPT-91-101] p 3859 N92-31521
Comparison of results: Technische Univ., Delft-Organisatie voor Toegepast Natuurwetenschappelijk Onderzoek expert judgement study of dispersion-deposition
[REPT-92-11] p 3856 N92-31522
Research and development of methods and tools for achieving and maintaining consensus processes in the face of change within and among government oversight agencies, volume 1
[DE92-014179] p 3852 N92-31592
Forms of memory for representation of visual objects
[AD-A250056] p 3871 N92-31779
Decision-making guide for the proposed Coast Guard differential global positioning system
[AD-A246046] p 3756 N92-32054
The impact of cognitive feedback on the performance of intelligence analysts
[AD-A252176] p 3871 N92-32063

DECISION THEORY
Heuristic sampling on DAGs
[DE92-017359] p 3917 N92-32037

DECODERS
ADIFOR: Automatic differentiation in a source translator environment
[DE92-016185] p 3886 N92-31311

DECODING
Optical interconnects in the computer environment
[AD-D015235] p 3873 N92-31269

DECOMMISSIONING
Laser decontamination: A new strategy for facility decommissioning
[DE92-014113] p 3831 N92-31775

DECOMPOSITION
The pathways and dynamics of molecular decomposition
[AD-A249627] p 3893 N92-31463
A task adaptive parallel graphics rendering algorithm
[DE92-008062] p 3878 N92-31739
Decomposition studies of triisopropylantimony and triallylantimony
[AD-A250671] p 3796 N92-31968
The hierarchical spatial decomposition of three-dimensional particle-in-cell plasma simulations on MIMD distributed memory multiprocessors
[DE92-016802] p 3883 N92-32034
Remote Data Transfer (RDT): An interprocess data transfer method for distributed environments
[AD-A250859] p 3920 N92-32102

DECONTAMINATION
EnviroTRADE: Its role in the cleanup of the environment
[DE92-013691] p 3851 N92-31427
Laser decontamination: A new strategy for facility decommissioning
[DE92-014113] p 3831 N92-31775

DEEP SPACE NETWORK
Mission and Safety Critical (MASC) plans for the MASC Kernel simulation
[NASA-CR-190708] p 3875 N92-31487
RL-34 ring laser gyro laboratory evaluation for the Deep Space Network antenna application
[NASA-CR-190481] p 3829 N92-32128

DEFENSE PROGRAM
Facilitating the transfer of scientific and technical information with scientific and technical numeric databases p 3922 N92-32192

DEFINITION
Type evolution and instance adaptation
[AD-A248435] p 3917 N92-31285
A dictionary of acquisition and contracting terms
[AD-A247053] p 3920 N92-31754
Correspondence dictionary from free English term to INIS descriptors
[DE92-782192] p 3920 N92-31859

DEFLECTION
Electrically-induced stresses and deflection in multiple plates
[DE92-012303] p 3841 N92-31844

DEFORMATION
A finite element procedure for analysis of laminated composite plates
[AD-A250902] p 3773 N92-31307

DEGRADATION
Radiolytic gas production in the alpha particle degradation of plastics
[DE92-011846] p 3795 N92-31938
Instabilities of damage and surface degradation mechanisms in brittle material structural systems
[AD-A250785] p 3842 N92-32168

DEGREES OF FREEDOM
Dynamic modeling and modal analysis of an air-to-air missile
[AD-A245957] p 3758 N92-32053

DEHYDRATION
Body water homeostasis and human performance in high heat environments: Fluid hydration recommendations for Operation Desert Storm
[AD-A249772] p 3868 N92-31492

DEICING
Digital analysis of wind tunnel imagery to measure fluid thickness
[NASA-CR-189234] p 3762 N92-31252
Analysis of three icing test flights reaching the aircraft-referred icing degree of severe
[ESA-TT-1254] p 3755 N92-31943

DELAMINATING
A finite element procedure for analysis of laminated composite plates
[AD-A250902] p 3773 N92-31307
Role of interfaces and interphases in the evolution mechanics of material systems
[AD-A250410] p 3774 N92-31604

DELAY
Design and specification of a high speed transport protocol
[AD-A248323] p 3804 N92-31284

DEMAGNETIZATION
Aluminum tunnel junction detector operation in an adiabatic demagnetization refrigerator
[DE92-013441] p 3913 N92-32166

DEMODULATION
A preliminary study in the use of phase demodulation techniques for the analysis of gear vibration data
[NRC-32083] p 3833 N92-31469
Beam position monitor electronics using DC coupled demodulating logarithmic amplifiers
[DE92-011697] p 3816 N92-31760

DEMOGRAPHY
Stress reactivity: Five-factor representation of a psychobiological typology
[AD-A252715] p 3872 N92-31327
Minorities and air quality non-attainment areas: A preliminary geo-demographic analysis
[DE92-013054] p 3852 N92-31591

DENSITY (MASS/VOLUME)
High density thin-walled syntactic foam
[DE92-013159] p 3797 N92-32136

DEPOLARIZATION
Analysis of random induced cross polarization
[AD-A249773] p 3806 N92-31569

DEPOSITION
Characterization of oxide formed on silicon by exposure to atomic oxygen in space
[AD-A249787] p 3778 N92-31301
Pulsed laser deposition of high Tc superconducting thin films
[AD-A250657] p 3830 N92-31319
Growth, nitrogen vacancy reduction and solid solution formation in cubic GaN thin films and the subsequent fabrication of superlattice structures using AlN and InN
[AD-A248058] p 3908 N92-31446
Sol-gel multilayers applied by a meniscus coating process
[DE92-012697] p 3794 N92-31560
Ion beam spectroscopy as a means of in-situ monitoring of thin film deposition
[DE92-014857] p 3909 N92-31652
Substrate surface effects on the properties of sputter-deposited and laser-irradiated films
[DE92-013850] p 3795 N92-31917
Ferroelectric thin films prepared by pulse laser deposition processing and characterization
[PB92-196088] p 3913 N92-32072
Supersonic pyrolysis jets for diamond film deposition
[AD-A251125] p 3798 N92-32198

DESCENT TRAJECTORIES
The use of high lift-to-drag hypersonic vehicles for aero-assisted orbital maneuvering p 3748 N92-31877

DESICCANTS
Desiccant cooling using unglazed transpired solar collectors
[DE92-010568] p 3849 N92-32112

DESIGN ANALYSIS
On the feasibility of a transient dynamic design analysis method
[AD-A250406] p 3838 N92-31337
ASTOVL combat aircraft design synthesis and optimization
[CRANFIELD-AERO-9201] p 3757 N92-31515
Design and analysis issues of integrated control systems for high-speed civil transports
[NASA-CR-186022] p 3761 N92-31656
Phase-locked arrays of antiguided diode lasers: Modelling, design, evaluation of performance limits
[LAAS-92034] p 3830 N92-31698
Performance tests of a fast-acting valve for the driver tubes of a large blast/thermal simulator
[AD-A250035] p 3835 N92-31807
Integrated computer systems in aircraft design and manufacture: Difficulties and implications
p 3746 N92-31864
Design, fabrication, and testing of a 30 kW(sub t) screen-wick heat-pipe solar receiver
[DE92-016500] p 3848 N92-32087
Design, analysis, and testing of the Phase 1 CSI Evolutionary Model erectable truss
[NASA-CR-4461] p 3767 N92-32100
Optimal design of geodesically stiffened composite cylindrical shells
[NASA-CR-190706] p 3842 N92-32235

DESORPTION
Dependence of secondary ion emission from organic material on the energy loss of the impacting heavy ion
[DE92-014845] p 3893 N92-31386
The collection, handling, transportation, and thermal desorption of explosive vapor using quartz collection tubes
[DE92-011441] p 3799 N92-31570
The thermal dissociation of decaborane on Si(111)-(7x7) and doping effects in the near surface region
[AD-A251057] p 3911 N92-31851
UV photochemistry of trivinylantimony adsorbed on quartz
[AD-A252215] p 3785 N92-32057

DESTRUCTIVE TESTS
Guidelines for generating acceptance sampling plans for continuous production
[DE92-010763] p 3837 N92-31753

DETECTION
Spacecraft dynamics characterization and control system failure detection. Volume 3: Control system failure monitoring
[NASA-CR-190529] p 3884 N92-31254
Systematic detection of parallelism in ordinary programs
[AD-A247514] p 3882 N92-31445
Readily implemented enhanced sinusoid detection in noise
[DE92-011359] p 3806 N92-31449
Real time detection in a laser bathymetry system
[PB92-195452] p 3866 N92-32069
Optimal targeting of evading objects
[DE92-014719] p 3889 N92-32119

DETONATION
Development of methodology and technology for identifying and quantifying emission products from open burning and open detonation thermal treatment methods. BangBox test series. Volume 1. Test summary
[AD-A250733] p 3800 N92-31969
Development of methodology and technology for identifying and quantifying emission products from open burning and open detonation thermal treatment methods. BangBox test series. Volume 2: Test development
[AD-A250734] p 3800 N92-31970
Development of methodology and technology for identifying and quantifying emission products from open burning and open detonation thermal treatment methods. Field test series A, B, and C. Volume 1: Test summary
[AD-A250735] p 3800 N92-31971
Development of methodology and technology for identifying and quantifying emission products from open burning and open detonation thermal treatment methods. Field test series A, B, and C. Volume 2, part A: Quality assurance and quality control
[AD-A250736] p 3801 N92-31972
Development of methodology and technology for identifying and quantifying emission products from open burning and open detonation thermal treatment methods. Field test series A, B, and C. Volume 2, part B: Quality assurance and quality control. Appendices
[AD-A250737] p 3801 N92-31973

DETONATION WAVES
Laser-initiated conical detonation wave for supersonic combustion, part 3
[AD-A250522] p 3785 N92-32076

DEUTERIUM
Fusion with highly spin polarized HD and D(2)
[DE92-017030] p 3898 N92-32007

DEUTERIUM PLASMA
Poloidal rotation and density asymmetries in a tokamak plasma with strong toroidal rotation
[PB92-182534] p 3904 N92-31613

DIAGNOSIS
Particle diagnostics in optically thick sprays
[AD-A250981] p 3897 N92-31936
DIAMAGNETISM
Rigid rotations in two-electron atoms in a uniform magnetic field
[DE92-624981] p 3896 N92-31836
DIAMINES
Photogenerated base as catalyst for imidization reactions: Design of photosensitive polyimides
[AD-A250067] p 3795 N92-31810
DIAMOND FILMS
Synthesis of diamond films with pulsed plasma
[AD-A250058] p 3791 N92-31356
Supersonic pyrolysis jets for diamond film deposition
[AD-A251125] p 3798 N92-32198
DIAMONDS
Transient internal probe diagnostic
[AD-A247306] p 3903 N92-31459
International Semiconductor Device Research Symposium (ISDRS-91)
[AD-A247394] p 3908 N92-31537
Fabrication of an insulated gate diamond FET for high temperature applications
[AD-A251042] p 3817 N92-31849
The synthesis and characterization of tribophysical layers on diamond and silicon carbide surfaces
[AD-A250983] p 3796 N92-32001
Supersonic pyrolysis jets for diamond film deposition
[AD-A251125] p 3798 N92-32198
DICTIONARIES
RCRIS data element dictionary, version 3.0.0: Data tape documentation
[PB92-145515] p 3918 N92-31398
A dictionary of acquisition and contracting terms
[AD-A247053] p 3920 N92-31754
Correspondence dictionary from free English term to INIS descriptors
[DE92-782192] p 3920 N92-31859
DIELECTRIC PROPERTIES
The role of metal structure in determining solvent orientation at the electrode/solution interface
[AD-A249751] p 3893 N92-31328
DIELECTRICS
High-frequency techniques for RCS prediction of plate geometries
[NASA-CR-190656] p 3804 N92-31273
The role of metal structure in determining solvent orientation at the electrode/solution interface
[AD-A249751] p 3893 N92-31328
Natural convection immersion cooling of an array of vertically oriented heated protrusions in an enclosure filled with a dielectric liquid: Effects of enclosure width, Prandtl number and component orientation
[AD-A245884] p 3914 N92-31489
Stress and phase transformation phenomena in oxide films
[DE92-014702] p 3910 N92-31665
Temperature-enhanced autodetachment from long-lived parent negative ions of gaseous dielectrics
[DE92-011108] p 3894 N92-31700
Compact millimeter-wave devices: Dielectric loaded carm, high voltage carm, slow wave crm and high harmonic gyrotron
[AD-A250497] p 3809 N92-31944
Mechanics of thin films
[AD-A247848] p 3912 N92-31984
Role of the double-layer cation on the potential-dependent stretching frequencies and binding geometries of carbon monoxide at platinum-nonaqueous interfaces
[AD-A246980] p 3784 N92-31998
Device for monitoring the thickness of a dielectric coating on a dielectric substrate
[DE92-014741] p 3829 N92-32174
Ba2Ti9O20 microwave dielectric resonator: Processing, phase synthesis and characterization
[INPE-5373-PRE/1747] p 3818 N92-32200
DIENES
Cyclopolymerization of metalloid-containing alpha, omega-dienes. 1,3-divinyltetramethyldisiloxane, 1,3-divinyltetramethyldisilazane and 1,3-divinylpentamethyldisilazane
[AD-A250347] p 3794 N92-31557
Unimolecular reaction mechanisms involving C3H4, C4H4, and C6H6 hydrocarbon species
[DE92-005326] p 3783 N92-31860
DIESEL ENGINES
Experimental evaluation of oxygen-enriched air and emulsified fuels in a single-cylinder diesel engine. Volume 1: Concept evaluation
[DE92-015999] p 3799 N92-31442
Effect of out-of-roundness on the performance of a diesel engine connecting-rod bearing
[NASA-TM-105600] p 3834 N92-31536
DIESEL FUELS
Experimental evaluation of oxygen-enriched air and emulsified fuels in a single-cylinder diesel engine. Volume 1: Concept evaluation
[DE92-015999] p 3799 N92-31442
DIFFERENTIAL AMPLIFIERS
Beam position monitor electronics using DC coupled demodulating logarithmic amplifiers
[DE92-011697] p 3816 N92-31760
DIFFERENTIAL CALCULUS
ADIFOR: Automatic differentiation in a source translator environment
[DE92-016185] p 3886 N92-31311
DIFFERENTIAL EQUATIONS
Phase portraits of non degenerate quadratic systems with zero finite multiplicity
[REPT-91-96] p 3886 N92-31520
Geometric theory of infinite dimensional dynamical systems
[AD-A252190] p 3915 N92-31585
An investigation of spinup dynamics of axial gyrostats using elliptic integrals and the method of averaging
[AD-A249728] p 3768 N92-31675
The Matrix Editor for symbolic Jacobians in ALPAL
[DE92-008076] p 3878 N92-31742
Heat transfer and flow of a modified second grade fluid
[DE92-014744] p 3824 N92-31895
ADIFOR: Fortran source translation for efficient derivatives
[DE92-016187] p 3879 N92-31899
DIFFRACTION
Electromagnetic scattering by coated convex surfaces and wedges simulated by approximate boundary conditions
[NASA-CR-190540] p 3803 N92-31238
High-frequency techniques for RCS prediction of plate geometries
[NASA-CR-190656] p 3804 N92-31273
DIFFUSION
Diffusion of camphorquinone in uniaxially drawn polycarbonate films
[AD-A252489] p 3796 N92-31961
Fundamental studies in oxidation-reduction in relation to water photolysis
[DE92-014333] p 3785 N92-32113
Diffusion in ordered and disordered media
[AD-A250949] p 3891 N92-32211
DIFFUSION COEFFICIENT
Diffusion of camphorquinone in uniaxially drawn polycarbonate films
[AD-A252489] p 3796 N92-31961
DIFFUSION FLAMES
Ignition and flame propagation studies over a flat fuel surface
[PB92-181056] p 3780 N92-31678
Dual gated imaging system for enhanced fluorescent diagnostics measurements
[AD-A249673] p 3828 N92-31694
Incipient and total group combustion of fuel sprays in air p 3749 N92-31883
Transport and evaporation effects in counterflow spray diffusion flames p 3749 N92-31884
DIFFUSIVITY
Theory of anomalous transport in toroidal helical plasmas
[NIFS-140] p 3904 N92-31659
Energy transport in the steady state plasma sustained by DC helicity current drive
[NIFS-127] p 3907 N92-32181
DIGITAL DATA
Digital analysis of wind tunnel imagery to measure fluid thickness
[NASA-CR-189234] p 3762 N92-31252
Compression of digitized map images
[AD-A250707] p 3843 N92-31323
Final report on DSA methods for monitoring alumina in aluminum reduction cells with cermet anodes
[DE92-013599] p 3813 N92-31440
Data compression techniques p 3922 N92-32190
Markovian fields as limits of Markov chains
[INPE-5395-PRE/1753] p 3889 N92-32225
DIGITAL SYSTEMS
A free-piston Stirling engine/linear alternator controls and load interaction test facility
[NASA-TM-105825] p 3845 N92-31262
Overview of integrated services digital network conformance testing
[PB92-181015] p 3881 N92-31365
VLSI for high-speed digital signal processing
[AD-A250365] p 3817 N92-32074
DIGITAL TECHNIQUES
Compression of digitized map images
[AD-A250707] p 3843 N92-31323
Problems with interleaved digitizers
[DE92-013369] p 3881 N92-32150
DIMERS
Synthesis of soluble alpha-thiophene oligomers. Monomer to octamer
[AD-A250082] p 3779 N92-31434
DIMETHYL COMPOUNDS
Synthesis of cresols and xylenols from phenol and methanol
[DE91-002141] p 3785 N92-32093
DIODES
The polarized electron gun for the SLC
[DE92-012418] p 3900 N92-32131
DIPOLE ANTENNAS
Scattering from a finite collection of transverse dipole and axial slot arrays with edge effects
[AD-A249622] p 3807 N92-31691
DIRAC EQUATION
The physical solution to the Lorentz-Dirac equations in a constant magnetic field
[DE92-013299] p 3890 N92-32140
DIRECT CURRENT
Energy transport in the steady state plasma sustained by DC helicity current drive
[NIFS-127] p 3907 N92-32181
DIRECTIONAL ANTENNAS
Analysis of random induced cross polarization
[AD-A249773] p 3806 N92-31569
DIRECTIONAL STABILITY
A computational examination of directional stability for smooth and chined forebodies at high-alpha
[NASA-CR-4465] p 3753 N92-32114
DIRECTORIES
Directory of IAEA databases
[DE92-628395] p 3920 N92-32058
DISCHARGE
Real time analysis of tokamak discharge parameters
[DE92-011394] p 3904 N92-31616
DISCONTINUITY
Highly accurate prediction of unsteady viscous flows
[AD-A250982] p 3825 N92-32000
DISCRIMINANT ANALYSIS (STATISTICS)
Empirical development of a scale for the prediction of performance on a sustained monitoring task
[AD-A252443] p 3872 N92-31294
DISPERSIONS
Application of Free-Air CO2 Enrichment (FACE) technology to a forest canopy: A simulation study
[DE92-013308] p 3851 N92-31422
DISPLAY DEVICES
Space constancy on video display terminals
[AD-A247290] p 3872 N92-32105
Engine monitoring display study
[NASA-CR-4463] p 3761 N92-32175
DISSIPATION
The prediction of the performance of a microcircuit heat sink in the boiling mode
[AD-A250045] p 3812 N92-31355
DISSOCIATION
Economics of microwave plasma dissociation of H2S
[DE92-014846] p 3779 N92-31441
DISSOLVING
Deterministic analysis of processes at corroding metal surfaces and the study of electrochemical noise in these systems
[DE92-016286] p 3788 N92-31733
DISTILLATION
Analysis and computer tools for separation processes involving nonideal mixtures
[DE92-015298] p 3781 N92-31752
DISTORTION
Research on aero-thermodynamic distortion induced structural dynamic response of multistage compressor blading
[AD-A250865] p 3760 N92-32059
Motion model for the correction of point source distortion in radiographs of honeycomb
[DREP-88-14] p 3777 N92-32215
DISTRIBUTED PROCESSING
A proposed group management scheme for XTP multicast
[NASA-CR-190633] p 3916 N92-31547
Using consistent subcuts for detecting stable properties
[NASA-CR-190443] p 3886 N92-31553
PARTI primitives for unstructured and block structured problems
[NASA-CR-189662] p 3876 N92-31561
A task adaptive parallel graphics rendering algorithm
[DE92-008062] p 3878 N92-31739
The multicomputer toolbox: Scalable parallel libraries for large-scale concurrent applications
[DE92-008068] p 3882 N92-31740
Specification and verification of secure concurrent and distributed software systems
[AD-A252477] p 3879 N92-31825

Remote Data Transfer (RDT): An interprocess data transfer method for distributed environments
[AD-A250859] p 3920 N92-32102

DISTRIBUTION FUNCTIONS
Independent sampling of a stochastic process
[AD-A249712] p 3888 N92-31600

DITCHING (LANDING)
Immersion suit usage within the RAAF
[AD-A250645] p 3755 N92-31562
Canadian aircrew sea water survival, 1952-1987
[DCIEM-88-RR-39] p 3756 N92-32219

DIURNAL VARIATIONS
Simulation of diurnally varying downslope winds over Northern Utah
[AD-A250568] p 3861 N92-31714
Probabilistic analysis of twenty-four hour weather data for Warsaw p 3863 N92-32097

DIVERTERS
Divertor material evaluation system at D3-D
[DE92-013696] p 3905 N92-31749
Power scaling of divertor plasma conditions during H-mode in D3-D
[DE92-012148] p 3906 N92-31771
Small tokamaks for fusion technology testing
[DE92-011790] p 3906 N92-31913

DIVING (UNDERWATER)
Canadian aircrew sea water survival, 1952-1987
[DCIEM-88-RR-39] p 3756 N92-32219

DO-28 AIRCRAFT
The icing of the elevator of the DLR icing research aircraft of Do 28 type
[DLR-MITT-91-12] p 3755 N92-31813

DOCUMENTATION
A model for extending the behavior of annotations
[DE92-011731] p 3920 N92-31934

DOCUMENTS
Next generation documents
[PB92-187103] p 3917 N92-31371
Automated payload experiment tool feasibility study
[NASA-CR-184256] p 3883 N92-31835
Use of expert systems as user interfaces in information retrieval p 3921 N92-32185
Non Boolean search methods in information retrieval p 3921 N92-32187
Data compression techniques p 3922 N92-32190

DONOR MATERIALS
Ultrafast experiments on the role of vibrational modes in electron transfer
[AD-A250630] p 3910 N92-31699

DOPED CRYSTALS
A comparison of interstitial oxygen calculated by different techniques
[DE92-011658] p 3910 N92-31668
Impurity effects on the magnetic ordering in chromium
[DE92-016165] p 3789 N92-31898
Absorption spectra and electronic properties of alkali metal doped C60
[AD-A251006] p 3912 N92-31937
Effect of synthesis temperature in the structure, doping level and charge-transport properties of polypyrrole
[AD-A250531] p 3796 N92-32079

DOPPLER EFFECT
Diagnostics for research in atomization and turbulent two-phase flows
[AD-A247201] p 3819 N92-31283
A data processing module for acoustic Doppler current meters
[AD-A250901] p 3891 N92-31563
Dicke narrowing in strong fields: The atom-as-antenna analogy
[AD-A252321] p 3807 N92-31629

DOPPLER RADAR
A comparison of the performance of two gust front detection algorithms using a length-based scoring technique
[AD-A250862] p 3863 N92-32103

DOSAGE
Noninvasive ambulatory assessment of cardiac function and myocardial ischemia in healthy subjects exposed to carbon monoxide
[AD-A252264] p 3870 N92-32107

DOSIMETERS
Use of tissue equivalent proportional counters to characterize radiation quality on the space shuttle
[DE92-012347] p 3768 N92-31846

DOUBLE BASE PROPELLANTS
Development of methodology and technology for identifying and quantifying emission products from open burning and open detonation thermal treatment methods. BangBox test series. Volume 1. Test summary
[AD-A250733] p 3800 N92-31969
Development of methodology and technology for identifying and quantifying emission products from open burning and open detonation thermal treatment methods. Field test series A, B, and C. Volume 1: Test summary
[AD-A250735] p 3800 N92-31971
Development of methodology and technology for identifying and quantifying emission products from open burning and open detonation thermal treatment methods. Field test series A, B, and C. Volume 2, part A: Quality assurance and quality control
[AD-A250736] p 3801 N92-31972
Development of methodology and technology for identifying and quantifying emission products from open burning and open detonation thermal treatment methods. Field test series A, B, and C. Volume 2, part B: Quality assurance and quality control. Appendices
[AD-A250737] p 3801 N92-31973

DRAG REDUCTION
Automatic design of transonic airfoils to reduce the shock induced pressure drag p 3745 N92-31863

DRAINAGE
Hydrological and geochemical response and recovery in disturbed Arctic ecosystems
[DE92-016223] p 3850 N92-31312

DRILLING
Proceedings of the 4th Atlantic OCS Region Information Transfer Meeting
[PB92-177690] p 3864 N92-31630
Cutting treatment by drilling of fiber bound synthetic materials
[MBB-UD-0609-91-PUB] p 3774 N92-31716
Geothermal materials development
[DE92-016940] p 3849 N92-32124

DRONE AIRCRAFT
Optimal trajectories for an unmanned air vehicle p 3748 N92-31880

DROP TRANSFER
Study of a spherical spinning combustion chamber for orbit insertion p 3746 N92-31869

DROPS (LIQUIDS)
Replaceable valve seat
[AD-D015250] p 3832 N92-31271
A model for the interfacial shear in vertical, adiabatic, annular-mist flow
[DE92-013537] p 3820 N92-31424

DUCTED FLOW
Three-dimensional compressible turbulent computations for a nondiffusing S-duct
[NASA-CR-4391] p 3754 N92-32240

DUCTILITY
J(sub 2) fracture toughness testing of Al 707 5-T7351 p 3747 N92-31872
The effect of thermomechanical processing parameters on the ambient behavior of 10 percent volume 6061 Al-Alumina
[AD-A252177] p 3776 N92-32064

DUMMIES
Vertical impact tests of humans and anthropomorphic manikins
[AD-A245866] p 3872 N92-31458

DUNES
Geomorphic variability in the coastal zone
[AD-A252713] p 3864 N92-31544

DURABILITY
Research into improving the durability of the hot section in the aircraft turbine engine
[AD-A250342] p 3759 N92-31439

DUST
Turbulent dusty boundary layer in an ANFO surface-burst explosion
[DE92-012101] p 3822 N92-31625

DYE LASERS
High performance of copper pumped dye lasers
[DE92-011763] p 3832 N92-31902

DYES
Diffusion of camphorquinone in uniaxially drawn polycarbonate films
[AD-A252489] p 3796 N92-31961

DYNAMIC CHARACTERISTICS
On the feasibility of a transient dynamic design analysis method
[AD-A250406] p 3838 N92-31337
Geomorphic variability in the coastal zone
[AD-A252713] p 3864 N92-31544
Advanced DAA methods for shock response analysis
[AD-A252696] p 3891 N92-31588
Studies in dynamic characterization and control of a flexible structure and optical beampath
[AD-A250555] p 3830 N92-31605
CSM solutions of rotating blade dynamics using integrating matrices
[NASA-CR-190577] p 3840 N92-31619
Static and dynamic properties of current sensing power VDMOS transistor
[LAAS-92032] p 3815 N92-31697
A comparative study of the dynamic performance of three bivanes
[AD-A250096] p 3862 N92-31784
Numerical simulation of tulip flame dynamics
[DE92-008553] p 3782 N92-31805

DYNAMIC CONTROL
Spacecraft dynamics characterization and control system failure detection. Volume 3: Control system failure monitoring
[NASA-CR-190529] p 3884 N92-31254
Studies in dynamic characterization and control of a flexible structure and optical beampath
[AD-A250555] p 3830 N92-31605

DYNAMIC MODELS
Fundamental studies of the structure of hypersonic attached and separated boundary layers over smooth, rough and transpiration-cooled surfaces
[AD-A250284] p 3819 N92-31286
Dynamic modeling of plasma-vapor interactions during plasma disruptions
[DE92-016183] p 3903 N92-31310
A dynamical model of the behaviour of hadronic and fundamental strings at finite densities
[DE92-630245] p 3914 N92-31402
Advanced thermally stable, jet fuels development program annual report. Volume 1: Model and experiment system development
[AD-A249625] p 3799 N92-31462
Modal simulation of gearbox vibration with experimental correlation
[NASA-TM-105702] p 3834 N92-31485
Dynamics of shuttle based flexible antenna system
[CRANFIELD-AERO-9203] p 3840 N92-31516
A dynamic model of terrestrial carbon cycling
[DE92-015130] p 3853 N92-31782
A simulation model of a single rotor helicopter p 3746 N92-31865
Mathematical modeling and numerical simulation of the dynamics of flexible structures undergoing large overall motions
[AD-A250202] p 3761 N92-31967
Dynamic modeling and modal analysis of an air-to-air missile
[AD-A245957] p 3758 N92-32053
Non-convex problems in PDE: Equilibrium theory and dynamics
[AD-A250549] p 3887 N92-32081

DYNAMIC RESPONSE
Mode methods for strain-hardening structures
[DE92-014855] p 3838 N92-31335
On the feasibility of a transient dynamic design analysis method
[AD-A250406] p 3838 N92-31337
Adaptive inverse filter
[DE92-011660] p 3878 N92-31669
Discrete optimal guidance for high order missile and maneuvering target p 3748 N92-31879
Research on aero-thermodynamic distortion induced structural dynamic response of multistage compressor blading
[AD-A250865] p 3760 N92-32059

DYNAMIC STABILITY
Studies in dynamic characterization and control of a flexible structure and optical beampath
[AD-A250555] p 3830 N92-31605

DYNAMIC STRUCTURAL ANALYSIS
A summary of the active flexible wing program
[NASA-TM-107655] p 3757 N92-31264
CSM solutions of rotating blade dynamics using integrating matrices
[NASA-CR-190577] p 3840 N92-31619
Mathematical modeling and numerical simulation of the dynamics of flexible structures undergoing large overall motions
[AD-A250202] p 3761 N92-31967
Optimal design of geodesically stiffened composite cylindrical shells
[NASA-CR-190706] p 3842 N92-32235

DYNAMIC TESTS
Studies of the effect of strain velocity on mechanical properties of the 34GS steel p 3786 N92-31243
Design, analysis, and testing of the Phase 1 CSI Evolutionary Model erectable truss
[NASA-CR-4461] p 3767 N92-32100

DYNAMICAL SYSTEMS
Geometric theory of infinite dimensional dynamical systems
[AD-A252190] p 3915 N92-31585
Noise-induced chaos and phase space flux: A sample-theoretic study
[PB92-172733] p 3915 N92-31645
Asymptotic modal analysis and statistical energy analysis
[NASA-CR-190516] p 3842 N92-32236

E

EARTH ATMOSPHERE
The detection of climate change due to the enhanced greenhouse effect
[NASA-TM-107965] p 3849 N92-31258
Annual dynamics within the active layer
[DE92-013520] p 3850 N92-31304
Numerical simulation of precipitation scavenging and comparison with observation of prescribed forest fires
[DE92-013513] p 3851 N92-31423
EnviroTRADE: Its role in the cleanup of the environment
[DE92-013691] p 3851 N92-31427
Response of a tundra ecosystem to elevated atmospheric carbon dioxide and CO2-induced climate change
[DE92-013925] p 3853 N92-31626
Analysis of the effects of aerosol distribution in the atmosphere on surface radiative measurements
[DE92-014189] p 3856 N92-31662
NASA High Speed Research Program, Emissions Scenarios Committee report of meetings on 26 September 1991 and 9 January 1992
[NASA-CR-190379] p 3855 N92-32147
Global trends in energy use: Indications for research
[DE92-014773] p 3855 N92-32155

EARTH ENVIRONMENT
Our changing planet: The FY 1993 US global change research program. A supplement to the US President's fiscal year 1993 budget
[NASA-CR-190675] p 3850 N92-31259

EARTH IONOSPHERE
Ionospheric communications channel modelling
[DE92-013039] p 3808 N92-31722
Impulsive magnetic perturbations of the high latitude, dayside ionosphere
[AD-A249872] p 3857 N92-31932
USU center of excellence in theory and analysis of the geo-plasma environment
[AD-A252189] p 3858 N92-32055

EARTH MAGNETOSPHERE
Mitigation of magnetohydrodynamic electromagnetic pulse (MHD-EMP) effects from commercial electric power systems
[AD-A249577] p 3804 N92-31354
Impulsive magnetic perturbations of the high latitude, dayside ionosphere
[AD-A249872] p 3857 N92-31932

EARTH MANTLE
Time domain regional discriminants
[AD-A249949] p 3855 N92-31509

EARTH MOVEMENTS
Advanced DAA methods for shock response analysis
[AD-A252696] p 3891 N92-31588

EARTH OBSERVATIONS (FROM SPACE)
Results of earth observation study on STS-31 for Terra Geode, January 1987 - June 1991
[AD-A250750] p 3844 N92-31621
Italian-US cooperation in space: The case of Tethered, IRIS/LAGEOS, and SPACEHAB
[TABES PAPER 92-467] p 3764 N92-32019
GIS: Geographic Information Systems. State of the art and future tendencies
[INPE-5358-NTC/301] p 3922 N92-32227

EARTH OBSERVING SYSTEM (EOS)
Advanced microwave sounding unit study for atmospheric infrared sounder
[NASA-CR-190628] p 3858 N92-32195

EARTH ORBITAL ENVIRONMENTS
Advances in small satellite communication systems
[TABES PAPER 92-411] p 3763 N92-32010

EARTH RADIATION BUDGET
Extended Kalman filter for attitude estimation of the Earth Radiation Budget Satellite p 3748 N92-31876
Mission description and in-flight operations of ERBE instruments on ERBS, NOAA 9, and NOAA 10 spacecraft
[NASA-RP-1279] p 3844 N92-32127

EARTH RADIATION BUDGET EXPERIMENT
Extended Kalman filter for attitude estimation of the Earth Radiation Budget Satellite p 3748 N92-31876
Mission description and in-flight operations of ERBE instruments on ERBS, NOAA 9, and NOAA 10 spacecraft
[NASA-RP-1279] p 3844 N92-32127

EARTH RESOURCES
ARO Geoscience Center fellowships
[AD-A249225] p 3857 N92-31964

EARTH SCIENCES
JPRS report: Science and technology. Central Eurasia: Earth sciences
[JPRS-UES-92-004] p 3843 N92-32132

EARTH TERMINALS
A prototype DND Ku band SATCOM system for ANIK-C2 (Project MASTER/MM2)
[DREO-1034] p 3810 N92-32176
EHF SATCOM frequency hopping pattern generator: Proof of concept
[DREO-89-32] p 3811 N92-32231
A frequency hopping synthesizer controller for EHF SATCOM
[DREO-89-29] p 3811 N92-32232

EARTHQUAKES
Time domain regional discriminants
[AD-A249949] p 3855 N92-31509

ECCENTRICITY
The stability of a slightly eccentric straight vortex filament in a circular tube p 3750 N92-31887

ECLIPSING BINARY STARS
Photometry of Nova Muscae 1983
[INPE-5339-PRE/1738] p 3923 N92-31344
The eclipsing cataclysmic variable AY Piscium
[INPE-5340-PRE/1739] p 3923 N92-31345
The eclipsing cataclysmic variable NSV 12615 (V4041 Sgr)
[INPE-5342-PRE/1741] p 3923 N92-31346

ECOLOGY
Extremely Low Frequency (ELF) communications system ecological monitoring program summary of 1990 progress
[AD-A246344] p 3809 N92-31996
Biology, oceanography, and fisheries of the North Pacific transition zone and subarctic frontal zone
[PB92-178128] p 3866 N92-32106
JPRS report: Science and technology. Central Eurasia: Earth sciences
[JPRS-UES-92-004] p 3843 N92-32132
A test of ecological optimality for semiarid vegetation
[NASA-CR-190705] p 3855 N92-32222

ECONOMIC ANALYSIS
Economics of microwave plasma dissociation of H2S
[DE92-014846] p 3779 N92-31441

ECONOMIC DEVELOPMENT
A program for the transfer of manufacturing technology from the national laboratories
[DE92-011905] p 3923 N92-31965

ECONOMIC FACTORS
Minorities and air quality non-attainment areas: A preliminary geo-demographic analysis
[DE92-013054] p 3852 N92-31591

ECOSYSTEMS
Hydrological and geochemical response and recovery in disturbed Arctic ecosystems
[DE92-016223] p 3850 N92-31312
Application of Free-Air CO2 Enrichment (FACE) technology to a forest canopy: A simulation study
[DE92-013308] p 3851 N92-31422
Response of a tundra ecosystem to elevated atmospheric carbon dioxide and CO2-induced climate change
[DE92-013925] p 3853 N92-31626
A dynamic model of terrestrial carbon cycling
[DE92-015130] p 3853 N92-31782
Ecosystems of the Florida Keys: A bibliography
[PB92-198910] p 3854 N92-32071

EDGE DETECTION
Detection of object edges in images containing cast shadows
[DE92-016092] p 3900 N92-31295

EDUCATION
Building an educational robot arm for under $1,000
[AD-A247499] p 3833 N92-31460
International mathematics and science assessments: What have we learned
[PB92-183599] p 3916 N92-32160

EFFICIENCY
Efficiency calculations of the hadron detector
[NIKHEF-K-EMIN-92-01] p 3896 N92-31814
New directions in network flows
[AD-A250499] p 3880 N92-32039

EFFLUX
Performance of multiple stream pulsed jet combustion systems
[AD-A249722] p 3780 N92-31671

EIGENVALUES
Sensitivity analysis of hydrodynamic stability operators
[NASA-CR-189683] p 3822 N92-31535
Eigensensitivity analysis of composite laminates: Effect of microstructure
[AD-A250864] p 3777 N92-32104
Diffusion in ordered and disordered media
[AD-A250949] p 3891 N92-32211

EIGENVECTORS
Diffusion in ordered and disordered media
[AD-A250949] p 3891 N92-32211

EINSTEIN EQUATIONS
Holographic grating relaxation and photon correlation spectroscopic studies of viscoelastic liquids above the glass transition
[AD-A252485] p 3828 N92-31828

ELASTIC CYLINDERS
A generalized plane-strain elastic stress solution for a multiorthotropic-layered cylinder
[AD-A250487] p 3838 N92-31331

ELASTIC PLATES
Applications of FEM and BEM in two-dimensional fracture mechanics problems
[NASA-TP-3277] p 3838 N92-31280

ELASTIC PROPERTIES
A generalized plane-strain elastic stress solution for a multiorthotropic-layered cylinder
[AD-A250487] p 3838 N92-31331
Modeling of composite beams and plates for static and dynamic analysis
[NASA-CR-190536] p 3839 N92-31339
The effect of elastic stress on Ostwald ripening phenomena
[DE92-015291] p 3839 N92-31400
US-Japan seminar on magnetic multilayered structures: Proceedings
[AD-A252440] p 3910 N92-31666

ELASTIC SCATTERING
The RQM triangle: A paradigm for relativistic quantum mechanics
[DE92-011583] p 3915 N92-31663

ELASTIC WAVES
Advanced DAA methods for shock response analysis
[AD-A252696] p 3891 N92-31588

ELASTODYNAMICS
Advanced DAA methods for shock response analysis
[AD-A252696] p 3891 N92-31588

ELASTOPLASTICITY
Effects of fiber and interfacial layer architectures on the thermoplastic response of metal matrix composites
[NASA-TM-105802] p 3777 N92-32234

ELECTRIC BATTERIES
Batteries and fuel cells
[DE92-011493] p 3847 N92-31571
Electric and hybrid vehicles program
[DE92-015200] p 3834 N92-31653

ELECTRIC CHARGE
Fundamental studies in oxidation-reduction in relation to water photolysis
[DE92-014333] p 3785 N92-32113
Structure and dynamics of Cl(H2O)20 clusters. The effect of the polarizability and the charge ofthe ion
[AD-A251094] p 3899 N92-32196

ELECTRIC CONTROL
A comparison of three self-tuning control algorithms developed for the Bristol-Babcock controller
[DE92-014472] p 3814 N92-31499

ELECTRIC CURRENT
Enhancement of fracture toughness using high intensity electric currents
[AD-A249809] p 3889 N92-31359
What can we learn from magnetization experiments on high T(sub c) superconductors? An overview
[DE92-014465] p 3815 N92-31650
Recent advances in high-temperature superconductor wire fabrication and applications development
[DE92-016634] p 3912 N92-31955

ELECTRIC EQUIPMENT
Analysis of systems hardware flown on LDEF. Results of the systems special investigation group
[NASA-CR-189628] p 3767 N92-31677

ELECTRIC EQUIPMENT TESTS
Measured responses of a munitions storage bunker to rocket-triggered lightning
[DE92-012628] p 3862 N92-31750

ELECTRIC FIELDS
Flow generation by turbulence
[DE92-013276] p 3906 N92-31829

ELECTRIC FILTERS
Adaptive inverse filter
[DE92-011660] p 3878 N92-31669

ELECTRIC GENERATORS
An evaluation of ionizing radiation emitted by high power microwave generators
[DE92-016160] p 3805 N92-31387
Hydrogenerator design manual, chapter 8
[PB92-173707] p 3919 N92-31682

ELECTRIC HYBRID VEHICLES
Electric and hybrid vehicles program
[DE92-015200] p 3834 N92-31653

ELECTRIC MOTOR VEHICLES
Research and development of advanced nickel-iron batteries for electric vehicle propulsion
[DE92-014099] p 3817 N92-31834

ELECTRIC MOTORS
Construction of a dual axis force reflection stick and test station
[AD-A250731] p 3803 N92-31890
ELECTRIC POTENTIAL
Calculational prediction of ultrawideband electromagnetic pulses by laser-initiated air avalanche switches
[DE92-011732] p 3812 N92-31334
Subnanosecond photoconductive switching in GaAs
[DE92-011521] p 3910 N92-31719
Dissociative electron attachment of O2: A solid-state effect on potential curve crossing
[AD-A246331] p 3913 N92-31995
Role of the double-layer cation on the potential-dependent stretching frequencies and binding geometries of carbon monoxide at platinum-nonaqueous interfaces
[AD-A246980] p 3784 N92-31998
Monolithic and mechanical multijunction space solar cells
[NASA-TM-105832] p 3818 N92-32233
ELECTRIC POWER SUPPLIES
External combustion engine technology (vapor and liquid cycles) for individual soldier power systems
[AD-A252754] p 3836 N92-32173
ELECTRIC POWER TRANSMISSION
Mitigation of magnetohydrodynamic electromagnetic pulse (MHD-EMP) effects from commercial electric power systems
[AD-A249577] p 3804 N92-31354
ELECTRIC PROPULSION
The evolutionary development of high specific impulse electric thruster technology
[NASA-TM-105712] p 3769 N92-31342
ELECTRIC SWITCHES
Calculational prediction of ultrawideband electromagnetic pulses by laser-initiated air avalanche switches
[DE92-011732] p 3812 N92-31334
Proposal for a workshop in the physics and application of hollow electrode glow switches
[AD-A247139] p 3814 N92-31490
High-pressure gas switch for a wideband source
[DE92-015822] p 3815 N92-31548
ANTHEM simulational studies of the plasma opening switch
[DE92-015247] p 3815 N92-31681
ELECTRICAL ENGINEERING
Electronics and electrical engineering laboratory technical publication announcements covering laboratory programs, July to September 1991, with 1992 EEEL events calendar
[PB92-181239] p 3813 N92-31367
Building an educational robot arm for under $1,000
[AD-A247499] p 3833 N92-31460
ELECTRICAL FAULTS
Calculational prediction of ultrawideband electromagnetic pulses by laser-initiated air avalanche switches
[DE92-011732] p 3812 N92-31334
ELECTRICAL IMPEDANCE
A three-gap klystron output cavity at X-band
[DE92-012417] p 3812 N92-31289
ELECTRICAL PROPERTIES
Real time investigations of the polymerization of 2-pentadecyl aniline on the Langmuir-Blodgett trough
[AD-A250994] p 3795 N92-31954
Physical characterization of magmatic liquids
[DE92-015302] p 3858 N92-32027
ELECTRICAL RESISTIVITY
Schwinger boson studies of the t-J model beyond mean-field approximation
[DE92-630650] p 3909 N92-31655
Synthesis, structure and properties of Ba6Co25S27: A Perovskite-like superstructure of Co8S6 and Ba6S clusters
[AD-A251041] p 3911 N92-31848
ELECTRO-OPTICS
Nonlinear optical acrylic polymers and use thereof in optical and electro-optic devices
[AD-D015236] p 3791 N92-31270
International Semiconductor Device Research Symposium (ISDRS-91)
[AD-A249348] p 3813 N92-31373
A microprism array for large-scale, wide-band interconnection of optoelectronic systems
[AD-A249380] p 3813 N92-31374
Laser material interactions
[AD-A250028] p 3831 N92-31802
Electro-optics and second harmonic generation of nonlinear optical polymers
[AD-A252488] p 3796 N92-31960
Single crystal growth optimization of magnesium-doped lithium niobate
[AD-A250781] p 3914 N92-32207
ELECTROCATALYSTS
Electrochemical oxidation of methane for fuel cells
[PB92-172303] p 3848 N92-31922
ELECTROCHEMICAL CELLS
Final report on DSA methods for monitoring alumina in aluminum reduction cells with cermet anodes
[DE92-013599] p 3813 N92-31440
ELECTROCHEMICAL OXIDATION
Electrochemical oxidation of methane for fuel cells
[PB92-172303] p 3848 N92-31922
ELECTROCHEMISTRY
Interfacial ion transport between immiscible liquids
[AD-A252424] p 3778 N92-31292
Development of an electrochemical method for field testing of protective coatings
[AD-A245872] p 3793 N92-31473
Deterministic analysis of processes at corroding metal surfaces and the study of electrochemical noise in these systems
[DE92-016286] p 3788 N92-31733
Near-IR absorption spectra for the Buckminsterfullerene Anions: An experimental and theoretical study
[AD-A250532] p 3785 N92-32080
Prediction of hydrogen entry and permeation in metals and alloys
[AD-A245286] p 3790 N92-32096
ELECTRODE MATERIALS
Electrochemical oxidation of methane for fuel cells
[PB92-172303] p 3848 N92-31922
ELECTRODES
The role of metal structure in determining solvent orientation at the electrode/solution interface
[AD-A249751] p 3893 N92-31328
High temperature superconducting films and multilayers for electronics
[AD-A250732] p 3813 N92-31451
Research and development of advanced nickel-iron batteries for electric vehicle propulsion
[DE92-014099] p 3817 N92-31834
Electrochemical oxidation of methane for fuel cells
[PB92-172303] p 3848 N92-31922
Role of the double-layer cation on the potential-dependent stretching frequencies and binding geometries of carbon monoxide at platinum-nonaqueous interfaces
[AD-A246980] p 3784 N92-31998
ELECTROHYDRODYNAMICS
ANTHEM simulational studies of the plasma opening switch
[DE92-015247] p 3815 N92-31681
ELECTROLUMINESCENCE
SiGe Si quantum wires for efficient, room temperature, tunable luminescence
[AD-A249651] p 3814 N92-31464
ELECTROLYTES
Application of the mean spherical approximation to the estimations of single ion thermodynamic quantities of solvation for monoatomic monovalent ions in aqueous solutions
[AD-A250190] p 3893 N92-31316
Role of the double-layer cation on the potential-dependent stretching frequencies and binding geometries of carbon monoxide at platinum-nonaqueous interfaces
[AD-A246980] p 3784 N92-31998
ELECTROMAGNETIC ABSORPTION
Photon absorption and the decay of surface excitation on sapphire (1120)-(3 x 1)
[DE92-011533] p 3910 N92-31661
Absorption spectra and electronic properties of alkali metal doped C60
[AD-A251006] p 3912 N92-31937
Electronic structure and photophysical properties of polyimides
[DE92-012353] p 3797 N92-32146
ELECTROMAGNETIC FIELDS
Modeling arbitrarily directed slots that are narrow both in width and depth with regard to the FDTD spatial cell
[DE92-008015] p 3808 N92-31738
Extremely Low Frequency (ELF) communications system ecological monitoring program summary of 1990 progress
[AD-A246344] p 3809 N92-31996
ELECTROMAGNETIC INTERACTIONS
Submillimeter wave spectroscopy of heterojunction superlattices
[AD-A250835] p 3908 N92-31496
ELECTROMAGNETIC INTERFERENCE
Electronics and electrical engineering laboratory technical publication announcements covering laboratory programs, July to September 1991, with 1992 EEEL events calendar
[PB92-181239] p 3813 N92-31367
ELECTROMAGNETIC PROPERTIES
Extremely Low Frequency (ELF) communications system ecological monitoring program summary of 1990 progress
[AD-A246344] p 3809 N92-31996
ELECTROMAGNETIC PULSES
Calculational prediction of ultrawideband electromagnetic pulses by laser-initiated air avalanche switches
[DE92-011732] p 3812 N92-31334
Mitigation of magnetohydrodynamic electromagnetic pulse (MHD-EMP) effects from commercial electric power systems
[AD-A249577] p 3804 N92-31354
Design of a TEM cell EMP simulator
[DREO-1084] p 3806 N92-31470
Subnanosecond photoconductive switching in GaAs
[DE92-011521] p 3910 N92-31719
Ionospheric communications channel modelling
[DE92-013039] p 3808 N92-31722
ELECTROMAGNETIC RADIATION
Algorithms for the determination of spatial and spectral distribution of electromagnetic energy in a simulated biostructure subjected to transient spatially heterogeneous radiation with applications to radar hazard assessment and cancer therapy
[AD-A250447] p 3805 N92-31381
Design of a TEM cell EMP simulator
[DREO-1084] p 3806 N92-31470
Changes in the reflectance of ex situ leaves: A methodological approach
[INPE-5407-PUD/051] p 3806 N92-31568
Scattering from a finite collection of transverse dipole and axial slot arrays with edge effects
[AD-A249622] p 3807 N92-31691
ELECTROMAGNETIC SCATTERING
Electromagnetic scattering by coated convex surfaces and wedges simulated by approximate boundary conditions
[NASA-CR-190540] p 3803 N92-31238
Scattering from a finite collection of transverse dipole and axial slot arrays with edge effects
[AD-A249622] p 3807 N92-31691
ELECTROMAGNETIC WAVE TRANSMISSION
Energy balance model for imagery and electromagnetic propagation
[AD-A250884] p 3806 N92-31543
ELECTROMAGNETISM
Validation of the Numerical Electro-magnetics Code (NEC) for antenna wire elements in proximity to Earth
[AD-A250507] p 3810 N92-32043
ELECTRON ACCELERATION
The physical solution to the Lorentz-Dirac equations in a constant magnetic field
[DE92-013299] p 3890 N92-32140
ELECTRON AFFINITY
Ionization potentials and electron affinities of semiconductor clusters determined via charge transfer reactions
[AD-A250943] p 3898 N92-32169
ELECTRON ATTACHMENT
Temperature-enhanced autodetachment from long-lived parent negative ions of gaseous dielectrics
[DE92-011108] p 3894 N92-31700
Dissociative electron attachment of O2: A solid-state effect on potential curve crossing
[AD-A246331] p 3913 N92-31995
ELECTRON BEAMS
Pulse-by-pulse energy measurement at the Stanford Linear Collider
[DE92-011520] p 3899 N92-31390
Microwave generation for magnetic fusion energy applications
[DE92-011424] p 3831 N92-31769
Theory for the CEBAF infrared and shipboard FELS
[AD-A252174] p 3832 N92-32061
Scaling of IFR propagation physics with beam/channel parameters
[DE92-015389] p 3900 N92-32123
Conversion of power and frequency
[DE92-012543] p 3810 N92-32134
The physical solution to the Lorentz-Dirac equations in a constant magnetic field
[DE92-013299] p 3890 N92-32140
ELECTRON BUNCHING
Calculations of emittance and damping time effects in the SLC damping rings
[DE92-012420] p 3900 N92-32133
Conversion of power and frequency
[DE92-012543] p 3810 N92-32134
ELECTRON CAPTURE
Theoretical atomic collision physics
[DE92-013571] p 3895 N92-31724

ELECTRON CYCLOTRON HEATING
Microwave generation for magnetic fusion energy applications
[DE92-011424] p 3831 N92-31769
Millimeter wave free electron laser amplifiers: Experiments and designs
[DE92-011813] p 3832 N92-31935
ELECTRON DENSITY (CONCENTRATION)
Characterization of oxides for low temperature solid oxide fuel cells
[PB92-152883] p 3848 N92-31903
ELECTRON ENERGY
Time and space resolved electron impact excitation rates in an RF glow discharge
[AD-A249614] p 3905 N92-31688
Electronic states in systems of reduced dimensionality
[DE92-013588] p 3912 N92-31945
ELECTRON FLUX DENSITY
Interaction of fast steady flow with slow transient flow: A new cause of interplanetary Bz events
[AD-A250273] p 3823 N92-31770
ELECTRON GUNS
Compact millimeter-wave devices: Dielectric loaded carm, high voltage carm, slow wave crm and high harmonic gyrotron
[AD-A250497] p 3809 N92-31944
The polarized electron gun for the SLC
[DE92-012418] p 3900 N92-32131
ELECTRON IMPACT
Electron impact excitation of positive ions: Partial wave approach in Coulomb-Eikonal approximation
[NIFS-106] p 3892 N92-31255
Time and space resolved electron impact excitation rates in an RF glow discharge
[AD-A249614] p 3905 N92-31688
UV photochemistry of trivinylantimony adsorbed on quartz
[AD-A252215] p 3785 N92-32057
ELECTRON MICROSCOPES
High brightness x ray source for directed energy and holographic imaging applications, phase 2
[AD-A248858] p 3827 N92-31475
Edge-on ion irradiation of electron microscope specimens
[DE92-014847] p 3894 N92-31595
ELECTRON MICROSCOPY
Edge-on ion irradiation of electron microscope specimens
[DE92-014847] p 3894 N92-31595
Imaging and spectrometry of bulk crystal surfaces and surface dynamical processes at high temperatures
[DE92-015235] p 3913 N92-32085
Incoherence effects in reflection electron microscopy
[DE92-016161] p 3829 N92-32086
ELECTRON PARAMAGNETIC RESONANCE
Many body perturbation theory using a Restricted Open-Shell Hartree-Fock (ROHF) reference function
[AD-A249725] p 3894 N92-31673
ELECTRON SCATTERING
Problems in neutrino electron scattering with 1-GeV neutrinos
[DE92-013535] p 3895 N92-31765
Electron scattering by atomic hydrogen: Elastic and inelastic phenomena at 13.9 to 200 eV
[DE92-625004] p 3896 N92-31837
ELECTRON SPECTROSCOPY
Auger line shapes as a probe of electronic structure in covalent systems
[AD-A246329] p 3912 N92-31994
Imaging and spectrometry of bulk crystal surfaces and surface dynamical processes at high temperatures
[DE92-015235] p 3913 N92-32085
ELECTRON STATES
Many body perturbation theory using a Restricted Open-Shell Hartree-Fock (ROHF) reference function
[AD-A249725] p 3894 N92-31673
Electronic states in systems of reduced dimensionality
[DE92-013588] p 3912 N92-31945
ELECTRON TRANSFER
Charge transfer processes in multiple site chemical systems
[AD-A249538] p 3791 N92-31358
Ultrafast experiments on the role of vibrational modes in electron transfer
[AD-A250630] p 3910 N92-31699
Vibrational modes and the dynamic solvent effect in electron and proton transfer
[AD-A250727] p 3897 N92-31950
Ultrafast studies on electron transfer in the betaines: Evidence for local heating
[AD-A250728] p 3897 N92-31999
ELECTRONIC EQUIPMENT
The sixteenth annual electronics manufacturing seminar proceedings
[AD-A247920] p 3814 N92-31461
The 193-pixel, three-dimensional capacitance imaging system
[DE92-001253] p 3919 N92-31731
A ban on use of lead-bearing solders: Implications for the electronics industry
[DE92-013291] p 3790 N92-32139
ELECTRONIC EQUIPMENT TESTS
New technology for remote testing of response time of installed thermocouples. Volume 2: Research data
[AD-A245821] p 3826 N92-31298
ELECTRONIC MAIL
Multimedia electronic mail: Standards and performance simulation
[AD-A250047] p 3808 N92-31809
ELECTRONIC MODULES
A data processing module for acoustic Doppler current meters
[AD-A250901] p 3891 N92-31563
ELECTRONIC PACKAGING
High-performance packaging for monolithic microwave and millimeter-wave integrated circuits
[NASA-TM-105744] p 3808 N92-31855
ELECTRONS
Ionization potentials and electron affinities of semiconductor clusters determined via charge transfer reactions
[AD-A250943] p 3898 N92-32169
ELECTROPHYSIOLOGY
The effects of hydrazines of neuronal excitability
[AD-A247142] p 3868 N92-31491
ELECTROPLATING
A fast laser alloying process for the selective electroplating of metal on SiO2 and polyimide
[DE92-011764] p 3788 N92-31759
ELECTROSTATIC PROBES
Electrostatic turbulence and transport in the RFP edge
[DE92-014322] p 3905 N92-31730
Power scaling of divertor plasma conditions during H-mode in D3-D
[DE92-012148] p 3906 N92-31771
Plasma channel generation using low energy electron beams
[DE92-013770] p 3906 N92-31949
ELECTROSTATICS
New high voltage parallel plate analyzer
[NIFS-128] p 3827 N92-31340
Electrostatic turbulence and transport in the RFP edge
[DE92-014322] p 3905 N92-31730
ELEVATION ANGLE
Analysis of random induced cross polarization
[AD-A249773] p 3806 N92-31569
ELEVATORS (CONTROL SURFACES)
The icing of the elevator of the DLR icing research aircraft of Do 28 type
[DLR-MITT-91-12] p 3755 N92-31813
ELLIPTIC FUNCTIONS
An investigation of spinup dynamics of axial gyrostats using elliptic integrals and the method of averaging
[AD-A249728] p 3768 N92-31675
EMBEDDING
The multicomputer toolbox: Scalable parallel libraries for large-scale concurrent applications
[DE92-008068] p 3882 N92-31740
EMERGENCIES
Immersion suit usage within the RAAF
[AD-A250645] p 3755 N92-31562
EMISSION
Development of methodology and technology for identifying and quantifying emission products from open burning and open detonation thermal treatment methods. BangBox test series. Volume 1. Test summary
[AD-A250733] p 3800 N92-31969
Development of methodology and technology for identifying and quantifying emission products from open burning and open detonation thermal treatment methods. BangBox test series. Volume 2: Test development
[AD-A250734] p 3800 N92-31970
Development of methodology and technology for identifying and quantifying emission products from open burning and open detonation thermal treatment methods. Field test series A, B, and C. Volume 2, part A: Quality assurance and quality control
[AD-A250736] p 3801 N92-31972
Development of methodology and technology for identifying and quantifying emission products from open burning and open detonation thermal treatment methods. Field test series A, B, and C. Volume 2, part B: Quality assurance and quality control. Appendices
[AD-A250737] p 3801 N92-31973
EMISSION SPECTRA
Real-time infrared spectroscopy of moving solids for on-line analyses
[DE92-012156] p 3782 N92-31772
The potential of passive-remote Fourier Transform Infrared (FTIR) spectroscopy to detect organic emissions under the Clean Air Act
[DE92-015224] p 3854 N92-32083
EMISSIVITY
Emissivity measurements in support of experiments on natural convection between a vertical cylinder and a surrounding array
[DE92-012321] p 3819 N92-31287
EMITTANCE
An evaluation of ionizing radiation emitted by high power microwave generators
[DE92-016160] p 3805 N92-31387
Calculations of emittance and damping time effects in the SLC damping rings
[DE92-012420] p 3900 N92-32133
EMITTERS
Effect of guard band reduction on marker beacon receiver performance
[DOT/FAA/CT-TN92/18] p 3807 N92-31617
EMOTIONS
Theory and test of stress resistance
[AD-A250741] p 3870 N92-31291
EMULSIONS
Experimental evaluation of oxygen-enriched air and emulsified fuels in a single-cylinder diesel engine. Volume 1: Concept evaluation
[DE92-015999] p 3799 N92-31442
ENAMELS
Development of an electrochemical method for field testing of protective coatings
[AD-A245872] p 3793 N92-31473
ENERGETIC PARTICLES
The interplanetary heavy ion environment for both galactic cosmic rays and solar energetic particles during the CRRES mission
[AD-A248942] p 3926 N92-31477
Injecting into AmPS when ring cavity operates at 476 MHz
[NIKHEF-K/AMPS/91-08] p 3899 N92-31815
Experimental particle physics at the University of Pittsburgh
[DE92-016182] p 3896 N92-31926
ENERGY BUDGETS
Effects of anthropogenic sulfur aerosols on climate
[DE92-016158] p 3850 N92-31297
Energy balance model for imagery and electromagnetic propagation
[AD-A250884] p 3806 N92-31543
User's guide for treetherm: A 3-D thermal model for single trees
[LTR91-003] p 3879 N92-31833
ENERGY CONSERVATION
Energy conservation: The main factor for reducing greenhouse gas emissions in the former Soviet Union
[DE92-012355] p 3852 N92-31574
ENERGY CONSUMPTION
World energy projection system: Model documentation
[DE92-014206] p 3847 N92-31594
Global trends in energy use: Indications for research
[DE92-014773] p 3855 N92-32155
ENERGY CONVERSION
Sodium Heat Engine Development Program
[DE92-012398] p 3846 N92-31531
Light alkane conversion processes: Suprabiotic catalyst systems for selective oxidation of light alkane gases to fuel oxygenates
[DE92-015229] p 3799 N92-31751
Probe molecule studies: Active species in alcohol synthesis
[DE92-015430] p 3784 N92-32029
ENERGY CONVERSION EFFICIENCY
Module process optimization and device efficiency improvement for stable, low-cost, large-area, cadmium telluride-based photovoltaic module production
[DE92-010564] p 3846 N92-31497
Energy conservation: The main factor for reducing greenhouse gas emissions in the former Soviet Union
[DE92-012355] p 3852 N92-31574
Advanced high efficiency concentrator cells
[DE92-010559] p 3848 N92-31893
Monolithic and mechanical multijunction space solar cells
[NASA-TM-105832] p 3818 N92-32233
ENERGY DISSIPATION
Injecting into AmPS when ring cavity operates at 476 MHz
[NIKHEF-K/AMPS/91-08] p 3899 N92-31815
Electronic states in systems of reduced dimensionality
[DE92-013588] p 3912 N92-31945
A self consistent generalized model for the calculation of minor loop excursions in the theory of hysteresis
[DE92-014394] p 3890 N92-32116
Reynolds stress calculations of homogeneous turbulent shear flow with bounded energy states
[NASA-CR-189682] p 3826 N92-32158

ENERGY GAPS (SOLID STATE)
International Semiconductor Device Research Symposium (ISDRS-91)
[AD-A247394] p 3908 N92-31537
ENERGY LEVELS
Rigid rotations in two-electron atoms in a uniform magnetic field
[DE92-624981] p 3896 N92-31836
Exotic nuclear shapes and configurations that can be studied at high spin using radioactive ion beams
[DE92-016800] p 3898 N92-32090
ENERGY SPECTRA
Use of tissue equivalent proportional counters to characterize radiation quality on the space shuttle
[DE92-012347] p 3768 N92-31846
ENERGY STORAGE
Chemical energy storage system for SEGS solar thermal power plant
[DE92-012327] p 3848 N92-31845
Solar thermal energy storage in phase change materials
[DE92-016908] p 3849 N92-32091
ENERGY TECHNOLOGY
Space nuclear power, propulsion, and related technologies
[SAND91-2617] p 3770 N92-31503
The 193-pixel, three-dimensional capacitance imaging system
[DE92-001253] p 3919 N92-31731
ENERGY TRANSFER
Advanced DAA methods for shock response analysis
[AD-A252696] p 3891 N92-31588
The chemistry and packaging of nanocomposite confined arrays
[AD-A250991] p 3817 N92-32002
Energy transport in the steady state plasma sustained by DC helicity current drive
[NIFS-127] p 3907 N92-32181
ENGINE CONTROL
Subsonic flight test evaluation of a performance seeking control algorithm on an F-15 airplane
[NASA-TM-4400] p 3759 N92-31275
A demonstration of an intelligent control system for a reusable rocket engine
[NASA-TM-105794] p 3770 N92-31507
ENGINE DESIGN
Free-piston Stirling engine conceptual design and technologies for space power, phase 1
[NASA-CR-182168] p 3769 N92-31245
Solid rocket combustion phenomena
[AD-A248006] p 3770 N92-31474
Sodium Heat Engine Development Program
[DE92-012398] p 3846 N92-31531
Gas engine heat recovery unit
[PB92-184373] p 3835 N92-31841
Orbital transfer rocket engine technology: Advanced engine study
[NASA-CR-187216] p 3771 N92-32129
ENGINE FAILURE
A demonstration of an intelligent control system for a reusable rocket engine
[NASA-TM-105794] p 3770 N92-31507
ENGINE MONITORING INSTRUMENTS
Engine monitoring display study
[NASA-CR-4463] p 3761 N92-32175
ENGINE PARTS
Research into improving the durability of the hot section in the aircraft turbine engine
[AD-A250342] p 3759 N92-31439
Life prediction and constitutive models for engine hot section anisotropic materials program
[NASA-CR-189222] p 3759 N92-31534
ENGINE TESTS
Gas engine heat recovery unit
[PB92-184373] p 3835 N92-31841
Low-Isp derated ion thruster operation
[NASA-TM-105787] p 3771 N92-32237
ENGLISH LANGUAGE
Correspondence dictionary from free English term to INIS descriptors
[DE92-782192] p 3920 N92-31859
ENRICHMENT
Experimental evaluation of oxygen-enriched air and emulsified fuels in a single-cylinder diesel engine. Volume 1: Concept evaluation
[DE92-015999] p 3799 N92-31442
ENTRAINMENT
Amending the w* velocity scale for surface layer, entrainment zone, and baroclinic shear in mixed Forced/Free turbulent convection
[AD-A250389] p 3859 N92-31540
ENTROPY
Geometric theory of infinite dimensional dynamical systems
[AD-A252190] p 3915 N92-31585
ENVIRONMENT EFFECTS
Numerical simulation of precipitation scavenging and comparison with observation of prescribed forest fires
[DE92-013513] p 3851 N92-31423
Wind tunnel aerodynamic characteristics of a transport-type airfoil in a simulated heavy rain environment
[NASA-TP-3184] p 3751 N92-31532
Acid deposition: State of science and technology. Summary report of the US National Acid Precipitation Assessment Program, volumes 1-4
[PB92-100353] p 3852 N92-31598
Methods of assessing responses of trees, stands and ecosystems to air pollution
[PB92-180231] p 3853 N92-31648
Multi-year strategic plan for the atmospheric studies in complex terrain: ASCOT program
[DE92-016646] p 3854 N92-31930
NASA High Speed Research Program, Emissions Scenarios Committee report of meetings on 26 September 1991 and 9 January 1992
[NASA-CR-190379] p 3855 N92-32147
ENVIRONMENT MANAGEMENT
EnviroTRADE: A technical perspective on the development of an information system providing data on environmental technologies and needs worldwide
[DE92-012625] p 3919 N92-31578
Development of methodology and technology for identifying and quantifying emission products from open burning and open detonation thermal treatment methods. Field test series A, B, and C. Volume 2, part A: Quality assurance and quality control
[AD-A250736] p 3801 N92-31972
ENVIRONMENT MODELS
A test of ecological optimality for semiarid vegetation
[NASA-CR-190705] p 3855 N92-32222
ENVIRONMENT POLLUTION
Anti-environmental warfare: Protecting the environment during wartime
[AD-A250337] p 3851 N92-31556
Global trends in energy use: Indications for research
[DE92-014773] p 3855 N92-32155
ENVIRONMENT PROTECTION
EnviroTRADE: Its role in the cleanup of the environment
[DE92-013691] p 3851 N92-31427
Anti-environmental warfare: Protecting the environment during wartime
[AD-A250337] p 3851 N92-31556
Our Changing Planet: The FY 1993 US Global Change Research Program. A report by the Committee on Earth and Environmental Sciences, a supplement to the US President's fiscal year 1993 budget
[PB92-156892] p 3852 N92-31620
Proceedings of the 4th Atlantic OCS Region Information Transfer Meeting
[PB92-177690] p 3864 N92-31630
Evolution of environmental protection strategies in the Soviet Union
[DE92-015090] p 3853 N92-31732
Development of methodology and technology for identifying and quantifying emission products from open burning and open detonation thermal treatment methods. Field test series A, B, and C. Volume 2, part B: Quality assurance and quality control. Appendices
[AD-A250737] p 3801 N92-31973
ENVIRONMENT SIMULATION
Development of quantitative specifications for simulating the stress environment
[AD-A250669] p 3870 N92-31321
Wind tunnel aerodynamic characteristics of a transport-type airfoil in a simulated heavy rain environment
[NASA-TP-3184] p 3751 N92-31532
ENVIRONMENT SIMULATORS
Application of Free-Air CO2 Enrichment (FACE) technology to a forest canopy: A simulation study
[DE92-013308] p 3851 N92-31422
ENVIRONMENTAL CHEMISTRY
Acid deposition: State of science and technology. Summary report of the US National Acid Precipitation Assessment Program, volumes 1-4
[PB92-100353] p 3852 N92-31598
Inorganic rings on carbon chains
[AD-A251043] p 3772 N92-31850
ENVIRONMENTAL MONITORING
Iterative functionalism and climate management regimes: From intergovernmental panel on climate change to intergovernmental negotiating committee
[DE92-014798] p 3853 N92-31896
Extremely Low Frequency (ELF) communications system ecological monitoring program summary of 1990 progress
[AD-A246344] p 3809 N92-31996
ENVIRONMENTAL QUALITY
Our changing planet: The FY 1993 US global change research program. A supplement to the US President's fiscal year 1993 budget
[NASA-CR-190675] p 3850 N92-31259
Evolution of environmental protection strategies in the Soviet Union
[DE92-015090] p 3853 N92-31732
ENZYMES
Evolution and analysis of the functional domains of the chimeric proteins that initiate pyrimidine biosynthesis
[AD-A250069] p 3866 N92-31465
EPHEMERIDES
The eclipsing cataclysmic variable AY Piscium
[INPE-5340-PRE/1739] p 3923 N92-31345
EPIDEMIOLOGY
JPRS report: Science and technology. Central Eurasia: Life sciences
[JPRS-ULS-92-015] p 3924 N92-32179
EPITAXY
He atom-surface scattering: Surface dynamics of insulators, overlayers and crystal growth
[DE92-011810] p 3911 N92-31914
Epitaxial iron films
[AD-A250402] p 3912 N92-31915
EPOXY MATRIX COMPOSITES
Role of interfaces and interphases in the evolution mechanics of material systems
[AD-A250410] p 3774 N92-31604
Flammability characteristics of glass reinforced epoxy composite materials
[AD-A251009] p 3775 N92-31940
EQUATIONS OF MOTION
Modal simulation of gearbox vibration with experimental correlation
[NASA-TM-105702] p 3834 N92-31485
Backlash control via redundant drives: An experimental verification
[DE92-016368] p 3835 N92-31929
Scaling of IFR propagation physics with beam/channel parameters
[DE92-015389] p 3900 N92-32123
EQUATIONS OF STATE
CAVEAT: A computer code for fluid dynamics problems with large distortion and internal slip
[DE92-014078] p 3825 N92-32022
EQUATORIAL REGIONS
The effects of magnetic storm phases on F-layer irregularities from auroral to equatorial latitudes
[AD-A249011] p 3855 N92-31478
An analysis of hydrographic data collected off Point Sur, California in June 1990
[AD-A246060] p 3866 N92-32056
EQUILIBRIUM METHODS
Non-convex problems in PDE: Equilibrium theory and dynamics
[AD-A250549] p 3887 N92-32081
EQUIVALENCE
A fundamental notion of equivalence for linear multivariable systems
[MATHS-REPT-A-153] p 3887 N92-31957
ERGODIC PROCESS
Independent sampling of a stochastic process
[AD-A249712] p 3888 N92-31600
EROSION
Dynamic modeling of plasma-vapor interactions during plasma disruptions
[DE92-016183] p 3903 N92-31310
Divertor material evaluation system at D3-D
[DE92-013696] p 3905 N92-31749
ERROR ANALYSIS
Reducing requirements errors through the use of Computer-Aided Software Engineering (CASE) tools and during requirements analysis
[AD-A246879] p 3874 N92-31299
Oscillating-flow regenerator test rig: Woven screen and metal felt results
[NASA-CR-190689] p 3820 N92-31352
Data parallel programming
[DE92-013981] p 3882 N92-31466
A simple linearized learning algorithm which outperforms back-propagation
[AD-A249697] p 3877 N92-31642
A continuing study of altitude determination deficiencies of the Service Aircraft Instrumentation Package (SAIP)
[AD-A245952] p 3758 N92-32051
Problems with interleaved digitizers
[DE92-013369] p 3881 N92-32150
ERROR DETECTION CODES
Problems with interleaved digitizers
[DE92-013369] p 3881 N92-32150
ERRORS
Procedures and errors in the determination of the bi-directional reflectance factor and other radiometric quantities
[INPE-5386-TDI/475] p 3843 N92-31277

Reducing requirements errors through the use of Computer-Aided Software Engineering (CASE) tools and during requirements analysis
[AD-A246879] p 3874 N92-31299
Signal and noise models arising from the theory of errors
[AD-A250222] p 3865 N92-31827
Artificial neural network implementation of a near-ideal error prediction controller
[NASA-CR-190694] p 3860 N92-32122

ERYTHROCYTES
Biodosimetry of ionizing radiation in humans using the glycophorin A genotoxicity assay
[DE92-011974] p 3869 N92-31608

ESTIMATES
Sun-view-target geometry effects on spectrally-derived vegetative index estimates of absorbed radiation and leaf area
[AD-A249984] p 3843 N92-31329
Estimation with multisensor/multiscan detection fusion
[AD-A250496] p 3804 N92-31333
Confidence interval estimation for output of discrete-event simulations using the Kalman filter
[AD-A248170] p 3880 N92-31991
Effects of fragmentation parameter variations on estimates of galactic cosmic ray exposure: Dose sensitivity studies for aluminum shields
[NASA-TM-4386] p 3926 N92-32193

ESTIMATING
Estimation with multisensor/multiscan detection fusion
[AD-A250496] p 3804 N92-31333
Two properties of uniform distributions, with applications to some nonparametric estimation problems
[REPT-91-94] p 3888 N92-31518
Nonparametric estimation in renewal theory, 1: The empirical renewal function
[REPT-91-95] p 3888 N92-31519
Analytic estimation of radiation effects in space using solid angles
[DE92-013282] p 3899 N92-31831
Confidence interval estimation for output of discrete-event simulations using the Kalman filter
[AD-A248170] p 3880 N92-31991
Determination of the matrix conditioning indicator. Comparison of approximate methods
p 3887 N92-32210

ETCHING
Metallization of ferrite ceramic couplings
[DE92-016573] p 3789 N92-32032
Movement of dislocations in quartz
[AD-A250527] p 3913 N92-32078

ETHANE
Light alkane conversion processes: Suprabiotic catalyst systems for selective oxidation of light alkane gases to fuel oxygenates
[DE92-015229] p 3799 N92-31751

ETHERS
High-temperature ignition of propane with MTBE as an additive: Shock-tube experiments and modeling
[DE92-008933] p 3778 N92-31415
Imide/arylene ether copolymers
[NASA-CASE-LAR-14159-1-CU] p 3794 N92-31792

ETHYL ALCOHOL
Analysis and computer tools for separation processes involving nonideal mixtures
[DE92-015298] p 3781 N92-31752
Unimolecular reaction mechanisms involving C3H4, C4H4, and C6H6 hydrocarbon species
[DE92-005326] p 3783 N92-31860

ETHYLENE
Diosmacycloalkanes as models for the formation of hydrocarbons from surface methylenes
[DE92-014588] p 3783 N92-31891

EULER EQUATIONS OF MOTION
Meteorological data, new series A monographs. Volume 5, no. 4: A three dimensional model simulation of the circulation in the middle atmosphere with cconsideration of tropospherical-stratospherical interactions
[ETN-92-91693] p 3861 N92-31708
Euler solver for arbitrary configurations: Further applications p 3750 N92-31888
An installed nacelle design code using a multiblock Euler solver. Volume 1: Theory document
[NASA-CR-189652-VOL-1] p 3754 N92-32226
An installed nacelle design code using a multiblock Euler solver. Volume 2: User guide
[NASA-CR-189652-VOL-2] p 3754 N92-32228

EUROPEAN SPACE AGENCY
Partnership in space: An introduction to Canada's special relationship with the European Space Agency
[ESA-BR-79] p 3922 N92-31947

EUROPEAN SPACE PROGRAMS
Partnership in space: An introduction to Canada's special relationship with the European Space Agency
[ESA-BR-79] p 3922 N92-31947

EUTECTICS
Solar thermal energy storage in phase change materials
[DE92-016908] p 3849 N92-32091

EVALUATION
Aviation safety: Changes needed in FAA's service difficulty reporting program
[GAO/RCED-91-24] p 3755 N92-31453
Minorities and air quality non-attainment areas: A preliminary geo-demographic analysis
[DE92-013054] p 3852 N92-31591
Divertor material evaluation system at D3-D
[DE92-013696] p 3905 N92-31749
Estimation of aircraft attitude by angular rate measurements p 3748 N92-31881

EVAPORATION
Transport and evaporation effects in counterflow spray diffusion flames p 3749 N92-31884

EVAPORATORS
Pressure loss and heat transfer in a toothed finned heat transfer medium
[MBB-UO-0163-91-PUB] p 3915 N92-31660

EXCIMER LASERS
Pulsed laser deposition of high Tc superconducting thin films
[AD-A250657] p 3830 N92-31319
UV photochemistry of trivinylantimony adsorbed on quartz
[AD-A252215] p 3785 N92-32057

EXCITATION
Electron impact excitation of positive ions: Partial wave approach in Coulomb-Eikonal approximation
[NIFS-106] p 3892 N92-31255
Photon absorption and the decay of surface excitation on sapphire (1120)-(3 x 1)
[DE92-011533] p 3910 N92-31661
Laser enhanced chemical reaction studies
[DE92-010772] p 3831 N92-31798
Turbine blade tip and seal clearance excitation forces
[NASA-CR-184341] p 3760 N92-31910
Alterations of multiphoton-resonant processes through wave-mixing effects
[DE92-016164] p 3896 N92-31923

EXCITONS
Theory of semiconducting superlattices and microstructures
[AD-A248758] p 3816 N92-31799

EXERCISE PHYSIOLOGY
Preliminary development of a protocol for determining heat stress caused by clothing
[DREO-PSD-EPS-05/89] p 3873 N92-32031

EXHAUST EMISSION
NASA High Speed Research Program, Emissions Scenarios Committee report of meetings on 26 September 1991 and 9 January 1992
[NASA-CR-190379] p 3855 N92-32147

EXPERIMENT DESIGN
Millimeter wave free electron laser amplifiers: Experiments and designs
[DE92-011813] p 3832 N92-31935

EXPERIMENTATION
Solar neutrinos: Theory versus experiment
[DE92-014327] p 3925 N92-32154

EXPERT SYSTEMS
Data to test and evaluate the performance of neural network architectures for seismic signal discrimination, neural computing for seismic phase identification, volume 2
[AD-A252442] p 3884 N92-31293
Automated payload experiment tool feasibility study
[NASA-CR-184256] p 3883 N92-31835
Development of a fault isolation system database manager
[AD-A248346] p 3916 N92-31992
Use of expert systems as user interfaces in information retrieval p 3921 N92-32185
Proceedings of the 53rd Symposium on Air Vehicle Mission Control and Management
[AGARD-AR-310] p 3889 N92-32229

EXPLOSIONS
Two-dimensional axisymmetric calculations of surface waves generated by an explosion in an island, mountain, and sedimentary basin
[AD-A249971] p 3856 N92-31510
Turbulent dusty boundary layer in an ANFO surface-burst explosion
[DE92-012101] p 3822 N92-31625
Energy and Environment: A Sandia Technology Bulletin
[DE92-016740] p 3854 N92-31931

EXPLOSIVES
The collection, handling, transportation, and thermal desorption of explosive vapor using quartz collection tubes
[DE92-011441] p 3799 N92-31570
Selective nitrations: The laser-induced nitration of three cycloalkanes, 1
[AD-A249942] p 3800 N92-31800
Development of methodology and technology for identifying and quantifying emission products from open burning and open detonation thermal treatment methods. Field test series A, B, and C. Volume 1: Test summary
[AD-A250735] p 3800 N92-31971
Development of methodology and technology for identifying and quantifying emission products from open burning and open detonation thermal treatment methods. Field test series A, B, and C. Volume 2, part B: Quality assurance and quality control. Appendices
[AD-A250737] p 3801 N92-31973
Estimation of metal acceleration by an SF5 containing explosive
[AD-A245338] p 3801 N92-32098

EXPONENTIAL FUNCTIONS
On a characterization of the exponential distribution based on a type 2 right censored sample
[CWI-BS-R9117] p 3888 N92-31517
Continuous time and discrete time hyperexponential model for dependability growth modeling
[LAAS-92002] p 3837 N92-31693

EXPOSURE
Characterization of oxide formed on silicon by exposure to atomic oxygen in space
[AD-A249787] p 3778 N92-31301
Outdoor testing of advanced optical materials for solar thermal electric applications
[DE92-010567] p 3847 N92-31623
Analysis of systems hardware flown on LDEF. Results of the systems special investigation group
[NASA-CR-189628] p 3767 N92-31677
Static magnetic fields: A summary of biological interactions, potential health effects, and exposure guidelines
[DE92-015218] p 3867 N92-31711
Effects of fragmentation parameter variations on estimates of galactic cosmic ray exposure: Dose sensitivity studies for aluminum shields
[NASA-TM-4386] p 3926 N92-32193
Demonstrated survivability of a high temperature optical fiber cable on a 1500 pound thrust rocket chamber
[NASA-TM-105835] p 3801 N92-32230

EXTERNAL COMBUSTION ENGINES
External combustion engine technology (vapor and liquid cycles) for individual soldier power systems
[AD-A252754] p 3836 N92-32173

EXTERNAL STORES
An investigation into the interface between three closely spaced axi-symmetric bodies at subsonic speed
[CRANFIELD-AERO-9114] p 3751 N92-31514

EXTRACTION
Analysis and computer tools for separation processes involving nonideal mixtures
[DE92-015298] p 3781 N92-31752
Ceramic membranes for high temperature hydrogen separation
[DE92-013342] p 3783 N92-31816
Wavelet signal processing for transient feature extraction
[AD-A250519] p 3890 N92-32046
Real time detection in a laser bathymetry system
[PB92-195452] p 3866 N92-32069

EXTRATERRESTRIAL LIFE
Methane-producing microorganisms: Component of Mars biosphere p 3924 N92-32180

EXTRATERRESTRIAL RADIATION
Combined Release and Radiation Effects Satellite (CRRES) experiments data collection, analysis, and publication
[NASA-CR-184361] p 3856 N92-31551
Relating space radiation environments to risk estimates
[DE92-010256] p 3926 N92-31756

EXTRATERRESTRIAL RESOURCES
Using space resources
[NASA-TM-107966] p 3924 N92-31781

EXTREME ULTRAVIOLET EXPLORER SATELLITE
True covariance simulation of the EUVE (extreme ultra violet explorer) update filter p 3748 N92-31878

EXTREMELY LOW FREQUENCIES
Extremely Low Frequency (ELF) communications system ecological monitoring program summary of 1990 progress
[AD-A246344] p 3809 N92-31996

EXTRUDING
Corrosion behavior of squeeze cast aluminum metal matrix composites
[AD-A250486] p 3774 N92-31382

EYE MOVEMENTS
Space constancy on video display terminals
[AD-A247290] p 3872 N92-32105

F

F REGION
The effects of magnetic storm phases on F-layer irregularities from auroral to equatorial latitudes
[AD-A249011] p 3855 N92-31478

F-15 AIRCRAFT
Subsonic flight test evaluation of a performance seeking control algorithm on an F-15 airplane
[NASA-TM-4400] p 3759 N92-31275

F-18 AIRCRAFT
In-flight leading-edge extension vortex flow-field survey measurements on a F-18 aircraft at high angle of attack
[NASA-TM-4398] p 3751 N92-31276

F-8 AIRCRAFT
Transonic wind tunnel test of a 14 percent thick oblique wing
[NASA-TM-102230] p 3754 N92-32213

FABRICATION
Corrosion behavior of squeeze cast aluminum metal matrix composites
[AD-A250486] p 3774 N92-31382
Prototype casting fabrication by stereolithography
[DE92-011489] p 3876 N92-31529
Ceramic surfaces and sintering
[DE92-011570] p 3793 N92-31538
MHD Contractors' Review Meeting: Abstracts
[DE92-011549] p 3904 N92-31576
Design and development of minilink video: A fiber-optic coupled video system
[AD-A249945] p 3808 N92-31801
Gas engine heat recovery unit
[PB92-184373] p 3835 N92-31841
Fabrication of an insulated gate diamond FET for high temperature applications
[AD-A251042] p 3817 N92-31849
Recent advances in high-temperature superconductor wire fabrication and applications development
[DE92-016634] p 3912 N92-31955
Metallization of ferrite ceramic couplings
[DE92-016573] p 3789 N92-32032
Design, fabrication, and testing of a 30 kW(sub t) screen-wick heat-pipe solar receiver
[DE92-016500] p 3848 N92-32087

FABRICS
High strength glass second source qualification to composite armor specification MIL-L-46197(MR)
[AD-A252114] p 3792 N92-31404
Polymer blends, volume 1
[AD-A252112] p 3792 N92-31419

FAILURE
Enhancement of fracture toughness using high intensity electric currents
[AD-A249809] p 3889 N92-31359
Motor-operated globe valve performance in a liquid sodium environment
[DE92-014456] p 3834 N92-31500

FAILURE ANALYSIS
Motor-operated globe valve performance in a liquid sodium environment
[DE92-014456] p 3834 N92-31500
Analysis of systems hardware flown on LDEF. Results of the systems special investigation group
[NASA-CR-189628] p 3767 N92-31677
Development of a fault isolation system database manager
[AD-A248346] p 3916 N92-31992
Composite failure analysis handbook. Volume 1: Program review
[AD-A250520] p 3776 N92-32047
Composite failure analysis handbook. Volume 2: Technical handbook. Part 1: Procedures and techniques
[AD-A250521] p 3776 N92-32048
Optimal design of geodesically stiffened composite cylindrical shells
[NASA-CR-190706] p 3842 N92-32235

FAILURE MODES
Motor-operated globe valve performance in a liquid sodium environment
[DE92-014456] p 3834 N92-31500
A demonstration of an intelligent control system for a reusable rocket engine
[NASA-TM-105794] p 3770 N92-31507
FCS skewed sensors array: Practical considerations
p 3746 N92-31868
Composite failure analysis handbook. Volume 1: Program review
[AD-A250520] p 3776 N92-32047
Composite failure analysis handbook. Volume 2: Technical handbook. Part 1: Procedures and techniques
[AD-A250521] p 3776 N92-32048

FALLOUT
Development of methodology and technology for identifying and quantifying emission products from open burning and open detonation thermal treatment methods. Field test series A, B, and C. Volume 1: Test summary
[AD-A250735] p 3800 N92-31971

FAR FIELDS
Near-field and far-field sound radiation from a line-driven fluid-loaded infinite flat plate having periodic and non-periodic attached rib stiffeners
[AD-A250100] p 3892 N92-31789

FAR INFRARED RADIATION
Submillimeter wave spectroscopy of heterojunction superlattices
[AD-A250835] p 3908 N92-31496

FARADAY EFFECT
Particle diagnostics in optically thick sprays
[AD-A250981] p 3897 N92-31936

FAST FOURIER TRANSFORMATIONS
Nonparametric estimation in renewal theory, 1: The empirical renewal function
[REPT-91-95] p 3888 N92-31519

FATIGUE (BIOLOGY)
Micro saint model of fatigue assessment
[AD-A249976] p 3868 N92-31554

FATIGUE (MATERIALS)
Analysis and prediction of Multiple-Site Damage (MSD) fatigue crack growth
[NASA-TP-3231] p 3838 N92-31279
A differential CDM model for fatigue of unidirectional metal matrix composites
[NASA-TM-105726] p 3840 N92-31505

FATIGUE LIFE
Cyclic hot firing results of tungsten-wire-reinforced, copper-lined thrust chambers
[NASA-TM-4214] p 3769 N92-31249
Life extending control for rocket engines
[NASA-TM-105789] p 3802 N92-31263
Research into improving the durability of the hot section in the aircraft turbine engine
[AD-A250342] p 3759 N92-31439
The influence of various spectrum parameters on fatigue life and residual stress relaxation
[FFA-TN-1991-44] p 3840 N92-31512
Life prediction and constitutive models for engine hot section anisotropic materials program
[NASA-CR-189222] p 3759 N92-31534
Role of interfaces and interphases in the evolution mechanics of material systems
[AD-A250410] p 3774 N92-31604
Aging fleet: Maintaining airworthiness
p 3745 N92-31862

FATIGUE TESTS
The influence of various spectrum parameters on fatigue life and residual stress relaxation
[FFA-TN-1991-44] p 3840 N92-31512
Cryogenic 4.4 MN mechanical test system for large scale tests of composite support struts
[PB92-181148] p 3774 N92-31609
Thermomechanical fatigue behavior of a silicone carbide fiber-reinforced calcium aluminosilicate glass-ceramic matrix composite
[AD-A249870] p 3775 N92-31823

FAULT TOLERANCE
Development of a fault isolation system database manager
[AD-A248346] p 3916 N92-31992
Fault tolerant parallel computing in orthogonal shared-memory and related architectures
[AD-A250504] p 3883 N92-32040

FEASIBILITY ANALYSIS
Computer-aided modeling tools for forging process feasibility studies
[DE92-012116] p 3838 N92-31303
Weld penetration and defect control
[DE92-015310] p 3836 N92-31336
Experimental testing of prototype face gears for helicopter transmissions
[NASA-TM-105434] p 3832 N92-31349
Feasibility study for a low-altitude wide and temperature profiler
[PB92-188200] p 3860 N92-31641
Application of reactor-pumped lasers to power beaming
[DE92-012370] p 3831 N92-31762
A detector for stationary gas bubbles: Feasibility studies
[AD-A250135] p 3828 N92-31794
Analytical and experimental studies of heat pipe radiation cooling of hypersonic propulsion systems
[DE92-013428] p 3759 N92-31817
Automated payload experiment tool feasibility study
[NASA-CR-184256] p 3883 N92-31835
Chemical energy storage system for SEGS solar thermal power plant
[DE92-012327] p 3848 N92-31845
An examination of the feasibility of a nuclear-pumped laser-driven inertial confinement fusion reactor with magnetically protected walls
[AD-A248163] p 3907 N92-31990
Laser-initiated conical detonation wave for supersonic combustion, part 3
[AD-A250522] p 3785 N92-32076

FEDERAL BUDGETS
Our changing planet: The FY 1993 US global change research program. A supplement to the US President's fiscal year 1993 budget
[NASA-CR-190675] p 3850 N92-31259

FEEDBACK
The impact of cognitive feedback on the performance of intelligence analysts
[AD-A252176] p 3871 N92-32063

FEEDBACK CONTROL
Subsonic flight test evaluation of a performance seeking control algorithm on an F-15 airplane
[NASA-TM-4400] p 3759 N92-31275
Adaptive and nonadaptive feedback control of global instabilities with application to a heated 2-D jet
[AD-A250700] p 3820 N92-31322
A comparison of three self-tuning control algorithms developed for the Bristol-Babcock controller
[DE92-014472] p 3814 N92-31499
A demonstration of an intelligent control system for a reusable rocket engine
[NASA-TM-105794] p 3770 N92-31507
Dynamics of shuttle based flexible antenna system
[CRANFIELD-AERO-9203] p 3840 N92-31516
Experimental feedback of fractional order states of a lightly damped structure
[AD-A248027] p 3842 N92-31989
A parameter optimization approach to controller partitioning for integrated flight/propulsion control application
[NASA-TM-105826] p 3761 N92-32241

FEEDFORWARD CONTROL
Analysis and design of neural networks
[AD-A250495] p 3864 N92-31332
The impact of cognitive feedback on the performance of intelligence analysts
[AD-A252176] p 3871 N92-32063

FERRITES
Improved ferrite biasing scheme for booster RF cavities
[DE92-011650] p 3815 N92-31664
Metallization of ferrite ceramic couplings
[DE92-016573] p 3789 N92-32032

FERROCENES
Organometallic Nonlinear Optical (NLO) polymers. Part 2: Synthesis of main-chain organometallic polymers and a structural study of ferrocene NLO-Phores
[AD-A250655] p 3791 N92-31318

FERROELECTRICITY
High temperature superconducting films and multilayers for electronics
[AD-A250732] p 3813 N92-31451
Ferroelectric thin films prepared by pulse laser deposition processing and characterization
[PB92-196088] p 3913 N92-32072

FERROMAGNETIC MATERIALS
A self consistent generalized model for the calculation of minor loop excursions in the theory of hysteresis
[DE92-014394] p 3890 N92-32116

FERROUS METALS
JPRS report: Science and technology. Central Eurasia: Materials science
[JPRS-UMS-92-010] p 3787 N92-31584

FEYNMAN DIAGRAMS
Feynman diagrams and Vassiliev invariants
[PB92-178284] p 3890 N92-31925

FIBER COMPOSITES
Cyclic hot firing results of tungsten-wire-reinforced, copper-lined thrust chambers
[NASA-TM-4214] p 3769 N92-31249
The 3-D analysis and verification of fracture growth mechanisms in fiber-reinforced ceramic composites
[AD-A250893] p 3773 N92-31305
Interface engineering in alumina/glass composites
[AD-A248587] p 3773 N92-31315
Polymer blends, volume 1
[AD-A252112] p 3792 N92-31419
Role of interfaces and interphases in the evolution mechanics of material systems
[AD-A250410] p 3774 N92-31604
Cutting treatment by drilling of fiber bound synthetic materials
[MBB-UD-0609-91-PUB] p 3774 N92-31716
Thermomechanical fatigue behavior of a silicone carbide fiber-reinforced calcium aluminosilicate glass-ceramic matrix composite
[AD-A249870] p 3775 N92-31823

Flammability characteristics of glass reinforced epoxy composite materials
[AD-A251009] p 3775 N92-31940

FIBER OPTICS
Three-wave envelope solitons: Can the speed of light in the fiber be controlled?
[AD-A247615] p 3901 N92-31611
Design and development of minilink video: A fiber-optic coupled video system
[AD-A249945] p 3808 N92-31801
Optical fiber sensors for organic matrix composite material cure monitoring
[AD-A247114] p 3776 N92-31979
Development and application of photosensitive device systems to studies of biological and organic materials
[DE92-014728] p 3867 N92-32120
Demonstrated survivability of a high temperature optical fiber cable on a 1500 pound thrust rocket chamber
[NASA-TM-105835] p 3801 N92-32230

FIBER ORIENTATION
Composite material shear property measurement using the Iosipescu specimen
[NASA-CR-190661] p 3772 N92-31274

FIBERS
Hollow fiber clinostat for simulating microgravity in cell culture
[NASA-CASE-MFS-28370-1] p 3828 N92-31790

FIELD ALIGNED CURRENTS
Impulsive magnetic perturbations of the high latitude, dayside ionosphere
[AD-A249872] p 3857 N92-31932

FIELD EFFECT TRANSISTORS
Stable integrated microwave to optical modulator
[AD-A249974] p 3813 N92-31431
Static and dynamic properties of current sensing power VDMOS transistor
[LAAS-92032] p 3815 N92-31697
Fabrication of an insulated gate diamond FET for high temperature applications
[AD-A251042] p 3817 N92-31849

FIELD EMISSION
Field-emitter arrays for RF vacuum microelectronics
[AD-A250101] p 3816 N92-31791

FIELD OF VIEW
Illusory self motion and disorientation
[CTN-92-60318] p 3871 N92-31472
Images simulation of sensors with large field of view from images of sensors with less field of view: The SSR/TM case
[INPE-5378-TDI/473] p 3845 N92-32220

FIELD THEORY (PHYSICS)
Modified black holes in two dimensional gravity
[DE92-630244] p 3924 N92-31401
A tumbling top-quark condensate model
[DE92-016194] p 3893 N92-31552
Schwinger boson studies of the t-J model beyond mean-field approximation
[DE92-630650] p 3909 N92-31655
Intermediate/high energy nuclear physics
[DE92-015363] p 3900 N92-32028

FIGHTER AIRCRAFT
A parameter optimization approach to controller partitioning for integrated flight/propulsion control application
[NASA-TM-105826] p 3761 N92-32241

FILM THICKNESS
Mechanics of thin films
[AD-A247848] p 3912 N92-31984

FINE STRUCTURE
Fine structure superimposed on mm-wavelength (18-23 GHz) spectra of solar active region
[INPE-5371-TDI/470] p 3926 N92-32221

FINITE DIFFERENCE THEORY
Monte Carlo simulations of random rough surface scattering with finite element and finite difference methods
[AD-A247528] p 3901 N92-31430
Two-dimensional axisymmetric calculations of surface waves generated by an explosion in an island, mountain, and sedimentary basin
[AD-A249971] p 3856 N92-31510
Modeling arbitrarily directed slots that are narrow both in width and depth with regard to the FDTD spatial cell
[DE92-008015] p 3808 N92-31738
Numerical simulation of tulip flame dynamics
[DE92-008553] p 3782 N92-31805
Three-dimensional finite difference modeling of surface wave propagation across the Barents Shelf
[AD-A249865] p 3865 N92-31821
CAVEAT: A computer code for fluid dynamics problems with large distortion and internal slip
[DE92-014078] p 3825 N92-32022
Nonlinearly stable compact schemes for shock calculations
[NASA-CR-189663] p 3887 N92-32164

FINITE ELEMENT METHOD
Composite material shear property measurement using the Iosipescu specimen
[NASA-CR-190661] p 3772 N92-31274
Applications of FEM and BEM in two-dimensional fracture mechanics problems
[NASA-TP-3277] p 3838 N92-31280
The 3-D analysis and verification of fracture growth mechanisms in fiber-reinforced ceramic composies
[AD-A250893] p 3773 N92-31305
A finite element procedure for analysis of laminated composite plates
[AD-A250902] p 3773 N92-31307
Transient fission gas behavior in uranium nitride fuel under proposed space applications
[AD-A252577] p 3899 N92-31325
Monte Carlo simulations of random rough surface scattering with finite element and finite difference methods
[AD-A247528] p 3901 N92-31430
Finite-element analyses and fracture simulation in thin-sheet aluminum alloy
[NASA-TM-107662] p 3839 N92-31504
Computational simulation of intermingled-fiber hybrid composite behavior
[NASA-TM-105666] p 3774 N92-31506
A finite element-boundary integral method for conformal antenna arrays on a circular cylinder
[NASA-CR-190534] p 3807 N92-31614
VAASEL-ANSYS comparison for a thermally loaded beam
[AD-A251003] p 3841 N92-31847
FEHMN 1.0: Finite element heat and mass transfer code
[DE92-013998] p 3825 N92-32008
Dynamic modeling and modal analysis of an air-to-air missile
[AD-A245957] p 3758 N92-32053
Time simulation of flutter with large stiffness changes
[NASA-TM-107650] p 3758 N92-32111
Optimal design of geodesically stiffened composite cylindrical shells
[NASA-CR-190706] p 3842 N92-32235

FINITE VOLUME METHOD
A general numerical model for wave rotor analysis
[NASA-TM-105740] p 3821 N92-31484
An installed nacelle design code using a multiblock Euler solver. Volume 1: Theory document
[NASA-CR-189652-VOL-1] p 3754 N92-32226

FINNED BODIES
Pressure loss and heat transfer in a toothed finned heat transfer medium
[MBB-UO-0163-91-PUB] p 3915 N92-31660
Further studies in filmwise condensation of steam on horizontal finned tubes
[AD-A252705] p 3915 N92-31767

FINS
Further studies in filmwise condensation of steam on horizontal finned tubes
[AD-A252705] p 3915 N92-31767

FIRE CONTROL
Simulation of a parallel processor based small tactical system
[AD-A245911] p 3882 N92-31443

FIRE PREVENTION
Flammability characteristics of glass reinforced epoxy composite materials
[AD-A251009] p 3775 N92-31940

FIRES
Nonthermal inhalation injury
[AD-A252532] p 3869 N92-31962

FISCHER-TROPSCH PROCESS
The development of precipitated iron catalysts with improved stability
[DE92-014630] p 3785 N92-32117

FISHERIES
Biology, oceanography, and fisheries of the North Pacific transition zone and subarctic frontal zone
[PB92-178128] p 3866 N92-32106

FISHES
Ecosystems of the Florida Keys: A bibliography
[PB92-198910] p 3854 N92-32071
Biology, oceanography, and fisheries of the North Pacific transition zone and subarctic frontal zone
[PB92-178128] p 3866 N92-32106

FISSION
Transient fission gas behavior in uranium nitride fuel under proposed space applications
[AD-A252577] p 3899 N92-31325

FITTING
Fitting and prediction uncertainty for a software reliability model
[AD-A252173] p 3880 N92-32060

FLAME PROPAGATION
Two-stage n-butane flame: A comparison between experimental measurements and modeling results
[DE92-009457] p 3779 N92-31416
Flame front geometry in premixed turbulent flames
[DE92-010310] p 3779 N92-31417
Ignition and flame propagation studies over a flat fuel surface
[PB92-181056] p 3780 N92-31678
Numerical simulation of tulip flame dynamics
[DE92-008553] p 3782 N92-31805
Incipient and total group combustion of fuel sprays in air p 3749 N92-31883
Transport and evaporation effects in counterflow spray diffusion flames p 3749 N92-31884
Flammability characteristics of glass reinforced epoxy composite materials
[AD-A251009] p 3775 N92-31940
Contribution to the modelling of turbulent combustion in the case of stabilisation by flame-lock
[ESA-TT-1229] p 3784 N92-31942

FLAME STABILITY
Contribution to the modelling of turbulent combustion in the case of stabilisation by flame-lock
[ESA-TT-1229] p 3784 N92-31942

FLAME TEMPERATURE
Two-stage n-butane flame: A comparison between experimental measurements and modeling results
[DE92-009457] p 3779 N92-31416
Absorption spectroscopy through the dark zone of solid propellant flames
[AD-A250033] p 3782 N92-31803

FLAMES
Absorption spectroscopy through the dark zone of solid propellant flames
[AD-A250033] p 3782 N92-31803
Numerical simulation of tulip flame dynamics
[DE92-008553] p 3782 N92-31805
Unimolecular reaction mechanisms involving C3H4, C4H4, and C6H6 hydrocarbon species
[DE92-005326] p 3783 N92-31860

FLAMMABILITY
Flammability limits and ballistic properties of fuel-rich propellants p 3749 N92-31885
Flammability characteristics of glass reinforced epoxy composite materials
[AD-A251009] p 3775 N92-31940

FLAT PLATES
Flat plates placed in depleted hypersonic flow
[SESSIA-430/91.960] p 3751 N92-31508
Near-field and far-field sound radiation from a line-driven fluid-loaded infinite flat plate having periodic and non-periodic attached rib stiffeners
[AD-A250100] p 3892 N92-31789

FLAT SURFACES
Ignition and flame propagation studies over a flat fuel surface
[PB92-181056] p 3780 N92-31678
Experimental studies of hypersonic shock-wave boundary-layer interactions
[NASA-CR-190731] p 3753 N92-32162

FLAVOR (PARTICLE PHYSICS)
Implications of the 17 keV neutrino
[DE92-017000] p 3898 N92-32006
Resonant enhancement of flavor-changing neutrino interactions
[DE92-013020] p 3898 N92-32167

FLEXIBILITY
Mission and Safety Critical (MASC) plans for the MASC Kernel simulation
[NASA-CR-190708] p 3875 N92-31487

FLEXIBLE BODIES
Flexible heating head for induction heating apparatus and method
[NASA-CASE-LAR-14418-1] p 3803 N92-31257
Dynamics of shuttle based flexible antenna system
[CRANFIELD-AERO-9203] p 3840 N92-31516
Studies in dynamic characterization and control of a flexible structure and optical beampath
[AD-A250555] p 3830 N92-31605
Mathematical modeling and numerical simulation of the dynamics of flexible structures undergoing large overall motions
[AD-A250202] p 3761 N92-31967

FLEXIBLE SPACECRAFT
Spacecraft dynamics characterization and control system failure detection. Volume 3: Control system failure monitoring
[NASA-CR-190529] p 3884 N92-31254

FLEXIBLE WINGS
Design and experimental validation of a flutter suppression controller for the active flexible wing
[NASA-TM-4381] p 3760 N92-31240
A summary of the active flexible wing program
[NASA-TM-107655] p 3757 N92-31264

FLEXING
The design and testing of an optimal beam composed of unimodal elements p 3747 N92-31873
FLIGHT CONDITIONS
Stagnation-point heat-transfer rate predictions at aeroassist flight conditions
[NASA-TP-3208] p 3819 N92-31281
FLIGHT CONTROL
Proceedings of the 53rd Symposium on Air Vehicle Mission Control and Management
[AGARD-AR-310] p 3889 N92-32229
A parameter optimization approach to controller partitioning for integrated flight/propulsion control application
[NASA-TM-105826] p 3761 N92-32241
FLIGHT CREWS
Immersion suit usage within the RAAF
[AD-A250645] p 3755 N92-31562
Pilot errors involving Head-Up Displays (HUDs), Helmet-Mounted Displays (HMDs), and Night Vision Goggles (NVGs)
[AD-A250719] p 3873 N92-32023
Canadian aircrew sea water survival, 1952-1987
[DCIEM-88-RR-39] p 3756 N92-32219
FLIGHT INSTRUMENTS
In-flight evaluation of aerodynamic predictions of an air-launched space booster
[NASA-TM-104246] p 3752 N92-31808
A continuing study of altitude determination deficiencies of the Service Aircraft Instrumentation Package (SAIP)
[AD-A245952] p 3758 N92-32051
FLIGHT PATHS
Optimal trajectories for an unmanned air vehicle
p 3748 N92-31880
FLIGHT SAFETY
In-flight decision making by high time and low time pilots during instrument operations
[AD-A249990] p 3871 N92-31392
Aviation safety: Changes needed in FAA's service difficulty reporting program
[GAO/RCED-91-24] p 3755 N92-31453
FLIGHT SIMULATION
Pilot errors involving Head-Up Displays (HUDs), Helmet-Mounted Displays (HMDs), and Night Vision Goggles (NVGs)
[AD-A250719] p 3873 N92-32023
Proceedings of the 53rd Symposium on Air Vehicle Mission Control and Management
[AGARD-AR-310] p 3889 N92-32229
FLIGHT TESTS
Overview of the NASA Dryden Flight Research Facility aeronautical flight projects
[NASA-TM-104254] p 3756 N92-31261
Subsonic flight test evaluation of a performance seeking control algorithm on an F-15 airplane
[NASA-TM-4400] p 3759 N92-31275
In-flight leading-edge extension vortex flow-field survey measurements on a F-18 aircraft at high angle of attack
[NASA-TM-4398] p 3751 N92-31276
In-flight evaluation of aerodynamic predictions of an air-launched space booster
[NASA-TM-104246] p 3752 N92-31808
System overview of the NASA Dryden Integrated Test Facility
[NASA-TM-104250] p 3762 N92-32201
FLIGHT TIME
In-flight decision making by high time and low time pilots during instrument operations
[AD-A249990] p 3871 N92-31392
FLOW CHARACTERISTICS
Flow generation by turbulence
[DE92-013276] p 3906 N92-31829
New techniques in computational fluid dynamics: Algorithms, analysis, applications
[AD-A250498] p 3825 N92-32038
Research on aero-thermodynamic distortion induced structural dynamic response of multistage compressor blading
[AD-A250865] p 3760 N92-32059
FLOW DISTORTION
An experimental investigation of the formation of secondary vortices and the generation of small-scale motion in a spanwise forced plane mixing layer
[AD-A250350] p 3822 N92-31559
FLOW DISTRIBUTION
Computer program to solve two-dimensional shock-wave interference problems with an equilibrium chemically reacting air model
[NASA-TM-4187] p 3818 N92-31247
NASA, Lewis Research Center supersonic throughflow fan program
[NASA-TM-103248] p 3759 N92-31250
In-flight leading-edge extension vortex flow-field survey measurements on a F-18 aircraft at high angle of attack
[NASA-TM-4398] p 3751 N92-31276
An experimental investigation of the formation of secondary vortices and the generation of small-scale motion in a spanwise forced plane mixing layer
[AD-A250350] p 3822 N92-31559
Ignition and flame propagation studies over a flat fuel surface
[PB92-181056] p 3780 N92-31678
On the spatial evolution of long-wavelength Goertler vortices governed by a viscous-inviscid interaction
[NASA-CR-189681] p 3822 N92-31687
Effects of flow conditioners and tap location on orifice flowmeter performance
[PB92-183730] p 3824 N92-31839
NAS (Numerical Aerodynamic Simulation Program) technical summaries, March 1989 - February 1990
[NASA-TM-107960] p 3926 N92-31852
The use of high lift-to-drag hypersonic vehicles for aero-assisted orbital maneuvering p 3748 N92-31877
The three-dimensional stability of the Foeppl vortices
p 3750 N92-31889
A computational examination of directional stability for smooth and chined forebodies at high-alpha
[NASA-CR-4465] p 3753 N92-32114
Control of unsteady separated flow associated with the dynamic stall of airfoils
[NASA-CR-190688] p 3753 N92-32177
An installed nacelle design code using a multiblock Euler solver. Volume 2: User guide
[NASA-CR-189652-VOL-2] p 3754 N92-32228
FLOW EQUATIONS
Use of a genetic algorithm to solve fluid flow problems on an NCUBE/2 multiprocessor computer
[DE92-014044] p 3824 N92-31832
FLOW GEOMETRY
Effect of inlet geometry on the flow and combustion processes in a solid fuel ramjet p 3747 N92-31871
FLOW MEASUREMENT
Effects of flow conditioners and tap location on orifice flowmeter performance
[PB92-183730] p 3824 N92-31839
Improvements to the Rocky Flats Metrology Laboratories velocity meter calibration system
[DE92-013162] p 3829 N92-32138
FLOW STABILITY
Flow instability in a vertical annulus under steady state and transient conditions
[DE92-013217] p 3820 N92-31421
Sensitivity analysis of hydrodynamic stability operators
[NASA-CR-189683] p 3822 N92-31535
Stability and transition of hypersonic boundary-layer flows
[AD-A250279] p 3752 N92-31555
The stability of a slightly eccentric straight vortex filament in a circular tube p 3750 N92-31887
The three-dimensional stability of the Foeppl vortices
p 3750 N92-31889
Turbine blade tip and seal clearance excitation forces
[NASA-CR-184341] p 3760 N92-31910
Contribution to the modelling of turbulent combustion in the case of stabilisation by flame-lock
[ESA-TT-1229] p 3784 N92-31942
FLOW THEORY
Pressure and temperature for B-1B transparency test
[AD-A252711] p 3752 N92-31674
FLOW VELOCITY
Granular flows down bumpy inclines
[DE92-013568] p 3820 N92-31425
Heat transfer and pressure drop in an annular channel with downflow
[DE92-014363] p 3825 N92-32115
Improvements to the Rocky Flats Metrology Laboratories velocity meter calibration system
[DE92-013162] p 3829 N92-32138
FLOW VISUALIZATION
In-flight leading-edge extension vortex flow-field survey measurements on a F-18 aircraft at high angle of attack
[NASA-TM-4398] p 3751 N92-31276
Active control of the separation region on a two-dimensional airfoil
[AD-A249739] p 3752 N92-31622
FLOWMETERS
Two-component flow study in large-diameter horizontal pipe
[DE92-013196] p 3820 N92-31420
Effects of flow conditioners and tap location on orifice flowmeter performance
[PB92-183730] p 3824 N92-31839
FLUENCE
Radiation damage in carbon-carbon composites
[DE92-011778] p 3775 N92-31912
FLUID BOUNDARIES
Advanced DAA methods for shock response analysis
[AD-A252696] p 3891 N92-31588
FLUID DYNAMICS
Diagnostics for research in atomization and turbulent two-phase flows
[AD-A247201] p 3819 N92-31283
Fundamental studies of the structure of hypersonic attached and separated boundary layers over smooth, rough and transpiration-cooled surfaces
[AD-A250284] p 3819 N92-31286
Stability of boundary layers at high supersonic and hypersonic speeds
[AD-A250900] p 3819 N92-31306
Description of a 1000 sensor constant current anemometer system for locating three-dimensional turbulent boundary layer separations
[AD-A250827] p 3821 N92-31452
CAVEAT: A computer code for fluid dynamics problems with large distortion and internal slip
[DE92-014078] p 3825 N92-32022
FLUID FLOW
CFD methods development considerations for unsteady aerodynamic analysis
[NASA-TM-107644] p 3750 N92-31239
Flow instability in a vertical annulus under steady state and transient conditions
[DE92-013217] p 3820 N92-31421
Use of a genetic algorithm to solve fluid flow problems on an NCUBE/2 multiprocessor computer
[DE92-014044] p 3824 N92-31832
Heat transfer and flow of a modified second grade fluid
[DE92-014744] p 3824 N92-31895
Heat transfer and pressure drop in an annular channel with downflow
[DE92-014363] p 3825 N92-32115
FLUID JETS
Evolution of reactants fluid volume in turbulent jets
[DE92-011298] p 3786 N92-32145
FLUID MANAGEMENT
Evaluation of proposed inservice testing procedures for check valves
[DE92-014502] p 3833 N92-31384
FLUID MECHANICS
Flow instability in a vertical annulus under steady state and transient conditions
[DE92-013217] p 3820 N92-31421
Plane stokes flow driven by capillarity on a free surface: Overview and status
[DE92-011469] p 3821 N92-31528
Iterative methods for large sparse linear systems arising from partial differential equations
[AD-A249524] p 3886 N92-31567
Pulse Combustion Engineering Research Laboratory: Exhaust energy
[PB92-172402] p 3783 N92-31918
Axisymmetric bluff-body flow: A vortex solver for thin shells
[DE92-016748] p 3824 N92-31933
FLUIDIZED BED PROCESSORS
Particle diagnostics in optically thick sprays
[AD-A250981] p 3897 N92-31936
FLUORESCENCE
Waveguide-binding sensor for use with assays
[AD-D015230] p 3777 N92-31268
Dual gated imaging system for enhanced fluorescent diagnostics measurements
[AD-A249673] p 3828 N92-31694
FLUORINATION
The synthesis and characterization of tribophysical layers on diamond and silicon carbide surfaces
[AD-A250983] p 3796 N92-32001
FLUORINE ORGANIC COMPOUNDS
Temperature-enhanced autodetachment from long-lived parent negative ions of gaseous dielectrics
[DE92-011108] p 3894 N92-31700
FLUOROCARBONS
World ocean circulation experiment. WOCE chlorofluorocarbon intercomparison cruise report
[PB92-185974] p 3865 N92-31842
FLUOROPOLYMERS
Development of methodology and technology for identifying and quantifying emission products from open burning and open detonation thermal treatment methods. Field test series A, B, and C. Volume 2, part A: Quality assurance and quality control
[AD-A250736] p 3801 N92-31972
Development of methodology and technology for identifying and quantifying emission products from open burning and open detonation thermal treatment methods. Field test series A, B, and C. Volume 2, part B: Quality assurance and quality control. Appendices
[AD-A250737] p 3801 N92-31973
FLUTTER
CFD methods development considerations for unsteady aerodynamic analysis
[NASA-TM-107644] p 3750 N92-31239

Design and experimental validation of a flutter suppression controller for the active flexible wing
[NASA-TM-4381] p 3760 N92-31240
Flutter suppression digital control law design and testing for the AFW wind-tunnel model
[NASA-TM-107652] p 3757 N92-31350
Time simulation of flutter with large stiffness changes
[NASA-TM-107650] p 3758 N92-32111

FLUTTER ANALYSIS
Flutter suppression digital control law design and testing for the AFW wind-tunnel model
[NASA-TM-107652] p 3757 N92-31350
Dynamic modeling and modal analysis of an air-to-air missile
[AD-A245957] p 3758 N92-32053

FLUX (RATE)
The interplanetary heavy ion environment for both galactic cosmic rays and solar energetic particles during the CRRES mission
[AD-A248942] p 3926 N92-31477

FLUX DENSITY
A dynamical model of the behaviour of hadronic and fundamental strings at finite densities
[DE92-630245] p 3914 N92-31402
Energy balance model for imagery and electromagnetic propagation
[AD-A250884] p 3806 N92-31543

FLUX TRANSFER EVENTS
Impulsive magnetic perturbations of the high latitude, dayside ionosphere
[AD-A249872] p 3857 N92-31932

FLY BY WIRE CONTROL
FCS skewed sensors array: Practical considerations
p 3746 N92-31868

FOAMS
Characterization of polymers for microcellular foams
[DE92-012444] p 3793 N92-31539
High density thin-walled syntactic foam
[DE92-013159] p 3797 N92-32136

FORCE DISTRIBUTION
Electrically-induced stresses and deflection in multiple plates
[DE92-012303] p 3841 N92-31844

FOREBODIES
A computational examination of directional stability for smooth and chined forebodies at high-alpha
[NASA-CR-4465] p 3753 N92-32114

FORECASTING
Modelling and prediction of regions of the North Pacific
[AD-A252144] p 3863 N92-31406

FOREST FIRES
Numerical simulation of precipitation scavenging and comparison with observation of prescribed forest fires
[DE92-013513] p 3851 N92-31423

FORESTS
Application of Free-Air CO2 Enrichment (FACE) technology to a forest canopy: A simulation study
[DE92-013308] p 3851 N92-31422
Numerical simulation of precipitation scavenging and comparison with observation of prescribed forest fires
[DE92-013513] p 3851 N92-31423
Methods of assessing responses of trees, stands and ecosystems to air pollution
[PB92-180231] p 3853 N92-31648
A dynamic model of terrestrial carbon cycling
[DE92-015130] p 3853 N92-31782
ARO Geoscience Center fellowships
[AD-A249225] p 3857 N92-31964

FORGING
Computer-aided modeling tools for forging process feasibility studies
[DE92-012116] p 3838 N92-31303

FORMALISM
Mathematical structures for qualitative calculus, a contribution to qualitative simulation
[LAAS-91475] p 3886 N92-31690

FORMAT
Objects used to implement intelligent databases
[DE92-013098] p 3919 N92-31581
Engine monitoring display study
[NASA-CR-4463] p 3761 N92-32175

FORTRAN
Quality Evaluation System (QUES), volume 1
[AD-A252679] p 3876 N92-31586
ADIFOR: Fortran source translation for efficient derivatives
[DE92-016187] p 3879 N92-31899

FORWARD SCATTERING
Three-wave envelope solitons: Can the speed of light in the fiber be controlled?
[AD-A247615] p 3901 N92-31611

FOSSIL FUELS
Global trends in energy use: Indications for research
[DE92-014773] p 3855 N92-32155

FOUR-WAVE MIXING
Saturation effects in degenerate four-wave mixing spectroscopy: Nonperturbative calculations
[DE92-012253] p 3782 N92-31773

FOURIER ANALYSIS
Detection of signal harmonic sets
[DREA-CR-89-420] p 3806 N92-31471
Wavelet signal processing for transient feature extraction
[AD-A250519] p 3890 N92-32046

FOURIER TRANSFORMATION
Gallium arsenide clusters and their interfacial physics and chemistry
[AD-A249565] p 3907 N92-31375
Ionospheric communications channel modelling
[DE92-013039] p 3808 N92-31722
Application of optical theory to quantitative surface FT-IR with emphasis on molecular depth profiling
[AD-A250525] p 3902 N92-32077
The potential of passive-remote Fourier Transform Infrared (FTIR) spectroscopy to detect organic emissions under the Clean Air Act
[DE92-015224] p 3854 N92-32083

FRACTALS
The mechanics of fractal damage
[AD-A250518] p 3776 N92-32075

FRACTIONATION
Supercritical fluid fractionation of JP-8
[AD-A247835] p 3801 N92-31982

FRACTOGRAPHY
Composite failure analysis handbook. Volume 2: Technical handbook. Part 1: Procedures and techniques
[AD-A250521] p 3776 N92-32048

FRACTURE MECHANICS
Cyclic hot firing results of tungsten-wire-reinforced, copper-lined thrust chambers
[NASA-TM-4214] p 3769 N92-31249
Applications of FEM and BEM in two-dimensional fracture mechanics problems
[NASA-TP-3277] p 3838 N92-31280
A finite element procedure for analysis of laminated composite plates
[AD-A250902] p 3773 N92-31307
Effect of fracture surface interference on shear crack growth
[DE92-011431] p 3839 N92-31389
Finite-element analyses and fracture simulation in thin-sheet aluminum alloy
[NASA-TM-107662] p 3839 N92-31504
J(sub 2) fracture toughness testing of Al 707 5-T7351
p 3747 N92-31872

FRACTURE STRENGTH
The 3-D analysis and verification of fracture growth mechanisms in fiber-reinforced ceramic composies
[AD-A250893] p 3773 N92-31305
Enhancement of fracture toughness using high intensity electric currents
[AD-A249809] p 3889 N92-31359
Mechanical strength and stability of lithium aluminate
[DE92-015998] p 3841 N92-31638
J(sub 2) fracture toughness testing of Al 707 5-T7351
p 3747 N92-31872
Tetragonal zirconia ceramics in ZrO2-CeO2 system (Ce-TZP): Preparation, characterization and mechanical properties
[INPE-5372-PRE/1746] p 3798 N92-32199

FRACTURES (MATERIALS)
Enhancement of fracture toughness using high intensity electric currents
[AD-A249809] p 3889 N92-31359

FRACTURING
The 3-D analysis and verification of fracture growth mechanisms in fiber-reinforced ceramic composies
[AD-A250893] p 3773 N92-31305
Effect of fracture surface interference on shear crack growth
[DE92-011431] p 3839 N92-31389
Research in regional seismology: The effect of anisotropy
[AD-A248940] p 3855 N92-31476
A differential CDM model for fatigue of unidirectional metal matrix composites
[NASA-TM-105726] p 3840 N92-31505
The structure and properties of grain boundaries in Ni3Al
[DE92-012143] p 3788 N92-31744
Particle emission and charging effects induced by fracture
[AD-A252182] p 3913 N92-32065

FRAGMENTATION
Effects of fragmentation parameter variations on estimates of galactic cosmic ray exposure: Dose sensitivity studies for aluminum shields
[NASA-TM-4386] p 3926 N92-32193

FREE CONVECTION
Emissivity measurements in support of experiments on natural convection between a vertical cylinder and a surrounding array
[DE92-012321] p 3819 N92-31287
Natural convection immersion cooling of an array of vertically oriented heated protrusions in an enclosure filled with a dielectric liquid: Effects of enclosure width, Prandtl number and component orientation
[AD-A245884] p 3914 N92-31489

FREE ELECTRON LASERS
Proposal for a workshop in the physics and application of hollow electrode glow switches
[AD-A247139] p 3814 N92-31490
Microwave generation for magnetic fusion energy applications
[DE92-011424] p 3831 N92-31769
Millimeter wave free electron laser amplifiers: Experiments and designs
[DE92-011813] p 3832 N92-31935
Theory for the CEBAF infrared and shipboard FELS
[AD-A252174] p 3832 N92-32061

FREE ENERGY
Theoretical studies of solid-fluid phase equilibria
[DE92-016598] p 3781 N92-31717

FREE JETS
Sizing supersonic freejet nozzle and inlet location for simulation of the transition phase in integral rocket ramjet
p 3747 N92-31870

FREQUENCIES
Optical oversampled analog-to-digital conversion
[AD-A252695] p 3877 N92-31587
Effect of guard band reduction on marker beacon receiver performance
[DOT/FAA/CT-TN92/18] p 3807 N92-31617

FREQUENCY CONTROL
Soviet precision timekeeping research and technology
[PB92-173046] p 3802 N92-31830
High performance of copper pumped dye lasers
[DE92-011763] p 3832 N92-31902
Movement of dislocations in quartz
[AD-A250527] p 3913 N92-32078
EHF SATCOM frequency hopping pattern generator: Proof of concept
[DREO-89-32] p 3811 N92-32231
A frequency hopping synthesizer controller for EHF SATCOM
[DREO-89-29] p 3811 N92-32232

FREQUENCY DISTRIBUTION
A preliminary study in the use of phase demodulation techniques for the analysis of gear vibration data
[NRC-32083] p 3833 N92-31469

FREQUENCY HOPPING
Experiment on a three-beam adaptive array for EHF frequency-hopped signals using a fast algorithm, phase-D
[CTN-92-60322] p 3810 N92-32203
EHF SATCOM frequency hopping pattern generator: Proof of concept
[DREO-89-32] p 3811 N92-32231
A frequency hopping synthesizer controller for EHF SATCOM
[DREO-89-29] p 3811 N92-32232

FREQUENCY MULTIPLIERS
CO2 laser frequency multiplication
[AD-A248574] p 3830 N92-31755

FREQUENCY SHIFT
Application of optical theory to quantitative surface FT-IR with emphasis on molecular depth profiling
[AD-A250525] p 3902 N92-32077

FREQUENCY SHIFT KEYING
Coherent/noncoherent detection of coherent optical heterodyne DPSK-CDMA and MFSK-CDMA signals
[AD-A246215] p 3809 N92-31993

FREQUENCY STANDARDS
Soviet precision timekeeping research and technology
[PB92-173046] p 3802 N92-31830

FREQUENCY SYNCHRONIZATION
EHF SATCOM frequency hopping pattern generator: Proof of concept
[DREO-89-32] p 3811 N92-32231
A frequency hopping synthesizer controller for EHF SATCOM
[DREO-89-29] p 3811 N92-32232

FRESNEL REGION
Validation of the Numerical Electro-magnetics Code (NEC) for antenna wire elements in proximity to Earth
[AD-A250507] p 3810 N92-32043

FRICTION
Tribology of Langmuir-Blodgett films
[AD-A250075] p 3833 N92-31363
Experimental studies of friction and heat transfer in enhanced passages
[DE92-011607] p 3890 N92-32099

FRICTION MEASUREMENT
Fundamental studies of the structure of hypersonic attached and separated boundary layers over smooth, rough and transpiration-cooled surfaces
[AD-A250284] p 3819 N92-31286
Description of a 1000 sensor constant current anemometer system for locating three-dimensional turbulent boundary layer separations
[AD-A250827] p 3821 N92-31452
FRONTS (METEOROLOGY)
A comparison of the performance of two gust front detection algorithms using a length-based scoring technique
[AD-A250862] p 3863 N92-32103
FUEL CELLS
Batteries and fuel cells
[DE92-011493] p 3847 N92-31571
Characterization of oxides for low temperature solid oxide fuel cells
[PB92-152883] p 3848 N92-31903
Electrochemical oxidation of methane for fuel cells
[PB92-172303] p 3848 N92-31922
FUEL COMBUSTION
Experimental evaluation of oxygen-enriched air and emulsified fuels in a single-cylinder diesel engine. Volume 1: Concept evaluation
[DE92-015999] p 3799 N92-31442
Hydrocarbon ignition: Automatic generation of reaction mechanisms and applications to modeling of engine knock
[DE92-011943] p 3780 N92-31607
Development of a core combustion research program plan for EPA
[PB92-180868] p 3781 N92-31683
Collection of papers of the 31st Israel Annual Conference on Aviation and Astronautics
[ITN-92-85124] p 3745 N92-31861
Effect of inlet geometry on the flow and combustion processes in a solid fuel ramjet p 3747 N92-31871
Incipient and total group combustion of fuel sprays in air p 3749 N92-31883
Transport and evaporation effects in counterflow spray diffusion flames p 3749 N92-31884
Pulse Combustion Engineering Research Laboratory: Exhaust energy
[PB92-172402] p 3783 N92-31918
Supercritical fluid fractionation of JP-8
[AD-A247835] p 3801 N92-31982
FUEL CONSUMPTION
Subsonic flight test evaluation of a performance seeking control algorithm on an F-15 airplane
[NASA-TM-4400] p 3759 N92-31275
Propane oxidation through the negative temperature coefficient region at 10 and 15 atmospheres: Results of experimental and modeling studies
[DE92-007902] p 3778 N92-31414
FUEL FLOW
Subsonic flight test evaluation of a performance seeking control algorithm on an F-15 airplane
[NASA-TM-4400] p 3759 N92-31275
FUEL INJECTION
Study of a spherical spinning combustion chamber for orbit insertion p 3746 N92-31869
FUEL OILS
Turbulent dusty boundary layer in an ANFO surface-burst explosion
[DE92-012101] p 3822 N92-31625
FUEL PUMPS
Orbit transfer vehicle engine technology program. Task B-6 high speed turbopump bearings
[NASA-CR-189230] p 3835 N92-31892
FUEL SPRAYS
Incipient and total group combustion of fuel sprays in air p 3749 N92-31883
Transport and evaporation effects in counterflow spray diffusion flames p 3749 N92-31884
FUEL TESTS
Advanced thermally stable, jet fuels development program annual report. Volume 1: Model and experiment system development
[AD-A249625] p 3799 N92-31462
Dual gated imaging system for enhanced fluorescent diagnostics measurements
[AD-A249673] p 3828 N92-31694
Shock tube study of the reaction of triethanol ammonium nitrate with N2O
[AD-A250034] p 3800 N92-31804
Flammability limits and ballistic properties of fuel-rich propellants p 3749 N92-31885
FUEL-AIR RATIO
Autoignition behavior of lean mixtures: Chemical and thermodynamics effects
[DE92-009690] p 3781 N92-31763
FUNCTION SPACE
Analysis and design of neural networks
[AD-A250495] p 3884 N92-31332
FUNCTIONAL DESIGN SPECIFICATIONS
Configuration management and software measurement in the Ground Systems Development Environment (GSDE)
[NASA-CR-190716] p 3879 N92-31787
FUNCTIONS (MATHEMATICS)
Nonparametric estimation in renewal theory, 1: The empirical renewal function
[REPT-91-95] p 3888 N92-31519
Lattice gaugefixing and other optics in lattice gauge theory
[DE92-016958] p 3901 N92-31737
FURNACES
Optimized photorefractive barium titanate
[AD-A250089] p 3908 N92-31438
FUSION REACTORS
Dynamic modeling of plasma-vapor interactions during plasma disruptions
[DE92-016183] p 3903 N92-31310
Divertor material evaluation system at D3-D
[DE92-013696] p 3905 N92-31749
An examination of the feasibility of a nuclear-pumped laser-driven inertial confinement fusion reactor with magnetically protected walls
[AD-A248163] p 3907 N92-31990
Fusion with highly spin polarized HD and D(2)
[DE92-017030] p 3898 N92-32007

G

GALACTIC COSMIC RAYS
The interplanetary heavy ion environment for both galactic cosmic rays and solar energetic particles during the CRRES mission
[AD-A248942] p 3926 N92-31477
Effects of fragmentation parameter variations on estimates of galactic cosmic ray exposure: Dose sensitivity studies for aluminum shields
[NASA-TM-4386] p 3926 N92-32193
GALLIUM ARSENIDE LASERS
Laser material interactions
[AD-A250028] p 3831 N92-31802
GALLIUM ARSENIDES
Pulsed laser deposition of high Tc superconducting thin films
[AD-A250657] p 3830 N92-31319
Gallium arsenide clusters and their interfacial physics and chemistry
[AD-A249565] p 3907 N92-31375
Phase-locked arrays of antiguided diode lasers: Modelling, design, evaluation of performance limits
[LAAS-92034] p 3830 N92-31698
Advanced high efficiency concentrator cells
[DE92-010559] p 3848 N92-31893
The polarized electron gun for the SLC
[DE92-012418] p 3900 N92-32131
GALLIUM NITRIDES
Growth, nitrogen vacancy reduction and solid solution formation in cubic GaN thin films and the subsequent fabrication of superlattice structures using AlN and InN
[AD-A248058] p 3908 N92-31446
GAME THEORY
An automated computational method for barrier construction in single and two-target differential games p 3749 N92-31882
Optimal targeting of evading objects
[DE92-014719] p 3889 N92-32119
GAMMA RAY ASTRONOMY
Institute of Geophysics and Planetary Physics, 1991
[DE92-016981] p 3923 N92-32005
GAMMA RAYS
Development of gamma ray imaging cameras
[DE92-015305] p 3828 N92-31919
GAS ANALYSIS
Dispersive-infrared gas sensor system design and operation manual
[DE92-011766] p 3828 N92-31909
GAS DETECTORS
A detector for stationary gas bubbles: Feasibility studies
[AD-A250135] p 3828 N92-31794
Dispersive-infrared gas sensor system design and operation manual
[DE92-011766] p 3828 N92-31909
GAS DISSOCIATION
Dissociative electron attachment of O2: A solid-state effect on potential curve crossing
[AD-A246331] p 3913 N92-31995
GAS DYNAMICS
Performance tests of a fast-acting valve for the driver tubes of a large blast/thermal simulator
[AD-A250035] p 3835 N92-31807
GAS GENERATORS
A semiconductor bridge ignited gas generator
[DE92-014049] p 3781 N92-31748
GAS JETS
Supersonic pyrolysis jets for diamond film deposition
[AD-A251125] p 3798 N92-32198
GAS TEMPERATURE
Monitoring gas temperatures entering an MHD superheater
[DE92-014200] p 3903 N92-31372
GAS TRANSPORT
Recent developments in the fundamentals of gas permeation in rubbery polymers
[AD-A249745] p 3794 N92-31624
GAS TUNGSTEN ARC WELDING
Weld penetration and defect control
[DE92-015310] p 3836 N92-31336
GAS TURBINE ENGINES
Research into improving the durability of the hot section in the aircraft turbine engine
[AD-A250342] p 3759 N92-31439
A general numerical model for wave rotor analysis
[NASA-TM-105740] p 3821 N92-31484
Life prediction and constitutive models for engine hot section anisotropic materials program
[NASA-CR-189222] p 3759 N92-31534
GAS TURBINES
Fatigue in single crystal nickel superalloys
[AD-A250068] p 3786 N92-31360
GASEOUS DIFFUSION
Recent developments in the fundamentals of gas permeation in rubbery polymers
[AD-A249745] p 3794 N92-31624
GASEOUS FUELS
Evolution of reactants fluid volume in turbulent jets
[DE92-011298] p 3786 N92-32145
GASES
Temperature-enhanced autodetachment from long-lived parent negative ions of gaseous dielectrics
[DE92-011108] p 3894 N92-31700
GAUGE INVARIANCE
Modified black holes in two dimensional gravity
[DE92-630244] p 3924 N92-31401
GAUGE THEORY
A tumbling top-quark condensate model
[DE92-016194] p 3893 N92-31552
Lattice gaugefixing and other optics in lattice gauge theory
[DE92-016958] p 3901 N92-31737
Minimal supersymmetric unification predictions
[RAL-92-005] p 3915 N92-31953
GEAR TEETH
A preliminary study in the use of phase demodulation techniques for the analysis of gear vibration data
[NRC-32083] p 3833 N92-31469
GEARS
Experimental testing of prototype face gears for helicopter transmissions
[NASA-TM-105434] p 3832 N92-31349
Modal simulation of gearbox vibration with experimental correlation
[NASA-TM-105702] p 3834 N92-31485
GELATION
Sol-gel multilayers applied by a meniscus coating process
[DE92-012697] p 3794 N92-31560
GELS
Rheology of zirconia-alumina gelcasting slurries
[DE92-016787] p 3797 N92-32089
GENERAL AVIATION AIRCRAFT
Effect of guard band reduction on marker beacon receiver performance
[DOT/FAA/CT-TN92/18] p 3807 N92-31617
GENES
Evolution and analysis of the functional domains of the chimeric proteins that initiate pyrimidine biosynthesis
[AD-A250069] p 3866 N92-31465
GENETICS
Biodosimetry of ionizing radiation in humans using the glycophorin A genotoxicity assay
[DE92-011974] p 3869 N92-31608
JPRS report: Science and technology. Central Eurasia: Life sciences
[JPRS-ULS-92-015] p 3924 N92-32179
GEOCHEMISTRY
Hydrological and geochemical response and recovery in disturbed Arctic ecosystems
[DE92-016223] p 3850 N92-31312
GEODETIC SATELLITES
Synthetic temperature profile in the Gulf of Mexico. Part 1: Statistical relationship between modal amplitudes and dynamic height at surface
[AD-A252701] p 3863 N92-31308
GEOGRAPHIC INFORMATION SYSTEMS
Enhancing GRASS data communication with videographic technology
[DE92-014852] p 3919 N92-31596
Technology Integration Workshop: Selected papers
[PB92-158278] p 3923 N92-31643

GIS: Geographic Information Systems. State of the art and future tendencies
[INPE-5358-NTC/301] p 3922 N92-32227

GEOGRAPHY
Minorities and air quality non-attainment areas: A preliminary geo-demographic analysis
[DE92-013054] p 3852 N92-31591
Enhancing GRASS data communication with videographic technology
[DE92-014852] p 3919 N92-31596

GEOLOGY
Lamont-Doherty Geological Observatory
[PB92-185040] p 3856 N92-31636
ARO Geoscience Center fellowships
[AD-A249225] p 3857 N92-31964

GEOMAGNETIC LATITUDE
The effects of magnetic storm phases on F-layer irregularities from auroral to equatorial latitudes
[AD-A249011] p 3855 N92-31478

GEOMAGNETISM
Solar-geophysical data number 572, April 1992. Part 1: (Prompt reports). Data for March, February 1992, and late data
[PB92-187723] p 3856 N92-31637

GEOMETRICAL THEORY OF DIFFRACTION
Electromagnetic scattering by coated convex surfaces and wedges simulated by approximate boundary conditions
[NASA-CR-190540] p 3803 N92-31238
High-frequency techniques for RCS prediction of plate geometries
[NASA-CR-190656] p 3804 N92-31273

GEOMETRY
CGVIEW: A program to generate isometric and perspective views of combinatorial geometries
[DE92-016979] p 3881 N92-32126

GEOMORPHOLOGY
Geomorphic variability in the coastal zone
[AD-A252713] p 3864 N92-31544

GEOPHYSICS
Solar-geophysical data number 572, April 1992. Part 1: (Prompt reports). Data for March, February 1992, and late data
[PB92-187723] p 3856 N92-31637
Solar-geophysical data number 572, April 1992. Part 2: (Comprehensive reports). Data for October 1991 and miscellaneous
[PB92-187731] p 3856 N92-31639
ARO Geoscience Center fellowships
[AD-A249225] p 3857 N92-31964
Institute of Geophysics and Planetary Physics, 1991
[DE92-016981] p 3923 N92-32005
USU center of excellence in theory and analysis of the geo-plasma environment
[AD-A252189] p 3858 N92-32055

GEOPOTENTIAL HEIGHT
Global atmospheric circulation statistics, 1000-1 mb
[PB92-186196] p 3853 N92-31649

GEOTHERMAL ENERGY CONVERSION
Materials for geothermal production
[DE92-014691] p 3849 N92-32118

GEOTHERMAL ENERGY UTILIZATION
World energy projection system: Model documentation
[DE92-014206] p 3847 N92-31594
Materials for geothermal production
[DE92-014691] p 3849 N92-32118
Geothermal materials development
[DE92-016940] p 3849 N92-32124

GEYSERS
Geothermal materials development
[DE92-016940] p 3849 N92-32124

GIBBS FREE ENERGY
Gibbs free energy of reactions involving SiC, Si3N4, H2, and H2O as a function of temperature and pressure
[NASA-TP-3275] p 3791 N92-31278
Application of the mean spherical approximation to the estimations of single ion thermodynamic quantities of solvation for monoatomic monovalent ions in aqueous solutions
[AD-A250190] p 3893 N92-31316

GLACIERS
Annual dynamics within the active layer
[DE92-013520] p 3850 N92-31304

GLASS
Interface engineering in alumina/glass composites
[AD-A248587] p 3773 N92-31315

GLASS FIBER REINFORCED PLASTICS
Flammability characteristics of glass reinforced epoxy composite materials
[AD-A251009] p 3775 N92-31940
Low thermal coefficient of expansion printed wiring boards
[DE92-013704] p 3817 N92-31946

GLASS FIBERS
High strength glass second source qualification to composite armor specification MIL-L-46197(MR)
[AD-A252114] p 3792 N92-31404

GLOBAL POSITIONING SYSTEM
Satellite positioning systems: A report to the director
[PB92-181270] p 3767 N92-31632
GPS satellite orbit determination using pseudorange data: Experiments and results
[PB92-178870] p 3765 N92-31685
Global positioning system runway incursion program static ground tests
[DOT/FAA/CT-TN91/44] p 3756 N92-31838
Decision-making guide for the proposed Coast Guard differential global positioning system
[AD-A246046] p 3756 N92-32054

GLOBAL WARMING
Our changing planet: The FY 1993 US global change research program. A supplement to the US President's fiscal year 1993 budget
[NASA-CR-190675] p 3850 N92-31259
Iterative functionalism and climate management regimes: From intergovernmental panel on climate change to intergovernmental negotiating committee
[DE92-014798] p 3853 N92-31896
The uncertainties of global temperatures in the global warming context
[TABES PAPER 92-447] p 3763 N92-32014

GLOW DISCHARGES
Time and space resolved electron impact excitation rates in an RF glow discharge
[AD-A249614] p 3905 N92-31688
An improved ion guide for external ion injection in glow discharge-Fourier transform ion cyclotron resonance (GD-FTICR) mass spectrometry
[AD-A250944] p 3900 N92-32170

GLUTAMINE
Evolution and analysis of the functional domains of the chimeric proteins that initiate pyrimidine biosynthesis
[AD-A250069] p 3866 N92-31465

GOERTLER INSTABILITY
On the spatial evolution of long-wavelength Goertler vortices governed by a viscous-inviscid interaction
[NASA-CR-189681] p 3822 N92-31687

GOGGLES
Pilot errors involving Head-Up Displays (HUDs), Helmet-Mounted Displays (HMDs), and Night Vision Goggles (NVGs)
[AD-A250719] p 3873 N92-32023

GOLD
Monte Carlo simulations of random rough surface scattering with finite element and finite difference methods
[AD-A247528] p 3901 N92-31430

GOVERNMENT/INDUSTRY RELATIONS
Small Business Innovation Research program solicitation. Closing date: July 21, 1992
[NASA-TM-107795] p 3916 N92-31253
NSF Tokyo reports. General outline of JFY 1991 government science and technology budget
[PB92-192640] p 3927 N92-32068

GOVERNMENTS
NSF Tokyo reports. General outline of JFY 1991 government science and technology budget
[PB92-192640] p 3927 N92-32068

GRAIN BOUNDARIES
The structure and properties of grain boundaries in Ni3Al
[DE92-012143] p 3788 N92-31744

GRAIN SIZE
Mechanics of thin films
[AD-A247848] p 3912 N92-31984

GRANULAR MATERIALS
Granular flows down bumpy inclines
[DE92-013568] p 3820 N92-31425
Steady flow of a fluid-solid mixture between parallel plates
[DE92-013645] p 3821 N92-31426

GRAPH THEORY
The Swendsen-Wang dynamics in the simulation of the Ising model
[INPE-5394-PRE/1752] p 3874 N92-31348
Decomposition of balanced matrices. Part 4: Connected squares
[AD-A247308] p 3888 N92-31768

GRAPHIC ARTS
Hyper-NPSNET: A virtual world with an integrated 3-D hypertext
[AD-A252726] p 3878 N92-31676

GRAPHITE
Electronic and total energy properties of ternary and quaternary semiconductor compounds, alloys, and superlattices: Theoretical study of Cu/graphite bonding
[NASA-CR-190691] p 3772 N92-31266
Auger line shapes as a probe of electronic structure in covalent systems
[AD-A246329] p 3912 N92-31994

GRAPHITE-EPOXY COMPOSITES
Graphite/epoxy composite adapters for the Space Shuttle/Centaur vehicle
[NASA-TP-3014] p 3765 N92-31251
Composite material shear property measurement using the Iosipescu specimen
[NASA-CR-190661] p 3772 N92-31274
Computational simulation of intermingled-fiber hybrid composite behavior
[NASA-TM-105666] p 3774 N92-31506

GRAPHS (CHARTS)
Development of the aspect graph representation for use in R version
[AD-A247109] p 3876 N92-31573
Trends 1991: A compendium of data on global change
[DE92-011733] p 3854 N92-31907

GRATINGS (SPECTRA)
Holographic grating relaxation and photon correlation spectroscopic studies of viscoelastic liquids above the glass transition
[AD-A252485] p 3828 N92-31828

GRAVITATION
Statistical analysis of anomalous transport in resistive interchange turbulence
[NIFS-125] p 3818 N92-31256
Research in elementary particle physics
[DE92-014585] p 3893 N92-31385

GRAVITATION THEORY
Modified black holes in two dimensional gravity
[DE92-630244] p 3924 N92-31401

GRAVITATIONAL EFFECTS
Hollow fiber clinostat for simulating microgravity in cell culture
[NASA-CASE-MFS-28370-1] p 3828 N92-31790

GRAVITATIONAL FIELDS
Satellite-to-satellite tracking in the high-low mode: Line-of-sight acceleration in a residual gravity field
[PL-TR-91-2209] p 3767 N92-32082

GRAVITY WAVES
Computation of nonlinear gravity waves by a desingularized boundary integral method
[AD-A251149] p 3857 N92-31766

GREASES
Surface analysis of stainless steel outer race bearing specimens
[AD-A250088] p 3833 N92-31437
Liquid lubrication for space applications
[NASA-TM-105198] p 3795 N92-31840

GREEN'S FUNCTIONS
Wavenumbers for currents on infinite- and finite-length wires in a chiral medium
[DE92-007565] p 3804 N92-31317
Schwinger boson studies of the t-J model beyond mean-field approximation
[DE92-630650] p 3909 N92-31655

GREENHOUSE EFFECT
The detection of climate change due to the enhanced greenhouse effect
[NASA-TM-107965] p 3849 N92-31258
Effects of anthropogenic sulfur aerosols on climate
[DE92-016158] p 3850 N92-31297
Energy conservation: The main factor for reducing greenhouse gas emissions in the former Soviet Union
[DE92-012355] p 3852 N92-31574
Trends 1991: A compendium of data on global change
[DE92-011733] p 3854 N92-31907

GREENLAND
Sensitivity of the tomographic inverse solution to acoustic path variability
[AD-A252146] p 3864 N92-31407

GRID GENERATION (MATHEMATICS)
Hypersonic code efficiency and validation studies
[NASA-CR-190680] p 3752 N92-31533
An installed nacelle design code using a multiblock Euler solver. Volume 1: Theory document
[NASA-CR-189652-VOL-1] p 3754 N92-32226
An installed nacelle design code using a multiblock Euler solver. Volume 2: User guide
[NASA-CR-189652-VOL-2] p 3754 N92-32228

GROUND STATE
Proceedings of the 2nd KUR symposium on hyperfine interactions
[DE92-789024] p 3895 N92-31728

GROUND SUPPORT EQUIPMENT
Ground based radar
[TABES PAPER 92-213] p 3764 N92-32021

GROUND SUPPORT SYSTEMS
Configuration management and software measurement in the Ground Systems Development Environment (GSDE)
[NASA-CR-190716] p 3879 N92-31787

GROUND TESTS
Global positioning system runway incursion program static ground tests
[DOT/FAA/CT-TN91/44] p 3756 N92-31838
GROUND WATER
Hydrological and geochemical response and recovery in disturbed Arctic ecosystems
[DE92-016223] p 3850 N92-31312
FEHMN 1.0: Finite element heat and mass transfer code
[DE92-013998] p 3825 N92-32008
GROUND WIND
A numerical, analytical, and observational study of the effect of clouds on surface wind and wind stress during the central Arctic winter
[AD-A252706] p 3860 N92-31670
GROUP DYNAMICS
Research and development of methods and tools for achieving and maintaining consensus processes in the face of change within and among government oversight agencies, volume 1
[DE92-014179] p 3852 N92-31592
GUIDANCE (MOTION)
Neural network perception for mobile robot guidance
[AD-A249972] p 3884 N92-31511
Discrete optimal guidance for high order missile and maneuvering target p 3748 N92-31879
GUIDANCE SENSORS
FCS skewed sensors array: Practical considerations p 3746 N92-31868
GULF OF MEXICO
Synthetic temperature profile in the Gulf of Mexico. Part 1: Statistical relationship between modal amplitudes and dynamic height at surface
[AD-A252701] p 3863 N92-31308
GULF STREAM
Synthetic temperature profile in the Gulf of Mexico. Part 1: Statistical relationship between modal amplitudes and dynamic height at surface
[AD-A252701] p 3863 N92-31308
GUST ALLEVIATORS
Rolling maneuver load alleviation using active controls
[NASA-TM-107654] p 3757 N92-31351
GUSTS
A comparison of the performance of two gust front detection algorithms using a length-based scoring technique
[AD-A250862] p 3863 N92-32103
GYROSCOPES
Spacecraft dynamics characterization and control system failure detection. Volume 3: Control system failure monitoring
[NASA-CR-190529] p 3884 N92-31254
An investigation of spinup dynamics of axial gyrostats using elliptic integrals and the method of averaging
[AD-A249728] p 3768 N92-31675

H

HADRONS
A dynamical model of the behaviour of hadronic and fundamental strings at finite densities
[DE92-630245] p 3914 N92-31402
Efficiency calculations of the hadron detector
[NIKHEF-K-EMIN-92-01] p 3896 N92-31814
Theoretical studies in nuclear reactions and nuclear structure
[DE92-016204] p 3897 N92-31927
Results of IR working group
[DE92-013294] p 3902 N92-32149
HANDBOOKS
STI handbook: Guidelines for producing, using, and managing scientific and technical information in the Department of the Navy. A handbook for Navy scientists and engineers on the use of scientific and technical information
[AD-A252439] p 3918 N92-31482
Marine structural steel toughness data bank, volume 1
[AD-A247923] p 3789 N92-31987
Composite failure analysis handbook. Volume 1: Program review
[AD-A250520] p 3776 N92-32047
Composite failure analysis handbook. Volume 2: Technical handbook. Part 1: Procedures and techniques
[AD-A250521] p 3776 N92-32048
HANDLING EQUIPMENT
Robotic soil sampler for hazardous waste clean up
[DE92-012693] p 3780 N92-31565
HARDENING (SYSTEMS)
Design of a TEM cell EMP simulator
[DREO-1084] p 3806 N92-31470
HARMONIC GENERATIONS
Detection of signal harmonic sets
[DREA-CR-89-420] p 3806 N92-31471
Dipolar interaction assisted effects on second harmonic generation
[AD-A252487] p 3784 N92-31959
Electro-optics and second harmonic generation of nonlinear optical polymers
[AD-A252488] p 3796 N92-31960
HARNESSES
Vertical impact tests of humans and anthropomorphic manikins
[AD-A245866] p 3872 N92-31458
HARTREE APPROXIMATION
Many body perturbation theory using a Restricted Open-Shell Hartree-Fock (ROHF) reference function
[AD-A249725] p 3894 N92-31673
HAZARDS
Algorithms for the determination of spatial and spectral distribution of electromagnetic energy in a simulated biostructure subjected to transient spatially heterogeneous radiation with applications to radar hazard assessment and cancer therapy
[AD-A250447] p 3805 N92-31381
Analysis of debris from Spacelab Space Life Sciences-1
[NASA-TM-103593] p 3765 N92-32148
HEAD MOVEMENT
Head tracking and head mounted displays for training simulations
[AD-A250866] p 3873 N92-31974
HEAD-UP DISPLAYS
Head tracking and head mounted displays for training simulations
[AD-A250866] p 3873 N92-31974
Pilot errors involving Head-Up Displays (HUDs), Helmet-Mounted Displays (HMDs), and Night Vision Goggles (NVGs)
[AD-A250719] p 3873 N92-32023
HEART FUNCTION
Noninvasive ambulatory assessment of cardiac function and myocardial ischemia in healthy subjects exposed to carbon monoxide
[AD-A252264] p 3870 N92-32107
HEAT
Body water homeostasis and human performance in high heat environments: Fluid hydration recommendations for Operation Desert Storm
[AD-A249772] p 3868 N92-31492
HEAT ACCLIMATIZATION
Body water homeostasis and human performance in high heat environments: Fluid hydration recommendations for Operation Desert Storm
[AD-A249772] p 3868 N92-31492
HEAT BALANCE
The structure and energetics of Amazon squall lines
[AD-A250182] p 3859 N92-31523
HEAT EXCHANGERS
Sodium Heat Engine Development Program
[DE92-012398] p 3846 N92-31531
Heat exchanger performance calculations for enhanced-tube condenser applications
[DE92-016603] p 3823 N92-31785
Gas engine heat recovery unit
[PB92-184373] p 3835 N92-31841
An overview of the Lewis Research Center CSTI thermal management program
[NASA-TM-105310] p 3771 N92-31916
HEAT FLUX
An airborne study of boundary layer heat and moisture fluxes for project FIFE
[NASA-CR-190665] p 3844 N92-31357
Energy balance model for imagery and electromagnetic propagation
[AD-A250884] p 3806 N92-31543
HEAT MEASUREMENT
An airborne study of boundary layer heat and moisture fluxes for project FIFE
[NASA-CR-190665] p 3844 N92-31357
Description of a 1000 sensor constant current anemometer system for locating three-dimensional turbulent boundary layer separations
[AD-A250827] p 3821 N92-31452
Energy balance model for imagery and electromagnetic propagation
[AD-A250884] p 3806 N92-31543
Calibration at 24 C of a heat-flow-meter apparatus having 610 mm square plates
[DE92-015954] p 3827 N92-31633
HEAT OF DISSOCIATION
Computational studies of metal-metal and metal-ligand interactions
[NASA-CR-190674] p 3790 N92-32156
HEAT PIPES
Establishing low-power operating limits for liquid metal heat pipes
[DE92-011367] p 3823 N92-31701
Analytical and experimental studies of heat pipe radiation cooling of hypersonic propulsion systems
[DE92-013428] p 3759 N92-31817
An overview of the Lewis Research Center CSTI thermal management program
[NASA-TM-105310] p 3771 N92-31916
Design, fabrication, and testing of a 30 kW(sub t) screen-wick heat-pipe solar receiver
[DE92-016500] p 3848 N92-32087
HEAT PUMPS
Heat and mass transfer considerations in advanced heat pump systems
[DE92-016635] p 3825 N92-32003
HEAT RESISTANT ALLOYS
Fatigue in single crystal nickel superalloys
[AD-A250068] p 3786 N92-31360
Chromium, nickel, and other alloying elements in US-produced stainless and heat-resisting steel
[PB92-178623] p 3788 N92-31797
Fatigue in single crystal nickel superalloys
[AD-A252492] p 3790 N92-32066
HEAT SINKS
The prediction of the performance of a microcircuit heat sink in the boiling mode
[AD-A250045] p 3812 N92-31355
HEAT STORAGE
Solar thermal energy storage in phase change materials
[DE92-016908] p 3849 N92-32091
HEAT TRANSFER
Effect of outer temperature changes and solar radiation on effective heat losses through external partitions of buildings p 3802 N92-31242
Free-piston Stirling engine conceptual design and technologies for space power, phase 1
[NASA-CR-182168] p 3769 N92-31245
Emissivity measurements in support of experiments on natural convection between a vertical cylinder and a surrounding array
[DE92-012321] p 3819 N92-31287
Annual dynamics within the active layer
[DE92-013520] p 3850 N92-31304
Weld penetration and defect control
[DE92-015310] p 3836 N92-31336
Oscillating-flow regenerator test rig: Woven screen and metal felt results
[NASA-CR-190689] p 3820 N92-31352
The prediction of the performance of a microcircuit heat sink in the boiling mode
[AD-A250045] p 3812 N92-31355
A model for the interfacial shear in vertical, adiabatic, annular-mist flow
[DE92-013537] p 3820 N92-31424
Description of a 1000 sensor constant current anemometer system for locating three-dimensional turbulent boundary layer separations
[AD-A250827] p 3821 N92-31452
Flat plates placed in depleted hypersonic flow
[SESSIA-430/91.960] p 3751 N92-31508
Pressure loss and heat transfer in a toothed finned heat transfer medium
[MBB-UO-0163-91-PUB] p 3915 N92-31660
A numerical, analytical, and observational study of the effect of clouds on surface wind and wind stress during the central Arctic winter
[AD-A252706] p 3860 N92-31670
Establishing low-power operating limits for liquid metal heat pipes
[DE92-011367] p 3823 N92-31701
Ion temperature gradient instability and transport
[DE92-013590] p 3905 N92-31727
Further studies in filmwise condensation of steam on horizontal finned tubes
[AD-A252705] p 3915 N92-31767
Heat exchanger performance calculations for enhanced-tube condenser applications
[DE92-016603] p 3823 N92-31785
Incipient and total group combustion of fuel sprays in air p 3749 N92-31883
Transport and evaporation effects in counterflow spray diffusion flames p 3749 N92-31884
Heat transfer and flow of a modified second grade fluid
[DE92-014744] p 3824 N92-31895
Condensation in a two-phase pool
[DE92-010048] p 3824 N92-31977
Heat and mass transfer considerations in advanced heat pump systems
[DE92-016635] p 3825 N92-32003
FEHMN 1.0: Finite element heat and mass transfer code
[DE92-013998] p 3825 N92-32008
Probabilistic analysis of twenty-four hour weather data for Warsaw p 3863 N92-32097

Experimental studies of friction and heat transfer in enhanced passages
[DE92-011607] p 3890 N92-32099
Heat transfer and pressure drop in an annular channel with downflow
[DE92-014363] p 3825 N92-32115
Thin polymer icemaker development and test program
[DE92-016941] p 3803 N92-32125

HEAT TRANSFER COEFFICIENTS
Description of a 1000 sensor constant current anemometer system for locating three-dimensional turbulent boundary layer separations
[AD-A250827] p 3821 N92-31452
Further studies in filmwise condensation of steam on horizontal finned tubes
[AD-A252705] p 3915 N92-31767

HEAT TRANSMISSION
Calibration at 24 C of a heat-flow-meter apparatus having 610 mm square plates
[DE92-015954] p 3827 N92-31633

HEATING
Simplified air change effectiveness modeling
[DE92-010577] p 3872 N92-31309
Enhancement of fracture toughness using high intensity electric currents
[AD-A249809] p 3889 N92-31359

HEAVY IONS
New high voltage parallel plate analyzer
[NIFS-128] p 3827 N92-31340
Dependence of secondary ion emission from organic material on the energy loss of the impacting heavy ion
[DE92-014845] p 3893 N92-31386
The interplanetary heavy ion environment for both galactic cosmic rays and solar energetic particles during the CRRES mission
[AD-A248942] p 3926 N92-31477

HELICOPTER DESIGN
Experimental testing of prototype face gears for helicopter transmissions
[NASA-TM-105434] p 3832 N92-31349

HELICOPTER PROPELLER DRIVE
Experimental testing of prototype face gears for helicopter transmissions
[NASA-TM-105434] p 3832 N92-31349
Modal simulation of gearbox vibration with experimental correlation
[NASA-TM-105702] p 3834 N92-31485

HELICOPTERS
A simulation model of a single rotor helicopter
p 3746 N92-31865
Report of the aviation safety review of Department of Energy helicopter operations
[DE92-016346] p 3755 N92-31928

HELIOSTATS
Computer simulation of shading and blocking: Discussion of accuracy and recommendations
[DE91-002146] p 3849 N92-32110

HELIOTRONS
Theory of anomalous transport in toroidal helical plasmas
[NIFS-140] p 3904 N92-31659

HELIUM
Comparison of double and single ionization in He by photons and by charged projectiles
[DE92-013411] p 3894 N92-31679
He atom-surface scattering: Surface dynamics of insulators, overlayers and crystal growth
[DE92-011810] p 3911 N92-31914
Laser-ablated copper condensation in helium
[DE92-016685] p 3789 N92-32004

HELIUM ISOTOPES
A sealed He-4 superfluid-transition fixed-point device
[DE92-014271] p 3908 N92-31403

HELMET MOUNTED DISPLAYS
Pilot errors involving Head-Up Displays (HUDs), Helmet-Mounted Displays (HMDs), and Night Vision Goggles (NVGs)
[AD-A250719] p 3873 N92-32023

HEPTANES
A study of the effect of hydrocarbon structure on the induction of male rat nephropathy and metabolite structure
[AD-A252192] p 3867 N92-31590

HERBIG-HARO OBJECTS
Molecular outflows associated with HH52-54 and IRAS 12496-7650
[PB92-184472] p 3924 N92-31635

HETEROCYCLIC COMPOUNDS
Synthesis of soluble alpha-thiophene oligomers. Monomer to octamer
[AD-A250082] p 3779 N92-31434
Supercritical fluid fractionation of JP-8
[AD-A247835] p 3801 N92-31982

HETERODYNING
Diagnostics for research in atomization and turbulent two-phase flows
[AD-A247201] p 3819 N92-31283

HETEROGENEITY
Prompt neutron lifetime in a strongly heterogeneous lattice
[DE92-013212] p 3898 N92-32165

HETEROJUNCTIONS
Submillimeter wave spectroscopy of heterojunction superlattices
[AD-A250835] p 3908 N92-31496

HEURISTIC METHODS
The vehicle routing problem: Some computational tests of savings method and its variations
[INPE-5361-RPQ/656] p 3886 N92-31241
Combining expert probabilistic weather forecasts: Results of post-hoc analyses of the Zierikzee experiment
[REPT-91-101] p 3859 N92-31521
Objects used to implement intelligent databases
[DE92-013098] p 3919 N92-31581
Artificial Intelligence in Training (AIT)
[AD-A250145] p 3885 N92-31811
Heuristic sampling on DAGs
[DE92-017359] p 3917 N92-32037

HIERARCHIES
Type evolution and instance adaptation
[AD-A248435] p 3917 N92-31285
Towards a complete hierarchy of compositional dataflow models
[RUU-CS-91-45] p 3807 N92-31715

HIGH ALTITUDE
Mitigation of magnetohydrodynamic electromagnetic pulse (MHD-EMP) effects from commercial electric power systems
[AD-A249577] p 3804 N92-31354

HIGH ENERGY INTERACTIONS
Theoretical high energy physics research at the University of Chicago, task A
[DE92-016288] p 3899 N92-31712
Participation in high energy physics. Task C: Particle physics and cosmology
[DE92-016290] p 3924 N92-31713

HIGH ENERGY PROPELLANTS
Selective nitrations: The laser-induced nitration of three cycloalkanes, 1
[AD-A249942] p 3800 N92-31800

HIGH FLUX BEAM REACTORS
Electrically-induced stresses and deflection in multiple plates
[DE92-012303] p 3841 N92-31844

HIGH FREQUENCIES
Injecting into AmPS when ring cavity operates at 476 MHz
[NIKHEF-K/AMPS/91-08] p 3899 N92-31815
Realization of lattice networks at MHz- and GHz-frequencies
[PB92-195437] p 3810 N92-32161

HIGH RESOLUTION
High-resolution microwave observations of the sun
[AD-A247869] p 3925 N92-31985

HIGH REYNOLDS NUMBER
High Reynolds number test of the Boeing TR77 airfoil in the Langley 0.3-meter transonic cryogenic tunnel
[NASA-TM-4189] p 3750 N92-31246

HIGH SPEED
A microprism array for large-scale, wide-band interconnection of optoelectronic systems
[AD-A249380] p 3813 N92-31374
Design and analysis issues of integrated control systems for high-speed civil transports
[NASA-CR-186022] p 3761 N92-31656
VLSI for high-speed digital signal processing
[AD-A250365] p 3817 N92-32074

HIGH STRENGTH
The effect of thermomechanical processing parameters on the ambient behavior of 10 percent volume 6061 Al-Alumina
[AD-A252177] p 3776 N92-32064

HIGH STRENGTH STEELS
Marine structural steel toughness data bank, volume 1
[AD-A247923] p 3789 N92-31987

HIGH TEMPERATURE
High-temperature ignition of propane with MTBE as an additive: Shock-tube experiments and modeling
[DE92-008933] p 3778 N92-31415
High temperature superconducting films and multilayers for electronics
[AD-A250732] p 3813 N92-31451
Elementary reaction rate measurements at high temperatures by tunable-laser flash-absorption
[DE92-015269] p 3830 N92-31684
Fabrication of an insulated gate diamond FET for high temperature applications
[AD-A251042] p 3817 N92-31849
Tailored metal matrix composites for high-temperature performance
[NASA-TM-105816] p 3775 N92-31854
An investigation of the thermoviscoplastic behavior of a metal matrix composite at elevated temperatures
[NASA-CR-190700] p 3777 N92-32159

HIGH TEMPERATURE ENVIRONMENTS
Demonstrated survivability of a high temperature optical fiber cable on a 1500 pound thrust rocket chamber
[NASA-TM-105835] p 3801 N92-32230

HIGH TEMPERATURE GASES
Ceramic membranes for high temperature hydrogen separation
[DE92-013342] p 3783 N92-31816

HIGH TEMPERATURE PLASMAS
New high voltage parallel plate analyzer
[NIFS-128] p 3827 N92-31340
Transient internal probe diagnostic
[AD-A247306] p 3903 N92-31459
Energy transport in the steady state plasma sustained by DC helicity current drive
[NIFS-127] p 3907 N92-32181

HIGH TEMPERATURE SUPERCONDUCTORS
Pulsed laser deposition of high Tc superconducting thin films
[AD-A250657] p 3830 N92-31319
High temperature superconducting films and multilayers for electronics
[AD-A250732] p 3813 N92-31451
Computer simulation of scattered ion and sputtered species effects in ion beam sputter-deposition of high temperature superconducting thin films
[DE92-015227] p 3909 N92-31546
Potential impact of high temperature superconductors on MAGLEV transportation
[DE92-012683] p 3834 N92-31720
Microstructure and properties of in-situ RF sputtered YBa2Cu3O7 thin films for microwave applications
[DE92-013379] p 3911 N92-31723
Recent advances in high-temperature superconductor wire fabrication and applications development
[DE92-016634] p 3912 N92-31955
Investigation of acoustic properties of high-temperature ceramic superconductors p 3914 N92-32209

HIGH TEMPERATURE TESTS
Thermomechanical fatigue behavior of a silicone carbide fiber-reinforced calcium aluminosilicate glass-ceramic matrix composite
[AD-A249870] p 3775 N92-31823

HIGH VOLTAGES
Calculational prediction of ultrawideband electromagnetic pulses by laser-initiated air avalanche switches
[DE92-011732] p 3812 N92-31334
New high voltage parallel plate analyzer
[NIFS-128] p 3827 N92-31340
Compact millimeter-wave devices: Dielectric loaded carm, high voltage carm, slow wave crm and high harmonic gyrotron
[AD-A250497] p 3809 N92-31944

HILBERT TRANSFORMATION
Phase characteristics and time responses of unknown linear systems determined from measured CW amplitude data
[PB92-183722] p 3805 N92-31368

HIPPOCAMPUS
The effects of hydrazines of neuronal excitability
[AD-A247142] p 3868 N92-31491

HMX
Estimation of metal acceleration by an SF5 containing explosive
[AD-A245338] p 3801 N92-32098

HOLLOW CATHODES
Proposal for a workshop in the physics and application of hollow electrode glow switches
[AD-A247139] p 3814 N92-31490

HOLOGRAPHIC INTERFEROMETRY
Effect of fracture surface interference on shear crack growth
[DE92-011431] p 3839 N92-31389

HOLOGRAPHY
A microprism array for large-scale, wide-band interconnection of optoelectronic systems
[AD-A249380] p 3813 N92-31374
High brightness x ray source for directed energy and holographic imaging applications, phase 2
[AD-A248858] p 3827 N92-31475
Holographic grating relaxation and photon correlation spectroscopic studies of viscoelastic liquids above the glass transition
[AD-A252485] p 3828 N92-31828
Diffusion of camphorquinone in uniaxially drawn polycarbonate films
[AD-A252489] p 3796 N92-31961

HOMEOSTASIS
Body water homeostasis and human performance in high heat environments: Fluid hydration recommendations for Operation Desert Storm
[AD-A249772] p 3868 N92-31492
HOMOGENEOUS TURBULENCE
Reynolds stress calculations of homogeneous turbulent shear flow with bounded energy states
[NASA-CR-189682] p 3826 N92-32158
HONEYCOMB STRUCTURES
Motion model for the correction of point source distortion in radiographs of honeycomb
[DREP-88-14] p 3777 N92-32215
HORIZON
A sensitivity study of daytime visibility determination with the horizon scanning imager
[SIO-91-15] p 3902 N92-32144
HORMONES
Acetylcholinesterase inhibitors on the spinal cord
[AD-A252694] p 3868 N92-31326
HORN ANTENNAS
Analysis and evaluation of Project Evergreen data
[AD-A245983] p 3804 N92-31314
HOT ATOMS
Laser enhanced chemical reaction studies
[DE92-010772] p 3831 N92-31798
HOT PRESSING
Effect of surface modifications on the properties of silicon nitride ceramics
[DE92-013848] p 3797 N92-32094
HOT WEATHER
Body water homeostasis and human performance in high heat environments: Fluid hydration recommendations for Operation Desert Storm
[AD-A249772] p 3868 N92-31492
HOT-WIRE ANEMOMETERS
Improvements to the Rocky Flats Metrology Laboratories velocity meter calibration system
[DE92-013162] p 3829 N92-32138
HULLS (STRUCTURES)
On the feasibility of a transient dynamic design analysis method
[AD-A250406] p 3838 N92-31337
HUMAN BEINGS
Body water homeostasis and human performance in high heat environments: Fluid hydration recommendations for Operation Desert Storm
[AD-A249772] p 3868 N92-31492
Organization of the human circadian system
[AD-A247498] p 3869 N92-31905
HUMAN BODY
Nonthermal inhalation injury
[AD-A252532] p 3869 N92-31962
HUMAN FACTORS ENGINEERING
Vertical impact tests of humans and anthropomorphic manikins
[AD-A245866] p 3872 N92-31458
Development of a fault isolation system database manager
[AD-A248346] p 3916 N92-31992
HUMAN PERFORMANCE
Theory and test of stress resistance
[AD-A250741] p 3870 N92-31291
Empirical development of a scale for the prediction of performance on a sustained monitoring task
[AD-A252443] p 3872 N92-31294
Development of quantitative specifications for simulating the stress environment
[AD-A250669] p 3870 N92-31321
Human image understanding
[AD-A250401] p 3872 N92-31330
Body water homeostasis and human performance in high heat environments: Fluid hydration recommendations for Operation Desert Storm
[AD-A249772] p 3868 N92-31492
Micro saint model of fatigue assessment
[AD-A249976] p 3868 N92-31554
HUMIDITY
Surface chemistry of MoS2 lubricant films: Effects of high humidity storage on sputtered films
[DE92-015392] p 3794 N92-31631
Advanced microwave sounding unit study for atmospheric infrared sounder
[NASA-CR-190628] p 3858 N92-32195
HUMIDITY MEASUREMENT
Energy balance model for imagery and electromagnetic propagation
[AD-A250884] p 3806 N92-31543
HURRICANES
Updated forecast of Atlantic seasonal hurricane activity for 1992 p 3859 N92-31583
HYBRID COMPOSITES
Computational simulation of intermingled-fiber hybrid composite behavior
[NASA-TM-105666] p 3774 N92-31506
HYDRAULIC EQUIPMENT
Hydrogenerator design manual, chapter 8
[PB92-173707] p 3919 N92-31682
HYDRAZINES
The effects of hydrazines of neuronal excitability
[AD-A247142] p 3868 N92-31491
HYDROCARBON FUELS
High-temperature ignition of propane with MTBE as an additive: Shock-tube experiments and modeling
[DE92-008933] p 3778 N92-31415
HYDROCARBONS
f Mo(CHCMe2Ph)(NAr)(OR)2 and relative reactivity toward 2,3-bis(trifluoromethyl) norbornadiene iene
[AD-A250234] p 3780 N92-31524
A study of the effect of hydrocarbon structure on the induction of male rat nephropathy and metabolite structure
[AD-A252192] p 3867 N92-31590
Hydrocarbon ignition: Automatic generation of reaction mechanisms and applications to modeling of engine knock
[DE92-011943] p 3780 N92-31607
HYDROCHLORIC ACID
Dispersive-infrared gas sensor system design and operation manual
[DE92-011766] p 3828 N92-31909
HYDROCYANIC ACID
Theoretical studies of the reactions and spectroscopy of radical species relevant to combustion reactions and diagnostics
[DE92-013484] p 3781 N92-31725
HYDRODYNAMICS
Macrostatistical hydrodynamics
[DE92-013589] p 3823 N92-31726
Numerical simulation of tulip flame dynamics
[DE92-008553] p 3782 N92-31805
HYDROELECTRICITY
World energy projection system: Model documentation
[DE92-014206] p 3847 N92-31594
HYDROGEN
Gibbs free energy of reactions involving SiC, Si3N4, H2, and H2O as a function of temperature and pressure
[NASA-TP-3275] p 3791 N92-31278
Ceramic membranes for high temperature hydrogen separation
[DE92-013342] p 3783 N92-31816
Electron scattering by atomic hydrogen: Elastic and inelastic phenomena at 13.9 to 200 eV
[DE92-625004] p 3896 N92-31837
Fusion with highly spin polarized HD and D(2)
[DE92-017030] p 3898 N92-32007
Prediction of hydrogen entry and permeation in metals and alloys
[AD-A245286] p 3790 N92-32096
HYDROGEN ATOMS
Nature of short Li-H-C contact interactions in organolithium compounds and its implication
[AD-A250992] p 3898 N92-32024
HYDROGEN BONDS
Structure and dynamics of Cl(H2O)20 clusters. The effect of the polarizability and the charge ofthe ion
[AD-A251094] p 3899 N92-32196
HYDROGEN IONS
Dependence of secondary ion emission from organic material on the energy loss of the impacting heavy ion
[DE92-014845] p 3893 N92-31386
Structure and dynamics of Cl(H2O)20 clusters. The effect of the polarizability and the charge ofthe ion
[AD-A251094] p 3899 N92-32196
HYDROGEN OXYGEN ENGINES
Demonstrated survivability of a high temperature optical fiber cable on a 1500 pound thrust rocket chamber
[NASA-TM-105835] p 3801 N92-32230
HYDROGEN PLASMA
Synthesis of diamond films with pulsed plasma
[AD-A250058] p 3791 N92-31356
HYDROGEN PRODUCTION
Catalytic carbon membranes for hydrogen production
[DE92-001269] p 3784 N92-31976
HYDROGEN SULFIDE
Economics of microwave plasma dissociation of H2S
[DE92-014846] p 3779 N92-31441
HYDROGENATION
The synthesis and characterization of tribophysical layers on diamond and silicon carbide surfaces
[AD-A250983] p 3796 N92-32001
Probe molecule studies: Active species in alcohol synthesis
[DE92-015430] p 3784 N92-32029
Catalyst dispersion and activity under conditions of temperature-staged liquefaction
[DE92-014112] p 3786 N92-32141
HYDROGEOLOGY
FEHMN 1.0: Finite element heat and mass transfer code
[DE92-013998] p 3825 N92-32008
HYDROGRAPHY
Hydrographic and Acoustic Doppler Current Profiler (ADCP) data from the Farallones shelf and slope study
[AD-A250834] p 3864 N92-31495
Hydrographic observations from the US/PRC cooperative program in the western equatorial Pacific Ocean: Cruises 5-8
[PB92-177054] p 3865 N92-31644
An analysis of hydrographic data collected off Point Sur, California in June 1990
[AD-A246060] p 3866 N92-32056
HYDROLOGICAL CYCLE
Our Changing Planet: The FY 1993 US Global Change Research Program. A report by the Committee on Earth and Environmental Sciences, a supplement to the US President's fiscal year 1993 budget
[PB92-156892] p 3852 N92-31620
HYDROLOGY
Annual dynamics within the active layer
[DE92-013520] p 3850 N92-31304
Hydrological and geochemical response and recovery in disturbed Arctic ecosystems
[DE92-016223] p 3850 N92-31312
A test of ecological optimality for semiarid vegetation
[NASA-CR-190705] p 3855 N92-32222
HYDROLOGY MODELS
ARO Geoscience Center fellowships
[AD-A249225] p 3857 N92-31964
HYDROLYSIS
Tris-triphenylsiloxy compounds of aluminum
[AD-A250141] p 3788 N92-31795
HYDROPHONES
Acoustic studies of ocean surface processes in SWAPP
[AD-A247519] p 3864 N92-31429
HYDROSTATICS
Orbit transfer vehicle engine technology program. Task B-6 high speed turbopump bearings
[NASA-CR-189230] p 3835 N92-31892
HYDROTHERMAL SYSTEMS
Materials for geothermal production
[DE92-014691] p 3849 N92-32118
HYGROSCOPICITY
Polyalphaolefins: A new improved cost effective aircraft radar coolant
[AD-A250517] p 3796 N92-32045
HYPERCUBE MULTIPROCESSORS
Use of a genetic algorithm to solve fluid flow problems on an NCUBE/2 multiprocessor computer
[DE92-014044] p 3824 N92-31832
The hierarchical spatial decomposition of three-dimensional particle-in-cell plasma simulations on MIMD distributed memory multiprocessors
[DE92-016802] p 3883 N92-32034
HYPERFINE STRUCTURE
Proceedings of the 2nd KUR symposium on hyperfine interactions
[DE92-789024] p 3895 N92-31728
HYPERSONIC BOUNDARY LAYER
Fundamental studies of the structure of hypersonic attached and separated boundary layers over smooth, rough and transpiration-cooled surfaces
[AD-A250284] p 3819 N92-31286
Stability and transition of hypersonic boundary-layer flows
[AD-A250279] p 3752 N92-31555
Experimental studies of hypersonic shock-wave boundary-layer interactions
[NASA-CR-190731] p 3753 N92-32162
HYPERSONIC FLIGHT
Analytical and experimental studies of heat pipe radiation cooling of hypersonic propulsion systems
[DE92-013428] p 3759 N92-31817
HYPERSONIC FLOW
Stagnation-point heat-transfer rate predictions at aeroassist flight conditions
[NASA-TP-3208] p 3819 N92-31281
Stability of boundary layers at high supersonic and hypersonic speeds
[AD-A250900] p 3819 N92-31306
Flat plates placed in depleted hypersonic flow
[SESSIA-430/91.960] p 3751 N92-31508
Hypersonic code efficiency and validation studies
[NASA-CR-190680] p 3752 N92-31533
Stability and transition of hypersonic boundary-layer flows
[AD-A250279] p 3752 N92-31555
Low density real gas flows about hypersonic vehicles
[AD-A250048] p 3752 N92-31777
HYPERSONIC HEAT TRANSFER
Stagnation-point heat-transfer rate predictions at aeroassist flight conditions
[NASA-TP-3208] p 3819 N92-31281

HYPERSONIC SPEED
Experimental studies of hypersonic shock-wave boundary-layer interactions
[NASA-CR-190731] p 3753 N92-32162
HYPERSONIC VEHICLES
Fundamental studies of the structure of hypersonic attached and separated boundary layers over smooth, rough and transpiration-cooled surfaces
[AD-A250284] p 3819 N92-31286
Low density real gas flows about hypersonic vehicles
[AD-A250048] p 3752 N92-31777
Analytical and experimental studies of heat pipe radiation cooling of hypersonic propulsion systems
[DE92-013428] p 3759 N92-31817
The use of high lift-to-drag hypersonic vehicles for aero-assisted orbital maneuvering p 3748 N92-31877
HYPERSONICS
Hypersonic code efficiency and validation studies
[NASA-CR-190680] p 3752 N92-31533
Experimental studies of hypersonic shock-wave boundary-layer interactions
[NASA-CR-190731] p 3753 N92-32162
HYPERVELOCITY PROJECTILES
Projectile development for railguns using hypervelocity preacceleration
[DE92-016741] p 3766 N92-31735
Problems associated with launching hypervelocity projectiles from the fast shock tube
[DE92-015276] p 3762 N92-32026
HYPOTHALAMUS
Organization of the human circadian system
[AD-A247498] p 3869 N92-31905
HYPOTHERMIA
Immersion suit usage within the RAAF
[AD-A250645] p 3755 N92-31562
HYSTERESIS
A self consistent generalized model for the calculation of minor loop excursions in the theory of hysteresis
[DE92-014394] p 3890 N92-32116

I

ICE
Thin polymer icemaker development and test program
[DE92-016941] p 3803 N92-32125
ICE FORMATION
The icing of the elevator of the DLR icing research aircraft of Do 28 type
[DLR-MITT-91-12] p 3755 N92-31813
Analysis of three icing test flights reaching the aircraft-referred icing degree of severe
[ESA-TT-1254] p 3755 N92-31943
IDENTIFYING
Results of earth observation study on STS-31 for Terra Geode, January 1987 - June 1991
[AD-A250750] p 3844 N92-31621
Development of methodology and technology for identifying and quantifying emission products from open burning and open detonation thermal treatment methods. BangBox test series. Volume 2: Test development
[AD-A250734] p 3800 N92-31970
Development of methodology and technology for identifying and quantifying emission products from open burning and open detonation thermal treatment methods. Field test series A, B, and C. Volume 1: Test summary
[AD-A250735] p 3800 N92-31971
Development of methodology and technology for identifying and quantifying emission products from open burning and open detonation thermal treatment methods. Field test series A, B, and C. Volume 2, part B: Quality assurance and quality control. Appendices
[AD-A250737] p 3801 N92-31973
Monitoring threats to satellite functions
[PB92-195445] p 3767 N92-32073
IGNITERS
A semiconductor bridge ignited gas generator
[DE92-014049] p 3781 N92-31748
IGNITION
High-temperature ignition of propane with MTBE as an additive: Shock-tube experiments and modeling
[DE92-008933] p 3778 N92-31415
Two-stage n-butane flame: A comparison between experimental measurements and modeling results
[DE92-009457] p 3779 N92-31416
Hydrocarbon ignition: Automatic generation of reaction mechanisms and applications to modeling of engine knock
[DE92-011943] p 3780 N92-31607
Ignition and flame propagation studies over a flat fuel surface
[PB92-181056] p 3780 N92-31678
A semiconductor bridge ignited gas generator
[DE92-014049] p 3781 N92-31748
Autoignition behavior of lean mixtures: Chemical and thermodynamics effects
[DE92-009690] p 3781 N92-31763
Flammability characteristics of glass reinforced epoxy composite materials
[AD-A251009] p 3775 N92-31940
IGNITION LIMITS
Flammability limits and ballistic properties of fuel-rich propellants p 3749 N92-31885
IGNITION TEMPERATURE
Shock tube study of the reaction of triethanol ammonium nitrate with N2O
[AD-A250034] p 3800 N92-31804
IMAGE ANALYSIS
A real time system for multisensor image analysis through pyramidal segmentation
[AD-A247169] p 3888 N92-31981
IMAGE CONTRAST
Radar backscatter from the sea: Controlled experiments
[AD-A250858] p 3810 N92-32101
IMAGE ENHANCEMENT
A characterization of the hot infrared background: The infrared cirrus, zodiacal dust bands, and solar system dust trails
[PL-TR-91-2065] p 3924 N92-32142
Images simulation of sensors with large field of view from images of sensors with less field of view: The SSR/TM case
[INPE-5378-TDI/473] p 3845 N92-32220
IMAGE INTENSIFIERS
Dual gated imaging system for enhanced fluorescent diagnostics measurements
[AD-A249673] p 3828 N92-31694
IMAGE MOTION COMPENSATION
Using the burst derivative measure to improve the computational efficiency of ISAR motion compensation algorithms
[AD-A250850] p 3805 N92-31369
IMAGE PROCESSING
Digital analysis of wind tunnel imagery to measure fluid thickness
[NASA-CR-189234] p 3762 N92-31252
Detection of object edges in images containing cast shadows
[DE92-016092] p 3900 N92-31295
Compression of digitized map images
[AD-A250707] p 3843 N92-31323
Novel chemically amplified dry-developing imaging materials for high resolution microlithography
[AD-A250085] p 3793 N92-31435
Logarithmic retinae
[PB92-183649] p 3885 N92-31680
The 193-pixel, three-dimensional capacitance imaging system
[DE92-001253] p 3919 N92-31731
Resolution limits for ground based astronomical imaging using adaptive optics
[DE92-011949] p 3902 N92-31761
Optical processing architectures for spaceborne SAR image generation and RF array beam forming
[TABES PAPER 92-444] p 3763 N92-32012
Wavelet signal processing for transient feature extraction
[AD-A250519] p 3890 N92-32046
Incoherence effects in reflection electron microscopy
[DE92-016161] p 3829 N92-32086
Motion model for the correction of point source distortion in radiographs of honeycomb
[DREP-88-14] p 3777 N92-32215
Images simulation of sensors with large field of view from images of sensors with less field of view: The SSR/TM case
[INPE-5378-TDI/473] p 3845 N92-32220
GIS: Geographic Information Systems. State of the art and future tendencies
[INPE-5358-NTC/301] p 3922 N92-32227
IMAGE RECONSTRUCTION
Accretion disk image reconstruction in cataclysmic variables
[INPE-5343-PRE/1742] p 3923 N92-31347
From perception to modelization in robotics using achromatic and chromatic cameras
[LAAS-91484] p 3901 N92-31692
IMAGE RESOLUTION
Development of the aspect graph representation for use in R version
[AD-A247109] p 3876 N92-31573
IMAGERY
Digital analysis of wind tunnel imagery to measure fluid thickness
[NASA-CR-189234] p 3762 N92-31252
Energy balance model for imagery and electromagnetic propagation
[AD-A250884] p 3806 N92-31543
Markovian fields as limits of Markov chains
[INPE-5395-PRE/1753] p 3889 N92-32225
IMAGES
Resolution limits for ground based astronomical imaging using adaptive optics
[DE92-011949] p 3902 N92-31761
Forms of memory for representation of visual objects
[AD-A250056] p 3871 N92-31779
IMAGING TECHNIQUES
High brightness x ray source for directed energy and holographic imaging applications, phase 2
[AD-A248858] p 3827 N92-31475
Utilization of gamma ray inspection system for tomographic imaging and dimensional analysis of complete model magnet cold masses and collared coil sections
[DE92-013466] p 3836 N92-31647
Logarithmic retinae
[PB92-183649] p 3885 N92-31680
Dual gated imaging system for enhanced fluorescent diagnostics measurements
[AD-A249673] p 3828 N92-31694
The 193-pixel, three-dimensional capacitance imaging system
[DE92-001253] p 3919 N92-31731
Resolution limits for ground based astronomical imaging using adaptive optics
[DE92-011949] p 3902 N92-31761
Development of gamma ray imaging cameras
[DE92-015305] p 3828 N92-31919
Imaging and spectrometry of bulk crystal surfaces and surface dynamical processes at high temperatures
[DE92-015235] p 3913 N92-32085
Radar backscatter from the sea: Controlled experiments
[AD-A250858] p 3810 N92-32101
A sensitivity study of daytime visibility determination with the horizon scanning imager
[SIO-91-15] p 3902 N92-32144
Wavelength-tunable liquid crystal imaging filters for remote sensing from geosynchronous platforms
[NASA-CR-190698] p 3845 N92-32223
IMIDES
Imide/arylene ether copolymers
[NASA-CASE-LAR-14159-1-CU] p 3794 N92-31792
IMINES
Cationic ring opening polymerization of oxazolines initiated by trimethylsilyl derivatives
[AD-A251109] p 3798 N92-32153
IMMUNOLOGY
JPRS report: Science and technology. Central Eurasia: Life sciences
[JPRS-ULS-92-015] p 3924 N92-32179
IMPACT DAMAGE
A penetration mechanics database
[AD-A246351] p 3767 N92-31997
IMPACT LOADS
On the feasibility of a transient dynamic design analysis method
[AD-A250406] p 3838 N92-31337
IMPACT RESISTANCE
Solid electrolytes and impact-resistant ceramics
[DE92-015297] p 3797 N92-32095
IMPACT TESTS
Vertical impact tests of humans and anthropomorphic manikins
[AD-A245866] p 3872 N92-31458
IMPEDANCE
High-frequency techniques for RCS prediction of plate geometries
[NASA-CR-190656] p 3804 N92-31273
IMPEDANCE MEASUREMENT
Stability testing and analysis of a PMAD DC test bed for the Space Station Freedom
[NASA-TM-105846] p 3812 N92-31282
Interfacial ion transport between immiscible liquids
[AD-A252424] p 3778 N92-31292
IMPULSE GENERATORS
Synthesis of diamond films with pulsed plasma
[AD-A250058] p 3791 N92-31356
IMPURITIES
Power scaling of divertor plasma conditions during H-mode in D3-D
[DE92-012148] p 3906 N92-31771
Impurity effects on the magnetic ordering in chromium
[DE92-016165] p 3789 N92-31898
IN-FLIGHT MONITORING
In-flight evaluation of aerodynamic predictions of an air-launched space booster
[NASA-TM-104246] p 3752 N92-31808
INCOHERENCE
Detection of signal harmonic sets
[DREA-CR-89-420] p 3806 N92-31471
INCOHERENT SCATTERING
Incoherence effects in reflection electron microscopy
[DE92-016161] p 3829 N92-32086

INCOMPRESSIBLE BOUNDARY LAYER
The calculation of incompressible separated turbulent boundary layers p 3749 N92-31886
INCOMPRESSIBLE FLOW
The discretization of the 2D incompressible Navier-Stokes equations on a collocated grid
[REPT-91-61] p 3821 N92-31513
INDEXES (DOCUMENTATION)
NASA patent abstracts bibliography: A continuing bibliography. Section 2: Indexes (supplement 41)
[NASA-SP-7039(41)-SECT-2] p 3918 N92-31455
Aeronautical engineering: A continuing bibliography with indexes (supplement 280)
[NASA-SP-7037(280)] p 3745 N92-31456
INDICATING INSTRUMENTS
Hollow fiber clinostat for simulating microgravity in cell culture
[NASA-CASE-MFS-28370-1] p 3828 N92-31790
INDICATORS
Determination of the matrix conditioning indicator. Comparison of approximate methods
p 3887 N92-32210
INDIUM ARSENIDES
Advanced high efficiency concentrator cells
[DE92-010559] p 3848 N92-31893
INDIUM COMPOUNDS
Development of a computer model for polycrystalline thin-film CuInSe2 and CdTe solar cells
[DE92-001242] p 3846 N92-31526
INDOOR AIR POLLUTION
Simplified air change effectiveness modeling
[DE92-010577] p 3872 N92-31309
INDUCTION HEATING
Flexible heating head for induction heating apparatus and method
[NASA-CASE-LAR-14418-1] p 3803 N92-31257
INDUSTRIAL ENERGY
Solar synthesis of advanced materials: A solar industrial program initiative
[DE92-010575] p 3845 N92-31481
INDUSTRIAL MANAGEMENT
Total quality management: A management philosophy for providing high quality construction
[AD-A252743] p 3837 N92-32172
INDUSTRIAL SAFETY
Report of the aviation safety review of Department of Energy helicopter operations
[DE92-016346] p 3755 N92-31928
INDUSTRIES
Report to the US Congress on minority small business and capital ownership development as required by the Business Opportunity Development Reform Act of 1988
[PB92-173681] p 3916 N92-31364
Energy conservation: The main factor for reducing greenhouse gas emissions in the former Soviet Union
[DE92-012355] p 3852 N92-31574
A ban on use of lead-bearing solders: Implications for the electronics industry
[DE92-013291] p 3790 N92-32139
INELASTIC COLLISIONS
Theoretical atomic collision physics
[DE92-013571] p 3895 N92-31724
INELASTIC SCATTERING
Electron scattering by atomic hydrogen: Elastic and inelastic phenomena at 13.9 to 200 eV
[DE92-625004] p 3896 N92-31837
Resolution function of an inelastic scattering spectrometer with a pulsed neutron source
[DE92-620889] p 3896 N92-31904
INEQUALITIES
Geometric theory of infinite dimensional dynamical systems
[AD-A252190] p 3915 N92-31585
INERT ATMOSPHERE
Controlled atmosphere soldering system
[DE92-012633] p 3802 N92-31580
INERTIAL CONFINEMENT FUSION
Light ion driven inertial confinement fusion
[DE92-011662] p 3905 N92-31707
An examination of the feasibility of a nuclear-pumped laser-driven inertial confinement fusion reactor with magnetically protected walls
[AD-A248163] p 3907 N92-31990
INERTIAL FUSION (REACTOR)
YLIFE-2 inertial fusion energy power plant design
[DE92-011965] p 3904 N92-31530
INFERENCE
Probability-based inference in a domain of proportional reasoning tasks
[AD-A247304] p 3871 N92-31444
Objects used to implement intelligent databases
[DE92-013096] p 3919 N92-31581
INFORMATION DISSEMINATION
FEDIX: The on-line database retrieval service of government information for colleges, universities, and other organizations
[DE92-012384] p 3917 N92-31288
EnviroTRADE: Its role in the cleanup of the environment
[DE92-013691] p 3851 N92-31427
Aviation safety: Changes needed in FAA's service difficulty reporting program
[GAO/RCED-91-24] p 3755 N92-31453
INFORMATION FLOW
Operating principles of MULTIKRON performance instrumentation for MIMD computers
[PB92-181072] p 3874 N92-31366
New directions in network flows
[AD-A250499] p 3880 N92-32039
INFORMATION MANAGEMENT
Hypertext and hypermedia systems in information retrieval p 3921 N92-32188
INFORMATION PROCESSING (BIOLOGY)
Modeling of learning-induced receptive field plasticity in auditory neocortex
[AD-A250348] p 3869 N92-31558
INFORMATION RETRIEVAL
Assessing repository technology. Where do we go from here?
[NASA-CR-190630] p 3917 N92-31272
FEDIX: The on-line database retrieval service of government information for colleges, universities, and other organizations
[DE92-012384] p 3917 N92-31288
Using neural networks in software repositories
[NASA-CR-190641] p 3885 N92-31597
Correspondence dictionary from free English term to INIS descriptors
[DE92-782192] p 3920 N92-31859
A model for extending the behavior of annotations
[DE92-011731] p 3920 N92-31934
Database explorer: Large scale database application
[AD-A252183] p 3920 N92-32049
Bringing Down the Barriers to Information Transfer
[AGARD-CP-505] p 3920 N92-32182
Local Area Networks (LAN) p 3874 N92-32183
Intelligent gateways p 3921 N92-32184
Use of expert systems as user interfaces in information retrieval p 3921 N92-32185
Search strategies in natural language p 3921 N92-32186
Non Boolean search methods in information retrieval p 3921 N92-32187
Hypertext and hypermedia systems in information retrieval p 3921 N92-32188
INFORMATION SYSTEMS
RCRIS data element dictionary, version 3.0.0: Data tape documentation
[PB92-145515] p 3918 N92-31398
EnviroTRADE: Its role in the cleanup of the environment
[DE92-013691] p 3851 N92-31427
EnviroTRADE: A technical perspective on the development of an information system providing data on environmental technologies and needs worldwide
[DE92-012625] p 3919 N92-31578
Research and development of methods and tools for achieving and maintaining consensus processes in the face of change within and among government oversight agencies, volume 1
[DE92-014179] p 3852 N92-31592
Continuous time and discrete time hyperexponential model for dependability growth modeling
[LAAS-92002] p 3837 N92-31693
Directory of IAEA databases
[DE92-628395] p 3920 N92-32058
Bringing Down the Barriers to Information Transfer
[AGARD-CP-505] p 3920 N92-32182
Local Area Networks (LAN) p 3874 N92-32183
Intelligent gateways p 3921 N92-32184
Non Boolean search methods in information retrieval p 3921 N92-32187
Hypertext and hypermedia systems in information retrieval p 3921 N92-32188
Automated input into databases: OCR and descriptive cataloguing p 3921 N92-32189
Facilitating the transfer of scientific and technical information with scientific and technical numeric databases p 3922 N92-32192
INFORMATION TRANSFER
Proceedings of the 4th Atlantic OCS Region Information Transfer Meeting
[PB92-177690] p 3864 N92-31630
Remote Data Transfer (RDT): An interprocess data transfer method for distributed environments
[AD-A250859] p 3920 N92-32102
Bringing Down the Barriers to Information Transfer
[AGARD-CP-505] p 3920 N92-32182
INFRARED ABSORPTION
Tomographic reconstruction of infrared spectra of nonhomogeneous media: Applications to a flat flame burner
[AD-A249999] p 3778 N92-31393
INFRARED ASTRONOMY SATELLITE
Molecular outflows associated with HH52-54 and IRAS 12496-7650
[PB92-184472] p 3924 N92-31635
INFRARED DETECTORS
Dispersive-infrared gas sensor system design and operation manual
[DE92-011766] p 3828 N92-31909
INFRARED IMAGERY
Cloud-to-ground lightning characteristics in mesoscale convective systems
[AD-A250418] p 3858 N92-31493
A coordinated study of a storm system over the South American continent
[INPE-5388-TDI/477] p 3863 N92-32212
INFRARED INSTRUMENTS
Advanced microwave sounding unit study for atmospheric infrared sounder
[NASA-CR-190628] p 3858 N92-32195
INFRARED INTERFEROMETERS
Absolute calibration of the Fourier interferometric transmissometer
[DREV-R-4511/88] p 3829 N92-32218
INFRARED LASERS
Selective nitrations: The laser-induced nitration of three cycloalkanes, 1
[AD-A249942] p 3800 N92-31800
INFRARED RADAR
OSRMS: The DREP near-nadir scatterometer
[DREP-88-15] p 3844 N92-32216
Characteristics of selected reference targets for calibrating 10.6 micron laser radars
[DREV-R-4487/88] p 3811 N92-32217
INFRARED RADIATION
Cellular localization of infrared sources
[AD-A249795] p 3866 N92-31302
Control of rapid thermal processing equipment for microelectronics applications
[LAAS-92013] p 3787 N92-31695
Theory for the CEBAF infrared and shipboard FELS
[AD-A252174] p 3832 N92-32061
A characterization of the hot infrared background: The infrared cirrus, zodiacal dust bands, and solar system dust trails
[PL-TR-91-2065] p 3924 N92-32142
INFRARED SPECTRA
Tomographic reconstruction of infrared spectra of nonhomogeneous media: Applications to a flat flame burner
[AD-A249999] p 3778 N92-31393
Role of the double-layer cation on the potential-dependent stretching frequencies and binding geometries of carbon monoxide at platinum-nonaqueous interfaces
[AD-A246980] p 3784 N92-31998
INFRARED SPECTROSCOPY
Tomographic reconstruction of infrared spectra of nonhomogeneous media: Applications to a flat flame burner
[AD-A249999] p 3778 N92-31393
Real-time infrared spectroscopy of moving solids for on-line analyses
[DE92-012156] p 3782 N92-31772
Application of optical theory to quantitative surface FT-IR with emphasis on molecular depth profiling
[AD-A250525] p 3902 N92-32077
The potential of passive-remote Fourier Transform Infrared (FTIR) spectroscopy to detect organic emissions under the Clean Air Act
[DE92-015224] p 3854 N92-32083
INHIBITION (PSYCHOLOGY)
Illusory self motion and disorientation
[CTN-92-60318] p 3871 N92-31472
INHIBITORS
Acetylcholinesterase inhibitors on the spinal cord
[AD-A252694] p 3868 N92-31326
INJURIES
Nonthermal inhalation injury
[AD-A252532] p 3869 N92-31962
INORGANIC MATERIALS
Inorganic rings on carbon chains
[AD-A251043] p 3772 N92-31850
INSPECTION
Replaceable valve seat
[AD-D015250] p 3832 N92-31271
Utilization of gamma ray inspection system for tomographic imaging and dimensional analysis of complete model magnet cold masses and collared coil sections
[DE92-013466] p 3836 N92-31647
EWE: A computer model for ultrasonic inspection
[DE92-627145] p 3837 N92-32143

INSTRUMENT ERRORS
A continuing study of altitude determination deficiencies of the Service Aircraft Instrumentation Package (SAIP)
[AD-A245952] p 3758 N92-32051
INSTRUMENT LANDING SYSTEMS
Effect of guard band reduction on marker beacon receiver performance
[DOT/FAA/CT-TN92/18] p 3807 N92-31617
INSULATION
Immersion suit usage within the RAAF
[AD-A250645] p 3755 N92-31562
INSULATORS
He atom-surface scattering: Surface dynamics of insulators, overlayers and crystal growth
[DE92-011810] p 3911 N92-31914
INTEGERS
The RQM triangle: A paradigm for relativistic quantum mechanics
[DE92-011583] p 3915 N92-31663
INTEGRAL EQUATIONS
The Matrix Editor for symbolic Jacobians in ALPAL
[DE92-008076] p 3878 N92-31742
Computation of nonlinear gravity waves by a desingularized boundary integral method
[AD-A251149] p 3857 N92-31766
INTEGRAL ROCKET RAMJETS
Sizing supersonic freejet nozzle and inlet location for simulation of the transition phase in integral rocket ramjet p 3747 N92-31870
INTEGRALS
Analytic estimation of radiation effects in space using solid angles
[DE92-013282] p 3899 N92-31831
INTEGRATED CIRCUITS
A fast laser alloying process for the selective electroplating of metal on SiO2 and polyimide
[DE92-011764] p 3788 N92-31759
High-performance packaging for monolithic microwave and millimeter-wave integrated circuits
[NASA-TM-105744] p 3808 N92-31855
INTELLIGENCE
The impact of cognitive feedback on the performance of intelligence analysts
[AD-A252176] p 3871 N92-32063
INTERACTIONAL AERODYNAMICS
On the spatial evolution of long-wavelength Goertler vortices governed by a viscous-inviscid interaction
[NASA-CR-189681] p 3822 N92-31687
In-flight evaluation of aerodynamic predictions of an air-launched space booster
[NASA-TM-104246] p 3752 N92-31808
INTERFACES
The role of metal structure in determining solvent orientation at the electrode/solution interface
[AD-A249751] p 3893 N92-31328
INTERFACIAL ENERGY
Real time investigations of the polymerization of 2-pentadecyl aniline on the Langmuir-Blodgett trough
[AD-A250994] p 3795 N92-31954
The chemistry and packaging of nanocomposite confined arrays
[AD-A250991] p 3817 N92-32002
INTERFACIAL TENSION
Epitaxial iron films
[AD-A250402] p 3912 N92-31915
INTERFEROMETERS
A phase contrast interferometer on D3-D
[DE92-012699] p 3905 N92-31764
Optical interferometric sensor detected intensity noise reductions means
[AD-D015296] p 3902 N92-32137
INTERFEROMETRY
Physical characterization of magmatic liquids
[DE92-015302] p 3858 N92-32027
Femtosecond photonics: Fundamental phenomena and device behavior
[AD-A250506] p 3832 N92-32042
INTERMETALLICS
Radiation-induced crystalline-to-amorphous transition in intermetallic compounds of the Cu-Ti alloy system
[DE92-010276] p 3787 N92-31575
Superplasticity in a nickel silicide alloy, Ni3Si(V, Mo)
[DE92-011651] p 3787 N92-31667
The structure and properties of grain boundaries in Ni3Al
[DE92-012143] p 3788 N92-31744
Quantum mechanical approach to understanding microstructural and mechanical properties in intermetallics
[AD-A250550] p 3790 N92-32084
INTERNAL COMBUSTION ENGINES
Hydrocarbon ignition: Automatic generation of reaction mechanisms and applications to modeling of engine knock
[DE92-011943] p 3780 N92-31607
Gas engine heat recovery unit
[PB92-184373] p 3835 N92-31841
INTERNAL ENERGY
Dicke narrowing in strong fields: The atom-as-antenna analogy
[AD-A252321] p 3807 N92-31629
INTERNATIONAL COOPERATION
International Semiconductor Device Research Symposium (ISDRS-91)
[AD-A247394] p 3908 N92-31537
EnviroTRADE: A technical perspective on the development of an information system providing data on environmental technologies and needs worldwide
[DE92-012625] p 3919 N92-31578
Iterative functionalism and climate management regimes: From intergovernmental panel on climate change to intergovernmental negotiating committee
[DE92-014798] p 3853 N92-31896
Partnership in space: An introduction to Canada's special relationship with the European Space Agency
[ESA-BR-79] p 3922 N92-31947
Italian-US cooperation in space: The case of Tethered, IRIS/LAGEOS, and SPACEHAB
[TABES PAPER 92-467] p 3764 N92-32019
INTERNATIONAL LAW
Anti-environmental warfare: Protecting the environment during wartime
[AD-A250337] p 3851 N92-31556
INTERPLANETARY SPACE
Interplanetary Program to Optimize Space Trajectories (IPOST). Volume 3: Programmer's manual
[NASA-CR-189653-VOL-3] p 3766 N92-32130
INTERPOLATION
A surface definition code for turbine blade surfaces
[DE92-010574] p 3846 N92-31498
INTERPROCESSOR COMMUNICATION
Performance measures of the Ada rendezvous
[AD-A250060] p 3877 N92-31601
Remote Data Transfer (RDT): An interprocess data transfer method for distributed environments
[AD-A250859] p 3920 N92-32102
INTERSTITIALS
A comparison of interstitial oxygen calculated by different techniques
[DE92-011658] p 3910 N92-31668
INVARIANCE
Geometric theory of infinite dimensional dynamical systems
[AD-A252190] p 3915 N92-31585
Theoretical high energy physics research at the University of Chicago, task A
[DE92-016288] p 3899 N92-31712
Feynman diagrams and Vassiliev invariants
[PB92-178284] p 3890 N92-31925
INVENTORY CONTROLS
Design and automated manufacturing p 3746 N92-31866
INVERSIONS
Using the burst derivative measure to improve the computational efficiency of ISAR motion compensation algorithms
[AD-A250850] p 3805 N92-31369
Sources of unbounded priority inversions in real-time systems and a comparative study of possible solutions
[NASA-CR-190711] p 3875 N92-31486
INVERTEBRATES
Ecosystems of the Florida Keys: A bibliography
[PB92-198910] p 3854 N92-32071
INVERTED CONVERTERS (DC TO AC)
Understanding and managing the effects of battery charger and inverter aging
[DE92-014473] p 3815 N92-31651
INVERTERS
MHD Contractors' Review Meeting: Abstracts
[DE92-011549] p 3904 N92-31576
INVESTMENT CASTING
Prototype casting fabrication by stereolithography
[DE92-011489] p 3876 N92-31529
INVISCID FLOW
A computational investigation of airfoil stall flutter
[AD-A247302] p 3751 N92-31300
On the spatial evolution of long-wavelength Goertler vortices governed by a viscous-inviscid interaction
[NASA-CR-189681] p 3822 N92-31687
IODIDES
Cationic ring opening polymerization of oxazolines initiated by trimethylsilyl derivatives
[AD-A251109] p 3798 N92-32153
IODINE
The crystal growth and characterization of the solid solutions (ZnS)(1-x)(CuMS2)(x)
[AD-A248029] p 3911 N92-31819
ION ACOUSTIC WAVES
Weak ion-acoustic shock waves and double layers in non-collision plasma p 3907 N92-32208
ION ATOM INTERACTIONS
Comparison of double and single ionization in He by photons and by charged projectiles
[DE92-013411] p 3894 N92-31679
ION BEAMS
Computer simulation of scattered ion and sputtered species effects in ion beam sputter-deposition of high temperature superconducting thin films
[DE92-015227] p 3909 N92-31546
Ion beam spectroscopy as a means of in-situ monitoring of thin film deposition
[DE92-014857] p 3909 N92-31652
Light ion driven inertial confinement fusion
[DE92-011662] p 3905 N92-31707
ION CYCLOTRON RADIATION
Gallium arsenide clusters and their interfacial physics and chemistry
[AD-A249565] p 3907 N92-31375
An improved ion guide for external ion injection in glow discharge-Fourier transform ion cyclotron resonance (GD-FTICR) mass spectrometry
[AD-A250944] p 3900 N92-32170
ION EMISSION
Dependence of secondary ion emission from organic material on the energy loss of the impacting heavy ion
[DE92-014845] p 3893 N92-31386
ION ENGINES
The evolutionary development of high specific impulse electric thruster technology
[NASA-TM-105712] p 3769 N92-31342
Krypton ion thruster performance
[NASA-TM-105818] p 3770 N92-31901
ION EXCHANGE MEMBRANE ELECTROLYTES
Interfacial ion transport between immiscible liquids
[AD-A252424] p 3778 N92-31292
Batteries and fuel cells
[DE92-011493] p 3847 N92-31571
ION IMPLANTATION
Strongly adherent ceramic surface layers by ion implantation
[AD-A248882] p 3792 N92-31388
Fabrication of an insulated gate diamond FET for high temperature applications
[AD-A251042] p 3817 N92-31849
ION INJECTION
An improved ion guide for external ion injection in glow discharge-Fourier transform ion cyclotron resonance (GD-FTICR) mass spectrometry
[AD-A250944] p 3900 N92-32170
ION IRRADIATION
Edge-on ion irradiation of electron microscope specimens
[DE92-014847] p 3894 N92-31595
Correlation from randomness. Quantitative analysis of sputtered graphite surfaces using the scanning tunneling microscope
[AD-A252420] p 3783 N92-31820
ION MOTION
Interfacial ion transport between immiscible liquids
[AD-A252424] p 3778 N92-31292
ION PROPULSION
Krypton ion thruster performance
[NASA-TM-105818] p 3770 N92-31901
Low-Isp derated ion thruster operation
[NASA-TM-105787] p 3771 N92-32237
ION TEMPERATURE
Vortices associated with toroidal ion temperature gradient driven fluctuations
[DE92-016180] p 3903 N92-31412
Ion temperature gradient instability and transport
[DE92-013590] p 3905 N92-31727
IONIC COLLISIONS
Comparison of double and single ionization in He by photons and by charged projectiles
[DE92-013411] p 3894 N92-31679
IONIZATION
Comparison of double and single ionization in He by photons and by charged projectiles
[DE92-013411] p 3894 N92-31679
Ionization potentials and electron affinities of semiconductor clusters determined via charge transfer reactions
[AD-A250943] p 3898 N92-32169
IONIZATION CHAMBERS
Use of tissue equivalent proportional counters to characterize radiation quality on the space shuttle
[DE92-012347] p 3768 N92-31846
IONIZATION CROSS SECTIONS
Comparison of double and single ionization in He by photons and by charged projectiles
[DE92-013411] p 3894 N92-31679
IONIZATION POTENTIALS
Ionization potentials and electron affinities of semiconductor clusters determined via charge transfer reactions
[AD-A250943] p 3898 N92-32169

IONIZED GASES
Plasma channel generation using low energy electron beams
[DE92-013770] p 3906 N92-31949
IONIZING RADIATION
An evaluation of ionizing radiation emitted by high power microwave generators
[DE92-016160] p 3805 N92-31387
Biodosimetry of ionizing radiation in humans using the glycophorin A genotoxicity assay
[DE92-011974] p 3869 N92-31608
IONOSPHERIC DISTURBANCES
Impulsive magnetic perturbations of the high latitude, dayside ionosphere
[AD-A249872] p 3857 N92-31932
USU center of excellence in theory and analysis of the geo-plasma environment
[AD-A252189] p 3858 N92-32055
IONOSPHERIC PROPAGATION
Ionospheric communications channel modelling
[DE92-013039] p 3808 N92-31722
IRON
Spin polarized photoemission studies of surfaces and thin-films
[DE92-016098] p 3907 N92-31296
Epitaxial iron films
[AD-A250402] p 3912 N92-31915
The development of precipitated iron catalysts with improved stability
[DE92-014630] p 3785 N92-32117
IRON ALLOYS
Oxidation/sulfidation behavior of Fe-Cr alloys: A reactive-element effect
[DE92-016172] p 3789 N92-31924
IRRADIATION
Dependence of secondary ion emission from organic material on the energy loss of the impacting heavy ion
[DE92-014845] p 3893 N92-31386
Novel chemically amplified dry-developing imaging materials for high resolution microlithography
[AD-A250085] p 3793 N92-31435
The photogeneration of polymeric amines: Synthesis and photocrosslinking of copolymers containing photoactive carbamate pendant groups
[AD-A250086] p 3793 N92-31436
Radiation-induced crystalline-to-amorphous transition in intermetallic compounds of the Cu-Ti alloy system
[DE92-010276] p 3787 N92-31575
Edge-on ion irradiation of electron microscope specimens
[DE92-014847] p 3894 N92-31595
Ion beam spectroscopy as a means of in-situ monitoring of thin film deposition
[DE92-014857] p 3909 N92-31652
Radiolytic gas production in the alpha particle degradation of plastics
[DE92-011846] p 3795 N92-31938
IRREGULARITIES
The effects of magnetic storm phases on F-layer irregularities from auroral to equatorial latitudes
[AD-A249011] p 3855 N92-31478
ISENTROPIC PROCESSES
A model for the interfacial shear in vertical, adiabatic, annular-mist flow
[DE92-013537] p 3820 N92-31424
ISING MODEL
The Swendsen-Wang dynamics in the simulation of the Ising model
[INPE-5394-PRE/1752] p 3874 N92-31348
Markovian fields as limits of Markov chains
[INPE-5395-PRE/1753] p 3889 N92-32225
ISLANDS
Two-dimensional axisymmetric calculations of surface waves generated by an explosion in an island, mountain, and sedimentary basin
[AD-A249971] p 3856 N92-31510
ISOLATION
One thousand days non-stop at sea: Lessons for a mission to Mars
[TABES PAPER 92-462] p 3764 N92-32020
ISOMERIZATION
Novel chemically amplified dry-developing imaging materials for high resolution microlithography
[AD-A250085] p 3793 N92-31435
Cationic ring opening polymerization of oxazolines initiated by trimethylsilyl derivatives
[AD-A251109] p 3798 N92-32153
ISOMERS
f Mo(CHCMe2Ph)(NAr)(OR)2 and relative reactivity toward 2,3-bis(trifluoromethyl) norbornadiene iene
[AD-A250234] p 3780 N92-31524
ISOTHERMAL PROCESSES
Control of rapid thermal processing equipment for microelectronics applications
[LAAS-92013] p 3787 N92-31695
ISOTOPE SEPARATION
Experimental and computer modeling studies of isotopically selective two-step laser photodissociation of small molecules
[DE92-011427] p 3894 N92-31606
ISOTOPIC ENRICHMENT
Experimental and computer modeling studies of isotopically selective two-step laser photodissociation of small molecules
[DE92-011427] p 3894 N92-31606
ISOTROPIC TURBULENCE
Towards understanding turbulent scalar mixing
[NASA-CR-4446] p 3826 N92-32242
ISOTROPY
A robust algorithm for isotropic reconstruction of magic-angle spinning solid-state NMR spectra
[AD-A249610] p 3874 N92-31379
ITALIAN SPACE PROGRAM
Italian-US cooperation in space: The case of Tethered, IRIS/LAGEOS, and SPACEHAB
[TABES PAPER 92-467] p 3764 N92-32019
ITERATIVE SOLUTION
A strictly improving phase 1 algorithm using least-squares subproblems
[DE92-015904] p 3875 N92-31410
Iterative methods for large sparse linear systems arising from partial differential equations
[AD-A249524] p 3886 N92-31567
The hierarchical spatial decomposition of three-dimensional particle-in-cell plasma simulations on MIMD distributed memory multiprocessors
[DE92-016802] p 3883 N92-32034
Determination of the matrix conditioning indicator. Comparison of approximate methods
p 3887 N92-32210

J

J INTEGRAL
J(sub 2) fracture toughness testing of Al 707 5-T7351
p 3747 N92-31872
JACOBI MATRIX METHOD
Singularity avoidance for SCARA-type robots
p 3746 N92-31867
JAMMING
Analysis of random induced cross polarization
[AD-A249773] p 3806 N92-31569
Experiment on a three-beam adaptive array for EHF frequency-hopped signals using a fast algorithm, phase-D
[CTN-92-60322] p 3810 N92-32203
JAPAN
The trading company in space development in Japan
[TABES PAPER 92-424] p 3764 N92-32015
NSF Tokyo reports. General outline of JFY 1991 government science and technology budget
[PB92-192640] p 3927 N92-32068
JET ENGINE FUELS
Advanced thermally stable jet fuel development program. Volume 2: Compositional factors affecting thermal degradation of jet fuels
[AD-A252656] p 3798 N92-31399
Advanced thermally stable, jet fuels development program annual report. Volume 1: Model and experiment system development
[AD-A249625] p 3799 N92-31462
JET ENGINES
Engine monitoring display study
[NASA-CR-4463] p 3761 N92-32175
JET FLOW
Adaptive and nonadaptive feedback control of global instabilities with application to a heated 2-D jet
[AD-A250700] p 3820 N92-31322
JET IMPINGEMENT
Computer program to solve two-dimensional shock-wave interference problems with an equilibrium chemically reacting air model
[NASA-TM-4187] p 3818 N92-31247
JET STREAMS (METEOROLOGY)
Upper tropospheric jet streams over North America during summer 1988
[AD-A249871] p 3857 N92-31906
JOINTS (JUNCTIONS)
Preliminary evaluation of adhesion strength measurement devices for ceramic/titanium matrix composite bonds
[NASA-TM-105803] p 3745 N92-31267
Torque linearizing hardware for the electric joint motors of a direct-drive robot
[DE92-012681] p 3816 N92-31718
Investigation into the ultrasonic NDE of adhesively bonded joints
[DREP-90-02] p 3837 N92-32202
JOSEPHSON JUNCTIONS
High temperature superconducting films and multilayers for electronics
[AD-A250732] p 3813 N92-31451
The physics of cellular automata and coherence and chaos in classical many-body systems
[DE92-016834] p 3890 N92-32035
Aluminum tunnel junction detector operation in an adiabatic demagnetization refrigerator
[DE92-013441] p 3913 N92-32166
JP-8 JET FUEL
Supercritical fluid fractionation of JP-8
[AD-A247835] p 3801 N92-31982

K

K-EPSILON TURBULENCE MODEL
Reynolds stress calculations of homogeneous turbulent shear flow with bounded energy states
[NASA-CR-189682] p 3826 N92-32158
KALMAN FILTERS
Extended Kalman filter for attitude estimation of the Earth Radiation Budget Satellite p 3748 N92-31876
True covariance simulation of the EUVE (extreme ultra violet explorer) update filter p 3748 N92-31878
Confidence interval estimation for output of discrete-event simulations using the Kalman filter
[AD-A248170] p 3880 N92-31991
KELVIN-HELMHOLTZ INSTABILITY
Evidence of stochastic diffusion across a cross-field sheath due to Kelvin-Helmholtz vortices
[AD-A247847] p 3907 N92-31983
KERNEL FUNCTIONS
Mission and Safety Critical (MASC) plans for the MASC Kernel simulation
[NASA-CR-190708] p 3875 N92-31487
KIDNEYS
A study of the effect of hydrocarbon structure on the induction of male rat nephropathy and metabolite structure
[AD-A252192] p 3867 N92-31590
KINEMATICS
Using the burst derivative measure to improve the computational efficiency of ISAR motion compensation algorithms
[AD-A250850] p 3805 N92-31369
Modeling and design of a closed kinematic chain robotic mechanism
[DE92-014777] p 3835 N92-32121
KINETIC THEORY
Weak ion-acoustic shock waves and double layers in non-collision plasma p 3907 N92-32208
KINETICS
Granular flows down bumpy inclines
[DE92-013568] p 3820 N92-31425
Diffusion in ordered and disordered media
[AD-A250949] p 3891 N92-32211
KLYSTRONS
A three-gap klystron output cavity at X-band
[DE92-012417] p 3812 N92-31289
KNOWLEDGE
Assessing repository technology. Where do we go from here?
[NASA-CR-190630] p 3917 N92-31272
KNOWLEDGE BASES (ARTIFICIAL INTELLIGENCE)
Artificial Intelligence in Training (AIT)
[AD-A250145] p 3885 N92-31811
KNOWLEDGE REPRESENTATION
Comparison of results: Technische Univ., Delft-Organisatie voor Toegepast Natuurwetenschappelijk Onderzoek expert judgement study of dispersion-deposition
[REPT-92-11] p 3856 N92-31522
Hypertext and hypermedia systems in information retrieval p 3921 N92-32188
KNUDSEN FLOW
Catalytic carbon membranes for hydrogen production
[DE92-001269] p 3784 N92-31976
KRYPTON
Krypton ion thruster performance
[NASA-TM-105818] p 3770 N92-31901

L

LABORATORIES
Space nuclear power, propulsion, and related technologies
[SAND91-2617] p 3770 N92-31503
A program for the transfer of manufacturing technology from the national laboratories
[DE92-011905] p 3923 N92-31965
LABYRINTH SEALS
Turbine blade tip and seal clearance excitation forces
[NASA-CR-184341] p 3760 N92-31910

LAGEOS (SATELLITE)
Italian-US cooperation in space: The case of Tethered, IRIS/LAGEOS, and SPACEHAB
[TABES PAPER 92-467] p 3764 N92-32019
LAGRANGE MULTIPLIERS
Diagnostics for research in atomization and turbulent two-phase flows
[AD-A247201] p 3819 N92-31283
New directions in network flows
[AD-A250499] p 3860 N92-32039
LAKE MICHIGAN
Extremely Low Frequency (ELF) communications system ecological monitoring program summary of 1990 progress
[AD-A246344] p 3809 N92-31996
LAMB WAVES
Investigation into the ultrasonic NDE of adhesively bonded joints
[DREP-90-02] p 3837 N92-32202
LAMINAR FLOW
Experimental studies of friction and heat transfer in enhanced passages
[DE92-011607] p 3890 N92-32099
LAMINATES
A finite element procedure for analysis of laminated composite plates
[AD-A250902] p 3773 N92-31307
Modeling of composite beams and plates for static and dynamic analysis
[NASA-CR-190536] p 3839 N92-31339
High strength glass second source qualification to composite armor specification MIL-L-46197(MR)
[AD-A252114] p 3792 N92-31404
An experimental procedure for the Iosipescu composite specimen tested in the modified Wyoming fixture
[NASA-CR-190660] p 3774 N92-31566
Role of interfaces and interphases in the evolution mechanics of material systems
[AD-A250410] p 3774 N92-31604
Cutting treatment by drilling of fiber bound synthetic materials
[MBB-UD-0609-91-PUB] p 3774 N92-31716
Tailored metal matrix composites for high-temperature performance
[NASA-TM-105816] p 3775 N92-31854
Structural similitude and scaling laws for laminated beam-plates
[NASA-CR-190585] p 3841 N92-31911
Flex circuit lamination
[DE92-016574] p 3817 N92-32033
Eigensensitivity analysis of composite laminates: Effect of microstructure
[AD-A250864] p 3777 N92-32104
LAND MOBILE SATELLITE SERVICE
A prototype DND Ku band SATCOM system for ANIK-C2 (Project MASTER/MM2)
[DREO-1034] p 3810 N92-32176
LAND USE
A dynamic model of terrestrial carbon cycling
[DE92-015130] p 3853 N92-31782
LANDAU-GINZBURG EQUATIONS
Adaptive and nonadaptive feedback control of global instabilities with application to a heated 2-D jet
[AD-A250700] p 3820 N92-31322
LANDING GEAR
An assessment of the B-747's capability to operate on rough surfaces
[AD-A250134] p 3757 N92-31793
LANDING LOADS
An assessment of the B-747's capability to operate on rough surfaces
[AD-A250134] p 3757 N92-31793
LANDSAT SATELLITES
Solar-geophysical data number 572, April 1992. Part 2: (Comprehensive reports). Data for October 1991 and miscellaneous
[PB92-187731] p 3856 N92-31639
LAPLACE TRANSFORMATION
Phase characteristics and time responses of unknown linear systems determined from measured CW amplitude data
[PB92-183722] p 3805 N92-31368
LARGE SPACE STRUCTURES
Spacecraft dynamics characterization and control system failure detection. Volume 3: Control system failure monitoring
[NASA-CR-190529] p 3884 N92-31254
Studies in dynamic characterization and control of a flexible structure and optical beampath
[AD-A250555] p 3830 N92-31605
USU center of excellence in theory and analysis of the geo-plasma environment
[AD-A252189] p 3858 N92-32055
LASER ABLATION
Particle emission and charging effects induced by fracture
[AD-A252182] p 3913 N92-32065
LASER APPLICATIONS
Pulsed laser deposition of high Tc superconducting thin films
[AD-A250657] p 3830 N92-31319
Calculational prediction of ultrawideband electromagnetic pulses by laser-initiated air avalanche switches
[DE92-011732] p 3812 N92-31334
Amplification mechanism of ion-ripple lasers and its possible application
[DE92-016155] p 3830 N92-31411
Experimental and computer modeling studies of isotopically selective two-step laser photodissociation of small molecules
[DE92-011427] p 3894 N92-31606
Non-equilibrium synthesis by laser cladding of Ni, Nb and Mg alloys for improved environmental resistance
[AD-A250552] p 3787 N92-31612
A fast laser alloying process for the selective electroplating of metal on SiO2 and polyimide
[DE92-011764] p 3788 N92-31759
Laser decontamination: A new strategy for facility decommissioning
[DE92-014113] p 3831 N92-31775
Technology advancing research combustion in burners
[PB92-164359] p 3782 N92-31776
Selective nitrations: The laser-induced nitration of three cycloalkanes, 1
[AD-A249942] p 3800 N92-31800
Substrate surface effects on the properties of sputter-deposited and laser-irradiated films
[DE92-013850] p 3795 N92-31917
Plasma channel generation using low energy electron beams
[DE92-013770] p 3906 N92-31949
Diffusion of camphorquinone in uniaxially drawn polycarbonate films
[AD-A252489] p 3796 N92-31961
Characteristics of selected reference targets for calibrating 10.6 micron laser radars
[DREV-R-4487/88] p 3811 N92-32217
LASER ARRAYS
Phase-locked arrays of antiguided diode lasers: Modelling, design, evaluation of performance limits
[LAAS-92034] p 3830 N92-31698
LASER BEAMS
Selective nitrations: The laser-induced nitration of three cycloalkanes, 1
[AD-A249942] p 3800 N92-31800
LASER DAMAGE
Mechanics of thin films
[AD-A247848] p 3912 N92-31984
LASER FUSION
An examination of the feasibility of a nuclear-pumped laser-driven inertial confinement fusion reactor with magnetically protected walls
[AD-A248163] p 3907 N92-31990
Fusion with highly spin polarized HD and D(2)
[DE92-017030] p 3898 N92-32007
LASER GYROSCOPES
RL-34 ring laser gyro laboratory evaluation for the Deep Space Network antenna application
[NASA-CR-190481] p 3829 N92-32128
LASER HEATING
VAASEL-ANSYS comparison for a thermally loaded beam
[AD-A251003] p 3841 N92-31847
LASER INDUCED FLUORESCENCE
Stress and phase transformation phenomena in oxide films
[DE92-014702] p 3910 N92-31665
LASER INTERFEROMETRY
Diagnostics for research in atomization and turbulent two-phase flows
[AD-A247201] p 3819 N92-31283
LASER MATERIALS
Laser material interactions
[AD-A250028] p 3831 N92-31802
LASER MODE LOCKING
CO2 laser frequency multiplication
[AD-A248574] p 3830 N92-31755
Method and circuit for controlling the evolution time interval of a laser output pulse
[NASA-CASE-LAR-13772-1] p 3831 N92-31788
LASER OUTPUTS
Amplification mechanism of ion-ripple lasers and its possible application
[DE92-016155] p 3830 N92-31411
CO2 laser frequency multiplication
[AD-A248574] p 3830 N92-31755
Saturation effects in degenerate four-wave mixing spectroscopy: Nonperturbative calculations
[DE92-012253] p 3782 N92-31773
Method and circuit for controlling the evolution time interval of a laser output pulse
[NASA-CASE-LAR-13772-1] p 3831 N92-31788
LASER PLASMA INTERACTIONS
Amplification mechanism of ion-ripple lasers and its possible application
[DE92-016155] p 3830 N92-31411
LASER PLASMAS
Transient internal probe diagnostic
[AD-A247306] p 3903 N92-31459
LASER POWER BEAMING
Application of reactor-pumped lasers to power beaming
[DE92-012370] p 3831 N92-31762
LASER PUMPING
Application of reactor-pumped lasers to power beaming
[DE92-012370] p 3831 N92-31762
An examination of the feasibility of a nuclear-pumped laser-driven inertial confinement fusion reactor with magnetically protected walls
[AD-A248163] p 3907 N92-31990
LASER SPECTROSCOPY
Saturation effects in degenerate four-wave mixing spectroscopy: Nonperturbative calculations
[DE92-012253] p 3782 N92-31773
LASER TARGETS
Fusion with highly spin polarized HD and D(2)
[DE92-017030] p 3898 N92-32007
LASERS
Studies in dynamic characterization and control of a flexible structure and optical beampath
[AD-A250555] p 3830 N92-31605
Laser enhanced chemical reaction studies
[DE92-010772] p 3831 N92-31798
Real time detection in a laser bathymetry system
[PB92-195452] p 3866 N92-32069
The polarized electron gun for the SLC
[DE92-012418] p 3900 N92-32131
LATENT HEAT
An airborne study of boundary layer heat and moisture fluxes for project FIFE
[NASA-CR-190665] p 3844 N92-31357
Energy balance model for imagery and electromagnetic propagation
[AD-A250884] p 3806 N92-31543
LATERAL CONTROL
Rolling maneuver load alleviation using active controls
[NASA-TM-107654] p 3757 N92-31351
LATEX
Development of an electrochemical method for field testing of protective coatings
[AD-A245872] p 3793 N92-31473
LATTICE PARAMETERS
Prompt neutron lifetime in a strongly heterogeneous lattice
[DE92-013212] p 3898 N92-32165
LATTICES (MATHEMATICS)
Realization of lattice networks at MHz- and GHz-frequencies
[PB92-195437] p 3810 N92-32161
LAUNCH VEHICLE CONFIGURATIONS
Graphite/epoxy composite adapters for the Space Shuttle/Centaur vehicle
[NASA-TP-3014] p 3765 N92-31251
LEACHING
Rainwater and throughfall chemistry in a terra firme rain forest: Central Amazonia
[INPE-5364-PRE/1744] p 3863 N92-32224
LEAD (METAL)
Microdistribution of lead in bone: A new approach
[DE92-013036] p 3869 N92-31589
LEAD ALLOYS
A ban on use of lead-bearing solders: Implications for the electronics industry
[DE92-013291] p 3790 N92-32139
LEADING EDGES
In-flight leading-edge extension vortex flow-field survey measurements on a F-18 aircraft at high angle of attack
[NASA-TM-4398] p 3751 N92-31276
LEAF AREA INDEX
Sun-view-target geometry effects on spectrally-derived vegetative index estimates of absorbed radiation and leaf area
[AD-A249984] p 3843 N92-31329
LEAKAGE
Replaceable valve seat
[AD-D015250] p 3832 N92-31271
Turbine blade tip and seal clearance excitation forces
[NASA-CR-184341] p 3760 N92-31910

LEARNING
Modeling of learning-induced receptive field plasticity in auditory neocortex
[AD-A250348] p 3869 N92-31558
LEARNING THEORY
A language for higher-order explanation-based learning
[AD-A251008] p 3880 N92-31939
LEAST SQUARES METHOD
A strictly improving phase 1 algorithm using least-squares subproblems
[DE92-015904] p 3875 N92-31410
Adaptive inverse filter
[DE92-011660] p 3878 N92-31669
LEAVES
Changes in the reflectance of ex situ leaves: A methodological approach
[INPE-5407-PUD/051] p 3806 N92-31568
LESIONS
Function of panel M pathways in primates
[AD-A250275] p 3871 N92-31758
LETHALITY
Modular UNIX (trade name)-based Vulnerability Estimation Suite (MUVES) analyst's guide
[AD-A245322] p 3876 N92-31488
LIE GROUPS
Modified black holes in two dimensional gravity
[DE92-630244] p 3924 N92-31401
LIFE (DURABILITY)
Subsonic flight test evaluation of a performance seeking control algorithm on an F-15 airplane
[NASA-TM-4400] p 3759 N92-31275
Life prediction and constitutive models for engine hot section anisotropic materials program
[NASA-CR-189222] p 3759 N92-31534
Outdoor testing of advanced optical materials for solar thermal electric applications
[DE92-010567] p 3847 N92-31623
Pressure and temperature for B-1B transparency test
[AD-A252711] p 3752 N92-31674
Low-Isp derated ion thruster operation
[NASA-TM-105787] p 3771 N92-32237
LIFE SCIENCES
JPRS report: Science and technology. Central Eurasia: Life sciences
[JPRS-ULS-92-015] p 3924 N92-32179
LIFTING ROTORS
A simulation model of a single rotor helicopter
p 3746 N92-31865
LIGANDS
Tris-triphenylsiloxy compounds of aluminum
[AD-A250141] p 3788 N92-31795
Computational studies of metal-metal and metal-ligand interactions
[NASA-CR-190674] p 3790 N92-32156
LIGHT (VISIBLE RADIATION)
Cellular localization of infrared sources
[AD-A249795] p 3866 N92-31302
New high voltage parallel plate analyzer
[NIFS-128] p 3827 N92-31340
LIGHT AMPLIFIERS
Amplification mechanism of ion-ripple lasers and its possible application
[DE92-016155] p 3830 N92-31411
Millimeter wave free electron laser amplifiers: Experiments and designs
[DE92-011813] p 3832 N92-31935
LIGHT BEAMS
Results of IR working group
[DE92-013294] p 3902 N92-32149
LIGHT EMITTING DIODES
SiGe Si quantum wires for efficient, room temperature, tunable luminescence
[AD-A249651] p 3814 N92-31464
LIGHT GAS GUNS
Transient internal probe diagnostic
[AD-A247306] p 3903 N92-31459
Projectile development for railguns using hypervelocity preacceleration
[DE92-016741] p 3766 N92-31735
LIGHT IONS
Light ion driven inertial confinement fusion
[DE92-011662] p 3905 N92-31707
LIGHT MODULATION
Stable integrated microwave to optical modulator
[AD-A249974] p 3813 N92-31431
LIGHT SCATTERING
Diagnostics for research in atomization and turbulent two-phase flows
[AD-A247201] p 3819 N92-31283
LIGHT SOURCES
Cellular localization of infrared sources
[AD-A249795] p 3866 N92-31302
LIGHT TRANSMISSION
Absorption spectra and electronic properties of alkali metal doped C60
[AD-A251006] p 3912 N92-31937
A sensitivity study of daytime visibility determination with the horizon scanning imager
[SIO-91-15] p 3902 N92-32144
LIGHT VALVES
Particle diagnostics in optically thick sprays
[AD-A250981] p 3897 N92-31936
LIGHTNING
Cloud-to-ground lightning characteristics in mesoscale convective systems
[AD-A250418] p 3858 N92-31493
A comparative analysis of the temporal variability of lightning observations and GOES imagery
[AD-A250185] p 3860 N92-31603
Using transfer functions as a method for predicting lightning effects on munitions storage bunkers
[DE92-012627] p 3861 N92-31709
Measured responses of a munitions storage bunker to rocket-triggered lightning
[DE92-012628] p 3862 N92-31750
LIMITERS (FUSION REACTORS)
Dynamic modeling of plasma-vapor interactions during plasma disruptions
[DE92-016183] p 3903 N92-31310
LINE OF SIGHT
Satellite-to-satellite tracking in the high-low mode: Line-of-sight acceleration in a residual gravity field
[PL-TR-91-2209] p 3767 N92-32082
LINEAR ACCELERATORS
A three-gap klystron output cavity at X-band
[DE92-012417] p 3812 N92-31289
Pulse-by-pulse energy measurement at the Stanford Linear Collider
[DE92-011520] p 3899 N92-31390
Beam position monitor electronics using DC coupled demodulating logarithmic amplifiers
[DE92-011697] p 3816 N92-31760
Theory for the CEBAF infrared and shipboard FELS
[AD-A252174] p 3832 N92-32061
The polarized electron gun for the SLC
[DE92-012418] p 3900 N92-32131
LINEAR ARRAYS
Field-emitter arrays for RF vacuum microelectronics
[AD-A250101] p 3816 N92-31791
LINEAR ENERGY TRANSFER (LET)
Relating space radiation environments to risk estimates
[DE92-010256] p 3926 N92-31756
LINEAR PROGRAMMING
A strictly improving phase 1 algorithm using least-squares subproblems
[DE92-015904] p 3875 N92-31410
The development of modularized software for empirical testing of new algorithms in linear programming
[AD-A250811] p 3875 N92-31480
LINEAR SYSTEMS
Phase characteristics and time responses of unknown linear systems determined from measured CW amplitude data
[PB92-183722] p 3805 N92-31368
Signal location using generalized linear constraints
[AD-A249580] p 3805 N92-31376
Iterative methods for large sparse linear systems arising from partial differential equations
[AD-A249524] p 3886 N92-31567
A fundamental notion of equivalence for linear multivariable systems
[MATHS-REPT-A-153] p 3887 N92-31957
Asymptotic modal analysis and statistical energy analysis
[NASA-CR-190516] p 3842 N92-32236
LINEARIZATION
A simple linearized learning algorithm which outperforms back-propagation
[AD-A249697] p 3877 N92-31642
LININGS
Materials for geothermal production
[DE92-014691] p 3849 N92-32118
LIQUID CRYSTALS
Synthesis of side chain liquid crystal polymers by living ring opening metathesis polymerization. 4: Synthesis of amorphous and side chain liquid crystal AB block copolymers
[AD-A250353] p 3792 N92-31394
Wavelength-tunable liquid crystal imaging filters for remote sensing from geosynchronous platforms
[NASA-CR-190698] p 3845 N92-32223
LIQUID FLOW
Decomposition studies of triisopropylantimony and triallylantimony
[AD-A250671] p 3796 N92-31968
LIQUID FUELS
Catalyst and feedstock effects in the thermochemical conversion of biomass to liquid transportation fuels
[DE92-010569] p 3799 N92-31593
Transport and evaporation effects in counterflow spray diffusion flames p 3749 N92-31884
LIQUID HYDROGEN
Orbital transfer rocket engine technology: Advanced engine study
[NASA-CR-187216] p 3771 N92-32129
LIQUID METAL FAST BREEDER REACTORS
Motor-operated globe valve performance in a liquid sodium environment
[DE92-014456] p 3834 N92-31500
Potassium Rankine cycle nuclear power systems for spacecraft and lunar-mass surface power
[DE92-016163] p 3770 N92-31897
LIQUID METALS
Establishing low-power operating limits for liquid metal heat pipes
[DE92-011367] p 3823 N92-31701
LIQUID OXIDIZERS
Evolution of reactants fluid volume in turbulent jets
[DE92-011298] p 3786 N92-32145
LIQUID OXYGEN
Orbital transfer rocket engine technology: Advanced engine study
[NASA-CR-187216] p 3771 N92-32129
LIQUID PROPELLANT ROCKET ENGINES
Pressure fed thrust chamber technology program
[NASA-CR-190666] p 3770 N92-31550
LIQUID ROCKET PROPELLANTS
The effects of hydrazines of neuronal excitability
[AD-A247142] p 3868 N92-31491
LIQUID SODIUM
Motor-operated globe valve performance in a liquid sodium environment
[DE92-014456] p 3834 N92-31500
LIQUID-LIQUID INTERFACES
Interfacial ion transport between immiscible liquids
[AD-A252424] p 3778 N92-31292
LIQUID-VAPOR INTERFACES
Condensation in a two-phase pool
[DE92-010048] p 3824 N92-31977
LIQUIDS
Steady flow of a fluid-solid mixture between parallel plates
[DE92-013645] p 3821 N92-31426
Ultrafast experiments on the role of vibrational modes in electron transfer
[AD-A250630] p 3910 N92-31699
Theoretical studies of solid-fluid phase equilibria
[DE92-016598] p 3781 N92-31717
Holographic grating relaxation and photon correlation spectroscopic studies of viscoelastic liquids above the glass transition
[AD-A252485] p 3828 N92-31828
Physical characterization of magmatic liquids
[DE92-015302] p 3858 N92-32027
EWE: A computer model for ultrasonic inspection
[DE92-627145] p 3837 N92-32143
LITHIUM
Mechanical strength and stability of lithium aluminate
[DE92-015998] p 3841 N92-31638
Light ion driven inertial confinement fusion
[DE92-011662] p 3905 N92-31707
LITHIUM BORATES
Development of high efficiency nonlinear optical materials
[AD-A249612] p 3901 N92-31380
LITHIUM COMPOUNDS
Mechanical strength and stability of lithium aluminate
[DE92-015998] p 3841 N92-31638
Solid electrolytes and impact-resistant ceramics
[DE92-015297] p 3797 N92-32095
LITHIUM NIOBATES
Single crystal growth optimization of magnesium-doped lithium niobate
[AD-A250781] p 3914 N92-32207
LITHOGRAPHY
Activities of the Center for X Ray Lithography, phase 1
[AD-A250446] p 3901 N92-31397
Novel chemically amplified dry-developing imaging materials for high resolution microlithography
[AD-A250085] p 3793 N92-31435
Prototype casting fabrication by stereolithography
[DE92-011489] p 3876 N92-31529
Photogenerated base as catalyst for imidization reactions: Design of photosensitive polyimides
[AD-A250067] p 3795 N92-31810
LOAD CARRYING CAPACITY
Tailored metal matrix composites for high-temperature performance
[NASA-TM-105816] p 3775 N92-31854
The design and testing of an optimal beam composed of unimodal elements p 3747 N92-31873

LOAD TESTING MACHINES
Automation of strain-gauge load-cell force calibration
[PB92-187087] p 3827 N92-31370
LOAD TESTS
A free-piston Stirling engine/linear alternator controls and load interaction test facility
[NASA-TM-105825] p 3845 N92-31262
LOADS (FORCES)
A free-piston Stirling engine/linear alternator controls and load interaction test facility
[NASA-TM-105825] p 3845 N92-31262
Automation of strain-gauge load-cell force calibration
[PB92-187087] p 3827 N92-31370
LOCAL AREA NETWORKS
Local Area Networks (LAN) p 3874 N92-32183
LOG PERIODIC ANTENNAS
Analysis and evaluation of Project Evergreen data
[AD-A245983] p 3804 N92-31314
LOGARITHMS
Beam position monitor electronics using DC coupled demodulating logarithmic amplifiers
[DE92-011697] p 3816 N92-31760
LOGISTICS
Next generation documents
[PB92-187103] p 3917 N92-31371
LONG DURATION EXPOSURE FACILITY
Characterization of oxide formed on silicon by exposure to atomic oxygen in space
[AD-A249787] p 3778 N92-31301
Analysis of systems hardware flown on LDEF. Results of the systems special investigation group
[NASA-CR-189628] p 3767 N92-31677
LONG DURATION SPACE FLIGHT
One thousand days non-stop at sea: Lessons for a mission to Mars
[TABES PAPER 92-462] p 3764 N92-32020
LONG WAVE RADIATION
A study of longwave radiation codes for climate studies: Validation with ARM observations and tests in general circulation models
[DE92-014100] p 3862 N92-31894
LONGERONS
Dynamics of shuttle based flexible antenna system
[CRANFIELD-AERO-9203] p 3840 N92-31516
LONGITUDE
The effects of magnetic storm phases on F-layer irregularities from auroral to equatorial latitudes
[AD-A249011] p 3855 N92-31478
LORENTZ TRANSFORMATIONS
The RQM triangle: A paradigm for relativistic quantum mechanics
[DE92-011583] p 3915 N92-31663
The physical solution to the Lorentz-Dirac equations in a constant magnetic field
[DE92-013299] p 3890 N92-32140
LOSS OF COOLANT
Emissivity measurements in support of experiments on natural convection between a vertical cylinder and a surrounding array
[DE92-012321] p 3819 N92-31287
Heat transfer and pressure drop in an annular channel with downflow
[DE92-014363] p 3825 N92-32115
LOW ALTITUDE
Spectrum modal analysis for the detection of low-altitude windshear with airborne Doppler radar
[NASA-CR-4457] p 3755 N92-31549
Feasibility study for a low-altitude wide and temperature profiler
[PB92-188200] p 3860 N92-31641
LOW FREQUENCIES
Stability testing and analysis of a PMAD DC test bed for the Space Station Freedom
[NASA-TM-105846] p 3812 N92-31282
An empirical prediction algorithm for low-frequency acoustic surface scattering strengths
[AD-A250508] p 3892 N92-32044
LOW MOLECULAR WEIGHTS
Cyclopolymerization of metalloid-containing alpha, omega-dienes. 1,3-divinyltetramethyldisiloxane, 1,3-divinyltetramethyldisilazane and 1,3-divinylpentamethyldisilazane
[AD-A250347] p 3794 N92-31557
Development of characterization techniques for polyurethanes 1. Characterization of SRM 1480, a low molecular weight polyurethane for SEC calibration
[PB92-172485] p 3794 N92-31618
LOW TEMPERATURE
Two-stage n-butane flame: A comparison between experimental measurements and modeling results
[DE92-009457] p 3779 N92-31416
Characterization of oxides for low temperature solid oxide fuel cells
[PB92-152883] p 3848 N92-31903
LUBRICANTS
Tribology of functionally-terminated oligomer films
[AD-A250076] p 3833 N92-31433
Surface analysis of stainless steel outer race bearing specimens
[AD-A250088] p 3833 N92-31437
Liquid lubrication for space applications
[NASA-TM-105198] p 3795 N92-31840
LUBRICATION
Tribology of Langmuir-Blodgett films
[AD-A250075] p 3833 N92-31363
Liquid lubrication for space applications
[NASA-TM-105198] p 3795 N92-31840
LUMINESCENCE
SiGe Si quantum wires for efficient, room temperature, tunable luminescence
[AD-A249651] p 3814 N92-31464
Proposal for a workshop in the physics and application of hollow electrode glow switches
[AD-A247139] p 3814 N92-31490
LUMINOSITY
Results of IR working group
[DE92-013294] p 3902 N92-32149
LUMINOUS INTENSITY
Saturation effects in degenerate four-wave mixing spectroscopy: Nonperturbative calculations
[DE92-012253] p 3782 N92-31773
LUNAR BASES
SP-100 reactor with Brayton conversion for lunar surface applications
[NASA-TM-105637] p 3771 N92-32108
LUNAR SURFACE
SP-100 reactor with Brayton conversion for lunar surface applications
[NASA-TM-105637] p 3771 N92-32108
LUNGS
Nonthermal inhalation injury
[AD-A252532] p 3869 N92-31962

M

MACH NUMBER
Transonic wind tunnel test of a 14 percent thick oblique wing
[NASA-TM-102230] p 3754 N92-32213
MACHINE LEARNING
Analysis and design of neural networks
[AD-A250495] p 3884 N92-31332
Acquisition and production of skilled behavior in dynamic decision-making tasks
[NASA-CR-190614] p 3870 N92-31341
A language for higher-order explanation-based learning
[AD-A251008] p 3880 N92-31939
MACHINE TOOLS
Shop of the 1990's project: An evaluation tool for wireframe CAD software
[PB92-181130] p 3877 N92-31628
Capabilities of the 3-axes modified FP42 Deckel milling machine
[DE92-011737] p 3803 N92-31908
MACHINING
Computer-aided modeling tools for forging process feasibility studies
[DE92-012116] p 3838 N92-31303
Shop of the 1990's project: An evaluation tool for wireframe CAD software
[PB92-181130] p 3877 N92-31628
MAGNESIUM ALLOYS
Non-equilibrium synthesis by laser cladding of Ni, Nb and Mg alloys for improved environmental resistance
[AD-A250552] p 3787 N92-31612
MAGNESIUM OXIDES
Single crystal growth optimization of magnesium-doped lithium niobate
[AD-A250781] p 3914 N92-32207
MAGNET COILS
Investigation of factors affecting the calibration of strain gage based transducers (Goodzeit gages) for SSC magnets
[DE92-010722] p 3826 N92-31313
Utilization of gamma ray inspection system for tomographic imaging and dimensional analysis of complete model magnet cold masses and collared coil sections
[DE92-013466] p 3836 N92-31647
MAGNETIC COMPRESSION
Interaction of fast steady flow with slow transient flow: A new cause of interplanetary Bz events
[AD-A250273] p 3823 N92-31770
MAGNETIC CONTROL
Spacecraft stability and control
[TABES PAPER 92-414] p 3763 N92-32011
MAGNETIC DIFFUSION
Solid-armature railguns without the velocity-skin effect
[DE92-012630] p 3765 N92-31542
MAGNETIC FIELD CONFIGURATIONS
Vortices associated with toroidal ion temperature gradient driven fluctuations
[DE92-016180] p 3903 N92-31412
MAGNETIC FIELD RECONNECTION
Simulation study of stepwise relaxation in a spheromak plasma
[DE92-782101] p 3906 N92-31843
MAGNETIC FIELDS
Static magnetic fields: A summary of biological interactions, potential health effects, and exposure guidelines
[DE92-015218] p 3867 N92-31711
Particle physics confronts the solar neutrino problem
[DE92-014013] p 3895 N92-31812
Rigid rotations in two-electron atoms in a uniform magnetic field
[DE92-624981] p 3896 N92-31836
The physical solution to the Lorentz-Dirac equations in a constant magnetic field
[DE92-013299] p 3890 N92-32140
MAGNETIC FILMS
Epitaxial iron films
[AD-A250402] p 3912 N92-31915
MAGNETIC FLUX
A dynamical model of the behaviour of hadronic and fundamental strings at finite densities
[DE92-630245] p 3914 N92-31402
Rigid rotations in two-electron atoms in a uniform magnetic field
[DE92-624981] p 3896 N92-31836
MAGNETIC LEVITATION VEHICLES
Potential impact of high temperature superconductors on MAGLEV transportation
[DE92-012683] p 3834 N92-31720
Preliminary design for a MAGLEV development facility
[DE92-012259] p 3835 N92-31774
MAGNETIC MEASUREMENT
Calculations of emittance and damping time effects in the SLC damping rings
[DE92-012420] p 3900 N92-32133
MAGNETIC MOMENTS
Particle physics confronts the solar neutrino problem
[DE92-014013] p 3895 N92-31812
Synthesis, structure and properties of Ba6Co25S27: A Perovskite-like superstructure of Co8S6 and Ba6S clusters
[AD-A251041] p 3911 N92-31848
MAGNETIC PERMEABILITY
Synthesis, structure and properties of Ba6Co25S27: A Perovskite-like superstructure of Co8S6 and Ba6S clusters
[AD-A251041] p 3911 N92-31848
MAGNETIC PROBES
Transient internal probe diagnostic
[AD-A247306] p 3903 N92-31459
MAGNETIC PROPERTIES
Impurity effects on the magnetic ordering in chromium
[DE92-016165] p 3789 N92-31898
Epitaxial iron films
[AD-A250402] p 3912 N92-31915
Physical characterization of magmatic liquids
[DE92-015302] p 3858 N92-32027
MAGNETIC STORMS
The effects of magnetic storm phases on F-layer irregularities from auroral to equatorial latitudes
[AD-A249011] p 3855 N92-31478
MAGNETIC SUSPENSION
Preliminary design for a MAGLEV development facility
[DE92-012259] p 3835 N92-31774
MAGNETIZATION
The Swendsen-Wang dynamics in the simulation of the Ising model
[INPE-5394-PRE/1752] p 3874 N92-31348
What can we learn from magnetization experiments on high T(sub c) superconductors? An overview
[DE92-014465] p 3815 N92-31650
A self consistent generalized model for the calculation of minor loop excursions in the theory of hysteresis
[DE92-014394] p 3890 N92-32116
MAGNETO-OPTICS
Transient internal probe diagnostic
[AD-A247306] p 3903 N92-31459
MAGNETOHYDRODYNAMIC FLOW
The flow of plasma in the solar terrestrial environment
[NASA-CR-190200] p 3925 N92-31338
MAGNETOHYDRODYNAMIC GENERATORS
Monitoring gas temperatures entering an MHD superheater
[DE92-014200] p 3903 N92-31372
MHD Contractors' Review Meeting: Abstracts
[DE92-011549] p 3904 N92-31576
MAGNETOHYDRODYNAMIC STABILITY
Ion temperature gradient instability and transport
[DE92-013590] p 3905 N92-31727

Flow generation by turbulence
[DE92-013276] p 3906 N92-31829
MAGNETOHYDRODYNAMIC WAVES
Vortices associated with toroidal ion temperature gradient driven fluctuations
[DE92-016180] p 3903 N92-31412
MAGNETOHYDRODYNAMICS
Statistical analysis of anomalous transport in resistive interchange turbulence
[NIFS-125] p 3818 N92-31256
Mitigation of magnetohydrodynamic electromagnetic pulse (MHD-EMP) effects from commercial electric power systems
[AD-A249577] p 3804 N92-31354
Monitoring gas temperatures entering an MHD superheater
[DE92-014200] p 3903 N92-31372
MHD Contractors' Review Meeting: Abstracts
[DE92-011549] p 3904 N92-31576
Simulation study of stepwise relaxation in a spheromak plasma
[DE92-782101] p 3906 N92-31843
Numerical simulation of geometric scale effects in cylindrical self-field MPD thrusters
[NASA-CR-189224] p 3772 N92-32239
MAGNETOPLASMADYNAMICS
Numerical simulation of geometric scale effects in cylindrical self-field MPD thrusters
[NASA-CR-189224] p 3772 N92-32239
MAGNETOSPHERE-IONOSPHERE COUPLING
The flow of plasma in the solar terrestrial environment
[NASA-CR-190200] p 3925 N92-31338
Impulsive magnetic perturbations of the high latitude, dayside ionosphere
[AD-A249872] p 3857 N92-31932
USU center of excellence in theory and analysis of the geo-plasma environment
[AD-A252189] p 3858 N92-32055
MAINTAINABILITY
The determination of operational and support requirements and costs during the conceptual design of space systems
[NASA-CR-190626] p 3766 N92-31260
MAINTENANCE
Replaceable valve seat
[AD-D015250] p 3832 N92-31271
Development of quantitative specifications for simulating the stress environment
[AD-A250669] p 3870 N92-31321
Sequential estimation of optimal age replacement policies when distribution of lifetimes is phase type
[AD-A249020] p 3836 N92-31479
MAN MACHINE SYSTEMS
Oracle and the end-user: Practical implementation of applications in a multi-user, multi-platform environment
[DE92-015223] p 3877 N92-31654
Pilot errors involving Head-Up Displays (HUDs), Helmet-Mounted Displays (HMDs), and Night Vision Goggles (NVGs)
[AD-A250719] p 3873 N92-32023
Local Area Networks (LAN) p 3874 N92-32183
MAN TENDED FREE FLYERS
COMET: Commercial space opportunities through developed technologies
[TABES PAPER 92-453] p 3764 N92-32017
MAN-COMPUTER INTERFACE
Acquisition and production of skilled behavior in dynamic decision-making tasks
[NASA-CR-190614] p 3870 N92-31341
Requirements Engineering and Analysis Workshop Proceedings
[AD-A250415] p 3876 N92-31541
Computer Aided Process Planning (CAPP): The user interface for the fabrication module of the rapid design system
[AD-A250095] p 3879 N92-31783
Automated payload experiment tool feasibility study
[NASA-CR-184256] p 3883 N92-31835
Navy Atmospheric Boundary Layer (NABL) model system: Software/Interface design document
[AD-A247903] p 3857 N92-31986
Development of a fault isolation system database manager
[AD-A248346] p 3916 N92-31992
Intelligent gateways p 3921 N92-32184
Hypertext and hypermedia systems in information retrieval p 3921 N92-32188
MANAGEMENT
Annual report to the Congress, fiscal year 1991 (Office of Technology Assessment)
[PB92-166549] p 3922 N92-31599
MANAGEMENT METHODS
A proposed group management scheme for XTP multicast
[NASA-CR-190633] p 3916 N92-31547
Report of the aviation safety review of Department of Energy helicopter operations
[DE92-016346] p 3755 N92-31928
Total quality management: A management philosophy for providing high quality construction
[AD-A252743] p 3837 N92-32172
MANAGEMENT PLANNING
Integrated Technology Plan for the Civil Space Program, 1991
[PB92-181692] p 3762 N92-31634
Total quality management: A management philosophy for providing high quality construction
[AD-A252743] p 3837 N92-32172
MANAGEMENT SYSTEMS
GNAS Maintenance Control Center (GMCC) Design Qualification Test and Evaluation (DQT/E) test report
[DOT/FAA/CT-TN91/39] p 3745 N92-31615
MANEUVERS
Optimal targeting of evading objects
[DE92-014719] p 3889 N92-32119
MANIPULATORS
Piezoelectric radiant-to-air ultrasonic transducers p 3811 N92-31244
Robotic soil sampler for hazardous waste clean up
[DE92-012693] p 3780 N92-31565
Torque linearizing hardware for the electric joint motors of a direct-drive robot
[DE92-012681] p 3816 N92-31718
Backlash control via redundant drives: An experimental verification
[DE92-016368] p 3835 N92-31929
Effective path planning through task restriction
[DE92-017351] p 3885 N92-32036
On dexterous rotations of polygons
[AD-A250967] p 3797 N92-32151
MANNED MANEUVERING UNITS
Mission and Safety Critical (MASC) plans for the MASC Kernel simulation
[NASA-CR-190708] p 3875 N92-31487
MANNED MARS MISSIONS
One thousand days non-stop at sea: Lessons for a mission to Mars
[TABES PAPER 92-462] p 3764 N92-32020
MANNED SPACE FLIGHT
TABES 92: 8th Annual Technical and Business Exhibition and Symposium. Executive summaries and submitted papers p 3763 N92-32009
Orbital transfer rocket engine technology: Advanced engine study
[NASA-CR-187216] p 3771 N92-32129
MANNED SPACECRAFT
Results of earth observation study on STS-31 for Terra Geode, January 1987 - June 1991
[AD-A250750] p 3844 N92-31621
MANUALS
Hydrogenerator design manual, chapter 8
[PB92-173707] p 3919 N92-31682
Capabilities of the 3-axes modified FP42 Deckel milling machine
[DE92-011737] p 3803 N92-31908
Dispersive-infrared gas sensor system design and operation manual
[DE92-011766] p 3828 N92-31909
MANUFACTURING
Weld penetration and defect control
[DE92-015310] p 3836 N92-31336
The sixteenth annual electronics manufacturing seminar proceedings
[AD-A247920] p 3814 N92-31461
Solar synthesis of advanced materials: A solar industrial program initiative
[DE92-010575] p 3845 N92-31481
Guidelines for generating acceptance sampling plans for continuous production
[DE92-010763] p 3837 N92-31753
A program for the transfer of manufacturing technology from the national laboratories
[DE92-011905] p 3923 N92-31965
MANY BODY PROBLEM
Schwinger boson studies of the t-J model beyond mean-field approximation
[DE92-630650] p 3909 N92-31655
Many body perturbation theory using a Restricted Open-Shell Hartree-Fock (ROHF) reference function
[AD-A249725] p 3894 N92-31673
Molecular interactions and properties with many-body methods
[AD-A247052] p 3896 N92-31858
The physics of cellular automata and coherence and chaos in classical many-body systems
[DE92-016834] p 3890 N92-32035
MAPPING
Lamont-Doherty Geological Observatory
[PB92-185040] p 3856 N92-31636
MARINE BIOLOGY
Proceedings of the 4th Atlantic OCS Region Information Transfer Meeting
[PB92-177690] p 3864 N92-31630
Ecosystems of the Florida Keys: A bibliography
[PB92-198910] p 3854 N92-32071
Biology, oceanography, and fisheries of the North Pacific transition zone and subarctic frontal zone
[PB92-178128] p 3866 N92-32106
MARINE ENVIRONMENTS
Hydrographic observations from the US/PRC cooperative program in the western equatorial Pacific Ocean: Cruises 5-8
[PB92-177054] p 3865 N92-31644
The KRAKEN normal mode program
[AD-A252409] p 3892 N92-31818
An empirical prediction algorithm for low-frequency acoustic surface scattering strengths
[AD-A250508] p 3892 N92-32044
MARINE MAMMALS
Ecosystems of the Florida Keys: A bibliography
[PB92-198910] p 3854 N92-32071
MARINE TECHNOLOGY
A proposal for the establishment of a Center for Advanced Composite Materials Research
[AD-A250072] p 3773 N92-31361
Naval Biodynamics Laboratory: 1989 and 1990 command history
[AD-A247185] p 3870 N92-31963
Development, testing and operation of a large suspended ocean measurement structure for deep-ocean use
[AD-A252188] p 3866 N92-32050
MARKERS
Effect of guard band reduction on marker beacon receiver performance
[DOT/FAA/CT-TN92/18] p 3807 N92-31617
MARKETING
Cooperative field test program for wind systems
[DE92-001209] p 3847 N92-31579
A program for the transfer of manufacturing technology from the national laboratories
[DE92-011905] p 3923 N92-31965
MARKOV CHAINS
Importance sampling for Markov chains: Asymptotics for the variance
[AD-A249804] p 3888 N92-31757
Markovian fields as limits of Markov chains
[INPE-5395-PRE/1753] p 3889 N92-32225
MARKOV PROCESSES
Maximum likelihood estimation of fractional Brownian motion and Markov noise parameters
[AD-A249623] p 3890 N92-31686
Importance sampling for Markov chains: Asymptotics for the variance
[AD-A249804] p 3888 N92-31757
A generalization to stochastic averaging in random vibration
[DE92-016747] p 3842 N92-32088
Markovian fields as limits of Markov chains
[INPE-5395-PRE/1753] p 3889 N92-32225
MARS (PLANET)
Using space resources
[NASA-TM-107966] p 3924 N92-31781
Methane-producing microorganisms: Component of Mars biosphere p 3924 N92-32180
MARS ATMOSPHERE
Methane-producing microorganisms: Component of Mars biosphere p 3924 N92-32180
MASS SPECTROMETERS
Gallium arsenide clusters and their interfacial physics and chemistry
[AD-A249565] p 3907 N92-31375
An improved ion guide for external ion injection in glow discharge-Fourier transform ion cyclotron resonance (GD-FTICR) mass spectrometry
[AD-A250944] p 3900 N92-32170
MASS SPECTROSCOPY
UV photochemistry of trivinylantimony adsorbed on quartz
[AD-A252215] p 3785 N92-32057
An improved ion guide for external ion injection in glow discharge-Fourier transform ion cyclotron resonance (GD-FTICR) mass spectrometry
[AD-A250944] p 3900 N92-32170
MASS TRANSFER
Hydrological and geochemical response and recovery in disturbed Arctic ecosystems
[DE92-016223] p 3850 N92-31312
Incipient and total group combustion of fuel sprays in air p 3749 N92-31883
Transport and evaporation effects in counterflow spray diffusion flames p 3749 N92-31884
Heat and mass transfer considerations in advanced heat pump systems
[DE92-016635] p 3825 N92-32003

FEHMN 1.0: Finite element heat and mass transfer code
[DE92-013998] p 3825 N92-32008
MASSIVELY PARALLEL PROCESSORS
Data parallel programming
[DE92-013981] p 3882 N92-31466
A sweep algorithm for massively parallel simulation of circuit-switched networks
[NASA-CR-189680] p 3881 N92-32157
MATERIAL ABSORPTION
Prediction of hydrogen entry and permeation in metals and alloys
[AD-A245286] p 3790 N92-32096
MATERIALS HANDLING
The collection, handling, transportation, and thermal desorption of explosive vapor using quartz collection tubes
[DE92-011441] p 3799 N92-31570
MATERIALS RECOVERY
Economics of microwave plasma dissociation of H2S
[DE92-014846] p 3779 N92-31441
Using space resources
[NASA-TM-107966] p 3924 N92-31781
Ceramic membranes for high temperature hydrogen separation
[DE92-013342] p 3783 N92-31816
MATERIALS SCIENCE
Mathematical problems in micromechanics and composite materials
[AD-A249584] p 3773 N92-31378
Computerized property data for engineering materials: An overview p 3922 N92-32191
MATERIALS TESTS
Finite-element analyses and fracture simulation in thin-sheet aluminum alloy
[NASA-TM-107662] p 3839 N92-31504
Development of characterization techniques for polyurethanes 1. Characterization of SRM 1480, a low molecular weight polyurethane for SEC calibration
[PB92-172485] p 3794 N92-31618
Radiolytic gas production in the alpha particle degradation of plastics
[DE92-011846] p 3795 N92-31938
Composite failure analysis handbook. Volume 1: Program review
[AD-A250520] p 3776 N92-32047
Composite failure analysis handbook. Volume 2: Technical handbook. Part 1: Procedures and techniques
[AD-A250521] p 3776 N92-32048
High density thin-walled syntactic foam
[DE92-013159] p 3797 N92-32136
MATHEMATICAL MODELS
Life extending control for rocket engines
[NASA-TM-105789] p 3802 N92-31263
Adaptive and nonadaptive feedback control of global instabilities with application to a heated 2-D jet
[AD-A250700] p 3820 N92-31322
The validation of atmospheric models
[DE92-013254] p 3850 N92-31324
Mode methods for strain-hardening structures
[DE92-014855] p 3838 N92-31335
Programming with inductive and co-inductive types
[AD-A249562] p 3874 N92-31353
A dynamical model of the behaviour of hadronic and fundamental strings at finite densities
[DE92-630245] p 3914 N92-31402
A general numerical model for wave rotor analysis
[NASA-TM-105740] p 3821 N92-31484
Modal simulation of gearbox vibration with experimental correlation
[NASA-TM-105702] p 3834 N92-31485
Development of a computer model for polycrystalline thin-film CuInSe2 and CdTe solar cells
[DE92-001242] p 3846 N92-31526
Life prediction and constitutive models for engine hot section anisotropic materials program
[NASA-CR-189222] p 3759 N92-31534
Effect of out-of-roundness on the performance of a diesel engine connecting-rod bearing
[NASA-TM-105600] p 3834 N92-31536
A tumbling top-quark condensate model
[DE92-016194] p 3893 N92-31552
Iterative methods for large sparse linear systems arising from partial differential equations
[AD-A249524] p 3886 N92-31567
Poloidal rotation and density asymmetries in a tokamak plasma with strong toroidal rotation
[PB92-182534] p 3904 N92-31613
Oxygen ordering and strain-related morphology in YBa2Cu(3-x)O7 systems
[DE92-014476] p 3909 N92-31627
Noise-induced chaos and phase space flux: A sample-theoretic study
[PB92-172733] p 3915 N92-31645
Mathematical structures for qualitative calculus, a contribution to qualitative simulation
[LAAS-91475] p 3886 N92-31690
Ionospheric communications channel modelling
[DE92-013039] p 3808 N92-31722
Low density real gas flows about hypersonic vehicles
[AD-A250048] p 3752 N92-31777
Three-dimensional finite difference modeling of surface wave propagation across the Barents Shelf
[AD-A249865] p 3865 N92-31821
Signal and noise models arising from the theory of errors
[AD-A250222] p 3885 N92-31827
User's guide for treetherm: A 3-D thermal model for single trees
[LTR91-003] p 3879 N92-31833
Integrated computer systems in aircraft design and manufacture: Difficulties and implications p 3746 N92-31864
A simulation model of a single rotor helicopter p 3746 N92-31865
True covariance simulation of the EUVE (extreme ultra violet explorer) update filter p 3748 N92-31878
Incipient and total group combustion of fuel sprays in air p 3749 N92-31883
A study of longwave radiation codes for climate studies: Validation with ARM observations and tests in general circulation models
[DE92-014100] p 3862 N92-31894
Contribution to the modelling of turbulent combustion in the case of stabilisation by flame-lock
[ESA-TT-1229] p 3784 N92-31942
The 6-D phase space tracking with acceleration: Modeling low energy proton synchrotrons, part 1
[DE92-013744] p 3899 N92-31948
An integrated research program for the modeling, analysis and control of aerospace systems
[AD-A250199] p 3761 N92-31966
Mathematical modeling and numerical simulation of the dynamics of flexible structures undergoing large overall motions
[AD-A250202] p 3761 N92-31967
Condensation in a two-phase pool
[DE92-010048] p 3824 N92-31977
A real time system for multisensor image analysis through pyramidal segmentation
[AD-A247169] p 3888 N92-31981
Seasonal wind and ocean thermal forcing influences on the generation of the Leeuwin current and its eddies
[AD-A246992] p 3865 N92-31988
Validation of the Numerical Electro-magnetics Code (NEC) for antenna wire elements in proximity to Earth
[AD-A250507] p 3810 N92-32043
A continuing study of altitude determination deficiencies of the Service Aircraft Instrumentation Package (SAIP)
[AD-A245952] p 3758 N92-32051
Results of IR working group
[DE92-013294] p 3902 N92-32149
Nonlinearly stable compact schemes for shock calculations
[NASA-CR-189663] p 3887 N92-32164
Prompt neutron lifetime in a strongly heterogeneous lattice
[DE92-013212] p 3898 N92-32165
Resonant enhancement of flavor-changing neutrino interactions
[DE92-013020] p 3898 N92-32167
Motion model for the correction of point source distortion in radiographs of honeycomb
[DREP-88-14] p 3777 N92-32215
Absolute calibration of the Fourier interferometric transmissometer
[DREV-R-4511/88] p 3829 N92-32218
Wavelength-tunable liquid crystal imaging filters for remote sensing from geosynchronous platforms
[NASA-CR-190698] p 3845 N92-32223
Markovian fields as limits of Markov chains
[INPE-5395-PRE/1753] p 3889 N92-32225
Optimal design of geodesically stiffened composite cylindrical shells
[NASA-CR-190706] p 3842 N92-32235
Numerical simulation of geometric scale effects in cylindrical self-field MPD thrusters
[NASA-CR-189224] p 3772 N92-32239
MATHEMATICAL PROGRAMMING
Decomposition of balanced matrices. Part 4: Connected squares
[AD-A247308] p 3888 N92-31768
MATHEMATICS
International mathematics and science assessments: What have we learned
[PB92-183599] p 3916 N92-32160
MATRICES (MATHEMATICS)
CSM solutions of rotating blade dynamics using integrating matrices
[NASA-CR-190577] p 3840 N92-31619
Lattice gaugefixing and other optics in lattice gauge theory
[DE92-016958] p 3901 N92-31737
Importance sampling for Markov chains: Asymptotics for the variance
[AD-A249804] p 3888 N92-31757
Decomposition of balanced matrices. Part 4: Connected squares
[AD-A247308] p 3888 N92-31768
A fundamental notion of equivalence for linear multivariable systems
[MATHS-REPT-A-153] p 3887 N92-31957
Determination of the matrix conditioning indicator. Comparison of approximate methods p 3887 N92-32210
MATRIX MATERIALS
Interface engineering in alumina/glass composites
[AD-A248587] p 3773 N92-31315
Corrosion behavior of squeeze cast aluminum metal matrix composites
[AD-A250486] p 3774 N92-31382
A differential CDM model for fatigue of unidirectional metal matrix composites
[NASA-TM-105726] p 3840 N92-31505
Optical fiber sensors for organic matrix composite material cure monitoring
[AD-A247114] p 3776 N92-31979
MATRIX METHODS
The effect of elastic stress on Ostwald ripening phenomena
[DE92-015291] p 3839 N92-31400
MATTER (PHYSICS)
Theoretical studies in nuclear reactions and nuclear structure
[DE92-016204] p 3897 N92-31927
MAXIMUM LIKELIHOOD ESTIMATES
Maximum likelihood estimation of fractional Brownian motion and Markov noise parameters
[AD-A249623] p 3890 N92-31686
MEAN SQUARE VALUES
Adaptive inverse filter
[DE92-011660] p 3878 N92-31669
Kernel optimum nearly-analytical discretization (KOND) method applied to parabolic equations KOND-P Scheme
[NIFS-118] p 3887 N92-32205
MEASURING INSTRUMENTS
Monitoring gas temperatures entering an MHD superheater
[DE92-014200] p 3903 N92-31372
Utilization of gamma ray inspection system for tomographic imaging and dimensional analysis of complete model magnet cold masses and collared coil sections
[DE92-013466] p 3836 N92-31647
The 193-pixel, three-dimensional capacitance imaging system
[DE92-001253] p 3919 N92-31731
FCS skewed sensors array: Practical considerations p 3746 N92-31868
Device for monitoring the thickness of a dielectric coating on a dielectric substrate
[DE92-014741] p 3829 N92-32174
MECHANICAL DRIVES
Torque linearizing hardware for the electric joint motors of a direct-drive robot
[DE92-012681] p 3816 N92-31718
Backlash control via redundant drives: An experimental verification
[DE92-016368] p 3835 N92-31929
MECHANICAL ENGINEERING
Building an educational robot arm for under $1,000
[AD-A247499] p 3833 N92-31460
MECHANICAL PROPERTIES
A proposal for the establishment of a Center for Advanced Composite Materials Research
[AD-A250072] p 3773 N92-31361
Role of interfaces and interphases in the evolution mechanics of material systems
[AD-A250410] p 3774 N92-31604
Superplasticity in a nickel silicide alloy, Ni3Si(V, Mo)
[DE92-011651] p 3787 N92-31667
The structure and properties of grain boundaries in Ni3Al
[DE92-012143] p 3788 N92-31744
Thermomechanical fatigue behavior of a silicone carbide fiber-reinforced calcium aluminosilicate glass-ceramic matrix composite
[AD-A249870] p 3775 N92-31823
A study of the microstructural basis for the strength and toughness properties of water-quenched and air-cooled HSLA-100, HSLA-100 with increased copper, and a ULCB steel
[AD-A245955] p 3789 N92-32052
Quantum mechanical approach to understanding microstructural and mechanical properties in intermetallics
[AD-A250550] p 3790 N92-32084

Effect of surface modifications on the properties of silicon nitride ceramics
[DE92-013848] p 3797 N92-32094
Computerized property data for engineering materials: An overview p 3922 N92-32191

MECHANICAL SHOCK
On the feasibility of a transient dynamic design analysis method
[AD-A250406] p 3838 N92-31337

MECHANICS (PHYSICS)
A penetration mechanics database
[AD-A246351] p 3767 N92-31997

MEDICAL SERVICES
Noninvasive ambulatory assessment of cardiac function and myocardial ischemia in healthy subjects exposed to carbon monoxide
[AD-A252264] p 3870 N92-32107

MELTING
Annual dynamics within the active layer
[DE92-013520] p 3850 N92-31304

MEMBRANE STRUCTURES
Ceramic membranes for high temperature hydrogen separation
[DE92-013342] p 3783 N92-31816
Catalytic carbon membranes for hydrogen production
[DE92-001269] p 3784 N92-31976

MEMBRANES
Fundamental studies in oxidation-reduction in relation to water photolysis
[DE92-014333] p 3785 N92-32113

MEMORY
In-flight decision making by high time and low time pilots during instrument operations
[AD-A249990] p 3871 N92-31392
Forms of memory for representation of visual objects
[AD-A250056] p 3871 N92-31779

MEMORY (COMPUTERS)
PARTI primitives for unstructured and block structured problems
[NASA-CR-189662] p 3876 N92-31561
The multicomputer toolbox: Scalable parallel libraries for large-scale concurrent applications
[DE92-008068] p 3882 N92-31740
PDDP: Data-driven parallelism and shared memory
[DE92-008073] p 3883 N92-31741
The hierarchical spatial decomposition of three-dimensional particle-in-cell plasma simulations on MIMD distributed memory multiprocessors
[DE92-016802] p 3883 N92-32034
Fault tolerant parallel computing in orthogonal shared-memory and related architectures
[AD-A250504] p 3883 N92-32040
Ferroelectric thin films prepared by pulse laser deposition processing and characterization
[PB92-196088] p 3913 N92-32072

MENISCI
Sol-gel multilayers applied by a meniscus coating process
[DE92-012697] p 3794 N92-31560

MENTAL PERFORMANCE
Human image understanding
[AD-A250401] p 3872 N92-31330
Probability-based inference in a domain of proportional reasoning tasks
[AD-A247304] p 3871 N92-31444
Forms of memory for representation of visual objects
[AD-A250056] p 3871 N92-31779
The impact of cognitive feedback on the performance of intelligence analysts
[AD-A252176] p 3871 N92-32063

MESONS
Theoretical high energy physics research at the University of Chicago, task A
[DE92-016288] p 3899 N92-31712

MESOSCALE PHENOMENA
The validation of atmospheric models
[DE92-013254] p 3850 N92-31324
Numerical simulation of precipitation scavenging and comparison with observation of prescribed forest fires
[DE92-013513] p 3851 N92-31423
Cloud-to-ground lightning characteristics in mesoscale convective systems
[AD-A250418] p 3858 N92-31493
The structure and energetics of Amazon squall lines
[AD-A250182] p 3859 N92-31523
A comparative analysis of the temporal variability of lightning observations and GOES imagery
[AD-A250185] p 3860 N92-31603
Impulsive magnetic perturbations of the high latitude, dayside ionosphere
[AD-A249872] p 3857 N92-31932
Biology, oceanography, and fisheries of the North Pacific transition zone and subarctic frontal zone
[PB92-178128] p 3866 N92-32106

MESSAGE PROCESSING
Methodology investigation final report: Automated real-time test scenario generation, phase 1
[AD-A250439] p 3884 N92-31395

MESSAGES
Issues in designing transport layer multicast facilities
[NASA-CR-190639] p 3882 N92-31483

METABOLITES
A study of the effect of hydrocarbon structure on the induction of male rat nephropathy and metabolite structure
[AD-A252192] p 3867 N92-31590

METAL COMPOUNDS
Tris-triphenylsiloxy compounds of aluminum
[AD-A250141] p 3788 N92-31795

METAL FATIGUE
A differential CDM model for fatigue of unidirectional metal matrix composites
[NASA-TM-105726] p 3840 N92-31505
Aging fleet: Maintaining airworthiness p 3745 N92-31862
Fatigue in single crystal nickel superalloys
[AD-A252492] p 3790 N92-32066

METAL FILMS
Spin polarized photoemission studies of surfaces and thin-films
[DE92-016098] p 3907 N92-31296
Epitaxial iron films
[AD-A250402] p 3912 N92-31915

METAL FUELS
Flammability limits and ballistic properties of fuel-rich propellants p 3749 N92-31885

METAL HALIDES
Application of the mean spherical approximation to the estimations of single ion thermodynamic quantities of solvation for monoatomic monovalent ions in aqueous solutions
[AD-A250190] p 3893 N92-31316

METAL IONS
Strongly adherent ceramic surface layers by ion implantation
[AD-A248882] p 3792 N92-31388
Experimental studies of aluminum solubility and speciation in brines
[DE92-010448] p 3786 N92-31418
Light ion driven inertial confinement fusion
[DE92-011662] p 3905 N92-31707

METAL MATRIX COMPOSITES
Cyclic hot firing results of tungsten-wire-reinforced, copper-lined thrust chambers
[NASA-TM-4214] p 3769 N92-31249
Preliminary evaluation of adhesion strength measurement devices for ceramic/titanium matrix composite bonds
[NASA-TM-105803] p 3745 N92-31267
A proposal for the establishment of a Center for Advanced Composite Materials Research
[AD-A250072] p 3773 N92-31361
Corrosion behavior of squeeze cast aluminum metal matrix composites
[AD-A250486] p 3774 N92-31382
A differential CDM model for fatigue of unidirectional metal matrix composites
[NASA-TM-105726] p 3840 N92-31505
Tailored metal matrix composites for high-temperature performance
[NASA-TM-105816] p 3775 N92-31854
The effect of thermomechanical processing parameters on the ambient behavior of 10 percent volume 6061 Al-Alumina
[AD-A252177] p 3776 N92-32064
An investigation of the thermoviscoplastic behavior of a metal matrix composite at elevated temperatures
[NASA-CR-190700] p 3777 N92-32159
Effects of fiber and interfacial layer architectures on the thermoplastic response of metal matrix composites
[NASA-TM-105802] p 3777 N92-32234

METAL NITRIDES
Transient fission gas behavior in uranium nitride fuel under proposed space applications
[AD-A252577] p 3899 N92-31325

METAL OXIDE SEMICONDUCTORS
Static and dynamic properties of current sensing power VDMOS transistor
[LAAS-92032] p 3815 N92-31697

METAL PLATES
Residual stress and strain measurements in an austenitic steel plate containing a multipass weld
[DE92-014478] p 3839 N92-31383
Residual stresses in a multipass ferritic weldment
[DE92-014467] p 3839 N92-31501
Electrically-induced stresses and deflection in multiple plates
[DE92-012303] p 3841 N92-31844

METAL SHEETS
Finite-element analyses and fracture simulation in thin-sheet aluminum alloy
[NASA-TM-107662] p 3839 N92-31504

METAL SURFACES
Spin polarized photoemission studies of surfaces and thin-films
[DE92-016098] p 3907 N92-31296
Surface analysis of stainless steel outer race bearing specimens
[AD-A250088] p 3833 N92-31437
Non-equilibrium synthesis by laser cladding of Ni, Nb and Mg alloys for improved environmental resistance
[AD-A250552] p 3787 N92-31612
Prediction of hydrogen entry and permeation in metals and alloys
[AD-A245286] p 3790 N92-32096

METAL VAPOR LASERS
High performance of copper pumped dye lasers
[DE92-011763] p 3832 N92-31902

METAL WORKING
JPRS report: Science and technology. Central Eurasia: Materials science
[JPRS-UMS-92-010] p 3787 N92-31584

METAL-METAL BONDING
Investigation into the ultrasonic NDE of adhesively bonded joints
[DREP-90-02] p 3837 N92-32202

METALLIZING
Metallization of ferrite ceramic couplings
[DE92-016573] p 3789 N92-32032

METALLURGY
A study of the microstructural basis for the strength and toughness properties of water-quenched and air-cooled HSLA-100, HSLA-100 with increased copper, and a ULCB steel
[AD-A245955] p 3789 N92-32052

METALORGANIC CHEMICAL VAPOR DEPOSITION
The preparation of (Al2O3)x(SiO2)y thin films using (Al(OSiEt3))2 as a single source precursor
[AD-A250142] p 3788 N92-31796

METALS
Deterministic analysis of processes at corroding metal surfaces and the study of electrochemical noise in these systems
[DE92-016286] p 3788 N92-31733
Laser decontamination: A new strategy for facility decommissioning
[DE92-014113] p 3831 N92-31775
Using space resources
[NASA-TM-107966] p 3924 N92-31781
Estimation of metal acceleration by an SF5 containing explosive
[AD-A245338] p 3801 N92-32098
Computational studies of metal-metal and metal-ligand interactions
[NASA-CR-190674] p 3790 N92-32156

METASTABLE STATE
Non-equilibrium synthesis by laser cladding of Ni, Nb and Mg alloys for improved environmental resistance
[AD-A250552] p 3787 N92-31612
Quantum mechanical approach to understanding microstructural and mechanical properties in intermetallics
[AD-A250550] p 3790 N92-32084

METATHESIS
Synthesis of side chain liquid crystal polymers by living ring opening metathesis polymerization. 4: Synthesis of amorphous and side chain liquid crystal AB block copolymers
[AD-A250353] p 3792 N92-31394

METEORITIC COMPOSITION
Methane-producing microorganisms: Component of Mars biosphere p 3924 N92-32180

METEOROLOGICAL BALLOONS
A coordinated study of a storm system over the South American continent
[INPE-5388-TDI/477] p 3863 N92-32212

METEOROLOGICAL CHARTS
Meteorological data, new series B basic material. Volume 53, no. 1: Daily altitude maps of the 30-hPa-area and monthly mean maps for the year 1986, part 1
[QR-1-VOL-53-NO-1-PT-1] p 3860 N92-31702
Meteorological data, new series B basic material. Volume 53, no. 2: Daily altitude maps of the 30-hPa-area and monthly mean maps for the year 1986, part 2
[QR-2-VOL-53-NO-2-PT-2] p 3860 N92-31704
Meteorological data, new series B basic material. Volume 53, no. 4: Daily altitude maps of the 30-hPa-area and monthly mean maps for the year 1986, part 4
[QR-4-VOL-53-NO-4-PT-4] p 3861 N92-31706

METEOROLOGICAL INSTRUMENTS
A sensitivity study of daytime visibility determination with the horizon scanning imager
[SIO-91-15] p 3902 N92-32144

METEOROLOGICAL PARAMETERS
Updated forecast of Atlantic seasonal hurricane activity for 1992 p 3859 N92-31583
Navy Atmospheric Boundary Layer (NABL) model system: Software/Interface design document [AD-A247903] p 3857 N92-31986
Probabilistic analysis of twenty-four hour weather data for Warsaw p 3863 N92-32097
METEOROLOGICAL RADAR
Feasibility study for a low-altitude wide and temperature profiler [PB92-188200] p 3860 N92-31641
A comparison of the performance of two gust front detection algorithms using a length-based scoring technique [AD-A250862] p 3863 N92-32103
METEOROLOGY
Annual dynamics within the active layer [DE92-013520] p 3850 N92-31304
Combining expert probabilistic weather forecasts: Results of post-hoc analyses of the Zierikzee experiment [REPT-91-101] p 3859 N92-31521
Acid deposition: State of science and technology. Summary report of the US National Acid Precipitation Assessment Program, volumes 1-4 [PB92-100353] p 3852 N92-31598
Global atmospheric circulation statistics, 1000-1 mb [PB92-186196] p 3853 N92-31649
Real-time statistical quality control and ARM [DE92-015253] p 3837 N92-31657
Comprehensive Aerological Reference Data Set (CARDS) [DE92-016469] p 3862 N92-31734
METHANE
Light alkane conversion processes: Suprabiotic catalyst systems for selective oxidation of light alkane gases to fuel oxygenates [DE92-015229] p 3799 N92-31751
Electrochemical oxidation of methane for fuel cells [PB92-172303] p 3848 N92-31922
Methane-producing microorganisms: Component of Mars biosphere p 3924 N92-32180
METHOD OF MOMENTS
Scattering from a finite collection of transverse dipole and axial slot arrays with edge effects [AD-A249622] p 3807 N92-31691
METHOXY SYSTEMS
Theoretical studies of the reactions and spectroscopy of radical species relevant to combustion reactions and diagnostics [DE92-013484] p 3781 N92-31725
METHYL ALCOHOL
Batteries and fuel cells [DE92-011493] p 3847 N92-31571
Synthesis of cresols and xylenols from phenol and methanol [DE91-002141] p 3785 N92-32093
METHYL COMPOUNDS
High-temperature ignition of propane with MTBE as an additive: Shock-tube experiments and modeling [DE92-008933] p 3778 N92-31415
Synthesis of soluble alpha-thiophene oligomers. Monomer to octamer [AD-A250082] p 3779 N92-31434
The photogeneration of polymeric amines: Synthesis and photocrosslinking of copolymers containing photoactive carbamate pendant groups [AD-A250086] p 3793 N92-31436
A study of the effect of hydrocarbon structure on the induction of male rat nephropathy and metabolite structure [AD-A252192] p 3867 N92-31590
Supersonic pyrolysis jets for diamond film deposition [AD-A251125] p 3798 N92-32198
METHYLATION
Synthesis of cresols and xylenols from phenol and methanol [DE91-002141] p 3785 N92-32093
METHYLENE
Diosmacycloalkanes as models for the formation of hydrocarbons from surface methylenes [DE92-014588] p 3783 N92-31891
METROLOGY
Soviet precision timekeeping research and technology [PB92-173046] p 3802 N92-31830
Improvements to the Rocky Flats Metrology Laboratories velocity meter calibration system [DE92-013162] p 3829 N92-32138
MICROANALYSIS
Incoherence effects in reflection electron microscopy [DE92-016161] p 3829 N92-32086
MICROBALLOONS
High density thin-walled syntactic foam [DE92-013159] p 3797 N92-32136
MICROBIOLOGY
JPRS report: Science and technology. Central Eurasia: Life sciences [JPRS-ULS-92-015] p 3924 N92-32179
MICROCRACKS
Enhancement of fracture toughness using high intensity electric currents [AD-A249809] p 3889 N92-31359
Particle emission and charging effects induced by fracture [AD-A252182] p 3913 N92-32065
MICROELECTRONICS
The prediction of the performance of a microcircuit heat sink in the boiling mode [AD-A250045] p 3812 N92-31355
Electronics and electrical engineering laboratory technical publication announcements covering laboratory programs, July to September 1991, with 1992 EEEL events calendar [PB92-181239] p 3813 N92-31367
Control of rapid thermal processing equipment for microelectronics applications [LAAS-92013] p 3787 N92-31695
Torque linearizing hardware for the electric joint motors of a direct-drive robot [DE92-012681] p 3816 N92-31718
Field-emitter arrays for RF vacuum microelectronics [AD-A250101] p 3816 N92-31791
Effect of synthesis temperature in the structure, doping level and charge-transport properties of polypyrrole [AD-A250531] p 3796 N92-32079
MICROMECHANICS
Mathematical problems in micromechanics and composite materials [AD-A249584] p 3773 N92-31378
Computational simulation of intermingled-fiber hybrid composite behavior [NASA-TM-105666] p 3774 N92-31506
The mechanics of fractal damage [AD-A250518] p 3776 N92-32075
Eigensensitivity analysis of composite laminates: Effect of microstructure [AD-A250864] p 3777 N92-32104
Effects of fiber and interfacial layer architectures on the thermoplastic response of metal matrix composites [NASA-TM-105802] p 3777 N92-32234
MICROMETEOROLOGY
Unified very low stratus cloud/subcloud microphysics model [AD-A250662] p 3858 N92-31320
MICROORGANISMS
Methane-producing microorganisms: Component of Mars biosphere p 3924 N92-32180
MICROPROCESSORS
Simulation of a parallel processor based small tactical system [AD-A245911] p 3882 N92-31443
MICROSCOPES
Cellular localization of infrared sources [AD-A249795] p 3866 N92-31302
MICROSTRIP TRANSMISSION LINES
Field-emitter arrays for RF vacuum microelectronics [AD-A250101] p 3816 N92-31791
MICROSTRUCTURE
Mathematical problems in micromechanics and composite materials [AD-A249584] p 3773 N92-31378
The effect of elastic stress on Ostwald ripening phenomena [DE92-015291] p 3839 N92-31400
Superplasticity in a nickel silicide alloy, Ni3Si(V, Mo) [DE92-011651] p 3787 N92-31667
Microstructure and properties of in-situ RF sputtered YBa2Cu3O7 thin films for microwave applications [DE92-013379] p 3911 N92-31723
Theory of semiconducting superlattices and microstructures [AD-A248758] p 3816 N92-31799
Mechanics of thin films [AD-A247848] p 3912 N92-31984
A study of the microstructural basis for the strength and toughness properties of water-quenched and air-cooled HSLA-100, HSLA-100 with increased copper, and a ULCB steel [AD-A245955] p 3789 N92-32052
The mechanics of fractal damage [AD-A250518] p 3776 N92-32075
Quantum mechanical approach to understanding microstructural and mechanical properties in intermetallics [AD-A250550] p 3790 N92-32084
Eigensensitivity analysis of composite laminates: Effect of microstructure [AD-A250864] p 3777 N92-32104
Tetragonal zirconia ceramics in ZrO2-CeO2 system (Ce-TZP): Preparation, characterization and mechanical properties [INPE-5372-PRE/1746] p 3798 N92-32199
MICROWAVE AMPLIFIERS
Microwave generation for magnetic fusion energy applications [DE92-011424] p 3831 N92-31769
Millimeter wave free electron laser amplifiers: Experiments and designs [DE92-011813] p 3832 N92-31935
MICROWAVE CIRCUITS
High-performance packaging for monolithic microwave and millimeter-wave integrated circuits [NASA-TM-105744] p 3808 N92-31855
MICROWAVE EMISSION
High-resolution microwave observations of the sun [AD-A247869] p 3925 N92-31985
MICROWAVE EQUIPMENT
An evaluation of ionizing radiation emitted by high power microwave generators [DE92-016160] p 3805 N92-31387
Stable integrated microwave to optical modulator [AD-A249974] p 3813 N92-31431
Microstructure and properties of in-situ RF sputtered YBa2Cu3O7 thin films for microwave applications [DE92-013379] p 3911 N92-31723
Advanced microwave sounding unit study for atmospheric infrared sounder [NASA-CR-190628] p 3858 N92-32195
MICROWAVE FREQUENCIES
Field-emitter arrays for RF vacuum microelectronics [AD-A250101] p 3816 N92-31791
MICROWAVE OSCILLATORS
Ba2Ti9O20 microwave dielectric resonator: Processing, phase synthesis and characterization [INPE-5373-PRE/1747] p 3818 N92-32200
MICROWAVE SOUNDING
High-resolution microwave observations of the sun [AD-A247869] p 3925 N92-31985
Advanced microwave sounding unit study for atmospheric infrared sounder [NASA-CR-190628] p 3858 N92-32195
MICROWAVE SPECTRA
High-resolution microwave observations of the sun [AD-A247869] p 3925 N92-31985
MICROWAVES
Synthesis of diamond films with pulsed plasma [AD-A250058] p 3791 N92-31356
An evaluation of ionizing radiation emitted by high power microwave generators [DE92-016160] p 3805 N92-31387
Economics of microwave plasma dissociation of H2S [DE92-014846] p 3779 N92-31441
Dicke narrowing in strong fields: The atom-as-antenna analogy [AD-A252321] p 3807 N92-31629
Subnanosecond photoconductive switching in GaAs [DE92-011521] p 3910 N92-31719
Microwave generation for magnetic fusion energy applications [DE92-011424] p 3831 N92-31769
High-resolution microwave observations of the sun [AD-A247869] p 3925 N92-31985
Ba2Ti9O20 microwave dielectric resonator: Processing, phase synthesis and characterization [INPE-5373-PRE/1747] p 3818 N92-32200
MIDDLE ATMOSPHERE
Meteorological data, new series A monographs. Volume 5, no. 4: A three dimensional model simulation of the circulation in the middle atmosphere with cconsideration of tropospherical-stratospherical interactions [ETN-92-91693] p 3861 N92-31708
MILITARY OPERATIONS
Body water homeostasis and human performance in high heat environments: Fluid hydration recommendations for Operation Desert Storm [AD-A249772] p 3868 N92-31492
Optimal targeting of evading objects [DE92-014719] p 3889 N92-32119
MILITARY PSYCHOLOGY
Development of quantitative specifications for simulating the stress environment [AD-A250669] p 3870 N92-31321
MILITARY TECHNOLOGY
Polyalphaolefins: A new improved cost effective aircraft radar coolant [AD-A250517] p 3796 N92-32045
External combustion engine technology (vapor and liquid cycles) for individual soldier power systems [AD-A252754] p 3836 N92-32173
MILLIMETER WAVES
International Semiconductor Device Research Symposium (ISDRS-91) [AD-A247394] p 3908 N92-31537

High-performance packaging for monolithic microwave and millimeter-wave integrated circuits
[NASA-TM-105744] p 3808 N92-31855
Millimeter wave free electron laser amplifiers: Experiments and designs
[DE92-011813] p 3832 N92-31935
Compact millimeter-wave devices: Dielectric loaded carm, high voltage carm, slow wave crm and high harmonic gyrotron
[AD-A250497] p 3809 N92-31944
Conversion of power and frequency
[DE92-012543] p 3810 N92-32134

MILLING MACHINES
Capabilities of the 3-axes modified FP42 Deckel milling machine
[DE92-011737] p 3803 N92-31908

MIMD (COMPUTERS)
Operating principles of MULTIKRON performance instrumentation for MIMD computers
[PB92-181072] p 3874 N92-31366
PDDP: Data-driven parallelism and shared memory
[DE92-008073] p 3883 N92-31741
A sweep algorithm for massively parallel simulation of circuit-switched networks
[NASA-CR-189680] p 3881 N92-32157

MINIATURIZATION
The chemistry and packaging of nanocomposite confined arrays
[AD-A250991] p 3817 N92-32002

MINING
JPRS report: Science and technology. Central Eurasia: Materials science
[JPRS-UMS-92-010] p 3787 N92-31584
Energy and Environment: A Sandia Technology Bulletin
[DE92-016740] p 3854 N92-31931

MINORITIES
Minorities and air quality non-attainment areas: A preliminary geo-demographic analysis
[DE92-013054] p 3852 N92-31591

MISSILE CONTROL
Collection of papers of the 31st Israel Annual Conference on Aviation and Astronautics
[ITN-92-85124] p 3745 N92-31861
Discrete optimal guidance for high order missile and maneuvering target p 3748 N92-31879

MISSILE DEFENSE
Ground based radar
[TABES PAPER 92-213] p 3764 N92-32021

MISSILE TRACKING
Ground based radar
[TABES PAPER 92-213] p 3764 N92-32021

MISSILE VIBRATION
Dynamic modeling and modal analysis of an air-to-air missile
[AD-A245957] p 3758 N92-32053

MISSILES
Discrete optimal guidance for high order missile and maneuvering target p 3748 N92-31879
Optimal targeting of evading objects
[DE92-014719] p 3889 N92-32119

MISSION PLANNING
A demonstration of an intelligent control system for a reusable rocket engine
[NASA-TM-105794] p 3770 N92-31507
Proceedings of the 53rd Symposium on Air Vehicle Mission Control and Management
[AGARD-AR-310] p 3889 N92-32229

MIXED CRYSTALS
Growth, nitrogen vacancy reduction and solid solution formation in cubic GaN thin films and the subsequent fabrication of superlattice structures using AlN and InN
[AD-A248058] p 3908 N92-31446

MIXED OXIDES
Characterization of oxides for low temperature solid oxide fuel cells
[PB92-152883] p 3848 N92-31903

MIXING LAYERS (FLUIDS)
An experimental investigation of the formation of secondary vortices and the generation of small-scale motion in a spanwise forced plane mixing layer
[AD-A250350] p 3822 N92-31559

MIXTURES
Steady flow of a fluid-solid mixture between parallel plates
[DE92-013645] p 3821 N92-31426
Theoretical studies of solid-fluid phase equilibria
[DE92-016598] p 3781 N92-31717

MODAL RESPONSE
Asymptotic modal analysis and statistical energy analysis
[NASA-CR-190516] p 3842 N92-32236

MODELS
Stress reactivity: Five-factor representation of a psychobiological typology
[AD-A252715] p 3872 N92-31327

MODEMS
Issues in designing transport layer multicast facilities
[NASA-CR-190639] p 3882 N92-31483

MODULATION
The investigation of bandwidth efficient coding and modulation techniques
[NASA-CR-190685] p 3806 N92-31468

MODULATORS
Optical oversampled analog-to-digital conversion
[AD-A252695] p 3877 N92-31587

MODULES
Data reduction formulas for the 16-foot transonic tunnel: NASA Langley Research Center, revision 2
[NASA-TM-107646] p 3762 N92-31900

MODULUS OF ELASTICITY
Development of effective quantum chemical method for polymers and solid
[AD-A250976] p 3795 N92-31951

MOIRE INTERFEROMETRY
Composite material shear property measurement using the Iosipescu specimen
[NASA-CR-190661] p 3772 N92-31274

MOISTURE CONTENT
Unified very low stratus cloud/subcloud microphysics model
[AD-A250662] p 3858 N92-31320

MOLECULAR BEAM EPITAXY
Growth, nitrogen vacancy reduction and solid solution formation in cubic GaN thin films and the subsequent fabrication of superlattice structures using AlN and InN
[AD-A248058] p 3908 N92-31446

MOLECULAR CHAINS
Photogenerated base as catalyst for imidization reactions: Design of photosensitive polyimides
[AD-A250067] p 3795 N92-31810

MOLECULAR DIFFUSION
Towards understanding turbulent scalar mixing
[NASA-CR-4446] p 3826 N92-32242

MOLECULAR ENERGY LEVELS
Many body perturbation theory using a Restricted Open-Shell Hartree-Fock (ROHF) reference function
[AD-A249725] p 3894 N92-31673
Theoretical studies of the reactions and spectroscopy of radical species relevant to combustion reactions and diagnostics
[DE92-013484] p 3781 N92-31725

MOLECULAR EXCITATION
The pathways and dynamics of molecular decomposition
[AD-A249627] p 3893 N92-31463

MOLECULAR INTERACTIONS
Molecular interactions and properties with many-body methods
[AD-A247052] p 3896 N92-31858

MOLECULAR IONS
Dependence of secondary ion emission from organic material on the energy loss of the impacting heavy ion
[DE92-014845] p 3893 N92-31386

MOLECULAR ORBITALS
Near-IR absorption spectra for the Buckminsterfullerene Anions: An experimental and theoretical study
[AD-A250532] p 3785 N92-32080
Electronic structure and photophysical properties of polyimides
[DE92-012353] p 3797 N92-32146

MOLECULAR OSCILLATIONS
Vibrational modes and the dynamic solvent effect in electron and proton transfer
[AD-A250727] p 3897 N92-31950

MOLECULAR PUMPS
Ultrafast studies on electron transfer in the betaines: Evidence for local heating
[AD-A250728] p 3897 N92-31999

MOLECULAR STRUCTURE
Linear and star-branched siloxy-silane polymers: One pot A-B polymerization and end-capping
[AD-A252195] p 3792 N92-31408
Tris-triphenylsiloxy compounds of aluminum
[AD-A250141] p 3788 N92-31795
Application of optical theory to quantitative surface FT-IR with emphasis on molecular depth profiling
[AD-A250525] p 3902 N92-32077

MOLECULAR WEIGHT
Ring-opening polymerization of strained cyclotetrasilanes as a new route towards well defined polysilylenes
[AD-A251020] p 3795 N92-31941

MOLECULES
Molecular outflows associated with HH52-54 and IRAS 12496-7650
[PB92-184472] p 3924 N92-31635
Many body perturbation theory using a Restricted Open-Shell Hartree-Fock (ROHF) reference function
[AD-A249725] p 3894 N92-31673

MOLTEN SALTS
YLIFE-2 inertial fusion energy power plant design
[DE92-011965] p 3904 N92-31530

MOLYBDENUM OXIDES
Surface chemistry of MoS2 lubricant films: Effects of high humidity storage on sputtered films
[DE92-015392] p 3794 N92-31631

MOLYBDENUM SULFIDES
Surface chemistry of MoS2 lubricant films: Effects of high humidity storage on sputtered films
[DE92-015392] p 3794 N92-31631

MONITORS
Spacecraft dynamics characterization and control system failure detection. Volume 3: Control system failure monitoring
[NASA-CR-190529] p 3884 N92-31254
Final report on DSA methods for monitoring alumina in aluminum reduction cells with cermet anodes
[DE92-013599] p 3813 N92-31440
Beam position monitor electronics using DC coupled demodulating logarithmic amplifiers
[DE92-011697] p 3816 N92-31760
Optical fiber sensors for organic matrix composite material cure monitoring
[AD-A247114] p 3776 N92-31979
Monitoring threats to satellite functions
[PB92-195445] p 3767 N92-32073
Device for monitoring the thickness of a dielectric coating on a dielectric substrate
[DE92-014741] p 3829 N92-32174
Engine monitoring display study
[NASA-CR-4463] p 3761 N92-32175

MONOMERS
Organometallic Nonlinear Optical (NLO) polymers. Part 2: Synthesis of main-chain organometallic polymers and a structural study of ferrocene NLO-Phores
[AD-A250655] p 3791 N92-31318
Synthesis of soluble alpha-thiophene oligomers. Monomer to octamer
[AD-A250082] p 3779 N92-31434
Ring-opening polymerization of strained cyclotetrasilanes as a new route towards well defined polysilylenes
[AD-A251020] p 3795 N92-31941
Real time investigations of the polymerization of 2-pentadecyl aniline on the Langmuir-Blodgett trough
[AD-A250994] p 3795 N92-31954
Polymerization of conducting polymers confined to free surfaces: A comparison of the Langmuir-Blodgett polymerization of 3-alkyl pyrroles and 2-alkyl anilines
[AD-A250966] p 3798 N92-32194

MONTE CARLO METHOD
Research in elementary particle physics
[DE92-014585] p 3893 N92-31385
Radiation protection for human exploration of the moon and Mars: Application of the MASH code system
[DE92-014416] p 3868 N92-31409
Comparison of effects of copropagated and precomputed atmosphere profiles on Monte Carlo trajectory simulation
[NASA-TM-102600] p 3766 N92-31457
Oxygen ordering and strain-related morphology in YBa2Cu(3-x)O7 systems
[DE92-014476] p 3909 N92-31627
Real time detection in a laser bathymetry system
[PB92-195452] p 3866 N92-32069

MOON
Using space resources
[NASA-TM-107966] p 3924 N92-31781

MORPHOLOGY
Oxygen ordering and strain-related morphology in YBa2Cu(3-x)O7 systems
[DE92-014476] p 3909 N92-31627

MOTION SIMULATION
Illusory self motion and disorientation
[CTN-92-60318] p 3871 N92-31472
Mathematical modeling and numerical simulation of the dynamics of flexible structures undergoing large overall motions
[AD-A250202] p 3761 N92-31967
Head tracking and head mounted displays for training simulations
[AD-A250866] p 3873 N92-31974

MOUNTAINS
Two-dimensional axisymmetric calculations of surface waves generated by an explosion in an island, mountain, and sedimentary basin
[AD-A249971] p 3856 N92-31510

MULTIBEAM ANTENNAS
Experiment on a three-beam adaptive array for EHF frequency-hopped signals using a fast algorithm, phase-D
[CTN-92-60322] p 3810 N92-32203

MULTIGRID METHODS
An installed nacelle design code using a multiblock Euler solver. Volume 1: Theory document
[NASA-CR-189652-VOL-1] p 3754 N92-32226
An installed nacelle design code using a multiblock Euler solver. Volume 2: User guide
[NASA-CR-189652-VOL-2] p 3754 N92-32228
MULTIPHASE FLOW
Steady flow of a fluid-solid mixture between parallel plates
[DE92-013645] p 3821 N92-31426
FEHMN 1.0: Finite element heat and mass transfer code
[DE92-013998] p 3825 N92-32008
MULTIPHOTON ABSORPTION
Alterations of multiphoton-resonant processes through wave-mixing effects
[DE92-016164] p 3896 N92-31923
MULTIPLIERS
VLSI for high-speed digital signal processing
[AD-A250365] p 3817 N92-32074
MULTIPROCESSING (COMPUTERS)
Graphical development tools for network-based concurrent supercomputing
[DE92-011144] p 3875 N92-31447
Performance measures of the Ada rendezvous
[AD-A250060] p 3877 N92-31601
A task adaptive parallel graphics rendering algorithm
[DE92-008062] p 3878 N92-31739
The multicomputer toolbox: Scalable parallel libraries for large-scale concurrent applications
[DE92-008068] p 3882 N92-31740
PDDP: Data-driven parallelism and shared memory
[DE92-008073] p 3883 N92-31741
Use of a genetic algorithm to solve fluid flow problems on an NCUBE/2 multiprocessor computer
[DE92-014044] p 3824 N92-31832
The hierarchical spatial decomposition of three-dimensional particle-in-cell plasma simulations on MIMD distributed memory multiprocessors
[DE92-016802] p 3883 N92-32034
VLSI for high-speed digital signal processing
[AD-A250365] p 3817 N92-32074
The data structure accelerator architecture
[AD-A250968] p 3883 N92-32152
MULTISENSOR APPLICATIONS
Estimation with multisensor/multiscan detection fusion
[AD-A250496] p 3804 N92-31333
A real time system for multisensor image analysis through pyramidal segmentation
[AD-A247169] p 3888 N92-31981
MULTISTATIC RADAR
Calibration network intended for phased-array antennas at 3 GHz
[PB92-195429] p 3810 N92-32070
MULTIVARIABLE CONTROL
A demonstration of an intelligent control system for a reusable rocket engine
[NASA-TM-105794] p 3770 N92-31507
MUONS
Proceedings of the 2nd KUR symposium on hyperfine interactions
[DE92-789024] p 3895 N92-31728
MUTATIONS
Biodosimetry of ionizing radiation in humans using the glycophorin A genotoxicity assay
[DE92-011974] p 3869 N92-31608
MYOCARDIUM
Noninvasive ambulatory assessment of cardiac function and myocardial ischemia in healthy subjects exposed to carbon monoxide
[AD-A252264] p 3870 N92-32107

N

NACELLES
Analytical and experimental studies of heat pipe radiation cooling of hypersonic propulsion systems
[DE92-013428] p 3759 N92-31817
An installed nacelle design code using a multiblock Euler solver. Volume 1: Theory document
[NASA-CR-189652-VOL-1] p 3754 N92-32226
An installed nacelle design code using a multiblock Euler solver. Volume 2: User guide
[NASA-CR-189652-VOL-2] p 3754 N92-32228
NASA PROGRAMS
Small Business Innovation Research program solicitation. Closing date: July 21, 1992
[NASA-TM-107795] p 3916 N92-31253
NASA patent abstracts bibliography: A continuing bibliography. Section 2: Indexes (supplement 41)
[NASA-SP-7039(41)-SECT-2] p 3918 N92-31455
System overview of the NASA Dryden Integrated Test Facility
[NASA-TM-104250] p 3762 N92-32201
NASA SPACE PROGRAMS
NASA programs --- nasa space programs
p 3765 N92-32238
NATIONAL AIRSPACE SYSTEM
GNAS Maintenance Control Center (GMCC) Design Qualification Test and Evaluation (DQT/E) test report
[DOT/FAA/CT-TN91/39] p 3745 N92-31615
NATURAL GAS
National Conference on Integrated Resource Planning: Proceedings
[DE92-013573] p 3845 N92-31290
World energy projection system: Model documentation
[DE92-014206] p 3847 N92-31594
Proceedings of the 4th Atlantic OCS Region Information Transfer Meeting
[PB92-177690] p 3864 N92-31630
Light alkane conversion processes: Suprabiotic catalyst systems for selective oxidation of light alkane gases to fuel oxygenates
[DE92-015229] p 3799 N92-31751
NATURAL LANGUAGE (COMPUTERS)
Use of expert systems as user interfaces in information retrieval p 3921 N92-32185
Search strategies in natural language
p 3921 N92-32186
NAVIER-STOKES EQUATION
Stagnation-point heat-transfer rate predictions at aeroassist flight conditions
[NASA-TP-3208] p 3819 N92-31281
A computational investigation of airfoil stall flutter
[AD-A247302] p 3751 N92-31300
The discretization of the 2D incompressible Navier-Stokes equations on a collocated grid
[REPT-91-61] p 3821 N92-31513
Hypersonic code efficiency and validation studies
[NASA-CR-190680] p 3752 N92-31533
Low density real gas flows about hypersonic vehicles
[AD-A250048] p 3752 N92-31777
Numerical simulation of tulip flame dynamics
[DE92-008553] p 3782 N92-31805
Use of a genetic algorithm to solve fluid flow problems on an NCUBE/2 multiprocessor computer
[DE92-014044] p 3824 N92-31832
The calculation of incompressible separated turbulent boundary layers p 3749 N92-31886
Three-dimensional compressible turbulent computations for a nondiffusing S-duct
[NASA-CR-4391] p 3754 N92-32240
NAVIGATION
Hyper-NPSNET: A virtual world with an integrated 3-D hypertext
[AD-A252726] p 3878 N92-31676
RL-34 ring laser gyro laboratory evaluation for the Deep Space Network antenna application
[NASA-CR-190481] p 3829 N92-32128
NAVIGATION AIDS
Satellite positioning systems: A report to the director
[PB92-181270] p 3767 N92-31632
Global positioning system runway incursion program static ground tests
[DOT/FAA/CT-TN91/44] p 3756 N92-31838
Decision-making guide for the proposed Coast Guard differential global positioning system
[AD-A246046] p 3756 N92-32054
NAVIGATION INSTRUMENTS
Techniques for autonomous navigation
[DE92-013458] p 3756 N92-31746
NAVIGATION SATELLITES
GPS satellite orbit determination using pseudorange data: Experiments and results
[PB92-178870] p 3765 N92-31685
NAVSTAR SATELLITES
Satellite positioning systems: A report to the director
[PB92-181270] p 3767 N92-31632
NAVY
STI handbook: Guidelines for producing, using, and managing scientific and technical information in the Department of the Navy. A handbook for Navy scientists and engineers on the use of scientific and technical information
[AD-A252439] p 3918 N92-31482
NEAR FIELDS
Near-field and far-field sound radiation from a line-driven fluid-loaded infinite flat plate having periodic and non-periodic attached rib stiffeners
[AD-A250100] p 3892 N92-31789
NEGATIVE IONS
Theoretical atomic collision physics
[DE92-013571] p 3895 N92-31724
Ring-opening polymerization of strained cyclotetrasilanes as a new route towards well defined polysilylenes
[AD-A251020] p 3795 N92-31941
NERVOUS SYSTEM
A biological model of the effects of toxic substances
[AD-A247138] p 3867 N92-31980
NETWORK ANALYSIS
New directions in network flows
[AD-A250499] p 3880 N92-32039
A sweep algorithm for massively parallel simulation of circuit-switched networks
[NASA-CR-189680] p 3881 N92-32157
Realization of lattice networks at MHz- and GHz-frequencies
[PB92-195437] p 3810 N92-32161
NETWORK CONTROL
EHF SATCOM frequency hopping pattern generator: Proof of concept
[DREO-89-32] p 3811 N92-32231
NEURAL NETS
Data to test and evaluate the performance of neural network architectures for seismic signal discrimination, neural computing for seismic phase identification, volume 2
[AD-A252442] p 3884 N92-31293
Human image understanding
[AD-A250401] p 3872 N92-31330
Analysis and design of neural networks
[AD-A250495] p 3884 N92-31332
Acquisition and production of skilled behavior in dynamic decision-making tasks
[NASA-CR-190614] p 3870 N92-31341
Neural network perception for mobile robot guidance
[AD-A249972] p 3884 N92-31511
Using neural networks in software repositories
[NASA-CR-190641] p 3885 N92-31597
A simple linearized learning algorithm which outperforms back-propagation
[AD-A249697] p 3877 N92-31642
Signal processing and recognition in adaptive neural networks
[AD-A250505] p 3885 N92-32041
Artificial neural network implementation of a near-ideal error prediction controller
[NASA-CR-190694] p 3880 N92-32122
NEURONS
Acetylcholinesterase inhibitors on the spinal cord
[AD-A252694] p 3868 N92-31326
The effects of hydrazines of neuronal excitability
[AD-A247142] p 3868 N92-31491
Organization of the human circadian system
[AD-A247498] p 3869 N92-31905
NEUROPHYSIOLOGY
The effects of hydrazines of neuronal excitability
[AD-A247142] p 3868 N92-31491
Modeling of learning-induced receptive field plasticity in auditory neocortex
[AD-A250348] p 3869 N92-31558
A biological model of the effects of toxic substances
[AD-A247138] p 3867 N92-31980
NEUROTRANSMITTERS
Acetylcholinesterase inhibitors on the spinal cord
[AD-A252694] p 3868 N92-31326
NEUTRAL BEAMS
A global fitting code for multichordal neutral beam spectroscopic data
[DE92-014258] p 3781 N92-31729
NEUTRINO BEAMS
Problems in neutrino electron scattering with 1-GeV neutrinos
[DE92-013535] p 3895 N92-31765
NEUTRINOS
Problems in neutrino electron scattering with 1-GeV neutrinos
[DE92-013535] p 3895 N92-31765
Implications of the 17 keV neutrino
[DE92-017000] p 3898 N92-32006
NEUTRON DECAY
Prompt neutron lifetime in a strongly heterogeneous lattice
[DE92-013212] p 3898 N92-32165
NEUTRON IRRADIATION
Radiation damage in carbon-carbon composites
[DE92-011778] p 3775 N92-31912
Neutron radiation damage to silicon detectors
[ITN-92-85162] p 3897 N92-31958
NEUTRON SOURCES
Resolution function of an inelastic scattering spectrometer with a pulsed neutron source
[DE92-620889] p 3896 N92-31904
NEUTRON SPECTRA
Resolution function of an inelastic scattering spectrometer with a pulsed neutron source
[DE92-620889] p 3896 N92-31904
NEUTRON SPECTROMETERS
Resolution function of an inelastic scattering spectrometer with a pulsed neutron source
[DE92-620889] p 3896 N92-31904
NEWTONIAN FLUIDS
Macrostatistical hydrodynamics
[DE92-013589] p 3823 N92-31726

NICKEL ALLOYS
Non-equilibrium synthesis by laser cladding of Ni, Nb and Mg alloys for improved environmental resistance
[AD-A250552] p 3787 N92-31612
Superplasticity in a nickel silicide alloy, Ni3Si(V, Mo)
[DE92-011651] p 3787 N92-31667
The structure and properties of grain boundaries in Ni3Al
[DE92-012143] p 3788 N92-31744
Fatigue in single crystal nickel superalloys
[AD-A252492] p 3790 N92-32066

NICKEL IRON BATTERIES
Research and development of advanced nickel-iron batteries for electric vehicle propulsion
[DE92-014099] p 3817 N92-31834

NICKEL STEELS
Chromium, nickel, and other alloying elements in US-produced stainless and heat-resisting steel
[PB92-178623] p 3788 N92-31797

NIGHT VISION
Pilot errors involving Head-Up Displays (HUDs), Helmet-Mounted Displays (HMDs), and Night Vision Goggles (NVGs)
[AD-A250719] p 3873 N92-32023

NIOBIUM ALLOYS
Non-equilibrium synthesis by laser cladding of Ni, Nb and Mg alloys for improved environmental resistance
[AD-A250552] p 3787 N92-31612

NITRATION
Selective nitrations: The laser-induced nitration of three cycloalkanes, 1
[AD-A249942] p 3800 N92-31800

NITRILES
Characterization of polymers for microcellular foams
[DE92-012444] p 3793 N92-31539

NITROGEN
Growth, nitrogen vacancy reduction and solid solution formation in cubic GaN thin films and the subsequent fabrication of superlattice structures using AlN and InN
[AD-A248058] p 3908 N92-31446
Theoretical studies of the reactions and spectroscopy of radical species relevant to combustion reactions and diagnostics
[DE92-013484] p 3781 N92-31725

NITROGEN OXIDES
Shock tube study of the reaction of triethanol ammonium nitrate with N2O
[AD-A250034] p 3800 N92-31804

NOAA 10 SATELLITE
Mission description and in-flight operations of ERBE instruments on ERBS, NOAA 9, and NOAA 10 spacecraft
[NASA-RP-1279] p 3844 N92-32127

NOAA 9 SATELLITE
Mission description and in-flight operations of ERBE instruments on ERBS, NOAA 9, and NOAA 10 spacecraft
[NASA-RP-1279] p 3844 N92-32127

NOISE INTENSITY
Aviation noise: Costs of phasing out noisy aircraft
[GAO/RCED-91-128] p 3891 N92-31454
Optical interferometric sensor detected intensity noise reductions means
[AD-D015296] p 3902 N92-32137

NOISE MEASUREMENT
Optical interferometric sensor detected intensity noise reductions means
[AD-D015296] p 3902 N92-32137

NOISE PREDICTION (AIRCRAFT)
High speed turboprop aeroacoustic study (counterrotation). Volume 2: Computer programs
[NASA-CR-185242] p 3891 N92-31248

NOISE REDUCTION
Aviation noise: Costs of phasing out noisy aircraft
[GAO/RCED-91-128] p 3891 N92-31454
Optical interferometric sensor detected intensity noise reductions means
[AD-D015296] p 3902 N92-32137

NOMENCLATURES
A dictionary of acquisition and contracting terms
[AD-A247053] p 3920 N92-31754
Correspondence dictionary from free English term to INIS descriptors
[DE92-782192] p 3920 N92-31859

NONDESTRUCTIVE TESTS
Residual stress and strain measurements in an austenitic steel plate containing a multipass weld
[DE92-014478] p 3839 N92-31383
Guidelines for generating acceptance sampling plans for continuous production
[DE92-010763] p 3837 N92-31753
Robotics development for the enhancement of space endeavors
[TABES PAPER 92-445] p 3763 N92-32013
Instabilities of damage and surface degradation mechanisms in brittle material structural systems
[AD-A250785] p 3842 N92-32168
Investigation into the ultrasonic NDE of adhesively bonded joints
[DREP-90-02] p 3837 N92-32202
Acoustic emission method applied to tests on concrete p 3842 N92-32206

NONEQUILIBRIUM CONDITIONS
A dynamical model of the behaviour of hadronic and fundamental strings at finite densities
[DE92-630245] p 3914 N92-31402
Non-equilibrium synthesis by laser cladding of Ni, Nb and Mg alloys for improved environmental resistance
[AD-A250552] p 3787 N92-31612

NONEQUILIBRIUM FLOW
An approximate local thermodynamic nonequilibrium radiation model for air
[NASA-CR-190580] p 3914 N92-31577

NONEQUILIBRIUM RADIATION
An approximate local thermodynamic nonequilibrium radiation model for air
[NASA-CR-190580] p 3914 N92-31577

NONFERROUS METALS
JPRS report: Science and technology. Central Eurasia: Materials science
[JPRS-UMS-92-010] p 3787 N92-31584

NONLINEAR EQUATIONS
Nonlinear partial differential equations and solitons
[MATHS-REPT-A-152] p 3886 N92-31956
Non-convex problems in PDE: Equilibrium theory and dynamics
[AD-A250549] p 3887 N92-32081

NONLINEAR OPTICS
Nonlinear optical acrylic polymers and use thereof in optical and electro-optic devices
[AD-D015236] p 3791 N92-31270
Organometallic Nonlinear Optical (NLO) polymers. Part 2: Synthesis of main-chain organometallic polymers and a structural study of ferrocene NLO-Phores
[AD-A250655] p 3791 N92-31318
Dipolar interaction assisted effects on second harmonic generation
[AD-A252487] p 3784 N92-31959
Optical computing and optical signal processing, phase 1
[AD-A250551] p 3902 N92-32092
Single crystal growth optimization of magnesium-doped lithium niobate
[AD-A250781] p 3914 N92-32207

NONLINEAR PROGRAMMING
Life extending control for rocket engines
[NASA-TM-105789] p 3802 N92-31263

NONLINEAR SYSTEMS
Electrostatic turbulence and transport in the RFP edge
[DE92-014322] p 3905 N92-31730
A generalization to stochastic averaging in random vibration
[DE92-016747] p 3842 N92-32088

NONLINEARITY
Analysis and design of neural networks
[AD-A250495] p 3884 N92-31332
Development of high efficiency nonlinear optical materials
[AD-A249612] p 3901 N92-31380
Computation of nonlinear gravity waves by a desingularized boundary integral method
[AD-A251149] p 3857 N92-31766
Electro-optics and second harmonic generation of nonlinear optical polymers
[AD-A252488] p 3796 N92-31960
Nonlinearly stable compact schemes for shock calculations
[NASA-CR-189663] p 3887 N92-32164

NORTH AMERICA
Upper tropospheric jet streams over North America during summer 1988
[AD-A249871] p 3857 N92-31906

NORTH CAROLINA
A case study of a prolonged sleet event: 16-17 February 1987 and climatology of sleet events for North Carolina, 1949-1989
[AD-A250184] p 3859 N92-31602

NORTHERN HEMISPHERE
Modelling and prediction of regions of the North Pacific
[AD-A252144] p 3863 N92-31406

NOZZLE GEOMETRY
Effect of inlet geometry on the flow and combustion processes in a solid fuel ramjet p 3747 N92-31871

NUCLEAR BINDING ENERGY
Nature of short Li-H-C contact interactions in organolithium compounds and its implication
[AD-A250992] p 3898 N92-32024
Computational studies of metal-metal and metal-ligand interactions
[NASA-CR-190674] p 3790 N92-32156

NUCLEAR DEFORMATION
The structure of nuclei far from beta stability
[DE92-012598] p 3895 N92-31721
Exotic nuclear shapes and configurations that can be studied at high spin using radioactive ion beams
[DE92-016800] p 3898 N92-32090

NUCLEAR DEVICES
Electrostatic turbulence and transport in the RFP edge
[DE92-014322] p 3905 N92-31730

NUCLEAR ELECTRIC POWER GENERATION
Space nuclear power, propulsion, and related technologies
[SAND91-2617] p 3770 N92-31503
YLIFE-2 inertial fusion energy power plant design
[DE92-011965] p 3904 N92-31530

NUCLEAR ENERGY
Space nuclear power, propulsion, and related technologies
[SAND91-2617] p 3770 N92-31503
Directory of IAEA databases
[DE92-626395] p 3920 N92-32058

NUCLEAR EXPLOSIONS
Mitigation of magnetohydrodynamic electromagnetic pulse (MHD-EMP) effects from commercial electric power systems
[AD-A249577] p 3804 N92-31354

NUCLEAR FUEL ELEMENTS
Emissivity measurements in support of experiments on natural convection between a vertical cylinder and a surrounding array
[DE92-012321] p 3819 N92-31287

NUCLEAR FUEL REPROCESSING
YLIFE-2 inertial fusion energy power plant design
[DE92-011965] p 3904 N92-31530

NUCLEAR FUELS
Transient fission gas behavior in uranium nitride fuel under proposed space applications
[AD-A252577] p 3899 N92-31325
Mechanical strength and stability of lithium aluminate
[DE92-015998] p 3841 N92-31638

NUCLEAR FUSION
Microwave generation for magnetic fusion energy applications
[DE92-011424] p 3831 N92-31769

NUCLEAR MAGNETIC RESONANCE
A robust algorithm for isotropic reconstruction of magic-angle spinning solid-state NMR spectra
[AD-A249610] p 3874 N92-31379
Characterization of polymers for microcellular foams
[DE92-012444] p 3793 N92-31539
Cationic ring opening polymerization of oxazolines initiated by trimethylsilyl derivatives
[AD-A251109] p 3798 N92-32153

NUCLEAR PHYSICS
Photon and electron data bases and their use in radiation transport calculations
[DE92-011458] p 3895 N92-31705
Experimental particle physics at the University of Pittsburgh
[DE92-016182] p 3896 N92-31926
Theoretical studies in nuclear reactions and nuclear structure
[DE92-016204] p 3897 N92-31927
Intermediate/high energy nuclear physics
[DE92-015363] p 3900 N92-32028

NUCLEAR POWER PLANTS
Emissivity measurements in support of experiments on natural convection between a vertical cylinder and a surrounding array
[DE92-012321] p 3819 N92-31287
YLIFE-2 inertial fusion energy power plant design
[DE92-011965] p 3904 N92-31530
Understanding and managing the effects of battery charger and inverter aging
[DE92-014473] p 3815 N92-31651
Heat transfer and pressure drop in an annular channel with downflow
[DE92-014363] p 3825 N92-32115

NUCLEAR POWER REACTORS
Potassium Rankine cycle nuclear power systems for spacecraft and lunar-mass surface power
[DE92-016163] p 3770 N92-31897

NUCLEAR PROPULSION
Space nuclear power, propulsion, and related technologies
[SAND91-2617] p 3770 N92-31503
A philosophy for space nuclear systems safety
[DE92-016501] p 3771 N92-32030

NUCLEAR REACTIONS
Photon and electron data bases and their use in radiation transport calculations
[DE92-011458] p 3895 N92-31705

Theoretical studies in nuclear reactions and nuclear structure
[DE92-016204] p 3897 N92-31927
NUCLEAR REACTOR CONTROL
Emissivity measurements in support of experiments on natural convection between a vertical cylinder and a surrounding array
[DE92-012321] p 3819 N92-31287
NUCLEAR REACTORS
Mechanical strength and stability of lithium aluminate
[DE92-015998] p 3841 N92-31638
Application of reactor-pumped lasers to power beaming
[DE92-012370] p 3831 N92-31762
Heat transfer and pressure drop in an annular channel with downflow
[DE92-014363] p 3825 N92-32115
NUCLEAR SPIN
Proceedings of the 2nd KUR symposium on hyperfine interactions
[DE92-789024] p 3895 N92-31728
Exotic nuclear shapes and configurations that can be studied at high spin using radioactive ion beams
[DE92-016800] p 3898 N92-32090
NUCLEAR STRUCTURE
The structure of nuclei far from beta stability
[DE92-012598] p 3895 N92-31721
Theoretical studies in nuclear reactions and nuclear structure
[DE92-016204] p 3897 N92-31927
Exotic nuclear shapes and configurations that can be studied at high spin using radioactive ion beams
[DE92-016800] p 3898 N92-32090
NUCLEAR WARFARE
B-1B nuclear certification tasks performed by the Aircraft Compatibility Department at Sandia National Laboratories
[DE92-016750] p 3757 N92-31736
NUCLEAR WEAPONS
B-1B nuclear certification tasks performed by the Aircraft Compatibility Department at Sandia National Laboratories
[DE92-016750] p 3757 N92-31736
NUCLEATE BOILING
Heat transfer and pressure drop in an annular channel with downflow
[DE92-014363] p 3825 N92-32115
NUCLEATION
Laser-ablated copper condensation in helium
[DE92-016685] p 3789 N92-32004
NUCLEI (NUCLEAR PHYSICS)
The structure of nuclei far from beta stability
[DE92-012598] p 3895 N92-31721
NUCLEON-NUCLEON INTERACTIONS
Intermediate/high energy nuclear physics
[DE92-015363] p 3900 N92-32028
NUCLEONS
Theoretical studies in nuclear reactions and nuclear structure
[DE92-016204] p 3897 N92-31927
NUMERICAL ANALYSIS
ADIFOR: Automatic differentiation in a source translator environment
[DE92-016185] p 3886 N92-31311
Ignition and flame propagation studies over a flat fuel surface
[PB92-181056] p 3780 N92-31678
The Matrix Editor for symbolic Jacobians in ALPAL
[DE92-008076] p 3878 N92-31742
NUMERICAL CONTROL
Flutter suppression digital control law design and testing for the AFW wind-tunnel model
[NASA-TM-107652] p 3757 N92-31350
Optimized photorefractive barium titanate
[AD-A250089] p 3908 N92-31438
A comparison of three self-tuning control algorithms developed for the Bristol-Babcock controller
[DE92-014472] p 3814 N92-31499
Real time analysis of tokamak discharge parameters
[DE92-011394] p 3904 N92-31616
Torque linearizing hardware for the electric joint motors of a direct-drive robot
[DE92-012681] p 3816 N92-31718
Techniques for autonomous navigation
[DE92-013458] p 3756 N92-31746
Integrated computer systems in aircraft design and manufacture: Difficulties and implications
p 3746 N92-31864
NUMERICAL FLOW VISUALIZATION
Evolution of reactants fluid volume in turbulent jets
[DE92-011298] p 3786 N92-32145
NUMERICAL INTEGRATION
CSM solutions of rotating blade dynamics using integrating matrices
[NASA-CR-190577] p 3840 N92-31619
NUMERICAL STABILITY
Nonlinearly stable compact schemes for shock calculations
[NASA-CR-189663] p 3887 N92-32164
NUTRIENTS
Rainwater and throughfall chemistry in a terra firme rain forest: Central Amazonia
[INPE-5364-PRE/1744] p 3863 N92-32224

O

O RING SEALS
Replaceable valve seat
[AD-D015250] p 3832 N92-31271
OBJECT-ORIENTED PROGRAMMING
A model for extending the behavior of annotations
[DE92-011731] p 3920 N92-31934
OBLIQUE SHOCK WAVES
Sizing supersonic freejet nozzle and inlet location for simulation of the transition phase in integral rocket ramjet p 3747 N92-31870
OBLIQUE WINGS
Transonic wind tunnel test of a 14 percent thick oblique wing
[NASA-TM-102230] p 3754 N92-32213
OBSERVATORIES
Lamont-Doherty Geological Observatory
[PB92-185040] p 3856 N92-31636
OCEAN BOTTOM
Sensitivity of the tomographic inverse solution to acoustic path variability
[AD-A252146] p 3864 N92-31407
Deep-tow acoustics/geophysics system compressional velocity database
[AD-A252700] p 3918 N92-31467
Hydrographic and Acoustic Doppler Current Profiler (ADCP) data from the Farallones shelf and slope study
[AD-A250834] p 3864 N92-31495
Steady-state and transient modeling of tracer and nutrient distributions in the global ocean
[DE92-011805] p 3864 N92-31572
Proceedings of the 4th Atlantic OCS Region Information Transfer Meeting
[PB92-177690] p 3864 N92-31630
Development, testing and operation of a large suspended ocean measurement structure for deep-ocean use
[AD-A252188] p 3866 N92-32050
OCEAN CURRENTS
Modelling and prediction of regions of the North Pacific
[AD-A252144] p 3863 N92-31406
Hydrographic and Acoustic Doppler Current Profiler (ADCP) data from the Farallones shelf and slope study
[AD-A250834] p 3864 N92-31495
Geomorphic variability in the coastal zone
[AD-A252713] p 3864 N92-31544
Steady-state and transient modeling of tracer and nutrient distributions in the global ocean
[DE92-011805] p 3864 N92-31572
World ocean circulation experiment. WOCE chlorofluorocarbon intercomparison cruise report
[PB92-185974] p 3865 N92-31842
Seasonal wind and ocean thermal forcing influences on the generation of the Leeuwin current and its eddies
[AD-A246992] p 3865 N92-31988
An analysis of hydrographic data collected off Point Sur, California in June 1990
[AD-A246060] p 3866 N92-32056
OCEAN DYNAMICS
Proceedings of the 4th Atlantic OCS Region Information Transfer Meeting
[PB92-177690] p 3864 N92-31630
Parameterization of directional spectra, part 2, volume 1
[DREA-CR-89-445-PT-2-VOL-1] p 3811 N92-32214
OCEAN MODELS
Modelling and prediction of regions of the North Pacific
[AD-A252144] p 3863 N92-31406
Steady-state and transient modeling of tracer and nutrient distributions in the global ocean
[DE92-011805] p 3864 N92-31572
Seasonal wind and ocean thermal forcing influences on the generation of the Leeuwin current and its eddies
[AD-A246992] p 3865 N92-31988
Parameterization of directional spectra, part 2, volume 1
[DREA-CR-89-445-PT-2-VOL-1] p 3811 N92-32214
OCEAN SURFACE
Synthetic temperature profile in the Gulf of Mexico. Part 1: Statistical relationship between modal amplitudes and dynamic height at surface
[AD-A252701] p 3863 N92-31308
Acoustic studies of ocean surface processes in SWAPP
[AD-A247519] p 3864 N92-31429
A numerical, analytical, and observational study of the effect of clouds on surface wind and wind stress during the central Arctic winter
[AD-A252706] p 3860 N92-31670
A diagnostic study of rapidly developing cyclones using surface-based Q vectors
[AD-A246993] p 3862 N92-31978
Radar backscatter from the sea: Controlled experiments
[AD-A250858] p 3810 N92-32101
OSRMS: The DREP near-nadir scatterometer
[DREP-88-15] p 3844 N92-32216
OCEAN TEMPERATURE
Synthetic temperature profile in the Gulf of Mexico. Part 1: Statistical relationship between modal amplitudes and dynamic height at surface
[AD-A252701] p 3863 N92-31308
OCEANOGRAPHIC PARAMETERS
Development, testing and operation of a large suspended ocean measurement structure for deep-ocean use
[AD-A252188] p 3866 N92-32050
OCEANOGRAPHY
Sensitivity of the tomographic inverse solution to acoustic path variability
[AD-A252146] p 3864 N92-31407
Hydrographic observations from the US/PRC cooperative program in the western equatorial Pacific Ocean: Cruises 5-8
[PB92-177054] p 3865 N92-31644
Computer simulation of acoustic fluctuations due to finescale temperature perturbations measured by thermistor chain
[AD-A252709] p 3892 N92-31672
Ecosystems of the Florida Keys: A bibliography
[PB92-198910] p 3854 N92-32071
Biology, oceanography, and fisheries of the North Pacific transition zone and subarctic frontal zone
[PB92-178128] p 3866 N92-32106
JPRS report: Science and technology. Central Eurasia: Earth sciences
[JPRS-UES-92-004] p 3843 N92-32132
OCEANS
Sensitivity of the tomographic inverse solution to acoustic path variability
[AD-A252146] p 3864 N92-31407
Two-dimensional axisymmetric calculations of surface waves generated by an explosion in an island, mountain, and sedimentary basin
[AD-A249971] p 3856 N92-31510
Geomorphic variability in the coastal zone
[AD-A252713] p 3864 N92-31544
The KRAKEN normal mode program
[AD-A252409] p 3892 N92-31818
Development, testing and operation of a large suspended ocean measurement structure for deep-ocean use
[AD-A252188] p 3866 N92-32050
OFFICE AUTOMATION
Automated input into databases: OCR and descriptive cataloguing p 3921 N92-32189
OIL ADDITIVES
Liquid lubrication for space applications
[NASA-TM-105198] p 3795 N92-31840
OIL POLLUTION
Proceedings of the 4th Atlantic OCS Region Information Transfer Meeting
[PB92-177690] p 3864 N92-31630
OIL SLICKS
Proceedings of the 4th Atlantic OCS Region Information Transfer Meeting
[PB92-177690] p 3864 N92-31630
OILS
Proceedings of the 4th Atlantic OCS Region Information Transfer Meeting
[PB92-177690] p 3864 N92-31630
OLIGOMERS
Tribology of functionally-terminated oligomer films
[AD-A250076] p 3833 N92-31433
Synthesis of soluble alpha-thiophene oligomers. Monomer to octamer
[AD-A250082] p 3779 N92-31434
Development of effective quantum chemical method for polymers and solid
[AD-A250976] p 3795 N92-31951
ON-LINE SYSTEMS
FEDIX: The on-line database retrieval service of government information for colleges, universities, and other organizations
[DE92-012384] p 3917 N92-31288
Real-time infrared spectroscopy of moving solids for on-line analyses
[DE92-012156] p 3782 N92-31772

The KRAKEN normal mode program
[AD-A252409] p 3892 N92-31818
Correspondence dictionary from free English term to INIS descriptors
[DE92-782192] p 3920 N92-31859
Intelligent gateways p 3921 N92-32184
Use of expert systems as user interfaces in information retrieval p 3921 N92-32185
Search strategies in natural language p 3921 N92-32186
Computerized property data for engineering materials: An overview p 3922 N92-32191

OPERATING SYSTEMS (COMPUTERS)
Operating principles of MULTIKRON performance instrumentation for MIMD computers
[PB92-181072] p 3874 N92-31366

OPERATIONAL PROBLEMS
Advanced thermally stable, jet fuels development program annual report. Volume 1: Model and experiment system development
[AD-A249625] p 3799 N92-31462

OPERATIONS
Annual report to the Congress, fiscal year 1991 (Office of Technology Assessment)
[PB92-166549] p 3922 N92-31599

OPERATOR PERFORMANCE
Acquisition and production of skilled behavior in dynamic decision-making tasks
[NASA-CR-190614] p 3870 N92-31341

OPTICAL COMMUNICATION
An improved ion guide for external ion injection in glow discharge-Fourier transform ion cyclotron resonance (GD-FTICR) mass spectrometry
[AD-A250944] p 3900 N92-32170

OPTICAL COMPUTERS
Optical processing architectures for spaceborne SAR image generation and RF array beam forming
[TABES PAPER 92-444] p 3763 N92-32012
Optical computing and optical signal processing, phase 1
[AD-A250551] p 3902 N92-32092

OPTICAL CORRECTION PROCEDURE
Resolution limits for ground based astronomical imaging using adaptive optics
[DE92-011949] p 3902 N92-31761

OPTICAL DATA PROCESSING
A microprism array for large-scale, wide-band interconnection of optoelectronic systems
[AD-A249380] p 3813 N92-31374
Optical oversampled analog-to-digital conversion
[AD-A252695] p 3877 N92-31587
Optical processing architectures for spaceborne SAR image generation and RF array beam forming
[TABES PAPER 92-444] p 3763 N92-32012
Optical computing and optical signal processing, phase 1
[AD-A250551] p 3902 N92-32092
Automated input into databases: OCR and descriptive cataloguing p 3921 N92-32189

OPTICAL EQUIPMENT
Analysis of systems hardware flown on LDEF. Results of the systems special investigation group
[NASA-CR-189628] p 3767 N92-31677

OPTICAL FIBERS
Three-wave envelope solitons: Can the speed of light in the fiber be controlled?
[AD-A247615] p 3901 N92-31611
Demonstrated survivability of a high temperature optical fiber cable on a 1500 pound thrust rocket chamber
[NASA-TM-105835] p 3801 N92-32230

OPTICAL HETERODYNING
Coherent/noncoherent detection of coherent optical heterodyne DPSK-CDMA and MFSK-CDMA signals
[AD-A246215] p 3809 N92-31993

OPTICAL ILLUSION
Illusory self motion and disorientation
[CTN-92-60318] p 3871 N92-31472

OPTICAL MATERIALS
Nonlinear optical acrylic polymers and use thereof in optical and electro-optic devices
[AD-D015236] p 3791 N92-31270
Organometallic Nonlinear Optical (NLO) polymers. Part 2: Synthesis of main-chain organometallic polymers and a structural study of ferrocene NLO-Phores
[AD-A250655] p 3791 N92-31318
Development of high efficiency nonlinear optical materials
[AD-A249612] p 3901 N92-31380
Optical computing and optical signal processing, phase 1
[AD-A250551] p 3902 N92-32092

OPTICAL MEASUREMENT
Absorption spectroscopy through the dark zone of solid propellant flames
[AD-A250033] p 3782 N92-31803
Application of optical theory to quantitative surface FT-IR with emphasis on molecular depth profiling
[AD-A250525] p 3902 N92-32077
Single crystal growth optimization of magnesium-doped lithium niobate
[AD-A250781] p 3914 N92-32207

OPTICAL MEASURING INSTRUMENTS
Waveguide-binding sensor for use with assays
[AD-D015230] p 3777 N92-31268
An innovative two axis rate gyro: Theory and principles of operation p 3748 N92-31875
Optical fiber sensors for organic matrix composite material cure monitoring
[AD-A247114] p 3776 N92-31979
Optical interferometric sensor detected intensity noise reductions means
[AD-D015296] p 3902 N92-32137

OPTICAL POLARIZATION
Single crystal growth optimization of magnesium-doped lithium niobate
[AD-A250781] p 3914 N92-32207

OPTICAL PROPERTIES
Development of high efficiency nonlinear optical materials
[AD-A249612] p 3901 N92-31380
Three-wave envelope solitons: Can the speed of light in the fiber be controlled?
[AD-A247615] p 3901 N92-31611
Dipolar interaction assisted effects on second harmonic generation
[AD-A252487] p 3784 N92-31959
Electronic structure and photophysical properties of polyimides
[DE92-012353] p 3797 N92-32146

OPTICAL PUMPING
High performance of copper pumped dye lasers
[DE92-011763] p 3832 N92-31902

OPTICAL RELAY SYSTEMS
A microprism array for large-scale, wide-band interconnection of optoelectronic systems
[AD-A249380] p 3813 N92-31374

OPTICAL SWITCHING
Static and dynamic properties of current sensing power VDMOS transistor
[LAAS-92032] p 3815 N92-31697
Femtosecond photonics: Fundamental phenomena and device behavior
[AD-A250506] p 3832 N92-32042

OPTICAL THICKNESS
Particle diagnostics in optically thick sprays
[AD-A250981] p 3897 N92-31936

OPTICAL WAVEGUIDES
Waveguide-binding sensor for use with assays
[AD-D015230] p 3777 N92-31268

OPTIMIZATION
In-flight decision making by high time and low time pilots during instrument operations
[AD-A249990] p 3871 N92-31392
The discretization of the 2D incompressible Navier-Stokes equations on a collocated grid
[REPT-91-61] p 3821 N92-31513
ASTOVL combat aircraft design synthesis and optimization
[CRANFIELD-AERO-9201] p 3757 N92-31515
Comparison of results: Technische Univ., Delft-Organisatie voor Toegepast Natuurwetenschappelijk Onderzoek expert judgement study of dispersion-deposition
[REPT-92-11] p 3856 N92-31522
Optimal targeting of evading objects
[DE92-014719] p 3889 N92-32119
Kernel optimum nearly-analytical discretization (KOND) method applied to parabolic equations KOND-P Scheme
[NIFS-118] p 3887 N92-32205
Optimal design of geodesically stiffened composite cylindrical shells
[NASA-CR-190706] p 3842 N92-32235

OPTOELECTRONIC DEVICES
Nonlinear optical acrylic polymers and use thereof in optical and electro-optic devices
[AD-D015236] p 3791 N92-31270
International Semiconductor Device Research Symposium (ISDRS-91)
[AD-A247394] p 3908 N92-31537

ORBIT CALCULATION
GPS satellite orbit determination using pseudorange data: Experiments and results
[PB92-178870] p 3765 N92-31685

ORBIT INSERTION
Study of a spherical spinning combustion chamber for orbit insertion p 3746 N92-31869

ORBIT TRANSFER VEHICLES
An approximate local thermodynamic nonequilibrium radiation model for air
[NASA-CR-190580] p 3914 N92-31577
Orbit transfer vehicle engine technology program. Task B-6 high speed turbopump bearings
[NASA-CR-189230] p 3835 N92-31892
Krypton ion thruster performance
[NASA-TM-105818] p 3770 N92-31901
Orbital transfer rocket engine technology: Advanced engine study
[NASA-CR-187216] p 3771 N92-32129

ORBITAL POSITION ESTIMATION
GPS satellite orbit determination using pseudorange data: Experiments and results
[PB92-178870] p 3765 N92-31685

ORBITS
Photometry of Nova Muscae 1983
[INPE-5339-PRE/1738] p 3923 N92-31344

ORDER-DISORDER TRANSFORMATIONS
Diffusion in ordered and disordered media
[AD-A250949] p 3891 N92-32211

ORDNANCE
Using transfer functions as a method for predicting lightning effects on munitions storage bunkers
[DE92-012627] p 3851 N92-31709
Measured responses of a munitions storage bunker to rocket-triggered lightning
[DE92-012628] p 3862 N92-31750

ORGANIC COMPOUNDS
Characterization of polymers for microcellular foams
[DE92-012444] p 3793 N92-31539
The potential of passive-remote Fourier Transform Infrared (FTIR) spectroscopy to detect organic emissions under the Clean Air Act
[DE92-015224] p 3854 N92-32083

ORGANIC LIQUIDS
Decomposition studies of triisopropylantimony and triallylantimony
[AD-A250671] p 3796 N92-31968

ORGANIC LITHIUM COMPOUNDS
Nature of short Li-H-C contact interactions in organolithium compounds and its implication
[AD-A250992] p 3898 N92-32024

ORGANIC MATERIALS
New sources for OMVPE
[AD-A250903] p 3909 N92-31582
A dynamic model of terrestrial carbon cycling
[DE92-015130] p 3853 N92-31782
Optical fiber sensors for organic matrix composite material cure monitoring
[AD-A247114] p 3776 N92-31979
Particle emission and charging effects induced by fracture
[AD-A252182] p 3913 N92-32065
Development and application of photosensitive device systems to studies of biological and organic materials
[DE92-014728] p 3867 N92-32120

ORGANIC PHOSPHORUS COMPOUNDS
Acetylcholinesterase inhibitors on the spinal cord
[AD-A252694] p 3868 N92-31326

ORGANIC SILICON COMPOUNDS
Cyclopolymerization of metalloid-containing alpha, omega-dienes. 1,3-divinyltetramethyldisiloxane, 1,3-divinyltetramethyldisilazane and 1,3-divinylpentamethyldisilazane
[AD-A250347] p 3794 N92-31557

ORGANOMETALLIC COMPOUNDS
Preparation of non-oxide ceramics by pyrolysis of organometallic precursors
[AD-A251112] p 3798 N92-32197

ORGANOMETALLIC POLYMERS
Organometallic Nonlinear Optical (NLO) polymers. Part 2: Synthesis of main-chain organometallic polymers and a structural study of ferrocene NLO-Phores
[AD-A250655] p 3791 N92-31318
The role of metal structure in determining solvent orientation at the electrode/solution interface
[AD-A249751] p 3893 N92-31328
Organic main-chain NLO polymers. 1: Copolymerization of bis(arylcarboxaldehyde) and bis(cyanoacetate) monomers via the Knoevenagel condensation
[AD-A250215] p 3802 N92-31826

ORIENTATION
Illusory self motion and disorientation
[CTN-92-60318] p 3871 N92-31472

ORIFICE FLOW
Effects of flow conditioners and tap location on orifice flowmeter performance
[PB92-183730] p 3824 N92-31839

ORIFICES
Effects of flow conditioners and tap location on orifice flowmeter performance
[PB92-183730] p 3824 N92-31839

ORTHOTROPIC CYLINDERS
A generalized plane-strain elastic stress solution for a multiorthotropic-layered cylinder
[AD-A250487] p 3838 N92-31331

ORTHOTROPIC PLATES
Structural similitude and scaling laws for laminated beam-plates
[NASA-CR-190585] p 3841 N92-31911
OSCILLATING FLOW
Oscillating-flow regenerator test rig: Woven screen and metal felt results
[NASA-CR-190689] p 3820 N92-31352
OSCILLATIONS
Organized turbulent structures and their induced wall pressure fluctuations p 3753 N92-31853
Pulse Combustion Engineering Research Laboratory: Exhaust energy
[PB92-172402] p 3783 N92-31918
Exploratory experimental investigation of a wave propeller
[AD-A252175] p 3753 N92-32062
A generalization to stochastic averaging in random vibration
[DE92-016747] p 3842 N92-32088
Time simulation of flutter with large stiffness changes
[NASA-TM-107650] p 3758 N92-32111
Nonlinearly stable compact schemes for shock calculations
[NASA-CR-189663] p 3887 N92-32164
OSCILLATORS
Dicke narrowing in strong fields: The atom-as-antenna analogy
[AD-A252321] p 3807 N92-31629
OSCILLOGRAPHS
Problems with interleaved digitizers
[DE92-013369] p 3881 N92-32150
OUTGASSING
Radiolytic gas production in the alpha particle degradation of plastics
[DE92-011846] p 3795 N92-31938
OUTPUT
Confidence interval estimation for output of discrete-event simulations using the Kalman filter
[AD-A248170] p 3880 N92-31991
OXIDATION
Propane oxidation through the negative temperature coefficient region at 10 and 15 atmospheres: Results of experimental and modeling studies
[DE92-007902] p 3778 N92-31414
Light alkane conversion processes: Suprabiotic catalyst systems for selective oxidation of light alkane gases to fuel oxygenates
[DE92-015229] p 3799 N92-31751
Incipient and total group combustion of fuel sprays in air p 3749 N92-31883
Oxidation/sulfidation behavior of Fe-Cr alloys: A reactive-element effect
[DE92-016172] p 3789 N92-31924
Effect of surface modifications on the properties of silicon nitride ceramics
[DE92-013848] p 3797 N92-32094
Fundamental studies in oxidation-reduction in relation to water photolysis
[DE92-014333] p 3785 N92-32113
OXIDATION-REDUCTION REACTIONS
Charge transfer processes in multiple site chemical systems
[AD-A249538] p 3791 N92-31358
Fundamental studies in oxidation-reduction in relation to water photolysis
[DE92-014333] p 3785 N92-32113
OXIDE FILMS
Characterization of oxide formed on silicon by exposure to atomic oxygen in space
[AD-A249787] p 3778 N92-31301
Stress and phase transformation phenomena in oxide films
[DE92-014702] p 3910 N92-31665
Preparation of non-oxide ceramics by pyrolysis of organometallic precursors
[AD-A251112] p 3798 N92-32197
OXIDES
Characterization of oxide formed on silicon by exposure to atomic oxygen in space
[AD-A249787] p 3778 N92-31301
Physical characterization of magmatic liquids
[DE92-015302] p 3858 N92-32027
OXYGEN
Experimental evaluation of oxygen-enriched air and emulsified fuels in a single-cylinder diesel engine. Volume 1: Concept evaluation
[DE92-015999] p 3799 N92-31442
A comparison of interstitial oxygen calculated by different techniques
[DE92-011658] p 3910 N92-31668
Dissociative electron attachment of O2: A solid-state effect on potential curve crossing
[AD-A246331] p 3913 N92-31995
OXYGEN ATOMS
Characterization of oxide formed on silicon by exposure to atomic oxygen in space
[AD-A249787] p 3778 N92-31301
Oxygen ordering and strain-related morphology in YBa2Cu(3-x)O7 systems
[DE92-014476] p 3909 N92-31627
OZONE DEPLETION
Our Changing Planet: The FY 1993 US Global Change Research Program. A report by the Committee on Earth and Environmental Sciences, a supplement to the US President's fiscal year 1993 budget
[PB92-156892] p 3852 N92-31620

P

PACIFIC OCEAN
Modelling and prediction of regions of the North Pacific
[AD-A252144] p 3863 N92-31406
Hydrographic observations from the US/PRC cooperative program in the western equatorial Pacific Ocean: Cruises 5-8
[PB92-177054] p 3865 N92-31644
An analysis of hydrographic data collected off Point Sur, California in June 1990
[AD-A246060] p 3866 N92-32056
Biology, oceanography, and fisheries of the North Pacific transition zone and subarctic frontal zone
[PB92-178128] p 3866 N92-32106
PAINTS
Device for monitoring the thickness of a dielectric coating on a dielectric substrate
[DE92-014741] p 3829 N92-32174
PALLADIUM
Energetics, bonding mechanism and electronic structure of metal/ceramic interfaces
[DE92-013401] p 3775 N92-31806
PARABOLIC DIFFERENTIAL EQUATIONS
Kernel optimum nearly-analytical discretization (KOND) method applied to parabolic equations KOND-P Scheme
[NIFS-118] p 3887 N92-32205
PARALLEL COMPUTERS
A task adaptive parallel graphics rendering algorithm
[DE92-008062] p 3878 N92-31739
Workshop on the Derivation of Parallel Programs and Architectures: Closing report
[AD-A252742] p 3883 N92-32109
PARALLEL PLATES
New high voltage parallel plate analyzer
[NIFS-128] p 3827 N92-31340
Steady flow of a fluid-solid mixture between parallel plates
[DE92-013645] p 3821 N92-31426
PARALLEL PROCESSING (COMPUTERS)
ADIFOR: Automatic differentiation in a source translator environment
[DE92-016185] p 3886 N92-31311
Simulation of a parallel processor based small tactical system
[AD-A245911] p 3882 N92-31443
Systematic detection of parallelism in ordinary programs
[AD-A247514] p 3882 N92-31445
Graphical development tools for network-based concurrent supercomputing
[DE92-011144] p 3875 N92-31447
Data parallel programming
[DE92-013981] p 3882 N92-31466
PARTI primitives for unstructured and block structured problems
[NASA-CR-189662] p 3876 N92-31561
Some computational challenges of developing efficient parallel algorithms for data-dependent computations in thermal-hydraulics supercomputer applications
[DE92-011368] p 3878 N92-31703
The multicomputer toolbox: Scalable parallel libraries for large-scale concurrent applications
[DE92-008068] p 3882 N92-31740
PDDP: Data-driven parallelism and shared memory
[DE92-008073] p 3883 N92-31741
New algorithms for the minimal form problem
[DE92-011963] p 3879 N92-31743
ADIFOR: Fortran source translation for efficient derivatives
[DE92-016187] p 3879 N92-31899
The hierarchical spatial decomposition of three-dimensional particle-in-cell plasma simulations on MIMD distributed memory multiprocessors
[DE92-016802] p 3883 N92-32034
Fault tolerant parallel computing in orthogonal shared-memory and related architectures
[AD-A250504] p 3883 N92-32040
A sweep algorithm for massively parallel simulation of circuit-switched networks
[NASA-CR-189680] p 3881 N92-32157
PARALLEL PROGRAMMING
Architectural adaptability in parallel programming
[AD-A247516] p 3881 N92-31428
Graphical development tools for network-based concurrent supercomputing
[DE92-011144] p 3875 N92-31447
Data parallel programming
[DE92-013981] p 3882 N92-31466
Some computational challenges of developing efficient parallel algorithms for data-dependent computations in thermal-hydraulics supercomputer applications
[DE92-011368] p 3878 N92-31703
The multicomputer toolbox: Scalable parallel libraries for large-scale concurrent applications
[DE92-008068] p 3882 N92-31740
PDDP: Data-driven parallelism and shared memory
[DE92-008073] p 3883 N92-31741
New algorithms for the minimal form problem
[DE92-011963] p 3879 N92-31743
Use of a genetic algorithm to solve fluid flow problems on an NCUBE/2 multiprocessor computer
[DE92-014044] p 3824 N92-31832
Workshop on the Derivation of Parallel Programs and Architectures: Closing report
[AD-A252742] p 3883 N92-32109
PARAMETERIZATION
Analysis and design of neural networks
[AD-A250495] p 3884 N92-31332
Parameterization of directional spectra, part 2, volume 1
[DREA-CR-89-445-PT-2-VOL-1] p 3811 N92-32214
PARTIAL DIFFERENTIAL EQUATIONS
Adaptive mesh strategies for the spectral element method
[NASA-CR-189686] p 3818 N92-31265
Mathematical problems in micromechanics and composite materials
[AD-A249584] p 3773 N92-31378
Iterative methods for large sparse linear systems arising from partial differential equations
[AD-A249524] p 3886 N92-31567
Nonlinear partial differential equations and solitons
[MATHS-REPT-A-152] p 3886 N92-31956
An integrated research program for the modeling, analysis and control of aerospace systems
[AD-A250199] p 3761 N92-31966
Non-convex problems in PDE: Equilibrium theory and dynamics
[AD-A250549] p 3887 N92-32081
Kernel optimum nearly-analytical discretization (KOND) method applied to parabolic equations KOND-P Scheme
[NIFS-118] p 3887 N92-32205
PARTICLE ACCELERATOR TARGETS
Resolution function of an inelastic scattering spectrometer with a pulsed neutron source
[DE92-620889] p 3896 N92-31904
PARTICLE ACCELERATORS
Light ion driven inertial confinement fusion
[DE92-011662] p 3905 N92-31707
PARTICLE BEAMS
Light ion driven inertial confinement fusion
[DE92-011662] p 3905 N92-31707
PARTICLE CHARGING
Particle emission and charging effects induced by fracture
[AD-A252182] p 3913 N92-32065
PARTICLE COLLISIONS
Pulse-by-pulse energy measurement at the Stanford Linear Collider
[DE92-011520] p 3899 N92-31390
A dynamical model of the behaviour of hadronic and fundamental strings at finite densities
[DE92-630245] p 3914 N92-31402
PARTICLE EMISSION
Development of methodology and technology for identifying and quantifying emission products from open burning and open detonation thermal treatment methods. Field test series A, B, and C. Volume 1: Test summary
[AD-A250735] p 3800 N92-31971
Particle emission and charging effects induced by fracture
[AD-A252182] p 3913 N92-32065
PARTICLE MOTION
Fundamental studies in oxidation-reduction in relation to water photolysis
[DE92-014333] p 3785 N92-32113
The physical solution to the Lorentz-Dirac equations in a constant magnetic field
[DE92-013299] p 3890 N92-32140
PARTICLE THEORY
Theoretical high energy physics research at the University of Chicago, task A
[DE92-016288] p 3899 N92-31712

Participation in high energy physics. Task C: Particle physics and cosmology
[DE92-016290] p 3924 N92-31713
PARTICLE TRAJECTORIES
Diagnostics for research in atomization and turbulent two-phase flows
[AD-A247201] p 3819 N92-31283
PARTICLES
Diagnostics for research in atomization and turbulent two-phase flows
[AD-A247201] p 3819 N92-31283
Analysis of debris from Spacelab Space Life Sciences-1
[NASA-TM-103593] p 3765 N92-32148
PARTICULATE SAMPLING
Development of methodology and technology for identifying and quantifying emission products from open burning and open detonation thermal treatment methods. BangBox test series. Volume 1. Test summary
[AD-A250733] p 3800 N92-31969
PATENT POLICY
NASA patent abstracts bibliography: A continuing bibliography. Section 2: Indexes (supplement 41)
[NASA-SP-7039(41)-SECT-2] p 3918 N92-31455
PATHOGENESIS
Relating space radiation environments to risk estimates
[DE92-010256] p 3926 N92-31756
PATHOLOGY
A study of the effect of hydrocarbon structure on the induction of male rat nephropathy and metabolite structure
[AD-A252192] p 3867 N92-31590
PATTERN RECOGNITION
Human image understanding
[AD-A250401] p 3872 N92-31330
Forms of memory for representation of visual objects
[AD-A250056] p 3871 N92-31779
Signal processing and recognition in adaptive neural networks
[AD-A250505] p 3885 N92-32041
Wavelet signal processing for transient feature extraction
[AD-A250519] p 3890 N92-32046
Artificial neural network implementation of a near-ideal error prediction controller
[NASA-CR-190694] p 3880 N92-32122
PAYLOADS
Automated payload experiment tool feasibility study
[NASA-CR-184256] p 3883 N92-31835
Optimum data analysis procedures for Titan 4 and Space Shuttle payload acoustic measurements during lift-off
[NASA-CR-190479] p 3892 N92-32178
PEGASUS AIR-LAUNCHED BOOSTER
In-flight evaluation of aerodynamic predictions of an air-launched space booster
[NASA-TM-104246] p 3752 N92-31808
PELLETS
Mechanical strength and stability of lithium aluminate
[DE92-015998] p 3841 N92-31638
PENETRATION
A penetration mechanics database
[AD-A246351] p 3767 N92-31997
PENTANES
Selective nitrations: The laser-induced nitration of three cycloalkanes, 1
[AD-A249942] p 3800 N92-31800
PENUMBRAS
Detection of object edges in images containing cast shadows
[DE92-016092] p 3900 N92-31295
PERCEPTION
Probability-based inference in a domain of proportional reasoning tasks
[AD-A247304] p 3871 N92-31444
PERCHLORATES
Effect of synthesis temperature in the structure, doping level and charge-transport properties of polypyrrole
[AD-A250531] p 3796 N92-32079
PERFORMANCE PREDICTION
Empirical development of a scale for the prediction of performance on a sustained monitoring task
[AD-A252443] p 3872 N92-31294
The prediction of the performance of a microcircuit heat sink in the boiling mode
[AD-A250045] p 3812 N92-31355
Wind tunnel aerodynamic characteristics of a transport-type airfoil in a simulated heavy rain environment
[NASA-TP-3184] p 3751 N92-31532
Effect of out-of-roundness on the performance of a diesel engine connecting-rod bearing
[NASA-TM-105600] p 3834 N92-31536
Recent developments in the fundamentals of gas permeation in rubbery polymers
[AD-A249745] p 3794 N92-31624
Heat exchanger performance calculations for enhanced-tube condenser applications
[DE92-016603] p 3823 N92-31785
Multimedia electronic mail: Standards and performance simulation
[AD-A250047] p 3808 N92-31809
Validation of the Numerical Electro-magnetics Code (NEC) for antenna wire elements in proximity to Earth
[AD-A250507] p 3810 N92-32043
Desiccant cooling using unglazed transpired solar collectors
[DE92-010568] p 3849 N92-32112
Numerical simulation of geometric scale effects in cylindrical self-field MPD thrusters
[NASA-CR-189224] p 3772 N92-32239
PERFORMANCE TESTS
Experimental testing of prototype face gears for helicopter transmissions
[NASA-TM-105434] p 3832 N92-31349
Evaluation of proposed inservice testing procedures for check valves
[DE92-014502] p 3833 N92-31384
Vertical impact tests of humans and anthropomorphic manikins
[AD-A245866] p 3872 N92-31458
Modular UNIX (trade name)-based Vulnerability Estimation Suite (MUVES) analyst's guide
[AD-A245322] p 3876 N92-31488
Research on stable, high-efficiency amorphous silicon multijunction modules
[DE92-001244] p 3814 N92-31525
Pressure fed thrust chamber technology program
[NASA-CR-190666] p 3770 N92-31550
GNAS Maintenance Control Center (GMCC) Design Qualification Test and Evaluation (DQT/E) test report
[DOT/FAA/CT-TN91/39] p 3745 N92-31615
Performance of multiple stream pulsed jet combustion systems
[AD-A249722] p 3780 N92-31671
Establishing low-power operating limits for liquid metal heat pipes
[DE92-011367] p 3823 N92-31701
Roundoff algorithms for digital phase shifters that minimize beam shift
[AD-A250094] p 3816 N92-31780
A comparative study of the dynamic performance of three bivanes
[AD-A250096] p 3862 N92-31784
Performance tests of a fast-acting valve for the driver tubes of a large blast/thermal simulator
[AD-A250035] p 3835 N92-31807
Effects of flow conditioners and tap location on orifice flowmeter performance
[PB92-183730] p 3824 N92-31839
FCS skewed sensors array: Practical considerations
p 3746 N92-31868
Construction of a dual axis force reflection stick and test station
[AD-A250731] p 3803 N92-31890
Estimation of metal acceleration by an SF5 containing explosive
[AD-A245338] p 3801 N92-32098
Titanium carbon nitride coating
[DE92-013158] p 3777 N92-32135
Problems with interleaved digitizers
[DE92-013369] p 3881 N92-32150
PERMEABILITY
Prediction of hydrogen entry and permeation in metals and alloys
[AD-A245286] p 3790 N92-32096
PERMEATING
Catalytic carbon membranes for hydrogen production
[DE92-001269] p 3784 N92-31976
Prediction of hydrogen entry and permeation in metals and alloys
[AD-A245286] p 3790 N92-32096
PERSONAL COMPUTERS
Oracle and the end-user: Practical implementation of applications in a multi-user, multi-platform environment
[DE92-015223] p 3877 N92-31654
PERSONALITY
Stress reactivity: Five-factor representation of a psychobiological typology
[AD-A252715] p 3872 N92-31327
PERSONALITY TESTS
Stress reactivity: Five-factor representation of a psychobiological typology
[AD-A252715] p 3872 N92-31327
PERSONNEL
Development of quantitative specifications for simulating the stress environment
[AD-A250669] p 3870 N92-31321
External combustion engine technology (vapor and liquid cycles) for individual soldier power systems
[AD-A252754] p 3836 N92-32173
PERTURBATION
Computer simulation of acoustic fluctuations due to finescale temperature perturbations measured by thermistor chain
[AD-A252709] p 3892 N92-31672
PERTURBATION THEORY
Signal location using generalized linear constraints
[AD-A249580] p 3805 N92-31376
Many body perturbation theory using a Restricted Open-Shell Hartree-Fock (ROHF) reference function
[AD-A249725] p 3894 N92-31673
Molecular interactions and properties with many-body methods
[AD-A247052] p 3896 N92-31858
PESTICIDES
Application of Free-Air CO2 Enrichment (FACE) technology to a forest canopy: A simulation study
[DE92-013308] p 3851 N92-31422
PETRI NETS
About real time industrial processes control: A methodology based on objects and Petri nets
[LAAS-91467] p 3878 N92-31689
PETROLEUM PRODUCTS
World energy projection system: Model documentation
[DE92-014206] p 3847 N92-31594
PH FACTOR
Experimental studies of aluminum solubility and speciation in brines
[DE92-010448] p 3786 N92-31418
PHASE CHANGE MATERIALS
Solar thermal energy storage in phase change materials
[DE92-016908] p 3849 N92-32091
PHASE CONJUGATION
Optimized photorefractive barium titanate
[AD-A250089] p 3908 N92-31438
PHASE CONTRAST
A phase contrast interferometer on D3-D
[DE92-012699] p 3905 N92-31764
PHASE DIAGRAMS
Thermodynamic assessment of the Cr-Zr system
[PB92-180645] p 3787 N92-31610
Analyses and predictions of the thermodynamic properties and phase diagrams of silicate systems
[DE92-016177] p 3783 N92-31857
PHASE ERROR
Signal location using generalized linear constraints
[AD-A249580] p 3805 N92-31376
Analysis of random induced cross polarization
[AD-A249773] p 3806 N92-31569
PHASE LOCKED SYSTEMS
Phase-locked arrays of antiguided diode lasers: Modelling, design, evaluation of performance limits
[LAAS-92034] p 3830 N92-31698
PHASE MODULATION
A preliminary study in the use of phase demodulation techniques for the analysis of gear vibration data
[NRC-32083] p 3833 N92-31469
PHASE SEPARATION (MATERIALS)
Condensation in a two-phase pool
[DE92-010048] p 3824 N92-31977
PHASE SHIFT KEYING
The investigation of bandwidth efficient coding and modulation techniques
[NASA-CR-190685] p 3806 N92-31468
Square-law device analysis for the detection and timing estimation of a burst BPSK signal
[DREO-91-6] p 3809 N92-31921
Coherent/noncoherent detection of coherent optical heterodyne DPSK-CDMA and MFSK-CDMA signals
[AD-A246215] p 3809 N92-31993
PHASE TRANSFORMATIONS
The effect of elastic stress on Ostwald ripening phenomena
[DE92-015291] p 3839 N92-31400
Radiation-induced crystalline-to-amorphous transition in intermetallic compounds of the Cu-Ti alloy system
[DE92-010276] p 3787 N92-31575
Stress and phase transformation phenomena in oxide films
[DE92-014702] p 3910 N92-31665
Participation in high energy physics. Task C: Particle physics and cosmology
[DE92-016290] p 3924 N92-31713
Theoretical studies of solid-fluid phase equilibria
[DE92-016598] p 3781 N92-31717
PHASE VELOCITY
Stability of boundary layers at high supersonic and hypersonic speeds
[AD-A250900] p 3819 N92-31306
Radar backscatter from the sea: Controlled experiments
[AD-A250858] p 3810 N92-32101

PHASED ARRAYS
Scattering from a finite collection of transverse dipole and axial slot arrays with edge effects
[AD-A249622] p 3807 N92-31691
Phase-locked arrays of antiguided diode lasers: Modelling, design, evaluation of performance limits
[LAAS-92034] p 3830 N92-31698
Roundoff algorithms for digital phase shifters that minimize beam shift
[AD-A250094] p 3816 N92-31780
High-performance packaging for monolithic microwave and millimeter-wave integrated circuits
[NASA-TM-105744] p 3808 N92-31855
Calibration network intended for phased-array antennas at 3 GHz
[PB92-195429] p 3810 N92-32070
PHENOLS
Synthesis of cresols and xylenols from phenol and methanol
[DE91-002141] p 3785 N92-32093
PHENYLS
Tris-triphenylsiloxy compounds of aluminum
[AD-A250141] p 3788 N92-31795
PHOSPHATES
Acetylcholinesterase inhibitors on the spinal cord
[AD-A252694] p 3868 N92-31326
PHOTOCATHODES
The polarized electron gun for the SLC
[DE92-012418] p 3900 N92-32131
PHOTOCHEMICAL REACTIONS
Charge transfer processes in multiple site chemical systems
[AD-A249538] p 3791 N92-31358
UV photochemistry of trivinylantimony adsorbed on quartz
[AD-A252215] p 3785 N92-32057
PHOTOCONDUCTIVITY
Subnanosecond photoconductive switching in GaAs
[DE92-011521] p 3910 N92-31719
PHOTODIODES
Laser material interactions
[AD-A250028] p 3831 N92-31802
Development of gamma ray imaging cameras
[DE92-015305] p 3828 N92-31919
PHOTODISSOCIATION
The pathways and dynamics of molecular decomposition
[AD-A249627] p 3893 N92-31463
Experimental and computer modeling studies of isotopically selective two-step laser photodissociation of small molecules
[DE92-011427] p 3894 N92-31606
PHOTOELECTRIC EMISSION
Spin polarized photoemission studies of surfaces and thin-films
[DE92-016098] p 3907 N92-31296
PHOTOIONIZATION
Comparison of double and single ionization in He by photons and by charged projectiles
[DE92-013411] p 3894 N92-31679
Theoretical studies of the reactions and spectroscopy of radical species relevant to combustion reactions and diagnostics
[DE92-013484] p 3781 N92-31725
Alterations of multiphoton-resonant processes through wave-mixing effects
[DE92-016164] p 3896 N92-31923
Supersonic pyrolysis jets for diamond film deposition
[AD-A251125] p 3798 N92-32198
PHOTOLITHOGRAPHY
Movement of dislocations in quartz
[AD-A250527] p 3913 N92-32078
PHOTOLUMINESCENCE
SiGe Si quantum wires for efficient, room temperature, tunable luminescence
[AD-A249651] p 3814 N92-31464
PHOTOLYSIS
The photogeneration of polymeric amines: Synthesis and photocrosslinking of copolymers containing photoactive carbamate pendant groups
[AD-A250086] p 3793 N92-31436
f Mo(CHCMe2Ph)(NAr)(OR)2 and relative reactivity toward 2,3-bis(trifluoromethyl) norbornadiene iene
[AD-A250234] p 3780 N92-31524
Photogenerated base as catalyst for imidization reactions: Design of photosensitive polyimides
[AD-A250067] p 3795 N92-31810
Fundamental studies in oxidation-reduction in relation to water photolysis
[DE92-014333] p 3785 N92-32113
PHOTONICS
The chemistry and packaging of nanocomposite confined arrays
[AD-A250991] p 3817 N92-32002
Femtosecond photonics: Fundamental phenomena and device behavior
[AD-A250506] p 3832 N92-32042
PHOTONS
Dynamic modeling of plasma-vapor interactions during plasma disruptions
[DE92-016183] p 3903 N92-31310
The NSLS 100 element solid state array detector
[DE92-014477] p 3827 N92-31502
Photon absorption and the decay of surface excitation on sapphire (1120)-(3 x 1)
[DE92-011533] p 3910 N92-31661
Comparison of double and single ionization in He by photons and by charged projectiles
[DE92-013411] p 3894 N92-31679
Photon and electron data bases and their use in radiation transport calculations
[DE92-011458] p 3895 N92-31705
Holographic grating relaxation and photon correlation spectroscopic studies of viscoelastic liquids above the glass transition
[AD-A252485] p 3828 N92-31828
Alterations of multiphoton-resonant processes through wave-mixing effects
[DE92-016164] p 3896 N92-31923
UV photochemistry of trivinylantimony adsorbed on quartz
[AD-A252215] p 3785 N92-32057
PHOTOPRODUCTION
Experimental particle physics at the University of Pittsburgh
[DE92-016182] p 3896 N92-31926
Intermediate/high energy nuclear physics
[DE92-015363] p 3900 N92-32028
PHOTOSENSITIVITY
Development and application of photosensitive device systems to studies of biological and organic materials
[DE92-014728] p 3867 N92-32120
PHOTOVOLTAIC CONVERSION
Advanced high efficiency concentrator cells
[DE92-010559] p 3848 N92-31893
PHOTOVOLTAIC EFFECT
Photovoltaic subcontract program, FY 1991
[DE92-001248] p 3847 N92-31646
PHYSICAL OPTICS
Remote sensing of trapping layer base height using ATIS transmissions
[AD-A250074] p 3844 N92-31362
Development of high efficiency nonlinear optical materials
[AD-A249612] p 3901 N92-31380
Results of IR working group
[DE92-013294] p 3902 N92-32149
PHYSICAL PROPERTIES
Computerized property data for engineering materials: An overview p 3922 N92-32191
PHYSICS
Correspondence dictionary from free English term to INIS descriptors
[DE92-782192] p 3920 N92-31859
PHYSIOLOGICAL EFFECTS
Algorithms for the determination of spatial and spectral distribution of electromagnetic energy in a simulated biostructure subjected to transient spatially heterogeneous radiation with applications to radar hazard assessment and cancer therapy
[AD-A250447] p 3805 N92-31381
Body water homeostasis and human performance in high heat environments: Fluid hydration recommendations for Operation Desert Storm
[AD-A249772] p 3868 N92-31492
Nonthermal inhalation injury
[AD-A252532] p 3869 N92-31962
Preliminary development of a protocol for determining heat stress caused by clothing
[DREO-PSD-EPS-05/89] p 3873 N92-32031
PHYSIOLOGICAL RESPONSES
Modeling of learning-induced receptive field plasticity in auditory neocortex
[AD-A250348] p 3869 N92-31558
PICOSECOND PULSES
Subnanosecond photoconductive switching in GaAs
[DE92-011521] p 3910 N92-31719
Femtosecond photonics: Fundamental phenomena and device behavior
[AD-A250506] p 3832 N92-32042
PIEZOELECTRIC TRANSDUCERS
Piezoelectric radiant-to-air ultrasonic transducers p 3811 N92-31244
PIEZOELECTRICITY
Ferroelectric thin films prepared by pulse laser deposition processing and characterization
[PB92-196088] p 3913 N92-32072
PILOT ERROR
Pilot errors involving Head-Up Displays (HUDs), Helmet-Mounted Displays (HMDs), and Night Vision Goggles (NVGs)
[AD-A250719] p 3873 N92-32023
PILOTS (PERSONNEL)
In-flight decision making by high time and low time pilots during instrument operations
[AD-A249990] p 3871 N92-31392
PIPE FLOW
Effects of flow conditioners and tap location on orifice flowmeter performance
[PB92-183730] p 3824 N92-31839
PIPES (TUBES)
Emissivity measurements in support of experiments on natural convection between a vertical cylinder and a surrounding array
[DE92-012321] p 3819 N92-31287
Two-component flow study in large-diameter horizontal pipe
[DE92-013196] p 3820 N92-31420
Heat exchanger performance calculations for enhanced-tube condenser applications
[DE92-016603] p 3823 N92-31785
Design, fabrication, and testing of a 30 kW(sub t) screen-wick heat-pipe solar receiver
[DE92-016500] p 3848 N92-32087
PISTON ENGINES
Free-piston Stirling engine conceptual design and technologies for space power, phase 1
[NASA-CR-182168] p 3769 N92-31245
A free-piston Stirling engine/linear alternator controls and load interaction test facility
[NASA-TM-105825] p 3845 N92-31262
Gas engine heat recovery unit
[PB92-184373] p 3835 N92-31841
PITCH (INCLINATION)
An investigation into the interface between three closely spaced axi-symmetric bodies at subsonic speed
[CRANFIELD-AERO-9114] p 3751 N92-31514
PITCHING MOMENTS
High Reynolds number test of the Boeing TR77 airfoil in the Langley 0.3-meter transonic cryogenic tunnel
[NASA-TM-4189] p 3750 N92-31246
PLANAR STRUCTURES
A finite element-boundary integral method for conformal antenna arrays on a circular cylinder
[NASA-CR-190534] p 3807 N92-31614
PLANE STRAIN
Applications of FEM and BEM in two-dimensional fracture mechanics problems
[NASA-TP-3277] p 3838 N92-31280
A generalized plane-strain elastic stress solution for a multiorthotropic-layered cylinder
[AD-A250487] p 3838 N92-31331
PLANE WAVES
High-frequency techniques for RCS prediction of plate geometries
[NASA-CR-190656] p 3804 N92-31273
Algorithms for the determination of spatial and spectral distribution of electromagnetic energy in a simulated biostructure subjected to transient spatially heterogeneous radiation with applications to radar hazard assessment and cancer therapy
[AD-A250447] p 3805 N92-31381
Monte Carlo simulations of random rough surface scattering with finite element and finite difference methods
[AD-A247528] p 3901 N92-31430
PLANET EPHEMERIDES
GPS satellite orbit determination using pseudorange data: Experiments and results
[PB92-178870] p 3765 N92-31685
PLANETS
Institute of Geophysics and Planetary Physics, 1991
[DE92-016981] p 3923 N92-32005
PLANNING
National Conference on Integrated Resource Planning: Proceedings
[DE92-013573] p 3845 N92-31290
Research and development of methods and tools for achieving and maintaining consensus processes in the face of change within and among government oversight agencies, volume 1
[DE92-014179] p 3852 N92-31592
Shop of the 1990's project: An evaluation tool for wireframe CAD software
[PB92-181130] p 3877 N92-31628
PLANT DESIGN
YLIFE-2 inertial fusion energy power plant design
[DE92-011965] p 3904 N92-31530
PLANTS (BOTANY)
A dynamic model of terrestrial carbon cycling
[DE92-015130] p 3853 N92-31782

Extremely Low Frequency (ELF) communications system ecological monitoring program summary of 1990 progress
[AD-A246344] p 3809 N92-31996

PLASMA COMPOSITION
Power scaling of divertor plasma conditions during H-mode in D3-D
[DE92-012148] p 3906 N92-31771

PLASMA CONTROL
Fusion development and technology
[DE92-014352] p 3904 N92-31545
Theory of anomalous transport in toroidal helical plasmas
[NIFS-140] p 3904 N92-31659
Light ion driven inertial confinement fusion
[DE92-011662] p 3905 N92-31707
Electrostatic turbulence and transport in the RFP edge
[DE92-014322] p 3905 N92-31730
Millimeter wave free electron laser amplifiers: Experiments and designs
[DE92-011813] p 3832 N92-31935
Fusion with highly spin polarized HD and D(2)
[DE92-017030] p 3898 N92-32007
Kernel optimum nearly-analytical discretization (KOND) method applied to parabolic equations KOND-P Scheme
[NIFS-118] p 3887 N92-32205

PLASMA CURRENTS
Radiation damage in carbon-carbon composites
[DE92-011778] p 3775 N92-31912
Energy transport in the steady state plasma sustained by DC helicity current drive
[NIFS-127] p 3907 N92-32181

PLASMA DENSITY
Power scaling of divertor plasma conditions during H-mode in D3-D
[DE92-012148] p 3906 N92-31771

PLASMA DIAGNOSTICS
Time and space resolved electron impact excitation rates in an RF glow discharge
[AD-A249614] p 3905 N92-31688
Electrostatic turbulence and transport in the RFP edge
[DE92-014322] p 3905 N92-31730
Plasma channel generation using low energy electron beams
[DE92-013770] p 3906 N92-31949

PLASMA DIFFUSION
Theory of anomalous transport in toroidal helical plasmas
[NIFS-140] p 3904 N92-31659
Evidence of stochastic diffusion across a cross-field sheath due to Kelvin-Helmholtz vortices
[AD-A247847] p 3907 N92-31983

PLASMA DYNAMICS
Vortices associated with toroidal ion temperature gradient driven fluctuations
[DE92-016180] p 3903 N92-31412
USU center of excellence in theory and analysis of the geo-plasma environment
[AD-A252189] p 3858 N92-32055

PLASMA ELECTRODES
USU center of excellence in theory and analysis of the geo-plasma environment
[AD-A252189] p 3858 N92-32055

PLASMA ENGINES
The evolutionary development of high specific impulse electric thruster technology
[NASA-TM-105712] p 3769 N92-31342
Numerical simulation of geometric scale effects in cylindrical self-field MPD thrusters
[NASA-CR-189224] p 3772 N92-32239

PLASMA GENERATORS
Plasma channel generation using low energy electron beams
[DE92-013770] p 3906 N92-31949

PLASMA HEATING
Synthesis of diamond films with pulsed plasma
[AD-A250058] p 3791 N92-31356
A global fitting code for multichordal neutral beam spectroscopic data
[DE92-014258] p 3781 N92-31729
Power scaling of divertor plasma conditions during H-mode in D3-D
[DE92-012148] p 3906 N92-31771
Small tokamaks for fusion technology testing
[DE92-011790] p 3906 N92-31913

PLASMA INTERACTIONS
Dynamic modeling of plasma-vapor interactions during plasma disruptions
[DE92-016183] p 3903 N92-31310
Evidence of stochastic diffusion across a cross-field sheath due to Kelvin-Helmholtz vortices
[AD-A247847] p 3907 N92-31983

PLASMA PHYSICS
New high voltage parallel plate analyzer
[NIFS-128] p 3827 N92-31340
Proposal for a workshop in the physics and application of hollow electrode glow switches
[AD-A247139] p 3814 N92-31490

PLASMA PROBES
Transient internal probe diagnostic
[AD-A247306] p 3903 N92-31459

PLASMA PROPULSION
Numerical simulation of geometric scale effects in cylindrical self-field MPD thrusters
[NASA-CR-189224] p 3772 N92-32239

PLASMA RADIATION
Time and space resolved electron impact excitation rates in an RF glow discharge
[AD-A249614] p 3905 N92-31688

PLASMA SHEATHS
Evidence of stochastic diffusion across a cross-field sheath due to Kelvin-Helmholtz vortices
[AD-A247847] p 3907 N92-31983

PLASMA SPRAYING
Strongly adherent ceramic surface layers by ion implantation
[AD-A248882] p 3792 N92-31388

PLASMA TEMPERATURE
Non-geothermal optics study of wave propagation
[DE92-011806] p 3903 N92-31494

PLASMA TURBULENCE
Vortices associated with toroidal ion temperature gradient driven fluctuations
[DE92-016180] p 3903 N92-31412
Electrostatic turbulence and transport in the RFP edge
[DE92-014322] p 3905 N92-31730
Flow generation by turbulence
[DE92-013276] p 3906 N92-31829
Evidence of stochastic diffusion across a cross-field sheath due to Kelvin-Helmholtz vortices
[AD-A247847] p 3907 N92-31983

PLASMAS (PHYSICS)
Statistical analysis of anomalous transport in resistive interchange turbulence
[NIFS-125] p 3818 N92-31256
Calculational prediction of ultrawideband electromagnetic pulses by laser-initiated air avalanche switches
[DE92-011732] p 3812 N92-31334
Economics of microwave plasma dissociation of H2S
[DE92-014846] p 3779 N92-31441
ANTHEM simulational studies of the plasma opening switch
[DE92-015247] p 3815 N92-31681
Time and space resolved electron impact excitation rates in an RF glow discharge
[AD-A249614] p 3905 N92-31688
Microwave generation for magnetic fusion energy applications
[DE92-011424] p 3831 N92-31769
Fusion with highly spin polarized HD and D(2)
[DE92-017030] p 3898 N92-32007
The hierarchical spatial decomposition of three-dimensional particle-in-cell plasma simulations on MIMD distributed memory multiprocessors
[DE92-016802] p 3883 N92-32034

PLASMASPHERE
The flow of plasma in the solar terrestrial environment
[NASA-CR-190200] p 3925 N92-31338

PLASTIC DEFORMATION
J(sub 2) fracture toughness testing of Al 707 5-T7351 p 3747 N92-31872
Mechanics of thin films
[AD-A247848] p 3912 N92-31984
Particle emission and charging effects induced by fracture
[AD-A252182] p 3913 N92-32065
Movement of dislocations in quartz
[AD-A250527] p 3913 N92-32078

PLASTIC FLOW
Studies of the effect of strain velocity on mechanical properties of the 34GS steel p 3786 N92-31243

PLASTIC PROPELLANTS
Development of methodology and technology for identifying and quantifying emission products from open burning and open detonation thermal treatment methods. BangBox test series. Volume 1. Test summary
[AD-A250733] p 3800 N92-31969

PLASTIC PROPERTIES
Mode methods for strain-hardening structures
[DE92-014855] p 3838 N92-31335
Modeling of learning-induced receptive field plasticity in auditory neocortex
[AD-A250348] p 3869 N92-31558

PLATE THEORY
Modeling of composite beams and plates for static and dynamic analysis
[NASA-CR-190536] p 3839 N92-31339

PLATES (STRUCTURAL MEMBERS)
Modeling of composite beams and plates for static and dynamic analysis
[NASA-CR-190536] p 3839 N92-31339

PLATING
Metallization of ferrite ceramic couplings
[DE92-016573] p 3789 N92-32032

PLATINUM
Role of the double-layer cation on the potential-dependent stretching frequencies and binding geometries of carbon monoxide at platinum-nonaqueous interfaces
[AD-A246980] p 3784 N92-31998

PLUMES
Numerical simulation of precipitation scavenging and comparison with observation of prescribed forest fires
[DE92-013513] p 3851 N92-31423
The potential of passive-remote Fourier Transform Infrared (FTIR) spectroscopy to detect organic emissions under the Clean Air Act
[DE92-015224] p 3854 N92-32083

PLY ORIENTATION
Tailored metal matrix composites for high-temperature performance
[NASA-TM-105816] p 3775 N92-31854

POISSON DENSITY FUNCTIONS
Two properties of uniform distributions, with applications to some nonparametric estimation problems
[REPT-91-94] p 3888 N92-31518

POLAR ORBITS
High-latitude spacecraft charging in low-Earth polar orbit
[AD-A249868] p 3767 N92-31822

POLAR REGIONS
Comprehensive Aerological Reference Data Set (CARDS)
[DE92-016469] p 3862 N92-31734

POLARIMETERS
A solar magnetic and velocity field measurement system for Spacelab 2: The Solar Optical Universal Polarimeter (SOUP)
[NASA-CR-190683] p 3925 N92-31856

POLARIZATION (CHARGE SEPARATION)
Dipolar interaction assisted effects on second harmonic generation
[AD-A252487] p 3784 N92-31959

POLARIZATION (SPIN ALIGNMENT)
Spin polarized photoemission studies of surfaces and thin-films
[DE92-016098] p 3907 N92-31296
Fusion with highly spin polarized HD and D(2)
[DE92-017030] p 3898 N92-32007

POLARIZATION (WAVES)
Wavenumbers for currents on infinite- and finite-length wires in a chiral medium
[DE92-007565] p 3804 N92-31317

POLARIZED RADIATION
The polarized electron gun for the SLC
[DE92-012418] p 3900 N92-32131

POLICIES
Report to the US Congress on minority small business and capital ownership development as required by the Business Opportunity Development Reform Act of 1988
[PB92-173681] p 3916 N92-31364
Anti-environmental warfare: Protecting the environment during wartime
[AD-A250337] p 3851 N92-31556
Our Changing Planet: The FY 1993 US Global Change Research Program. A report by the Committee on Earth and Environmental Sciences, a supplement to the US President's fiscal year 1993 budget
[PB92-156892] p 3852 N92-31620

POLLUTION
EnviroTRADE: Its role in the cleanup of the environment
[DE92-013691] p 3851 N92-31427

POLLUTION CONTROL
EnviroTRADE: Its role in the cleanup of the environment
[DE92-013691] p 3851 N92-31427
Anti-environmental warfare: Protecting the environment during wartime
[AD-A250337] p 3851 N92-31556
Energy conservation: The main factor for reducing greenhouse gas emissions in the former Soviet Union
[DE92-012355] p 3852 N92-31574
Methods of assessing responses of trees, stands and ecosystems to air pollution
[PB92-180231] p 3853 N92-31648
Development of a core combustion research program plan for EPA
[PB92-180868] p 3781 N92-31683

POLLUTION MONITORING
World ocean circulation experiment. WOCE chlorofluorocarbon intercomparison cruise report
[PB92-185974] p 3865 N92-31842

POLYATOMIC MOLECULES
Laser enhanced chemical reaction studies
[DE92-010772] p 3831 N92-31798
POLYBUTADIENE
Flammability limits and ballistic properties of fuel-rich propellants p 3749 N92-31885
POLYCARBONATES
Diffusion of camphorquinone in uniaxially drawn polycarbonate films
[AD-A252489] p 3796 N92-31961
POLYCRYSTALS
Development of a computer model for polycrystalline thin-film CuInSe2 and CdTe solar cells
[DE92-001242] p 3846 N92-31526
The structure and properties of grain boundaries in Ni3Al
[DE92-012143] p 3788 N92-31744
The crystal growth and characterization of the solid solutions (ZnS)(1-x)(CuMS2)(x)
[AD-A248029] p 3911 N92-31819
POLYESTER RESINS
High strength glass second source qualification to composite armor specification MIL-L-46197(MR)
[AD-A252114] p 3792 N92-31404
Development of an electrochemical method for field testing of protective coatings
[AD-A245872] p 3793 N92-31473
POLYETHYLENES
Characterization of polymers for microcellular foams
[DE92-012444] p 3793 N92-31539
Radiolytic gas production in the alpha particle degradation of plastics
[DE92-011846] p 3795 N92-31938
Auger line shapes as a probe of electronic structure in covalent systems
[AD-A246329] p 3912 N92-31994
POLYHEDRONS
Development of the aspect graph representation for use in R version
[AD-A247109] p 3876 N92-31573
POLYIMIDE RESINS
Low thermal coefficient of expansion printed wiring boards
[DE92-013704] p 3817 N92-31946
POLYIMIDES
A fast laser alloying process for the selective electroplating of metal on SiO2 and polyimide
[DE92-011764] p 3788 N92-31759
Photogenerated base as catalyst for imidization reactions: Design of photosensitive polyimides
[AD-A250067] p 3795 N92-31810
Electronic structure and photophysical properties of polyimides
[DE92-012353] p 3797 N92-32146
POLYMER CHEMISTRY
Polymer blends, volume 1
[AD-A252112] p 3792 N92-31419
Thin polymer icemaker development and test program
[DE92-016941] p 3803 N92-32125
POLYMERIC FILMS
Charge transfer processes in multiple site chemical systems
[AD-A249538] p 3791 N92-31358
Tribology of Langmuir-Blodgett films
[AD-A250075] p 3833 N92-31363
Tribology of functionally-terminated oligomer films
[AD-A250076] p 3833 N92-31433
The effect of surface pressure on Langmuir-Blodgett polymerization of 2-pentadecyl aniline
[AD-A250993] p 3795 N92-31952
Dipolar interaction assisted effects on second harmonic generation
[AD-A252487] p 3784 N92-31959
POLYMERIZATION
Organometallic Nonlinear Optical (NLO) polymers. Part 2: Synthesis of main-chain organometallic polymers and a structural study of ferrocene NLO-Phores
[AD-A250655] p 3791 N92-31318
Synthesis of side chain liquid crystal polymers by living ring opening metathesis polymerization. 4: Synthesis of amorphous and side chain liquid crystal AB block copolymers
[AD-A250353] p 3792 N92-31394
Linear and star-branched siloxy-silane polymers: One pot A-B polymerization and end-capping
[AD-A252195] p 3792 N92-31408
Cyclopolymerization of metalloid-containing alpha, omega-dienes. 1,3-divinyltetramethyldisiloxane, 1,3-divinyltetramethyldisilazane and 1,3-divinylpentamethyldisilazane
[AD-A250347] p 3794 N92-31557
Ring-opening polymerization of strained cyclotetrasilanes as a new route towards well defined polysilylenes
[AD-A251020] p 3795 N92-31941
The effect of surface pressure on Langmuir-Blodgett polymerization of 2-pentadecyl aniline
[AD-A250993] p 3795 N92-31952
Real time investigations of the polymerization of 2-pentadecyl aniline on the Langmuir-Blodgett trough
[AD-A250994] p 3795 N92-31954
Catalytic carbon membranes for hydrogen production
[DE92-001269] p 3784 N92-31976
Cationic ring opening polymerization of oxazolines initiated by trimethylsilyl derivatives
[AD-A251109] p 3798 N92-32153
Polymerization of conducting polymers confined to free surfaces: A comparison of the Langmuir-Blodgett polymerization of 3-alkyl pyrroles and 2-alkyl anilines
[AD-A250966] p 3798 N92-32194
POLYMERS
Nonlinear optical acrylic polymers and use thereof in optical and electro-optic devices
[AD-D015236] p 3791 N92-31270
Recent developments in the fundamentals of gas permeation in rubbery polymers
[AD-A249745] p 3794 N92-31624
Development of effective quantum chemical method for polymers and solid
[AD-A250976] p 3795 N92-31951
POLYMORPHISM
Polymorphic type assignment and CPS conversion
[AD-A250954] p 3887 N92-32171
POLYNOMIALS
A fundamental notion of equivalence for linear multivariable systems
[MATHS-REPT-A-153] p 3887 N92-31957
POLYPEPTIDES
Evolution and analysis of the functional domains of the chimeric proteins that initiate pyrimidine biosynthesis
[AD-A250069] p 3866 N92-31465
POLYSTYRENE
Characterization of polymers for microcellular foams
[DE92-012444] p 3793 N92-31539
POLYURETHANE RESINS
Development of characterization techniques for polyurethanes 1. Characterization of SRM 1480, a low molecular weight polyurethane for SEC calibration
[PB92-172485] p 3794 N92-31618
POLYVINYL CHLORIDE
Radiolytic gas production in the alpha particle degradation of plastics
[DE92-011846] p 3795 N92-31938
POPULATIONS
Multiple electron populations accelerated in solar bursts
[INPE-5377-TDI/472] p 3925 N92-32025
POROSITY
Tetragonal zirconia ceramics in ZrO2-CeO2 system (Ce-TZP): Preparation, characterization and mechanical properties
[INPE-5372-PRE/1746] p 3798 N92-32199
PORTABLE EQUIPMENT
Robotic soil sampler for hazardous waste clean up
[DE92-012693] p 3780 N92-31565
Development of gamma ray imaging cameras
[DE92-015305] p 3828 N92-31919
External combustion engine technology (vapor and liquid cycles) for individual soldier power systems
[AD-A252754] p 3836 N92-32173
POSITION (LOCATION)
Signal location using generalized linear constraints
[AD-A249580] p 3805 N92-31376
Cloud-to-ground lightning characteristics in mesoscale convective systems
[AD-A250418] p 3858 N92-31493
Satellite positioning systems: A report to the director
[PB92-181270] p 3767 N92-31632
Beam position monitor electronics using DC coupled demodulating logarithmic amplifiers
[DE92-011697] p 3816 N92-31760
POSITION INDICATORS
Techniques for autonomous navigation
[DE92-013458] p 3756 N92-31746
POSITIONING DEVICES (MACHINERY)
Piezoelectric radiant-to-air ultrasonic transducers p 3811 N92-31244
POSITIVE IONS
Electron impact excitation of positive ions: Partial wave approach in Coulomb-Eikonal approximation
[NIFS-106] p 3892 N92-31255
Theoretical atomic collision physics
[DE92-013571] p 3895 N92-31724
POSITRONS
Pulse-by-pulse energy measurement at the Stanford Linear Collider
[DE92-011520] p 3899 N92-31390
POTASSIUM
Establishing low-power operating limits for liquid metal heat pipes
[DE92-011367] p 3823 N92-31701
Potassium Rankine cycle nuclear power systems for spacecraft and lunar-mass surface power
[DE92-016163] p 3770 N92-31897
POTENTIAL ENERGY
Molecular interactions and properties with many-body methods
[AD-A247052] p 3896 N92-31858
POTENTIAL FIELDS
Balanced, potential vorticity dynamics in the tropics
[AD-A249981] p 3858 N92-31432
POTENTIAL FLOW
Pressure and temperature for B-1B transparency test
[AD-A252711] p 3752 N92-31674
The three-dimensional stability of the Foeppl vortices p 3750 N92-31889
POWDER (PARTICLES)
Ceramic surfaces and sintering
[DE92-011570] p 3793 N92-31538
Effect of surface modifications on the properties of silicon nitride ceramics
[DE92-013848] p 3797 N92-32094
Preparation of non-oxide ceramics by pyrolysis of organometallic precursors
[AD-A251112] p 3798 N92-32197
Tetragonal zirconia ceramics in ZrO2-CeO2 system (Ce-TZP): Preparation, characterization and mechanical properties
[INPE-5372-PRE/1746] p 3798 N92-32199
POWER AMPLIFIERS
Conversion of power and frequency
[DE92-012543] p 3810 N92-32134
POWER CONDITIONING
Stability testing and analysis of a PMAD DC test bed for the Space Station Freedom
[NASA-TM-105846] p 3812 N92-31282
Optical oversampled analog-to-digital conversion
[AD-A252695] p 3877 N92-31587
POWER CONVERTERS
Stability testing and analysis of a PMAD DC test bed for the Space Station Freedom
[NASA-TM-105846] p 3812 N92-31282
Conversion of power and frequency
[DE92-012543] p 3810 N92-32134
POWER REACTORS
Some computational challenges of developing efficient parallel algorithms for data-dependent computations in thermal-hydraulics supercomputer applications
[DE92-011368] p 3878 N92-31703
POWER SPECTRA
Dicke narrowing in strong fields: The atom-as-antenna analogy
[AD-A252321] p 3807 N92-31629
PRE-MAIN SEQUENCE STARS
Molecular outflows associated with HH52-54 and IRAS 12496-7650
[PB92-184472] p 3924 N92-31635
PRECIPITATION (CHEMISTRY)
Numerical simulation of precipitation scavenging and comparison with observation of prescribed forest fires
[DE92-013513] p 3851 N92-31423
The development of precipitated iron catalysts with improved stability
[DE92-014630] p 3785 N92-32117
PRECIPITATION (METEOROLOGY)
Hydrological and geochemical response and recovery in disturbed Arctic ecosystems
[DE92-016223] p 3850 N92-31312
A case study of a prolonged sleet event: 16-17 February 1987 and climatology of sleet events for North Carolina, 1949-1989
[AD-A250184] p 3859 N92-31602
Meteorological data, new series A monographs. Volume 6, no. 2: Case study on the congruence of precipitation data from SYNOP-MODELL and Meteosat data
[ETN-92-91694] p 3861 N92-31710
PRECISION
Estimation of aircraft attitude by angular rate measurements p 3748 N92-31881
PREDICTION ANALYSIS TECHNIQUES
The determination of operational and support requirements and costs during the conceptual design of space systems
[NASA-CR-190626] p 3766 N92-31260
Life extending control for rocket engines
[NASA-TM-105789] p 3802 N92-31263
The validation of atmospheric models
[DE92-013254] p 3850 N92-31324
Mode methods for strain-hardening structures
[DE92-014855] p 3838 N92-31335
Life prediction and constitutive models for engine hot section anisotropic materials program
[NASA-CR-189222] p 3759 N92-31534
Micro saint model of fatigue assessment
[AD-A249976] p 3868 N92-31554
World energy projection system: Model documentation
[DE92-014206] p 3847 N92-31594

Using transfer functions as a method for predicting lightning effects on munitions storage bunkers
[DE92-012627] p 3861 N92-31709
In-flight evaluation of aerodynamic predictions of an air-launched space booster
[NASA-TM-104246] p 3752 N92-31808
The KRAKEN normal mode program
[AD-A252409] p 3892 N92-31818
Highly accurate prediction of unsteady viscous flows
[AD-A250982] p 3825 N92-32000
Fitting and prediction uncertainty for a software reliability model
[AD-A252173] p 3880 N92-32060
Prediction of hydrogen entry and permeation in metals and alloys
[AD-A245286] p 3790 N92-32096
Artificial neural network implementation of a near-ideal error prediction controller
[NASA-CR-190694] p 3880 N92-32122
An investigation of the thermoviscoplastic behavior of a metal matrix composite at elevated temperatures
[NASA-CR-190700] p 3777 N92-32159

PREDICTIONS
Our changing planet: The FY 1993 US global change research program. A supplement to the US President's fiscal year 1993 budget
[NASA-CR-190675] p 3850 N92-31259
Calculational prediction of ultrawideband electromagnetic pulses by laser-initiated air avalanche switches
[DE92-011732] p 3812 N92-31334
Analyses and predictions of the thermodynamic properties and phase diagrams of silicate systems
[DE92-016177] p 3783 N92-31857
Minimal supersymmetric unification predictions
[RAL-92-005] p 3915 N92-31953

PREMIXED FLAMES
Tomographic reconstruction of infrared spectra of nonhomogeneous media: Applications to a flat flame burner
[AD-A249999] p 3778 N92-31393
Flame front geometry in premixed turbulent flames
[DE92-010310] p 3779 N92-31417
Ignition and flame propagation studies over a flat fuel surface
[PB92-181056] p 3780 N92-31678

PRESIDENTIAL REPORTS
Our Changing Planet: The FY 1993 US Global Change Research Program. A report by the Committee on Earth and Environmental Sciences, a supplement to the US President's fiscal year 1993 budget
[PB92-156892] p 3852 N92-31620

PRESSING (FORMING)
Sodium Heat Engine Development Program
[DE92-012398] p 3846 N92-31531
Flex circuit lamination
[DE92-016574] p 3817 N92-32033

PRESSURE
Pressure and temperature for B-1B transparency test
[AD-A252711] p 3752 N92-31674
The effect of surface pressure on Langmuir-Blodgett polymerization of 2-pentadecyl aniline
[AD-A250993] p 3795 N92-31952

PRESSURE DEPENDENCE
Gibbs free energy of reactions involving SiC, Si3N4, H2, and H2O as a function of temperature and pressure
[NASA-TP-3275] p 3791 N92-31278

PRESSURE DISTRIBUTION
The discretization of the 2D incompressible Navier-Stokes equations on a collocated grid
[REPT-91-61] p 3821 N92-31513
Pressure loss and heat transfer in a toothed finned heat transfer medium
[MBB-UO-0163-91-PUB] p 3915 N92-31660
Exploratory experimental investigation of a wave propeller
[AD-A252175] p 3753 N92-32062
Three-dimensional compressible turbulent computations for a nondiffusing S-duct
[NASA-CR-4391] p 3754 N92-32240

PRESSURE DRAG
Automatic design of transonic airfoils to reduce the shock induced pressure drag p 3745 N92-31863

PRESSURE EFFECTS
Pressure fed thrust chamber technology program
[NASA-CR-190666] p 3770 N92-31550
Pressure and temperature for B-1B transparency test
[AD-A252711] p 3752 N92-31674
The effect of surface pressure on Langmuir-Blodgett polymerization of 2-pentadecyl aniline
[AD-A250993] p 3795 N92-31952

PRESSURE GRADIENTS
Heat transfer and flow of a modified second grade fluid
[DE92-014744] p 3824 N92-31895

PRESSURE MEASUREMENT
Active control of the separation region on a two-dimensional airfoil
[AD-A249739] p 3752 N92-31622

PRESSURE OSCILLATIONS
Organized turbulent structures and their induced wall pressure fluctuations p 3753 N92-31853

PRESSURE PULSES
Performance of multiple stream pulsed jet combustion systems
[AD-A249722] p 3780 N92-31671

PRESSURE REDUCTION
Oscillating-flow regenerator test rig: Woven screen and metal felt results
[NASA-CR-190689] p 3820 N92-31352

PRESSURE SENSORS
A continuing study of altitude determination deficiencies of the Service Aircraft Instrumentation Package (SAIP)
[AD-A245952] p 3758 N92-32051

PRESSURIZED WATER REACTORS
Evaluation of proposed inservice testing procedures for check valves
[DE92-014502] p 3833 N92-31384

PRETREATMENT
Catalyst dispersion and activity under conditions of temperature-staged liquefaction
[DE92-014112] p 3786 N92-32141

PRIMATES
Stress reactivity: Five-factor representation of a psychobiological typology
[AD-A252715] p 3872 N92-31327
Function of P and M pathways in primates
[AD-A250055] p 3867 N92-31778

PRINTED CIRCUITS
Low thermal coefficient of expansion printed wiring boards
[DE92-013704] p 3817 N92-31946
Flex circuit lamination
[DE92-016574] p 3817 N92-32033
Modeling and design of a closed kinematic chain robotic mechanism
[DE92-014777] p 3835 N92-32121

PRIORITIES
Sources of unbounded priority inversions in real-time systems and a comparative study of possible solutions
[NASA-CR-190711] p 3875 N92-31486

PRISMS
A microprism array for large-scale, wide-band interconnection of optoelectronic systems
[AD-A249380] p 3813 N92-31374

PROBABILITY DENSITY FUNCTIONS
Towards understanding turbulent scalar mixing
[NASA-CR-4446] p 3826 N92-32242

PROBABILITY THEORY
Probability-based inference in a domain of proportional reasoning tasks
[AD-A247304] p 3871 N92-31444
Combining expert probabilistic weather forecasts: Results of post-hoc analyses of the Zierikzee experiment
[REPT-91-101] p 3859 N92-31521
Importance sampling for Markov chains: Asymptotics for the variance
[AD-A249804] p 3868 N92-31757
Signal and noise models arising from the theory of errors
[AD-A250222] p 3885 N92-31827
Probabilistic analysis of twenty-four hour weather data for Warsaw p 3863 N92-32097
A comparison of the performance of two gust front detection algorithms using a length-based scoring technique
[AD-A250862] p 3863 N92-32103

PROBLEM SOLVING
The development of modularized software for empirical testing of new algorithms in linear programming
[AD-A250811] p 3875 N92-31480
Two properties of uniform distributions, with applications to some nonparametric estimation problems
[REPT-91-94] p 3888 N92-31518

PROCESS CONTROL (INDUSTRY)
Weld penetration and defect control
[DE92-015310] p 3836 N92-31336
The sixteenth annual electronics manufacturing seminar proceedings
[AD-A247920] p 3814 N92-31461
About real time industrial processes control: A methodology based on objects and Petri nets
[LAAS-91467] p 3878 N92-31689
Guidelines for generating acceptance sampling plans for continuous production
[DE92-010763] p 3837 N92-31753
Computer Aided Process Planning (CAPP): The user interface for the fabrication module of the rapid design system
[AD-A250095] p 3879 N92-31783

PROCUREMENT
Building an educational robot arm for under $1,000
[AD-A247499] p 3833 N92-31460

PRODUCT DEVELOPMENT
Development of high efficiency nonlinear optical materials
[AD-A249612] p 3901 N92-31380
Design and automated manufacturing p 3746 N92-31866

PRODUCTION MANAGEMENT
Design and automated manufacturing p 3746 N92-31866

PROGRAM VERIFICATION (COMPUTERS)
The development of modularized software for empirical testing of new algorithms in linear programming
[AD-A250811] p 3875 N92-31480
Specification and verification of secure concurrent and distributed software systems
[AD-A252477] p 3879 N92-31825
A language for higher-order explanation-based learning
[AD-A251008] p 3880 N92-31939
A frequency hopping synthesizer controller for EHF SATCOM
[DREO-89-29] p 3811 N92-32232

PROGRAMMING LANGUAGES
Architectural adaptability in parallel programming
[AD-A247516] p 3881 N92-31428
Implementing relational operations in an object-oriented database
[AD-A249332] p 3918 N92-31450
The data structure accelerator architecture
[AD-A250968] p 3883 N92-32152
Full abstraction and the context lemma
[AD-A247062] p 3887 N92-32163
Polymorphic type assignment and CPS conversion
[AD-A250954] p 3887 N92-32171

PROJECT MANAGEMENT
Report to the US Congress on minority small business and capital ownership development as required by the Business Opportunity Development Reform Act of 1988
[PB92-173681] p 3916 N92-31364

PROJECT PLANNING
Requirements Engineering and Analysis Workshop Proceedings
[AD-A250415] p 3876 N92-31541
Our Changing Planet: The FY 1993 US Global Change Research Program. A report by the Committee on Earth and Environmental Sciences, a supplement to the US President's fiscal year 1993 budget
[PB92-156892] p 3852 N92-31620
Development of a core combustion research program plan for EPA
[PB92-180868] p 3781 N92-31683

PROJECTILES
Comparison of double and single ionization in He by photons and by charged projectiles
[DE92-013411] p 3894 N92-31679
Problems associated with launching hypervelocity projectiles from the fast shock tube
[DE92-015276] p 3762 N92-32026

PROLOG (PROGRAMMING LANGUAGE)
A language for higher-order explanation-based learning
[AD-A251008] p 3880 N92-31939

PROPANE
Propane oxidation through the negative temperature coefficient region at 10 and 15 atmospheres: Results of experimental and modeling studies
[DE92-007902] p 3778 N92-31414
High-temperature ignition of propane with MTBE as an additive: Shock-tube experiments and modeling
[DE92-008933] p 3778 N92-31415
Light alkane conversion processes: Suprabiotic catalyst systems for selective oxidation of light alkane gases to fuel oxygenates
[DE92-015229] p 3799 N92-31751

PROPELLANT BINDERS
Estimation of metal acceleration by an SF5 containing explosive
[AD-A245338] p 3801 N92-32098

PROPELLANT CHEMISTRY
Advanced thermally stable jet fuel development program. Volume 2: Compositional factors affecting thermal degradation of jet fuels
[AD-A252656] p 3798 N92-31399
A semiconductor bridge ignited gas generator
[DE92-014049] p 3781 N92-31748
Estimation of metal acceleration by an SF5 containing explosive
[AD-A245338] p 3801 N92-32098

PROPELLANT COMBUSTION
A semiconductor bridge ignited gas generator
[DE92-014049] p 3781 N92-31748

Autoignition behavior of lean mixtures: Chemical and thermodynamics effects
[DE92-009690] p 3781 N92-31763
Shock tube study of the reaction of triethanol ammonium nitrate with N2O
[AD-A250034] p 3800 N92-31804
Flammability limits and ballistic properties of fuel-rich propellants p 3749 N92-31885
Development of methodology and technology for identifying and quantifying emission products from open burning and open detonation thermal treatment methods. Field test series A, B, and C. Volume 2, part A: Quality assurance and quality control
[AD-A250736] p 3801 N92-31972
Development of methodology and technology for identifying and quantifying emission products from open burning and open detonation thermal treatment methods. Field test series A, B, and C. Volume 2, part B: Quality assurance and quality control. Appendices
[AD-A250737] p 3801 N92-31973

PROPELLANT GRAINS
A semiconductor bridge ignited gas generator
[DE92-014049] p 3781 N92-31748

PROPELLANT STORAGE
Development of methodology and technology for identifying and quantifying emission products from open burning and open detonation thermal treatment methods. Field test series A, B, and C. Volume 2, part A: Quality assurance and quality control
[AD-A250736] p 3801 N92-31972
Development of methodology and technology for identifying and quantifying emission products from open burning and open detonation thermal treatment methods. Field test series A, B, and C. Volume 2, part B: Quality assurance and quality control. Appendices
[AD-A250737] p 3801 N92-31973

PROPELLANT TESTS
Autoignition behavior of lean mixtures: Chemical and thermodynamics effects
[DE92-009690] p 3781 N92-31763
Estimation of metal acceleration by an SF5 containing explosive
[AD-A245338] p 3801 N92-32098

PROPELLANTS
Flammability limits and ballistic properties of fuel-rich propellants p 3749 N92-31885
Krypton ion thruster performance
[NASA-TM-105818] p 3770 N92-31901
Orbital transfer rocket engine technology: Advanced engine study
[NASA-CR-187216] p 3771 N92-32129

PROPELLER NOISE
High speed turboprop aeroacoustic study (counterrotation). Volume 2: Computer programs
[NASA-CR-185242] p 3691 N92-31248

PROPELLERS
Exploratory experimental investigation of a wave propeller
[AD-A252175] p 3753 N92-32062

PROPORTIONAL CONTROL
Control of rapid thermal processing equipment for microelectronics applications
[LAAS-92013] p 3787 N92-31695

PROPORTIONAL COUNTERS
Use of tissue equivalent proportional counters to characterize radiation quality on the space shuttle
[DE92-012347] p 3768 N92-31846

PROPULSION
A parameter optimization approach to controller partitioning for integrated flight/propulsion control application
[NASA-TM-105826] p 3761 N92-32241

PROPULSION SYSTEM CONFIGURATIONS
Pressure fed thrust chamber technology program
[NASA-CR-190666] p 3770 N92-31550
Supersonic Throughflow Fan Test Facility at NASA. Lewis Research Center
[NASA-TP-3038] p 3762 N92-31640
Electric and hybrid vehicles program
[DE92-015200] p 3834 N92-31653
Analytical and experimental studies of heat pipe radiation cooling of hypersonic propulsion systems
[DE92-013428] p 3759 N92-31817

PROPULSION SYSTEM PERFORMANCE
Subsonic flight test evaluation of a performance seeking control algorithm on an F-15 airplane
[NASA-TM-4400] p 3759 N92-31275
Supersonic Throughflow Fan Test Facility at NASA. Lewis Research Center
[NASA-TP-3038] p 3762 N92-31640
Electric and hybrid vehicles program
[DE92-015200] p 3834 N92-31653
Analytical and experimental studies of heat pipe radiation cooling of hypersonic propulsion systems
[DE92-013428] p 3759 N92-31817
Numerical simulation of geometric scale effects in cylindrical self-field MPD thrusters
[NASA-CR-189224] p 3772 N92-32239

PROTECTIVE CLOTHING
Immersion suit usage within the RAAF
[AD-A250645] p 3755 N92-31562
Preliminary development of a protocol for determining heat stress caused by clothing
[DREO-PSD-EPS-05/89] p 3873 N92-32031

PROTECTIVE COATINGS
Strongly adherent ceramic surface layers by ion implantation
[AD-A248882] p 3792 N92-31388
Development of an electrochemical method for field testing of protective coatings
[AD-A245872] p 3793 N92-31473
Life prediction and constitutive models for engine hot section anisotropic materials program
[NASA-CR-189222] p 3759 N92-31534
JPRS report: Science and technology. Central Eurasia: Materials science
[JPRS-UMS-92-010] p 3787 N92-31584
The preparation of (Al2O3)x(SiO2)y thin films using (Al(OSiEt3))2 as a single source precursor
[AD-A250142] p 3788 N92-31796
Titanium carbon nitride coating
[DE92-013158] p 3777 N92-32135

PROTOCOL (COMPUTERS)
Design and specification of a high speed transport protocol
[AD-A248323] p 3804 N92-31284
Overview of integrated services digital network conformance testing
[PB92-181015] p 3881 N92-31365
Issues in designing transport layer multicast facilities
[NASA-CR-190639] p 3882 N92-31483
Sources of unbounded priority inversions in real-time systems and a comparative study of possible solutions
[NASA-CR-190711] p 3875 N92-31486
Using consistent subcuts for detecting stable properties
[NASA-CR-190443] p 3886 N92-31553

PROTON BEAMS
Light ion driven inertial confinement fusion
[DE92-011662] p 3905 N92-31707

PROTON ENERGY
Vibrational modes and the dynamic solvent effect in electron and proton transfer
[AD-A250727] p 3897 N92-31950

PROTON FLUX DENSITY
Interaction of fast steady flow with slow transient flow: A new cause of interplanetary Bz events
[AD-A250273] p 3823 N92-31770

PROTONS
Efficiency calculations of the hadron detector
[NIKHEF-K-EMIN-92-01] p 3896 N92-31814
The 6-D phase space tracking with acceleration: Modeling low energy proton synchrotrons, part 1
[DE92-013744] p 3899 N92-31948

PROTOSTARS
G305.8 - 0.2 water vapour source: A young object
[INPE-5337-PRE/1736] p 3923 N92-31343

PROTOTYPES
Ariel database rule system project
[AD-A250443] p 3917 N92-31396
Mission and Safety Critical (MASC) plans for the MASC Kernel simulation
[NASA-CR-190708] p 3875 N92-31487
Prototype casting fabrication by stereolithography
[DE92-011489] p 3876 N92-31529
Artificial Intelligence in Training (AIT)
[AD-A250145] p 3885 N92-31811
Construction of a dual axis force reflection stick and test station
[AD-A250731] p 3803 N92-31890

PROVING
The validation of atmospheric models
[DE92-013254] p 3850 N92-31324
Modular UNIX (trade name)-based Vulnerability Estimation Suite (MUVES) analyst's guide
[AD-A245322] p 3876 N92-31488

PSYCHOACOUSTICS
Signal processing and recognition in adaptive neural networks
[AD-A250505] p 3885 N92-32041

PSYCHOLOGICAL EFFECTS
One thousand days non-stop at sea: Lessons for a mission to Mars
[TABES PAPER 92-462] p 3764 N92-32020

PSYCHOLOGICAL TESTS
Theory and test of stress resistance
[AD-A250741] p 3870 N92-31291

PSYCHOLOGY
Stress reactivity: Five-factor representation of a psychobiological typology
[AD-A252715] p 3872 N92-31327

PSYCHOPHYSIOLOGY
Function of panel M pathways in primates
[AD-A250275] p 3871 N92-31758
Function of P and M pathways in primates
[AD-A250055] p 3867 N92-31778

PUBLIC HEALTH
JPRS report: Science and technology. Central Eurasia: Life sciences
[JPRS-ULS-92-015] p 3924 N92-32179

PULSE COMMUNICATION
Ionospheric communications channel modelling
[DE92-013039] p 3808 N92-31722

PULSE DOPPLER RADAR
Spectrum modal analysis for the detection of low-altitude windshear with airborne Doppler radar
[NASA-CR-4457] p 3755 N92-31549

PULSE DURATION
Synthesis of diamond films with pulsed plasma
[AD-A250058] p 3791 N92-31356
Method and circuit for controlling the evolution time interval of a laser output pulse
[NASA-CASE-LAR-13772-1] p 3831 N92-31788

PULSE GENERATORS
Design of a TEM cell EMP simulator
[DREO-1084] p 3806 N92-31470

PULSE RADAR
Square-law device analysis for the detection and timing estimation of a burst BPSK signal
[DREO-91-6] p 3809 N92-31921

PULSED JET ENGINES
Performance of multiple stream pulsed jet combustion systems
[AD-A249722] p 3780 N92-31671

PULSED LASERS
Pulsed laser deposition of high Tc superconducting thin films
[AD-A250657] p 3830 N92-31319
Photon absorption and the decay of surface excitation on sapphire (1120)-(3 x 1)
[DE92-011533] p 3910 N92-31661
Laser decontamination: A new strategy for facility decommissioning
[DE92-014113] p 3831 N92-31775
Ferroelectric thin films prepared by pulse laser deposition processing and characterization
[PB92-196088] p 3913 N92-32072
Laser-initiated conical detonation wave for supersonic combustion, part 3
[AD-A250522] p 3785 N92-32076

PULSED RADIATION
Design of a TEM cell EMP simulator
[DREO-1084] p 3806 N92-31470
UV photochemistry of trivinylantimony adsorbed on quartz
[AD-A252215] p 3785 N92-32057

PULSES
Analysis and evaluation of Project Evergreen data
[AD-A245983] p 3804 N92-31314
CO2 laser frequency multiplication
[AD-A248574] p 3830 N92-31755
Injecting into AmPS when ring cavity operates at 476 MHz
[NIKHEF-K/AMPS/91-08] p 3899 N92-31815
Pulse Combustion Engineering Research Laboratory: Exhaust energy
[PB92-172402] p 3783 N92-31918

PYRAMIDS
A real time system for multisensor image analysis through pyramidal segmentation
[AD-A247169] p 3888 N92-31981

PYRIMIDINES
Evolution and analysis of the functional domains of the chimeric proteins that initiate pyrimidine biosynthesis
[AD-A250069] p 3866 N92-31485

PYROLYSIS
New sources for OMVPE
[AD-A250903] p 3909 N92-31582
Catalyst and feedstock effects in the thermochemical conversion of biomass to liquid transportation fuels
[DE92-010569] p 3799 N92-31593
Preparation of non-oxide ceramics by pyrolysis of organometallic precursors
[AD-A251112] p 3798 N92-32197
Supersonic pyrolysis jets for diamond film deposition
[AD-A251125] p 3798 N92-32198

PYROLYTIC GRAPHITE
Correlation from randomness: Quantitative analysis of sputtered graphite surfaces using the scanning tunneling microscope
[AD-A252420] p 3783 N92-31820

PYROLYTIC MATERIALS
Decomposition studies of triisopropylantimony and triallylantimony
[AD-A250671] p 3796 N92-31968

PYROTECHNICS
A semiconductor bridge ignited gas generator
[DE92-014049] p 3781 N92-31748
PYRROLES
Charge transfer processes in multiple site chemical systems
[AD-A249538] p 3791 N92-31358
Polymerization of conducting polymers confined to free surfaces: A comparison of the Langmuir-Blodgett polymerization of 3-alkyl pyrroles and 2-alkyl anilines
[AD-A250966] p 3798 N92-32194

Q

Q SWITCHED LASERS
Method and circuit for controlling the evolution time interval of a laser output pulse
[NASA-CASE-LAR-13772-1] p 3831 N92-31788
QUADRATIC EQUATIONS
Phase portraits of non degenerate quadratic systems with zero finite multiplicity
[REPT-91-96] p 3886 N92-31520
QUALIFICATIONS
High strength glass second source qualification to composite armor specification MIL-L-46197(MR)
[AD-A252114] p 3792 N92-31404
QUALITATIVE ANALYSIS
Mathematical structures for qualitative calculus, a contribution to qualitative simulation
[LAAS-91475] p 3886 N92-31690
The potential of passive-remote Fourier Transform Infrared (FTIR) spectroscopy to detect organic emissions under the Clean Air Act
[DE92-015224] p 3854 N92-32083
Ba2Ti9O20 microwave dielectric resonator: Processing, phase synthesis and characterization
[INPE-5373-PRE/1747] p 3818 N92-32200
QUALITY CONTROL
Overview of integrated services digital network conformance testing
[PB92-181015] p 3881 N92-31365
Quality Evaluation System (QUES), volume 1
[AD-A252679] p 3876 N92-31586
Real-time statistical quality control and ARM
[DE92-015253] p 3837 N92-31657
Guidelines for generating acceptance sampling plans for continuous production
[DE92-010763] p 3837 N92-31753
Total quality management: A management philosophy for providing high quality construction
[AD-A252743] p 3837 N92-32172
QUANTITATIVE ANALYSIS
Dispersive-infrared gas sensor system design and operation manual
[DE92-011766] p 3828 N92-31909
QUANTUM CHEMISTRY
Development of effective quantum chemical method for polymers and solid
[AD-A250976] p 3795 N92-31951
Computational studies of metal-metal and metal-ligand interactions
[NASA-CR-190674] p 3790 N92-32156
QUANTUM CHROMODYNAMICS
Research in elementary particle physics
[DE92-014585] p 3893 N92-31385
Lattice gaugefixing and other optics in lattice gauge theory
[DE92-016958] p 3901 N92-31737
Theoretical studies in nuclear reactions and nuclear structure
[DE92-016204] p 3897 N92-31927
Intermediate/high energy nuclear physics
[DE92-015363] p 3900 N92-32028
QUANTUM EFFICIENCY
Research on stable, high-efficiency amorphous silicon multijunction modules
[DE92-001244] p 3814 N92-31525
QUANTUM ELECTRODYNAMICS
Schwinger boson studies of the t-J model beyond mean-field approximation
[DE92-630650] p 3909 N92-31655
QUANTUM ELECTRONICS
Electronic structure and photophysical properties of polyimides
[DE92-012353] p 3797 N92-32146
QUANTUM MECHANICS
Dicke narrowing in strong fields: The atom-as-antenna analogy
[AD-A252321] p 3807 N92-31629
The RQM triangle: A paradigm for relativistic quantum mechanics
[DE92-011583] p 3915 N92-31663
Quantum mechanical approach to understanding microstructural and mechanical properties in intermetallics
[AD-A250550] p 3790 N92-32084
QUANTUM THEORY
Research in elementary particle physics
[DE92-014585] p 3893 N92-31385
Molecular interactions and properties with many-body methods
[AD-A247052] p 3896 N92-31858
Intermediate/high energy nuclear physics
[DE92-015363] p 3900 N92-32028
QUANTUM WELLS
Stable integrated microwave to optical modulator
[AD-A249974] p 3813 N92-31431
QUARK MODELS
Theoretical studies in nuclear reactions and nuclear structure
[DE92-016204] p 3897 N92-31927
Intermediate/high energy nuclear physics
[DE92-015363] p 3900 N92-32028
QUARKS
A tumbling top-quark condensate model
[DE92-016194] p 3893 N92-31552
Intermediate/high energy nuclear physics
[DE92-015363] p 3900 N92-32028
QUARTZ
Low thermal coefficient of expansion printed wiring boards
[DE92-013704] p 3817 N92-31946
QUARTZ CRYSTALS
Movement of dislocations in quartz
[AD-A250527] p 3913 N92-32078
QUATERNARY ALLOYS
Electronic and total energy properties of ternary and quaternary semiconductor compounds, alloys, and superlattices: Theoretical study of Cu/graphite bonding
[NASA-CR-190691] p 3772 N92-31266
QUENCHING (COOLING)
A study of the microstructural basis for the strength and toughness properties of water-quenched and air-cooled HSLA-100, HSLA-100 with increased copper, and a ULCB steel
[AD-A245955] p 3789 N92-32052
QUERY LANGUAGES
Non Boolean search methods in information retrieval
p 3921 N92-32187

R

RACE FACTORS
Minorities and air quality non-attainment areas: A preliminary geo-demographic analysis
[DE92-013054] p 3852 N92-31591
RACES (ANTHROPOLOGY)
Minorities and air quality non-attainment areas: A preliminary geo-demographic analysis
[DE92-013054] p 3852 N92-31591
RADAR
Simulation of a parallel processor based small tactical system
[AD-A245911] p 3882 N92-31443
Readily implemented enhanced sinusoid detection in noise
[DE92-011359] p 3806 N92-31449
RADAR EQUIPMENT
Ground based radar
[TABES PAPER 92-213] p 3764 N92-32021
Polyalphaolefins: A new improved cost effective aircraft radar coolant
[AD-A250517] p 3796 N92-32045
RADAR IMAGERY
An airborne study of boundary layer heat and moisture fluxes for project FIFE
[NASA-CR-190665] p 3844 N92-31357
RADAR NETWORKS
Calibration network intended for phased-array antennas at 3 GHz
[PB92-195429] p 3810 N92-32070
RADAR TARGETS
Characteristics of selected reference targets for calibrating 10.6 micron laser radars
[DREV-R-4487/88] p 3811 N92-32217
RADAR TRANSMITTERS
Feasibility study for a low-altitude wide and temperature profiler
[PB92-188200] p 3860 N92-31641
RADIAL FLOW
Flow generation by turbulence
[DE92-013276] p 3906 N92-31829
RADIANCE
A sensitivity study of daytime visibility determination with the horizon scanning imager
[SIO-91-15] p 3902 N92-32144
RADIANT COOLING
Analytical and experimental studies of heat pipe radiation cooling of hypersonic propulsion systems
[DE92-013428] p 3759 N92-31817
RADIATION ABSORPTION
Dicke narrowing in strong fields: The atom-as-antenna analogy
[AD-A252321] p 3807 N92-31629
RADIATION CHEMISTRY
The Radiological Research Accelerator Facility
[DE92-013674] p 3867 N92-31747
RADIATION COUNTERS
Research in elementary particle physics
[DE92-014585] p 3893 N92-31385
Development and application of photosensitive device systems to studies of biological and organic materials
[DE92-014728] p 3867 N92-32120
Aluminum tunnel junction detector operation in an adiabatic demagnetization refrigerator
[DE92-013441] p 3913 N92-32166
RADIATION DAMAGE
Analysis of systems hardware flown on LDEF. Results of the systems special investigation group
[NASA-CR-189628] p 3767 N92-31677
Radiation damage in carbon-carbon composites
[DE92-011778] p 3775 N92-31912
Neutron radiation damage to silicon detectors
[ITN-92-85162] p 3897 N92-31958
RADIATION DETECTORS
Waveguide-binding sensor for use with assays
[AD-D015230] p 3777 N92-31268
Pulse-by-pulse energy measurement at the Stanford Linear Collider
[DE92-011520] p 3899 N92-31390
Dispersive-infrared gas sensor system design and operation manual
[DE92-011766] p 3828 N92-31909
Aluminum tunnel junction detector operation in an adiabatic demagnetization refrigerator
[DE92-013441] p 3913 N92-32166
RADIATION DOSAGE
Biodosimetry of ionizing radiation in humans using the glycophorin A genotoxicity assay
[DE92-011974] p 3869 N92-31608
Relating space radiation environments to risk estimates
[DE92-010256] p 3926 N92-31756
Use of tissue equivalent proportional counters to characterize radiation quality on the space shuttle
[DE92-012347] p 3768 N92-31846
Effects of fragmentation parameter variations on estimates of galactic cosmic ray exposure: Dose sensitivity studies for aluminum shields
[NASA-TM-4386] p 3926 N92-32193
RADIATION EFFECTS
Mitigation of magnetohydrodynamic electromagnetic pulse (MHD-EMP) effects from commercial electric power systems
[AD-A249577] p 3804 N92-31354
Algorithms for the determination of spatial and spectral distribution of electromagnetic energy in a simulated biostructure subjected to transient spatially heterogeneous radiation with applications to radar hazard assessment and cancer therapy
[AD-A250447] p 3805 N92-31381
Economics of microwave plasma dissociation of H2S
[DE92-014846] p 3779 N92-31441
Design of a TEM cell EMP simulator
[DREO-1084] p 3806 N92-31470
The interplanetary heavy ion environment for both galactic cosmic rays and solar energetic particles during the CRRES mission
[AD-A248942] p 3926 N92-31477
Combined Release and Radiation Effects Satellite (CRRES) experiments data collection, analysis, and publication
[NASA-CR-184361] p 3856 N92-31551
Radiation-induced crystalline-to-amorphous transition in intermetallic compounds of the Cu-Ti alloy system
[DE92-010276] p 3787 N92-31575
An approximate local thermodynamic nonequilibrium radiation model for air
[NASA-CR-190580] p 3914 N92-31577
Biodosimetry of ionizing radiation in humans using the glycophorin A genotoxicity assay
[DE92-011974] p 3869 N92-31608
Static magnetic fields: A summary of biological interactions, potential health effects, and exposure guidelines
[DE92-015218] p 3867 N92-31711
Divertor material evaluation system at D3-D
[DE92-013696] p 3905 N92-31749
Relating space radiation environments to risk estimates
[DE92-010256] p 3926 N92-31756

Selective nitrations: The laser-induced nitration of three cycloalkanes, 1
[AD-A249942] p 3800 N92-31800
Analytic estimation of radiation effects in space using solid angles
[DE92-013282] p 3899 N92-31831
Radiation damage in carbon-carbon composites
[DE92-011778] p 3775 N92-31912
Substrate surface effects on the properties of sputter-deposited and laser-irradiated films
[DE92-013850] p 3795 N92-31917
Extremely Low Frequency (ELF) communications system ecological monitoring program summary of 1990 progress
[AD-A246344] p 3809 N92-31996
Effects of fragmentation parameter variations on estimates of galactic cosmic ray exposure: Dose sensitivity studies for aluminum shields
[NASA-TM-4386] p 3926 N92-32193

RADIATION HARDENING
Wavelength-tunable liquid crystal imaging filters for remote sensing from geosynchronous platforms
[NASA-CR-190698] p 3845 N92-32223

RADIATION HAZARDS
Algorithms for the determination of spatial and spectral distribution of electromagnetic energy in a simulated biostructure subjected to transient spatially heterogeneous radiation with applications to radar hazard assessment and cancer therapy
[AD-A250447] p 3805 N92-31381

RADIATION MEASUREMENT
Combined Release and Radiation Effects Satellite (CRRES) experiments data collection, analysis, and publication
[NASA-CR-184361] p 3856 N92-31551
Real-time statistical quality control and ARM
[DE92-015253] p 3837 N92-31657
Analysis of the effects of aerosol distribution in the atmosphere on surface radiative measurements
[DE92-014189] p 3856 N92-31662
A study of longwave radiation codes for climate studies: Validation with ARM observations and tests in general circulation models
[DE92-014100] p 3862 N92-31894

RADIATION SHIELDING
Radiation protection for human exploration of the moon and Mars: Application of the MASH code system
[DE92-014416] p 3868 N92-31409
Effects of fragmentation parameter variations on estimates of galactic cosmic ray exposure: Dose sensitivity studies for aluminum shields
[NASA-TM-4386] p 3926 N92-32193

RADIATION SOURCES
An evaluation of ionizing radiation emitted by high power microwave generators
[DE92-016160] p 3805 N92-31387

RADIATION TRANSPORT
Photon and electron data bases and their use in radiation transport calculations
[DE92-011458] p 3895 N92-31705
Analytic estimation of radiation effects in space using solid angles
[DE92-013282] p 3899 N92-31831
Effects of fragmentation parameter variations on estimates of galactic cosmic ray exposure: Dose sensitivity studies for aluminum shields
[NASA-TM-4386] p 3926 N92-32193

RADIATIVE HEAT TRANSFER
Stagnation-point heat-transfer rate predictions at aeroassist flight conditions
[NASA-TP-3208] p 3819 N92-31281

RADIATIVE TRANSFER
An approximate local thermodynamic nonequilibrium radiation model for air
[NASA-CR-190580] p 3914 N92-31577

RADICALS
Propane oxidation through the negative temperature coefficient region at 10 and 15 atmospheres: Results of experimental and modeling studies
[DE92-007902] p 3778 N92-31414
Theoretical studies of the reactions and spectroscopy of radical species relevant to combustion reactions and diagnostics
[DE92-013484] p 3781 N92-31725
Supersonic pyrolysis jets for diamond film deposition
[AD-A251125] p 3798 N92-32198

RADIO ASTRONOMY
High-resolution microwave observations of the sun
[AD-A247869] p 3925 N92-31985

RADIO FREQUENCIES
Improved ferrite biasing scheme for booster RF cavities
[DE92-011650] p 3815 N92-31664
Field-emitter arrays for RF vacuum microelectronics
[AD-A250101] p 3816 N92-31791
Optical processing architectures for spaceborne SAR image generation and RF array beam forming
[TABES PAPER 92-444] p 3763 N92-32012

RADIO TRANSMISSION
Remote sensing of trapping layer base height using ATIS transmissions
[AD-A250074] p 3844 N92-31362
Exponential representation and consistency checking for M layer
[AD-A250423] p 3805 N92-31413

RADIOACTIVE DECAY
The structure of nuclei far from beta stability
[DE92-012598] p 3895 N92-31721
Experimental particle physics at the University of Pittsburgh
[DE92-016182] p 3896 N92-31926
Implications of the 17 keV neutrino
[DE92-017000] p 3898 N92-32006
Resonant enhancement of flavor-changing neutrino interactions
[DE92-013020] p 3898 N92-32167

RADIOACTIVE ISOTOPES
Proceedings of the 2nd KUR symposium on hyperfine interactions
[DE92-789024] p 3895 N92-31728

RADIOACTIVE WASTES
EnviroTRADE: Its role in the cleanup of the environment
[DE92-013691] p 3851 N92-31427

RADIOACTIVITY
Exotic nuclear shapes and configurations that can be studied at high spin using radioactive ion beams
[DE92-016800] p 3898 N92-32090

RADIOBIOLOGY
The Radiological Research Accelerator Facility
[DE92-013674] p 3867 N92-31747
Use of tissue equivalent proportional counters to characterize radiation quality on the space shuttle
[DE92-012347] p 3768 N92-31846

RADIOGRAPHY
Motion model for the correction of point source distortion in radiographs of honeycomb
[DREP-88-14] p 3777 N92-32215

RADIOLOGY
The Radiological Research Accelerator Facility
[DE92-013674] p 3867 N92-31747

RADIOMETERS
Procedures and errors in the determination of the bi-directional reflectance factor and other radiometric quantities
[INPE-5386-TDI/475] p 3843 N92-31277
Mission description and in-flight operations of ERBE instruments on ERBS, NOAA 9, and NOAA 10 spacecraft
[NASA-RP-1279] p 3844 N92-32127
Fine structure superimposed on mm-wavelength (18-23 GHz) spectra of solar active region
[INPE-5371-TDI/470] p 3926 N92-32221

RADOMES
Analysis of random induced cross polarization
[AD-A249773] p 3806 N92-31569
Scattering from a finite collection of transverse dipole and axial slot arrays with edge effects
[AD-A249622] p 3807 N92-31691

RAIL TRANSPORTATION
Potential impact of high temperature superconductors on MAGLEV transportation
[DE92-012683] p 3834 N92-31720
Preliminary design for a MAGLEV development facility
[DE92-012259] p 3835 N92-31774

RAILGUN ACCELERATORS
Solid-armature railguns without the velocity-skin effect
[DE92-012630] p 3765 N92-31542
Projectile development for railguns using hypervelocity preacceleration
[DE92-016741] p 3766 N92-31735

RAIN
The structure and energetics of Amazon squall lines
[AD-A250182] p 3859 N92-31523
Wind tunnel aerodynamic characteristics of a transport-type airfoil in a simulated heavy rain environment
[NASA-TP-3184] p 3751 N92-31532

RAIN FORESTS
Rainwater and throughfall chemistry in a terra firme rain forest: Central Amazonia
[INPE-5364-PRE/1744] p 3863 N92-32224

RAMAN SPECTRA
Stress and phase transformation phenomena in oxide films
[DE92-014702] p 3910 N92-31665

RAMAN SPECTROSCOPY
Electronic states in systems of reduced dimensionality
[DE92-013588] p 3912 N92-31945

RAMJET ENGINES
Collection of papers of the 31st Israel Annual Conference on Aviation and Astronautics
[ITN-92-85124] p 3745 N92-31861
Sizing supersonic freejet nozzle and inlet location for simulation of the transition phase in integral rocket ramjet p 3747 N92-31870
Effect of inlet geometry on the flow and combustion processes in a solid fuel ramjet p 3747 N92-31871

RANDOM NOISE
Noise-induced chaos and phase space flux: A sample-theoretic study
[PB92-172733] p 3915 N92-31645

RANDOM PROCESSES
Guidelines for generating acceptance sampling plans for continuous production
[DE92-010763] p 3837 N92-31753
Correlation from randomness: Quantitative analysis of sputtered graphite surfaces using the scanning tunneling microscope
[AD-A252420] p 3783 N92-31820
Signal and noise models arising from the theory of errors
[AD-A250222] p 3885 N92-31827
The physics of cellular automata and coherence and chaos in classical many-body systems
[DE92-016834] p 3890 N92-32035
A generalization to stochastic averaging in random vibration
[DE92-016747] p 3842 N92-32088

RANDOM VARIABLES
Signal and noise models arising from the theory of errors
[AD-A250222] p 3885 N92-31827

RANDOM VIBRATION
A generalization to stochastic averaging in random vibration
[DE92-016747] p 3842 N92-32088

RANDOM WALK
Maximum likelihood estimation of fractional Brownian motion and Markov noise parameters
[AD-A249623] p 3890 N92-31686
Diffusion in ordered and disordered media
[AD-A250949] p 3891 N92-32211

RANKINE CYCLE
Potassium Rankine cycle nuclear power systems for spacecraft and lunar-mass surface power
[DE92-016163] p 3770 N92-31897
External combustion engine technology (vapor and liquid cycles) for individual soldier power systems
[AD-A252754] p 3836 N92-32173

RAPID TRANSIT SYSTEMS
NASA High Speed Research Program, Emissions Scenarios Committee report of meetings on 26 September 1991 and 9 January 1992
[NASA-CR-190379] p 3855 N92-32147

RAREFIED GASES
Low density real gas flows about hypersonic vehicles
[AD-A250048] p 3752 N92-31777

RASTER SCANNING
Multimedia electronic mail: Standards and performance simulation
[AD-A250047] p 3808 N92-31809

RATES (PER TIME)
The effect of surface pressure on Langmuir-Blodgett polymerization of 2-pentadecyl aniline
[AD-A250993] p 3795 N92-31952

RATS
A study of the effect of hydrocarbon structure on the induction of male rat nephropathy and metabolite structure
[AD-A252192] p 3867 N92-31590

RDX
Development of methodology and technology for identifying and quantifying emission products from open burning and open detonation thermal treatment methods. Field test series A, B, and C. Volume 1: Test summary
[AD-A250735] p 3800 N92-31971
Development of methodology and technology for identifying and quantifying emission products from open burning and open detonation thermal treatment methods. Field test series A, B, and C. Volume 2, part B: Quality assurance and quality control. Appendices
[AD-A250737] p 3801 N92-31973

REACTING FLOW
Stagnation-point heat-transfer rate predictions at aeroassist flight conditions
[NASA-TP-3208] p 3819 N92-31281

REACTION KINETICS
Propane oxidation through the negative temperature coefficient region at 10 and 15 atmospheres: Results of experimental and modeling studies
[DE92-007902] p 3778 N92-31414
The pathways and dynamics of molecular decomposition
[AD-A249627] p 3893 N92-31463

Hydrocarbon ignition: Automatic generation of reaction mechanisms and applications to modeling of engine knock
[DE92-011943] p 3780 N92-31607
Elementary reaction rate measurements at high temperatures by tunable-laser flash-absorption
[DE92-015269] p 3830 N92-31684
Theoretical studies of the reactions and spectroscopy of radical species relevant to combustion reactions and diagnostics
[DE92-013484] p 3781 N92-31725
Deterministic analysis of processes at corroding metal surfaces and the study of electrochemical noise in these systems
[DE92-016286] p 3788 N92-31733
Application of reactor-pumped lasers to power beaming
[DE92-012370] p 3831 N92-31762
Molecular interactions and properties with many-body methods
[AD-A247052] p 3896 N92-31858
Unimolecular reaction mechanisms involving C3H4, C4H4, and C6H6 hydrocarbon species
[DE92-005326] p 3783 N92-31860
Diosmacycloalkanes as models for the formation of hydrocarbons from surface methylenes
[DE92-014588] p 3783 N92-31891
Electrochemical oxidation of methane for fuel cells
[PB92-172303] p 3848 N92-31922
Laser-ablated copper condensation in helium
[DE92-016685] p 3789 N92-32004
Probe molecule studies: Active species in alcohol synthesis
[DE92-015430] p 3784 N92-32029
The development of precipitated iron catalysts with improved stability
[DE92-014630] p 3785 N92-32117
Evolution of reactants fluid volume in turbulent jets
[DE92-011298] p 3786 N92-32145
Prompt neutron lifetime in a strongly heterogeneous lattice
[DE92-013212] p 3898 N92-32165

REACTION WHEELS
Spacecraft stability and control
[TABES PAPER 92-414] p 3763 N92-32011

REACTIVITY
Stress reactivity: Five-factor representation of a psychobiological typology
[AD-A252715] p 3872 N92-31327
Inorganic rings on carbon chains
[AD-A251043] p 3772 N92-31850

REACTOR DESIGN
A model for the interfacial shear in vertical, adiabatic, annular-mist flow
[DE92-013537] p 3820 N92-31424
Small tokamaks for fusion technology testing
[DE92-011790] p 3906 N92-31913

REACTOR MATERIALS
Divertor material evaluation system at D3-D
[DE92-013696] p 3905 N92-31749
Radiation damage in carbon-carbon composites
[DE92-011778] p 3775 N92-31912
Heat transfer and pressure drop in an annular channel with downflow
[DE92-014363] p 3825 N92-32115

REACTOR SAFETY
Radiation protection for human exploration of the moon and Mars: Application of the MASH code system
[DE92-014416] p 3868 N92-31409
EnviroTRADE: Its role in the cleanup of the environment
[DE92-013691] p 3851 N92-31427
Non-geothermal optics study of wave propagation
[DE92-011806] p 3903 N92-31494
YLIFE-2 inertial fusion energy power plant design
[DE92-011965] p 3904 N92-31530
Fusion development and technology
[DE92-014352] p 3904 N92-31545
A philosophy for space nuclear systems safety
[DE92-016501] p 3771 N92-32030
Heat transfer and pressure drop in an annular channel with downflow
[DE92-014363] p 3825 N92-32115

REACTOR TECHNOLOGY
Transient fission gas behavior in uranium nitride fuel under proposed space applications
[AD-A252577] p 3899 N92-31325

READING
Space constancy on video display terminals
[AD-A247290] p 3872 N92-32105

REAL GASES
Low density real gas flows about hypersonic vehicles
[AD-A250048] p 3752 N92-31777

REAL TIME OPERATION
Methodology investigation final report: Automated real-time test scenario generation, phase 1
[AD-A250439] p 3884 N92-31395
Sources of unbounded priority inversions in real-time systems and a comparative study of possible solutions
[NASA-CR-190711] p 3875 N92-31486
Neural network perception for mobile robot guidance
[AD-A249972] p 3884 N92-31511
A data processing module for acoustic Doppler current meters
[AD-A250901] p 3891 N92-31563
Real time analysis of tokamak discharge parameters
[DE92-011394] p 3904 N92-31616
Real-time statistical quality control and ARM
[DE92-015253] p 3837 N92-31657
Hyper-NPSNET: A virtual world with an integrated 3-D hypertext
[AD-A252726] p 3878 N92-31676
About real time industrial processes control: A methodology based on objects and Petri nets
[LAAS-91467] p 3878 N92-31689
Real-time infrared spectroscopy of moving solids for on-line analyses
[DE92-012156] p 3782 N92-31772
Real time investigations of the polymerization of 2-pentadecyl aniline on the Langmuir-Blodgett trough
[AD-A250994] p 3795 N92-31954
A real time system for multisensor image analysis through pyramidal segmentation
[AD-A247169] p 3888 N92-31981
Real time detection in a laser bathymetry system
[PB92-195452] p 3866 N92-32089
System overview of the NASA Dryden Integrated Test Facility
[NASA-TM-104250] p 3762 N92-32201

REATTACHED FLOW
The calculation of incompressible separated turbulent boundary layers p 3749 N92-31886

RECEIVERS
Effect of guard band reduction on marker beacon receiver performance
[DOT/FAA/CT-TN92/18] p 3807 N92-31617

RECEPTORS (PHYSIOLOGY)
Modeling of learning-induced receptive field plasticity in auditory neocortex
[AD-A250348] p 3869 N92-31558

RECOMMENDATIONS
Aviation safety: Changes needed in FAA's service difficulty reporting program
[GAO/RCED-91-24] p 3755 N92-31453
Canadian aircrew sea water survival, 1952-1987
[DCIEM-88-RR-39] p 3756 N92-32219

RECTANGULAR PLATES
High-frequency techniques for RCS prediction of plate geometries
[NASA-CR-190656] p 3804 N92-31273

REDUCED GRAVITY
Hollow fiber clinostat for simulating microgravity in cell culture
[NASA-CASE-MFS-28370-1] p 3828 N92-31790
SPACEHAB: A giant step in the commercial development of space
[TABES PAPER 92-454] p 3764 N92-32018

REDUCTION (CHEMISTRY)
Final report on DSA methods for monitoring alumina in aluminum reduction cells with cermet anodes
[DE92-013599] p 3813 N92-31440

REDUNDANCY
FCS skewed sensors array: Practical considerations p 3746 N92-31868

REFLECTANCE
Changes in the reflectance of ex situ leaves: A methodological approach
[INPE-5407-PUD/051] p 3806 N92-31568
Characteristics of selected reference targets for calibrating 10.6 micron laser radars
[DREV-R-4487/88] p 3811 N92-32217

REFLECTORS
Analysis of random induced cross polarization
[AD-A249773] p 3806 N92-31569

REFLEXES
Acetylcholinesterase inhibitors on the spinal cord
[AD-A252694] p 3868 N92-31326

REFRACTIVITY
Exponential representation and consistency checking for M layer
[AD-A250423] p 3805 N92-31413
Optimized photorefractive barium titanate
[AD-A250089] p 3908 N92-31438
Computer simulation of acoustic fluctuations due to finescale temperature perturbations measured by thermistor chain
[AD-A252709] p 3892 N92-31672

REFRACTORY METALS
Potassium Rankine cycle nuclear power systems for spacecraft and lunar-mass surface power
[DE92-016163] p 3770 N92-31897

REFRIGERATING
Heat and mass transfer considerations in advanced heat pump systems
[DE92-016635] p 3825 N92-32003

REFRIGERATORS
Aluminum tunnel junction detector operation in an adiabatic demagnetization refrigerator
[DE92-013441] p 3913 N92-32166

REGENERATORS
Oscillating-flow regenerator test rig: Woven screen and metal felt results
[NASA-CR-190689] p 3820 N92-31352

REGRESSION COEFFICIENTS
Sun-view-target geometry effects on spectrally-derived vegetative index estimates of absorbed radiation and leaf area
[AD-A249984] p 3843 N92-31329

REGULATIONS
National Conference on Integrated Resource Planning: Proceedings
[DE92-013573] p 3845 N92-31290
Aviation noise: Costs of phasing out noisy aircraft
[GAO/RCED-91-128] p 3891 N92-31454
Evolution of environmental protection strategies in the Soviet Union
[DE92-015090] p 3853 N92-31732
Report of the aviation safety review of Department of Energy helicopter operations
[DE92-016346] p 3755 N92-31928
A ban on use of lead-bearing solders: Implications for the electronics industry
[DE92-013291] p 3790 N92-32139

REINFORCED PLASTICS
High strength glass second source qualification to composite armor specification MIL-L-46197(MR)
[AD-A252114] p 3792 N92-31404

RELATIVISTIC ELECTRON BEAMS
Amplification mechanism of ion-ripple lasers and its possible application
[DE92-016155] p 3830 N92-31411
Plasma channel generation using low energy electron beams
[DE92-013770] p 3906 N92-31949

RELATIVISTIC VELOCITY
The physical solution to the Lorentz-Dirac equations in a constant magnetic field
[DE92-013299] p 3890 N92-32140

RELATIVITY
Modified black holes in two dimensional gravity
[DE92-630244] p 3924 N92-31401
The RQM triangle: A paradigm for relativistic quantum mechanics
[DE92-011583] p 3915 N92-31663
Lattice gaugefixing and other optics in lattice gauge theory
[DE92-016958] p 3901 N92-31737

RELAXATION (MECHANICS)
Holographic grating relaxation and photon correlation spectroscopic studies of viscoelastic liquids above the glass transition
[AD-A252485] p 3828 N92-31828
Simulation study of stepwise relaxation in a spheromak plasma
[DE92-782101] p 3906 N92-31843

RELAY SATELLITES
Soviet satellite communications science and technology
[PB92-173038] p 3809 N92-31920

RELIABILITY
Design and specification of a high speed transport protocol
[AD-A248323] p 3804 N92-31284
Continuous time and discrete time hyperexponential model for dependability growth modeling
[LAAS-92002] p 3837 N92-31693
Guidelines for generating acceptance sampling plans for continuous production
[DE92-010763] p 3837 N92-31753
Low thermal coefficient of expansion printed wiring boards
[DE92-013704] p 3817 N92-31946

RELIABILITY ANALYSIS
Cryogenic 4.4 MN mechanical test system for large scale tests of composite support struts
[PB92-181148] p 3774 N92-31609
Fitting and prediction uncertainty for a software reliability model
[AD-A252173] p 3880 N92-32060

RELIABILITY ENGINEERING
Weld penetration and defect control
[DE92-015310] p 3836 N92-31336

Continuous time and discrete time hyperexponential model for dependability growth modeling
[LAAS-92002] p 3837 N92-31693
Fitting and prediction uncertainty for a software reliability model
[AD-A252173] p 3880 N92-32060

RELIEF VALVES
Performance tests of a fast-acting valve for the driver tubes of a large blast/thermal simulator
[AD-A250035] p 3835 N92-31807

REMOTE HANDLING
Robotic soil sampler for hazardous waste clean up
[DE92-012693] p 3780 N92-31565

REMOTE SENSING
The detection of climate change due to the enhanced greenhouse effect
[NASA-TM-107965] p 3849 N92-31258
Procedures and errors in the determination of the bi-directional reflectance factor and other radiometric quantities
[INPE-5386-TDI/475] p 3843 N92-31277
An airborne study of boundary layer heat and moisture fluxes for project FIFE
[NASA-CR-190665] p 3844 N92-31357
Remote sensing of trapping layer base height using ATIS transmissions
[AD-A250074] p 3844 N92-31362
Changes in the reflectance of ex situ leaves: A methodological approach
[INPE-5407-PUD/051] p 3806 N92-31568
ARO Geoscience Center fellowships
[AD-A249225] p 3857 N92-31964
Optical processing architectures for spaceborne SAR image generation and RF array beam forming
[TABES PAPER 92-444] p 3763 N92-32012
OSRMS: The DREP near-nadir scatterometer
[DREP-88-15] p 3844 N92-32216
Images simulation of sensors with large field of view from images of sensors with less field of view: The SSR/TM case
[INPE-5378-TDI/473] p 3845 N92-32220
Wavelength-tunable liquid crystal imaging filters for remote sensing from geosynchronous platforms
[NASA-CR-190698] p 3845 N92-32223
GIS: Geographic Information Systems. State of the art and future tendencies
[INPE-5358-NTC/301] p 3922 N92-32227

REMOTELY PILOTED VEHICLES
Optimal trajectories for an unmanned air vehicle
p 3748 N92-31880

REPLACING
Sequential estimation of optimal age replacement policies when distribution of lifetimes is phase type
[AD-A249020] p 3836 N92-31479

REQUIREMENTS
Requirements Engineering and Analysis Workshop Proceedings
[AD-A250415] p 3876 N92-31541

RESEARCH
Development of a core combustion research program plan for EPA
[PB92-180868] p 3781 N92-31683

RESEARCH AIRCRAFT
Overview of the NASA Dryden Flight Research Facility aeronautical flight projects
[NASA-TM-104254] p 3756 N92-31261
System overview of the NASA Dryden Integrated Test Facility
[NASA-TM-104250] p 3762 N92-32201
Transonic wind tunnel test of a 14 percent thick oblique wing
[NASA-TM-102230] p 3754 N92-32213

RESEARCH AND DEVELOPMENT
Small Business Innovation Research program solicitation. Closing date: July 21, 1992
[NASA-TM-107795] p 3916 N92-31253
Space nuclear power, propulsion, and related technologies
[SAND91-2617] p 3770 N92-31503
Technology Integration Workshop: Selected papers
[PB92-158278] p 3923 N92-31643
Technology advancing research combustion in burners
[PB92-164359] p 3782 N92-31776
Femtosecond photonics: Fundamental phenomena and device behavior
[AD-A250506] p 3832 N92-32042
NSF Tokyo reports. 1991 survey of research and development in Japan
[PB92-192624] p 3927 N92-32067
NSF Tokyo reports. General outline of JFY 1991 government science and technology budget
[PB92-192640] p 3927 N92-32068

RESEARCH FACILITIES
Overview of the NASA Dryden Flight Research Facility aeronautical flight projects
[NASA-TM-104254] p 3756 N92-31261
The Radiological Research Accelerator Facility
[DE92-013674] p 3867 N92-31747
Technology advancing research combustion in burners
[PB92-164359] p 3782 N92-31776
Naval Biodynamics Laboratory: 1989 and 1990 command history
[AD-A247185] p 3870 N92-31963
System overview of the NASA Dryden Integrated Test Facility
[NASA-TM-104250] p 3762 N92-32201

RESEARCH MANAGEMENT
Fusion development and technology
[DE92-014352] p 3904 N92-31545
Cooperative field test program for wind systems
[DE92-001209] p 3847 N92-31579
Research and development of methods and tools for achieving and maintaining consensus processes in the face of change within and among government oversight agencies, volume 1
[DE92-014179] p 3852 N92-31592
Photovoltaic subcontract program, FY 1991
[DE92-001248] p 3847 N92-31646
Iterative functionalism and climate management regimes: From intergovernmental panel on climate change to intergovernmental negotiating committee
[DE92-014798] p 3853 N92-31896
Experimental particle physics at the University of Pittsburgh
[DE92-016182] p 3896 N92-31926

RESEARCH PROJECTS
The Radiological Research Accelerator Facility
[DE92-013674] p 3867 N92-31747
Femtosecond photonics: Fundamental phenomena and device behavior
[AD-A250506] p 3832 N92-32042

RESIDUAL STRESS
Residual stress and strain measurements in an austenitic steel plate containing a multipass weld
[DE92-014478] p 3839 N92-31383
Residual stresses in a multipass ferritic weldment
[DE92-014467] p 3839 N92-31501
The influence of various spectrum parameters on fatigue life and residual stress relaxation
[FFA-TN-1991-44] p 3840 N92-31512
Tailored metal matrix composites for high-temperature performance
[NASA-TM-105816] p 3775 N92-31854
Effects of fiber and interfacial layer architectures on the thermoplastic response of metal matrix composites
[NASA-TM-105802] p 3777 N92-32234

RESIDUES
Development of methodology and technology for identifying and quantifying emission products from open burning and open detonation thermal treatment methods. BangBox test series. Volume 1. Test summary
[AD-A250733] p 3800 N92-31969
Development of methodology and technology for identifying and quantifying emission products from open burning and open detonation thermal treatment methods. Field test series A, B, and C. Volume 1: Test summary
[AD-A250735] p 3800 N92-31971
Development of methodology and technology for identifying and quantifying emission products from open burning and open detonation thermal treatment methods. Field test series A, B, and C. Volume 2, part A: Quality assurance and quality control
[AD-A250736] p 3801 N92-31972
Development of methodology and technology for identifying and quantifying emission products from open burning and open detonation thermal treatment methods. Field test series A, B, and C. Volume 2, part B: Quality assurance and quality control. Appendices
[AD-A250737] p 3801 N92-31973

RESIN MATRIX COMPOSITES
Optical fiber sensors for organic matrix composite material cure monitoring
[AD-A247114] p 3776 N92-31979

RESINS
High density thin-walled syntactic foam
[DE92-013159] p 3797 N92-32136

RESISTOJET ENGINES
The evolutionary development of high specific impulse electric thruster technology
[NASA-TM-105712] p 3769 N92-31342

RESONANCE
Dicke narrowing in strong fields: The atom-as-antenna analogy
[AD-A252321] p 3807 N92-31629
Alterations of multiphoton-resonant processes through wave-mixing effects
[DE92-016164] p 3896 N92-31923

RESONANT FREQUENCIES
Asymptotic modal analysis and statistical energy analysis
[NASA-CR-190516] p 3842 N92-32236

RESONATORS
Movement of dislocations in quartz
[AD-A250527] p 3913 N92-32078
Ba2Ti9O20 microwave dielectric resonator: Processing, phase synthesis and characterization
[INPE-5373-PRE/1747] p 3818 N92-32200

RESOURCES MANAGEMENT
National Conference on Integrated Resource Planning: Proceedings
[DE92-013573] p 3845 N92-31290
RCRIS data element dictionary, version 3.0.0: Data tape documentation
[PB92-145515] p 3918 N92-31398

RESPIRATION
Nonthermal inhalation injury
[AD-A252532] p 3869 N92-31962

RESPIRATORY SYSTEM
The effects of hydrazines of neuronal excitability
[AD-A247142] p 3868 N92-31491

RESPONSE TIME (COMPUTERS)
Performance measures of the Ada rendezvous
[AD-A250060] p 3877 N92-31601

RESTORATION
EnviroTRADE: A technical perspective on the development of an information system providing data on environmental technologies and needs worldwide
[DE92-012625] p 3919 N92-31578

RETINAL IMAGES
Human image understanding
[AD-A250401] p 3872 N92-31330

REUSABLE ROCKET ENGINES
A demonstration of an intelligent control system for a reusable rocket engine
[NASA-TM-105794] p 3770 N92-31507

REVERBERATION
An empirical prediction algorithm for low-frequency acoustic surface scattering strengths
[AD-A250508] p 3892 N92-32044

REVERSE FIELD PINCH
Electrostatic turbulence and transport in the RFP edge
[DE92-014322] p 3905 N92-31730

REVISIONS
Type evolution and instance adaptation
[AD-A248435] p 3917 N92-31285

REYNOLDS NUMBER
Transonic wind tunnel test of a 14 percent thick oblique wing
[NASA-TM-102230] p 3754 N92-32213

REYNOLDS STRESS
Reynolds stress calculations of homogeneous turbulent shear flow with bounded energy states
[NASA-CR-189682] p 3826 N92-32158

RHEOLOGY
Macrostatistical hydrodynamics
[DE92-013589] p 3823 N92-31726
Rheology of zirconia-alumina gelcasting slurries
[DE92-016787] p 3797 N92-32089

RIBS (SUPPORTS)
Near-field and far-field sound radiation from a line-driven fluid-loaded infinite flat plate having periodic and non-periodic attached rib stiffeners
[AD-A250100] p 3892 N92-31789

RIGID STRUCTURES
An investigation of spinup dynamics of axial gyrostats using elliptic integrals and the method of averaging
[AD-A249728] p 3768 N92-31675

RING LASERS
RL-34 ring laser gyro laboratory evaluation for the Deep Space Network antenna application
[NASA-CR-190481] p 3829 N92-32128

RING STRUCTURES
Flow instability in a vertical annulus under steady state and transient conditions
[DE92-013217] p 3820 N92-31421

RISK
Relating space radiation environments to risk estimates
[DE92-010256] p 3926 N92-31756

ROBOT ARMS
Building an educational robot arm for under $1,000
[AD-A247499] p 3833 N92-31460
Singularity avoidance for SCARA-type robots
p 3746 N92-31867

ROBOT CONTROL
Torque linearizing hardware for the electric joint motors of a direct-drive robot
[DE92-012681] p 3816 N92-31718
Techniques for autonomous navigation
[DE92-013458] p 3756 N92-31746
Singularity avoidance for SCARA-type robots
p 3746 N92-31867
Robotics development for the enhancement of space endeavors
[TABES PAPER 92-445] p 3763 N92-32013

ROBOT DYNAMICS
Techniques for autonomous navigation
[DE92-013458] p 3756 N92-31746
ROBOTICS
Piezoelectric radiant-to-air ultrasonic transducers
p 3811 N92-31244
Building an educational robot arm for under $1,000
[AD-A247499] p 3833 N92-31460
Robotic soil sampler for hazardous waste clean up
[DE92-012693] p 3780 N92-31565
From perception to modelization in robotics using achromatic and chromatic cameras
[LAAS-91484] p 3901 N92-31692
Robotics development for the enhancement of space endeavors
[TABES PAPER 92-445] p 3763 N92-32013
Modeling and design of a closed kinematic chain robotic mechanism
[DE92-014777] p 3835 N92-32121
On dexterous rotations of polygons
[AD-A250967] p 3797 N92-32151
ROBOTS
Building an educational robot arm for under $1,000
[AD-A247499] p 3833 N92-31460
Neural network perception for mobile robot guidance
[AD-A249972] p 3884 N92-31511
Robotic soil sampler for hazardous waste clean up
[DE92-012693] p 3780 N92-31565
Singularity avoidance for SCARA-type robots
p 3746 N92-31867
Robotics development for the enhancement of space endeavors
[TABES PAPER 92-445] p 3763 N92-32013
Effective path planning through task restriction
[DE92-017351] p 3885 N92-32036
Modeling and design of a closed kinematic chain robotic mechanism
[DE92-014777] p 3835 N92-32121
On dexterous rotations of polygons
[AD-A250967] p 3797 N92-32151
ROBUSTNESS (MATHEMATICS)
A robust algorithm for isotropic reconstruction of magic-angle spinning solid-state NMR spectra
[AD-A249610] p 3874 N92-31379
Estimation of aircraft attitude by angular rate measurements p 3748 N92-31881
ROCKET ENGINES
Life extending control for rocket engines
[NASA-TM-105789] p 3802 N92-31263
Solid rocket combustion phenomena
[AD-A248006] p 3770 N92-31474
Study of a spherical spinning combustion chamber for orbit insertion p 3746 N92-31869
Orbital transfer rocket engine technology: Advanced engine study
[NASA-CR-187216] p 3771 N92-32129
Demonstrated survivability of a high temperature optical fiber cable on a 1500 pound thrust rocket chamber
[NASA-TM-105835] p 3801 N92-32230
ROCKET LININGS
Cyclic hot firing results of tungsten-wire-reinforced, copper-lined thrust chambers
[NASA-TM-4214] p 3769 N92-31249
ROCKS
Instabilities of damage and surface degradation mechanisms in brittle material structural systems
[AD-A250785] p 3842 N92-32168
RODS
Emissivity measurements in support of experiments on natural convection between a vertical cylinder and a surrounding array
[DE92-012321] p 3819 N92-31287
Effect of out-of-roundness on the performance of a diesel engine connecting-rod bearing
[NASA-TM-105600] p 3834 N92-31536
ROLL
A summary of the active flexible wing program
[NASA-TM-107655] p 3757 N92-31264
Rolling maneuver load alleviation using active controls
[NASA-TM-107654] p 3757 N92-31351
ROOM TEMPERATURE
SiGe Si quantum wires for efficient, room temperature, tunable luminescence
[AD-A249651] p 3814 N92-31464
ROTARY GYROSCOPES
An innovative two axis rate gyro: Theory and principles of operation p 3748 N92-31875
ROTATING BODIES
CSM solutions of rotating blade dynamics using integrating matrices
[NASA-CR-190577] p 3840 N92-31619
An innovative two axis rate gyro: Theory and principles of operation p 3748 N92-31875
Extended Kalman filter for attitude estimation of the Earth Radiation Budget Satellite p 3748 N92-31876
ROTATION
f Mo(CHCMe2Ph)(NAr)(OR)2 and relative reactivity toward 2,3-bis(trifluoromethyl) norbornadiene iene
[AD-A250234] p 3780 N92-31524
Poloidal rotation and density asymmetries in a tokamak plasma with strong toroidal rotation
[PB92-182534] p 3904 N92-31613
Rigid rotations in two-electron atoms in a uniform magnetic field
[DE92-624981] p 3896 N92-31836
On dexterous rotations of polygons
[AD-A250967] p 3797 N92-32151
ROTOR AERODYNAMICS
A general numerical model for wave rotor analysis
[NASA-TM-105740] p 3821 N92-31484
ROTOR BLADES
CSM solutions of rotating blade dynamics using integrating matrices
[NASA-CR-190577] p 3840 N92-31619
ROTOR DYNAMICS
CSM solutions of rotating blade dynamics using integrating matrices
[NASA-CR-190577] p 3840 N92-31619
A simulation model of a single rotor helicopter
p 3746 N92-31865
An innovative two axis rate gyro: Theory and principles of operation p 3748 N92-31875
Orbit transfer vehicle engine technology program. Task B-6 high speed turbopump bearings
[NASA-CR-189230] p 3835 N92-31892
ROTOR LIFT
A simulation model of a single rotor helicopter
p 3746 N92-31865
ROTORS
A general numerical model for wave rotor analysis
[NASA-TM-105740] p 3821 N92-31484
ROUTES
The vehicle routing problem: Some computational tests of savings method and its variations
[INPE-5361-RPQ/656] p 3886 N92-31241
RUBBER
Recent developments in the fundamentals of gas permeation in rubbery polymers
[AD-A249745] p 3794 N92-31624
RUN TIME (COMPUTERS)
Using the burst derivative measure to improve the computational efficiency of ISAR motion compensation algorithms
[AD-A250850] p 3805 N92-31369
New directions in network flows
[AD-A250499] p 3880 N92-32039
RUNGE-KUTTA METHOD
Nonlinearly stable compact schemes for shock calculations
[NASA-CR-189663] p 3887 N92-32164
RUNWAYS
An assessment of the B-747's capability to operate on rough surfaces
[AD-A250134] p 3757 N92-31793
Global positioning system runway incursion program static ground tests
[DOT/FAA/CT-TN91/44] p 3756 N92-31838

S

S GLASS
Computational simulation of intermingled-fiber hybrid composite behavior
[NASA-TM-105666] p 3774 N92-31506
S WAVES
Time domain regional discriminants
[AD-A249949] p 3855 N92-31509
SAMPLED DATA SYSTEMS
Artificial neural network implementation of a near-ideal error prediction controller
[NASA-CR-190694] p 3880 N92-32122
SAMPLERS
Robotic soil sampler for hazardous waste clean up
[DE92-012693] p 3780 N92-31565
SAMPLING
Hydrographic and Acoustic Doppler Current Profiler (ADCP) data from the Farallones shelf and slope study
[AD-A250834] p 3864 N92-31495
Robotic soil sampler for hazardous waste clean up
[DE92-012693] p 3780 N92-31565
The collection, handling, transportation, and thermal desorption of explosive vapor using quartz collection tubes
[DE92-011441] p 3799 N92-31570
Independent sampling of a stochastic process
[AD-A249712] p 3888 N92-31600
Guidelines for generating acceptance sampling plans for continuous production
[DE92-010763] p 3837 N92-31753
Importance sampling for Markov chains: Asymptotics for the variance
[AD-A249804] p 3888 N92-31757
Heuristic sampling on DAGs
[DE92-017359] p 3917 N92-32037
SAPPHIRE
Photon absorption and the decay of surface excitation on sapphire (1120)-(3 x 1)
[DE92-011533] p 3910 N92-31661
SATELLITE ATTITUDE CONTROL
Extended Kalman filter for attitude estimation of the Earth Radiation Budget Satellite p 3748 N92-31876
SATELLITE COMMUNICATION
Soviet satellite communications science and technology
[PB92-173038] p 3809 N92-31920
Advances in small satellite communication systems
[TABES PAPER 92-411] p 3763 N92-32010
Decision-making guide for the proposed Coast Guard differential global positioning system
[AD-A246046] p 3756 N92-32054
EHF SATCOM frequency hopping pattern generator: Proof of concept
[DREO-89-32] p 3811 N92-32231
SATELLITE CONTROL
Extended Kalman filter for attitude estimation of the Earth Radiation Budget Satellite p 3748 N92-31876
SATELLITE DESIGN
Advances in small satellite communication systems
[TABES PAPER 92-411] p 3763 N92-32010
Spacecraft stability and control
[TABES PAPER 92-414] p 3763 N92-32011
SATELLITE IMAGERY
Cloud-to-ground lightning characteristics in mesoscale convective systems
[AD-A250418] p 3858 N92-31493
A comparative analysis of the temporal variability of lightning observations and GOES imagery
[AD-A250185] p 3860 N92-31603
A real time system for multisensor image analysis through pyramidal segmentation
[AD-A247169] p 3888 N92-31981
SATELLITE INSTRUMENTS
True covariance simulation of the EUVE (extreme ultra violet explorer) update filter p 3748 N92-31878
SATELLITE INTERCEPTORS
Monitoring threats to satellite functions
[PB92-195445] p 3767 N92-32073
SATELLITE NETWORKS
Advances in small satellite communication systems
[TABES PAPER 92-411] p 3763 N92-32010
SATELLITE OBSERVATION
Images simulation of sensors with large field of view from images of sensors with less field of view: The SSR/TM case
[INPE-5378-TDI/473] p 3845 N92-32220
SATELLITE ORBITS
GPS satellite orbit determination using pseudorange data: Experiments and results
[PB92-178870] p 3765 N92-31685
SATELLITE ORIENTATION
True covariance simulation of the EUVE (extreme ultra violet explorer) update filter p 3748 N92-31878
SATELLITE POWER TRANSMISSION
Application of reactor-pumped lasers to power beaming
[DE92-012370] p 3831 N92-31762
SATELLITE ROTATION
True covariance simulation of the EUVE (extreme ultra violet explorer) update filter p 3748 N92-31878
SATELLITE-TO-SATELLITE TRACKING
Satellite-to-satellite tracking in the high-low mode: Line-of-sight acceleration in a residual gravity field
[PL-TR-91-2209] p 3767 N92-32082
SCALARS
Towards understanding turbulent scalar mixing
[NASA-CR-4446] p 3826 N92-32242
SCALE (CORROSION)
Oxidation/sulfidation behavior of Fe-Cr alloys: A reactive-element effect
[DE92-016172] p 3789 N92-31924
SCALE EFFECT
Numerical simulation of geometric scale effects in cylindrical self-field MPD thrusters
[NASA-CR-189224] p 3772 N92-32239
SCALE MODELS
Wind tunnel aerodynamic characteristics of a transport-type airfoil in a simulated heavy rain environment
[NASA-TP-3184] p 3751 N92-31532
Preliminary design for a MAGLEV development facility
[DE92-012259] p 3835 N92-31774
Structural similitude and scaling laws for laminated beam-plates
[NASA-CR-190585] p 3841 N92-31911

Transonic wind tunnel test of a 14 percent thick oblique wing
[NASA-TM-102230] p 3754 N92-32213

SCALING LAWS
Amending the w* velocity scale for surface layer, entrainment zone, and baroclinic shear in mixed Forced/Free turbulent convection
[AD-A250389] p 3859 N92-31540
Structural similitude and scaling laws for laminated beam-plates
[NASA-CR-190585] p 3841 N92-31911

SCANNERS
A sensitivity study of daytime visibility determination with the horizon scanning imager
[SIO-91-15] p 3902 N92-32144

SCANNING
Analysis of random induced cross polarization
[AD-A249773] p 3806 N92-31569

SCANNING TUNNELING MICROSCOPY
Surface structures and surface processes of ceramics with atomic resolutions: A study by scanning tunneling microscopy
[AD-A249581] p 3792 N92-31377
Correlation from randomness: Quantitative analysis of sputtered graphite surfaces using the scanning tunneling microscope
[AD-A252420] p 3783 N92-31820

SCATTER PROPAGATION
Single crystal growth optimization of magnesium-doped lithium niobate
[AD-A250781] p 3914 N92-32207

SCATTERING
Monte Carlo simulations of random rough surface scattering with finite element and finite difference methods
[AD-A247528] p 3901 N92-31430
Research in regional seismology: The effect of anisotropy
[AD-A248940] p 3855 N92-31476
Computer simulation of scattered ion and sputtered species effects in ion beam sputter-deposition of high temperature superconducting thin films
[DE92-015227] p 3909 N92-31546

SCATTERING AMPLITUDE
Theoretical atomic collision physics
[DE92-013571] p 3895 N92-31724

SCATTEROMETERS
OSRMS: The DREP near-nadir scatterometer
[DREP-88-15] p 3844 N92-32216

SCAVENGING
Numerical simulation of precipitation scavenging and comparison with observation of prescribed forest fires
[DE92-013513] p 3851 N92-31423

SCHEDULING
Sequential estimation of optimal age replacement policies when distribution of lifetimes is phase type
[AD-A249020] p 3836 N92-31479
Sources of unbounded priority inversions in real-time systems and a comparative study of possible solutions
[NASA-CR-190711] p 3875 N92-31486
Heuristic sampling on DAGs
[DE92-017359] p 3917 N92-32037

SCHOOLS
International mathematics and science assessments: What have we learned
[PB92-183599] p 3916 N92-32160

SCHOTTKY DIODES
Laser material interactions
[AD-A250028] p 3831 N92-31602

SCIENCE
International mathematics and science assessments: What have we learned
[PB92-183599] p 3916 N92-32160

SCIENTIFIC SATELLITES
The interplanetary heavy ion environment for both galactic cosmic rays and solar energetic particles during the CRRES mission
[AD-A248942] p 3926 N92-31477

SCIENTISTS
Results of earth observation study on STS-31 for Terra Geode, January 1987 - June 1991
[AD-A250750] p 3844 N92-31621

SCINTILLATION COUNTERS
Efficiency calculations of the hadron detector
[NIKHEF-K-EMIN-92-01] p 3896 N92-31814

SCORING
A comparison of the performance of two gust front detection algorithms using a length-based scoring technique
[AD-A250862] p 3863 N92-32103

SEA STATES
Parameterization of directional spectra, part 2, volume 1
[DREA-CR-89-445-PT-2-VOL-1] p 3811 N92-32214

SEA SURFACE TEMPERATURE
Updated forecast of Atlantic seasonal hurricane activity for 1992 p 3859 N92-31583

SEA WATER
World ocean circulation experiment. WOCE chlorofluorocarbon intercomparison cruise report
[PB92-185974] p 3865 N92-31842

SEARCH PROFILES
Non Boolean search methods in information retrieval p 3921 N92-32187

SEARCHING
Search strategies in natural language p 3921 N92-32186

SEAS
One thousand days non-stop at sea: Lessons for a mission to Mars
[TABES PAPER 92-462] p 3764 N92-32020

SEATS
Vertical impact tests of humans and anthropomorphic manikins
[AD-A245866] p 3872 N92-31458

SECONDARY EMISSION
Dependence of secondary ion emission from organic material on the energy loss of the impacting heavy ion
[DE92-014845] p 3893 N92-31386

SEDIMENT TRANSPORT
Geomorphic variability in the coastal zone
[AD-A252713] p 3864 N92-31544

SEDIMENTS
Deep-tow acoustics/geophysics system compressional velocity database
[AD-A252700] p 3918 N92-31467

SEGMENTS
A real time system for multisensor image analysis through pyramidal segmentation
[AD-A247169] p 3888 N92-31981

SEISMIC WAVES
Data to test and evaluate the performance of neural network architectures for seismic signal discrimination, neural computing for seismic phase identification, volume 2
[AD-A252442] p 3884 N92-31293
Time domain regional discriminants
[AD-A249949] p 3855 N92-31509

SEISMOLOGY
Data to test and evaluate the performance of neural network architectures for seismic signal discrimination, neural computing for seismic phase identification, volume 2
[AD-A252442] p 3884 N92-31293
Deep-tow acoustics/geophysics system compressional velocity database
[AD-A252700] p 3918 N92-31467
Research in regional seismology: The effect of anisotropy
[AD-A248940] p 3855 N92-31476
Time domain regional discriminants
[AD-A249949] p 3855 N92-31509
Two-dimensional axisymmetric calculations of surface waves generated by an explosion in an island, mountain, and sedimentary basin
[AD-A249971] p 3856 N92-31510

SELECTIVE DISSEMINATION OF INFORMATION
An alternative to sneakernet
[DE92-011146] p 3918 N92-31448

SELENIDES
Development of a computer model for polycrystalline thin-film CuInSe2 and CdTe solar cells
[DE92-001242] p 3846 N92-31526

SELF ORGANIZING SYSTEMS
A simple linearized learning algorithm which outperforms back-propagation
[AD-A249697] p 3877 N92-31642

SEMANTICS
Programming with inductive and co-inductive types
[AD-A249562] p 3874 N92-31353
Systematic detection of parallelism in ordinary programs
[AD-A247514] p 3882 N92-31445
Towards a complete hierarchy of compositional dataflow models
[RUU-CS-91-45] p 3807 N92-31715
Full abstraction and the context lemma
[AD-A247062] p 3887 N92-32163
Polymorphic type assignment and CPS conversion
[AD-A250954] p 3887 N92-32171

SEMICONDUCTING FILMS
Development of a computer model for polycrystalline thin-film CuInSe2 and CdTe solar cells
[DE92-001242] p 3846 N92-31526

SEMICONDUCTOR DEVICES
International Semiconductor Device Research Symposium (ISDRS-91)
[AD-A249348] p 3813 N92-31373
International Semiconductor Device Research Symposium (ISDRS-91)
[AD-A247394] p 3908 N92-31537
A semiconductor bridge ignited gas generator
[DE92-014049] p 3781 N92-31748
Femtosecond photonics: Fundamental phenomena and device behavior
[AD-A250506] p 3832 N92-32042

SEMICONDUCTOR JUNCTIONS
Advanced high efficiency concentrator cells
[DE92-010559] p 3848 N92-31893

SEMICONDUCTOR LASERS
Stable integrated microwave to optical modulator
[AD-A249974] p 3813 N92-31431

SEMICONDUCTORS (MATERIALS)
Electronic and total energy properties of ternary and quaternary semiconductor compounds, alloys, and superlattices: Theoretical study of Cu/graphite bonding
[NASA-CR-190691] p 3772 N92-31266
Electronics and electrical engineering laboratory technical publication announcements covering laboratory programs, July to September 1991, with 1992 EEEL events calendar
[PB92-181239] p 3813 N92-31367
International Semiconductor Device Research Symposium (ISDRS-91)
[AD-A249348] p 3813 N92-31373
Synthesis of soluble alpha-thiophene oligomers. Monomer to octamer
[AD-A250082] p 3779 N92-31434
Submillimeter wave spectroscopy of heterojunction superlattices
[AD-A250835] p 3908 N92-31496
Research on stable, high-efficiency amorphous silicon multijunction modules
[DE92-001244] p 3814 N92-31525
New sources for OMVPE
[AD-A250903] p 3909 N92-31582
Stress and phase transformation phenomena in oxide films
[DE92-014702] p 3910 N92-31665
A comparison of interstitial oxygen calculated by different techniques
[DE92-011658] p 3910 N92-31668
Theory of semiconducting superlattices and microstructures
[AD-A248758] p 3816 N92-31799
Laser material interactions
[AD-A250028] p 3831 N92-31802
Advanced high efficiency concentrator cells
[DE92-010559] p 3848 N92-31893
Ionization potentials and electron affinities of semiconductor clusters determined via charge transfer reactions
[AD-A250943] p 3898 N92-32169

SENSITIVITY
Sensitivity analysis of hydrodynamic stability operators
[NASA-CR-189683] p 3822 N92-31535
A sensitivity study of daytime visibility determination with the horizon scanning imager
[SIO-91-15] p 3902 N92-32144

SEPARATED FLOW
Fundamental studies of the structure of hypersonic attached and separated boundary layers over smooth, rough and transpiration-cooled surfaces
[AD-A250284] p 3819 N92-31286
A computational investigation of airfoil stall flutter
[AD-A247302] p 3751 N92-31300
Control of unsteady separated flow associated with the dynamic stall of airfoils
[NASA-CR-190688] p 3753 N92-32177

SEPARATORS
Ceramic membranes for high temperature hydrogen separation
[DE92-013342] p 3783 N92-31816

SEQUENCING
Programming with inductive and co-inductive types
[AD-A249562] p 3874 N92-31353

SERVICE LIFE
Research into improving the durability of the hot section in the aircraft turbine engine
[AD-A250342] p 3759 N92-31439
Understanding and managing the effects of battery charger and inverter aging
[DE92-014473] p 3815 N92-31651
Aging fleet: Maintaining airworthiness p 3745 N92-31862

SERVICE MODULES
Space Station mini pressurised logistics modules: An opportunity to enlarge and reinforce international cooperation
[TABES PAPER 92-425] p 3764 N92-32016
COMET: Commercial space opportunities through developed technologies
[TABES PAPER 92-453] p 3764 N92-32017

SERVOMECHANISMS
Backlash control via redundant drives: An experimental verification
[DE92-016368] p 3835 N92-31929
SERVOMOTORS
Dynamics of shuttle based flexible antenna system
[CRANFIELD-AERO-9203] p 3840 N92-31516
SETTLING
Macrostatistical hydrodynamics
[DE92-013589] p 3823 N92-31726
SHADES
Computer simulation of shading and blocking: Discussion of accuracy and recommendations
[DE91-002146] p 3849 N92-32110
SHADOWS
Detection of object edges in images containing cast shadows
[DE92-016092] p 3900 N92-31295
SHALLOW WATER
Computation of nonlinear gravity waves by a desingularized boundary integral method
[AD-A251149] p 3857 N92-31766
SHAPES
Exotic nuclear shapes and configurations that can be studied at high spin using radioactive ion beams
[DE92-016800] p 3898 N92-32090
SHEAR FLOW
A model for the interfacial shear in vertical, adiabatic, annular-mist flow
[DE92-013537] p 3820 N92-31424
Solid rocket combustion phenomena
[AD-A248006] p 3770 N92-31474
Heat transfer and flow of a modified second grade fluid
[DE92-014744] p 3824 N92-31895
Reynolds stress calculations of homogeneous turbulent shear flow with bounded energy states
[NASA-CR-189682] p 3826 N92-32158
SHEAR PROPERTIES
Composite material shear property measurement using the losipescu specimen
[NASA-CR-190661] p 3772 N92-31274
An experimental procedure for the losipescu composite specimen tested in the modified Wyoming fixture
[NASA-CR-190660] p 3774 N92-31566
Composite failure analysis handbook. Volume 1: Program review
[AD-A250520] p 3776 N92-32047
SHEAR STRESS
Composite material shear property measurement using the losipescu specimen
[NASA-CR-190661] p 3772 N92-31274
A numerical, analytical, and observational study of the effect of clouds on surface wind and wind stress during the central Arctic winter
[AD-A252706] p 3860 N92-31670
Electrically-induced stresses and deflection in multiple plates
[DE92-012303] p 3841 N92-31844
The design and testing of an optimal beam composed of unimodal elements p 3747 N92-31873
SHIELDING
Dynamic modeling of plasma-vapor interactions during plasma disruptions
[DE92-016183] p 3903 N92-31310
SHIFT REGISTERS
Optical interconnects in the computer environment
[AD-D015235] p 3873 N92-31269
SHIPS
One thousand days non-stop at sea: Lessons for a mission to Mars
[TABES PAPER 92-462] p 3764 N92-32020
SHOCK HEATING
Computer program to solve two-dimensional shock-wave interference problems with an equilibrium chemically reacting air model
[NASA-TM-4187] p 3818 N92-31247
SHOCK LAYERS
Stagnation-point heat-transfer rate predictions at aeroassist flight conditions
[NASA-TP-3208] p 3819 N92-31281
Stability of boundary layers at high supersonic and hypersonic speeds
[AD-A250900] p 3819 N92-31306
An approximate local thermodynamic nonequilibrium radiation model for air
[NASA-CR-190580] p 3914 N92-31577
The structure and control of three-dimensional shock wave turbulent boundary layer interactions
[AD-A250209] p 3823 N92-31824
Highly accurate prediction of unsteady viscous flows
[AD-A250982] p 3825 N92-32000
SHOCK SIMULATORS
Performance tests of a fast-acting valve for the driver tubes of a large blast/thermal simulator
[AD-A250035] p 3835 N92-31807
SHOCK TUBES
High-temperature ignition of propane with MTBE as an additive: Shock-tube experiments and modeling
[DE92-008933] p 3778 N92-31415
Elementary reaction rate measurements at high temperatures by tunable-laser flash-absorption
[DE92-015269] p 3830 N92-31684
Shock tube study of the reaction of triethanol ammonium nitrate with N2O
[AD-A250034] p 3800 N92-31804
Problems associated with launching hypervelocity projectiles from the fast shock tube
[DE92-015276] p 3762 N92-32026
SHOCK WAVE INTERACTION
Computer program to solve two-dimensional shock-wave interference problems with an equilibrium chemically reacting air model
[NASA-TM-4187] p 3818 N92-31247
The structure and control of three-dimensional shock wave turbulent boundary layer interactions
[AD-A250209] p 3823 N92-31824
Experimental studies of hypersonic shock-wave boundary-layer interactions
[NASA-CR-190731] p 3753 N92-32162
SHOCK WAVES
Advanced DAA methods for shock response analysis
[AD-A252696] p 3891 N92-31588
Turbulent dusty boundary layer in an ANFO surface-burst explosion
[DE92-012101] p 3822 N92-31625
Performance tests of a fast-acting valve for the driver tubes of a large blast/thermal simulator
[AD-A250035] p 3835 N92-31807
Automatic design of transonic airfoils to reduce the shock induced pressure drag p 3745 N92-31863
The use of high lift-to-drag hypersonic vehicles for aero-assisted orbital maneuvering p 3748 N92-31877
Experimental studies of hypersonic shock-wave boundary-layer interactions
[NASA-CR-190731] p 3753 N92-32162
Nonlinearly stable compact schemes for shock calculations
[NASA-CR-189663] p 3887 N92-32164
Weak ion-acoustic shock waves and double layers in non-collision plasma p 3907 N92-32208
SHOPS
Shop of the 1990's project: An evaluation tool for wireframe CAD software
[PB92-181130] p 3877 N92-31628
SHORELINES
Geomorphic variability in the coastal zone
[AD-A252713] p 3864 N92-31544
SHORT TAKEOFF AIRCRAFT
ASTOVL combat aircraft design synthesis and optimization
[CRANFIELD-AERO-9201] p 3757 N92-31515
SHORT WAVE RADIATION
Conversion of power and frequency
[DE92-012543] p 3810 N92-32134
SHROUDED TURBINES
Turbine blade tip and seal clearance excitation forces
[NASA-CR-184341] p 3760 N92-31910
SICKNESSES
Body water homeostasis and human performance in high heat environments: Fluid hydration recommendations for Operation Desert Storm
[AD-A249772] p 3868 N92-31492
SIGNAL ANALYZERS
An improved ion guide for external ion injection in glow discharge-Fourier transform ion cyclotron resonance (GD-FTICR) mass spectrometry
[AD-A250944] p 3900 N92-32170
SIGNAL DETECTION
Signal location using generalized linear constraints
[AD-A249580] p 3805 N92-31376
Detection of signal harmonic sets
[DREA-CR-89-420] p 3806 N92-31471
Time domain regional discriminants
[AD-A249949] p 3855 N92-31509
Coherent/noncoherent detection of coherent optical heterodyne DPSK-CDMA and MFSK-CDMA signals
[AD-A246215] p 3809 N92-31993
SIGNAL ENCODING
Optical oversampled analog-to-digital conversion
[AD-A252695] p 3877 N92-31587
Data compression techniques p 3922 N92-32190
SIGNAL MEASUREMENT
Remote sensing of trapping layer base height using ATIS transmissions
[AD-A250074] p 3844 N92-31362
SIGNAL PROCESSING
Electronics and electrical engineering laboratory technical publication announcements covering laboratory programs, July to September 1991, with 1992 EEEL events calendar
[PB92-181239] p 3813 N92-31367
Acoustic studies of ocean surface processes in SWAPP
[AD-A247519] p 3864 N92-31429
Final report on DSA methods for monitoring alumina in aluminum reduction cells with cermet anodes
[DE92-013599] p 3813 N92-31440
Readily implemented enhanced sinusoid detection in noise
[DE92-011359] p 3806 N92-31449
Detection of signal harmonic sets
[DREA-CR-89-420] p 3806 N92-31471
Optical oversampled analog-to-digital conversion
[AD-A252695] p 3877 N92-31587
Beam position monitor electronics using DC coupled demodulating logarithmic amplifiers
[DE92-011697] p 3816 N92-31760
Signal processing and recognition in adaptive neural networks
[AD-A250505] p 3885 N92-32041
Wavelet signal processing for transient feature extraction
[AD-A250519] p 3890 N92-32046
VLSI for high-speed digital signal processing
[AD-A250365] p 3817 N92-32074
Optical computing and optical signal processing, phase 1
[AD-A250551] p 3902 N92-32092
Experiment on a three-beam adaptive array for EHF frequency-hopped signals using a fast algorithm, phase-D
[CTN-92-60322] p 3810 N92-32203
SIGNAL REFLECTION
An empirical prediction algorithm for low-frequency acoustic surface scattering strengths
[AD-A250508] p 3892 N92-32044
SIGNAL TO NOISE RATIOS
Data to test and evaluate the performance of neural network architectures for seismic signal discrimination, neural computing for seismic phase identification, volume 2
[AD-A252442] p 3884 N92-31293
A robust algorithm for isotropic reconstruction of magic-angle spinning solid-state NMR spectra
[AD-A249610] p 3874 N92-31379
Readily implemented enhanced sinusoid detection in noise
[DE92-011359] p 3806 N92-31449
The NSLS 100 element solid state array detector
[DE92-014477] p 3827 N92-31502
A detector for stationary gas bubbles: Feasibility studies
[AD-A250135] p 3828 N92-31794
Square-law device analysis for the detection and timing estimation of a burst BPSK signal
[DREO-91-6] p 3809 N92-31921
SIGNAL TRANSMISSION
Electronics and electrical engineering laboratory technical publication announcements covering laboratory programs, July to September 1991, with 1992 EEEL events calendar
[PB92-181239] p 3813 N92-31367
Optical interferometric sensor detected intensity noise reductions means
[AD-D015296] p 3902 N92-32137
SILANES
Linear and star-branched siloxy-silane polymers: One pot A-B polymerization and end-capping
[AD-A252195] p 3792 N92-31408
Ring-opening polymerization of strained cyclotetrasilanes as a new route towards well defined polysilylenes
[AD-A251020] p 3795 N92-31941
Cationic ring opening polymerization of oxazolines initiated by trimethylsilyl derivatives
[AD-A251109] p 3798 N92-32153
SILICA GEL
Polyalphaolefins: A new improved cost effective aircraft radar coolant
[AD-A250517] p 3796 N92-32045
SILICATES
Analyses and predictions of the thermodynamic properties and phase diagrams of silicate systems
[DE92-016177] p 3783 N92-31857
Physical characterization of magmatic liquids
[DE92-015302] p 3858 N92-32027
SILICIDES
Superplasticity in a nickel silicide alloy, Ni3Si(V, Mo)
[DE92-011651] p 3787 N92-31667
SILICON
Characterization of oxide formed on silicon by exposure to atomic oxygen in space
[AD-A249787] p 3778 N92-31301
A comparison of interstitial oxygen calculated by different techniques
[DE92-011658] p 3910 N92-31688

SILICON ALLOYS
Research on stable, high-efficiency amorphous silicon multijunction modules
[DE92-001244] p 3814 N92-31525
SILICON CARBIDES
Gibbs free energy of reactions involving SiC, Si3N4, H2, and H2O as a function of temperature and pressure
[NASA-TP-3275] p 3791 N92-31278
Interface engineering in alumina/glass composites
[AD-A248587] p 3773 N92-31315
Surface structures and surface processes of ceramics with atomic resolutions: A study by scanning tunneling microscopy
[AD-A249581] p 3792 N92-31377
International Semiconductor Device Research Symposium (ISDRS-91)
[AD-A247394] p 3908 N92-31537
Thermomechanical fatigue behavior of a silicone carbide fiber-reinforced calcium aluminosilicate glass-ceramic matrix composite
[AD-A249870] p 3775 N92-31823
The synthesis and characterization of tribophysical layers on diamond and silicon carbide surfaces
[AD-A250983] p 3796 N92-32001
Effects of fiber and interfacial layer architectures on the thermoplastic response of metal matrix composites
[NASA-TM-105802] p 3777 N92-32234
SILICON COMPOUNDS
Linear and star-branched siloxy-silane polymers: One pot A-B polymerization and end-capping
[AD-A252195] p 3792 N92-31408
SiGe Si quantum wires for efficient, room temperature, tunable luminescence
[AD-A249651] p 3814 N92-31464
SILICON FILMS
Pulsed laser deposition of high Tc superconducting thin films
[AD-A250657] p 3830 N92-31319
Growth, nitrogen vacancy reduction and solid solution formation in cubic GaN thin films and the subsequent fabrication of superlattice structures using AlN and InN
[AD-A248058] p 3908 N92-31446
SILICON JUNCTIONS
SiGe Si quantum wires for efficient, room temperature, tunable luminescence
[AD-A249651] p 3814 N92-31464
SILICON NITRIDES
Gibbs free energy of reactions involving SiC, Si3N4, H2, and H2O as a function of temperature and pressure
[NASA-TP-3275] p 3791 N92-31278
Growth, nitrogen vacancy reduction and solid solution formation in cubic GaN thin films and the subsequent fabrication of superlattice structures using AlN and InN
[AD-A248058] p 3908 N92-31446
Effect of surface modifications on the properties of silicon nitride ceramics
[DE92-013848] p 3797 N92-32094
SILICON OXIDES
Sol-gel multilayers applied by a meniscus coating process
[DE92-012697] p 3794 N92-31560
A fast laser alloying process for the selective electroplating of metal on SiO2 and polyimide
[DE92-011764] p 3788 N92-31759
SILICON RADIATION DETECTORS
The NSLS 100 element solid state array detector
[DE92-014477] p 3827 N92-31502
Neutron radiation damage to silicon detectors
[ITN-92-85162] p 3897 N92-31958
SILICONE RUBBER
High density thin-walled syntactic foam
[DE92-013159] p 3797 N92-32136
SILOXANES
Linear and star-branched siloxy-silane polymers: One pot A-B polymerization and end-capping
[AD-A252195] p 3792 N92-31408
Cyclopolymerization of metalloid-containing alpha, omega-dienes. 1,3-divinyltetramethyldisiloxane, 1,3-divinyltetramethyldisilazane and 1,3-divinylpentamethyldisilazane
[AD-A250347] p 3794 N92-31557
SILVER ALLOYS
The role of metal structure in determining solvent orientation at the electrode/solution interface
[AD-A249751] p 3893 N92-31328
SIMD (COMPUTERS)
A sweep algorithm for massively parallel simulation of circuit-switched networks
[NASA-CR-189680] p 3881 N92-32157
SIMILARITY THEOREM
Structural similitude and scaling laws for laminated beam-plates
[NASA-CR-190585] p 3841 N92-31911
SIMILITUDE LAW
Structural similitude and scaling laws for laminated beam-plates
[NASA-CR-190585] p 3841 N92-31911
SIMPLEX METHOD
A strictly improving phase 1 algorithm using least-squares subproblems
[DE92-015904] p 3875 N92-31410
SIMULATION
The Swendsen-Wang dynamics in the simulation of the Ising model
[INPE-5394-PRE/1752] p 3874 N92-31348
Modal simulation of gearbox vibration with experimental correlation
[NASA-TM-105702] p 3834 N92-31485
Importance sampling for Markov chains: Asymptotics for the variance
[AD-A249804] p 3888 N92-31757
Simulation study of stepwise relaxation in a spheromak plasma
[DE92-782101] p 3906 N92-31843
A simulation model of a single rotor helicopter
p 3746 N92-31865
Time simulation of flutter with large stiffness changes
[NASA-TM-107650] p 3758 N92-32111
A sweep algorithm for massively parallel simulation of circuit-switched networks
[NASA-CR-189680] p 3881 N92-32157
SIMULATORS
Design of a TEM cell EMP simulator
[DREO-1084] p 3806 N92-31470
A frequency hopping synthesizer controller for EHF SATCOM
[DREO-89-29] p 3811 N92-32232
SINE WAVES
Readily implemented enhanced sinusoid detection in noise
[DE92-011359] p 3806 N92-31449
SINGLE CRYSTALS
Electronic and total energy properties of ternary and quaternary semiconductor compounds, alloys, and superlattices: Theoretical study of Cu/graphite bonding
[NASA-CR-190691] p 3772 N92-31266
Organometallic Nonlinear Optical (NLO) polymers. Part 2: Synthesis of main-chain organometallic polymers and a structural study of ferrocene NLO-Phores
[AD-A250655] p 3791 N92-31318
The role of metal structure in determining solvent orientation at the electrode/solution interface
[AD-A249751] p 3893 N92-31328
Fatigue in single crystal nickel superalloys
[AD-A250068] p 3786 N92-31360
Surface structures and surface processes of ceramics with atomic resolutions: A study by scanning tunneling microscopy
[AD-A249581] p 3792 N92-31377
The synthesis and characterization of new copper coordination complexes containing an asymmetric coordinating chelate ligand: Application to enzyme active site modeling
[DE92-011532] p 3786 N92-31391
Growth, nitrogen vacancy reduction and solid solution formation in cubic GaN thin films and the subsequent fabrication of superlattice structures using AlN and InN
[AD-A248058] p 3908 N92-31446
The crystal growth and characterization of the solid solutions (ZnS)(1-x)(CuMS2)(x)
[AD-A248029] p 3911 N92-31819
Synthesis, structure and properties of Ba6Co25S27: A Perovskite-like superstructure of Co8S6 and Ba6S clusters
[AD-A251041] p 3911 N92-31848
The synthesis and characterization of tribophysical layers on diamond and silicon carbide surfaces
[AD-A250983] p 3796 N92-32001
The chemistry and packaging of nanocomposite confined arrays
[AD-A250991] p 3817 N92-32002
Fatigue in single crystal nickel superalloys
[AD-A252492] p 3790 N92-32066
Single crystal growth optimization of magnesium-doped lithium niobate
[AD-A250781] p 3914 N92-32207
SINGULARITY (MATHEMATICS)
Phase portraits of non degenerate quadratic systems with zero finite multiplicity
[REPT-91-96] p 3886 N92-31520
Feynman diagrams and Vassiliev invariants
[PB92-178284] p 3890 N92-31925
SINTERING
Ceramic surfaces and sintering
[DE92-011570] p 3793 N92-31538
Effect of surface modifications on the properties of silicon nitride ceramics
[DE92-013848] p 3797 N92-32094
Tetragonal zirconia ceramics in ZrO2-CeO2 system (Ce-TZP): Preparation, characterization and mechanical properties
[INPE-5372-PRE/1746] p 3798 N92-32199
Ba2Ti9O20 microwave dielectric resonator: Processing, phase synthesis and characterization
[INPE-5373-PRE/1747] p 3818 N92-32200
SISO (CONTROL SYSTEMS)
Flutter suppression digital control law design and testing for the AFW wind-tunnel model
[NASA-TM-107652] p 3757 N92-31350
SITE SELECTION
Outdoor testing of advanced optical materials for solar thermal electric applications
[DE92-010567] p 3847 N92-31623
Preliminary design for a MAGLEV development facility
[DE92-012259] p 3835 N92-31774
SIZE DETERMINATION
A detector for stationary gas bubbles: Feasibility studies
[AD-A250135] p 3828 N92-31794
SIZE DISTRIBUTION
Acoustic studies of ocean surface processes in SWAPP
[AD-A247519] p 3864 N92-31429
A detector for stationary gas bubbles: Feasibility studies
[AD-A250135] p 3828 N92-31794
The mechanics of fractal damage
[AD-A250518] p 3776 N92-32075
SKIN FRICTION
Fundamental studies of the structure of hypersonic attached and separated boundary layers over smooth, rough and transpiration-cooled surfaces
[AD-A250284] p 3819 N92-31286
SLEEP DEPRIVATION
Micro saint model of fatigue assessment
[AD-A249976] p 3868 N92-31554
SLIDING FRICTION
Tribology of functionally-terminated oligomer films
[AD-A250076] p 3833 N92-31433
SLOPES
Granular flows down bumpy inclines
[DE92-013568] p 3820 N92-31425
Hydrographic and Acoustic Doppler Current Profiler (ADCP) data from the Farallones shelf and slope study
[AD-A250834] p 3864 N92-31495
SLOT ANTENNAS
Scattering from a finite collection of transverse dipole and axial slot arrays with edge effects
[AD-A249622] p 3807 N92-31691
SLOTS
Modeling arbitrarily directed slots that are narrow both in width and depth with regard to the FDTD spatial cell
[DE92-008015] p 3808 N92-31738
SLURRIES
Research and development of advanced nickel-iron batteries for electric vehicle propulsion
[DE92-014099] p 3817 N92-31834
Rheology of zirconia-alumina gelcasting slurries
[DE92-016787] p 3797 N92-32089
The development of precipitated iron catalysts with improved stability
[DE92-014630] p 3785 N92-32117
Thin polymer icemaker development and test program
[DE92-016941] p 3803 N92-32125
SMOKE
Numerical simulation of precipitation scavenging and comparison with observation of prescribed forest fires
[DE92-013513] p 3851 N92-31423
Nonthermal inhalation injury
[AD-A252532] p 3869 N92-31962
SNOW
Annual dynamics within the active layer
[DE92-013520] p 3850 N92-31304
Hydrological and geochemical response and recovery in disturbed Arctic ecosystems
[DE92-016223] p 3850 N92-31312
A numerical, analytical, and observational study of the effect of clouds on surface wind and wind stress during the central Arctic winter
[AD-A252706] p 3860 N92-31670
SOCIAL FACTORS
Minorities and air quality non-attainment areas: A preliminary geo-demographic analysis
[DE92-013054] p 3852 N92-31591
SODIUM
Sodium Heat Engine Development Program
[DE92-012398] p 3846 N92-31531
SOFTWARE ENGINEERING
Assessing repository technology. Where do we go from here?
[NASA-CR-190630] p 3917 N92-31272

Reducing requirements errors through the use of Computer-Aided Software Engineering (CASE) tools and during requirements analysis
[AD-A246879] p 3874 N92-31299
Architectural adaptability in parallel programming
[AD-A247516] p 3881 N92-31428
The development of modularized software for empirical testing of new algorithms in linear programming
[AD-A250811] p 3875 N92-31480
Requirements Engineering and Analysis Workshop Proceedings
[AD-A250415] p 3876 N92-31541
About real time industrial processes control: A methodology based on objects and Petri nets
[LAAS-91467] p 3878 N92-31689
Configuration management and software measurement in the Ground Systems Development Environment (GSDE)
[NASA-CR-190716] p 3879 N92-31787

SOFTWARE TOOLS
Reducing requirements errors through the use of Computer-Aided Software Engineering (CASE) tools and during requirements analysis
[AD-A246879] p 3874 N92-31299
A performance-based comparison of object-oriented simulation tools
[AD-A252125] p 3875 N92-31405
The development of modularized software for empirical testing of new algorithms in linear programming
[AD-A250811] p 3875 N92-31480
PARTI primitives for unstructured and block structured problems
[NASA-CR-189662] p 3876 N92-31561
Development of wavelet analysis tools for turbulence
[NASA-CR-189674] p 3822 N92-31564
Quality Evaluation System (QUES), volume 1
[AD-A252679] p 3876 N92-31586
The Matrix Editor for symbolic Jacobians in ALPAL
[DE92-008076] p 3878 N92-31742
New algorithms for the minimal form problem
[DE92-011963] p 3879 N92-31743
Hypertext and hypermedia systems in information retrieval p 3921 N92-32188

SOIL EROSION
Geomorphic variability in the coastal zone
[AD-A252713] p 3864 N92-31544

SOIL MOISTURE
An airborne study of boundary layer heat and moisture fluxes for project FIFE
[NASA-CR-190665] p 3844 N92-31357
A test of ecological optimality for semiarid vegetation
[NASA-CR-190705] p 3855 N92-32222

SOIL SCIENCE
A test of ecological optimality for semiarid vegetation
[NASA-CR-190705] p 3855 N92-32222

SOILS
Robotic soil sampler for hazardous waste clean up
[DE92-012693] p 3780 N92-31565
A dynamic model of terrestrial carbon cycling
[DE92-015130] p 3853 N92-31782
Development of methodology and technology for identifying and quantifying emission products from open burning and open detonation thermal treatment methods. Field test series A, B, and C. Volume 1: Test summary
[AD-A250735] p 3800 N92-31971
Development of methodology and technology for identifying and quantifying emission products from open burning and open detonation thermal treatment methods. Field test series A, B, and C. Volume 2, part A: Quality assurance and quality control
[AD-A250736] p 3801 N92-31972
Development of methodology and technology for identifying and quantifying emission products from open burning and open detonation thermal treatment methods. Field test series A, B, and C. Volume 2, part B: Quality assurance and quality control. Appendices
[AD-A250737] p 3801 N92-31973

SOL-GEL PROCESSES
Sol-gel multilayers applied by a meniscus coating process
[DE92-012697] p 3794 N92-31560

SOLAR ACTIVITY
Solar-geophysical data number 572, April 1992. Part 1: (Prompt reports). Data for March, February 1992, and late data
[PB92-187723] p 3856 N92-31637
Solar-geophysical data number 572, April 1992. Part 2: (Comprehensive reports). Data for October 1991 and miscellaneous
[PB92-187731] p 3856 N92-31639
High-resolution microwave observations of the sun
[AD-A247869] p 3925 N92-31985
Fine structure superimposed on mm-wavelength (18-23 GHz) spectra of solar active region
[INPE-5371-TDI/470] p 3926 N92-32221

SOLAR ACTIVITY EFFECTS
Evolution of the solar and coronal field structure: 1976-1991
[AD-A250097] p 3925 N92-31786
High-latitude spacecraft charging in low-Earth polar orbit
[AD-A249868] p 3767 N92-31822

SOLAR ATMOSPHERE
A solar magnetic and velocity field measurement system for Spacelab 2: The Solar Optical Universal Polarimeter (SOUP)
[NASA-CR-190683] p 3925 N92-31856

SOLAR CELLS
Module process optimization and device efficiency improvement for stable, low-cost, large-area, cadmium telluride-based photovoltaic module production
[DE92-010564] p 3846 N92-31497
Research on stable, high-efficiency amorphous silicon multijunction modules
[DE92-001244] p 3814 N92-31525
Development of a computer model for polycrystalline thin-film CuInSe2 and CdTe solar cells
[DE92-001242] p 3846 N92-31526
Photovoltaic subcontract program, FY 1991
[DE92-001248] p 3847 N92-31646
Advanced high efficiency concentrator cells
[DE92-010559] p 3848 N92-31893
Monolithic and mechanical multijunction space solar cells
[NASA-TM-105832] p 3818 N92-32233

SOLAR COLLECTORS
Module process optimization and device efficiency improvement for stable, low-cost, large-area, cadmium telluride-based photovoltaic module production
[DE92-010564] p 3846 N92-31497
Outdoor testing of advanced optical materials for solar thermal electric applications
[DE92-010567] p 3847 N92-31623
Advanced high efficiency concentrator cells
[DE92-010559] p 3848 N92-31893
Design, fabrication, and testing of a 30 kW(sub t) screen-wick heat-pipe solar receiver
[DE92-016500] p 3848 N92-32087
Desiccant cooling using unglazed transpired solar collectors
[DE92-010568] p 3849 N92-32112

SOLAR CORONA
Evolution of the solar and coronal field structure: 1976-1991
[AD-A250097] p 3925 N92-31786

SOLAR CYCLES
Evolution of the solar and coronal field structure: 1976-1991
[AD-A250097] p 3925 N92-31786
High-latitude spacecraft charging in low-Earth polar orbit
[AD-A249868] p 3767 N92-31822

SOLAR ENERGY
Solar synthesis of advanced materials: A solar industrial program initiative
[DE92-010575] p 3845 N92-31481
Solar thermal energy storage in phase change materials
[DE92-016908] p 3849 N92-32091

SOLAR ENERGY CONVERSION
Solar synthesis of advanced materials: A solar industrial program initiative
[DE92-010575] p 3845 N92-31481
Outdoor testing of advanced optical materials for solar thermal electric applications
[DE92-010567] p 3847 N92-31623
Photovoltaic subcontract program, FY 1991
[DE92-001248] p 3847 N92-31646
Design, fabrication, and testing of a 30 kW(sub t) screen-wick heat-pipe solar receiver
[DE92-016500] p 3848 N92-32087

SOLAR FLARES
The interplanetary heavy ion environment for both galactic cosmic rays and solar energetic particles during the CRRES mission
[AD-A248942] p 3926 N92-31477
Solar-geophysical data number 572, April 1992. Part 1: (Prompt reports). Data for March, February 1992, and late data
[PB92-187723] p 3856 N92-31637
Solar-geophysical data number 572, April 1992. Part 2: (Comprehensive reports). Data for October 1991 and miscellaneous
[PB92-187731] p 3856 N92-31639

SOLAR FLUX
Computer simulation of shading and blocking: Discussion of accuracy and recommendations
[DE91-002146] p 3849 N92-32110
Solar neutrinos: Theory versus experiment
[DE92-014327] p 3925 N92-32154

SOLAR FURNACES
Solar synthesis of advanced materials: A solar industrial program initiative
[DE92-010575] p 3845 N92-31481

SOLAR GENERATORS
Chemical energy storage system for SEGS solar thermal power plant
[DE92-012327] p 3848 N92-31845

SOLAR INTERIOR
Particle physics confronts the solar neutrino problem
[DE92-014013] p 3895 N92-31812

SOLAR MAGNETIC FIELD
Solar-geophysical data number 572, April 1992. Part 1: (Prompt reports). Data for March, February 1992, and late data
[PB92-187723] p 3856 N92-31637
Evolution of the solar and coronal field structure: 1976-1991
[AD-A250097] p 3925 N92-31786
A solar magnetic and velocity field measurement system for Spacelab 2: The Solar Optical Universal Polarimeter (SOUP)
[NASA-CR-190683] p 3925 N92-31856

SOLAR NEUTRINOS
Particle physics confronts the solar neutrino problem
[DE92-014013] p 3895 N92-31812
Solar neutrinos: Theory versus experiment
[DE92-014327] p 3925 N92-32154
Resonant enhancement of flavor-changing neutrino interactions
[DE92-013020] p 3898 N92-32167

SOLAR OSCILLATIONS
Solar neutrinos: Theory versus experiment
[DE92-014327] p 3925 N92-32154

SOLAR PHYSICS
Solar-geophysical data number 572, April 1992. Part 2: (Comprehensive reports). Data for October 1991 and miscellaneous
[PB92-187731] p 3856 N92-31639
Particle physics confronts the solar neutrino problem
[DE92-014013] p 3895 N92-31812

SOLAR POSITION
Sun-view-target geometry effects on spectrally-derived vegetative index estimates of absorbed radiation and leaf area
[AD-A249984] p 3843 N92-31329

SOLAR PROBES
A solar magnetic and velocity field measurement system for Spacelab 2: The Solar Optical Universal Polarimeter (SOUP)
[NASA-CR-190683] p 3925 N92-31856

SOLAR RADIATION
Effect of outer temperature changes and solar radiation on effective heat losses through external partitions of buildings p 3802 N92-31242

SOLAR RADIO BURSTS
Multiple electron populations accelerated in solar bursts
[INPE-5377-TDI/472] p 3925 N92-32025

SOLAR RADIO EMISSION
Solar-geophysical data number 572, April 1992. Part 1: (Prompt reports). Data for March, February 1992, and late data
[PB92-187723] p 3856 N92-31637

SOLAR TERRESTRIAL INTERACTIONS
The flow of plasma in the solar terrestrial environment
[NASA-CR-190200] p 3925 N92-31338

SOLAR THERMAL ELECTRIC POWER PLANTS
Chemical energy storage system for SEGS solar thermal power plant
[DE92-012327] p 3848 N92-31845

SOLAR WIND
Interaction of fast steady flow with slow transient flow: A new cause of interplanetary Bz events
[AD-A250273] p 3823 N92-31770
Impulsive magnetic perturbations of the high latitude, dayside ionosphere
[AD-A249872] p 3857 N92-31932

SOLDERED JOINTS
A ban on use of lead-bearing solders: Implications for the electronics industry
[DE92-013291] p 3790 N92-32139

SOLDERING
The sixteenth annual electronics manufacturing seminar proceedings
[AD-A247920] p 3814 N92-31461
Controlled atmosphere soldering system
[DE92-012633] p 3802 N92-31580
Energy and Environment: A Sandia Technology Bulletin
[DE92-016740] p 3854 N92-31931
Metallization of ferrite ceramic couplings
[DE92-016573] p 3789 N92-32032

SOLDERS
Controlled atmosphere soldering system
[DE92-012633] p 3802 N92-31580

A ban on use of lead-bearing solders: Implications for the electronics industry
[DE92-013291] p 3790 N92-32139
SOLID ELECTROLYTES
Sodium Heat Engine Development Program
[DE92-012398] p 3846 N92-31531
Batteries and fuel cells
[DE92-011493] p 3847 N92-31571
Solid electrolytes and impact-resistant ceramics
[DE92-015297] p 3797 N92-32095
SOLID LUBRICANTS
Tribology of Langmuir-Blodgett films
[AD-A250075] p 3833 N92-31363
Surface chemistry of MoS2 lubricant films: Effects of high humidity storage on sputtered films
[DE92-015392] p 3794 N92-31631
SOLID PROPELLANT COMBUSTION
Absorption spectroscopy through the dark zone of solid propellant flames
[AD-A250033] p 3782 N92-31803
Effect of inlet geometry on the flow and combustion processes in a solid fuel ramjet p 3747 N92-31871
SOLID SOLUTIONS
The crystal growth and characterization of the solid solutions (ZnS)(1-x)(CuMS2)(x)
[AD-A248029] p 3911 N92-31819
SOLID STATE
A robust algorithm for isotropic reconstruction of magic-angle spinning solid-state NMR spectra
[AD-A249610] p 3874 N92-31379
Synthesis, structure and properties of Ba6Co25S27: A Perovskite-like superstructure of Co8S6 and Ba6S clusters
[AD-A251041] p 3911 N92-31848
Dissociative electron attachment of O2: A solid-state effect on potential curve crossing
[AD-A246331] p 3913 N92-31995
SOLID STATE DEVICES
The NSLS 100 element solid state array detector
[DE92-014477] p 3827 N92-31502
SOLID STATE LASERS
Application of reactor-pumped lasers to power beaming
[DE92-012370] p 3831 N92-31762
SOLID STATE PHYSICS
Electronic states in systems of reduced dimensionality
[DE92-013588] p 3912 N92-31945
SOLID-SOLID INTERFACES
Role of interfaces and interphases in the evolution mechanics of material systems
[AD-A250410] p 3774 N92-31604
Energetics, bonding mechanism and electronic structure of metal/ceramic interfaces
[DE92-013401] p 3775 N92-31806
SOLIDIFICATION
Corrosion behavior of squeeze cast aluminum metal matrix composites
[AD-A250486] p 3774 N92-31382
SOLIDS
Steady flow of a fluid-solid mixture between parallel plates
[DE92-013645] p 3821 N92-31426
Development of the aspect graph representation for use in R version
[AD-A247109] p 3876 N92-31573
Theoretical studies of solid-fluid phase equilibria
[DE92-016598] p 3781 N92-31717
Real-time infrared spectroscopy of moving solids for on-line analyses
[DE92-012156] p 3782 N92-31772
EWE: A computer model for ultrasonic inspection
[DE92-627145] p 3837 N92-32143
SOLIDS FLOW
Granular flows down bumpy inclines
[DE92-013568] p 3820 N92-31425
SOLITARY WAVES
Three-wave envelope solitons: Can the speed of light in the fiber be controlled?
[AD-A247615] p 3901 N92-31611
Computation of nonlinear gravity waves by a desingularized boundary integral method
[AD-A251149] p 3857 N92-31766
Nonlinear partial differential equations and solitons
[MATHS-REPT-A-152] p 3886 N92-31956
Weak ion-acoustic shock waves and double layers in non-collision plasma p 3907 N92-32208
SOLUBILITY
Experimental studies of aluminum solubility and speciation in brines
[DE92-010448] p 3786 N92-31418
Recent developments in the fundamentals of gas permeation in rubbery polymers
[AD-A249745] p 3794 N92-31624
SOLUTIONS
Analyses and predictions of the thermodynamic properties and phase diagrams of silicate systems
[DE92-016177] p 3783 N92-31857
SOLVATION
Application of the mean spherical approximation to the estimations of single ion thermodynamic quantities of solvation for monoatomic monovalent ions in aqueous solutions
[AD-A250190] p 3893 N92-31316
Structure and dynamics of Cl(H2O)20 clusters. The effect of the polarizability and the charge ofthe ion
[AD-A251094] p 3899 N92-32196
SOLVENTS
The role of metal structure in determining solvent orientation at the electrode/solution interface
[AD-A249751] p 3893 N92-31328
Imide/arylene ether copolymers
[NASA-CASE-LAR-14159-1-CU] p 3794 N92-31792
Tris-triphenylsiloxy compounds of aluminum
[AD-A250141] p 3788 N92-31795
Vibrational modes and the dynamic solvent effect in electron and proton transfer
[AD-A250727] p 3897 N92-31950
Ultrafast studies on electron transfer in the betaines: Evidence for local heating
[AD-A250728] p 3897 N92-31999
SONAR
Acoustic studies of ocean surface processes in SWAPP
[AD-A247519] p 3864 N92-31429
Readily implemented enhanced sinusoid detection in noise
[DE92-011359] p 3806 N92-31449
SOUND PRESSURE
Near-field and far-field sound radiation from a line-driven fluid-loaded infinite flat plate having periodic and non-periodic attached rib stiffeners
[AD-A250100] p 3892 N92-31789
Optimum data analysis procedures for Titan 4 and Space Shuttle payload acoustic measurements during lift-off
[NASA-CR-190479] p 3892 N92-32178
Asymptotic modal analysis and statistical energy analysis
[NASA-CR-190516] p 3842 N92-32236
SOUND TRANSMISSION
Sensitivity of the tomographic inverse solution to acoustic path variability
[AD-A252146] p 3864 N92-31407
SOUND WAVES
Solid rocket combustion phenomena
[AD-A248006] p 3770 N92-31474
Three-wave envelope solitons: Can the speed of light in the fiber be controlled?
[AD-A247615] p 3901 N92-31611
Computer simulation of acoustic fluctuations due to finescale temperature perturbations measured by thermistor chain
[AD-A252709] p 3892 N92-31672
Near-field and far-field sound radiation from a line-driven fluid-loaded infinite flat plate having periodic and non-periodic attached rib stiffeners
[AD-A250100] p 3892 N92-31789
SOUNDING ROCKETS
Combined Release and Radiation Effects Satellite (CRRES) experiments data collection, analysis, and publication
[NASA-CR-184361] p 3856 N92-31551
SOURCE PROGRAMS
Computer applications for engineering/structural analysis
[DE92-013070] p 3841 N92-31745
SOUTH AMERICA
A coordinated study of a storm system over the South American continent
[INPE-5388-TDI/477] p 3863 N92-32212
SPACE BASES
Radiation protection for human exploration of the moon and Mars: Application of the MASH code system
[DE92-014416] p 3868 N92-31409
SPACE CHARGE
The 6-D phase space tracking with acceleration: Modeling low energy proton synchrotrons, part 1
[DE92-013744] p 3899 N92-31948
SPACE COMMERCIALIZATION
TABES 92: 8th Annual Technical and Business Exhibition and Symposium. Executive summaries and submitted papers p 3763 N92-32009
Robotics development for the enhancement of space endeavors
[TABES PAPER 92-445] p 3763 N92-32013
The trading company in space development in Japan
[TABES PAPER 92-424] p 3764 N92-32015
COMET: Commercial space opportunities through developed technologies
[TABES PAPER 92-453] p 3764 N92-32017
SPACEHAB: A giant step in the commercial development of space
[TABES PAPER 92-454] p 3764 N92-32018
NASA programs --- nasa space programs p 3765 N92-32238
SPACE EXPLORATION
Using space resources
[NASA-TM-107966] p 3924 N92-31781
Robotics development for the enhancement of space endeavors
[TABES PAPER 92-445] p 3763 N92-32013
NASA programs --- nasa space programs p 3765 N92-32238
SPACE FLIGHT
Relating space radiation environments to risk estimates
[DE92-010256] p 3926 N92-31756
SPACE HABITATS
Radiation protection for human exploration of the moon and Mars: Application of the MASH code system
[DE92-014416] p 3868 N92-31409
SPACE LABORATORIES
SPACEHAB: A giant step in the commercial development of space
[TABES PAPER 92-454] p 3764 N92-32018
SPACE LOGISTICS
Space Station mini pressurised logistics modules: An opportunity to enlarge and reinforce international cooperation
[TABES PAPER 92-425] p 3764 N92-32016
SPACE MISSIONS
Integrated Technology Plan for the Civil Space Program, 1991
[PB92-181692] p 3762 N92-31634
Soviet satellite communications science and technology
[PB92-173038] p 3809 N92-31920
TABES 92: 8th Annual Technical and Business Exhibition and Symposium. Executive summaries and submitted papers p 3763 N92-32009
Italian-US cooperation in space: The case of Tethered, IRIS/LAGEOS, and SPACEHAB
[TABES PAPER 92-467] p 3764 N92-32019
Monolithic and mechanical multijunction space solar cells
[NASA-TM-105832] p 3818 N92-32233
NASA programs --- nasa space programs p 3765 N92-32238
SPACE PLASMAS
The flow of plasma in the solar terrestrial environment
[NASA-CR-190200] p 3925 N92-31338
High-latitude spacecraft charging in low-Earth polar orbit
[AD-A249868] p 3767 N92-31822
SPACE POWER REACTORS
Free-piston Stirling engine conceptual design and technologies for space power, phase 1
[NASA-CR-182168] p 3769 N92-31245
Radiation protection for human exploration of the moon and Mars: Application of the MASH code system
[DE92-014416] p 3868 N92-31409
Potassium Rankine cycle nuclear power systems for spacecraft and lunar-mass surface power
[DE92-016163] p 3770 N92-31897
An overview of the Lewis Research Center CSTI thermal management program
[NASA-TM-105310] p 3771 N92-31916
A philosophy for space nuclear systems safety
[DE92-016501] p 3771 N92-32030
SP-100 reactor with Brayton conversion for lunar surface applications
[NASA-TM-105637] p 3771 N92-32108
SPACE PROGRAMS
Integrated Technology Plan for the Civil Space Program, 1991
[PB92-181692] p 3762 N92-31634
SPACE SHUTTLE ORBITERS
Ground and flight calibration assessment of HiRAP accelerometer data from missions STS-35 and STS-40
[NASA-TM-107602] p 3769 N92-32204
SPACE SHUTTLE PAYLOADS
Graphite/epoxy composite adapters for the Space Shuttle/Centaur vehicle
[NASA-TP-3014] p 3765 N92-31251
Optimum data analysis procedures for Titan 4 and Space Shuttle payload acoustic measurements during lift-off
[NASA-CR-190479] p 3892 N92-32178
SPACE SHUTTLES
Use of tissue equivalent proportional counters to characterize radiation quality on the space shuttle
[DE92-012347] p 3768 N92-31846
Optimum data analysis procedures for Titan 4 and Space Shuttle payload acoustic measurements during lift-off
[NASA-CR-190479] p 3892 N92-32178

SPACE STATION FREEDOM
Stability testing and analysis of a PMAD DC test bed for the Space Station Freedom
[NASA-TM-105846] p 3812 N92-31282
Configuration management and software measurement in the Ground Systems Development Environment (GSDE)
[NASA-CR-190716] p 3879 N92-31787
Space Station mini pressurised logistics modules: An opportunity to enlarge and reinforce international cooperation
[TABES PAPER 92-425] p 3764 N92-32016
SPACEHAB: A giant step in the commercial development of space
[TABES PAPER 92-454] p 3764 N92-32018

SPACE STATION POWER SUPPLIES
Stability testing and analysis of a PMAD DC test bed for the Space Station Freedom
[NASA-TM-105846] p 3812 N92-31282

SPACE TRANSPORTATION SYSTEM FLIGHTS
A solar magnetic and velocity field measurement system for Spacelab 2: The Solar Optical Universal Polarimeter (SOUP)
[NASA-CR-190683] p 3925 N92-31856

SPACE WEAPONS
Monitoring threats to satellite functions
[PB92-195445] p 3767 N92-32073

SPACE-TIME FUNCTIONS
Modified black holes in two dimensional gravity
[DE92-630244] p 3924 N92-31401

SPACEBORNE EXPERIMENTS
Analysis of systems hardware flown on LDEF. Results of the systems special investigation group
[NASA-CR-189628] p 3767 N92-31677
COMET: Commercial space opportunities through developed technologies
[TABES PAPER 92-453] p 3764 N92-32017
SPACEHAB: A giant step in the commercial development of space
[TABES PAPER 92-454] p 3764 N92-32018
NASA programs --- nasa space programs
p 3765 N92-32238

SPACECRAFT ANTENNAS
Dynamics of shuttle based flexible antenna system
[CRANFIELD-AERO-9203] p 3840 N92-31516

SPACECRAFT CHARGING
High-latitude spacecraft charging in low-Earth polar orbit
[AD-A249868] p 3767 N92-31822
USU center of excellence in theory and analysis of the geo-plasma environment
[AD-A252189] p 3858 N92-32055

SPACECRAFT CONSTRUCTION MATERIALS
Graphite/epoxy composite adapters for the Space Shuttle/Centaur vehicle
[NASA-TP-3014] p 3765 N92-31251

SPACECRAFT CONTAMINATION
Analysis of debris from Spacelab Space Life Sciences-1
[NASA-TM-103593] p 3765 N92-32148

SPACECRAFT CONTROL
Spacecraft dynamics characterization and control system failure detection. Volume 3: Control system failure monitoring
[NASA-CR-190529] p 3884 N92-31254
A novel control-guidance law for low-thrust orbit maneuver p 3747 N92-31874
Spacecraft stability and control
[TABES PAPER 92-414] p 3763 N92-32011

SPACECRAFT DESIGN
Graphite/epoxy composite adapters for the Space Shuttle/Centaur vehicle
[NASA-TP-3014] p 3765 N92-31251
The determination of operational and support requirements and costs during the conceptual design of space systems
[NASA-CR-190626] p 3766 N92-31260

SPACECRAFT EQUIPMENT
Analysis of systems hardware flown on LDEF. Results of the systems special investigation group
[NASA-CR-189628] p 3767 N92-31677

SPACECRAFT GUIDANCE
A novel control-guidance law for low-thrust orbit maneuver p 3747 N92-31874

SPACECRAFT INSTRUMENTS
Mission description and in-flight operations of ERBE instruments on ERBS, NOAA 9, and NOAA 10 spacecraft
[NASA-RP-1279] p 3844 N92-32127

SPACECRAFT LAUNCHING
Optimum data analysis procedures for Titan 4 and Space Shuttle payload acoustic measurements during lift-off
[NASA-CR-190479] p 3892 N92-32178

SPACECRAFT MAINTENANCE
The determination of operational and support requirements and costs during the conceptual design of space systems
[NASA-CR-190626] p 3766 N92-31260
Space Station mini pressurised logistics modules: An opportunity to enlarge and reinforce international cooperation
[TABES PAPER 92-425] p 3764 N92-32016

SPACECRAFT MANEUVERS
A novel control-guidance law for low-thrust orbit maneuver p 3747 N92-31874

SPACECRAFT MODULES
Space Station mini pressurised logistics modules: An opportunity to enlarge and reinforce international cooperation
[TABES PAPER 92-425] p 3764 N92-32016
COMET: Commercial space opportunities through developed technologies
[TABES PAPER 92-453] p 3764 N92-32017
SPACEHAB: A giant step in the commercial development of space
[TABES PAPER 92-454] p 3764 N92-32018

SPACECRAFT ORBITS
A novel control-guidance law for low-thrust orbit maneuver p 3747 N92-31874

SPACECRAFT POWER SUPPLIES
Space nuclear power, propulsion, and related technologies
[SAND91-2617] p 3770 N92-31503
Analysis of systems hardware flown on LDEF. Results of the systems special investigation group
[NASA-CR-189628] p 3767 N92-31677

SPACECRAFT PROPULSION
The evolutionary development of high specific impulse electric thruster technology
[NASA-TM-105712] p 3769 N92-31342
Space nuclear power, propulsion, and related technologies
[SAND91-2617] p 3770 N92-31503

SPACECRAFT RADIATORS
An overview of the Lewis Research Center CSTI thermal management program
[NASA-TM-105310] p 3771 N92-31916

SPACECRAFT RELIABILITY
The determination of operational and support requirements and costs during the conceptual design of space systems
[NASA-CR-190626] p 3766 N92-31260

SPACECRAFT STABILITY
Spacecraft stability and control
[TABES PAPER 92-414] p 3763 N92-32011

SPACECRAFT STRUCTURES
Graphite/epoxy composite adapters for the Space Shuttle/Centaur vehicle
[NASA-TP-3014] p 3765 N92-31251
USU center of excellence in theory and analysis of the geo-plasma environment
[AD-A252189] p 3858 N92-32055
Design, analysis, and testing of the Phase 1 CSI Evolutionary Model erectable truss
[NASA-CR-4461] p 3767 N92-32100

SPACECRAFT TRAJECTORIES
The use of high lift-to-drag hypersonic vehicles for aero-assisted orbital maneuvering p 3748 N92-31877
Interplanetary Program to Optimize Space Trajectories (IPOST). Volume 3: Programmer's manual
[NASA-CR-189653-VOL-3] p 3766 N92-32130

SPACELAB
Analysis of debris from Spacelab Space Life Sciences-1
[NASA-TM-103593] p 3765 N92-32148

SPARK GAPS
High-pressure gas switch for a wideband source
[DE92-015822] p 3815 N92-31548

SPATIAL DISTRIBUTION
Algorithms for the determination of spatial and spectral distribution of electromagnetic energy in a simulated biostructure subjected to transient spatially heterogeneous radiation with applications to radar hazard assessment and cancer therapy
[AD-A250447] p 3805 N92-31381
Steady-state and transient modeling of tracer and nutrient distributions in the global ocean
[DE92-011805] p 3864 N92-31572
Analysis of the effects of aerosol distribution in the atmosphere on surface radiative measurements
[DE92-014189] p 3856 N92-31662
The mechanics of fractal damage
[AD-A250518] p 3776 N92-32075

SPECIFIC HEAT
High density thin-walled syntactic foam
[DE92-013159] p 3797 N92-32138

SPECIFIC IMPULSE
The evolutionary development of high specific impulse electric thruster technology
[NASA-TM-105712] p 3769 N92-31342

SPECIFICATIONS
High strength glass second source qualification to composite armor specification MIL-L-46197(MR)
[AD-A252114] p 3792 N92-31404
Requirements Engineering and Analysis Workshop Proceedings
[AD-A250415] p 3876 N92-31541
B-1B nuclear certification tasks performed by the Aircraft Compatibility Department at Sandia National Laboratories
[DE92-016750] p 3757 N92-31736
Specification and verification of secure concurrent and distributed software systems
[AD-A252477] p 3879 N92-31825
Capabilities of the 3-axes modified FP42 Deckel milling machine
[DE92-011737] p 3803 N92-31908

SPECTRA
Time domain regional discriminants
[AD-A249949] p 3855 N92-31509

SPECTRAL METHODS
Adaptive mesh strategies for the spectral element method
[NASA-CR-189686] p 3818 N92-31265

SPECTRAL REFLECTANCE
Sun-view-target geometry effects on spectrally-derived vegetative index estimates of absorbed radiation and leaf area
[AD-A249984] p 3843 N92-31329

SPECTROMETERS
Use of tissue equivalent proportional counters to characterize radiation quality on the space shuttle
[DE92-012347] p 3768 N92-31846
Imaging and spectrometry of bulk crystal surfaces and surface dynamical processes at high temperatures
[DE92-015235] p 3913 N92-32085

SPECTROSCOPIC ANALYSIS
Cyclopolymerization of metalloid-containing alpha, omega-dienes. 1,3-divinyltetramethyldisiloxane, 1,3-divinyltetramethyldisilazane and 1,3-divinylpentamethyldisilazane
[AD-A250347] p 3794 N92-31557
Holographic grating relaxation and photon correlation spectroscopic studies of viscoelastic liquids above the glass transition
[AD-A252485] p 3828 N92-31828

SPECTROSCOPY
Submillimeter wave spectroscopy of heterojunction superlattices
[AD-A250835] p 3908 N92-31496
Ion beam spectroscopy as a means of in-situ monitoring of thin film deposition
[DE92-014857] p 3909 N92-31652
A global fitting code for multichordal neutral beam spectroscopic data
[DE92-014258] p 3781 N92-31729
Ultrafast studies on electron transfer in the betaines: Evidence for local heating
[AD-A250728] p 3897 N92-31999
Cationic ring opening polymerization of oxazolines initiated by trimethylsilyl derivatives
[AD-A251109] p 3798 N92-32153

SPECTRUM ANALYSIS
Spectrum modal analysis for the detection of low-altitude windshear with airborne Doppler radar
[NASA-CR-4457] p 3755 N92-31549
Real time analysis of tokamak discharge parameters
[DE92-011394] p 3904 N92-31616
Maximum likelihood estimation of fractional Brownian motion and Markov noise parameters
[AD-A249623] p 3890 N92-31686
Meteorological data, new series A monographs. Volume 6, no. 2: Case study on the congruence of precipitation data from SYNOP-MODELL and Meteosat data
[ETN-92-91694] p 3861 N92-31710
Method and circuit for controlling the evolution time interval of a laser output pulse
[NASA-CASE-LAR-13772-1] p 3831 N92-31788
Determination of the matrix conditioning indicator. Comparison of approximate methods
p 3887 N92-32210
Parameterization of directional spectra, part 2, volume 1
[DREA-CR-89-445-PT-2-VOL-1] p 3811 N92-32214

SPEED INDICATORS
Estimation of aircraft attitude by angular rate measurements p 3748 N92-31881

SPHERES
Granular flows down bumpy inclines
[DE92-013568] p 3820 N92-31425

SPHEROMAKS
Simulation study of stepwise relaxation in a spheromak plasma
[DE92-782101] p 3906 N92-31843
SPIN STABILIZATION
An investigation of spinup dynamics of axial gyrostats using elliptic integrals and the method of averaging
[AD-A249728] p 3768 N92-31675
Spacecraft stability and control
[TABES PAPER 92-414] p 3763 N92-32011
SPIN-LATTICE RELAXATION
Fusion with highly spin polarized HD and D(2)
[DE92-017030] p 3898 N92-32007
SPINAL CORD
Acetylcholinesterase inhibitors on the spinal cord
[AD-A252694] p 3868 N92-31326
SPLINES
Non-geothermal optics study of wave propagation
[DE92-011806] p 3903 N92-31494
SPRAY CHARACTERISTICS
Study of a spherical spinning combustion chamber for orbit insertion p 3746 N92-31869
SPRAYERS
Diagnostics for research in atomization and turbulent two-phase flows
[AD-A247201] p 3819 N92-31283
Particle diagnostics in optically thick sprays
[AD-A250981] p 3897 N92-31936
SPUTTERING
Dependence of secondary ion emission from organic material on the energy loss of the impacting heavy ion
[DE92-014845] p 3893 N92-31386
High temperature superconducting films and multilayers for electronics
[AD-A250732] p 3813 N92-31451
Computer simulation of scattered ion and sputtered species effects in ion beam sputter-deposition of high temperature superconducting thin films
[DE92-015227] p 3909 N92-31546
Surface chemistry of MoS2 lubricant films: Effects of high humidity storage on sputtered films
[DE92-015392] p 3794 N92-31631
Correlation from randomness: Quantitative analysis of sputtered graphite surfaces using the scanning tunneling microscope
[AD-A252420] p 3783 N92-31820
Substrate surface effects on the properties of sputter-deposited and laser-irradiated films
[DE92-013850] p 3795 N92-31917
Metallization of ferrite ceramic couplings
[DE92-016573] p 3789 N92-32032
SQUALLS
The structure and energetics of Amazon squall lines
[AD-A250182] p 3859 N92-31523
SQUARES (MATHEMATICS)
Decomposition of balanced matrices. Part 4: Connected squares
[AD-A247308] p 3888 N92-31768
STABILITY
Mechanical strength and stability of lithium aluminate
[DE92-015998] p 3841 N92-31638
STABILITY TESTS
Rigid rotations in two-electron atoms in a uniform magnetic field
[DE92-624981] p 3896 N92-31836
STABILIZERS
Stable integrated microwave to optical modulator
[AD-A249974] p 3813 N92-31431
STAGNATION POINT
Stagnation-point heat-transfer rate predictions at aeroassist flight conditions
[NASA-TP-3208] p 3819 N92-31281
Flame front geometry in premixed turbulent flames
[DE92-010310] p 3779 N92-31417
An approximate local thermodynamic nonequilibrium radiation model for air
[NASA-CR-190580] p 3914 N92-31577
STAINLESS STEELS
Surface analysis of stainless steel outer race bearing specimens
[AD-A250088] p 3833 N92-31437
Surface chemistry of MoS2 lubricant films: Effects of high humidity storage on sputtered films
[DE92-015392] p 3794 N92-31631
Chromium, nickel, and other alloying elements in US-produced stainless and heat-resisting steel
[PB92-178623] p 3788 N92-31797
STANDARDIZATION
Multimedia electronic mail: Standards and performance simulation
[AD-A250047] p 3808 N92-31809
Full abstraction and the context lemma
[AD-A247062] p 3887 N92-32163
STANDARDS
Simplified air change effectiveness modeling
[DE92-010577] p 3872 N92-31309
Overview of integrated services digital network conformance testing
[PB92-181015] p 3881 N92-31365
Operating principles of MULTIKRON performance instrumentation for MIMD computers
[PB92-181072] p 3874 N92-31366
Next generation documents
[PB92-187103] p 3917 N92-31371
Technology Integration Workshop: Selected papers
[PB92-158278] p 3923 N92-31643
A detector for stationary gas bubbles: Feasibility studies
[AD-A250135] p 3828 N92-31794
International mathematics and science assessments: What have we learned
[PB92-183599] p 3916 N92-32160
Characteristics of selected reference targets for calibrating 10.6 micron laser radars
[DREV-R-4487/88] p 3811 N92-32217
STAR FORMATION
Molecular outflows associated with HH52-54 and IRAS 12496-7650
[PB92-184472] p 3924 N92-31635
STARK EFFECT
A global fitting code for multichordal neutral beam spectroscopic data
[DE92-014258] p 3781 N92-31729
STATIC CHARACTERISTICS
Static and dynamic properties of current sensing power VDMOS transistor
[LAAS-92032] p 3815 N92-31697
STATIC TESTS
Global positioning system runway incursion program static ground tests
[DOT/FAA/CT-TN91/44] p 3756 N92-31838
Design, analysis, and testing of the Phase 1 CSI Evolutionary Model erectable truss
[NASA-CR-4461] p 3767 N92-32100
STATISTICAL ANALYSIS
The vehicle routing problem: Some computational tests of savings method and its variations
[INPE-5361-RPQ/656] p 3886 N92-31241
Statistical analysis of anomalous transport in resistive interchange turbulence
[NIFS-125] p 3818 N92-31256
Stress reactivity: Five-factor representation of a psychobiological typology
[AD-A252715] p 3872 N92-31327
Accretion disk image reconstruction in cataclysmic variables
[INPE-5343-PRE/1742] p 3923 N92-31347
Non-geothermal optics study of wave propagation
[DE92-011806] p 3903 N92-31494
On a characterization of the exponential distribution based on a type 2 right censored sample
[CWI-BS-R9117] p 3888 N92-31517
Independent sampling of a stochastic process
[AD-A249712] p 3888 N92-31600
Real-time statistical quality control and ARM
[DE92-015253] p 3837 N92-31657
Macrostatistical hydrodynamics
[DE92-013589] p 3823 N92-31726
Guidelines for generating acceptance sampling plans for continuous production
[DE92-010763] p 3837 N92-31753
NSF Tokyo reports. 1991 survey of research and development in Japan
[PB92-192624] p 3927 N92-32067
A generalization to stochastic averaging in random vibration
[DE92-016747] p 3842 N92-32088
Asymptotic modal analysis and statistical energy analysis
[NASA-CR-190516] p 3842 N92-32236
STATISTICAL CORRELATION
Synthetic temperature profile in the Gulf of Mexico. Part 1: Statistical relationship between modal amplitudes and dynamic height at surface
[AD-A252701] p 3863 N92-31308
STATISTICAL DISTRIBUTIONS
On a characterization of the exponential distribution based on a type 2 right censored sample
[CWI-BS-R9117] p 3888 N92-31517
Two properties of uniform distributions, with applications to some nonparametric estimation problems
[REPT-91-94] p 3888 N92-31518
Nonparametric estimation in renewal theory, 1: The empirical renewal function
[REPT-91-95] p 3888 N92-31519
Independent sampling of a stochastic process
[AD-A249712] p 3888 N92-31600
STATISTICAL MECHANICS
Application of the mean spherical approximation to the estimations of single ion thermodynamic quantities of solvation for monoatomic monovalent ions in aqueous solutions
[AD-A250190] p 3893 N92-31316
Motor-operated globe valve performance in a liquid sodium environment
[DE92-014456] p 3834 N92-31500
Theoretical studies of solid-fluid phase equilibria
[DE92-016598] p 3781 N92-31717
STATISTICS
Global atmospheric circulation statistics, 1000-1 mb
[PB92-186196] p 3853 N92-31649
STEADY FLOW
A computational investigation of airfoil stall flutter
[AD-A247302] p 3751 N92-31300
Steady flow of a fluid-solid mixture between parallel plates
[DE92-013645] p 3821 N92-31426
STEADY STATE
Flow instability in a vertical annulus under steady state and transient conditions
[DE92-013217] p 3820 N92-31421
Absorption spectroscopy through the dark zone of solid propellant flames
[AD-A250033] p 3782 N92-31803
Small tokamaks for fusion technology testing
[DE92-011790] p 3906 N92-31913
STEEL STRUCTURES
Marine structural steel toughness data bank, volume 1
[AD-A247923] p 3789 N92-31987
STEELS
Studies of the effect of strain velocity on mechanical properties of the 34GS steel p 3786 N92-31243
Marine structural steel toughness data bank, volume 1
[AD-A247923] p 3789 N92-31987
A study of the microstructural basis for the strength and toughness properties of water-quenched and air-cooled HSLA-100, HSLA-100 with increased copper, and a ULCB steel
[AD-A245955] p 3789 N92-32052
STEERING
Studies in dynamic characterization and control of a flexible structure and optical beampath
[AD-A250555] p 3830 N92-31605
STELLAR EVOLUTION
G305.8 - 0.2 water vapour source: A young object
[INPE-5337-PRE/1736] p 3923 N92-31343
Molecular outflows associated with HH52-54 and IRAS 12496-7650
[PB92-184472] p 3924 N92-31635
Evolution of the solar and coronal field structure: 1976-1991
[AD-A250097] p 3925 N92-31786
STELLAR LUMINOSITY
Molecular outflows associated with HH52-54 and IRAS 12496-7650
[PB92-184472] p 3924 N92-31635
STELLAR MASS EJECTION
Molecular outflows associated with HH52-54 and IRAS 12496-7650
[PB92-184472] p 3924 N92-31635
Interaction of fast steady flow with slow transient flow: A new cause of interplanetary Bz events
[AD-A250273] p 3823 N92-31770
STELLAR MODELS
Solar neutrinos: Theory versus experiment
[DE92-014327] p 3925 N92-32154
STELLAR STRUCTURE
Evolution of the solar and coronal field structure: 1976-1991
[AD-A250097] p 3925 N92-31786
STELLAR WINDS
Molecular outflows associated with HH52-54 and IRAS 12496-7650
[PB92-184472] p 3924 N92-31635
STIFFNESS
Time simulation of flutter with large stiffness changes
[NASA-TM-107650] p 3758 N92-32111
STIRLING CYCLE
A free-piston Stirling engine/linear alternator controls and load interaction test facility
[NASA-TM-105825] p 3845 N92-31262
Oscillating-flow regenerator test rig: Woven screen and metal felt results
[NASA-CR-190689] p 3820 N92-31352
STIRLING ENGINES
Free-piston Stirling engine conceptual design and technologies for space power, phase 1
[NASA-CR-182168] p 3769 N92-31245
STOCHASTIC PROCESSES
Mathematical problems in micromechanics and composite materials
[AD-A249584] p 3773 N92-31378

Comparison of effects of copropagated and precomputed atmosphere profiles on Monte Carlo trajectory simulation
[NASA-TM-102600] p 3766 N92-31457
Two properties of uniform distributions, with applications to some nonparametric estimation problems
[REPT-91-94] p 3888 N92-31518
Nonparametric estimation in renewal theory, 1: The empirical renewal function
[REPT-91-95] p 3888 N92-31519
Independent sampling of a stochastic process
[AD-A249712] p 3888 N92-31600
Noise-induced chaos and phase space flux: A sample-theoretic study
[PB92-172733] p 3915 N92-31645
Evidence of stochastic diffusion across a cross-field sheath due to Kelvin-Helmholtz vortices
[AD-A247847] p 3907 N92-31983
A generalization to stochastic averaging in random vibration
[DE92-016747] p 3842 N92-32088

STOCKPILING
Using transfer functions as a method for predicting lightning effects on munitions storage bunkers
[DE92-012627] p 3861 N92-31709
Measured responses of a munitions storage bunker to rocket-triggered lightning
[DE92-012628] p 3862 N92-31750

STOKES FLOW
Plane stokes flow driven by capillarity on a free surface: Overview and status
[DE92-011469] p 3821 N92-31528

STOKES LAW (FLUID MECHANICS)
Plane stokes flow driven by capillarity on a free surface: Overview and status
[DE92-011469] p 3821 N92-31528

STORAGE
Measured responses of a munitions storage bunker to rocket-triggered lightning
[DE92-012628] p 3862 N92-31750

STORAGE RINGS (PARTICLE ACCELERATORS)
Injecting into AmPS when ring cavity operates at 476 MHz
[NIKHEF-K/AMPS/91-08] p 3899 N92-31815

STORMS
A case study of a prolonged sleet event: 16-17 February 1987 and climatology of sleet events for North Carolina, 1949-1989
[AD-A250184] p 3859 N92-31602

STORMS (METEOROLOGY)
A coordinated study of a storm system over the South American continent
[INPE-5388-TDI/477] p 3863 N92-32212

STRAIN DISTRIBUTION
Modeling of composite beams and plates for static and dynamic analysis
[NASA-CR-190536] p 3839 N92-31339

STRAIN GAGES
Investigation of factors affecting the calibration of strain gage based transducers (Goodzeit gages) for SSC magnets
[DE92-010722] p 3826 N92-31313
Automation of strain-gauge load-cell force calibration
[PB92-187087] p 3827 N92-31370
An experimental procedure for the Iosipescu composite specimen tested in the modified Wyoming fixture
[NASA-CR-190660] p 3774 N92-31566

STRAIN HARDENING
Mode methods for strain-hardening structures
[DE92-014855] p 3838 N92-31335
Superplasticity in a nickel silicide alloy, Ni3Si(V, Mo)
[DE92-011651] p 3787 N92-31667
Effects of fiber and interfacial layer architectures on the thermoplastic response of metal matrix composites
[NASA-TM-105802] p 3777 N92-32234

STRAIN MEASUREMENT
Residual stress and strain measurements in an austenitic steel plate containing a multipass weld
[DE92-014478] p 3839 N92-31383

STRAIN RATE
Superplasticity in a nickel silicide alloy, Ni3Si(V, Mo)
[DE92-011651] p 3787 N92-31667

STRATOSPHERE
Meteorological data, new series B basic material. Volume 53, no. 1: Daily altitude maps of the 30-hPa-area and monthly mean maps for the year 1986, part 1
[QR-1-VOL-53-NO-1-PT-1] p 3860 N92-31702
Meteorological data, new series B basic material. Volume 53, no. 2: Daily altitude maps of the 30-hPa-area and monthly mean maps for the year 1986, part 2
[QR-2-VOL-53-NO-2-PT-2] p 3860 N92-31704
Meteorological data, new series B basic material. Volume 53, no. 4: Daily altitude maps of the 30-hPa-area and monthly mean maps for the year 1986, part 4
[QR-4-VOL-53-NO-4-PT-4] p 3861 N92-31706
Comprehensive Aerological Reference Data Set (CARDS)
[DE92-016469] p 3862 N92-31734
A coordinated study of a storm system over the South American continent
[INPE-5388-TDI/477] p 3863 N92-32212

STRATUS CLOUDS
Unified very low stratus cloud/subcloud microphysics model
[AD-A250662] p 3858 N92-31320

STRESS (PHYSIOLOGY)
Body water homeostasis and human performance in high heat environments: Fluid hydration recommendations for Operation Desert Storm
[AD-A249772] p 3868 N92-31492

STRESS (PSYCHOLOGY)
Theory and test of stress resistance
[AD-A250741] p 3870 N92-31291
Development of quantitative specifications for simulating the stress environment
[AD-A250669] p 3870 N92-31321
Stress reactivity: Five-factor representation of a psychobiological typology
[AD-A252715] p 3872 N92-31327

STRESS ANALYSIS
A finite element procedure for analysis of laminated composite plates
[AD-A250902] p 3773 N92-31307
Mode methods for strain-hardening structures
[DE92-014855] p 3838 N92-31335
The effect of elastic stress on Ostwald ripening phenomena
[DE92-015291] p 3839 N92-31400
Sodium Heat Engine Development Program
[DE92-012398] p 3846 N92-31531
Role of interfaces and interphases in the evolution mechanics of material systems
[AD-A250410] p 3774 N92-31604
Electrically-induced stresses and deflection in multiple plates
[DE92-012303] p 3841 N92-31844
Instabilities of damage and surface degradation mechanisms in brittle material structural systems
[AD-A250785] p 3842 N92-32168
Effects of fiber and interfacial layer architectures on the thermoplastic response of metal matrix composites
[NASA-TM-105802] p 3777 N92-32234

STRESS CONCENTRATION
Optimal design of geodesically stiffened composite cylindrical shells
[NASA-CR-190706] p 3842 N92-32235

STRESS DISTRIBUTION
Composite material shear property measurement using the Iosipescu specimen
[NASA-CR-190661] p 3772 N92-31274
Computer-aided modeling tools for forging process feasibility studies
[DE92-012116] p 3838 N92-31303
Modeling of composite beams and plates for static and dynamic analysis
[NASA-CR-190536] p 3839 N92-31339
Residual stresses in a multipass ferritic weldment
[DE92-014467] p 3839 N92-31501
Effects of fiber and interfacial layer architectures on the thermoplastic response of metal matrix composites
[NASA-TM-105802] p 3777 N92-32234

STRESS FUNCTIONS
A differential CDM model for fatigue of unidirectional metal matrix composites
[NASA-TM-105726] p 3840 N92-31505

STRESS INTENSITY FACTORS
Analysis and prediction of Multiple-Site Damage (MSD) fatigue crack growth
[NASA-TP-3231] p 3838 N92-31279
Applications of FEM and BEM in two-dimensional fracture mechanics problems
[NASA-TP-3277] p 3838 N92-31280
Effect of fracture surface interference on shear crack growth
[DE92-011431] p 3839 N92-31389

STRESS MEASUREMENT
Investigation of factors affecting the calibration of strain gage based transducers (Goodzeit gages) for SSC magnets
[DE92-010722] p 3826 N92-31313

STRESS RELAXATION
The influence of various spectrum parameters on fatigue life and residual stress relaxation
[FFA-TN-1991-44] p 3840 N92-31512

STRESS-STRAIN RELATIONSHIPS
Residual stress and strain measurements in an austenitic steel plate containing a multipass weld
[DE92-014478] p 3839 N92-31383
The effect of elastic stress on Ostwald ripening phenomena
[DE92-015291] p 3839 N92-31400
Role of interfaces and interphases in the evolution mechanics of material systems
[AD-A250410] p 3774 N92-31604

STRESSES
Oxygen ordering and strain-related morphology in YBa2Cu(3-x)O7 systems
[DE92-014476] p 3909 N92-31627

STRETCHING
Injecting into AmPS when ring cavity operates at 476 MHz
[NIKHEF-K/AMPS/91-08] p 3899 N92-31815

STRING THEORY
A dynamical model of the behaviour of hadronic and fundamental strings at finite densities
[DE92-630245] p 3914 N92-31402
Theoretical high energy physics research at the University of Chicago, task A
[DE92-016288] p 3899 N92-31712
Minimal supersymmetric unification predictions
[RAL-92-005] p 3915 N92-31953

STRUCTURAL ANALYSIS
Graphite/epoxy composite adapters for the Space Shuttle/Centaur vehicle
[NASA-TP-3014] p 3765 N92-31251
Organometallic Nonlinear Optical (NLO) polymers. Part 2: Synthesis of main-chain organometallic polymers and a structural study of ferrocene NLO-Phores
[AD-A250655] p 3791 N92-31318
Mode methods for strain-hardening structures
[DE92-014855] p 3838 N92-31335
On the feasibility of a transient dynamic design analysis method
[AD-A250406] p 3838 N92-31337
Modeling of composite beams and plates for static and dynamic analysis
[NASA-CR-190536] p 3839 N92-31339
Research into improving the durability of the hot section in the aircraft turbine engine
[AD-A250342] p 3759 N92-31439
Iterative methods for large sparse linear systems arising from partial differential equations
[AD-A249524] p 3886 N92-31567
Cryogenic 4.4 MN mechanical test system for large scale tests of composite support struts
[PB92-181148] p 3774 N92-31609
Computer applications for engineering/structural analysis
[DE92-013070] p 3841 N92-31745
Marine structural steel toughness data bank, volume 1
[AD-A247923] p 3789 N92-31987

STRUCTURAL BASINS
Two-dimensional axisymmetric calculations of surface waves generated by an explosion in an island, mountain, and sedimentary basin
[AD-A249971] p 3856 N92-31510
The structure and energetics of Amazon squall lines
[AD-A250182] p 3859 N92-31523

STRUCTURAL DESIGN
Design, fabrication, and testing of a 30 kW(sub t) screen-wick heat-pipe solar receiver
[DE92-016500] p 3848 N92-32087

STRUCTURAL ENGINEERING
Building an educational robot arm for under $1,000
[AD-A247499] p 3833 N92-31460
Geomorphic variability in the coastal zone
[AD-A252713] p 3864 N92-31544

STRUCTURAL PROPERTIES (GEOLOGY)
Geomorphic variability in the coastal zone
[AD-A252713] p 3864 N92-31544

STRUCTURAL RELIABILITY
Weld penetration and defect control
[DE92-015310] p 3836 N92-31336

STRUCTURAL STABILITY
The effect of elastic stress on Ostwald ripening phenomena
[DE92-015291] p 3839 N92-31400
Design, analysis, and testing of the Phase 1 CSI Evolutionary Model erectable truss
[NASA-CR-4461] p 3767 N92-32100

STRUCTURAL VIBRATION
Experimental feedback of fractional order states of a lightly damped structure
[AD-A248027] p 3842 N92-31989
Asymptotic modal analysis and statistical energy analysis
[NASA-CR-190516] p 3842 N92-32236

STRUCTURAL WEIGHT
The design and testing of an optimal beam composed of unimodal elements p 3747 N92-31873

STRUTS
Cryogenic 4.4 MN mechanical test system for large scale tests of composite support struts
[PB92-181148] p 3774 N92-31609
Design, analysis, and testing of the Phase 1 CSI Evolutionary Model erectable truss
[NASA-CR-4461] p 3767 N92-32100

STUDENTS
USU center of excellence in theory and analysis of the geo-plasma environment
[AD-A252189] p 3858 N92-32055
International mathematics and science assessments: What have we learned
[PB92-183599] p 3916 N92-32160
STYRENES
The photogeneration of polymeric amines: Synthesis and photocrosslinking of copolymers containing photoactive carbamate pendant groups
[AD-A250086] p 3793 N92-31436
SUBARCTIC REGIONS
An analysis of hydrographic data collected off Point Sur, California in June 1990
[AD-A246060] p 3866 N92-32056
SUBMARINES
Description of a 1000 sensor constant current anemometer system for locating three-dimensional turbulent boundary layer separations
[AD-A250827] p 3821 N92-31452
SUBMERGING
Natural convection immersion cooling of an array of vertically oriented heated protrusions in an enclosure filled with a dielectric liquid: Effects of enclosure width, Prandtl number and component orientation
[AD-A245884] p 3914 N92-31489
SUBMILLIMETER WAVES
Submillimeter wave spectroscopy of heterojunction superlattices
[AD-A250835] p 3908 N92-31496
SUBROUTINES
The development of modularized software for empirical testing of new algorithms in linear programming
[AD-A250811] p 3875 N92-31480
SUBSONIC FLUTTER
A computational investigation of airfoil stall flutter
[AD-A247302] p 3751 N92-31300
SUBSONIC SPEED
An investigation into the interface between three closely spaced axi-symmetric bodies at subsonic speed
[CRANFIELD-AERO-9114] p 3751 N92-31514
SUBSTRATES
Growth, nitrogen vacancy reduction and solid solution formation in cubic GaN thin films and the subsequent fabrication of superlattice structures using AlN and InN
[AD-A248058] p 3908 N92-31446
High temperature superconducting films and multilayers for electronics
[AD-A250732] p 3813 N92-31451
Sol-gel multilayers applied by a meniscus coating process
[DE92-012697] p 3794 N92-31560
Substrate surface effects on the properties of sputter-deposited and laser-irradiated films
[DE92-013850] p 3795 N92-31917
SUITS
Immersion suit usage within the RAAF
[AD-A250645] p 3755 N92-31562
SULFIDATION
Oxidation/sulfidation behavior of Fe-Cr alloys: A reactive-element effect
[DE92-016172] p 3789 N92-31924
SULFUR
Effects of anthropogenic sulfur aerosols on climate
[DE92-016158] p 3850 N92-31297
SULFUR FLUORIDES
Estimation of metal acceleration by an SF5 containing explosive
[AD-A245338] p 3801 N92-32098
SUMMER
Upper tropospheric jet streams over North America during summer 1988
[AD-A249871] p 3857 N92-31906
SUN
Interaction of fast steady flow with slow transient flow: A new cause of interplanetary Bz events
[AD-A250273] p 3823 N92-31770
Multiple electron populations accelerated in solar bursts
[INPE-5377-TDI/472] p 3925 N92-32025
SUPERCOMPUTERS
Simulation of a parallel processor based small tactical system
[AD-A245911] p 3882 N92-31443
Some computational challenges of developing efficient parallel algorithms for data-dependent computations in thermal-hydraulics supercomputer applications
[DE92-011368] p 3878 N92-31703
NAS (Numerical Aerodynamic Simulation Program) technical summaries, March 1989 - February 1990
[NASA-TM-107960] p 3926 N92-31852
SUPERCONDUCTING FILMS
Pulsed laser deposition of high Tc superconducting thin films
[AD-A250657] p 3830 N92-31319
High temperature superconducting films and multilayers for electronics
[AD-A250732] p 3813 N92-31451
Computer simulation of scattered ion and sputtered species effects in ion beam sputter-deposition of high temperature superconducting thin films
[DE92-015227] p 3909 N92-31546
Microstructure and properties of in-situ RF sputtered YBa2Cu3O7 thin films for microwave applications
[DE92-013379] p 3911 N92-31723
SUPERCONDUCTING MAGNETS
Investigation of factors affecting the calibration of strain gage based transducers (Goodzeit gages) for SSC magnets
[DE92-010722] p 3826 N92-31313
Utilization of gamma ray inspection system for tomographic imaging and dimensional analysis of complete model magnet cold masses and collared coil sections
[DE92-013466] p 3836 N92-31647
Potential impact of high temperature superconductors on MAGLEV transportation
[DE92-012683] p 3834 N92-31720
Connectivity among computer-aided engineering methods, procedures, and tools used in developing the SSC collider magnets
[DE92-013954] p 3900 N92-31975
SUPERCONDUCTING SUPER COLLIDER
Investigation of factors affecting the calibration of strain gage based transducers (Goodzeit gages) for SSC magnets
[DE92-010722] p 3826 N92-31313
Utilization of gamma ray inspection system for tomographic imaging and dimensional analysis of complete model magnet cold masses and collared coil sections
[DE92-013466] p 3836 N92-31647
Improved ferrite biasing scheme for booster RF cavities
[DE92-011650] p 3815 N92-31664
Beam position monitor electronics using DC coupled demodulating logarithmic amplifiers
[DE92-011697] p 3816 N92-31760
Experimental particle physics at the University of Pittsburgh
[DE92-016182] p 3896 N92-31926
Connectivity among computer-aided engineering methods, procedures, and tools used in developing the SSC collider magnets
[DE92-013954] p 3900 N92-31975
SUPERCONDUCTIVITY
Aluminum tunnel junction detector operation in an adiabatic demagnetization refrigerator
[DE92-013441] p 3913 N92-32166
Investigation of acoustic properties of high-temperature ceramic superconductors p 3914 N92-32209
SUPERCONDUCTORS
What can we learn from magnetization experiments on high T(sub c) superconductors? An overview
[DE92-014465] p 3815 N92-31650
SUPERCOOLING
Holographic grating relaxation and photon correlation spectroscopic studies of viscoelastic liquids above the glass transition
[AD-A252485] p 3828 N92-31828
SUPERCRITICAL FLUIDS
Supercritical fluid fractionation of JP-8
[AD-A247835] p 3801 N92-31982
SUPERFLUIDITY
A sealed He-4 superfluid-transition fixed-point device
[DE92-014271] p 3908 N92-31403
SUPERHIGH FREQUENCIES
A three-gap klystron output cavity at X-band
[DE92-012417] p 3812 N92-31289
SUPERLATTICES
Electronic and total energy properties of ternary and quaternary semiconductor compounds, alloys, and superlattices: Theoretical study of Cu/graphite bonding
[NASA-CR-190691] p 3772 N92-31266
Growth, nitrogen vacancy reduction and solid solution formation in cubic GaN thin films and the subsequent fabrication of superlattice structures using AlN and InN
[AD-A248058] p 3908 N92-31446
Submillimeter wave spectroscopy of heterojunction superlattices
[AD-A250835] p 3908 N92-31496
US-Japan seminar on magnetic multilayered structures: Proceedings
[AD-A252440] p 3910 N92-31666
Theory of semiconducting superlattices and microstructures
[AD-A248758] p 3816 N92-31799
SUPERPLASTICITY
Superplasticity in a nickel silicide alloy, Ni3Si(V, Mo)
[DE92-011651] p 3787 N92-31667
SUPERSONIC COMBUSTION
Laser-initiated conical detonation wave for supersonic combustion, part 3
[AD-A250522] p 3785 N92-32076
SUPERSONIC COMPRESSORS
NASA. Lewis Research Center supersonic throughflow fan program
[NASA-TM-103248] p 3759 N92-31250
SUPERSONIC FLOW
NASA. Lewis Research Center supersonic throughflow fan program
[NASA-TM-103248] p 3759 N92-31250
Stability of boundary layers at high supersonic and hypersonic speeds
[AD-A250900] p 3819 N92-31306
Hypersonic code efficiency and validation studies
[NASA-CR-190680] p 3752 N92-31533
Stability and transition of hypersonic boundary-layer flows
[AD-A250279] p 3752 N92-31555
Supersonic Throughflow Fan Test Facility at NASA. Lewis Research Center
[NASA-TP-3038] p 3762 N92-31640
Euler solver for arbitrary configurations: Further applications p 3750 N92-31888
Laser-initiated conical detonation wave for supersonic combustion, part 3
[AD-A250522] p 3785 N92-32076
SUPERSONIC INLETS
NASA. Lewis Research Center supersonic throughflow fan program
[NASA-TM-103248] p 3759 N92-31250
Sizing supersonic freejet nozzle and inlet location for simulation of the transition phase in integral rocket ramjet p 3747 N92-31870
SUPERSONIC JET FLOW
Supersonic pyrolysis jets for diamond film deposition
[AD-A251125] p 3798 N92-32198
SUPERSONIC NOZZLES
Sizing supersonic freejet nozzle and inlet location for simulation of the transition phase in integral rocket ramjet p 3747 N92-31870
SUPERSONIC SPEED
Supersonic Throughflow Fan Test Facility at NASA. Lewis Research Center
[NASA-TP-3038] p 3762 N92-31640
SUPERSONIC TEST APPARATUS
Supersonic Throughflow Fan Test Facility at NASA. Lewis Research Center
[NASA-TP-3038] p 3762 N92-31640
SUPERSONIC TRANSPORTS
NASA. Lewis Research Center supersonic throughflow fan program
[NASA-TM-103248] p 3759 N92-31250
Design and analysis issues of integrated control systems for high-speed civil transports
[NASA-CR-186022] p 3761 N92-31656
SUPERSONIC TURBINES
Supersonic Throughflow Fan Test Facility at NASA. Lewis Research Center
[NASA-TP-3038] p 3762 N92-31640
SUPERSONIC WIND TUNNELS
Supersonic Throughflow Fan Test Facility at NASA. Lewis Research Center
[NASA-TP-3038] p 3762 N92-31640
SUPERSYMMETRY
Minimal supersymmetric unification predictions
[RAL-92-005] p 3915 N92-31953
Resonant enhancement of flavor-changing neutrino interactions
[DE92-013020] p 3898 N92-32167
SUPPORT SYSTEMS
The determination of operational and support requirements and costs during the conceptual design of space systems
[NASA-CR-190626] p 3766 N92-31260
SURFACE CRACKS
The 3-D analysis and verification of fracture growth mechanisms in fiber-reinforced ceramic composies
[AD-A250893] p 3773 N92-31305
Effect of fracture surface interference on shear crack growth
[DE92-011431] p 3839 N92-31389
SURFACE DEFECTS
Instabilities of damage and surface degradation mechanisms in brittle material structural systems
[AD-A250785] p 3842 N92-32168
SURFACE DISTORTION
Application of optical theory to quantitative surface FT-IR with emphasis on molecular depth profiling
[AD-A250525] p 3902 N92-32077
SURFACE EMITTING LASERS
Laser material interactions
[AD-A250028] p 3831 N92-31802

SURFACE ENERGY
Electronic and total energy properties of ternary and quaternary semiconductor compounds, alloys, and superlattices: Theoretical study of Cu/graphite bonding
[NASA-CR-190691] p 3772 N92-31266
SURFACE LAYERS
Strongly adherent ceramic surface layers by ion implantation
[AD-A248882] p 3792 N92-31388
He atom-surface scattering: Surface dynamics of insulators, overlayers and crystal growth
[DE92-011810] p 3911 N92-31914
SURFACE PROPERTIES
Surface structures and surface processes of ceramics with atomic resolutions: A study by scanning tunneling microscopy
[AD-A249581] p 3792 N92-31377
A surface definition code for turbine blade surfaces
[DE92-010574] p 3846 N92-31498
On the spatial evolution of long-wavelength Goertler vortices governed by a viscous-inviscid interaction
[NASA-CR-189681] p 3822 N92-31687
Microstructure and properties of in-situ RF sputtered YBa2Cu3O7 thin films for microwave applications
[DE92-013379] p 3911 N92-31723
He atom-surface scattering: Surface dynamics of insulators, overlayers and crystal growth
[DE92-011810] p 3911 N92-31914
Substrate surface effects on the properties of sputter-deposited and laser-irradiated films
[DE92-013850] p 3795 N92-31917
Effect of surface modifications on the properties of silicon nitride ceramics
[DE92-013848] p 3797 N92-32094
SURFACE REACTIONS
Gibbs free energy of reactions involving SiC, Si3N4, H2, and H2O as a function of temperature and pressure
[NASA-TP-3275] p 3791 N92-31278
Tribology of functionally-terminated oligomer films
[AD-A250076] p 3833 N92-31433
Surface chemistry of MoS2 lubricant films: Effects of high humidity storage on sputtered films
[DE92-015392] p 3794 N92-31631
The synthesis and characterization of tribophysical layers on diamond and silicon carbide surfaces
[AD-A250983] p 3796 N92-32001
SURFACE ROUGHNESS
Fundamental studies of the structure of hypersonic attached and separated boundary layers over smooth, rough and transpiration-cooled surfaces
[AD-A250284] p 3819 N92-31286
Monte Carlo simulations of random rough surface scattering with finite element and finite difference methods
[AD-A247528] p 3901 N92-31430
An assessment of the B-747's capability to operate on rough surfaces
[AD-A250134] p 3757 N92-31793
The icing of the elevator of the DLR icing research aircraft of Do 28 type
[DLR-MITT-91-12] p 3755 N92-31813
Correlation from randomness: Quantitative analysis of sputtered graphite surfaces using the scanning tunneling microscope
[AD-A252420] p 3783 N92-31820
OSRMS: The DREP near-nadir scatterometer
[DREP-88-15] p 3844 N92-32216
SURFACE STABILITY
Instabilities of damage and surface degradation mechanisms in brittle material structural systems
[AD-A250785] p 3842 N92-32168
SURFACE TEMPERATURE
Ignition and flame propagation studies over a flat fuel surface
[PB92-181056] p 3780 N92-31678
The uncertainties of global temperatures in the global warming context
[TABES PAPER 92-447] p 3763 N92-32014
SURFACE TREATMENT
Laser decontamination: A new strategy for facility decommissioning
[DE92-014113] p 3831 N92-31775
SURFACE WATER
Hydrological and geochemical response and recovery in disturbed Arctic ecosystems
[DE92-016223] p 3850 N92-31312
SURFACE WAVES
Electromagnetic scattering by coated convex surfaces and wedges simulated by approximate boundary conditions
[NASA-CR-190540] p 3803 N92-31238
High-frequency techniques for RCS prediction of plate geometries
[NASA-CR-190656] p 3804 N92-31273
Acoustic studies of ocean surface processes in SWAPP
[AD-A247519] p 3864 N92-31429
Two-dimensional axisymmetric calculations of surface waves generated by an explosion in an island, mountain, and sedimentary basin
[AD-A249971] p 3856 N92-31510
Three-dimensional finite difference modeling of surface wave propagation across the Barents Shelf
[AD-A249865] p 3865 N92-31821
SURGES
Wavelet signal processing for transient feature extraction
[AD-A250519] p 3890 N92-32046
SURVEILLANCE
Results of earth observation study on STS-31 for Terra Geode, January 1987 - June 1991
[AD-A250750] p 3844 N92-31621
SURVEYS
NSF Tokyo reports. 1991 survey of research and development in Japan
[PB92-192624] p 3927 N92-32067
International mathematics and science assessments: What have we learned
[PB92-183599] p 3916 N92-32160
SURVIVAL
Immersion suit usage within the RAAF
[AD-A250645] p 3755 N92-31562
Canadian aircrew sea water survival, 1952-1987
[DCIEM-88-RR-39] p 3756 N92-32219
Demonstrated survivability of a high temperature optical fiber cable on a 1500 pound thrust rocket chamber
[NASA-TM-105835] p 3801 N92-32230
SURVIVAL EQUIPMENT
Immersion suit usage within the RAAF
[AD-A250645] p 3755 N92-31562
SWIMMING
Canadian aircrew sea water survival, 1952-1987
[DCIEM-88-RR-39] p 3756 N92-32219
SWITCHES
Calculational prediction of ultrawideband electromagnetic pulses by laser-initiated air avalanche switches
[DE92-011732] p 3812 N92-31334
Subnanosecond photoconductive switching in GaAs
[DE92-011521] p 3910 N92-31719
SWITCHING
Subnanosecond photoconductive switching in GaAs
[DE92-011521] p 3910 N92-31719
A sweep algorithm for massively parallel simulation of circuit-switched networks
[NASA-CR-189680] p 3881 N92-32157
SWITCHING CIRCUITS
Static and dynamic properties of current sensing power VDMOS transistor
[LAAS-92032] p 3815 N92-31697
SYMBOLIC PROGRAMMING
New algorithms for the minimal form problem
[DE92-011963] p 3879 N92-31743
SYMMETRY
Two-dimensional axisymmetric calculations of surface waves generated by an explosion in an island, mountain, and sedimentary basin
[AD-A249971] p 3856 N92-31510
Development of effective quantum chemical method for polymers and solid
[AD-A250976] p 3795 N92-31951
SYNAPSES
Acetylcholinesterase inhibitors on the spinal cord
[AD-A252694] p 3868 N92-31326
Organization of the human circadian system
[AD-A247498] p 3869 N92-31905
SYNCHRONISM
The investigation of bandwidth efficient coding and modulation techniques
[NASA-CR-190685] p 3806 N92-31468
Square-law device analysis for the detection and timing estimation of a burst BPSK signal
[DREO-91-6] p 3809 N92-31921
SYNCHRONIZERS
Square-law device analysis for the detection and timing estimation of a burst BPSK signal
[DREO-91-6] p 3809 N92-31921
SYNCHRONOUS PLATFORMS
Wavelength-tunable liquid crystal imaging filters for remote sensing from geosynchronous platforms
[NASA-CR-190698] p 3845 N92-32223
SYNCHROTRON RADIATION
Pulse-by-pulse energy measurement at the Stanford Linear Collider
[DE92-011520] p 3899 N92-31390
Microdistribution of lead in bone: A new approach
[DE92-013036] p 3869 N92-31589
SYNCHROTRONS
Activities of the Center for X Ray Lithography, phase 1
[AD-A250446] p 3901 N92-31397
The NSLS 100 element solid state array detector
[DE92-014477] p 3827 N92-31502
The 6-D phase space tracking with acceleration: Modeling low energy proton synchrotrons, part 1
[DE92-013744] p 3899 N92-31948
SYNOPTIC METEOROLOGY
The structure and energetics of Amazon squall lines
[AD-A250182] p 3859 N92-31523
A case study of a prolonged sleet event: 16-17 February 1987 and climatology of sleet events for North Carolina, 1949-1989
[AD-A250184] p 3859 N92-31602
SYNTHESIS (CHEMISTRY)
The role of metal structure in determining solvent orientation at the electrode/solution interface
[AD-A249751] p 3893 N92-31328
Imide/arylene ether copolymers
[NASA-CASE-LAR-14159-1-CU] p 3794 N92-31792
Organic main-chain NLO polymers. 1: Copolymerization of bis(arylcarboxaldehyde) and bis(cyanoacetate) monomers via the Knoevenagel condensation
[AD-A250215] p 3802 N92-31826
Probe molecule studies: Active species in alcohol synthesis
[DE92-015430] p 3784 N92-32029
Synthesis of cresols and xylenols from phenol and methanol
[DE91-002141] p 3785 N92-32093
SYNTHETIC APERTURE RADAR
Using the burst derivative measure to improve the computational efficiency of ISAR motion compensation algorithms
[AD-A250850] p 3805 N92-31369
Optical processing architectures for spaceborne SAR image generation and RF array beam forming
[TABES PAPER 92-444] p 3763 N92-32012
Radar backscatter from the sea: Controlled experiments
[AD-A250858] p 3810 N92-32101
SYNTHETIC FUELS
Light alkane conversion processes: Suprabiotic catalyst systems for selective oxidation of light alkane gases to fuel oxygenates
[DE92-015229] p 3799 N92-31751
Probe molecule studies: Active species in alcohol synthesis
[DE92-015430] p 3784 N92-32029
SYSTEM FAILURES
Spacecraft dynamics characterization and control system failure detection. Volume 3: Control system failure monitoring
[NASA-CR-190529] p 3884 N92-31254
Sequential estimation of optimal age replacement policies when distribution of lifetimes is phase type
[AD-A249020] p 3836 N92-31479
Continuous time and discrete time hyperexponential model for dependability growth modeling
[LAAS-92002] p 3837 N92-31693
Development of a fault isolation system database manager
[AD-A248346] p 3916 N92-31992
SYSTEM IDENTIFICATION
Maximum likelihood estimation of fractional Brownian motion and Markov noise parameters
[AD-A249623] p 3890 N92-31686
SYSTEMS ANALYSIS
Type evolution and instance adaptation
[AD-A248435] p 3917 N92-31285
Methodology investigation final report: Automated real-time test scenario generation, phase 1
[AD-A250439] p 3884 N92-31395
An alternative to sneakernet
[DE92-011146] p 3918 N92-31448
Requirements Engineering and Analysis Workshop Proceedings
[AD-A250415] p 3876 N92-31541
Analysis of systems hardware flown on LDEF. Results of the systems special investigation group
[NASA-CR-189628] p 3767 N92-31677
About real time industrial processes control: A methodology based on objects and Petri nets
[LAAS-91467] p 3878 N92-31689
SYSTEMS ENGINEERING
Implementing relational operations in an object-oriented database
[AD-A249332] p 3918 N92-31450
Advanced thermally stable, jet fuels development program annual report. Volume 1: Model and experiment system development
[AD-A249625] p 3799 N92-31462
Requirements Engineering and Analysis Workshop Proceedings
[AD-A250415] p 3876 N92-31541
Establishing low-power operating limits for liquid metal heat pipes
[DE92-011367] p 3823 N92-31701

Configuration management and software measurement in the Ground Systems Development Environment (GSDE)
[NASA-CR-190716] p 3879 N92-31787
Development of a fault isolation system database manager
[AD-A248346] p 3916 N92-31992

SYSTEMS INTEGRATION
A microprism array for large-scale, wide-band interconnection of optoelectronic systems
[AD-A249380] p 3813 N92-31374
Methodology investigation final report: Automated real-time test scenario generation, phase 1
[AD-A250439] p 3884 N92-31395
Stable integrated microwave to optical modulator
[AD-A249974] p 3813 N92-31431
Design and analysis issues of integrated control systems for high-speed civil transports
[NASA-CR-186022] p 3761 N92-31656
System overview of the NASA Dryden Integrated Test Facility
[NASA-TM-104250] p 3762 N92-32201

SYSTEMS STABILITY
Stability testing and analysis of a PMAD DC test bed for the Space Station Freedom
[NASA-TM-105846] p 3812 N92-31282
Stable integrated microwave to optical modulator
[AD-A249974] p 3813 N92-31431

T

TABLES (DATA)
Solar-geophysical data number 572, April 1992. Part 2: (Comprehensive reports). Data for October 1991 and miscellaneous
[PB92-187731] p 3856 N92-31639
Trends 1991: A compendium of data on global change
[DE92-011733] p 3854 N92-31907

TACHOMETERS
An innovative two axis rate gyro: Theory and principles of operation p 3748 N92-31875

TACTICS
Optimal targeting of evading objects
[DE92-014719] p 3889 N92-32119

TAKEOFF RUNS
An assessment of the B-747's capability to operate on rough surfaces
[AD-A250134] p 3757 N92-31793

TANGENTS
Analysis of random induced cross polarization
[AD-A249773] p 3806 N92-31569

TANKS (COMBAT VEHICLES)
Head tracking and head mounted displays for training simulations
[AD-A250866] p 3873 N92-31974

TAPS
Effects of flow conditioners and tap location on orifice flowmeter performance
[PB92-183730] p 3824 N92-31839

TARGET ACQUISITION
Empirical development of a scale for the prediction of performance on a sustained monitoring task
[AD-A252443] p 3872 N92-31294
Estimation with multisensor/multiscan detection fusion
[AD-A250496] p 3804 N92-31333
Discrete optimal guidance for high order missile and maneuvering target p 3748 N92-31879
Ground based radar
[TABES PAPER 92-213] p 3764 N92-32021
RL-34 ring laser gyro laboratory evaluation for the Deep Space Network antenna application
[NASA-CR-190481] p 3829 N92-32128

TARGET RECOGNITION
Piezoelectric radiant-to-air ultrasonic transducers p 3811 N92-31244
Using the burst derivative measure to improve the computational efficiency of ISAR motion compensation algorithms
[AD-A250850] p 3805 N92-31369
Results of earth observation study on STS-31 for Terra Geode, January 1987 - June 1991
[AD-A250750] p 3844 N92-31621

TARGETS
Using the burst derivative measure to improve the computational efficiency of ISAR motion compensation algorithms
[AD-A250850] p 3805 N92-31369
Modular UNIX (trade name)-based Vulnerability Estimation Suite (MUVES) analyst's guide
[AD-A245322] p 3876 N92-31488
An automated computational method for barrier construction in single and two-target differential games p 3749 N92-31882

TASK PLANNING (ROBOTICS)
Singularity avoidance for SCARA-type robots p 3746 N92-31867

TASKS
Heuristic sampling on DAGs
[DE92-017359] p 3917 N92-32037

TECHNOLOGIES
STI handbook: Guidelines for producing, using, and managing scientific and technical information in the Department of the Navy. A handbook for Navy scientists and engineers on the use of scientific and technical information
[AD-A252439] p 3918 N92-31482

TECHNOLOGY ASSESSMENT
The evolutionary development of high specific impulse electric thruster technology
[NASA-TM-105712] p 3769 N92-31342
International Semiconductor Device Research Symposium (ISDRS-91)
[AD-A249348] p 3813 N92-31373
Pressure fed thrust chamber technology program
[NASA-CR-190666] p 3770 N92-31550
Annual report to the Congress, fiscal year 1991 (Office of Technology Assessment)
[PB92-166549] p 3922 N92-31599
Specification and verification of secure concurrent and distributed software systems
[AD-A252477] p 3879 N92-31825
Potassium Rankine cycle nuclear power systems for spacecraft and lunar-mass surface power
[DE92-016163] p 3770 N92-31897
Soviet satellite communications science and technology
[PB92-173038] p 3809 N92-31920
A program for the transfer of manufacturing technology from the national laboratories
[DE92-011905] p 3923 N92-31965
GIS: Geographic Information Systems. State of the art and future tendencies
[INPE-5358-NTC/301] p 3922 N92-32227

TECHNOLOGY TRANSFER
International Semiconductor Device Research Symposium (ISDRS-91)
[AD-A249348] p 3813 N92-31373
EnviroTRADE: Its role in the cleanup of the environment
[DE92-013691] p 3851 N92-31427
Cooperative field test program for wind systems
[DE92-001209] p 3847 N92-31579
Technology Integration Workshop: Selected papers
[PB92-158278] p 3923 N92-31643
Iterative functionalism and climate management regimes: From intergovernmental panel on climate change to intergovernmental negotiating committee
[DE92-014798] p 3853 N92-31896
A program for the transfer of manufacturing technology from the national laboratories
[DE92-011905] p 3923 N92-31965
Workshop on the Derivation of Parallel Programs and Architectures: Closing report
[AD-A252742] p 3883 N92-32109
Facilitating the transfer of scientific and technical information with scientific and technical numeric databases p 3922 N92-32192
NASA programs --- nasa space programs p 3765 N92-32238

TECHNOLOGY UTILIZATION
Transient fission gas behavior in uranium nitride fuel under proposed space applications
[AD-A252577] p 3899 N92-31325
Small tokamaks for fusion technology testing
[DE92-011790] p 3906 N92-31913
GIS: Geographic Information Systems. State of the art and future tendencies
[INPE-5358-NTC/301] p 3922 N92-32227

TELECOMMUNICATION
Design and specification of a high speed transport protocol
[AD-A248323] p 3804 N92-31284

TELEMETRY
A data processing module for acoustic Doppler current meters
[AD-A250901] p 3891 N92-31563

TELEROBOTICS
Robotics development for the enhancement of space endeavors
[TABES PAPER 92-445] p 3763 N92-32013

TELESCOPES
Resolution limits for ground based astronomical imaging using adaptive optics
[DE92-011949] p 3902 N92-31761
A solar magnetic and velocity field measurement system for Spacelab 2: The Solar Optical Universal Polarimeter (SOUP)
[NASA-CR-190683] p 3925 N92-31856

TELEVISION CAMERAS
Design and development of minilink video: A fiber-optic coupled video system
[AD-A249945] p 3808 N92-31801

TELEVISION SYSTEMS
Space constancy on video display terminals
[AD-A247290] p 3872 N92-32105

TEMPERATURE
Pressure and temperature for B-1B transparency test
[AD-A252711] p 3752 N92-31674
Meteorological data, new series B basic material. Volume 53, no. 1: Daily altitude maps of the 30-hPa-area and monthly mean maps for the year 1986, part 1
[QR-1-VOL-53-NO-1-PT-1] p 3860 N92-31702
Meteorological data, new series B basic material. Volume 53, no. 4: Daily altitude maps of the 30-hPa-area and monthly mean maps for the year 1986, part 4
[QR-4-VOL-53-NO-4-PT-4] p 3861 N92-31706

TEMPERATURE CONTROL
Subsonic flight test evaluation of a performance seeking control algorithm on an F-15 airplane
[NASA-TM-4400] p 3759 N92-31275
Control of rapid thermal processing equipment for microelectronics applications
[LAAS-92013] p 3787 N92-31695
An overview of the Lewis Research Center CSTI thermal management program
[NASA-TM-105310] p 3771 N92-31916

TEMPERATURE DEPENDENCE
Gibbs free energy of reactions involving SiC, Si3N4, H2, and H2O as a function of temperature and pressure
[NASA-TP-3275] p 3791 N92-31278
Heat transfer and flow of a modified second grade fluid
[DE92-014744] p 3824 N92-31895
Epitaxial iron films
[AD-A250402] p 3912 N92-31915
Radiolytic gas production in the alpha particle degradation of plastics
[DE92-011846] p 3795 N92-31938
Solid electrolytes and impact-resistant ceramics
[DE92-015297] p 3797 N92-32095
Effects of fiber and interfacial layer architectures on the thermoplastic response of metal matrix composites
[NASA-TM-105802] p 3777 N92-32234

TEMPERATURE EFFECTS
Cryogenic 4.4 MN mechanical test system for large scale tests of composite support struts
[PB92-181148] p 3774 N92-31609
Pressure and temperature for B-1B transparency test
[AD-A252711] p 3752 N92-31674
Temperature-enhanced autodetachment from long-lived parent negative ions of gaseous dielectrics
[DE92-011108] p 3894 N92-31700
VAASEL-ANSYS comparison for a thermally loaded beam
[AD-A251003] p 3841 N92-31847
Movement of dislocations in quartz
[AD-A250527] p 3913 N92-32078
Effect of synthesis temperature in the structure, doping level and charge-transport properties of polypyrrole
[AD-A250531] p 3796 N92-32079
Probabilistic analysis of twenty-four hour weather data for Warsaw p 3863 N92-32097
An investigation of the thermoviscoplastic behavior of a metal matrix composite at elevated temperatures
[NASA-CR-190700] p 3777 N92-32159

TEMPERATURE GRADIENTS
Vortices associated with toroidal ion temperature gradient driven fluctuations
[DE92-016180] p 3903 N92-31412
Ion temperature gradient instability and transport
[DE92-013590] p 3905 N92-31727

TEMPERATURE MEASUREMENT
Monitoring gas temperatures entering an MHD superheater
[DE92-014200] p 3903 N92-31372
Feasibility study for a low-altitude wide and temperature profiler
[PB92-188200] p 3860 N92-31641

TEMPERATURE PROFILES
Synthetic temperature profile in the Gulf of Mexico. Part 1: Statistical relationship between modal amplitudes and dynamic height at surface
[AD-A252701] p 3863 N92-31308
Propane oxidation through the negative temperature coefficient region at 10 and 15 atmospheres: Results of experimental and modeling studies
[DE92-007902] p 3778 N92-31414
Non-geothermal optics study of wave propagation
[DE92-011806] p 3903 N92-31494
User's guide for treetherm: A 3-D thermal model for single trees
[LTR91-003] p 3879 N92-31833

TEMPORAL DISTRIBUTION
A comparative analysis of the temporal variability of lightning observations and GOES imagery
[AD-A250185] p 3860 N92-31603
TEMPORAL RESOLUTION
Fine structure superimposed on mm-wavelength (18-23 GHz) spectra of solar active region
[INPE-5371-TDI/470] p 3926 N92-32221
TENSILE PROPERTIES
Imide/arylene ether copolymers
[NASA-CASE-LAR-14159-1-CU] p 3794 N92-31792
TENSILE STRESS
Residual stresses in a multipass ferritic weldment
[DE92-014467] p 3839 N92-31501
TENSILE TESTS
Thermomechanical fatigue behavior of a silicone carbide fiber-reinforced calcium aluminosilicate glass-ceramic matrix composite
[AD-A249870] p 3775 N92-31823
TENSION
An experimental procedure for the Iosipescu composite specimen tested in the modified Wyoming fixture
[NASA-CR-190660] p 3774 N92-31566
TERMINAL BALLISTICS
Modular UNIX (trade name)-based Vulnerability Estimation Suite (MUVES) analyst's guide
[AD-A245322] p 3876 N92-31488
A penetration mechanics database
[AD-A246351] p 3767 N92-31997
TERMINOLOGY
A dictionary of acquisition and contracting terms
[AD-A247053] p 3920 N92-31754
Correspondence dictionary from free English term to INIS descriptors
[DE92-782192] p 3920 N92-31859
TERMS
A dictionary of acquisition and contracting terms
[AD-A247053] p 3920 N92-31754
Correspondence dictionary from free English term to INIS descriptors
[DE92-782192] p 3920 N92-31859
TERNARY ALLOYS
Non-equilibrium synthesis by laser cladding of Ni, Nb and Mg alloys for improved environmental resistance
[AD-A250552] p 3787 N92-31612
TERRAIN
Results of earth observation study on STS-31 for Terra Geode, January 1987 - June 1991
[AD-A250750] p 3844 N92-31621
Multi-year strategic plan for the atmospheric studies in complex terrain: ASCOT program
[DE92-016646] p 3854 N92-31930
TEST EQUIPMENT
New technology for remote testing of response time of installed thermocouples. Volume 2: Research data
[AD-A245821] p 3826 N92-31298
Orbit transfer vehicle engine technology program. Task B-6 high speed turbopump bearings
[NASA-CR-189230] p 3835 N92-31892
System overview of the NASA Dryden Integrated Test Facility
[NASA-TM-104250] p 3762 N92-32201
Acoustic emission method applied to tests on concrete p 3842 N92-32206
TEST FACILITIES
A free-piston Stirling engine/linear alternator controls and load interaction test facility
[NASA-TM-105825] p 3845 N92-31262
Space nuclear power, propulsion, and related technologies
[SAND91-2617] p 3770 N92-31503
Outdoor testing of advanced optical materials for solar thermal electric applications
[DE92-010567] p 3847 N92-31623
Preliminary design for a MAGLEV development facility
[DE92-012259] p 3835 N92-31774
Turbine blade tip and seal clearance excitation forces
[NASA-CR-184341] p 3760 N92-31910
System overview of the NASA Dryden Integrated Test Facility
[NASA-TM-104250] p 3762 N92-32201
TEST FIRING
Cyclic hot firing results of tungsten-wire-reinforced, copper-lined thrust chambers
[NASA-TM-4214] p 3769 N92-31249
TEST STANDS
Design, analysis, and testing of the Phase 1 CSI Evolutionary Model erectable truss
[NASA-CR-4461] p 3767 N92-32100
TEST VEHICLES
Preliminary design for a MAGLEV development facility
[DE92-012259] p 3835 N92-31774
TETHERED SATELLITES
Italian-US cooperation in space: The case of Tethered, IRIS/LAGEOS, and SPACEHAB
[TABES PAPER 92-467] p 3764 N92-32019
TETRAHYDROFURAN
Development of characterization techniques for polyurethanes 1. Characterization of SRM 1480, a low molecular weight polyurethane for SEC calibration
[PB92-172485] p 3794 N92-31618
TEXTILES
Device for monitoring the thickness of a dielectric coating on a dielectric substrate
[DE92-014741] p 3829 N92-32174
TEXTS
Use of expert systems as user interfaces in information retrieval p 3921 N92-32185
Automated input into databases: OCR and descriptive cataloguing p 3921 N92-32189
THEMATIC MAPPERS (LANDSAT)
Images simulation of sensors with large field of view from images of sensors with less field of view: The SSR/TM case
[INPE-5378-TDI/473] p 3845 N92-32220
THEOREM PROVING
A language for higher-order explanation-based learning
[AD-A251008] p 3880 N92-31939
THEORETICAL PHYSICS
Theoretical high energy physics research at the University of Chicago, task A
[DE92-016288] p 3899 N92-31712
Theoretical atomic collision physics
[DE92-013571] p 3895 N92-31724
Feynman diagrams and Vassiliev invariants
[PB92-178284] p 3890 N92-31925
Solar neutrinos: Theory versus experiment
[DE92-014327] p 3925 N92-32154
THERMAL ABSORPTION
Heat and mass transfer considerations in advanced heat pump systems
[DE92-016635] p 3825 N92-32003
THERMAL ANALYSIS
Research into improving the durability of the hot section in the aircraft turbine engine
[AD-A250342] p 3759 N92-31439
Control of rapid thermal processing equipment for microelectronics applications
[LAAS-92013] p 3787 N92-31695
Thin polymer icemaker development and test program
[DE92-016941] p 3803 N92-32125
THERMAL CONDUCTIVITY
A numerical, analytical, and observational study of the effect of clouds on surface wind and wind stress during the central Arctic winter
[AD-A252706] p 3860 N92-31670
An overview of the Lewis Research Center CSTI thermal management program
[NASA-TM-105310] p 3771 N92-31916
Mechanics of thin films
[AD-A247848] p 3912 N92-31984
High density thin-walled syntactic foam
[DE92-013159] p 3797 N92-32136
THERMAL CYCLING TESTS
Cyclic hot firing results of tungsten-wire-reinforced, copper-lined thrust chambers
[NASA-TM-4214] p 3769 N92-31249
THERMAL DECOMPOSITION
Inorganic rings on carbon chains
[AD-A251043] p 3772 N92-31850
The thermal dissociation of decaborane on Si(111)-(7x7) and doping effects in the near surface region
[AD-A251057] p 3911 N92-31851
THERMAL DEGRADATION
Advanced thermally stable jet fuel development program. Volume 2: Compositional factors affecting thermal degradation of jet fuels
[AD-A252656] p 3798 N92-31399
THERMAL DISSOCIATION
The thermal dissociation of decaborane on Si(111)-(7x7) and doping effects in the near surface region
[AD-A251057] p 3911 N92-31851
THERMAL ENERGY
Solar thermal energy storage in phase change materials
[DE92-016908] p 3849 N92-32091
THERMAL ENVIRONMENTS
Technology advancing research combustion in burners
[PB92-164359] p 3782 N92-31776
Ultrafast studies on electron transfer in the betaines: Evidence for local heating
[AD-A250728] p 3897 N92-31999
THERMAL EXPANSION
Low thermal coefficient of expansion printed wiring boards
[DE92-013704] p 3817 N92-31946
THERMAL FATIGUE
Fatigue in single crystal nickel superalloys
[AD-A250068] p 3786 N92-31360
Fatigue in single crystal nickel superalloys
[AD-A252492] p 3790 N92-32066
THERMAL NEUTRONS
Prompt neutron lifetime in a strongly heterogeneous lattice
[DE92-013212] p 3898 N92-32165
THERMAL REACTORS
Some computational challenges of developing efficient parallel algorithms for data-dependent computations in thermal-hydraulics supercomputer applications
[DE92-011368] p 3878 N92-31703
THERMAL RESISTANCE
Further studies in filmwise condensation of steam on horizontal finned tubes
[AD-A252705] p 3915 N92-31767
Mechanics of thin films
[AD-A247848] p 3912 N92-31984
THERMAL SHOCK
Mechanical strength and stability of lithium aluminate
[DE92-015998] p 3841 N92-31638
THERMAL SIMULATION
Control of rapid thermal processing equipment for microelectronics applications
[LAAS-92013] p 3787 N92-31695
THERMAL STABILITY
Advanced thermally stable jet fuel development program. Volume 2: Compositional factors affecting thermal degradation of jet fuels
[AD-A252656] p 3798 N92-31399
Advanced thermally stable, jet fuels development program annual report. Volume 1: Model and experiment system development
[AD-A249625] p 3799 N92-31462
The crystal growth and characterization of the solid solutions (ZnS)(1-x)(CuMS2)(x)
[AD-A248029] p 3911 N92-31819
Supercritical fluid fractionation of JP-8
[AD-A247835] p 3801 N92-31982
THERMAL STRESSES
Research into improving the durability of the hot section in the aircraft turbine engine
[AD-A250342] p 3759 N92-31439
Low thermal coefficient of expansion printed wiring boards
[DE92-013704] p 3817 N92-31946
Effects of fiber and interfacial layer architectures on the thermoplastic response of metal matrix composites
[NASA-TM-105802] p 3777 N92-32234
THERMIONIC CONVERTERS
Potassium Rankine cycle nuclear power systems for spacecraft and lunar-mass surface power
[DE92-016163] p 3770 N92-31897
THERMISTORS
Computer simulation of acoustic fluctuations due to finescale temperature perturbations measured by thermistor chain
[AD-A252709] p 3892 N92-31672
THERMOCHEMISTRY
Catalyst and feedstock effects in the thermochemical conversion of biomass to liquid transportation fuels
[DE92-010569] p 3799 N92-31593
Unimolecular reaction mechanisms involving C3H4, C4H4, and C6H6 hydrocarbon species
[DE92-005326] p 3783 N92-31860
THERMOCOUPLES
New technology for remote testing of response time of installed thermocouples. Volume 2: Research data
[AD-A245821] p 3826 N92-31298
Monitoring gas temperatures entering an MHD superheater
[DE92-014200] p 3903 N92-31372
THERMODYNAMIC CYCLES
Heat and mass transfer considerations in advanced heat pump systems
[DE92-016635] p 3825 N92-32003
THERMODYNAMIC PROPERTIES
Application of the mean spherical approximation to the estimations of single ion thermodynamic quantities of solvation for monoatomic monovalent ions in aqueous solutions
[AD-A250190] p 3893 N92-31316
Thermodynamic assessment of the Cr-Zr system
[PB92-180645] p 3787 N92-31610
Establishing low-power operating limits for liquid metal heat pipes
[DE92-011367] p 3823 N92-31701
Autoignition behavior of lean mixtures: Chemical and thermodynamics effects
[DE92-009690] p 3781 N92-31763
Analyses and predictions of the thermodynamic properties and phase diagrams of silicate systems
[DE92-016177] p 3783 N92-31857
Potassium Rankine cycle nuclear power systems for spacecraft and lunar-mass surface power
[DE92-016163] p 3770 N92-31897
Physical characterization of magmatic liquids
[DE92-015302] p 3858 N92-32027

Solar thermal energy storage in phase change materials
[DE92-016908] p 3849 N92-32091

THERMODYNAMICS
Gibbs free energy of reactions involving SiC, Si3N4, H2, and H2O as a function of temperature and pressure
[NASA-TP-3275] p 3791 N92-31278
An approximate local thermodynamic nonequilibrium radiation model for air
[NASA-CR-190580] p 3914 N92-31577
Geometric theory of infinite dimensional dynamical systems
[AD-A252190] p 3915 N92-31585
Thermomechanical fatigue behavior of a silicone carbide fiber-reinforced calcium aluminosilicate glass-ceramic matrix composite
[AD-A249870] p 3775 N92-31823
Tailored metal matrix composites for high-temperature performance
[NASA-TM-105816] p 3775 N92-31854

THERMOELECTRIC GENERATORS
Sodium Heat Engine Development Program
[DE92-012398] p 3846 N92-31531
Outdoor testing of advanced optical materials for solar thermal electric applications
[DE92-010567] p 3847 N92-31623

THERMOELECTRIC MATERIALS
Outdoor testing of advanced optical materials for solar thermal electric applications
[DE92-010567] p 3847 N92-31623

THERMOHYDRAULICS
Pressure loss and heat transfer in a toothed finned heat transfer medium
[MBB-UO-0163-91-PUB] p 3915 N92-31660

THERMOLUMINESCENCE
An evaluation of ionizing radiation emitted by high power microwave generators
[DE92-016160] p 3805 N92-31387

THERMOMECHANICAL TREATMENT
The effect of thermomechanical processing parameters on the ambient behavior of 10 percent volume 6061 Al-Alumina
[AD-A252177] p 3776 N92-32064

THERMOMETERS
A sealed He-4 superfluid-transition fixed-point device
[DE92-014271] p 3908 N92-31403

THERMONUCLEAR REACTIONS
Institute of Geophysics and Planetary Physics, 1991
[DE92-016981] p 3923 N92-32005
Exotic nuclear shapes and configurations that can be studied at high spin using radioactive ion beams
[DE92-016800] p 3898 N92-32090

THERMOPLASTIC RESINS
Preparation of non-oxide ceramics by pyrolysis of organometallic precursors
[AD-A251112] p 3798 N92-32197

THERMOPLASTICITY
An investigation of the thermoviscoplastic behavior of a metal matrix composite at elevated temperatures
[NASA-CR-190700] p 3777 N92-32159
Effects of fiber and interfacial layer architectures on the thermoplastic response of metal matrix composites
[NASA-TM-105802] p 3777 N92-32234

THESAURI
Correspondence dictionary from free English term to INIS descriptors
[DE92-782192] p 3920 N92-31859
Search strategies in natural language
p 3921 N92-32186

THICK FILMS
Absorption spectra and electronic properties of alkali metal doped C60
[AD-A251006] p 3912 N92-31937

THICK PLATES
A finite element procedure for analysis of laminated composite plates
[AD-A250902] p 3773 N92-31307

THICKNESS
Digital analysis of wind tunnel imagery to measure fluid thickness
[NASA-CR-189234] p 3762 N92-31252
Device for monitoring the thickness of a dielectric coating on a dielectric substrate
[DE92-014741] p 3829 N92-32174

THIN FILMS
Tribology of Langmuir-Blodgett films
[AD-A250075] p 3833 N92-31363
Tribology of functionally-terminated oligomer films
[AD-A250076] p 3833 N92-31433
Growth, nitrogen vacancy reduction and solid solution formation in cubic GaN thin films and the subsequent fabrication of superlattice structures using AlN and InN
[AD-A248058] p 3908 N92-31446
High temperature superconducting films and multilayers for electronics
[AD-A250732] p 3813 N92-31451
Module process optimization and device efficiency improvement for stable, low-cost, large-area, cadmium telluride-based photovoltaic module production
[DE92-010564] p 3846 N92-31497
Development of a computer model for polycrystalline thin-film CuInSe2 and CdTe solar cells
[DE92-001242] p 3846 N92-31526
Effect of out-of-roundness on the performance of a diesel engine connecting-rod bearing
[NASA-TM-105600] p 3834 N92-31536
Computer simulation of scattered ion and sputtered species effects in ion beam sputter-deposition of high temperature superconducting thin films
[DE92-015227] p 3909 N92-31546
Sol-gel multilayers applied by a meniscus coating process
[DE92-012697] p 3794 N92-31560
Surface chemistry of MoS2 lubricant films: Effects of high humidity storage on sputtered films
[DE92-015392] p 3794 N92-31631
Ion beam spectroscopy as a means of in-situ monitoring of thin film deposition
[DE92-014857] p 3909 N92-31652
Microstructure and properties of in-situ RF sputtered YBa2Cu3O7 thin films for microwave applications
[DE92-013379] p 3911 N92-31723
The preparation of (Al2O3)x(SiO2)y thin films using (Al(OSiEt3))2 as a single source precursor
[AD-A250142] p 3788 N92-31796
Energetics, bonding mechanism and electronic structure of metal/ceramic interfaces
[DE92-013401] p 3775 N92-31806
Photogenerated base as catalyst for imidization reactions: Design of photosensitive polyimides
[AD-A250067] p 3795 N92-31810
Characterization of oxides for low temperature solid oxide fuel cells
[PB92-152883] p 3848 N92-31903
Epitaxial iron films
[AD-A250402] p 3912 N92-31915
Substrate surface effects on the properties of sputter-deposited and laser-irradiated films
[DE92-013850] p 3795 N92-31917
Real time investigations of the polymerization of 2-pentadecyl aniline on the Langmuir-Blodgett trough
[AD-A250994] p 3795 N92-31954
Mechanics of thin films
[AD-A247848] p 3912 N92-31984
The chemistry and packaging of nanocomposite confined arrays
[AD-A250991] p 3817 N92-32002
Ferroelectric thin films prepared by pulse laser deposition processing and characterization
[PB92-196088] p 3913 N92-32072
Preparation of non-oxide ceramics by pyrolysis of organometallic precursors
[AD-A251112] p 3798 N92-32197

THIN WALLS
Strength tests of cold-formed channel sections undergoing local and distortional buckling
[PB92-180835] p 3841 N92-31658
High density thin-walled syntactic foam
[DE92-013159] p 3797 N92-32136

THREE DIMENSIONAL BODIES
High brightness x ray source for directed energy and holographic imaging applications, phase 2
[AD-A248858] p 3827 N92-31475

THREE DIMENSIONAL BOUNDARY LAYER
The structure and control of three-dimensional shock wave turbulent boundary layer interactions
[AD-A250209] p 3823 N92-31824
Navy Atmospheric Boundary Layer (NABL) model system: Software/Interface design document
[AD-A247903] p 3857 N92-31986

THREE DIMENSIONAL COMPOSITES
The 3-D analysis and verification of fracture growth mechanisms in fiber-reinforced ceramic composies
[AD-A250893] p 3773 N92-31305
The chemistry and packaging of nanocomposite confined arrays
[AD-A250991] p 3817 N92-32002

THREE DIMENSIONAL FLOW
Description of a 1000 sensor constant current anemometer system for locating three-dimensional turbulent boundary layer separations
[AD-A250827] p 3821 N92-31452
The three-dimensional stability of the Foeppl vortices
p 3750 N92-31889
New techniques in computational fluid dynamics: Algorithms, analysis, applications
[AD-A250498] p 3825 N92-32038
Three-dimensional compressible turbulent computations for a nondiffusing S-duct
[NASA-CR-4391] p 3754 N92-32240

THREE DIMENSIONAL MODELS
Modal simulation of gearbox vibration with experimental correlation
[NASA-TM-105702] p 3834 N92-31485
From perception to modelization in robotics using achromatic and chromatic cameras
[LAAS-91484] p 3901 N92-31692
Three-dimensional finite difference modeling of surface wave propagation across the Barents Shelf
[AD-A249865] p 3865 N92-31821
User's guide for treetherm: A 3-D thermal model for single trees
[LTR91-003] p 3879 N92-31833
Euler solver for arbitrary configurations: Further applications p 3750 N92-31888
The hierarchical spatial decomposition of three-dimensional particle-in-cell plasma simulations on MIMD distributed memory multiprocessors
[DE92-016802] p 3883 N92-32034

THREE DIMENSIONAL MOTION
Development and application of new algorithms for the simulation of compressible flows with moving bodies in three dimensions
[AD-A250232] p 3823 N92-31696

THRESHOLDS (PERCEPTION)
Function of panel M pathways in primates
[AD-A250275] p 3871 N92-31758
Function of P and M pathways in primates
[AD-A250055] p 3867 N92-31778

THROTTLING
Orbital transfer rocket engine technology: Advanced engine study
[NASA-CR-187216] p 3771 N92-32129

THRUST
Krypton ion thruster performance
[NASA-TM-105818] p 3770 N92-31901

THRUST CHAMBERS
Cyclic hot firing results of tungsten-wire-reinforced, copper-lined thrust chambers
[NASA-TM-4214] p 3769 N92-31249
Pressure fed thrust chamber technology program
[NASA-CR-190666] p 3770 N92-31550
Demonstrated survivability of a high temperature optical fiber cable on a 1500 pound thrust rocket chamber
[NASA-TM-105835] p 3801 N92-32230

THRUST CONTROL
Subsonic flight test evaluation of a performance seeking control algorithm on an F-15 airplane
[NASA-TM-4400] p 3759 N92-31275

THRUSTORS
The evolutionary development of high specific impulse electric thruster technology
[NASA-TM-105712] p 3769 N92-31342
Numerical simulation of geometric scale effects in cylindrical self-field MPD thrusters
[NASA-CR-189224] p 3772 N92-32239

THUNDERSTORMS
Cloud-to-ground lightning characteristics in mesoscale convective systems
[AD-A250418] p 3858 N92-31493
A comparative analysis of the temporal variability of lightning observations and GOES imagery
[AD-A250185] p 3860 N92-31603

TIME CONSTANT
Importance sampling for Markov chains: Asymptotics for the variance
[AD-A249804] p 3888 N92-31757

TIME DEPENDENCE
On the spatial evolution of long-wavelength Goertler vortices governed by a viscous-inviscid interaction
[NASA-CR-189681] p 3822 N92-31687
Calculations of emittance and damping time effects in the SLC damping rings
[DE92-012420] p 3900 N92-32133

TIME MARCHING
CAVEAT: A computer code for fluid dynamics problems with large distortion and internal slip
[DE92-014078] p 3825 N92-32022

TIME MEASUREMENT
Time and space resolved electron impact excitation rates in an RF glow discharge
[AD-A249614] p 3905 N92-31688
Soviet precision timekeeping research and technology
[PB92-173046] p 3802 N92-31830
Energy and Environment: A Sandia Technology Bulletin
[DE92-016740] p 3854 N92-31931

TIME OF FLIGHT SPECTROMETERS
Ion beam spectroscopy as a means of in-situ monitoring of thin film deposition
[DE92-014857] p 3909 N92-31652

TIME OPTIMAL CONTROL
Optimal trajectories for an unmanned air vehicle
p 3748 N92-31880

TIME RESPONSE
Phase characteristics and time responses of unknown linear systems determined from measured CW amplitude data
[PB92-183722] p 3805 N92-31368
TIME TEMPERATURE PARAMETER
Controlled atmosphere soldering system
[DE92-012633] p 3802 N92-31580
TIN
Interface engineering in alumina/glass composites
[AD-A248587] p 3773 N92-31315
TISSUES (BIOLOGY)
Cellular localization of infrared sources
[AD-A249795] p 3866 N92-31302
A biological model of the effects of toxic substances
[AD-A247138] p 3867 N92-31980
TITAN
Optimum data analysis procedures for Titan 4 and Space Shuttle payload acoustic measurements during lift-off
[NASA-CR-190479] p 3892 N92-32178
TITANIUM
Preliminary evaluation of adhesion strength measurement devices for ceramic/titanium matrix composite bonds
[NASA-TM-105803] p 3745 N92-31267
TITANIUM ALLOYS
Radiation-induced crystalline-to-amorphous transition in intermetallic compounds of the Cu-Ti alloy system
[DE92-010276] p 3787 N92-31575
TITANIUM CARBIDES
Titanium carbon nitride coating
[DE92-013158] p 3777 N92-32135
TITANIUM NITRIDES
Titanium carbon nitride coating
[DE92-013158] p 3777 N92-32135
TITANIUM OXIDES
Ba2Ti9O20 microwave dielectric resonator: Processing, phase synthesis and characterization
[INPE-5373-PRE/1747] p 3818 N92-32200
TOKAMAK DEVICES
Non-geothermal optics study of wave propagation
[DE92-011806] p 3903 N92-31494
Fusion development and technology
[DE92-014352] p 3904 N92-31545
Poloidal rotation and density asymmetries in a tokamak plasma with strong toroidal rotation
[PB92-182534] p 3904 N92-31613
Real time analysis of tokamak discharge parameters
[DE92-011394] p 3904 N92-31616
Ion temperature gradient instability and transport
[DE92-013590] p 3905 N92-31727
A global fitting code for multichordal neutral beam spectroscopic data
[DE92-014258] p 3781 N92-31729
Electrostatic turbulence and transport in the RFP edge
[DE92-014322] p 3905 N92-31730
Divertor material evaluation system at D3-D
[DE92-013696] p 3905 N92-31749
A phase contrast interferometer on D3-D
[DE92-012699] p 3905 N92-31764
Power scaling of divertor plasma conditions during H-mode in D3-D
[DE92-012148] p 3906 N92-31771
Flow generation by turbulence
[DE92-013276] p 3906 N92-31829
Simulation study of stepwise relaxation in a spheromak plasma
[DE92-782101] p 3906 N92-31843
Radiation damage in carbon-carbon composites
[DE92-011778] p 3775 N92-31912
Small tokamaks for fusion technology testing
[DE92-011790] p 3906 N92-31913
Energy transport in the steady state plasma sustained by DC helicity current drive
[NIFS-127] p 3907 N92-32181
TOLERANCES (PHYSIOLOGY)
Body water homeostasis and human performance in high heat environments: Fluid hydration recommendations for Operation Desert Storm
[AD-A249772] p 3868 N92-31492
TOLUENE
f Mo(CHCMe2Ph)(NAr)(OR)2 and relative reactivity toward 2,3-bis(trifluoromethyl) norbornadiene iene
[AD-A250234] p 3780 N92-31524
TOMOGRAPHY
Sensitivity of the tomographic inverse solution to acoustic path variability
[AD-A252146] p 3864 N92-31407
Utilization of gamma ray inspection system for tomographic imaging and dimensional analysis of complete model magnet cold masses and collared coil sections
[DE92-013466] p 3836 N92-31647
TOOLING
Capabilities of the 3-axes modified FP42 Deckel milling machine
[DE92-011737] p 3803 N92-31908
Titanium carbon nitride coating
[DE92-013158] p 3777 N92-32135
TOPOGRAPHY
Sensitivity of the tomographic inverse solution to acoustic path variability
[AD-A252146] p 3864 N92-31407
Results of earth observation study on STS-31 for Terra Geode, January 1987 - June 1991
[AD-A250750] p 3844 N92-31621
Lamont-Doherty Geological Observatory
[PB92-185040] p 3856 N92-31636
TOROIDAL DISCHARGE
Real time analysis of tokamak discharge parameters
[DE92-011394] p 3904 N92-31616
TOROIDAL PLASMAS
Vortices associated with toroidal ion temperature gradient driven fluctuations
[DE92-016180] p 3903 N92-31412
Poloidal rotation and density asymmetries in a tokamak plasma with strong toroidal rotation
[PB92-182534] p 3904 N92-31613
Theory of anomalous transport in toroidal helical plasmas
[NIFS-140] p 3904 N92-31659
Simulation study of stepwise relaxation in a spheromak plasma
[DE92-782101] p 3906 N92-31843
Small tokamaks for fusion technology testing
[DE92-011790] p 3906 N92-31913
Energy transport in the steady state plasma sustained by DC helicity current drive
[NIFS-127] p 3907 N92-32181
TORQUE
Backlash control via redundant drives: An experimental verification
[DE92-016368] p 3835 N92-31929
TORQUE MOTORS
Torque linearizing hardware for the electric joint motors of a direct-drive robot
[DE92-012681] p 3816 N92-31718
TOTAL QUALITY MANAGEMENT
Total quality management: A management philosophy for providing high quality construction
[AD-A252743] p 3837 N92-32172
TOUGHNESS
The 3-D analysis and verification of fracture growth mechanisms in fiber-reinforced ceramic composies
[AD-A250893] p 3773 N92-31305
Marine structural steel toughness data bank, volume 1
[AD-A247923] p 3789 N92-31987
TOWED BODIES
Deep-tow acoustics/geophysics system compressional velocity database
[AD-A252700] p 3918 N92-31467
TOXIC HAZARDS
Robotic soil sampler for hazardous waste clean up
[DE92-012693] p 3780 N92-31565
TOXICITY
Microdistribution of lead in bone: A new approach
[DE92-013036] p 3869 N92-31589
A study of the effect of hydrocarbon structure on the induction of male rat nephropathy and metabolite structure
[AD-A252192] p 3867 N92-31590
Biodosimetry of ionizing radiation in humans using the glycophorin A genotoxicity assay
[DE92-011974] p 3869 N92-31608
A biological model of the effects of toxic substances
[AD-A247138] p 3867 N92-31980
TOXICITY AND SAFETY HAZARD
The effects of hydrazines of neuronal excitability
[AD-A247142] p 3868 N92-31491
TOXINS AND ANTITOXINS
A biological model of the effects of toxic substances
[AD-A247138] p 3867 N92-31980
TRACE ELEMENTS
Tomographic reconstruction of infrared spectra of nonhomogeneous media: Applications to a flat flame burner
[AD-A249999] p 3778 N92-31393
The NSLS 100 element solid state array detector
[DE92-014477] p 3827 N92-31502
TRACKING (POSITION)
Roundoff algorithms for digital phase shifters that minimize beam shift
[AD-A250094] p 3816 N92-31780
RL-34 ring laser gyro laboratory evaluation for the Deep Space Network antenna application
[NASA-CR-190481] p 3829 N92-32128
TRAINING DEVICES
Artificial Intelligence in Training (AIT)
[AD-A250145] p 3885 N92-31811
Head tracking and head mounted displays for training simulations
[AD-A250866] p 3873 N92-31974
TRAJECTORIES
Optimal targeting of evading objects
[DE92-014719] p 3889 N92-32119
Interplanetary Program to Optimize Space Trajectories (IPOST). Volume 3: Programmer's manual
[NASA-CR-189653-VOL-3] p 3766 N92-32130
TRAJECTORY ANALYSIS
Interplanetary Program to Optimize Space Trajectories (IPOST). Volume 3: Programmer's manual
[NASA-CR-189653-VOL-3] p 3766 N92-32130
TRAJECTORY OPTIMIZATION
Comparison of effects of copropagated and precomputed atmosphere profiles on Monte Carlo trajectory simulation
[NASA-TM-102600] p 3766 N92-31457
Optimal trajectories for an unmanned air vehicle
p 3748 N92-31880
An automated computational method for barrier construction in single and two-target differential games
p 3749 N92-31882
Proceedings of the 53rd Symposium on Air Vehicle Mission Control and Management
[AGARD-AR-310] p 3889 N92-32229
TRAJECTORY PLANNING
Singularity avoidance for SCARA-type robots
p 3746 N92-31867
An automated computational method for barrier construction in single and two-target differential games
p 3749 N92-31882
Effective path planning through task restriction
[DE92-017351] p 3885 N92-32036
TRANSCONDUCTANCE
Fabrication of an insulated gate diamond FET for high temperature applications
[AD-A251042] p 3817 N92-31849
TRANSDUCERS
Investigation of factors affecting the calibration of strain gage based transducers (Goodzeit gages) for SSC magnets
[DE92-010722] p 3826 N92-31313
TRANSFER FUNCTIONS
Using transfer functions as a method for predicting lightning effects on munitions storage bunkers
[DE92-012627] p 3861 N92-31709
TRANSFER ORBITS
Comparison of effects of copropagated and precomputed atmosphere profiles on Monte Carlo trajectory simulation
[NASA-TM-102600] p 3766 N92-31457
A novel control-guidance law for low-thrust orbit maneuver p 3747 N92-31874
TRANSFERRING
Design and specification of a high speed transport protocol
[AD-A248323] p 3804 N92-31284
TRANSIENT RESPONSE
A free-piston Stirling engine/linear alternator controls and load interaction test facility
[NASA-TM-105825] p 3845 N92-31262
Sensitivity analysis of hydrodynamic stability operators
[NASA-CR-189683] p 3822 N92-31535
TRANSITION FLOW
Solid rocket combustion phenomena
[AD-A248006] p 3770 N92-31474
Stability and transition of hypersonic boundary-layer flows
[AD-A250279] p 3752 N92-31555
An experimental investigation of the formation of secondary vortices and the generation of small-scale motion in a spanwise forced plane mixing layer
[AD-A250350] p 3822 N92-31559
Experimental studies of friction and heat transfer in enhanced passages
[DE92-011607] p 3890 N92-32099
TRANSITION METALS
Ring-opening polymerization of strained cyclotetrasilanes as a new route towards well defined polysilylenes
[AD-A251020] p 3795 N92-31941
TRANSITION PROBABILITIES
Diffusion in ordered and disordered media
[AD-A250949] p 3891 N92-32211
TRANSMISSION LOSS
The KRAKEN normal mode program
[AD-A252409] p 3892 N92-31818
TRANSMISSIONS (MACHINE ELEMENTS)
Experimental testing of prototype face gears for helicopter transmissions
[NASA-TM-105434] p 3832 N92-31349
Modal simulation of gearbox vibration with experimental correlation
[NASA-TM-105702] p 3834 N92-31485
TRANSMISSOMETERS
Absolute calibration of the Fourier interferometric transmissometer
[DREV-R-4511/88] p 3829 N92-32218

TRANSMITTANCE
Design and specification of a high speed transport protocol
[AD-A248323] p 3804 N92-31284
Absolute calibration of the Fourier interferometric transmissometer
[DREV-R-4511/88] p 3829 N92-32218
TRANSONIC FLOW
Automatic design of transonic airfoils to reduce the shock induced pressure drag p 3745 N92-31863
TRANSONIC WIND TUNNELS
High Reynolds number test of the Boeing TR77 airfoil in the Langley 0.3-meter transonic cryogenic tunnel
[NASA-TM-4189] p 3750 N92-31246
Data reduction formulas for the 16-foot transonic tunnel: NASA Langley Research Center, revision 2
[NASA-TM-107646] p 3762 N92-31900
Transonic wind tunnel test of a 14 percent thick oblique wing
[NASA-TM-102230] p 3754 N92-32213
TRANSPORT PROPERTIES
Statistical analysis of anomalous transport in resistive interchange turbulence
[NIFS-125] p 3818 N92-31256
Interfacial ion transport between immiscible liquids
[AD-A252424] p 3778 N92-31292
Theory of anomalous transport in toroidal helical plasmas
[NIFS-140] p 3904 N92-31659
Epitaxial iron films
[AD-A250402] p 3912 N92-31915
Electronic states in systems of reduced dimensionality
[DE92-013588] p 3912 N92-31945
Reynolds stress calculations of homogeneous turbulent shear flow with bounded energy states
[NASA-CR-189682] p 3826 N92-32158
TRANSPORTATION
The collection, handling, transportation, and thermal desorption of explosive vapor using quartz collection tubes
[DE92-011441] p 3799 N92-31570
TRANSPORTER
COMET: Commercial space opportunities through developed technologies
[TABES PAPER 92-453] p 3764 N92-32017
TRANSVERSE LOADS
Structural similitude and scaling laws for laminated beam-plates
[NASA-CR-190585] p 3841 N92-31911
TRANSVERSE OSCILLATION
Conversion of power and frequency
[DE92-012543] p 3810 N92-32134
TRAVELING SALESMAN PROBLEM
The vehicle routing problem: Some computational tests of savings method and its variations
[INPE-5361-RPQ/656] p 3886 N92-31241
TREES (MATHEMATICS)
Heuristic sampling on DAGs
[DE92-017359] p 3917 N92-32037
TREES (PLANTS)
User's guide for treetherm: A 3-D thermal model for single trees
[LTR91-003] p 3879 N92-31833
TRENDS
Trends 1991: A compendium of data on global change
[DE92-011733] p 3854 N92-31907
Global trends in energy use: Indications for research
[DE92-014773] p 3855 N92-32155
TRIBOLOGY
Tribology of Langmuir-Blodgett films
[AD-A250075] p 3833 N92-31363
Tribology of functionally-terminated oligomer films
[AD-A250076] p 3833 N92-31433
Surface chemistry of MoS2 lubricant films: Effects of high humidity storage on sputtered films
[DE92-015392] p 3794 N92-31631
Experimental studies of friction and heat transfer in enhanced passages
[DE92-011607] p 3890 N92-32099
TRIETHYL COMPOUNDS
Shock tube study of the reaction of triethanol ammonium nitrate with N2O
[AD-A250034] p 3800 N92-31804
TRIGGER CIRCUITS
Experimental particle physics at the University of Pittsburgh
[DE92-016182] p 3896 N92-31926
TRIMERS
Synthesis of soluble alpha-thiophene oligomers. Monomer to octamer
[AD-A250082] p 3779 N92-31434
TRINITROTOLUENE
The collection, handling, transportation, and thermal desorption of explosive vapor using quartz collection tubes
[DE92-011441] p 3799 N92-31570
Development of methodology and technology for identifying and quantifying emission products from open burning and open detonation thermal treatment methods. BangBox test series. Volume 1. Test summary
[AD-A250733] p 3800 N92-31969
Development of methodology and technology for identifying and quantifying emission products from open burning and open detonation thermal treatment methods. Field test series A, B, and C. Volume 1: Test summary
[AD-A250735] p 3800 N92-31971
Development of methodology and technology for identifying and quantifying emission products from open burning and open detonation thermal treatment methods. Field test series A, B, and C. Volume 2, part B: Quality assurance and quality control. Appendices
[AD-A250737] p 3801 N92-31973
TRIPODS
Development, testing and operation of a large suspended ocean measurement structure for deep-ocean use
[AD-A252188] p 3866 N92-32050
TRITIUM
YLIFE-2 inertial fusion energy power plant design
[DE92-011965] p 3904 N92-31530
Divertor material evaluation system at D3-D
[DE92-013696] p 3905 N92-31749
TROPICAL METEOROLOGY
Balanced, potential vorticity dynamics in the tropics
[AD-A249981] p 3858 N92-31432
TROPICAL REGIONS
Balanced, potential vorticity dynamics in the tropics
[AD-A249981] p 3858 N92-31432
Hydrographic observations from the US/PRC cooperative program in the western equatorial Pacific Ocean: Cruises 5-8
[PB92-177054] p 3865 N92-31644
TROPOSPHERE
Exponential representation and consistency checking for M layer
[AD-A250423] p 3805 N92-31413
Upper tropospheric jet streams over North America during summer 1988
[AD-A249871] p 3857 N92-31906
Rainwater and throughfall chemistry in a terra firme rain forest: Central Amazonia
[INPE-5364-PRE/1744] p 3863 N92-32224
TRUSSES
Studies in dynamic characterization and control of a flexible structure and optical beampath
[AD-A250555] p 3830 N92-31605
Design, analysis, and testing of the Phase 1 CSI Evolutionary Model erectable truss
[NASA-CR-4461] p 3767 N92-32100
TUBES
The stability of a slightly eccentric straight vortex filament in a circular tube p 3750 N92-31887
TUNDRA
Hydrological and geochemical response and recovery in disturbed Arctic ecosystems
[DE92-016223] p 3850 N92-31312
Response of a tundra ecosystem to elevated atmospheric carbon dioxide and CO2-induced climate change
[DE92-013925] p 3853 N92-31626
TUNGSTEN
Residual stress and strain measurements in an austenitic steel plate containing a multipass weld
[DE92-014478] p 3839 N92-31383
TUNING
A comparison of three self-tuning control algorithms developed for the Bristol-Babcock controller
[DE92-014472] p 3814 N92-31499
TURBINE BLADES
Fatigue in single crystal nickel superalloys
[AD-A250068] p 3786 N92-31360
A surface definition code for turbine blade surfaces
[DE92-010574] p 3846 N92-31498
Turbine blade tip and seal clearance excitation forces
[NASA-CR-184341] p 3760 N92-31910
Fatigue in single crystal nickel superalloys
[AD-A252492] p 3790 N92-32066
TURBINE PUMPS
Orbit transfer vehicle engine technology program. Task B-6 high speed turbopump bearings
[NASA-CR-189230] p 3835 N92-31892
TURBOCOMPRESSORS
Research on aero-thermodynamic distortion induced structural dynamic response of multistage compressor blading
[AD-A250865] p 3760 N92-32059
TURBOFAN ENGINES
Subsonic flight test evaluation of a performance seeking control algorithm on an F-15 airplane
[NASA-TM-4400] p 3759 N92-31275
TURBOFANS
Supersonic Throughflow Fan Test Facility at NASA. Lewis Research Center
[NASA-TP-3038] p 3762 N92-31640
TURBOPROP ENGINES
High speed turboprop aeroacoustic study (counterrotation). Volume 2: Computer programs
[NASA-CR-185242] p 3891 N92-31248
TURBULENCE
Statistical analysis of anomalous transport in resistive interchange turbulence
[NIFS-125] p 3818 N92-31256
Amending the w* velocity scale for surface layer, entrainment zone, and baroclinic shear in mixed Forced/Free turbulent convection
[AD-A250389] p 3859 N92-31540
Energy balance model for imagery and electromagnetic propagation
[AD-A250884] p 3806 N92-31543
Development of wavelet analysis tools for turbulence
[NASA-CR-189674] p 3822 N92-31564
Simulation of diurnally varying downslope winds over Northern Utah
[AD-A250568] p 3861 N92-31714
Organized turbulent structures and their induced wall pressure fluctuations p 3753 N92-31853
TURBULENCE MODELS
A computational investigation of airfoil stall flutter
[AD-A247302] p 3751 N92-31300
NAS (Numerical Aerodynamic Simulation Program) technical summaries, March 1989 - February 1990
[NASA-TM-107960] p 3926 N92-31852
A computational examination of directional stability for smooth and chined forebodies at high-alpha
[NASA-CR-4465] p 3753 N92-32114
Towards understanding turbulent scalar mixing
[NASA-CR-4446] p 3826 N92-32242
TURBULENT BOUNDARY LAYER
Description of a 1000 sensor constant current anemometer system for locating three-dimensional turbulent boundary layer separations
[AD-A250827] p 3821 N92-31452
Amending the w* velocity scale for surface layer, entrainment zone, and baroclinic shear in mixed Forced/Free turbulent convection
[AD-A250389] p 3859 N92-31540
Turbulent dusty boundary layer in an ANFO surface-burst explosion
[DE92-012101] p 3822 N92-31625
The structure and control of three-dimensional shock wave turbulent boundary layer interactions
[AD-A250209] p 3823 N92-31824
Organized turbulent structures and their induced wall pressure fluctuations p 3753 N92-31853
The calculation of incompressible separated turbulent boundary layers p 3749 N92-31886
TURBULENT FLOW
Statistical analysis of anomalous transport in resistive interchange turbulence
[NIFS-125] p 3818 N92-31256
Diagnostics for research in atomization and turbulent two-phase flows
[AD-A247201] p 3819 N92-31283
Flame front geometry in premixed turbulent flames
[DE92-010310] p 3779 N92-31417
An experimental investigation of the formation of secondary vortices and the generation of small-scale motion in a spanwise forced plane mixing layer
[AD-A250350] p 3822 N92-31559
Flow generation by turbulence
[DE92-013276] p 3906 N92-31829
Organized turbulent structures and their induced wall pressure fluctuations p 3753 N92-31853
Contribution to the modelling of turbulent combustion in the case of stabilisation by flame-lock
[ESA-TT-1229] p 3784 N92-31942
Experimental studies of friction and heat transfer in enhanced passages
[DE92-011607] p 3890 N92-32099
Reynolds stress calculations of homogeneous turbulent shear flow with bounded energy states
[NASA-CR-189682] p 3826 N92-32158
Experimental studies of hypersonic shock-wave boundary-layer interactions
[NASA-CR-190731] p 3753 N92-32162
Three-dimensional compressible turbulent computations for a nondiffusing S-duct
[NASA-CR-4391] p 3754 N92-32240
Towards understanding turbulent scalar mixing
[NASA-CR-4446] p 3826 N92-32242
TURBULENT JETS
Performance of multiple stream pulsed jet combustion systems
[AD-A249722] p 3780 N92-31671
Evolution of reactants fluid volume in turbulent jets
[DE92-011298] p 3786 N92-32145

TURBULENT MIXING
Simulation of diurnally varying downslope winds over Northern Utah
[AD-A250568] p 3861 N92-31714
Evolution of reactants fluid volume in turbulent jets
[DE92-011298] p 3786 N92-32145
Towards understanding turbulent scalar mixing
[NASA-CR-4446] p 3826 N92-32242
TWO DIMENSIONAL FLOW
Solid rocket combustion phenomena
[AD-A248006] p 3770 N92-31474
The discretization of the 2D incompressible Navier-Stokes equations on a collocated grid
[REPT-91-61] p 3821 N92-31513
Automatic design of transonic airfoils to reduce the shock induced pressure drag p 3745 N92-31863
TWO DIMENSIONAL JETS
Adaptive and nonadaptive feedback control of global instabilities with application to a heated 2-D jet
[AD-A250700] p 3820 N92-31322
TWO DIMENSIONAL MODELS
Finite-element analyses and fracture simulation in thin-sheet aluminum alloy
[NASA-TM-107662] p 3839 N92-31504
TWO FLUID MODELS
Weak ion-acoustic shock waves and double layers in non-collision plasma p 3907 N92-32208
TWO PHASE FLOW
Diagnostics for research in atomization and turbulent two-phase flows
[AD-A247201] p 3819 N92-31283
Two-component flow study in large-diameter horizontal pipe
[DE92-013196] p 3820 N92-31420
A model for the interfacial shear in vertical, adiabatic, annular-mist flow
[DE92-013537] p 3820 N92-31424
Use of a genetic algorithm to solve fluid flow problems on an NCUBE/2 multiprocessor computer
[DE92-014044] p 3824 N92-31832
Study of a spherical spinning combustion chamber for orbit insertion p 3746 N92-31869
Condensation in a two-phase pool
[DE92-010048] p 3824 N92-31977

U

U.S.S.R.
Energy conservation: The main factor for reducing greenhouse gas emissions in the former Soviet Union
[DE92-012355] p 3852 N92-31574
Evolution of environmental protection strategies in the Soviet Union
[DE92-015090] p 3853 N92-31732
Soviet precision timekeeping research and technology
[PB92-173046] p 3802 N92-31830
Soviet satellite communications science and technology
[PB92-173038] p 3809 N92-31920
ULTRAHIGH VACUUM
The synthesis and characterization of tribophysical layers on diamond and silicon carbide surfaces
[AD-A250983] p 3796 N92-32001
ULTRASONIC FLAW DETECTION
Investigation into the ultrasonic NDE of adhesively bonded joints
[DREP-90-02] p 3837 N92-32202
ULTRASONIC TESTS
Physical characterization of magmatic liquids
[DE92-015302] p 3858 N92-32027
EWE: A computer model for ultrasonic inspection
[DE92-627145] p 3837 N92-32143
Instabilities of damage and surface degradation mechanisms in brittle material structural systems
[AD-A250785] p 3842 N92-32168
ULTRASONIC WAVE TRANSDUCERS
Piezoelectric radiant-to-air ultrasonic transducers p 3811 N92-31244
ULTRAVIOLET LASERS
Particle emission and charging effects induced by fracture
[AD-A252182] p 3913 N92-32065
ULTRAVIOLET RADIATION
New high voltage parallel plate analyzer
[NIFS-128] p 3827 N92-31340
UNDERWATER ACOUSTICS
The KRAKEN normal mode program
[AD-A252409] p 3892 N92-31818
An empirical prediction algorithm for low-frequency acoustic surface scattering strengths
[AD-A250508] p 3892 N92-32044
Development, testing and operation of a large suspended ocean measurement structure for deep-ocean use
[AD-A252188] p 3866 N92-32050
UNDERWATER ENGINEERING
Development, testing and operation of a large suspended ocean measurement structure for deep-ocean use
[AD-A252188] p 3866 N92-32050
UNIQUENESS THEOREM
Feynman diagrams and Vassiliev invariants
[PB92-178284] p 3890 N92-31925
UNIVERSITIES
Building an educational robot arm for under $1,000
[AD-A247499] p 3833 N92-31460
UNIVERSITY PROGRAM
ARO Geoscience Center fellowships
[AD-A249225] p 3857 N92-31964
An integrated research program for the modeling, analysis and control of aerospace systems
[AD-A250199] p 3761 N92-31966
UNIX (OPERATING SYSTEM)
Modular UNIX (trade name)-based Vulnerability Estimation Suite (MUVES) analyst's guide
[AD-A245322] p 3876 N92-31488
An installed nacelle design code using a multiblock Euler solver. Volume 2: User guide
[NASA-CR-189652-VOL-2] p 3754 N92-32228
UNSTEADY AERODYNAMICS
CFD methods development considerations for unsteady aerodynamic analysis
[NASA-TM-107644] p 3750 N92-31239
Active control of the separation region on a two-dimensional airfoil
[AD-A249739] p 3752 N92-31622
Research on aero-thermodynamic distortion induced structural dynamic response of multistage compressor blading
[AD-A250865] p 3760 N92-32059
UNSTEADY FLOW
A computational investigation of airfoil stall flutter
[AD-A247302] p 3751 N92-31300
Adaptive and nonadaptive feedback control of global instabilities with application to a heated 2-D jet
[AD-A250700] p 3820 N92-31322
The discretization of the 2D incompressible Navier-Stokes equations on a collocated grid
[REPT-91-61] p 3821 N92-31513
Active control of the separation region on a two-dimensional airfoil
[AD-A249739] p 3752 N92-31622
Highly accurate prediction of unsteady viscous flows
[AD-A250982] p 3825 N92-32000
Control of unsteady separated flow associated with the dynamic stall of airfoils
[NASA-CR-190688] p 3753 N92-32177
UPPER ATMOSPHERE
Combined Release and Radiation Effects Satellite (CRRES) experiments data collection, analysis, and publication
[NASA-CR-184361] p 3856 N92-31551
UPPER IONOSPHERE
High-latitude spacecraft charging in low-Earth polar orbit
[AD-A249868] p 3767 N92-31822
UPPER STAGE ROCKET ENGINES
Graphite/epoxy composite adapters for the Space Shuttle/Centaur vehicle
[NASA-TP-3014] p 3765 N92-31251
UPWELLING WATER
An analysis of hydrographic data collected off Point Sur, California in June 1990
[AD-A246060] p 3866 N92-32056
URANIUM COMPOUNDS
Transient fission gas behavior in uranium nitride fuel under proposed space applications
[AD-A252577] p 3899 N92-31325
USER MANUALS (COMPUTER PROGRAMS)
The KRAKEN normal mode program
[AD-A252409] p 3892 N92-31818
User's guide for treetherm: A 3-D thermal model for single trees
[LTR91-003] p 3879 N92-31833
FEHMN 1.0: Finite element heat and mass transfer code
[DE92-013998] p 3825 N92-32008
Interplanetary Program to Optimize Space Trajectories (IPOST). Volume 3: Programmer's manual
[NASA-CR-189653-VOL-3] p 3766 N92-32130
An installed nacelle design code using a multiblock Euler solver. Volume 2: User guide
[NASA-CR-189652-VOL-2] p 3754 N92-32228
USER REQUIREMENTS
Next generation documents
[PB92-187103] p 3917 N92-31371
Hydrogenerator design manual, chapter 8
[PB92-173707] p 3919 N92-31682
Computer Aided Process Planning (CAPP): The user interface for the fabrication module of the rapid design system
[AD-A250095] p 3879 N92-31783
UTAH
Simulation of diurnally varying downslope winds over Northern Utah
[AD-A250568] p 3861 N92-31714
UTILIZATION
Solar synthesis of advanced materials: A solar industrial program initiative
[DE92-010575] p 3845 N92-31481

V

VACANCIES (CRYSTAL DEFECTS)
Growth, nitrogen vacancy reduction and solid solution formation in cubic GaN thin films and the subsequent fabrication of superlattice structures using AlN and InN
[AD-A248058] p 3908 N92-31446
VACUUM
Activities of the Center for X Ray Lithography, phase 1
[AD-A250446] p 3901 N92-31397
Field-emitter arrays for RF vacuum microelectronics
[AD-A250101] p 3816 N92-31791
VACUUM APPARATUS
The synthesis and characterization of tribophysical layers on diamond and silicon carbide surfaces
[AD-A250983] p 3796 N92-32001
VACUUM CHAMBERS
Controlled atmosphere soldering system
[DE92-012633] p 3802 N92-31580
VALVES
Replaceable valve seat
[AD-D015250] p 3832 N92-31271
Motor-operated globe valve performance in a liquid sodium environment
[DE92-014456] p 3834 N92-31500
VAN DE GRAAFF ACCELERATORS
The Radiological Research Accelerator Facility
[DE92-013674] p 3867 N92-31747
VAN DER WAALS FORCES
Theoretical studies of solid-fluid phase equilibria
[DE92-016598] p 3781 N92-31717
VANADIUM
Resolution function of an inelastic scattering spectrometer with a pulsed neutron source
[DE92-620889] p 3896 N92-31904
VAPOR PHASE EPITAXY
New sources for OMVPE
[AD-A250903] p 3909 N92-31582
VAPOR PHASES
Saturation effects in degenerate four-wave mixing spectroscopy: Nonperturbative calculations
[DE92-012253] p 3782 N92-31773
VAPORS
Dynamic modeling of plasma-vapor interactions during plasma disruptions
[DE92-016183] p 3903 N92-31310
The collection, handling, transportation, and thermal desorption of explosive vapor using quartz collection tubes
[DE92-011441] p 3799 N92-31570
Further studies in filmwise condensation of steam on horizontal finned tubes
[AD-A252705] p 3915 N92-31767
Condensation in a two-phase pool
[DE92-010048] p 3824 N92-31977
Laser-ablated copper condensation in helium
[DE92-016685] p 3789 N92-32004
VARIABILITY
Geomorphic variability in the coastal zone
[AD-A252713] p 3864 N92-31544
A comparative analysis of the temporal variability of lightning observations and GOES imagery
[AD-A250185] p 3860 N92-31603
The uncertainties of global temperatures in the global warming context
[TABES PAPER 92-447] p 3763 N92-32014
VARIATIONAL PRINCIPLES
A finite element procedure for analysis of laminated composite plates
[AD-A250902] p 3773 N92-31307
CAVEAT: A computer code for fluid dynamics problems with large distortion and internal slip
[DE92-014078] p 3825 N92-32022
VARIATIONS
Effects of fragmentation parameter variations on estimates of galactic cosmic ray exposure: Dose sensitivity studies for aluminum shields
[NASA-TM-4386] p 3926 N92-32193
VECTOR PROCESSING (COMPUTERS)
CAVEAT: A computer code for fluid dynamics problems with large distortion and internal slip
[DE92-014078] p 3825 N92-32022

VECTOR QUANTIZATION
Compression of digitized map images
[AD-A250707] p 3843 N92-31323
VECTORS (MATHEMATICS)
A diagnostic study of rapidly developing cyclones using surface-based Q vectors
[AD-A246993] p 3862 N92-31978
VEGETATION
A test of ecological optimality for semiarid vegetation
[NASA-CR-190705] p 3855 N92-32222
VEGETATIVE INDEX
Sun-view-target geometry effects on spectrally-derived vegetative index estimates of absorbed radiation and leaf area
[AD-A249984] p 3843 N92-31329
VELOCITY
Solid-armature railguns without the velocity-skin effect
[DE92-012630] p 3765 N92-31542
Problems associated with launching hypervelocity projectiles from the fast shock tube
[DE92-015276] p 3762 N92-32026
VELOCITY DISTRIBUTION
An experimental investigation of the formation of secondary vortices and the generation of small-scale motion in a spanwise forced plane mixing layer
[AD-A250350] p 3822 N92-31559
Simulation of diurnally varying downslope winds over Northern Utah
[AD-A250568] p 3861 N92-31714
Macrostatistical hydrodynamics
[DE92-013589] p 3823 N92-31726
Three-dimensional compressible turbulent computations for a nondiffusing S-duct
[NASA-CR-4391] p 3754 N92-32240
Towards understanding turbulent scalar mixing
[NASA-CR-4446] p 3826 N92-32242
VELOCITY MEASUREMENT
A comparative study of the dynamic performance of three bivanes
[AD-A250096] p 3862 N92-31784
Improvements to the Rocky Flats Metrology Laboratories velocity meter calibration system
[DE92-013162] p 3829 N92-32138
VENTILATION
Simplified air change effectiveness modeling
[DE92-010577] p 3872 N92-31309
VERTICAL LANDING
ASTOVL combat aircraft design synthesis and optimization
[CRANFIELD-AERO-9201] p 3757 N92-31515
VERY LARGE SCALE INTEGRATION
VLSI for high-speed digital signal processing
[AD-A250365] p 3817 N92-32074
VIBRATION
Modal simulation of gearbox vibration with experimental correlation
[NASA-TM-105702] p 3834 N92-31485
Ultrafast experiments on the role of vibrational modes in electron transfer
[AD-A250630] p 3910 N92-31699
VIBRATION DAMPING
Design and experimental validation of a flutter suppression controller for the active flexible wing
[NASA-TM-4381] p 3760 N92-31240
A summary of the active flexible wing program
[NASA-TM-107655] p 3757 N92-31264
Flutter suppression digital control law design and testing for the AFW wind-tunnel model
[NASA-TM-107652] p 3757 N92-31350
Rolling maneuver load alleviation using active controls
[NASA-TM-107654] p 3757 N92-31351
Dynamics of shuttle based flexible antenna system
[CRANFIELD-AERO-9203] p 3840 N92-31516
Experimental feedback of fractional order states of a lightly damped structure
[AD-A248027] p 3842 N92-31989
Eigensensitivity analysis of composite laminates: Effect of microstructure
[AD-A250864] p 3777 N92-32104
VIBRATION MEASUREMENT
A preliminary study in the use of phase demodulation techniques for the analysis of gear vibration data
[NRC-32083] p 3833 N92-31469
VIBRATION MODE
Modal simulation of gearbox vibration with experimental correlation
[NASA-TM-105702] p 3834 N92-31485
Time simulation of flutter with large stiffness changes
[NASA-TM-107650] p 3758 N92-32111
Asymptotic modal analysis and statistical energy analysis
[NASA-CR-190516] p 3842 N92-32236
VIBRATION TESTS
Dynamic modeling and modal analysis of an air-to-air missile
[AD-A245957] p 3758 N92-32053
VIDEO EQUIPMENT
Enhancing GRASS data communication with videographic technology
[DE92-014852] p 3919 N92-31596
Design and development of minilink video: A fiber-optic coupled video system
[AD-A249945] p 3808 N92-31801
Space constancy on video display terminals
[AD-A247290] p 3872 N92-32105
VIDEO SIGNALS
Design and development of minilink video: A fiber-optic coupled video system
[AD-A249945] p 3808 N92-31801
VIEW EFFECTS
Sun-view-target geometry effects on spectrally-derived vegetative index estimates of absorbed radiation and leaf area
[AD-A249984] p 3843 N92-31329
VINYL POLYMERS
Cyclopolymerization of metalloid-containing alpha, omega-dienes. 1,3-divinyltetramethyldisiloxane, 1,3-divinyltetramethyldisilazane and 1,3-divinylpentamethyldisilazane
[AD-A250347] p 3794 N92-31557
VIRTUAL REALITY
Hyper-NPSNET: A virtual world with an integrated 3-D hypertext
[AD-A252726] p 3878 N92-31676
VISCOELASTICITY
Holographic grating relaxation and photon correlation spectroscopic studies of viscoelastic liquids above the glass transition
[AD-A252485] p 3828 N92-31828
VISCOPLASTICITY
An investigation of the thermoviscoplastic behavior of a metal matrix composite at elevated temperatures
[NASA-CR-190700] p 3777 N92-32159
VISCOSITY
Development of characterization techniques for polyurethanes 1. Characterization of SRM 1480, a low molecular weight polyurethane for SEC calibration
[PB92-172485] p 3794 N92-31618
Macrostatistical hydrodynamics
[DE92-013589] p 3823 N92-31726
Heat transfer and flow of a modified second grade fluid
[DE92-014744] p 3824 N92-31895
VISCOUS FLOW
Adaptive mesh strategies for the spectral element method
[NASA-CR-189686] p 3818 N92-31265
Stagnation-point heat-transfer rate predictions at aeroassist flight conditions
[NASA-TP-3208] p 3819 N92-31281
Plane stokes flow driven by capillarity on a free surface: Overview and status
[DE92-011469] p 3821 N92-31528
On the spatial evolution of long-wavelength Goertler vortices governed by a viscous-inviscid interaction
[NASA-CR-189681] p 3822 N92-31687
Highly accurate prediction of unsteady viscous flows
[AD-A250982] p 3825 N92-32000
VISIBILITY
A sensitivity study of daytime visibility determination with the horizon scanning imager
[SIO-91-15] p 3902 N92-32144
VISUAL ACUITY
Function of panel M pathways in primates
[AD-A250275] p 3871 N92-31758
Function of P and M pathways in primates
[AD-A250055] p 3867 N92-31778
VISUAL FIELDS
Logarithmic retinae
[PB92-183649] p 3885 N92-31680
Function of P and M pathways in primates
[AD-A250055] p 3867 N92-31778
VISUAL OBSERVATION
Replaceable valve seat
[AD-D015250] p 3832 N92-31271
Results of earth observation study on STS-31 for Terra Geode, January 1987 - June 1991
[AD-A250750] p 3844 N92-31621
VISUAL PERCEPTION
Human image understanding
[AD-A250401] p 3872 N92-31330
Illusory self motion and disorientation
[CTN-92-60318] p 3871 N92-31472
Function of P and M pathways in primates
[AD-A250055] p 3867 N92-31778
Forms of memory for representation of visual objects
[AD-A250056] p 3871 N92-31779
VISUAL SIGNALS
Modeling of learning-induced receptive field plasticity in auditory neocortex
[AD-A250348] p 3869 N92-31558
VISUAL STIMULI
Illusory self motion and disorientation
[CTN-92-60318] p 3871 N92-31472
Function of P and M pathways in primates
[AD-A250055] p 3867 N92-31778
Forms of memory for representation of visual objects
[AD-A250056] p 3871 N92-31779
VOID RATIO
Flow instability in a vertical annulus under steady state and transient conditions
[DE92-013217] p 3820 N92-31421
VOIDS
Analytic estimation of radiation effects in space using solid angles
[DE92-013282] p 3899 N92-31831
VOLTAGE CONVERTERS (DC TO DC)
Stability testing and analysis of a PMAD DC test bed for the Space Station Freedom
[NASA-TM-105846] p 3812 N92-31282
VOLTMETERS
Automation of strain-gauge load-cell force calibration
[PB92-187087] p 3827 N92-31370
VORTEX BREAKDOWN
In-flight leading-edge extension vortex flow-field survey measurements on a F-18 aircraft at high angle of attack
[NASA-TM-4398] p 3751 N92-31276
The stability of a slightly eccentric straight vortex filament in a circular tube p 3750 N92-31887
VORTEX FILAMENTS
The stability of a slightly eccentric straight vortex filament in a circular tube p 3750 N92-31887
The three-dimensional stability of the Foeppl vortices p 3750 N92-31889
VORTEX GENERATORS
On the spatial evolution of long-wavelength Goertler vortices governed by a viscous-inviscid interaction
[NASA-CR-189681] p 3822 N92-31687
VORTICES
In-flight leading-edge extension vortex flow-field survey measurements on a F-18 aircraft at high angle of attack
[NASA-TM-4398] p 3751 N92-31276
Vortices associated with toroidal ion temperature gradient driven fluctuations
[DE92-016180] p 3903 N92-31412
An experimental investigation of the formation of secondary vortices and the generation of small-scale motion in a spanwise forced plane mixing layer
[AD-A250350] p 3822 N92-31559
On the spatial evolution of long-wavelength Goertler vortices governed by a viscous-inviscid interaction
[NASA-CR-189681] p 3822 N92-31687
Numerical simulation of tulip flame dynamics
[DE92-008553] p 3782 N92-31805
The stability of a slightly eccentric straight vortex filament in a circular tube p 3750 N92-31887
Turbine blade tip and seal clearance excitation forces
[NASA-CR-184341] p 3760 N92-31910
Axisymmetric bluff-body flow: A vortex solver for thin shells
[DE92-016748] p 3824 N92-31933
Evidence of stochastic diffusion across a cross-field sheath due to Kelvin-Helmholtz vortices
[AD-A247847] p 3907 N92-31983
Seasonal wind and ocean thermal forcing influences on the generation of the Leeuwin current and its eddies
[AD-A246992] p 3865 N92-31988
VORTICITY
Balanced, potential vorticity dynamics in the tropics
[AD-A249981] p 3858 N92-31432
Reynolds stress calculations of homogeneous turbulent shear flow with bounded energy states
[NASA-CR-189682] p 3826 N92-32158
VULNERABILITY
Modular UNIX (trade name)-based Vulnerability Estimation Suite (MUVES) analyst's guide
[AD-A245322] p 3876 N92-31488

W

WAFERS
Control of rapid thermal processing equipment for microelectronics applications
[LAAS-92013] p 3787 N92-31695
WAKES
Fundamental studies of the structure of hypersonic attached and separated boundary layers over smooth, rough and transpiration-cooled surfaces
[AD-A250284] p 3819 N92-31286
Computation of nonlinear gravity waves by a desingularized boundary integral method
[AD-A251149] p 3857 N92-31766
WALL PRESSURE
Flat plates placed in depleted hypersonic flow
[SESSIA-430/91.960] p 3751 N92-31508

Organized turbulent structures and their induced wall pressure fluctuations p 3753 N92-31853

WALLS
Effect of outer temperature changes and solar radiation on effective heat losses through external partitions of buildings p 3802 N92-31242

WARFARE
Anti-environmental warfare: Protecting the environment during wartime
[AD-A250337] p 3851 N92-31556

WARNING SYSTEMS
Engine monitoring display study
[NASA-CR-4463] p 3761 N92-32175

WASTE DISPOSAL
EnviroTRADE: Its role in the cleanup of the environment
[DE92-013691] p 3851 N92-31427
EnviroTRADE: A technical perspective on the development of an information system providing data on environmental technologies and needs worldwide
[DE92-012625] p 3919 N92-31578

WASTE ENERGY UTILIZATION
Gas engine heat recovery unit
[PB92-184373] p 3835 N92-31841

WASTE TREATMENT
Economics of microwave plasma dissociation of H2S
[DE92-014846] p 3779 N92-31441
EnviroTRADE: A technical perspective on the development of an information system providing data on environmental technologies and needs worldwide
[DE92-012625] p 3919 N92-31578

WASTES
Robotic soil sampler for hazardous waste clean up
[DE92-012693] p 3780 N92-31565

WATER
Gibbs free energy of reactions involving SiC, Si3N4, H2, and H2O as a function of temperature and pressure
[NASA-TP-3275] p 3791 N92-31278
An experimental investigation of the formation of secondary vortices and the generation of small-scale motion in a spanwise forced plane mixing layer
[AD-A250350] p 3822 N92-31559
Analysis and computer tools for separation processes involving nonideal mixtures
[DE92-015298] p 3781 N92-31752
Fundamental studies in oxidation-reduction in relation to water photolysis
[DE92-014333] p 3785 N92-32113
Thin polymer icemaker development and test program
[DE92-016941] p 3803 N92-32125
Structure and dynamics of Cl(H2O)20 clusters. The effect of the polarizability and the charge ofthe ion
[AD-A251094] p 3899 N92-32196

WATER BALANCE
A test of ecological optimality for semiarid vegetation
[NASA-CR-190705] p 3855 N92-32222

WATER IMMERSION
Immersion suit usage within the RAAF
[AD-A250645] p 3755 N92-31562
A study of the microstructural basis for the strength and toughness properties of water-quenched and air-cooled HSLA-100, HSLA-100 with increased copper, and a ULCB steel
[AD-A245955] p 3789 N92-32052
Canadian aircrew sea water survival, 1952-1987
[DCIEM-88-RR-39] p 3756 N92-32219

WATER MASERS
G305.8 - 0.2 water vapour source: A young object
[INPE-5337-PRE/1736] p 3923 N92-31343

WATER MODERATED REACTORS
Evaluation of proposed inservice testing procedures for check valves
[DE92-014502] p 3833 N92-31384
A model for the interfacial shear in vertical, adiabatic, annular-mist flow
[DE92-013537] p 3820 N92-31424

WATER POLLUTION
Acid deposition: State of science and technology. Summary report of the US National Acid Precipitation Assessment Program, volumes 1-4
[PB92-100353] p 3852 N92-31598
World ocean circulation experiment. WOCE chlorofluorocarbon intercomparison cruise report
[PB92-185974] p 3865 N92-31842

WATER VAPOR
The detection of climate change due to the enhanced greenhouse effect
[NASA-TM-107965] p 3849 N92-31258

WATER WAVES
Geomorphic variability in the coastal zone
[AD-A252713] p 3864 N92-31544
Computation of nonlinear gravity waves by a desingularized boundary integral method
[AD-A251149] p 3857 N92-31766
Radar backscatter from the sea: Controlled experiments
[AD-A250858] p 3810 N92-32101
Parameterization of directional spectra, part 2, volume 1
[DREA-CR-89-445-PT-2-VOL-1] p 3811 N92-32214

WATERPROOFING
Immersion suit usage within the RAAF
[AD-A250645] p 3755 N92-31562

WATERSHEDS
Hydrological and geochemical response and recovery in disturbed Arctic ecosystems
[DE92-016223] p 3850 N92-31312

WAVE EQUATIONS
Intermediate/high energy nuclear physics
[DE92-015363] p 3900 N92-32028
EWE: A computer model for ultrasonic inspection
[DE92-627145] p 3837 N92-32143

WAVE FUNCTIONS
Electron impact excitation of positive ions: Partial wave approach in Coulomb-Eikonal approximation
[NIFS-106] p 3892 N92-31255
Wavelet signal processing for transient feature extraction
[AD-A250519] p 3890 N92-32046

WAVE GENERATION
Two-dimensional axisymmetric calculations of surface waves generated by an explosion in an island, mountain, and sedimentary basin
[AD-A249971] p 3856 N92-31510
EWE: A computer model for ultrasonic inspection
[DE92-627145] p 3837 N92-32143

WAVE INTERACTION
Three-wave envelope solitons: Can the speed of light in the fiber be controlled?
[AD-A247615] p 3901 N92-31611
Compact millimeter-wave devices: Dielectric loaded carm, high voltage carm, slow wave crm and high harmonic gyrotron
[AD-A250497] p 3809 N92-31944

WAVE PROPAGATION
Wavenumbers for currents on infinite- and finite-length wires in a chiral medium
[DE92-007565] p 3804 N92-31317
Exponential representation and consistency checking for M layer
[AD-A250423] p 3805 N92-31413
Non-geothermal optics study of wave propagation
[DE92-011806] p 3903 N92-31494
Time domain regional discriminants
[AD-A249949] p 3855 N92-31509
Development of wavelet analysis tools for turbulence
[NASA-CR-189674] p 3822 N92-31564
Computer simulation of acoustic fluctuations due to finescale temperature perturbations measured by thermistor chain
[AD-A252709] p 3892 N92-31672
ANTHEM simulational studies of the plasma opening switch
[DE92-015247] p 3815 N92-31681
Three-dimensional finite difference modeling of surface wave propagation across the Barents Shelf
[AD-A249865] p 3865 N92-31821
Radar backscatter from the sea: Controlled experiments
[AD-A250858] p 3810 N92-32101
EWE: A computer model for ultrasonic inspection
[DE92-627145] p 3837 N92-32143

WAVE SCATTERING
Three-dimensional finite difference modeling of surface wave propagation across the Barents Shelf
[AD-A249865] p 3865 N92-31821

WAVEGUIDES
A three-gap klystron output cavity at X-band
[DE92-012417] p 3812 N92-31289
Conversion of power and frequency
[DE92-012543] p 3810 N92-32134

WAVELENGTHS
Wavenumbers for currents on infinite- and finite-length wires in a chiral medium
[DE92-007565] p 3804 N92-31317

WAVERIDERS
The use of high lift-to-drag hypersonic vehicles for aero-assisted orbital maneuvering p 3748 N92-31877

WEAK ENERGY INTERACTIONS
Problems in neutrino electron scattering with 1-GeV neutrinos
[DE92-013535] p 3895 N92-31765

WEAR
Tribology of Langmuir-Blodgett films
[AD-A250075] p 3833 N92-31363
Surface analysis of stainless steel outer race bearing specimens
[AD-A250088] p 3833 N92-31437

WEAR RESISTANCE
The preparation of (Al2O3)x(SiO2)y thin films using (Al(OSiEt3))2 as a single source precursor
[AD-A250142] p 3788 N92-31796

WEAR TESTS
A preliminary study in the use of phase demodulation techniques for the analysis of gear vibration data
[NRC-32083] p 3833 N92-31469

WEATHER FORECASTING
Combining expert probabilistic weather forecasts: Results of post-hoc analyses of the Zierikzee experiment
[REPT-91-101] p 3859 N92-31521
Updated forecast of Atlantic seasonal hurricane activity for 1992 p 3859 N92-31583
A case study of a prolonged sleet event: 16-17 February 1987 and climatology of sleet events for North Carolina, 1949-1989
[AD-A250184] p 3859 N92-31602
Meteorological data, new series A monographs. Volume 5, no. 4: A three dimensional model simulation of the circulation in the middle atmosphere with cconsideration of tropospherical-stratospherical interactions
[ETN-92-91693] p 3861 N92-31708
Simulation of diurnally varying downslope winds over Northern Utah
[AD-A250568] p 3861 N92-31714
A diagnostic study of rapidly developing cyclones using surface-based Q vectors
[AD-A246993] p 3862 N92-31978
Navy Atmospheric Boundary Layer (NABL) model system: Software/Interface design document
[AD-A247903] p 3857 N92-31986

WEATHERING
Outdoor testing of advanced optical materials for solar thermal electric applications
[DE92-010567] p 3847 N92-31623

WEDGES
High-frequency techniques for RCS prediction of plate geometries
[NASA-CR-190656] p 3804 N92-31273

WEIGHT REDUCTION
The design and testing of an optimal beam composed of unimodal elements p 3747 N92-31873

WEIGHTLESSNESS SIMULATION
Hollow fiber clinostat for simulating microgravity in cell culture
[NASA-CASE-MFS-28370-1] p 3828 N92-31790

WELD TESTS
Investigation into the ultrasonic NDE of adhesively bonded joints
[DREP-90-02] p 3837 N92-32202

WELDED JOINTS
Weld penetration and defect control
[DE92-015310] p 3836 N92-31336
Residual stresses in a multipass ferritic weldment
[DE92-014467] p 3839 N92-31501

WELDED STRUCTURES
Weld penetration and defect control
[DE92-015310] p 3836 N92-31336

WELLS
Materials for geothermal production
[DE92-014691] p 3849 N92-32118
Geothermal materials development
[DE92-016940] p 3849 N92-32124

WETTING
Controlled atmosphere soldering system
[DE92-012633] p 3802 N92-31580

WIGGLER MAGNETS
Microwave generation for magnetic fusion energy applications
[DE92-011424] p 3831 N92-31769

WIND (METEOROLOGY)
A numerical, analytical, and observational study of the effect of clouds on surface wind and wind stress during the central Arctic winter
[AD-A252706] p 3860 N92-31670
Simulation of diurnally varying downslope winds over Northern Utah
[AD-A250568] p 3861 N92-31714
Seasonal wind and ocean thermal forcing influences on the generation of the Leeuwin current and its eddies
[AD-A246992] p 3865 N92-31988

WIND DIRECTION
A comparative study of the dynamic performance of three bivanes
[AD-A250096] p 3862 N92-31784

WIND SHEAR
Spectrum modal analysis for the detection of low-altitude windshear with airborne Doppler radar
[NASA-CR-4457] p 3755 N92-31549
A numerical, analytical, and observational study of the effect of clouds on surface wind and wind stress during the central Arctic winter
[AD-A252706] p 3860 N92-31670

WIND TUNNEL DRIVES
Supersonic Throughflow Fan Test Facility at NASA. Lewis Research Center
[NASA-TP-3038] p 3762 N92-31640
WIND TUNNEL MODELS
Time simulation of flutter with large stiffness changes
[NASA-TM-107650] p 3758 N92-32111
WIND TUNNEL TESTS
High Reynolds number test of the Boeing TR77 airfoil in the Langley 0.3-meter transonic cryogenic tunnel
[NASA-TM-4189] p 3750 N92-31246
Flutter suppression digital control law design and testing for the AFW wind-tunnel model
[NASA-TM-107652] p 3757 N92-31350
Description of a 1000 sensor constant current anemometer system for locating three-dimensional turbulent boundary layer separations
[AD-A250827] p 3821 N92-31452
Flat plates placed in depleted hypersonic flow
[SESSIA-430/91.960] p 3751 N92-31508
Wind tunnel aerodynamic characteristics of a transport-type airfoil in a simulated heavy rain environment
[NASA-TP-3184] p 3751 N92-31532
A comparative study of the dynamic performance of three bivanes
[AD-A250096] p 3862 N92-31784
Euler solver for arbitrary configurations: Further applications p 3750 N92-31888
Exploratory experimental investigation of a wave propeller
[AD-A252175] p 3753 N92-32062
Experimental studies of hypersonic shock-wave boundary-layer interactions
[NASA-CR-190731] p 3753 N92-32162
Transonic wind tunnel test of a 14 percent thick oblique wing
[NASA-TM-102230] p 3754 N92-32213
WIND TUNNELS
Digital analysis of wind tunnel imagery to measure fluid thickness
[NASA-CR-189234] p 3762 N92-31252
WIND TURBINES
A surface definition code for turbine blade surfaces
[DE92-010574] p 3846 N92-31498
Cooperative field test program for wind systems
[DE92-001209] p 3847 N92-31579
WIND VANES
A comparative study of the dynamic performance of three bivanes
[AD-A250096] p 3862 N92-31784
WIND VELOCITY
Amending the w* velocity scale for surface layer, entrainment zone, and baroclinic shear in mixed Forced/Free turbulent convection
[AD-A250389] p 3859 N92-31540
Spectrum modal analysis for the detection of low-altitude windshear with airborne Doppler radar
[NASA-CR-4457] p 3755 N92-31549
Simulation of diurnally varying downslope winds over Northern Utah
[AD-A250568] p 3861 N92-31714
A comparative study of the dynamic performance of three bivanes
[AD-A250096] p 3862 N92-31784
Upper tropospheric jet streams over North America during summer 1988
[AD-A249871] p 3857 N92-31906
A comparison of the performance of two gust front detection algorithms using a length-based scoring technique
[AD-A250862] p 3863 N92-32103
WINDPOWER UTILIZATION
Cooperative field test program for wind systems
[DE92-001209] p 3847 N92-31579
WINDPOWERED GENERATORS
Cooperative field test program for wind systems
[DE92-001209] p 3847 N92-31579
WINDS ALOFT
Updated forecast of Atlantic seasonal hurricane activity for 1992 p 3859 N92-31583
WINDSHIELDS
Pressure and temperature for B-1B transparency test
[AD-A252711] p 3752 N92-31674
WINGS
Analysis of three icing test flights reaching the aircraft-referred icing degree of severe
[ESA-TT-1254] p 3755 N92-31943
Exploratory experimental investigation of a wave propeller
[AD-A252175] p 3753 N92-32062
WINTER
A case study of a prolonged sleet event: 16-17 February 1987 and climatology of sleet events for North Carolina, 1949-1989
[AD-A250184] p 3859 N92-31602
A numerical, analytical, and observational study of the effect of clouds on surface wind and wind stress during the central Arctic winter
[AD-A252706] p 3860 N92-31670
WIRE
Flexible heating head for induction heating apparatus and method
[NASA-CASE-LAR-14418-1] p 3803 N92-31257
SiGe Si quantum wires for efficient, room temperature, tunable luminescence
[AD-A249651] p 3814 N92-31464
Recent advances in high-temperature superconductor wire fabrication and applications development
[DE92-016634] p 3912 N92-31955
WIRE CLOTH
Oscillating-flow regenerator test rig: Woven screen and metal felt results
[NASA-CR-190689] p 3820 N92-31352
WORDS (LANGUAGE)
Optical interconnects in the computer environment
[AD-D015235] p 3873 N92-31269
A dictionary of acquisition and contracting terms
[AD-A247053] p 3920 N92-31754
WORK-REST CYCLE
Micro saint model of fatigue assessment
[AD-A249976] p 3868 N92-31554
WORKING FLUIDS
Natural convection immersion cooling of an array of vertically oriented heated protrusions in an enclosure filled with a dielectric liquid: Effects of enclosure width, Prandtl number and component orientation
[AD-A245884] p 3914 N92-31489
Establishing low-power operating limits for liquid metal heat pipes
[DE92-011367] p 3823 N92-31701
Heat transfer and flow of a modified second grade fluid
[DE92-014744] p 3824 N92-31895
WORKSTATIONS
Intelligent gateways p 3921 N92-32184

X

X RAY ABSORPTION
The NSLS 100 element solid state array detector
[DE92-014477] p 3827 N92-31502
X RAY DIFFRACTION
US-Japan seminar on magnetic multilayered structures: Proceedings
[AD-A252440] p 3910 N92-31666
Development and application of photosensitive device systems to studies of biological and organic materials
[DE92-014728] p 3867 N92-32120
X RAY IMAGERY
High brightness x ray source for directed energy and holographic imaging applications, phase 2
[AD-A248858] p 3827 N92-31475
X RAY INSPECTION
Motion model for the correction of point source distortion in radiographs of honeycomb
[DREP-88-14] p 3777 N92-32215
X RAY SOURCES
Activities of the Center for X Ray Lithography, phase 1
[AD-A250446] p 3901 N92-31397
High brightness x ray source for directed energy and holographic imaging applications, phase 2
[AD-A248858] p 3827 N92-31475
X RAY SPECTRA
Multiple electron populations accelerated in solar bursts
[INPE-5377-TDI/472] p 3925 N92-32025
X RAYS
Activities of the Center for X Ray Lithography, phase 1
[AD-A250446] p 3901 N92-31397
Microdistribution of lead in bone: A new approach
[DE92-013036] p 3869 N92-31589
XENON
Low-Isp derated ion thruster operation
[NASA-TM-105787] p 3771 N92-32237

Y

YAW
An investigation into the interface between three closely spaced axi-symmetric bodies at subsonic speed
[CRANFIELD-AERO-9114] p 3751 N92-31514
YIELD POINT
Studies of the effect of strain velocity on mechanical properties of the 34GS steel p 3786 N92-31243
YIELD STRENGTH
Strength tests of cold-formed channel sections undergoing local and distortional buckling
[PB92-180835] p 3841 N92-31658
YTTRIUM OXIDES
Oxygen ordering and strain-related morphology in YBa2Cu(3-x)O7 systems
[DE92-014476] p 3909 N92-31627
Effect of surface modifications on the properties of silicon nitride ceramics
[DE92-013848] p 3797 N92-32094

Z

ZENITH
Sun-view-target geometry effects on spectrally-derived vegetative index estimates of absorbed radiation and leaf area
[AD-A249984] p 3843 N92-31329
ZINC SULFIDES
The crystal growth and characterization of the solid solutions (ZnS)(1-x)(CuMS2)(x)
[AD-A248029] p 3911 N92-31819
ZIRCONIUM
Strongly adherent ceramic surface layers by ion implantation
[AD-A248882] p 3792 N92-31388
ZIRCONIUM ALLOYS
Thermodynamic assessment of the Cr-Zr system
[PB92-180645] p 3787 N92-31610
ZIRCONIUM OXIDES
Tetragonal zirconia ceramics in ZrO2-CeO2 system (Ce-TZP): Preparation, characterization and mechanical properties
[INPE-5372-PRE/1746] p 3798 N92-32199
ZODIACAL DUST
A characterization of the hot infrared background: The infrared cirrus, zodiacal dust bands, and solar system dust trails
[PL-TR-91-2065] p 3924 N92-32142

PERSONAL AUTHOR INDEX

Typical Personal Author Index Listing

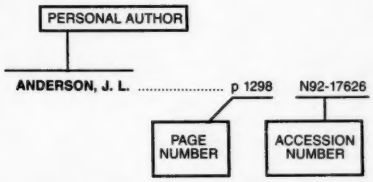

Listings in this index are arranged alphabetically by personal author. The page number helps you locate the citation in the abstract section. The accession number denotes the number by which the citation is identified.

A

AARONS, JULES ..... p 3855 N92-31478
ABE, Y. ..... p 3827 N92-31340
ABERCROMBIE, K. R. ..... p 3829 N92-32138
ABID, R. ..... p 3826 N92-32158
ABREVAYA, H. ..... p 3785 N92-32117
ABROMAVAGE, M. M. ..... p 3809 N92-31996
ACKERMAN, B. ..... p 3846 N92-31497
ADAMS, J. W. ..... p 3805 N92-31368
ADAMS, R. G. ..... p 3905 N92-31707
ADDESSIO, F. L. ..... p 3825 N92-32022
ADOLPH, HORST G. ..... p 3801 N92-32098
AGAMI, D. ..... p 3746 N92-31868
AGARWALA, VINOD S. ..... p 3774 N92-31382
AGBLEVOR, F. A. ..... p 3799 N92-31593
AGGARWAL, S. ..... p 3815 N92-31651
AHLERS, G. ..... p 3908 N92-31403
AIELLO, G. R. ..... p 3816 N92-31760
AINGER, R. ..... p 3864 N92-31630
AKESSON, EVA ..... p 3897 N92-31999
AKLUFI, M. ..... p 3791 N92-31356
ALAM, S. ..... p 3785 N92-32093
ALBIN, G. ..... p 3828 N92-31794
ALBRECHT-BUEHLER, GUENTER
..... p 3866 N92-31302
ALBRIGHT, S. P. ..... p 3846 N92-31497
ALBUS, J. S. ..... p 3885 N92-31680
ALEXANDER, Y. ..... p 3851 N92-31422
ALFONSI, ERIC A. ..... p 3873 N92-31269
ALIKAKOS, NICHOLAS ..... p 3887 N92-32081
ALLAN, D. W. ..... p 3802 N92-31830
ALLEGRE, J. ..... p 3751 N92-31508
ALLEN, C. W. ..... p 3894 N92-31595
ALLEN, CHRISTOPHER W. ..... p 3772 N92-31850
ALLUISI, EARL A. ..... p 3873 N92-32023
ALVES-FOSS, J. ..... p 3879 N92-31825
ALZMANN, MELANIE O. ..... p 3856 N92-31551
AMIN, N. ..... p 3810 N92-32203
AMOS, B. T. ..... p 3780 N92-31678
ANDERSON, CHARLES E., JR. ..... p 3767 N92-31997
ANDERSON, H. U. ..... p 3848 N92-31903
ANDERSON, R. ..... p 3872 N92-31309
ANDERSON, TED L. ..... p 3776 N92-32075
ANDRAKA, C. E. ..... p 3848 N92-32087
ANG, J. A. ..... p 3766 N92-31735
ANGELL, C. A. ..... p 3797 N92-32095
ANNIS, CHARLES ..... p 3786 N92-31360
ANSELMO, ESTELLE R. ..... p 3841 N92-31847
ANTONSEN, T. M., JR. ..... p 3831 N92-31769
..... p 3832 N92-31935
APBLETT, ALLEN W. ..... p 3788 N92-31795
ARCHAMBAULT, D. ..... p 3921 N92-32185
ARCHER, M. ..... p 3879 N92-31825
ARFIELD, NEWELL ..... p 3864 N92-31495
ARNOLD, S. M. ..... p 3840 N92-31505
ARNOLD, STEVEN M. ..... p 3777 N92-32234
ARTOK, L. ..... p 3786 N92-32141
ASAY, J. R. ..... p 3766 N92-31735
ASHURST, W. T. ..... p 3779 N92-31417
ASSINK, R. A. ..... p 3793 N92-31539
ATKINS, E. M. ..... p 3767 N92-32100
ATKINSON, L. ..... p 3864 N92-31630
AUBERT, J. H. ..... p 3905 N92-31707
AUCIELLO, O. ..... p 3909 N92-31546
AVELLANEDA, MARCO ..... p 3773 N92-31378
AVITAL, G. ..... p 3746 N92-31869
AZUMA, Y. ..... p 3894 N92-31679

B

BACH, S. H. ..... p 3898 N92-32169
BACHALO, WILLIAM D. ..... p 3819 N92-31283
BACON, L. D. ..... p 3905 N92-31707
BADDING, MICHAEL E. ..... p 3911 N92-31848
BADINELLI, MARTIN ..... p 3807 N92-31617
BAER, F. ..... p 3862 N92-31894
BAHR, R. K. ..... p 3808 N92-31722
BAILEY, J. E. ..... p 3905 N92-31707
BAILLY, F. MORET ..... p 3822 N92-31564
BALANIS, CONSTANTINE A. ..... p 3804 N92-31273
BALDWIN, C. ..... p 3882 N92-31740
BALDWIN, D. P. ..... p 3831 N92-31775
BANERJEE, A. ..... p 3814 N92-31525
BANKS-SILLS, LESLIE ..... p 3747 N92-31872
BAPTISTA, RAYMUNDO ..... p 3923 N92-31346
..... p 3923 N92-31347
BAR-AVI, P. ..... p 3748 N92-31875
BAR-ITZHACK, I. Y. ..... p 3748 N92-31878
BAR-ITZHACK, ITZHACK Y. ..... p 3748 N92-31876
BAR-SHALOM, Y. ..... p 3804 N92-31333
BARBARA, PAUL F. ..... p 3910 N92-31699
..... p 3897 N92-31950
..... p 3897 N92-31999
BARCLAY, C. B. ..... p 3916 N92-31992
BARKER, T. G. ..... p 3865 N92-31821
BARNES, J. M. ..... p 3868 N92-31409
BARNES, LESLIE A. ..... p 3790 N92-32156
BARNES, NORMAN P. ..... p 3831 N92-31788
BARNES, P. R. ..... p 3804 N92-31354
BARON, THIERRY ..... p 3901 N92-31692
BARRET, CHRIS ..... p 3763 N92-32011
BARRON, ANDREW R. ..... p 3788 N92-31795
..... p 3788 N92-31796
BARSHICK, CHRISTOPHER M. ..... p 3900 N92-32170
BARTLETT, RODNEY J. ..... p 3896 N92-31858
BARTO, SAM ..... p 3807 N92-31617
BASHMAKOV, I. A. ..... p 3852 N92-31574
BASS, ROBERT G. ..... p 3794 N92-31792
BASSANO, J.-C. ..... p 3921 N92-32185
BASTASZ, R. ..... p 3905 N92-31749
BATCHELOR, CHERYL L. ..... p 3870 N92-31321
BATINA, JOHN T. ..... p 3750 N92-31239
BAUMANN, N. P. ..... p 3898 N92-32165
BAUMGARDNER, J. R. ..... p 3825 N92-32022
BAYLER, ERIC J. ..... p 3865 N92-31988
BAYRAKAL, S. ..... p 3831 N92-31775
BEALE, WILLIAM T. ..... p 3769 N92-31245
BEASLEY, KENNETH D. ..... p 3766 N92-31260
BECKWITH, PAUL D. ..... p 3837 N92-32172
BEECHER, J. E. ..... p 3793 N92-31436
BEGUELIN, A. ..... p 3875 N92-31447
BEHUNEK, JAN L. ..... p 3857 N92-31964
BEIGELMAN, Z. ..... p 3746 N92-31865
BEIN, D. ..... p 3836 N92-31647
BEINER, L. ..... p 3746 N92-31867
BELAND, ANNE ..... p 3871 N92-31444
BELISLE, CLAUDE ..... p 3811 N92-32231
BELL, J. ..... p 3786 N92-32145
BELL, K. J. ..... p 3825 N92-32003
BEN-ASHER, JOSEPH Z. ..... p 3748 N92-31880
BENNETT, B. L. ..... p 3868 N92-31492
BENNETT, BRADFORD C. ..... p 3752 N92-31533
BENSEN, D. M. ..... p 3832 N92-31935
BENSLEY, EDWARD H. ..... p 3875 N92-31405
BENTLEY, J. ..... p 3913 N92-32085
BENYAMINI, GIDEON ..... p 3747 N92-31873
BEREN, J. ..... p 3827 N92-31502
BERGER, J. R. ..... p 3774 N92-31609
BERGER, T. ..... p 3864 N92-31630
BERGQUIST, A. ..... p 3810 N92-32070
..... p 3810 N92-32161
BERKOWITZ, M. ..... p 3899 N92-32196
BERMAN, MARSHALL ..... p 3770 N92-31503
BERMINGHAM, WILLIAM J. ..... p 3873 N92-31269
BERNHARDT, A. F. ..... p 3788 N92-31759
BERRAH-MANSOUR, N. ..... p 3894 N92-31679
BERRIER, BOBBY L. ..... p 3762 N92-31900
BERRY, H. G. ..... p 3894 N92-31679
BERTELRUD, A. ..... p 3822 N92-31564
BEUTTENMULLER, R. H. ..... p 3827 N92-31502
BEYER, RICHARD A. ..... p 3800 N92-31804
BEZOS, GAUDY M. ..... p 3751 N92-31532
BHATTACHARYYA, A. K. ..... p 3804 N92-31317
BIBERMAN, LUCIEN M. ..... p 3873 N92-32023
BICKES, R. W., JR. ..... p 3781 N92-31748
BIDWELL, S. W. ..... p 3832 N92-31935
BIEDERMAN, IRVING ..... p 3872 N92-31330
BIGBEE, W. L. ..... p 3869 N92-31608
BIGELOW, C. A. ..... p 3839 N92-31504
BINKLEY, ROBERT L. ..... p 3762 N92-32201
BIRCH, J. N. ..... p 3809 N92-31920
BIRD, C. D. ..... p 3914 N92-32207
BIRDSALL, C. K. ..... p 3907 N92-31983
BIRMINGHAM, T. J. ..... p 3925 N92-31338
BISCHOF, C. ..... p 3886 N92-31311
..... p 3879 N92-31899
BLACKMOND, D. G. ..... p 3784 N92-32029
BLAHA, GEORGES ..... p 3767 N92-32082
BLANCHARD, ROBERT C. ..... p 3769 N92-32204
BLAND, R. W. ..... p 3893 N92-31385
..... p 3913 N92-32166
BLANDER, M. ..... p 3783 N92-31857
BLAYLOCK, G. ..... p 3899 N92-31390
BLEIER, A. ..... p 3797 N92-32089
BLOOM, CHARLES P. ..... p 3885 N92-31811
BLOOMQUIST, D. D. ..... p 3905 N92-31707
BLOUGH, D. K. ..... p 3837 N92-31657
BLUETHMANN, B. ..... p 3877 N92-31628
BLUM, LESSER ..... p 3893 N92-31316
BOCKER, R. P. ..... p 3805 N92-31369
BOCKMAN, R. S. ..... p 3869 N92-31589
BODEN, T. A. ..... p 3854 N92-31907
BOETTICHER, G. ..... p 3885 N92-31597
BOGDONOFF, SEYMOUR M. ..... p 3823 N92-31824
BOGREN, JONAS ..... p 3840 N92-31512
BOHNHOFF-HLAVACEK, GAIL L. ..... p 3767 N92-31677
BOLCH, W. EMMETT ..... p 3805 N92-31387
BOLGER, J. ..... p 3836 N92-31647
BOLLMEIER, W. S., II ..... p 3847 N92-31579
BONICAMP, JUDITH M. ..... p 3800 N92-31800
BORDUI, P. F. ..... p 3914 N92-32207
BOSSLER, R. ..... p 3832 N92-31349
BOUILLARD, J. X. ..... p 3835 N92-31774
BOURKE, M. A. M. ..... p 3839 N92-31383
BOUSSO, EHUD ..... p 3747 N92-31873
BOWYER, KEVIN ..... p 3876 N92-31573
BOYCE, J. B. ..... p 3830 N92-31319
BOYD, J. E. ..... p 3777 N92-32215
BOYES, J. D. ..... p 3905 N92-31707
BOZEN, RALPH M. ..... p 3792 N92-31408
BRABY, L. A. ..... p 3768 N92-31846
BRACKENBUSH, L. W. ..... p 3768 N92-31846
BRADLEY, M. M. ..... p 3851 N92-31423
BRAITHWAITE, W. W. ..... p 3746 N92-31864
BRANDEMUEHL, M. J. ..... p 3872 N92-31309
BRASE, J. M. ..... p 3902 N92-31761
BRAY, IGOR ..... p 3896 N92-31837
BRENNAN, J. A. ..... p 3824 N92-31839
BRENNER, H. ..... p 3823 N92-31726
BREUER, L. ..... p 3749 N92-31882
BREWE, D. E. ..... p 3834 N92-31536
BRICOUT, F. A. ..... p 3785 N92-32093
BRIDGEMAN, BRUCE ..... p 3872 N92-32105
BRIGGS, D. ..... p 3899 N92-31390
BRILLHART, R. D. ..... p 3767 N92-32100
BRIMHALL, J. L. ..... p 3841 N92-31638
BRINGI, VISWANATHAN N. ..... p 3857 N92-31964
BRITTEN, J. A. ..... p 3794 N92-31560
BROCHU, CLAUDE ..... p 3811 N92-32231
..... p 3811 N92-32232
BROCK, D. ..... p 3791 N92-31356
BRODKIN, JUDITH S. ..... p 3778 N92-31301

BROECKER, W. S. ..... p 3864 N92-31572
BRONNER, F. ..... p 3869 N92-31589
BROOKES, N. ..... p 3907 N92-31296
BROOKS, C. J. ..... p 3756 N92-32219
BROOKS, J. ..... p 3905 N92-31749
BROOME, S. ..... p 3864 N92-31630
BROOME, TAFT H. ..... p 3777 N92-32104
BROWN, D. R. ..... p 3848 N92-31845
BROWN, G. ..... p 3864 N92-31630
BROWN, JEFFREY C. ..... p 3762 N92-31640
BROWN, MARK A. ..... p 3920 N92-31754
BRUBAKER, THOMAS H. ..... p 3857 N92-31964
BRUCE, J. E. ..... p 3898 N92-32169
BRUECK, S. R. ..... p 3831 N92-31802
BRUNNBERG, MATS ..... p 3840 N92-31512
BRUNS, J. E. ..... p 3754 N92-32240
BRUSH, ANDREW S. ..... p 3812 N92-31282
BRYAN, J. R. ..... p 3816 N92-31718
BUCHENAUER, D. ..... p 3905 N92-31749
p 3906 N92-31771
BUDIMAN, HARYANTO T. ..... p 3772 N92-31274
BUDWINE, C. M. ..... p 3923 N92-32005
BUHRMAN, JOHN R. ..... p 3872 N92-31458
BULLEMER, PETER T. ..... p 3885 N92-31811
BUNKER, STEPHEN N. ..... p 3792 N92-31388
BURCHELL, T. D. ..... p 3775 N92-31912
BURDEN, J. ..... p 3789 N92-32032
BURDICK, L. J. ..... p 3855 N92-31509
BURKE, G. J. ..... p 3804 N92-31317
BURNS, J. A. ..... p 3761 N92-31966
BURNS, T. J. ..... p 3881 N92-32126
BURRELL, K. H. ..... p 3781 N92-31729
BUSH, KATHRYN A. ..... p 3844 N92-32127
BUSTOS, OSCAR H. ..... p 3889 N92-32225
BUTKUS, LAWRENCE M. ..... p 3775 N92-31823
BUTTON, ROBERT M. ..... p 3812 N92-31282
BYRNE, R. H. ..... p 3756 N92-31746
BZOWSKA, DOROTA ..... p 3863 N92-32097

C

CABELLO, JEAN ..... p 3823 N92-31696
CAI, Y. ..... p 3835 N92-31774
CAMERON, J. F. ..... p 3793 N92-31436
p 3795 N92-31810
CAMPANELLA, S. J. ..... p 3809 N92-31920
CAMPARO, J. C. ..... p 3807 N92-31629
CAO, YUSONG ..... p 3857 N92-31766
CAPONE, FRANCIS J. ..... p 3762 N92-31900
CAPPIELLO, M. W. ..... p 3820 N92-31424
CARLE, A. ..... p 3886 N92-31311
p 3879 N92-31899
CARLSON, LELAND A. ..... p 3914 N92-31577
CARLSTROM, T. N. ..... p 3905 N92-31764
CARMICHAEL, RALPH L. ..... p 3754 N92-32213
CARPENTER, R. J. ..... p 3874 N92-31366
CARPINO, M. ..... p 3802 N92-31263
CARRANO, V. ..... p 3820 N92-31421
CARRERAS, B. A. ..... p 3906 N92-31829
CARRIER, G. F. ..... p 3785 N92-32076
CARTAYA, CHRISTINE M. ..... p 3879 N92-31783
CARTER, J. G. ..... p 3894 N92-31700
CARUSO, CARL ..... p 3756 N92-31838
CARUSO, S. V. ..... p 3765 N92-32148
CASADA, D. A. ..... p 3833 N92-31384
CATHCART, M. E. ..... p 3918 N92-31482
CECATTO, JOSE ROBERTO ..... p 3926 N92-32221
CERNANSKY, N. P. ..... p 3778 N92-31414
CHA, ZHI-XIONG ..... p 3909 N92-31627
CHAMBERLIN, R. R. ..... p 3846 N92-31497
CHAMIS, C. C. ..... p 3775 N92-31854
CHAMIS, CHRISTOS C. ..... p 3774 N92-31506
CHAN, CHI H. ..... p 3901 N92-31430
CHANDLER, G. A. ..... p 3905 N92-31707
CHANG, S. L. ..... p 3835 N92-31774
p 3835 N92-31929
CHANG, Y. ..... p 3907 N92-31296
CHAPLIN, K. R. ..... p 3837 N92-32143
CHASE, L. L. ..... p 3910 N92-31661
CHAWLA, K. K. ..... p 3773 N92-31315
CHEATHAM, LINDA K. ..... p 3788 N92-31796
CHELETTE, TAMARA L. ..... p 3803 N92-31890
CHEN, C. ..... p 3848 N92-31922
CHEN, C. P. ..... p 3885 N92-32036
CHEN, E. ..... p 3814 N92-31525
CHEN, H. C. ..... p 3754 N92-32226
p 3754 N92-32228
CHEN, K. R. ..... p 3830 N92-31411
CHEN, P. J. ..... p 3911 N92-31851
CHEN, PANG-CHIEH ..... p 3917 N92-32037
CHEN, PETER ..... p 3798 N92-32198
CHEN, RAY T. ..... p 3813 N92-31374
CHEN, S. S. ..... p 3835 N92-31774
CHEVALIER, C. ..... p 3780 N92-31607
CHIANG, C. K. ..... p 3913 N92-32072
CHIEFA, M. A. ..... p 3861 N92-31709
CHIEN, K. Y. ..... p 3822 N92-31625
p 3786 N92-32145
CHIMA, RODRICK V. ..... p 3759 N92-31250
CHIN, B. A. ..... p 3836 N92-31336
CHOI, NAG J. ..... p 3808 N92-31809
CHOU, M. S. ..... p 3785 N92-32076
CHOUDHARI, MEELAN ..... p 3822 N92-31687
CHOY, FRED K. ..... p 3834 N92-31485
CHPOUN, A. ..... p 3751 N92-31508
CHRISTIANSEN, WALTER H. ..... p 3903 N92-31459
CHRISTOPHOROU, L. G. ..... p 3894 N92-31700
CHRISTY, JOHN R. ..... p 3763 N92-32014
CHRUSCIEL, JEREZY ..... p 3795 N92-31941
CHU, JULIO ..... p 3750 N92-31246
CHUANG, C. C. ..... p 3850 N92-31297
CHUNG, C. M. ..... p 3795 N92-31810
CHUPYATOV, V. P. ..... p 3852 N92-31574
CHURCH, VICTOR E. ..... p 3879 N92-31787
CLAMEN, STEWART M. ..... p 3917 N92-31285
CLARK, DARWIN L. ..... p 3832 N92-32061
CLARK, JAMES ..... p 3883 N92-31835
CLARKE, JERRY A. ..... p 3920 N92-32102
CLARKE, MARGARET M. ..... p 3763 N92-32013
CLARKSON, JEFFREY D. ..... p 3751 N92-31300
CLEARY, M. P. ..... p 3773 N92-31305
CLELAND, W. E. ..... p 3896 N92-31926
CLENDENIN, J. ..... p 3900 N92-32131
CLIFF, E. M. ..... p 3761 N92-31966
CLINE, D. D. ..... p 3824 N92-31832
CLINE, S. P. ..... p 3853 N92-31648
CLOUGH, R. ..... p 3814 N92-31525
CLOUTMAN, L. D. ..... p 3782 N92-31805
COATS, R. S. ..... p 3905 N92-31707
COATS, WILLIAM G., JR. ..... p 3862 N92-31784
COCKBURN, BERNARDO ..... p 3887 N92-32164
CODA, S. ..... p 3905 N92-31764
COFFEY, H. T. ..... p 3835 N92-31774
COFFEY, HELEN E. ..... p 3856 N92-31637
p 3856 N92-31639
COHEN, P. I. ..... p 3912 N92-31915
COHOON, D. K. ..... p 3805 N92-31381
COLAIANNI, M. L. ..... p 3911 N92-31851
COLE, R. L. ..... p 3799 N92-31442
COLE, STANLEY R. ..... p 3757 N92-31264
COLEMAN, M. M. ..... p 3798 N92-31399
COLLICA, L. A. ..... p 3881 N92-31365
COLLINS, B. ..... p 3899 N92-31390
COLLINS, CURTIS A. ..... p 3864 N92-31495
COLLINS, J. P. ..... p 3822 N92-31625
p 3786 N92-32145
CONFORTI, MICHELE ..... p 3888 N92-31768
CONNELL, G. A. ..... p 3830 N92-31319
CONROY, T. J. ..... p 3768 N92-31846
COOK, D. L. ..... p 3905 N92-31707
COOK, E. R. ..... p 3853 N92-31648
COOK, G. O., JR. ..... p 3879 N92-31743
COOK, L. P. ..... p 3913 N92-32072
COOKE, R. M. ..... p 3859 N92-31521
COOKE, ROGER M. ..... p 3856 N92-31522
CORLEY, J. P. ..... p 3905 N92-31707
CORLISS, G. ..... p 3886 N92-31311
p 3879 N92-31899
CORNELL, DANIEL ..... p 3843 N92-31329
CORNUEJOLS, GERARD ..... p 3888 N92-31768
CORRE, C. ..... p 3779 N92-31416
COSGROVE, B. A. ..... p 3745 N92-31862
COULTRIP, ROBERT H. ..... p 3803 N92-31257
COUZY, W. ..... p 3821 N92-31513
COWAN, M. ..... p 3765 N92-31542
CRABTREE, GREGORY D. ..... p 3892 N92-31672
CRAMER, S. N. ..... p 3899 N92-31831
CRAMER, S. P. ..... p 3827 N92-31502
CRAMPTON, S. J. B. ..... p 3802 N92-31830
CRANE, B. ..... p 3836 N92-31647
CRAVEY, W. R. ..... p 3815 N92-31548
CRAY, BENJAMIN A. ..... p 3892 N92-31789
CRIM, F. F. ..... p 3893 N92-31463
CROMWELL, W. E. ..... p 3876 N92-31529
CROWL, LAWRENCE A. ..... p 3881 N92-31428
CROWLEY, C. J. ..... p 3825 N92-32115
CROWLEY, KAY ..... p 3876 N92-31561
CRUICKSHANK, J. M. ..... p 3811 N92-32217
CRUMLEY, LLOYD M. ..... p 3872 N92-31294
CRUZDOSSANTOS, AILTON ..... p 3845 N92-32220
CUCINOTTA, FRANCIS A. ..... p 3926 N92-32193
CULLEN, D. E. ..... p 3895 N92-31705
CUNNAN, WALTER S. ..... p 3762 N92-31640
CUNNIFF, PATRICK F. ..... p 3838 N92-31337
CURL, ROBERT F. ..... p 3907 N92-31375
CURRY, ROBERT E. ..... p 3752 N92-31808
CURTIS, S. B. ..... p 3926 N92-31756
CUSHMAN, ARTHUR ..... p 3807 N92-31617
CUTHBERTSON, J. W. ..... p 3906 N92-31771
CUTLER, L. S. ..... p 3802 N92-31830
CUTRI, ROC M. ..... p 3924 N92-32142
CYBENKO, GEORGE ..... p 3884 N92-31332
CYPRYK, MAREK ..... p 3795 N92-31941

D

DAFERMOS, C. ..... p 3915 N92-31585
DAHLBERG, E. D. ..... p 3912 N92-31915
DALEY, JOHN A. ..... p 3878 N92-31676
DAMLE, A. S. ..... p 3784 N92-31976
DANE, CARL W. ..... p 3753 N92-32062
DANIEL, B. R. ..... p 3783 N92-31916
DANIELS, E. J. ..... p 3779 N92-31441
DANTZIG, G. B. ..... p 3875 N92-31410
DARVAS, RAFAEL ..... p 3897 N92-31958
DAS, L. ..... p 3890 N92-32099
DAS, RAJA ..... p 3876 N92-31561
DASH, Z. ..... p 3825 N92-32008
DATSKOS, P. G. ..... p 3894 N92-31700
DAVARI, SADEGH ..... p 3875 N92-31486
DAVID, S. A. ..... p 3839 N92-31383
p 3839 N92-31501
DAVIDSON, M. ..... p 3826 N92-31313
DAVIS, A. ..... p 3786 N92-32141
DAVIS, B. ..... p 3831 N92-31775
DAVIS, D. A. ..... p 3767 N92-32100
DAVIS, J. W. ..... p 3875 N92-31410
DAVIS, ROBERT F. ..... p 3908 N92-31446
DAWICKE, D. S. ..... p 3838 N92-31279
p 3839 N92-31504
DAWSON, J. M. ..... p 3830 N92-31411
DAWSON, RONALD A. ..... p 3762 N92-31640
DAY, S. M. ..... p 3856 N92-31510
p 3865 N92-31821
DEBONIS, J. R. ..... p 3754 N92-32240
DECASTRO, PEDRO JOSE ..... p 3818 N92-32200
DEFOREST, DANIEL L. ..... p 3899 N92-31325
DEGNAN, KEITH T. ..... p 3844 N92-32127
DELLER, J. R., JR. ..... p 3877 N92-31642
DELORENZO, ROBERT J. ..... p 3868 N92-31491
DELUGACH, HARRY ..... p 3883 N92-31835
DEMENDONCAMOTTA, IAMARA VIRGINIA
p 3886 N92-31241
DEMIRGIAN, J. C. ..... p 3854 N92-32083
DEMMEL, JOHANN ..... p 3755 N92-31813
p 3755 N92-31943
DEMPSEY, BERT J. ..... p 3882 N92-31483
p 3916 N92-31547
DENNISON, THOMAS E. ..... p 3880 N92-32060
DESAI, C. S. ..... p 3842 N92-32168
DESCH, J. K. ..... p 3817 N92-31946
DESPER, C. R. ..... p 3794 N92-31624
DESROCQUES, G. ..... p 3921 N92-32185
DESTLER, W. W. ..... p 3831 N92-31769
p 3832 N92-31935
DEUTSCHMANN, JULIE ..... p 3748 N92-31876
DEVANATHAN, R. ..... p 3787 N92-31575
DIAZ, MARCOS P. ..... p 3923 N92-31344
p 3923 N92-31345
DICKINSON, J. T. ..... p 3913 N92-32065
DICKSON, S. C. ..... p 3913 N92-32166
DIECKMAN, S. L. ..... p 3846 N92-31531
DIETRICH, LECH ..... p 3786 N92-31243
DIETZEN, SCOTT ..... p 3880 N92-31939
DIGNAN, T. G. ..... p 3913 N92-32166
DIJKSTRA, F. ..... p 3747 N92-31871
DILLARD, D. ..... p 3774 N92-31604
DISALVO, F. J. ..... p 3911 N92-31848
DIVER, R. B. ..... p 3848 N92-32087
DJELLABI, KAMEL ..... p 3815 N92-31697
DO, Y. R. ..... p 3911 N92-31819
DOCARMOANONO, MARIA ..... p 3818 N92-32200
DOCARMODEANONO, MARIA ..... p 3798 N92-32199
DOCTOR, R. D. ..... p 3779 N92-31441
DODGE, D. M. ..... p 3847 N92-31579
DODSON, T. A. ..... p 3839 N92-31501
DOLAN, F. X. ..... p 3825 N92-32115
DONGARRA, J. ..... p 3875 N92-31447
DONOVAN, M. F. ..... p 3863 N92-32103
DORHOUT, PETER K. ..... p 3785 N92-32080
DORRIS, S. ..... p 3846 N92-31531
DOUGHERTY, M. ..... p 3826 N92-31313
DOUGLAS, S. R. ..... p 3837 N92-32143
DOW, JOHN D. ..... p 3816 N92-31799
DOWELL, EARL H. ..... p 3842 N92-32236
DRISCHLER, J. D. ..... p 3868 N92-31409
p 3834 N92-31500
DRISKELL, JAMES E. ..... p 3870 N92-31321
DROEGE, M. W. ..... p 3786 N92-31391
DRUCE, R. L. ..... p 3910 N92-31719
DRYER, F. L. ..... p 3779 N92-31416
DUAN, YUN-BO ..... p 3892 N92-31255
DUFFEY, R. B. ..... p 3824 N92-31977
DUKOWICZ, J. K. ..... p 3825 N92-32022
DUNCAN, R. V. ..... p 3908 N92-31403
DUNHAM, R. EARL, JR. ..... p 3751 N92-31532

DUNN-ROBERTS, RICHARD ..... p 3873 N92-31974
DUNN, GLEN M. ..... p 3770 N92-31550
DURAN, R. S. ..... p 3795 N92-31952
p 3795 N92-31954
p 3798 N92-32194
DURISCOE, D. M. ..... p 3853 N92-31648
DURSCH, HARRY W. ..... p 3767 N92-31677
DUSSOUILLEZ, PH. ..... p 3822 N92-31564
DWIGHT, K. ..... p 3911 N92-31819
DYKMAN, JOHN R. ..... p 3761 N92-31656
DYKOV, A. N. ..... p 3829 N92-32174
DYSON, KAREN A. ..... p 3876 N92-31586

E

EAGLESON, PETER S. ..... p 3855 N92-32222
EARTHERLY, W. P. ..... p 3775 N92-31912
EASTON, ROGER L., JR. ..... p 3762 N92-31252
EASTWOOD, DAVID, JR. ..... p 3776 N92-32064
EBELING, CHARLES ..... p 3766 N92-31260
EBELING, W. D. ..... p 3915 N92-31660
EBERHARDT, J. ..... p 3847 N92-31571
ECONOMY, JAMES ..... p 3773 N92-31361
EDELMAN, JOEL ..... p 3767 N92-31677
EDELSON, M. C. ..... p 3831 N92-31775
EGHBALI, D. A. ..... p 3820 N92-31420
EHST, D. A. ..... p 3903 N92-31310
EICHMANN, DAVID ..... p 3917 N92-31272
p 3885 N92-31597
EKBLAD, U. ..... p 3767 N92-32073
EKLUND, E. A. ..... p 3783 N92-31820
EL-GIZAWY, A. S. ..... p 3838 N92-31303
ELBAUM, NICK C. ..... p 3874 N92-31379
ELDER, M. G. ..... p 3759 N92-31817
ELEGY, D. C. ..... p 3768 N92-31846
ELLINGSON, R. G. ..... p 3862 N92-31894
ELLIOTT, C. MICHAEL ..... p 3785 N92-32080
ELMAN, HOWARD C. ..... p 3886 N92-31567
ELSWICK, S. ..... p 3854 N92-32071
EMANUEL, W. R. ..... p 3853 N92-31782
EMERY, J. ..... p 3795 N92-31938
ENDRES, D. ..... p 3890 N92-32140
ENGE, JAMES ..... p 3762 N92-31252
ENGELS, E., JR. ..... p 3896 N92-31926
ENGLE, STANLEY E. ..... p 3816 N92-31780
ENGLISH, GARY E. ..... p 3864 N92-31407
EPSTEIN, B. ..... p 3750 N92-31888
ERICKSON, S. A., JR. ..... p 3889 N92-32119
ERIKSSON, G. ..... p 3783 N92-31857
ERLEBACHER, G. ..... p 3822 N92-31564
ERSKINE, FRED T. ..... p 3892 N92-32044
ESEN, E. B. ..... p 3890 N92-32099
ESER, S. ..... p 3798 N92-31399
ESKRIDGE, R. E. ..... p 3862 N92-31734
EVANS, DAVID R. ..... p 3866 N92-31465
EVANS, R. J. ..... p 3799 N92-31593
EVLETH, E. M. ..... p 3783 N92-31860
EXARHOS, G. J. ..... p 3910 N92-31665
EYLER, JOHN R. ..... p 3900 N92-32170

F

FABISZEWSKI, ALAN S. ..... p 3774 N92-31382
FAGOT, M. G. ..... p 3866 N92-32050
FAHEY, J. ..... p 3793 N92-31435
FAIN, D. E. ..... p 3783 N92-31816
FARLEY, G. L. ..... p 3774 N92-31566
FARLEY, GARY L. ..... p 3772 N92-31274
FARMER, D. M. ..... p 3864 N92-31429
FARQUHAR, G. ..... p 3874 N92-32183
FARROW, R. L. ..... p 3782 N92-31773
FASCHING, G. E. ..... p 3919 N92-31731
FAWCETT, W. R. ..... p 3893 N92-31316
p 3893 N92-31328
FEATHER, JOHN B. ..... p 3761 N92-31656
FEHRINGER, W. ..... p 3774 N92-31609
FEIGELSON, ROBERT S. ..... p 3901 N92-31380
FELDHEIM, DANIEL L. ..... p 3785 N92-32080
FELDMAN, D. D. ..... p 3805 N92-31376
FELDMAN, D. L. ..... p 3853 N92-31896
FENDELL, F. E. ..... p 3785 N92-32076
FERGUSON, R. E. ..... p 3822 N92-31625
p 3786 N92-32145
FERRON, J. R. ..... p 3904 N92-31616
FIFER, ROBERT A. ..... p 3778 N92-31393
FIGHETTI, C. ..... p 3820 N92-31421
FILIPPI, STEPHEN C. ..... p 3918 N92-31450
FIREY, B. ..... p 3836 N92-31647
FISHER, DAVID F. ..... p 3751 N92-31276
FISHER, G. ..... p 3879 N92-31825
FISHER, R. J. ..... p 3862 N92-31750
FISHMAN, R. S. ..... p 3789 N92-31898
FLECHNER, STUART G. ..... p 3750 N92-31246
FLEETER, SANFORD ..... p 3760 N92-32059
FLOOD, DENNIS J. ..... p 3818 N92-32233
FLOYD, H. ..... p 3854 N92-31931
FLUHR, CHRISTIAN ..... p 3921 N92-32184
FOILES, S. M. ..... p 3788 N92-31744
FOOTE, J. P. ..... p 3903 N92-31372
FORTI, MARIA CRISTINA ..... p 3863 N92-32224
FOSS, COLBY A. ..... p 3785 N92-32080
FOSSUM, ERIC ..... p 3795 N92-31941
FOUKAL, PETER ..... p 3845 N92-32223
FOX, ROBERT L. ..... p 3803 N92-31257
FRANTZISKONIS, G. N. ..... p 3842 N92-32168
FREAR, D. R. ..... p 3802 N92-31580
FRECHET, J. M. ..... p 3793 N92-31435
p 3793 N92-31436
p 3795 N92-31810
FREED, ALAN D. ..... p 3777 N92-32234
FREEMAN, A. J. ..... p 3775 N92-31806
FREEMAN, ARTHUR J. ..... p 3790 N92-32084
FRENCH, JONATHAN ..... p 3868 N92-31554
FRERY, ALEJANDRO C. ..... p 3874 N92-31348
p 3889 N92-32225
FRESE, K. W. ..... p 3848 N92-31922
FREUND, H. P. ..... p 3832 N92-31935
FREY, M. ..... p 3915 N92-31645
FRISCH, J. ..... p 3900 N92-32131
FRNZEN, WOLFGANG ..... p 3778 N92-31301
FRONEK, DENNIS L. ..... p 3762 N92-31640
FROONINCKX, THOMAS B. ..... p 3767 N92-31822
FRUEHOLZ, R. P. ..... p 3807 N92-31629
FUCHS, MOSHE B. ..... p 3747 N92-31873
FUJIMOTO, J. G. ..... p 3832 N92-32042
FUJISAWA, A. ..... p 3827 N92-31340
FUKUYAMA, A. ..... p 3904 N92-31659
p 3907 N92-32181
FUNG, J. ..... p 3810 N92-32203
FURENLID, L. R. ..... p 3827 N92-31502
FUSARO, ROBERT L. ..... p 3795 N92-31840

G

GALA, ANTONIO ..... p 3804 N92-31314
GALAMBOS, J. D. ..... p 3906 N92-31913
GALE, R. ..... p 3848 N92-31893
GALLY, THOMAS A. ..... p 3914 N92-31577
GAMBLE, RICHARD O., II ..... p 3851 N92-31556
GANGWAL, S. K. ..... p 3784 N92-31976
GANY, ALON ..... p 3749 N92-31885
GARCIA, A. M. ..... p 3920 N92-31934
GARCIA, L. ..... p 3906 N92-31829
GARG, SANJAY ..... p 3761 N92-32241
GARNERO, E. J. ..... p 3855 N92-31509
GARRETT, J. D. ..... p 3898 N92-32090
GARRETT, W. R. ..... p 3896 N92-31923
GARVIS, D. ..... p 3828 N92-31909
GARZON, F. H. ..... p 3911 N92-31723
GATES, W. L. ..... p 3850 N92-31324
GAUJAL, BRUNO ..... p 3881 N92-32157
GAUL, K. ..... p 3831 N92-31775
GAVALER, JOHN R. ..... p 3813 N92-31451
GAVEL, D. T. ..... p 3902 N92-31761
GEDEON, D. ..... p 3820 N92-31352
GEDRIDGE, R. W., JR. ..... p 3796 N92-31968
GEERS, THOMAS L. ..... p 3891 N92-31588
GEIST, A. ..... p 3875 N92-31447
GENDRON, G. ..... p 3842 N92-32235
GENTRY, GARL L., JR. ..... p 3751 N92-31532
GERDES, D. ..... p 3919 N92-31596
GESELL, LESLIE H. ..... p 3763 N92-32012
GETTRUST, J. F. ..... p 3918 N92-31467
GIBSON, RICHARD L., JR. ..... p 3855 N92-31476
GIDDINGS, VICTOR T. ..... p 3875 N92-31405
GIEL, T. V. ..... p 3903 N92-31372
GILBANK, PASCALE ..... p 3784 N92-31942
GILBERTSON, A. ..... p 3826 N92-31313
GILYARD, GLENN B. ..... p 3759 N92-31275
GIN, ROSANGELA BARRETO BIASI
p 3863 N92-32212
GIRIMAJI, SHARATH S. ..... p 3826 N92-32242
GLASS, CHRISTOPHER E. ..... p 3818 N92-31247
GLATFELTER, T. ..... p 3814 N92-31525
GLEZER, A. ..... p 3822 N92-31559
GLIEBE, P. R. ..... p 3891 N92-31248
GLYNN, PETER W. ..... p 3888 N92-31600
p 3888 N92-31757
GODBEY, SUSAN E. ..... p 3800 N92-31800
GODBOLE, M. J. ..... p 3795 N92-31917
GOGGIN, R. M. ..... p 3847 N92-31623
GOLDSTONE, J. ..... p 3839 N92-31383
GONDA, TOSHI N. ..... p 3764 N92-32015
GONG, S. S. ..... p 3828 N92-31828
GONZALES, J. A. ..... p 3813 N92-31367
GONZALEZ, CESAR A. ..... p 3882 N92-31445
GOODS, S. H. ..... p 3788 N92-31744
GOPALSAMI, N. ..... p 3846 N92-31531
GORDA, B. C. ..... p 3882 N92-31466
p 3883 N92-31741
GORDON, G. S. ..... p 3809 N92-31920
GOSWAMI, D. Y. ..... p 3849 N92-32091
GOTTESDIENER, L. ..... p 3751 N92-31508
GRANATSTEIN, V. L. ..... p 3831 N92-31769
p 3832 N92-31935
GRANT, S. G. ..... p 3869 N92-31608
GRAVES, W. E. ..... p 3898 N92-32165
GRAY, J. A. ..... p 3778 N92-31415
GRAY, J. L. ..... p 3846 N92-31526
GRAY, WILLIAM M. ..... p 3859 N92-31583
GRAYSTON, ALAN M. ..... p 3762 N92-31900
GREENBERG, ALBERT G. ..... p 3881 N92-32157
GREENBERG, HARVEY J. ..... p 3875 N92-31480
GREENBERG, I. ..... p 3747 N92-31870
GREENBERG, J. B. ..... p 3746 N92-31869
p 3749 N92-31884
GREENSITE, J. ..... p 3893 N92-31385
GREGAR, J. S. ..... p 3846 N92-31531
GREINER, JOHN ..... p 3874 N92-31353
GREMILLION, JEFFREY C. ..... p 3902 N92-32137
GRENERT, J. E. ..... p 3861 N92-31709
GRIEWANK, A. ..... p 3886 N92-31311
p 3879 N92-31899
GRIFFIN, K. L. ..... p 3910 N92-31719
GRIFFITH, J. E. ..... p 3916 N92-32160
GRIFFITHS, LLOYD J. ..... p 3805 N92-31376
GROEBNER, R. J. ..... p 3781 N92-31729
GRONET, M. J. ..... p 3767 N92-32100
GROSS, T. S. ..... p 3839 N92-31389
GRUBELICH, M. C. ..... p 3781 N92-31748
GRUEBEL, R. ..... p 3888 N92-31518
GRUEBEL, RUDOLF ..... p 3888 N92-31519
GRUEN, D. M. ..... p 3909 N92-31652
GRUNER, S. M. ..... p 3867 N92-32120
GUAN, H. W. ..... p 3784 N92-31959
p 3796 N92-31960
GUERDAL, Z. ..... p 3842 N92-32235
GUERRIERO, LUCIANO ..... p 3764 N92-32016
GUEST, PETER S. ..... p 3860 N92-31670
GUHA, S. ..... p 3814 N92-31525
GUNDERSEN, MARTIN ..... p 3814 N92-31490
GUNTHER, W. ..... p 3815 N92-31651
GUPTA, G. ..... p 3824 N92-31895
GUPTA, ROOP N. ..... p 3819 N92-31281
GUPTA, S. ..... p 3876 N92-31561
GURLAND, J. ..... p 3889 N92-31359
GUTMARK, E. ..... p 3747 N92-31871
GUTTMAN, C. M. ..... p 3794 N92-31618
GUZIK, T. G. ..... p 3926 N92-31477

H

HACKEL, R. P. ..... p 3832 N92-31902
HAEMAELAEINEN, M. ..... p 3787 N92-31610
HALL, C. A. ..... p 3766 N92-31735
HALL, CHRISTOPHER D. ..... p 3768 N92-31675
HALL, E. J. ..... p 3867 N92-31747
HALL, L. J. ..... p 3898 N92-32006
HALL, PHILIP ..... p 3822 N92-31687
HALLER, H. ..... p 3922 N92-32192
HAMADA, Y. ..... p 3827 N92-31340
p 3765 N92-31685
HAMLEY, JOHN A. ..... p 3769 N92-31342
HAMMER, C. L. ..... p 3854 N92-32083
HAMMOND, G. ..... p 3814 N92-31525
HAMMONS, CHARLES ..... p 3883 N92-31835
HAMRICK, Y. M. ..... p 3831 N92-31775
HAMZA, A. V. ..... p 3910 N92-31661
HAN, C. C. ..... p 3794 N92-31618
HAN, YIN Y. ..... p 3805 N92-31413
HANCOCK, G. J. ..... p 3841 N92-31658
HAND, H. M. ..... p 3833 N92-31437
HANDSCHUH, R. ..... p 3832 N92-31349
HANES, PHILLIP J. ..... p 3876 N92-31488
HANLON, JAMES C. ..... p 3771 N92-32108
HANSON, ERIC N. ..... p 3917 N92-31396
HAQUE, S. A. ..... p 3795 N92-31810
HARDING, KENNETH W. ..... p 3858 N92-31432
HARKNESS, J. B. L. ..... p 3779 N92-31441
HARLAN, C. P. ..... p 3851 N92-31427
p 3919 N92-31578
HARLOFF, G. J. ..... p 3754 N92-32240
HARMAN, R. R. ..... p 3748 N92-31878
HARPER, ROBERT ..... p 3887 N92-32171
HARRINGTON, M. W. ..... p 3851 N92-31427
p 3919 N92-31578
HARRISON, ALBERT A. ..... p 3764 N92-32020
HARTENSTEIN, RAY ..... p 3879 N92-31787
HASHEMIAN, H. M. ..... p 3826 N92-31298
HASKELL, WILLIAM E., III ..... p 3792 N92-31404
HASSANEIN, A. ..... p 3903 N92-31310
HATCHER, P. G. ..... p 3798 N92-31399
HAUS, H. A. ..... p 3832 N92-32042
HAW, JAMES F. ..... p 3874 N92-31379
HAWKE, R. S. ..... p 3766 N92-31735

HAWLEY, M. p 3911 N92-31723
HAXTON, W. C. p 3925 N92-32154
HAYDEN, WARREN R. p 3771 N92-32129
HAYTON, G. E. p 3887 N92-31957
HAZUCHA, MILAN J. p 3870 N92-32107
HE, J. L. p 3835 N92-31774
HELMBERGER, D. V. p 3855 N92-31509
HENDREY, G. R. p 3851 N92-31422
HENNINGSON, DAN S. p 3822 N92-31535
HENRY, SCOTT L. p 3876 N92-31488
HENSHALL, H. p 3811 N92-32217
HENSINGER, D. M. p 3780 N92-31671
HERBERT, THORWALD p 3819 N92-31306
HERDMAN, T. L. p 3761 N92-31966
HERGENROTHER, PAUL M. p 3794 N92-31792
HERMAN, WARREN N. p 3791 N92-31270
HERNANDEZ, C. L. p 3802 N92-31580
HESS, N. J. p 3910 N92-31665
HESSLER, J. P. p 3830 N92-31684
HEWETT, C. A. p 3817 N92-31849
HEY, N. S. p 3854 N92-31931
HILL, ACQUILLA S. p 3750 N92-31246
HILL, D. N. p 3906 N92-31771
HIMM, J. p 3828 N92-31794
HIRLEMAN, E. D. p 3897 N92-31936
HO, HENJEN p 3772 N92-31274
p 3774 N92-31566
HO, M. J. p 3846 N92-31498
HOBBS, D. p 3795 N92-31938
HOBSON, J. p 3856 N92-31662
HODGES, DEWEY H. p 3839 N92-31339
HODGKINSON, JOHN p 3761 N92-31656
HOEKSEMA, J. T. p 3925 N92-31786
HOENSELAERS, C. p 3886 N92-31956
HOFFMAN, J. J. p 3752 N92-31777
HOFFMANN, HANS-EBERHARD p 3755 N92-31813
p 3755 N92-31943
HOGENDOORN, R. A. p 3922 N92-32190
HOH, J. p 3795 N92-31938
HOLA, JERZY p 3842 N92-32206
HOLCOMB, R. S. p 3770 N92-31897
HOLDEN, MICHAEL S. p 3819 N92-31286
HOLDEN, T. M. p 3839 N92-31383
p 3839 N92-31501
HOLDER, DARRYL p 3808 N92-31801
HOLOWECKY, BRIAN p 3761 N92-32241
HOM, K. p 3780 N92-31671
HONG, P. E. p 3766 N92-32130
HONIG, A. p 3898 N92-32007
HOPPER, R. W. p 3821 N92-31528
HOPPIE, L. O. p 3835 N92-31774
HOPSON, M. p 3814 N92-31525
HORIUCHI, RITOKU p 3906 N92-31843
HORNSBY, MARY E. p 3761 N92-32175
HORTON, W. p 3903 N92-31412
HOSAKA, Y. p 3887 N92-32205
HOSKING, F. M. p 3802 N92-31580
HOULTON, R. J. p 3911 N92-31723
HOVLAND, P. p 3879 N92-31899
HOWARD, IAN P. p 3871 N92-31472
HOWARD, RANDALL B. p 3880 N92-31991
HOWELL, T. A. p 3866 N92-32050
HOWERTON, CLAYTON E. p 3844 N92-32127
HOWIE, A. p 3829 N92-32086
HOYT, E. p 3900 N92-32131
HRKACH, JEFFREY S. p 3798 N92-32153
HSU, W. p 3905 N92-31749
HU, JIH-PERNG p 3841 N92-31844
HUBBARD, C. A. p 3839 N92-31501
HUFF, T. L. p 3765 N92-32148
HUGHES, B. A. p 3844 N92-32216
HUGHES, E. D. p 3824 N92-31977
HUGHES, R. S., JR. p 3910 N92-31661
HUGHES, S. J. p 3844 N92-32216
HUGHES, SANDY p 3870 N92-31321
HULL, J. R. p 3834 N92-31720
p 3912 N92-31955
HUMANIC, T. J. p 3896 N92-31926
HUNT, J. E. p 3893 N92-31386
HUNT, S. D. p 3877 N92-31642
HURST, J. K. p 3785 N92-32113

I

IGUCHI, H. p 3827 N92-31340
IMRE, K. p 3903 N92-31494
INGERSOLL, D. p 3799 N92-31570
INOE, MARIO TAKAO p 3806 N92-31568
INTERRANTE, L. V. p 3798 N92-32197
IPPEN, E. P. p 3832 N92-32042
IRVING, P. M. p 3852 N92-31598
ISHAM, M. A. p 3791 N92-31278
ISHIDA, HATSUO p 3902 N92-32077
ITOH, K. p 3904 N92-31659
p 3907 N92-32181
ITOH, S.-I. p 3907 N92-32181
ITOH, SANAE-I. p 3904 N92-31659
IVANOV, M. V. p 3924 N92-32180

J

JABLONSKI, FRANCISCO J. p 3923 N92-31346
JACKETT, N. p 3814 N92-31525
JACKSON, J. A. p 3757 N92-31736
JACOBSON, JOHN M. p 3907 N92-31990
JAFFE, MICHAEL p 3792 N92-31419
JAGLER, KARL B. p 3890 N92-32046
JAGODA, J. I. p 3783 N92-31918
JAIN, HIMANSHU p 3791 N92-31270
JAIN, RAJ K. p 3818 N92-32233
JAKUBEK, DAVID A. p 3809 N92-31993
JALLOH, A. R. p 3900 N92-31975
JAMESON, ANTONY p 3745 N92-31863
JANKOVSKY, ROBERT S. p 3769 N92-31249
JAOUABI, K. p 3778 N92-31414
JARBOE, THOMAS R. p 3903 N92-31459
JAROSS, R. A. p 3846 N92-31531
JAROUX, B. p 3760 N92-31910
JASELSKIS, E. J. p 3780 N92-31565
JAYARAMAN, K. p 3774 N92-31604
JELLINECK, R. p 3856 N92-31636
JENSEN, BRIAN J. p 3794 N92-31792
JENSEN, R. H. p 3869 N92-31608
JENSSEN, HANS P. p 3908 N92-31438
JESSEN, PAUL F. p 3864 N92-31495
JETTE, M. p 3873 N92-32031
JHA, NIRAJ K. p 3883 N92-32040
JILES, D. C. p 3890 N92-32116
JIM, TREVOR p 3887 N92-32163
JOHNSON, ALAN E. p 3910 N92-31699
p 3897 N92-31999
JOHNSON, CRAIG p 3870 N92-31321
JOHNSON, D. L. p 3846 N92-31531
JOHNSON, G. p 3821 N92-31426
JOHNSON, J. p 3877 N92-31628
JOHNSON, J. O. p 3868 N92-31409
JOHNSON, MACDONALD p 3800 N92-31969
p 3800 N92-31970
p 3800 N92-31971
p 3801 N92-31972
p 3801 N92-31973
JOHNSON, N. L. p 3825 N92-32022
JOHNSON, P. D. p 3907 N92-31296
JOHNSON, R. T. p 3913 N92-32166
JOHNSON, R. W. p 3902 N92-32144
JOHNSON, SAMUEL D. p 3803 N92-31257
JOHNSON, W. C. p 3839 N92-31400
JONES, JAMES R. p 3879 N92-31833
JONES, JIM J. p 3819 N92-31281
JONES, K. W. p 3869 N92-31589
JONES, R. W. p 3782 N92-31772
JONES, S. A. p 3805 N92-31369
JONSSON, BENGT p 3807 N92-31715
JORDAN, J. F. p 3846 N92-31497
JORDAN, J. R. p 3860 N92-31641
JORDAN, RAYMOND W. p 3832 N92-31271
JORGENSEN, G. p 3847 N92-31623
JORGENSON, R. E. p 3861 N92-31709
JOTSHI, C. K. p 3849 N92-32091
JOVANOVIC, D. p 3903 N92-31412
JOYCE, T. p 3865 N92-31842
JUHASZ, ALBERT J. p 3771 N92-31916
JULIEN, PIERRE Y. p 3857 N92-31964
JUNGLE, R. p 3905 N92-31749
JUSZKO, BARBARA-ANN p 3811 N92-32214

K

KAANICHE, MOHAMED p 3837 N92-31693
KAFAFI, S. A. p 3797 N92-32146
KAISER, D. P. p 3851 N92-31527
KALB, J. p 3878 N92-31669
KALKHORAN, NADER M. p 3814 N92-31464
KALLAS, N. p 3900 N92-31975
KAMADA, R. F. p 3859 N92-31540
KANKAM, M. DAVID p 3845 N92-31262
KANTOR, B. p 3749 N92-31882
KANURY, A. M. p 3749 N92-31883
KAR, A. p 3787 N92-31612
KAR, R. J. p 3776 N92-32047
p 3776 N92-32048
KARAMPETAKIS, N. P. p 3887 N92-31957
KARPEL, MORDECHAY p 3758 N92-32111
KARPISCAK, JOHN, III p 3844 N92-31621
KARR, M. E. p 3902 N92-32144
KASHIWA, B. A. p 3825 N92-32022
KASPER, HAROLD J. p 3765 N92-31251
KASSOY, DAVID R. p 3770 N92-31474
KAUFMAN, J. G. p 3789 N92-31987
KAWASE, Y. p 3895 N92-31728
KAWASUMI, Y. p 3827 N92-31340
KAYE, K. M. p 3921 N92-32188
KAZAROFF, JOHN M. p 3769 N92-31249
KAZOVSKY, L. G. p 3901 N92-31611
KEAT, W. D. p 3773 N92-31305
KEDDY, E. S. p 3759 N92-31817
KEDDY, M. D. p 3823 N92-31701
KEHAYAS, N. p 3757 N92-31515
KEICHER, D. M. p 3802 N92-31580
KEITH, T. G., JR. p 3834 N92-31536
KELKAR, S. p 3825 N92-32008
KELLER, N. p 3894 N92-31679
KELLY, ROBERT D. p 3844 N92-31357
KEMPEL, LEO C. p 3807 N92-31614
KEMPER, KENNETH L. p 3871 N92-31392
KENNEDY, R. p 3828 N92-31909
KENNELLY, ROBERT A., JR. p 3754 N92-32213
KENNEY, S. B. p 3897 N92-31936
KENT, P. D. p 3766 N92-32130
KERN, R. H. p 3802 N92-31830
KERRISK, J. F. p 3762 N92-32026
KERTESZ, M. p 3795 N92-31951
KEY, MARVIN B., JR. p 3874 N92-31299
KHEMANI, K. C. p 3912 N92-31937
KHONSARI, MICHAEL M. p 3795 N92-31840
KHORRAMI, MEHDI R. p 3822 N92-31535
KIEKEL, P. D. p 3906 N92-31949
KING, A. W. p 3853 N92-31782
KINTIS, D. H. p 3767 N92-32100
KIRK, C. L. p 3840 N92-31516
KIRLIK, ALEX p 3870 N92-31341
KIZAKEVICH, PAUL N. p 3870 N92-32107
KLAISNER, L. p 3900 N92-32131
KLARER, P. R. p 3756 N92-31746
KLAVETTER, ELMER p 3799 N92-31462
KLEPPER, C. p 3906 N92-31771
KLINE, TODD A. p 3873 N92-31269
KLINER, DAHV A. p 3910 N92-31699
KLINGLE-WILSON, D. L. p 3863 N92-32103
KNEE, L. B. G. p 3924 N92-31635
KNOLL, G. F. p 3828 N92-31919
KNORZ, GERHARD E. p 3921 N92-32189
KO, D. S. p 3863 N92-31308
KO, K. p 3812 N92-31289
KOBERSTEIN, J. T. p 3833 N92-31363
p 3833 N92-31433
KOEPFLER, G. p 3888 N92-31981
KOERT, D. N. p 3778 N92-31414
KOGAN, A. p 3749 N92-31886
KOHN, ROBERT V. p 3773 N92-31378
KOIFMAN, M. p 3748 N92-31881
KOK, JOOST N. p 3807 N92-31715
KOK, M. p 3859 N92-31521
KOKOLIS, S. p 3820 N92-31421
KOMIYA, ZEN p 3792 N92-31394
KONDOH, Y. p 3887 N92-32205
KONOVALOV, D. A. p 3896 N92-31837
KONRAD, C. H. p 3766 N92-31735
KORTING, P. A. O. G. p 3747 N92-31871
KOSSECKA, ELZBIETA p 3863 N92-32097
KOTLAR, ANTHONY J. p 3782 N92-31803
KRAJNAK, MICHAEL D. p 3857 N92-31932
KRANER, H. W. p 3827 N92-31502
KRAUSS, A. R. p 3909 N92-31546
p 3909 N92-31652
KRAUSS, J. K. p 3752 N92-31777
KREMER, P. p 3810 N92-32203
KRISHNAPPA, G. p 3833 N92-31469
KRISHNAPRASAD, P. S. p 3885 N92-32041
KROLL, N. p 3812 N92-31289
KROO, ILAN M. p 3754 N92-32213
KROTOW, GERALDINE S. p 3871 N92-32063
KROUTIL, R. T. p 3854 N92-32083
KRUCH, S. p 3840 N92-31505
KRUKONIS, V. J. p 3801 N92-31982
KRZAK, JERZY p 3914 N92-32209
KUBASCO, A. J. p 3835 N92-31841
KUHL, A. L. p 3822 N92-31625
p 3786 N92-32145
KUHN, A. D. p 3921 N92-32188
KUKACKA, L. E. p 3849 N92-32118
p 3849 N92-32124
KULP, T. J. p 3828 N92-31909
KUMAR, P. R. p 3884 N92-31332
KUNKEL, MATTHEW W. p 3755 N92-31549
KUPPERMAN, D. S. p 3846 N92-31531
KUX, HERMANN JOHANN HEINRICH p 3922 N92-32227
KWON, Y. B. p 3841 N92-31658

L

LABOV, S. p 3913 N92-32166
LAFEMINA, J. P. p 3797 N92-32146

LAFUSE, JAMES L. p 3763 N92-32012
LAKE, B. J. p 3865 N92-31644
LAKIN, WILLIAM D. p 3840 N92-31619
LAM, N. Q. p 3787 N92-31575
LAMARCHE, J. L. p 3848 N92-31845
LAMBERT, JAMES D. p 3810 N92-32176
LAMBRECHT, WALTER R. L. p 3772 N92-31266
LAMBROPOULOS, J. C. p 3912 N92-31984
LAMICH, G. p 3909 N92-31652
LANDERS, DAVID E. p 3857 N92-31906
LANDGREBE, A. p 3847 N92-31571
LANDRY, CHRISTOPHER C. p 3788 N92-31796
LANE, N. F. p 3895 N92-31724
LANG, KENNETH R. p 3925 N92-31985
LANGEMATZ, ULRIKE p 3861 N92-31708
LANGLOIS, R. G. p 3869 N92-31608
LANGSETH, M. p 3856 N92-31636
LANTHAM, P. E. p 3832 N92-31935
LANTZ, RICHARD L. p 3762 N92-31640
LANZEROTTI, M. Y. p 3829 N92-32086
LAPOINTE, M. p 3772 N92-32239
LAREDO, D. p 3746 N92-31869
LARKIN, JOHN W. p 3812 N92-31355
LARMAN, KEVIN T. p 3769 N92-32204
LARSEN, C. A. p 3796 N92-31968
LARSON, M. C. p 3773 N92-31305
LARSSON, C. p 3866 N92-32069
LATAITIS, R. J. p 3860 N92-31641
LATANISION, R. M. p 3788 N92-31733
LAUDERDALE, WALTER J. p 3894 N92-31673
LAWRENCE, G. W. p 3801 N92-32098
LAWS, K. p 3913 N92-32166
LAWSON, DEL R. p 3785 N92-32080
LEE, H. W.H. p 3910 N92-31661
LEE, HUNG-MOU p 3805 N92-31413
LEE, S. M. p 3793 N92-31435
LEE, S. P. p 3785 N92-32057
LEE, T. G. p 3812 N92-31289
LEE, Y. J. p 3846 N92-31526
LEFEVRE, DON K. p 3763 N92-32010
LEGROS, M. p 3913 N92-32166
LEI, JUNTING p 3796 N92-32079
LEICHNER, S. A. p 3875 N92-31410
LEIDINGER, B. J. G. p 3915 N92-31660
LEIGH, R. W. p 3803 N92-32125
LEIN, A. YU. p 3924 N92-32180
LEIVENT, JONATHAN I. p 3875 N92-31405
LENGRAND, J. C. p 3751 N92-31508
LEPAGE, RAOUL p 3885 N92-31827
LESLIE, JULIAN p 3888 N92-31517
LESPERANCE, A. M. p 3853 N92-31732
LEVIN, J. p 3894 N92-31679
LEVINGER, NANCY E. p 3910 N92-31699
p 3897 N92-31999
LEVITT, K. p 3879 N92-31825
LEVUSH, B. p 3831 N92-31769
p 3832 N92-31935
LEVY, Y. p 3746 N92-31869
LEWANDOWSKI, A. p 3845 N92-31481
LEWICKI, D. p 3832 N92-31349
LEWIN, K. L. p 3851 N92-31422
LEWIS, BRETT A. p 3891 N92-31588
LEWIS, M. A. p 3824 N92-31839
LEWIS, MARK J. p 3748 N92-31877
LI, K. p 3808 N92-31855
LI, S. H. p 3796 N92-31968
LI, Y. M. p 3909 N92-31655
LI, YUAN p 3905 N92-31688
LIANDRAT, J. p 3822 N92-31564
LIANDRAT, M. P. p 3822 N92-31564
LIANG, WENBIN p 3796 N92-32079
LICHTENBERG, A. J. p 3907 N92-31983
LICITRA, B. A. p 3827 N92-31633
LILLIBRIDGE, MARK p 3887 N92-32171
LILLIE, KENNETH A. p 3833 N92-31460
LIMBERG, T. p 3900 N92-32133
LIN, M. C. p 3785 N92-32057
LINDSAY, K. V. p 3806 N92-31449
LIPERT, R. J. p 3831 N92-31775
LIPFERT, F. W. p 3851 N92-31422
LIPPS, F. W. p 3849 N92-32110
LITT, JONATHAN S. p 3770 N92-31507
LITTLEFIELD, DAVID L. p 3767 N92-31997
LIU, S. H. p 3789 N92-31898
LIZZI, F. p 3914 N92-31402
LLEWELYN-DAVIES, D. I. T. P. p 3751 N92-31514
LOGAN, JULIE p 3883 N92-31835
LOHNER, RAINALD p 3823 N92-31696
LONG, D. p 3879 N92-31787
LONG, TERRY N. p 3856 N92-31551
LONGDON, NORMAN p 3922 N92-31947
LOPEZMARTINEZ, LUIS p 3840 N92-31512
LORENZO, C. F. p 3802 N92-31263
LOTTES, S. A. p 3835 N92-31774
LOUDIN, W. J. p 3919 N92-31731
LOVATO, JULIE A. p 3752 N92-31622
LOVELL, C. DAVID p 3805 N92-31387
LOW, FRANK J. p 3924 N92-32142
LU, FRANK K. p 3753 N92-32162
LUCHT, R. P. p 3782 N92-31773
LUCIA, A. p 3781 N92-31752
LUDWICK, LARRY M. p 3800 N92-31800
LUHMANN, NEVILLE, JR. p 3809 N92-31944
LUIZHI, Z. p 3865 N92-31644
LUNTZ, A. L. p 3750 N92-31888
LUO, S. p 3782 N92-31772
LUOMA, R. p 3787 N92-31610
LYCETTE, M. p 3814 N92-31525
LYNCH, V. E. p 3906 N92-31829
LYONS, J. E. p 3799 N92-31751

M

MA, M. T. p 3805 N92-31368
MAAS, R. p 3899 N92-31815
MACHARD, CLAUDINE p 3921 N92-32184
MACHIDA, S. p 3899 N92-31948
MACIEL, G. E. p 3798 N92-32197
MACINNES, ANDREW N. p 3788 N92-31796
MACIUCA, C. p 3820 N92-31421
MACKALL, DALE p 3762 N92-32201
MADDUX, GARY A. p 3883 N92-31835
MADI, FRANK J. p 3845 N92-31262
MAHECHAG, J. p 3896 N92-31836
MAJUMDAR, S. p 3846 N92-31531
MAKAOUCHE, A. p 3921 N92-32185
MALBA, V. p 3788 N92-31759
MALIK, MUJEEB R. p 3822 N92-31535
MALLET-PARET, J. p 3915 N92-31585
MANCHEK, R. p 3875 N92-31447
MANDREKAR, V. p 3885 N92-31827
MANGHNANI, M. H. p 3858 N92-32027
MANI, R. p 3891 N92-31248
MANSFELD, FLORIAN p 3793 N92-31473
MANSFIELD, BRIAN C. p 3771 N92-32108
MARCHETTI, P. S. p 3798 N92-32197
MARCINIAK, T. J. p 3799 N92-31442
MARCONI, F. p 3825 N92-32000
MARENGONI, MAURICIO p 3874 N92-31348
MARGOLESE, D. p 3912 N92-31937
MARKS, L. D. p 3793 N92-31538
MARR, W. W. p 3799 N92-31442
MARSHALL, A. C. p 3771 N92-32030
MARTIN, CHARLES R. p 3796 N92-32079
p 3785 N92-32080
MARTIN, G. B. p 3781 N92-31683
MARTIN, R. A. p 3759 N92-31817
MARTIN, R. E. p 3820 N92-31425
MARTIN, S. P. p 3893 N92-31552
MARTIN, STEVE p 3799 N92-31462
MARTINEC, E. J. p 3899 N92-31712
MARTINEZ-SANCHEZ, M. p 3760 N92-31910
MARUSKA, H. P. p 3814 N92-31464
MARZULLO, KEITH p 3886 N92-31553
MASAI, K. p 3827 N92-31340
MASON, LEE S. p 3771 N92-32108
MASON, RODNEY J. p 3815 N92-31681
MASON, WILLIAM H. p 3753 N92-32114
MASSELL, P. p 3828 N92-31794
MASSIE, CURTIS p 3884 N92-31395
MASSIE, HAROLD L., JR. p 3859 N92-31523
MASSOUDI, M. p 3821 N92-31426
p 3824 N92-31895
MATHIAS, LON J. p 3792 N92-31408
MATHUR, M. P. p 3821 N92-31426
MATTHEWS, SCOTT T. p 3914 N92-31489
MATUSZCZAK, S. p 3793 N92-31435
MATYJASZEWSKI, KRZYSZTOF p 3795 N92-31941
p 3798 N92-32153
MAUCERI, A. J. p 3763 N92-32013
MAUREY, J. R. p 3794 N92-31618
MAVRIPLIS, CATHERINE p 3818 N92-31265
MAVRIPLIS, DIMITRI p 3876 N92-31561
MAX, C. E. p 3902 N92-31761
MAXSON, J. A. p 3780 N92-31671
MAYHALL, D. J. p 3812 N92-31334
MAZUMDER, J. p 3787 N92-31612
MCARTHUR, ROBERT C. p 3804 N92-31284
MCASSEY, E., JR. p 3820 N92-31421
MCCALL, ROBERT C. p 3842 N92-31989
MCCARDLE, G. D. p 3866 N92-32050
MCCARTHY, I. E. p 3896 N92-31837
MCCARTNEY, MICHAEL L. p 3870 N92-32107
MCCARTY, CRAIG A. p 3761 N92-31656
MCCLELLAND, J. F. p 3782 N92-31772
MCCOLSKEY, J. D. p 3774 N92-31609
MCELROY, D. R. p 3809 N92-31920
MCEWEN, ALLEN H. p 3810 N92-32176
MCGRATH, DANIEL T. p 3806 N92-31569
MCIVER, DUNCAN E. p 3889 N92-32229
MCKAY, DAVID S. p 3924 N92-31781
MCKENNA, FRANK P. p 3870 N92-31291
MCKISSOCK, BARBARA I. p 3771 N92-32108
MCLAUGHLIN, K. L. p 3856 N92-31510
p 3865 N92-31821
MCNESBY, KEVIN L. p 3778 N92-31393
MCPHERSON, ARMON p 3827 N92-31475
MCRAE, K. I. p 3837 N92-32202
MCRAE, T. G. p 3828 N92-31909
MCVEY, EUGENE S. p 3880 N92-32122
MEDERNACH, J. W. p 3910 N92-31668
MEDRICH, E. A. p 3916 N92-32160
MEIER, J. K. p 3762 N92-32026
MEISBURGER, EDWARD P. p 3864 N92-31544
MEKATA, M. p 3895 N92-31728
MELIUS, C. F. p 3783 N92-31860
MELSON, W. EDWARD, JR. p 3751 N92-31532
MELTON, LYNN A. p 3828 N92-31694
MENDELSOHN, D. A. p 3839 N92-31389
MENDENHALL, MICHAEL R. p 3752 N92-31808
MENDILLO, MICHAEL p 3855 N92-31478
MERCER, CHARLES E. p 3762 N92-31900
MERHAV, S. J. p 3748 N92-31881
MERIGAN, WILLIAM p 3871 N92-31758
p 3867 N92-31778
MERRIGAN, M. A. p 3823 N92-31701
p 3759 N92-31817
MERRILL, WALTER C. p 3770 N92-31507
MEYER, ALBERT R. p 3887 N92-32163
MEYER, ROBERT R., JR. p 3756 N92-31261
MEYER, T. G. p 3759 N92-31534
MEYER, THOMAS J. p 3791 N92-31358
MIGEMI, S. p 3749 N92-31886
MILLARD, R. C. p 3865 N92-31644
MILLER, D. L. p 3778 N92-31414
MILLER, E. K. p 3804 N92-31317
MILLER, EMMETT A. p 3767 N92-31677
MILLER, GERALD D. p 3757 N92-31264
MILLER, J. A. p 3783 N92-31860
MILLER, PATRICIA M. p 3869 N92-31962
MILLER, R. p 3894 N92-31679
MILLER, TERESA Y. p 3828 N92-31790
MILLS, M. J. p 3788 N92-31744
MILLS, M. R. p 3816 N92-31760
MILTON, GRAEME W. p 3773 N92-31378
MIN, J. B. p 3838 N92-31280
MINAMISONO, T. p 3895 N92-31728
MINEI, M. p 3877 N92-31601
MINGORI, D. L. p 3820 N92-31322
MINK, A. p 3874 N92-31366
MINTS, W. p 3828 N92-31794
MIRLEY, C. L. p 3833 N92-31363
p 3833 N92-31433
MISLEVY, ROBERT J. p 3871 N92-31444
MISSIER, ANTOINE p 3886 N92-31690
MITAL, SUBODH K. p 3774 N92-31506
MITCHELL, D. W. p 3826 N92-31298
MITCHELL, G. D. p 3786 N92-32141
MIYAHARA, M. p 3927 N92-32067
p 3927 N92-32068
MOATS, CHRISTINA D. p 3769 N92-32204
MOAZZAMI, M. p 3773 N92-31307
MOCH, M. p 3840 N92-31516
MOHAMMEDI, N. p 3924 N92-31401
MOHR, THOMAS C. p 3789 N92-32052
MOINZADEH, K. p 3785 N92-32093
MOIR, R. W. p 3904 N92-31530
MOLENKAMP, C. R. p 3851 N92-31423
MOLNAR, J. A. p 3916 N92-31992
MONEY, JOHN M. p 3908 N92-31537
MONKEWITZ, PETER A. p 3820 N92-31322
MONSON, P. A. p 3781 N92-31717
MONTGOMERY, D. B. p 3904 N92-31545
MOORE, R. K. p 3810 N92-32101
MOORE, ROBERT Y. p 3869 N92-31905
MOORE, ROYCE D. p 3759 N92-31250
MORANG, ANDREW p 3864 N92-31544
MOREIRA-NORDEMANN, LYCIA MARIA p 3863 N92-32224
MOREL, J. M. p 3888 N92-31981
MOREL, M. R. p 3775 N92-31854
MORETTI, GINO p 3825 N92-32000
MORGAN, L. p 3836 N92-31647
MORGENSTERN, CAROLYN D. p 3858 N92-31493
MORRIS, BRUCE L. p 3767 N92-31997
MORRIS, M. E. p 3861 N92-31709
MORTON, JOHN p 3772 N92-31274
p 3774 N92-31566
MOSHAMMER, H. p 3900 N92-32133
MOSHELL, J. M. p 3873 N92-31974
MOSKAL, PAT p 3873 N92-31974
MOSS, GARY S. p 3876 N92-31488
MOSSA, JOANN p 3864 N92-31544
MOULTON, BRYAN p 3752 N92-31808
MOYERS, J. C. p 3833 N92-31384
MUIR, P. F. p 3816 N92-31718
MUKHOPADHYAY, VIVEK p 3757 N92-31350

MULLEN, BRIAN p 3870 N92-31321
MULLICK, SANJOY p 3802 N92-31826
MURATA, M. p 3765 N92-31685
MURNICK, DANIEL E. p 3905 N92-31688
MURPHY, CLARENCE J. p 3791 N92-31270
MURRAY, KAREN R. p 3876 N92-31488
MURRAY, R. A. p 3913 N92-32078
MUSGRAVE, JEFFREY L. p 3770 N92-31507
MUSICK, DAVID R. p 3859 N92-31602
MYERS, CARTER H. p 3764 N92-32017
MYERS, ROGER M. p 3769 N92-31342

N

NACHSHON, A. p 3750 N92-31888
NAKANISHI, HISAO p 3891 N92-32211
NAMAVAR, FEREYDOON p 3814 N92-31464
NANCE, S. D. p 3777 N92-32135
NARUMI, H. p 3892 N92-31255
NASIRUDDIN, MOHAMMED p 3885 N92-31811
NASRALLAH, M. M. p 3848 N92-31903
NATANSOHN, S. p 3797 N92-32094
NATESAN, K. p 3789 N92-31924
NAUJOKAT, BARBARA p 3860 N92-31702
p 3860 N92-31704
p 3861 N92-31706
NELLIS, W. J. p 3923 N92-32005
NELSON, G. E. p 3775 N92-31912
NETZER, E. p 3748 N92-31875
NEVESDASILVAFILHO, PEDRO p 3843 N92-31277
NEWMAN, J. C., JR. p 3838 N92-31279
p 3839 N92-31504
NGUYEN, R. p 3817 N92-31849
NICKS, J. p 3833 N92-31469
NICOL, DAVID M. p 3881 N92-32157
NICOLAIDES, R. A. p 3825 N92-32038
NIEVES, L. p 3852 N92-31591
NISSLEY, D. M. p 3759 N92-31534
NOCH, J. p 3814 N92-31525
NOLHIER, NICOLAS p 3787 N92-31695
NORTON, J. R. p 3783 N92-31891
NOVOA, JUAN J. p 3898 N92-32024
NOYES, H. P. p 3915 N92-31663

O

OBOT, N. T. p 3890 N92-32099
OBRIEN, J. E. p 3819 N92-31287
OECHEL, W. C. p 3853 N92-31626
OGDEN, PETER M. p 3892 N92-32044
OHARA, GEORGE J. p 3838 N92-31337
OHERN, TIM p 3799 N92-31462
OHLHAUSEN, J. A. p 3794 N92-31631
OKAMOTO, P. R. p 3787 N92-31575
OLEN, ANDREA L. p 3891 N92-31563
OLIVEIRA, J. S. p 3879 N92-31743
OLIVIER, S. S. p 3902 N92-31761
OLSON, D. W. p 3766 N92-32130
OLSON, S. H. p 3863 N92-32103
OLSSON, R. p 3879 N92-31825
OMARA, THOMAS M. p 3766 N92-31457
OMATETE, O. O. p 3797 N92-32089
OPILSKI, ALEKSANDER p 3914 N92-32209
OPPENHEIM, A. K. p 3780 N92-31671
ORHAUG, T. p 3767 N92-32073
ORLIN, JAMES B. p 3880 N92-32039
ORME, JOHN S. p 3759 N92-31275
ORRELL, S. p 3918 N92-31448
ORSER, D. J. p 3885 N92-31680
ORYANG, D. p 3846 N92-31498
OSBOURN, G. C. p 3900 N92-31295
OSHER, S. p 3888 N92-31981
OSKAM, JOHN H. p 3780 N92-31524
OSWALD, FRED B. p 3834 N92-31485
OTERO, M. P. p 3894 N92-31595
OVERMAN, DAVID L. p 3836 N92-32173

P

PAGE, MARK A. p 3761 N92-31656
PAIGE, ROBERT p 3883 N92-32109
PAINTER, J. F. p 3878 N92-31742
PAJEWSKI, WINCENTY p 3811 N92-31244
PAL, P. B. p 3895 N92-31812
PALMER, D. A. p 3786 N92-31418
PALUDETTO, MARIO p 3878 N92-31689
PAN, J. J. p 3902 N92-32092
PANCHAL, C. B. p 3825 N92-32003
PANG, H. M. p 3831 N92-31775
PAPP, J. F. p 3788 N92-31797
PARK, J. H. p 3789 N92-31924
PARKER, S. E. p 3907 N92-31983
PARKINSON, BRUCE A. p 3785 N92-32080
PARKS, W. S. p 3919 N92-31581
PARROTT, L. p 3854 N92-31931
PASTO, A. E. p 3797 N92-32094
PATNAIK, GAGAN B. p 3884 N92-31293
PATTERSON, F. T. p 3773 N92-31305
PATTERSON, MICHAEL J. p 3769 N92-31342
p 3770 N92-31901
p 3771 N92-32237
PATTIPATI, K. R. p 3804 N92-31333
PAXSON, DANIEL E. p 3770 N92-31507
PAXSON, DANIEL W. p 3821 N92-31484
PAYNE, R. p 3782 N92-31776
PECKERAR, MARTIN p 3901 N92-31397
PEDRAZA, A. J. p 3795 N92-31917
PEEBLES, D. E. p 3794 N92-31631
PELEG, I. p 3749 N92-31883
PELTON, A. p 3783 N92-31857
PELZL, J. p 3774 N92-31716
PENG, Y. K. M. p 3906 N92-31913
PENNER, J. E. p 3850 N92-31297
PENNER, ROBIN R. p 3885 N92-31811
PENSWICK, L. BARRY p 3769 N92-31245
PERERA, L. p 3899 N92-32196
PERERA, U. p 3896 N92-31926
PEREZ-DAVILA, ALFREDO p 3879 N92-31787
PERKINS, S. T. p 3895 N92-31705
PERRY, BOYD, III p 3757 N92-31264
PESARAN, A. A. p 3849 N92-32112
PETIT, PIERRE A. p 3857 N92-31986
PETREE, M. p 3899 N92-31390
PETRIE, T. W. p 3906 N92-31771
PETUSKEY, WILLIAM T. p 3792 N92-31377
PHELPS, R. D. p 3905 N92-31749
PHILLIPS, W. MORRIS p 3803 N92-31257
PIANTELLA, PAOLO p 3764 N92-32019
PICKERING, HOWARD W. p 3790 N92-32096
PIERCE, LINDA G. p 3872 N92-31294
PIERSOL, ALLAN G. p 3892 N92-32178
PIKULA, L. p 3854 N92-32071
PINCOSY, P. A. p 3815 N92-31548
PINDERA, MAREK-JERZY p 3777 N92-32234
PINK, S. E. p 3757 N92-31736
PITTS, SUSAN M. p 3888 N92-31519
PITZ, W. J. p 3778 N92-31414
p 3779 N92-31416
p 3780 N92-31607
p 3781 N92-31763
PIZA, M. E. p 3911 N92-31723
PLETTA, J. B. p 3756 N92-31746
PLUEDDEMANN, ALBERT J. p 3891 N92-31563
PLUTA, ZBYSLAW p 3802 N92-31242
POCHA, M. D. p 3910 N92-31719
POEPPEL, R. B. p 3846 N92-31531
POHLCHUCK, BOBBY p 3745 N92-31267
POLITZER, P. p 3905 N92-31749
POLKA, LESLEY A. p 3804 N92-31273
POMERLEAU, DEAN A. p 3884 N92-31511
PONNUSAMY, RAVI p 3876 N92-31561
PONZONI, FLAVIO JORGE p 3806 N92-31568
POOLMAN, E. p 3912 N92-31937
PORAT, I. p 3748 N92-31875
PORKOLAB, M. p 3905 N92-31764
PORTER, M. B. p 3892 N92-31818
POST, W. M. p 3853 N92-31782
POTOTZKY, ANTHONY S. p 3757 N92-31351
POULSEN, P. p 3815 N92-31548
PRAGER, MARTIN p 3789 N92-31987
PRAIRIE, R. R. p 3837 N92-31753
PREISS, KENNETH p 3746 N92-31866
PRENGLE, H. W., JR. p 3785 N92-32093
PRITCHARD, W. L. p 3809 N92-31920
PROVANCHA, ANNA p 3883 N92-31835
PRYOR, R. J. p 3824 N92-31832
PU, S. p 3865 N92-31644
PUGH, A. C. p 3887 N92-31957
PUGH, COLEEN p 3792 N92-31394
PUHN, F. p 3905 N92-31749
PUMPICHED, PATCHARA p 3836 N92-31479
PURTILL, M. R. p 3879 N92-31743

Q

QIAN, WEN-JIA p 3892 N92-31255
QUEEN, ERIC M. p 3766 N92-31457
QUENNEVILLE, J. p 3873 N92-32031
QURESHI, Z. p 3820 N92-31421
QURESHI, Z. H. p 3825 N92-32115

R

RABAEY, G. p 3836 N92-31647
RABAS, T. J. p 3823 N92-31785
RACHELE, HENRY p 3858 N92-31320
p 3806 N92-31543
RAFFIN, M. p 3751 N92-31508
RAISTRICK, I. D. p 3911 N92-31723
RAJAGOPAL, K. R. p 3821 N92-31426
RAKESTRAW, D. J. p 3782 N92-31773
RALSTIN, S. p 3918 N92-31448
RAMAKER, DAVID E. p 3912 N92-31994
p 3913 N92-31995
RAMANATHAN, R. p 3898 N92-32169
RAMP, STEVEN R. p 3864 N92-31495
RANACHOWSKI, ZBIGNIEW p 3842 N92-32206
RANDEL, WILLIAM J. p 3853 N92-31649
RANGASWAMY, M. p 3909 N92-31652
RAO, M. R. p 3888 N92-31768
RASMUSSEN, J. J. p 3903 N92-31412
RAUBENHEIMER, T. p 3900 N92-32133
RAUCH, JEFFREY S. p 3845 N92-31262
RAUENZAHN, R. M. p 3825 N92-32022
RAVI, RAMAKRISHNAN p 3753 N92-32114
RAVIV, D. p 3885 N92-31680
RAWLIN, VINCENT K. p 3769 N92-31342
RAY, A. p 3802 N92-31263
RAY, JODI p 3885 N92-31811
REAGOR, D. W. p 3911 N92-31723
RED-HORSE, J. R. p 3842 N92-32088
REDDY, D. G. p 3820 N92-31421
REED, D. T. p 3795 N92-31938
REED, HELEN L. p 3752 N92-31555
REED, R. P. p 3774 N92-31609
REGLAT, MURIEL p 3830 N92-31698
REIBOLD, R. A. p 3786 N92-31391
REIFSNIDER, K. p 3774 N92-31604
REISS, ROBERT p 3777 N92-32104
REJAI, B. p 3799 N92-31593
REMPEL, L. C. p 3844 N92-32216
REPETTI, T. E. p 3831 N92-31762
REPPERGER, DANIEL E. p 3803 N92-31890
REYN, J. W. p 3886 N92-31520
REYNOLDS, G. T. p 3867 N92-32120
REZAEEPAZHAND, JALIL p 3841 N92-31911
RHODES, CHARLES K. p 3827 N92-31475
RHODES, PERCY H. p 3828 N92-31790
RIBAUDO, C. R. p 3787 N92-31612
RICE, B. p 3836 N92-31647
RICHMAN, M. W. p 3820 N92-31425
RICHWINE, DAVID M. p 3751 N92-31276
RIECHERS, JOHN T. p 3752 N92-31674
p 3757 N92-31793
RIGLING, KIM M. p 3861 N92-31714
RILEY, D. J. p 3808 N92-31738
RING, DARRYL S. p 3765 N92-31251
RITSON, D. p 3902 N92-32149
ROBERTS, K. M. p 3881 N92-31365
ROBERTS, R. G. p 3915 N92-31953
ROBINSON, ALLAN R. p 3863 N92-31406
ROBINSON, H. G. p 3807 N92-31629
ROBISON, JENNIFER L. p 3794 N92-31557
ROCHELLE, WILLIAM C. p 3819 N92-31281
ROCK, B. A. p 3872 N92-31309
RODACY, P. J. p 3799 N92-31570
RODGERS, E. B. p 3765 N92-32148
RODGERS, J. p 3832 N92-31935
RODRIGUEZ, CARLOS D. p 3771 N92-32108
ROELEVEN, D. p 3859 N92-31521
ROETTGER, G. E. p 3783 N92-31816
ROGACKI, JOHN R. p 3777 N92-32159
ROGERS, L. C. p 3827 N92-31502
ROMANA, L. p 3795 N92-31917
RONEY, P. L. p 3829 N92-32218
RONNEY, P. D. p 3781 N92-31763
ROOHR, PETER B. p 3860 N92-31603
ROOT, J. H. p 3839 N92-31383
p 3839 N92-31501
ROSEN, A. p 3746 N92-31865
ROSEN, L. C. p 3856 N92-31662
ROSEN, WARREN A. p 3873 N92-31269
p 3791 N92-31270
ROSENBERG, J. p 3748 N92-31875
ROSENFELD, LESLIE K. p 3864 N92-31495
ROSENGREEN, A. p 3816 N92-31791
ROSENKRANZ, PHILIP W. p 3858 N92-32195
ROSNER, J. L. p 3899 N92-31712
ROSS, G. G. p 3915 N92-31953
ROTE, D. M. p 3835 N92-31774
ROTH, JOSEPH D. p 3784 N92-31998
ROULET, E. p 3898 N92-32167
ROURKE, W. J. p 3797 N92-32094
ROUTE, ROGER K. p 3901 N92-31380
ROWE, M. M. p 3918 N92-31467
ROZENDAAL, ROGER A. p 3750 N92-31246
RUAN, YEEFENG F. p 3834 N92-31485
RUDIN, L. p 3888 N92-31981
RUGGIERO, A. G. p 3810 N92-32134
RUS, DANIELA p 3797 N92-32151
RUSAK, Z. p 3750 N92-31887
p 3750 N92-31889
RUSNAK, ILAN p 3748 N92-31879
RUSSELL, ROBERT J. p 3758 N92-32051

RYAN, WILLIAM W. ..... p 3764 N92-32021

S

SAAB, A. P. ..... p 3912 N92-31937
SABEL, LAURA ..... p 3886 N92-31553
SABOCHICK, M. J. ..... p 3787 N92-31575
SACHS, R. G. ..... p 3899 N92-31712
SAGALYN, PAUL L. ..... p 3778 N92-31301
SAIKIA, C. K. ..... p 3855 N92-31509
SALTZ, JOEL ..... p 3876 N92-31561
SALVUCCI, GUIDO D. ..... p 3855 N92-32222
SAMADDAR, S. K. ..... p 3841 N92-31745
SAMBE, HIDEO ..... p 3913 N92-31995
SAMUELSEN, G. S. ..... p 3782 N92-31776
SANDHU, R. S. ..... p 3773 N92-31307
SANTIAGO, WALTER ..... p 3845 N92-31262
SANTORO, R. T. ..... p 3868 N92-31409
SANZOVO, C. G. ..... p 3923 N92-31343
SARAVANOS, D. A. ..... p 3775 N92-31854
SARIC, WILLIAM S. ..... p 3752 N92-31555
SARIG, N. ..... p 3749 N92-31884
SARIN, V. K. ..... p 3889 N92-31359
SATCHER, J. H., JR. ..... p 3786 N92-31391
SATO, TETSUYA ..... p 3906 N92-31843
SAUS, J. R. ..... p 3802 N92-31263
SAUVE, G. L. ..... p 3766 N92-31735
SCALISE, E., JR. ..... p 3923 N92-31343
SCARBOROUGH, ERIC L. ..... p 3803 N92-31890
SCHACTER, DANIEL L. ..... p 3871 N92-31779
SCHADOW, K. C. ..... p 3747 N92-31871
SCHAFFER, D. K. ..... p 3833 N92-31437
SCHAFFER, G. ..... p 3815 N92-31664
SCHENCK, P. K. ..... p 3913 N92-32072
SCHERSON, ISAAC D. ..... p 3883 N92-32040
SCHIFFER, ROBERT A. ..... p 3849 N92-31258
SCHLECHT, A. M. ..... p 3914 N92-32207
SCHLECHT, R. G. ..... p 3914 N92-32207
SCHMID, PETER J. ..... p 3822 N92-31535
SCHMIDT, H. ..... p 3909 N92-31652
SCHMIDT, PHILLIP ..... p 3761 N92-32241
SCHMIDT, W. R. ..... p 3798 N92-32197
SCHNEIDER, D. A. ..... p 3793 N92-31539
SCHNETZER, G. H. ..... p 3862 N92-31750
SCHOBERT, H. H. ..... p 3798 N92-31399
p 3786 N92-32141
SCHOCK, R. N. ..... p 3855 N92-32155
SCHOLL, MARGIT CHRISTA ..... p 3861 N92-31710
SCHROCK, RICHARD R. ..... p 3792 N92-31394
p 3780 N92-31524
SCHROEDER, J. ..... p 3839 N92-31501
SCHULTHESS, MARCUS R. ..... p 3830 N92-31605
SCHULTZ, D. C. ..... p 3900 N92-32131
SCHULTZ, J. A. ..... p 3909 N92-31652
SCHUNK, R. W. ..... p 3925 N92-31338
SCHUNK, ROBERT W. ..... p 3858 N92-32055
SCHUSTER, JOACHIM ..... p 3755 N92-31813
SCHWARTZ, R. J. ..... p 3846 N92-31526
SCOTT, J. L. ..... p 3824 N92-31839
SECARY, J. ..... p 3823 N92-31701
SEED, W. R. ..... p 3809 N92-31921
SEGINER, A. ..... p 3750 N92-31887
p 3750 N92-31889
SEKAR, R. R. ..... p 3799 N92-31442
SELLIN, I. ..... p 3894 N92-31679
SELTZER, S. M. ..... p 3895 N92-31705
SENA, J. T. ..... p 3759 N92-31817
SENDA, I. ..... p 3914 N92-31402
SENGUPTA, LOUISE C. ..... p 3778 N92-31301
SEPANSKI, R. J. ..... p 3854 N92-31907
SERAYDARIAN, R. P. ..... p 3781 N92-31729
SERENO, THOMAS J., JR. ..... p 3884 N92-31293
SERVE, M. P. ..... p 3867 N92-31590
SEVAT, PETE ..... p 3806 N92-31470
SEYFERTH, DIETMAR ..... p 3794 N92-31557
SHA, LUI ..... p 3875 N92-31486
SHACHAM-DIAMOND, Y. ..... p 3793 N92-31435
SHACKSON, R. H. ..... p 3923 N92-31965
SHALKHAUSER, K. A. ..... p 3808 N92-31855
SHALOM, ABRAHAM ..... p 3749 N92-31885
SHAMMA, SHIHAB A. ..... p 3885 N92-32041
SHARMA, DINKAR ..... p 3870 N92-31291
SHENG, D. N. ..... p 3909 N92-31655
SHEPARD, JAMES E. ..... p 3764 N92-32018
SHEPARD, P. F. ..... p 3896 N92-31926
SHEPHERD, I. G. ..... p 3779 N92-31417
SHERMAN, DOV ..... p 3747 N92-31872
SHIELDS, J. E. ..... p 3902 N92-32144
SHIH, Y. C. ..... p 3808 N92-31855
SHINAR, J. ..... p 3749 N92-31882
SHINN, JUDY L. ..... p 3926 N92-32193
SHINPAUGH, K. A. ..... p 3821 N92-31452
SHIPE, P. C. ..... p 3906 N92-31913
SHKOLLER, B. ..... p 3856 N92-31510
p 3865 N92-31821
SHODA, M. ..... p 3781 N92-31763
SHOKAIR, I. R. ..... p 3900 N92-32123
SHOKRON, E. ..... p 3747 N92-31870
SHOOP, BARRY L. ..... p 3877 N92-31587
SHU, CHI-WANG ..... p 3887 N92-32164
SHUR, MICHAEL ..... p 3813 N92-31373
p 3908 N92-31537
SHUTTY, MICHAEL A. ..... p 3758 N92-32053
SIDI, MARCEL ..... p 3747 N92-31874
SIEMANN, R. ..... p 3900 N92-32133
SIES, ROGER F. ..... p 3917 N92-31371
SIGMAN, KARL ..... p 3888 N92-31600
SILVER, E. ..... p 3913 N92-32166
SILVERSTEIN, C. C. ..... p 3759 N92-31817
SIMITSES, GEORGE J. ..... p 3841 N92-31911
SIMIU, E. ..... p 3915 N92-31645
SIMO, J. C. ..... p 3761 N92-31967
SIMON, M. W. ..... p 3913 N92-32166
SIMPSON, R. L. ..... p 3821 N92-31452
SINDT, C. F. ..... p 3824 N92-31839
SINGER, ROBIN C. ..... p 3891 N92-31563
SINGH, J. P. ..... p 3846 N92-31531
SKEEN, MATTHEW E. ..... p 3890 N92-31686
SKINNER, J. P. ..... p 3807 N92-31691
SKJELLUM, A. ..... p 3882 N92-31740
SKLANSKY, JACK ..... p 3869 N92-31558
SKRIPNIK, YU. A. ..... p 3829 N92-32174
SLIWOWSKI, MAREK ..... p 3786 N92-31243
SMALLEY, RICHARD E. ..... p 3907 N92-31375
SMITH, C. F. ..... p 3754 N92-32240
SMITH, E. ..... p 3852 N92-31598
SMITH, M. S. ..... p 3834 N92-31500
SMITH, N. S. ..... p 3919 N92-31731
SMITH, STEPHEN P. ..... p 3891 N92-31563
SMITH, TERRANCE P. ..... p 3897 N92-31950
SMITS, ALEXANDER J. ..... p 3823 N92-31824
SNYDER, E. J. ..... p 3783 N92-31820
SNYDER, G. J. ..... p 3911 N92-31848
SNYDER, ROBERT S. ..... p 3828 N92-31790
SONG, C. ..... p 3798 N92-31399
SOSSINSKY, A. B. ..... p 3890 N92-31925
SOUGANIDIS, P. ..... p 3915 N92-31585
SOUTHARD, D. A. ..... p 3843 N92-31323
SOVEY, JAMES S. ..... p 3769 N92-31342
SOVIE, AMY L. ..... p 3801 N92-32230
SPANJERS, GREGORY G. ..... p 3903 N92-31459
SPANNER, G. E. ..... p 3848 N92-31845
SPEAR, W. STEVE ..... p 3767 N92-31677
SPENCER, J. ..... p 3900 N92-32133
SPERLING, LESLIE H. ..... p 3791 N92-31270
SPEZIALE, CHARLES G. ..... p 3826 N92-32158
SPINDT, C. A. ..... p 3816 N92-31791
SPOONER, S. ..... p 3839 N92-31383
p 3839 N92-31501
SPRAGINS, C. W. ..... p 3905 N92-31730
SRDANOV, V. I. ..... p 3912 N92-31937
SRINATHKUMAR, S. ..... p 3760 N92-31240
SRINIVAS, KANKANAHALLI ..... p 3885 N92-31597
STACEY, MARCELA R. ..... p 3835 N92-31807
STACEY, W. M., JR. ..... p 3904 N92-31613
STAELIN, DAVID H. ..... p 3858 N92-32195
STAGGS, W. A. ..... p 3797 N92-32136
STANLEY, ANN E. ..... p 3800 N92-31800
STEEVE, B. E. ..... p 3838 N92-31280
STEINER, JOAO E. ..... p 3923 N92-31344
p 3923 N92-31345
p 3923 N92-31346
p 3923 N92-31347
STEPHANI, D. ..... p 3827 N92-31502
STERRETT, A. ..... p 3877 N92-31601
STEVENS, J. L. ..... p 3856 N92-31510
p 3865 N92-31821
STEVENSON, J. O. ..... p 3910 N92-31668
STIKAR, JOHN A. ..... p 3770 N92-31503
STINCHCOMB, W. ..... p 3774 N92-31604
STOCKER, T. F. ..... p 3864 N92-31572
STOLTE, K. W. ..... p 3853 N92-31648
STONER, S. L. ..... p 3787 N92-31667
STOSS, F. W. ..... p 3854 N92-31907
STOWE, REID ..... p 3764 N92-32020
STRAIT, E. J. ..... p 3904 N92-31616
STRAUSS, W. A. ..... p 3915 N92-31585
STREETT, CRAIG ..... p 3822 N92-31687
STRICKER, D. A. ..... p 3913 N92-32166
STRICKLAND, J. H. ..... p 3824 N92-31933
STRINGFELLOW, G. B. ..... p 3909 N92-31582
p 3796 N92-31968
STROBEL, G. L. ..... p 3789 N92-32004
STRONG, JAMES M. ..... p 3754 N92-32213
STROPKI, MICHAEL A. ..... p 3796 N92-32045
STRUCK, J. K. ..... p 3861 N92-31709
STUCKY, G. D. ..... p 3817 N92-32002
STUCKY, GALEN D. ..... p 3898 N92-32024
STUPAK, A. I. ..... p 3896 N92-31904
SU, D. ..... p 3881 N92-31365
SU, Z. B. ..... p 3909 N92-31655
SUGAMA, HIDEO ..... p 3818 N92-31256
SULLIVAN, R. G. ..... p 3919 N92-31596
SULLIVAN, THOMAS A. ..... p 3924 N92-31781
SUSOEFF, A. R. ..... p 3766 N92-31735
SUSSMAN, ALAN ..... p 3876 N92-31561
SVIRIDOV, N. M. ..... p 3829 N92-32174
SWAIN, R. ..... p 3774 N92-31604
SWANSON, G. R. ..... p 3838 N92-31280
SWANSSON, N. S. ..... p 3759 N92-31439
SWENSEN, KEITH A. ..... p 3915 N92-31767
SWENSON, R. C. ..... p 3866 N92-32050
SYED, H. H. ..... p 3803 N92-31238
SYKES, M. ..... p 3924 N92-32142
SZALEWSKI, MAREK ..... p 3811 N92-31244

T

TALVACCHIO, JOHN ..... p 3813 N92-31451
TAMBOUR, Y. ..... p 3746 N92-31869
TANG, F. F. ..... p 3842 N92-32168
TAPP, P. A. ..... p 3814 N92-31499
TARANENKO, Y. N. ..... p 3901 N92-31611
TARBELL, THEODORE D. ..... p 3925 N92-31856
TARR, J. A. ..... p 3785 N92-32057
TAYLOR, LYNORE DENISE ..... p 3880 N92-32122
TCHAMITCHIAN, PH. ..... p 3822 N92-31564
TEAGUE, M. W. ..... p 3782 N92-31803
TENFORDE, T. S. ..... p 3867 N92-31711
TESCHE, F. M. ..... p 3804 N92-31354
TEWARI, S. K. ..... p 3787 N92-31612
TEWARSON, ARCHIBALD ..... p 3775 N92-31940
THERIAULT, J.-M. ..... p 3829 N92-32218
THODEN, J. S. ..... p 3873 N92-32031
THOMAS, I. M. ..... p 3794 N92-31560
THOMPSON, J. A. ..... p 3896 N92-31926
THOMPSON, J. R. ..... p 3815 N92-31650
THOMPSON, RICHARD B. ..... p 3777 N92-31268
TICHLER, P. R. ..... p 3841 N92-31844
TIMNAT, Y. M. ..... p 3746 N92-31869
TITLE, ALAN M. ..... p 3925 N92-31856
TITLEY, DAVID W. ..... p 3862 N92-31978
TITTEL, FRANK K. ..... p 3907 N92-31375
TOKSOZ, M. N. ..... p 3855 N92-31476
TOLSON, CAROL J. ..... p 3844 N92-32127
TOM, H. ..... p 3923 N92-31643
TOMINAGA, KEISUKE ..... p 3910 N92-31699
TOMLINSON, J. J. ..... p 3849 N92-32091
TONEGAWA, S. ..... p 3812 N92-31289
TOPLIKAR, EDWARD G. ..... p 3791 N92-31318
TOUR, JAMES M. ..... p 3779 N92-31434
TOWNSEND, LAWRENCE W. ..... p 3926 N92-32193
TROTT, WAYNE ..... p 3799 N92-31462
TRUMBLE, E. F. ..... p 3898 N92-32165
TRUONG, Y. VIET ..... p 3807 N92-31617
TSAI, L. W. ..... p 3835 N92-31929
TSAI, MING-YI ..... p 3772 N92-31274
p 3774 N92-31566
TSANG, LEUNG ..... p 3901 N92-31430
TSONG, IGNATIUS S. ..... p 3792 N92-31377
TSUI, D. C. ..... p 3908 N92-31496
TUCKETT, ROBERT P. ..... p 3867 N92-31980
TUNICK, ARNOLD ..... p 3806 N92-31543
TURNER, C. D. ..... p 3808 N92-31738
TURNER, EDMUND K. ..... p 3855 N92-32222
TURNER, ELIJAH W. ..... p 3752 N92-31674
p 3757 N92-31793
TURNER, M. S. ..... p 3924 N92-31713
TURPIN, TERRY M. ..... p 3763 N92-32012
TUTTLE, MARK E. ..... p 3777 N92-32159
TWEEDT, DANIEL L. ..... p 3759 N92-31250
TYRKIEL, ELZBIETA ..... p 3887 N92-32210
TZIAGIDIS, GEORGIOS TH. ..... p 3866 N92-32056

U

UCHIDA, MASAYA ..... p 3906 N92-31843
UHERKA, K. L. ..... p 3912 N92-31955
ULLOA, S. E. ..... p 3912 N92-31945
UNNINAYAR, SUSHEL ..... p 3849 N92-31258
URASEK, DONALD C. ..... p 3762 N92-31640

V

VALLADO, C. A. ..... p 3766 N92-32130
VALLERANI, ERNESTO ..... p 3764 N92-32016
VANCE, E. F. ..... p 3804 N92-31354
VANDERHOFF, JOHN A. ..... p 3782 N92-31803
VANEEDEN, CONSTANCE ..... p 3888 N92-31517
VANRIJSBERGEN, C. J. ..... p 3921 N92-32187
VANSCHALKWYK, CHRISTIAAN M. ..... p 3884 N92-31254
VANSUETENDAEL, RICHARD ..... p 3745 N92-31615
VANTRAN, X. ..... p 3785 N92-32093
VANYSEK, PETR ..... p 3778 N92-31292

VARDULAKIS, A. I. G. ..... p 3887 N92-31957
VARY, J. P. ..... p 3900 N92-32028
VAZ, ANA MARIA ZODI ..... p 3925 N92-32025
VERDIER, P. H. ..... p 3794 N92-31618
VESSOT, R. F. C. ..... p 3802 N92-31830
VIANCO, P. T. ..... p 3790 N92-32139
VICKERS, ROSS R., JR. ..... p 3872 N92-31327
VIJAYARAGHAVAN, D. ..... p 3834 N92-31536
VILASBOAS, J. W. S. ..... p 3923 N92-31343
VILLARREAL, E. ..... p 3803 N92-31908
VILLARRUEL, CARL A. ..... p 3777 N92-31268
VISWANATHAN, R. R. ..... p 3914 N92-31402
VOLAKIS, JOHN L. ..... p 3803 N92-31238
p 3807 N92-31614
VONDERHAAR, THOMAS H. ..... p 3857 N92-31964
VONSPRECKELSEN, PAUL ..... p 3896 N92-31814
VUONG, T. M. ..... p 3844 N92-31362

W

WAIDA, S. T. ..... p 3781 N92-31763
WAKATANI, MASAHIRO ..... p 3818 N92-31256
WALKER, D. A. ..... p 3821 N92-31452
WALKER, D. W. ..... p 3883 N92-32034
WALKER, GILBERT C. ..... p 3897 N92-31950
p 3897 N92-31999
WALLACE, DOUGLAS W. R. ..... p 3865 N92-31842
WALSH, R. P. ..... p 3774 N92-31609
WALTON, D. L. ..... p 3866 N92-32050
WANG, C. H. ..... p 3828 N92-31828
p 3784 N92-31959
p 3796 N92-31960
p 3796 N92-31961
WANG, D. ..... p 3799 N92-31593
WANG, F. ..... p 3848 N92-31922
WANG, F. W. ..... p 3794 N92-31618
WANG, MENG ..... p 3770 N92-31474
WANG, RONG-LONG ..... p 3892 N92-31255
WANG, Z. L. ..... p 3913 N92-32085
p 3829 N92-32086
WARD, B. R. ..... p 3808 N92-31722
WARDE, CARDINAL ..... p 3908 N92-31438
WARNATZ, J. ..... p 3780 N92-31607
WARNICK, JORDAN E. ..... p 3868 N92-31326
WARREN, ALISON C. ..... p 3788 N92-31795
WARREN, K. H. ..... p 3883 N92-31741
WASZAK, MARTIN R. ..... p 3760 N92-31240
WATKINS, JAMES J. ..... p 3801 N92-31982
WATRO, RONALD J. ..... p 3875 N92-31405
WATSON, C. H. ..... p 3898 N92-32169
WATSON, D. B. ..... p 3755 N92-31562
WATT, D. W. ..... p 3839 N92-31389
WEAKELY, T. J. R. ..... p 3786 N92-31391
WEAVER, ALFRED C. ..... p 3882 N92-31483
p 3916 N92-31547
WEAVER, MICHAEL J. ..... p 3784 N92-31998
WEAVER, WILLIAM L. ..... p 3844 N92-32127
WEBER, L. H. ..... p 3927 N92-32067
p 3927 N92-32068
WEFEL, JOHN P. ..... p 3926 N92-31477
WEHE, D. K. ..... p 3828 N92-31919
WEI, J. ..... p 3810 N92-32134
WEINBERGER, NORMAN M. ..... p 3869 N92-31558
WEINER, M. M. ..... p 3810 N92-32043
WEISS, R. ..... p 3865 N92-31842
WELCH, D. O. ..... p 3909 N92-31627
WENDELIN, T. J. ..... p 3847 N92-31623
WERNETTE, D. ..... p 3852 N92-31591
WESICK, J. ..... p 3836 N92-31647
WESOLOWSKI, D. J. ..... p 3786 N92-31418
WEST, W. P. ..... p 3905 N92-31749
WESTBROOK, C. K. ..... p 3778 N92-31414
p 3778 N92-31415
p 3779 N92-31416
p 3780 N92-31607
p 3781 N92-31763
WESTMORELAND, C. G. ..... p 3797 N92-32089
WETHERALL, J. A. ..... p 3866 N92-32106
WHANBO, MYUNG-HWAN ..... p 3898 N92-32024
WHITE, D. E. ..... p 3783 N92-31816
WHITE, D. H. ..... p 3895 N92-31765
WHITFIELD, C. E. ..... p 3891 N92-31248
WHITMAN, S. ..... p 3878 N92-31739
WIEN, K. ..... p 3893 N92-31386
WIESEMAN, CAROL D. ..... p 3758 N92-32111
WILCZYNSKI, VINCENT ..... p 3753 N92-31853
WILDER, MICHAEL C. ..... p 3753 N92-32177
WILDERS, P. ..... p 3821 N92-31513
WILLIAMS, GEORGE J. ..... p 3770 N92-31901
WILLIAMS, R. S. ..... p 3783 N92-31820
WILLSON, ALAN N., JR. ..... p 3817 N92-32074
WILLSON, C. G. ..... p 3795 N92-31810
WILSON, F. W. ..... p 3863 N92-32103
WILSON, JOHN W. ..... p 3926 N92-32193
WILSON, K. J. ..... p 3747 N92-31871
WILSON, ROBERT J. ..... p 3756 N92-32054
WILSON, RONALD B. ..... p 3917 N92-31371
WINDISCH, C. F., JR. ..... p 3813 N92-31440
WINKLEMAN, B. C. ..... p 3903 N92-31372
WINNER, WENDY A. ..... p 3876 N92-31488
WIPKE, K. ..... p 3849 N92-32112
WITHERELL, MARK D. ..... p 3838 N92-31331
WOLD, A. ..... p 3911 N92-31819
WOLF, D. A. ..... p 3848 N92-32087
WOLFE, L. ..... p 3817 N92-32033
WOLFE, W. E. ..... p 3773 N92-31307
WONG, C. P. C. ..... p 3905 N92-31749
WONG, KON M. ..... p 3806 N92-31471
WONG, R. S. ..... p 3752 N92-31777
WOOD, D. H. ..... p 3834 N92-31500
WOOD, GORDON H. ..... p 3922 N92-32191
WOOD, J. G. ..... p 3820 N92-31352
WOOD, J. GARY ..... p 3769 N92-31245
WOODRUFF, S. B. ..... p 3878 N92-31703
WOODS-VEDELER, JESSICA A. ..... p 3757 N92-31351
WOODS, M. ..... p 3900 N92-32131
WRIGHT, BRADFORD L. ..... p 3903 N92-31459
WRIGHT, D. ..... p 3900 N92-32131
WRIGHT, MICHAEL E. ..... p 3791 N92-31318
p 3802 N92-31826
WU, M.-K. ..... p 3802 N92-31263
WU, RUILIAN ..... p 3779 N92-31434
WUEBBLES, D. J. ..... p 3855 N92-32147
WURDEN, GLEN A. ..... p 3903 N92-31459

X

XIA, J. L. ..... p 3796 N92-31961
XU, X. Q. ..... p 3907 N92-31983

Y

YAHIA, H. ..... p 3746 N92-31868
YAMAMOTO, T. ..... p 3765 N92-31685
YANASSE, HORACIO HIDEKI ..... p 3886 N92-31241
YANG, B. ..... p 3820 N92-31421
YANG, K. ..... p 3865 N92-31644
YANG, S. L. ..... p 3846 N92-31498
YARKONY, D. R. ..... p 3781 N92-31725
YATES, J. T., JR. ..... p 3911 N92-31851
YATES, JOHN T., JR. ..... p 3796 N92-32001
YEE, J. H. ..... p 3812 N92-31334
YEE, KEN ..... p 3901 N92-31737
YEE, KENNETH W. ..... p 3827 N92-31370
YEN, J. L. ..... p 3810 N92-32203
YONGQI, SUN ..... p 3776 N92-32075
YOST, F. G. ..... p 3790 N92-32139
YOUNG, K. D. ..... p 3835 N92-32121
YOUNGDAHL, C. K. ..... p 3838 N92-31335
YOUNGS, D. ..... p 3919 N92-31596
YU, L. ..... p 3909 N92-31655
YUKTADATTA, PANURIT ..... p 3882 N92-31443

Z

ZAKRAJSEK, JAMES J. ..... p 3834 N92-31485
ZANELLI, C. I. ..... p 3914 N92-32207
ZAPOTOSKY, J. E. ..... p 3809 N92-31996
ZARR, R. R. ..... p 3827 N92-31633
ZASLAWSKY, M. ..... p 3841 N92-31745
ZBASNIK, J. ..... p 3836 N92-31647
ZEIDLER, J. R. ..... p 3817 N92-31849
ZEISSE, C. R. ..... p 3817 N92-31849
ZELLER, MARY V. ..... p 3745 N92-31267
ZEMACH, C. ..... p 3825 N92-32022
ZENG, K. ..... p 3787 N92-31610
ZEYTINOGLU, MEHMET ..... p 3806 N92-31471
ZGANJAR, E. F. ..... p 3895 N92-31721
ZHANG, PEIZHEN ..... p 3891 N92-31588
ZHANG, Z. X. ..... p 3832 N92-31935
ZHANG, Z. Y. ..... p 3835 N92-31774
ZHAO, QING ..... p 3770 N92-31474
ZHAO, XUEPU ..... p 3823 N92-31770
ZHOU, H. C. ..... p 3795 N92-31954
p 3798 N92-32194
ZHOU, H.-C. ..... p 3795 N92-31952
ZHU, YIMEI ..... p 3909 N92-31627
ZIJLSTRA, B. H. A. ..... p 3921 N92-32186
ZIMMERMAN, J. A. ..... p 3898 N92-32169
ZIMMERMANN, BERND D. ..... p 3776 N92-31979
ZINN, B. T. ..... p 3783 N92-31918
ZIPPEL, RICHARD ..... p 3883 N92-32152
ZITTEL, P. F. ..... p 3894 N92-31606
ZOLOTOREV, M. ..... p 3900 N92-32131
ZUCHOWSKI, KRZYSZTOF ..... p 3907 N92-32208
ZYTKOW, JAN M. ..... p 3920 N92-32049
ZYVOLOSKI, G. ..... p 3825 N92-32008

Typical Corporate Source Index Listing

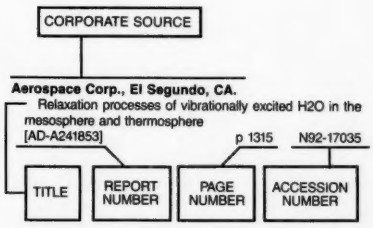

Listings in this index are arranged alphabetically by corporate source. The title of the document provides the user with a brief description of the subject matter. The report number helps to indicate the type of document cited (e.g., NASA report, translation, NASA contractor report). The accession number denotes the number by which the citation is identified. The page number helps you locate the citation in the abstract section. The titles are arranged under each corporate source in ascending accession number order.

A

ADVISORY GROUP FOR AEROSPACE RESEARCH AND DEVELOPMENT, NEUILLY-SUR-SEINE (FRANCE).
Bringing Down the Barriers to Information Transfer
[AGARD-CP-505] p 3920 N92-32182
Proceedings of the 53rd Symposium on Air Vehicle Mission Control and Management
[AGARD-AR-310] p 3889 N92-32229

AEROMETRICS, INC., SUNNYVALE, CA.
Diagnostics for research in atomization and turbulent two-phase flows
[AD-A247201] p 3819 N92-31283

AERONAUTICAL RESEARCH INST. OF SWEDEN, STOCKHOLM.
The influence of various spectrum parameters on fatigue life and residual stress relaxation
[FFA-TN-1991-44] p 3840 N92-31512

AERONAUTICAL RESEARCH LABS., MELBOURNE (AUSTRALIA).
Research into improving the durability of the hot section in the aircraft turbine engine
[AD-A250342] p 3759 N92-31439
Polyalphaolefins: A new improved cost effective aircraft radar coolant
[AD-A250517] p 3796 N92-32045

AEROSPACE CORP., EL SEGUNDO, CA.
Experimental and computer modeling studies of isotopically selective two-step laser photodissociation of small molecules
[DE92-011427] p 3894 N92-31606
Dicke narrowing in strong fields: The atom-as-antenna analogy
[AD-A252321] p 3807 N92-31629

AEROSPACE MEDICAL RESEARCH LABS., WRIGHT-PATTERSON AFB, OH.
Vertical impact tests of humans and anthropomorphic manikins
[AD-A245866] p 3872 N92-31458
Construction of a dual axis force reflection stick and test station
[AD-A250731] p 3803 N92-31890

AIR FORCE ACADEMY, CO.
Building an educational robot arm for under $1,000
[AD-A247499] p 3833 N92-31460
Active control of the separation region on a two-dimensional airfoil
[AD-A249739] p 3752 N92-31622

AIR FORCE INST. OF TECH., WRIGHT-PATTERSON AFB, OH.
Reducing requirements errors through the use of Computer-Aided Software Engineering (CASE) tools and during requirements analysis
[AD-A246879] p 3874 N92-31299
Transient fission gas behavior in uranium nitride fuel under proposed space applications
[AD-A252577] p 3899 N92-31325
Sun-view-target geometry effects on spectrally-derived vegetative index estimates of absorbed radiation and leaf area
[AD-A249984] p 3843 N92-31329
In-flight decision making by high time and low time pilots during instrument operations
[AD-A249990] p 3871 N92-31392
Balanced, potential vorticity dynamics in the tropics
[AD-A249981] p 3858 N92-31432
Cloud-to-ground lightning characteristics in mesoscale convective systems
[AD-A250418] p 3858 N92-31493
The structure and energetics of Amazon squall lines
[AD-A250182] p 3859 N92-31523
A case study of a prolonged sleet event: 16-17 February 1987 and climatology of sleet events for North Carolina, 1949-1989
[AD-A250184] p 3859 N92-31602
A comparative analysis of the temporal variability of lightning observations and GOES imagery
[AD-A250185] p 3860 N92-31603
Studies in dynamic characterization and control of a flexible structure and optical beampath
[AD-A250555] p 3830 N92-31605
Many body perturbation theory using a Restricted Open-Shell Hartree-Fock (ROHF) reference function
[AD-A249725] p 3894 N92-31673
An investigation of spinup dynamics of axial gyrostats using elliptic integrals and the method of averaging
[AD-A249728] p 3768 N92-31675
Maximum likelihood estimation of fractional Brownian motion and Markov noise parameters
[AD-A249623] p 3890 N92-31686
Scattering from a finite collection of transverse dipole and axial slot arrays with edge effects
[AD-A249622] p 3807 N92-31691
Simulation of diurnally varying downslope winds over Northern Utah
[AD-A250568] p 3861 N92-31714
Computer Aided Process Planning (CAPP): The user interface for the fabrication module of the rapid design system
[AD-A250095] p 3879 N92-31783
A comparative study of the dynamic performance of three bivanes
[AD-A250096] p 3862 N92-31784
High-latitude spacecraft charging in low-Earth polar orbit
[AD-A249868] p 3767 N92-31822
Thermomechanical fatigue behavior of a silicone carbide fiber-reinforced calcium aluminosilicate glass-ceramic matrix composite
[AD-A249870] p 3775 N92-31823
Upper tropospheric jet streams over North America during summer 1988
[AD-A249871] p 3857 N92-31906
Impulsive magnetic perturbations of the high latitude, dayside ionosphere
[AD-A249872] p 3857 N92-31932
Nonthermal inhalation injury
[AD-A252532] p 3869 N92-31962
Experimental feedback of fractional order states of a lightly damped structure
[AD-A248027] p 3842 N92-31989
An examination of the feasibility of a nuclear-pumped laser-driven inertial confinement fusion reactor with magnetically protected walls
[AD-A248163] p 3907 N92-31990
Confidence interval estimation for output of discrete-event simulations using the Kalman filter
[AD-A248170] p 3860 N92-31991

ALABAMA UNIV., HUNTSVILLE.
Combined Release and Radiation Effects Satellite (CRRES) experiments data collection, analysis, and publication
[NASA-CR-184361] p 3856 N92-31551
Automated payload experiment tool feasibility study
[NASA-CR-184256] p 3883 N92-31835
The uncertainties of global temperatures in the global warming context
[TABES PAPER 92-447] p 3763 N92-32014

ALASKA UNIV., FAIRBANKS.
Annual dynamics within the active layer
[DE92-013520] p 3850 N92-31304

ALENIA SPAZIO S.P.A., ROME (ITALY).
Space Station mini pressurised logistics modules: An opportunity to enlarge and reinforce international cooperation
[TABES PAPER 92-425] p 3764 N92-32016

ALENIA SPAZIO S.P.A., TURIN (ITALY).
Italian-US cooperation in space: The case of Tethered, IRIS/LAGEOS, and SPACEHAB
[TABES PAPER 92-467] p 3764 N92-32019

ALLIED-SIGNAL AEROSPACE CO., KANSAS CITY, MO.
Computer-aided modeling tools for forging process feasibility studies
[DE92-012116] p 3838 N92-31303
Prototype casting fabrication by stereolithography
[DE92-011489] p 3876 N92-31529
Low thermal coefficient of expansion printed wiring boards
[DE92-013704] p 3817 N92-31946
Metallization of ferrite ceramic couplings
[DE92-016573] p 3789 N92-32032
Flex circuit lamination
[DE92-016574] p 3817 N92-32033
Titanium carbon nitride coating
[DE92-013158] p 3777 N92-32135
High density thin-walled syntactic foam
[DE92-013159] p 3797 N92-32136

ALLIED-SIGNAL AEROSPACE CO., TETERBORO, NJ.
RL-34 ring laser gyro laboratory evaluation for the Deep Space Network antenna application
[NASA-CR-190481] p 3829 N92-32128

AMES LAB., IA.
Robotic soil sampler for hazardous waste clean up
[DE92-012693] p 3780 N92-31565
Real-time infrared spectroscopy of moving solids for on-line analyses
[DE92-012156] p 3782 N92-31772
Laser decontamination: A new strategy for facility decommissioning
[DE92-014113] p 3831 N92-31775
A self consistent generalized model for the calculation of minor loop excursions in the theory of hysteresis
[DE92-014394] p 3890 N92-32116

ANALYSIS AND MEASUREMENT SERVICES CORP., KNOXVILLE, TN.
New technology for remote testing of response time of installed thermocouples. Volume 2: Research data
[AD-A245821] p 3826 N92-31298

ANALYTICAL SERVICES AND MATERIALS, INC., HAMPTON, VA.
Towards understanding turbulent scalar mixing
[NASA-CR-4446] p 3826 N92-32242

ANDRULIS RESEARCH CORP., SALT LAKE CITY, UT.
Development of methodology and technology for identifying and quantifying emission products from open burning and open detonation thermal treatment methods. BangBox test series. Volume 1. Test summary
[AD-A250733] p 3800 N92-31969
Development of methodology and technology for identifying and quantifying emission products from open burning and open detonation thermal treatment methods. BangBox test series. Volume 2: Test development
[AD-A250734] p 3800 N92-31970

Development of methodology and technology for identifying and quantifying emission products from open burning and open detonation thermal treatment methods. Field test series A, B, and C. Volume 1: Test summary
[AD-A250735] p 3800 N92-31971
Development of methodology and technology for identifying and quantifying emission products from open burning and open detonation thermal treatment methods. Field test series A, B, and C. Volume 2, part A: Quality assurance and quality control
[AD-A250736] p 3801 N92-31972
Development of methodology and technology for identifying and quantifying emission products from open burning and open detonation thermal treatment methods. Field test series A, B, and C. Volume 2, part B: Quality assurance and quality control. Appendices
[AD-A250737] p 3801 N92-31973

ARGONNE NATIONAL LAB., IL.
Dynamic modeling of plasma-vapor interactions during plasma disruptions
[DE92-016183] p 3903 N92-31310
ADIFOR: Automatic differentiation in a source translator environment
[DE92-016185] p 3886 N92-31311
Mode methods for strain-hardening structures
[DE92-014855] p 3838 N92-31335
Dependence of secondary ion emission from organic material on the energy loss of the impacting heavy ion
[DE92-014845] p 3893 N92-31386
Economics of microwave plasma dissociation of H2S
[DE92-014846] p 3779 N92-31441
Experimental evaluation of oxygen-enriched air and emulsified fuels in a single-cylinder diesel engine. Volume 1: Concept evaluation
[DE92-015999] p 3799 N92-31442
Sodium Heat Engine Development Program
[DE92-012398] p 3846 N92-31531
Computer simulation of scattered ion and sputtered species effects in ion beam sputter-deposition of high temperature superconducting thin films
[DE92-015227] p 3909 N92-31546
Radiation-induced crystalline-to-amorphous transition in intermetallic compounds of the Cu-Ti alloy system
[DE92-010276] p 3787 N92-31575
Minorities and air quality non-attainment areas: A preliminary geo-demographic analysis
[DE92-013054] p 3852 N92-31591
Edge-on ion irradiation of electron microscope specimens
[DE92-014847] p 3894 N92-31595
Enhancing GRASS data communication with videographic technology
[DE92-014852] p 3919 N92-31596
Ion beam spectroscopy as a means of in-situ monitoring of thin film deposition
[DE92-014857] p 3909 N92-31652
Oracle and the end-user: Practical implementation of applications in a multi-user, multi-platform environment
[DE92-015223] p 3877 N92-31654
Elementary reaction rate measurements at high temperatures by tunable-laser flash-absorption
[DE92-015269] p 3830 N92-31684
Potential impact of high temperature superconductors on MAGLEV transportation
[DE92-012683] p 3834 N92-31720
Preliminary design for a MAGLEV development facility
[DE92-012259] p 3835 N92-31774
Heat exchanger performance calculations for enhanced-tube condenser applications
[DE92-016603] p 3823 N92-31785
Analyses and predictions of the thermodynamic properties and phase diagrams of silicate systems
[DE92-016177] p 3783 N92-31857
ADIFOR: Fortran source translation for efficient derivatives
[DE92-016187] p 3879 N92-31899
Oxidation/sulfidation behavior of Fe-Cr alloys: A reactive-element effect
[DE92-016172] p 3789 N92-31924
Radiolytic gas production in the alpha particle degradation of plastics
[DE92-011846] p 3795 N92-31938
Recent advances in high-temperature superconductor wire fabrication and applications development
[DE92-016634] p 3912 N92-31955
Heat and mass transfer considerations in advanced heat pump systems
[DE92-016635] p 3825 N92-32003
The potential of passive-remote Fourier Transform Infrared (FTIR) spectroscopy to detect organic emissions under the Clean Air Act
[DE92-015224] p 3854 N92-32083

ARIZONA STATE UNIV., TEMPE.
High-frequency techniques for RCS prediction of plate geometries
[NASA-CR-190656] p 3804 N92-31273
Surface structures and surface processes of ceramics with atomic resolutions: A study by scanning tunneling microscopy
[AD-A249581] p 3792 N92-31377
Stability and transition of hypersonic boundary-layer flows
[AD-A250279] p 3752 N92-31555
Particle diagnostics in optically thick sprays
[AD-A250981] p 3897 N92-31936
Solid electrolytes and impact-resistant ceramics
[DE92-015297] p 3797 N92-32095

ARIZONA UNIV., TUCSON.
An experimental investigation of the formation of secondary vortices and the generation of small-scale motion in a spanwise forced plane mixing layer
[AD-A250350] p 3822 N92-31559
A characterization of the hot infrared background: The infrared cirrus, zodiacal dust bands, and solar system dust trails
[PL-TR-91-2065] p 3924 N92-32142
Instabilities of damage and surface degradation mechanisms in brittle material structural systems
[AD-A250785] p 3842 N92-32168

ARMY ARMAMENT RESEARCH, DEVELOPMENT AND ENGINEERING CENTER, WATERVLIET, NY.
A generalized plane-strain elastic stress solution for a multiorthotropic-layered cylinder
[AD-A250487] p 3838 N92-31331

ARMY AVIATION SYSTEMS COMMAND, CLEVELAND, OH.
Experimental testing of prototype face gears for helicopter transmissions
[NASA-TM-105434] p 3832 N92-31349
A demonstration of an intelligent control system for a reusable rocket engine
[NASA-TM-105794] p 3770 N92-31507

ARMY CHEMICAL RESEARCH AND DEVELOPMENT CENTER, ABERDEEN PROVING GROUND, MD.
Remote Data Transfer (RDT): An interprocess data transfer method for distributed environments
[AD-A250859] p 3920 N92-32102

ARMY ELECTRONIC PROVING GROUND, FORT HUACHUCA, AZ.
Methodology investigation final report: Automated real-time test scenario generation, phase 1
[AD-A250439] p 3884 N92-31395

ARMY ENGINEER SCHOOL, FORT LEONARD WOOD, MO.
Results of earth observation study on STS-31 for Terra Geode, January 1987 - June 1991
[AD-A250750] p 3844 N92-31621

ARMY LAB. COMMAND, FORT MONMOUTH, NJ.
Movement of dislocations in quartz
[AD-A250527] p 3913 N92-32078

ARMY LAB. COMMAND, WATERTOWN, MA.
Characterization of oxide formed on silicon by exposure to atomic oxygen in space
[AD-A249787] p 3778 N92-31301
High strength glass second source qualification to composite armor specification MIL-L-46197(MR)
[AD-A252114] p 3792 N92-31404
Recent developments in the fundamentals of gas permeation in rubbery polymers
[AD-A249745] p 3794 N92-31624

ARMY LAB. COMMAND, WHITE SANDS MISSILE RANGE, NM.
Unified very low stratus cloud/subcloud microphysics model
[AD-A250662] p 3858 N92-31320

ARMY MISSILE COMMAND, REDSTONE ARSENAL, AL.
Selective nitrations: The laser-induced nitration of three cycloalkanes, 1
[AD-A249942] p 3800 N92-31800
Design and development of minilink video: A fiber-optic coupled video system
[AD-A249945] p 3808 N92-31801

ARMY RESEARCH INST. FOR THE BEHAVIORAL AND SOCIAL SCIENCES, ALEXANDRIA, VA.
Empirical development of a scale for the prediction of performance on a sustained monitoring task
[AD-A252443] p 3872 N92-31294

ARMY STRATEGIC DEFENSE COMMAND, HUNTSVILLE, AL.
Ground based radar
[TABES PAPER 92-213] p 3764 N92-32021

ATMOSPHERIC SCIENCES LAB., WHITE SANDS MISSILE RANGE, NM.
Energy balance model for imagery and electromagnetic propagation
[AD-A250884] p 3806 N92-31543

ATOMIC ENERGY OF CANADA LTD., CHALK RIVER (ONTARIO).
EWE: A computer model for ultrasonic inspection
[DE92-627145] p 3837 N92-32143

AUBURN UNIV., AL.
Weld penetration and defect control
[DE92-015310] p 3836 N92-31336

AWARE, INC., CAMBRIDGE, MA.
Wavelet signal processing for transient feature extraction
[AD-A250519] p 3890 N92-32046

B

BALLISTIC RESEARCH LABS., ABERDEEN PROVING GROUND, MD.
Tomographic reconstruction of infrared spectra of nonhomogeneous media: Applications to a flat flame burner
[AD-A249999] p 3778 N92-31393
Modular UNIX (trade name)-based Vulnerability Estimation Suite (MUVES) analyst's guide
[AD-A245322] p 3876 N92-31488
Absorption spectroscopy through the dark zone of solid propellant flames
[AD-A250033] p 3782 N92-31803
Shock tube study of the reaction of triethanol ammonium nitrate with N2O
[AD-A250034] p 3800 N92-31804

BOEING AEROSPACE AND ELECTRONICS CO., SEATTLE, WA.
Low density real gas flows about hypersonic vehicles
[AD-A250048] p 3752 N92-31777

BOEING CO., SEATTLE, WA.
Analysis of systems hardware flown on LDEF. Results of the systems special investigation group
[NASA-CR-189628] p 3767 N92-31677

BOEING COMMERCIAL AIRPLANE CO., SEATTLE, WA.
Aging fleet: Maintaining airworthiness
p 3745 N92-31862
Integrated computer systems in aircraft design and manufacture: Difficulties and implications
p 3746 N92-31864
Engine monitoring display study
[NASA-CR-4463] p 3761 N92-32175
An installed nacelle design code using a multiblock Euler solver. Volume 1: Theory document
[NASA-CR-189652-VOL-1] p 3754 N92-32226
An installed nacelle design code using a multiblock Euler solver. Volume 2: User guide
[NASA-CR-189652-VOL-2] p 3754 N92-32228

BOSTON UNIV., MA.
Enhancement of fracture toughness using high intensity electric currents
[AD-A249809] p 3889 N92-31359
The effects of magnetic storm phases on F-layer irregularities from auroral to equatorial latitudes
[AD-A249011] p 3855 N92-31478

BROOKHAVEN NATIONAL LAB., UPTON, NY.
Spin polarized photoemission studies of surfaces and thin-films
[DE92-016098] p 3907 N92-31296
Application of Free-Air CO2 Enrichment (FACE) technology to a forest canopy: A simulation study
[DE92-013308] p 3851 N92-31422
The NSLS 100 element solid state array detector
[DE92-014477] p 3827 N92-31502
Microdistribution of lead in bone: A new approach
[DE92-013036] p 3869 N92-31589
Oxygen ordering and strain-related morphology in YBa2Cu(3-x)O7 systems
[DE92-014476] p 3909 N92-31627
Understanding and managing the effects of battery charger and inverter aging
[DE92-014473] p 3815 N92-31651
Lattice gaugefixing and other optics in lattice gauge theory
[DE92-016958] p 3901 N92-31737
Electrically-induced stresses and deflection in multiple plates
[DE92-012303] p 3841 N92-31844
Condensation in a two-phase pool
[DE92-010048] p 3824 N92-31977
Materials for geothermal production
[DE92-014691] p 3849 N92-32118
Geothermal materials development
[DE92-016940] p 3849 N92-32124
Thin polymer icemaker development and test program
[DE92-016941] p 3803 N92-32125
Conversion of power and frequency
[DE92-012543] p 3810 N92-32134

BROWN UNIV., PROVIDENCE, RI.
Geometric theory of infinite dimensional dynamical systems
[AD-A252190] p 3915 N92-31585
The crystal growth and characterization of the solid solutions (ZnS)(1-x)(CuMS2)(x)
[AD-A248029] p 3911 N92-31819

BUREAU OF LAND MANAGEMENT, WASHINGTON, DC.
Satellite positioning systems: A report to the director
[PB92-181270] p 3767 N92-31632
BUREAU OF MINES, WASHINGTON, DC.
Chromium, nickel, and other alloying elements in US-produced stainless and heat-resisting steel
[PB92-178623] p 3788 N92-31797
BUREAU OF RECLAMATION, DENVER, CO.
Hydrogenerator design manual, chapter 8
[PB92-173707] p 3919 N92-31682

C

CALIFORNIA UNIV., BERKELEY.
Ignition and flame propagation studies over a flat fuel surface
[PB92-181056] p 3780 N92-31678
Evidence of stochastic diffusion across a cross-field sheath due to Kelvin-Helmholtz vortices
[AD-A247847] p 3907 N92-31983
CALIFORNIA UNIV., BERKELEY. LAWRENCE BERKELEY LAB.
Flame front geometry in premixed turbulent flames
[DE92-010310] p 3779 N92-31417
Performance of multiple stream pulsed jet combustion systems
[AD-A249722] p 3780 N92-31671
Relating space radiation environments to risk estimates
[DE92-010256] p 3926 N92-31756
Implications of the 17 keV neutrino
[DE92-017000] p 3898 N92-32006
CALIFORNIA UNIV., DAVIS.
Application of the mean spherical approximation to the estimations of single ion thermodynamic quantities of solvation for monoatomic monovalent ions in aqueous solutions
[AD-A250190] p 3893 N92-31316
The role of metal structure in determining solvent orientation at the electrode/solution interface
[AD-A249751] p 3893 N92-31328
Specification and verification of secure concurrent and distributed software systems
[AD-A252477] p 3879 N92-31825
CALIFORNIA UNIV., IRVINE.
Modeling of learning-induced receptive field plasticity in auditory neocortex
[AD-A250348] p 3869 N92-31558
Technology advancing research combustion in burners
[PB92-164359] p 3782 N92-31776
CALIFORNIA UNIV., LOS ANGELES.
Adaptive and nonadaptive feedback control of global instabilities with application to a heated 2-D jet
[AD-A250700] p 3820 N92-31322
Signal location using generalized linear constraints
[AD-A249580] p 3805 N92-31376
Correlation from randomness: Quantitative analysis of sputtered graphite surfaces using the scanning tunneling microscope
[AD-A252420] p 3783 N92-31820
Compact millimeter-wave devices: Dielectric loaded carm, high voltage carm, slow wave crm and high harmonic gyrotron
[AD-A250497] p 3809 N92-31944
VLSI for high-speed digital signal processing
[AD-A250365] p 3817 N92-32074
CALIFORNIA UNIV., SAN DIEGO.
A sensitivity study of daytime visibility determination with the horizon scanning imager
[SIO-91-15] p 3902 N92-32144
CALIFORNIA UNIV., SANTA BARBARA.
Absorption spectra and electronic properties of alkali metal doped C60
[AD-A251006] p 3912 N92-31937
The chemistry and packaging of nanocomposite confined arrays
[AD-A250991] p 3817 N92-32002
Nature of short Li-H-C contact interactions in organolithium compounds and its implication
[AD-A250992] p 3898 N92-32024
CALIFORNIA UNIV., SANTA CRUZ.
Space constancy on video display terminals
[AD-A247290] p 3872 N92-32105
CALSPAN-BUFFALO UNIV. RESEARCH CENTER, NY.
Fundamental studies of the structure of hypersonic attached and separated boundary layers over smooth, rough and transpiration-cooled surfaces
[AD-A250284] p 3819 N92-31286
CAMBRIDGE RESEARCH AND INSTRUMENTATION, INC., MA.
Wavelength-tunable liquid crystal imaging filters for remote sensing from geosynchronous platforms
[NASA-CR-190698] p 3845 N92-32223
CANADA INST. FOR SCIENTIFIC AND TECHNICAL INFORMATION, OTTAWA (ONTARIO).
Computerized property data for engineering materials: An overview p 3922 N92-32191
CARNEGIE-MELLON UNIV., PITTSBURGH, PA.
Type evolution and instance adaptation
[AD-A248435] p 3917 N92-31285
Programming with inductive and co-inductive types
[AD-A249562] p 3874 N92-31353
The effect of elastic stress on Ostwald ripening phenomena
[DE92-015291] p 3839 N92-31400
Neural network perception for mobile robot guidance
[AD-A249972] p 3884 N92-31511
Requirements Engineering and Analysis Workshop Proceedings
[AD-A250415] p 3876 N92-31541
Decomposition of balanced matrices. Part 4: Connected squares
[AD-A247308] p 3888 N92-31768
A language for higher-order explanation-based learning
[AD-A251008] p 3880 N92-31939
Ring-opening polymerization of strained cyclotetrasilanes as a new route towards well defined polysilylenes
[AD-A251020] p 3795 N92-31941
New techniques in computational fluid dynamics: Algorithms, analysis, applications
[AD-A250498] p 3825 N92-32038
Cationic ring opening polymerization of oxazolines initiated by trimethylsilyl derivatives
[AD-A251109] p 3798 N92-32153
Polymorphic type assignment and CPS conversion
[AD-A250954] p 3887 N92-32171
CASE WESTERN RESERVE UNIV., CLEVELAND, OH.
Electronic and total energy properties of ternary and quaternary semiconductor compounds, alloys, and superlattices: Theoretical study of Cu/graphite bonding
[NASA-CR-190691] p 3772 N92-31266
Application of optical theory to quantitative surface FT-IR with emphasis on molecular depth profiling
[AD-A250525] p 3902 N92-32077
CATHOLIC UNIV. OF AMERICA, WASHINGTON, DC.
Organized turbulent structures and their induced wall pressure fluctuations p 3753 N92-31853
CENTER FOR MATHEMATICS AND COMPUTER SCIENCE, AMSTERDAM (NETHERLANDS).
On a characterization of the exponential distribution based on a type 2 right censored sample
[CWI-BS-R9117] p 3888 N92-31517
CHICAGO UNIV., IL.
Theoretical high energy physics research at the University of Chicago, task A
[DE92-016288] p 3899 N92-31712
Participation in high energy physics. Task C: Particle physics and cosmology
[DE92-016290] p 3924 N92-31713
CINCINNATI UNIV., OH.
Structural similitude and scaling laws for laminated beam-plates
[NASA-CR-190585] p 3841 N92-31911
CITY UNIV. OF NEW YORK, STATEN ISLAND.
Non-geothermal optics study of wave propagation
[DE92-011806] p 3903 N92-31494
CLARKSON UNIV., POTSDAM, NY.
Analysis and computer tools for separation processes involving nonideal mixtures
[DE92-015298] p 3781 N92-31752
Experimental studies of friction and heat transfer in enhanced passages
[DE92-011607] p 3890 N92-32099
CLEMSON UNIV., SC.
Spectrum modal analysis for the detection of low-altitude windshear with airborne Doppler radar
[NASA-CR-4457] p 3755 N92-31549
COGNITECH, INC., SANTA MONICA, CA.
A real time system for multisensor image analysis through pyramidal segmentation
[AD-A247169] p 3888 N92-31981
COLORADO STATE UNIV., FORT COLLINS.
Updated forecast of Atlantic seasonal hurricane activity for 1992 p 3859 N92-31583
Diosmacycloalkanes as models for the formation of hydrocarbons from surface methylenes
[DE92-014588] p 3783 N92-31891
Effect of synthesis temperature in the structure, doping level and charge-transport properties of polypyrrole
[AD-A250531] p 3796 N92-32079
Near-IR absorption spectra for the Buckminsterfullerene Anions: An experimental and theoretical study
[AD-A250532] p 3785 N92-32080
COLORADO UNIV., BOULDER.
Solid rocket combustion phenomena
[AD-A248006] p 3770 N92-31474
Advanced DAA methods for shock response analysis
[AD-A252696] p 3891 N92-31588
COLORADO UNIV., DENVER.
The development of modularized software for empirical testing of new algorithms in linear programming
[AD-A250811] p 3875 N92-31480
COLUMBIA UNIV., NEW YORK, NY.
Ion temperature gradient instability and transport
[DE92-013590] p 3905 N92-31727
The Radiological Research Accelerator Facility
[DE92-013674] p 3867 N92-31747
Laser enhanced chemical reaction studies
[DE92-010772] p 3831 N92-31798
CONNECTICUT UNIV., STORRS.
Estimation with multisensor/multiscan detection fusion
[AD-A250496] p 3804 N92-31333
Tribology of Langmuir-Blodgett films
[AD-A250075] p 3833 N92-31363
Tribology of functionally-terminated oligomer films
[AD-A250076] p 3833 N92-31433
COOPERATIVE INST. FOR RESEARCH IN THE ATMOSPHERE, FORT COLLINS, CO.
ARO Geoscience Center fellowships
[AD-A249225] p 3857 N92-31964
CORNELL UNIV., ITHACA, NY.
Novel chemically amplified dry-developing imaging materials for high resolution microlithography
[AD-A250085] p 3793 N92-31435
The photogeneration of polymeric amines: Synthesis and photocrosslinking of copolymers containing photoactive carbamate pendant groups
[AD-A250086] p 3793 N92-31436
Using consistent subcuts for detecting stable properties
[NASA-CR-190443] p 3886 N92-31553
Photogenerated base as catalyst for imidization reactions: Design of photosensitive polyimides
[AD-A250067] p 3795 N92-31810
Synthesis, structure and properties of Ba6Co25S27: A Perovskite-like superstructure of Co8S6 and Ba6S clusters
[AD-A251041] p 3911 N92-31848
On dexterous rotations of polygons
[AD-A250967] p 3797 N92-32151
The data structure accelerator architecture
[AD-A250968] p 3883 N92-32152
CORVALLIS ENVIRONMENTAL RESEARCH LAB., OR.
Methods of assessing responses of trees, stands and ecosystems to air pollution
[PB92-180231] p 3853 N92-31648
CRANFIELD INST. OF TECH., BEDFORD (ENGLAND).
An investigation into the interface between three closely spaced axi-symmetric bodies at subsonic speed
[CRANFIELD-AERO-9114] p 3751 N92-31514
ASTOVL combat aircraft design synthesis and optimization
[CRANFIELD-AERO-9201] p 3757 N92-31515
Dynamics of shuttle based flexible antenna system
[CRANFIELD-AERO-9203] p 3840 N92-31516
CYNETICS CORP., RAPID CITY, SD.
Advances in small satellite communication systems
[TABES PAPER 92-411] p 3763 N92-32010

D

DAYTON UNIV., OH.
The determination of operational and support requirements and costs during the conceptual design of space systems
[NASA-CR-190626] p 3766 N92-31260
DEFENCE AND CIVIL INST. OF ENVIRONMENTAL MEDICINE, DOWNSVIEW (ONTARIO).
Canadian aircrew sea water survival, 1952-1987
[DCIEM-88-RR-39] p 3756 N92-32219
DEFENCE RESEARCH ESTABLISHMENT, OTTAWA (ONTARIO).
Design of a TEM cell EMP simulator
[DREO-1084] p 3806 N92-31470
Square-law device analysis for the detection and timing estimation of a burst BPSK signal
[DREO-91-6] p 3809 N92-31921
A prototype DND Ku band SATCOM system for ANIK-C2 (Project MASTER/MM2)
[DREO-1034] p 3810 N92-32176
EHF SATCOM frequency hopping pattern generator: Proof of concept
[DREO-89-32] p 3811 N92-32231
A frequency hopping synthesizer controller for EHF SATCOM
[DREO-89-29] p 3811 N92-32232
DEFENCE RESEARCH ESTABLISHMENT PACIFIC, VICTORIA (BRITISH COLUMBIA).
Investigation into the ultrasonic NDE of adhesively bonded joints
[DREP-90-02] p 3837 N92-32202

Motion model for the correction of point source distortion in radiographs of honeycomb
[DREP-88-14] p 3777 N92-32215
OSRMS: The DREP near-nadir scatterometer
[DREP-88-15] p 3844 N92-32216
DEFENCE RESEARCH ESTABLISHMENT VALCARTIER (QUEBEC).
Characteristics of selected reference targets for calibrating 10.6 micron laser radars
[DREV-R-4487/88] p 3811 N92-32217
Absolute calibration of the Fourier interferometric transmissometer
[DREV-R-4511/88] p 3829 N92-32218
DEFENCE RESEARCH INFORMATION CENTRE, GLASGOW (SCOTLAND).
Local Area Networks (LAN) p 3874 N92-32183
DEFENSE TECHNICAL INFORMATION CENTER, ALEXANDRIA, VA.
Facilitating the transfer of scientific and technical information with scientific and technical numeric databases p 3922 N92-32192
DEPARTMENT OF ENERGY, WASHINGTON, DC.
FEDIX: The on-line database retrieval service of government information for colleges, universities, and other organizations
[DE92-012384] p 3917 N92-31288
Electric and hybrid vehicles program
[DE92-015200] p 3834 N92-31653
Report of the aviation safety review of Department of Energy helicopter operations
[DE92-016346] p 3755 N92-31928
Multi-year strategic plan for the atmospheric studies in complex terrain: ASCOT program
[DE92-016646] p 3854 N92-31930
DEPARTMENT OF THE NAVY, WASHINGTON, DC.
Waveguide-binding sensor for use with assays
[AD-D015230] p 3777 N92-31268
Optical interconnects in the computer environment
[AD-D015235] p 3873 N92-31269
Nonlinear optical acrylic polymers and use thereof in optical and electro-optic devices
[AD-D015236] p 3791 N92-31270
Replaceable valve seat
[AD-D015250] p 3832 N92-31271
Optical interferometric sensor detected intensity noise reductions means
[AD-D015296] p 3902 N92-32137
DEUTSCHE FORSCHUNGSANSTALT FUER LUFT- UND RAUMFAHRT, OBERPFAFFENHOFEN (GERMANY, F.R.).
The icing of the elevator of the DLR icing research aircraft of Do 28 type
[DLR-MITT-91-12] p 3755 N92-31813
DOUGLAS AIRCRAFT CO., INC., LONG BEACH, CA.
Design and analysis issues of integrated control systems for high-speed civil transports
[NASA-CR-186022] p 3761 N92-31656
DUKE UNIV., DURHAM, NC.
Asymptotic modal analysis and statistical energy analysis
[NASA-CR-190516] p 3842 N92-32236

E

E-TEK DYNAMICS, INC., SAN JOSE, CA.
Optical computing and optical signal processing, phase 1
[AD-A250551] p 3902 N92-32092
EAGLE-PICHER INDUSTRIES, INC., JOPLIN, MO.
Research and development of advanced nickel-iron batteries for electric vehicle propulsion
[DE92-014099] p 3817 N92-31834
EAGLE TECHNOLOGY, INC., WINTER PARK, FL.
Development of quantitative specifications for simulating the stress environment
[AD-A250669] p 3870 N92-31321
EDGERTON, GERMESHAUSEN AND GRIER, INC., IDAHO FALLS, ID.
Application of reactor-pumped lasers to power beaming
[DE92-012370] p 3831 N92-31762
Performance tests of a fast-acting valve for the driver tubes of a large blast/thermal simulator
[AD-A250035] p 3835 N92-31807
EDUCATIONAL TESTING SERVICE, PRINCETON, NJ.
Probability-based inference in a domain of proportional reasoning tasks
[AD-A247304] p 3871 N92-31444
EG AND G ENERGY MEASUREMENTS, INC., ALBUQUERQUE, NM.
An alternative to sneakernet
[DE92-011146] p 3918 N92-31448
EG AND G ENERGY MEASUREMENTS, INC., IDAHO FALLS.
Emissivity measurements in support of experiments on natural convection between a vertical cylinder and a surrounding array
[DE92-012321] p 3819 N92-31287
EG AND G ENERGY MEASUREMENTS, INC., LOS ALAMOS, NM.
Problems with interleaved digitizers
[DE92-013369] p 3881 N92-32150
EG AND G ROCKY FLATS, INC., GOLDEN, CO.
Improvements to the Rocky Flats Metrology Laboratories velocity meter calibration system
[DE92-013162] p 3829 N92-32138
ELORET CORP., SUNNYVALE, CA.
Computational studies of metal-metal and metal-ligand interactions
[NASA-CR-190674] p 3790 N92-32156
EMORY UNIV., ATLANTA, GA.
UV photochemistry of trivinylantimony adsorbed on quartz
[AD-A252215] p 3785 N92-32057
ENERGY AND ENVIRONMENTAL RESEARCH CORP., IRVINE, CA.
Technology advancing research combustion in burners
[PB92-164359] p 3782 N92-31776
ENERGY INFORMATION ADMINISTRATION, WASHINGTON, DC.
World energy projection system: Model documentation
[DE92-014206] p 3847 N92-31594
ENVIRONMENTAL PROTECTION AGENCY, RESEARCH TRIANGLE PARK, NC.
Development of a core combustion research program plan for EPA
[PB92-180868] p 3781 N92-31683
ENVIRONMENTAL PROTECTION AGENCY, WASHINGTON, DC.
RCRIS data element dictionary, version 3.0.0: Data tape documentation
[PB92-145515] p 3918 N92-31398
ESSEX CORP., COLUMBIA, MD.
Optical processing architectures for spaceborne SAR image generation and RF array beam forming
[TABES PAPER 92-444] p 3763 N92-32012
EUROPEAN SPACE AGENCY, PARIS (FRANCE).
Contribution to the modelling of turbulent combustion in the case of stabilisation by flame-lock
[ESA-TT-1229] p 3784 N92-31942
Analysis of three icing test flights reaching the aircraft-referred icing degree of severe
[ESA-TT-1254] p 3755 N92-31943
Partnership in space: An introduction to Canada's special relationship with the European Space Agency
[ESA-BR-79] p 3922 N92-31947

F

FACHHOCHSCHULE, DARMSTADT (GERMANY, F.R.).
Automated input into databases: OCR and descriptive cataloguing p 3921 N92-32189
FACTORY MUTUAL RESEARCH CORP., NORWOOD, MA.
Flammability characteristics of glass reinforced epoxy composite materials
[AD-A251009] p 3775 N92-31940
FEDERAL AVIATION ADMINISTRATION, ATLANTIC CITY, NJ.
GNAS Maintenance Control Center (GMCC) Design Qualification Test and Evaluation (DQT/E) test report
[DOT/FAA/CT-TN91/39] p 3745 N92-31615
Effect of guard band reduction on marker beacon receiver performance
[DOT/FAA/CT-TN92/18] p 3807 N92-31617
Global positioning system runway incursion program static ground tests
[DOT/FAA/CT-TN91/44] p 3756 N92-31838
FEDERAL COORDINATING COUNCIL FOR SCIENCE, ENGINEERING AND TECHNOLOGY, WASHINGTON, DC.
Our Changing Planet: The FY 1993 US Global Change Research Program. A report by the Committee on Earth and Environmental Sciences, a supplement to the US President's fiscal year 1993 budget
[PB92-156892] p 3852 N92-31620
FERMI NATIONAL ACCELERATOR LAB., BATAVIA, IL.
Investigation of factors affecting the calibration of strain gage based transducers (Goodzeit gages) for SSC magnets
[DE92-010722] p 3826 N92-31313
Resonant enhancement of flavor-changing neutrino interactions
[DE92-013020] p 3898 N92-32167
FIMOD CORP., BLACKSBURG, VA.
Optical fiber sensors for organic matrix composite material cure monitoring
[AD-A247114] p 3776 N92-31979
FLINDERS UNIV., ADELAIDE (AUSTRALIA).
Electron scattering by atomic hydrogen: Elastic and inelastic phenomena at 13.9 to 200 eV
[DE92-625004] p 3896 N92-31837
FLORIDA ATLANTIC UNIV., BOCA RATON.
Logarithmic retinae
[PB92-183649] p 3885 N92-31680
FLORIDA STATE UNIV., TALLAHASSEE.
He atom-surface scattering: Surface dynamics of insulators, overlayers and crystal growth
[DE92-011810] p 3911 N92-31914
FLORIDA UNIV., GAINESVILLE.
Geomorphic variability in the coastal zone
[AD-A252713] p 3864 N92-31544
A tumbling top-quark condensate model
[DE92-016194] p 3893 N92-31552
Molecular interactions and properties with many-body methods
[AD-A247052] p 3896 N92-31858
The effect of surface pressure on Langmuir-Blodgett polymerization of 2-pentadecyl aniline
[AD-A250993] p 3795 N92-31952
Real time investigations of the polymerization of 2-pentadecyl aniline on the Langmuir-Blodgett trough
[AD-A250994] p 3795 N92-31954
Ionization potentials and electron affinities of semiconductor clusters determined via charge transfer reactions
[AD-A250943] p 3898 N92-32169
An improved ion guide for external ion injection in glow discharge-Fourier transform ion cyclotron resonance (GD-FTICR) mass spectrometry
[AD-A250944] p 3900 N92-32170
Polymerization of conducting polymers confined to free surfaces: A comparison of the Langmuir-Blodgett polymerization of 3-alkyl pyrroles and 2-alkyl anilines
[AD-A250966] p 3798 N92-32194
FOREST SERVICE, RESEARCH TRIANGLE PARK, NC.
Methods of assessing responses of trees, stands and ecosystems to air pollution
[PB92-180231] p 3853 N92-31648
FREIE UNIV., BERLIN (GERMANY, F.R.).
Meteorological data, new series B basic material. Volume 53, no. 1: Daily altitude maps of the 30-hPa-area and monthly mean maps for the year 1986, part 1
[QR-1-VOL-53-NO-1-PT-1] p 3860 N92-31702
Meteorological data, new series B basic material. Volume 53, no. 2: Daily altitude maps of the 30-hPa-area and monthly mean maps for the year 1986, part 2
[QR-2-VOL-53-NO-2-PT-2] p 3860 N92-31704
Meteorological data, new series B basic material. Volume 53, no. 4: Daily altitude maps of the 30-hPa-area and monthly mean maps for the year 1986, part 4
[QR-4-VOL-53-NO-4-PT-4] p 3861 N92-31706
Meteorological data, new series A monographs. Volume 5, no. 4: A three dimensional model simulation of the circulation in the middle atmosphere with cconsideration of tropospherical-stratospherical interactions
[ETN-92-91693] p 3861 N92-31708
Meteorological data, new series A monographs. Volume 6, no. 2: Case study on the congruence of precipitation data from SYNOP-MODELL and Meteosat data
[ETN-92-91694] p 3861 N92-31710

G

GENCORP AEROJET, SACRAMENTO, CA.
Pressure fed thrust chamber technology program
[NASA-CR-190666] p 3770 N92-31550
Orbital transfer rocket engine technology: Advanced engine study
[NASA-CR-187216] p 3771 N92-32129
GENERAL ACCOUNTING OFFICE, WASHINGTON, DC.
Aviation safety: Changes needed in FAA's service difficulty reporting program
[GAO/RCED-91-24] p 3755 N92-31453
Aviation noise: Costs of phasing out noisy aircraft
[GAO/RCED-91-128] p 3891 N92-31454
GENERAL ATOMIC CO., SAN DIEGO, CA.
Real time analysis of tokamak discharge parameters
[DE92-011394] p 3904 N92-31616
A global fitting code for multichordal neutral beam spectroscopic data
[DE92-014258] p 3781 N92-31729
Divertor material evaluation system at D3-D
[DE92-013696] p 3905 N92-31749
A phase contrast interferometer on D3-D
[DE92-012699] p 3905 N92-31764

GENERAL ELECTRIC CO., CINCINNATI, OH.
High speed turboprop aeroacoustic study (counterrotation). Volume 2: Computer programs
[NASA-CR-185242] p 3891 N92-31248
GEORGE WASHINGTON UNIV., WASHINGTON, DC.
Development and application of new algorithms for the simulation of compressible flows with moving bodies in three dimensions
[AD-A250232] p 3823 N92-31696
Auger line shapes as a probe of electronic structure in covalent systems
[AD-A246329] p 3912 N92-31994
Dissociative electron attachment of O2: A solid-state effect on potential curve crossing
[AD-A246331] p 3913 N92-31995
GEORGETOWN UNIV., WASHINGTON, DC.
Development of effective quantum chemical method for polymers and solid
[AD-A250976] p 3795 N92-31951
GEORGIA INST. OF TECH., ATLANTA.
Modeling of composite beams and plates for static and dynamic analysis
[NASA-CR-190536] p 3839 N92-31339
Acquisition and production of skilled behavior in dynamic decision-making tasks
[NASA-CR-190614] p 3870 N92-31341
Poloidal rotation and density asymmetries in a tokamak plasma with strong toroidal rotation
[PB92-182534] p 3904 N92-31613
Pulse Combustion Engineering Research Laboratory: Exhaust energy
[PB92-172402] p 3783 N92-31918
GHG CORP., HOUSTON, TX.
Mission and Safety Critical (MASC) plans for the MASC Kernel simulation
[NASA-CR-190708] p 3875 N92-31487
GLASGOW UNIV. (SCOTLAND).
Non Boolean search methods in information retrieval
p 3921 N92-32187
GOSUDARSTVENNYI KOMITET PO ISPOLZOVANIYU ATOMNOI ENERGII, OBNINSK (USSR).
Resolution function of an inelastic scattering spectrometer with a pulsed neutron source
[DE92-620889] p 3896 N92-31904
GRUMMAN AEROSPACE CORP., BETHPAGE, NY.
Highly accurate prediction of unsteady viscous flows
[AD-A250982] p 3825 N92-32000

H

HARRY DIAMOND LABS., ADELPHI, MD.
External combustion engine technology (vapor and liquid cycles) for individual soldier power systems
[AD-A252754] p 3836 N92-32173
HARVARD UNIV., CAMBRIDGE, MA.
Modelling and prediction of regions of the North Pacific
[AD-A252144] p 3863 N92-31406
Forms of memory for representation of visual objects
[AD-A250056] p 3871 N92-31779
Tris-triphenylsiloxy compounds of aluminum
[AD-A250141] p 3788 N92-31795
The preparation of (Al2O3)x(SiO2)y thin films using (Al(OSiEt3))2 as a single source precursor
[AD-A250142] p 3788 N92-31796
Supersonic pyrolysis jets for diamond film deposition
[AD-A251125] p 3798 N92-32198
HAWAII UNIV., HONOLULU.
Physical characterization of magmatic liquids
[DE92-015302] p 3858 N92-32027
HCC SCIENCE AND TECHNOLOGY CO., SUMMIT, NJ.
Polymer blends, volume 1
[AD-A252112] p 3792 N92-31419
HELSINKI UNIV. OF TECHNOLOGY, ESPOO (FINLAND).
Thermodynamic assessment of the Cr-Zr system
[PB92-180645] p 3787 N92-31610
HONEYWELL, INC., MINNEAPOLIS, MN.
Artificial Intelligence in Training (AIT)
[AD-A250145] p 3885 N92-31811
HOWARD UNIV., WASHINGTON, DC.
Eigensensitivity analysis of composite laminates: Effect of microstructure
[AD-A250864] p 3777 N92-32104
HUMAN SYSTEMS DIV., BROOKS AFB, TX.
Micro saint model of fatigue assessment
[AD-A249976] p 3868 N92-31554
HUNTSVILLE ASSOCIATION OF TECHNICAL SOCIETIES, AL.
TABES 92: 8th Annual Technical and Business Exhibition and Symposium. Executive summaries and submitted papers p 3763 N92-32009

I

IIT RESEARCH INST., CHICAGO, IL.
Extremely Low Frequency (ELF) communications system ecological monitoring program summary of 1990 progress
[AD-A246344] p 3809 N92-31996
ILLINOIS UNIV., URBANA.
Analysis and design of neural networks
[AD-A250495] p 3884 N92-31332
Non-equilibrium synthesis by laser cladding of Ni, Nb and Mg alloys for improved environmental resistance
[AD-A250552] p 3787 N92-31612
ILLINOIS UNIV., URBANA-CHAMPAIGN.
A proposal for the establishment of a Center for Advanced Composite Materials Research
[AD-A250072] p 3773 N92-31361
IMPLANT SCIENCES CORP., WAKEFIELD, MA.
Strongly adherent ceramic surface layers by ion implantation
[AD-A248882] p 3792 N92-31388
INDUSTRIAL TECHNOLOGY INST., ANN ARBOR, MI.
A program for the transfer of manufacturing technology from the national laboratories
[DE92-011905] p 3923 N92-31965
INSTITUT DES HAUTES ETUDES SCIENTIFIQUES, BURES-SUR-YVETTE (FRANCE).
Feynman diagrams and Vassiliev invariants
[PB92-178284] p 3890 N92-31925
INSTITUT NATIONAL DES SCIENCES ET TECHNIQUES NUCLEAIRES, SACLAY (FRANCE).
Intelligent gateways p 3921 N92-32184
INSTITUTE FOR COMPUTER APPLICATIONS IN SCIENCE AND ENGINEERING, HAMPTON, VA.
Adaptive mesh strategies for the spectral element method
[NASA-CR-189686] p 3818 N92-31265
Sensitivity analysis of hydrodynamic stability operators
[NASA-CR-189683] p 3822 N92-31535
PARTI primitives for unstructured and block structured problems
[NASA-CR-189662] p 3876 N92-31561
Development of wavelet analysis tools for turbulence
[NASA-CR-189674] p 3822 N92-31564
On the spatial evolution of long-wavelength Goertler vortices governed by a viscous-inviscid interaction
[NASA-CR-189681] p 3822 N92-31687
A sweep algorithm for massively parallel simulation of circuit-switched networks
[NASA-CR-189680] p 3881 N92-32157
Reynolds stress calculations of homogeneous turbulent shear flow with bounded energy states
[NASA-CR-189682] p 3826 N92-32158
Nonlinearly stable compact schemes for shock calculations
[NASA-CR-189663] p 3887 N92-32164
INSTITUTE FOR DEFENSE ANALYSES, ALEXANDRIA, VA.
Pilot errors involving Head-Up Displays (HUDs), Helmet-Mounted Displays (HMDs), and Night Vision Goggles (NVGs)
[AD-A250719] p 3873 N92-32023
INSTITUTE FOR NAVAL OCEANOGRAPHY, BAY SAINT LOUIS, MS.
Synthetic temperature profile in the Gulf of Mexico. Part 1: Statistical relationship between modal amplitudes and dynamic height at surface
[AD-A252701] p 3863 N92-31308
INSTITUTE OF OCEAN SCIENCES, SIDNEY (BRITISH COLUMBIA).
Acoustic studies of ocean surface processes in SWAPP
[AD-A247519] p 3864 N92-31429
INSTITUTO DE PESQUISAS ESPACIAIS, SAO JOSE DOS CAMPOS (BRAZIL).
The vehicle routing problem: Some computational tests of savings method and its variations
[INPE-5361-RPQ/656] p 3886 N92-31241
Procedures and errors in the determination of the bi-directional reflectance factor and other radiometric quantities
[INPE-5386-TDI/475] p 3843 N92-31277
G305.8 - 0.2 water vapour source: A young object
[INPE-5337-PRE/1736] p 3923 N92-31343
Photometry of Nova Muscae 1983
[INPE-5339-PRE/1738] p 3923 N92-31344
The eclipsing cataclysmic variable AY Piscium
[INPE-5340-PRE/1739] p 3923 N92-31345
The eclipsing cataclysmic variable NSV 12615 (V4041 Sgr)
[INPE-5342-PRE/1741] p 3923 N92-31346
Accretion disk image reconstruction in cataclysmic variables
[INPE-5343-PRE/1742] p 3923 N92-31347
The Swendsen-Wang dynamics in the simulation of the Ising model
[INPE-5394-PRE/1752] p 3874 N92-31348
Changes in the reflectance of ex situ leaves: A methodological approach
[INPE-5407-PUD/051] p 3806 N92-31568
Multiple electron populations accelerated in solar bursts
[INPE-5377-TDI/472] p 3925 N92-32025
Tetragonal zirconia ceramics in ZrO2-CeO2 system (Ce-TZP): Preparation, characterization and mechanical properties
[INPE-5372-PRE/1746] p 3798 N92-32199
Ba2Ti9O20 microwave dielectric resonator: Processing, phase synthesis and characterization
[INPE-5373-PRE/1747] p 3818 N92-32200
A coordinated study of a storm system over the South American continent
[INPE-5388-TDI/477] p 3863 N92-32212
Images simulation of sensors with large field of view from images of sensors with less field of view: The SSR/TM case
[INPE-5378-TDI/473] p 3845 N92-32220
Fine structure superimposed on mm-wavelength (18-23 GHz) spectra of solar active region
[INPE-5371-TDI/470] p 3926 N92-32221
Rainwater and throughfall chemistry in a terra firme rain forest: Central Amazonia
[INPE-5364-PRE/1744] p 3863 N92-32224
Markovian fields as limits of Markov chains
[INPE-5395-PRE/1753] p 3889 N92-32225
GIS: Geographic Information Systems. State of the art and future tendencies
[INPE-5358-NTC/301] p 3922 N92-32227
INTERFACIAL SCIENCES, INC., SANTA CLARA, CA.
Electrochemical oxidation of methane for fuel cells
[PB92-172303] p 3848 N92-31922
INTERNATIONAL ATOMIC ENERGY AGENCY, VIENNA (AUSTRIA).
Directory of IAEA databases
[DE92-628395] p 3920 N92-32058
INTERNATIONAL CENTRE FOR THEORETICAL PHYSICS, TRIESTE (ITALY).
Modified black holes in two dimensional gravity
[DE92-630244] p 3924 N92-31401
A dynamical model of the behaviour of hadronic and fundamental strings at finite densities
[DE92-630245] p 3914 N92-31402
Schwinger boson studies of the t-J model beyond mean-field approximation
[DE92-630650] p 3909 N92-31655
Rigid rotations in two-electron atoms in a uniform magnetic field
[DE92-624981] p 3896 N92-31836
IOWA STATE UNIV. OF SCIENCE AND TECHNOLOGY, AMES.
Intermediate/high energy nuclear physics
[DE92-015363] p 3900 N92-32028
ISRAEL AIRCRAFT INDUSTRIES LTD., BEN-GURION AIRPORT.
The calculation of incompressible separated turbulent boundary layers p 3749 N92-31886
Euler solver for arbitrary configurations: Further applications p 3750 N92-31888
ISRAEL AIRCRAFT INDUSTRIES LTD., LOD.
FCS skewed sensors array: Practical considerations
p 3746 N92-31868
ISRAEL AIRCRAFT INDUSTRIES LTD., YEHUD.
A novel control-guidance law for low-thrust orbit maneuver p 3747 N92-31874
ISRAEL MILITARY INDUSTRIES, RAMAT-HASHARON (ISRAEL).
Optimal trajectories for an unmanned air vehicle
p 3748 N92-31880
Flammability limits and ballistic properties of fuel-rich propellants p 3749 N92-31885
ISRAEL SOCIETY OF AERONAUTICS AND ASTRONAUTICS, TEL AVIV.
Collection of papers of the 31st Israel Annual Conference on Aviation and Astronautics
[ITN-92-85124] p 3745 N92-31861
ITALIAN SPACE AGENCY, ROME.
Space Station mini pressurised logistics modules: An opportunity to enlarge and reinforce international cooperation
[TABES PAPER 92-425] p 3764 N92-32016

J

JAPAN ATOMIC ENERGY RESEARCH INST., TOKYO.
Correspondence dictionary from free English term to INIS descriptors
[DE92-782192] p 3920 N92-31859

JOHNS HOPKINS UNIV., BALTIMORE, MD.
Noise-induced chaos and phase space flux: A sample-theoretic study
[PB92-172733] p 3915 N92-31645
Theoretical studies of the reactions and spectroscopy of radical species relevant to combustion reactions and diagnostics
[DE92-013484] p 3781 N92-31725
JOINT INST. FOR MARINE AND ATMOSPHERIC RESEARCH, HONOLULU, HI.
Biology, oceanography, and fisheries of the North Pacific transition zone and subarctic frontal zone
[PB92-178128] p 3866 N92-32106
JOINT PUBLICATIONS RESEARCH SERVICE, ARLINGTON, VA.
JPRS report: Science and technology. Central Eurasia: Materials science
[JPRS-UMS-92-010] p 3787 N92-31584
JPRS report: Science and technology. Central Eurasia: Earth sciences
[JPRS-UES-92-004] p 3843 N92-32132
JPRS report: Science and technology. Central Eurasia: Life sciences
[JPRS-ULS-92-015] p 3924 N92-32179
Methane-producing microorganisms: Component of Mars biosphere p 3924 N92-32180
JUSZKO SCIENTIFIC SERVICES, VICTORIA (BRITISH COLUMBIA).
Parameterization of directional spectra, part 2, volume 1
[DREA-CR-89-445-PT-2-VOL-1] p 3811 N92-32214

K

KANSAS UNIV., LAWRENCE.
Radar backscatter from the sea: Controlled experiments
[AD-A250858] p 3810 N92-32101
KYOTO UNIV., KUMATORI (JAPAN).
Proceedings of the 2nd KUR symposium on hyperfine interactions
[DE92-789024] p 3895 N92-31728

L

LABORATOIRE D'AEROTHERMIQUE DU CNRS, MEUDON (FRANCE).
Flat plates placed in depleted hypersonic flow
[SESSIA-430/91.960] p 3751 N92-31508
LABORATOIRE D'AUTOMATIQUE ET D'ANALYSE DES SYSTEMES, TOULOUSE (FRANCE).
About real time industrial processes control: A methodology based on objects and Petri nets
[LAAS-91467] p 3878 N92-31689
Mathematical structures for qualitative calculus, a contribution to qualitative simulation
[LAAS-91475] p 3886 N92-31690
From perception to modelization in robotics using achromatic and chromatic cameras
[LAAS-91484] p 3901 N92-31692
Continuous time and discrete time hyperexponential model for dependability growth modeling
[LAAS-92002] p 3837 N92-31693
Control of rapid thermal processing equipment for microelectronics applications
[LAAS-92013] p 3787 N92-31695
Static and dynamic properties of current sensing power VDMOS transistor
[LAAS-92032] p 3815 N92-31697
Phase-locked arrays of antiguided diode lasers: Modelling, design, evaluation of performance limits
[LAAS-92034] p 3830 N92-31698
LAMONT-DOHERTY GEOLOGICAL INST., PALISADES, NY.
Steady-state and transient modeling of tracer and nutrient distributions in the global ocean
[DE92-011805] p 3864 N92-31572
Methods of assessing responses of trees, stands and ecosystems to air pollution
[PB92-180231] p 3853 N92-31648
LAMONT-DOHERTY GEOLOGICAL OBSERVATORY, PALISADES, NY.
Lamont-Doherty Geological Observatory
[PB92-185040] p 3856 N92-31636
LASERGENICS CORP., SAN JOSE, CA.
Single crystal growth optimization of magnesium-doped lithium niobate
[AD-A250781] p 3914 N92-32207
LAWRENCE LIVERMORE NATIONAL LAB., CA.
Effects of anthropogenic sulfur aerosols on climate
[DE92-016158] p 3850 N92-31297
The validation of atmospheric models
[DE92-013254] p 3850 N92-31324
Calculational prediction of ultrawideband electromagnetic pulses by laser-initiated air avalanche switches
[DE92-011732] p 3812 N92-31334
The synthesis and characterization of new copper coordination complexes containing an asymmetric coordinating chelate ligand: Application to enzyme active site modeling
[DE92-011532] p 3786 N92-31391
Propane oxidation through the negative temperature coefficient region at 10 and 15 atmospheres: Results of experimental and modeling studies
[DE92-007902] p 3778 N92-31414
High-temperature ignition of propane with MTBE as an additive: Shock-tube experiments and modeling
[DE92-008933] p 3778 N92-31415
Two-stage n-butane flame: A comparison between experimental measurements and modeling results
[DE92-009457] p 3779 N92-31416
Numerical simulation of precipitation scavenging and comparison with observation of prescribed forest fires
[DE92-013513] p 3851 N92-31423
Data parallel programming
[DE92-013981] p 3882 N92-31466
Plane stokes flow driven by capillarity on a free surface: Overview and status
[DE92-011469] p 3821 N92-31528
YLIFE-2 inertial fusion energy power plant design
[DE92-011965] p 3904 N92-31530
High-pressure gas switch for a wideband source
[DE92-015822] p 3815 N92-31548
Sol-gel multilayers applied by a meniscus coating process
[DE92-012697] p 3794 N92-31560
Hydrocarbon ignition: Automatic generation of reaction mechanisms and applications to modeling of engine knock
[DE92-011943] p 3780 N92-31607
Biodosimetry of ionizing radiation in humans using the glycophorin A genotoxicity assay
[DE92-011974] p 3869 N92-31608
Turbulent dusty boundary layer in an ANFO surface-burst explosion
[DE92-012101] p 3822 N92-31625
Photon absorption and the decay of surface excitation on sapphire (1120)-(3 x 1)
[DE92-011533] p 3910 N92-31661
Analysis of the effects of aerosol distribution in the atmosphere on surface radiative measurements
[DE92-014189] p 3856 N92-31662
Superplasticity in a nickel silicide alloy, Ni3Si(V, Mo)
[DE92-011651] p 3787 N92-31667
Photon and electron data bases and their use in radiation transport calculations
[DE92-011458] p 3895 N92-31705
Subnanosecond photoconductive switching in GaAs
[DE92-011521] p 3910 N92-31719
Ionospheric communications channel modelling
[DE92-013039] p 3808 N92-31722
Projectile development for railguns using hypervelocity preacceleration
[DE92-016741] p 3766 N92-31735
A task adaptive parallel graphics rendering algorithm
[DE92-008062] p 3878 N92-31739
The multicomputer toolbox: Scalable parallel libraries for large-scale concurrent applications
[DE92-008068] p 3882 N92-31740
PDDP: Data-driven parallelism and shared memory
[DE92-008073] p 3883 N92-31741
The Matrix Editor for symbolic Jacobians in ALPAL
[DE92-008076] p 3878 N92-31742
New algorithms for the minimal form problem
[DE92-011963] p 3879 N92-31743
A fast laser alloying process for the selective electroplating of metal on SiO2 and polyimide
[DE92-011764] p 3788 N92-31759
Resolution limits for ground based astronomical imaging using adaptive optics
[DE92-011949] p 3902 N92-31761
Autoignition behavior of lean mixtures: Chemical and thermodynamics effects
[DE92-009690] p 3781 N92-31763
Numerical simulation of tulip flame dynamics
[DE92-008553] p 3782 N92-31805
High performance of copper pumped dye lasers
[DE92-011763] p 3832 N92-31902
Capabilities of the 3-axes modified FP42 Deckel milling machine
[DE92-011737] p 3803 N92-31908
Dispersive-infrared gas sensor system design and operation manual
[DE92-011766] p 3828 N92-31909
A model for extending the behavior of annotations
[DE92-011731] p 3920 N92-31934
Institute of Geophysics and Planetary Physics, 1991
[DE92-016981] p 3923 N92-32005
Optimal targeting of evading objects
[DE92-014719] p 3889 N92-32119
Modeling and design of a closed kinematic chain robotic mechanism
[DE92-014777] p 3835 N92-32121
Evolution of reactants fluid volume in turbulent jets
[DE92-011298] p 3786 N92-32145
NASA High Speed Research Program, Emissions Scenarios Committee report of meetings on 26 September 1991 and 9 January 1992
[NASA-CR-190379] p 3855 N92-32147
Global trends in energy use: Indications for research
[DE92-014773] p 3855 N92-32155
Aluminum tunnel junction detector operation in an adiabatic demagnetization refrigerator
[DE92-013441] p 3913 N92-32166
LEHIGH UNIV., BETHLEHEM, PA.
Design and automated manufacturing p 3746 N92-31866
LOCKHEED MISSILES AND SPACE CO., CALABASAS, CA.
NASA programs p 3765 N92-32238
LOCKHEED MISSILES AND SPACE CO., PALO ALTO, CA.
A solar magnetic and velocity field measurement system for Spacelab 2: The Solar Optical Universal Polarimeter (SOUP)
[NASA-CR-190683] p 3925 N92-31856
LOCKHEED MISSILES AND SPACE CO., SUNNYVALE, CA.
Design, analysis, and testing of the Phase 1 CSI Evolutionary Model erectable truss
[NASA-CR-4461] p 3767 N92-32100
LOS ALAMOS NATIONAL LAB., NM.
Wavenumbers for currents on infinite- and finite-length wires in a chiral medium
[DE92-007565] p 3804 N92-31317
A model for the interfacial shear in vertical, adiabatic, annular-mist flow
[DE92-013537] p 3820 N92-31424
Readily implemented enhanced sinusoid detection in noise
[DE92-011359] p 3806 N92-31449
Batteries and fuel cells
[DE92-011493] p 3847 N92-31571
ANTHEM simulational studies of the plasma opening switch
[DE92-015247] p 3815 N92-31681
Establishing low-power operating limits for liquid metal heat pipes
[DE92-011367] p 3823 N92-31701
Some computational challenges of developing efficient parallel algorithms for data-dependent computations in thermal-hydraulics supercomputer applications
[DE92-011368] p 3878 N92-31703
Microstructure and properties of in-situ RF sputtered YBa2Cu3O7 thin films for microwave applications
[DE92-013379] p 3911 N92-31723
Problems in neutrino electron scattering with 1-GeV neutrinos
[DE92-013535] p 3895 N92-31765
Analytical and experimental studies of heat pipe radiation cooling of hypersonic propulsion systems
[DE92-013428] p 3759 N92-31817
Laser-ablated copper condensation in helium
[DE92-016685] p 3789 N92-32004
FEHMN 1.0: Finite element heat and mass transfer code
[DE92-013998] p 3825 N92-32008
CAVEAT: A computer code for fluid dynamics problems with large distortion and internal slip
[DE92-014078] p 3825 N92-32022
Problems associated with launching hypervelocity projectiles from the fast shock tube
[DE92-015276] p 3762 N92-32026
LOUGHBOROUGH UNIV. OF TECHNOLOGY (ENGLAND).
Nonlinear partial differential equations and solitons
[MATHS-REPT-A-152] p 3886 N92-31956
A fundamental notion of equivalence for linear multivariable systems
[MATHS-REPT-A-153] p 3887 N92-31957
LOUISIANA STATE UNIV., BATON ROUGE.
The interplanetary heavy ion environment for both galactic cosmic rays and solar energetic particles during the CRRES mission
[AD-A248942] p 3926 N92-31477
The structure of nuclei far from beta stability
[DE92-012598] p 3895 N92-31721

M

MANTECH ENVIRONMENTAL TECHNOLOGY, INC., CORVALLIS, OR.
Methods of assessing responses of trees, stands and ecosystems to air pollution
[PB92-180231] p 3853 N92-31648

MARTIN MARIETTA CORP., DENVER, CO.
Interplanetary Program to Optimize Space Trajectories (IPOST). Volume 3: Programmer's manual
[NASA-CR-189653-VOL-3] p 3766 N92-32130

MARTIN MARIETTA LABS., BALTIMORE, MD.
Surface analysis of stainless steel outer race bearing specimens
[AD-A250088] p 3833 N92-31437

MARYLAND UNIV., BALTIMORE.
Acetylcholinesterase inhibitors on the spinal cord
[AD-A252694] p 3868 N92-31326
Total quality management: A management philosophy for providing high quality construction
[AD-A252743] p 3837 N92-32172

MARYLAND UNIV., COLLEGE PARK.
On the feasibility of a transient dynamic design analysis method
[AD-A250406] p 3838 N92-31337
Iterative methods for large sparse linear systems arising from partial differential equations
[AD-A249524] p 3886 N92-31567
Microwave generation for magnetic fusion energy applications
[DE92-011424] p 3831 N92-31769
The use of high lift-to-drag hypersonic vehicles for aero-assisted orbital maneuvering p 3748 N92-31877
A study of longwave radiation codes for climate studies: Validation with ARM observations and tests in general circulation models
[DE92-014100] p 3862 N92-31894
Theoretical studies in nuclear reactions and nuclear structure
[DE92-016204] p 3897 N92-31927
Backlash control via redundant drives: An experimental verification
[DE92-016368] p 3835 N92-31929
Millimeter wave free electron laser amplifiers: Experiments and designs
[DE92-011813] p 3832 N92-31935
Signal processing and recognition in adaptive neural networks
[AD-A250505] p 3885 N92-32041

MASSACHUSETTS INST. OF TECH., CAMBRIDGE.
Spacecraft dynamics characterization and control system failure detection. Volume 3: Control system failure monitoring
[NASA-CR-190529] p 3884 N92-31254
The 3-D analysis and verification of fracture growth mechanisms in fiber-reinforced ceramic composies
[AD-A250893] p 3773 N92-31305
Synthesis of side chain liquid crystal polymers by living ring opening metathesis polymerization. 4: Synthesis of amorphous and side chain liquid crystal AB block copolymers
[AD-A250353] p 3792 N92-31394
Optimized photorefractive barium titanate
[AD-A250089] p 3908 N92-31438
Research in regional seismology: The effect of anisotropy
[AD-A248940] p 3855 N92-31476
f Mo(CHCMe2Ph)(NAr)(OR)2 and relative reactivity toward 2,3-bis(trifluoromethyl) norbornadiene iene
[AD-A250234] p 3780 N92-31524
Fusion development and technology
[DE92-014352] p 3904 N92-31545
Cyclopolymerization of metalloid-containing alpha, omega-dienes. 1,3-divinyltetramethyldisiloxane, 1,3-divinyltetramethyldisilazane and 1,3-divinylpentamethyldisilazane
[AD-A250347] p 3794 N92-31557
Macrostatistical hydrodynamics
[DE92-013589] p 3823 N92-31726
Deterministic analysis of processes at corroding metal surfaces and the study of electrochemical noise in these systems
[DE92-016286] p 3788 N92-31733
Turbine blade tip and seal clearance excitation forces
[NASA-CR-184341] p 3760 N92-31910
New directions in network flows
[AD-A250499] p 3880 N92-32039
Femtosecond photonics: Fundamental phenomena and device behavior
[AD-A250506] p 3832 N92-32042
A comparison of the performance of two gust front detection algorithms using a length-based scoring technique
[AD-A250862] p 3863 N92-32103
Full abstraction and the context lemma
[AD-A247062] p 3887 N92-32163
Advanced microwave sounding unit study for atmospheric infrared sounder
[NASA-CR-190628] p 3858 N92-32195
A test of ecological optimality for semiarid vegetation
[NASA-CR-190705] p 3855 N92-32222

MASSACHUSETTS UNIV., AMHERST.
Theoretical studies of solid-fluid phase equilibria
[DE92-016598] p 3781 N92-31717

MCAT INST., SAN JOSE, CA.
Hypersonic code efficiency and validation studies
[NASA-CR-190680] p 3752 N92-31533
Control of unsteady separated flow associated with the dynamic stall of airfoils
[NASA-CR-190688] p 3753 N92-32177

MCDONNELL-DOUGLAS CORP., HUNTSVILLE, AL.
SPACEHAB: A giant step in the commercial development of space
[TABES PAPER 92-454] p 3764 N92-32018

MCMASTER UNIV., HAMILTON (ONTARIO).
Detection of signal harmonic sets
[DREA-CR-89-420] p 3806 N92-31471

MCR TECHNOLOGY, INC., CHICAGO, IL.
High brightness x ray source for directed energy and holographic imaging applications, phase 2
[AD-A248858] p 3827 N92-31475

MEDICAL COLL. OF VIRGINIA, RICHMOND.
The effects of hydrazines of neuronal excitability
[AD-A247142] p 3868 N92-31491

MESSERSCHMITT-BOELKOW-BLOHM G.M.B.H., MUNICH (GERMANY, F.R.).
Pressure loss and heat transfer in a toothed finned heat transfer medium
[MBB-UO-0163-91-PUB] p 3915 N92-31660
Cutting treatment by drilling of fiber bound synthetic materials
[MBB-UD-0609-91-PUB] p 3774 N92-31716

MICHIGAN STATE UNIV., EAST LANSING.
A simple linearized learning algorithm which outperforms back-propagation
[AD-A249697] p 3877 N92-31642
Signal and noise models arising from the theory of errors
[AD-A250222] p 3885 N92-31827

MICHIGAN UNIV., ANN ARBOR.
Electromagnetic scattering by coated convex surfaces and wedges simulated by approximate boundary conditions
[NASA-CR-190540] p 3803 N92-31238
A finite element-boundary integral method for conformal antenna arrays on a circular cylinder
[NASA-CR-190534] p 3807 N92-31614
Computation of nonlinear gravity waves by a desingularized boundary integral method
[AD-A251149] p 3857 N92-31766
Development of gamma ray imaging cameras
[DE92-015305] p 3828 N92-31919

MIDWEST RESEARCH INST., GOLDEN, CO.
Simplified air change effectiveness modeling
[DE92-010577] p 3872 N92-31309
Solar synthesis of advanced materials: A solar industrial program initiative
[DE92-010575] p 3845 N92-31481
Module process optimization and device efficiency improvement for stable, low-cost, large-area, cadmium telluride-based photovoltaic module production
[DE92-010564] p 3846 N92-31497
A surface definition code for turbine blade surfaces
[DE92-010574] p 3846 N92-31498
Research on stable, high-efficiency amorphous silicon multijunction modules
[DE92-001244] p 3814 N92-31525
Development of a computer model for polycrystalline thin-film CuInSe2 and CdTe solar cells
[DE92-001242] p 3846 N92-31526
Cooperative field test program for wind systems
[DE92-001209] p 3847 N92-31579
Catalyst and feedstock effects in the thermochemical conversion of biomass to liquid transportation fuels
[DE92-010569] p 3799 N92-31593
Outdoor testing of advanced optical materials for solar thermal electric applications
[DE92-010567] p 3847 N92-31623
Photovoltaic subcontract program, FY 1991
[DE92-001248] p 3847 N92-31646
Advanced high efficiency concentrator cells
[DE92-010559] p 3848 N92-31893
Synthesis of cresols and xylenols from phenol and methanol
[DE91-002141] p 3785 N92-32093
Computer simulation of shading and blocking: Discussion of accuracy and recommendations
[DE91-002146] p 3849 N92-32110
Desiccant cooling using unglazed transpired solar collectors
[DE92-010568] p 3849 N92-32112

MINNESOTA UNIV., MINNEAPOLIS.
Human image understanding
[AD-A250401] p 3872 N92-31330
Ultrafast experiments on the role of vibrational modes in electron transfer
[AD-A250630] p 3910 N92-31699
Epitaxial iron films
[AD-A250402] p 3912 N92-31915
Vibrational modes and the dynamic solvent effect in electron and proton transfer
[AD-A250727] p 3897 N92-31950
Ultrafast studies on electron transfer in the betaines: Evidence for local heating
[AD-A250728] p 3897 N92-31999

MISSOURI UNIV., ROLLA.
Characterization of oxides for low temperature solid oxide fuel cells
[PB92-152883] p 3848 N92-31903

MITRE CORP., BEDFORD, MA.
Compression of digitized map images
[AD-A250707] p 3843 N92-31323
A performance-based comparison of object-oriented simulation tools
[AD-A252125] p 3875 N92-31405
Validation of the Numerical Electro-magnetics Code (NEC) for antenna wire elements in proximity to Earth
[AD-A250507] p 3810 N92-32043

MORGANTOWN TECHNOLOGY CENTER, WV.
The 193-pixel, three-dimensional capacitance imaging system
[DE92-001253] p 3919 N92-31731

N

NATIONAAL INST. VOOR KERNFYSICA EN HOGE ENERGIEFYSICA, AMSTERDAM (NETHERLANDS).
Efficiency calculations of the hadron detector
[NIKHEF-K-EMIN-92-01] p 3896 N92-31814
Injecting into AmPS when ring cavity operates at 476 MHz
[NIKHEF-K/AMPS/91-08] p 3899 N92-31815

NATIONAL ACID PRECIPITATION ASSESSMENT PROGRAM, WASHINGTON, DC.
Acid deposition: State of science and technology. Summary report of the US National Acid Precipitation Assessment Program, volumes 1-4
[PB92-100353] p 3852 N92-31598

NATIONAL AERONAUTICS AND SPACE ADMINISTRATION, WASHINGTON, DC.
Small Business Innovation Research program solicitation. Closing date: July 21, 1992
[NASA-TM-107795] p 3916 N92-31253
The detection of climate change due to the enhanced greenhouse effect
[NASA-TM-107965] p 3849 N92-31258
NASA patent abstracts bibliography: A continuing bibliography. Section 2: Indexes (supplement 41)
[NASA-SP-7039(41)-SECT-2] p 3918 N92-31455
Aeronautical engineering: A continuing bibliography with indexes (supplement 280)
[NASA-SP-7037(280)] p 3745 N92-31456
Integrated Technology Plan for the Civil Space Program, 1991
[PB92-181692] p 3762 N92-31634
Hypertext and hypermedia systems in information retrieval p 3921 N92-32188

NATIONAL AERONAUTICS AND SPACE ADMINISTRATION. AMES RESEARCH CENTER, MOFFETT FIELD, CA.
NAS (Numerical Aerodynamic Simulation Program) technical summaries, March 1989 - February 1990
[NASA-TM-107960] p 3926 N92-31852
Transonic wind tunnel test of a 14 percent thick oblique wing
[NASA-TM-102230] p 3754 N92-32213

NATIONAL AERONAUTICS AND SPACE ADMINISTRATION. GODDARD SPACE FLIGHT CENTER, GREENBELT, MD.
Extended Kalman filter for attitude estimation of the Earth Radiation Budget Satellite p 3748 N92-31876
True covariance simulation of the EUVE (extreme ultra violet explorer) update filter p 3748 N92-31878

NATIONAL AERONAUTICS AND SPACE ADMINISTRATION. HUGH L. DRYDEN FLIGHT RESEARCH FACILITY, EDWARDS, CA.
Overview of the NASA Dryden Flight Research Facility aeronautical flight projects
[NASA-TM-104254] p 3756 N92-31261
Subsonic flight test evaluation of a performance seeking control algorithm on an F-15 airplane
[NASA-TM-4400] p 3759 N92-31275

In-flight leading-edge extension vortex flow-field survey measurements on a F-18 aircraft at high angle of attack
[NASA-TM-4398] p 3751 N92-31276
In-flight evaluation of aerodynamic predictions of an air-launched space booster
[NASA-TM-104246] p 3752 N92-31808
System overview of the NASA Dryden Integrated Test Facility
[NASA-TM-104250] p 3762 N92-32201

NATIONAL AERONAUTICS AND SPACE ADMINISTRATION. LYNDON B. JOHNSON SPACE CENTER, HOUSTON, TX.

Using space resources
[NASA-TM-107966] p 3924 N92-31781

NATIONAL AERONAUTICS AND SPACE ADMINISTRATION. LANGLEY RESEARCH CENTER, HAMPTON, VA.

CFD methods development considerations for unsteady aerodynamic analysis
[NASA-TM-107644] p 3750 N92-31239
Design and experimental validation of a flutter suppression controller for the active flexible wing
[NASA-TM-4381] p 3760 N92-31240
High Reynolds number test of the Boeing TR77 airfoil in the Langley 0.3-meter transonic cryogenic tunnel
[NASA-TM-4189] p 3750 N92-31246
Computer program to solve two-dimensional shock-wave interference problems with an equilibrium chemically reacting air model
[NASA-TM-4187] p 3818 N92-31247
Flexible heating head for induction heating apparatus and method
[NASA-CASE-LAR-14418-1] p 3803 N92-31257
A summary of the active flexible wing program
[NASA-TM-107655] p 3757 N92-31264
Analysis and prediction of Multiple-Site Damage (MSD) fatigue crack growth
[NASA-TP-3231] p 3838 N92-31279
Stagnation-point heat-transfer rate predictions at aeroassist flight conditions
[NASA-TP-3208] p 3819 N92-31281
Flutter suppression digital control law design and testing for the AFW wind-tunnel model
[NASA-TM-107652] p 3757 N92-31350
Rolling maneuver load alleviation using active controls
[NASA-TM-107654] p 3757 N92-31351
Comparison of effects of copropagated and precomputed atmosphere profiles on Monte Carlo trajectory simulation
[NASA-TM-102600] p 3766 N92-31457
Finite-element analyses and fracture simulation in thin-sheet aluminum alloy
[NASA-TM-107662] p 3839 N92-31504
Wind tunnel aerodynamic characteristics of a transport-type airfoil in a simulated heavy rain environment
[NASA-TP-3184] p 3751 N92-31532
Method and circuit for controlling the evolution time interval of a laser output pulse
[NASA-CASE-LAR-13772-1] p 3831 N92-31788
Imide/arylene ether copolymers
[NASA-CASE-LAR-14159-1-CU] p 3794 N92-31792
Data reduction formulas for the 16-foot transonic tunnel: NASA Langley Research Center, revision 2
[NASA-TM-107646] p 3762 N92-31900
Time simulation of flutter with large stiffness changes
[NASA-TM-107650] p 3758 N92-32111
Mission description and in-flight operations of ERBE instruments on ERBS, NOAA 9, and NOAA 10 spacecraft
[NASA-RP-1279] p 3844 N92-32127
Effects of fragmentation parameter variations on estimates of galactic cosmic ray exposure: Dose sensitivity studies for aluminum shields
[NASA-TM-4386] p 3926 N92-32193
Ground and flight calibration assessment of HiRAP accelerometer data from missions STS-35 and STS-40
[NASA-TM-107602] p 3769 N92-32204

NATIONAL AERONAUTICS AND SPACE ADMINISTRATION. LEWIS RESEARCH CENTER, CLEVELAND, OH.

Cyclic hot firing results of tungsten-wire-reinforced, copper-lined thrust chambers
[NASA-TM-4214] p 3769 N92-31249
NASA Lewis Research Center supersonic throughflow fan program
[NASA-TM-103248] p 3759 N92-31250
Graphite/epoxy composite adapters for the Space Shuttle/Centaur vehicle
[NASA-TP-3014] p 3765 N92-31251
A free-piston Stirling engine/linear alternator controls and load interaction test facility
[NASA-TM-105825] p 3845 N92-31262
Life extending control for rocket engines
[NASA-TM-105789] p 3802 N92-31263
Preliminary evaluation of adhesion strength measurement devices for ceramic/titanium matrix composite bonds
[NASA-TM-105803] p 3745 N92-31267
Stability testing and analysis of a PMAD DC test bed for the Space Station Freedom
[NASA-TM-105846] p 3812 N92-31282
The evolutionary development of high specific impulse electric thruster technology
[NASA-TM-105712] p 3769 N92-31342
Experimental testing of prototype face gears for helicopter transmissions
[NASA-TM-105434] p 3832 N92-31349
A general numerical model for wave rotor analysis
[NASA-TM-105740] p 3821 N92-31484
Modal simulation of gearbox vibration with experimental correlation
[NASA-TM-105702] p 3834 N92-31485
A differential CDM model for fatigue of unidirectional metal matrix composites
[NASA-TM-105726] p 3840 N92-31505
Computational simulation of interningled-fiber hybrid composite behavior
[NASA-TM-105666] p 3774 N92-31506
A demonstration of an intelligent control system for a reusable rocket engine
[NASA-TM-105794] p 3770 N92-31507
Effect of out-of-roundness on the performance of a diesel engine connecting-rod bearing
[NASA-TM-105600] p 3834 N92-31536
Supersonic Throughflow Fan Test Facility at NASA. Lewis Research Center
[NASA-TP-3038] p 3762 N92-31640
Liquid lubrication for space applications
[NASA-TM-105198] p 3795 N92-31840
High-performance packaging for monolithic microwave and millimeter-wave integrated circuits
[NASA-TM-105744] p 3808 N92-31855
Krypton ion thruster performance
[NASA-TM-105818] p 3770 N92-31901
An overview of the Lewis Research Center CSTI thermal management program
[NASA-TM-105310] p 3771 N92-31916
SP-100 reactor with Brayton conversion for lunar surface applications
[NASA-TM-105637] p 3771 N92-32108
Demonstrated survivability of a high temperature optical fiber cable on a 1500 pound thrust rocket chamber
[NASA-TM-105835] p 3801 N92-32230
Monolithic and mechanical multijunction space solar cells
[NASA-TM-105832] p 3818 N92-32233
Effects of fiber and interfacial layer architectures on the thermoplastic response of metal matrix composites
[NASA-TM-105802] p 3777 N92-32234
Low-Isp derated ion thruster operation
[NASA-TM-105787] p 3771 N92-32237
A parameter optimization approach to controller partitioning for integrated flight/propulsion control application
[NASA-TM-105826] p 3761 N92-32241

NATIONAL AERONAUTICS AND SPACE ADMINISTRATION. MARSHALL SPACE FLIGHT CENTER, HUNTSVILLE, AL.

Gibbs free energy of reactions involving SiC, Si3N4, H2, and H2O as a function of temperature and pressure
[NASA-TP-3275] p 3791 N92-31278
Applications of FEM and BEM in two-dimensional fracture mechanics problems
[NASA-TP-3277] p 3838 N92-31280
Hollow fiber clinostat for simulating microgravity in cell culture
[NASA-CASE-MFS-28370-1] p 3828 N92-31790
Spacecraft stability and control
[TABES PAPER 92-414] p 3763 N92-32011
Analysis of debris from Spacelab Space Life Sciences-1
[NASA-TM-103593] p 3765 N92-32148

NATIONAL AEROSPACE LAB., EMMELOORD (NETHERLANDS).

Data compression techniques p 3922 N92-32190

NATIONAL AEROSPACE LAB., TOKYO (JAPAN).

GPS satellite orbit determination using pseudorange data: Experiments and results
[PB92-178870] p 3765 N92-31685

NATIONAL ASSOCIATION OF REGULATORY UTILITY COMMISSIONERS, WASHINGTON, DC.

National Conference on Integrated Resource Planning: Proceedings
[DE92-013573] p 3845 N92-31290

NATIONAL CENTER FOR ATMOSPHERIC RESEARCH, BOULDER, CO.

Global atmospheric circulation statistics, 1000-1 mb
[PB92-186196] p 3853 N92-31649

NATIONAL CENTER FOR EDUCATION STATISTICS, WASHINGTON, DC.

International mathematics and science assessments: What have we learned
[PB92-183599] p 3916 N92-32160

NATIONAL CLIMATIC DATA CENTER, ASHEVILLE, NC.

Comprehensive Aerological Reference Data Set (CARDS)
[DE92-016469] p 3862 N92-31734

NATIONAL GEOPHYSICAL DATA CENTER, BOULDER, CO.

Solar-geophysical data number 572, April 1992. Part 1: (Prompt reports). Data for March, February 1992, and late data
[PB92-187723] p 3856 N92-31637
Solar-geophysical data number 572, April 1992. Part 2: (Comprehensive reports). Data for October 1991 and miscellaneous
[PB92-187731] p 3856 N92-31639

NATIONAL INST. FOR FUSION SCIENCE, NAGOYA (JAPAN).

Electron impact excitation of positive ions: Partial wave approach in Coulomb-Eikonal approximation
[NIFS-106] p 3892 N92-31255
Statistical analysis of anomalous transport in resistive interchange turbulence
[NIFS-125] p 3818 N92-31256
New high voltage parallel plate analyzer
[NIFS-128] p 3827 N92-31340
Theory of anomalous transport in toroidal helical plasmas
[NIFS-140] p 3904 N92-31659
Simulation study of stepwise relaxation in a spheromak plasma
[DE92-782101] p 3906 N92-31843
Energy transport in the steady state plasma sustained by DC helicity current drive
[NIFS-127] p 3907 N92-32181
Kernel optimum nearly-analytical discretization (KOND) method applied to parabolic equations KOND-P Scheme
[NIFS-118] p 3887 N92-32205

NATIONAL INST. OF STANDARDS AND TECHNOLOGY, BOULDER, CO.

Phase characteristics and time responses of unknown linear systems determined from measured CW amplitude data
[PB92-183722] p 3805 N92-31368
Cryogenic 4.4 MN mechanical test system for large scale tests of composite support struts
[PB92-181148] p 3774 N92-31609
Effects of flow conditioners and tap location on orifice flowmeter performance
[PB92-183730] p 3824 N92-31839

NATIONAL INST. OF STANDARDS AND TECHNOLOGY, GAITHERSBURG, MD.

Overview of integrated services digital network conformance testing
[PB92-181015] p 3881 N92-31365
Operating principles of MULTIKRON performance instrumentation for MIMD computers
[PB92-181072] p 3874 N92-31366
Electronics and electrical engineering laboratory technical publication announcements covering laboratory programs, July to September 1991, with 1992 EEEL events calendar
[PB92-181239] p 3813 N92-31367
Automation of strain-gauge load-cell force calibration
[PB92-187087] p 3827 N92-31370
Next generation documents
[PB92-187103] p 3917 N92-31371
Development of characterization techniques for polyurethanes 1. Characterization of SRM 1480, a low molecular weight polyurethane for SEC calibration
[PB92-172485] p 3794 N92-31618
Shop of the 1990's project: An evaluation tool for wireframe CAD software
[PB92-181130] p 3877 N92-31628
Calibration at 24 C of a heat-flow-meter apparatus having 610 mm square plates
[DE92-015954] p 3827 N92-31633
Technology Integration Workshop: Selected papers
[PB92-158278] p 3923 N92-31643
Noise-induced chaos and phase space flux: A sample-theoretic study
[PB92-172733] p 3915 N92-31645
Logarithmic retinae
[PB92-183649] p 3885 N92-31680
Ferroelectric thin films prepared by pulse laser deposition processing and characterization
[PB92-196088] p 3913 N92-32072

NATIONAL MARINE FISHERIES SERVICE, HONOLULU, HI.

Biology, oceanography, and fisheries of the North Pacific transition zone and subarctic frontal zone
[PB92-178128] p 3866 N92-32106

NATIONAL MATERIALS PROPERTY DATA NETWORK, INC., COLUMBUS, OH.
Marine structural steel toughness data bank, volume 1
[AD-A247923] p 3789 N92-31987
NATIONAL OCEANIC AND ATMOSPHERIC ADMINISTRATION, BOULDER, CO.
Feasibility study for a low-altitude wide and temperature profiler
[PB92-188200] p 3860 N92-31641
NATIONAL OCEANOGRAPHIC DATA CENTER, ROCKVILLE, MD.
Ecosystems of the Florida Keys: A bibliography
[PB92-198910] p 3854 N92-32071
NATIONAL PARK SERVICE, THREE RIVERS, CA.
Methods of assessing responses of trees, stands and ecosystems to air pollution
[PB92-180231] p 3853 N92-31648
NATIONAL RESEARCH COUNCIL OF CANADA, OTTAWA (ONTARIO).
A preliminary study in the use of phase demodulation techniques for the analysis of gear vibration data
[NRC-32083] p 3833 N92-31469
NATIONAL SCIENCE FOUNDATION, WASHINGTON, DC.
Our changing planet: The FY 1993 US global change research program. A supplement to the US President's fiscal year 1993 budget
[NASA-CR-190675] p 3850 N92-31259
NATIONAL SCIENCE FOUNDATION OF US, TOKYO (JAPAN).
NSF Tokyo reports. 1991 survey of research and development in Japan
[PB92-192624] p 3927 N92-32067
NSF Tokyo reports. General outline of JFY 1991 government science and technology budget
[PB92-192640] p 3927 N92-32068
NAVAL AIR DEVELOPMENT CENTER, WARMINSTER, PA.
Corrosion behavior of squeeze cast aluminum metal matrix composites
[AD-A250486] p 3774 N92-31382
NAVAL BIODYNAMICS LAB., NEW ORLEANS, LA.
Naval Biodynamics Laboratory: 1989 and 1990 command history
[AD-A247185] p 3870 N92-31963
NAVAL COMMAND, CONTROL AND OCEAN SURVEILLANCE CENTER, SAN DIEGO, CA.
Using the burst derivative measure to improve the computational efficiency of ISAR motion compensation algorithms
[AD-A250850] p 3805 N92-31369
STI handbook: Guidelines for producing, using, and managing scientific and technical information in the Department of the Navy. A handbook for Navy scientists and engineers on the use of scientific and technical information
[AD-A252439] p 3918 N92-31482
Fabrication of an insulated gate diamond FET for high temperature applications
[AD-A251042] p 3817 N92-31849
NAVAL HEALTH RESEARCH CENTER, SAN DIEGO, CA.
Stress reactivity: Five-factor representation of a psychobiological typology
[AD-A252715] p 3872 N92-31327
Body water homeostasis and human performance in high heat environments: Fluid hydration recommendations for Operation Desert Storm
[AD-A249772] p 3868 N92-31492
NAVAL MEDICAL RESEARCH INST., BETHESDA, MD.
A detector for stationary gas bubbles: Feasibility studies
[AD-A250135] p 3828 N92-31794
NAVAL OCEAN SYSTEMS CENTER, SAN DIEGO, CA.
Synthesis of diamond films with pulsed plasma
[AD-A250058] p 3791 N92-31356
Remote sensing of trapping layer base height using ATIS transmissions
[AD-A250074] p 3844 N92-31362
Performance measures of the Ada rendezvous
[AD-A250060] p 3877 N92-31601
NAVAL OCEANOGRAPHIC AND ATMOSPHERIC RESEARCH LAB., BAY SAINT LOUIS, MS.
Deep-tow acoustics/geophysics system compressional velocity database
[AD-A252700] p 3918 N92-31467
Development, testing and operation of a large suspended ocean measurement structure for deep-ocean use
[AD-A252188] p 3866 N92-32050
NAVAL POSTGRADUATE SCHOOL, MONTEREY, CA.
Design and specification of a high speed transport protocol
[AD-A248323] p 3804 N92-31284
A computational investigation of airfoil stall flutter
[AD-A247302] p 3751 N92-31300
Analysis and evaluation of Project Evergreen data
[AD-A245983] p 3804 N92-31314
The prediction of the performance of a microcircuit heat sink in the boiling mode
[AD-A250045] p 3812 N92-31355
Sensitivity of the tomographic inverse solution to acoustic path variability
[AD-A252146] p 3864 N92-31407
Exponential representation and consistency checking for M layer
[AD-A250423] p 3805 N92-31413
Simulation of a parallel processor based small tactical system
[AD-A245911] p 3882 N92-31443
Implementing relational operations in an object-oriented database
[AD-A249332] p 3918 N92-31450
Sequential estimation of optimal age replacement policies when distribution of lifetimes is phase type
[AD-A249020] p 3836 N92-31479
Natural convection immersion cooling of an array of vertically oriented heated protrusions in an enclosure filled with a dielectric liquid: Effects of enclosure width, Prandtl number and component orientation
[AD-A245884] p 3914 N92-31489
Hydrographic and Acoustic Doppler Current Profiler (ADCP) data from the Farallones shelf and slope study
[AD-A250834] p 3864 N92-31495
Amending the w* velocity scale for surface layer, entrainment zone, and baroclinic shear in mixed Forced/Free turbulent convection
[AD-A250389] p 3859 N92-31540
A numerical, analytical, and observational study of the effect of clouds on surface wind and wind stress during the central Arctic winter
[AD-A252706] p 3860 N92-31670
Computer simulation of acoustic fluctuations due to finescale temperature perturbations measured by thermistor chain
[AD-A252709] p 3892 N92-31672
Hyper-NPSNET: A virtual world with an integrated 3-D hypertext
[AD-A252726] p 3878 N92-31676
A dictionary of acquisition and contracting terms
[AD-A247053] p 3920 N92-31754
Further studies in filmwise condensation of steam on horizontal finned tubes
[AD-A252705] p 3915 N92-31767
Roundoff algorithms for digital phase shifters that minimize beam shift
[AD-A250094] p 3816 N92-31780
Multimedia electronic mail: Standards and performance simulation
[AD-A250047] p 3808 N92-31809
A diagnostic study of rapidly developing cyclones using surface-based Q vectors
[AD-A246993] p 3862 N92-31978
Seasonal wind and ocean thermal forcing influences on the generation of the Leeuwin current and its eddies
[AD-A246992] p 3865 N92-31988
Coherent/noncoherent detection of coherent optical heterodyne DPSK-CDMA and MFSK-CDMA signals
[AD-A246215] p 3809 N92-31993
A continuing study of altitude determination deficiencies of the Service Aircraft Instrumentation Package (SAIP)
[AD-A245952] p 3758 N92-32051
A study of the microstructural basis for the strength and toughness properties of water-quenched and air-cooled HSLA-100, HSLA-100 with increased copper, and a ULCB steel
[AD-A245955] p 3789 N92-32052
Dynamic modeling and modal analysis of an air-to-air missile
[AD-A245957] p 3758 N92-32053
Decision-making guide for the proposed Coast Guard differential global positioning system
[AD-A246046] p 3756 N92-32054
An analysis of hydrographic data collected off Point Sur, California in June 1990
[AD-A246060] p 3866 N92-32056
Fitting and prediction uncertainty for a software reliability model
[AD-A252173] p 3880 N92-32060
Theory for the CEBAF infrared and shipboard FELS
[AD-A252174] p 3832 N92-32061
Exploratory experimental investigation of a wave propeller
[AD-A252175] p 3753 N92-32062
The impact of cognitive feedback on the performance of intelligence analysts
[AD-A252176] p 3871 N92-32063
The effect of thermomechanical processing parameters on the ambient behavior of 10 percent volume 6061 Al-Alumina
[AD-A252177] p 3776 N92-32064
NAVAL RESEARCH LAB., WASHINGTON, DC.
The KRAKEN normal mode program
[AD-A252409] p 3892 N92-31818
Development of a fault isolation system database manager
[AD-A248346] p 3916 N92-31992
An empirical prediction algorithm for low-frequency acoustic surface scattering strengths
[AD-A250508] p 3892 N92-32044
NAVAL SURFACE WARFARE CENTER, SILVER SPRING, MD.
Estimation of metal acceleration by an SF5 containing explosive
[AD-A245338] p 3801 N92-32098
NAVAL UNDERSEA WARFARE CENTER, NEW LONDON, CT.
Near-field and far-field sound radiation from a line-driven fluid-loaded infinite flat plate having periodic and non-periodic attached rib stiffeners
[AD-A250100] p 3892 N92-31789
NAVAL WAR COLL., NEWPORT, RI.
Anti-environmental warfare: Protecting the environment during wartime
[AD-A250337] p 3851 N92-31556
NAVAL WEAPONS CENTER, CHINA LAKE, CA.
The sixteenth annual electronics manufacturing seminar proceedings
[AD-A247920] p 3814 N92-31461
Effect of inlet geometry on the flow and combustion processes in a solid fuel ramjet p 3747 N92-31871
NEBRASKA UNIV., LINCOLN.
Holographic grating relaxation and photon correlation spectroscopic studies of viscoelastic liquids above the glass transition
[AD-A252485] p 3828 N92-31828
Dipolar interaction assisted effects on second harmonic generation
[AD-A252487] p 3784 N92-31959
Electro-optics and second harmonic generation of nonlinear optical polymers
[AD-A252488] p 3796 N92-31960
Diffusion of camphorquinone in uniaxially drawn polycarbonate films
[AD-A252489] p 3796 N92-31961
NEW HAMPSHIRE UNIV., DURHAM.
Effect of fracture surface interference on shear crack growth
[DE92-011431] p 3839 N92-31389
NEW MEXICO INST. OF MINING AND TECHNOLOGY, SOCORRO.
Interface engineering in alumina/glass composites
[AD-A248587] p 3773 N92-31315
NEW MEXICO STATE UNIV., LAS CRUCES.
The investigation of bandwidth efficient coding and modulation techniques
[NASA-CR-190685] p 3806 N92-31468
NEW MEXICO UNIV., ALBUQUERQUE.
Laser material interactions
[AD-A250028] p 3831 N92-31802
NEW YORK UNIV., NEW YORK.
Mathematical problems in micromechanics and composite materials
[AD-A249584] p 3773 N92-31378
US-Japan seminar on magnetic multilayered structures: Proceedings
[AD-A252440] p 3910 N92-31666
Workshop on the Derivation of Parallel Programs and Architectures: Closing report
[AD-A252742] p 3883 N92-32109
NISSHO IWAI CORP., TOKYO (JAPAN).
The trading company in space development in Japan
[TABES PAPER 92-424] p 3764 N92-32015
NORTH CAROLINA STATE UNIV., RALEIGH.
Growth, nitrogen vacancy reduction and solid solution formation in cubic GaN thin films and the subsequent fabrication of superlattice structures using AlN and InN
[AD-A248058] p 3908 N92-31446
NORTH CAROLINA UNIV., CHAPEL HILL.
Charge transfer processes in multiple site chemical systems
[AD-A249538] p 3791 N92-31358
Structure and dynamics of Cl(H2O)20 clusters. The effect of the polarizability and the charge ofthe ion
[AD-A251094] p 3899 N92-32196
NORTHROP CORP., HAWTHORNE, CA.
Composite failure analysis handbook. Volume 1: Program review
[AD-A250520] p 3776 N92-32047
Composite failure analysis handbook. Volume 2: Technical handbook. Part 1: Procedures and techniques
[AD-A250521] p 3776 N92-32048
NORTHWESTERN UNIV., CHICAGO, IL.
Cellular localization of infrared sources
[AD-A249795] p 3866 N92-31302

NORTHWESTERN UNIV., EVANSTON, IL.
Ceramic surfaces and sintering
[DE92-011570] p 3793 N92-31538
Energetics, bonding mechanism and electronic structure of metal/ceramic interfaces
[DE92-013401] p 3775 N92-31806
Quantum mechanical approach to understanding microstructural and mechanical properties in intermetallics
[AD-A250550] p 3790 N92-32084
NOTRE DAME UNIV., IN.
Theory of semiconducting superlattices and microstructures
[AD-A248758] p 3816 N92-31799
NOVA UNIV., DANIA, FL.
Satellite-to-satellite tracking in the high-low mode: Line-of-sight acceleration in a residual gravity field
[PL-TR-91-2209] p 3767 N92-32082

O

OAK RIDGE K-25 SITE, TN.
Ceramic membranes for high temperature hydrogen separation
[DE92-013342] p 3783 N92-31816
OAK RIDGE NATIONAL LAB., TN.
Mitigation of magnetohydrodynamic electromagnetic pulse (MHD-EMP) effects from commercial electric power systems
[AD-A249577] p 3804 N92-31354
Residual stress and strain measurements in an austenitic steel plate containing a multipass weld
[DE92-014478] p 3839 N92-31383
Evaluation of proposed inservice testing procedures for check valves
[DE92-014502] p 3833 N92-31384
Radiation protection for human exploration of the moon and Mars: Application of the MASH code system
[DE92-014416] p 3868 N92-31409
Experimental studies of aluminum solubility and speciation in brines
[DE92-010448] p 3786 N92-31418
Graphical development tools for network-based concurrent supercomputing
[DE92-011144] p 3875 N92-31447
A comparison of three self-tuning control algorithms developed for the Bristol-Babcock controller
[DE92-014472] p 3814 N92-31499
Motor-operated globe valve performance in a liquid sodium environment
[DE92-014456] p 3834 N92-31500
Residual stresses in a multipass ferritic weldment
[DE92-014467] p 3839 N92-31501
Two long-term instrumental climatic data bases of the People's Republic of China
[DE92-010378] p 3851 N92-31527
What can we learn from magnetization experiments on high T(sub c) superconductors? An overview
[DE92-014465] p 3815 N92-31650
Comparison of double and single ionization in He by photons and by charged projectiles
[DE92-013411] p 3894 N92-31679
Temperature-enhanced autodetachment from long-lived parent negative ions of gaseous dielectrics
[DE92-011108] p 3894 N92-31700
A dynamic model of terrestrial carbon cycling
[DE92-015130] p 3853 N92-31782
Flow generation by turbulence
[DE92-013276] p 3906 N92-31829
Analytic estimation of radiation effects in space using solid angles
[DE92-013282] p 3899 N92-31831
Iterative functionalism and climate management regimes: From intergovernmental panel on climate change to intergovernmental negotiating committee
[DE92-014798] p 3853 N92-31896
Potassium Rankine cycle nuclear power systems for spacecraft and lunar-mass surface power
[DE92-016163] p 3770 N92-31897
Impurity effects on the magnetic ordering in chromium
[DE92-016165] p 3789 N92-31898
Trends 1991: A compendium of data on global change
[DE92-011733] p 3854 N92-31907
Radiation damage in carbon-carbon composites
[DE92-011778] p 3775 N92-31912
Small tokamaks for fusion technology testing
[DE92-011790] p 3906 N92-31913
Substrate surface effects on the properties of sputter-deposited and laser-irradiated films
[DE92-013850] p 3795 N92-31917
Alterations of multiphoton-resonant processes through wave-mixing effects
[DE92-016164] p 3896 N92-31923
The hierarchical spatial decomposition of three-dimensional particle-in-cell plasma simulations on MIMD distributed memory multiprocessors
[DE92-016802] p 3883 N92-32034
Imaging and spectrometry of bulk crystal surfaces and surface dynamical processes at high temperatures
[DE92-015235] p 3913 N92-32085
Incoherence effects in reflection electron microscopy
[DE92-016161] p 3829 N92-32086
Rheology of zirconia-alumina gelcasting slurries
[DE92-016787] p 3797 N92-32089
Exotic nuclear shapes and configurations that can be studied at high spin using radioactive ion beams
[DE92-016800] p 3898 N92-32090
Solar thermal energy storage in phase change materials
[DE92-016908] p 3849 N92-32091
Effect of surface modifications on the properties of silicon nitride ceramics
[DE92-013848] p 3797 N92-32094
CGVIEW: A program to generate isometric and perspective views of combinatorial geometries
[DE92-016979] p 3881 N92-32126
OCEAN PLANET ODYSSEY, NEW YORK, NY.
One thousand days non-stop at sea: Lessons for a mission to Mars
[TABES PAPER 92-462] p 3764 N92-32020
OFFICE OF TECHNOLOGY ASSESSMENT, WASHINGTON, DC.
Annual report to the Congress, fiscal year 1991 (Office of Technology Assessment)
[PB92-166549] p 3922 N92-31599
OHIO STATE UNIV., COLUMBUS.
Stability of boundary layers at high supersonic and hypersonic speeds
[AD-A250900] p 3819 N92-31306
A finite element procedure for analysis of laminated composite plates
[AD-A250902] p 3773 N92-31307
Hydrological and geochemical response and recovery in disturbed Arctic ecosystems
[DE92-016223] p 3850 N92-31312
The physics of cellular automata and coherence and chaos in classical many-body systems
[DE92-016834] p 3890 N92-32035
OHIO UNIV., ATHENS.
Oscillating-flow regenerator test rig: Woven screen and metal felt results
[NASA-CR-190689] p 3820 N92-31352
Electronic states in systems of reduced dimensionality
[DE92-013588] p 3912 N92-31945
ONSALA SPACE OBSERVATORY (SWEDEN).
Molecular outflows associated with HH52-54 and IRAS 12496-7650
[PB92-184472] p 3924 N92-31635
OREGON GRADUATE CENTER FOR STUDY AND RESEARCH, BEAVERTON.
Fundamental studies in oxidation-reduction in relation to water photolysis
[DE92-014333] p 3785 N92-32113
OREGON STATE UNIV., CORVALLIS.
Incipient and total group combustion of fuel sprays in air p 3749 N92-31883
OREGON UNIV., EUGENE.
Particle physics confronts the solar neutrino problem
[DE92-014013] p 3895 N92-31812
ORLEANS UNIV. (FRANCE).
Use of expert systems as user interfaces in information retrieval p 3921 N92-32185
OTTAWA UNIV. (ONTARIO).
Preliminary development of a protocol for determining heat stress caused by clothing
[DREO-PSD-EPS-05/89] p 3873 N92-32031

P

PACIFIC NORTHWEST LAB., RICHLAND, WA.
Final report on DSA methods for monitoring alumina in aluminum reduction cells with cermet anodes
[DE92-013599] p 3813 N92-31440
Energy conservation: The main factor for reducing greenhouse gas emissions in the former Soviet Union
[DE92-012355] p 3852 N92-31574
Mechanical strength and stability of lithium aluminate
[DE92-015998] p 3841 N92-31638
Real-time statistical quality control and ARM
[DE92-015253] p 3837 N92-31657
Stress and phase transformation phenomena in oxide films
[DE92-014702] p 3910 N92-31665
Static magnetic fields: A summary of biological interactions, potential health effects, and exposure guidelines
[DE92-015218] p 3867 N92-31711
Evolution of environmental protection strategies in the Soviet Union
[DE92-015090] p 3853 N92-31732
Chemical energy storage system for SEGS solar thermal power plant
[DE92-012327] p 3848 N92-31845
Use of tissue equivalent proportional counters to characterize radiation quality on the space shuttle
[DE92-012347] p 3768 N92-31846
Electronic structure and photophysical properties of polyimides
[DE92-012353] p 3797 N92-32146
PENNSYLVANIA STATE UNIV., UNIVERSITY PARK.
Advanced thermally stable jet fuel development program. Volume 2: Compositional factors affecting thermal degradation of jet fuels
[AD-A252656] p 3798 N92-31399
Prediction of hydrogen entry and permeation in metals and alloys
[AD-A245286] p 3790 N92-32096
Catalyst dispersion and activity under conditions of temperature-staged liquefaction
[DE92-014112] p 3786 N92-32141
PHASEX CORP., LAWRENCE, MA.
Supercritical fluid fractionation of JP-8
[AD-A247835] p 3801 N92-31982
PHYSICAL OPTICS CORP., TORRANCE, CA.
A microprism array for large-scale, wide-band interconnection of optoelectronic systems
[AD-A249380] p 3813 N92-31374
PIERSOL ENGINEERING CO., WOODLAND HILLS, CA.
Optimum data analysis procedures for Titan 4 and Space Shuttle payload acoustic measurements during lift-off
[NASA-CR-190479] p 3892 N92-32178
PITTSBURGH ENERGY TECHNOLOGY CENTER, PA.
Steady flow of a fluid-solid mixture between parallel plates
[DE92-013645] p 3821 N92-31426
MHD Contractors' Review Meeting: Abstracts
[DE92-011549] p 3904 N92-31576
Heat transfer and flow of a modified second grade fluid
[DE92-014744] p 3824 N92-31895
PITTSBURGH UNIV., PA.
The thermal dissociation of decaborane on Si(111)-(7x7) and doping effects in the near surface region
[AD-A251057] p 3911 N92-31851
Organization of the human circadian system
[AD-A247498] p 3869 N92-31905
Experimental particle physics at the University of Pittsburgh
[DE92-016182] p 3896 N92-31926
The synthesis and characterization of tribophysical layers on diamond and silicon carbide surfaces
[AD-A250983] p 3796 N92-32001
Probe molecule studies: Active species in alcohol synthesis
[DE92-015430] p 3784 N92-32029
POLISH ACADEMY OF SCIENCES, WARSAW.
Effect of outer temperature changes and solar radiation on effective heat losses through external partitions of buildings p 3802 N92-31242
Studies of the effect of strain velocity on mechanical properties of the 34GS steel p 3786 N92-31243
Piezoelectric radiant-to-air ultrasonic transducers p 3811 N92-31244
Probabilistic analysis of twenty-four hour weather data for Warsaw p 3863 N92-32097
Acoustic emission method applied to tests on concrete p 3842 N92-32206
Weak ion-acoustic shock waves and double layers in non-collision plasma p 3907 N92-32208
Investigation of acoustic properties of high-temperature ceramic superconductors p 3914 N92-32209
Determination of the matrix conditioning indicator. Comparison of approximate methods p 3887 N92-32210
PRATT AND WHITNEY AIRCRAFT, WEST PALM BEACH, FL.
Fatigue in single crystal nickel superalloys
[AD-A250068] p 3786 N92-31360
Fatigue in single crystal nickel superalloys
[AD-A252492] p 3790 N92-32066
PRC KENTRON, INC., EDWARDS, CA.
Design and analysis issues of integrated control systems for high-speed civil transports
[NASA-CR-186022] p 3761 N92-31656
PRINCETON UNIV., NJ.
Submillimeter wave spectroscopy of heterojunction superlattices
[AD-A250835] p 3908 N92-31496
The structure and control of three-dimensional shock wave turbulent boundary layer interactions
[AD-A250209] p 3823 N92-31824
Automatic design of transonic airfoils to reduce the shock induced pressure drag p 3745 N92-31863

Fault tolerant parallel computing in orthogonal shared-memory and related architectures
[AD-A250504] p 3883 N92-32040
Development and application of photosensitive device systems to studies of biological and organic materials
[DE92-014728] p 3867 N92-32120

PURDUE UNIV., WEST LAFAYETTE, IN.
Role of the double-layer cation on the potential-dependent stretching frequencies and binding geometries of carbon monoxide at platinum-nonaqueous interfaces
[AD-A246980] p 3784 N92-31998
Research on aero-thermodynamic distortion induced structural dynamic response of multistage compressor blading
[AD-A250865] p 3760 N92-32059
Diffusion in ordered and disordered media
[AD-A250949] p 3891 N92-32211

R

RAFAEL ARMAMENT DEVELOPMENT AUTHORITY, HAIFA (ISRAEL).
Sizing supersonic freejet nozzle and inlet location for simulation of the transition phase in integral rocket ramjet p 3747 N92-31870
An innovative two axis rate gyro: Theory and principles of operation p 3748 N92-31875
Discrete optimal guidance for high order missile and maneuvering target p 3748 N92-31879

READING UNIV. (ENGLAND).
Theory and test of stress resistance
[AD-A250741] p 3870 N92-31291

RENSSELAER POLYTECHNIC INST., TROY, NY.
Preparation of non-oxide ceramics by pyrolysis of organometallic precursors
[AD-A251112] p 3798 N92-32197

RESEARCH INST. FOR COMPUTING AND INFORMATION SYSTEMS, HOUSTON, TX.
Assessing repository technology. Where do we go from here?
[NASA-CR-190630] p 3917 N92-31272
Issues in designing transport layer multicast facilities
[NASA-CR-190639] p 3882 N92-31483
Sources of unbounded priority inversions in real-time systems and a comparative study of possible solutions
[NASA-CR-190711] p 3875 N92-31486
Mission and Safety Critical (MASC) plans for the MASC Kernel simulation
[NASA-CR-190708] p 3875 N92-31487
A proposed group management scheme for XTP multicast
[NASA-CR-190633] p 3916 N92-31547
Using neural networks in software repositories
[NASA-CR-190641] p 3885 N92-31597
Configuration management and software measurement in the Ground Systems Development Environment (GSDE)
[NASA-CR-190716] p 3879 N92-31787

RESEARCH INST. OF NATIONAL DEFENCE, LINKOEPING (SWEDEN).
Real time detection in a laser bathymetry system
[PB92-195452] p 3866 N92-32069
Calibration network intended for phased-array antennas at 3 GHz
[PB92-195429] p 3810 N92-32070
Realization of lattice networks at MHz- and GHz-frequencies
[PB92-195437] p 3810 N92-32161

RESEARCH INST. OF NATIONAL DEFENCE, STOCKHOLM (SWEDEN).
Monitoring threats to satellite functions
[PB92-195445] p 3767 N92-32073

RESEARCH TRIANGLE INST., RESEARCH TRIANGLE PARK, NC.
Catalytic carbon membranes for hydrogen production
[DE92-001269] p 3784 N92-31976
Noninvasive ambulatory assessment of cardiac function and myocardial ischemia in healthy subjects exposed to carbon monoxide
[AD-A252264] p 3870 N92-32107

RICE UNIV., HOUSTON, TX.
Gallium arsenide clusters and their interfacial physics and chemistry
[AD-A249565] p 3907 N92-31375
Theoretical atomic collision physics
[DE92-013571] p 3895 N92-31724

ROCHESTER INST. OF TECH., NY.
Digital analysis of wind tunnel imagery to measure fluid thickness
[NASA-CR-189234] p 3762 N92-31252

ROCHESTER UNIV., NY.
Architectural adaptability in parallel programming
[AD-A247516] p 3881 N92-31428
Systematic detection of parallelism in ordinary programs
[AD-A247514] p 3882 N92-31445
Function of panel M pathways in primates
[AD-A250275] p 3871 N92-31758
Function of P and M pathways in primates
[AD-A250055] p 3867 N92-31778
Mechanics of thin films
[AD-A247848] p 3912 N92-31984

ROCKWELL INTERNATIONAL CORP., CANOGA PARK, CA.
Orbit transfer vehicle engine technology program. Task B-6 high speed turbopump bearings
[NASA-CR-189230] p 3835 N92-31892

ROCKWELL INTERNATIONAL CORP., DOWNEY, CA.
Robotics development for the enhancement of space endeavors
[TABES PAPER 92-445] p 3763 N92-32013

ROYAL AUSTRALIAN AIR FORCE, VICTORIA.
Immersion suit usage within the RAAF
[AD-A250645] p 3755 N92-31562

RUTGERS - THE STATE UNIV., NEWARK, NJ.
Time and space resolved electron impact excitation rates in an RF glow discharge
[AD-A249614] p 3905 N92-31688

RUTHERFORD APPLETON LAB., CHILTON (ENGLAND).
Minimal supersymmetric unification predictions
[RAL-92-005] p 3915 N92-31953

S

SAN DIEGO STATE UNIV., CA.
Response of a tundra ecosystem to elevated atmospheric carbon dioxide and CO2-induced climate change
[DE92-013925] p 3853 N92-31626

SAN FRANCISCO STATE UNIV., CA.
Research in elementary particle physics
[DE92-014585] p 3893 N92-31385

SANDIA NATIONAL LABS., ALBUQUERQUE, NM.
Detection of object edges in images containing cast shadows
[DE92-016092] p 3900 N92-31295
An evaluation of ionizing radiation emitted by high power microwave generators
[DE92-016160] p 3805 N92-31387
A sealed He-4 superfluid-transition fixed-point device
[DE92-014271] p 3908 N92-31403
EnviroTRADE: Its role in the cleanup of the environment
[DE92-013691] p 3851 N92-31427
Advanced thermally stable, jet fuels development program annual report. Volume 1: Model and experiment system development
[AD-A249625] p 3799 N92-31462
Space nuclear power, propulsion, and related technologies
[SAND91-2617] p 3770 N92-31503
Characterization of polymers for microcellular foams
[DE92-012444] p 3793 N92-31539
Solid-armature railguns without the velocity-skin effect
[DE92-012630] p 3765 N92-31542
The collection, handling, transportation, and thermal desorption of explosive vapor using quartz collection tubes
[DE92-011441] p 3799 N92-31570
EnviroTRADE: A technical perspective on the development of an information system providing data on environmental technologies and needs worldwide
[DE92-012625] p 3919 N92-31578
Controlled atmosphere soldering system
[DE92-012633] p 3802 N92-31580
Surface chemistry of MoS2 lubricant films: Effects of high humidity storage on sputtered films
[DE92-015392] p 3794 N92-31631
A comparison of interstitial oxygen calculated by different techniques
[DE92-011658] p 3910 N92-31668
Adaptive inverse filter
[DE92-011660] p 3878 N92-31669
Light ion driven inertial confinement fusion
[DE92-011662] p 3905 N92-31707
Using transfer functions as a method for predicting lightning effects on munitions storage bunkers
[DE92-012627] p 3861 N92-31709
Torque linearizing hardware for the electric joint motors of a direct-drive robot
[DE92-012681] p 3816 N92-31718
B-1B nuclear certification tasks performed by the Aircraft Compatibility Department at Sandia National Laboratories
[DE92-016750] p 3757 N92-31736
Modeling arbitrarily directed slots that are narrow both in width and depth with regard to the FDTD spatial cell
[DE92-008015] p 3808 N92-31738
Techniques for autonomous navigation
[DE92-013458] p 3756 N92-31746
A semiconductor bridge ignited gas generator
[DE92-014049] p 3781 N92-31748
Measured responses of a munitions storage bunker to rocket-triggered lightning
[DE92-012628] p 3862 N92-31750
Guidelines for generating acceptance sampling plans for continuous production
[DE92-010763] p 3837 N92-31753
Use of a genetic algorithm to solve fluid flow problems on an NCUBE/2 multiprocessor computer
[DE92-014044] p 3824 N92-31832
Energy and Environment: A Sandia Technology Bulletin
[DE92-016740] p 3854 N92-31931
Axisymmetric bluff-body flow: A vortex solver for thin shells
[DE92-016748] p 3824 N92-31933
Plasma channel generation using low energy electron beams
[DE92-013770] p 3906 N92-31949
A philosophy for space nuclear systems safety
[DE92-016501] p 3771 N92-32030
Effective path planning through task restriction
[DE92-017351] p 3885 N92-32036
Heuristic sampling on DAGs
[DE92-017359] p 3917 N92-32037
Design, fabrication, and testing of a 30 kW(sub t) screen-wick heat-pipe solar receiver
[DE92-016500] p 3848 N92-32087
A generalization to stochastic averaging in random vibration
[DE92-016747] p 3842 N92-32088
Scaling of IFR propagation physics with beam/channel parameters
[DE92-015389] p 3900 N92-32123
A ban on use of lead-bearing solders: Implications for the electronics industry
[DE92-013291] p 3790 N92-32139
Device for monitoring the thickness of a dielectric coating on a dielectric substrate
[DE92-014741] p 3829 N92-32174

SANDIA NATIONAL LABS., LIVERMORE, CA.
The structure and properties of grain boundaries in Ni3Al
[DE92-012143] p 3788 N92-31744
Power scaling of divertor plasma conditions during H-mode in D3-D
[DE92-012148] p 3906 N92-31771
Saturation effects in degenerate four-wave mixing spectroscopy: Nonperturbative calculations
[DE92-012253] p 3782 N92-31773
Unimolecular reaction mechanisms involving C3H4, C4H4, and C6H6 hydrocarbon species
[DE92-005326] p 3783 N92-31860

SCIENCE APPLICATIONS INTERNATIONAL CORP., SAN DIEGO, CA.
Data to test and evaluate the performance of neural network architectures for seismic signal discrimination, neural computing for seismic phase identification, volume 2
[AD-A252442] p 3884 N92-31293
Soviet precision timekeeping research and technology
[PB92-173046] p 3802 N92-31830
Soviet satellite communications science and technology
[PB92-173038] p 3809 N92-31920

SMALL BUSINESS ADMINISTRATION, WASHINGTON, DC.
Report to the US Congress on minority small business and capital ownership development as required by the Business Opportunity Development Reform Act of 1988
[PB92-173681] p 3916 N92-31364

SOFTWARE PRODUCTIVITY SOLUTIONS, INC., INDIALANTIC, FL.
Quality Evaluation System (QUES), volume 1
[AD-A252679] p 3876 N92-31586

SOLAR TURBINES, INC. SAN DIEGO, CA.
Gas engine heat recovery unit
[PB92-184373] p 3835 N92-31841

SOUTH CAROLINA UNIV., COLUMBIA.
Synthesis of soluble alpha-thiophene oligomers. Monomer to octamer
[AD-A250082] p 3779 N92-31434

SOUTHWEST RESEARCH INST., SAN ANTONIO, TX.
A penetration mechanics database
[AD-A246351] p 3767 N92-31997

SPARTA, INC., LEXINGTON, MA.
User's guide for treetherm: A 3-D thermal model for single trees
[LTR91-003] p 3879 N92-31833

SPIRE CORP., BEDFORD, MA.
SiGe Si quantum wires for efficient, room temperature, tunable luminescence
[AD-A249651] p 3814 N92-31464

SRI INTERNATIONAL CORP., MENLO PARK, CA.
Field-emitter arrays for RF vacuum microelectronics
[AD-A250101] p 3816 N92-31791
ST SYSTEMS CORP., PACIFIC GROVE, CA.
Navy Atmospheric Boundary Layer (NABL) model system: Software/Interface design document
[AD-A247903] p 3857 N92-31986
STANFORD LINEAR ACCELERATOR CENTER, CA.
A three-gap klystron output cavity at X-band
[DE92-012417] p 3812 N92-31289
Pulse-by-pulse energy measurement at the Stanford Linear Collider
[DE92-011520] p 3899 N92-31390
The RQM triangle: A paradigm for relativistic quantum mechanics
[DE92-011583] p 3915 N92-31663
The polarized electron gun for the SLC
[DE92-012418] p 3900 N92-32131
Calculations of emittance and damping time effects in the SLC damping rings
[DE92-012420] p 3900 N92-32133
Results of IR working group
[DE92-013294] p 3902 N92-32149
STANFORD UNIV., CA.
Development of high efficiency nonlinear optical materials
[AD-A249612] p 3901 N92-31380
A strictly improving phase 1 algorithm using least-squares subproblems
[DE92-015904] p 3875 N92-31410
Optical oversampled analog-to-digital conversion
[AD-A252695] p 3877 N92-31587
Independent sampling of a stochastic process
[AD-A249712] p 3888 N92-31600
Three-wave envelope solitons: Can the speed of light in the fiber be controlled?
[AD-A247615] p 3901 N92-31611
Importance sampling for Markov chains: Asymptotics for the variance
[AD-A249804] p 3888 N92-31757
Interaction of fast steady flow with slow transient flow: A new cause of interplanetary Bz events
[AD-A250273] p 3823 N92-31770
Evolution of the solar and coronal field structure: 1976-1991
[AD-A250097] p 3925 N92-31786
Mathematical modeling and numerical simulation of the dynamics of flexible structures undergoing large overall motions
[AD-A250202] p 3761 N92-31967
SUN OIL CO., MARCUS HOOK, PA.
Light alkane conversion processes: Suprabiotic catalyst systems for selective oxidation of light alkane gases to fuel oxygenates
[DE92-015229] p 3799 N92-31751
SUNPOWER, INC., ATHENS, OH.
Free-piston Stirling engine conceptual design and technologies for space power, phase 1
[NASA-CR-182168] p 3769 N92-31245
SUPERCONDUCTING SUPER COLLIDER LAB., DALLAS, TX.
Utilization of gamma ray inspection system for tomographic imaging and dimensional analysis of complete model magnet cold masses and collared coil sections
[DE92-013466] p 3836 N92-31647
Improved ferrite biasing scheme for booster RF cavities
[DE92-011650] p 3815 N92-31664
Beam position monitor electronics using DC coupled demodulating logarithmic amplifiers
[DE92-011697] p 3816 N92-31760
The 6-D phase space tracking with acceleration: Modeling low energy proton synchrotrons, part 1
[DE92-013744] p 3899 N92-31948
Connectivity among computer-aided engineering methods, procedures, and tools used in developing the SSC collider magnets
[DE92-013954] p 3900 N92-31975
The physical solution to the Lorentz-Dirac equations in a constant magnetic field
[DE92-013299] p 3890 N92-32140
SVERDRUP TECHNOLOGY, INC., BROOK PARK, OH.
Tailored metal matrix composites for high-temperature performance
[NASA-TM-105816] p 3775 N92-31854
Numerical simulation of geometric scale effects in cylindrical self-field MPD thrusters
[NASA-CR-189224] p 3772 N92-32239
Three-dimensional compressible turbulent computations for a nondiffusing S-duct
[NASA-CR-4391] p 3754 N92-32240
SYDNEY UNIV. (AUSTRALIA).
Strength tests of cold-formed channel sections undergoing local and distortional buckling
[PB92-180835] p 3841 N92-31658
SYRACUSE UNIV., NY.
Fusion with highly spin polarized HD and D(2)
[DE92-017030] p 3898 N92-32007
SYSTEMS SCIENCE AND SOFTWARE, LA JOLLA, CA.
Two-dimensional axisymmetric calculations of surface waves generated by an explosion in an island, mountain, and sedimentary basin
[AD-A249971] p 3856 N92-31510
Three-dimensional finite difference modeling of surface wave propagation across the Barents Shelf
[AD-A249865] p 3865 N92-31821

T

TECHNION - ISRAEL INST. OF TECH., HAIFA.
A simulation model of a single rotor helicopter
p 3746 N92-31865
Study of a spherical spinning combustion chamber for orbit insertion p 3746 N92-31869
Estimation of aircraft attitude by angular rate measurements p 3748 N92-31881
An automated computational method for barrier construction in single and two-target differential games
p 3749 N92-31882
Transport and evaporation effects in counterflow spray diffusion flames p 3749 N92-31884
The stability of a slightly eccentric straight vortex filament in a circular tube p 3750 N92-31887
The three-dimensional stability of the Foeppl vortices
p 3750 N92-31889
TECHNISCH DOCUMENTATIE EN INFORMATIE CENTRUM VOOR DE KRIJGSMACHT, THE HAGUE (NETHERLANDS).
Search strategies in natural language
p 3921 N92-32186
TECHNISCHE UNIV., DELFT (NETHERLANDS).
The discretization of the 2D incompressible Navier-Stokes equations on a collocated grid
[REPT-91-61] p 3821 N92-31513
Two properties of uniform distributions, with applications to some nonparametric estimation problems
[REPT-91-94] p 3888 N92-31518
Nonparametric estimation in renewal theory, 1: The empirical renewal function
[REPT-91-95] p 3888 N92-31519
Phase portraits of non degenerate quadratic systems with zero finite multiplicity
[REPT-91-96] p 3886 N92-31520
Combining expert probabilistic weather forecasts: Results of post-hoc analyses of the Zierikzee experiment
[REPT-91-101] p 3859 N92-31521
Comparison of results: Technische Univ., Delft-Organisatie voor Toegepast Natuurwetenschappelijk Onderzoek expert judgement study of dispersion-deposition
[REPT-92-11] p 3856 N92-31522
TEL-AVIV UNIV. (ISRAEL).
Singularity avoidance for SCARA-type robots
p 3746 N92-31867
J(sub 2) fracture toughness testing of Al 707 5-T7351
p 3747 N92-31872
The design and testing of an optimal beam composed of unimodal elements p 3747 N92-31873
Neutron radiation damage to silicon detectors
[ITN-92-85162] p 3897 N92-31958
TENNESSEE UNIV., KNOXVILLE.
Non-convex problems in PDE: Equilibrium theory and dynamics
[AD-A250549] p 3887 N92-32081
TENNESSEE UNIV. SPACE INST., TULLAHOMA.
Monitoring gas temperatures entering an MHD superheater
[DE92-014200] p 3903 N92-31372
COMET: Commercial space opportunities through developed technologies
[TABES PAPER 92-453] p 3764 N92-32017
TEXAS A&M UNIV., COLLEGE STATION.
A robust algorithm for isotropic reconstruction of magic-angle spinning solid-state NMR spectra
[AD-A249610] p 3874 N92-31379
An approximate local thermodynamic nonequilibrium radiation model for air
[NASA-CR-190580] p 3914 N92-31577
The mechanics of fractal damage
[AD-A250518] p 3776 N92-32075
TEXAS UNIV., ARLINGTON.
Experimental studies of hypersonic shock-wave boundary-layer interactions
[NASA-CR-190731] p 3753 N92-32162
TEXAS UNIV., AUSTIN.
Amplification mechanism of ion-ripple lasers and its possible application
[DE92-016155] p 3830 N92-31411
Vortices associated with toroidal ion temperature gradient driven fluctuations
[DE92-016180] p 3903 N92-31412
TEXAS UNIV. AT DALLAS, RICHARDSON.
Dual gated imaging system for enhanced fluorescent diagnostics measurements
[AD-A249673] p 3828 N92-31694
TEXTRON DEFENSE SYSTEMS, EVERETT, MA.
CO2 laser frequency multiplication
[AD-A248574] p 3830 N92-31755
TOPICAL TESTING, INC., SALT LAKE CITY, UT.
A biological model of the effects of toxic substances
[AD-A247138] p 3867 N92-31980
TORONTO UNIV. (ONTARIO).
Experiment on a three-beam adaptive array for EHF frequency-hopped signals using a fast algorithm, phase-D
[CTN-92-60322] p 3810 N92-32203
TRW SPACE TECHNOLOGY LABS., REDONDO BEACH, CA.
Laser-initiated conical detonation wave for supersonic combustion, part 3
[AD-A250522] p 3785 N92-32076
TUFTS UNIV., MEDFORD, MA.
High-resolution microwave observations of the sun
[AD-A247869] p 3925 N92-31985

U

UNITED SOLAR SYSTEMS CORP., TROY, MI.
Research on stable, high-efficiency amorphous silicon multijunction modules
[DE92-001244] p 3814 N92-31525
UNITED TECHNOLOGIES CORP., EAST HARTFORD, CT.
Life prediction and constitutive models for engine hot section anisotropic materials program
[NASA-CR-189222] p 3759 N92-31534
UNIVERSITY OF CENTRAL FLORIDA, ORLANDO.
Head tracking and head mounted displays for training simulations
[AD-A250866] p 3873 N92-31974
UNIVERSITY OF NORTHERN ILLINOIS, DE KALB.
Interfacial ion transport between immiscible liquids
[AD-A252424] p 3778 N92-31292
UNIVERSITY OF SOUTH FLORIDA, TAMPA.
Development of the aspect graph representation for use in R version
[AD-A247109] p 3876 N92-31573
UNIVERSITY OF SOUTHERN CALIFORNIA, LOS ANGELES.
Development of an electrochemical method for field testing of protective coatings
[AD-A245872] p 3793 N92-31473
Proposal for a workshop in the physics and application of hollow electrode glow switches
[AD-A247139] p 3814 N92-31490
UNIVERSITY OF SOUTHERN MISSISSIPPI, HATTIESBURG.
Linear and star-branched siloxy-silane polymers: One pot A-B polymerization and end-capping
[AD-A252195] p 3792 N92-31408
UOP, INC., DES PLAINES, IL.
The development of precipitated iron catalysts with improved stability
[DE92-014630] p 3785 N92-32117
UTAH STATE UNIV., LOGAN.
Organometallic Nonlinear Optical (NLO) polymers. Part 2: Synthesis of main-chain organometallic polymers and a structural study of ferrocene NLO-Phores
[AD-A250655] p 3791 N92-31318
The flow of plasma in the solar terrestrial environment
[NASA-CR-190200] p 3925 N92-31338
Organic main-chain NLO polymers. 1: Copolymerization of bis(arylcarboxaldehyde) and bis(cyanoacetate) monomers via the Knoevenagel condensation
[AD-A250215] p 3802 N92-31826
USU center of excellence in theory and analysis of the geo-plasma environment
[AD-A252189] p 3858 N92-32055
UTAH UNIV., SALT LAKE CITY.
New sources for OMVPE
[AD-A250903] p 3909 N92-31582
Decomposition studies of triisopropylantimony and triallylantimony
[AD-A250671] p 3796 N92-31968
UTRECHT STATE UNIV. (NETHERLANDS).
Towards a complete hierarchy of compositional dataflow models
[RUU-CS-91-45] p 3807 N92-31715

V

VARIAN ASSOCIATES, PALO ALTO, CA.
Advanced high efficiency concentrator cells
[DE92-010559] p 3848 N92-31893
VERMONT UNIV., BURLINGTON.
CSM solutions of rotating blade dynamics using integrating matrices
[NASA-CR-190577] p 3840 N92-31619
Inorganic rings on carbon chains
[AD-A251043] p 3772 N92-31850
VIRGINIA POLYTECHNIC INST. AND STATE UNIV., BLACKSBURG.
Composite material shear property measurement using the Iosipescu specimen
[NASA-CR-190661] p 3772 N92-31274
Description of a 1000 sensor constant current anemometer system for locating three-dimensional turbulent boundary layer separations
[AD-A250827] p 3821 N92-31452
An experimental procedure for the Iosipescu composite specimen tested in the modified Wyoming fixture
[NASA-CR-190660] p 3774 N92-31566
Research and development of methods and tools for achieving and maintaining consensus processes in the face of change within and among government oversight agencies, volume 1
[DE92-014179] p 3852 N92-31592
Role of interfaces and interphases in the evolution mechanics of material systems
[AD-A250410] p 3774 N92-31604
An integrated research program for the modeling, analysis and control of aerospace systems
[AD-A250199] p 3761 N92-31966
A computational examination of directional stability for smooth and chined forebodies at high-alpha
[NASA-CR-4465] p 3753 N92-32114
Optimal design of geodesically stiffened composite cylindrical shells
[NASA-CR-190706] p 3842 N92-32235
VIRGINIA UNIV., CHARLOTTESVILLE.
International Semiconductor Device Research Symposium (ISDRS-91)
[AD-A249348] p 3813 N92-31373
International Semiconductor Device Research Symposium (ISDRS-91)
[AD-A247394] p 3908 N92-31537
Artificial neural network implementation of a near-ideal error prediction controller
[NASA-CR-190694] p 3880 N92-32122

W

WALCOFF AND ASSOCIATES, INC., ALEXANDRIA, VA.
Proceedings of the 4th Atlantic OCS Region Information Transfer Meeting
[PB92-177690] p 3864 N92-31630
WASHINGTON STATE UNIV., PULLMAN.
Particle emission and charging effects induced by fracture
[AD-A252182] p 3913 N92-32065
WASHINGTON UNIV., SEATTLE.
Monte Carlo simulations of random rough surface scattering with finite element and finite difference methods
[AD-A247528] p 3901 N92-31430
Transient internal probe diagnostic
[AD-A247306] p 3903 N92-31459
Solar neutrinos: Theory versus experiment
[DE92-014327] p 3925 N92-32154
An investigation of the thermoviscoplastic behavior of a metal matrix composite at elevated temperatures
[NASA-CR-190700] p 3777 N92-32159
WAYNE STATE UNIV., DETROIT, MI.
Evolution and analysis of the functional domains of the chimeric proteins that initiate pyrimidine biosynthesis
[AD-A250069] p 3866 N92-31465
WEST CHESTER UNIV., PA.
Algorithms for the determination of spatial and spectral distribution of electromagnetic energy in a simulated biostructure subjected to transient spatially heterogeneous radiation with applications to radar hazard assessment and cancer therapy
[AD-A250447] p 3805 N92-31381
WESTINGHOUSE DEFENSE AND ELECTRONIC SYSTEMS CENTER, BALTIMORE, MD.
Stable integrated microwave to optical modulator
[AD-A249974] p 3813 N92-31431
WESTINGHOUSE SAVANNAH RIVER CO., AIKEN, SC.
Two-component flow study in large-diameter horizontal pipe
[DE92-013196] p 3820 N92-31420
Flow instability in a vertical annulus under steady state and transient conditions
[DE92-013217] p 3820 N92-31421
Objects used to implement intelligent databases
[DE92-013098] p 3919 N92-31581
Computer applications for engineering/structural analysis
[DE92-013070] p 3841 N92-31745
Heat transfer and pressure drop in an annular channel with downflow
[DE92-014363] p 3825 N92-32115
Prompt neutron lifetime in a strongly heterogeneous lattice
[DE92-013212] p 3898 N92-32165
WESTINGHOUSE SCIENCE AND TECHNOLOGY CENTER, PITTSBURGH, PA.
High temperature superconducting films and multilayers for electronics
[AD-A250732] p 3813 N92-31451
WICHITA STATE UNIV., KS.
Database explorer: Large scale database application
[AD-A252183] p 3920 N92-32049
WISCONSIN UNIV., MADISON.
Activities of the Center for X Ray Lithography, phase 1
[AD-A250446] p 3901 N92-31397
The pathways and dynamics of molecular decomposition
[AD-A249627] p 3893 N92-31463
Electrostatic turbulence and transport in the RFP edge
[DE92-014322] p 3905 N92-31730
WOODS HOLE OCEANOGRAPHIC INST., MA.
A data processing module for acoustic Doppler current meters
[AD-A250901] p 3891 N92-31563
Hydrographic observations from the US/PRC cooperative program in the western equatorial Pacific Ocean: Cruises 5-8
[PB92-177054] p 3865 N92-31644
World ocean circulation experiment. WOCE chlorofluorocarbon intercomparison cruise report
[PB92-185974] p 3865 N92-31842
WOODWARD-CLYDE CONSULTANTS, PASADENA, CA.
Time domain regional discriminants
[AD-A249949] p 3855 N92-31509
WORCESTER POLYTECHNIC INST., MA.
Granular flows down bumpy inclines
[DE92-013568] p 3820 N92-31425
WRIGHT LAB., WRIGHT-PATTERSON AFB, OH.
Analysis of random induced cross polarization
[AD-A249773] p 3806 N92-31569
Pressure and temperature for B-1B transparency test
[AD-A252711] p 3752 N92-31674
An assessment of the B-747's capability to operate on rough surfaces
[AD-A250134] p 3757 N92-31793
VAASEL-ANSYS comparison for a thermally loaded beam
[AD-A251003] p 3841 N92-31847
WRIGHT STATE UNIV., DAYTON, OH.
Ariel database rule system project
[AD-A250443] p 3917 N92-31396
A study of the effect of hydrocarbon structure on the induction of male rat nephropathy and metabolite structure
[AD-A252192] p 3867 N92-31590
WYOMING UNIV., LARAMIE.
An airborne study of boundary layer heat and moisture fluxes for project FIFE
[NASA-CR-190665] p 3844 N92-31357

X

XEROX PALO ALTO RESEARCH CENTER, CA.
Pulsed laser deposition of high Tc superconducting thin films
[AD-A250657] p 3830 N92-31319

Y

YORK UNIV. (ONTARIO).
Illusory self motion and disorientation
[CTN-92-60318] p 3871 N92-31472

Typical Contract Number Index Listing

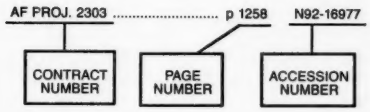

Listings in this index are arranged alphanumerically by contract number. Under each contract number the accession numbers denoting documents that have been produced as a result of research done under that contract are arranged in ascending order. The page number helps to locate the citation in the abstract section. The accession number denotes the number by which the citation is identified.

AF PROJ. S321 ..... p 3924 N92-32142
AF PROJ. 2300 ..... p 3752 N92-31622
AF PROJ. 2401 ..... p 3752 N92-31674
AF PROJ. 2688 ..... p 3902 N92-32144
AF PROJ. 3048 ..... p 3799 N92-31462
AF PROJ. 7231 ..... p 3872 N92-31458
AF-AFOSR-0005-89 ..... p 3773 N92-31305
AF-AFOSR-0005-90 ..... p 3809 N92-31944
AF-AFOSR-0023-89 ..... p 3770 N92-31474
AF-AFOSR-0026-90 ..... p 3858 N92-32055
AF-AFOSR-0033-89 ..... p 3823 N92-31824
AF-AFOSR-0036-89 ..... p 3876 N92-31573
AF-AFOSR-0041-89 ..... p 3871 N92-31758
p 3867 N92-31778
AF-AFOSR-0061-89 ..... p 3787 N92-31612
AF-AFOSR-0079-90 ..... p 3896 N92-31858
AF-AFOSR-0088-88 ..... p 3880 N92-32039
AF-AFOSR-0095-90 ..... p 3872 N92-32105
AF-AFOSR-0144-90 ..... p 3883 N92-32040
AF-AFOSR-0147-89 ..... p 3925 N92-31985
AF-AFOSR-0175-91 ..... p 3869 N92-31905
AF-AFOSR-0182-91 ..... p 3871 N92-31779
AF-AFOSR-0183-90 ..... p 3805 N92-31381
AF-AFOSR-0204-88 ..... p 3885 N92-32041
AF-AFOSR-0216-89 ..... p 3774 N92-31604
AF-AFOSR-0223-88 ..... p 3819 N92-31286
AF-AFOSR-0229-89 ..... p 3795 N92-31951
AF-AFOSR-0231-88 ..... p 3872 N92-31330
AF-AFOSR-0232-91 ..... p 3887 N92-32081
AF-AFOSR-0235-87 ..... p 3868 N92-31491
AF-AFOSR-0248-89 ..... p 3912 N92-31915
AF-AFOSR-0271-88 ..... p 3822 N92-31559
AF-AFOSR-0286-89 ..... p 3917 N92-31396
AF-AFOSR-0292-91 ..... p 3804 N92-31333
AF-AFOSR-0292-92 ..... p 3761 N92-31966
AF-AFOSR-0294-89 ..... p 3761 N92-31967
AF-AFOSR-0337-89 ..... p 3831 N92-31802
AF-AFOSR-0342-89 ..... p 3814 N92-31490
AF-AFOSR-0345-90 ..... p 3903 N92-31459
AF-AFOSR-0346-88 ..... p 3790 N92-32084
AF-AFOSR-0358-90 ..... p 3897 N92-31936
AF-AFOSR-0359-89 ..... p 3825 N92-32038
AF-AFOSR-0364-89 ..... p 3796 N92-32001
AF-AFOSR-0373-90 ..... p 3776 N92-32075
AF-AFOSR-0396-89 ..... p 3867 N92-31590
AF-AFOSR-0421-89 ..... p 3820 N92-31322
AF-AFOSR-0460-89 ..... p 3842 N92-32168
AF-AFOSR-0536-89 ..... p 3884 N92-31332
AF-AFOSR-0540-89 ..... p 3823 N92-31696
AF-AFOSR-2048-88 ..... p 3908 N92-31496
ARPA ORDER 5404 ..... p 3874 N92-31353
ARPA ORDER 8162 ..... p 3816 N92-31791
ATD-91-DAC-7103 ..... p 3761 N92-31656
BMFT-KF-20128 ..... p 3861 N92-31708
DA PROJ. M00-94 ..... p 3868 N92-31492
DA PROJ. RJ1-4-C-02 ..... p 3892 N92-31818
DA PROJ. 1L1-61102-AH-42 ..... p 3794 N92-31624
DA PROJ. 1L1-61102-AH-43 ..... p 3778 N92-31393
p 3782 N92-31803
p 3800 N92-31804
DA PROJ. 1L1-62211-A-47-A ..... p 3832 N92-31349
p 3834 N92-31485
DA PROJ. 1L1-62705-AH-94 ..... p 3913 N92-32078
DA PROJ. 162-63102-D-071 ..... p 3775 N92-31940
DA PROJ. 3MI-62770-A-871 ..... p 3868 N92-31326
DA PROJ. 3M1-62787-A-878 ..... p 3870 N92-32107
DA PROJ. 3M2-63002-D-995 ..... p 3868 N92-31554
DAAD09-87-D-0008 ..... p 3800 N92-31969
p 3800 N92-31970
p 3800 N92-31971
p 3801 N92-31972
p 3801 N92-31973
DAAL03-86-D-0001 ..... p 3800 N92-31800
DAAL03-86-G-0190 ..... p 3857 N92-31964
DAAL03-86-K-0129 ..... p 3901 N92-31380
DAAL03-87-K-0123 ..... p 3780 N92-31671
DAAL03-88-K-0039 ..... p 3907 N92-31375
DAAL03-88-K-0098 ..... p 3792 N92-31377
DAAL03-88-K-0189 ..... p 3893 N92-31463
DAAL03-88-K-0192 ..... p 3791 N92-31358
DAAL03-89-K-0016 ..... p 3886 N92-31567
DAAL03-89-K-0127 ..... p 3805 N92-31376
DAAL03-91-C-0014 ..... p 3792 N92-31388
DAAL03-91-C-0021 ..... p 3767 N92-31997
DAAL03-91-C-0030 ..... p 3813 N92-31374
DAAL03-91-C-0033 ..... p 3814 N92-31464
DAAL03-91-G-0084 ..... p 3773 N92-31378
DAAL03-91-G-0101 ..... p 3888 N92-31600
p 3888 N92-31757
DAAL03-91-G-0123 ..... p 3887 N92-32164
DAAL03-91-G-0139 ..... p 3833 N92-31363
p 3833 N92-31433
DAAL03-91-G-0148 ..... p 3828 N92-31694
DAAL03-91-G-0217 ..... p 3901 N92-31430
DAAL03-91-G-0240 ..... p 3889 N92-31359
DAAL03-91-G-0297 ..... p 3905 N92-31688
DAAL03-91-G-0338 ..... p 3813 N92-31373
DAAL04-88-C-0029 ..... p 3914 N92-32207
DAAL04-90-C-0013 ..... p 3776 N92-31979
DAAL04-90-M-0746 ..... p 3775 N92-31940
DACA76-85-C-0002 ..... p 3884 N92-31511
DACA76-85-C-0003 ..... p 3884 N92-31511
DAJA45-90-C-0031 ..... p 3870 N92-31291
DAMD17-86-C-66030 ..... p 3868 N92-31326
DAMD17-91-C-1007 ..... p 3870 N92-32107
DCIEM-07SE-W7711-7-7012 ..... p 3871 N92-31472
DE-AC02-76CH-00016 ..... p 3907 N92-31296
p 3851 N92-31422
p 3827 N92-31502
p 3869 N92-31589
p 3909 N92-31627
p 3815 N92-31651
p 3894 N92-31679
p 3901 N92-31737
p 3865 N92-31842
p 3841 N92-31844
p 3824 N92-31977
p 3849 N92-32118
p 3849 N92-32124
p 3803 N92-32125
p 3810 N92-32134
DE-AC02-76CH-03000 ..... p 3826 N92-31313
p 3898 N92-32167
DE-AC02-79ET-10815 ..... p 3903 N92-31372
DE-AC02-80ER-10667 ..... p 3896 N92-31926
DE-AC02-83CH-10093 ..... p 3872 N92-31309
p 3845 N92-31481
p 3846 N92-31497
p 3846 N92-31498
p 3814 N92-31525
p 3846 N92-31526
p 3847 N92-31579
p 3799 N92-31593
p 3847 N92-31623
p 3847 N92-31646
p 3848 N92-31893
p 3785 N92-32093
p 3849 N92-32110
p 3849 N92-32112
DE-AC02-92CH-10510 ..... p 3817 N92-31834
DE-AC03-76SF-00098 ..... p 3779 N92-31417
p 3926 N92-31756
p 3898 N92-32006
DE-AC03-76SF-00515 ..... p 3812 N92-31289
p 3899 N92-31390
p 3915 N92-31663
p 3900 N92-32131
p 3900 N92-32133
p 3902 N92-32149
DE-AC03-81ER-40009 ..... p 3893 N92-31385
DE-AC03-89ER-51114 ..... p 3904 N92-31616
p 3781 N92-31729
p 3905 N92-31764
DE-AC03-89ER-52153 ..... p 3905 N92-31749
DE-AC04-76DP-00613 ..... p 3838 N92-31303
p 3876 N92-31529
p 3817 N92-31946
p 3789 N92-32032
p 3817 N92-32033
p 3777 N92-32135
p 3797 N92-32136
DE-AC04-76DP-00789 ..... p 3900 N92-31295
p 3805 N92-31387
p 3908 N92-31403
p 3851 N92-31427
p 3793 N92-31539
p 3765 N92-31542
p 3799 N92-31570
p 3919 N92-31578
p 3802 N92-31580
p 3794 N92-31631
p 3910 N92-31668
p 3878 N92-31669
p 3905 N92-31707
p 3861 N92-31709
p 3816 N92-31718
p 3766 N92-31735
p 3757 N92-31736
p 3808 N92-31738
p 3756 N92-31746
p 3781 N92-31748
p 3862 N92-31750
p 3837 N92-31753
p 3824 N92-31832
p 3854 N92-31931
p 3824 N92-31933
p 3906 N92-31949
p 3771 N92-32030
p 3885 N92-32036
p 3917 N92-32037
p 3848 N92-32087
p 3842 N92-32088
p 3900 N92-32123
p 3790 N92-32139
p 3829 N92-32174
DE-AC04-76DR-00789 ..... p 3779 N92-31417
p 3788 N92-31744
p 3906 N92-31771
p 3782 N92-31773
p 3783 N92-31860
DE-AC04-90AL-58770 ..... p 3767 N92-31997
DE-AC05-76OR-00033 ..... p 3821 N92-31426
DE-AC05-84OR-21400 ..... p 3804 N92-31354
p 3839 N92-31383
p 3833 N92-31384
p 3868 N92-31409
p 3786 N92-31418
p 3875 N92-31447
p 3814 N92-31499
p 3834 N92-31500
p 3839 N92-31501
p 3851 N92-31527
p 3815 N92-31650
p 3894 N92-31679
p 3894 N92-31700
p 3853 N92-31782
p 3906 N92-31829
p 3899 N92-31831
p 3853 N92-31896
p 3770 N92-31897
p 3789 N92-31898
p 3854 N92-31907
p 3775 N92-31912
p 3906 N92-31913
p 3795 N92-31917
p 3896 N92-31923
p 3883 N92-32034

DE-AC05-84OT-21400 p 3783 N92-31816
DE-AC06-76RL-01830 p 3813 N92-31440
p 3852 N92-31574
p 3841 N92-31638
p 3837 N92-31657
p 3910 N92-31665
p 3867 N92-31711
p 3853 N92-31732
p 3848 N92-31845
p 3768 N92-31846
p 3797 N92-32146
DE-AC07-76ID-01570 p 3819 N92-31287
p 3831 N92-31762
p 3835 N92-31807
p 3824 N92-31977
DE-AC08-88NV-10617 p 3918 N92-31448
p 3881 N92-32150
DE-AC09-89SR-18035 p 3820 N92-31420
p 3820 N92-31421
p 3919 N92-31581
p 3841 N92-31745
p 3825 N92-32115
p 3898 N92-32165
DE-AC21-89MC-26034 p 3784 N92-31976
DE-AC22-87PC-79812 p 3785 N92-32117
DE-AC22-89PC-89877 p 3786 N92-32141
DE-AC22-91PC-90185 p 3820 N92-31425
DE-AC34-90DP-62349 p 3829 N92-32138
DE-AC35-89ER-40486 p 3836 N92-31647
p 3815 N92-31664
p 3816 N92-31760
p 3899 N92-31948
p 3900 N92-31975
p 3890 N92-32140
DE-AI01-90CE-21041 p 3827 N92-31633
DE-AI05-90ER-61011 p 3862 N92-31734
DE-AS03-89ER-40527 p 3812 N92-31289
DE-FC21-90MC-26029 p 3799 N92-31751
DE-FG01-89CE-28301 p 3845 N92-31290
DE-FG02-84ER-13299 p 3783 N92-31891
DE-FG02-84ER-45166 p 3839 N92-31400
DE-FG02-84ER-60246 p 3850 N92-31312
DE-FG02-85ER-53198 p 3905 N92-31730
DE-FG02-86ER-13552 p 3781 N92-31752
DE-FG02-87ER-40371 p 3900 N92-32028
DE-FG02-87ER-45309 p 3793 N92-31538
DE-FG02-87ER-45334 p 3912 N92-31945
DE-FG02-87ER-53257 p 3905 N92-31727
DE-FG02-87ER-60522 p 3867 N92-32120
DE-FG02-88DP-48058 p 3852 N92-31592
DE-FG02-88ER-12817 p 3836 N92-31336
DE-FG02-88ER-13896 p 3823 N92-31726
DE-FG02-88ER-13916 p 3890 N92-32035
DE-FG02-88ER-13937 p 3831 N92-31798
DE-FG02-88ER-45372 p 3775 N92-31806
DE-FG02-88ER-60631 p 3867 N92-31747
DE-FG02-89CE-90029 p 3890 N92-32099
DE-FG02-89ER-45388 p 3788 N92-31733
DE-FG02-89ER-45398 p 3797 N92-32095
DE-FG02-90ER-12932 p 3828 N92-31919
DE-FG02-90ER-14150 p 3781 N92-31717
DE-FG02-90ER-40560 p 3899 N92-31712
p 3924 N92-31713
DE-FG02-90ER-45433 p 3839 N92-31389
DE-FG02-90ER-75564 p 3923 N92-31965
DE-FG02-91ER-14189 p 3781 N92-31725
DE-FG02-91ER-54110 p 3904 N92-31545
DE-FG02-91ER-54131 p 3903 N92-31494
DE-FG02-91ER-61202 p 3864 N92-31572
DE-FG03-85ER-13418 p 3858 N92-32027
DE-FG03-86ER-53225 p 3830 N92-31411
DE-FG03-86ER-60479 p 3853 N92-31626
DE-FG03-87ER-13657 p 3894 N92-31606
DE-FG03-91SF-18862 p 3898 N92-32007
DE-FG03-92ER-25116 p 3875 N92-31410
DE-FG04-87AL-43771 p 3779 N92-31416
DE-FG05-80ET-53088 p 3830 N92-31411
p 3903 N92-31412
DE-FG05-84ER-40159 p 3895 N92-31721
DE-FG05-85ER-45208 p 3911 N92-31914
DE-FG05-86ER-40272 p 3893 N92-31552
DE-FG05-87ER-13751 p 3895 N92-31724
DE-FG05-87ER-40322 p 3897 N92-31927
DE-FG05-87ER-51112 p 3904 N92-31613
DE-FG05-87ER-52147 p 3831 N92-31769
p 3832 N92-31935
DE-FG05-88ER-13977 p 3835 N92-31929
DE-FG05-90ER-61075 p 3862 N92-31894
DE-FG06-84ER-60247 p 3850 N92-31304
DE-FG06-85ER-40224 p 3895 N92-31812
DE-FG06-87ER-13664 p 3785 N92-32113
DE-FG06-88ER-40427 p 3925 N92-32154
DE-FG22-90PC-90305 p 3784 N92-32029
DI-14-12-0001-30583 p 3864 N92-31630
DNA001-88-C-0057 p 3891 N92-31588
DNA0046-C156-AI p 3804 N92-31354
DREA-W7707-7-7926 p 3806 N92-31471
DREA-W77707-9-0214-01-OCS p 3811 N92-32214
DREO-55SS.W7714-8-5725 p 3873 N92-32031
DRET-88-521 p 3751 N92-31508
DSS-36001-8-3527-01-SS p 3810 N92-32203
DTCG23-86-C-20062 p 3789 N92-31987
DTFA01-89-Z-02033 p 3863 N92-32103
EPA-68-02-3365 p 3781 N92-31683
FAA-T0704-E p 3756 N92-31838
FY1455-89-N-0635 p 3798 N92-31399
F04701-88-C-0089 p 3807 N92-31629
F08606-89-C-0022 p 3856 N92-31510
p 3865 N92-31821
F19628-87-C-0173 p 3908 N92-31438
F19628-87-K-0045 p 3924 N92-32142
F19628-88-C-0038 p 3879 N92-31833
F19628-88-C-0154 p 3902 N92-32144
F19628-89-C-0001 p 3843 N92-31323
F19628-89-K-0016 p 3767 N92-32082
F19628-90-C-0003 p 3876 N92-31541
F19628-90-C-0156 p 3884 N92-31293
F19628-90-C-0194 p 3855 N92-31509
F19628-90-K-0026 p 3926 N92-31477
F19628-90-K-0057 p 3855 N92-31476
F19628-91-C-0168 p 3887 N92-32171
F30602-88-C-0019 p 3876 N92-31586
F30602-88-D-0025 p 3879 N92-31825
F33615-85-C-3213 p 3773 N92-31307
F33615-86-C-3006 p 3752 N92-31777
F33615-87-C-5212 p 3776 N92-32047
p 3776 N92-32048
F33615-89-C-0008 p 3870 N92-31321
F33615-90-C-0013 p 3885 N92-31811
F33615-90-C-2075 p 3801 N92-31982
F40600-87-C-0003 p 3826 N92-31298
F49620-86-C-0078 p 3819 N92-31283
F49620-88-C-0014 p 3792 N92-31419
F49620-88-C-0022 p 3760 N92-32059
F49620-88-C-0076 p 3752 N92-31555
F49620-88-C-0082 p 3819 N92-31306
F49620-88-C-0089 p 3832 N92-32042
F49620-88-C-0129 p 3915 N92-31585
F49620-89-C-0003 p 3777 N92-32104
F49620-90-C-0069 p 3830 N92-31319
F49620-90-C-0070 p 3785 N92-32076
F49620-91-C-0012 p 3867 N92-31980
F49620-91-C-0015 p 3825 N92-32000
F49620-91-C-0034 p 3813 N92-31451
F49620-91-C-0036 p 3888 N92-31981
F49620-91-C-0089 p 3890 N92-32046
F49620-91-C-0090 p 3902 N92-32092
GRI-5083-243-0787 p 3835 N92-31841
GRI-5088-271-1680 p 3824 N92-31839
GRI-5089-260-1828 p 3782 N92-31776
GRI-5089-260-1839 p 3783 N92-31918
GRI-5090-260-2048 p 3848 N92-31922
GRI-5090-260-2069 p 3848 N92-31903
JPL-959072 p 3829 N92-32128
JPL-9950-1365 p 3892 N92-32178
MDA972-90-C-0013 p 3821 N92-31452
MDA972-91-C-0029 p 3816 N92-31791
MIPR-FY76169100412 p 3859 N92-31540
MIPR-113-90 p 3866 N92-31302
MIPR-122-89 p 3866 N92-31302
MITRE RP-91260 p 3810 N92-32043
NAGW-1696 p 3855 N92-32222
NAGW-1708 p 3758 N92-32111
NAG1-1003 p 3914 N92-31577
NAG1-1037 p 3753 N92-32114
NAG1-1053 p 3772 N92-31274
p 3774 N92-31566
NAG1-1060 p 3881 N92-32157
NAG1-1094 p 3839 N92-31339
NAG1-1097 p 3840 N92-31619
NAG1-1145 p 3887 N92-32164
NAG1-1280 p 3841 N92-31911
NAG1-1327 p 3766 N92-31260
NAG1-562 p 3804 N92-31273
NAG1-643 p 3842 N92-32235
NAG1-709 p 3842 N92-32236
NAG1-891 p 3753 N92-32162
NAG1-928 p 3755 N92-31549
NAG1-968 p 3884 N92-31254
NAG1-974 p 3777 N92-32159
NAG1-995 p 3881 N92-32157
NAG2-541 p 3803 N92-31238
NAG2-593 p 3886 N92-31553
NAG2-656 p 3870 N92-31341
NAG3-1202 p 3762 N92-31252
NAG3-1269 p 3820 N92-31352
NAG3-954 p 3772 N92-31266
NAG5-1392 p 3806 N92-31468
NAG5-1484 p 3925 N92-31338
NAG5-913 p 3844 N92-31357
NANB7D737 p 3780 N92-31678
NASA ORDER H-11987-D p 3845 N92-32223
NASW-16215 p 3853 N92-31649
NAS1-18027 p 3761 N92-32175
NAS1-18147 p 3766 N92-32130
NAS1-18240 p 3822 N92-31535
NAS1-18599 p 3826 N92-32242
NAS1-18605 p 3822 N92-31535
p 3876 N92-31561
p 3822 N92-31564
p 3822 N92-31687
p 3758 N92-32111
p 3881 N92-32157
p 3826 N92-32158
p 3887 N92-32164
NAS1-18703 p 3754 N92-32226
p 3754 N92-32228
NAS1-19241 p 3767 N92-32100
NAS1-19247 p 3767 N92-31677
NAS1-19480 p 3818 N92-31265
p 3822 N92-31535
p 3881 N92-32157
p 3826 N92-32158
NAS2-12722 p 3761 N92-31656
NAS3-2290 p 3765 N92-31251
NAS3-23721 p 3891 N92-31248
NAS3-23772 p 3771 N92-32129
NAS3-23773 p 3835 N92-31892
NAS3-23885 p 3769 N92-31245
NAS3-23939 p 3759 N92-31534
NAS3-25266 p 3845 N92-31262
p 3769 N92-31342
p 3772 N92-32239
p 3754 N92-32240
NAS3-25870 p 3808 N92-31855
NAS5-30791 p 3858 N92-32195
NAS7-1170 p 3845 N92-32223
NAS8-32805 p 3925 N92-31856
NAS8-35018 p 3760 N92-31910
NAS8-36955 p 3883 N92-31835
NAS8-37365 p 3770 N92-31550
NAS8-38609 p 3856 N92-31551
NA85AA-D-AC117 p 3865 N92-31644
NCA2-543 p 3807 N92-31614
NCC2-522 p 3752 N92-31533
NCC2-637 p 3753 N92-32177
NCC2-741 p 3790 N92-32156
NCC3-189 p 3745 N92-31267
NCC9-16 p 3917 N92-31272
p 3882 N92-31483
p 3875 N92-31486
p 3875 N92-31487
p 3916 N92-31547
p 3885 N92-31597
p 3879 N92-31787
NGT-70172 p 3880 N92-32122
NR PROJ. MM3-3-P-30 p 3828 N92-31794
NR PROJ. MR0-4101 p 3872 N92-31327
NR PROJ. RR0-4106 p 3866 N92-31465
NR PROJ. 627838 p 3785 N92-32080
NSF ASC-88-19373 p 3881 N92-32157
NSF ASC-88-19374 p 3876 N92-31561
NSF ATM-90-22249 p 3925 N92-31786
NSF CCR-92-01195 p 3881 N92-32157
NSF CHE-85-16904 p 3785 N92-32080
NSF DDM-88-00281 p 3888 N92-31768
NSF DDM-89-01495 p 3888 N92-31768
NSF DDM-90-01705 p 3888 N92-31768
NSF DMR-88-09714 p 3772 N92-31274
NSF DSM-91-03997 p 3887 N92-32164
NSF MIP-90-16734 p 3877 N92-31642
NSF OCE-86-13321 p 3865 N92-31842
NSF OCE-92-06184 p 3865 N92-31842
N00014-82-K-0193 p 3881 N92-31428
p 3882 N92-31445
N00014-82-K-0280 p 3911 N92-31851
N00014-82-K-0612 p 3796 N92-32079
p 3785 N92-32080
N00014-84-K-0415 p 3874 N92-31353
p 3880 N92-31939
N00014-85-K-0150 p 3885 N92-31827
N00014-86-K-0684 p 3857 N92-31766
N00014-86-K-0686 p 3908 N92-31446
N00014-86-K-0799 p 3773 N92-31361
N00014-87-J-1248 p 3898 N92-32169
p 3900 N92-32170
N00014-87-K-0081 p 3866 N92-31465
N00014-87-K-0488 p 3912 N92-31984
N00014-87-K-0514 p 3913 N92-32065
N00014-87-K-0548 p 3881 N92-31428
N00014-87-K-6009 p 3863 N92-31406

N00014-88-D-0333 ..... p 3857 N92-31986
N00014-88-K-0104 ..... p 3875 N92-31480
N00014-88-K-0304 ..... p 3871 N92-31444
N00014-88-K-0591 ..... p 3797 N92-32151
p 3883 N92-32152
N00014-88-K-0641 ..... p 3917 N92-31285
N00014-88-R-0330 ..... p 3902 N92-32077
N00014-89-C-2274 ..... p 3827 N92-31475
N00014-89-J-1024 ..... p 3823 N92-31770
p 3925 N92-31786
N00014-89-J-1041 ..... p 3772 N92-31850
N00014-89-J-1097 ..... p 3907 N92-31983
N00014-89-J-1136 ..... p 3816 N92-31799
N00014-89-J-1169 ..... p 3899 N92-32196
N00014-89-J-1225 ..... p 3792 N92-31408
N00014-89-J-1235 ..... p 3785 N92-32057
N00014-89-J-1288 ..... p 3891 N92-31563
N00014-89-J-1459 ..... p 3773 N92-31315
N00014-89-J-1542 ..... p 3792 N92-31394
p 3780 N92-31524
N00014-89-J-1746 ..... p 3910 N92-31699
p 3897 N92-31950
p 3897 N92-31999
N00014-89-J-1754 ..... p 3855 N92-31478
N00014-89-J-1849 ..... p 3911 N92-31819
N00014-89-J-1946 ..... p 3797 N92-32151
p 3883 N92-32152
N00014-89-J-1988 ..... p 3887 N92-32163
N00014-89-J-2017 ..... p 3901 N92-31397
N00014-89-J-3062 ..... p 3779 N92-31434
N00014-89-J-3187 ..... p 3869 N92-31558
N00014-90-C-0073 ..... p 3813 N92-31431
N00014-90-J-1028 ..... p 3891 N92-32211
N00014-90-J-1159 ..... p 3912 N92-31937
p 3817 N92-32002
p 3898 N92-32024
N00014-90-J-1178 ..... p 3783 N92-31820
N00014-90-J-1186 ..... p 3795 N92-31941
p 3798 N92-32153
N00014-90-J-1198 ..... p 3907 N92-31983
N00014-90-J-1235 ..... p 3893 N92-31316
p 3893 N92-31328
N00014-90-J-1421 ..... p 3883 N92-32109
N00014-90-J-1494 ..... p 3828 N92-31828
p 3784 N92-31959
p 3796 N92-31960
p 3796 N92-31961
N00014-90-J-4044 ..... p 3810 N92-32101
N00014-90-J-4123 ..... p 3793 N92-31473
N00014-91-C-0124 ..... p 3786 N92-31360
N00014-91-C-2279 ..... p 3830 N92-31755
N00014-91-J-1012 ..... p 3798 N92-32198
N00014-91-J-1036 ..... p 3864 N92-31429
N00014-91-J-1058 ..... p 3778 N92-31292
N00014-91-J-1189 ..... p 3790 N92-32096
N00014-91-J-1269 ..... p 3911 N92-31848
N00014-91-J-1329 ..... p 3877 N92-31642
N00014-91-J-1338 ..... p 3793 N92-31435
p 3793 N92-31436
p 3795 N92-31810
N00014-91-J-1362 ..... p 3920 N92-32049
N00014-91-J-1409 ..... p 3784 N92-31998
N00014-91-J-1447 ..... p 3909 N92-31582
p 3796 N92-31968
N00014-91-J-1475 ..... p 3874 N92-31379
N00014-91-J-1590 ..... p 3794 N92-31557
N00014-91-J-1625 ..... p 3791 N92-31318
p 3802 N92-31826
N00014-91-J-1655 ..... p 3795 N92-31952
p 3795 N92-31954
p 3798 N92-32194
N00014-91-J-1852 ..... p 3817 N92-32074
N00014-91-J-1857 ..... p 3901 N92-31611
N00014-91-J-1896 ..... p 3912 N92-31994
p 3913 N92-31995
N00014-91-J-1917 ..... p 3798 N92-32197
N00014-91-J-1925 ..... p 3753 N92-31853
N00014-91-J-1934 ..... p 3788 N92-31795
p 3788 N92-31796
N00014-91-J-4059 ..... p 3838 N92-31337
N00014-91-J-4101 ..... p 3871 N92-31444
N00014-92-J-1386 ..... p 3910 N92-31666
N00039-88-C-0065 ..... p 3809 N92-31996
N61339-90-C-0041 ..... p 3873 N92-31974
N62269-90-M-7269 ..... p 3833 N92-31437
RICIS PROJ. SE-16 ..... p 3875 N92-31487
RICIS PROJ. SE-31 ..... p 3882 N92-31483
p 3916 N92-31547
RICIS PROJ. SE-34 ..... p 3879 N92-31787
RICIS PROJ. SE-43 ..... p 3917 N92-31272
p 3885 N92-31597
RTOP 474-42-10 ..... p 3812 N92-31282
RTOP 505-01-11 ..... p 3769 N92-31249
RTOP 505-02-40 ..... p 3752 N92-31808
RTOP 505-61-01-01 ..... p 3750 N92-31246
RTOP 505-62-10 ..... p 3821 N92-31484
RTOP 505-62-30-01 ..... p 3762 N92-31900
RTOP 505-62-40-06 ..... p 3826 N92-32242
RTOP 505-62-50 ..... p 3761 N92-32241
RTOP 505-62-61 ..... p 3759 N92-31250
p 3762 N92-31640
RTOP 505-63-36 ..... p 3832 N92-31349
p 3834 N92-31485
RTOP 505-63-5A ..... p 3834 N92-31536
RTOP 505-63-5B ..... p 3795 N92-31840
RTOP 505-63-50-04 ..... p 3838 N92-31279
RTOP 505-63-50-12 ..... p 3750 N92-31239
RTOP 505-63-50-15 ..... p 3757 N92-31264
p 3757 N92-31350
p 3757 N92-31351
p 3758 N92-32111
RTOP 505-64-12-02 ..... p 3755 N92-31549
RTOP 505-64-20-01 ..... p 3760 N92-31240
RTOP 505-66-41-04 ..... p 3761 N92-32175
RTOP 505-68-01-02 ..... p 3751 N92-31532
RTOP 505-68-27 ..... p 3762 N92-32201
RTOP 505-68-30-03 ..... p 3753 N92-32114
RTOP 505-68-50 ..... p 3756 N92-31261
RTOP 505-68-71 ..... p 3751 N92-31276
RTOP 505-90-52-01 ..... p 3818 N92-31265
p 3822 N92-31535
p 3876 N92-31561
p 3822 N92-31564
p 3822 N92-31687
p 3881 N92-32157
p 3826 N92-32158
p 3887 N92-32164
RTOP 506-40-21-01 ..... p 3818 N92-31247
RTOP 506-40-91-02 ..... p 3819 N92-31281
RTOP 506-41-11 ..... p 3818 N92-32233
RTOP 506-42-31 ..... p 3769 N92-31342
p 3770 N92-31901
p 3771 N92-32237
RTOP 506-46-21-01 ..... p 3766 N92-31457
RTOP 506-48-11-05 ..... p 3769 N92-32204
RTOP 506-48-91-08 ..... p 3767 N92-31677
RTOP 506-49-11-02 ..... p 3766 N92-32130
RTOP 506-49-11 ..... p 3771 N92-32108
RTOP 506-72-1C ..... p 3808 N92-31855
RTOP 510-01-08 ..... p 3775 N92-31854
RTOP 510-01-50 ..... p 3840 N92-31505
p 3774 N92-31506
RTOP 519-01-50 ..... p 3777 N92-32234
RTOP 533-02-30 ..... p 3754 N92-32240
RTOP 533-02-36 ..... p 3759 N92-31275
RTOP 533-06-01 ..... p 3754 N92-32213
RTOP 535-05-01 ..... p 3891 N92-31248
RTOP 538-02-10 ..... p 3839 N92-31504
RTOP 582-01-11 ..... p 3770 N92-31507
RTOP 586-01-11 ..... p 3769 N92-31245
RTOP 590-13-11 ..... p 3845 N92-31262
RTOP 590-13-21 ..... p 3771 N92-31916
RTOP 590-14-61-01 ..... p 3767 N92-32100
RTOP 590-21-11 ..... p 3802 N92-31263
RTOP 590-21-41 ..... p 3801 N92-32230
RTOP 593-42-21-01 ..... p 3926 N92-32193
RTOP 593-71-51 ..... p 3791 N92-31278
RTOP 665-45-20 ..... p 3844 N92-32127
RTOP 763-22-51 ..... p 3745 N92-31267
STU-89-01220P ..... p 3807 N92-31715
W-31-109-ENG-38 ..... p 3903 N92-31310
p 3886 N92-31311
p 3838 N92-31335
p 3893 N92-31386
p 3779 N92-31441
p 3799 N92-31442
p 3846 N92-31531
p 3909 N92-31546
p 3787 N92-31575
p 3852 N92-31591
p 3894 N92-31595
p 3919 N92-31596
p 3909 N92-31652
p 3877 N92-31654
p 3894 N92-31679
p 3830 N92-31684
p 3834 N92-31720
p 3835 N92-31774
p 3823 N92-31785
p 3817 N92-31834
p 3783 N92-31857
p 3879 N92-31899
p 3789 N92-31924
p 3795 N92-31938
p 3912 N92-31955
p 3825 N92-32003
p 3854 N92-32083
W-7405-ENG-36 ..... p 3804 N92-31317
p 3820 N92-31424
p 3806 N92-31449
p 3847 N92-31571
p 3815 N92-31681
p 3823 N92-31701
p 3878 N92-31703
p 3911 N92-31723
p 3895 N92-31765
p 3759 N92-31817
p 3789 N92-32004
p 3825 N92-32008
p 3825 N92-32022
p 3762 N92-32026
W-7405-ENG-48 ..... p 3850 N92-31297
p 3850 N92-31324
p 3812 N92-31334
p 3786 N92-31391
p 3778 N92-31414
p 3778 N92-31415
p 3779 N92-31416
p 3851 N92-31423
p 3882 N92-31466
p 3821 N92-31528
p 3904 N92-31530
p 3815 N92-31548
p 3794 N92-31560
p 3780 N92-31607
p 3869 N92-31608
p 3822 N92-31625
p 3910 N92-31661
p 3856 N92-31662
p 3787 N92-31667
p 3895 N92-31705
p 3910 N92-31719
p 3808 N92-31722
p 3766 N92-31735
p 3878 N92-31739
p 3882 N92-31740
p 3883 N92-31741
p 3878 N92-31742
p 3879 N92-31743
p 3788 N92-31759
p 3902 N92-31761
p 3781 N92-31763
p 3782 N92-31805
p 3832 N92-31902
p 3803 N92-31308
p 3828 N92-31909
p 3920 N92-31934
p 3923 N92-32005
p 3889 N92-32119
p 3835 N92-32121
p 3786 N92-32145
p 3855 N92-32147
p 3855 N92-32155
p 3913 N92-32166
W-7405-ENG-82 ..... p 3780 N92-31565
p 3782 N92-31772
p 3831 N92-31775
p 3890 N92-32116

Typical Report Number Index Listing

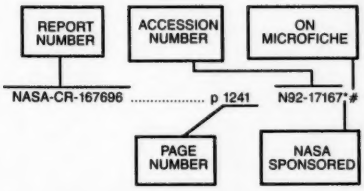

Listings in this index are arranged alphanumerically by report number. The accession number denotes the number by which the citation is identified. The page number helps to locate the citation in the abstract section. An asterisk (*) indicates that the item is a NASA report. A pound sign (#) indicates that the item is available on microfiche.

A-89236 ..... p 3754 N92-32213 * #

AD-A245286 ..... p 3790 N92-32096 #
AD-A245322 ..... p 3876 N92-31488 #
AD-A245338 ..... p 3801 N92-32098 #
AD-A245821 ..... p 3826 N92-31298 #
AD-A245866 ..... p 3872 N92-31458 #
AD-A245872 ..... p 3793 N92-31473 #
AD-A245884 ..... p 3914 N92-31489 #
AD-A245911 ..... p 3882 N92-31443 #
AD-A245952 ..... p 3758 N92-32051 #
AD-A245955 ..... p 3789 N92-32052 #
AD-A245957 ..... p 3758 N92-32053 #
AD-A245983 ..... p 3804 N92-31314 #
AD-A246046 ..... p 3756 N92-32054 #
AD-A246060 ..... p 3866 N92-32056 #
AD-A246215 ..... p 3809 N92-31993 #
AD-A246329 ..... p 3912 N92-31994 #
AD-A246331 ..... p 3913 N92-31995 #
AD-A246344 ..... p 3809 N92-31996 #
AD-A246351 ..... p 3767 N92-31997 #
AD-A246879 ..... p 3874 N92-31299 #
AD-A246980 ..... p 3784 N92-31998 #
AD-A246992 ..... p 3865 N92-31988 #
AD-A246993 ..... p 3862 N92-31978 #
AD-A247052 ..... p 3896 N92-31858 #
AD-A247053 ..... p 3920 N92-31754 #
AD-A247062 ..... p 3887 N92-32163 #
AD-A247109 ..... p 3876 N92-31573 #
AD-A247114 ..... p 3776 N92-31979 #
AD-A247138 ..... p 3867 N92-31980 #
AD-A247139 ..... p 3814 N92-31490 #
AD-A247142 ..... p 3868 N92-31491 #
AD-A247169 ..... p 3888 N92-31981 #
AD-A247185 ..... p 3870 N92-31963 #
AD-A247201 ..... p 3819 N92-31283 #
AD-A247290 ..... p 3872 N92-32105 #
AD-A247302 ..... p 3751 N92-31300 #
AD-A247304 ..... p 3871 N92-31444 #
AD-A247306 ..... p 3903 N92-31459 #
AD-A247308 ..... p 3888 N92-31768 #
AD-A247394 ..... p 3908 N92-31537 #
AD-A247498 ..... p 3869 N92-31905 #
AD-A247499 ..... p 3833 N92-31460 #
AD-A247514 ..... p 3882 N92-31445 #
AD-A247516 ..... p 3881 N92-31428 #
AD-A247519 ..... p 3864 N92-31429 #
AD-A247528 ..... p 3901 N92-31430 #
AD-A247615 ..... p 3901 N92-31611 #
AD-A247835 ..... p 3801 N92-31982 #
AD-A247847 ..... p 3907 N92-31983 #
AD-A247848 ..... p 3912 N92-31984 #
AD-A247869 ..... p 3925 N92-31985 #
AD-A247903 ..... p 3857 N92-31986 #
AD-A247920 ..... p 3814 N92-31461 #
AD-A247923 ..... p 3789 N92-31987 #
AD-A248006 ..... p 3770 N92-31474 #
AD-A248027 ..... p 3842 N92-31989 #
AD-A248029 ..... p 3911 N92-31819 #
AD-A248058 ..... p 3908 N92-31446 #
AD-A248163 ..... p 3907 N92-31990 #
AD-A248170 ..... p 3880 N92-31991 #
AD-A248323 ..... p 3804 N92-31284 #
AD-A248346 ..... p 3916 N92-31992 #
AD-A248435 ..... p 3917 N92-31285 #
AD-A248574 ..... p 3830 N92-31755 #
AD-A248587 ..... p 3773 N92-31315 #
AD-A248758 ..... p 3816 N92-31799 #
AD-A248858 ..... p 3827 N92-31475 #
AD-A248882 ..... p 3792 N92-31388 #
AD-A248940 ..... p 3855 N92-31476 #
AD-A248942 ..... p 3926 N92-31477 #
AD-A249011 ..... p 3855 N92-31478 #
AD-A249020 ..... p 3836 N92-31479 #
AD-A249225 ..... p 3857 N92-31964 #
AD-A249332 ..... p 3918 N92-31450 #
AD-A249348 ..... p 3813 N92-31373 #
AD-A249380 ..... p 3813 N92-31374 #
AD-A249524 ..... p 3886 N92-31567 #
AD-A249538 ..... p 3791 N92-31358 #
AD-A249562 ..... p 3874 N92-31353 #
AD-A249565 ..... p 3907 N92-31375 #
AD-A249577 ..... p 3804 N92-31354 #
AD-A249580 ..... p 3805 N92-31376 #
AD-A249581 ..... p 3792 N92-31377 #
AD-A249584 ..... p 3773 N92-31378 #
AD-A249610 ..... p 3874 N92-31379 #
AD-A249612 ..... p 3901 N92-31380 #
AD-A249614 ..... p 3905 N92-31688 #
AD-A249622 ..... p 3807 N92-31691 #
AD-A249623 ..... p 3890 N92-31686 #
AD-A249625 ..... p 3799 N92-31462 #
AD-A249627 ..... p 3893 N92-31463 #
AD-A249651 ..... p 3814 N92-31464 #
AD-A249673 ..... p 3828 N92-31694 #
AD-A249697 ..... p 3877 N92-31642 #
AD-A249712 ..... p 3888 N92-31600 #
AD-A249722 ..... p 3780 N92-31671 #
AD-A249725 ..... p 3894 N92-31673 #
AD-A249728 ..... p 3768 N92-31675 #
AD-A249739 ..... p 3752 N92-31622 #
AD-A249745 ..... p 3794 N92-31624 #
AD-A249751 ..... p 3893 N92-31328 #
AD-A249772 ..... p 3868 N92-31492 #
AD-A249773 ..... p 3806 N92-31569 #
AD-A249787 ..... p 3778 N92-31301 #
AD-A249795 ..... p 3866 N92-31302 #
AD-A249804 ..... p 3888 N92-31757 #
AD-A249809 ..... p 3889 N92-31359 #
AD-A249865 ..... p 3865 N92-31821 #
AD-A249868 ..... p 3767 N92-31822 #
AD-A249870 ..... p 3775 N92-31823 #
AD-A249871 ..... p 3857 N92-31906 #
AD-A249872 ..... p 3857 N92-31932 #
AD-A249942 ..... p 3800 N92-31800 #
AD-A249945 ..... p 3808 N92-31801 #
AD-A249949 ..... p 3855 N92-31509 #
AD-A249971 ..... p 3856 N92-31510 #
AD-A249972 ..... p 3884 N92-31511 #
AD-A249974 ..... p 3813 N92-31431 #
AD-A249976 ..... p 3868 N92-31554 #
AD-A249981 ..... p 3858 N92-31432 #
AD-A249984 ..... p 3843 N92-31329 #
AD-A249990 ..... p 3871 N92-31392 #
AD-A249999 ..... p 3778 N92-31393 #
AD-A250028 ..... p 3831 N92-31802 #
AD-A250033 ..... p 3782 N92-31803 #
AD-A250034 ..... p 3800 N92-31804 #
AD-A250035 ..... p 3835 N92-31807 #
AD-A250045 ..... p 3812 N92-31355 #
AD-A250047 ..... p 3808 N92-31809 #
AD-A250048 ..... p 3752 N92-31777 #
AD-A250055 ..... p 3867 N92-31778 #
AD-A250056 ..... p 3871 N92-31779 #
AD-A250058 ..... p 3791 N92-31356 #
AD-A250060 ..... p 3877 N92-31601 #
AD-A250067 ..... p 3795 N92-31810 #
AD-A250068 ..... p 3786 N92-31360 #
AD-A250069 ..... p 3866 N92-31465 #
AD-A250072 ..... p 3773 N92-31361 #
AD-A250074 ..... p 3844 N92-31362 #
AD-A250075 ..... p 3833 N92-31363 #
AD-A250076 ..... p 3833 N92-31433 #
AD-A250082 ..... p 3779 N92-31434 #
AD-A250085 ..... p 3793 N92-31435 #
AD-A250086 ..... p 3793 N92-31436 #
AD-A250088 ..... p 3833 N92-31437 #
AD-A250089 ..... p 3908 N92-31438 #
AD-A250094 ..... p 3816 N92-31780 #
AD-A250095 ..... p 3879 N92-31783 #
AD-A250096 ..... p 3862 N92-31784 #
AD-A250097 ..... p 3925 N92-31786 #
AD-A250100 ..... p 3892 N92-31789 #
AD-A250101 ..... p 3816 N92-31791 #
AD-A250134 ..... p 3757 N92-31793 #
AD-A250135 ..... p 3828 N92-31794 #
AD-A250141 ..... p 3788 N92-31795 #
AD-A250142 ..... p 3788 N92-31796 #
AD-A250145 ..... p 3885 N92-31811 #
AD-A250182 ..... p 3859 N92-31523 #
AD-A250184 ..... p 3859 N92-31602 #
AD-A250185 ..... p 3860 N92-31603 #
AD-A250190 ..... p 3893 N92-31316 #
AD-A250199 ..... p 3761 N92-31966 #
AD-A250202 ..... p 3761 N92-31967 #
AD-A250209 ..... p 3823 N92-31824 #
AD-A250215 ..... p 3802 N92-31826 #
AD-A250222 ..... p 3885 N92-31827 #
AD-A250232 ..... p 3823 N92-31696 #
AD-A250234 ..... p 3780 N92-31524 #
AD-A250273 ..... p 3823 N92-31770 #
AD-A250275 ..... p 3871 N92-31758 #
AD-A250279 ..... p 3752 N92-31555 #
AD-A250284 ..... p 3819 N92-31286 #
AD-A250337 ..... p 3851 N92-31556 #
AD-A250342 ..... p 3759 N92-31439 #
AD-A250347 ..... p 3794 N92-31557 #
AD-A250348 ..... p 3869 N92-31558 #
AD-A250350 ..... p 3822 N92-31559 #
AD-A250353 ..... p 3792 N92-31394 #
AD-A250365 ..... p 3817 N92-32074 #
AD-A250389 ..... p 3859 N92-31540 #
AD-A250401 ..... p 3872 N92-31330 #
AD-A250402 ..... p 3912 N92-31915 #
AD-A250406 ..... p 3838 N92-31337 #
AD-A250410 ..... p 3774 N92-31604 #
AD-A250415 ..... p 3876 N92-31541 #
AD-A250418 ..... p 3858 N92-31493 #
AD-A250423 ..... p 3805 N92-31413 #
AD-A250439 ..... p 3884 N92-31395 #
AD-A250443 ..... p 3917 N92-31396 #
AD-A250446 ..... p 3901 N92-31397 #
AD-A250447 ..... p 3805 N92-31381 #
AD-A250486 ..... p 3774 N92-31382 #
AD-A250487 ..... p 3838 N92-31331 #
AD-A250495 ..... p 3884 N92-31332 #
AD-A250496 ..... p 3804 N92-31333 #
AD-A250497 ..... p 3809 N92-31944 #
AD-A250498 ..... p 3825 N92-32038 #
AD-A250499 ..... p 3880 N92-32039 #
AD-A250504 ..... p 3883 N92-32040 #
AD-A250505 ..... p 3885 N92-32041 #
AD-A250506 ..... p 3832 N92-32042 #
AD-A250507 ..... p 3810 N92-32043 #
AD-A250508 ..... p 3892 N92-32044 #
AD-A250517 ..... p 3796 N92-32045 #
AD-A250518 ..... p 3776 N92-32075 #
AD-A250519 ..... p 3890 N92-32046 #
AD-A250520 ..... p 3776 N92-32047 #
AD-A250521 ..... p 3776 N92-32048 #
AD-A250522 ..... p 3785 N92-32076 #
AD-A250525 ..... p 3902 N92-32077 #
AD-A250527 ..... p 3913 N92-32078 #
AD-A250531 ..... p 3796 N92-32079 #
AD-A250532 ..... p 3785 N92-32080 #
AD-A250549 ..... p 3887 N92-32081 #
AD-A250550 ..... p 3790 N92-32084 #
AD-A250551 ..... p 3902 N92-32092 #
AD-A250552 ..... p 3787 N92-31612 #
AD-A250555 ..... p 3830 N92-31605 #
AD-A250568 ..... p 3861 N92-31714 #

AD-A250630 ..... p 3910 N92-31699 #
AD-A250645 ..... p 3755 N92-31562 #
AD-A250655 ..... p 3791 N92-31318 #
AD-A250657 ..... p 3830 N92-31319 #
AD-A250662 ..... p 3858 N92-31320 #
AD-A250669 ..... p 3870 N92-31321 #
AD-A250671 ..... p 3796 N92-31968 #
AD-A250700 ..... p 3820 N92-31322 #
AD-A250707 ..... p 3843 N92-31323 #
AD-A250719 ..... p 3873 N92-32023 #
AD-A250727 ..... p 3897 N92-31950 #
AD-A250728 ..... p 3897 N92-31999 #
AD-A250731 ..... p 3803 N92-31890 #
AD-A250732 ..... p 3813 N92-31451 #
AD-A250733 ..... p 3800 N92-31969 #
AD-A250734 ..... p 3800 N92-31970 #
AD-A250735 ..... p 3800 N92-31971 #
AD-A250736 ..... p 3801 N92-31972 #
AD-A250737 ..... p 3801 N92-31973 #
AD-A250741 ..... p 3870 N92-31291 #
AD-A250750 ..... p 3844 N92-31621 #
AD-A250781 ..... p 3914 N92-32207 #
AD-A250785 ..... p 3842 N92-32168 #
AD-A250811 ..... p 3875 N92-31480 #
AD-A250827 ..... p 3821 N92-31452 #
AD-A250834 ..... p 3864 N92-31495 #
AD-A250835 ..... p 3908 N92-31496 #
AD-A250850 ..... p 3805 N92-31369 #
AD-A250858 ..... p 3810 N92-32101 #
AD-A250859 ..... p 3920 N92-32102 #
AD-A250862 ..... p 3863 N92-32103 #
AD-A250864 ..... p 3777 N92-32104 #
AD-A250865 ..... p 3760 N92-32059 #
AD-A250866 ..... p 3873 N92-31974 #
AD-A250884 ..... p 3806 N92-31543 #
AD-A250893 ..... p 3773 N92-31305 #
AD-A250900 ..... p 3819 N92-31306 #
AD-A250901 ..... p 3891 N92-31563 #
AD-A250902 ..... p 3773 N92-31307 #
AD-A250903 ..... p 3909 N92-31582 #
AD-A250943 ..... p 3898 N92-32169 #
AD-A250944 ..... p 3900 N92-32170 #
AD-A250949 ..... p 3891 N92-32211 #
AD-A250954 ..... p 3887 N92-32171 #
AD-A250966 ..... p 3798 N92-32194 #
AD-A250967 ..... p 3797 N92-32151 #
AD-A250968 ..... p 3883 N92-32152 #
AD-A250976 ..... p 3795 N92-31951 #
AD-A250981 ..... p 3897 N92-31936 #
AD-A250982 ..... p 3825 N92-32000 #
AD-A250983 ..... p 3796 N92-32001 #
AD-A250991 ..... p 3817 N92-32002 #
AD-A250992 ..... p 3898 N92-32024 #
AD-A250993 ..... p 3795 N92-31952 #
AD-A250994 ..... p 3795 N92-31954 #
AD-A251003 ..... p 3841 N92-31647 #
AD-A251006 ..... p 3912 N92-31937 #
AD-A251008 ..... p 3880 N92-31939 #
AD-A251009 ..... p 3775 N92-31940 #
AD-A251020 ..... p 3795 N92-31941 #
AD-A251041 ..... p 3911 N92-31848 #
AD-A251042 ..... p 3817 N92-31849 #
AD-A251043 ..... p 3772 N92-31850 #
AD-A251057 ..... p 3911 N92-31851 #
AD-A251094 ..... p 3899 N92-32196 #
AD-A251109 ..... p 3798 N92-32153 #
AD-A251112 ..... p 3798 N92-32197 #
AD-A251125 ..... p 3798 N92-32198 #
AD-A251149 ..... p 3857 N92-31766 #
AD-A252112 ..... p 3792 N92-31419 #
AD-A252114 ..... p 3792 N92-31404 #
AD-A252125 ..... p 3875 N92-31405 #
AD-A252144 ..... p 3863 N92-31406 #
AD-A252146 ..... p 3864 N92-31407 #
AD-A252173 ..... p 3880 N92-32060 #
AD-A252174 ..... p 3832 N92-32061 #
AD-A252175 ..... p 3753 N92-32062 #
AD-A252176 ..... p 3871 N92-32063 #
AD-A252177 ..... p 3776 N92-32064 #
AD-A252182 ..... p 3913 N92-32065 #
AD-A252183 ..... p 3920 N92-32049 #
AD-A252188 ..... p 3866 N92-32050 #
AD-A252189 ..... p 3858 N92-32055 #
AD-A252190 ..... p 3915 N92-31585 #
AD-A252192 ..... p 3867 N92-31590 #
AD-A252195 ..... p 3792 N92-31408 #
AD-A252215 ..... p 3785 N92-32057 #
AD-A252264 ..... p 3870 N92-32107 #
AD-A252321 ..... p 3807 N92-31629 #
AD-A252409 ..... p 3892 N92-31818 #
AD-A252420 ..... p 3783 N92-31820 #
AD-A252424 ..... p 3778 N92-31292 #
AD-A252439 ..... p 3918 N92-31482 #
AD-A252440 ..... p 3910 N92-31666 #
AD-A252442 ..... p 3884 N92-31293 #
AD-A252443 ..... p 3872 N92-31294 #
AD-A252477 ..... p 3879 N92-31825 #
AD-A252485 ..... p 3828 N92-31828 #
AD-A252487 ..... p 3784 N92-31959 #
AD-A252488 ..... p 3796 N92-31960 #
AD-A252489 ..... p 3796 N92-31961 #
AD-A252492 ..... p 3790 N92-32066 #
AD-A252532 ..... p 3869 N92-31962 #
AD-A252577 ..... p 3899 N92-31325 #
AD-A252656 ..... p 3798 N92-31399 #
AD-A252679 ..... p 3876 N92-31586 #
AD-A252694 ..... p 3868 N92-31326 #
AD-A252695 ..... p 3877 N92-31587 #
AD-A252696 ..... p 3891 N92-31588 #
AD-A252700 ..... p 3918 N92-31467 #
AD-A252701 ..... p 3863 N92-31308 #
AD-A252705 ..... p 3915 N92-31767 #
AD-A252706 ..... p 3860 N92-31670 #
AD-A252709 ..... p 3892 N92-31672 #
AD-A252711 ..... p 3752 N92-31674 #
AD-A252713 ..... p 3864 N92-31544 #
AD-A252715 ..... p 3872 N92-31327 #
AD-A252726 ..... p 3878 N92-31676 #
AD-A252742 ..... p 3883 N92-32109 #
AD-A252743 ..... p 3837 N92-32172 #
AD-A252754 ..... p 3836 N92-32173 #

AD-D015230 ..... p 3777 N92-31268
AD-D015235 ..... p 3873 N92-31269
AD-D015236 ..... p 3791 N92-31270
AD-D015250 ..... p 3832 N92-31271
AD-D015296 ..... p 3902 N92-32137

AD-E200945 ..... p 3855 N92-31509 #
AD-E200988 ..... p 3926 N92-31477 #
AD-E200990 ..... p 3855 N92-31476 #
AD-E501523 ..... p 3873 N92-32023 #
AD-E951775 ..... p 3800 N92-31800 #
AD-E951785 ..... p 3808 N92-31801 #

AD-920315 ..... p 3890 N92-32046 #

AECL-10507 ..... p 3837 N92-32143 #

AEDC-TR-91-26-VOL-2 ..... p 3826 N92-31298 #

AEROJET-2459-31-1 ..... p 3771 N92-32129 * #

AFIT/CI-CIA-92-010 ..... p 3869 N92-31962 #

AFIT/CI/CIA-91-025D ..... p 3807 N92-31691 #
AFIT/CI/CIA-91-026D ..... p 3768 N92-31675 #
AFIT/CI/CIA-91-027D ..... p 3859 N92-31523 #
AFIT/CI/CIA-91-028D ..... p 3894 N92-31673 #
AFIT/CI/CIA-91-105 ..... p 3858 N92-31432 #
AFIT/CI/CIA-91-107 ..... p 3862 N92-31784 #
AFIT/CI/CIA-91-109 ..... p 3860 N92-31603 #
AFIT/CI/CIA-91-110 ..... p 3857 N92-31932 #
AFIT/CI/CIA-91-112 ..... p 3859 N92-31602 #
AFIT/CI/CIA-91-114 ..... p 3843 N92-31329 #
AFIT/CI/CIA-91-115 ..... p 3857 N92-31906 #
AFIT/CI/CIA-91-116 ..... p 3861 N92-31714 #
AFIT/CI/CIA-91-119 ..... p 3767 N92-31822 #
AFIT/CI/CIA-91-120 ..... p 3858 N92-31493 #
AFIT/CI/CIA-91-126 ..... p 3775 N92-31823 #
AFIT/CI/CIA-91-129 ..... p 3879 N92-31783 #
AFIT/CI/CIA-91-130 ..... p 3830 N92-31605 #
AFIT/CI/CIA-91-132 ..... p 3890 N92-31686 #
AFIT/CI/CIA-92-001D ..... p 3899 N92-31325 #

AFIT/GA/ENY/90M-01 ..... p 3842 N92-31989 #

AFIT/GA/92M/01 ..... p 3842 N92-31989 #

AFIT/GNE/ENP/92M-4 ..... p 3907 N92-31990 #

AFIT/GOR/ENS/92M-15 ..... p 3880 N92-31991 #

AFIT/GSS/ENG/91D-07 ..... p 3874 N92-31299 #

AFOSR-92-0004TR ..... p 3867 N92-31980 #
AFOSR-92-0021TR ..... p 3888 N92-31981 #
AFOSR-92-0034TR ..... p 3819 N92-31283 #
AFOSR-92-0071TR ..... p 3876 N92-31573 #
AFOSR-92-0101TR ..... p 3903 N92-31459 #
AFOSR-92-0111TR ..... p 3868 N92-31491 #
AFOSR-92-0126TR ..... p 3896 N92-31858 #
AFOSR-92-0142TR ..... p 3872 N92-32105 #
AFOSR-92-0149TR ..... p 3814 N92-31490 #
AFOSR-92-0208TR ..... p 3770 N92-31474 #
AFOSR-92-0219TR ..... p 3869 N92-31905 #
AFOSR-92-0221TR ..... p 3925 N92-31985 #
AFOSR-92-0234TR ..... p 3871 N92-31779 #
AFOSR-92-0272TR ..... p 3917 N92-31396 #
AFOSR-92-0276TR ..... p 3912 N92-31915 #
AFOSR-92-0282TR ..... p 3832 N92-32042 #
AFOSR-92-0286TR ..... p 3813 N92-31451 #
AFOSR-92-0287TR ..... p 3761 N92-31967 #
AFOSR-92-0290TR ..... p 3805 N92-31381 #
AFOSR-92-0292TR ..... p 3761 N92-31966 #
AFOSR-92-0304TR ..... p 3908 N92-31496 #
AFOSR-92-0305TR ..... p 3787 N92-31612 #
AFOSR-92-0310TR ..... p 3867 N92-31778 #
AFOSR-92-0312TR ..... p 3831 N92-31802 #
AFOSR-92-0345TR ..... p 3830 N92-31319 #
AFOSR-92-0347TR ..... p 3871 N92-31758 #
AFOSR-92-0350TR ..... p 3809 N92-31944 #
AFOSR-92-0352TR ..... p 3880 N92-32039 #
AFOSR-92-0353TR ..... p 3825 N92-32038 #
AFOSR-92-0355TR ..... p 3884 N92-31332 #
AFOSR-92-0357TR ..... p 3885 N92-32041 #
AFOSR-92-0360TR ..... p 3872 N92-31330 #
AFOSR-92-0361TR ..... p 3822 N92-31559 #
AFOSR-92-0366TR ..... p 3842 N92-32168 #
AFOSR-92-0368TR ..... p 3883 N92-32040 #
AFOSR-92-0369TR ..... p 3823 N92-31696 #
AFOSR-92-0372TR ..... p 3804 N92-31333 #
AFOSR-92-0388TR ..... p 3823 N92-31824 #
AFOSR-92-0394TR ..... p 3819 N92-31286 #
AFOSR-92-0397TR ..... p 3776 N92-32075 #
AFOSR-92-0398TR ..... p 3774 N92-31604 #
AFOSR-92-0399TR ..... p 3752 N92-31555 #
AFOSR-92-0401TR ..... p 3777 N92-32104 #
AFOSR-92-0402TR ..... p 3890 N92-32046 #
AFOSR-92-0403TR ..... p 3760 N92-32059 #
AFOSR-92-0404TR ..... p 3902 N92-32092 #
AFOSR-92-0412TR ..... p 3887 N92-32081 #
AFOSR-92-0414TR ..... p 3790 N92-32084 #
AFOSR-92-0415TR ..... p 3792 N92-31419 #
AFOSR-92-0416TR ..... p 3819 N92-31306 #
AFOSR-92-0417TR ..... p 3773 N92-31305 #
AFOSR-92-0420TR ..... p 3785 N92-32076 #
AFOSR-92-0427TR ..... p 3820 N92-31322 #
AFOSR-92-0429TR ..... p 3825 N92-32000 #
AFOSR-92-0444TR ..... p 3796 N92-32001 #
AFOSR-92-0446TR ..... p 3897 N92-31936 #
AFOSR-92-0457TR ..... p 3795 N92-31951 #
AFOSR-92-0545TR ..... p 3915 N92-31585 #
AFOSR-92-0547TR ..... p 3858 N92-32055 #
AFOSR-92-0559TR ..... p 3867 N92-31590 #

AGARD-AR-310 ..... p 3889 N92-32229 #

AGARD-CP-505 ..... p 3920 N92-32182 #

AGARD-16 ..... p 3756 N92-31261 * #

AIAA PAPER 91-3528 ..... p 3771 N92-31916 * #
AIAA PAPER 92-1556 ..... p 3769 N92-31342 * #
AIAA PAPER 92-2095-CP ..... p 3757 N92-31350 * #
AIAA PAPER 92-3494 ..... p 3834 N92-31485 * #

AL-TP-1992-0010 ..... p 3885 N92-31811 #

AL-TR-1991-0109 ..... p 3870 N92-31321 #
AL-TR-1991-0129 ..... p 3872 N92-31458 #
AL-TR-1992-0041 ..... p 3803 N92-31890 #

ALS/TR-92-008 ..... p 3829 N92-32174 #

AMSMI/TR-RD-WS-91-12 ..... p 3800 N92-31800 #
AMSMI/TR-RD-WS-92-2 ..... p 3808 N92-31801 #

ANL-91/45 ..... p 3846 N92-31531 #

ANL/CP-74821 ..... p 3894 N92-31595 #
ANL/CP-74880 ..... p 3903 N92-31310 #
ANL/CP-75260 ..... p 3879 N92-31899 #
ANL/CP-75330 ..... p 3825 N92-32003 #
ANL/CP-75440 ..... p 3852 N92-31591 #
ANL/CP-75477 ..... p 3912 N92-31955 #
ANL/CP-75497 ..... p 3886 N92-31311 #
ANL/CP-75586 ..... p 3787 N92-31575 #
ANL/CP-75684 ..... p 3795 N92-31938 #
ANL/CP-75787 ..... p 3789 N92-31924 #
ANL/CP-75799 ..... p 3909 N92-31652 #
ANL/CP-75853 ..... p 3854 N92-32083 #
ANL/CP-75935 ..... p 3830 N92-31684 #
ANL/CP-75955 ..... p 3877 N92-31654 #
ANL/CP-75978 ..... p 3919 N92-31596 #
ANL/CP-75985 ..... p 3823 N92-31785 #
ANL/CP-76034 ..... p 3779 N92-31441 #
ANL/CP-76036 ..... p 3893 N92-31386 #
ANL/CP-76120 ..... p 3838 N92-31335 #
ANL/CP-76122 ..... p 3909 N92-31546 #
ANL/CP-76308 ..... p 3783 N92-31857 #

ANL/ESD-14 ..... p 3835 N92-31774 #

ANL/ESD/TM-27 ..... p 3834 N92-31720 #
ANL/ESD/TM-30-VOL-1 ..... p 3799 N92-31442 #

ARCCB-TR-92013 ..... p 3838 N92-31331 #

ARI-RN-92-22 ..... p 3870 N92-31291 #
ARI-RN-92-36 ..... p 3872 N92-31294 #

ARL-MAT-R-124 ..... p 3796 N92-32045 #

ARL-PROP-TM-473 ..... p 3759 N92-31439 #

ARO-23577.6-MS ..... p 3901 N92-31380 #
ARO-24610.1-GS-UIF ..... p 3857 N92-31964 #
ARO-24845.15-MS ..... p 3792 N92-31377 #
ARO-25222.8-CH ..... p 3907 N92-31375 #
ARO-25245.4-EG ..... p 3780 N92-31671 #
ARO-25586.14-CH ..... p 3791 N92-31358 #
ARO-26049.2-CH ..... p 3893 N92-31463 #
ARO-26385.6-LS ..... p 3866 N92-31302 #
ARO-26391.10-MA ..... p 3886 N92-31567 #
ARO-27032.1-EL ..... p 3805 N92-31376 #
ARO-27863.1-MS ..... p 3833 N92-31363 #
ARO-27863.2-MS ..... p 3833 N92-31433 #
ARO-28283.3-EG ..... p 3773 N92-31378 #
ARO-28436.1-MS-SBI ..... p 3792 N92-31388 #
ARO-28809.5-MA-SDI ..... p 3888 N92-31757 #
ARO-28809.6-MASDI ..... p 3888 N92-31600 #
ARO-28821.1-MS ..... p 3889 N92-31359 #
ARO-28890.1-EG-EQ ..... p 3828 N92-31694 #
ARO-29005.1-EL-SBI ..... p 3813 N92-31374 #
ARO-29008.1-EL-SBI ..... p 3814 N92-31464 #
ARO-29276-GS ..... p 3901 N92-31430 #
ARO-29342.2-EL-CF ..... p 3813 N92-31373 #

ASL-TR-0309 ..... p 3858 N92-31320 #
ASL-TR-0311 ..... p 3806 N92-31543 #

ATC-185 ..... p 3863 N92-32103 #

AVMED-8-92 ..... p 3755 N92-31562 #

AVSCOM-TR-92-C-008 ..... p 3832 N92-31349 * #
AVSCOM-TR-92-C-018 ..... p 3834 N92-31485 * #
AVSCOM-TR-92-C-029 ..... p 3834 N92-31536 * #

A015-VOL-1 ..... p 3876 N92-31586 #

B-238393 ..... p 3755 N92-31453 #
B-239410 ..... p 3891 N92-31454 #

BNL-NUREG-47472 ..... p 3815 N92-31651 #

BNL-46678 ..... p 3810 N92-32134 #
BNL-47120 ..... p 3824 N92-31977 #
BNL-47331 ..... p 3841 N92-31844 #
BNL-47370 ..... p 3869 N92-31589 #
BNL-47392 ..... p 3851 N92-31422 #
BNL-47474 ..... p 3909 N92-31627 #
BNL-47475 ..... p 3827 N92-31502 #
BNL-47508 ..... p 3849 N92-32118 #
BNL-47529 ..... p 3849 N92-32124 #
BNL-47549 ..... p 3803 N92-32125 #
BNL-47636 ..... p 3907 N92-31296 #
BNL-47668 ..... p 3901 N92-31737 #

BRL-CR-687 ..... p 3835 N92-31807 #

BRL-MR-3954 ..... p 3876 N92-31488 #

BRL-TR-3329 ..... p 3800 N92-31804 #
BRL-TR-3333 ..... p 3778 N92-31393 #
BRL-TR-3334 ..... p 3782 N92-31803 #

BUMINES-IC-9275 ..... p 3788 N92-31797 #

B91-0161 ..... p 3774 N92-31609 #
B91-0281 ..... p 3824 N92-31839 #

CCMS-92-23 ..... p 3842 N92-32235 * #

CCR-92-01 ..... p 3770 N92-31474 #

CMC-6730-15 ..... p 3776 N92-32075 #

CMR-92-2 ..... p 3901 N92-31380 #

CMU-CS-92-109 ..... p 3874 N92-31353 #
CMU-CS-92-115 ..... p 3884 N92-31511 #

CMU/CS-92-110 ..... p 3880 N92-31939 #
CMU/CS-92-122 ..... p 3887 N92-32171 #

CMU/SEI-91-TR-30 ..... p 3876 N92-31541 #

CNRS-RC-91-1 ..... p 3751 N92-31508 #

COG-91-261 ..... p 3837 N92-32143 #

CONF-900397-3-REV-1 ..... p 3910 N92-31719 #
CONF-900684-1-REV-2 ..... p 3821 N92-31528 #
CONF-910340-54 ..... p 3826 N92-31313 #
CONF-910406-41 ..... p 3907 N92-31296 #
CONF-9104196 ..... p 3845 N92-31290 #
CONF-9104363-1 ..... p 3869 N92-31589 #
CONF-9105121-2 ..... p 3898 N92-32006 #
CONF-9107136-11 ..... p 3869 N92-31608 #
CONF-9107216 ..... p 3895 N92-31728 #
CONF-9108146-2 ..... p 3832 N92-31935 #
CONF-9108199-1 ..... p 3893 N92-31386 #
CONF-9109182-2 ..... p 3898 N92-32167 #
CONF-9109182-6 ..... p 3925 N92-32154 #
CONF-9109297-2 ..... p 3782 N92-31772 #
CONF-9109317-2 ..... p 3913 N92-32166 #
CONF-9109340-4 ..... p 3853 N92-31782 #
CONF-9110003-24 ..... p 3787 N92-31575 #
CONF-9110127-4 ..... p 3855 N92-32155 #
CONF-9110146-18 ..... p 3827 N92-31502 #
CONF-9110312-2 ..... p 3926 N92-31756 #
CONF-9110341-3 ..... p 3919 N92-31581 #
CONF-9110344-8-REV-1 ..... p 3841 N92-31745 #
CONF-9110369-1 ..... p 3820 N92-31425 #
CONF-9110374-1 ..... p 3850 N92-31324 #
CONF-911064-9 ..... p 3910 N92-31661 #
CONF-911103-8 ..... p 3875 N92-31447 #
CONF-9111208-2 ..... p 3902 N92-32149 #
CONF-9111227-1 ..... p 3889 N92-32119 #
CONF-911202-76 ..... p 3788 N92-31759 #
CONF-911202-77 ..... p 3788 N92-31744 #
CONF-911202-79 ..... p 3795 N92-31917 #
CONF-9112112-1 ..... p 3847 N92-31571 #
CONF-911296-9 ..... p 3832 N92-31902 #
CONF-9201101-1 ..... p 3899 N92-31390 #
CONF-9201102-ABSTS ..... p 3904 N92-31576 #
CONF-920124-21 ..... p 3812 N92-31334 #
CONF-920124-23 ..... p 3812 N92-31289 #
CONF-920142-1 ..... p 3906 N92-31829 #
CONF-9202100-1 ..... p 3915 N92-31663 #
CONF-9202106-1 ..... p 3895 N92-31765 #
CONF-9202113-1 ..... p 3835 N92-32121 #
CONF-920307-72 ..... p 3795 N92-31938 #
CONF-920308-21 ..... p 3898 N92-32165 #
CONF-920310-10 ..... p 3779 N92-31441 #
CONF-920311-18 ..... p 3903 N92-31310 #
CONF-920311-5 ..... p 3906 N92-31771 #
CONF-920311-8 ..... p 3905 N92-31749 #
CONF-9203139-1 ..... p 3902 N92-31761 #
CONF-9203146-1 ..... p 3894 N92-31679 #
CONF-920315-18 ..... p 3816 N92-31760 #
CONF-920315-20 ..... p 3815 N92-31664 #
CONF-920315-23 ..... p 3900 N92-32131 #
CONF-920315-24 ..... p 3900 N92-32133 #
CONF-920315-33 ..... p 3810 N92-32134 #
CONF-9203156-1 ..... p 3919 N92-31596 #
CONF-9203164-1 ..... p 3898 N92-32090 #
CONF-920331-10 ..... p 3900 N92-31975 #
CONF-920331-5 ..... p 3836 N92-31647 #
CONF-920362-20 ..... p 3904 N92-31616 #
CONF-920362-24 ..... p 3905 N92-31764 #
CONF-920362-32 ..... p 3781 N92-31729 #
CONF-920375-18 ..... p 3815 N92-31651 #
CONF-920402-11 ..... p 3815 N92-31650 #
CONF-920402-16 ..... p 3910 N92-31665 #
CONF-920402-1 ..... p 3794 N92-31560 #
CONF-920402-25 ..... p 3894 N92-31595 #
CONF-920402-31 ..... p 3909 N92-31546 #
CONF-920402-39 ..... p 3797 N92-32089 #
CONF-920402-3 ..... p 3911 N92-31723 #
CONF-920408-2 ..... p 3890 N92-32116 #
CONF-9204102-8 ..... p 3765 N92-31542 #
CONF-9204114-1 ..... p 3876 N92-31529 #
CONF-9204121-2 ..... p 3919 N92-31578 #
CONF-9204124-3 ..... p 3881 N92-32150 #
CONF-9204136-2 ..... p 3882 N92-31466 #
CONF-920423-5 ..... p 3908 N92-31403 #
CONF-920429-2 ..... p 3848 N92-31845 #
CONF-920431-24 ..... p 3768 N92-31846 #
CONF-920439-7 ..... p 3909 N92-31652 #
CONF-920443-1 ..... p 3854 N92-32083 #
CONF-920444-21 ..... p 3786 N92-31391 #
CONF-920444-27 ..... p 3797 N92-32146 #
CONF-920448-5 ..... p 3797 N92-32094 #
CONF-920501-22 ..... p 3867 N92-31711 #
CONF-9205123-1 ..... p 3783 N92-31816 #
CONF-9205123-7 ..... p 3789 N92-31924 #
CONF-9205130-1 ..... p 3918 N92-31448 #
CONF-920514-3 ..... p 3910 N92-31668 #
CONF-9205141-1 ..... p 3878 N92-31669 #
CONF-9205141-2 ..... p 3816 N92-31718 #
CONF-9205145-1 ..... p 3841 N92-31844 #
CONF-9205147-1 ..... p 3838 N92-31335 #
CONF-920515-12 ..... p 3815 N92-31681 #
CONF-920515-19 ..... p 3815 N92-31548 #
CONF-9205167-1 ..... p 3853 N92-31896 #
CONF-920519-3 ..... p 3853 N92-31732 #
CONF-9205190-1 ..... p 3837 N92-31657 #
CONF-9205200-1 ..... p 3877 N92-31654 #
CONF-920573-8 ..... p 3782 N92-31773 #
CONF-920574-7 ..... p 3896 N92-31923 #
CONF-920584-22 ..... p 3799 N92-31751 #
CONF-920607-10 ..... p 3904 N92-31530 #
CONF-920607-9 ..... p 3906 N92-31913 #
CONF-9206154-1 ..... p 3802 N92-31580 #
CONF-9206157-1 ..... p 3780 N92-31565 #
CONF-9206158-3 ..... p 3852 N92-31591 #
CONF-9206173-1 ..... p 3839 N92-31383 #
CONF-9206173-2 ..... p 3839 N92-31501 #
CONF-9206180-3 ..... p 3830 N92-31684 #
CONF-9206196-1 ..... p 3783 N92-31857 #
CONF-920628-2-EXTD-ABST ..... p 3775 N92-31912 #
CONF-920677-3 ..... p 3903 N92-31372 #
CONF-920678-5 ..... p 3847 N92-31623 #
CONF-920678-6 ..... p 3849 N92-32112 #
CONF-920678-7 ..... p 3799 N92-31593 #
CONF-920678-8 ..... p 3849 N92-32091 #
CONF-920707-20 ..... p 3782 N92-31805 #
CONF-920707-22 ..... p 3778 N92-31415 #
CONF-920707-23 ..... p 3776 N92-31414 #
CONF-920707-24 ..... p 3781 N92-31763 #
CONF-920707-25 ..... p 3779 N92-31416 #
CONF-920707-26 ..... p 3779 N92-31417 #
CONF-920707-27 ..... p 3786 N92-32145 #
CONF-920707-28 ..... p 3822 N92-31625 #
CONF-920707-29 ..... p 3780 N92-31607 #
CONF-920707-5 ..... p 3783 N92-31860 #
CONF-920722-1 ..... p 3909 N92-31627 #
CONF-920730-1 ..... p 3883 N92-31741 #
CONF-920730-2 ..... p 3882 N92-31740 #
CONF-920730-4 ..... p 3879 N92-31899 #
CONF-920732-4 ..... p 3833 N92-31384 #
CONF-920747-2 ..... p 3759 N92-31817 #
CONF-920750-2 ..... p 3804 N92-31317 #
CONF-920750-3 ..... p 3808 N92-31738 #
CONF-920759-1 ..... p 3878 N92-31739 #
CONF-920760-1 ..... p 3878 N92-31742 #
CONF-920760-3 ..... p 3879 N92-31743 #
CONF-920760-5 ..... p 3886 N92-31311 #
CONF-920761-4 ..... p 3786 N92-31418 #
CONF-920762-2 ..... p 3789 N92-31898 #
CONF-920795-2 ..... p 3900 N92-31295 #
CONF-920796-1 ..... p 3781 N92-31748 #
CONF-920801-12 ..... p 3912 N92-31955 #
CONF-920801-13 ..... p 3825 N92-32003 #
CONF-920801-5 ..... p 3848 N92-32087 #
CONF-920803-10 ..... p 3770 N92-31897 #
CONF-920803-12 ..... p 3771 N92-32030 #
CONF-920803-3 ..... p 3899 N92-31831 #
CONF-920803-5 ..... p 3868 N92-31409 #
CONF-920804-10 ..... p 3825 N92-32115 #
CONF-920804-17 ..... p 3823 N92-31785 #
CONF-920804-7 ..... p 3820 N92-31421 #
CONF-920804-8 ..... p 3820 N92-31424 #
CONF-920804-9 ..... p 3820 N92-31420 #
CONF-9208100-1 ..... p 3850 N92-31297 #
CONF-920814-4 ..... p 3851 N92-31422 #
CONF-920818-2 ..... p 3834 N92-31500 #
CONF-920851-12 ..... p 3831 N92-31775 #
CONF-920851-8 ..... p 3851 N92-31427 #
CONF-920881-1 ..... p 3851 N92-31423 #
CONF-920891-1 ..... p 3913 N92-32085 #
CONF-920891-2 ..... p 3829 N92-32086 #
CONF-920903-4 ..... p 3878 N92-31703 #
CONF-9209107-1 ..... p 3861 N92-31709 #
CONF-9209107-2 ..... p 3862 N92-31750 #
CONF-920913-1 ..... p 3905 N92-31707 #
CONF-9209143-1 ..... p 3835 N92-31929 #
CONF-920919-1 ..... p 3895 N92-31705 #
CONF-920928-1 ..... p 3824 N92-31977 #
CONF-920939-1 ..... p 3894 N92-31700 #
CONF-920981-1 ..... p 3823 N92-31701 #

CP-504S ..... p 3889 N92-32229 #
CP-504 ..... p 3889 N92-32229 #

CRANFIELD-AERO-9114 ..... p 3751 N92-31514 #
CRANFIELD-AERO-9201 ..... p 3757 N92-31515 #
CRANFIELD-AERO-9203 ..... p 3840 N92-31516 #

CREC-TR-92-4 ..... p 3864 N92-31544 #

CRI-P45-1 ..... p 3845 N92-32223 * #

CTN-92-60310 ..... p 3833 N92-31469 #
CTN-92-60311 ..... p 3806 N92-31470 #
CTN-92-60315 ..... p 3806 N92-31471 #
CTN-92-60318 ..... p 3871 N92-31472 #
CTN-92-60321 ..... p 3837 N92-32202 #
CTN-92-60322 ..... p 3810 N92-32203 #
CTN-92-60323 ..... p 3811 N92-32231 #
CTN-92-60324 ..... p 3811 N92-32232 #
CTN-92-60327 ..... p 3811 N92-32214 #
CTN-92-60329 ..... p 3873 N92-32031 #
CTN-92-60331 ..... p 3809 N92-31921 #

CTN-92-60332 ..... p 3810 N92-32176 #
CTN-92-60337 ..... p 3777 N92-32215 #
CTN-92-60338 ..... p 3844 N92-32216 #
CTN-92-60339 ..... p 3811 N92-32217 #
CTN-92-60343 ..... p 3829 N92-32218 #
CTN-92-60344 ..... p 3756 N92-32219 #

CU-TR-15 ..... p 3755 N92-31549 * #
CU-TR-26 ..... p 3893 N92-31328 #

CURRENT-REF-92-1 ..... p 3854 N92-32071 #

CWI-BS-R9117 ..... p 3888 N92-31517 #

CWRU/DMS/TR-45 ..... p 3902 N92-32077 #

DCIEM-88-RR-39 ..... p 3756 N92-32219 #

DE91-002141 ..... p 3785 N92-32093 #
DE91-002146 ..... p 3849 N92-32110 #
DE92-001209 ..... p 3847 N92-31579 #
DE92-001242 ..... p 3846 N92-31526 #
DE92-001244 ..... p 3814 N92-31525 #
DE92-001248 ..... p 3847 N92-31646 #
DE92-001253 ..... p 3919 N92-31731 #
DE92-001269 ..... p 3784 N92-31976 #
DE92-005326 ..... p 3783 N92-31860 #
DE92-007565 ..... p 3804 N92-31317 #
DE92-007902 ..... p 3778 N92-31414 #
DE92-008015 ..... p 3808 N92-31738 #
DE92-008062 ..... p 3878 N92-31739 #
DE92-008068 ..... p 3882 N92-31740 #
DE92-008073 ..... p 3883 N92-31741 #
DE92-008076 ..... p 3878 N92-31742 #
DE92-008553 ..... p 3782 N92-31805 #
DE92-008933 ..... p 3778 N92-31415 #
DE92-009457 ..... p 3779 N92-31416 #
DE92-009690 ..... p 3781 N92-31763 #
DE92-010048 ..... p 3824 N92-31977 #
DE92-010256 ..... p 3926 N92-31756 #
DE92-010276 ..... p 3787 N92-31575 #
DE92-010310 ..... p 3779 N92-31417 #
DE92-010378 ..... p 3851 N92-31527 #
DE92-010448 ..... p 3786 N92-31418 #
DE92-010559 ..... p 3848 N92-31893 #
DE92-010564 ..... p 3846 N92-31497 #
DE92-010567 ..... p 3847 N92-31623 #
DE92-010568 ..... p 3849 N92-32112 #
DE92-010569 ..... p 3799 N92-31593 #
DE92-010574 ..... p 3846 N92-31498 #
DE92-010575 ..... p 3845 N92-31481 #
DE92-010577 ..... p 3872 N92-31309 #
DE92-010722 ..... p 3826 N92-31313 #
DE92-010763 ..... p 3837 N92-31753 #
DE92-010772 ..... p 3831 N92-31798 #
DE92-011108 ..... p 3894 N92-31700 #
DE92-011144 ..... p 3875 N92-31447 #
DE92-011146 ..... p 3918 N92-31448 #
DE92-011298 ..... p 3786 N92-32145 #
DE92-011359 ..... p 3806 N92-31449 #
DE92-011367 ..... p 3823 N92-31701 #
DE92-011368 ..... p 3878 N92-31703 #
DE92-011394 ..... p 3904 N92-31616 #
DE92-011424 ..... p 3831 N92-31769 #
DE92-011427 ..... p 3894 N92-31606 #
DE92-011431 ..... p 3839 N92-31389 #
DE92-011441 ..... p 3799 N92-31570 #
DE92-011458 ..... p 3895 N92-31705 #
DE92-011469 ..... p 3821 N92-31528 #
DE92-011489 ..... p 3876 N92-31529 #
DE92-011493 ..... p 3847 N92-31571 #
DE92-011520 ..... p 3899 N92-31390 #
DE92-011521 ..... p 3910 N92-31719 #
DE92-011532 ..... p 3786 N92-31391 #
DE92-011533 ..... p 3910 N92-31661 #
DE92-011549 ..... p 3904 N92-31576 #
DE92-011570 ..... p 3793 N92-31538 #
DE92-011583 ..... p 3915 N92-31663 #
DE92-011607 ..... p 3890 N92-32099 #
DE92-011650 ..... p 3815 N92-31664 #
DE92-011651 ..... p 3787 N92-31667 #
DE92-011658 ..... p 3910 N92-31668 #
DE92-011660 ..... p 3878 N92-31669 #
DE92-011662 ..... p 3905 N92-31707 #
DE92-011697 ..... p 3816 N92-31760 #
DE92-011731 ..... p 3920 N92-31934 #
DE92-011732 ..... p 3812 N92-31334 #
DE92-011733 ..... p 3854 N92-31907 #
DE92-011737 ..... p 3803 N92-31908 #
DE92-011763 ..... p 3832 N92-31902 #
DE92-011764 ..... p 3788 N92-31759 #
DE92-011766 ..... p 3828 N92-31909 #
DE92-011778 ..... p 3775 N92-31912 #
DE92-011790 ..... p 3906 N92-31913 #
DE92-011805 ..... p 3864 N92-31572 #
DE92-011806 ..... p 3903 N92-31494 #

DE92-011810 ..... p 3911 N92-31914 #
DE92-011813 ..... p 3832 N92-31935 #
DE92-011846 ..... p 3795 N92-31938 #
DE92-011905 ..... p 3923 N92-31965 #
DE92-011943 ..... p 3780 N92-31607 #
DE92-011949 ..... p 3902 N92-31761 #
DE92-011963 ..... p 3879 N92-31743 #
DE92-011965 ..... p 3904 N92-31530 #
DE92-011974 ..... p 3869 N92-31608 #
DE92-012101 ..... p 3822 N92-31625 #
DE92-012116 ..... p 3838 N92-31303 #
DE92-012143 ..... p 3788 N92-31744 #
DE92-012148 ..... p 3906 N92-31771 #
DE92-012156 ..... p 3782 N92-31772 #
DE92-012253 ..... p 3782 N92-31773 #
DE92-012259 ..... p 3835 N92-31774 #
DE92-012303 ..... p 3841 N92-31844 #
DE92-012321 ..... p 3819 N92-31287 #
DE92-012327 ..... p 3848 N92-31845 #
DE92-012347 ..... p 3768 N92-31846 #
DE92-012353 ..... p 3797 N92-32146 #
DE92-012355 ..... p 3852 N92-31574 #
DE92-012370 ..... p 3831 N92-31762 #
DE92-012384 ..... p 3917 N92-31288 #
DE92-012398 ..... p 3846 N92-31531 #
DE92-012409 ..... p 3855 N92-32147 * #
DE92-012417 ..... p 3812 N92-31289 #
DE92-012418 ..... p 3900 N92-32131 #
DE92-012420 ..... p 3900 N92-32133 #
DE92-012444 ..... p 3793 N92-31539 #
DE92-012543 ..... p 3810 N92-32134 #
DE92-012598 ..... p 3895 N92-31721 #
DE92-012625 ..... p 3919 N92-31578 #
DE92-012627 ..... p 3861 N92-31709 #
DE92-012628 ..... p 3862 N92-31750 #
DE92-012630 ..... p 3765 N92-31542 #
DE92-012633 ..... p 3802 N92-31580 #
DE92-012681 ..... p 3816 N92-31718 #
DE92-012683 ..... p 3834 N92-31720 #
DE92-012693 ..... p 3780 N92-31565 #
DE92-012697 ..... p 3794 N92-31560 #
DE92-012699 ..... p 3905 N92-31764 #
DE92-013020 ..... p 3898 N92-32167 #
DE92-013036 ..... p 3869 N92-31589 #
DE92-013039 ..... p 3808 N92-31722 #
DE92-013054 ..... p 3852 N92-31591 #
DE92-013070 ..... p 3841 N92-31745 #
DE92-013098 ..... p 3919 N92-31581 #
DE92-013158 ..... p 3777 N92-32135 #
DE92-013159 ..... p 3797 N92-32136 #
DE92-013162 ..... p 3829 N92-32138 #
DE92-013196 ..... p 3820 N92-31420 #
DE92-013212 ..... p 3898 N92-32165 #
DE92-013217 ..... p 3820 N92-31421 #
DE92-013254 ..... p 3850 N92-31324 #
DE92-013276 ..... p 3906 N92-31829 #
DE92-013282 ..... p 3899 N92-31831 #
DE92-013291 ..... p 3790 N92-32139 #
DE92-013294 ..... p 3902 N92-32149 #
DE92-013299 ..... p 3890 N92-32140 #
DE92-013308 ..... p 3851 N92-31422 #
DE92-013342 ..... p 3783 N92-31816 #
DE92-013369 ..... p 3881 N92-32150 #
DE92-013379 ..... p 3911 N92-31723 #
DE92-013401 ..... p 3775 N92-31806 #
DE92-013411 ..... p 3894 N92-31679 #
DE92-013428 ..... p 3759 N92-31817 #
DE92-013441 ..... p 3913 N92-32166 #
DE92-013458 ..... p 3756 N92-31746 #
DE92-013466 ..... p 3836 N92-31647 #
DE92-013484 ..... p 3781 N92-31725 #
DE92-013513 ..... p 3851 N92-31423 #
DE92-013520 ..... p 3850 N92-31304 #
DE92-013535 ..... p 3895 N92-31765 #
DE92-013537 ..... p 3820 N92-31424 #
DE92-013568 ..... p 3820 N92-31425 #
DE92-013571 ..... p 3895 N92-31724 #
DE92-013573 ..... p 3845 N92-31290 #
DE92-013588 ..... p 3912 N92-31945 #
DE92-013589 ..... p 3823 N92-31726 #
DE92-013590 ..... p 3905 N92-31727 #
DE92-013599 ..... p 3813 N92-31440 #
DE92-013645 ..... p 3821 N92-31426 #
DE92-013674 ..... p 3867 N92-31747 #
DE92-013691 ..... p 3851 N92-31427 #
DE92-013696 ..... p 3905 N92-31749 #
DE92-013704 ..... p 3817 N92-31946 #
DE92-013744 ..... p 3899 N92-31948 #
DE92-013770 ..... p 3906 N92-31949 #
DE92-013848 ..... p 3797 N92-32094 #
DE92-013850 ..... p 3795 N92-31917 #
DE92-013925 ..... p 3853 N92-31626 #
DE92-013954 ..... p 3900 N92-31975 #
DE92-013981 ..... p 3882 N92-31466 #
DE92-013998 ..... p 3825 N92-32008 #
DE92-014013 ..... p 3895 N92-31812 #

DE92-014044 ..... p 3824 N92-31832 #
DE92-014049 ..... p 3781 N92-31748 #
DE92-014078 ..... p 3825 N92-32022 #
DE92-014099 ..... p 3817 N92-31834 #
DE92-014100 ..... p 3862 N92-31894 #
DE92-014112 ..... p 3786 N92-32141 #
DE92-014113 ..... p 3831 N92-31775 #
DE92-014179 ..... p 3852 N92-31592 #
DE92-014189 ..... p 3856 N92-31662 #
DE92-014200 ..... p 3903 N92-31372 #
DE92-014206 ..... p 3847 N92-31594 #
DE92-014258 ..... p 3781 N92-31729 #
DE92-014271 ..... p 3908 N92-31403 #
DE92-014322 ..... p 3905 N92-31730 #
DE92-014327 ..... p 3925 N92-32154 #
DE92-014333 ..... p 3785 N92-32113 #
DE92-014352 ..... p 3904 N92-31545 #
DE92-014363 ..... p 3825 N92-32115 #
DE92-014394 ..... p 3890 N92-32116 #
DE92-014416 ..... p 3868 N92-31409 #
DE92-014456 ..... p 3834 N92-31500 #
DE92-014465 ..... p 3815 N92-31650 #
DE92-014467 ..... p 3839 N92-31501 #
DE92-014472 ..... p 3814 N92-31499 #
DE92-014473 ..... p 3815 N92-31651 #
DE92-014476 ..... p 3909 N92-31627 #
DE92-014477 ..... p 3827 N92-31502 #
DE92-014478 ..... p 3839 N92-31383 #
DE92-014502 ..... p 3833 N92-31384 #
DE92-014585 ..... p 3893 N92-31385 #
DE92-014588 ..... p 3783 N92-31891 #
DE92-014630 ..... p 3785 N92-32117 #
DE92-014691 ..... p 3849 N92-32118 #
DE92-014702 ..... p 3910 N92-31665 #
DE92-014719 ..... p 3889 N92-32119 #
DE92-014728 ..... p 3867 N92-32120 #
DE92-014741 ..... p 3829 N92-32174 #
DE92-014744 ..... p 3824 N92-31895 #
DE92-014773 ..... p 3855 N92-32155 #
DE92-014777 ..... p 3835 N92-32121 #
DE92-014798 ..... p 3853 N92-31896 #
DE92-014845 ..... p 3893 N92-31386 #
DE92-014846 ..... p 3779 N92-31441 #
DE92-014847 ..... p 3894 N92-31595 #
DE92-014852 ..... p 3919 N92-31596 #
DE92-014855 ..... p 3838 N92-31335 #
DE92-014857 ..... p 3909 N92-31652 #
DE92-015090 ..... p 3853 N92-31732 #
DE92-015130 ..... p 3853 N92-31782 #
DE92-015200 ..... p 3834 N92-31653 #
DE92-015218 ..... p 3867 N92-31711 #
DE92-015223 ..... p 3877 N92-31654 #
DE92-015224 ..... p 3854 N92-32083 #
DE92-015227 ..... p 3909 N92-31546 #
DE92-015229 ..... p 3799 N92-31751 #
DE92-015235 ..... p 3913 N92-32085 #
DE92-015247 ..... p 3815 N92-31681 #
DE92-015253 ..... p 3837 N92-31657 #
DE92-015269 ..... p 3830 N92-31684 #
DE92-015276 ..... p 3762 N92-32026 #
DE92-015291 ..... p 3839 N92-31400 #
DE92-015297 ..... p 3797 N92-32095 #
DE92-015298 ..... p 3781 N92-31752 #
DE92-015302 ..... p 3858 N92-32027 #
DE92-015305 ..... p 3828 N92-31919 #
DE92-015310 ..... p 3836 N92-31336 #
DE92-015363 ..... p 3900 N92-32028 #
DE92-015389 ..... p 3900 N92-32123 #
DE92-015392 ..... p 3794 N92-31631 #
DE92-015430 ..... p 3784 N92-32029 #
DE92-015822 ..... p 3815 N92-31548 #
DE92-015904 ..... p 3875 N92-31410 #
DE92-015954 ..... p 3827 N92-31633 #
DE92-015998 ..... p 3841 N92-31638 #
DE92-015999 ..... p 3799 N92-31442 #
DE92-016092 ..... p 3900 N92-31295 #
DE92-016098 ..... p 3907 N92-31296 #
DE92-016155 ..... p 3830 N92-31411 #
DE92-016158 ..... p 3850 N92-31297 #
DE92-016160 ..... p 3805 N92-31387 #
DE92-016161 ..... p 3829 N92-32086 #
DE92-016163 ..... p 3770 N92-31897 #
DE92-016164 ..... p 3896 N92-31923 #
DE92-016165 ..... p 3789 N92-31898 #
DE92-016172 ..... p 3789 N92-31924 #
DE92-016177 ..... p 3783 N92-31857 #
DE92-016180 ..... p 3903 N92-31412 #
DE92-016182 ..... p 3896 N92-31926 #
DE92-016183 ..... p 3903 N92-31310 #
DE92-016185 ..... p 3886 N92-31311 #
DE92-016187 ..... p 3879 N92-31899 #
DE92-016194 ..... p 3893 N92-31552 #
DE92-016204 ..... p 3897 N92-31927 #
DE92-016223 ..... p 3850 N92-31312 #
DE92-016286 ..... p 3788 N92-31733 #
DE92-016288 ..... p 3899 N92-31712 #

DE92-016290 ..... p 3924 N92-31713 #
DE92-016346 ..... p 3755 N92-31928 #
DE92-016368 ..... p 3835 N92-31929 #
DE92-016469 ..... p 3862 N92-31734 #
DE92-016500 ..... p 3848 N92-32087 #
DE92-016501 ..... p 3771 N92-32030 #
DE92-016573 ..... p 3789 N92-32032 #
DE92-016574 ..... p 3817 N92-32033 #
DE92-016598 ..... p 3781 N92-31717 #
DE92-016603 ..... p 3823 N92-31785 #
DE92-016634 ..... p 3912 N92-31955 #
DE92-016635 ..... p 3825 N92-32003 #
DE92-016646 ..... p 3854 N92-31930 #
DE92-016685 ..... p 3789 N92-32004 #
DE92-016740 ..... p 3854 N92-31931 #
DE92-016741 ..... p 3766 N92-31735 #
DE92-016747 ..... p 3842 N92-32088 #
DE92-016748 ..... p 3824 N92-31933 #
DE92-016750 ..... p 3757 N92-31736 #
DE92-016787 ..... p 3797 N92-32089 #
DE92-016800 ..... p 3898 N92-32090 #
DE92-016802 ..... p 3883 N92-32034 #
DE92-016834 ..... p 3890 N92-32035 #
DE92-016908 ..... p 3849 N92-32091 #
DE92-016940 ..... p 3849 N92-32124 #
DE92-016941 ..... p 3803 N92-32125 #
DE92-016958 ..... p 3901 N92-31737 #
DE92-016979 ..... p 3881 N92-32126 #
DE92-016981 ..... p 3923 N92-32005 #
DE92-017000 ..... p 3898 N92-32006 #
DE92-017030 ..... p 3898 N92-32007 #
DE92-017351 ..... p 3885 N92-32036 #
DE92-017359 ..... p 3917 N92-32037 #
DE92-620889 ..... p 3896 N92-31904 #
DE92-624981 ..... p 3896 N92-31836 #
DE92-625004 ..... p 3896 N92-31837 #
DE92-627145 ..... p 3837 N92-32143 #
DE92-628395 ..... p 3920 N92-32058 #
DE92-630244 ..... p 3924 N92-31401 #
DE92-630245 ..... p 3914 N92-31402 #
DE92-630650 ..... p 3909 N92-31655 #
DE92-782101 ..... p 3906 N92-31843 #
DE92-782192 ..... p 3920 N92-31859 #
DE92-789024 ..... p 3895 N92-31728 #

DLR-FB-90-34 ..... p 3755 N92-31943 #

DLR-MITT-91-12 ..... p 3755 N92-31813 #

DNA-TR-91-69 ..... p 3891 N92-31588 #

DODA-AR-006-607 ..... p 3796 N92-32045 #
DODA-AR-006-651 ..... p 3759 N92-31439 #
DODA-AR-006-814 ..... p 3755 N92-31562 #

DOE/CE-0357P ..... p 3834 N92-31653 #
DOE/CE-90029/7 ..... p 3890 N92-32099 #

DOE/CH-10510-01 ..... p 3817 N92-31834 #

DOE/DP-48058/4-VOL-1 ..... p 3852 N92-31592 #

DOE/EH-0242P ..... p 3755 N92-31928 #

DOE/EIA-M050(92) ..... p 3847 N92-31594 #

DOE/ER-0533P ..... p 3917 N92-31288 #
DOE/ER-0549T ..... p 3854 N92-31930 #
DOE/ER-10667/11 ..... p 3896 N92-31926 #
DOE/ER-12817/T1 ..... p 3836 N92-31336 #
DOE/ER-12932/2 ..... p 3828 N92-31919 #
DOE/ER-13299/8 ..... p 3783 N92-31891 #
DOE/ER-13418/T1 ..... p 3858 N92-32027 #
DOE/ER-13552/7 ..... p 3781 N92-31752 #
DOE/ER-13657/T1 ..... p 3894 N92-31606 #
DOE/ER-13664/5 ..... p 3785 N92-32113 #
DOE/ER-13751/5 ..... p 3895 N92-31724 #
DOE/ER-13896/4 ..... p 3823 N92-31726 #
DOE/ER-13916/4 ..... p 3890 N92-32035 #
DOE/ER-13937/4 ..... p 3831 N92-31798 #
DOE/ER-14150/2 ..... p 3781 N92-31717 #
DOE/ER-14189/1 ..... p 3781 N92-31725 #
DOE/ER-40009/T3 ..... p 3893 N92-31385 #
DOE/ER-40159/182 ..... p 3895 N92-31721 #
DOE/ER-40224/205 ..... p 3895 N92-31812 #
DOE/ER-40272/T1 ..... p 3893 N92-31552 #
DOE/ER-40322/165 ..... p 3897 N92-31927 #
DOE/ER-40371/5 ..... p 3900 N92-32028 #
DOE/ER-40427/2-N92 ..... p 3925 N92-32154 #
DOE/ER-40560/3A ..... p 3899 N92-31712 #
DOE/ER-40560/3C ..... p 3924 N92-31713 #
DOE/ER-45166/4 ..... p 3839 N92-31400 #
DOE/ER-45208/7 ..... p 3911 N92-31914 #
DOE/ER-45309/4 ..... p 3793 N92-31538 #
DOE/ER-45334/5 ..... p 3912 N92-31945 #
DOE/ER-45372/4 ..... p 3775 N92-31806 #

DOE/ER-45388/T1 ..... p 3788 N92-31733 #
DOE/ER-45398/3 ..... p 3797 N92-32095 #
DOE/ER-45433/1 ..... p 3839 N92-31389 #
DOE/ER-52147/5 ..... p 3831 N92-31769 #
DOE/ER-53198/196 ..... p 3905 N92-31730 #
DOE/ER-53257/5 ..... p 3905 N92-31727 #
DOE/ER-54110/2 ..... p 3904 N92-31545 #
DOE/ER-54131/1 ..... p 3903 N92-31494 #
DOE/ER-60246/5 ..... p 3850 N92-31312 #
DOE/ER-60247/T1 ..... p 3850 N92-31304 #
DOE/ER-60479/T1 ..... p 3853 N92-31626 #
DOE/ER-60522/6 ..... p 3867 N92-32120 #
DOE/ER-60631/9 ..... p 3867 N92-31747 #
DOE/ER-61011/T2 ..... p 3862 N92-31734 #
DOE/ER-61075/T1 ..... p 3862 N92-31894 #
DOE/ER-61202/1 ..... p 3864 N92-31572 #
DOE/ER-75564/9 ..... p 3923 N92-31965 #

DOE/ET-10815/182 ..... p 3903 N92-31372 #
DOE/ET-53088/549 ..... p 3903 N92-31412 #
DOE/ET-53088/554 ..... p 3830 N92-31411 #

DOE/MC-26029/92/C0037 ..... p 3799 N92-31751 #
DOE/MC-26034/3083 ..... p 3784 N92-31976 #

DOE/METC-92-4109 ..... p 3919 N92-31731 #

DOE/OR-00033/T476 ..... p 3821 N92-31426 #

DOE/PC-79812/T7 ..... p 3785 N92-32117 #
DOE/PC-89877/9 ..... p 3786 N92-32141 #
DOE/PC-90305/T6 ..... p 3784 N92-32029 #

DOE/PETC-TR/92/6 ..... p 3824 N92-31895 #

DOE/SF-18862/T1 ..... p 3898 N92-32007 #

DOT/FAA/CT-TN91/39 ..... p 3745 N92-31615 #
DOT/FAA/CT-TN91/44 ..... p 3756 N92-31838 #
DOT/FAA/CT-TN92/18 ..... p 3807 N92-31617 #

DOT/FAA/CT-91-23-VOL-2-PT-1 p 3776 N92-32048 #
DOT/FAA/CT-91/23-VOL-1 ..... p 3776 N92-32047 #

DOT/FAA/NR-92/1 ..... p 3863 N92-32103 #

DOT/FAA/RD-92/21 ..... p 3755 N92-31549 * #

DREA-CR-89-420 ..... p 3806 N92-31471 #
DREA-CR-89-445-PT-2-VOL-1 ..... p 3811 N92-32214 #

DREO-PSD-EPS-05/89 ..... p 3873 N92-32031 #

DREO-1034 ..... p 3810 N92-32176 #
DREO-1084 ..... p 3806 N92-31470 #
DREO-89-29 ..... p 3811 N92-32232 #
DREO-89-32 ..... p 3811 N92-32231 #
DREO-91-6 ..... p 3809 N92-31921 #

DREP-88-14 ..... p 3777 N92-32215 #
DREP-88-15 ..... p 3844 N92-32216 #
DREP-90-02 ..... p 3837 N92-32202 #

DREV-R-4487/88 ..... p 3811 N92-32217 #
DREV-R-4511/88 ..... p 3829 N92-32218 #

E-4969 ..... p 3765 N92-31251 * #
E-5337 ..... p 3769 N92-31249 * #
E-5398 ..... p 3762 N92-31640 * #
E-5675 ..... p 3759 N92-31250 * #
E-6173 ..... p 3754 N92-32240 * #
E-6500 ..... p 3795 N92-31840 * #
E-6542 ..... p 3771 N92-31916 * #
E-6863 ..... p 3834 N92-31536 * #
E-6983 ..... p 3771 N92-32108 * #
E-7009-1 ..... p 3818 N92-32233 * #
E-7028 ..... p 3774 N92-31506 * #
E-7084 ..... p 3832 N92-31349 * #
E-7090 ..... p 3834 N92-31485 * #
E-7104 ..... p 3769 N92-31342 * #
E-7128 ..... p 3840 N92-31505 * #
E-7141 ..... p 3821 N92-31484 * #
E-7149 ..... p 3808 N92-31855 * #
E-7217 ..... p 3771 N92-32237 * #
E-7219 ..... p 3802 N92-31263 * #
E-7224 ..... p 3770 N92-31507 * #
E-7232 ..... p 3777 N92-32234 * #
E-7233 ..... p 3745 N92-31267 * #
E-7247 ..... p 3775 N92-31854 * #
E-7249 ..... p 3770 N92-31901 * #
E-7259 ..... p 3845 N92-31262 * #
E-7260 ..... p 3761 N92-32241 * #
E-7270 ..... p 3801 N92-32230 * #
E-7277 ..... p 3772 N92-32239 * #
E-7289 ..... p 3812 N92-31282 * #

EGG-ME-10066 ..... p 3835 N92-31807 #

EGG-NE-10083 ..... p 3819 N92-31287 #

EGG-PHY-9978 ..... p 3831 N92-31762 #

EGG-10617-5103 ..... p 3881 N92-32150 #
EGG-10617-6085 ..... p 3918 N92-31448 #

EPA/600/A-92/104 ..... p 3853 N92-31648 #
EPA/600/R-92/084 ..... p 3781 N92-31683 #

ESA-BR-79 ..... p 3922 N92-31947 #

ESA-TT-1229 ..... p 3784 N92-31942 #
ESA-TT-1254 ..... p 3755 N92-31943 #

ESD-TR-91-30 ..... p 3876 N92-31541 #
ESD-TR-92-052 ..... p 3843 N92-31323 #

ESD-3746 ..... p 3854 N92-31907 #

ESDP-3747 ..... p 3851 N92-31527 #

ESM-31 ..... p 3896 N92-31837 #

ETN-92-91319 ..... p 3751 N92-31508 #
ETN-92-91387 ..... p 3784 N92-31942 #
ETN-92-91393 ..... p 3840 N92-31512 #
ETN-92-91425 ..... p 3821 N92-31513 #
ETN-92-91679 ..... p 3878 N92-31689 #
ETN-92-91680 ..... p 3886 N92-31690 #
ETN-92-91681 ..... p 3901 N92-31692 #
ETN-92-91682 ..... p 3837 N92-31693 #
ETN-92-91683 ..... p 3787 N92-31695 #
ETN-92-91684 ..... p 3815 N92-31697 #
ETN-92-91685 ..... p 3830 N92-31698 #
ETN-92-91690 ..... p 3860 N92-31702 #
ETN-92-91691 ..... p 3860 N92-31704 #
ETN-92-91692 ..... p 3861 N92-31706 #
ETN-92-91693 ..... p 3861 N92-31708 #
ETN-92-91694 ..... p 3861 N92-31710 #
ETN-92-91711 ..... p 3755 N92-31943 #
ETN-92-91712 ..... p 3922 N92-31947 #
ETN-92-91721 ..... p 3915 N92-31953 #
ETN-92-91725 ..... p 3886 N92-31956 #
ETN-92-91726 ..... p 3887 N92-31957 #
ETN-92-91727 ..... p 3751 N92-31514 #
ETN-92-91728 ..... p 3757 N92-31515 #
ETN-92-91729 ..... p 3840 N92-31516 #
ETN-92-91732 ..... p 3755 N92-31813 #
ETN-92-91738 ..... p 3896 N92-31814 #
ETN-92-91739 ..... p 3899 N92-31815 #
ETN-92-91784 ..... p 3888 N92-31517 #
ETN-92-91811 ..... p 3807 N92-31715 #
ETN-92-91844 ..... p 3888 N92-31518 #
ETN-92-91845 ..... p 3888 N92-31519 #
ETN-92-91846 ..... p 3886 N92-31520 #
ETN-92-91851 ..... p 3859 N92-31521 #
ETN-92-91863 ..... p 3856 N92-31522 #
ETN-92-91889 ..... p 3774 N92-31716 #
ETN-92-91891 ..... p 3915 N92-31660 #

ETS-RR-92-15-ONR ..... p 3871 N92-31444 #

FEI-2187 ..... p 3896 N92-31904 #

FFA-TN-1991-44 ..... p 3840 N92-31512 #

FJSRL-TR-92-0001 ..... p 3752 N92-31622 #

FNAL-TM-1724 ..... p 3826 N92-31313 #

FNAL/C-91/295-A ..... p 3898 N92-32167 #

FOA-C-30642-3.1 ..... p 3866 N92-32069 #
FOA-C-30647-9.4 ..... p 3767 N92-32073 #
FOA-C-30649-3.2 ..... p 3810 N92-32161 #
FOA-C-30650-8.4,3.2 ..... p 3810 N92-32070 #

FRACTO-92 ..... p 3913 N92-32065 #

GA-A-20860 ..... p 3904 N92-31616 #
GA-A-20876 ..... p 3905 N92-31764 #
GA-A-20877 ..... p 3905 N92-31749 #
GA-A-20915 ..... p 3781 N92-31729 #

GAO/RCED-91-128 ..... p 3891 N92-31454 #
GAO/RCED-91-24 ..... p 3755 N92-31453 #

GIT-AER-E-16-616 ..... p 3783 N92-31918 #

GRI-91/0229 ..... p 3824 N92-31839 #
GRI-91/0352 ..... p 3783 N92-31918 #
GRI-91/0354 ..... p 3835 N92-31841 #
GRI-91/0397 ..... p 3848 N92-31903 #

GRI-92/0021 ..... p 3848 N92-31922 #
GRI-92/0068 ..... p 3782 N92-31776 #

GTRF-101 ..... p 3904 N92-31613 #

H-1783 ..... p 3751 N92-31276 * #
H-1787 ..... p 3761 N92-31656 * #
H-1803 ..... p 3752 N92-31808 * #
H-1808 ..... p 3759 N92-31275 * #
H-1831 ..... p 3762 N92-32201 * #
H-1847 ..... p 3756 N92-31261 * #

HDL-TR-2212 ..... p 3836 N92-32173 #

IC-91/384 ..... p 3924 N92-31401 #
IC-91/388 ..... p 3914 N92-31402 #
IC-91/391 ..... p 3909 N92-31655 #

ICASE-IR-22 ..... p 3876 N92-31561 * #
ICASE-IR-23 ..... p 3822 N92-31564 * #

ICASE-92-21 ..... p 3887 N92-32164 * #
ICASE-92-30 ..... p 3881 N92-32157 * #
ICASE-92-31 ..... p 3822 N92-31687 * #
ICASE-92-32 ..... p 3826 N92-32158 * #
ICASE-92-33 ..... p 3822 N92-31535 * #
ICASE-92-36 ..... p 3818 N92-31265 * #

IDA-P-2638 ..... p 3873 N92-32023 #

IDA/HQ-91-40259 ..... p 3873 N92-32023 #

IFSR-549 ..... p 3903 N92-31412 #
IFSR-554 ..... p 3830 N92-31411 #

IHES/M/92/13 ..... p 3890 N92-31925 #

IITRI-D06200-1 ..... p 3809 N92-31996 #

INIS-JP-002 ..... p 3920 N92-31859 #

INIS-MF-13154 ..... p 3920 N92-32058 #

INO-TM-8-PT-1 ..... p 3863 N92-31308 #

INPE-5337-PRE/1736 ..... p 3923 N92-31343 #
INPE-5339-PRE/1738 ..... p 3923 N92-31344 #
INPE-5340-PRE/1739 ..... p 3923 N92-31345 #
INPE-5342-PRE/1741 ..... p 3923 N92-31346 #
INPE-5343-PRE/1742 ..... p 3923 N92-31347 #
INPE-5358-NTC/301 ..... p 3922 N92-32227 #
INPE-5361-RPQ/656 ..... p 3886 N92-31241 #
INPE-5364-PRE/1744 ..... p 3863 N92-32224 #
INPE-5371-TDI/470 ..... p 3926 N92-32221 #
INPE-5372-PRE/1746 ..... p 3798 N92-32199 #
INPE-5373-PRE/1747 ..... p 3818 N92-32200 #
INPE-5377-TDI/472 ..... p 3925 N92-32025 #
INPE-5378-TDI/473 ..... p 3845 N92-32220 #
INPE-5386-TDI/475 ..... p 3843 N92-31277 #
INPE-5388-TDI/477 ..... p 3863 N92-32212 #
INPE-5394-PRE/1752 ..... p 3874 N92-31348 #
INPE-5395-PRE/1753 ..... p 3889 N92-32225 #
INPE-5407-PUD/051 ..... p 3806 N92-31568 #

INT-PATENT-CLASS-C08L-79/08 p 3794 N92-31792 *
INT-PATENT-CLASS-C12M-1/10 p 3828 N92-31790 *
INT-PATENT-CLASS-C12M-1/12 p 3828 N92-31790 *
INT-PATENT-CLASS-C12M-3/00 p 3828 N92-31790 *
INT-PATENT-CLASS-C12M-3/02 p 3828 N92-31790 *

INT-PATENT-CLASS-H01S-3/10 . p 3831 N92-31788 *

IS-M-686 ..... p 3782 N92-31772 #
IS-M-703 ..... p 3780 N92-31565 #
IS-M-709 ..... p 3831 N92-31775 #
IS-M-711 ..... p 3890 N92-32116 #

ISBN-0-16-035925-2 ..... p 3852 N92-31598 #
ISBN-1-871564-360 ..... p 3757 N92-31515 #
ISBN-1-871564-379 ..... p 3840 N92-31516 #
ISBN-1-871564-387 ..... p 3751 N92-31514 #
ISBN-92-835-0655-3 ..... p 3920 N92-32182 #
ISBN-92-835-0678-2 ..... p 3889 N92-32229 #
ISBN-92-9092-095-5 ..... p 3922 N92-31947 #
ISBN-951-22-0857-1 ..... p 3787 N92-31610 #

ISSN-0038-0911 ..... p 3856 N92-31637 #
ISSN-0038-0911 ..... p 3856 N92-31639 #
ISSN-0915-633X ..... p 3827 N92-31340 #
ISSN-0939-298X ..... p 3755 N92-31813 #

IST-TR-92-12 ..... p 3873 N92-31974 #

ITN-92-85124 ..... p 3745 N92-31861 #
ITN-92-85162 ..... p 3897 N92-31958

JPC-92-3144 ..... p 3770 N92-31901 * #
JPC-92-3203 ..... p 3771 N92-32237 * #

JPR-584243 ..... p 3892 N92-32178 * #
JPR-9950-1368 ..... p 3829 N92-32128 * #

JPRS-UES-92-004 ..... p 3843 N92-32132 #

JPRS-ULS-92-015 ..... p 3924 N92-32179 #

JPRS-UMS-92-010 ..... p 3787 N92-31584 #

K/TCD-1020 ..... p 3783 N92-31816 #

KCP-613-4503 ..... p 3838 N92-31303 #
KCP-613-4650 ..... p 3777 N92-32135 #
KCP-613-4661 ..... p 3797 N92-32136 #
KCP-613-4747 ..... p 3789 N92-32032 #
KCP-613-4748 ..... p 3817 N92-31946 #
KCP-613-4804 ..... p 3817 N92-32033 #
KCP-613-4837 ..... p 3876 N92-31529 #

KURRI-TR-358 ..... p 3895 N92-31728 #

L-16709 ..... p 3818 N92-31247 * #
L-16724 ..... p 3750 N92-31246 * #
L-16959 ..... p 3751 N92-31532 * #
L-16977 ..... p 3760 N92-31240 * #
L-17006 ..... p 3838 N92-31279 * #
L-17039 ..... p 3819 N92-31281 * #
L-17069 ..... p 3844 N92-32127 * #
L-17082 ..... p 3926 N92-32193 * #

LA-UR-92-1271 ..... p 3820 N92-31424 #
LA-UR-92-1302 ..... p 3895 N92-31765 #
LA-UR-92-1390 ..... p 3759 N92-31817 #
LA-UR-92-1435 ..... p 3911 N92-31723 #
LA-UR-92-1528 ..... p 3839 N92-31383 #
LA-UR-92-1529 ..... p 3762 N92-32026 #
LA-UR-92-1705 ..... p 3815 N92-31681 #
LA-UR-92-296 ..... p 3804 N92-31317 #
LA-UR-92-789 ..... p 3806 N92-31449 #
LA-UR-92-849 ..... p 3823 N92-31701 #
LA-UR-92-859 ..... p 3878 N92-31703 #
LA-UR-92-984 ..... p 3847 N92-31571 #

LA-10613-MS-REV-1 ..... p 3825 N92-32022 #
LA-12062-MS-REV-1 ..... p 3825 N92-32008 #
LA-12291-MS ..... p 3789 N92-32004 #

LAAS-91467 ..... p 3878 N92-31689 #
LAAS-91475 ..... p 3886 N92-31690 #
LAAS-91484 ..... p 3901 N92-31692 #
LAAS-92002 ..... p 3837 N92-31693 #
LAAS-92013 ..... p 3787 N92-31695 #
LAAS-92032 ..... p 3815 N92-31697 #
LAAS-92034 ..... p 3830 N92-31698 #

LAMP-91/10 ..... p 3896 N92-31836 #

LBL-30841 ..... p 3898 N92-32006 #
LBL-31590 ..... p 3779 N92-31417 #
LBL-31685 ..... p 3926 N92-31756 #

LC-79-640375 ..... p 3856 N92-31637 #
LC-79-640375 ..... p 3856 N92-31639 #
LC-88-600144 ..... p 3788 N92-31797 #

LMSC-F404726 ..... p 3925 N92-31856 * #

LMSC-PO35355 ..... p 3925 N92-31856 * #

LMSC/P024859 ..... p 3767 N92-32100 * #

LTR91-003 ..... p 3879 N92-31833 #

M-694 ..... p 3791 N92-31278 * #
M-695 ..... p 3838 N92-31280 * #

MATHS-REPT-A-152 ..... p 3886 N92-31956 #
MATHS-REPT-A-153 ..... p 3887 N92-31957 #

MBB-UD-0609-91-PUB ..... p 3774 N92-31716 #

MBB-UO-0163-91-PUB ..... p 3915 N92-31660 #

MCAT-92-014 ..... p 3752 N92-31533 * #
MCAT-92-015 ..... p 3753 N92-32177 * #

MIT-R92-17 ..... p 3855 N92-32222 * #

MIT-TR-16 ..... p 3792 N92-31394 #
MIT-TR-17 ..... p 3780 N92-31524 #

MIT-335 ..... p 3855 N92-32222 * #

MIT/LCS/TR-524 ..... p 3887 N92-32163 #

MML-TR-91-16C ..... p 3833 N92-31437 #

MPL-U-25/91 ..... p 3902 N92-32144 #

MSRR-572 ..... p 3888 N92-31768 #

MTL-TR-92-14 ..... p 3794 N92-31624 #
MTL-TR-92-1 ..... p 3778 N92-31301 #
MTL-TR-92-24 ..... p 3914 N92-32207 #
MTL-TR-92-30 ..... p 3792 N92-31404 #
MTL-TR-92-8 ..... p 3775 N92-31940 #

MTR-11201 ..... p 3843 N92-31323 #
MTR-11278 ..... p 3810 N92-32043 #

NADC-91093-60 ..... p 3833 N92-31437 #
NADC-91122-60 ..... p 3774 N92-31382 #

NAL-TR-1110T ..... p 3765 N92-31685 #

NAS 1.15:102230 ..... p 3754 N92-32213 * #
NAS 1.15:102600 ..... p 3766 N92-31457 * #
NAS 1.15:103248 ..... p 3759 N92-31250 * #
NAS 1.15:103593 ..... p 3765 N92-32148 * #
NAS 1.15:104246 ..... p 3752 N92-31808 * #
NAS 1.15:104250 ..... p 3762 N92-32201 * #
NAS 1.15:104254 ..... p 3756 N92-31261 * #
NAS 1.15:105198 ..... p 3795 N92-31840 * #
NAS 1.15:105310 ..... p 3771 N92-31916 * #
NAS 1.15:105434 ..... p 3832 N92-31349 * #
NAS 1.15:105600 ..... p 3834 N92-31536 * #
NAS 1.15:105637 ..... p 3771 N92-32108 * #
NAS 1.15:105666 ..... p 3774 N92-31506 * #
NAS 1.15:105702 ..... p 3834 N92-31485 * #
NAS 1.15:105712 ..... p 3769 N92-31342 * #
NAS 1.15:105726 ..... p 3840 N92-31505 * #
NAS 1.15:105740 ..... p 3821 N92-31484 * #
NAS 1.15:105744 ..... p 3808 N92-31855 * #
NAS 1.15:105787 ..... p 3771 N92-32237 * #
NAS 1.15:105789 ..... p 3802 N92-31263 * #
NAS 1.15:105794 ..... p 3770 N92-31507 * #
NAS 1.15:105802 ..... p 3777 N92-32234 * #
NAS 1.15:105803 ..... p 3745 N92-31267 * #
NAS 1.15:105816 ..... p 3775 N92-31854 * #
NAS 1.15:105818 ..... p 3770 N92-31901 * #
NAS 1.15:105825 ..... p 3845 N92-31262 * #
NAS 1.15:105826 ..... p 3761 N92-32241 * #
NAS 1.15:105832 ..... p 3818 N92-32233 * #
NAS 1.15:105835 ..... p 3801 N92-32230 * #
NAS 1.15:105846 ..... p 3812 N92-31282 * #
NAS 1.15:107602 ..... p 3769 N92-32204 * #
NAS 1.15:107644 ..... p 3750 N92-31239 * #
NAS 1.15:107646 ..... p 3762 N92-31900 * #
NAS 1.15:107650 ..... p 3758 N92-32111 * #
NAS 1.15:107652 ..... p 3757 N92-31350 * #
NAS 1.15:107654 ..... p 3757 N92-31351 * #
NAS 1.15:107655 ..... p 3757 N92-31264 * #
NAS 1.15:107662 ..... p 3839 N92-31504 * #
NAS 1.15:107795 ..... p 3916 N92-31253 * #
NAS 1.15:107980 ..... p 3926 N92-31852 * #
NAS 1.15:107965 ..... p 3849 N92-31258 * #
NAS 1.15:107966 ..... p 3924 N92-31781 * #
NAS 1.15:4187 ..... p 3818 N92-31247 * #
NAS 1.15:4189 ..... p 3750 N92-31246 * #
NAS 1.15:4214 ..... p 3769 N92-31249 * #
NAS 1.15:4381 ..... p 3760 N92-31240 * #
NAS 1.15:4386 ..... p 3926 N92-32193 * #
NAS 1.15:4398 ..... p 3751 N92-31276 * #
NAS 1.15:4400 ..... p 3759 N92-31275 * #
NAS 1.21:7037(280) ..... p 3745 N92-31456 *
NAS 1.21:7039(41)-SECT-2 ..... p 3918 N92-31455 *
NAS 1.26:182168 ..... p 3769 N92-31245 * #
NAS 1.26:184256 ..... p 3883 N92-31835 * #
NAS 1.26:184341 ..... p 3760 N92-31910 * #
NAS 1.26:184361 ..... p 3856 N92-31551 * #
NAS 1.26:185242 ..... p 3891 N92-31248 * #
NAS 1.26:186022 ..... p 3761 N92-31656 * #
NAS 1.26:187216 ..... p 3771 N92-32129 * #
NAS 1.26:189222 ..... p 3759 N92-31534 * #
NAS 1.26:189224 ..... p 3772 N92-32239 * #
NAS 1.26:189230 ..... p 3835 N92-31892 * #
NAS 1.26:189234 ..... p 3762 N92-31252 * #
NAS 1.26:189628 ..... p 3767 N92-31677 * #
NAS 1.26:189652-VOL-1 ..... p 3754 N92-32226 * #
NAS 1.26:189652-VOL-2 ..... p 3754 N92-32228 * #
NAS 1.26:189653-VOL-3 ..... p 3766 N92-32130 * #
NAS 1.26:189662 ..... p 3876 N92-31561 * #
NAS 1.26:189663 ..... p 3887 N92-32164 * #
NAS 1.26:189674 ..... p 3822 N92-31564 * #
NAS 1.26:189680 ..... p 3881 N92-32157 * #
NAS 1.26:189681 ..... p 3822 N92-31687 * #
NAS 1.26:189682 ..... p 3826 N92-32158 * #
NAS 1.26:189683 ..... p 3822 N92-31535 * #
NAS 1.26:189686 ..... p 3818 N92-31265 * #

NAS 1.26:190200 ..... p 3925 N92-31338 * #
NAS 1.26:190379 ..... p 3855 N92-32147 * #
NAS 1.26:190443 ..... p 3886 N92-31553 * #
NAS 1.26:190479 ..... p 3892 N92-32178 * #
NAS 1.26:190481 ..... p 3829 N92-32128 * #
NAS 1.26:190516 ..... p 3842 N92-32236 * #
NAS 1.26:190529 ..... p 3884 N92-31254 * #
NAS 1.26:190534 ..... p 3807 N92-31614 * #
NAS 1.26:190536 ..... p 3839 N92-31339 * #
NAS 1.26:190540 ..... p 3803 N92-31238 * #
NAS 1.26:190577 ..... p 3840 N92-31619 * #
NAS 1.26:190580 ..... p 3914 N92-31577 * #
NAS 1.26:190585 ..... p 3841 N92-31911 * #
NAS 1.26:190614 ..... p 3870 N92-31341 * #
NAS 1.26:190626 ..... p 3766 N92-31260 * #
NAS 1.26:190628 ..... p 3858 N92-32195 * #
NAS 1.26:190630 ..... p 3917 N92-31272 * #
NAS 1.26:190633 ..... p 3916 N92-31547 * #
NAS 1.26:190639 ..... p 3882 N92-31483 * #
NAS 1.26:190641 ..... p 3885 N92-31597 * #
NAS 1.26:190656 ..... p 3804 N92-31273 * #
NAS 1.26:190660 ..... p 3774 N92-31566 * #
NAS 1.26:190661 ..... p 3772 N92-31274 * #
NAS 1.26:190665 ..... p 3844 N92-31357 * #
NAS 1.26:190666 ..... p 3770 N92-31550 * #
NAS 1.26:190674 ..... p 3790 N92-32156 * #
NAS 1.26:190675 ..... p 3850 N92-31259 * #
NAS 1.26:190680 ..... p 3752 N92-31533 * #
NAS 1.26:190683 ..... p 3925 N92-31856 * #
NAS 1.26:190685 ..... p 3806 N92-31468 * #
NAS 1.26:190688 ..... p 3753 N92-32177 * #
NAS 1.26:190689 ..... p 3820 N92-31352 * #
NAS 1.26:190691 ..... p 3772 N92-31266 * #
NAS 1.26:190694 ..... p 3880 N92-32122 * #
NAS 1.26:190698 ..... p 3845 N92-32223 * #
NAS 1.26:190700 ..... p 3777 N92-32159 * #
NAS 1.26:190705 ..... p 3855 N92-32222 * #
NAS 1.26:190706 ..... p 3842 N92-32235 * #
NAS 1.26:190708 ..... p 3875 N92-31487 * #
NAS 1.26:190711 ..... p 3875 N92-31486 * #
NAS 1.26:190716 ..... p 3879 N92-31787 * #
NAS 1.26:190731 ..... p 3753 N92-32162 * #
NAS 1.26:4391 ..... p 3754 N92-32240 * #
NAS 1.26:4446 ..... p 3826 N92-32242 * #
NAS 1.26:4457 ..... p 3755 N92-31549 * #
NAS 1.26:4461 ..... p 3767 N92-32100 * #
NAS 1.26:4463 ..... p 3761 N92-32175 * #
NAS 1.26:4465 ..... p 3753 N92-32114 * #
NAS 1.60:3014 ..... p 3765 N92-31251 * #
NAS 1.60:3038 ..... p 3762 N92-31640 * #
NAS 1.60:3184 ..... p 3751 N92-31532 * #
NAS 1.60:3208 ..... p 3819 N92-31281 * #
NAS 1.60:3231 ..... p 3838 N92-31279 * #
NAS 1.60:3275 ..... p 3791 N92-31278 * #
NAS 1.60:3277 ..... p 3838 N92-31280 * #
NAS 1.61:1279 ..... p 3844 N92-32127 * #
NAS 1.71:LAR-14418-1 ..... p 3803 N92-31257 * #

NASA-CASE-LAR-13772-1 ..... p 3831 N92-31788 *
NASA-CASE-LAR-14159-1-CU ..... p 3794 N92-31792 *
NASA-CASE-LAR-14418-1 ..... p 3803 N92-31257 * #

NASA-CASE-MFS-28370-1 ..... p 3828 N92-31790 *

NASA-CR-182168 ..... p 3769 N92-31245 * #
NASA-CR-184256 ..... p 3883 N92-31835 * #
NASA-CR-184341 ..... p 3760 N92-31910 * #
NASA-CR-184361 ..... p 3856 N92-31551 * #
NASA-CR-185242 ..... p 3891 N92-31248 * #
NASA-CR-186022 ..... p 3761 N92-31656 * #
NASA-CR-187216 ..... p 3771 N92-32129 * #
NASA-CR-189222 ..... p 3759 N92-31534 * #
NASA-CR-189224 ..... p 3772 N92-32239 * #
NASA-CR-189230 ..... p 3835 N92-31892 * #
NASA-CR-189234 ..... p 3762 N92-31252 * #
NASA-CR-189628 ..... p 3767 N92-31677 * #
NASA-CR-189652-VOL-1 ..... p 3754 N92-32226 * #
NASA-CR-189652-VOL-2 ..... p 3754 N92-32228 * #
NASA-CR-189653-VOL-3 ..... p 3766 N92-32130 * #
NASA-CR-189662 ..... p 3876 N92-31561 * #
NASA-CR-189663 ..... p 3887 N92-32164 * #
NASA-CR-189674 ..... p 3822 N92-31564 * #
NASA-CR-189680 ..... p 3881 N92-32157 * #
NASA-CR-189681 ..... p 3822 N92-31687 * #
NASA-CR-189682 ..... p 3826 N92-32158 * #
NASA-CR-189683 ..... p 3822 N92-31535 * #
NASA-CR-189686 ..... p 3818 N92-31265 * #
NASA-CR-190200 ..... p 3925 N92-31338 * #
NASA-CR-190379 ..... p 3855 N92-32147 * #
NASA-CR-190443 ..... p 3886 N92-31553 * #
NASA-CR-190479 ..... p 3892 N92-32178 * #
NASA-CR-190481 ..... p 3829 N92-32128 * #
NASA-CR-190516 ..... p 3842 N92-32236 * #
NASA-CR-190529 ..... p 3884 N92-31254 * #
NASA-CR-190534 ..... p 3807 N92-31614 * #
NASA-CR-190536 ..... p 3839 N92-31339 * #
NASA-CR-190540 ..... p 3803 N92-31238 * #
NASA-CR-190577 ..... p 3840 N92-31619 * #
NASA-CR-190580 ..... p 3914 N92-31577 * #
NASA-CR-190585 ..... p 3841 N92-31911 * #
NASA-CR-190614 ..... p 3870 N92-31341 * #
NASA-CR-190626 ..... p 3766 N92-31260 * #
NASA-CR-190628 ..... p 3858 N92-32195 * #
NASA-CR-190630 ..... p 3917 N92-31272 * #
NASA-CR-190633 ..... p 3916 N92-31547 * #
NASA-CR-190639 ..... p 3882 N92-31483 * #
NASA-CR-190641 ..... p 3885 N92-31597 * #
NASA-CR-190656 ..... p 3804 N92-31273 * #
NASA-CR-190660 ..... p 3774 N92-31566 * #
NASA-CR-190661 ..... p 3772 N92-31274 * #
NASA-CR-190665 ..... p 3844 N92-31357 * #
NASA-CR-190666 ..... p 3770 N92-31550 * #
NASA-CR-190674 ..... p 3790 N92-32156 * #
NASA-CR-190675 ..... p 3850 N92-31259 * #
NASA-CR-190680 ..... p 3752 N92-31533 * #
NASA-CR-190683 ..... p 3925 N92-31856 * #
NASA-CR-190685 ..... p 3806 N92-31468 * #
NASA-CR-190688 ..... p 3753 N92-32177 * #
NASA-CR-190689 ..... p 3820 N92-31352 * #
NASA-CR-190691 ..... p 3772 N92-31266 * #
NASA-CR-190694 ..... p 3880 N92-32122 * #
NASA-CR-190698 ..... p 3845 N92-32223 * #
NASA-CR-190700 ..... p 3777 N92-32159 * #
NASA-CR-190705 ..... p 3855 N92-32222 * #
NASA-CR-190706 ..... p 3842 N92-32235 * #
NASA-CR-190708 ..... p 3875 N92-31487 * #
NASA-CR-190711 ..... p 3875 N92-31486 * #
NASA-CR-190716 ..... p 3879 N92-31787 * #
NASA-CR-190731 ..... p 3753 N92-32162 * #
NASA-CR-4391 ..... p 3754 N92-32240 * #
NASA-CR-4446 ..... p 3826 N92-32242 * #
NASA-CR-4457 ..... p 3755 N92-31549 * #
NASA-CR-4461 ..... p 3767 N92-32100 * #
NASA-CR-4463 ..... p 3761 N92-32175 * #
NASA-CR-4465 ..... p 3753 N92-32114 * #

NASA-RP-1279 ..... p 3844 N92-32127 * #

NASA-SBIR-92-1 ..... p 3916 N92-31253 * #

NASA-SP-7037(280) ..... p 3745 N92-31456 *
NASA-SP-7039(41)-SECT-2 ..... p 3918 N92-31455 *

NASA-TM-102230 ..... p 3754 N92-32213 * #
NASA-TM-102600 ..... p 3766 N92-31457 * #
NASA-TM-103248 ..... p 3759 N92-31250 * #
NASA-TM-103593 ..... p 3765 N92-32148 * #
NASA-TM-104246 ..... p 3752 N92-31808 * #
NASA-TM-104250 ..... p 3762 N92-32201 * #
NASA-TM-104254 ..... p 3756 N92-31261 * #
NASA-TM-105198 ..... p 3795 N92-31840 * #
NASA-TM-105310 ..... p 3771 N92-31916 * #
NASA-TM-105434 ..... p 3832 N92-31349 * #
NASA-TM-105600 ..... p 3834 N92-31536 * #
NASA-TM-105637 ..... p 3771 N92-32108 * #
NASA-TM-105666 ..... p 3774 N92-31506 * #
NASA-TM-105702 ..... p 3834 N92-31485 * #
NASA-TM-105712 ..... p 3769 N92-31342 * #
NASA-TM-105726 ..... p 3840 N92-31505 * #
NASA-TM-105740 ..... p 3821 N92-31484 * #
NASA-TM-105744 ..... p 3808 N92-31855 * #
NASA-TM-105787 ..... p 3771 N92-32237 * #
NASA-TM-105789 ..... p 3802 N92-31263 * #
NASA-TM-105794 ..... p 3770 N92-31507 * #
NASA-TM-105802 ..... p 3777 N92-32234 * #
NASA-TM-105803 ..... p 3745 N92-31267 * #
NASA-TM-105816 ..... p 3775 N92-31854 * #
NASA-TM-105818 ..... p 3770 N92-31901 * #
NASA-TM-105825 ..... p 3845 N92-31262 * #
NASA-TM-105826 ..... p 3761 N92-32241 * #
NASA-TM-105832 ..... p 3818 N92-32233 * #
NASA-TM-105835 ..... p 3801 N92-32230 * #
NASA-TM-105846 ..... p 3812 N92-31282 * #
NASA-TM-107602 ..... p 3769 N92-32204 * #
NASA-TM-107644 ..... p 3750 N92-31239 * #
NASA-TM-107646 ..... p 3762 N92-31900 * #
NASA-TM-107650 ..... p 3758 N92-32111 * #
NASA-TM-107652 ..... p 3757 N92-31350 * #
NASA-TM-107654 ..... p 3757 N92-31351 * #
NASA-TM-107655 ..... p 3757 N92-31264 * #
NASA-TM-107662 ..... p 3839 N92-31504 * #
NASA-TM-107795 ..... p 3916 N92-31253 * #
NASA-TM-107960 ..... p 3926 N92-31852 * #
NASA-TM-107965 ..... p 3849 N92-31258 * #
NASA-TM-107966 ..... p 3924 N92-31781 * #
NASA-TM-4187 ..... p 3818 N92-31247 * #
NASA-TM-4189 ..... p 3750 N92-31246 * #
NASA-TM-4214 ..... p 3769 N92-31249 * #
NASA-TM-4381 ..... p 3760 N92-31240 * #
NASA-TM-4386 ..... p 3926 N92-32193 * #
NASA-TM-4398 ..... p 3751 N92-31276 * #
NASA-TM-4400 ..... p 3759 N92-31275 * #

NASA-TP-3014 ..... p 3765 N92-31251 * #
NASA-TP-3038 ..... p 3762 N92-31640 * #
NASA-TP-3184 ..... p 3751 N92-31532 * #
NASA-TP-3208 ..... p 3819 N92-31281 * #
NASA-TP-3231 ..... p 3838 N92-31279 * #
NASA-TP-3275 ..... p 3791 N92-31278 * #
NASA-TP-3277 ..... p 3838 N92-31280 * #

NAVSWC-TR-91-250 ..... p 3801 N92-32096 #

NCAR/TN-366+STR ..... p 3853 N92-31649 * #

NCES-92-011 ..... p 3916 N92-32160 #

NDP-039 ..... p 3851 N92-31527 #

NHRC-91-13 ..... p 3868 N92-31492 #
NHRC-91-26 ..... p 3872 N92-31327 #

NIFS-106 ..... p 3892 N92-31255 #
NIFS-111 ..... p 3906 N92-31843 #
NIFS-118 ..... p 3887 N92-32205 #
NIFS-125 ..... p 3818 N92-31256 #
NIFS-127 ..... p 3907 N92-32181 #
NIFS-128 ..... p 3827 N92-31340 #
NIFS-140 ..... p 3904 N92-31659 #

NIKHEF-K-EMIN-92-01 ..... p 3896 N92-31814 #

NIKHEF-K/AMPS/91-08 ..... p 3899 N92-31815 #

NIST/GCR-92/604 ..... p 3780 N92-31678 #

NIST/SP-823/1 ..... p 3881 N92-31365 #

NIST/TN-1349 ..... p 3805 N92-31368 #
NIST/TN-1352 ..... p 3824 N92-31839 #

NISTIR-3966 ..... p 3774 N92-31609 #
NISTIR-4539 ..... p 3827 N92-31633 #
NISTIR-4703 ..... p 3923 N92-31643 #
NISTIR-4737 ..... p 3874 N92-31366 #
NISTIR-4788 ..... p 3794 N92-31618 #
NISTIR-4791 ..... p 3915 N92-31645 #
NISTIR-4803 ..... p 3813 N92-31367 #
NISTIR-4807 ..... p 3885 N92-31680 #
NISTIR-4813 ..... p 3877 N92-31628 #
NISTIR-4823 ..... p 3827 N92-31370 #
NISTIR-4830 ..... p 3917 N92-31371 #
NISTIR-4844 ..... p 3913 N92-32072 #

NMRI-92-25 ..... p 3828 N92-31794 #

NOAA-TM-ERL-WPL-222 ..... p 3860 N92-31641 #

NOAA-TM-NMFS-105 ..... p 3866 N92-32106 #

NOARL-CR-044-91 ..... p 3863 N92-31406 #

NOARL-PR-91-132-253 ..... p 3866 N92-32050 #

NOARL-TN-204 ..... p 3857 N92-31986 #
NOARL-TN-257 ..... p 3918 N92-31467 #

NOSC/TR-1487 ..... p 3844 N92-31362 #

NPS-OC-91-003 ..... p 3865 N92-31988 #
NPS-OC-92-003 ..... p 3864 N92-31495 #

NPS-PH-92-007 ..... p 3859 N92-31540 #

NPSEC-92-005 ..... p 3805 N92-31413 #

NRAD-TD-2278 ..... p 3805 N92-31369 #

NRC-TR-ENG-005 ..... p 3833 N92-31469 #

NRC-32083 ..... p 3833 N92-31469 #

NREL/TP-253-4252 ..... p 3847 N92-31579 #
NREL/TP-253-4276 ..... p 3785 N92-32093 #
NREL/TP-253-4281 ..... p 3849 N92-32110 #
NREL/TP-257-4099 ..... p 3846 N92-31498 #
NREL/TP-410-4724 ..... p 3847 N92-31646 #
NREL/TP-411-4840 ..... p 3814 N92-31525 #
NREL/TP-413-4835 ..... p 3846 N92-31526 #
NREL/TP-413-4873 ..... p 3846 N92-31497 #
NREL/TP-431-4831 ..... p 3799 N92-31593 #
NREL/TP-432-4734 ..... p 3845 N92-31481 #
NREL/TP-432-4737 ..... p 3872 N92-31309 #
NREL/TP-432-4827 ..... p 3849 N92-32112 #
NREL/TP-441-4801 ..... p 3847 N92-31623 #
NREL/TP-451-4855 ..... p 3848 N92-31893 #

NRL/FR/5160-92-9377 ..... p 3892 N92-32044 #

NRL/MR/5120-92-6920 ..... p 3892 N92-31818 #
NRL/MR/5524-92-6944 ..... p 3916 N92-31992 #

NUWC-NL-TD-10023 ..... p 3892 N92-31789 #

NWC-TP-7163 ..... p 3814 N92-31461 #

OCS/MMS-92/0001 ..... p 3864 N92-31630 #

OITS-470 ..... p 3895 N92-31812 #

ONERA-NT-1989-8 ..... p 3784 N92-31942 #

ORNL-6709 ..... p 3804 N92-31354 #

ORNL/CDIAC-46 ..... p 3854 N92-31907 #
ORNL/CDIAC-47 ..... p 3851 N92-31527 #

ORNL/TM-12019 ..... p 3881 N92-32126 #
ORNL/TM-12040 ..... p 3814 N92-31499 #
ORNL/TM-12071 ..... p 3883 N92-32034 #

OTA-A-530 ..... p 3922 N92-31599 #

PB92-100353 ..... p 3852 N92-31598 #
PB92-145515 ..... p 3918 N92-31398 #
PB92-152883 ..... p 3848 N92-31903 #
PB92-156892 ..... p 3852 N92-31620 #
PB92-158278 ..... p 3923 N92-31643 #
PB92-164359 ..... p 3782 N92-31776 #
PB92-166549 ..... p 3922 N92-31599 #
PB92-172303 ..... p 3848 N92-31922 #
PB92-172402 ..... p 3783 N92-31918 #
PB92-172485 ..... p 3794 N92-31618 #
PB92-172733 ..... p 3915 N92-31645 #
PB92-173038 ..... p 3809 N92-31920 #
PB92-173046 ..... p 3802 N92-31830 #
PB92-173681 ..... p 3916 N92-31364 #
PB92-173707 ..... p 3919 N92-31682 #
PB92-177054 ..... p 3865 N92-31644 #
PB92-177690 ..... p 3864 N92-31630 #
PB92-178128 ..... p 3866 N92-32106 #
PB92-178284 ..... p 3890 N92-31925 #
PB92-178623 ..... p 3788 N92-31797 #
PB92-178870 ..... p 3765 N92-31685 #
PB92-180231 ..... p 3853 N92-31648 #
PB92-180645 ..... p 3787 N92-31610 #
PB92-180835 ..... p 3841 N92-31658 #
PB92-180868 ..... p 3781 N92-31683 #
PB92-181015 ..... p 3881 N92-31365 #
PB92-181056 ..... p 3780 N92-31678 #
PB92-181072 ..... p 3874 N92-31366 #
PB92-181130 ..... p 3877 N92-31628 #
PB92-181148 ..... p 3774 N92-31609 #
PB92-181239 ..... p 3813 N92-31367 #
PB92-181270 ..... p 3767 N92-31632 #
PB92-181692 ..... p 3762 N92-31634 * #
PB92-182534 ..... p 3904 N92-31613 #
PB92-183599 ..... p 3916 N92-32160 #
PB92-183649 ..... p 3885 N92-31680 #
PB92-183722 ..... p 3805 N92-31368 #
PB92-183730 ..... p 3824 N92-31839 #
PB92-184373 ..... p 3835 N92-31841 #
PB92-184472 ..... p 3924 N92-31635 #
PB92-185040 ..... p 3856 N92-31636 #
PB92-185974 ..... p 3865 N92-31842 #
PB92-186196 ..... p 3853 N92-31649 * #
PB92-187087 ..... p 3827 N92-31370 #
PB92-187103 ..... p 3917 N92-31371 #
PB92-187723 ..... p 3856 N92-31637 #
PB92-187731 ..... p 3856 N92-31639 #
PB92-188200 ..... p 3860 N92-31641 #
PB92-192624 ..... p 3927 N92-32067 #
PB92-192640 ..... p 3927 N92-32068 #
PB92-195429 ..... p 3810 N92-32070 #
PB92-195437 ..... p 3810 N92-32161 #
PB92-195445 ..... p 3767 N92-32073 #
PB92-195452 ..... p 3866 N92-32069 #
PB92-196088 ..... p 3913 N92-32072 #
PB92-198910 ..... p 3854 N92-32071 #

PL-TR-91-2065 ..... p 3924 N92-32142 #
PL-TR-91-2109 ..... p 3879 N92-31833 #
PL-TR-91-2189 ..... p 3902 N92-32144 #
PL-TR-91-2209 ..... p 3767 N92-32082 #
PL-TR-91-2252 ..... p 3926 N92-31477 #
PL-TR-91-2278 ..... p 3855 N92-31509 #
PL-TR-91-2297 ..... p 3855 N92-31476 #
PL-TR-92-2110 ..... p 3884 N92-31293 #

PNL-SA-19467 ..... p 3848 N92-31845 #
PNL-SA-19981 ..... p 3768 N92-31846 #
PNL-SA-19989 ..... p 3837 N92-31657 #
PNL-SA-20340 ..... p 3867 N92-31711 #
PNL-SA-20358 ..... p 3797 N92-32146 #
PNL-SA-20400 ..... p 3852 N92-31574 #
PNL-SA-20767 ..... p 3853 N92-31732 #
PNL-SA-20854 ..... p 3910 N92-31665 #

PNL-8076 ..... p 3813 N92-31440 #
PNL-8088 ..... p 3841 N92-31638 #

PWA-FR2198-06 ..... p 3786 N92-31360 #
PWA-FR21998-08 ..... p 3790 N92-32066 #

PWA-5968-80 ..... p 3759 N92-31534 * #

QR-1-VOL-53-NO-1-PT-1 ..... p 3860 N92-31702 #
QR-2-VOL-53-NO-2-PT-2 ..... p 3860 N92-31704 #
QR-4-VOL-53-NO-4-PT-4 ..... p 3861 N92-31706 #

R-640 ..... p 3841 N92-31658 #

RAL-92-005 ..... p 3915 N92-31953 #

REPT-MEMO-221 ..... p 3927 N92-32067 #
REPT-MEMO-222 ..... p 3927 N92-32068 #

REPT-3128 ..... p 3813 N92-31374 #
REPT-5-32746 ..... p 3856 N92-31551 * #
REPT-74527 ..... p 3855 N92-31476 #
REPT-91-101 ..... p 3859 N92-31521 #
REPT-91-61 ..... p 3821 N92-31513 #
REPT-91-94 ..... p 3888 N92-31518 #
REPT-91-95 ..... p 3888 N92-31519 #
REPT-91-96 ..... p 3886 N92-31520 #
REPT-92-RC-09071 ..... p 3835 N92-31892 * #
REPT-92-11 ..... p 3856 N92-31522 #
REPT-92-9SL2-SUPER-R1 ..... p 3813 N92-31451 #

RFP-4529 ..... p 3829 N92-32138 #

RI/RD-92-114 ..... p 3835 N92-31892 * #

RL-TR-91-407-VOL-1 ..... p 3876 N92-31586 #
RL-TR-92-16 ..... p 3879 N92-31825 #

RSL-TR-8960-1 ..... p 3810 N92-32101 #

RUU-CS-91-45 ..... p 3807 N92-31715 #

SAND-88-3185 ..... p 3837 N92-31753 #
SAND-89-2608 ..... p 3842 N92-32088 #
SAND-90-0444 ..... p 3917 N92-32037 #
SAND-90-1326 ..... p 3799 N92-31570 #
SAND-91-1591 ..... p 3793 N92-31539 #
SAND-91-1615C ..... p 3908 N92-31403 #
SAND-91-1626 ..... p 3906 N92-31949 #
SAND-91-1964 ..... p 3885 N92-32036 #
SAND-91-2061C ..... p 3862 N92-31750 #
SAND-91-2208C ..... p 3765 N92-31542 #
SAND-91-2350C ..... p 3816 N92-31718 #
SAND-91-2532 ..... p 3824 N92-31832 #
SAND-91-2693C ..... p 3910 N92-31668 #
SAND-91-2760 ..... p 3824 N92-31933 #
SAND-91-2910C ..... p 3808 N92-31738 #
SAND-91-7061 ..... p 3805 N92-31387 #
SAND-91-8718 ..... p 3783 N92-31860 #
SAND-92-0021C ..... p 3781 N92-31748 #
SAND-92-0052 ..... p 3794 N92-31631 #
SAND-92-0211 ..... p 3790 N92-32139 #
SAND-92-0457 ..... p 3756 N92-31746 #
SAND-92-0458C ..... p 3851 N92-31427 #
SAND-92-0467 ..... p 3854 N92-31931 #
SAND-92-0637C ..... p 3919 N92-31578 #
SAND-92-0747 ..... p 3900 N92-32123 #
SAND-92-0795C ..... p 3848 N92-32087 #
SAND-92-0806C ..... p 3905 N92-31707 #
SAND-92-0816C ..... p 3878 N92-31669 #
SAND-92-0830C ..... p 3900 N92-31295 #
SAND-92-0849C ..... p 3802 N92-31580 #
SAND-92-0912 ..... p 3757 N92-31736 #
SAND-92-1008C ..... p 3861 N92-31709 #
SAND-92-1223C ..... p 3771 N92-32030 #
SAND-92-8411C ..... p 3788 N92-31744 #
SAND-92-8489C ..... p 3906 N92-31771 #
SAND-92-8495C ..... p 3782 N92-31773 #
SAND-92-8504C ..... p 3779 N92-31417 #

SAND91-2617 ..... p 3770 N92-31503 #

SESSIA-430/91.960 ..... p 3751 N92-31508 #

SGD-572-PT-1 ..... p 3856 N92-31637 #
SGD-572-PT-2 ..... p 3856 N92-31639 #

SIO-91-15 ..... p 3902 N92-32144 #

SLAC-PUB-5649 ..... p 3899 N92-31390 #

SLCET-TR-92-2 ..... p 3913 N92-32078 #
SPIRE-FR-60208 ..... p 3814 N92-31464 #

SR-1 ..... p 3884 N92-31293 #

SR83-R-5092-90 ..... p 3835 N92-31841 #

SSC-SSR-1311-VOL-1 ..... p 3789 N92-31987 #

SSC-352-VOL-1 ..... p 3789 N92-31987 #

SSCL-PREPRINT-57 ..... p 3836 N92-31647 #
SSCL-PREPRINT-60 ..... p 3900 N92-31975 #
SSCL-PREPRINT-74 ..... p 3816 N92-31760 #
SSCL-PREPRINT-79 ..... p 3815 N92-31664 #

SSCL-530 ..... p 3890 N92-32140 #
SSCL-570 ..... p 3899 N92-31948 #

SSD-TR-92-10 ..... p 3807 N92-31629 #

SSS-TR-91-12828 ..... p 3865 N92-31821 #
SSS-TR-91-12833 ..... p 3856 N92-31510 #

SU-SLAC-PUB-5752 ..... p 3915 N92-31663 #
SU-SLAC-PUB-5760 ..... p 3812 N92-31289 #
SU-SLAC-PUB-5768 ..... p 3900 N92-32131 #
SU-SLAC-PUB-5774 ..... p 3902 N92-32149 #
SU-SLAC-PUB-5789 ..... p 3900 N92-32133 #

SU-SOL-92-1 ..... p 3875 N92-31410 #

SU-TR-74 ..... p 3888 N92-31600 #

SWRI-3593/001 ..... p 3767 N92-31997 #

TABES PAPER 92-213 ..... p 3764 N92-32021
TABES PAPER 92-411 ..... p 3763 N92-32010
TABES PAPER 92-414 ..... p 3763 N92-32011 *
TABES PAPER 92-424 ..... p 3764 N92-32015
TABES PAPER 92-425 ..... p 3764 N92-32016
TABES PAPER 92-444 ..... p 3763 N92-32012
TABES PAPER 92-445 ..... p 3763 N92-32013
TABES PAPER 92-447 ..... p 3763 N92-32014
TABES PAPER 92-453 ..... p 3764 N92-32017
TABES PAPER 92-454 ..... p 3764 N92-32018
TABES PAPER 92-462 ..... p 3764 N92-32020
TABES PAPER 92-467 ..... p 3764 N92-32019

TEC-0009 ..... p 3844 N92-31621 #

TKK-V-B66 ..... p 3787 N92-31610 #

TR-0089(4945-05)-1 ..... p 3807 N92-31629 #
TR-042 ..... p 3778 N92-31292 #
TR-116 ..... p 3784 N92-31998 #
TR-12 ..... p 3828 N92-31828 #
TR-12 ..... p 3897 N92-31950 #
TR-13 ..... p 3897 N92-31999 #
TR-14 ..... p 3796 N92-31961 #
TR-16 ..... p 3783 N92-31820 #
TR-16 ..... p 3784 N92-31959 #
TR-17 ..... p 3796 N92-31960 #
TR-19 ..... p 3772 N92-31850 #
TR-1 ..... p 3833 N92-31363 #
TR-20 ..... p 3911 N92-31819 #
TR-22 ..... p 3796 N92-31968 #
TR-24 ..... p 3893 N92-31316 #
TR-2 ..... p 3833 N92-31433 #
TR-2 ..... p 3798 N92-32198 #
TR-30 ..... p 3909 N92-31582 #
TR-31 ..... p 3798 N92-32153 #
TR-34 ..... p 3795 N92-31941 #
TR-351 ..... p 3882 N92-31445 #
TR-37 ..... p 3900 N92-32170 #
TR-381 ..... p 3881 N92-31428 #
TR-38 ..... p 3898 N92-32169 #
TR-3 ..... p 3874 N92-31379 #
TR-3 ..... p 3795 N92-31952 #
TR-44 ..... p 3911 N92-31851 #
TR-45 ..... p 3792 N92-31408 #
TR-57 ..... p 3912 N92-31994 #
TR-58 ..... p 3913 N92-31995 #
TR-6 ..... p 3793 N92-31435 #
TR-6 ..... p 3795 N92-31954 #
TR-71 ..... p 3785 N92-32080 #
TR-72 ..... p 3796 N92-32079 #
TR-7 ..... p 3791 N92-31318 #
TR-7 ..... p 3793 N92-31436 #
TR-8 ..... p 3795 N92-31810 #
TR-8 ..... p 3899 N92-32196 #
TR-91-1205 ..... p 3886 N92-31553 * #
TR-91-1256 ..... p 3883 N92-32152 #
TR-91-1258 ..... p 3797 N92-32151 #
TR-91-13 ..... p 3857 N92-31766 #
TR-92-1277 ..... p 3886 N92-31553 * #
TR-9 ..... p 3779 N92-31434 #

TSPC-TR-92-10 ..... p 3760 N92-32059 #

UAH-5-32559 ..... p 3883 N92-31835 * #

UCB-PTH-91/28 ..... p 3898 N92-32006 #

UCB/ERL-M91/79 ..... p 3907 N92-31983 #

UCLA-ENG-92-28 ..... p 3820 N92-31322 #

UCRL-CR-103698 ..... p 3828 N92-31909 #
UCRL-CR-110002 ..... p 3808 N92-31722 #

UCRL-ID-107571 ..... p 3803 N92-31908 #
UCRL-ID-109283-REV-1 ..... p 3766 N92-31735 #
UCRL-ID-109810 ..... p 3850 N92-31324 #
UCRL-ID-109860 ..... p 3855 N92-32147 * #
UCRL-ID-110395 ..... p 3856 N92-31662 #

UCRL-JC-103243-REV-2 ..... p 3821 N92-31528 #
UCRL-JC-103782-REV-1 ..... p 3910 N92-31719 #
UCRL-JC-106910 ..... p 3778 N92-31415 #
UCRL-JC-107443 ..... p 3812 N92-31334 #
UCRL-JC-108024 ..... p 3869 N92-31608 #
UCRL-JC-108146 ..... p 3832 N92-31902 #
UCRL-JC-108521 ..... p 3850 N92-31297 #
UCRL-JC-108771 ..... p 3889 N92-32119 #
UCRL-JC-108827 ..... p 3815 N92-31548 #
UCRL-JC-108985 ..... p 3822 N92-31625 #
UCRL-JC-108986 ..... p 3786 N92-32145 #
UCRL-JC-109018 ..... p 3855 N92-32155 #
UCRL-JC-109083 ..... p 3782 N92-31805 #
UCRL-JC-109152 ..... p 3835 N92-32121 #
UCRL-JC-109179 ..... p 3851 N92-31423 #
UCRL-JC-109210 ..... p 3786 N92-31391 #
UCRL-JC-109219 ..... p 3902 N92-31761 #
UCRL-JC-109225 ..... p 3879 N92-31743 #
UCRL-JC-109251 ..... p 3882 N92-31740 #
UCRL-JC-109266 ..... p 3878 N92-31742 #
UCRL-JC-109268 ..... p 3788 N92-31759 #
UCRL-JC-109496 ..... p 3883 N92-31741 #
UCRL-JC-109522 ..... p 3904 N92-31530 #
UCRL-JC-109627 ..... p 3910 N92-31661 #
UCRL-JC-109659 ..... p 3878 N92-31739 #
UCRL-JC-109673 ..... p 3781 N92-31763 #
UCRL-JC-109756 ..... p 3779 N92-31416 #
UCRL-JC-109757 ..... p 3778 N92-31414 #
UCRL-JC-109758 ..... p 3780 N92-31607 #
UCRL-JC-109763 ..... p 3895 N92-31705 #
UCRL-JC-110033 ..... p 3913 N92-32166 #
UCRL-JC-110152 ..... p 3794 N92-31560 #
UCRL-JC-110439 ..... p 3882 N92-31466 #

UCRL-LR-109425 ..... p 3787 N92-31667 #
UCRL-LR-109666 ..... p 3920 N92-31934 #

UCRL-53809-91 ..... p 3923 N92-32005 #

UFIFT-HEP-92-07 ..... p 3893 N92-31552 #

UMICH-025921-30-T ..... p 3803 N92-31238 * #
UMICH-027723-6-T ..... p 3807 N92-31614 * #

US-PATENT-APPL-SN-359460 ..... p 3831 N92-31788 *
US-PATENT-APPL-SN-386175 ..... p 3828 N92-31790 *
US-PATENT-APPL-SN-439317 ..... p 3794 N92-31792 *
US-PATENT-APPL-SN-474941 ..... p 3902 N92-32137
US-PATENT-APPL-SN-552658 ..... p 3791 N92-31270
US-PATENT-APPL-SN-580043 ..... p 3873 N92-31269
US-PATENT-APPL-SN-610895 ..... p 3777 N92-31268
US-PATENT-APPL-SN-691287 ..... p 3832 N92-31271
US-PATENT-APPL-SN-790723 ..... p 3803 N92-31257 * #

US-PATENT-CLASS-137-1 ..... p 3832 N92-31271
US-PATENT-CLASS-250-458.1 .... p 3777 N92-31268
US-PATENT-CLASS-372-25 ..... p 3831 N92-31788 *
US-PATENT-CLASS-372-30 ..... p 3831 N92-31788 *
US-PATENT-CLASS-375-116 ..... p 3873 N92-31269
US-PATENT-CLASS-435-286 ..... p 3828 N92-31790 *
US-PATENT-CLASS-435-311 ..... p 3828 N92-31790 *
US-PATENT-CLASS-435-312 ..... p 3828 N92-31790 *
US-PATENT-CLASS-525-420 ..... p 3794 N92-31792 *
US-PATENT-CLASS-525-434 ..... p 3794 N92-31792 *
US-PATENT-CLASS-525-436 ..... p 3794 N92-31792 *
US-PATENT-CLASS-526-311 ..... p 3791 N92-31270

US-PATENT-5,061,857 ..... p 3777 N92-31268
US-PATENT-5,068,880 ..... p 3873 N92-31269
US-PATENT-5,079,321 ..... p 3791 N92-31270
US-PATENT-5,080,120 ..... p 3832 N92-31271
US-PATENT-5,104,223 ..... p 3902 N92-32137
US-PATENT-5,104,802 ..... p 3828 N92-31790 *
US-PATENT-5,112,923 ..... p 3794 N92-31792 *
US-PATENT-5,128,949 ..... p 3831 N92-31788 *

USAEPG-FR-1425 ..... p 3884 N92-31395 #

USAFA-TR-92-1 ..... p 3833 N92-31460 #

UVA/525291/EE92/101 ..... p 3813 N92-31373 #
UVA/525465/EE92/101 ..... p 3908 N92-31537 #
UVA/528352/EE93/102 ..... p 3880 N92-32122 * #

VPI-AERO-182 ..... p 3753 N92-32114 * #

VPI-AOE-185 ..... p 3821 N92-31452 #

VPI-E-92-20 ..... p 3842 N92-32235 * #

WHOI-91-19 ..... p 3865 N92-31644 #
WHOI-92-05 ..... p 3891 N92-31563 #

WHPO-92-1 ..... p 3865 N92-31842 #

WL-TM-92-308-FIBE ..... p 3841 N92-31847 #
WL-TM-92-312-FIBE ..... p 3752 N92-31674 #
WL-TM-92-313-FIBE ..... p 3757 N92-31793 #
WL-TM-92-700-XPN ..... p 3806 N92-31569 #

WL-TR-91-2083 ..... p 3801 N92-31982 #
WL-TR-91-2099 ..... p 3799 N92-31462 #
WL-TR-91-2117-VOL-2 ..... p 3798 N92-31399 #
WL-TR-91-3023 ..... p 3773 N92-31307 #
WL-TR-91-3072 ..... p 3752 N92-31777 #
WL-TR-91-4032-VOL-1 ..... p 3776 N92-32047 #
WL-TR-91-4032-VOL-2-PT-1 ..... p 3776 N92-32048 #

WOCE-83/92 ..... p 3865 N92-31842 #

WSRC-MS-91-230-REV-1 ..... p 3841 N92-31745 #
WSRC-MS-91-313 ..... p 3898 N92-32165 #
WSRC-MS-91-393 ..... p 3820 N92-31420 #
WSRC-MS-91-439 ..... p 3919 N92-31581 #
WSRC-MS-92-123 ..... p 3825 N92-32115 #
WSRC-MS-92-132 ..... p 3820 N92-31421 #

Typical Accession Number Index Listing

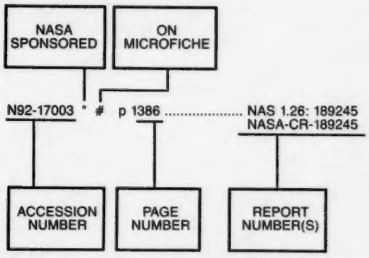

Listings in this index are arranged alphanumerically by accession number. The page number helps to locate the citation in the abstract section. An asterisk (*) indicates that the item is a NASA report. A pound sign (#) indicates that the item is available on microfiche.

N92-31238* # p 3803 NAS 1.26:190540
N92-31238* # p 3803 NASA-CR-190540
UMICH-025921-30-T
N92-31239* # p 3750 NAS 1.15:107644
NASA-TM-107644
N92-31240* # p 3760 L-16977
NAS 1.15:4381
NASA-TM-4381
N92-31241 # p 3886 INPE-5361-RPQ/656
N92-31242 # p 3802 NO REPORT NUMBER
N92-31243 # p 3786 NO REPORT NUMBER
N92-31244 # p 3811 NO REPORT NUMBER
N92-31245* # p 3769 NAS 1.26:182168
NASA-CR-182168
N92-31246* # p 3750 L-16724
NAS 1.15:4189
NASA-TM-4189
N92-31247* # p 3818 L-16709
NAS 1.15:4187
NASA-TM-4187
N92-31248* # p 3891 NAS 1.26:185242
NASA-CR-185242
N92-31249* # p 3769 E-5337
NAS 1.15:4214
NASA-TM-4214
N92-31250* # p 3759 E-5675
NAS 1.15:103248
NASA-TM-103248
N92-31251* # p 3765 E-4969
NAS 1.60:3014
NASA-TP-3014
N92-31252* # p 3762 NAS 1.26:189234
NASA-CR-189234
N92-31253* # p 3916 NAS 1.15:107795
NASA-SBIR-92-1
NASA-TM-107795
N92-31254* # p 3884 NAS 1.26:190529
NASA-CR-190529
N92-31255 # p 3892 NIFS-106
N92-31256 # p 3818 NIFS-125
N92-31257* # p 3803 NAS 1.71:LAR-14418-1
NASA-CASE-LAR-14418-1
US-PATENT-APPL-SN-790723
N92-31258* # p 3849 NAS 1.15:107965
NASA-TM-107965
N92-31259* # p 3850 NAS 1.26:190675
NASA-CR-190675
N92-31260* # p 3766 NAS 1.26:190626
NASA-CR-190626
N92-31261* # p 3756 AGARD-16
H-1847
NAS 1.15:104254
NASA-TM-104254
N92-31262* # p 3845 E-7259
NAS 1.15:105825
NASA-TM-105825
N92-31263* # p 3802 E-7219
NAS 1.15:105789
NASA-TM-105789
N92-31264* # p 3757 NAS 1.15:107655
NASA-TM-107655
N92-31265* # p 3818 ICASE-92-36
NAS 1.26:189686
NASA-CR-189686
N92-31266* # p 3772 NAS 1.26:190691
NASA-CR-190691
N92-31267* # p 3745 E-7233
NAS 1.15:105803
NASA-TM-105803
N92-31268 p 3777 AD-D015230
US-PATENT-APPL-SN-610895
US-PATENT-CLASS-250-458.1
US-PATENT-5,061,857
N92-31269 p 3873 AD-D015235
US-PATENT-APPL-SN-580043
US-PATENT-CLASS-375-116
US-PATENT-5,068,880
N92-31270 p 3791 AD-D015236
US-PATENT-APPL-SN-552658
US-PATENT-CLASS-526-311
US-PATENT-5,079,321
N92-31271 p 3832 AD-D015250
US-PATENT-APPL-SN-691287
US-PATENT-CLASS-137-1
US-PATENT-5,080,120
N92-31272* # p 3917 NAS 1.26:190630
NASA-CR-190630
N92-31273* # p 3804 NAS 1.26:190656
NASA-CR-190656
N92-31274* # p 3772 NAS 1.26:190661
NASA-CR-190661
N92-31275* # p 3759 H-1808
NAS 1.15:4400
NASA-TM-4400
N92-31276* # p 3751 H-1783
NAS 1.15:4398
NASA-TM-4398
N92-31277 # p 3843 INPE-5386-TDI/475
N92-31278* # p 3791 M-694
NAS 1.60:3275
NASA-TP-3275
N92-31279* # p 3838 L-17006
NAS 1.60:3231
NASA-TP-3231
N92-31280* # p 3838 M-695
NAS 1.60:3277
NASA-TP-3277
N92-31281* # p 3819 L-17039
NAS 1.60:3208
NASA-TP-3208
N92-31282* # p 3812 E-7289
NAS 1.15:105846
NASA-TM-105846
N92-31283 # p 3819 AD-A247201
AFOSR-92-0034TR
N92-31284 # p 3804 AD-A248323
N92-31285 # p 3917 AD-A248435
N92-31286 # p 3819 AD-A250284
AFOSR-92-0394TR
N92-31287 # p 3819 DE92-012321
EGG-NE-10083
N92-31288 # p 3917 DE92-012384
DOE/ER-0533P
N92-31289 # p 3812 CONF-920124-23
DE92-012417
SU-SLAC-PUB-5760
N92-31290 # p 3845 CONF-9104196
DE92-013573
N92-31291 # p 3870 AD-A250741
ARI-RN-92-22
N92-31292 # p 3778 AD-A252424
TR-042
N92-31293 # p 3884 AD-A252442
PL-TR-92-2110
SR-1
N92-31294 # p 3872 AD-A252443
ARI-RN-92-36
N92-31295 # p 3900 CONF-920795-2
DE92-016092
SAND-92-0830C
N92-31296 # p 3907 BNL-47636
CONF-910406-41
N92-31297 # p 3850 DE92-016098
CONF-9208100-1
DE92-016158
UCRL-JC-108521
N92-31298 # p 3826 AD-A245821
AEDC-TR-91-26-VOL-2
N92-31299 # p 3874 AD-A246879
AFIT/GSS/ENG/91D-07
N92-31300 # p 3751 AD-A247302
N92-31301 # p 3778 AD-A249787
MTL-TR-92-1
N92-31302 # p 3866 AD-A249795
ARO-26385.6-LS
N92-31303 # p 3838 DE92-012116
KCP-613-4503
N92-31304 # p 3850 DE92-013520
DOE/ER-60247/T1
N92-31305 # p 3773 AD-A250893
AFOSR-92-0417TR
N92-31306 # p 3819 AD-A250900
AFOSR-92-0416TR
N92-31307 # p 3773 AD-A250902
WL-TR-91-3023
N92-31308 # p 3863 AD-A252701
INO-TM-8-PT-1
N92-31309 # p 3872 DE92-010577
NREL/TP-432-4737
N92-31310 # p 3903 ANL/CP-74880
CONF-920311-18
DE92-016183
N92-31311 # p 3886 ANL/CP-75497
CONF-920760-5
DE92-016185
N92-31312 # p 3850 DE92-016223
DOE/ER-60246/5
N92-31313 # p 3826 CONF-910340-54
DE92-010722
FNAL-TM-1724
N92-31314 # p 3804 AD-A245983
N92-31315 # p 3773 AD-A248587
N92-31316 # p 3893 AD-A250190
TR-24
N92-31317 # p 3804 CONF-920750-2
DE92-007565
LA-UR-92-296
N92-31318 # p 3791 AD-A250655
TR-7
N92-31319 # p 3830 AD-A250657
AFOSR-92-0345TR
N92-31320 # p 3858 AD-A250662
ASL-TR-0309
N92-31321 # p 3870 AD-A250669
AL-TR-1991-0109
N92-31322 # p 3820 AD-A250700
AFOSR-92-0427TR
UCLA-ENG-92-28
N92-31323 # p 3843 AD-A250707
ESD-TR-92-052
MTR-11201
N92-31324 # p 3850 CONF-9110374-1
DE92-013254
UCRL-ID-109810
N92-31325 # p 3899 AD-A252577
AFIT/CI/CIA-92-001D
N92-31326 # p 3868 AD-A252694
N92-31327 # p 3872 AD-A252715
NHRC-91-26
N92-31328 # p 3893 AD-A249751
CU-TR-26
N92-31329 # p 3843 AD-A249984
AFIT/CI/CIA-91-114
N92-31330 # p 3872 AD-A250401
AFOSR-92-0360TR
N92-31331 # p 3838 AD-A250487
ARCCB-TR-92013
N92-31332 # p 3884 AD-A250495
AFOSR-92-0355TR
N92-31333 # p 3804 AD-A250496
AFOSR-92-0372TR

N92-31334 # p 3812 ..... CONF-920124-21
DE92-011732
UCRL-JC-107443
N92-31335 # p 3838 ..... ANL/CP-76120
CONF-9205147-1
DE92-014855
N92-31336 # p 3836 ..... DE92-015310
DOE/ER-12817/T1
N92-31337 # p 3836 ..... AD-A250406
N92-31338* # p 3925 ..... NAS 1.26:190200
NASA-CR-190200
N92-31339* # p 3839 ..... NAS 1.26:190536
NASA-CR-190536
N92-31340 # p 3827 ..... ISSN-0915-633X
NIFS-128
N92-31341* # p 3870 ..... NAS 1.26:190614
NASA-CR-190614
N92-31342* # p 3769 ..... AIAA PAPER 92-1556
E-7104
NAS 1.15:105712
NASA-TM-105712
N92-31343 # p 3923 ..... INPE-5337-PRE/1736
N92-31344 # p 3923 ..... INPE-5339-PRE/1738
N92-31345 # p 3923 ..... INPE-5340-PRE/1739
N92-31346 # p 3923 ..... INPE-5342-PRE/1741
N92-31347 # p 3923 ..... INPE-5343-PRE/1742
N92-31348 # p 3874 ..... INPE-5394-PRE/1752
N92-31349* # p 3832 ..... AVSCOM-TR-92-C-008
E-7084
NAS 1.15:105434
NASA-TM-105434
N92-31350* # p 3757 ..... AIAA PAPER 92-2095-CP
NAS 1.15:107652
NASA-TM-107652
N92-31351* # p 3757 ..... NAS 1.15:107654
NASA-TM-107654
N92-31352* # p 3820 ..... NAS 1.26:190689
NASA-CR-190689
N92-31353 # p 3874 ..... AD-A249562
CMU-CS-92-109
N92-31354 # p 3804 ..... AD-A249577
ORNL-6709
N92-31355 # p 3812 ..... AD-A250045
N92-31356 # p 3791 ..... AD-A250058
N92-31357* # p 3844 ..... NAS 1.26:190665
NASA-CR-190665
N92-31358 # p 3791 ..... AD-A249538
ARO-25586.14-CH
N92-31359 # p 3889 ..... AD-A249809
ARO-28821.1-MS
N92-31360 # p 3786 ..... AD-A250068
PWA-FR2198-06
N92-31361 # p 3773 ..... AD-A250072
N92-31362 # p 3844 ..... AD-A250074
NOSC/TR-1487
N92-31363 # p 3833 ..... AD-A250075
ARO-27863.1-MS
TR-1
N92-31364 # p 3916 ..... PB92-173681
N92-31365 # p 3881 ..... NIST/SP-823/1
PB92-181015
N92-31366 # p 3874 ..... NISTIR-4737
PB92-181072
N92-31367 # p 3813 ..... NISTIR-4803
PB92-181239
N92-31368 # p 3805 ..... NIST/TN-1349
PB92-183722
N92-31369 # p 3805 ..... AD-A250850
NRAD-TD-2278
N92-31370 # p 3827 ..... NISTIR-4823
PB92-187087
N92-31371 # p 3917 ..... NISTIR-4830
PB92-187103
N92-31372 # p 3903 ..... CONF-920677-3
DE92-014200
DOE/ET-10815/182
N92-31373 # p 3813 ..... AD-A249348
ARO-29342.2-EL-CF
UVA/525291/EE92/101
N92-31374 # p 3813 ..... AD-A249380
ARO-29005.1-EL-SBI
REPT-3128
N92-31375 # p 3907 ..... AD-A249565
ARO-25222.8-CH
N92-31376 # p 3805 ..... AD-A249580
ARO-27032.1-EL
N92-31377 # p 3792 ..... AD-A249581
ARO-24845.15-MS
N92-31378 # p 3773 ..... AD-A249584
ARO-28283.3-EG
N92-31379 # p 3874 ..... AD-A249610
TR-3
N92-31380 # p 3901 ..... AD-A249612
ARO-23577.6-MS
CMR-92-2
N92-31381 # p 3805 ..... AD-A250447
AFOSR-92-0290TR
N92-31382 # p 3774 ..... AD-A250486
NADC-91122-60
N92-31383 # p 3839 ..... CONF-9206173-1
DE92-014478
LA-UR-92-1528
N92-31384 # p 3833 ..... CONF-920732-4
DE92-014502
N92-31385 # p 3893 ..... DE92-014585
DOE/ER-40009/T3
N92-31386 # p 3893 ..... ANL/CP-76036
CONF-9108199-1
DE92-014845
N92-31387 # p 3805 ..... DE92-016160
SAND-91-7061
N92-31388 # p 3792 ..... AD-A248882
ARO-28436.1-MS-SBI
N92-31389 # p 3839 ..... DE92-011431
DOE/ER-45433/1
N92-31390 # p 3899 ..... CONF-9201101-1
DE92-011520
SLAC-PUB-5649
N92-31391 # p 3786 ..... CONF-920444-21
DE92-011532
UCRL-JC-109210
N92-31392 # p 3871 ..... AD-A249990
N92-31393 # p 3778 ..... AD-A249999
BRL-TR-3333
N92-31394 # p 3792 ..... AD-A250353
MIT-TR-16
N92-31395 # p 3884 ..... AD-A250439
USAEPG-FR-1425
N92-31396 # p 3917 ..... AD-A250443
AFOSR-92-0272TR
N92-31397 # p 3901 ..... AD-A250446
N92-31398 # p 3918 ..... PB92-145515
N92-31399 # p 3798 ..... AD-A252656
WL-TR-91-2117-VOL-2
N92-31400 # p 3839 ..... DE92-015291
DOE/ER-45166/4
N92-31401 # p 3924 ..... DE92-630244
IC-91/384
N92-31402 # p 3914 ..... DE92-630245
IC-91/388
N92-31403 # p 3908 ..... CONF-920423-5
DE92-014271
SAND-91-1615C
N92-31404 # p 3792 ..... AD-A252114
MTL-TR-92-30
N92-31405 # p 3875 ..... AD-A252125
N92-31406 # p 3863 ..... AD-A252144
NOARL-CR-044-91
N92-31407 # p 3864 ..... AD-A252146
N92-31408 # p 3792 ..... AD-A252195
TR-45
N92-31409 # p 3868 ..... CONF-920803-5
DE92-014416
N92-31410 # p 3875 ..... DE92-015904
SU-SOL-92-1
N92-31411 # p 3830 ..... DE92-016155
DOE/ET-53088/554
IFSR-554
N92-31412 # p 3903 ..... DE92-016180
DOE/ET-53088/549
IFSR-549
N92-31413 # p 3805 ..... AD-A250423
NPSEC-92-005
N92-31414 # p 3778 ..... CONF-920707-23
DE92-007902
UCRL-JC-109757
N92-31415 # p 3778 ..... CONF-920707-22
DE92-008933
UCRL-JC-106910
N92-31416 # p 3779 ..... CONF-920707-25
DE92-009457
UCRL-JC-109756
N92-31417 # p 3779 ..... CONF-920707-26
DE92-010310
LBL-31590
SAND-92-8504C
N92-31418 # p 3786 ..... CONF-920761-4
DE92-010448
N92-31419 # p 3792 ..... AD-A252112
AFOSR-92-0415TR
N92-31420 # p 3820 ..... CONF-920804-9
DE92-013196
WSRC-MS-91-393
N92-31421 # p 3820 ..... CONF-920804-7
DE92-013217
WSRC-MS-92-132
N92-31422 # p 3851 ..... BNL-47392
CONF-920814-4
DE92-013308
N92-31423 # p 3851 ..... CONF-920881-1
DE92-013513
UCRL-JC-109179
N92-31424 # p 3820 ..... CONF-920804-8
DE92-013537
LA-UR-92-1271
N92-31425 # p 3820 ..... CONF-9110369-1
DE92-013568
N92-31426 # p 3821 ..... DE92-013645
DOE/OR-00033/T476
N92-31427 # p 3851 ..... CONF-920851-8
DE92-013691
SAND-92-0458C
N92-31428 # p 3881 ..... AD-A247516
TR-381
N92-31429 # p 3864 ..... AD-A247519
N92-31430 # p 3901 ..... AD-A247528
ARO-29276-GS
N92-31431 # p 3813 ..... AD-A249974
N92-31432 # p 3858 ..... AD-A249981
AFIT/CI/CIA-91-105
N92-31433 # p 3833 ..... AD-A250076
ARO-27863.2-MS
TR-2
N92-31434 # p 3779 ..... AD-A250082
TR-9
N92-31435 # p 3793 ..... AD-A250085
TR-6
N92-31436 # p 3793 ..... AD-A250086
TR-7
N92-31437 # p 3833 ..... AD-A250088
MML-TR-91-16C
NADC-91093-60
N92-31438 # p 3908 ..... AD-A250089
N92-31439 # p 3759 ..... AD-A250342
ARL-PROP-TM-473
DODA-AR-006-651
N92-31440 # p 3813 ..... DE92-013599
PNL-8076
N92-31441 # p 3779 ..... ANL/CP-76034
CONF-920310-10
DE92-014846
N92-31442 # p 3799 ..... ANL/ESD/TM-30-VOL-1
DE92-015999
N92-31443 # p 3882 ..... AD-A245911
N92-31444 # p 3871 ..... AD-A247304
ETS-RR-92-15-ONR
N92-31445 # p 3882 ..... AD-A247514
TR-351
N92-31446 # p 3908 ..... AD-A248058
N92-31447 # p 3875 ..... CONF-911103-8
DE92-011144
N92-31448 # p 3918 ..... CONF-9205130-1
DE92-011146
EGG-10617-6085
N92-31449 # p 3806 ..... DE92-011359
LA-UR-92-789
N92-31450 # p 3918 ..... AD-A249332
N92-31451 # p 3813 ..... AD-A250732
AFOSR-92-0286TR
REPT-92-9SL2-SUPER-R1
N92-31452 # p 3821 ..... AD-A250827
VPI-AOE-185
N92-31453 # p 3755 ..... B-238393
GAO/RCED-91-24
N92-31454 # p 3891 ..... B-239410
GAO/RCED-91-128
N92-31455* p 3918 ..... NAS 1.21:7039(41)-SECT-2
NASA-SP-7039(41)-SECT-2
N92-31456* p 3745 ..... NAS 1.21:7037(280)
NASA-SP-7037(280)
N92-31457* # p 3766 ..... NAS 1.15:102600
NASA-TM-102600
N92-31458 # p 3872 ..... AD-A245866
AL-TR-1991-0129
N92-31459 # p 3903 ..... AD-A247306
AFOSR-92-0101TR
N92-31460 # p 3833 ..... AD-A247499
USAFA-TR-92-1
N92-31461 # p 3814 ..... AD-A247920
NWC-TP-7163
N92-31462 # p 3799 ..... AD-A249625
WL-TR-91-2099
N92-31463 # p 3893 ..... AD-A249627
ARO-26049.2-CH
N92-31464 # p 3814 ..... AD-A249651
ARO-29008.1-EL-SBI
SPIRE-FR-60208
N92-31465 # p 3866 ..... AD-A250069
N92-31466 # p 3882 ..... CONF-9204136-2
DE92-013981
UCRL-JC-110439
N92-31467 # p 3918 ..... AD-A252700
NOARL-TN-257
N92-31468* # p 3806 ..... NAS 1.26:190685
NASA-CR-190685
N92-31469 # p 3833 ..... CTN-92-60310
NRC-TR-ENG-005
NRC-32083

N92-31470 # p 3806 ..... CTN-92-60311
DREO-1084
N92-31471 # p 3806 ..... CTN-92-60315
DREA-CR-89-420
N92-31472 # p 3871 ..... CTN-92-60318
N92-31473 # p 3793 ..... AD-A245872
N92-31474 # p 3770 ..... AD-A248006
AFOSR-92-0208TR
CCR-92-01
N92-31475 # p 3827 ..... AD-A248858
N92-31476 # p 3855 ..... AD-A248940
AD-E200990
PL-TR-91-2297
REPT-74527
N92-31477 # p 3926 ..... AD-A248942
AD-E200988
PL-TR-91-2252
N92-31478 # p 3855 ..... AD-A249011
N92-31479 # p 3836 ..... AD-A249020
N92-31480 # p 3875 ..... AD-A250811
N92-31481 # p 3845 ..... DE92-010575
NREL/TP-432-4734
N92-31482 # p 3918 ..... AD-A252439
N92-31483*# p 3882 ..... NAS 1.26:190639
NASA-CR-190639
N92-31484*# p 3821 ..... E-7141
NAS 1.15:105740
NASA-TM-105740
N92-31485*# p 3834 ..... AIAA PAPER 92-3494
AVSCOM-TR-92-C-018
E-7090
NAS 1.15:105702
NASA-TM-105702
N92-31486*# p 3875 ..... NAS 1.26:190711
NASA-CR-190711
N92-31487*# p 3875 ..... NAS 1.26:190708
NASA-CR-190708
N92-31488 # p 3876 ..... AD-A245322
BRL-MR-3954
N92-31489 # p 3914 ..... AD-A245884
N92-31490 # p 3814 ..... AD-A247139
AFOSR-92-0149TR
N92-31491 # p 3868 ..... AD-A247142
AFOSR-92-0111TR
N92-31492 # p 3868 ..... AD-A249772
NHRC-91-13
N92-31493 # p 3858 ..... AD-A250418
AFIT/CI/CIA-91-120
N92-31494 # p 3903 ..... DE92-011806
DOE/ER-54131/1
N92-31495 # p 3864 ..... AD-A250834
NPS-OC-92-003
N92-31496 # p 3908 ..... AD-A250835
AFOSR-92-0304TR
N92-31497 # p 3846 ..... DE92-010564
NREL/TP-413-4873
N92-31498 # p 3846 ..... DE92-010574
NREL/TP-257-4099
N92-31499 # p 3814 ..... DE92-014472
ORNL/TM-12040
N92-31500 # p 3834 ..... CONF-920818-2
DE92-014456
N92-31501 # p 3839 ..... CONF-9206173-2
DE92-014467
N92-31502 # p 3827 ..... BNL-47475
CONF-9110146-18
DE92-014477
N92-31503 # p 3770 ..... SAND91-2617
N92-31504*# p 3839 ..... NAS 1.15:107662
NASA-TM-107662
N92-31505*# p 3840 ..... E-7128
NAS 1.15:105726
NASA-TM-105726
N92-31506*# p 3774 ..... E-7028
NAS 1.15:105666
NASA-TM-105666
N92-31507*# p 3770 ..... E-7224
NAS 1.15:105794
NASA-TM-105794
N92-31508 # p 3751 ..... CNRS-RC-91-1
ETN-92-91319
SESSIA-430/91.960
N92-31509 # p 3855 ..... AD-A249949
AD-E200945
PL-TR-91-2278
N92-31510 # p 3856 ..... AD-A249971
SSS-TR-91-12833
N92-31511 # p 3884 ..... AD-A249972
CMU-CS-92-115
N92-31512 # p 3840 ..... ETN-92-91393
FFA-TN-1991-44
N92-31513 # p 3821 ..... ETN-92-91425
REPT-91-61
N92-31514 # p 3751 ..... CRANFIELD-AERO-9114
ETN-92-91727
ISBN-1-871564-387
N92-31515 # p 3757 ..... CRANFIELD-AERO-9201
ETN-92-91728
ISBN-1-871564-360
N92-31516 # p 3840 ..... CRANFIELD-AERO-9203
ETN-92-91729
ISBN-1-871564-379
N92-31517 # p 3888 ..... CWI-BS-R9117
ETN-92-91784
N92-31518 # p 3888 ..... ETN-92-91844
REPT-91-94
N92-31519 # p 3888 ..... ETN-92-91845
REPT-91-95
N92-31520 # p 3886 ..... ETN-92-91846
REPT-91-96
N92-31521 # p 3859 ..... ETN-92-91851
REPT-91-101
N92-31522 # p 3856 ..... ETN-92-91863
REPT-92-11
N92-31523 # p 3859 ..... AD-A250182
AFIT/CI/CIA-91-027D
N92-31524 # p 3780 ..... AD-A250234
MIT-TR-17
N92-31525 # p 3814 ..... DE92-001244
NREL/TP-411-4840
N92-31526 # p 3846 ..... DE92-001242
NREL/TP-413-4835
N92-31527 # p 3851 ..... DE92-010378
ESDP-3747
NDP-039
ORNL/CDIAC-47
N92-31528 # p 3821 ..... CONF-900684-1-REV-2
DE92-011469
UCRL-JC-103243-REV-2
N92-31529 # p 3876 ..... CONF-9204114-1
DE92-011489
KCP-613-4837
N92-31530 # p 3904 ..... CONF-920607-10
DE92-011965
UCRL-JC-109522
N92-31531 # p 3846 ..... ANL-91/45
DE92-012398
N92-31532*# p 3751 ..... L-16959
NAS 1.60:3184
NASA-TP-3184
N92-31533*# p 3752 ..... MCAT-92-014
NAS 1.26:190680
NASA-CR-190680
N92-31534*# p 3759 ..... NAS 1.26:189222
NASA-CR-189222
PWA-5968-80
N92-31535*# p 3822 ..... ICASE-92-33
NAS 1.26:189683
NASA-CR-189683
N92-31536*# p 3834 ..... AVSCOM-TR-92-C-029
E-6863
NAS 1.15:105600
NASA-TM-105600
N92-31537 # p 3908 ..... AD-A247394
UVA/525465/EE92/101
N92-31538 # p 3793 ..... DE92-011570
DOE/ER-45309/4
N92-31539 # p 3793 ..... DE92-012444
SAND-91-1591
N92-31540 # p 3859 ..... AD-A250389
NPS-PH-92-007
N92-31541 # p 3876 ..... AD-A250415
CMU/SEI-91-TR-30
ESD-TR-91-30
N92-31542 # p 3765 ..... CONF-9204102-8
DE92-012630
SAND-91-2208C
N92-31543 # p 3806 ..... AD-A250884
ASL-TR-0311
N92-31544 # p 3864 ..... AD-A252713
CREC-TR-92-4
N92-31545 # p 3904 ..... DE92-014352
DOE/ER-54110/2
N92-31546 # p 3909 ..... ANL/CP-76122
CONF-920402-31
DE92-015227
N92-31547*# p 3916 ..... NAS 1.26:190633
NASA-CR-190633
N92-31548 # p 3815 ..... CONF-920515-19
DE92-015822
UCRL-JC-108827
N92-31549*# p 3755 ..... CU-TR-15
DOT/FAA/RD-92/21
NAS 1.26:4457
NASA-CR-4457
N92-31550*# p 3770 ..... NAS 1.26:190666
NASA-CR-190666
N92-31551*# p 3856 ..... NAS 1.26:184361
NASA-CR-184361
REPT-5-32746
N92-31552 # p 3893 ..... DE92-016194
DOE/ER-40272/T1
UFIFT-HEP-92-07
N92-31553*# p 3886 ..... NAS 1.26:190443
NASA-CR-190443
TR-91-1205
TR-92-1277
N92-31554 # p 3868 ..... AD-A249976
N92-31555 # p 3752 ..... AD-A250279
AFOSR-92-0399TR
N92-31556 # p 3851 ..... AD-A250337
N92-31557 # p 3794 ..... AD-A250347
N92-31558 # p 3869 ..... AD-A250348
N92-31559 # p 3822 ..... AD-A250350
AFOSR-92-0361TR
N92-31560 # p 3794 ..... CONF-920402-1
DE92-012697
UCRL-JC-110152
N92-31561*# p 3876 ..... ICASE-IR-22
NAS 1.26:189662
NASA-CR-189662
N92-31562 # p 3755 ..... AD-A250645
AVMED-8-92
DODA-AR-006-814
N92-31563 # p 3891 ..... AD-A250901
WHOI-92-05
N92-31564*# p 3822 ..... ICASE-IR-23
NAS 1.26:189674
NASA-CR-189674
N92-31565 # p 3780 ..... CONF-9206157-1
DE92-012693
IS-M-703
N92-31566*# p 3774 ..... NAS 1.26:190660
NASA-CR-190660
N92-31567 # p 3886 ..... AD-A249524
ARO-26391.10-MA
N92-31568 # p 3806 ..... INPE-5407-PUD/051
N92-31569 # p 3806 ..... AD-A249773
WL-TM-92-700-XPN
N92-31570 # p 3799 ..... DE92-011441
SAND-90-1326
N92-31571 # p 3847 ..... CONF-9112112-1
DE92-011493
LA-UR-92-984
N92-31572 # p 3864 ..... DE92-011805
DOE/ER-61202/1
N92-31573 # p 3876 ..... AD-A247109
AFOSR-92-0071TR
N92-31574 # p 3852 ..... DE92-012355
PNL-SA-20400
N92-31575 # p 3787 ..... ANL/CP-75586
CONF-911003-24
DE92-010276
N92-31576 # p 3904 ..... CONF-9201102-ABSTS
DE92-011549
N92-31577*# p 3914 ..... NAS 1.26:190580
NASA-CR-190580
N92-31578 # p 3919 ..... CONF-9204121-2
DE92-012625
SAND-92-0637C
N92-31579 # p 3847 ..... DE92-001209
NREL/TP-253-4252
N92-31580 # p 3802 ..... CONF-9206154-1
DE92-012633
SAND-92-0849C
N92-31581 # p 3919 ..... CONF-9110341-3
DE92-013098
WSRC-MS-91-439
N92-31582 # p 3909 ..... AD-A250903
TR-30
N92-31583 # p 3859 ..... NO REPORT NUMBER
N92-31584 # p 3787 ..... JPRS-UMS-92-010
N92-31585 # p 3915 ..... AD-A252190
AFOSR-92-0545TR
N92-31586 # p 3876 ..... AD-A252679
A015-VOL-1
RL-TR-91-407-VOL-1
N92-31587 # p 3877 ..... AD-A252695
N92-31588 # p 3891 ..... AD-A252696
DNA-TR-91-69
N92-31589 # p 3869 ..... BNL-47370
CONF-9104363-1
DE92-013036
N92-31590 # p 3867 ..... AD-A252192
AFOSR-92-0559TR
N92-31591 # p 3852 ..... ANL/CP-75440
CONF-9206158-3
DE92-013054
N92-31592 # p 3852 ..... DE92-014179
DOE/DP-48058/4-VOL-1
N92-31593 # p 3799 ..... CONF-920678-7
DE92-010569
NREL/TP-431-4831
N92-31594 # p 3847 ..... DE92-014206
DOE/EIA-M050(92)
N92-31595 # p 3894 ..... ANL/CP-74821
CONF-920402-25
DE92-014847

N92-31596 # p 3919 ..... ANL/CP-75978
CONF-9203156-1
DE92-014852
N92-31597* # p 3885 ..... NAS 1.26:190641
NASA-CR-190641
N92-31598 # p 3852 ..... ISBN-0-16-035925-2
PB92-100353
N92-31599 # p 3922 ..... OTA-A-530
PB92-166549
N92-31600 # p 3888 ..... AD-A249712
ARO-28809.6-MASDI
SU-TR-74
N92-31601 # p 3877 ..... AD-A250060
N92-31602 # p 3859 ..... AD-A250184
AFIT/CI/CIA-91-112
N92-31603 # p 3860 ..... AD-A250185
AFIT/CI/CIA-91-109
N92-31604 # p 3774 ..... AD-A250410
AFOSR-92-0398TR
N92-31605 # p 3830 ..... AD-A250555
AFIT/CI/CIA-91-130
N92-31606 # p 3894 ..... DE92-011427
DOE/ER-13657/T1
N92-31607 # p 3780 ..... CONF-920707-29
DE92-011943
UCRL-JC-109758
N92-31608 # p 3869 ..... CONF-9107136-11
DE92-011974
UCRL-JC-108024
N92-31609 # p 3774 ..... B91-0161
NISTIR-3966
PB92-181148
N92-31610 # p 3787 ..... ISBN-951-22-0857-1
PB92-180645
TKK-V-B66
N92-31611 # p 3901 ..... AD-A247615
N92-31612 # p 3787 ..... AD-A250552
AFOSR-92-0305TR
N92-31613 # p 3904 ..... GTRF-101
PB92-182534
N92-31614* # p 3807 ..... NAS 1.26:190534
NASA-CR-190534
UMICH-027723-6-T
N92-31615 # p 3745 ..... DOT/FAA/CT-TN91/39
N92-31616 # p 3904 ..... CONF-920362-20
DE92-011394
GA-A-20860
N92-31617 # p 3807 ..... DOT/FAA/CT-TN92/18
N92-31618 # p 3794 ..... NISTIR-4788
PB92-172485
N92-31619* # p 3840 ..... NAS 1.26:190577
NASA-CR-190577
N92-31620 # p 3852 ..... PB92-156892
N92-31621 # p 3844 ..... AD-A250750
TEC-0009
N92-31622 # p 3752 ..... AD-A249739
FJSRL-TR-92-0001
N92-31623 # p 3847 ..... CONF-920678-5
DE92-010567
NREL/TP-441-4801
N92-31624 # p 3794 ..... AD-A249745
MTL-TR-92-14
N92-31625 # p 3822 ..... CONF-920707-28
DE92-012101
UCRL-JC-108985
N92-31626 # p 3853 ..... DE92-013925
DOE/ER-60479/T1
N92-31627 # p 3909 ..... BNL-47474
CONF-920722-1
DE92-014476
N92-31628 # p 3877 ..... NISTIR-4813
PB92-181130
N92-31629 # p 3807 ..... AD-A252321
SSD-TR-92-10
TR-0089(4945-05)-1
N92-31630 # p 3864 ..... OCS/MMS-92/0001
PB92-177690
N92-31631 # p 3794 ..... DE92-015392
SAND-92-0052
N92-31632 # p 3767 ..... PB92-181270
N92-31633 # p 3827 ..... DE92-015954
NISTIR-4539
N92-31634* # p 3762 ..... PB92-181692
N92-31635 # p 3924 ..... PB92-184472
N92-31636 # p 3856 ..... PB92-185040
N92-31637 # p 3856 ..... ISSN-0038-0911
LC-79-640375
PB92-187723
SGD-572-PT-1
N92-31638 # p 3841 ..... DE92-015998
PNL-8088
N92-31639 # p 3856 ..... ISSN-0038-0911
LC-79-640375
PB92-187731
SGD-572-PT-2
N92-31640* # p 3762 ..... E-5398
NAS 1.60:3038
NASA-TP-3038
N92-31641 # p 3860 ..... NOAA-TM-ERL-WPL-222
PB92-188200
N92-31642 # p 3877 ..... AD-A249697
N92-31643 # p 3923 ..... NISTIR-4703
PB92-158278
N92-31644 # p 3865 ..... PB92-177054
WHOI-91-19
N92-31645 # p 3915 ..... NISTIR-4791
PB92-172733
N92-31646 # p 3847 ..... DE92-001248
NREL/TP-410-4724
N92-31647 # p 3836 ..... CONF-920331-5
DE92-013466
SSCL-PREPRINT-57
N92-31648 # p 3853 ..... EPA/600/A-92/104
PB92-180231
N92-31649* # p 3853 ..... NCAR/TN-366+STR
PB92-186196
N92-31650 # p 3815 ..... CONF-920402-11
DE92-014465
N92-31651 # p 3815 ..... BNL-NUREG-47472
CONF-920375-18
DE92-014473
N92-31652 # p 3909 ..... ANL/CP-75799
CONF-920439-7
DE92-014857
N92-31653 # p 3834 ..... DE92-015200
DOE/CE-0357P
N92-31654 # p 3877 ..... ANL/CP-75955
CONF-9205200-1
DE92-015223
N92-31655 # p 3909 ..... DE92-630650
IC-91/391
N92-31656* # p 3761 ..... H-1787
NAS 1.26:186022
NASA-CR-186022
N92-31657 # p 3837 ..... CONF-9205190-1
DE92-015253
PNL-SA-19989
N92-31658 # p 3841 ..... PB92-180835
R-640
N92-31659 # p 3904 ..... NIFS-140
N92-31660 # p 3915 ..... ETN-92-91891
MBB-UO-0163-91-PUB
N92-31661 # p 3910 ..... CONF-911064-9
DE92-011533
UCRL-JC-109627
N92-31662 # p 3856 ..... DE92-014189
UCRL-ID-110395
N92-31663 # p 3915 ..... CONF-9202100-1
DE92-011583
SU-SLAC-PUB-5752
N92-31664 # p 3815 ..... CONF-920315-20
DE92-011650
SSCL-PREPRINT-79
N92-31665 # p 3910 ..... CONF-920402-16
DE92-014702
PNL-SA-20854
N92-31666 # p 3910 ..... AD-A252440
N92-31667 # p 3787 ..... DE92-011651
UCRL-LR-109425
N92-31668 # p 3910 ..... CONF-920514-3
DE92-011658
SAND-91-2693C
N92-31669 # p 3878 ..... CONF-9205141-1
DE92-011660
SAND-92-0816C
N92-31670 # p 3860 ..... AD-A252706
N92-31671 # p 3780 ..... AD-A249722
ARO-25245.4-EG
N92-31672 # p 3892 ..... AD-A252709
N92-31673 # p 3894 ..... AD-A249725
AFIT/CI/CIA-91-028D
N92-31674 # p 3752 ..... AD-A252711
WL-TM-92-312-FIBE
N92-31675 # p 3768 ..... AD-A249728
AFIT/CI/CIA-91-026D
N92-31676 # p 3878 ..... AD-A252726
N92-31677* # p 3767 ..... NAS 1.26:189628
NASA-CR-189628
N92-31678 # p 3780 ..... NIST/GCR-92/604
PB92-181056
N92-31679 # p 3894 ..... CONF-9203146-1
DE92-013411
N92-31680 # p 3885 ..... NISTIR-4807
PB92-183649
N92-31681 # p 3815 ..... CONF-920515-12
DE92-015247
LA-UR-92-1705
N92-31682 # p 3919 ..... PB92-173707
N92-31683 # p 3781 ..... EPA/600/R-92/084
PB92-180868
N92-31684 # p 3830 ..... ANL/CP-75935
CONF-9206180-3
DE92-015269
N92-31685 # p 3765 ..... NAL-TR-1110T
PB92-178870
N92-31686 # p 3890 ..... AD-A249623
AFIT/CI/CIA-91-132
N92-31687* # p 3822 ..... ICASE-92-31
NAS 1.26:189681
NASA-CR-189681
N92-31688 # p 3905 ..... AD-A249614
N92-31689 # p 3878 ..... ETN-92-91679
LAAS-91467
N92-31690 # p 3886 ..... ETN-92-91680
LAAS-91475
N92-31691 # p 3807 ..... AD-A249622
AFIT/CI/CIA-91-025D
N92-31692 # p 3901 ..... ETN-92-91681
LAAS-91484
N92-31693 # p 3837 ..... ETN-92-91682
LAAS-92002
N92-31694 # p 3828 ..... AD-A249673
ARO-28890.1-EG-EQ
N92-31695 # p 3787 ..... ETN-92-91683
LAAS-92013
N92-31696 # p 3823 ..... AD-A250232
AFOSR-92-0369TR
N92-31697 # p 3815 ..... ETN-92-91684
LAAS-92032
N92-31698 # p 3830 ..... ETN-92-91685
LAAS-92034
N92-31699 # p 3910 ..... AD-A250630
N92-31700 # p 3894 ..... CONF-920939-1
DE92-011108
N92-31701 # p 3823 ..... CONF-920981-1
DE92-011367
LA-UR-92-849
N92-31702 # p 3860 ..... ETN-92-91690
QR-1-VOL-53-NO-1-PT-1
N92-31703 # p 3878 ..... CONF-920903-4
DE92-011368
LA-UR-92-859
N92-31704 # p 3860 ..... ETN-92-91691
QR-2-VOL-53-NO-2-PT-2
N92-31705 # p 3895 ..... CONF-920919-1
DE92-011458
UCRL-JC-109763
N92-31706 # p 3861 ..... ETN-92-91692
QR-4-VOL-53-NO-4-PT-4
N92-31707 # p 3905 ..... CONF-920913-1
DE92-011662
SAND-92-0806C
N92-31708 # p 3861 ..... ETN-92-91693
N92-31709 # p 3861 ..... CONF-9209107-1
DE92-012627
SAND-92-1008C
N92-31710 # p 3861 ..... ETN-92-91694
N92-31711 # p 3867 ..... CONF-920501-22
DE92-015218
PNL-SA-20340
N92-31712 # p 3899 ..... DE92-016288
DOE/ER-40560/3A
N92-31713 # p 3924 ..... DE92-016290
DOE/ER-40560/3C
N92-31714 # p 3861 ..... AD-A250568
AFIT/CI/CIA-91-116
N92-31715 # p 3807 ..... ETN-92-91811
RUU-CS-91-45
N92-31716 # p 3774 ..... ETN-92-91889
MBB-UD-0609-91-PUB
N92-31717 # p 3781 ..... DE92-016598
DOE/ER-14150/2
N92-31718 # p 3816 ..... CONF-9205141-2
DE92-012681
SAND-91-2350C
N92-31719 # p 3910 ..... CONF-900397-3-REV-1
DE92-011521
UCRL-JC-103782-REV-1
N92-31720 # p 3834 ..... ANL/ESD/TM-27
DE92-012683
N92-31721 # p 3895 ..... DE92-012598
DOE/ER-40159/182
N92-31722 # p 3808 ..... DE92-013039
UCRL-CR-110002
N92-31723 # p 3911 ..... CONF-920402-3
DE92-013379
LA-UR-92-1435
N92-31724 # p 3895 ..... DE92-013571
DOE/ER-13751/5
N92-31725 # p 3781 ..... DE92-013484
DOE/ER-14189/1
N92-31726 # p 3823 ..... DE92-013589
DOE/ER-13896/4
N92-31727 # p 3905 ..... DE92-013590
DOE/ER-53257/5
N92-31728 # p 3895 ..... CONF-9107216
DE92-789024
KURRI-TR-358

N92-31729 # p 3781 ..... CONF-920362-32
DE92-014258
GA-A-20915
N92-31730 # p 3905 ..... DE92-014322
DOE/ER-53198/196
N92-31731 # p 3919 ..... DE92-001253
DOE/METC-92-4109
N92-31732 # p 3853 ..... CONF-920519-3
DE92-015090
PNL-SA-20767
N92-31733 # p 3788 ..... DE92-016286
DOE/ER-45388/T1
N92-31734 # p 3862 ..... DE92-016469
DOE/ER-61011/T2
N92-31735 # p 3766 ..... DE92-016741
UCRL-ID-109283-REV-1
N92-31736 # p 3757 ..... DE92-016750
SAND-92-0912
N92-31737 # p 3901 ..... BNL-47668
DE92-016958
N92-31738 # p 3808 ..... CONF-920750-3
DE92-008015
SAND-91-2910C
N92-31739 # p 3878 ..... CONF-920759-1
DE92-008062
UCRL-JC-109659
N92-31740 # p 3882 ..... CONF-920730-2
DE92-008068
UCRL-JC-109251
N92-31741 # p 3883 ..... CONF-920730-1
DE92-008073
UCRL-JC-109496
N92-31742 # p 3878 ..... CONF-920760-1
DE92-008076
UCRL-JC-109266
N92-31743 # p 3879 ..... CONF-920760-3
DE92-011963
UCRL-JC-109225
N92-31744 # p 3788 ..... CONF-911202-77
DE92-012143
SAND-92-8411C
N92-31745 # p 3841 ..... CONF-9110344-8-REV-1
DE92-013070
WSRC-MS-91-230-REV-1
N92-31746 # p 3756 ..... DE92-013458
SAND-92-0457
N92-31747 # p 3867 ..... DE92-013674
DOE/ER-60631/9
N92-31748 # p 3781 ..... CONF-920796-1
DE92-014049
SAND-92-0021C
N92-31749 # p 3905 ..... CONF-920311-8
DE92-013696
GA-A-20877
N92-31750 # p 3862 ..... CONF-9209107-2
DE92-012628
SAND-91-2061C
N92-31751 # p 3799 ..... CONF-920584-22
DE92-015229
DOE/MC-26029/92/C0037
N92-31752 # p 3781 ..... DE92-015298
DOE/ER-13552/7
N92-31753 # p 3837 ..... DE92-010763
SAND-88-3185
N92-31754 # p 3920 ..... AD-A247053
N92-31755 # p 3830 ..... AD-A248574
N92-31756 # p 3926 ..... CONF-9110312-2
DE92-010256
LBL-31685
N92-31757 # p 3888 ..... AD-A249804
ARO-28809.5-MA-SDI
N92-31758 # p 3871 ..... AD-A250275
AFOSR-92-0347TR
N92-31759 # p 3788 ..... CONF-911202-76
DE92-011764
UCRL-JC-109268
N92-31760 # p 3816 ..... CONF-920315-18
DE92-011697
SSCL-PREPRINT-74
N92-31761 # p 3902 ..... CONF-9203139-1
DE92-011949
UCRL-JC-109219
N92-31762 # p 3831 ..... DE92-012370
EGG-PHY-9978
N92-31763 # p 3781 ..... CONF-920707-24
DE92-009690
UCRL-JC-109673
N92-31764 # p 3905 ..... CONF-920362-24
DE92-012699
GA-A-20876
N92-31765 # p 3895 ..... CONF-9202106-1
DE92-013535
LA-UR-92-1302
N92-31766 # p 3857 ..... AD-A251149
TR-91-13
N92-31767 # p 3915 ..... AD-A252705
N92-31768 # p 3888 ..... AD-A247308
MSRR-572
N92-31769 # p 3831 ..... DE92-011424
DOE/ER-52147/5
N92-31770 # p 3823 ..... AD-A250273
N92-31771 # p 3908 ..... CONF-920311-5
DE92-012148
SAND-92-8489C
N92-31772 # p 3782 ..... CONF-9109297-2
DE92-012156
IS-M-686
N92-31773 # p 3782 ..... CONF-920573-8
DE92-012253
SAND-92-8495C
N92-31774 # p 3835 ..... ANL/ESD-14
DE92-012259
N92-31775 # p 3831 ..... CONF-920851-12
DE92-014113
IS-M-709
N92-31776 # p 3782 ..... GRI-92/0068
PB92-164359
N92-31777 # p 3752 ..... AD-A250048
WL-TR-91-3072
N92-31778 # p 3867 ..... AD-A250055
AFOSR-92-0310TR
N92-31779 # p 3871 ..... AD-A250056
AFOSR-92-0234TR
N92-31780 # p 3816 ..... AD-A250094
N92-31781*# p 3924 ..... NAS 1.15:107966
NASA-TM-107966
N92-31782 # p 3853 ..... CONF-9109340-4
DE92-015130
N92-31783 # p 3879 ..... AD-A250095
AFIT/CI/CIA-91-129
N92-31784 # p 3862 ..... AD-A250096
AFIT/CI/CIA-91-107
N92-31785 # p 3823 ..... ANL/CP-75985
CONF-920804-17
DE92-016603
N92-31786 # p 3925 ..... AD-A250097
N92-31787*# p 3879 ..... NAS 1.26:190716
NASA-CR-190716
N92-31788* p 3831 INT-PATENT-CLASS-H01S-3/10
NASA-CASE-LAR-13772-1
US-PATENT-APPL-SN-359460
US-PATENT-CLASS-372-25
US-PATENT-CLASS-372-30
US-PATENT-5,128,949
N92-31789 # p 3892 ..... AD-A250100
NUWC-NL-TD-10023
N92-31790* p 3828 INT-PATENT-CLASS-C12M-1/10
INT-PATENT-CLASS-C12M-1/12
INT-PATENT-CLASS-C12M-3/00
INT-PATENT-CLASS-C12M-3/02
NASA-CASE-MFS-28370-1
US-PATENT-APPL-SN-386175
US-PATENT-CLASS-435-286
US-PATENT-CLASS-435-311
US-PATENT-CLASS-435-312
US-PATENT-5,104,802
N92-31791 # p 3816 ..... AD-A250101
N92-31792* p 3794 INT-PATENT-CLASS-C08L-79/08
NASA-CASE-LAR-14159-1-CU
US-PATENT-APPL-SN-439317
US-PATENT-CLASS-525-420
US-PATENT-CLASS-525-434
US-PATENT-CLASS-525-436
US-PATENT-5,112,923
N92-31793 # p 3757 ..... AD-A250134
WL-TM-92-313-FIBE
N92-31794 # p 3828 ..... AD-A250135
NMRI-92-25
N92-31795 # p 3788 ..... AD-A250141
N92-31796 # p 3788 ..... AD-A250142
N92-31797 # p 3788 ..... BUMINES-IC-9275
LC-88-600144
PB92-178623
N92-31798 # p 3831 ..... DE92-010772
DOE/ER-13937/4
N92-31799 # p 3816 ..... AD-A248758
N92-31800 # p 3800 ..... AD-A249942
AD-E951775
AMSMI/TR-RD-WS-91-12
N92-31801 # p 3808 ..... AD-A249945
AD-E951785
AMSMI/TR-RD-WS-92-2
N92-31802 # p 3831 ..... AD-A250028
AFOSR-92-0312TR
N92-31803 # p 3782 ..... AD-A250033
BRL-TR-3334
N92-31804 # p 3800 ..... AD-A250034
BRL-TR-3329
N92-31805 # p 3782 ..... CONF-920707-20
DE92-008553
UCRL-JC-109083
N92-31806 # p 3775 ..... DE92-013401
DOE/ER-45372/4
N92-31807 # p 3835 ..... AD-A250035
BRL-CR-687
EGG-ME-10066
N92-31808*# p 3752 ..... H-1803
NAS 1.15:104246
NASA-TM-104246
N92-31809 # p 3808 ..... AD-A250047
N92-31810 # p 3795 ..... AD-A250067
TR-8
N92-31811 # p 3885 ..... AD-A250145
AL-TP-1992-0010
N92-31812 # p 3895 ..... DE92-014013
DOE/ER-40224/205
OITS-470
N92-31813 # p 3755 ..... DLR-MITT-91-12
ETN-92-91732
ISSN-0939-298X
N92-31814 # p 3896 ..... ETN-92-91738
NIKHEF-K-EMIN-92-01
N92-31815 # p 3899 ..... ETN-92-91739
NIKHEF-K/AMPS/91-08
N92-31816 # p 3783 ..... CONF-9205123-1
DE92-013342
K/TCD-1020
N92-31817 # p 3759 ..... CONF-920747-2
DE92-013428
LA-UR-92-1390
N92-31818 # p 3892 ..... AD-A252409
NRL/MR/5120-92-6920
N92-31819 # p 3911 ..... AD-A248029
TR-20
N92-31820 # p 3783 ..... AD-A252420
TR-16
N92-31821 # p 3865 ..... AD-A249865
SSS-TR-91-12828
N92-31822 # p 3767 ..... AD-A249868
AFIT/CI/CIA-91-119
N92-31823 # p 3775 ..... AD-A249870
AFIT/CI/CIA-91-126
N92-31824 # p 3823 ..... AD-A250209
AFOSR-92-0388TR
N92-31825 # p 3879 ..... AD-A252477
RL-TR-92-16
N92-31826 # p 3802 ..... AD-A250215
N92-31827 # p 3885 ..... AD-A250222
N92-31828 # p 3828 ..... AD-A252485
TR-12
N92-31829 # p 3906 ..... CONF-920142-1
DE92-013276
N92-31830 # p 3802 ..... PB92-173046
N92-31831 # p 3899 ..... CONF-920803-3
DE92-013282
N92-31832 # p 3824 ..... DE92-014044
SAND-91-2532
N92-31833 # p 3879 ..... LTR91-003
PL-TR-91-2109
N92-31834 # p 3817 ..... DE92-014099
DOE/CH-10510-01
N92-31835*# p 3883 ..... NAS 1.26:184256
NASA-CR-184256
UAH-5-32559
N92-31836 # p 3896 ..... DE92-624981
LAMP-91/10
N92-31837 # p 3896 ..... DE92-625004
ESM-31
N92-31838 # p 3756 ..... DOT/FAA/CT-TN91/44
N92-31839 # p 3824 ..... B91-0281
GRI-91/0229
NIST/TN-1352
PB92-183730
N92-31840*# p 3795 ..... E-6500
NAS 1.15:105198
NASA-TM-105198
N92-31841 # p 3835 ..... GRI-91/0354
PB92-184373
SR83-R-5092-90
N92-31842 # p 3865 ..... PB92-185974
WHPO-92-1
WOCE-83/92
N92-31843 # p 3906 ..... DE92-782101
NIFS-111
N92-31844 # p 3841 ..... BNL-47331
CONF-9205145-1
DE92-012303
N92-31845 # p 3848 ..... CONF-920429-2
DE92-012327
PNL-SA-19467
N92-31846 # p 3768 ..... CONF-920431-24
DE92-012347
PNL-SA-19981
N92-31847 # p 3841 ..... AD-A251003
WL-TM-92-308-FIBE
N92-31848 # p 3911 ..... AD-A251041
N92-31849 # p 3817 ..... AD-A251042
N92-31850 # p 3772 ..... AD-A251043

TR-19
N92-31851 # p 3911 ..... AD-A251057
TR-44
N92-31852* # p 3926 ..... NAS 1.15:107960
NASA-TM-107960
N92-31853 # p 3753 ..... NO REPORT NUMBER
N92-31854* # p 3775 ..... E-7247
NAS 1.15:105816
NASA-TM-105816
N92-31855* # p 3808 ..... E-7149
NAS 1.15:105744
NASA-TM-105744
N92-31856* # p 3925 ..... LMSC-F404726
LMSC-PO35355
NAS 1.26:190683
NASA-CR-190683
N92-31857 # p 3763 ..... ANL/CP-76308
CONF-9206196-1
DE92-016177
N92-31858 # p 3896 ..... AD-A247052
AFOSR-92-0126TR
N92-31859 # p 3920 ..... DE92-782192
INIS-JP-002
N92-31860 # p 3783 ..... CONF-920707-5
DE92-005326
SAND-91-8718
N92-31861 # p 3745 ..... ITN-92-85124
N92-31862 # p 3745 ..... NO REPORT NUMBER
N92-31863 # p 3745 ..... NO REPORT NUMBER
N92-31864 # p 3746 ..... NO REPORT NUMBER
N92-31865 # p 3746 ..... NO REPORT NUMBER
N92-31866 # p 3746 ..... NO REPORT NUMBER
N92-31867 # p 3746 ..... NO REPORT NUMBER
N92-31868 # p 3746 ..... NO REPORT NUMBER
N92-31869 # p 3746 ..... NO REPORT NUMBER
N92-31870 # p 3747 ..... NO REPORT NUMBER
N92-31871 # p 3747 ..... NO REPORT NUMBER
N92-31872 # p 3747 ..... NO REPORT NUMBER
N92-31873 # p 3747 ..... NO REPORT NUMBER
N92-31874 # p 3747 ..... NO REPORT NUMBER
N92-31875 # p 3748 ..... NO REPORT NUMBER
N92-31876* # p 3748 ..... NO REPORT NUMBER
N92-31877 # p 3748 ..... NO REPORT NUMBER
N92-31878* # p 3748 ..... NO REPORT NUMBER
N92-31879 # p 3748 ..... NO REPORT NUMBER
N92-31880 # p 3748 ..... NO REPORT NUMBER
N92-31881 # p 3748 ..... NO REPORT NUMBER
N92-31882 # p 3749 ..... NO REPORT NUMBER
N92-31883 # p 3749 ..... NO REPORT NUMBER
N92-31884 # p 3749 ..... NO REPORT NUMBER
N92-31885 # p 3749 ..... NO REPORT NUMBER
N92-31886 # p 3749 ..... NO REPORT NUMBER
N92-31887 # p 3750 ..... NO REPORT NUMBER
N92-31888 # p 3750 ..... NO REPORT NUMBER
N92-31889 # p 3750 ..... NO REPORT NUMBER
N92-31890 # p 3803 ..... AD-A250731
AL-TR-1992-0041
N92-31891 # p 3783 ..... DE92-014588
DOE/ER-13299/8
N92-31892* # p 3835 ..... NAS 1.26:189230
NASA-CR-189230
REPT-92-RC-09071
RI/RD-92-114
N92-31893 # p 3848 ..... DE92-010559
NREL/TP-451-4855
N92-31894 # p 3862 ..... DE92-014100
DOE/ER-61075/T1
N92-31895 # p 3824 ..... DE92-014744
DOE/PETC-TR/92/6
N92-31896 # p 3853 ..... CONF-9205167-1
DE92-014798
N92-31897 # p 3770 ..... CONF-920803-10
DE92-016163
N92-31898 # p 3789 ..... CONF-920762-2
DE92-016165
N92-31899 # p 3879 ..... ANL/CP-75260
CONF-920730-4
DE92-016187
N92-31900* # p 3762 ..... NAS 1.15:107646
NASA-TM-107646
N92-31901* # p 3770 ..... E-7249
JPC-92-3144
NAS 1.15:105818
NASA-TM-105818
N92-31902 # p 3832 ..... CONF-911296-9
DE92-011763
UCRL-JC-108146
N92-31903 # p 3848 ..... GRI-91/0397
PB92-152883
N92-31904 # p 3896 ..... DE92-620889
FEI-2187
N92-31905 # p 3869 ..... AD-A247498
AFOSR-92-0219TR
N92-31906 # p 3857 ..... AD-A249871
AFIT/CI/CIA-91-115
N92-31907 # p 3854 ..... DE92-011733
ESD-3746
ORNL/CDIAC-46
N92-31908 # p 3803 ..... DE92-011737
UCRL-ID-107571
N92-31909 # p 3828 ..... DE92-011766
UCRL-CR-103698
N92-31910* # p 3760 ..... NAS 1.26:184341
NASA-CR-184341
N92-31911* # p 3841 ..... NAS 1.26:190585
NASA-CR-190585
N92-31912 # p 3775 ..... CONF-920628-2-EXTD-ABST
DE92-011778
N92-31913 # p 3906 ..... CONF-920607-9
DE92-011790
N92-31914 # p 3911 ..... DE92-011810
DOE/ER-45208/7
N92-31915 # p 3912 ..... AD-A250402
AFOSR-92-0276TR
N92-31916* # p 3771 ..... AIAA PAPER 91-3528
E-6542
NAS 1.15:105310
NASA-TM-105310
N92-31917 # p 3795 ..... CONF-911202-79
DE92-013850
N92-31918 # p 3783 ..... GIT-AER-E-16-616
GRI-91/0352
PB92-172402
N92-31919 # p 3828 ..... DE92-015305
DOE/ER-12932/2
N92-31920 # p 3809 ..... PB92-173038
N92-31921 # p 3809 ..... CTN-92-60331
DREO-91-6
N92-31922 # p 3848 ..... GRI-92/0021
PB92-172303
N92-31923 # p 3896 ..... CONF-920574-7
DE92-016164
N92-31924 # p 3789 ..... ANL/CP-75787
CONF-9205123-7
DE92-016172
N92-31925 # p 3890 ..... IHES/M/92/13
PB92-178284
N92-31926 # p 3896 ..... DE92-016182
DOE/ER-10667/11
N92-31927 # p 3897 ..... DE92-016204
DOE/ER-40322/165
N92-31928 # p 3755 ..... DE92-016346
DOE/EH-0242P
N92-31929 # p 3835 ..... CONF-9209143-1
DE92-016368
N92-31930 # p 3854 ..... DE92-016646
DOE/ER-0549T
N92-31931 # p 3854 ..... DE92-016740
SAND-92-0467
N92-31932 # p 3857 ..... AD-A249872
AFIT/CI/CIA-91-110
N92-31933 # p 3824 ..... DE92-016748
SAND-91-2760
N92-31934 # p 3920 ..... DE92-011731
UCRL-LR-109666
N92-31935 # p 3832 ..... CONF-9108146-2
DE92-011813
N92-31936 # p 3897 ..... AD-A250981
AFOSR-92-0446TR
N92-31937 # p 3912 ..... AD-A251006
N92-31938 # p 3795 ..... ANL/CP-75684
CONF-920307-72
DE92-011846
N92-31939 # p 3880 ..... AD-A251008
CMU/CS-92-110
N92-31940 # p 3775 ..... AD-A251009
MTL-TR-92-8
N92-31941 # p 3795 ..... AD-A251020
TR-34
N92-31942 # p 3784 ..... ESA-TT-1229
ETN-92-91387
ONERA-NT-1989-8
N92-31943 # p 3755 ..... DLR-FB-90-34
ESA-TT-1254
ETN-92-91711
N92-31944 # p 3809 ..... AD-A250497
AFOSR-92-0350TR
N92-31945 # p 3912 ..... DE92-013588
DOE/ER-45334/5
N92-31946 # p 3817 ..... DE92-013704
KCP-613-4748
N92-31947 # p 3922 ..... ESA-BR-79
ETN-92-91712
ISBN-92-9092-095-5
N92-31948 # p 3899 ..... DE92-013744
SSCL-570
N92-31949 # p 3906 ..... DE92-013770
SAND-91-1626
N92-31950 # p 3897 ..... AD-A250727
TR-12
N92-31951 # p 3795 ..... AD-A250976
AFOSR-92-0457TR
N92-31952 # p 3795 ..... AD-A250993
TR-3
N92-31953 # p 3915 ..... ETN-92-91721
RAL-92-005
N92-31954 # p 3795 ..... AD-A250994
TR-6
N92-31955 # p 3912 ..... ANL/CP-75477
CONF-920801-12
DE92-016634
N92-31956 # p 3886 ..... ETN-92-91725
MATHS-REPT-A-152
N92-31957 # p 3887 ..... ETN-92-91726
MATHS-REPT-A-153
N92-31958 p 3897 ..... ITN-92-85162
N92-31959 # p 3784 ..... AD-A252487
TR-16
N92-31960 # p 3796 ..... AD-A252488
TR-17
N92-31961 # p 3796 ..... AD-A252489
TR-14
N92-31962 # p 3869 ..... AD-A252532
AFIT/CI-CIA-92-010
N92-31963 # p 3870 ..... AD-A247185
N92-31964 # p 3857 ..... AD-A249225
ARO-24610.1-GS-UIF
N92-31965 # p 3923 ..... DE92-011905
DOE/ER-75564/9
N92-31966 # p 3761 ..... AD-A250199
AFOSR-92-0292TR
N92-31967 # p 3761 ..... AD-A250202
AFOSR-92-0287TR
N92-31968 # p 3796 ..... AD-A250671
TR-22
N92-31969 # p 3800 ..... AD-A250733
N92-31970 # p 3800 ..... AD-A250734
N92-31971 # p 3800 ..... AD-A250735
N92-31972 # p 3801 ..... AD-A250736
N92-31973 # p 3801 ..... AD-A250737
N92-31974 # p 3873 ..... AD-A250866
IST-TR-92-12
N92-31975 # p 3900 ..... CONF-920331-10
DE92-013954
SSCL-PREPRINT-60
N92-31976 # p 3784 ..... DE92-001269
DOE/MC-26034/3083
N92-31977 # p 3824 ..... BNL-47120
CONF-920928-1
DE92-010048
N92-31978 # p 3862 ..... AD-A246993
N92-31979 # p 3776 ..... AD-A247114
N92-31980 # p 3867 ..... AD-A247138
AFOSR-92-0004TR
N92-31981 # p 3888 ..... AD-A247169
AFOSR-92-0021TR
N92-31982 # p 3801 ..... AD-A247835
WL-TR-91-2083
N92-31983 # p 3907 ..... AD-A247847
UCB/ERL-M91/79
N92-31984 # p 3912 ..... AD-A247848
N92-31985 # p 3925 ..... AD-A247869
AFOSR-92-0221TR
N92-31986 # p 3857 ..... AD-A247903
NOARL-TN-204
N92-31987 # p 3789 ..... AD-A247923
SSC-SSR-1311-VOL-1
SSC-352-VOL-1
N92-31988 # p 3865 ..... AD-A246992
NPS-OC-91-003
N92-31989 # p 3842 ..... AD-A248027
AFIT/GA/ENY/90M-01
AFIT/GA/92M/01
N92-31990 # p 3907 ..... AD-A248163
AFIT/GNE/ENP/92M-4
N92-31991 # p 3880 ..... AD-A248170
AFIT/GOR/ENS/92M-15
N92-31992 # p 3916 ..... AD-A248346
NRL/MR/5524-92-6944
N92-31993 # p 3809 ..... AD-A246215
N92-31994 # p 3912 ..... AD-A246329
TR-57
N92-31995 # p 3913 ..... AD-A248331
TR-58
N92-31996 # p 3809 ..... AD-A246344
IITRI-D06200-1
N92-31997 # p 3767 ..... AD-A248351
SWRI-3593/001
N92-31998 # p 3784 ..... AD-A246980
TR-116
N92-31999 # p 3897 ..... AD-A250728
TR-13
N92-32000 # p 3825 ..... AD-A250982
AFOSR-92-0429TR
N92-32001 # p 3796 ..... AD-A250983
AFOSR-92-0444TR
N92-32002 # p 3817 ..... AD-A250991
N92-32003 # p 3825 ..... ANL/CP-75330

CONF-920801-13
DE92-016635
N92-32004 # p 3789 ..... DE92-016685
LA-12291-MS
N92-32005 # p 3923 ..... DE92-016981
UCRL-53809-91
N92-32006 # p 3898 ..... CONF-9105121-2
DE92-017000
LBL-30841
UCB-PTH-91/28
N92-32007 # p 3898 ..... DE92-017030
DOE/SF-19862/T1
N92-32008 # p 3825 ..... DE92-013998
LA-12062-MS-REV-1
N92-32009 p 3763 ..... NO REPORT NUMBER
N92-32010 p 3763 ..... TABES PAPER 92-411
N92-32011* p 3763 ..... TABES PAPER 92-414
N92-32012 p 3763 ..... TABES PAPER 92-444
N92-32013 p 3763 ..... TABES PAPER 92-445
N92-32014 p 3763 ..... TABES PAPER 92-447
N92-32015 p 3764 ..... TABES PAPER 92-424
N92-32016 p 3764 ..... TABES PAPER 92-425
N92-32017 p 3764 ..... TABES PAPER 92-453
N92-32018 p 3764 ..... TABES PAPER 92-454
N92-32019 p 3764 ..... TABES PAPER 92-467
N92-32020 p 3764 ..... TABES PAPER 92-462
N92-32021 p 3764 ..... TABES PAPER 92-213
N92-32022 # p 3825 ..... DE92-014078
LA-10613-MS-REV-1
N92-32023 # p 3873 ..... AD-A250719
AD-E501523
IDA-P-2638
IDA/HQ-91-40259
N92-32024 # p 3898 ..... AD-A250992
N92-32025 # p 3925 ..... INPE-5377-TDI/472
N92-32026 # p 3762 ..... DE92-015276
LA-UR-92-1529
N92-32027 # p 3858 ..... DE92-015302
DOE/ER-13418/T1
N92-32028 # p 3900 ..... DE92-015363
DOE/ER-40371/5
N92-32029 # p 3784 ..... DE92-015430
DOE/PC-90305/T6
N92-32030 # p 3771 ..... CONF-920803-12
DE92-016501
SAND-92-1223C
N92-32031 # p 3873 ..... CTN-92-60329
DREO-PSD-EPS-05/89
N92-32032 # p 3789 ..... DE92-016573
KCP-613-4747
N92-32033 # p 3817 ..... DE92-016574
KCP-613-4804
N92-32034 # p 3883 ..... DE92-016802
ORNL/TM-12071
N92-32035 # p 3890 ..... DE92-016834
DOE/ER-13916/4
N92-32036 # p 3885 ..... DE92-017351
SAND-91-1964
N92-32037 # p 3917 ..... DE92-017359
SAND-90-0444
N92-32038 # p 3825 ..... AD-A250498
AFOSR-92-0353TR
N92-32039 # p 3880 ..... AD-A250499
AFOSR-92-0352TR
N92-32040 # p 3883 ..... AD-A250504
AFOSR-92-0368TR
N92-32041 # p 3885 ..... AD-A250505
AFOSR-92-0357TR
N92-32042 # p 3832 ..... AD-A250506
AFOSR-92-0282TR
N92-32043 # p 3810 ..... AD-A250507
MTR-11278
N92-32044 # p 3892 ..... AD-A250508
NRL/FR/5160-92-9377
N92-32045 # p 3796 ..... AD-A250517
ARL-MAT-R-124
DODA-AR-006-607
N92-32046 # p 3890 ..... AD-A250519
AD-920315
AFOSR-92-0402TR
N92-32047 # p 3776 ..... AD-A250520
DOT/FAA/CT-91/23-VOL-1
WL-TR-91-4032-VOL-1
N92-32048 # p 3776 ..... AD-A250521
DOT/FAA/CT-91-23-VOL-2-PT-1
WL-TR-91-4032-VOL-2-PT-1
N92-32049 # p 3920 ..... AD-A252183
N92-32050 # p 3866 ..... AD-A252188
NOARL-PR-91-132-253
N92-32051 # p 3758 ..... AD-A245952
N92-32052 # p 3789 ..... AD-A245955
N92-32053 # p 3758 ..... AD-A245957
N92-32054 # p 3756 ..... AD-A246046
N92-32055 # p 3858 ..... AD-A252189
AFOSR-92-0547TR
N92-32056 # p 3866 ..... AD-A246080
N92-32057 # p 3785 ..... AD-A252215
N92-32058 # p 3920 ..... DE92-628395
INIS-MF-13154
N92-32059 # p 3760 ..... AD-A250865
AFOSR-92-0403TR
TSPC-TR-92-10
N92-32060 # p 3880 ..... AD-A252173
N92-32061 # p 3832 ..... AD-A252174
N92-32062 # p 3753 ..... AD-A252175
N92-32063 # p 3871 ..... AD-A252176
N92-32064 # p 3776 ..... AD-A252177
N92-32065 # p 3913 ..... AD-A252182
FRACTO-92
N92-32066 # p 3790 ..... AD-A252492
PWA-FR21998-08
N92-32067 # p 3927 ..... PB92-192624
REPT-MEMO-221
N92-32068 # p 3927 ..... PB92-192640
REPT-MEMO-222
N92-32069 # p 3866 ..... FOA-C-30642-3.1
PB92-195452
N92-32070 # p 3810 ..... FOA-C-30650-8.4,3.2
PB92-195429
N92-32071 # p 3854 ..... CURRENT-REF-92-1
PB92-198910
N92-32072 # p 3913 ..... NISTIR-4844
PB92-196088
N92-32073 # p 3767 ..... FOA-C-30647-9.4
PB92-195445
N92-32074 # p 3817 ..... AD-A250365
N92-32075 # p 3776 ..... AD-A250518
AFOSR-92-0397TR
CMC-6730-15
N92-32076 # p 3785 ..... AD-A250522
AFOSR-92-0420TR
N92-32077 # p 3902 ..... AD-A250525
CWRU/DMS/TR-45
N92-32078 # p 3913 ..... AD-A250527
SLCET-TR-92-2
N92-32079 # p 3796 ..... AD-A250531
TR-72
N92-32080 # p 3785 ..... AD-A250532
TR-71
N92-32081 # p 3887 ..... AD-A250549
AFOSR-92-0412TR
N92-32082 # p 3767 ..... PL-TR-91-2209
N92-32083 # p 3854 ..... ANL/CP-75853
CONF-920443-1
DE92-015224
N92-32084 # p 3790 ..... AD-A250550
AFOSR-92-0414TR
N92-32085 # p 3913 ..... CONF-920891-1
DE92-015235
N92-32086 # p 3829 ..... CONF-920891-2
DE92-016161
N92-32087 # p 3848 ..... CONF-920801-5
DE92-016500
SAND-92-0795C
N92-32088 # p 3842 ..... DE92-016747
SAND-89-2608
N92-32089 # p 3797 ..... CONF-920402-39
DE92-016787
N92-32090 # p 3898 ..... CONF-9203164-1
DE92-016800
N92-32091 # p 3849 ..... CONF-920878-8
DE92-016908
N92-32092 # p 3902 ..... AD-A250551
AFOSR-92-0404TR
N92-32093 # p 3785 ..... DE91-002141
NREL/TP-253-4276
N92-32094 # p 3797 ..... CONF-920448-5
DE92-013848
N92-32095 # p 3797 ..... DE92-015297
DOE/ER-45398/3
N92-32096 # p 3790 ..... AD-A245286
N92-32097 # p 3863 ..... NO REPORT NUMBER
N92-32098 # p 3801 ..... AD-A245338
NAVSWC-TR-91-250
N92-32099 # p 3890 ..... DE92-011607
DOE/CE-90029/7
N92-32100* # p 3767 ..... LMSC/P024859
NAS 1.26:4461
NASA-CR-4461
N92-32101 # p 3810 ..... AD-A250858
RSL-TR-8960-1
N92-32102 # p 3920 ..... AD-A250859
N92-32103 # p 3863 ..... AD-A250862
ATC-185
DOT/FAA/NR-92/1
N92-32104 # p 3777 ..... AD-A250864
AFOSR-92-0401TR
N92-32105 # p 3872 ..... AD-A247290
AFOSR-92-0142TR
N92-32106 # p 3866 ..... NOAA-TM-NMFS-105
PB92-178128
N92-32107 # p 3870 ..... AD-A252264
N92-32108* # p 3771 ..... E-6983
NAS 1.15:105637
NASA-TM-105637
N92-32109 # p 3883 ..... AD-A252742
N92-32110 # p 3849 ..... DE91-002146
NREL/TP-253-4281
N92-32111* # p 3758 ..... NAS 1.15:107650
NASA-TM-107650
N92-32112 # p 3849 ..... CONF-920678-6
DE92-010568
NREL/TP-432-4827
N92-32113 # p 3785 ..... DE92-014333
DOE/ER-13664/5
N92-32114* # p 3753 ..... NAS 1.26:4465
NASA-CR-4465
VPI-AERO-182
N92-32115 # p 3825 ..... CONF-920804-10
DE92-014363
WSRC-MS-92-123
N92-32116 # p 3890 ..... CONF-920408-2
DE92-014394
IS-M-711
N92-32117 # p 3785 ..... DE92-014630
DOE/PC-79812/T7
N92-32118 # p 3849 ..... BNL-47508
DE92-014691
N92-32119 # p 3889 ..... CONF-9111227-1
DE92-014719
UCRL-JC-108771
N92-32120 # p 3867 ..... DE92-014728
DOE/ER-60522/6
N92-32121 # p 3835 ..... CONF-9202113-1
DE92-014777
UCRL-JC-109152
N92-32122* # p 3880 ..... NAS 1.26:190894
NASA-CR-190894
UVA/528352/EE93/102
N92-32123 # p 3900 ..... DE92-015389
SAND-92-0747
N92-32124 # p 3849 ..... BNL-47529
DE92-016940
N92-32125 # p 3803 ..... BNL-47549
DE92-016941
N92-32126 # p 3881 ..... DE92-016979
ORNL/TM-12019
N92-32127* # p 3844 ..... L-17069
NAS 1.61:1279
NASA-RP-1279
N92-32128* # p 3829 ..... JPR-9950-1368
NAS 1.26:190481
NASA-CR-190481
N92-32129* # p 3771 ..... AEROJET-2459-31-1
NAS 1.26:187216
NASA-CR-187216
N92-32130* # p 3766 ..... NAS 1.26:189653-VOL-3
NASA-CR-189653-VOL-3
N92-32131 # p 3900 ..... CONF-920315-23
DE92-012418
SU-SLAC-PUB-5768
N92-32132 # p 3843 ..... JPRS-UES-92-004
N92-32133 # p 3900 ..... CONF-920315-24
DE92-012420
SU-SLAC-PUB-5789
N92-32134 # p 3810 ..... BNL-46678
CONF-920315-33
DE92-012543
N92-32135 # p 3777 ..... DE92-013158
KCP-613-4650
N92-32136 # p 3797 ..... DE92-013159
KCP-613-4661
N92-32137 p 3902 ..... AD-D015296
US-PATENT-APPL-SN-474941
US-PATENT-5,104,223
N92-32138 # p 3829 ..... DE92-013162
RFP-4529
N92-32139 # p 3790 ..... DE92-013291
SAND-92-0211
N92-32140 # p 3890 ..... DE92-013299
SSCL-530
N92-32141 # p 3786 ..... DE92-014112
DOE/PC-89877/9
N92-32142 # p 3924 ..... PL-TR-91-2065
N92-32143 # p 3837 ..... AECL-10507
COG-91-261
DE92-627145
N92-32144 # p 3902 ..... MPL-U-25/91
PL-TR-91-2189
SIO-91-15
N92-32145 # p 3786 ..... CONF-920707-27
DE92-011298
UCRL-JC-108986
N92-32146 # p 3797 ..... CONF-920444-27
DE92-012353
PNL-SA-20358
N92-32147* # p 3855 ..... DE92-012409
NAS 1.26:190379

NASA-CR-190379
UCRL-ID-109860
N92-32148* # p 3765 ..... NAS 1.15:103593
NASA-TM-103593
N92-32149 # p 3902 ..... CONF-9111208-2
DE92-013294
SU-SLAC-PUB-5774
N92-32150 # p 3881 ..... CONF-9204124-3
DE92-013369
EGG-10617-5103
N92-32151 # p 3797 ..... AD-A250967
TR-91-1258
N92-32152 # p 3883 ..... AD-A250968
TR-91-1256
N92-32153 # p 3798 ..... AD-A251109
TR-31
N92-32154 # p 3925 ..... CONF-9109182-6
DE92-014327
DOE/ER-40427/2-N92
N92-32155 # p 3855 ..... CONF-9110127-4
DE92-014773
UCRL-JC-109018
N92-32156* # p 3790 ..... NAS 1.26:190674
NASA-CR-190674
N92-32157* # p 3881 ..... ICASE-92-30
NAS 1.26:189680
NASA-CR-189680
N92-32158* # p 3826 ..... ICASE-92-32
NAS 1.26:189682
NASA-CR-189682
N92-32159* # p 3777 ..... NAS 1.26:190700
NASA-CR-190700
N92-32160 # p 3916 ..... NCES-92-011
PB92-193599
N92-32161 # p 3810 ..... FOA-C-30649-3.2
PB92-195437
N92-32162* # p 3753 ..... NAS 1.26:190731
NASA-CR-190731
N92-32163 # p 3887 ..... AD-A247062
MIT/LCS/TR-524
N92-32164* # p 3887 ..... ICASE-92-21
NAS 1.26:189663
NASA-CR-189663
N92-32165 # p 3898 ..... CONF-920308-21
DE92-013212
WSRC-MS-91-313
N92-32166 # p 3913 ..... CONF-9109317-2
DE92-013441
UCRL-JC-110033
N92-32167 # p 3898 ..... CONF-9109182-2
DE92-013020
FNAL/C-91/295-A
N92-32168 # p 3842 ..... AD-A250785
AFOSR-92-0366TR
N92-32169 # p 3898 ..... AD-A250943
TR-38
N92-32170 # p 3900 ..... AD-A250944
TR-37
N92-32171 # p 3887 ..... AD-A250954
CMU/CS-92-122
N92-32172 # p 3837 ..... AD-A252743
N92-32173 # p 3836 ..... AD-A252754
HDL-TR-2212
N92-32174 # p 3829 ..... ALS/TR-92-008
DE92-014741
N92-32175* # p 3761 ..... NAS 1.26:4463
NASA-CR-4463
N92-32176 # p 3810 ..... CTN-92-60332
DREO-1034
N92-32177* # p 3753 ..... MCAT-92-015
NAS 1.26:190688
NASA-CR-190688
N92-32178* # p 3892 ..... JPR-584243
NAS 1.26:190479
NASA-CR-190479
N92-32179 # p 3924 ..... JPRS-ULS-92-015
N92-32180 # p 3924 ..... NO REPORT NUMBER
N92-32181 # p 3907 ..... NIFS-127
N92-32182 # p 3920 ..... AGARD-CP-505
ISBN-92-835-0655-3
N92-32183 # p 3874 ..... NO REPORT NUMBER
N92-32184 # p 3921 ..... NO REPORT NUMBER
N92-32185 # p 3921 ..... NO REPORT NUMBER
N92-32186 # p 3921 ..... NO REPORT NUMBER
N92-32187 # p 3921 ..... NO REPORT NUMBER
N92-32188* # p 3921 ..... NO REPORT NUMBER
N92-32189 # p 3921 ..... NO REPORT NUMBER
N92-32190 # p 3922 ..... NO REPORT NUMBER
N92-32191 # p 3922 ..... NO REPORT NUMBER
N92-32192 # p 3922 ..... NO REPORT NUMBER
N92-32193* # p 3926 ..... L-17082
NAS 1.15:4386
NASA-TM-4386
N92-32194 # p 3798 ..... AD-A250966
N92-32195* # p 3858 ..... NAS 1.26:190628
NASA-CR-190628
N92-32196 # p 3899 ..... AD-A251094
TR-8
N92-32197 # p 3798 ..... AD-A251112
N92-32198 # p 3798 ..... AD-A251125
TR-2
N92-32199 # p 3798 ..... INPE-5372-PRE/1746
N92-32200 # p 3818 ..... INPE-5373-PRE/1747
N92-32201* # p 3762 ..... H-1831
NAS 1.15:104250
NASA-TM-104250
N92-32202 # p 3837 ..... CTN-92-60321
DREP-90-02
N92-32203 # p 3810 ..... CTN-92-60322
N92-32204* # p 3769 ..... NAS 1.15:107602
NASA-TM-107602
N92-32205 # p 3887 ..... NIFS-118
N92-32206 # p 3842 ..... NO REPORT NUMBER
N92-32207 # p 3914 ..... AD-A250781
MTL-TR-92-24
N92-32208 # p 3907 ..... NO REPORT NUMBER
N92-32209 # p 3914 ..... NO REPORT NUMBER
N92-32210 # p 3887 ..... NO REPORT NUMBER
N92-32211 # p 3891 ..... AD-A250949
N92-32212 # p 3863 ..... INPE-5388-TDI/477
N92-32213* # p 3754 ..... A-89236
NAS 1.15:102230
NASA-TM-102230
N92-32214 # p 3811 ..... CTN-92-60327
DREA-CR-89-445-PT-2-VOL-1
N92-32215 # p 3777 ..... CTN-92-60337
DREP-88-14
N92-32216 # p 3844 ..... CTN-92-60338
DREP-88-15
N92-32217 # p 3811 ..... CTN-92-60339
DREV-R-4487/88
N92-32218 # p 3829 ..... CTN-92-60343
DREV-R-4511/88
N92-32219 # p 3756 ..... CTN-92-60344
DCIEM-88-RR-39
N92-32220 # p 3845 ..... INPE-5378-TDI/473
N92-32221 # p 3926 ..... INPE-5371-TDI/470
N92-32222* # p 3855 ..... MIT-R92-17
MIT-335
NAS 1.26:190705
NASA-CR-190705
N92-32223* # p 3845 ..... CRI-P45-1
NAS 1.26:190698
NASA-CR-190698
N92-32224 # p 3863 ..... INPE-5364-PRE/1744
N92-32225 # p 3889 ..... INPE-5395-PRE/1753
N92-32226* # p 3754 ..... NAS 1.26:189652-VOL-1
NASA-CR-189652-VOL-1
N92-32227 # p 3922 ..... INPE-5358-NTC/301
N92-32228* # p 3754 ..... NAS 1.26:189652-VOL-2
NASA-CR-189652-VOL-2
N92-32229 # p 3889 ..... AGARD-AR-310
CP-504
CP-504S
ISBN-92-835-0678-2
N92-32230* # p 3801 ..... E-7270
NAS 1.15:105835
NASA-TM-105835
N92-32231 # p 3811 ..... CTN-92-60323
DREO-89-32
N92-32232 # p 3811 ..... CTN-92-60324
DREO-89-29
N92-32233* # p 3818 ..... E-7009-1
NAS 1.15:105832
NASA-TM-105832
N92-32234* # p 3777 ..... E-7232
NAS 1.15:105802
NASA-TM-105802
N92-32235* # p 3842 ..... CCMS-92-23
NAS 1.26:190706
NASA-CR-190706
VPI-E-92-20
N92-32236* # p 3842 ..... NAS 1.26:190516
NASA-CR-190516
N92-32237* # p 3771 ..... E-7217
JPC-92-3203
NAS 1.15:105787
NASA-TM-105787
N92-32238 # p 3765 ..... NO REPORT NUMBER
N92-32239* # p 3772 ..... E-7277
NAS 1.26:189224
NASA-CR-189224
N92-32240* # p 3754 ..... E-6173
NAS 1.26:4391
NASA-CR-4391
N92-32241* # p 3761 ..... E-7260
NAS 1.15:105826
NASA-TM-105826
N92-32242* # p 3826 ..... NAS 1.26:4446
NASA-CR-4446

Appendix

NASA SCIENTIFIC AND TECHNICAL INFORMATION PROGRAM PRODUCTS AND SERVICES

The NASA Scientific and Technical Information (STI) Program provides for the collection and announcement of aerospace-related reports and literature obtained worldwide through agreements and exchanges. The result of the collection is the comprehensive NASA STI Database that covers aeronautics, space, and supporting disciplines.

The STI Database, documents generated or obtained by NASA, and products and services derived from or supporting the database are made available to the NASA research community and to the public. Descriptions and sources of these items are presented in the following pages.

Scientific and Technical Aerospace Reports (*STAR*) is an abstract journal, listing citations with abstracts for aerospace-related reports obtained from worldwide sources. *STAR* is issued on the 8th and 23rd of each month and announces current documents that have been entered into the NASA STI Database during the previous two weeks. The reports are of the following types:

- NASA, NASA contractor, and NASA grantee reports;
- Reports issued by other U.S. Government agencies, domestic and foreign institutions, universities, and private firms;
- Translations in report form;
- NASA-owned patents and patent applications;
- Other U.S. Government agency and foreign patents and patent applications;
- Domestic and foreign dissertations and theses.

Journal, book, and conference literature, journal translations, and certain foreign dissertations having the same subject scope as *STAR* are announced in a companion journal, *International Aerospace Abstracts* (*IAA*). *IAA* is issued on the 1st and 15th of each month and is available from the American Institute of Aeronautics and Astronautics, Technical Information Service, 555 West 57th Street, 12th Floor, New York, NY 10019.

ELIGIBILITY AND REGISTRATION FOR NASA STI PRODUCTS AND SERVICES

Organizations of the type listed below that have registered with NASA can receive products and services.

- NASA offices and installations, contractors, subcontractors, grantees, and consultants;
- Other U.S. Government agencies and their contractors;
- Libraries in the United States that have arrangements with NASA to maintain collections of NASA documents for public reference;
- Other organizations in the United States having a need for NASA documents in work related to aeronautics and space research;
- Organizations abroad that have established reciprocal documents exchange arrangements with NASA.

The central service points — central points of document acquisition and control within qualified organizations — or individuals are eligible to register for NASA STI products and services. Domestic organizations or individuals may be eligible to receive various classes of NASA publications and services and should address their requests for registration or further information to:

NASA Center for AeroSpace Information
ATTN: Registration Services
P.O. Box 8757
Baltimore, MD 21240-0757
301-621-0390

Organizations abroad should direct requests to:

National Aeronautics and Space Administration
Scientific and Technical Information Program (JTT)
International STI Program
Washington, DC 20546-0001
USA
703-271-5640

SUBJECT SCOPE

The subject scope of *STAR* and *IAA* includes all aspects of aeronautics and space research and development, supporting basic and applied research, and applications. Aerospace aspects of Earth resources, energy development, conservation, oceanography, environmental protection, urban transportation, and other topics of high national priority are also covered.

HOW TO USE *STAR* SUBJECT CATEGORIES

Abstracts in *STAR* are categorized by 10 major subject divisions that are divided further into 76 specific subject categories. The subject divisions and categories are listed in the Table of Contents together with a note for each that defines its scope and provides any cross-references. For example:

16 SPACE TRANSPORTATION
Includes passenger and cargo space transportation, e.g., shuttle operations; and space rescue techniques. For related information see also *03 Air Transportation and Safety* and *18 Spacecraft Design, Testing and Performance*. For space suits see *54 Man/System Technology and Life Support*.

CROSS-REFERENCES

Individual *STAR* abstracts are not ordinarily cross-referenced, except for certain conference reports or book translations that have had separate abstracts written for their component papers or chapters. Citations and abstracts of the components follow immediately after those of the parent document. When the subject content of a component differs sufficiently from the general content of the parent, a cross-reference citation also is printed at the end of the category to which it normally would have been assigned if it were independent.

DOCUMENTS ON MICROFICHE

Documents available on microfiche are designated by a pound sign (#) following the accession number.

LIMITED REPRODUCIBILITY

A note of limited reproducibility appears in the citation, if there are factors affecting the reproducibility of more than 20% of the document. These factors include faint or broken type, color photographs, black and white photographs, foldouts, dot matrix print, or some other factor that limits the reproducibility of the document. This notation also appears on the microfiche header.

COLOR COPIES

An increasing number of NASA scientific and technical reports are being produced with color graphs, charts, illustrations, and photographs. An indication that a document has color pages follows the source and pricing (SAP) information in the *STAR* citation.

Registered users of the NASA Scientific and Technical Information Program will receive ordered documents with color at no additional cost, as long as stock copies of the document are available. Otherwise, an additional fee of $2.00 per color page will be charged. The NASA Center for AeroSpace Information staff will contact registered users to determine individual user's needs.

NASA PATENTS AND PATENT APPLICATIONS

Patents and patent applications owned by NASA are announced in *STAR* under appropriate subject categories and are referenced in the *STAR* indexes. In the Report/Accession Number Index, patents are indexed by the NASA Case Number, and the U.S. Patent Class. Patent applications are indexed by the NASA Case Number and the U.S. Patent Application Serial Number.

Printed copies of patents (which are not microfiched) are available for purchase from the U.S. Patent and Trademark Office.

When ordering patents, the U.S. Patent Number should be used, and payment must be remitted in advance, by money order or check payable to the Commissioner of Patents and Trademarks. Prepaid purchase coupons for ordering are also available from the U.S. Patent and Trademark Office.

NASA patent application specifications are sold in both paper copy and microfiche by the NASA Center for AeroSpace Information (CASI). The N accession number should be used in ordering either paper copy or microfiche from CASI.

The patents and patent applications announced in *STAR* are owned by NASA and are available for royalty-free licensing. Requests for licensing terms and further information should be addressed to:

National Aeronautics and Space Administration
Associate General Counsel for Intellectual Property
Code GP
Washington, DC 20546-0001

SOURCES FOR DOCUMENTS

One or more sources from which a document announced in *STAR* is available to the public is given in each citation. The most commonly indicated sources and their acronyms or abbreviations are listed, below, and their addresses are listed on page A-6. If the publication is available from a source other than those listed, the publisher and address will be displayed on the availability line or in combination with the corporate source line.

Avail: CASI. Sold by the NASA Center for AeroSpace Information. Prices for hard copy (HC) and microfiche (MF) are indicated by a price code following the letters HC or MF in the *STAR* citation. Current values for the price codes are given in the tables on page A-7.

NOTE ON ORDERING DOCUMENTS: When ordering publications from CASI, use the N accession number or other report number. It is also advisable to cite the title and other bibliographic identification.

Avail: SOD (or GPO). Sold by the Superintendent of Documents, U.S. Government Printing Office, in hard copy.

Avail: BLL (formerly NLL): British Library Lending Division, Boston Spa, Wetherby, Yorkshire, England. Photocopies available from this organization at the price shown. (If none is given, address inquiry to the BLL.)

Avail: DOE Depository Libraries. Organizations in U.S. cities and abroad that maintain collections of Department of Energy reports, usually in microfiche form, are listed in *Energy Research Abstracts*. Services available from the DOE and its depositories are described in a booklet, *DOE Technical Information Center - Its Functions and Services* (TID-4660), which may be obtained without charge from the DOE Technical Information Center.

Avail: ESDU. Pricing information on specific data, computer programs, and details on Engineering Sciences Data Unit (ESDU) topic categories can be obtained from ESDU International Ltd. Requesters in North America should use the Virginia address while all other requesters should use the London address, both of which are on page A-6.

Avail: Fachinformationszentrum, Karlsruhe. Gesellschaft für wissenschaftlich-technische Information mbH 7514 Eggenstein-Leopoldshafen 2, Germany.

Avail: HMSO. Publications of Her Majesty's Stationery Office are sold in the U.S. by Pendragon House, Inc. (PHI), Redwood City, CA. The U.S. price (including a service and mailing charge) is given, or a conversion table may be obtained from PHI.

Avail: Issuing Activity, or Corporate Author, or no indication of availability. Inquiries as to the availability of these documents should be addressed to the organization shown in the citation as the corporate author of the document.

Avail: NASA Public Document Rooms. Documents so indicated may be examined at or purchased from the National Aeronautics and Space Administration (JBD-4), Public Documents Room (Room 1H23), Washington, DC 20546-0001, or public document rooms located at NASA installations, and the NASA Pasadena Office at the Jet Propulsion Laboratory.

Avail: NTIS. Sold by the National Technical Information Service. Initially distributed microfiche under the NTIS SRIM (Selected Research in Microfiche) are available. For information concerning this service, consult the NTIS Subscription Section, Springfield, VA 22161.

Avail: Univ. Microfilms. Documents so indicated are dissertations selected from *Dissertation Abstracts* and are sold by University Microfilms as xerographic copy (HC) and microfilm. All requests should cite the author and the Order Number as they appear in the citation.

Avail: US Patent and Trademark Office. Sold by Commissioner of Patents and Trademarks, U.S. Patent and Trademark Office, at the standard price of $1.50 each, postage free. (See discussion of NASA patents and patent applications below.)

Avail: (US Sales Only). These foreign documents are available to users within the United States from the National Technical Information Service (NTIS). They are available to users outside the United States through the International Nuclear Information Service (INIS) representative in their country, or by applying directly to the issuing organization.

Avail: USGS. Originals of many reports from the U.S. Geological Survey, which may contain color illustrations, or otherwise may not have the quality of illustrations preserved in the microfiche or facsimile reproduction, may be examined by the public at the libraries of the USGS field offices whose addresses are listed on page A-6. The libraries may be queried concerning the availability of specific documents and the possible utilization of local copying services, such as color reproduction.

FEDERAL DEPOSITORY LIBRARIES: To provide the general public with greater access to U.S. Government publications, Congress established the Federal Depository Library Program under the Government Printing Office (GPO), with 53 regional depositories responsible for permanent retention of material, inter-library loan, and reference services. (These libraries are not sales outlets.) At least one copy of nearly every NASA and NASA-sponsored publication, either in printed or microfiche format, is received and retained by the 53 regional depositories. A list of the regional GPO libraries, appears on page A-8. A local library can contact a regional depository library to help locate specific reports, or direct contact may be made by an individual.

PUBLIC COLLECTION OF NASA DOCUMENTS

An extensive collection of NASA and NASA-sponsored publications is maintianed by the British Library Lending Divison, Boston Spa, Wetherby, Yorkshire, England, for public access. The British Library Lending Division also has available many of the non-NASA publications cited in *STAR*.

European requesters may purchase facsimile copy or microfiche of NASA and NASA-sponsored documents, those identified by both the symbols # and * from ESA—Information Retrieval Service, European Space Agency, 8-10 rue Mario-Nikis, 75738 Paris CEDEX 15, France.

SUBMITTING DOCUMENTS

All users of this abstract service are urged to forward reports to be considered for announcement in *STAR*. This will aid NASA in its efforts to provide the fullest possible coverage of all scientific and technical publications that might support aeronautics and space research and development. If you have prepared relevant reports (other than those you will transmit to NASA, DOD, or DOE through the usual contract- or grant-reporting channels), please send them for consideration to the NASA Center for AeroSpace Information, P.O. Box 8757, Baltimore, MD 21240-0757.

Reprints of journal articles, book chapters, and conference papers are also welcome. These will be considered for announcement in *STAR*'s companion journal, *IAA*.

You may specify a particular source to be included in a report announcement if you wish; otherwise the report will be placed on a public sale at the NASA Center for AeroSpace Information. Copyrighted publications will be announced but not distributed or sold.

PURCHASE OF *STAR*

STAR is publicly available on annual subscription from the NASA Center for AeroSpace Information (CASI) at $114.00.

STAR is available to registered users on annual subscription from the NASA Center for AeroSpace Information, ATTN: Registration Services, P.O. Box 8757, Baltimore, MD 21240-0757.

Microfiche of the abstract sections of *STAR* are available, on annual subscription, from CASI. Annual subscription rates are $216.00 North America; $432.00 foreign.

ADDRESSES OF ORGANIZATIONS

American Institute of Aeronautics and Astronautics
Technical Information Service
555 West 57th Street, 12th Floor
New York, New York 10019

British Library Lending Division,
Boston Spa, Wetherby, Yorkshire,
England

Commissioner of Patents and Trademarks
U.S. Patent and Trademark Office
Washington, DC 20231

Department of Energy
Technical Information Center
P.O. Box 62
Oak Ridge, Tennessee 37830

European Space Agency-Information Retrieval Service
ESRIN
Via Galileo Galilei
00044 Frascati (Rome) Italy

Engineering Sciences Data Unit International
P.O. Box 1633
Manassas, Virginia 22110

Engineering Sciences Data Unit International, Ltd.
251-259 Regent Street
London, W1R 7AD, England

Fachinformationszentrum Karlsruhe
Gesellschaft für wissenschaftlich-technische
Information mbH
7514 Eggenstein-Leopoldshafen 2, Germany

Her Majesty's Stationery Office
P.O. Box 569, S.E. 1
London, England

NASA Center for AeroSpace Information
P.O. Box 8757
Baltimore, Maryland 21240-0757

National Aeronautics and Space Administration
Scientific and Technical Information Program (JTT)
Washington, DC 20546-0001

National Technical Information Service
5285 Port Royal Road
Springfield, Virginia 22161

Pendragon House, Inc.
899 Broadway Avenue
Redwood City, California 94063

Superintendent of Documents
U.S. Government Printing Office
Washington, DC 20402

University Microfilms
A Xerox Company
300 North Zeeb Road
Ann Arbor, Michigan 48106

University Microfilms, Ltd.
Tylers Green
London, England

U.S. Geological Survey Library National Center
MS 950
12201 Sunrise Valley Drive
Reston, Virginia 22092

U.S. Geological Survey Library
2255 North Gemini Drive
Flagstaff, Arizona 86001

U.S. Geological Survey
345 Middlefield Road
Menlo Park, California 94025

U.S. Geological Survey Library
Box 25046
Denver Federal Center, MS914
Denver, Colorado 80225

CASI PRICE TABLES

(Effective October 1, 1991)

STANDARD PRICE DOCUMENTS

PRICE CODE	NORTH AMERICAN PRICE	FOREIGN PRICE
A01	$ 9.00	$ 18.00
A02	12.50	25.00
A03	17.00	34.00
A04-A05	19.00	38.00
A06-A09	26.00	52.00
A10-A13	35.00	70.00
A14-A17	43.00	86.00
A18-A21	50.00	100.00
A22-A25	59.00	118.00
A99	69.00	138.00

MICROFICHE

PRICE CODE	NORTH AMERICAN PRICE	FOREIGN PRICE
A01	$ 9.00	$ 18.00
A02	12.50	25.00
A03	17.00	34.00
A04	19.00	38.00
A06	26.00	52.00
A10	35.00	70.00

IMPORTANT NOTICE

CASI Shipping and Handling Charges
U.S. — ADD $3.00 per TOTAL ORDER
Canada and Mexico — ADD $3.50 per TOTAL ORDER
All Other Countries — ADD $7.50 per TOTAL ORDER
Does NOT apply to orders
requesting CASI RUSH HANDLING.
Contact CASI for charge.

FEDERAL REGIONAL DEPOSITORY LIBRARIES

ALABAMA

AUBURN UNIV. AT MONTGOMERY LIBRARY
Documents Dept.
7300 University Drive
Montgomery, AL 36117-3596
(205) 244-3650 FAX: (205) 244-0678

UNIV. OF ALABAMA
Amelia Gayle Gorgas Library
Govt. Documents
Box 870266
Tuscaloosa, AL 35487-0266
(205) 348-6046 FAX: (205) 348-8833

ARIZONA

DEPT. OF LIBRARY, ARCHIVES, AND PUBLIC RECORDS
Federal Documents
Third Floor State Capitol
1700 West Washington
Phoenix, AZ 85007
(602) 542-4121 FAX: (602) 542-4400; 542-4500

ARKANSAS

ARKANSAS STATE LIBRARY
State Library Services
One Capitol Mall
Little Rock, AR 72201
(501) 682-2869

CALIFORNIA

CALIFORNIA STATE LIBRARY
Govt. Publications Section
914 Capitol Mall - P.O. Box 942837
Sacramento, CA 94237-0001
(916) 322-4572 FAX: (916) 324-8120

COLORADO

UNIV. OF COLORADO - BOULDER
Norlin Library
Govt. Publications
Campus Box 184
Boulder, CO 80309-0184
(303) 492-8834 FAX: (303) 492-2185

DENVER PUBLIC LIBRARY
Govt. Publications Dept. BS/GPD
1357 Broadway
Denver, CO 80203
(303) 571-2135

CONNECTICUT

CONNECTICUT STATE LIBRARY
231 Capitol Avenue
Hartford, CT 06106
(203) 566-4971 FAX: (203) 566-3322

FLORIDA

UNIV. OF FLORIDA LIBRARIES
Documents Dept.
Library West
Gainesville, FL 32611-2048
(904) 392-0366 FAX: (904) 392-7251

GEORGIA

UNIV. OF GEORGIA LIBRARIES
Govt. Documents Dept.
Jackson Street
Athens, GA 30602
(404) 542-8949 FAX: (404) 542-6522

HAWAII

UNIV. OF HAWAII
Hamilton Library
Govt. Documents Collection
2550 The Mall
Honolulu, HI 96822
(808) 948-8230 FAX: (808) 956-5968

IDAHO

UNIV. OF IDAHO LIBRARY
Documents Section
Moscow, ID 83843
(208) 885-6344 FAX: (208) 885-6817

ILLINOIS

ILLINOIS STATE LIBRARY
Reference Dept.
300 South Second
Springfield, IL 62701-1796
(217) 782-7596 FAX: (217) 524-0041

INDIANA

INDIANA STATE LIBRARY
Serials/Documents Section
140 North Senate Avenue
Indianapolis, IN 46204
(317) 232-3678 FAX: (317) 232-3728

IOWA

UNIV. OF IOWA LIBRARIES
Govt. Publications Dept.
Washington & Madison Streets
Iowa City, IA 52242
(319) 335-5926 FAX: (319) 335-5830

KANSAS

UNIV. OF KANSAS
Govt. Documents & Map Library
6001 Malatt Hall
Lawrence, KS 66045-2800
(913) 864-4660 FAX: (913) 864-5380

KENTUCKY

UNIV. OF KENTUCKY LIBRARIES
Govt. Publications/Maps Dept.
Lexington, KY 40506-0039
(606) 257-3139 FAX: (606) 257-1563; 257-8379

LOUISIANA

LOUISIANA STATE UNIV.
Middleton Library
Govt. Documents Dept.
Baton Rouge, LA 70803
(504) 388-2570 FAX: (504) 388-6992

LOUISIANA TECHNICAL UNIV.
Prescott Memorial Library
Govt. Documents Dept.
305 Wisteria Street
Ruston, LA 71270-9985
(318) 257-4962 FAX: (318) 257-2447

MAINE

TRI-STATE DOCUMENTS DEPOSITORY
Raymond H. Fogler Library
Govt. Documents & Microforms Dept.
Univ. of Maine
Orono, ME 04469
(207) 581-1680

MARYLAND

UNIV. OF MARYLAND
Hornbake Library
Govt. Documents/Maps Unit
College Park, MD 20742
(301) 454-3034 FAX: (301) 454-4985

MASSACHUSETTS

BOSTON PUBLIC LIBRARY
Govt. Documents Dept.
666 Boylston Street
Boston, MA 02117
(617) 536-5400 ext. 226
FAX: (617) 267-8273; 267-8248

MICHIGAN

DETROIT PUBLIC LIBRARY
5201 Woodward Avenue
Detroit, MI 48202-4093
(313) 833-1440; 833-1409
FAX: (313) 833-5039

LIBRARY OF MICHIGAN
Govt. Documents Unit
P.O. Box 30007
Lansing, MI 48909
(517) 373-0640 FAX: (517) 373-3381

MINNESOTA

UNIV. OF MINNESOTA
Wilson Library
Govt. Publications Library
309 19th Avenue South
Minneapolis, MN 55455
(612) 624-5073 FAX: (612) 626-9353

MISSISSIPPI

UNIV. OF MISSISSIPPI
J.D. Williams Library
Federal Documents Dept.
106 Old Gym Bldg.
University, MS 38677
(601) 232-5857 FAX: (601) 232-5453

MISSOURI

UNIV. OF MISSOURI - COLUMBIA
Ellis Library
Govt. Documents
Columbia, MO 65201
(314) 882-6733 FAX: (314) 882-8044

MONTANA

UNIV. OF MONTANA
Maureen & Mike Mansfield Library
Documents Div.
Missoula, MT 59812-1195
(406) 243-6700 FAX: (406) 243-2060

NEBRASKA

UNIV. OF NEBRASKA - LINCOLN
D.L. Love Memorial Library
Documents Dept.
Lincoln, NE 68588
(402) 472-2562

NEVADA

UNIV. OF NEVADA
Reno Library
Govt. Publications Dept.
Reno, NV 89557
(702) 784-6579 FAX: (702) 784-1751

NEW JERSEY

NEWARK PUBLIC LIBRARY
U.S. Documents Div.
5 Washington Street - P.O. Box 630
Newark, NJ 07101-0630
(201) 733-7812 FAX: (201) 733-5648

NEW MEXICO

UNIV. OF NEW MEXICO
General Library
Govt. Publications Dept.
Albuquerque, NM 87131-1466
(505) 277-5441 FAX: (505) 277-6019

NEW MEXICO STATE LIBRARY
325 Don Gaspar Avenue
Santa Fe, NM 87503
(505) 827-3826 FAX: (505) 827-3820

NEW YORK

NEW YORK STATE LIBRARY
Documents/Gift & Exchange Section
Federal Depository Program
Cultural Education Center
Albany, NY 12230
(518) 474-5563 FAX: (518) 474-5786

NORTH CAROLINA

UNIV. OF NORTH CAROLINA - CHAPEL HILL
CB#3912, Davis Library
BA/SS Dept.—Documents
Chapel Hill, NC 27599
(919) 962-1151 FAX: (919) 962-0484

NORTH DAKOTA

NORTH DAKOTA STATE UNIV. LIBRARY
Documents Office
Fargo, ND 58105
(701) 237-8886 FAX: (701) 237-7138
In cooperation with Univ. of North Dakota, Chester Fritz Library
Grand Forks

OHIO

STATE LIBRARY OF OHIO
Documents Dept.
65 South Front Street
Columbus, OH 43266
(614) 644-7051 FAX: (614) 752-9178

OKLAHOMA

OKLAHOMA DEPT. OF LIBRARIES
U.S. Govt. Information Div.
200 NE 18th Street
Oklahoma City, OK 73105-3298
(405) 521-2502, ext. 252, 253
FAX: (405) 525-7804

OKLAHOMA STATE UNIV.
Edmon Low Library
Documents Dept.
Stillwater, OK 74078
(405) 744-6546 FAX: (405) 744-5183 *U.S. G.P.O.:1992-342-599-60022

OREGON

PORTLAND STATE UNIV.
Millar Library
934 SW Harrison - P.O. Box 1151
Portland, OR 97207
(503) 725-3673 FAX: (503) 725-4527

PENNSYLVANIA

STATE LIBRARY OF PENN.
Govt. Publications Section
Walnut St. & Commonwealth Ave. - P.O. Box 1601
Harrisburg, PA 17105
(717) 787-3752

SOUTH CAROLINA

CLEMSON UNIV.
Cooper Library
Public Documents Unit
Clemson, SC 29634-3001
(803) 656-5174 FAX: (803) 656-3025
In cooperation with Univ. of South Carolina, Thomas Cooper Library, Columbia

TENNESSEE

MEMPHIS STATE UNIV. LIBRARIES
Govt. Documents
Memphis, TN 38152
(901) 678-2586 FAX: (901) 678-2511

TEXAS

TEXAS STATE LIBRARY
United States Documents
P.O. Box 12927 - 1201 Brazos
Austin, TX 78711
(512) 463-5455 FAX: (512) 463-5436

TEXAS TECH. UNIV. LIBRARY
Documents Dept.
Lubbock, TX 79409
(806) 742-2268 FAX: (806) 742-1920

UTAH

UTAH STATE UNIV.
Merrill Library & Learning Resources Center, UMC-3000
Documents Dept.
Logan, UT 84322-3000
(801) 750-2684 FAX: (801) 750-2677

VIRGINIA

UNIV. OF VIRGINIA
Alderman Library
Govt. Documents
Charlottesville, VA 22903-2498
(804) 924-3133 FAX: (804) 924-4337

WASHINGTON

WASHINGTON STATE LIBRARY
Document Section
MS AJ-11
Olympia, WA 98504-0111
(206) 753-4027 FAX: (206) 753-3546

WEST VIRGINIA

WEST VIRGINIA UNIV. LIBRARY
Govt. Documents Section
P.O. Box 6069
Morgantown, WV 26506
(304) 293-3640

WISCONSIN

ST. HIST. SOC. OF WISCONSIN LIBRARY
Govt. Publications Section
816 State Street
Madison, WI 53706
(608) 262-2781 FAX: (608) 262-4711
In cooperation with Univ. of Wisconsin-Madison, Memorial Library

MILWAUKEE PUBLIC LIBRARY
Documents Div.
814 West Wisconsin Avenue
Milwaukee, WI 53233
(414) 278-2167 FAX: (414) 278-2137

National Aeronautics and
Space Administration
Code JTT
Washington, D.C.
20546-0001

Official Business
Penalty for Private Use, $300

SPECIAL FOURTH-CLASS RATE
POSTAGE & FEES PAID
NASA
PERMIT No. G27

POSTMASTER: If Undeliverable (Section 158
Postal Manual) Do Not Return

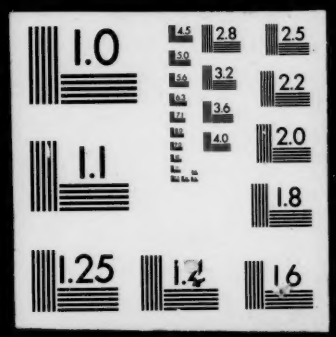
1.0
1.1
1.25
1.4
1.6
2.0
2.2
2.5
2.8
3.2
3.6
4.0
4.5
5.0
5.6
6.3